AD-A248 085

DTIC
ELECTE
MAR 3 1 1992
S B D

**DESIGN AND ANALYSIS OF ELECTRICAL CIRCUITS
THAT PRODUCE
FRACTIONAL-ORDER DIFFERENTIATION**

THESIS

Richard N. Hughes, Captain, USAF

AFIT/GE/ENG/92M-05

92-08103

92 3 31 049

DEPARTMENT OF THE AIR FORCE

AIR UNIVERSITY

AIR FORCE INSTITUTE OF TECHNOLOGY

Wright-Patterson Air Force Base, Ohio

AFIT/GE/ENG/92M-05

DESIGN AND ANALYSIS OF ELECTRICAL CIRCUITS
THAT PRODUCE
FRACTIONAL-ORDER DIFFERENTIATION

THESIS

Richard N. Hughes, Captain, USAF

AFIT/GE/ENG/92M-05

REPORT DOCUMENTATION PAGE

1. AGENCY USE ONLY (Leave blank)	2. REPORT DATE March 1992	3. REPORT TYPE AND DATES COVERED Master's Thesis

4. TITLE AND SUBTITLE
DESIGN AND ANALYSIS OF ELECTRICAL CIRCUITS THAT PRODUCE FRACTIONAL-ORDER DIFFERENTIATION

5. FUNDING NUMBERS

6. AUTHOR(S)

Richard N. Hughes

7. PERFORMING ORGANIZATION NAME(S) AND ADDRESS(ES)

Air Force Institute of Technology, WPAFB, OH 45433

8. PERFORMING ORGANIZATION REPORT NUMBER

AFIT/GE/ENG/92M-05

9. SPONSORING/MONITORING AGENCY NAME(S) AND ADDRESS(ES)

Wright Laboratory (WL/FIBG)
WPAFB, OH 45433

10. SPONSORING/MONITORING AGENCY REPORT NUMBER

11. SUPPLEMENTARY NOTES

12a. DISTRIBUTION/AVAILABILITY STATEMENT

Unlimited

12b. DISTRIBUTION CODE

13. ABSTRACT (Maximum 200 words)

Two half-order differentiator circuit designs were investigated and their electrical performance evaluated (Oldham and Oldfield). Initially, each circuit design was computer modelled and simulated using the HSPICE computer analysis program. Then, each circuit design (Oldham and Oldfield) was fabricated with two different component technologies. This resulted in four circuits, realized on printed circuit boards, to be evaluated--Oldham discrete component; Oldham hybrid component; Oldfield discrete component; and Oldfield surface mount component. The characterizations of each circuit's electrical performance is documented with time, phase, gain, noise and spectrum responses. A comparison of each circuit's performance versus the design criteria and computer model performance is presented. Based upon the comparison of the circuit's electrical performances, the circuits were rank ordered as follows: 1. Oldham integrated chip technology (hybrid) component circuit design; 2. Oldham discrete component circuit design; 3. Oldfield surface mount component circuit design; 4. Oldfield discrete component design.

14. SUBJECT TERMS
Electrical Circuits, Fractional Calculus, Very Large Scale Integration, Printed Circuit Boards, Half-Order Differentiation

15. NUMBER OF PAGES
717

16. PRICE CODE

17. SECURITY CLASSIFICATION OF REPORT	18. SECURITY CLASSIFICATION OF THIS PAGE	19. SECURITY CLASSIFICATION OF ABSTRACT	20. LIMITATION OF ABSTRACT
UNCLASSIFIED	UNCLASSIFIED	UNCLASSIFIED	UL

AFIT/GE/ENG/92M-05

DESIGN AND ANALYSIS OF ELECTRICAL CIRCUITS THAT PRODUCE

FRACTIONAL-ORDER DIFFERENTIATION

THESIS

Presented to the Faculty of the School of Engineering

of the Air Force Institute of Technology

Air University

In Partial Fulfillment of the

Requirements for the Degree of

Master of Science in Electrical Engineering

Richard N. Hughes, B.S.E.E.

Captain, USAF

March 1992

Approved for public release; distribution unlimited

Preface

The original intent of this effort was to produce a half-order differentiator on a single micro-chip. However, the background investigation proved that with the chip · fabrication technology available at this time it was not possible. The goal had to modified to produce a circuit with existing technology. This goal was achieved and four circuits were fabricated and demonstrated the function of a half-order differentiator.

I am forever indebted to my advisor, Lt Col Kolesar, for his guidance and understanding throughout this effort. Capt Jenkins, thanks for your insights and help with Hspice. And a special thanks to Lt Col Bagely, your expertise in fractional calculus was invaluable during the background research. I also wish to thank Mr. Bruce Clay of the AFIT VLSI lab and Mr. Rick Fultz of the 4950th test wing for their assistance and cooperation during the design of the printed circuit boards. It was the final push over the mountain.

Finally, words can not express the thanks that's due my family -- Kay and Christina. The sacrifices you made were beyond description. Again Thanks.

ii

Table of Contents

List of Figures

List of Tables

xii

AFIT/ENG/GE/92M-05

Abstract

Two half-order differentiator circuit designs were
investigated and their electrical performance evaluated·
(Oldham and Oldfield). Initially, each circuit design was
computer modelled and simulated using the HSPICE computer
analysis program. Then, each circuit design (Oldham and
Oldfield) was fabricated with two different component
technologies. This resulted in four circuits, realized on
printed circuit boards, to be evaluated--Oldham discrete
component; Oldham hybrid component; Oldfield discrete
component; and Oldfield surface mount component. The
characterizations of each circuit's electrical performance
is documented with time, phase, gain, noise and spectrum
responses. A comparison of each circuit's performance
versus the design criteria and computer model performance is
presented. Based upon the comparison of the circuit's
electrical performances, the circuits were rank ordered as
follows: 1. Oldham integrated chip technology (hybrid)
component circuit design; 2. Oldham discrete component
circuit design; 3. Oldfield surface mount component circuit
design; 4. Oldfield discrete component circuit design.

DESIGN AND ANALYSIS OF ELECTRICAL CIRCUITS
THAT PRODUCE
FRACTIONAL-ORDER DIFFERENTIATION

I. Introduction

The continuing search for more accurate feedback and control systems has motivated research focused toward applying fractional-order differentiator circuits. To date, experiments and analyses have only been accomplished with electrical circuits fabricated from discrete devices. Although the theoretical analysis has proven the concept of fractional-order differentiation, practical circuits for widespread applications have not been fully developed. To date, fractional-order differentiator circuits have only been designed and used in problem specific applications.

The current solution for control system problems is to produce the desired fractional-order differentiation control signals mathematically (computationally), which inherently induces a time delay. Since fractional-order differ-integral circuits produce the desired signals in essentially real-time, a control system's delay time should be significantly reduced.

Problem Statement

A comprehensive analysis of the discrete electrical circuits which can be used for fractional-order differentiation is warranted, along with an analysis of

I-1

other circuit realization technologies--namely, more
advanced technology components (for example, integrated
circuit technology) and circuit realization techniques.
There are two critical technologies applicable for realizing
fractional-order differentiator circuits--printed circuit
board and very large scale integrated (VLSI) circuits. The
printed circuit board technology option can be further
subdivided to include discrete components and dual-in-line
package (DIP) devices.

The design options are outlined in Figure 1. There are
two fractional-Ooder differentiator circuit designs (Oldham
[1] and Oldfield [2]) and three options for realizing each
fundamental circuit.

Scope

The goal of this research effort is to design,
fabricate, and evaluate the performance of two fractional-
order differentatior circuit designs (Oldham and Oldfield)
realized with both discrete and integrated circuit[1]
components. Their performance will be compared and
analyzed, and the circuits will be rank ordered based upon
their test results. A secondary objective is to realize as
much of one circuit variant (Oldham or Oldfield) in VLSI
technology, and correspondingly evaluate the effects on

---

[1] The integrated circuit technology is broader in scope than
conventional DIPs. That is, the anticipated circuit realizations
will have a mix of DIPs and surface mount devices. For the
purposes of this thesis, the nomenclature--integrated circuit
encompasses DIP components.
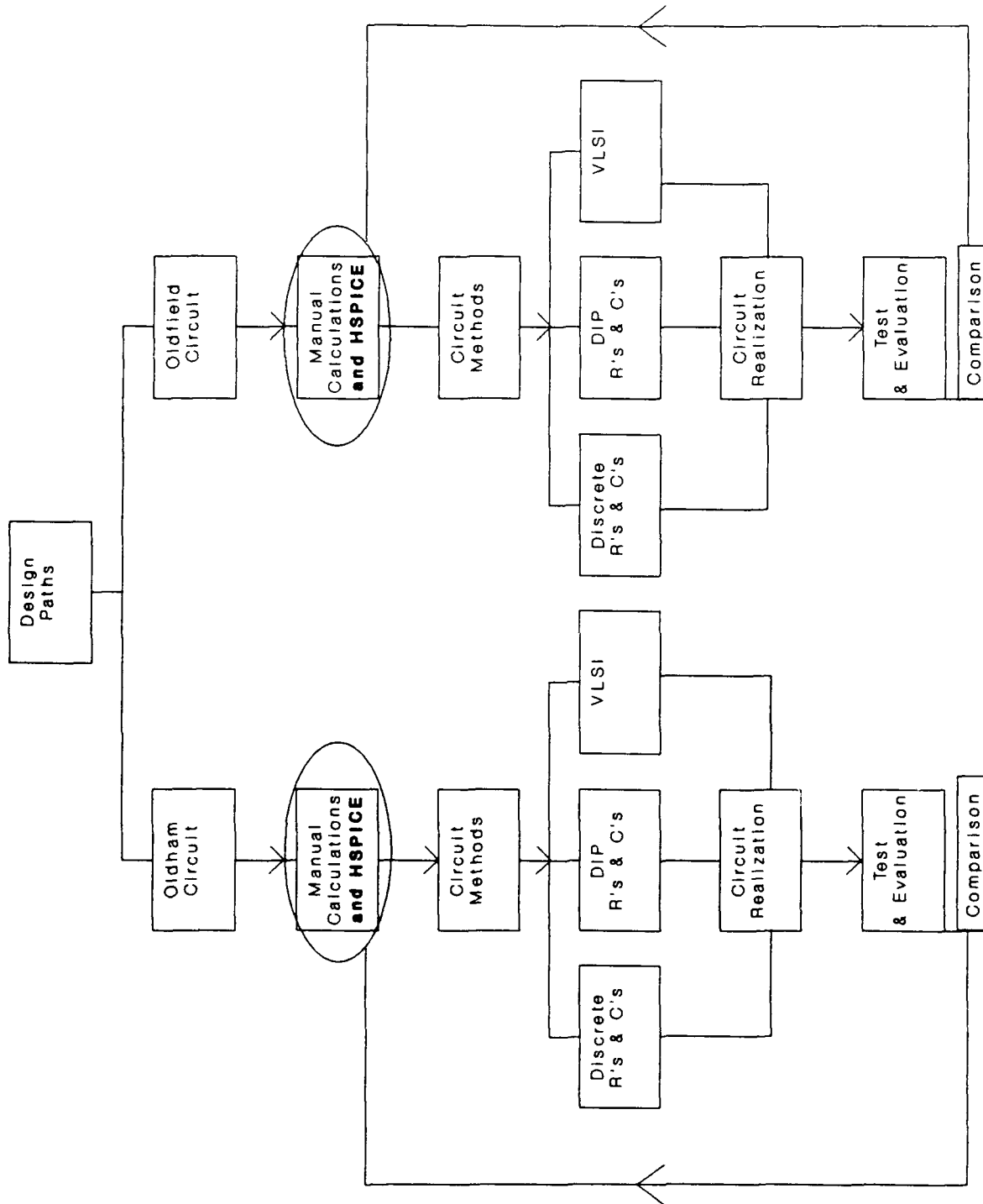
Figure 1. Fractional-Order Differentiator Circuit Design Tree.

overall circuit performance.

The performance specifications are listed below:

1. The fractional-order differentiator circuit should produce a half-order derivative of an input signal. The initial input signal will be a sine wave, for which the half-order derivative is known to be a sine wave with a relative phase shift of 45 degrees (Figure 2) [3:29].

2. The fractional-order differentiator circuit should produce the desired output over the frequency range spanning 0.01 Hz to 1000 Hz, and it should have a Bode plot with a slope of 10 dB per decade (another indicator of a 1/2-order derivative) (Figure 3) [3:28].

3. A computer simulation of both fractional-order differentiator circuit options (Oldham and Oldfield) will be performed. The goal is two-fold: first, to verify the manual calculations, and second, to develop a method for evaluating the sensitivity of the circuit's performance with respect to variations in individual component values. The computer simulation tool, HSPICE, possesses an automated component variation option to facilitate this analysis. Therefore, the component values within individual cells will be systematically varied, and the effect on circuit performance will be documented.

Approach

The approach of this research effort can be partioned into the following steps and sub-goals.
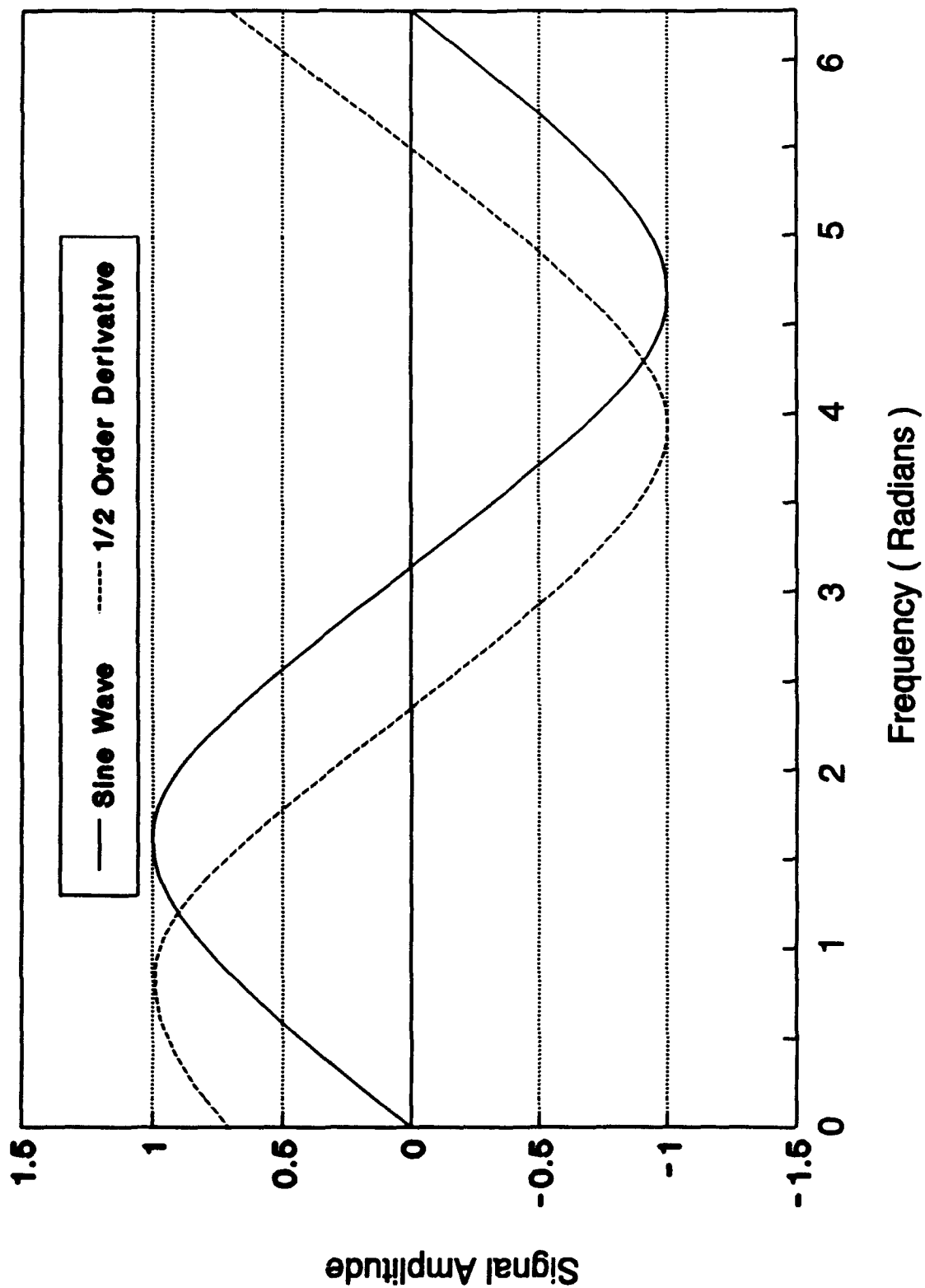
Figure 2. Ideal Half - Order Derivative of a Sine Wave
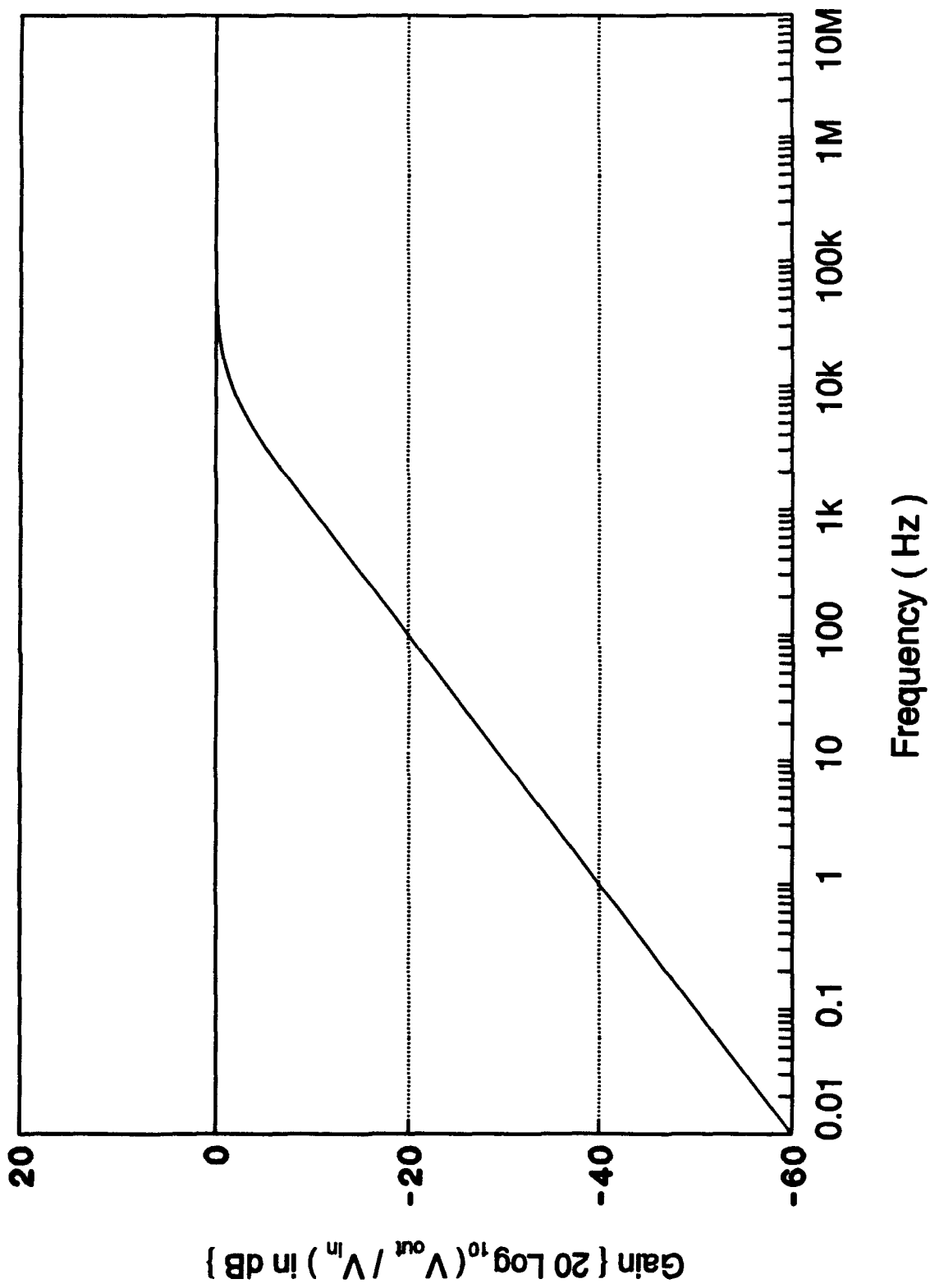
Figure 3. Ideal Half - Order Differentiator Bode Gain Plot.

Circuit Design. Each circuit design (Oldham and Oldfield) will follow the same fundamental process. First, for each circuit option, the component values (resistor and capacitor values) will be determined from the design equations (references [1] and [2]) based upon the performance specifications. The critical factor in both circuit designs is the desired operating frequency range, which directly affects the number of cells and the component values. As stated above, for the purposes of this research effort, the frequency range will span 0.01 Hz to 1000 Hz. The number of cells will be chosen to facilitate establishing common performance criteria (that is, the operational frequency range of both fractional-order differentiator circuits will be the same, even though they will likely possess different numbers of cells and components). The calculated values of the resistors and capacitors will then be incorporated into a basic circuit design for each circuit variant. Next, each circuit variant will be realized. The designs will also be simulated using computer circuit analysis tools to verify and optimize the component values[2]. The computer simulation tools that will be utilized will include SPICE and HSPICE--two common computer circuit analysis programs. Utilizing the features

---

[2] The reality of the time and budget cycle does not permit all circuits to be optimized in this manner. Therefore, only the hybrid design will utilize the full design tree. The circuit realizations in discrete and IC die components will be realized the with manually calculated values.

of SPICE and HSPICE, the "ideal" one-half order
differentiator response will be calculated and plotted.
Then, using a component variational technique available in
HSPICE, each circuit's sensitivity to individual component
value variation can be ascertained. After the computer
simulations verify the component value calculations, the
actual components will be selected, and the circuits will be
fabricated[3].

Once the component values are known, the design
processes will progress simultaneously. Since the specific
component dimensions are available from the vendors, the
artwork required for the printed circuit boards can be
designed and prepared.

One circuit design variant, based upon the computer
simulation results, will be selected for a hybrid design;
that is, a combination of VLSI and printed circuit board
techniques.

Analysis and Comparison. In order to form a basis for
comparison, each circuit's performance will be
characterized. That is, for each circuit, the deviations
from the computer simulated and experimentally measured
values will be determined. The circuits will be evaluated

---

[3] There will be two procurement actions. One for the manually
calculated component values. These will be used to realize the
discrete and IC die variants. The second procurement action will
be accomplished for the computer HSPICE verified component values.
These results will be used to realize the hybrid variant and to
facilitate improving the discrete component and IC die variants.

relative to the performance specifications discussed in the Scope section. The results of all the tests will be analyzed, and a rank ordering of circuit performance will be determined. This analysis will consider the design criteria, with the most significant weighting factor being how close the actual output resembles the predicted (ideal) results. The second factor to consider in this analysis will focus on how the circuit performs the desired function relative to the frequency range of interest.

Sequence of Presentation

Chapter 1 presents the Introduction, Problem Statement, and Scope of this thesis effort. Also, Chapter 1 includes a general approach which outlines the design criteria and the analysis to be performed. Since one of this thesis effort's foundations emerged from the mathematics of fractional calculus, a historical perspective is presented in Chapter 2. A summary of the design equations is also presented. The detailed methodology and findings of the computer simulation techniques are documented in Chapter 3. The component selection process and printed circuit board designs are also addressed. The detailed experimental approach, including equipment used, testing procedures, circuit fabrication, and findings of the experimental efforts are reported in Chapter 4. Chapter 5 focuses on analyzing the data and determining its significance. Conclusions and recommendations constitute Chapter 6.

II. Literature Review

Historical Perspective

The concept of a fractional-order derivative was originally addressed by L'Hospital and Leibnitz [4:115]. Since that time, members of the scientific research community have had little difficulty recognizing equation (1) as the general form of the νth derivative of a function of x with respect to time (t) [3:1]. That is,

$$\frac{d^{\nu}[f(x)]}{dt^{\nu}} = f^{(\nu)}(x) \ .$$

(1)

However, most engineers and scientists assume ν is a positive integer.

In 1695, L'Hopital first posed the question, "What if ν is one-half?" [4:115]. Since then, many noted scientists and mathematicians have developed the mathematical foundations for fractional-order calculus. Among them are, G. F. A. De L'Hospital, G. W. Leibnitz, S. F. Lacroix, Neils Henrik Abel, G. Bernhard Riemann, Joseph Liouville and Harold T. Davis, to name a few. Figure 4 depicts a timeline that portrays significant events in fractional-order calculus history, and it is by no means, comprehensive or all inclusive. Today, there are at least four definitions of fractional-order calculus that are prevalent. "These are the generalized Cauchy integral, power function,

Figure 4. Significant Milestones in Fractional-Order Calculus History [4; 5].

the differintegral, and the Riemann-Liouville definition"
[5:iv]. (For further historical details, the reader is
directed to references [4] and [5]).

The recent emphasis on the Strategic Defense Initiative
(SDI) has revitalized the study of fractional-order
calculus. SDI will likely require the use of large flexible
space structures. Control requirements of these structures
drive the need for fast, accurate control of their state
[6:297-298; 7:1]. The primary emphasis in the past has
focused on purely elastic structures which can be controlled
by externally applied forces and torques determined by
feedback and control systems [7:1]. A major limitation of
the large structures envisaged is that they tend to have a
large number of excitable vibrational modes at low
frequencies (that is, a particular vibrational mode
characterizes the structure's motion whereby its mass moves
sinusoidally at a common frequency) [7:1]. These excitable
vibrational modes are also very closely spaced with respect
to frequency, such that the control of one mode excites or
perturbs the balance and control of one or more of the
neighboring closely-spaced modes [7:1]. However the
incorporation of viscoelastic materials into these large
structure designs promises to improve control performance
considerably [6:294]. Nevertheless, a prime reason
viscoelastic materials have not been readily utilized is
that classical models of viscoelastic behavior are extremely

complex [7:8-9].

Beginning in 1979, R. Bagley and P. Torvik developed a method for modelling the behavior of viscoelastic materials using fractional-order derivatives in a finite element formulation [3:8-10]. Previous methods of modelling viscoelastic materials were computationally difficult except for steady-state conditions [7:1-2]. However, Bagley showed that a fractional-order derivative model, utilizing three to five parameters, could be used to accurately describe the behavior of viscoelastic materials [3; 8]. This analysis and subsequent research by Bagley and Torvik successfully demonstrated the usefulness of fractional-order calculus applied to large structure analysis [3; 9].

With the renewed interest in fractional-order calculus, Bagley and Torvik successfully demonstrated that the solution to viscoelastic material control problems is analogous to the solution of the generalized diffusion equation. Using a Newtonian fluid model that is bounded by a rigid plate (Figure 5), and the stress-strain rate constitutive relation defined as

$$\sigma = \mu \frac{\partial v}{\partial z} \qquad (2)$$

where

μ = viscosity of the fluid
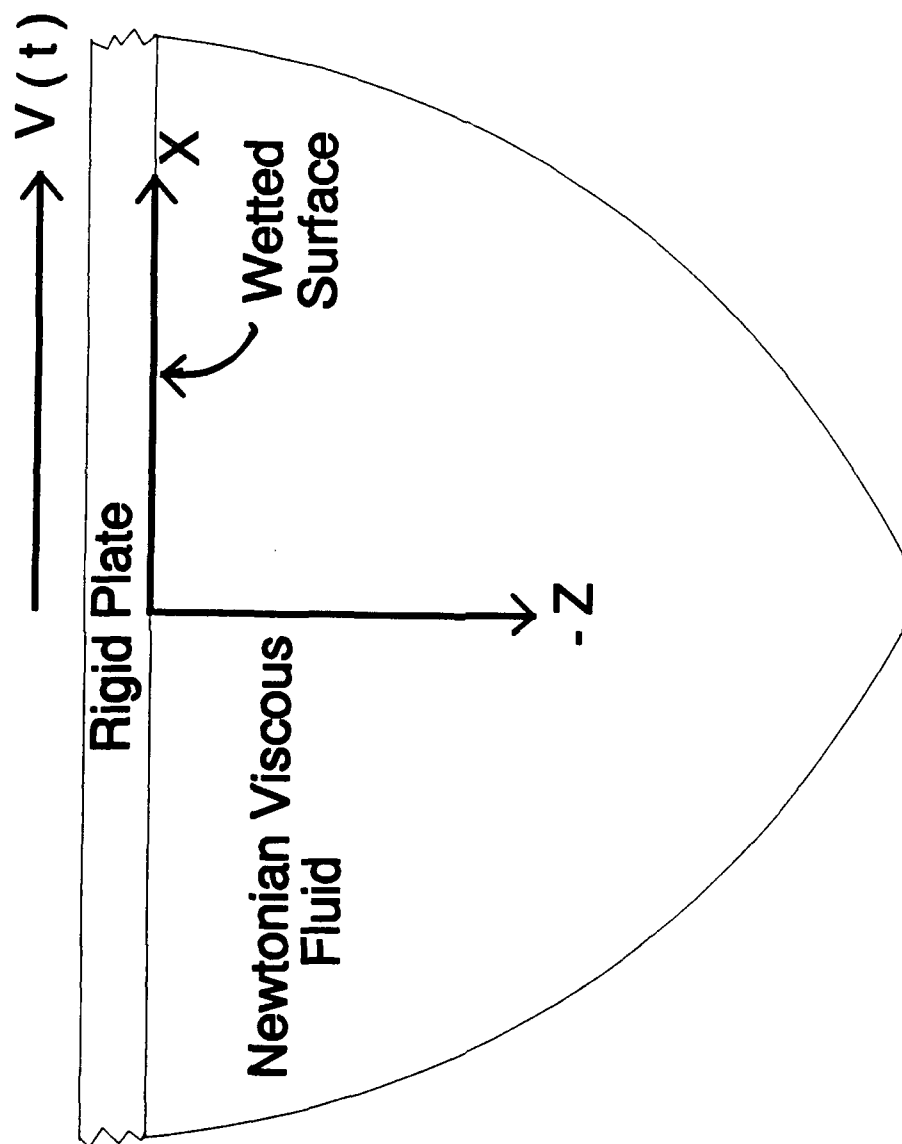
Figure 5.   Semi - infinite Fluid Sheared by a Rigid Plate [3: 245].

$$v = \text{transverse velocity profile of the fluid}$$

$$z = \text{vertical distance from the surface of the}$$
$$\text{plate,}$$

and the one-dimensional momentum equation

$$\rho \frac{\partial v}{\partial t} = \frac{\partial \sigma}{\partial z} \qquad (3)$$

where

$$\rho = \text{density of the fluid}$$

$$t = \text{time,}$$

Bagley noted that when equation (2) is introduced into the one-dimensional momentum equation (equation (3)), the resulting differential equation is a form of the one-dimensional diffusion equation [10:119]. That is,

$$\rho \frac{\partial v}{\partial t} = \mu \frac{\partial^2 v}{\partial z^2}. \qquad (4)$$

Bagley and Torvik further demonstrated that a solution to equation (4) is a fractional-order derivative whose order is equal to one-half [6:295; 10:124] (equation (5)). (For a full development, the reader is directed to references [6] and [10]). That is,

$$\sigma(t,z) = \sqrt{\mu\,\rho}\,\frac{d^{1/2}}{dt^{1/2}}[v(t,z)]. \qquad (5)$$

Therefore, one could reasonably expect that any physical system or quantity that can be related to, or modelled by, the generalized diffusion equation represents a potential candidate for the application of fractional-order calculus.

Fractional-order calculus has been used to solve differential equations in a wide variety of scientific applications and disciplines. These applications span from electro-chemical reactions to control systems. In control systems, the additional signals provided by fractional-order differintegral responses provide greater control, and they facilitate creating more flexible back-up systems [7]. This particular engineering application has captured the greatest interest for military use at this time.

Thus, numerous studies have been conducted at AFIT regarding the control theory application of fractional-order calculus. Bagley has continued his research focused on the control of viscoelastically damped structures [11]. As a result of this effort, Bagley and Calico demonstrated that a fractional-order derivative model provides additional forms of feedback that improve system performance [11:495]. Still, there was a need for a solid link between fractional-order calculus control theory and system realization. Toward this end, Bagley and Swinney developed a novel approach toward modelling unsteady aerodynamic forces and systems with fractional-order calculus techniques [12:1]. Their research motivates the merging of fractional-order

calculus control theory and system realization.

Theory and Design Equations.

In 1988, Klonoski fabricated an electrical circuit that could produce fractional-order derivative feedback signals [3]. In doing so, Klonoski provided a link between theory and practice. Klonoski used an electrical circuit realization method developed by Oldham [1] to produce fractional-order derivative feedback signals (Figure 6). Klonoski's implementation of Oldham's circuit design utilized seven cells, but it produced a relatively narrow bandwidth spanning 0.01 to 10 Hz (two decades), even though the design goal spanned 0.01 to 1000 Hz [3]. A literature search also yielded a fractional-order derivative circuit developed by Oldfield et al [2] (Figure 7). Oldfield's circuit, on the other hand, incorporated 9 cells, and it had a bandwidth of 0.1 Hz to 100 KHz [2]. There are three major differences between these two circuits. The Oldham design can be utilized as a generalized fractional-order differintegral circuit; it operates with voltage input and output signals; and it has cells composed of parallel combinations of resistors and capacitors which form the ladder circuit [1]. In contrast, the Oldfield design can only produce a half-order derivative response; it operates with an input current signal and produces an output voltage signal; and it has cells composed of resistors and capacitors in a "T" configuration which form the ladder
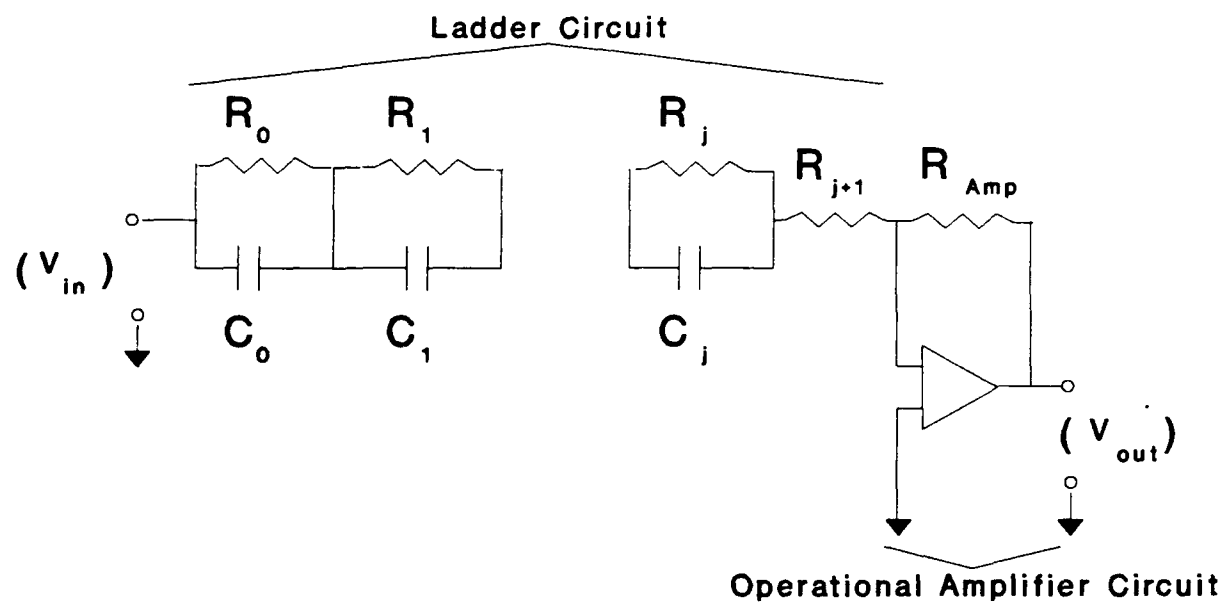
Ladder Circuit

Figure 6. Oldham Fractional-Order Calculus
Electrical Circuit [10].
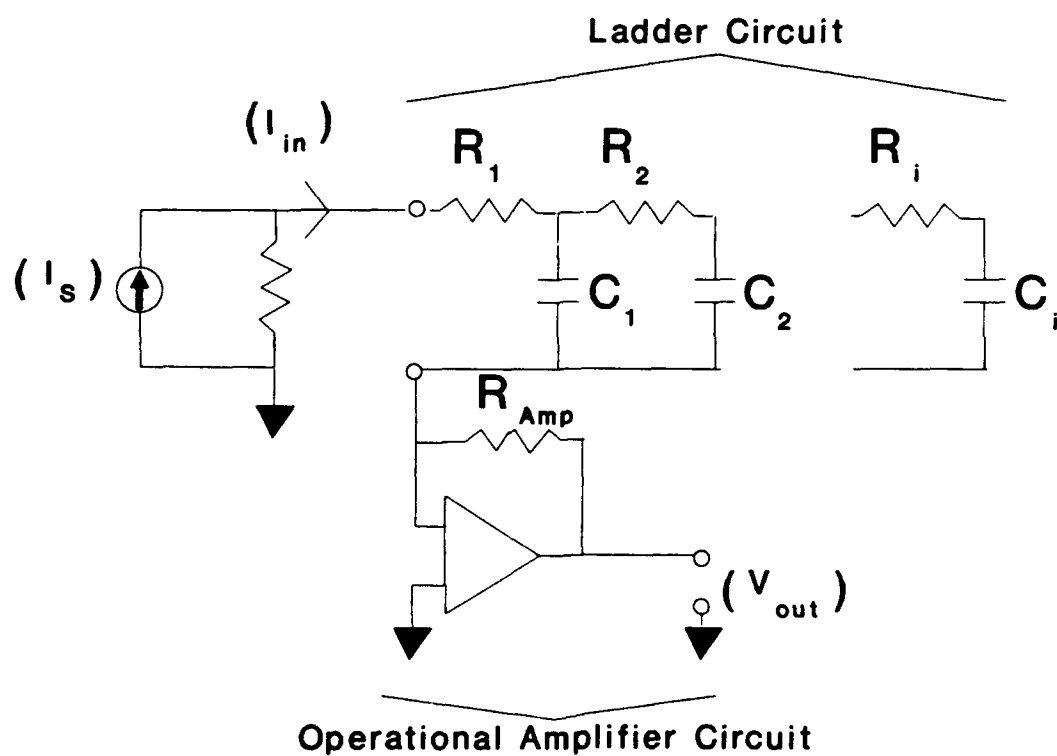
Ladder Circuit

Figure 7. Oldfield Fractional-Order Calculus
Electrical Circuit [11].

circuit [2].

In the Oldham and Oldfield design, the T-cell or ladder circuit does not, on its own accord, produce the differ-integral result desired. That is, the T-Cell or ladder circuit must be utilized in a classical operational amplifier circuit to achieve the desired result. That is, as depicted in Figure 8, the feedback resistor, R_{Amp}, controls the gain, and the "Ladder Network" contributes to the gain [13:579-581].

In the Oldham circuit, the scaling factor (F_h) (in the time domain) that contributes to the gain is [1:30]:

$$F_h = \frac{R_o C_o^{1-v} \ln(Gg)}{R_o^v \pi \, csc(v\pi)} \tag{6}$$

where

R_o = first resistor in the ladder circuit

C_o = first capacitor in the ladder circuit

v = desired fractional-order

G = capacitive geometric ratio

g = resistive geometric ratio.

On the other hand, the scaling factor (F_f) (in the frequency domain) that contributes to the gain for the Oldfield circuit is [2:236]:

$$F_f = \frac{\sqrt{I}}{\sqrt{\omega \, C}} \tag{7}$$
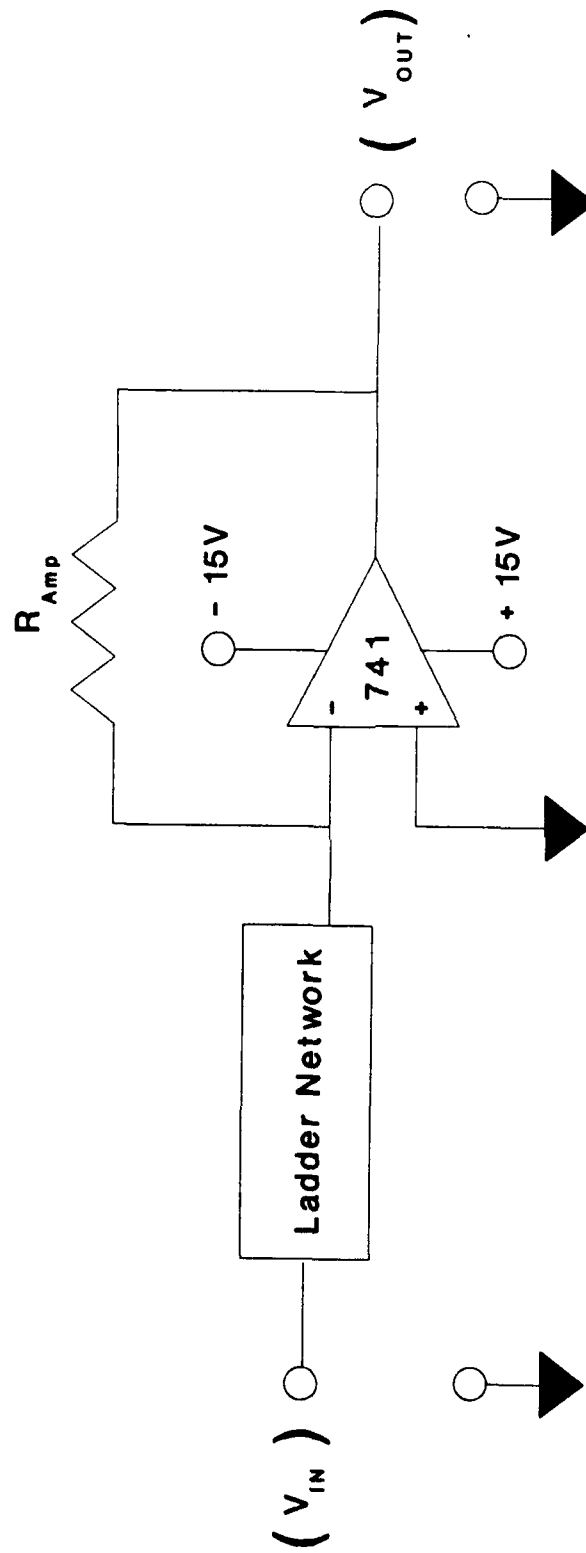
Figure 8. Basic Circuit Design of a Fractional-Order Differentiator.

where

r = resistance per unit length

c = capacitance per unit length.

However, in both designs, the "Ladder Network" circuit's function is to provide the mathematical relationship required to obtain the desired fractional-order calculus output signal. The theoretical development for the Oldham circuit is discussed in reference [1], and the theoretical development for the Oldfield circuit is presented in reference [2].

Since the motivation for this effort is a fractional-order system circuit realization through implementation of Oldham's and Oldfield's circuits, a summary of the design equations follows.

Oldham Circuit Design Summary. The design objective involves realizing the Oldham resistor/capacitor domino-ladder circuit to perform the operation d^v/dt^v on the input voltage signal [3]. The detailed design equations and procedures are developed in [1] and [3]. Presented here is a summary of the design process.

The factor v is the order of fractional differintegration. The valid range for v is:

$$-1 < v < 1 \tag{8}$$

where v less than zero indicates integration [3:145].

The basic circuit is referred to as a domino-ladder,

and it consists of a chain of resistors and capacitors. The chain is connected at each node as illustrated in Figure 1 [1; 3]. Each resistor is a constant factor multiple of its predecessor, as is each capacitor, according to the following relationship:

$$R_j = R_0 \ g^{-j} \quad and \quad C_j = C_0 \ G^{-j} \tag{9}$$

where both (g) and (G) are greater than unity. The subscripts refer to the "cell number" within the domino-ladder circuit (See Figure 6). The subscript "o" is used to denote the first resistor and capacitor pair, and the subscript "j" is used for each succeeding pair (j ranges from 1 to N, where N equals the number of cells).

To design a specific fractional-order Oldham circuit, a value of v must first be specified. Next the values of (G) and (g) are estimated from:

$$\ln G \le \frac{3}{2} \ v^{\frac{2}{3}} \tag{10}$$

and

$$\ln g = (1-v) \ v^{-1} \ \ln G . \tag{11}$$

The remainder of the method follows the basic guidelines established in [1] and [3]. However, the derivation is cast in terms of frequency rather than time,

as was done in the original Oldham article and demonstrated by Klonoski [3]. First, a minimum frequency (f_m) is selected for the particular application (f_m is in Hz). The time constant of the first resistor-capacitor pair is:

$$R_o C_o = \frac{111 \exp\ (-3v^{2/3})}{f_m\ Gg} \ . \tag{12}$$

Any combination of resistors and capacitors which produces this time constant is acceptable [1; 3]. It is advantageous to limit the tolerance on the components to be less than two percent [1; 3]. This limitation is necessary to produce acceptable circuit performance.

To calculate the number of cells required in the domino-ladder, the desired upper frequency limit (f_M) is specified. The number of cells (N) required is:

$$N+1 \geq [5.5 + \ln(\frac{f_M}{f_m}) - 3v^{2/3}]\ [\ln(Gg)]^{-1} \ . \tag{13}$$

There are other techniques discussed in [1] and [3] for further circuit enhancement (For further information on the Oldham circuit, the reader is directed to references [1] and [3]).

Oldfield Circuit Design Summary. The Oldfield circuit design involves realizing the resistor/capacitor T-cell ladder circuit to perform the operation $d^{\frac{1}{2}}/dt^{\frac{1}{2}}$ on an input

current signal (See Figure 7) [2]. The detailed design

equations and procedures are developed in reference [2].

Presented here is a summary of the design process.

First, the maximum operating frequency (f_M) and the

minimum operating frequency (f_m) are established [2].

Oldfield determined the logarithmic scaling constant (γ) to

be 2.154 [2:246]. Next, the linear scaling factor (F_L) is

determined from;

$$F_L = \frac{f_M}{f_m} \tag{14}$$

and the resistor dividing ratio (β) is calculated from:

$$\beta = \frac{1}{1+\sqrt{\gamma}} \cdot \tag{15}$$

Next, the number of cells, N, is determined by:

$$N = \frac{\log\left[1+\beta\,(\gamma-1)\sqrt{F}\right]}{\log(\gamma)} \cdot \tag{16}$$

However, if N is not an integer, it should be rounded

upwards, and F_L is recalculated as:

$$F_L = \left[\frac{(\gamma^N-1)}{\beta\,(\gamma-1)}\right]^2 \cdot \tag{17}$$

The frequency limits are converted to the radian measure (ω)

to facilitate calculating the component values. That is,

$$\omega_2 = \frac{2 \pi f_M}{0.95} \quad and \quad \omega_1 = \frac{\omega_2}{F_L} . \tag{18}$$

The next step is to choose a nominal value for R_1 and determine an estimate of C_1 from:

$$C_1 = \frac{1}{\beta R_1 \omega_2} . \tag{19}$$

The specific values for C_1 thru C_N can then be selected using the nearest convenient standard value for C_1, and utilizing a standard capacitor sequence [2]. This technique facilitates selecting standard capacitor values. However, once a value of C_1 is specified, R_1 needs to be recalculated using:

$$R_1 = \frac{1}{\omega_2 \beta C_1} . \tag{20}$$

With R_1 baselined and C_1 established, the ratio, r/c, is calculated from:

$$\frac{r}{c} = \frac{1}{\omega_2 \beta^2 C_1^2} \tag{21}$$

where r is the resistance per length and c is the

capacitance per length. With the capacitor values
determined, R_1 thru R_N can be finalized using the following
three equations:

$$\gamma_i = \frac{C_i}{C_{i-1}} \ , \ i = 2, \ldots N \tag{22}$$

$$R_i = \frac{r}{c} \frac{C_i}{\sqrt{\gamma_i}} = \frac{r}{c} \sqrt{C_i C_{i-1}} \ , \ i = 2, \ldots N \tag{23}$$

$$R_1 = \frac{r}{c} \frac{C_1}{1 + \sqrt{\gamma_2}} . \tag{24}$$

There are other techniques discussed in [2] that
enhance the circuit's performance. (For additional
information concerning the Oldfield circuit, the reader is
directed to reference [2]).

Summary

With the theory of fractional-order calculus being well
developed and the foundation established for control theory,
the next logical step is to physically realize systems which
test the combination of the two theories.

Toward this end, the two circuit analogues outlined
(Oldham and Oldfield designs) will be investigated relative

to their application in a control system function.

III. Design, Computer Simulation, and Component Selection Techniques and Their Results

This portion of the effort establishes the circuit component values required for fabricating the electrical circuits. The component selection process is defined, and the electrical performance of the circuits are examined. Also, the general trend of the effects of deviations relative to the "ideal" component values with respect to circuit performance via the computer modelling program known as HSPICE, is presented. The electrical circuits required for this effort were designed and simulated via computer analysis using the following techniques and procedures.

The Oldham and Oldfield electrical circuit design equations were utilized to calculate the resistor and capacitor values required to satisfy the performance criteria specified in Chapter 1 (See Chapter 1, Scope) [1; 2]. This design process was accomplished in three steps. First, the component values were calculated using direct application of the design equations. Second, the calculated values were then used to simulate the circuit's performance (Figure 6, Oldham, and Figure 7, Oldfield) using the HSPICE computer program. Next, the results from the HSPICE simulation were used to incrementally adjust and tune each circuit's performance to satisfy the design criteria. The final set of component values are tabulated in Table 1 and

Table 2.

Table 1 Oldham Ladder Circuit Component Values		
jth (cell #)	jth Resistor (MΩ)	jth Capacitor (nF)
0	68.99	16510.0
1	25.4	10000.0
2	9.85	3880.0
3	3.83	1514.0
4	1.488	587.3
5	0.5785	228.3
6	0.2249	88.73
7	0.0874	34.49
8	0.03397	13.41
9	0.01321	5.211
10	0.005133	2.026
11	0.0009975	1.575
12	0.00211	

The initial computer results revealed that the response of each circuit did not satisfy the performance criteria.

Therefore, further design work was required to satisfy the design goals. The development of each circuit is addressed separately.

Table 2		
Oldfield Ladder Circuit Component Values		
ith (cell #)	ith Resistor (MΩ)	ith Capacitor (nF) .
1	0.0001802	22.0
2	0.000630	47.0
3	0.001313	100.0
4	0.002798	220.0
5	0.006009	470.0
6	0.01311	1000.0
7	0.02857	2200.0
8	0.06044	4700.0
9	0.1296	10000.0

Oldham Circuit Computer Simulation Induced Design Changes

The initial computer simulation of the Oldham circuit design did not satisfy the design criteria. Although, the gain and phase plots satisfied the design criteria, the output signal developed a **25 KHz** oscillation with a peak

amplitude of 175 millivolts that was superimposed on the
circuit's output signal whose peak amplitude was 100
millivolts at 500 Hz (Figure 9). Rather than focus on the
source of this perturbation, a decision was made to
incorporate a low-pass filter in the overall fractional-
order differentiator circuit design. The low-pass filter
was designed using the equations and tables in reference 14
(abbreviated low-pass filter design equations are presented
in Appendix A). The schematic of the low-pass filter is
depicted in Figure 10. Since the initially designed circuit
also required amplification of the output signal, the low-
pass filter was adopted to perform both functions.

Next, the improved circuit with the "ideal" component
values was simulated using the HSPICE computer program.
The circuit's electrical performance only satisfied the
design criteria from 0.01 Hz to 55 Hz. The amplification of
the output signal was not adjusted correctly. At 55 Hz, the
output signal's peak amplitude was greater than the peak
operating voltage of the operational amplifier. Therefore,
no amplification of the output signal was implemented.
Finally, the redesigned circuit was simulated using the
HSPICE computer program. The circuit's electrical
performance satisfied the gain response design criteria from
0.01 Hz to 1925 Hz (Figure 11) and phase response design
criteria from 0.01 Hz to 10 KHz (Figure 12).

With the component values and circuit design specified
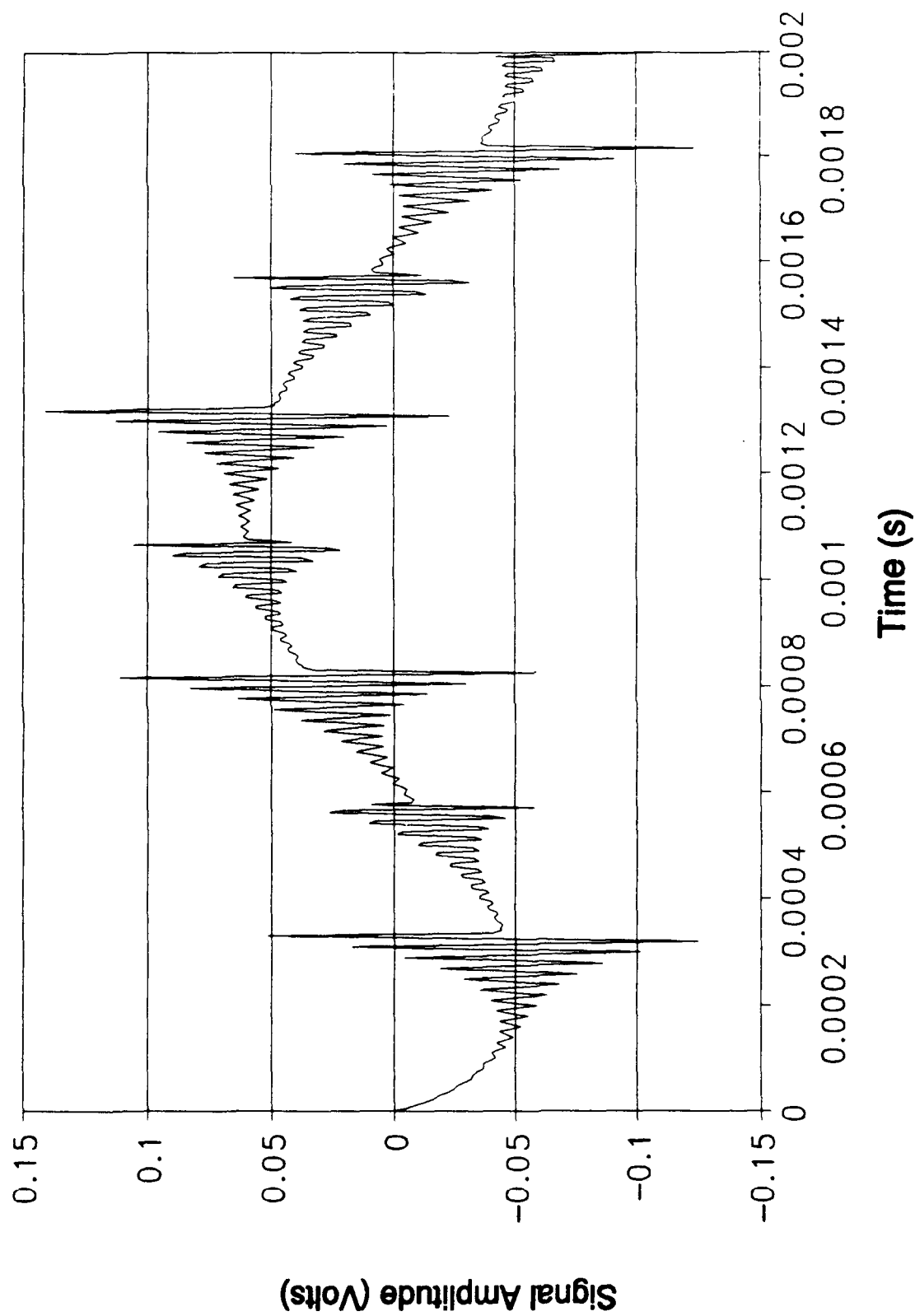
Figure 9. Time Response of the Oldham Circuit Design Without a Low-Pass Filter Simulated Using the HSPICE Computer Program.
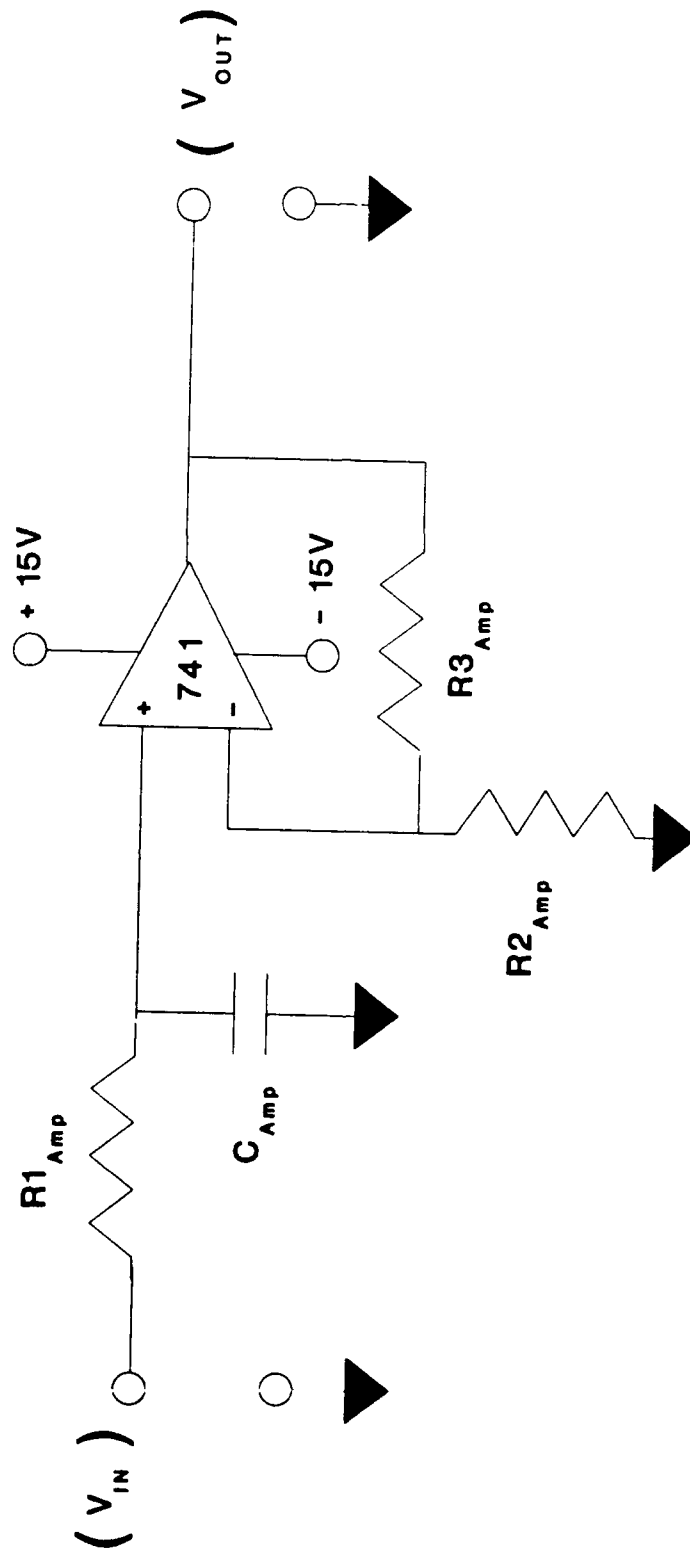
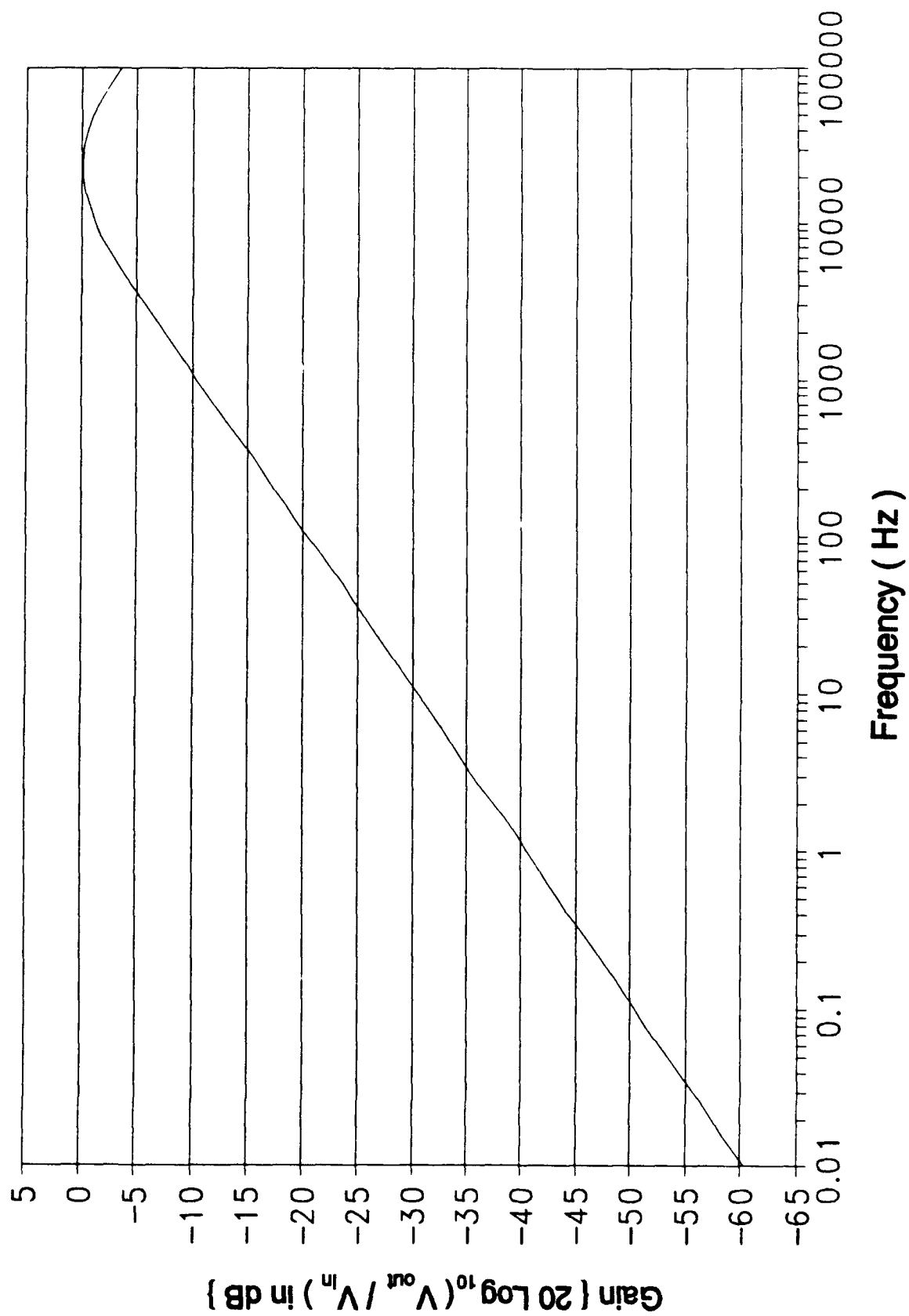Figure 10. Circuit Design of a Low-Pass Filter With Amplification.

Figure 11. Gain Response of the Oldham Circuit Design Using HSPICE Computer Analysis.
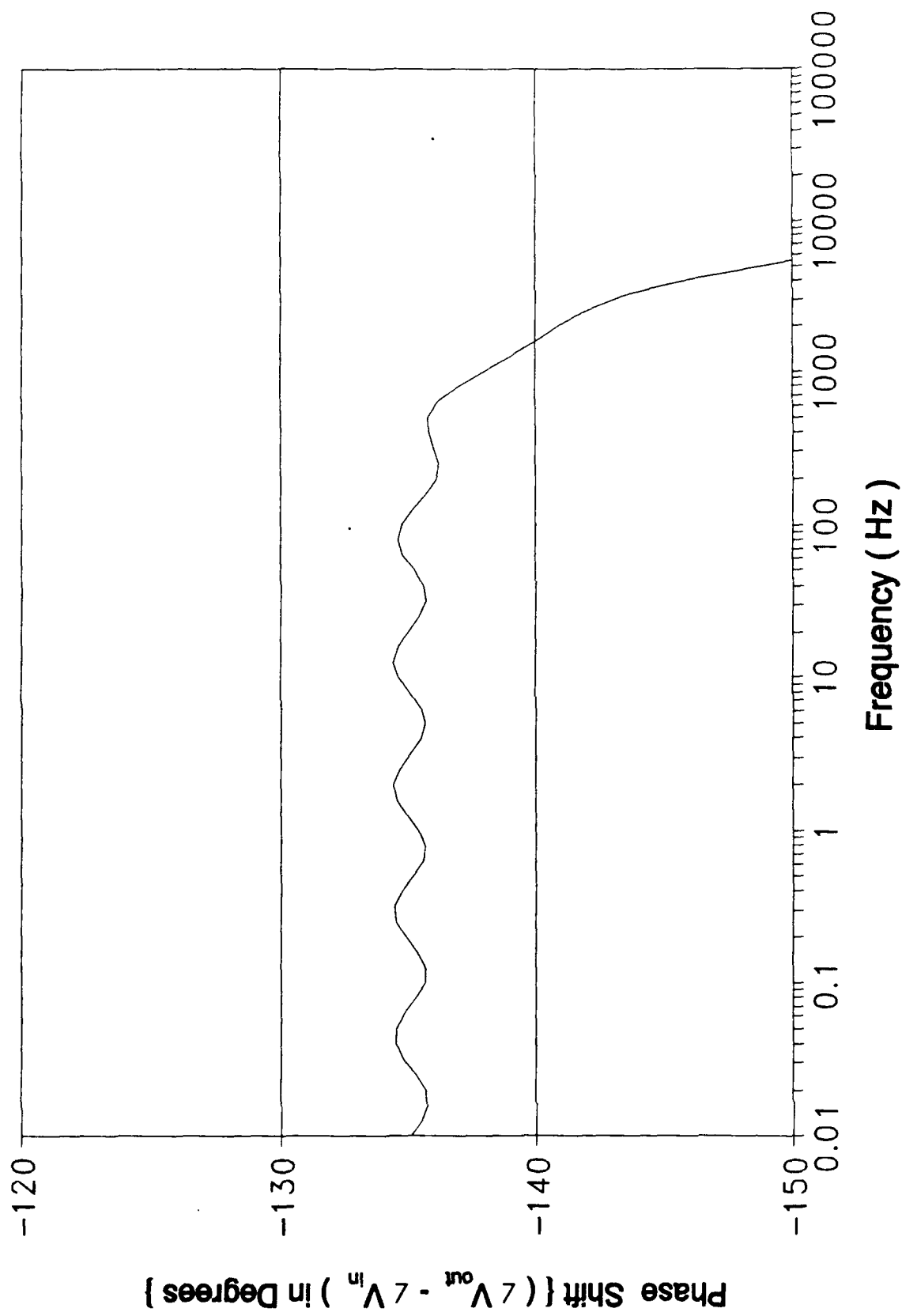
Figure 12. Phase Response of the Oldham Circuit Design Using HSPICE Computer Analysis.

III-8

and tested using computer simulations, the robustness of the
design was tested. The limitations of the design were found
using two techniques available in HSPICE: parameter variation
and MONTE CARLO analysis [15]. The parameter variation
technique allows for component values to be systematically
varied by user defined scaling factors. While the MONTE CARLO
analysis allows the component values to be varied by a
statistically based program that generates a random number
scaling factor from user defined limitations. First, the
parameter variation method was used to stress the Oldham
ladder circuit by varying each cell's component values
separately while holding all other components at their "ideal"
values. The factors used to vary the circuit component values
were 0.1, 0.4, 1, 1.6, 2, and 5. Second, the MONTE CARLO
analysis method was used to vary each of the cell component
values while holding all other cell component values at their
"ideal" values. Then, again utilizing the MONTE CARLO
analysis, all the cell component values were varied $\pm$ 20
percent. The Oldham circuit's baseline HSPICE deck and
graphical performance data is presented in Appendix B. Figure
13 depicts a sample of the results obtained. The variations
of the Oldham circuit component values demonstrated that the
general trend was that the circuit was robust and not
extremely sensitive to discrete component or cell value
variations. The detailed analysis and comparison of these
results is discussed in Chapter 5.

Capacitor Values for Figure 13						
Plot Symbol	——	-+-	-*-	-□-	×_ -×-	-▲-
Capac-itor. Value (μF)	.02283	.09132	.2283 (Ideal)	.36528	.4566	1.1415

Figure 13. Graphical Symbols and Capacitor Values Corresponding to the Plot in Figure 13 (cont).
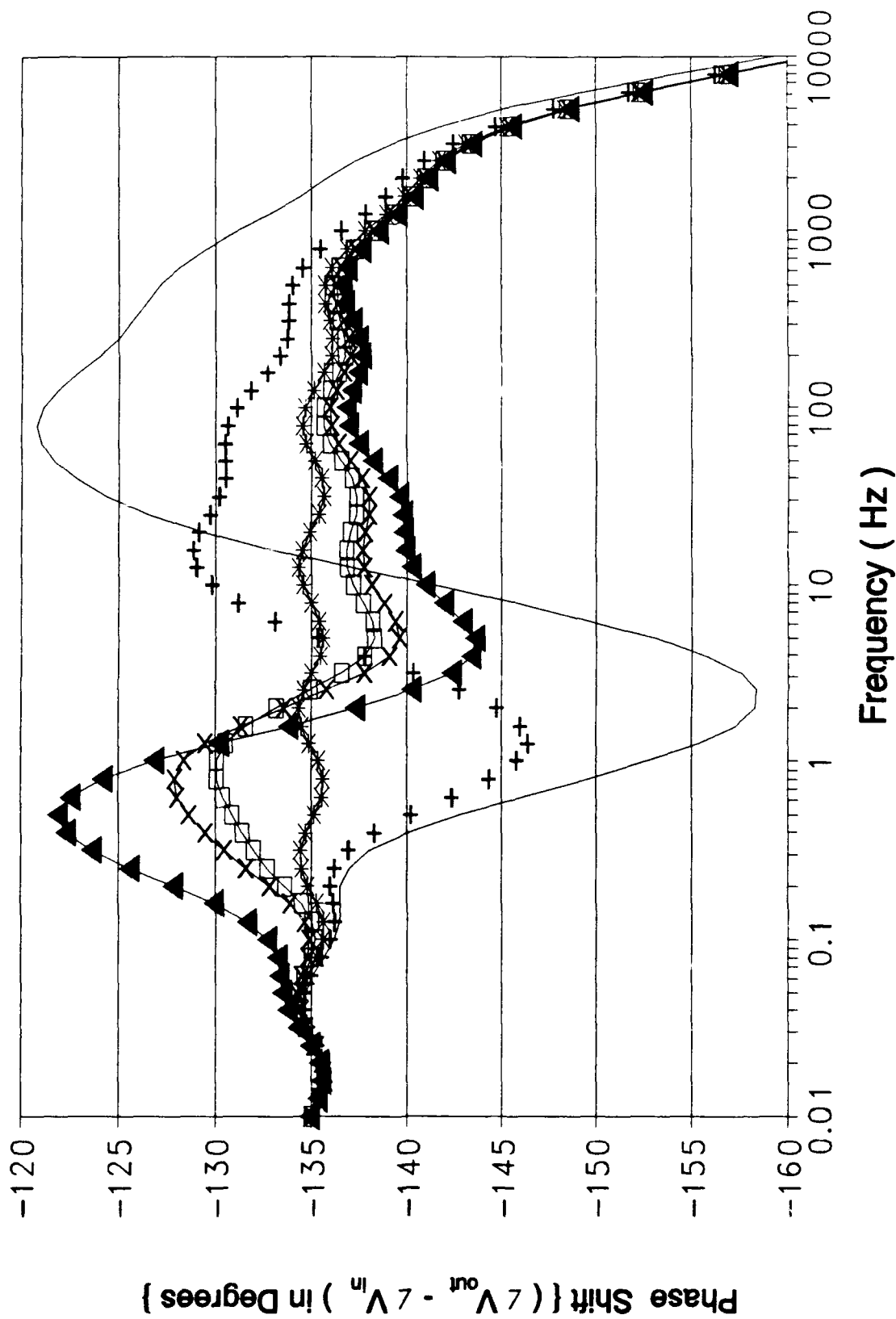
III-10

Figure 13 (cont). Phase Response of the Oldham Circuit Design Simulated Using HSPICE Computer Analysis for a Variation in the Value of Capacitor 5.

III-11

Oldfield Circuit Computer Simulation Induced Design Changes

In contrast with the Oldham circuit, the initial computer simulation of the Oldfield circuit did satisfy the design criteria. However, there was a difference between the two design options that presented a formidable performance comparison task. That is, the difference in the form of the input signals. The Oldham design is based upon an input voltage signal. In contrast, the Oldfield design is based upon an input current signal. This difference was resolved before the computer simulations were accomplished. That is, the basic Oldfield circuit design was modified to accept an equivalent input voltage signal (Figure 14). This new variation was simulated, but, the time response was "weak" and amplification of the output signal would be required (That is, for a 5-volt peak amplitude input signal, the output signal peak amplitude was 50 millivolts). Therefore, a design decision was made, not only to amplify, but, to incorporate a low-pass filter, as was initially implemented in the Oldham circuit. The purpose of this filter was two-fold. The first objective was to improve the time response of the output signal and to facilitate characterization in the laboratory. The second objective was to design the two circuits so that the differences were minimized to simplify their comparison (Oldfield versus Oldham).

Next, the improved circuit with "ideal" component values was simulated in HSPICE. The circuit now satisfied
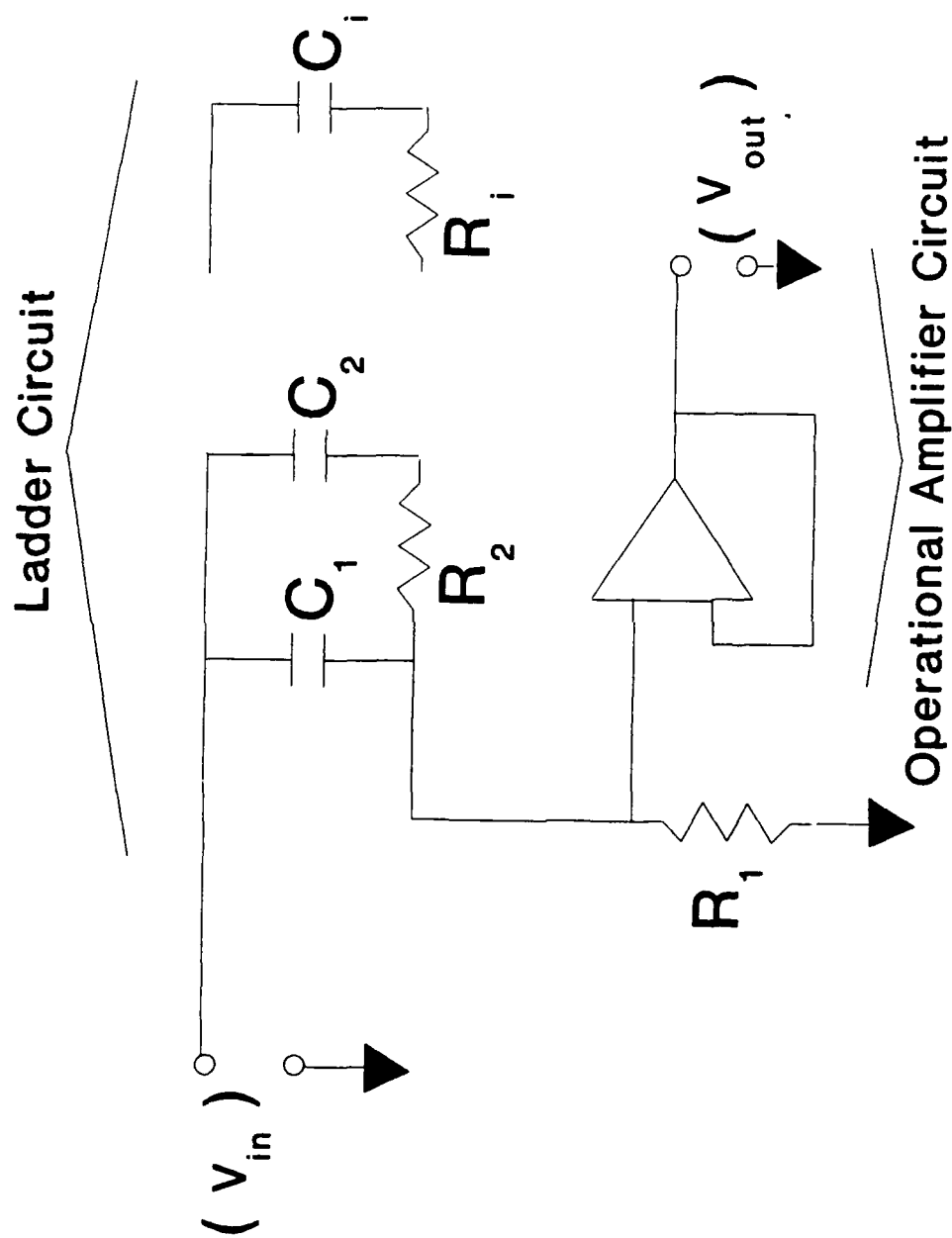
Figure 14. Modified Oldfield Circuit for a Voltage Input.

the gain response design criteria from 0.05 Hz to 10 KHz
(Figure 15) and the phase response design criteria from
0.06 Hz to 19.25 KHz (Figure 16). Since the Oldfield
circuit satisfied the performance criteria with
amplification, a decision was made to accept this difference
in circuit designs.

As with the Oldham circuit, the robustness of the
design was tested using a similar computer simulation
technique that was previously addressed. The Oldfield
circuit baseline HSPICE deck and graphical performance data
is presented in Appendix C. Figure 17 illustrates a sample
of the results obtained. The component value variations of
the Oldfield circuit demonstrated the general trend that the
circuit was not sufficiently robust to facilitate the design
with ± 20 percent component tolerances. The detailed
analysis and comparison of these results is discussed in
Chapter 5.

Component Selection For The Discrete Device, Integrated Circuit, VLSI, And Hybrid Circuit Realizations

The component selection effort was sub-divided based
upon the mode of "component technology" implemented. The
separate efforts involved the selection of the discrete
components, surface mount components, VLSI components, and
hybrid components. Although each selection process shared
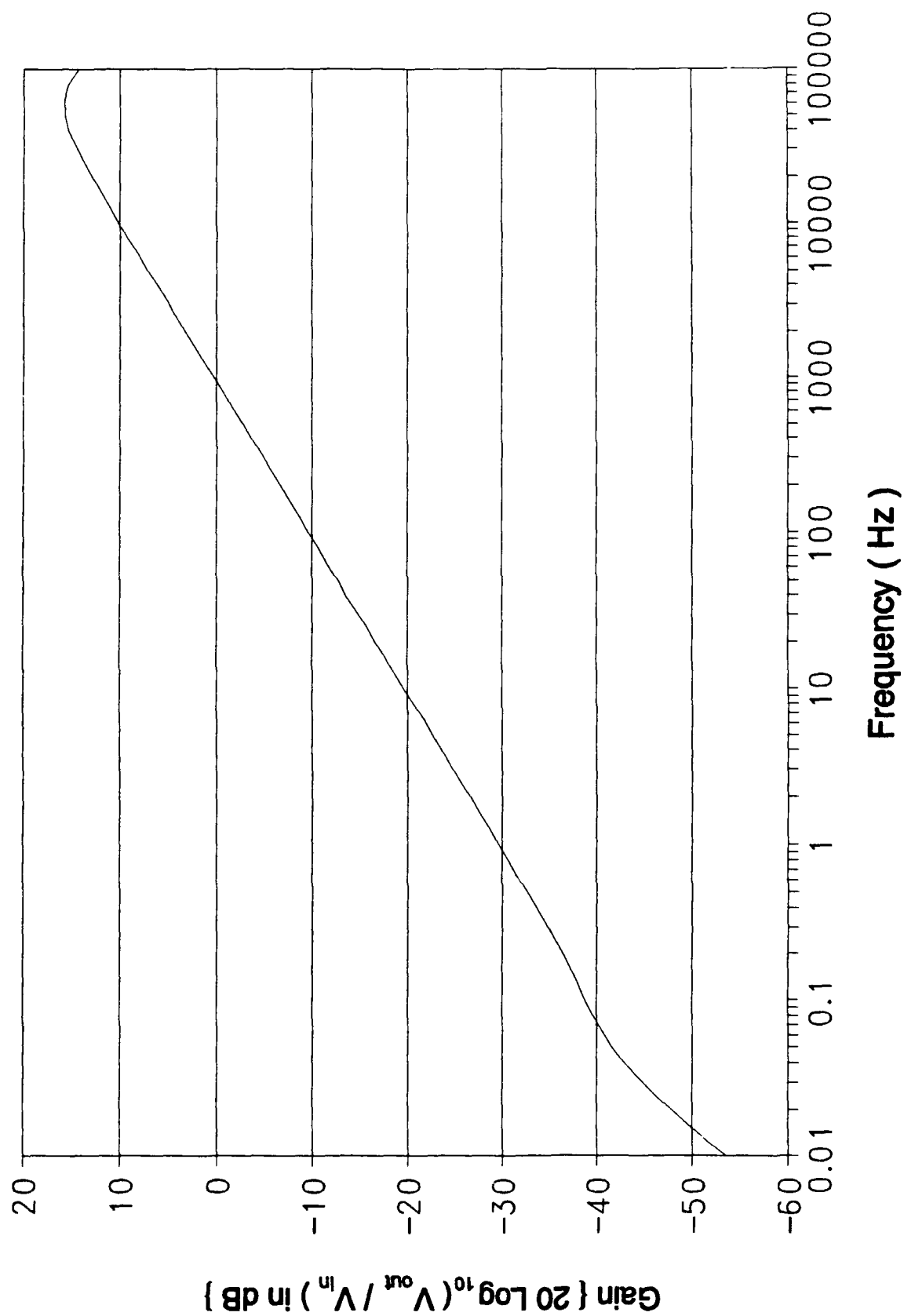similar steps, each will be described separately.

Figure 15.   Gain Response of the Oldfield Circuit Design Using
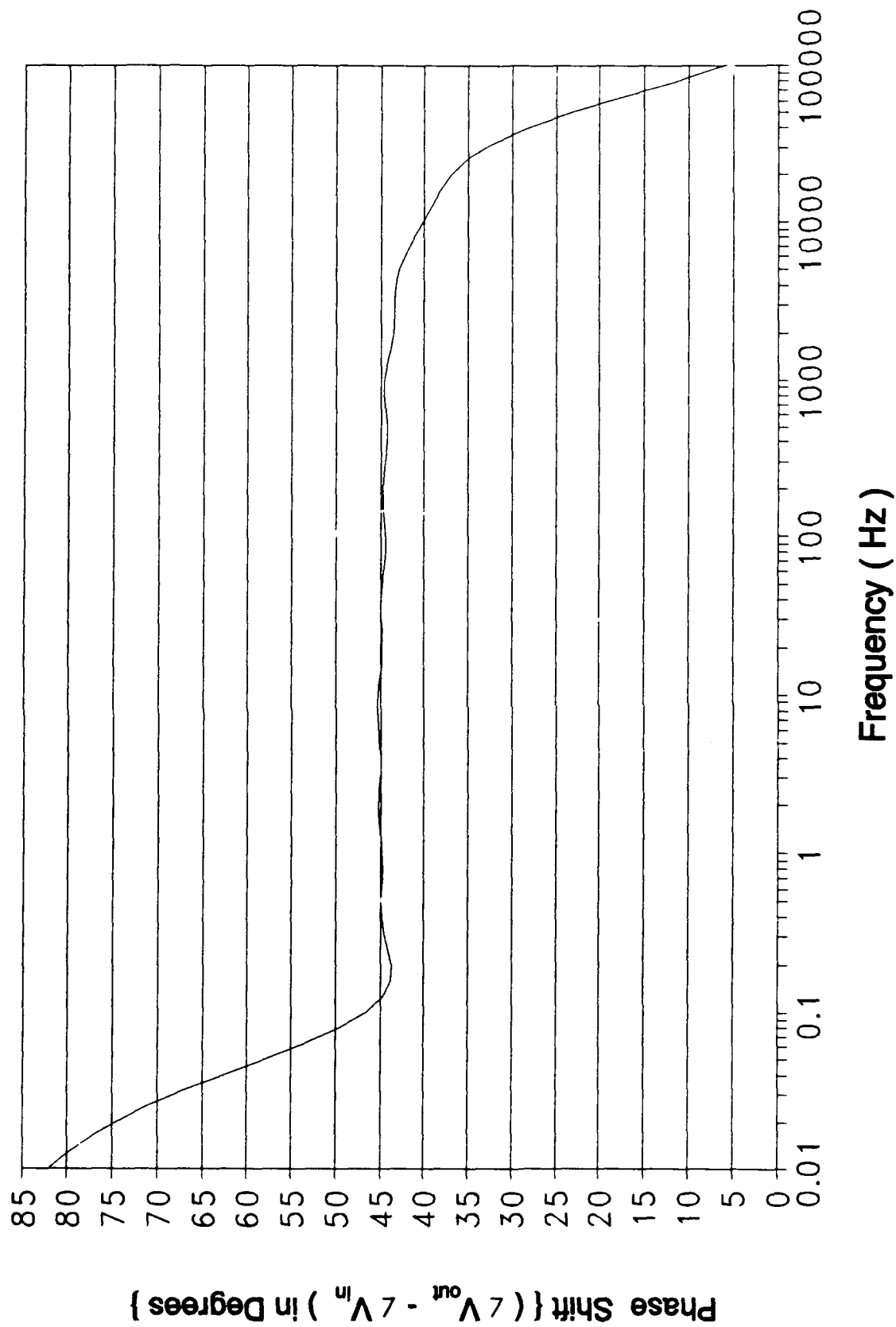HSPICE Computer Analysis.

Figure 16. Phase Response of the Oldfield Circuit Design Using HSPICE Computer Analysis.

Capacitor Values for Figure 17						
Plot Symbol	——	−+−	−*−	−□−	× −−−	−▲−
Capac- itor Value (nF)	47	188	470 (Ideal)	752	940	2350

**Figure 17. Graphical Symbols and Capacitor Values
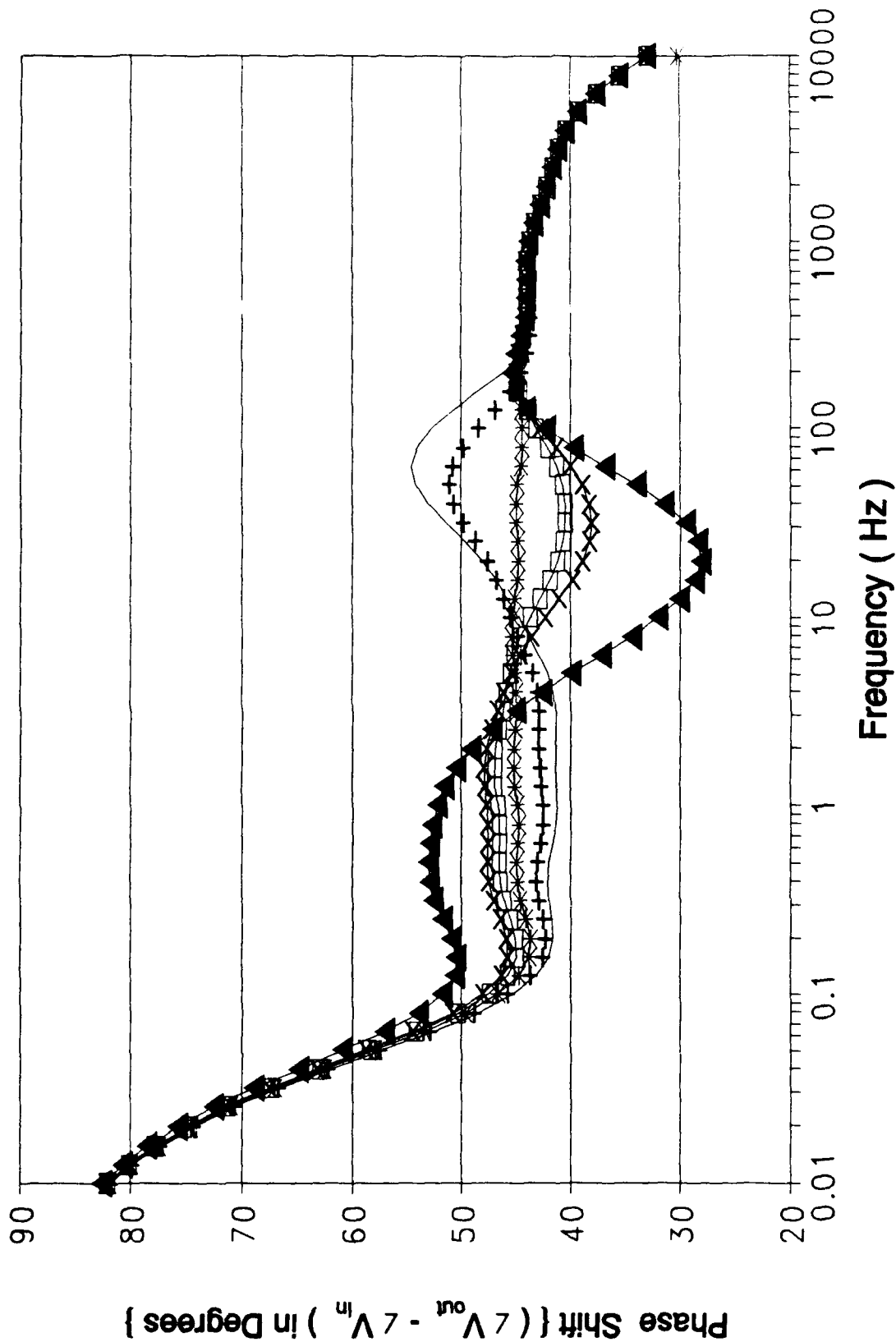Corresponding to the Plot in Figure 17
(cont).**

Figure 17 (cont). Phase Response of the Oldfield Circuit Design Simulated Using HSPICE Computer Analysis for a Variation in the Value of Capacitor 5.

Discrete Component Selection. The selection process for the discrete components involved a manual sorting process of available stock resistors and capacitors. The goal was to obtain components that were within ± 0.1 percent of the "ideal" component values.

The resistors were presorted using a Fluke multimeter (John Fluke Mfg. Co. Inc., Model 77/AN, 1420 75th Street S.W., Everett, WA 98203) to obtain a lot of parts to select from. Since the components were to be utilized over a frequency range of six decades (0.01 Hz to 10 KHz), a frequency scanning measurement instrument was required. An Impedance Analyzer (Hewlett-Packard, Model HP4192A, 8600 Soper Hill Road, Evertt, WA 98205) facilitated resistor value measurements over the frequency range required. The presorted resistors were then characterized with the HP4192A. Although the original goal was to obtain components with a ± 0.1 percent tolerance, the limited stock of parts to select from prevented 100 percent accomplishment of this goal. Therefore, the "best" fit components were selected. Since each component value changes with frequency, a strict, quantifiable percent error is not possible.

The capacitors were not presorted. Because of the limited stock of parts, the goal of identifying capacitors with a tolerance of ± 0.1 percent was not achieved. However, the "best" fit capacitors were selected using the

HP4192A. Since each component value changes with frequency, a strict, quantifiable percent error is not possible.

Therefore, the value of each discrete component over the desired frequency range for both circuit options is documented in Appendix D. Figure 18 illustrates a sample of the results obtained.

Integrated Circuit (IC) Technology Component Selection. The component selection process for the surface mount components parallelled that of the discrete component screening process. This process was subsequently expanded to include the hybrid components. The value of each component relative to the desired frequency range is documented in Appendix E. Figure 19 is a sample of the results obtained.

VLSI Component Selection. The VLSI component selection process was actually a fabrication technique and a geometrical layout selection process. The KΩ and MΩ resistors, and the μF and nF capacitors required high density ohms-per-square and thin dielectric layers, respectively. A preliminary investigation revealed that the Oldfield and Oldham circuit designs could not be implemented with the standard CMOS IC fabrication process. However, through MOSIS, the Orbit Semiconductor vender offered an analog CMOS fabrication process. The higher ohms-per-square (2500 versus 75) and the thinner dielectric oxides (394 versus 700 angstroms) provided the means to design the Oldfield resistive ladder and one capacitor per IC die
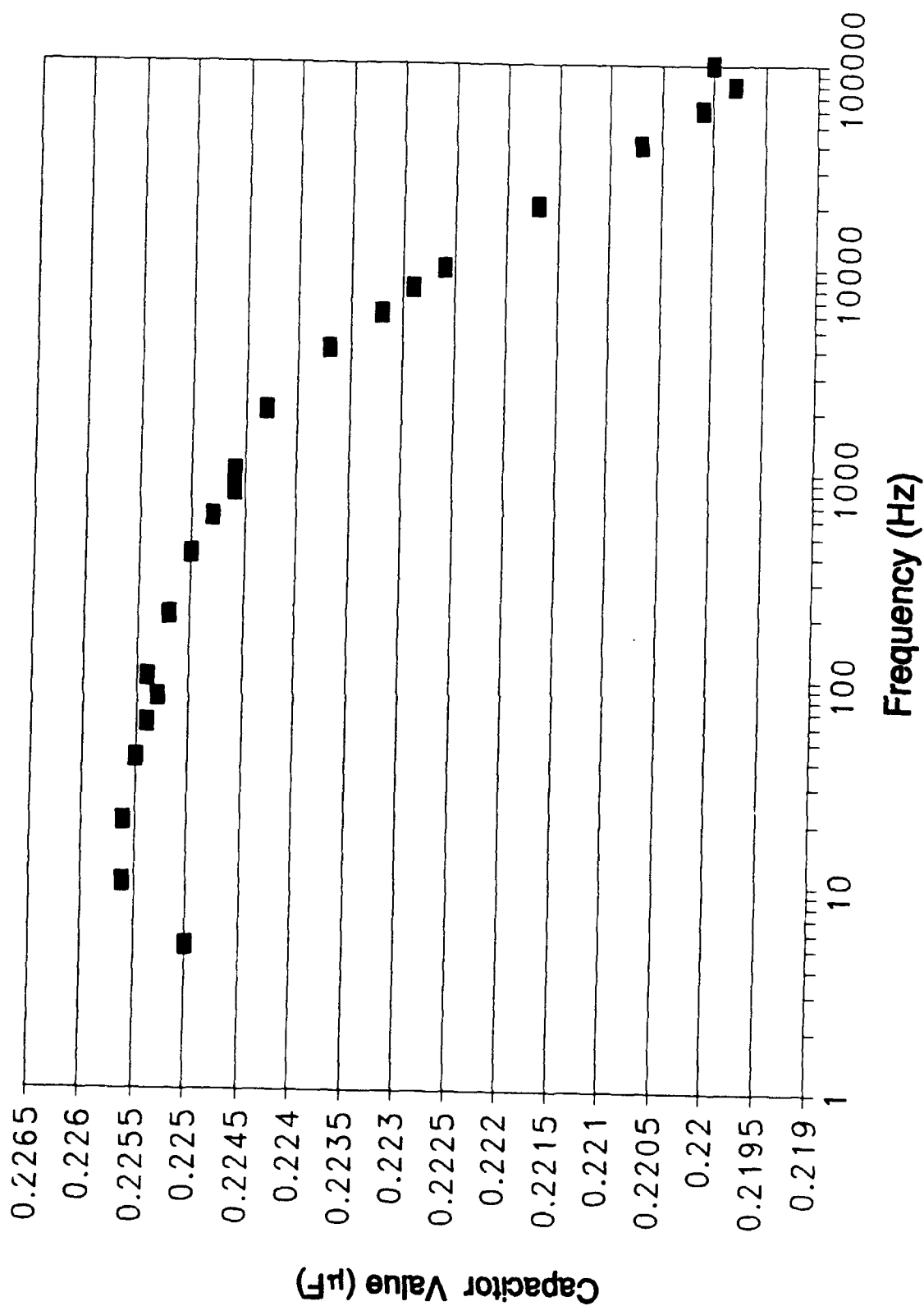
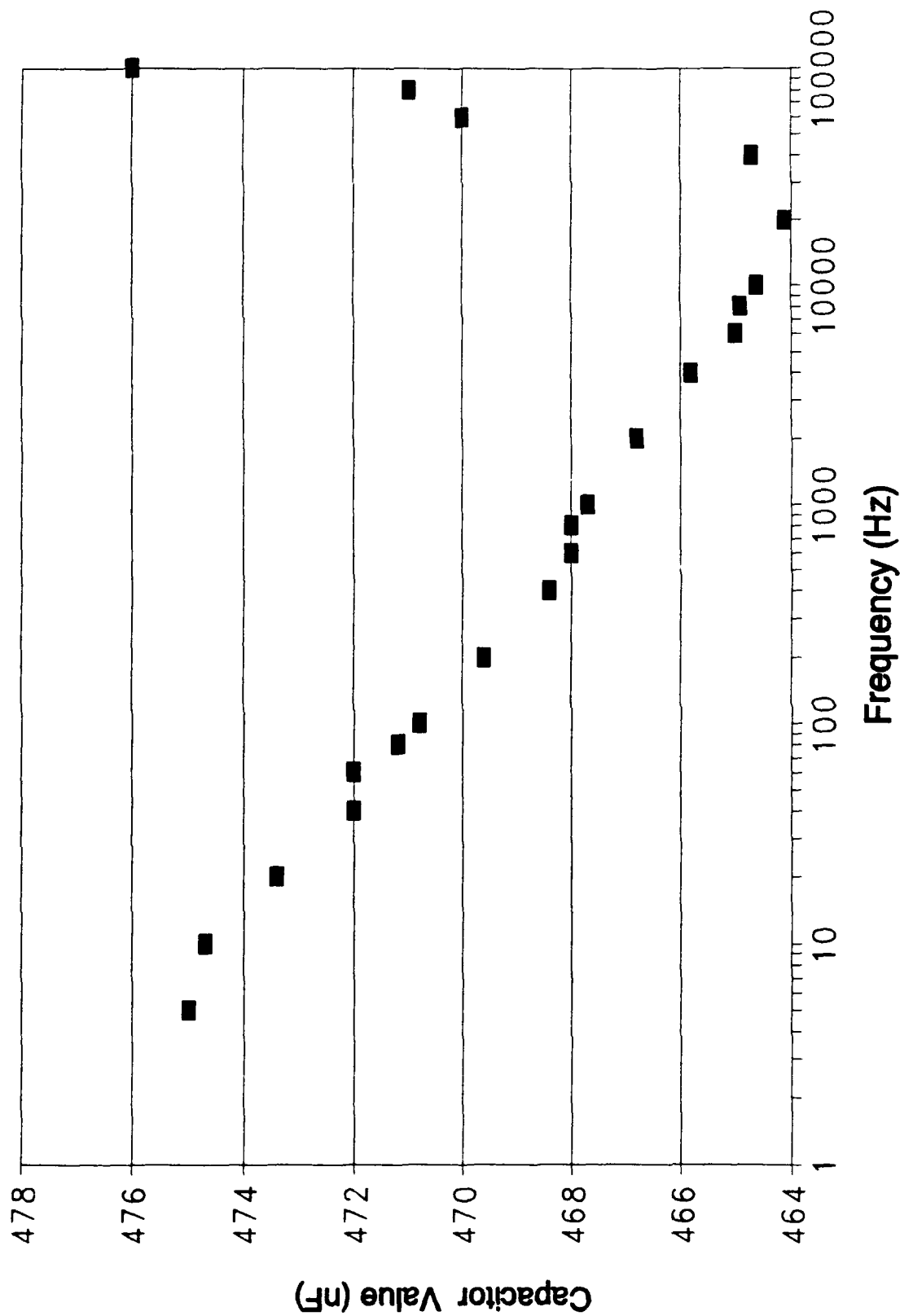Figure 18. Oldham Circuit Design -- Variation in the Value of Capacitor C5 versus Frequency (Ideal Value -- .2283 µf).

Figure 19. Oldfield Circuit Design -- Variation in the Value of Capacitor C5 versus Frequency (Ideal Value -- 470 nF).

(22 mm x 22 mm) [16]. The design rules and constraints used are detailed in reference 17 and the MOSIS fabrication data sheets. The MAGIC CAD tool was used to implement the design of the resistive network. The final design of the Oldfield resistive network is presented in Figure 20. The design permitted four resistive ladders to be realized on each IC die. This scheme was adopted to compensate for defects in the fabrication process and to improve the yield. The final design of the capacitor is presented in Figure 21. The goal of the capacitor design was to realize the largest capacitor possible on the IC die (22 mm x 22 mm).

The designs were submitted to MOSIS for fabrication. The fabrication process resulted in the production of 20 of each IC die type (resistive ladder and capacitor). The next step was to test the chips and to implement the component selection process adopted for the other two technologies. However, the resistive ladder IC die circuit design did not function properly. That is, the Fluke multimeter and the HP 4192A both measured infinite resistance. As a result, three troubleshooting efforts were initiated to discover the reason for the open circuits. In the first effort, five IC die were set aside to be destructively sacrificed to determine the cause of the open circuit. In the second effort, one IC die was examined and probed with the Micromanipulator probe station (The Micromanipulator Co., Model 6200, Carson City, NV 89701). The results were also

Legend

▢ Metal 2 Line
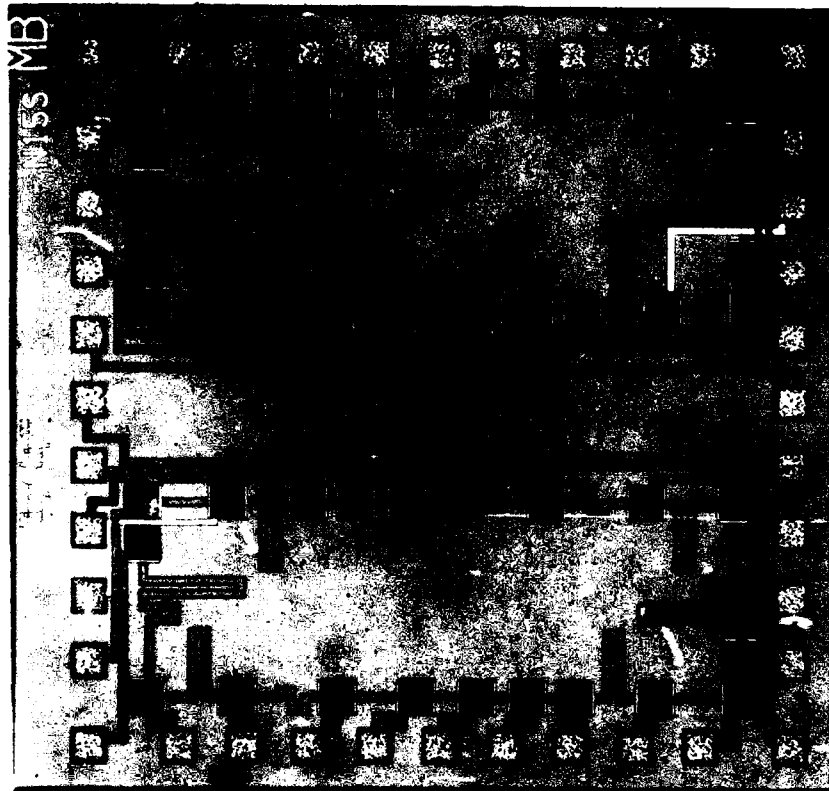▬ Metal 1 Line

▪ Probe Pad
▨ Output Pad
▪— Resistor

Figure 20. Oldfield Resistive Ladder Design That Was Fabricated.

Figure 21. Capacitor Design That Was Fabricated.

Legend

■ Input/Output Pads

■ Dielectric Layers

negative. Next, two IC die were "cut" using the ultrasonic
cutter (The Micromanipulator Co., model 700-MUC, Carson
City, NV 89701) in an attempt to expose the buried layer
connections, and hence, to determine the value of the
resistors. These results were also negative. Finally, the
IC die design was re-evaluated relative to the design rules
in place at the time the design was accomplished. This
check was initially positive, and the IC die design passed
the examination. However, a subsequent evaluation revealed
that the MAGIC layout tool design rules had not been updated
in accorance with the current MOSIS analog fabrication
process. As a consequence, the IC die design was modified
for the new design rules and submitted for fabrication. The
revised IC die designs were not available for testing in
this investigation due to the timing of the MOSIS analog
fabrication run.

The capacitor was tested, and its performance revealed
positive results. A sample lot of five (arbitrarily
selected) IC die was characterized. The results are
summarized in Table 3. Since these results revealed that
the resistor and capacitor IC die were not within 20 percent
of the ideal component values, a design decision was made
not to fabricate a circuit with these components.

Final Circuit Designs

With the two circuit designs tuned via the computer
simulation process, they were ready to be implemented.

III-26

Table 3					
Capacitor IC Die Values					
Design Value (nF)	Chip #1 (nF)	Chip #2 (nF)	Chip #3 (nF)	Chip #4 (nF)	Chip #5 (nF)
1.87	2.276	2.357	2.313	2.367	2.306
percent error	21.71	26.04	23.69	26.57	23.31

The schematics used to fabricate the two circuits are illustrated in Figure 22 (Oldham) and Figure 23 (Oldfield). The format selected to realize the two circuits was the conventional printed circuit board technology. Therefore, each circuit option had to be realized on a printed circuit board (Oldfield discrete component, Oldfield IC, Oldham discrete component, and due to the capacitor and resistor values, the Oldham hybrid technology). The four printed circuit boards were designed using the guidelines established in reference 18. However, space savings was not a prime consideration. Since this was a research effort, the optimization of the printed circuit board space utilization was sacrificed to accommodate overall testability and accessablity of the individual components.

The tool used to design the printed circuit board layout was AutoCad (Auto Desk Inc., AUTOCAD Design Tool, 2320 Marineship Way, Sausalito, CA 94965). The printed circuit boards were initially designed with AutoCad
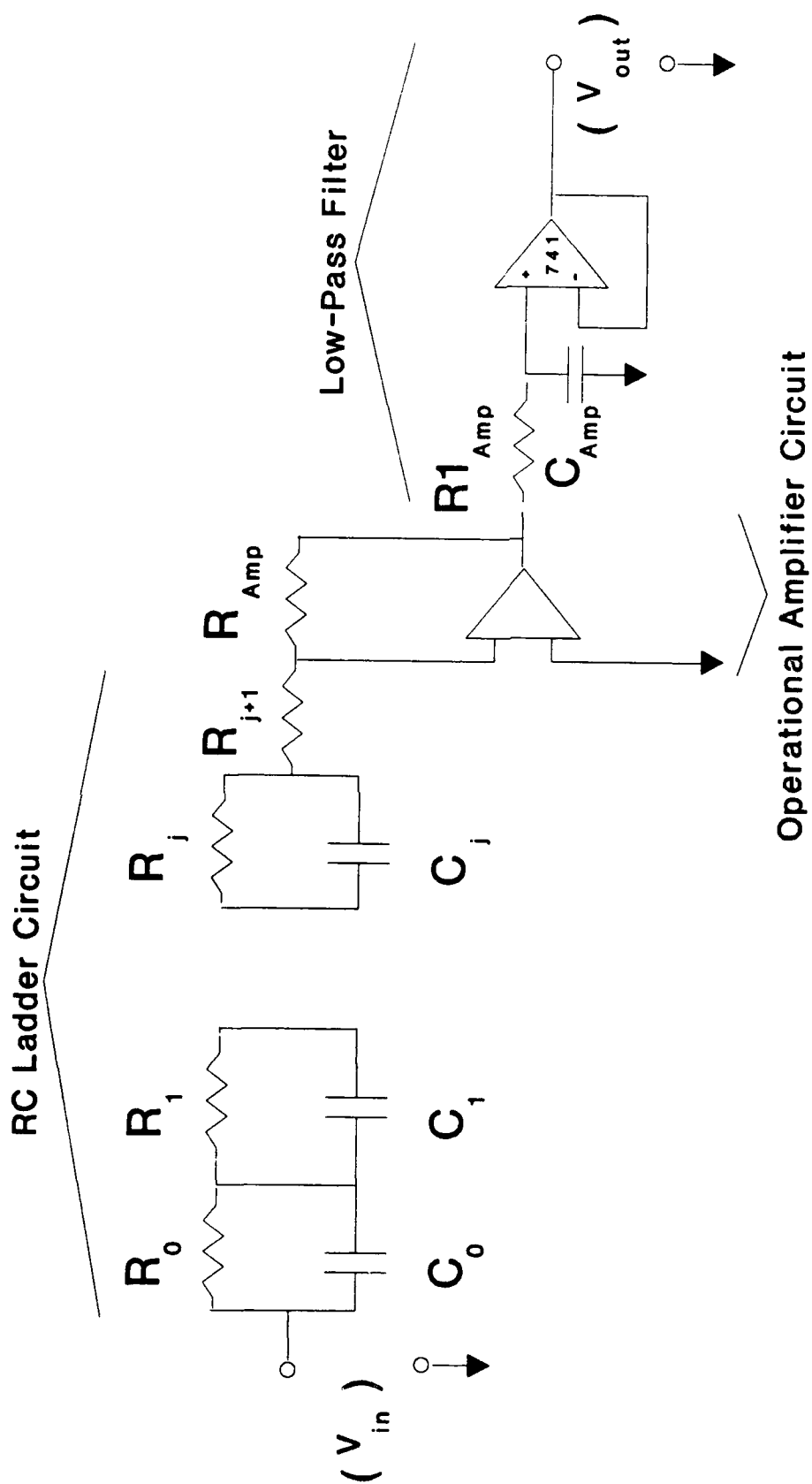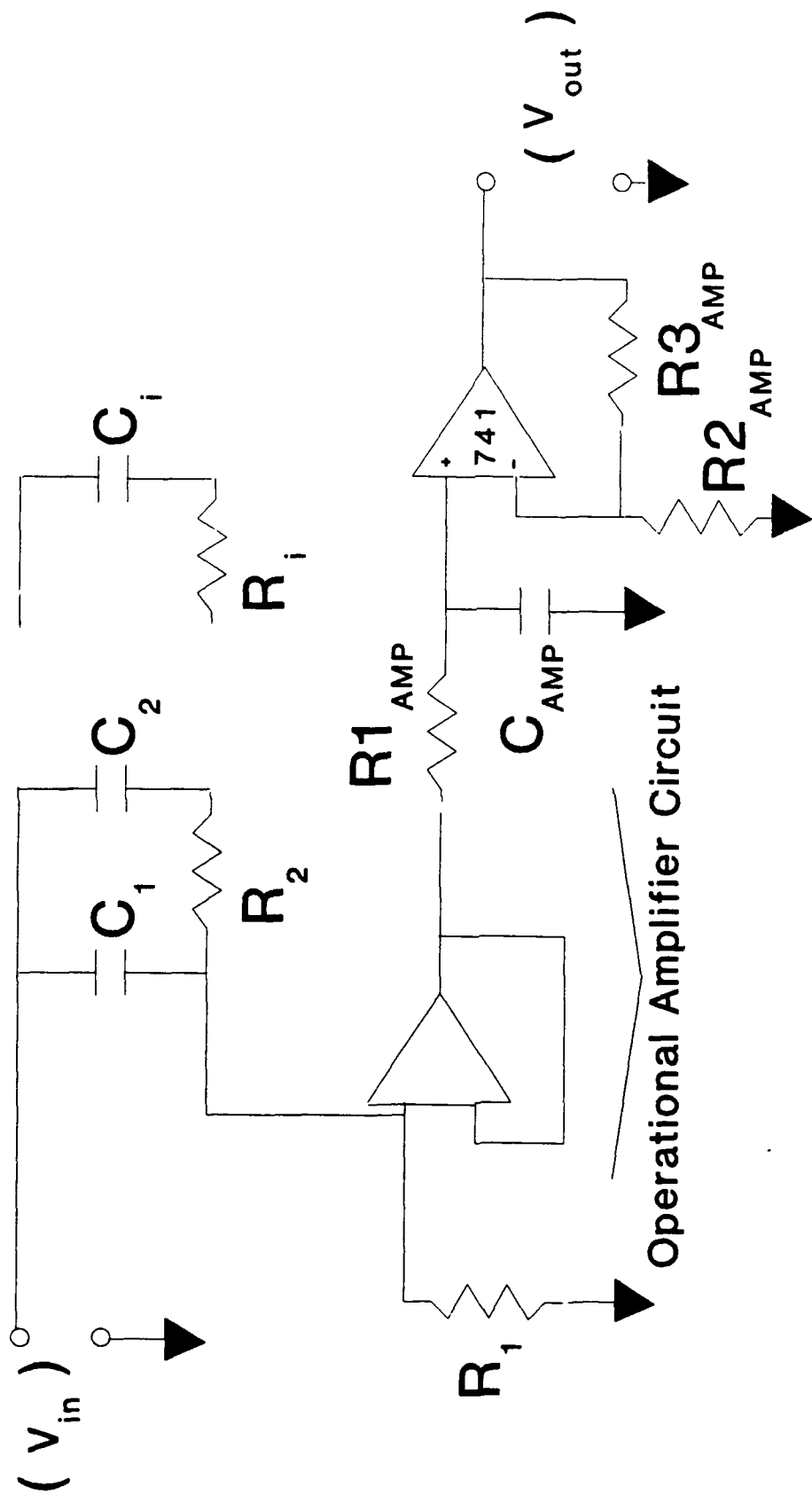
Figure 22. Implemented Oldham Circuit Design

Figure 23.   Implemented Oldfield Circuit Design.

and converted to the Gerber format. The Gerber plots were utilized by the fabrication branch of the 2950 Test Wing to manufacture the desired printed circuit boards. Figure 24 illustrates the Oldham discrete component printed circuit board design; Figure 25 depicts 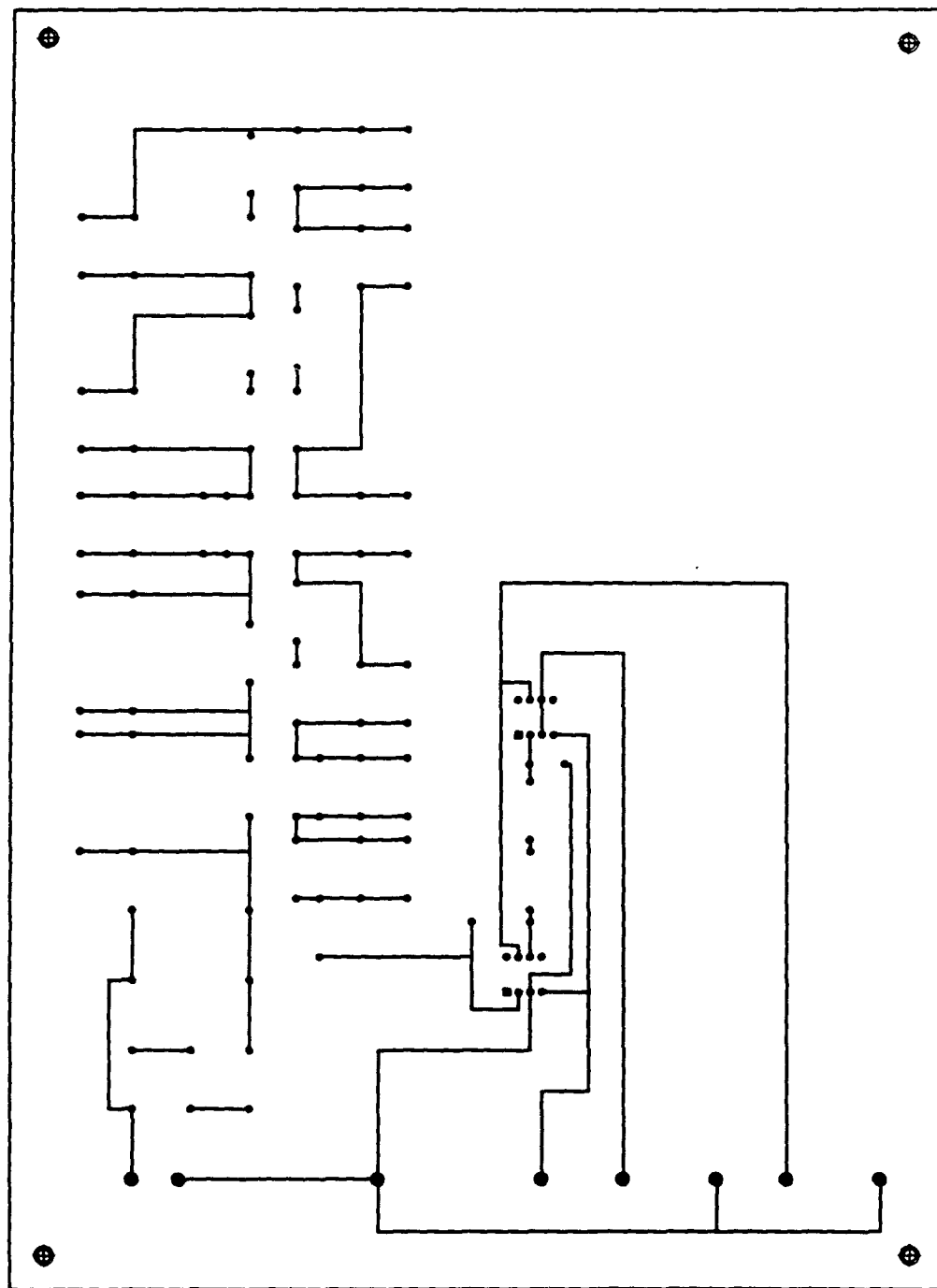the Oldfield discrete component printed circuit board design; Figure 26 depicts the Oldham hybrid component printed circuit board design; and Figure 27 depicts the Oldfield surface mount component printed circuit board design.

Figure 24. Artwork for the Oldham Discrete Component Printed Circuit Board Design (scale 1 : 1.43).
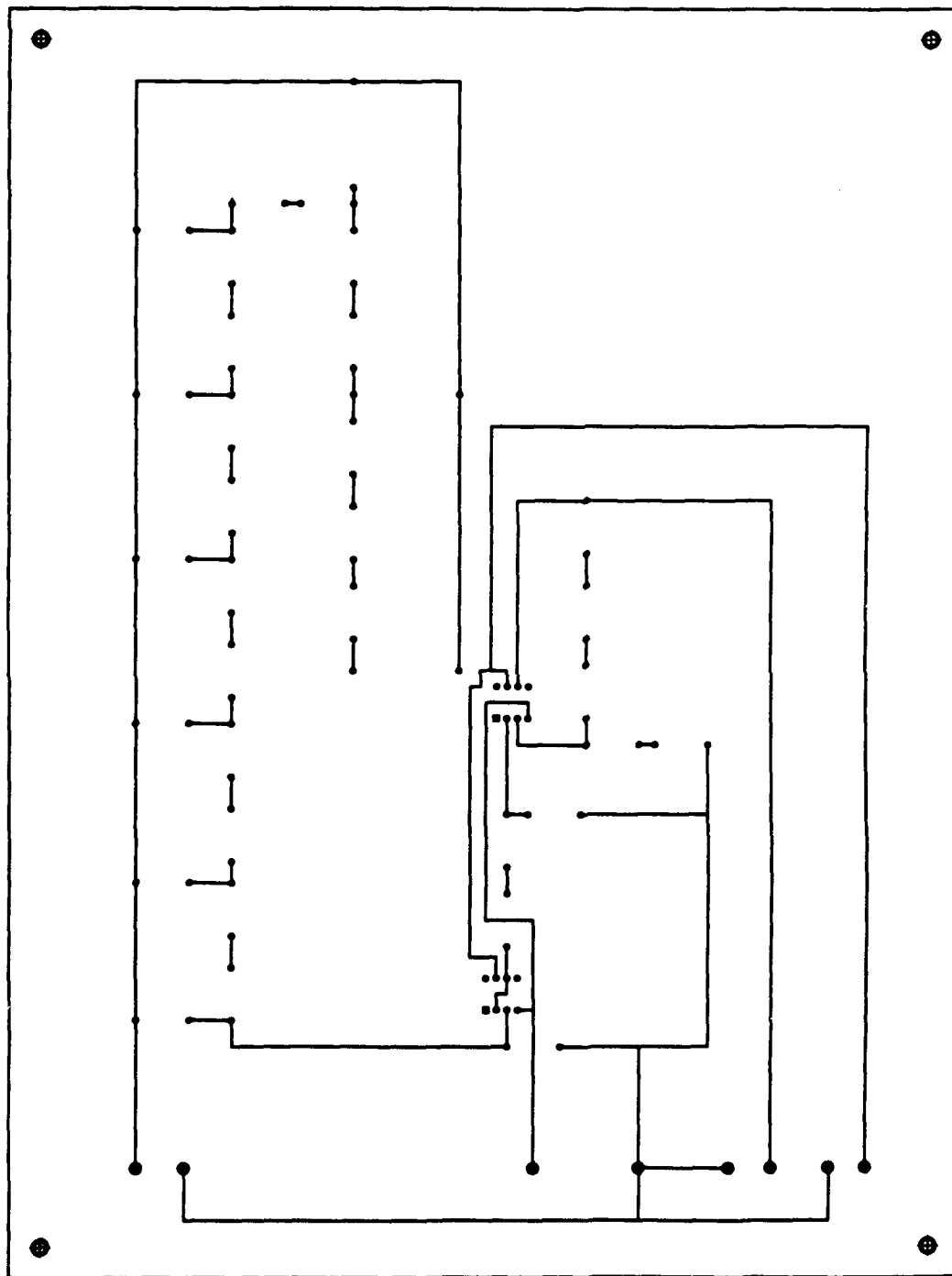
Figure 25. Artwork for the Oldfield Discrete Component Printed Circuit Board Design (scale 1 : 1.43).
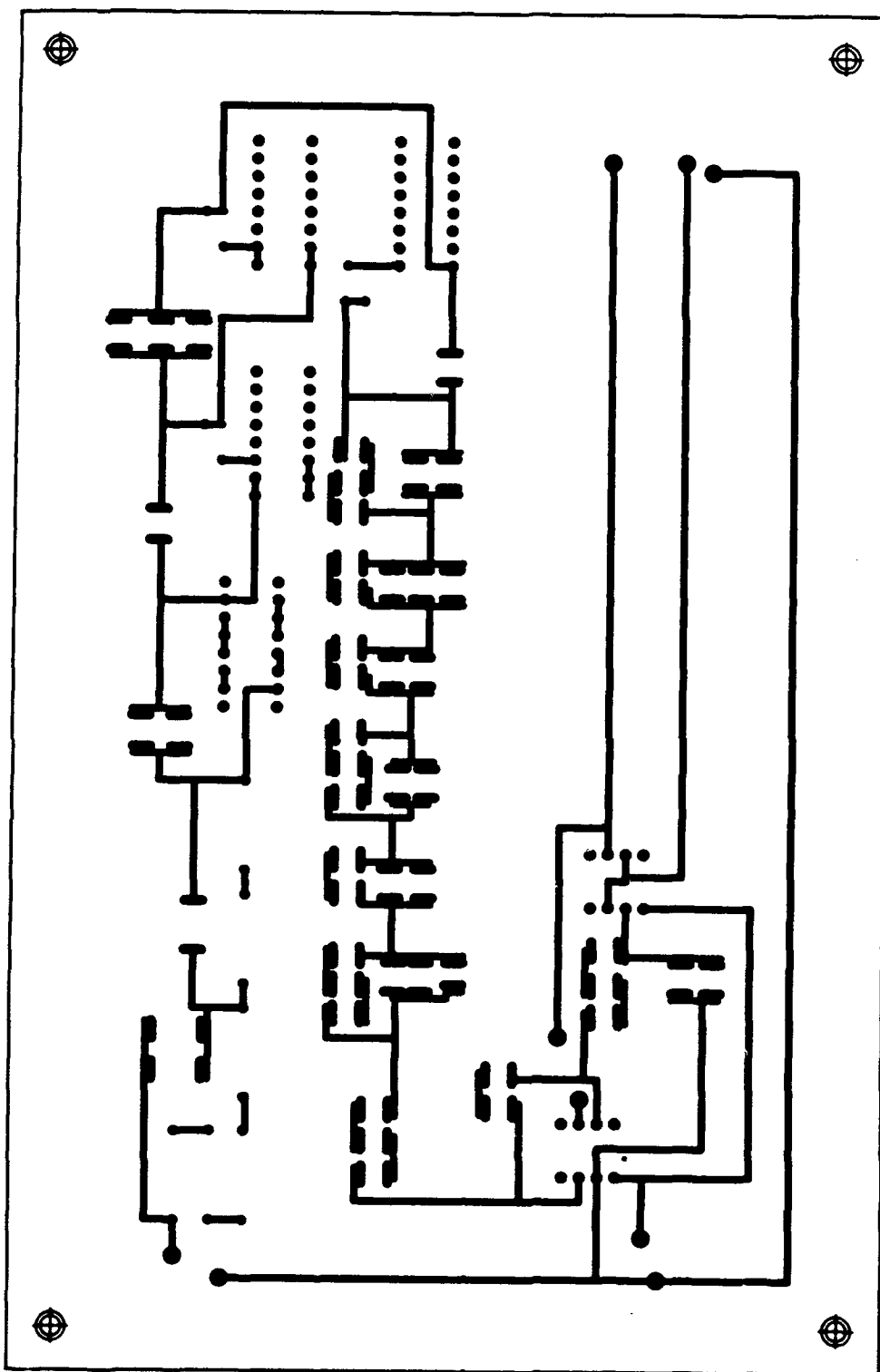
Figure 26. Artwork for the Oldham Hybrid Component Printed Circuit Board Design (scale 1 : 1).
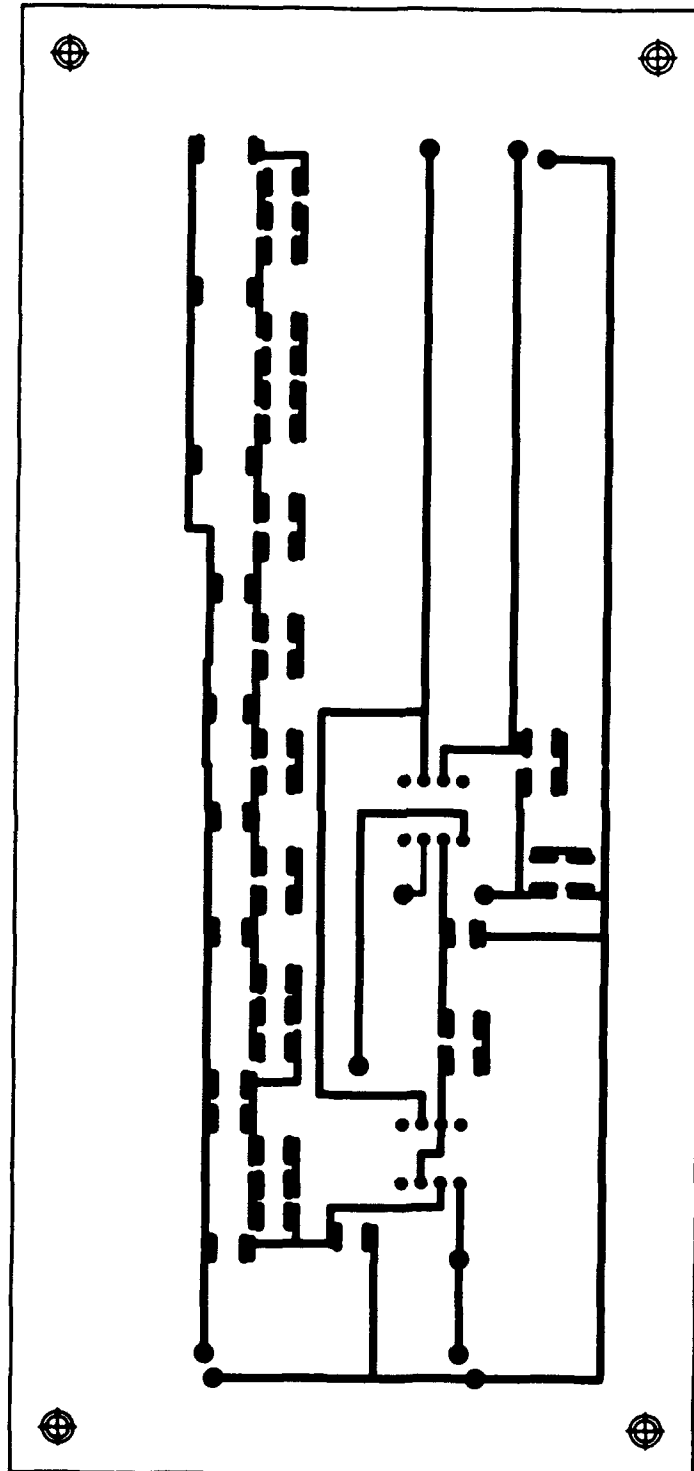
Figure 27. Artwork for the Oldfield Surface Mount Component Printed Circuit Board Design (scale 1 : 1).

IV. Circuit Fabrication And Electrical Performance Evaluation

The next phase of the research effort was focused toward fabricating and evaluating the electrical performance of the circuits. Each process is described separately in this chapter. However, before the final fabrication and electrical performance evaluation phases were implemented, the Oldfield and the Oldham discrete component circuits were configured on breadboards. The purpose of this diversion was two-fold. First, the circuits were evaluated to ascertain their general compliance with the design criteria. Secondly, the electrical performance evaluation procedures and instrumentation configuration were finalized. The breadboard Oldfield circuit is shown in Figure 28, and the breadboard Oldham circuit is shown in Figure 29.

The instrumentation configuration for evaluating the performance of these circuits is displayed in Figure 30. The HP3314A function generator (Heweltt-Packard, Model HP3314A, 8600 Soper HIll Road, Everett, WA 98205) was used to supply the excitation signal and the dual-channel LeCroy digital storage oscilloscope (LeCroy Corporation, Model 9400A, 700 Chestnut Ridge Road, Chestnut Ridge, NY 10977) was used to display the excitation and response signals. A dual power supply (Heweltt-Packard, Model HP6236B, 8600 Soper Hill Road, Everett, WA 98205) was used to provide the
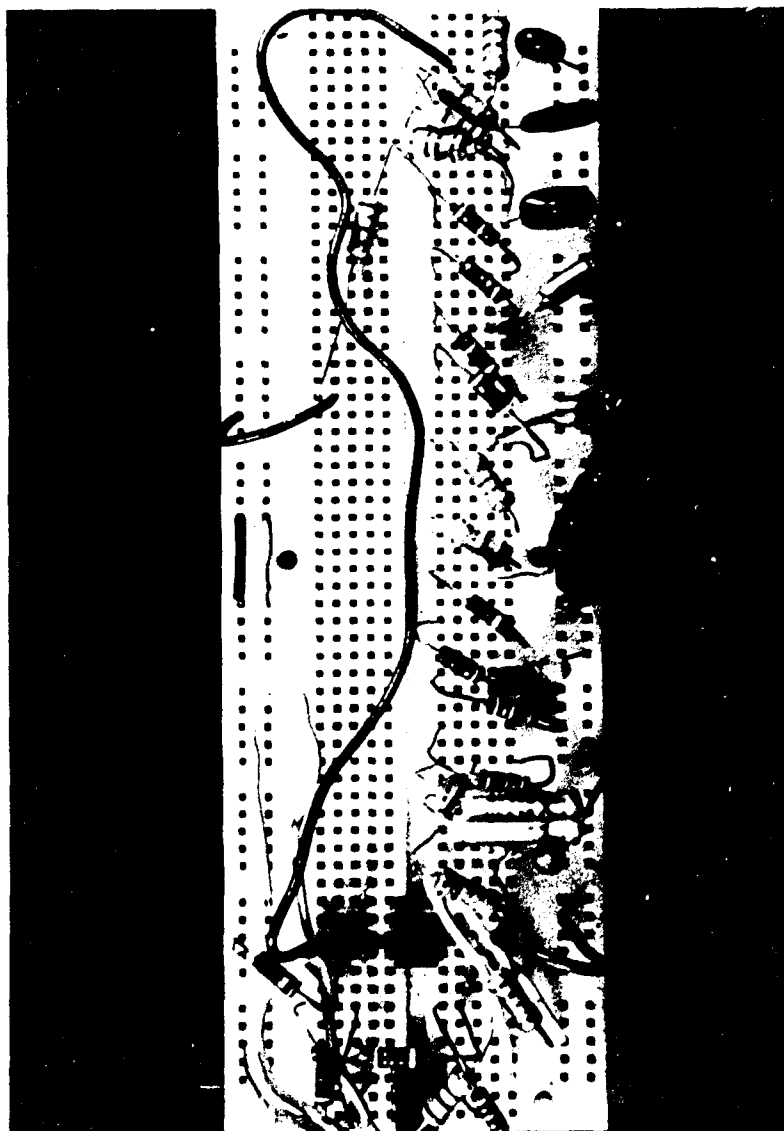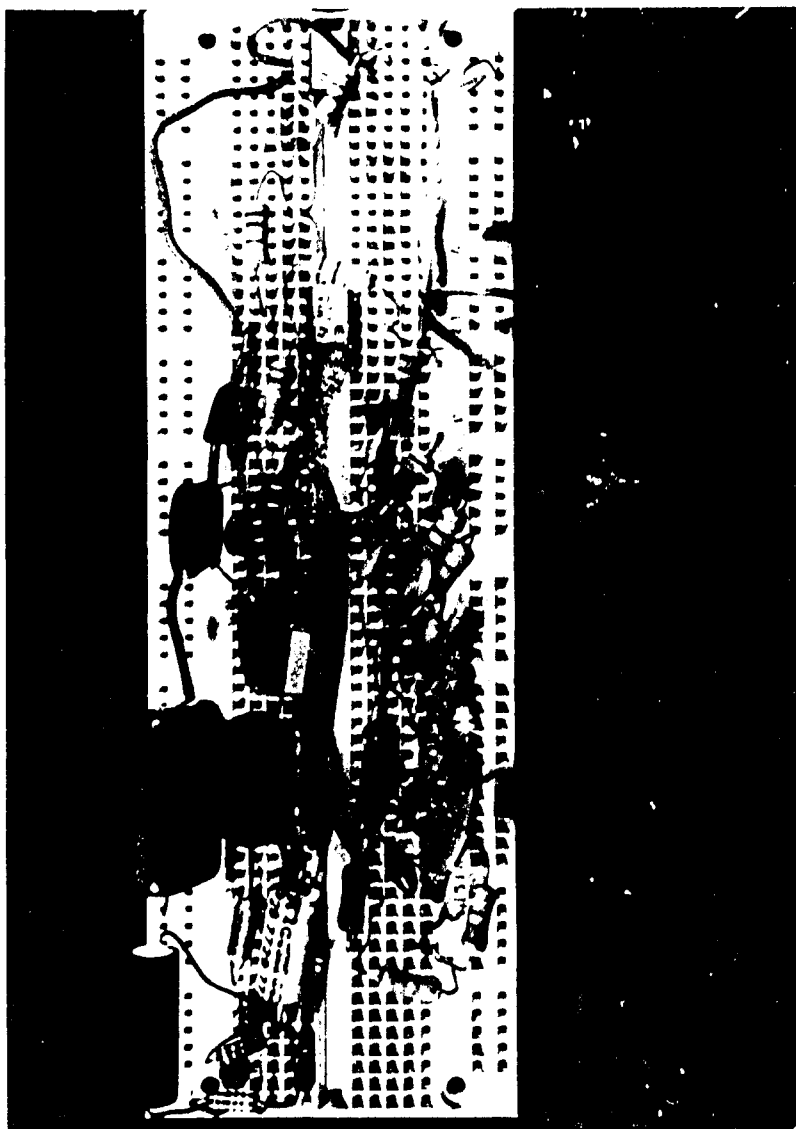
Figure 28. Oldfield Breadboard Circuit
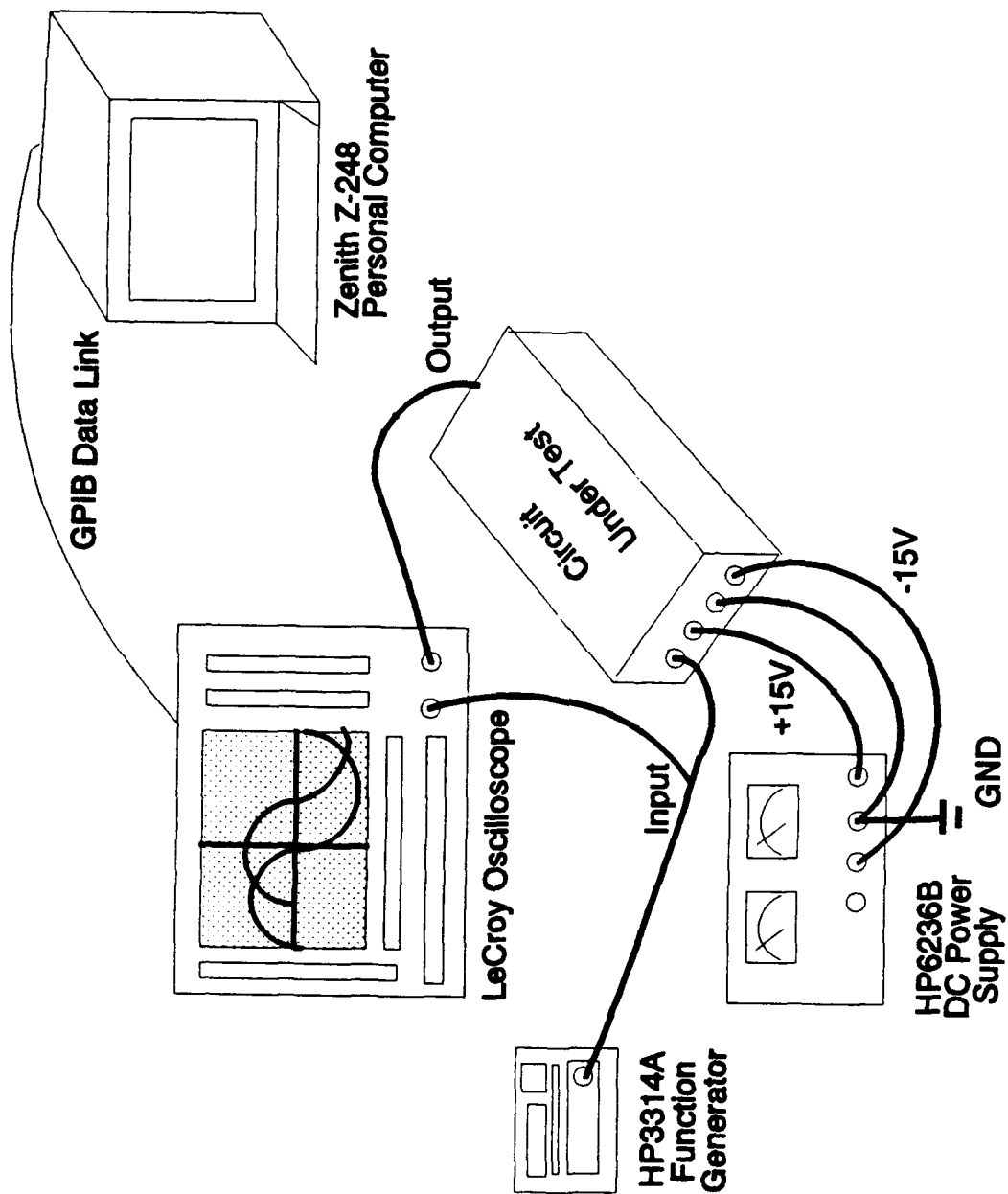
Figure 29. Oldham Breadboard Circuit

Figure 30. Test and Data Acqusition Circuit

DC operating biases for the AN-741 operational amplifiers. Additionally, a method for recording the data was required. The method adopted to collect the data involved connecting a GPIB cable from the LeCroy oscilloscope to the Zenith personal computer. This arrangement facilitated the data acquisition process.

Since the breadboard circuit was only an interim "test" step, a limited frequency range was tested (Bode plots 10 Hz to 100 KHz and the time response at 500 Hz). The data is presented in Appendix F. A sample of the data is shown in Figure 31 and Figure 31a.

During the electrical performance evaluation of the breadboard circuits, it was discovered that Building 125 (the testing facility), Wright-Patterson Air Force Base, had an electrical noise background that inhibited low-level data acquisition. This problem was rectified by inserting the final printed circuit board variants into a "Bud" box to electrically isolate them. Otherwise, the preliminary results from the breadboard circuits demonstrated that the designs could perform within the design specifications.

Circuit Fabrication

The four fractional-order differentiator circuits were fabricated from the characterized components, the printed circuit boards, and the "Bud" boxes. The components were manually soldered onto the printed circiut boards. Then.
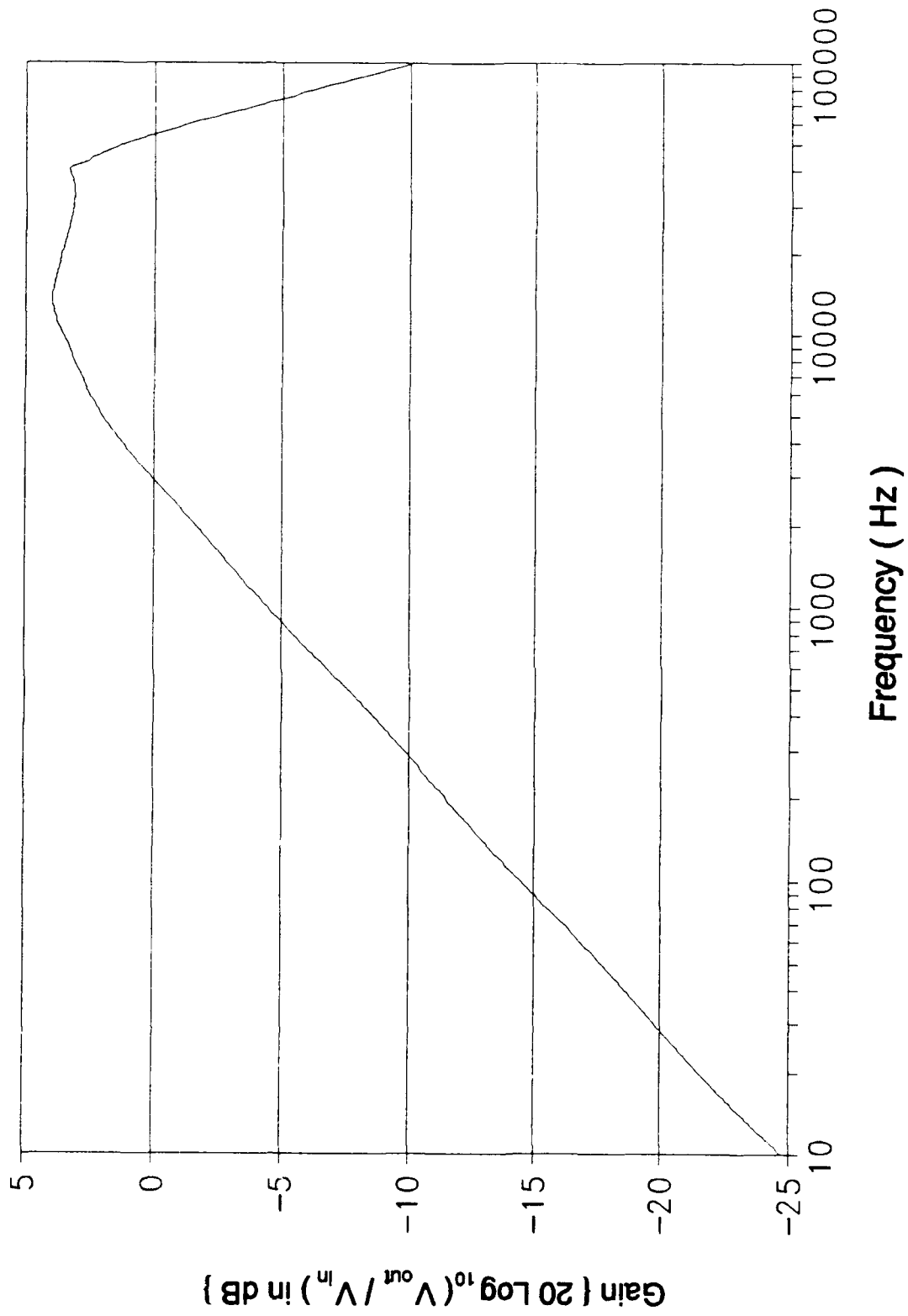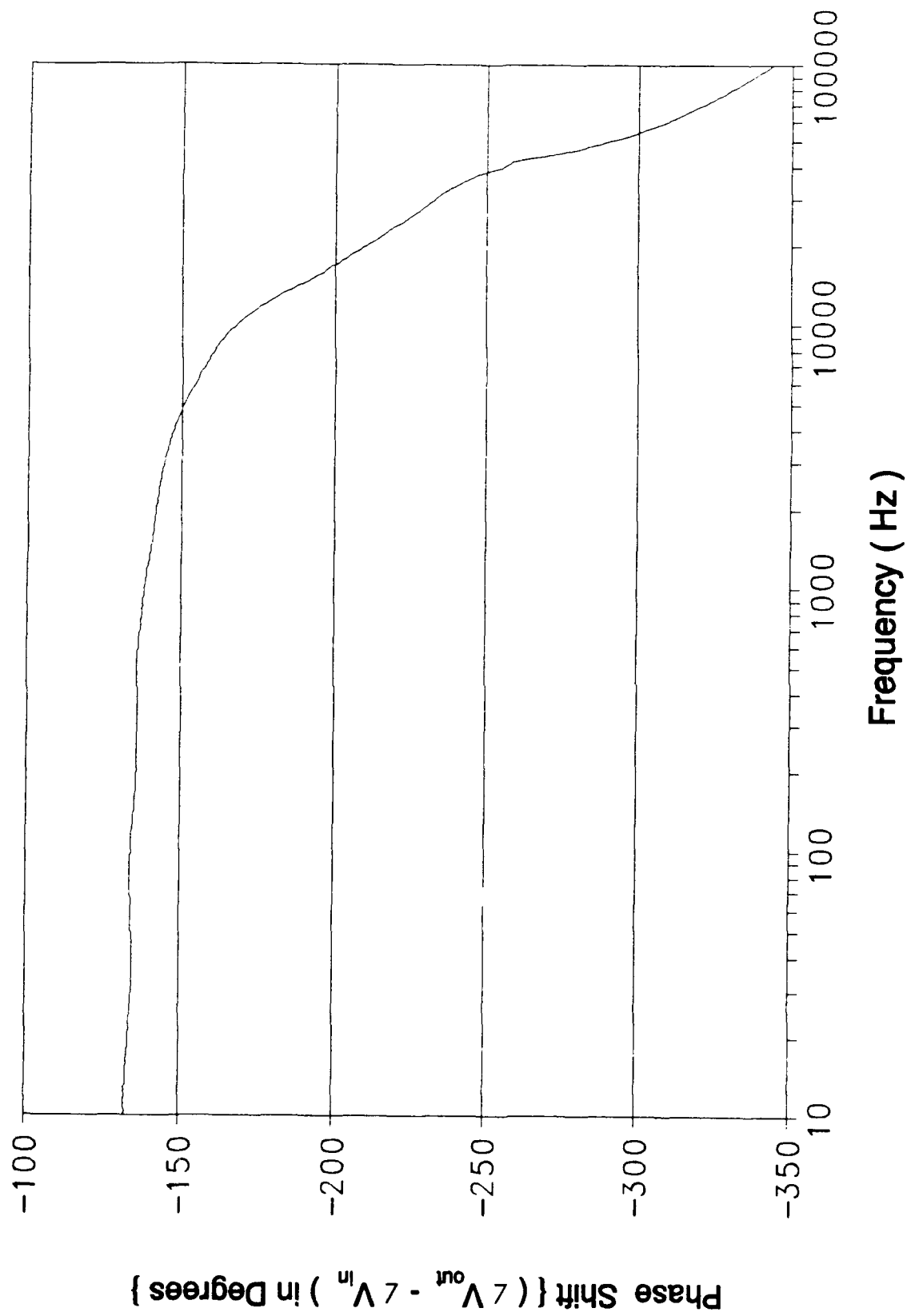
Figure 31. Gain Response of the Oldham Discrete Component Circuit
Realized on a Breadboard.

Figure 31a. Phase Response of the Oldham Discrete Component Circuit Realized on a Breadboard.

Frequency (Hz)

Phase Shift { (∠V_{out} − ∠V_{in}) in Degrees }

five BNCs were mounted on each "Bud" box to provide access
to the input, output, ground, +15 volt, and -15 volt ports.
Next, the printed circuit boards, with components installed,
were mounted in the "Bud" boxes.   The fabricated circuits
are shown in Figure 32 (Oldfield discrete component), Figure
33 (Oldfield surface mount component), Figure 34 (Oldham
discrete component), and Figure 35 (Oldham hybrid circuit
technology).

Electrical Performance Evaluation

The performance of each circuit was evaluated using the
instrumentation configuration illustrated in Figure 30.   A
sample of the results obtained is presented in Figures 36a
and 36b, and the remainder of the data is presented in
Appendix G.

Throughout the design effort, periodic design reviews
were held to keep this effort focused.   During the 1 Aug 91
review, a request was made to portray the data in Nichols
plot format.   Therefore, an alternate method of testing was
required.

The test instrumentation configuration (Figure 30) was
realigned by substituting a spectrum analyzer (Bruel & Kjaer
(B & K), Model 2032, Naerum, Denmark) for the LeCroy
oscilloscope.   The spectrum analyzer facilitated three
further data acquisitions.   Namely, noise, spectral data,
and Nichols plot information.   Since the test
instrumentation (B&K) also provided the same data as the
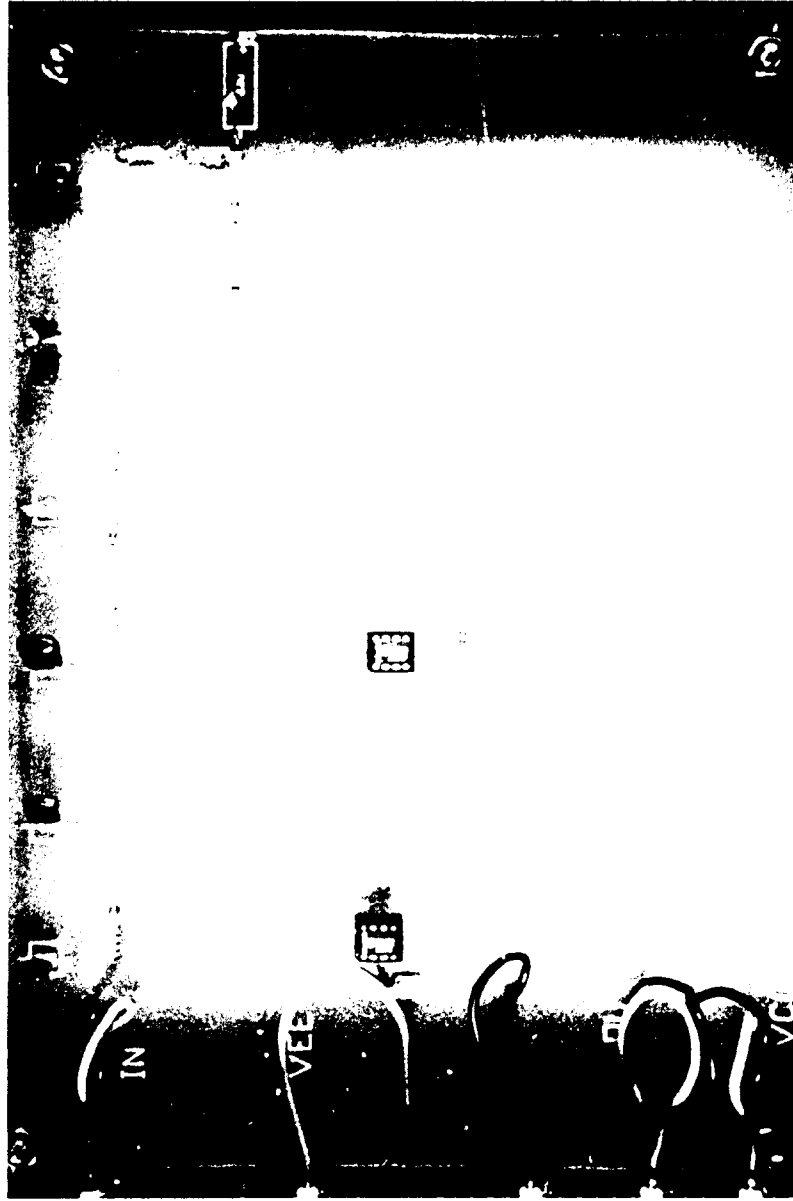
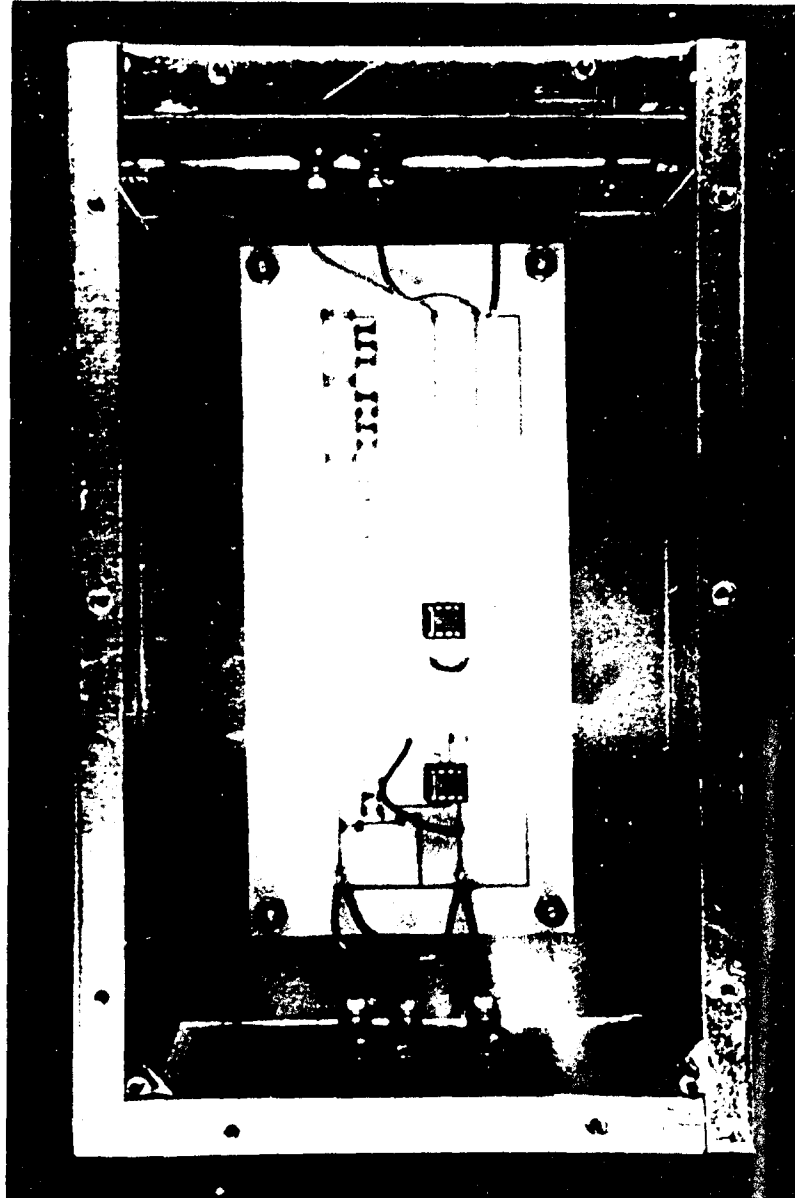Figure 32. Oldfield Discrete Component Circuit Realized on a Printed Circuit Board.

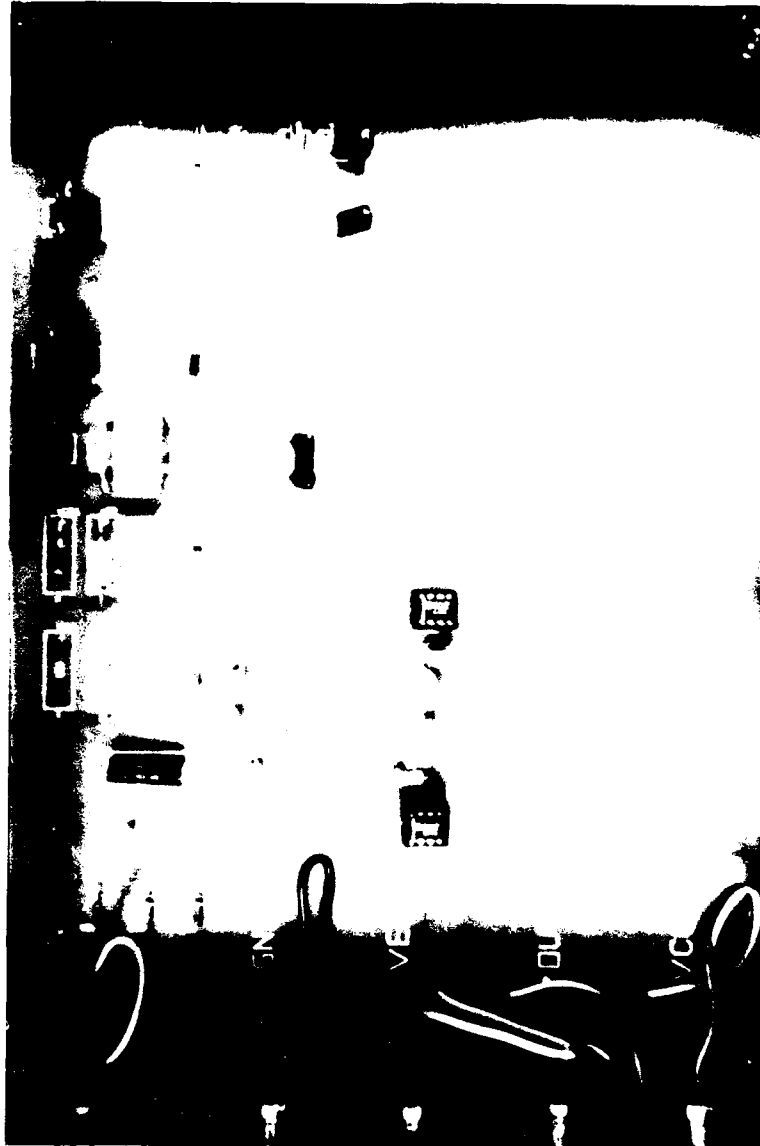Figure 33. Oldfield Surface Mount Component Circuit Realized on a Printed Circuit Board.

Figure 34. Oldham Discrete Component Circuit Realized on a Printed Circuit Board.

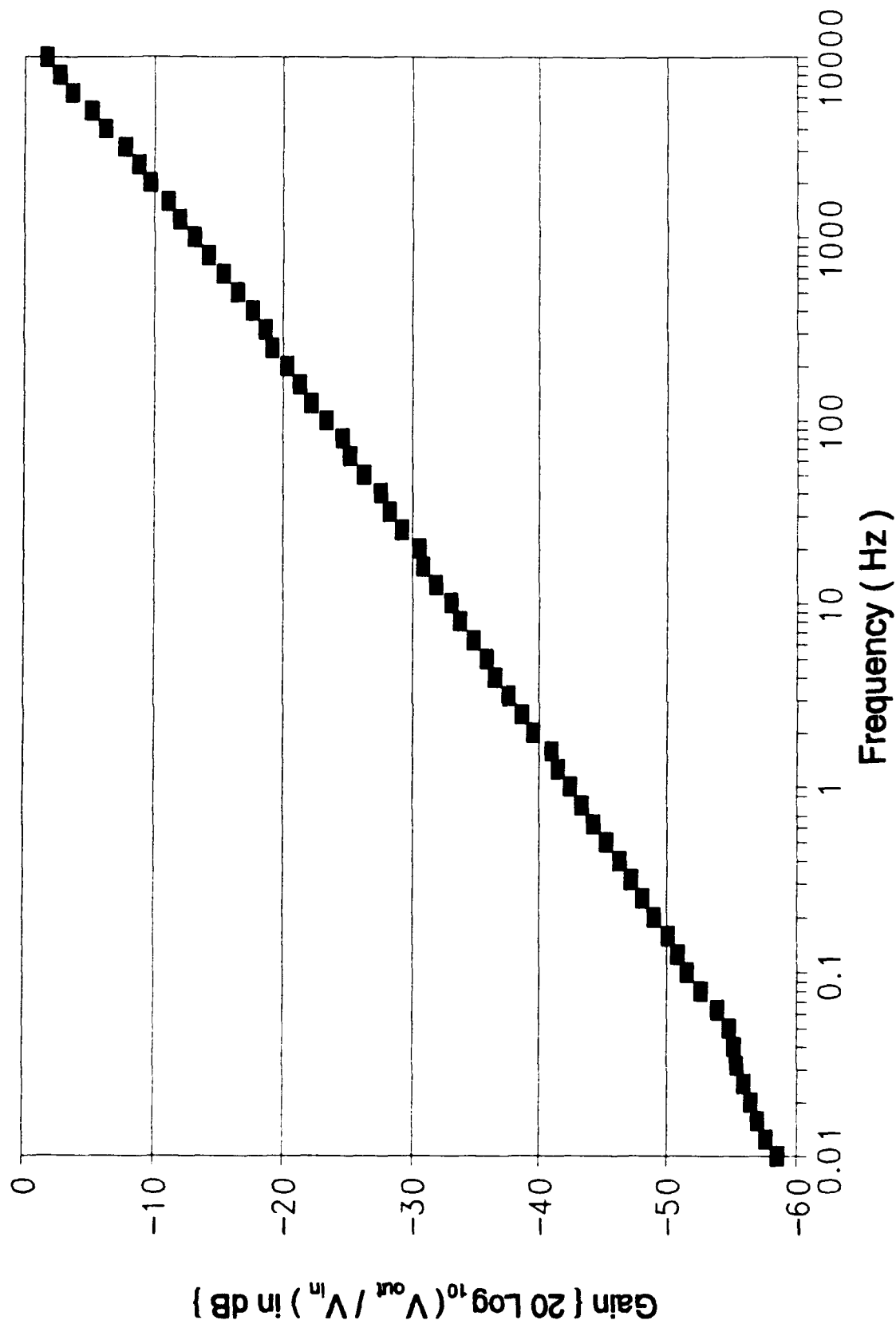Figure 35. Oldham Hybrid Component Circuit Realized on a Printed Circuit Board.

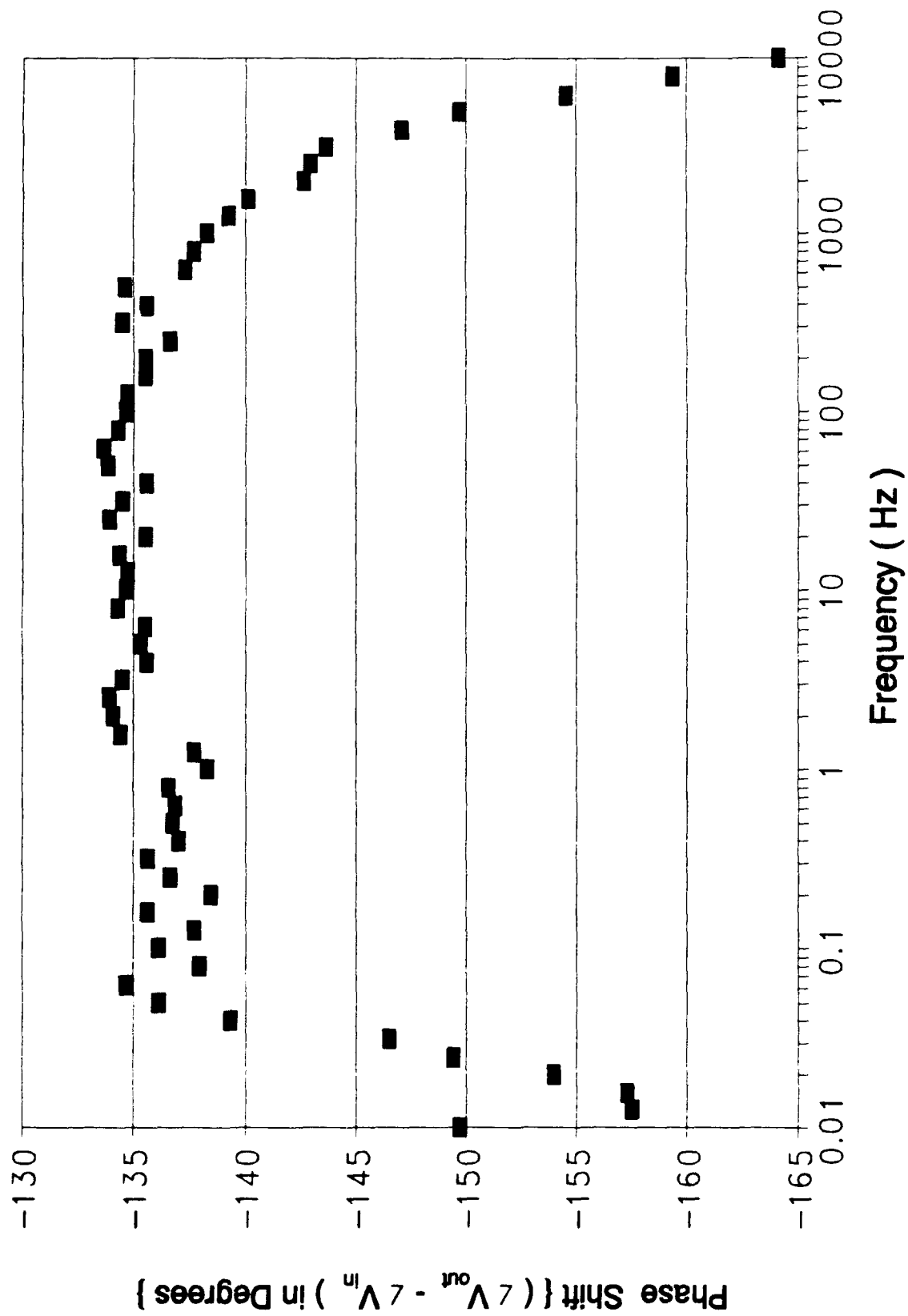**Figure 36a. Gain Response of the Oldham Discrete Component Circuit.**

Gain { 20 Log$_{10}$ (V$_{out}$ / V$_{in}$) in dB }

Figure 36b. Phase Response of the Oldham Discrete Component Circuit.

Output Signal Amplitude (Volts)

Input Signal Amplitude (Volts)

Time (10E-4 seconds)

Legend

Input ■
Output ○
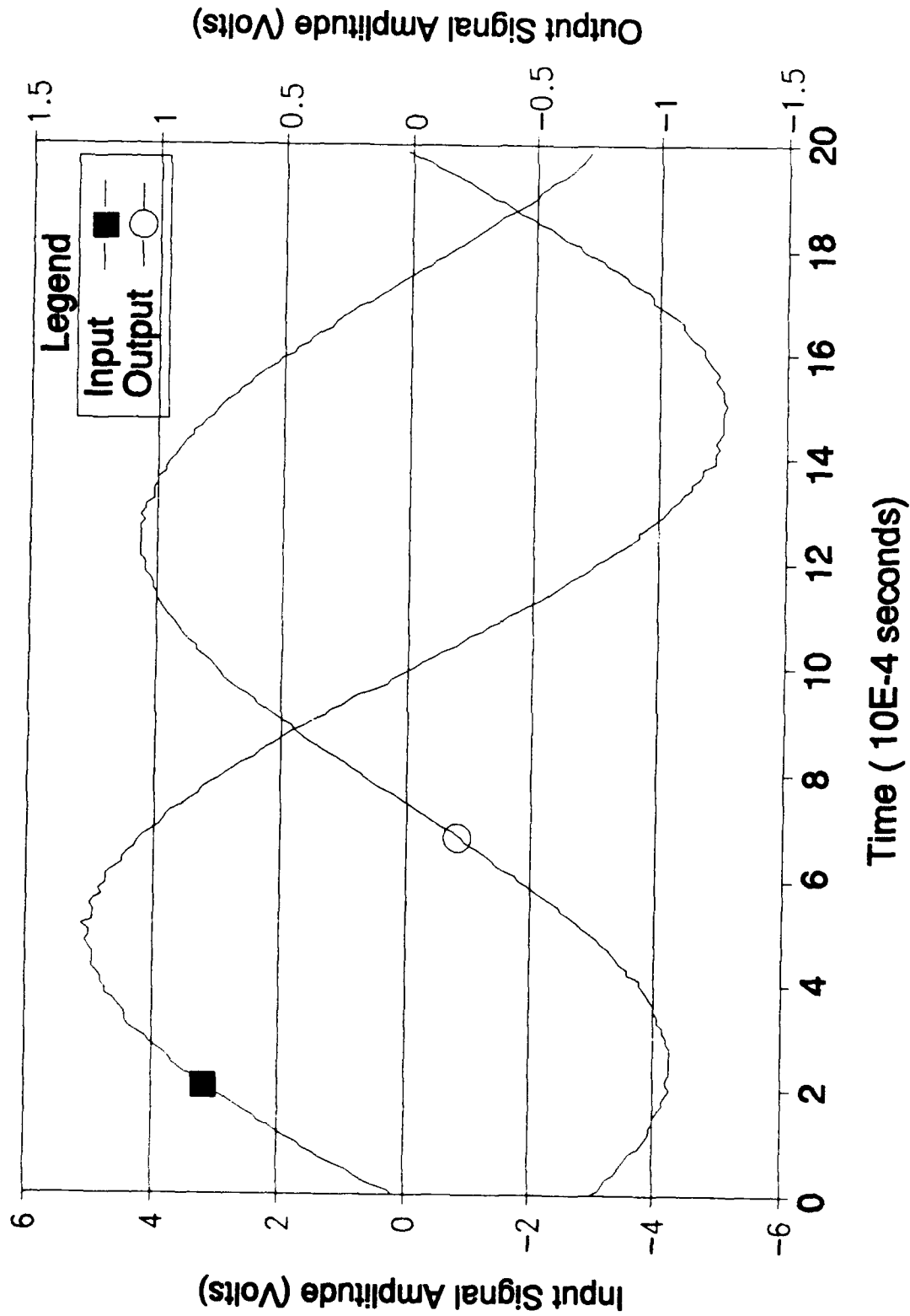
Figure 36c. Time Response of the Oldham Discrete Component Circuit Design with a 500 Hz Excitation Signal.

Lecroy oscilloscope, both data sets were collected to verify the results.

Sample Nichols plots, spectrum plots, gain plots and phase plots are presented in Figure 37, Figure 38, Figure 39 and Figure 40, respectively. A complete set of Nichols plots are organized in Appendix H, while the spectral plots are collected in Appendix I. The corresponding gain and phase plots are reported in Appendix J.

Phase Shift (Degrees)
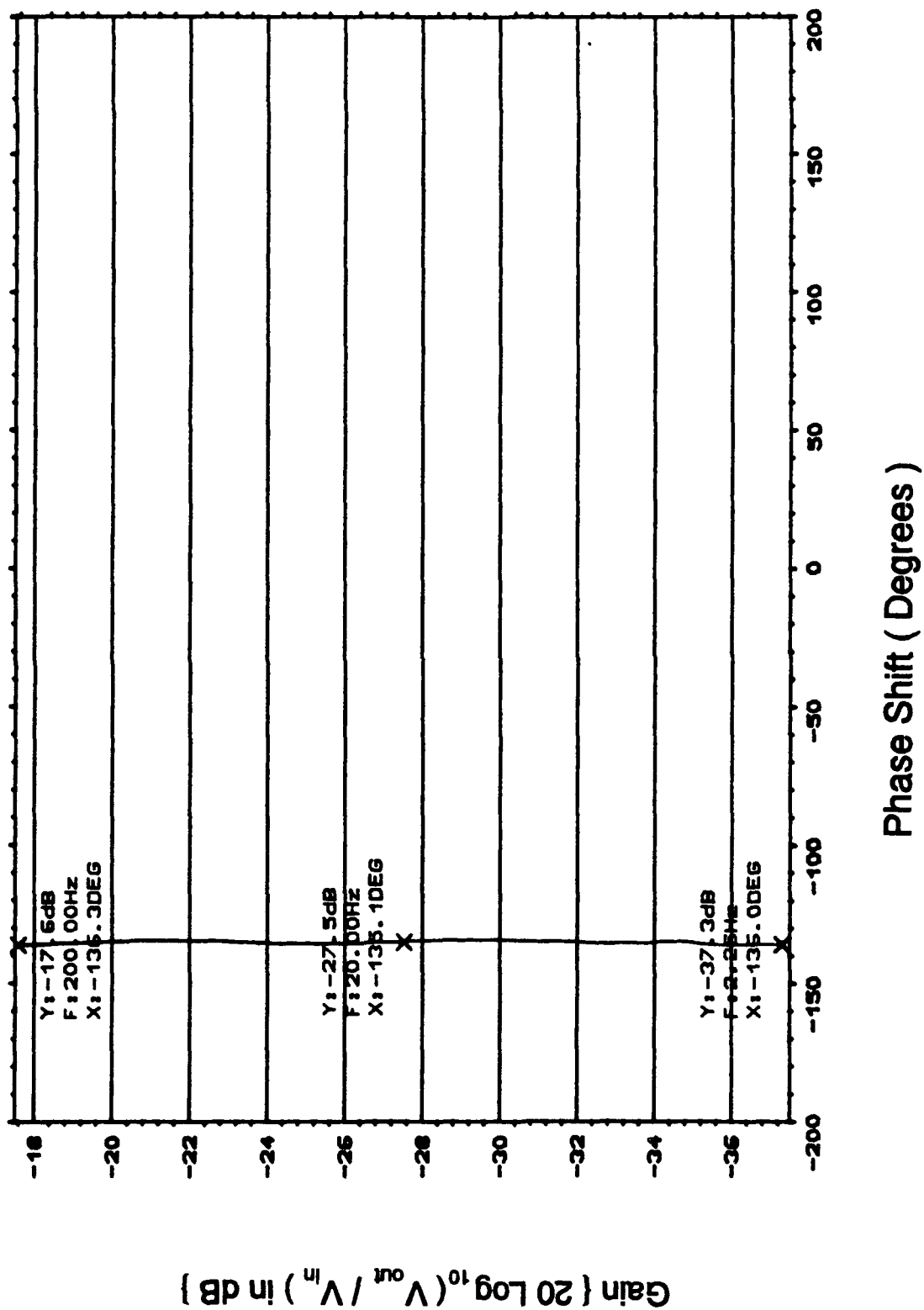
Figure 37.   Nichols Plot for the Oldham Hybrid Component Circuit
(Frequency Range 2.25 Hz to 200 Hz).

Gain { 20 Log₁₀(V$_{out}$ / V$_{in}$) in dB }

Y:-17.6dB
F:200.00Hz
X:-135.3DEG

Y:-27.5dB
F:20.00Hz
X:-135.1DEG

Y:-37.3dB
F:2.25Hz
X:-135.0DEG
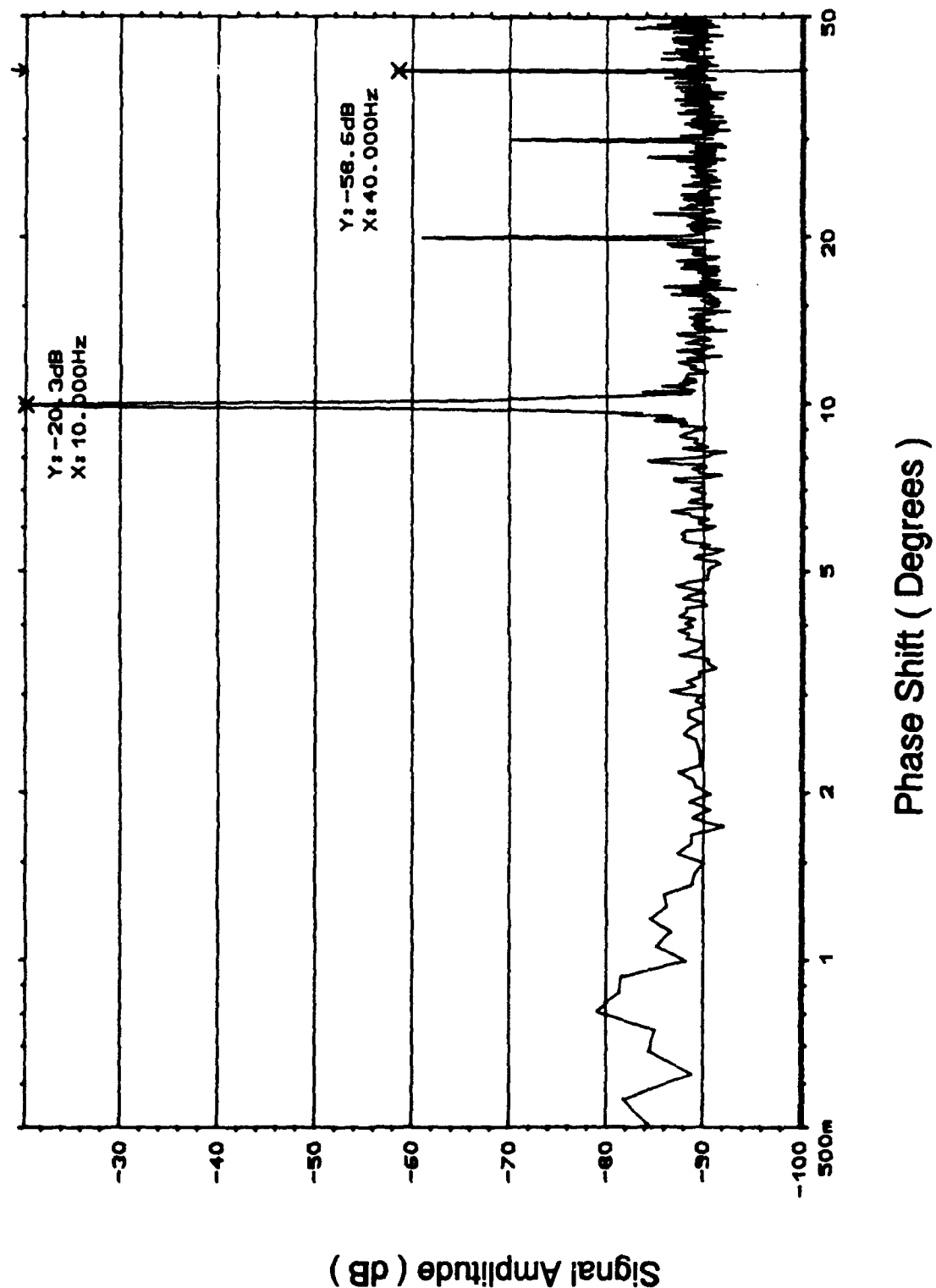
Figure 38. Spectrum Analysis of the Oldham Hybrid Component Circuit With a 10.0 Hz Excitation Signal.
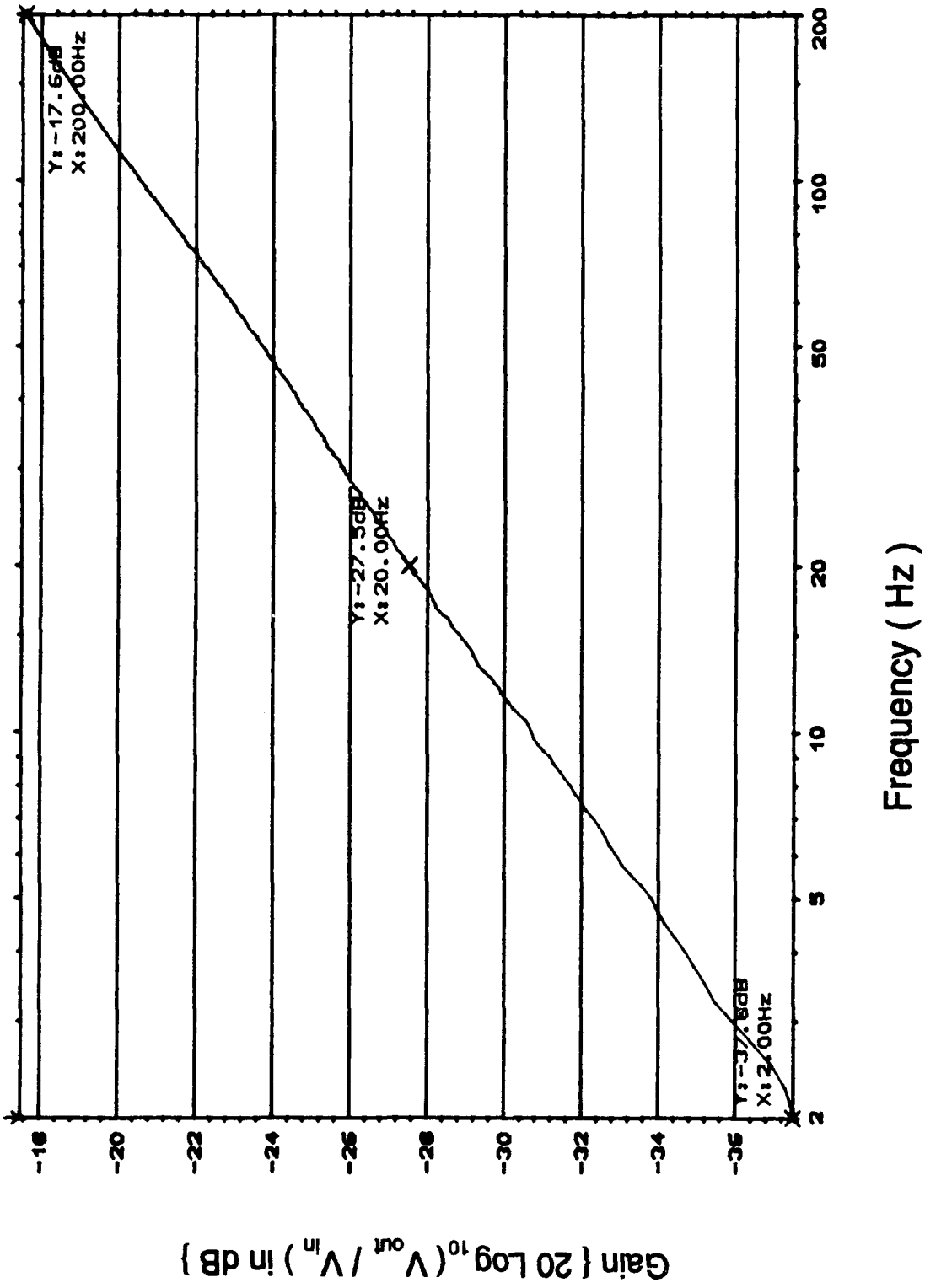
Figure 39. Gain Response of the Oldham Hybrid Component Circuit.
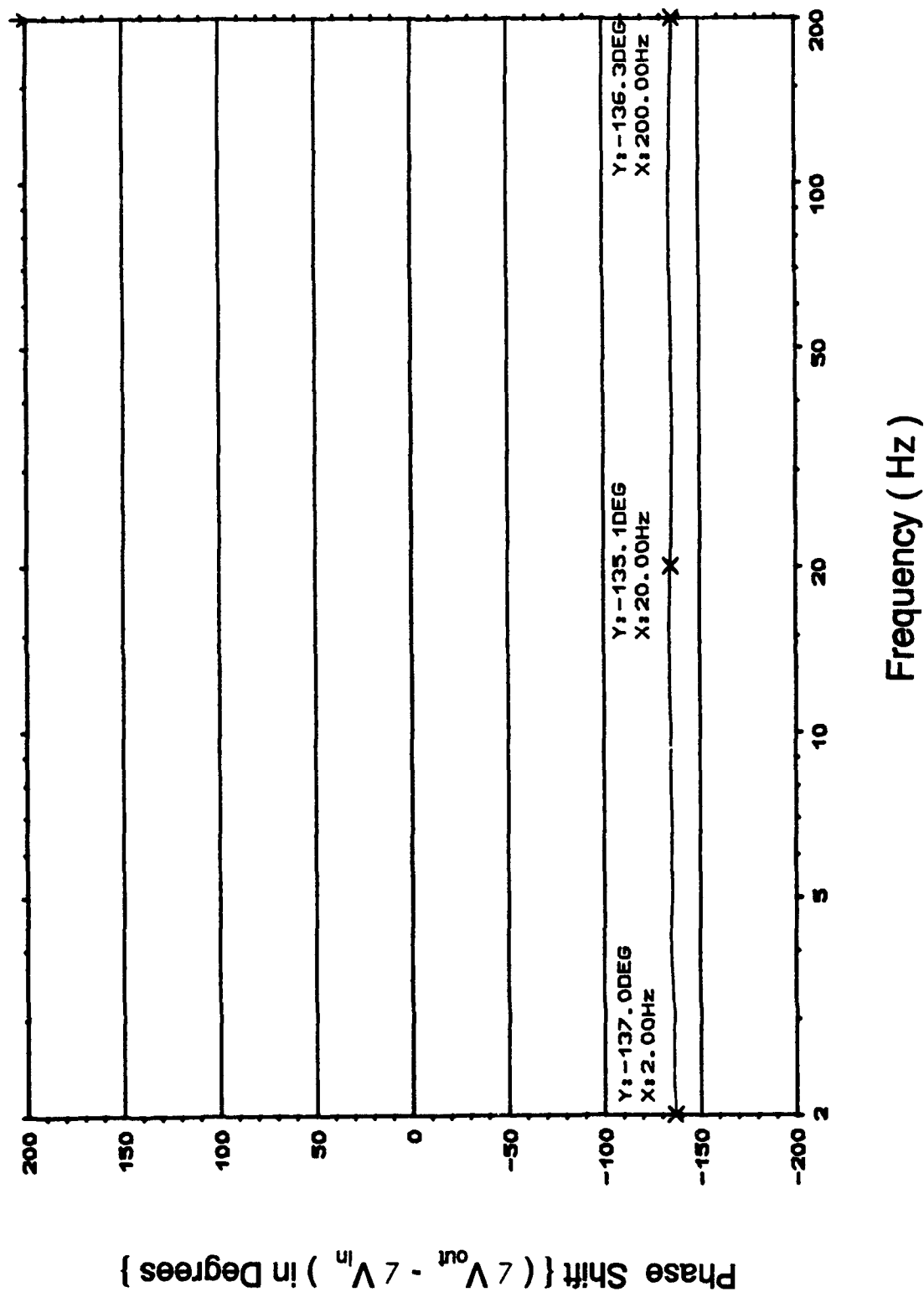
Figure 40. Phase Response of the Oldham Hybrid Component Circuit.

V. Analysis and Comparison of the Data

With the electrical performance test completed, a comparison of the data was motivated. The task of the data analysis is divided into three categories. First, the analysis of the computer simulation results is discussed. Namely, the component value variation analysis and the associated effects on the two circuit's electrical performance is presented. Second, the analysis of the experimental data recorded with the LeCroy digital storage oscilloscope and its significance is developed. Finally, the analysis of the data recorded from the B & K spectrum analyzer is accomplished.

Analysis of Computer Simulation Results

This portion of the analysis is subdivided into two sections, with three subdivisions each. The two circuit variations, Oldham and Oldfield, comprise the two sections. The three subdivisions are organized according to the three types of simulations that were completed, namely, individual component value variations, individual cell component value variations, and all the cells component value variations. Each circuit variant (Oldham and Oldfield) is analyzed separately below. Since a major concern was the frequency range of the circuit's performance, the analysis focuses on the frequency range affected by each variation category. The frequency range affected is reported in two ways.

First, the frequency interval that the component value variation affects is identified, and second, the frequency interval over which the component value variation had "negative effects" is cited ("negative effects" imply that either the tolerance on the phase shift or the slope of the gain, or both, are not satisfied -- see Chapter 1, Scope section).

Oldham Computer Simulation Analysis. The Oldham circuit design was accomplished using 12 cells, it was simulated computationally and the results were analyzed by using the three categories described below.

Oldham Circuit Individual Component Value Variations. The value of each component was systematically varied using the following scaling factors: 0.1, 0.4, 1.6, 2.0, and 5.0. That is, the value of the simulated component was

$$N = C \times F \tag{25}$$

where

C = "ideal" component value,

F = the scaling factor, and

N = the simulated component value.

The specific values of the scaling factors were strongly influenced by the initial computer simulation results where all the cell values were varied. The computer simulation results for the all-cell component value variations in

Appendix A and Appendix B reveal that the 0.4 and 1.6 factors were the approximate lower and upper limits that permitted the circuit's performance to remain within the design criteria (see Chapter 1, Scope section). The detailed effect of varying each component's value is documented in Appendix K. However, the frequency interval over which each component's value displayed undesirable effects is summarized in Figure 41 (Oldham circuit resistors) and Figure 42 (Oldham circuit capacitors). The results displayed in Figure 41 and Figure 42 reveal that the interior-section cell component values have the most significant influence on circuit's performance. Specifically, R0, R1, R11, C0, C1, C9, C10, and C11 (the components in the terminal cells) have the least effect on circuit performance.

Oldham Circuit Individual Cell Component Value Variations. As stated in Chapter 3, the cell (resistor-capacitor pair) component value computer variation used the Monte Carlo technique. The detailed effect of each cell's value variations is documented in Appendix K. As discussed above, the frequency interval over which each component's value variation displayed undesirable performance effects is summarized in Figure 43. The results displayed in Figure 43 further demonstrate that the component values of the interior cells have the most significant influence on the circuit's performance. Specifically, cell 0, cell 1,
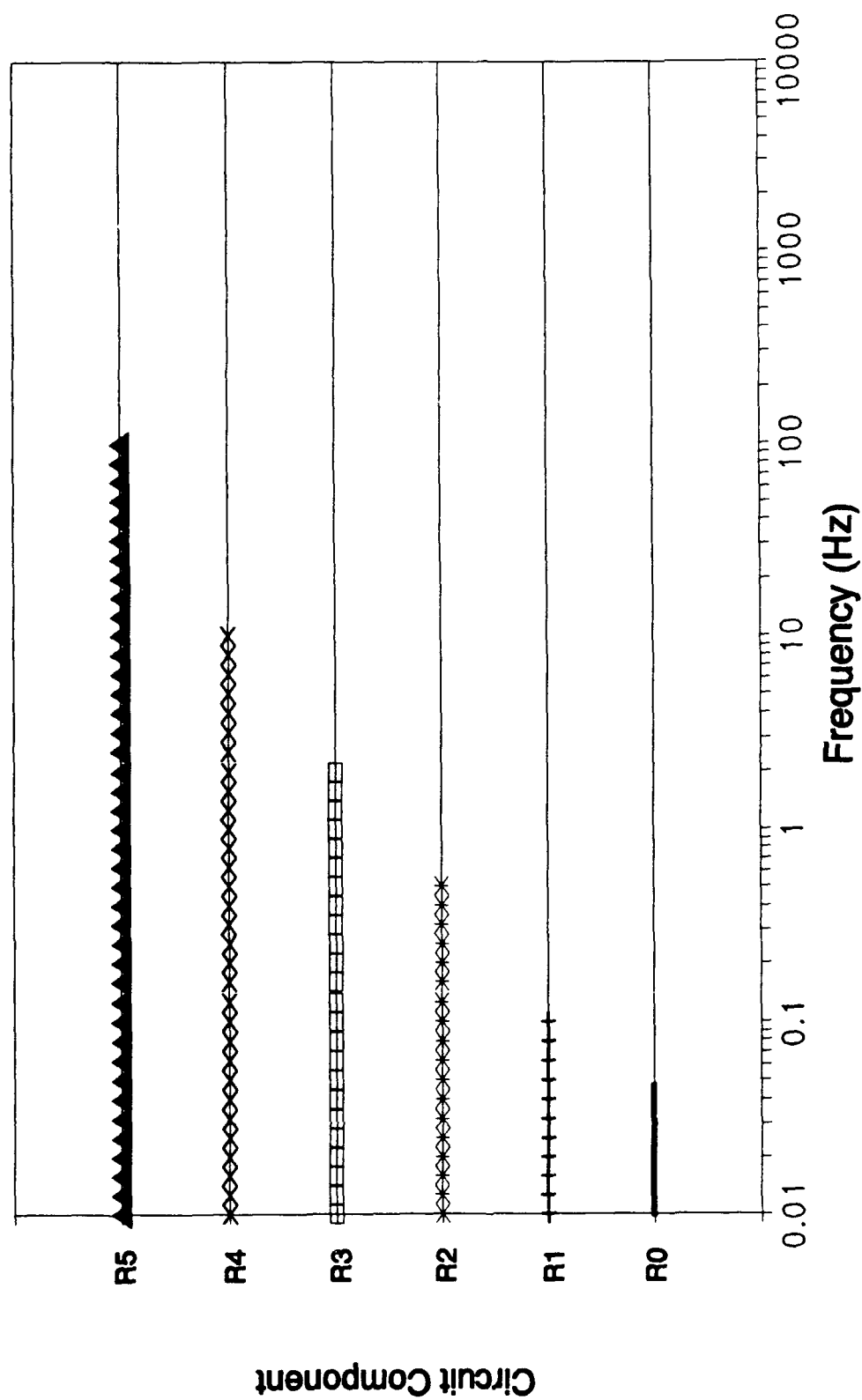
Figure 41. Frequency Interval (as indicated by the plot symbols) Over Which the Oldham Resistor Components (when varied by 0.1 ≤ F ≤ 5.0) Caused the Circuit's Performance to Deviate from the "Ideal" Response (cont).
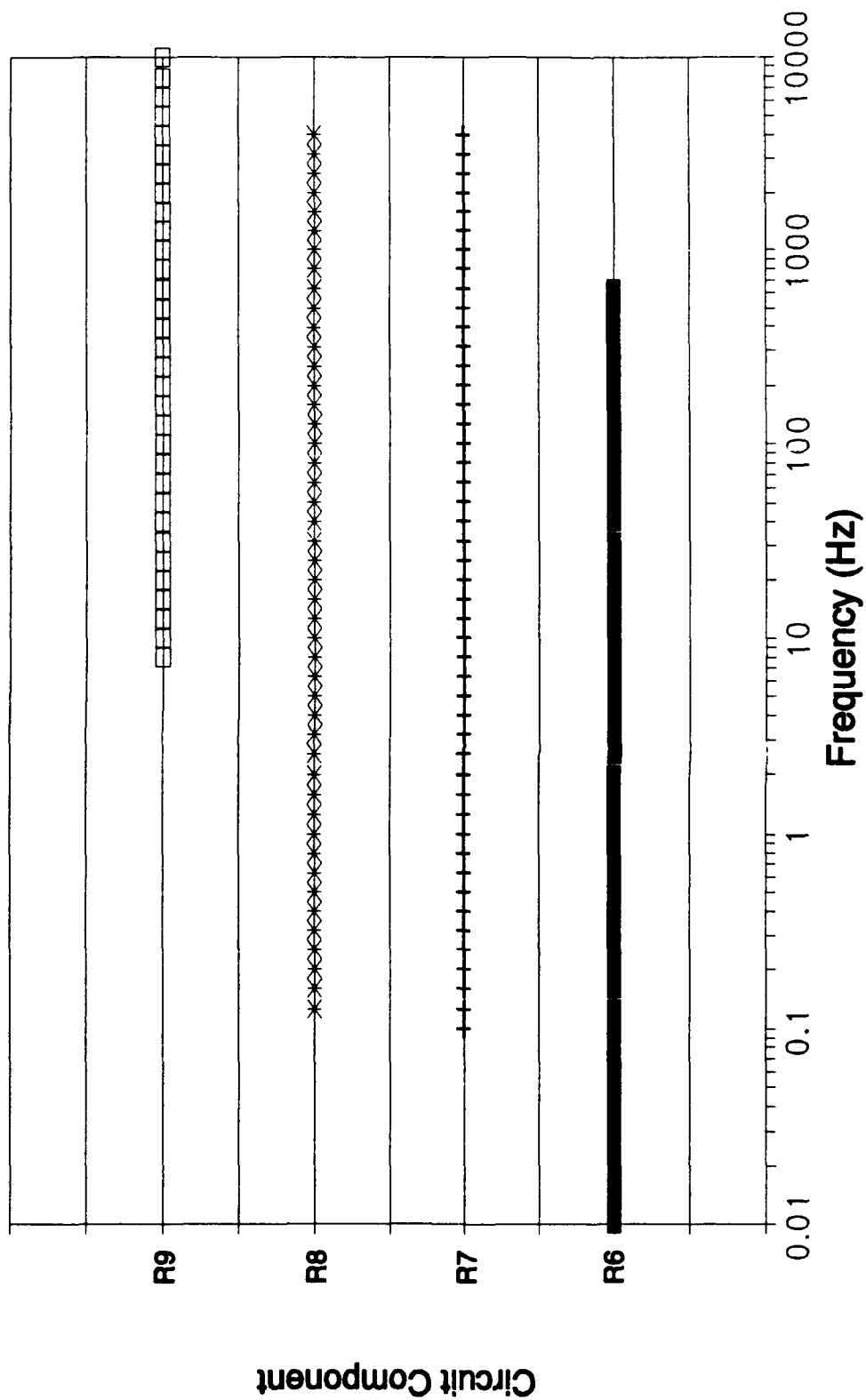
Figure 41 (cont). Frequency Interval (as indicated by the plot symbols) Over Which the Oldham Resistor Components (when varied by $0.1 \leq F \leq 5.0$) Caused the Circuit's Performance to Deviate from the "Ideal" Response (cont).
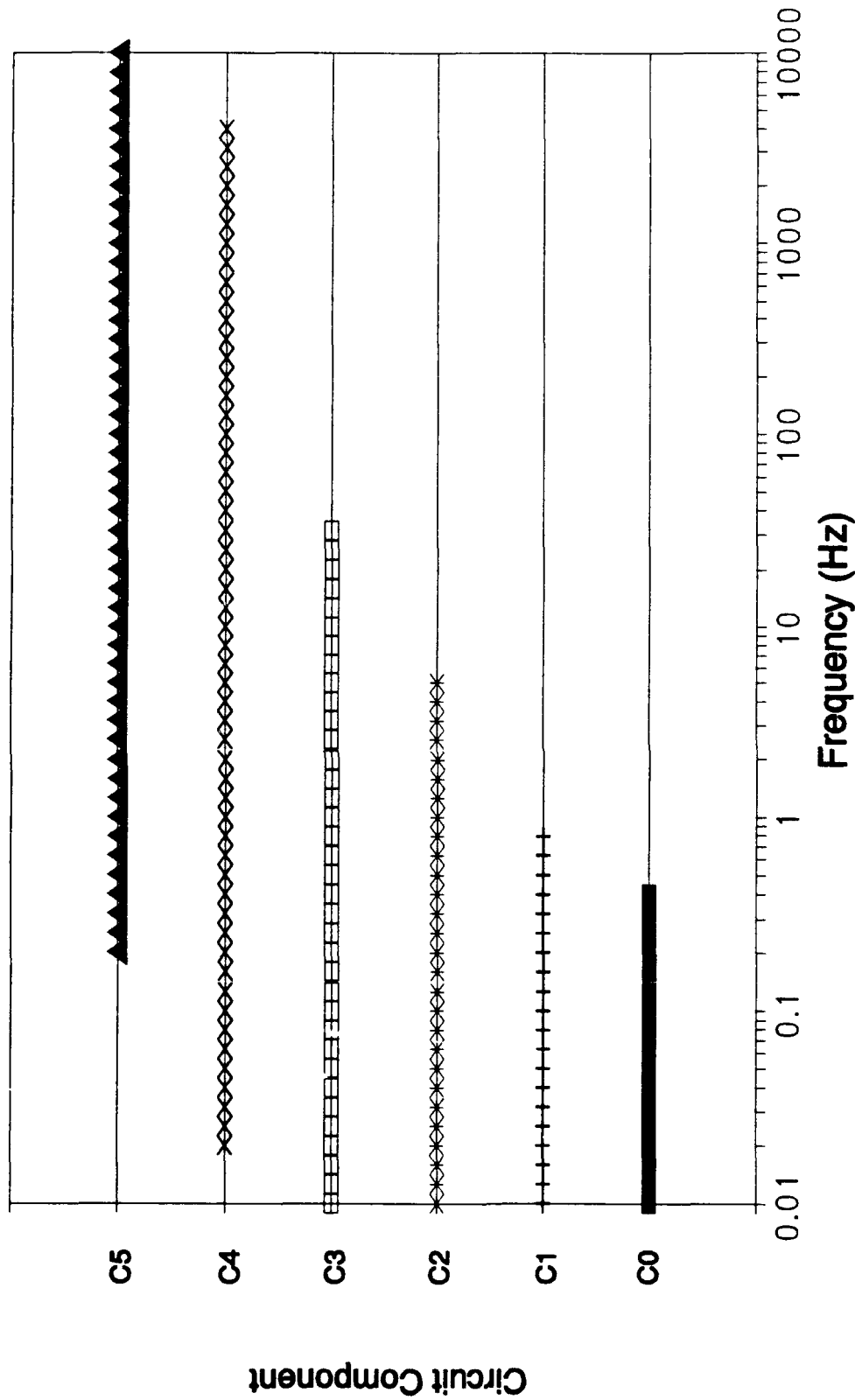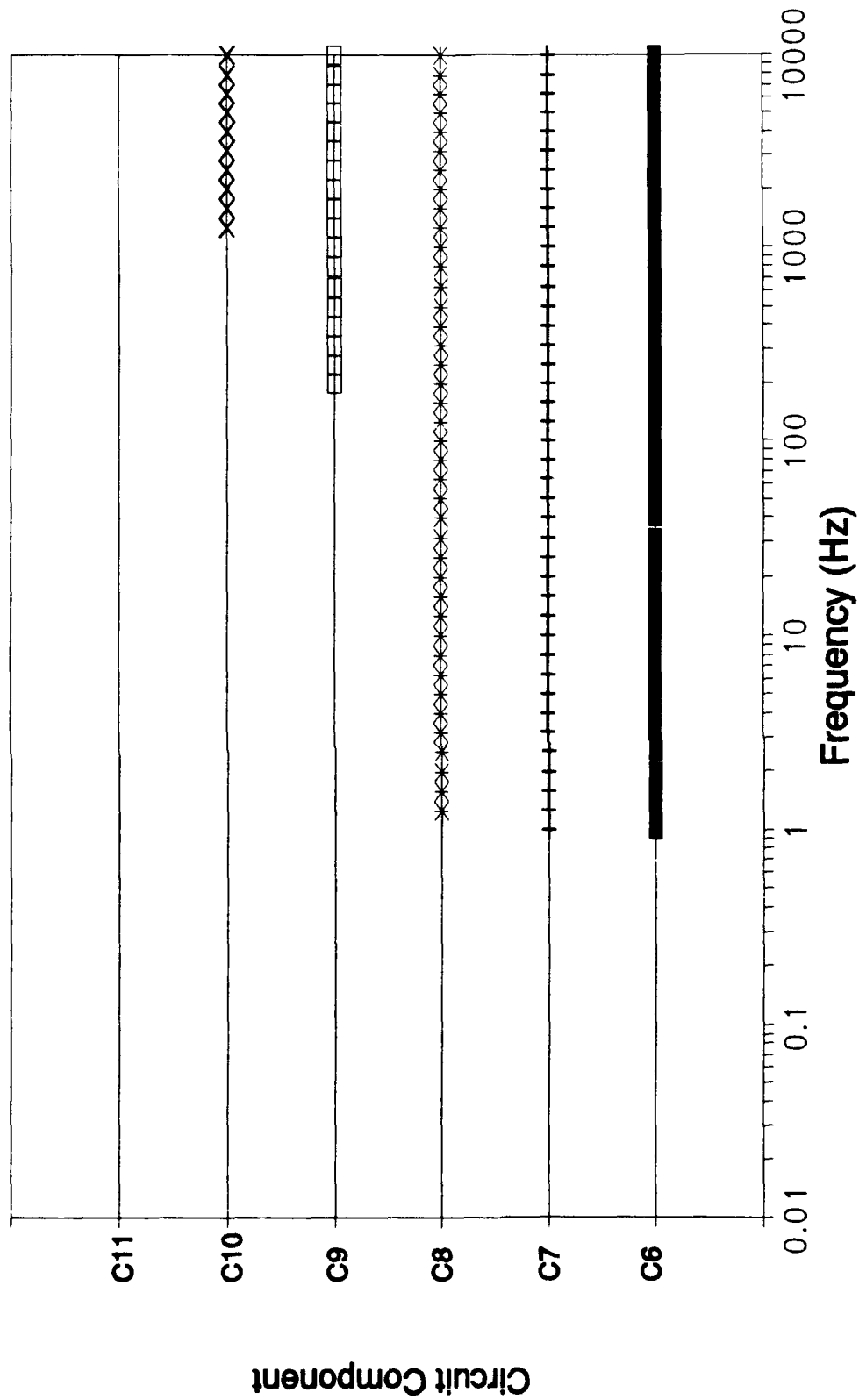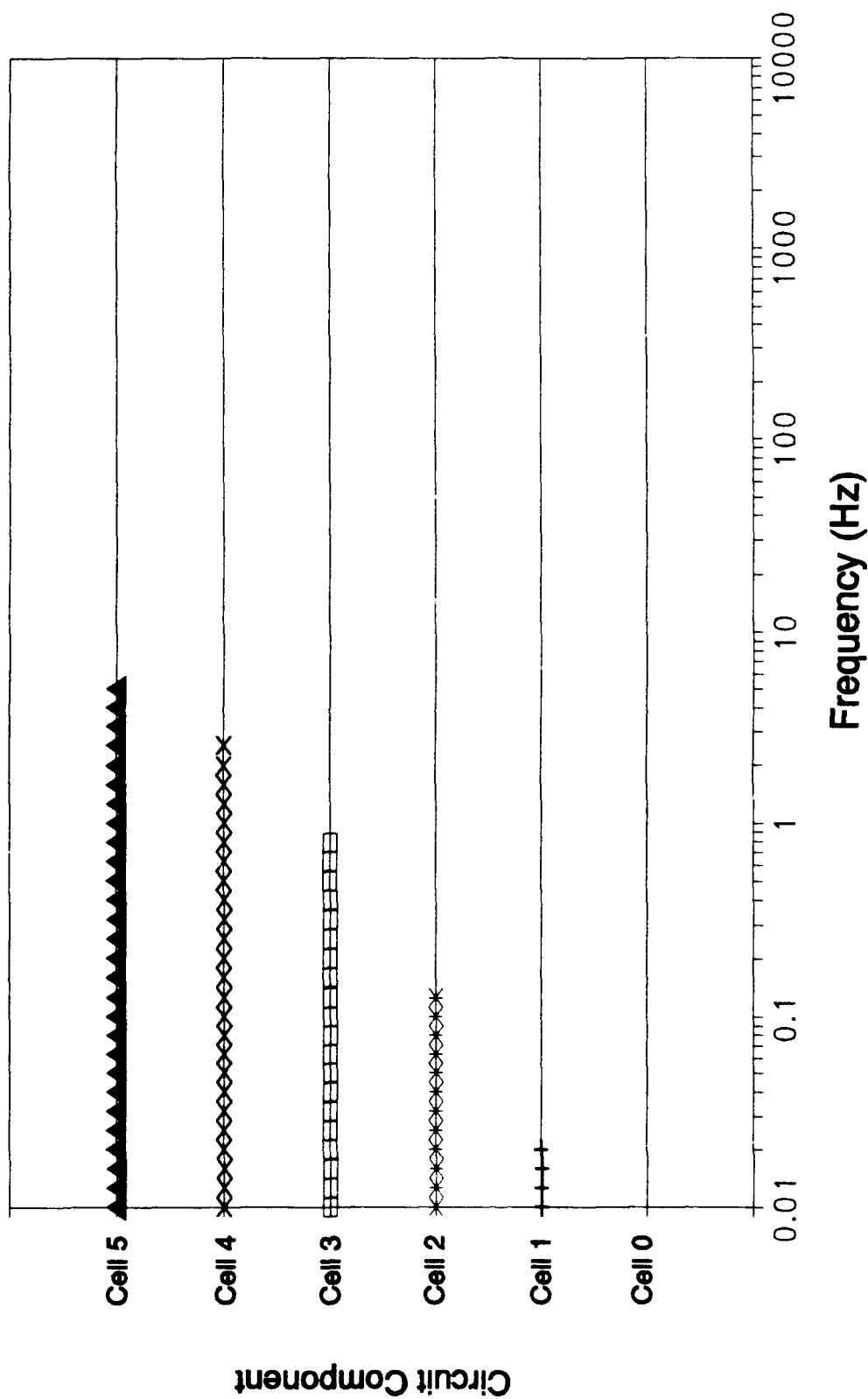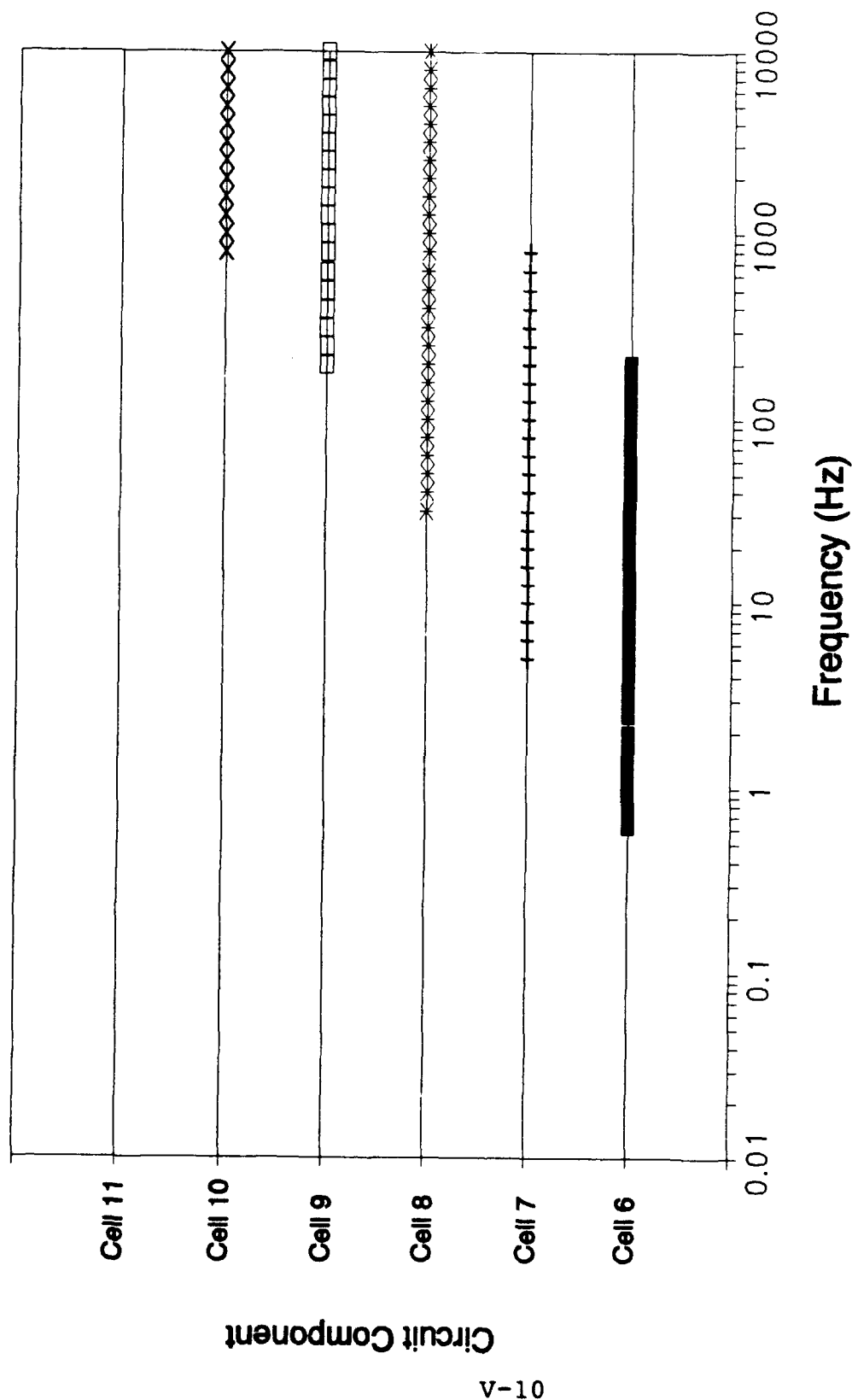
V-5
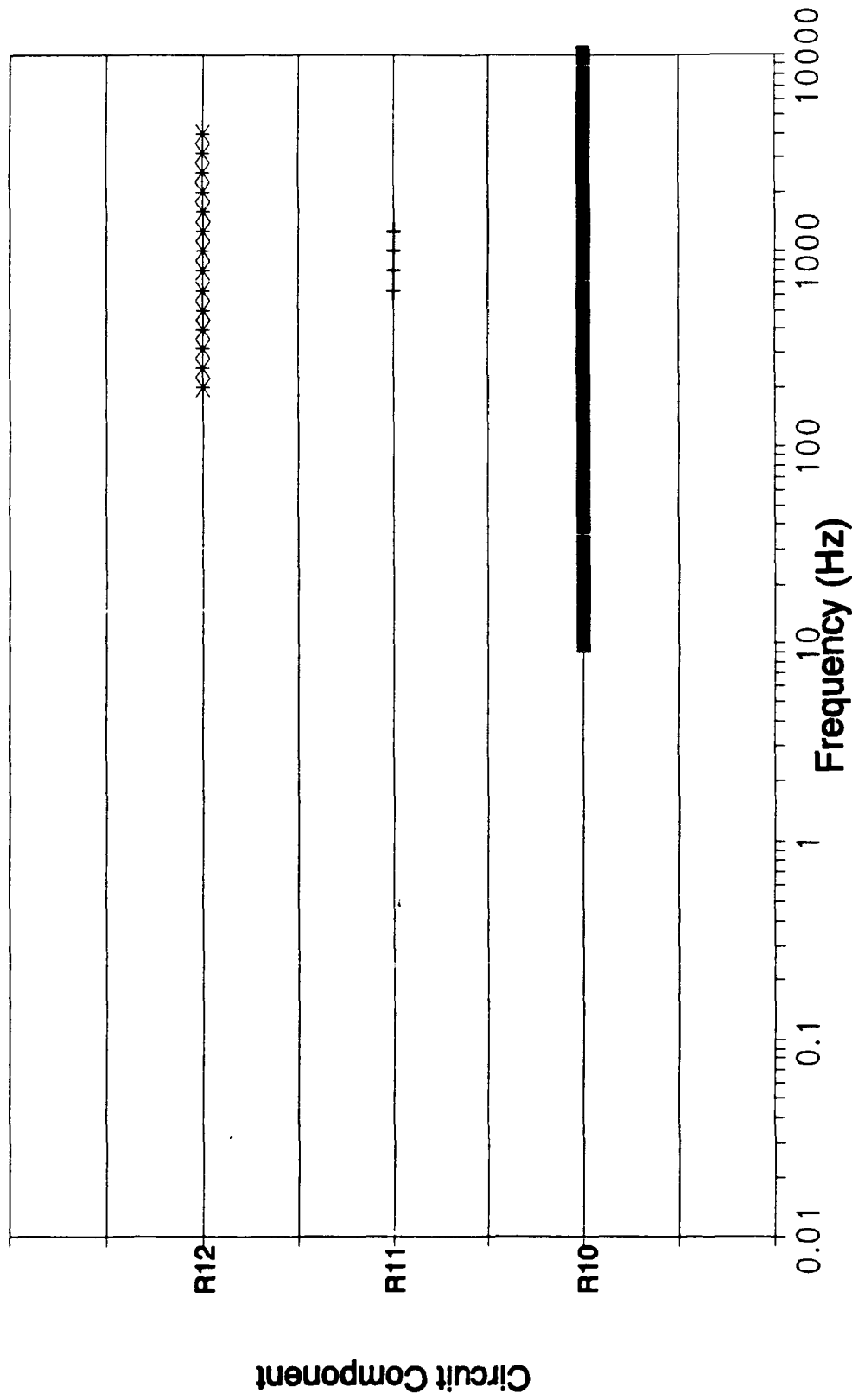
Figure 41 (cont). Frequency Interval (as indicated by the plot symbols) Over Which the "Oldham Resistor Components (when varied by 0.1 ≤ F ≤ 5.0) Caused the Circuit's Performance to Deviate from the "Ideal" Response.

Figure 42. Frequency Interval (as indicated by the plot symbols) Over Which the Oldham Capacitor Components (when varied by $0.1 \leq F \leq 5.0$) Caused the Circuit's Performance to Deviate from the "Ideal" Response (cont).

Figure 42 (cont). Frequency Interval (as indicated by the plot symbols) Over Which the Oldham Capacitor Components (when varied by $0.1 \leq F \leq 5.0$) Caused the Circuit's Performance to Deviate from the "Ideal" Response.

Figure 43. Frequency Interval (as indicated by the plot symbols) Over Which the Oldham Cell Components (when varied by $0.4 \leq F \leq 1.8$) Caused the Circuit's Performance to Deviate from the "Ideal" Response (cont).

Figure 43 (cont). Frequency Interval (as indicated by the plot symbols) Over Which the Oldham Cell Components (when varied by $0.4 \leq F \leq 1.8$) Caused the Circuit's Performance to Deviate from the "Ideal" Response.

cell 9, cell 10 and cell 11 have the least affect on circuit performance.

Oldham Circuit Component Values Variations Involving All of the Cells. A similar computer simulation scheme (Monte Carlo technique) was performed in this segment of the analysis except that "all-cell" component values were varied. The purpose of this analysis was twofold. First, it was accomplished to define the upper and lower tolerance limits of the cell component value variations, and secondly, to determine if a random selection of conventional ± 20 percent components would produce circuits that could satisfy the design specifications. The computer simulation results are displayed in Figure B-38 (Appendix B). The results show that the Oldham circuit design satisfies the design criteria for the phase and gain specifications described earlier under these test conditions.

The frequency intervals undesirably affected by component value variations are also summarized in Table 4 in a slightly different manner. That is, Table 4 documents each component's and cell's affect on the frequency intervals over which the gain and phase responses displayed undesirable effects.

Table 4

Frequency Intervals Over Which the Oldham Circuit Design Components Demonstrated Undesirable Effects for the Gain and Phase Responses

Component	Gain Response Frequency Interval (GF[4] in Hz)	Phase Response Frequency Interval (PF[5] in Hz)
R0	None	None
C0	$0.01 < GF < 0.041$	$0.01 < PF < 0.041$
R1	None	$0.01 < PF < 0.1$
C1	$0.01 < GF < 0.6$	$0.01 < PF < 0.82$
R2	None	$0.01 < PF < 0.52$
C2	$0.01 < GF < 5.2$	$0.01 < PF < 5.2$
R3	$0.01 < GF < 0.3$	$0.01 < PF < 2.0$
C3	$0.02 < GF < 32$	$0.01 < PF < 32$

---

[4] The GF represents the value of frequency at which the circuit's gain performance is undesirably affected when the circuit's component values are varied from their "ideal" value.

[5] Correspondingly, the PF represents the value of frequency at which the circuit's gain performance is undesirably affected when the circuit's component values are varied from their "ideal" value.

Table 4 (cont)		
R4	0.01 < GF < 1.0	0.01 < PF < 10.5
C4	0.08 < GF < 300	0.02 < PF < 4K
R5	0.02 < GF < 6.5	0.01 < PF < 100
C5	0.62 < GF < 2K	0.18 < PF < 10K
R6	0.03 < GF < 35	0.01 < PF < 650
C6	0.3 < GF < 10K	1.0 < PF < 10K
R7	0.1 < GF < 450	0.01 < PF < 4K
C7	3.6 < GF < 10K	1.0 < PF < 10K
R8	0.2 < GF < 290	0.01 < PF < 4K
C8	4.0 < GF < 10K	1.1 < PF < 10K
R9	10 < GF < 10K	0.2 < PF < 10K
C9	800 < GF < 10K	200 < PF < 10K
R10	11 < GF < 10K	0.5 < PF < 10K
C10	None	1.2K < PF < 10K
R11	900 < GF < 10K	3.0 < PF < 2.5K
C11	None	None
R12	300 < GF < 10K	4.0 < PF < 3.9K
Cell 0	None	None

Table 4 (cont)		
Cell 1	0.01 < GF < 0.04	0.01 < PF < 5.8
Cell 2	0.01 < GF < 0.2	0.01 < PF < 0.12
Cell 3	0.01 < GF < 3.0	0.01 < PF < 0.9
Cell 4	0.01 < GF < 20	0.019 < PF < 5.0
Cell 5	0.04 < GF < 200	0.1 < PF < 50
Cell 6	0.01 < GF < 1K	0.7 < PF < 1K
Cell 7	1.0 < GF < 2K	5.0 < PF < 900
Cell 8	10 < GF < 10K	30 < PF < 10K
Cell 9	50 < GF < 10K	200 < PF < 10K
Cell 10	200 < GF < 10K	800 < PF < 10K
Cell 11	None	None

Oldfield Circuit Computer Simulation Analysis. As described earlier, the Oldfield circuit was designed and simulated with 9 cells, and the results are analyzed using an analogous scheme that was employed for the Oldham circuit.

Oldfield Circuit Component Value Variations. Again, the value of each component was varied by the factors established earlier for the same reasons. The detailed affect of each component's value variation is documented in

Appendix L. The frequency interval over which each component displayed undesirable effects is summarized in Figure 44 (Oldfield circuit resistors) and Figure 45 (Oldfield circuit capacitors). The results displayed in Figure 44 and Figure 45 reveal that all the component value variations have a critical impact on the frequency range when the circuit performs as desired.

Oldfield Circuit Individual Cell Component Value Variations. As stated in Chapter 3, and as for the Oldham circuit, the cell (resistor-capacitor pair) component value computer variation used the Monte Carlo technique. The detailed effect of varying the values of the components in each cell is documented in Appendix L. As described above, the frequency interval over which each component displayed undesirable effects is summarized in Figure 46. These results further demonstrate that each component, and thus, each cell, has a specific frequency interval over which it dominates the circuit's performance.

Oldfield Circuit Component Value Variations Involving All the Cells. Again, as discussed above, and in Chapter 3, the "all-cell" computer simulation used the Monte Carlo technique. The computer simulation results are displayed in Figures C-28.1 through Figure C-28.2 (Appendix C). The results demonstrate the influence of each component's value relative to a specific frequency interval, and they reveal that the Oldfield circuit design DOES NOT
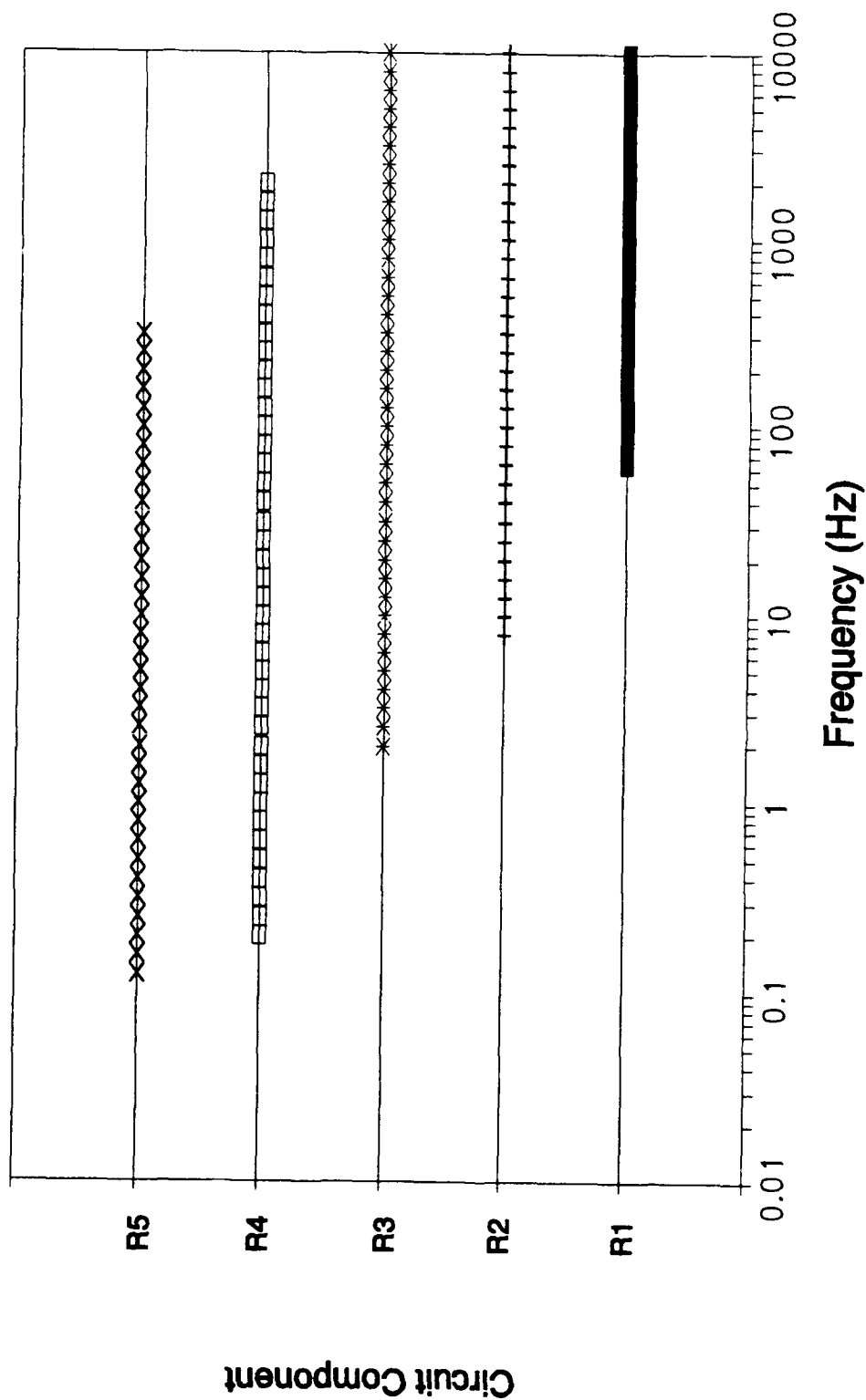
Figure 44. Frequency Interval (as indicated by the plot symbols) Over Which the Oldfield Resistor Components (when varied by $0.1 \leq F \leq 5.0$) Caused the Circuit's Performance to Deviate from the "Ideal" Response (cont).
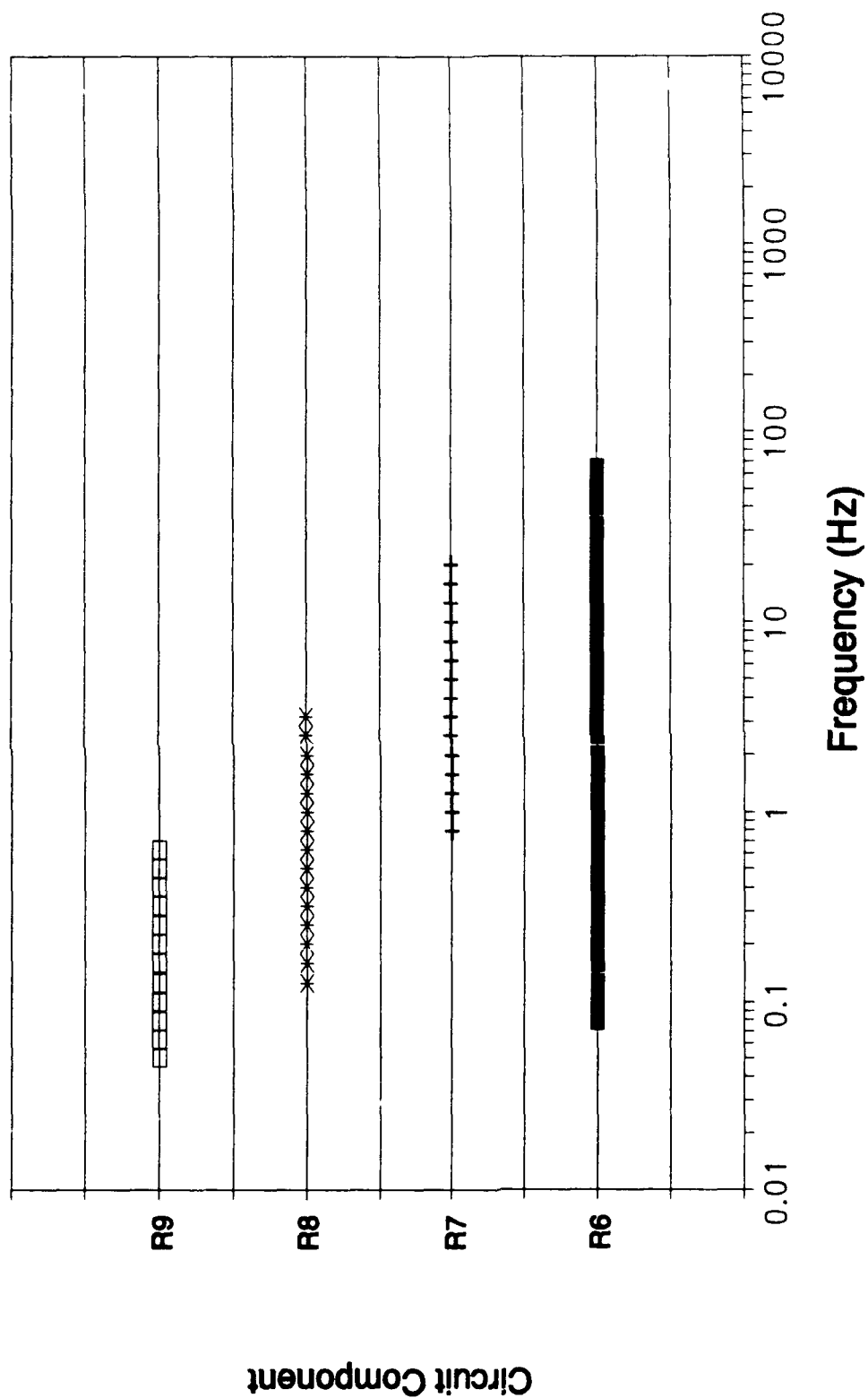
Figure 44 (cont). Frequency Interval (as indicated by the plot symbols) Over Which the Oldfield Resistor Components (when varied by $0.1 \le F \le 5.0$) Caused the Circuit's Perfor,ance to Deviate from the "Ideal" Response.
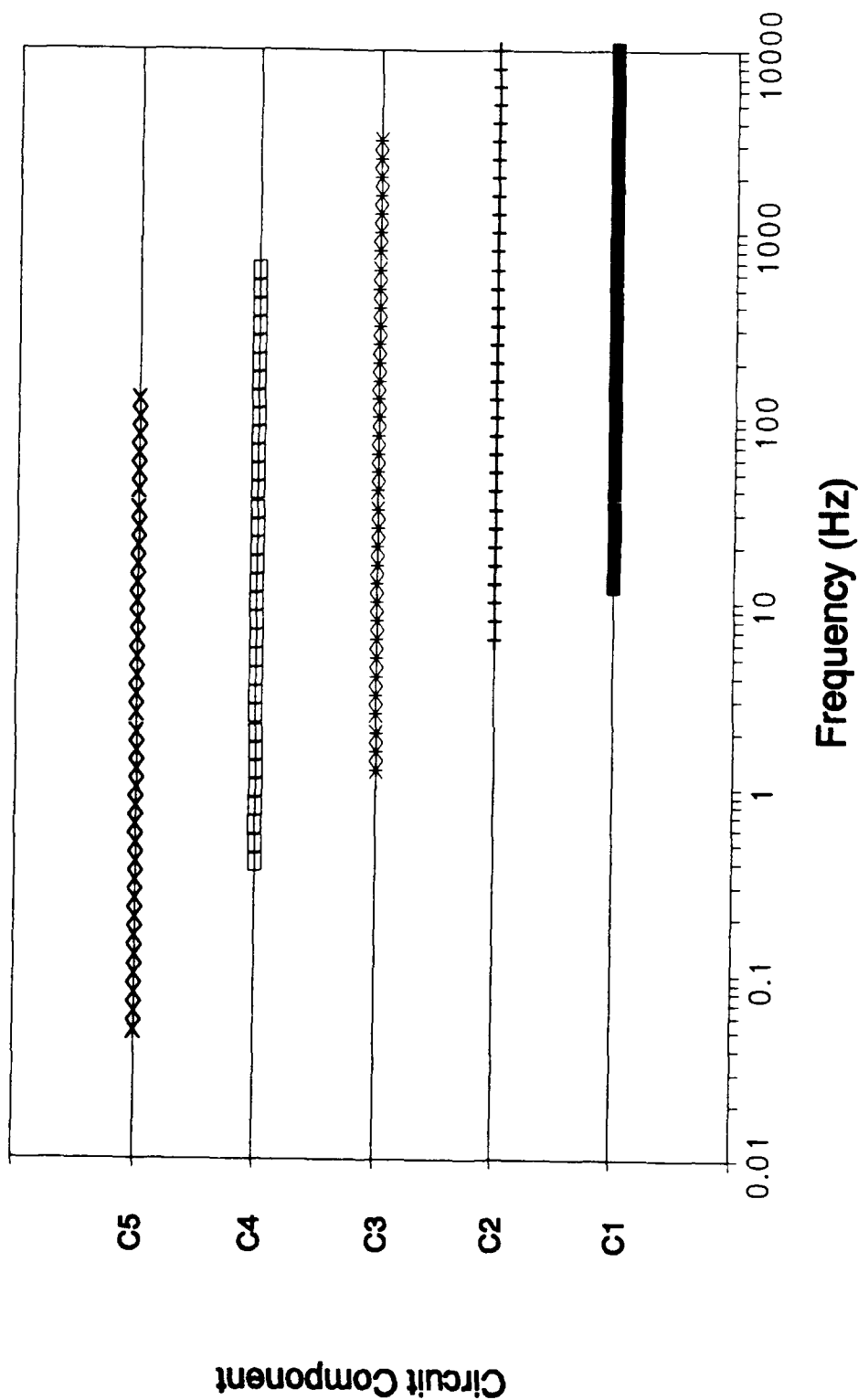
Figure 45. Frequency Interval (as indicated bt the plot symbols) Over Which the Oldfield Capacitor Components (when varied by $0.1 \leq F \leq 5.0$) Caused the Circuit's Performance to Deviate from the "Ideal" Response (cont).
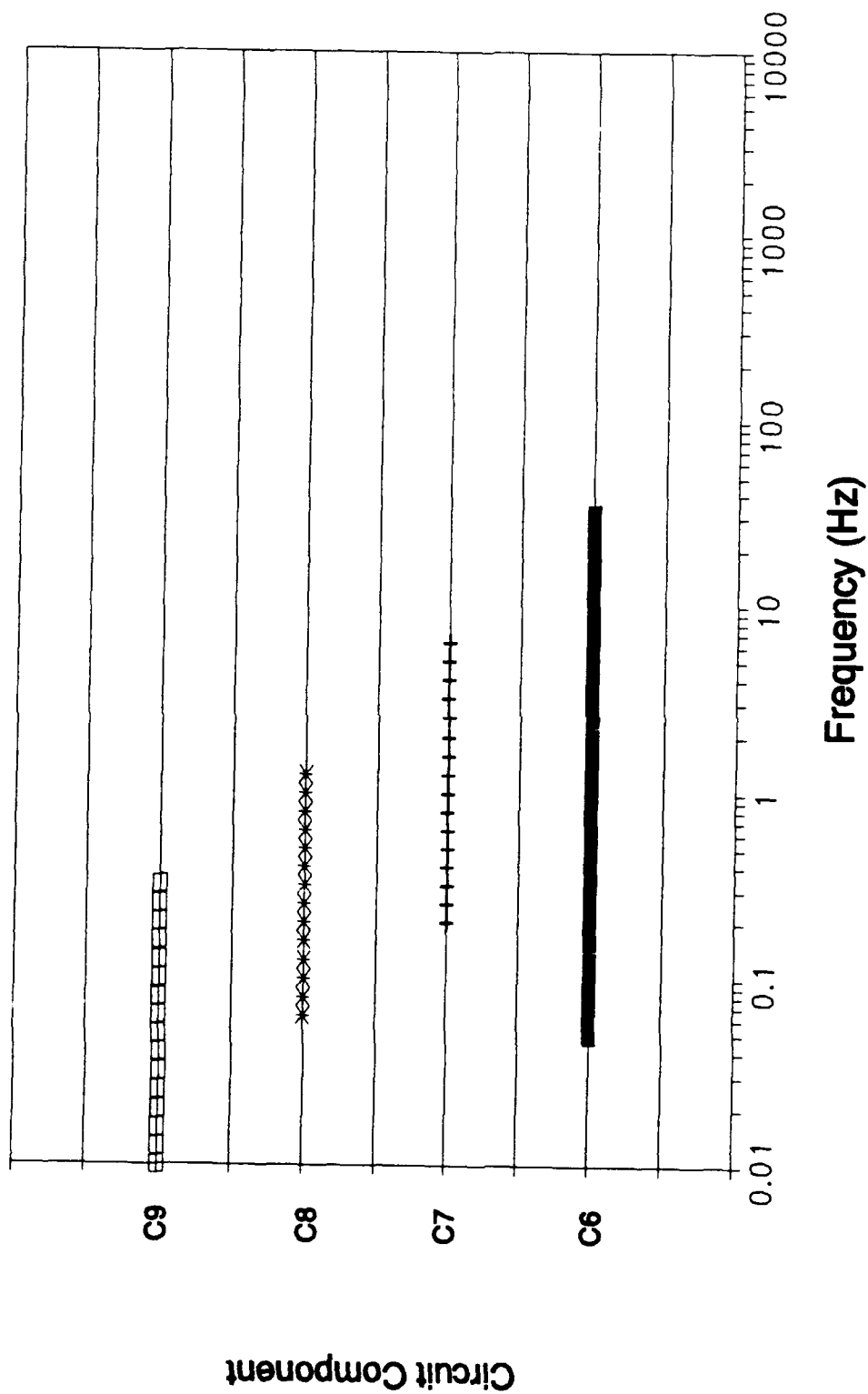
Figure 45 (cont). Frequency Interval (as indicated by the plot symbols) Over Which the Oldfield Capacitor Components (when varied by 0.1 ≤ F ≤ 5.0) Caused the Circuit's Performance to Deviate from the "Ideal" Response.
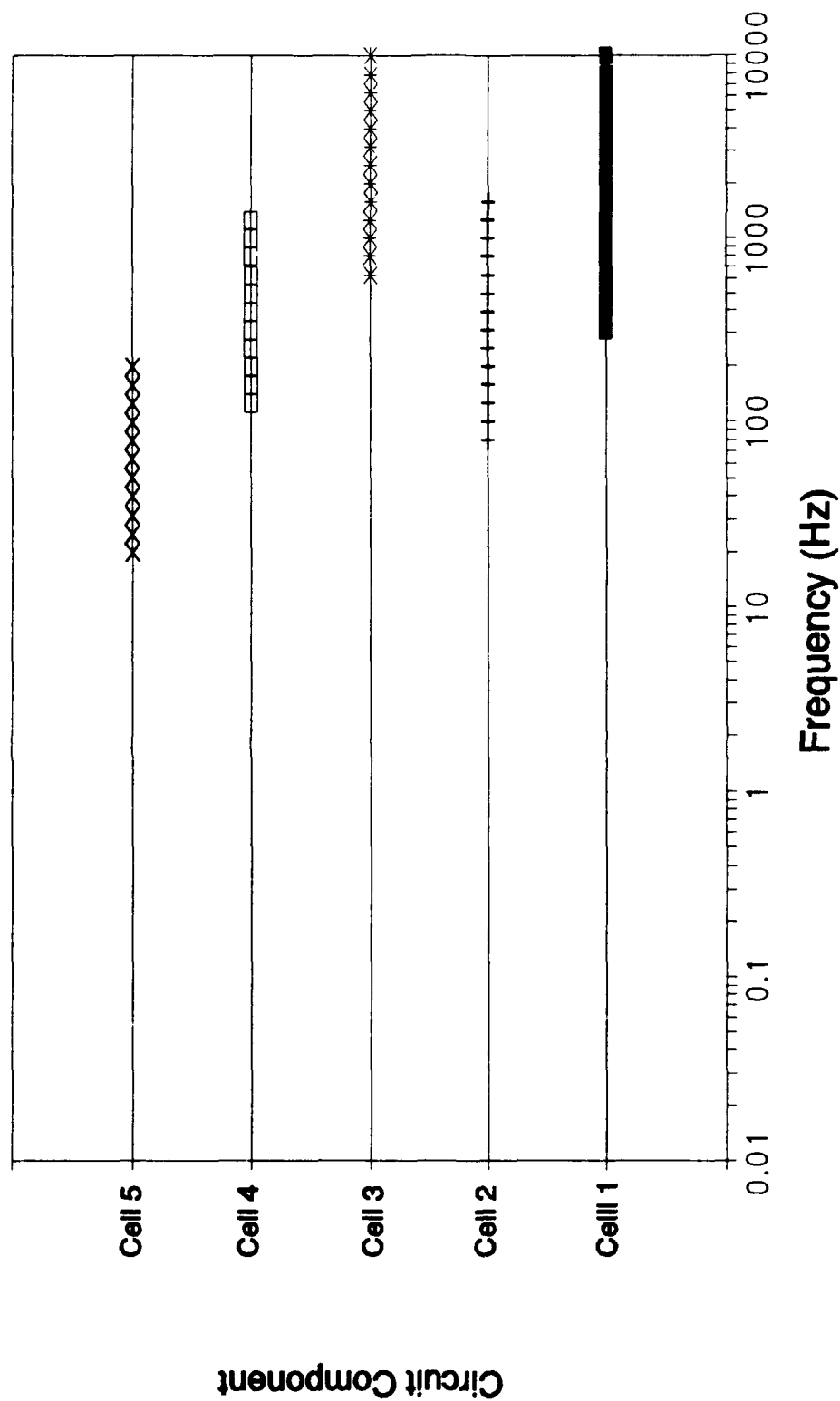
Figure 46. Frequency Interval (as indicated by the plot symbols) Over Which the Oldfield Cell Components (when varied by $0.4 \leq F \leq 1.8$) Caused the Circuit's Performance to Deviate from the "Ideal" Response (cont).
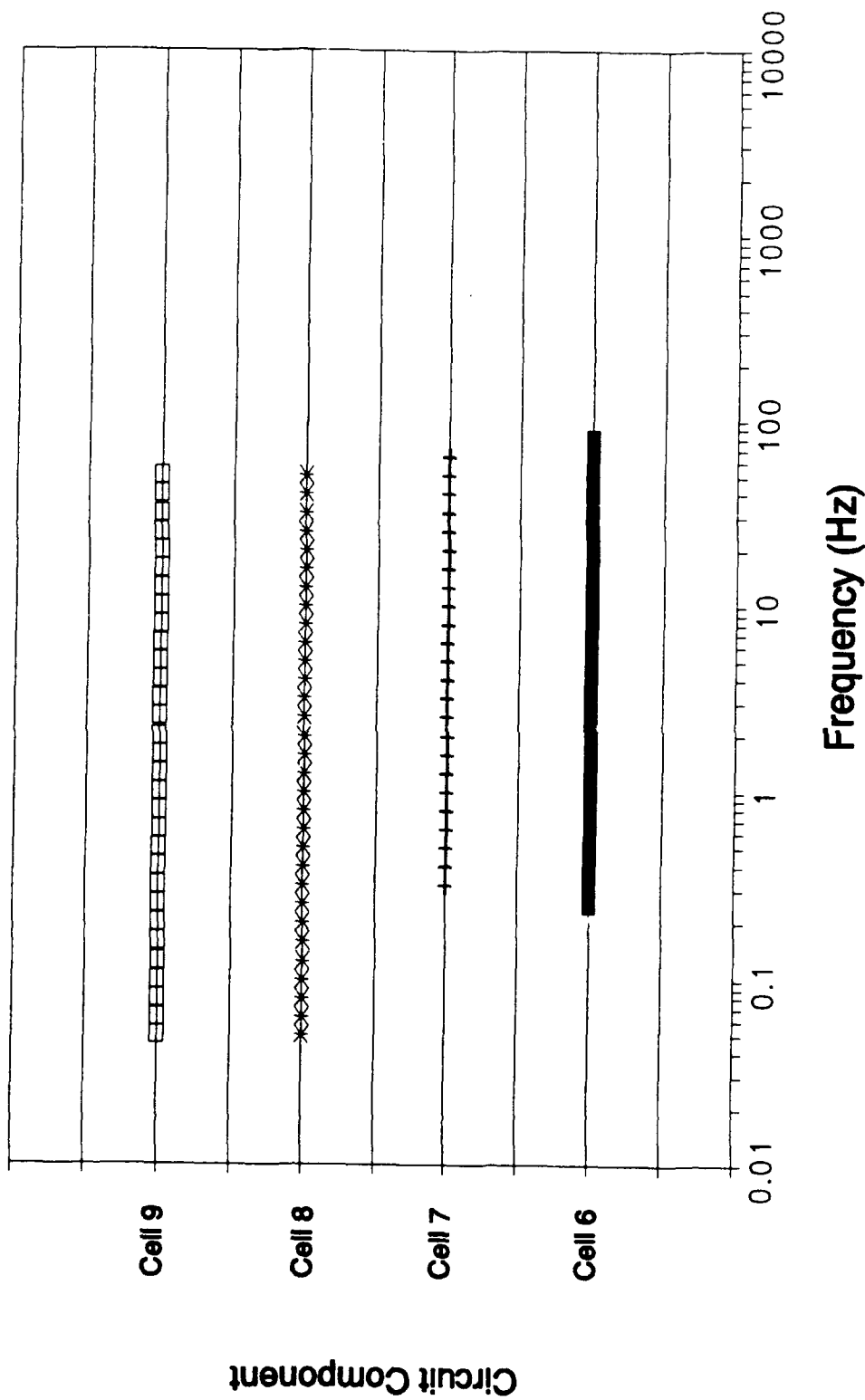
Figure 46 (cont). Frequency Interval (as indicated bt the plot symbols) Over Which the Oldfield Cell Components (when varied by $0.4 \leq F \leq 1.8$) Caused the Circuit's Performance to Deviate from the "Ideal" Response.

satisfy the gain and phase design specifications (Chapter 1, Scope section) under these test conditions.

The frequency intervals affected by component value variations are also summarized in Table 5 in a slightly different manner. That is, Table 5 documents each component's and cell's affect on the frequency intervals over which the gain and phase responses displayed undesirable effects.

Table 5		
Frequency Intervals Over Which the Oldfield Circuit Design Components Demonstrated Undesirable Effects for the Gain and Phase Responses		
Component	Gain Response Frequency Interval (GF[6] in Hz)	Phase Response Frequency Interval (PF[7] in Hz)
R1	$0.01 < GF < 10K$	$62 < PF < 10K$
C1	$10 < GF < 10K$	$11.4 < PF < 10K$
R2	$3.0 < GF < 10K$	$8.0 < PF < 10K$

---

[6] The GF represents the value of frequency at which the circuit's gain performance is undesirably affected when the circuit's component values are varied from their "ideal" value.

[7] Correspondingly, the PF represents the value of frequency at which the circuit's phase performance is undesirably affected when the circuit's component values are varied from their "ideal" value.

Table 5 (cont)		
C2	7.0 < GF < 10K	5.7 < PF < 10K
R3	0.3 < GF < 5K	2.0 < PF < 10K
C3	0.6 < GF < 3K	1.4 < PF < 4K
R4	0.1 < GF < 2K	0.05 < PF < 2K
C4	0.3 < GF < 700	0.4 < PF < 700
R5	0.1 < GF < 500	0.05 < PF < 2K
C5	0.1 < GF < 160	0.05 < PF < 140
R6	0.05 < GF < 60	0.9 < PF < 70
C6	0.01 < GF < 2K	0.05 < PF < 100
R7	0.03 < GF < 20	0.9 < PF < 18
C7	0.01 < GF < 4.0	0.2 < PF < 6.0
R8	0.18 < GF < 4.0	0.12 < PF < 3.0
C8	0.01 < GF < 2.0	0.05 < PF < 4.0
R9	0.01 < GF < 0.9	0.05 < PF < 0.64
C9	0.01 < GF < 0.6	0.01 < PF < 0.3
Cell 1	0.01 < GF < 10K	300 < PF < 10K
Cell 2	10 < GF < 10K	80 < PF < 1.4K
Cell 3	1.0 < GF < 4K	620 < PF < 10K

Table 5 (cont)		
Cell 4	0.1 < GF < 1K	100 < PF < 1.2K
Cell 5	0.09 < GF < 500	21 < PF < 200
Cell 6	0.8 < GF < 100	0.25 < PF < 82
Cell 7	0.05 < GF < 800	0.3 < PF < 62
Cell 8	0.01 < GF < 60	0.025 < PF < 82˙
Cell 9	0.01 < GF < 5.0	0.05 < PF < 52

Analysis of the Experimental Data Recorded with the LeCroy Digital Storage Oscilloscope.

This portion of the analysis focuses on the experimental data recorded using the LeCroy digital storage oscilloscope. Since the design criteria is specified by bode plot parameters, the circuits' performances are analyzed and compared using the bode plot data. The metric used to accomplish the comparison was a conventional point-by-point percent error analysis. That is,

$$E = ((\ I - T\ )/I\ ) \times 100 \ \%\ \tag{26}$$

where,

I = ideal (calculated) value

T = experimentally measured value, and

E = percent error.

The gain data for each circuit is presented in Figures 47 through 54 (Oldham discrete, Oldham hybrid, Oldfield discrete and Oldfield surface mount, respectively). The corresponding phase data is displayed in Figures 55 through 58.

The gain data were initially compared on a point-by-point basis. However, the gain criteria was not a single-valued parameter (Chapter 1, Scope section). That is, the gain design criteria is actually a rate of change parameter. Hence, the discrete error values involving a point-by-point comparison could be misleading. Consequently, a different metric was be developed to compare the gain responses. The metric chosen was a comparison of the slopes of the actual experimental response versus the ideal design slope parameter. The slope calculated from the experimental data was determined using a weighted average:

$$S = \frac{(DP_{i+10} - DP_i)}{(1 \; Decade)} \qquad (27)$$

where

        DPi   = a data point (in dB)

        $DP_{i\pm10}$ = a data point one decade larger or less

                (as measured along the frequency axis)

                (in dB) and,

        S   = the calculated slope (dB/decade).

Then, Equation 26 was utilized to perform the error
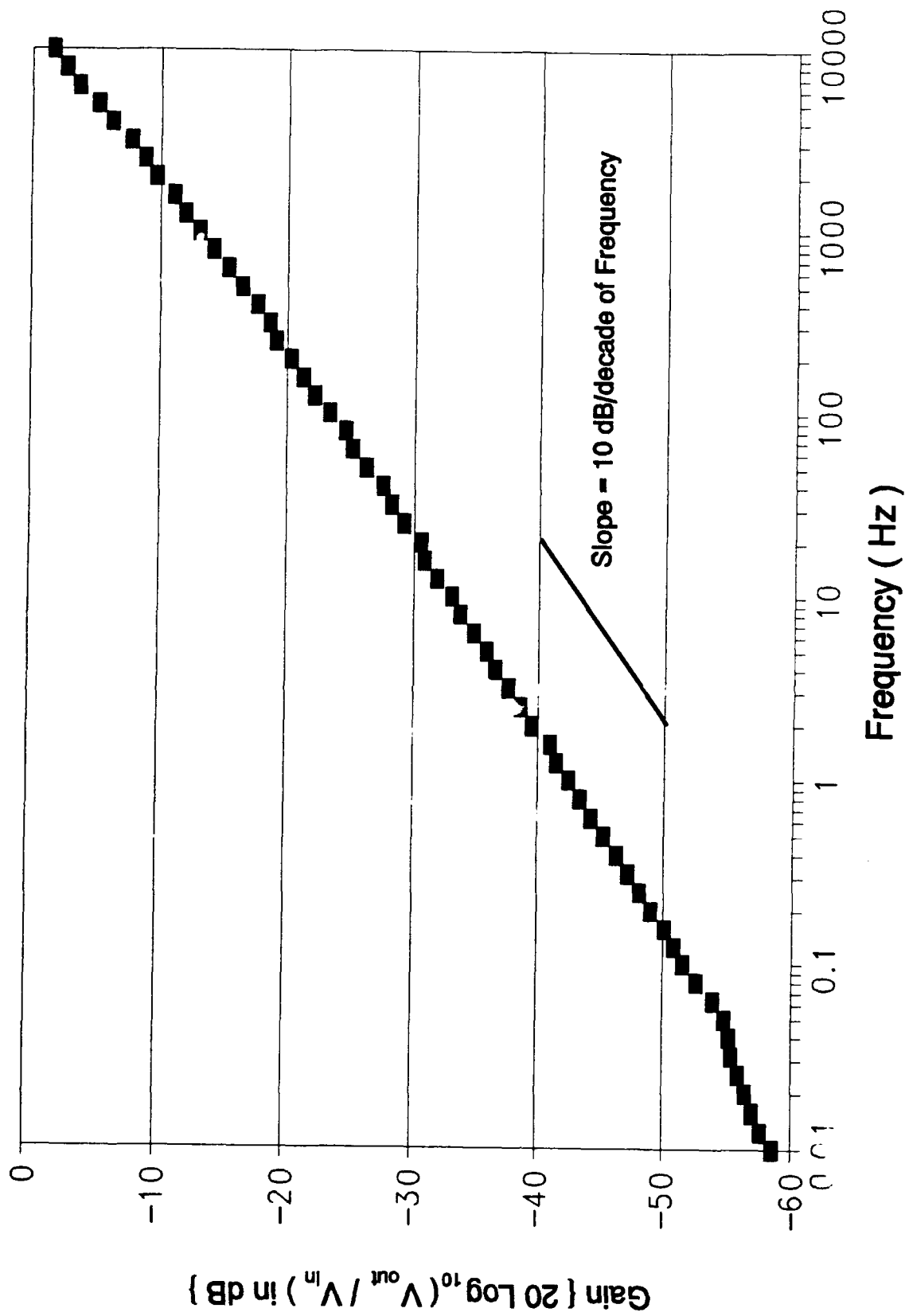
Figure 47. Oldham Circuit Discrete Component Gain Response.

The figure plots Gain { 20 Log_{10} (V_{out} / V_{in}) in dB } on the vertical axis versus Frequency (Hz) on the horizontal axis. A reference line is marked: Slope = 10 dB/decade of Frequency.
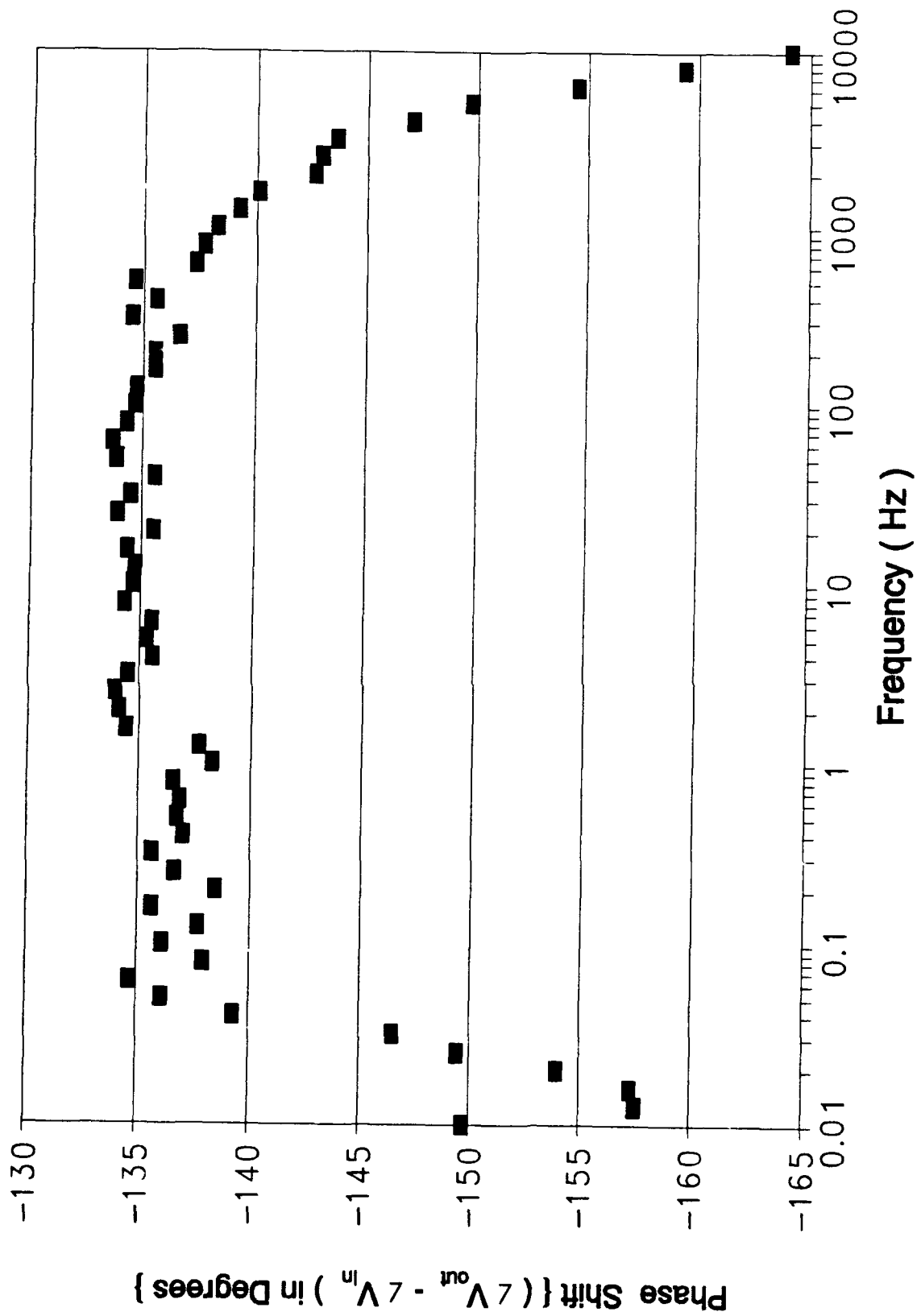
Figure 48. Oldham Circuit Discrete Component Phase Response.
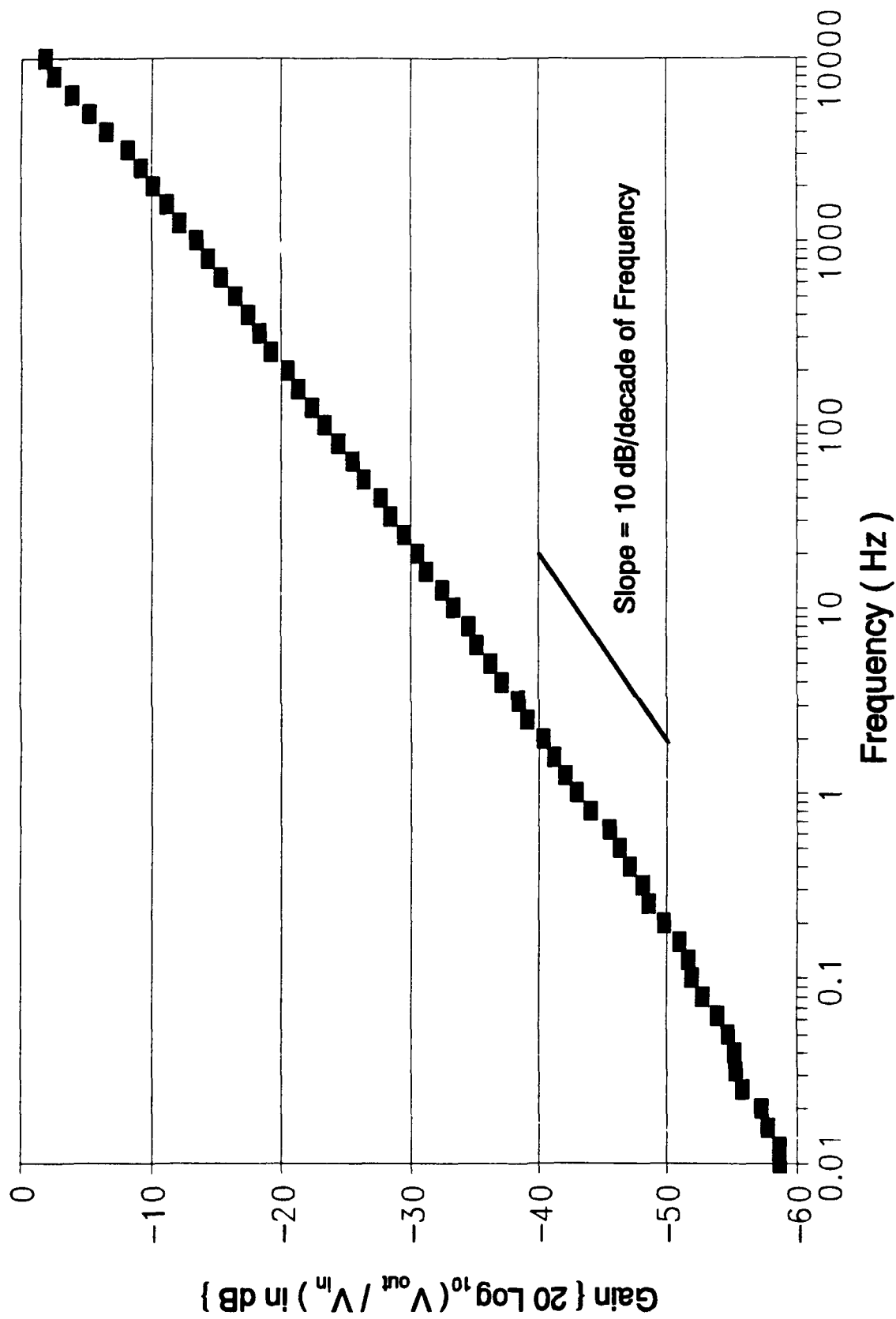
Figure 49. Oldham Circuit Hybrid Component Gain Response.

Slope = 10 dB/decade of Frequency

Frequency (Hz)

Gain { 20 Log₁₀(Vₒᵤₜ / Vᵢₙ) in dB }
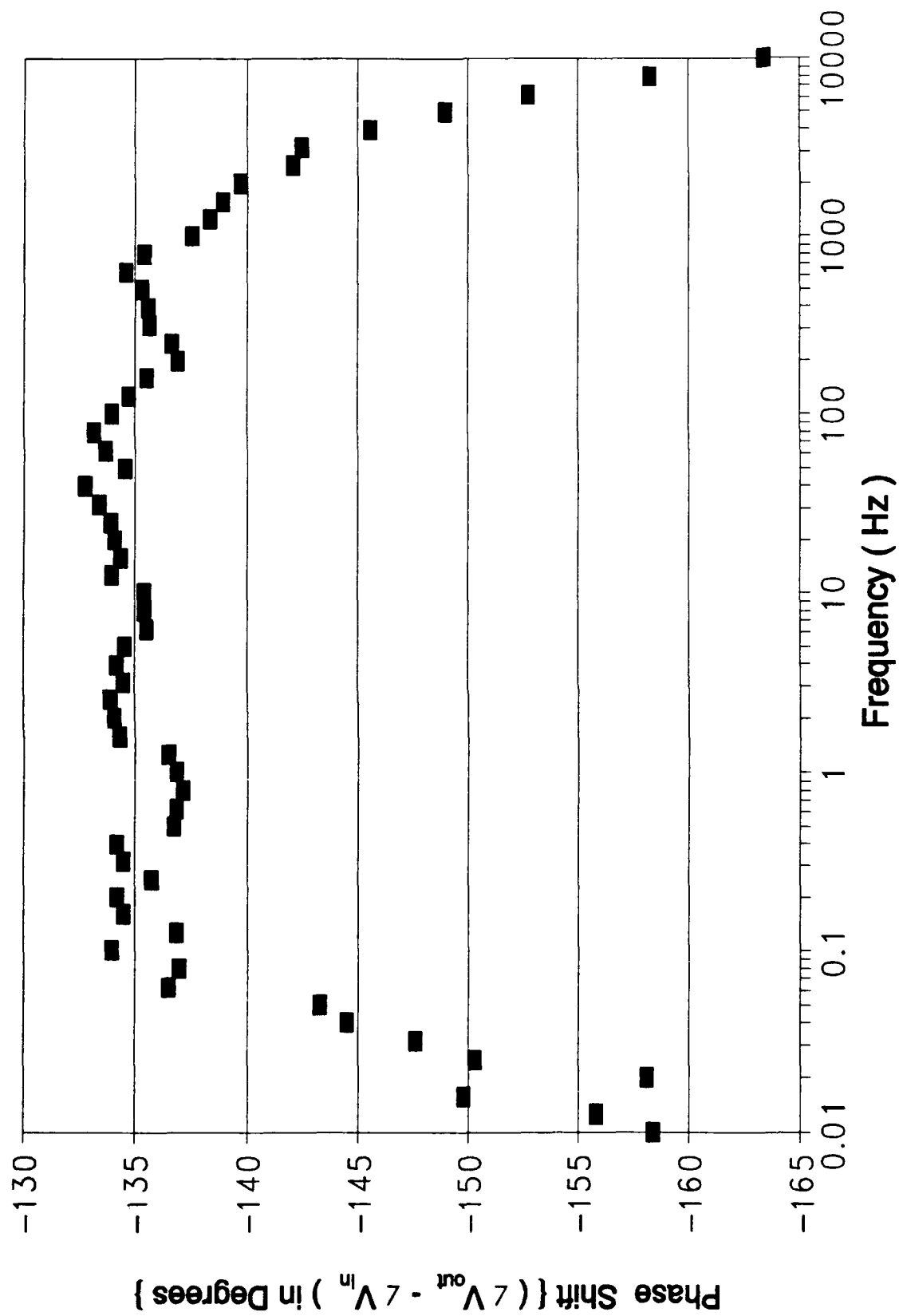
Figure 50. Oldham Circuit Hybrid Component Phase Response.
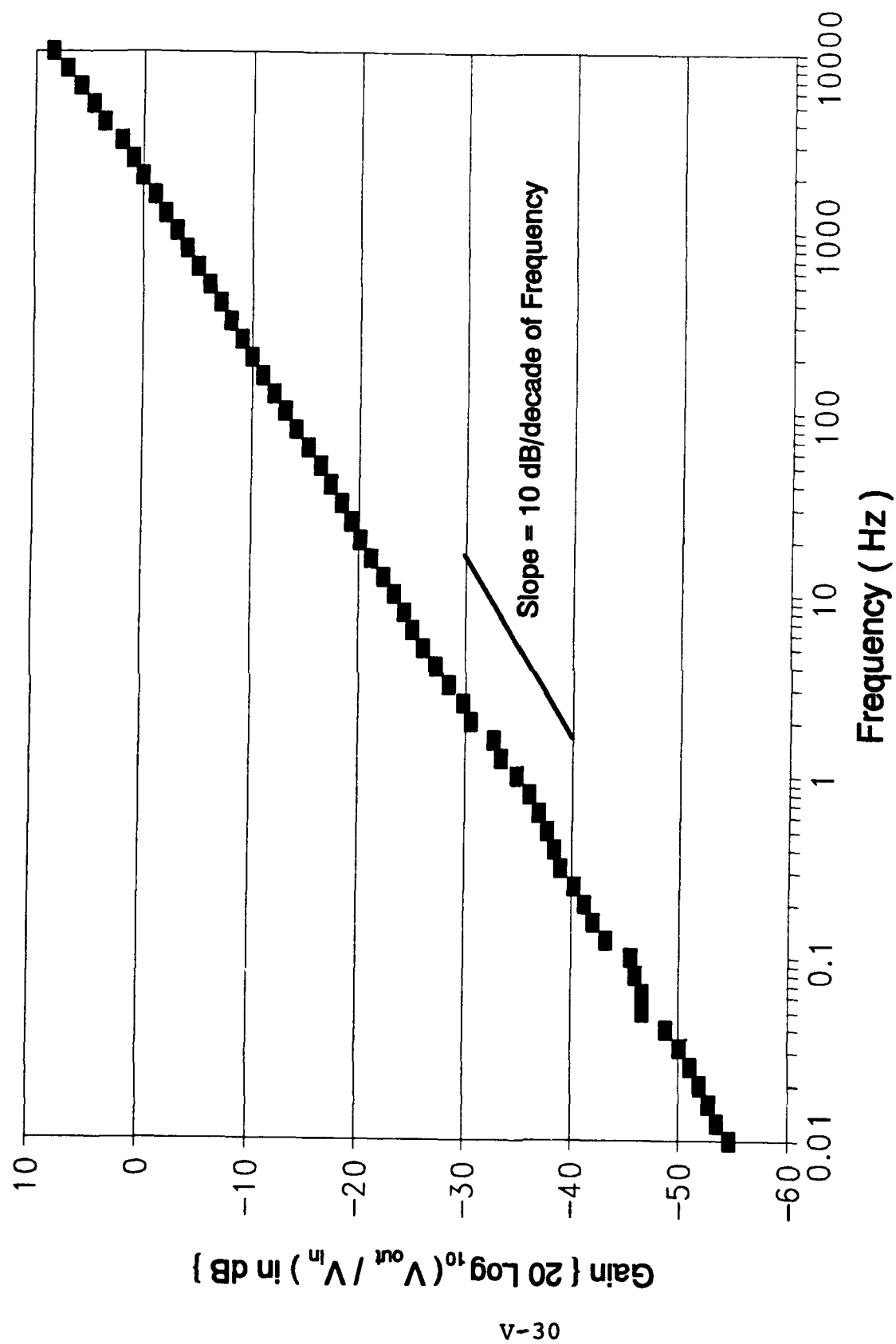
Figure 51. Oldfield Circuit Discrete Component Gain Response.
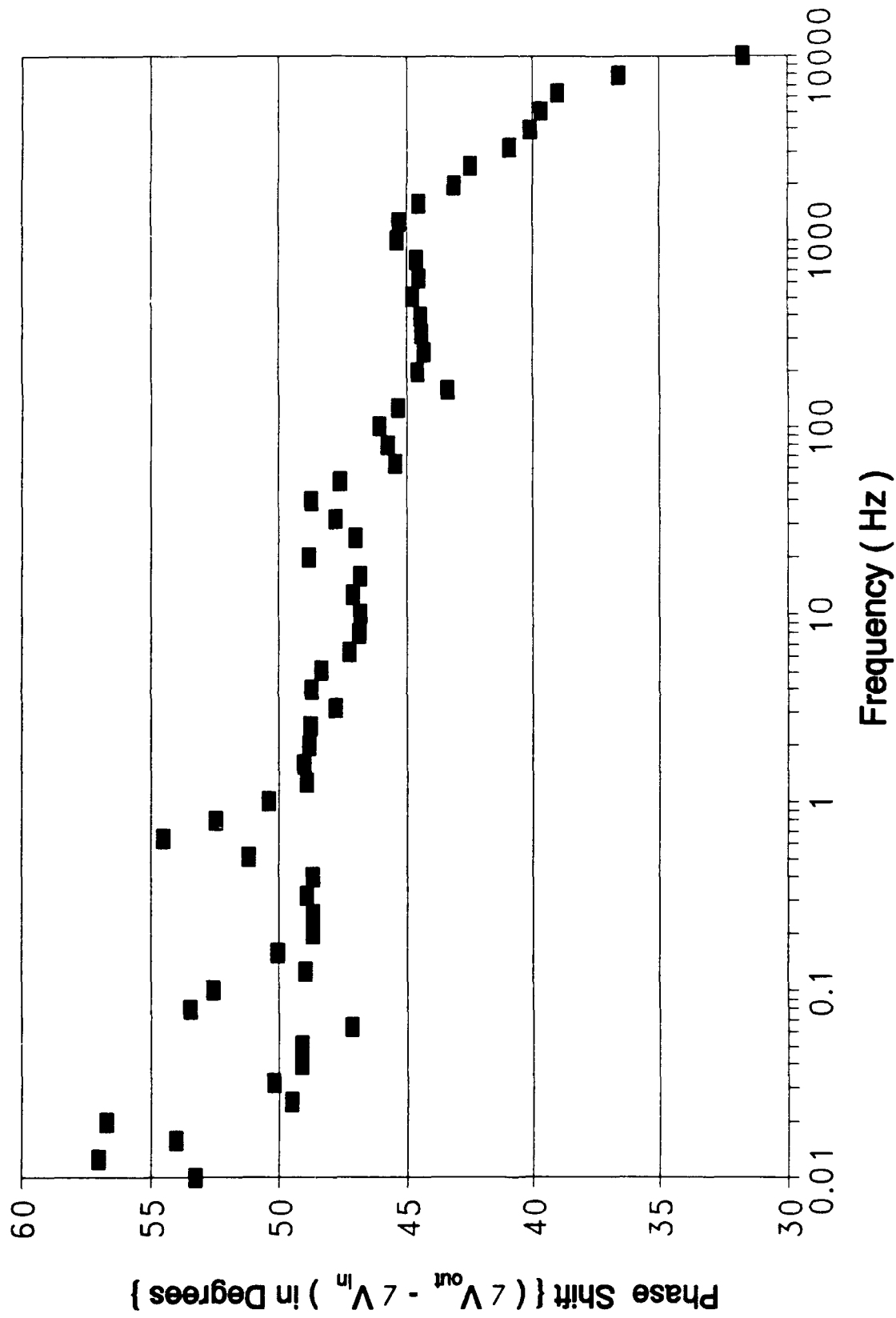
Figure 52. Oldfield Circuit Discrete Component Phase Response.
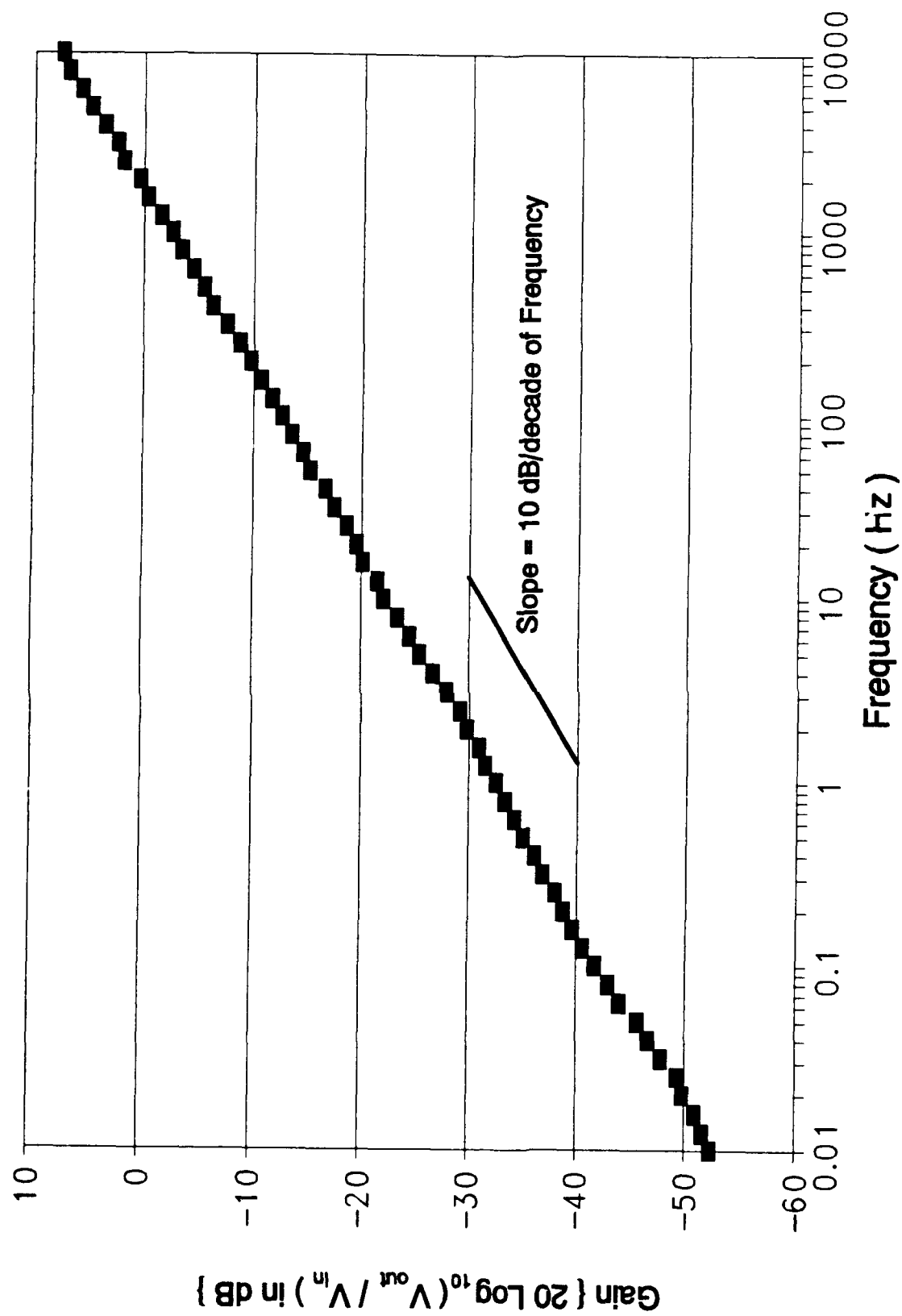
Figure 53. Oldfield Circuit Surface Mount Component Gain Response.

Slope = 10 dB/decade of Frequency

Gain { 20 Log$_{10}$ (V$_{out}$ / V$_{in}$) in dB }

Frequency (Hz)
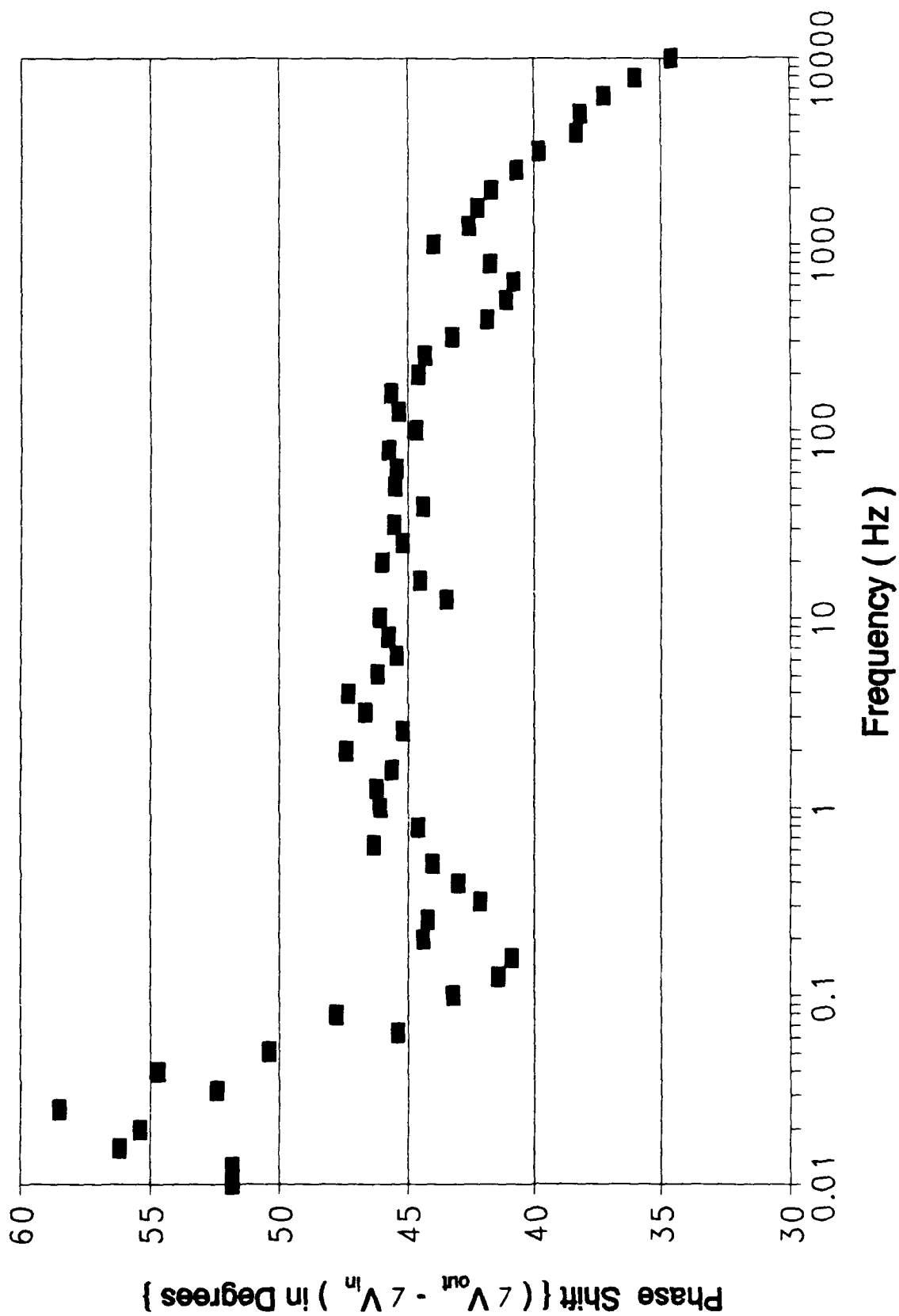
Figure 54. Oldfield Circuit Surface Mount Component Phase Response.
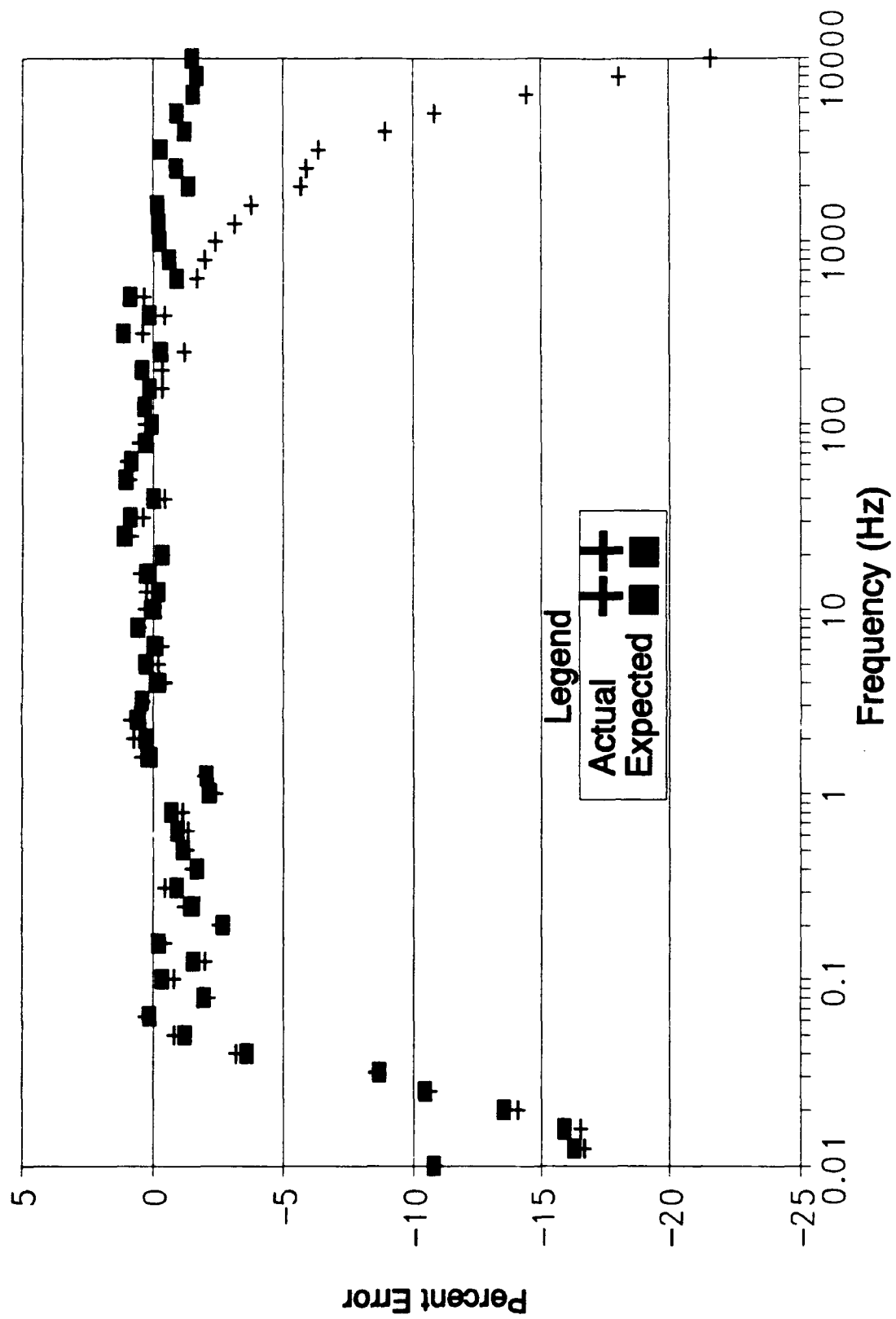
Figure 55.   Oldham Circuit Discrete Component Phase Shift Error.
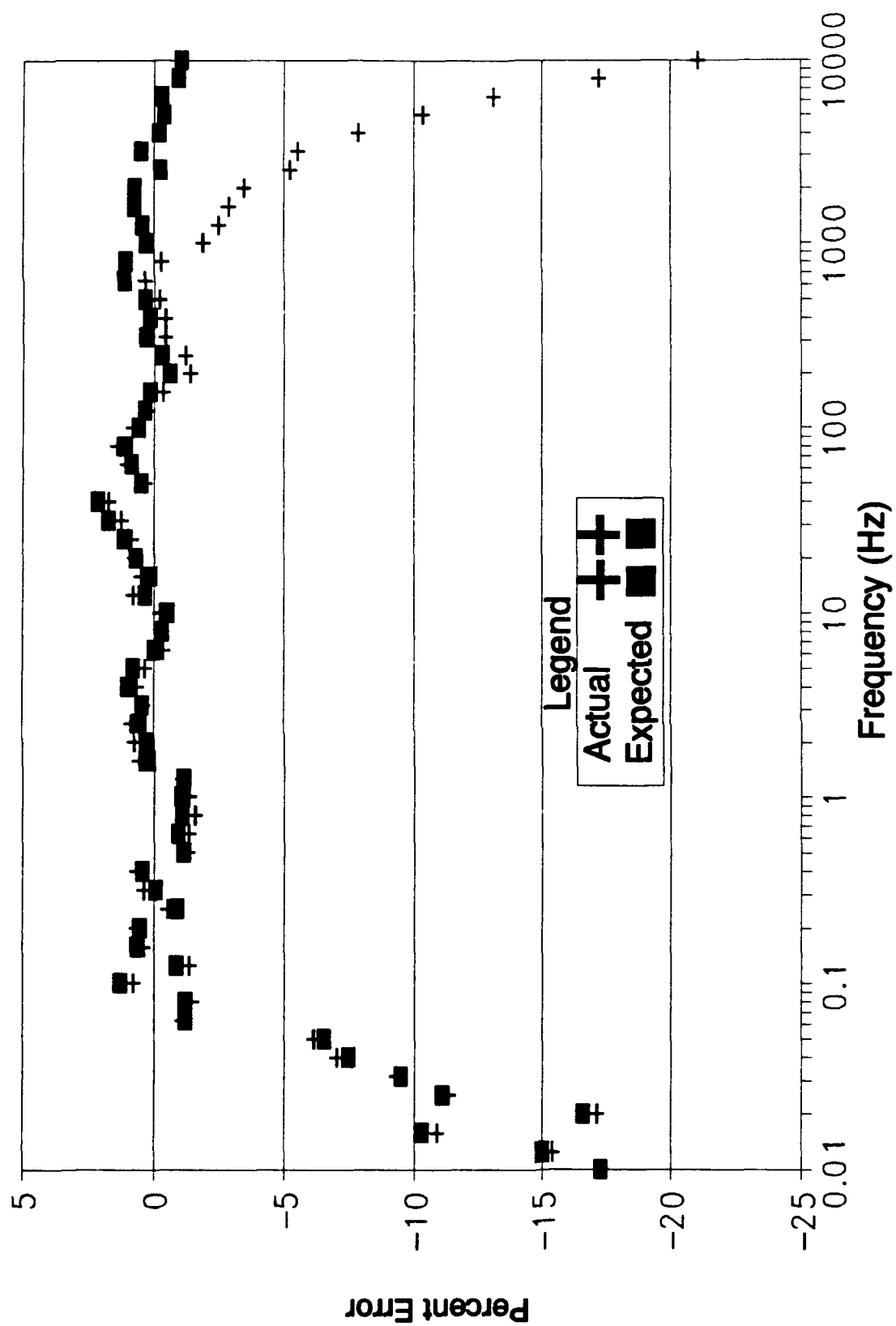
Figure 56. Oldham Circuit Hybrid Component Phase Shift Error.
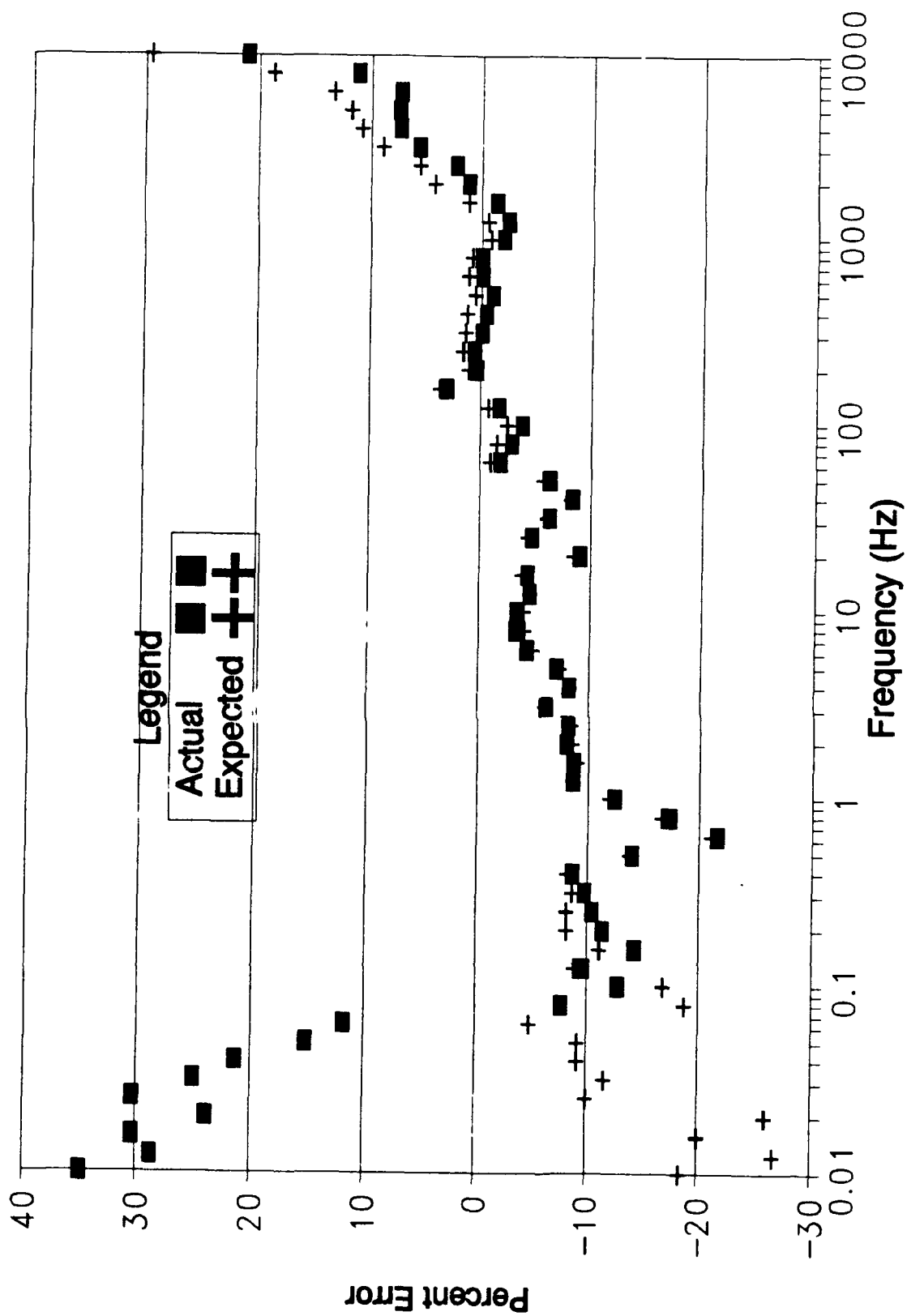
Figure 57. Oldfield Circuit Discrete Component Phase Shift Error.
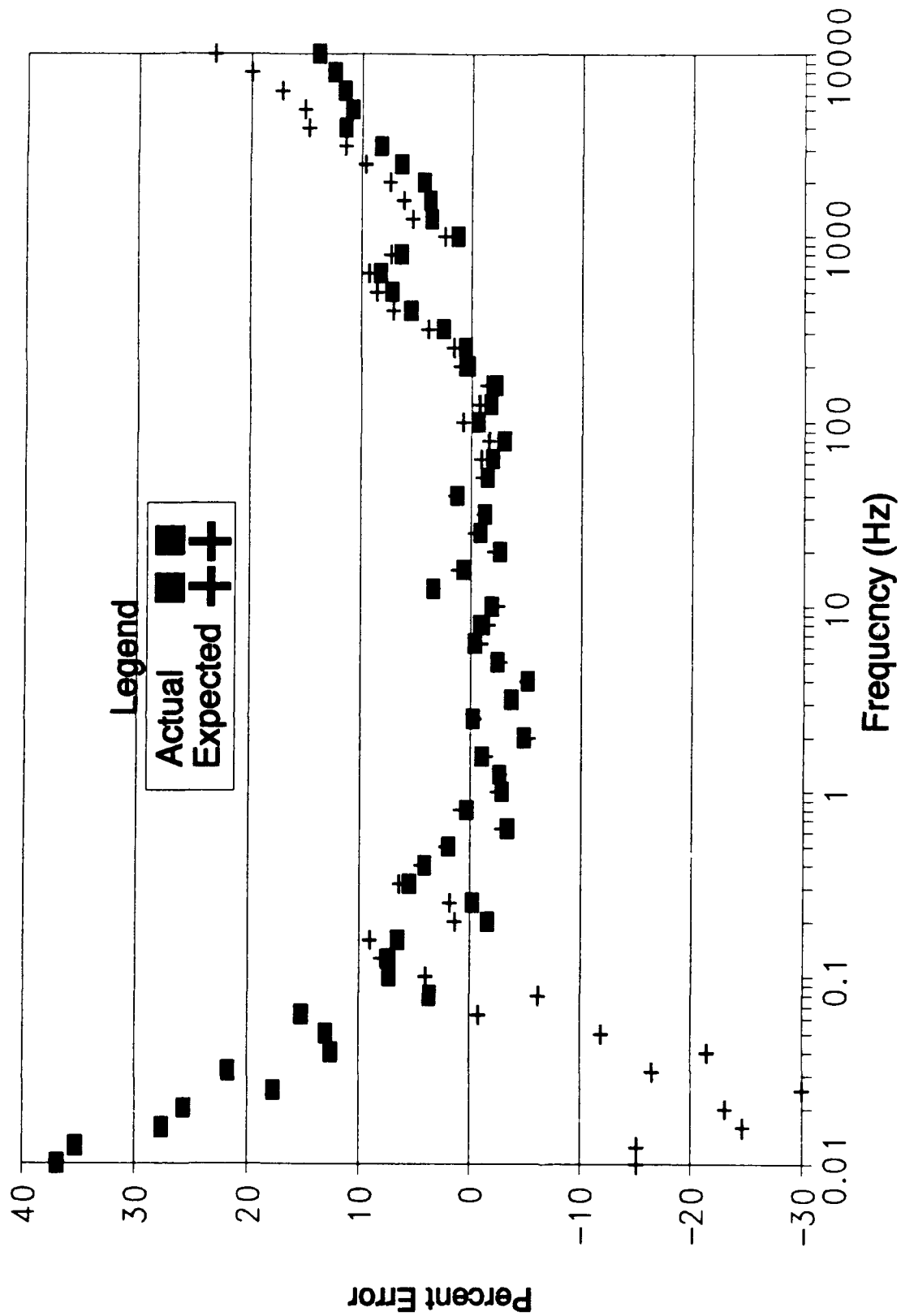
Figure 58. Oldfield Circuit Surface Mount Component Phase Shift Error.

analysis on the slope data. The results are portrayed in Figures 59 through 62.

The error analysis and experimental gain and phase data provided a means for evaluating the four circuits based upon their performance versus the ideal expectations. Each circuit variant was evaluated based upon the frequency interval over which it satisfies the design specifications (Chapter 1, Scope section).

Oldham Discrete Component Circuit. The Oldham discrete component circuit's phase shift response exceeded the design expectations (Figure 55). Consequently, the frequency range was extended from 1925 Hz to 10 KHz. In contrast, the gain (reported as the slope) response (Figure 59) frequency range was less than expected. Specifically, the slope deviated relative to the design specifications over the intervals 0.01 Hz to 0.05 Hz, 2 Hz to 2.8 Hz, and from 3 KHz to 10 KHz.

Oldham Hybrid Component Circuit. The Oldham hybrid component circuit's phase shift response exceeded the design expectations (Figure 56). Consequently, the frequency range was similarly extended from 1925 Hz to 10 KHz. The gain (reported as the slope) response (Figure 60) was less than expected, but it also represented an improvement relative to the discrete component circuit variant. Specifically, the slope deviated from the expected and design criteria over the frequency intervals 0.01 Hz to
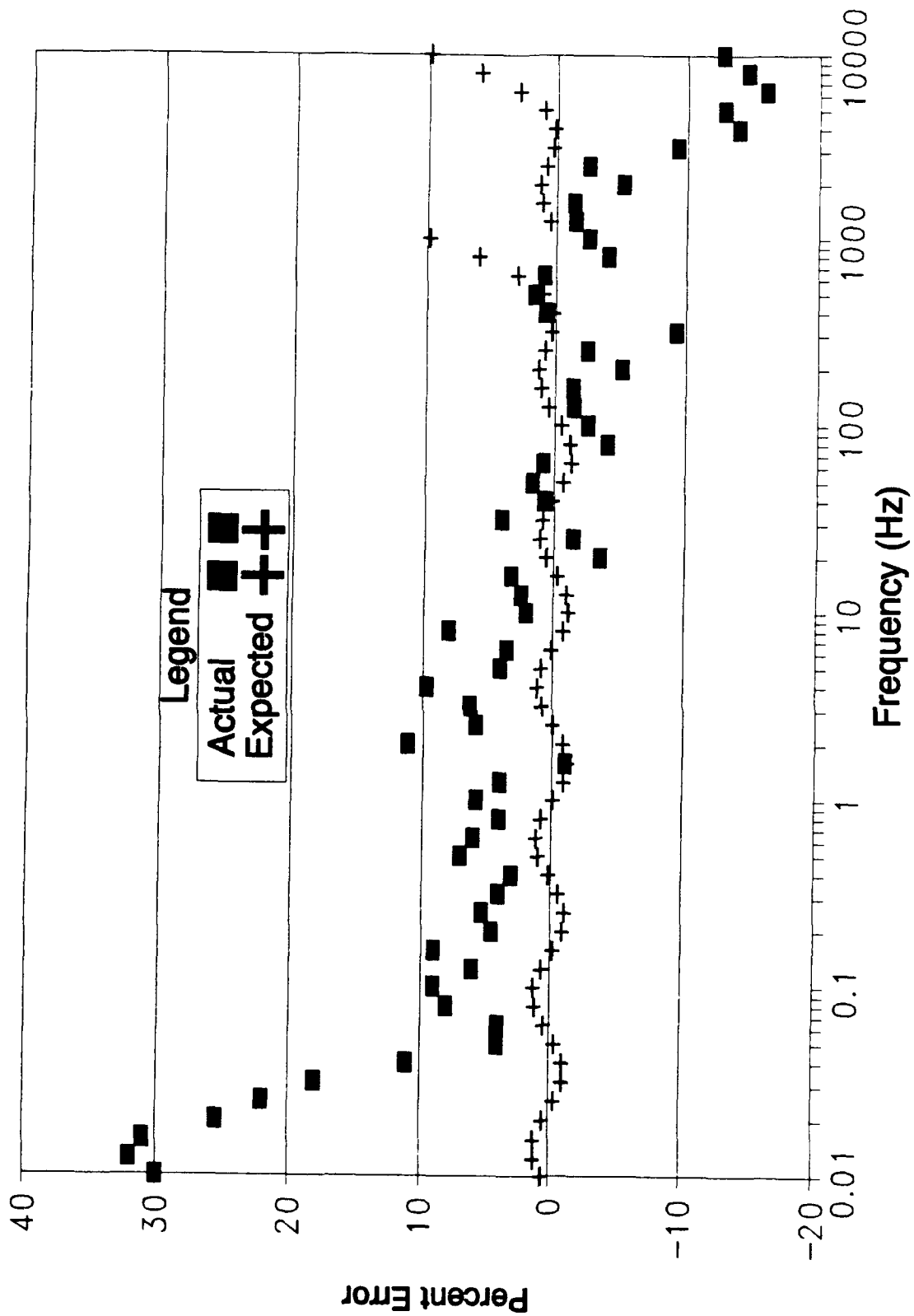
Figure 59.   Oldham Circuit Discrete Component Gain Slope Error.
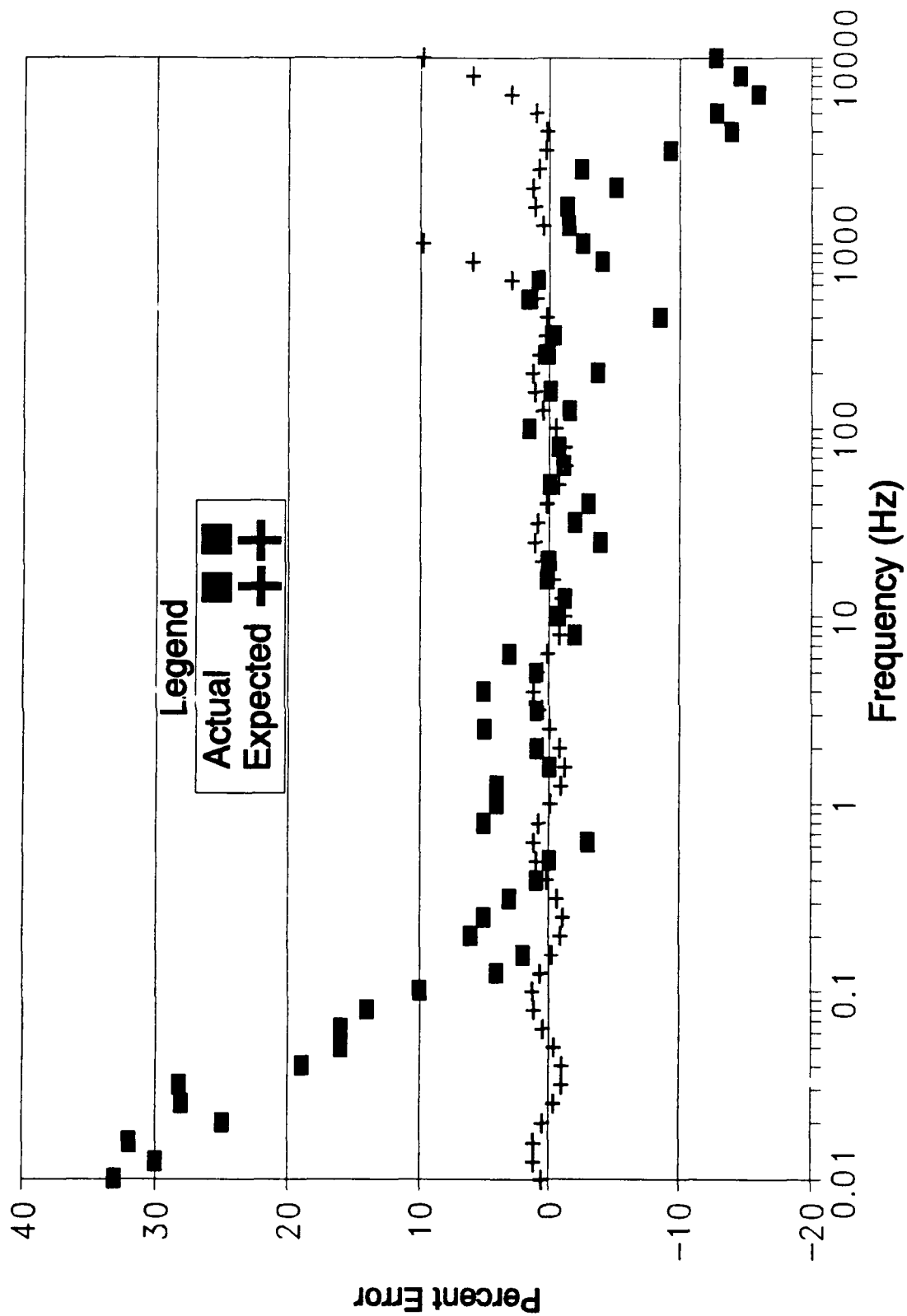
Figure 60. Oldham Circuit Hybrid Component Gain Slope Error.
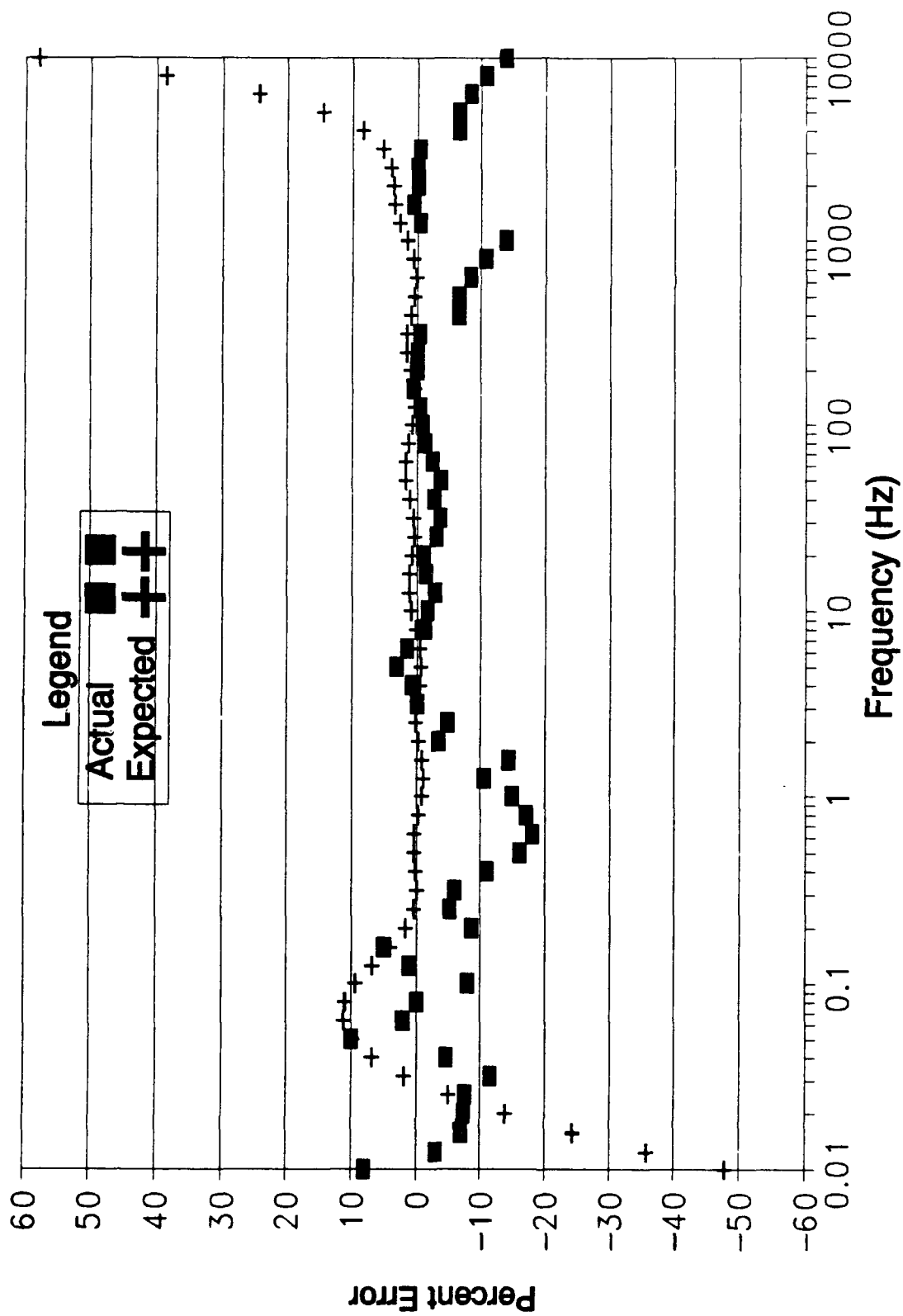
Figure 61. Oldfield Circuit Discrete Component Gain Slope Error.
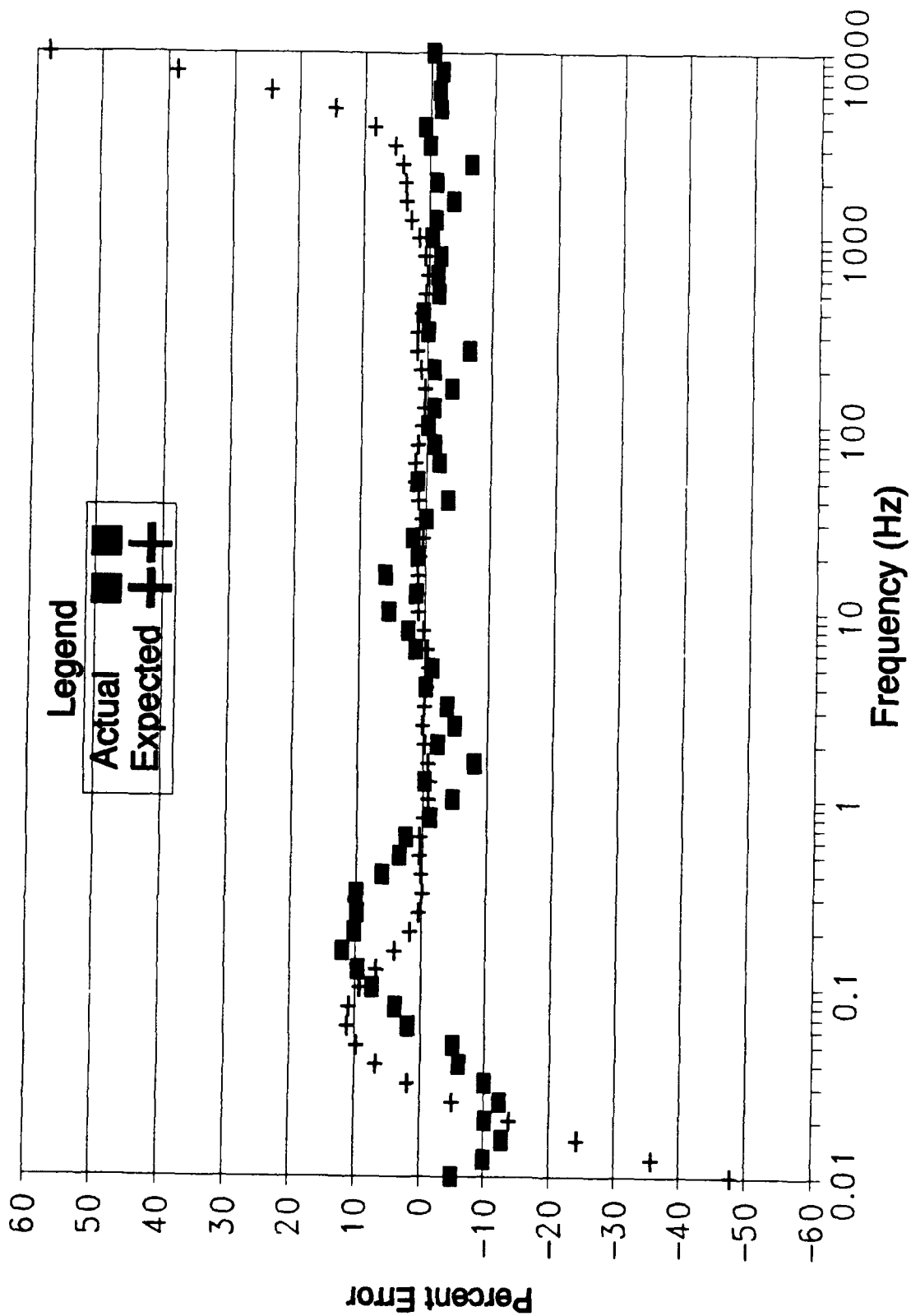
Figure 62. Oldfield Circuit Surface Mount Component Gain Slope Error

0.1 Hz and from 2.1 KHz to 10 KHz.

Oldfield Discrete Component Circuit. The Oldfield discrete component circuit's phase shift response performed as expected over the frequency interval 0.5 Hz to 10 KHz (Figure 57), but, it deviated from the expected and design specifications over the interval 0.01 Hz to 0.69 Hz. The gain (reported as the slope) response (Figure 61) deviated from the expected and ideal conditions relative to specific frequency intervals. The frequency intervals where the design specifications were not satisfied spanned 0.02 Hz to 0.03 Hz, 0.05 Hz to 2.6 Hz, 1 KHz to 1.2 KHz, and from 9 KHz to 10 KHz.

Oldfield Surface Mount Component Circuit. The Oldfield surface mount component circuit's phase shift response performed as expected from 0.1 Hz to 1 KHz (Figure 58). However, the circuit's phase shift response did not satisfy the design specifications over the frequency interval 0.01 Hz to 0.06 Hz. The gain (reported as the slope) response (Figure 62) exceeded the design expectations over the frequency interval 1.2 KHz to 10 KHz, but it did not satisfy the design specifications from 0.012 Hz to 0.05 Hz and from 0.02 Hz to 0.05 Hz.

Analysis of the Experimental Data Recorded with the B & K Spectrum Analyzer

This section of the analysis focuses on the experimental data recorded using the B & K spectrum

analyzer. The bode plot data, displayed in Appendix J, verifies the data recorded on the LeCroy digital storage oscilloscope with only minor deviations (since graphical data could only be obtained from the B & K spectrum analyzer, only a relative comparison and verification was accomplished).

The Nichols plots display the frequency, phase shift, and gain in a different format (Appendix H). The Nichols plots also verify the experimental data collected with the LeCroy digital storage oscilloscope. Specifically, the experimental data demonstrates an excellent correlation at the lower frequencies where the performance of all four circuit variants was severely degraded. However, at the higher frequencies (1 Hz to 10 KHz), the Nichols plots show that all four circuits are stable.

The spectral analysis accomplished with the B & K spectrum analyzer also served to reinforce the weakness of the four circuit variants at the lower frequencies. The data from the spectral plots is displayed in a different format in Figures 63 through 66. The signal amplitude (dB) is plotted versus frequency along the highest "noise" peak signal from the spectrum graph. In each case, the noise is greatest at the lower frequencies. Specifically, the spectral plots reveal that the effective frequency range (noise more than 10 dB below the signal) for each circuit is approximately 0.5 Hz to 10 KHz.
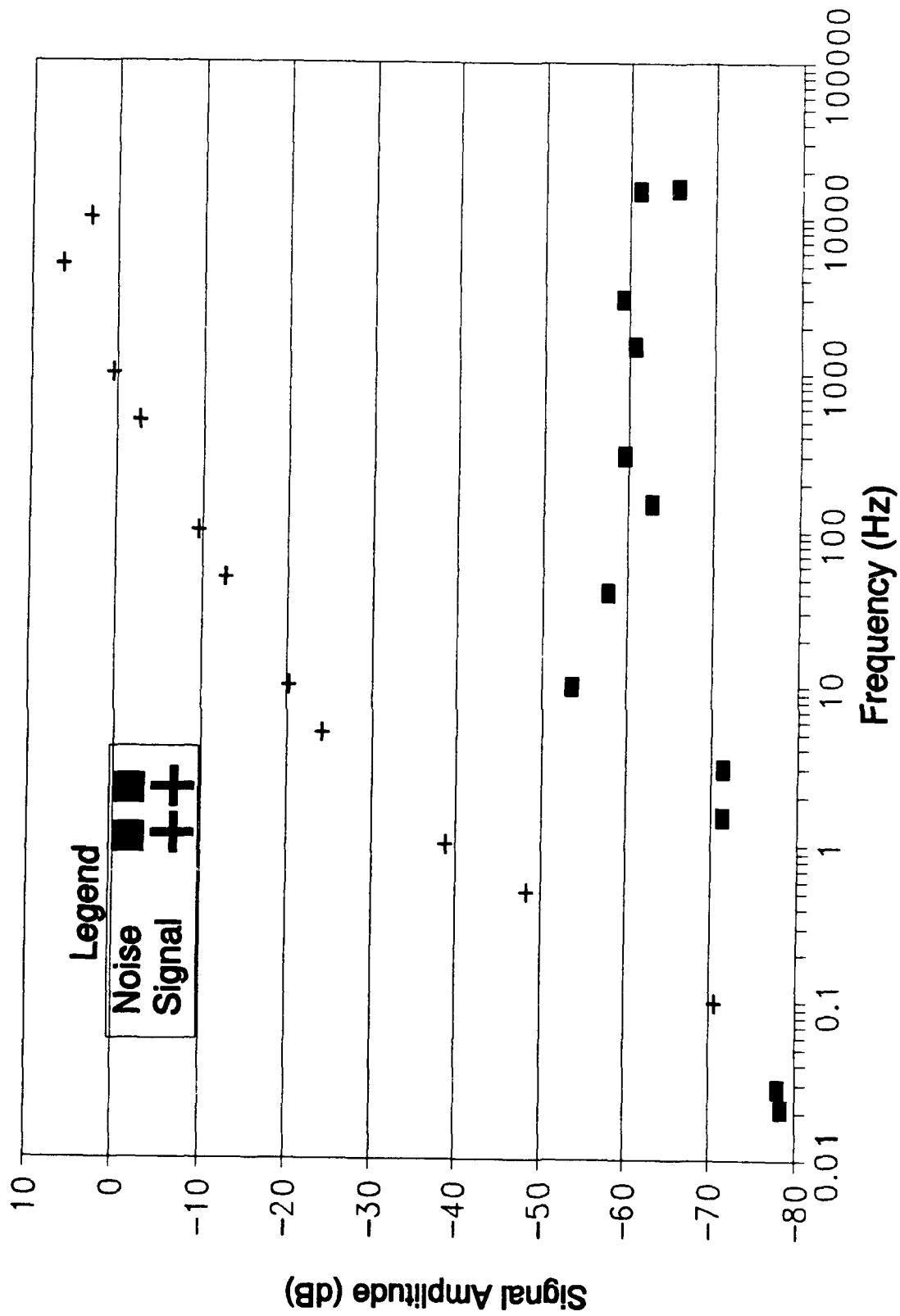
Figure 63. Signal and Noise Responses the for Oldham Discrete Component Circuit.
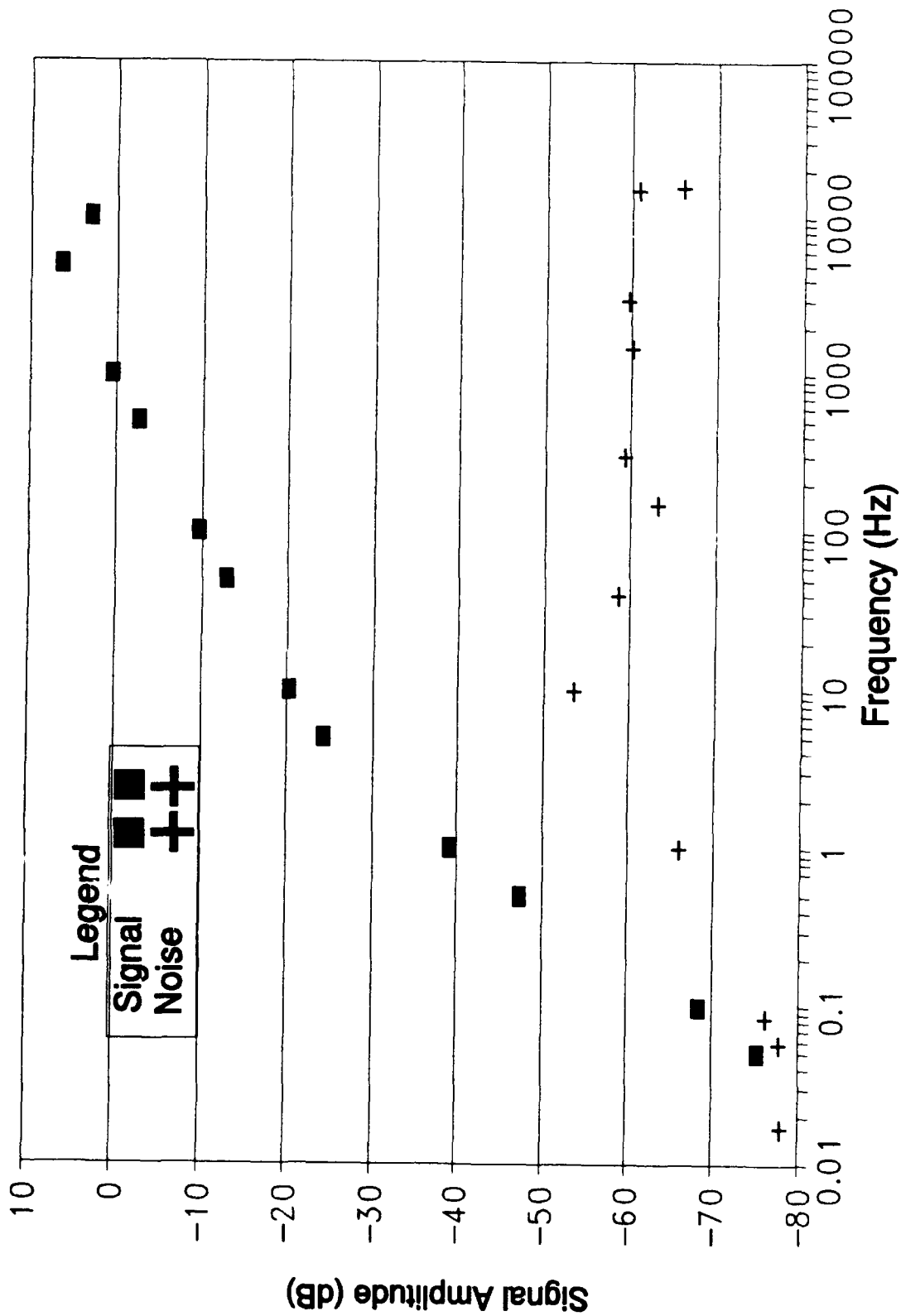
Figure 64. Signal and Noise Responses for the Oldham Hybrid Component Circuit.
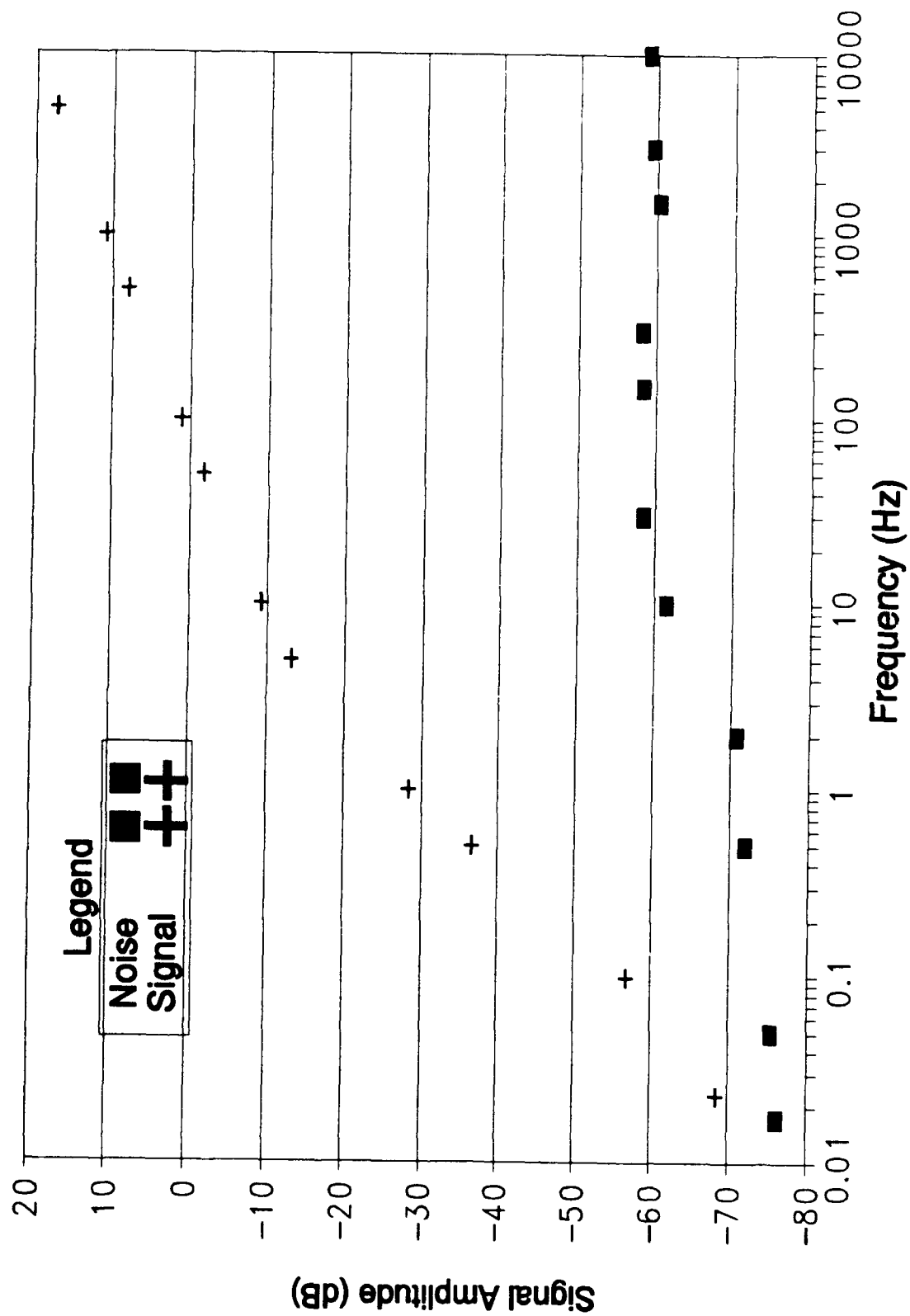
Figure 65. Signal and Noise Responses for the Oldfield Discrete Component Circuit.
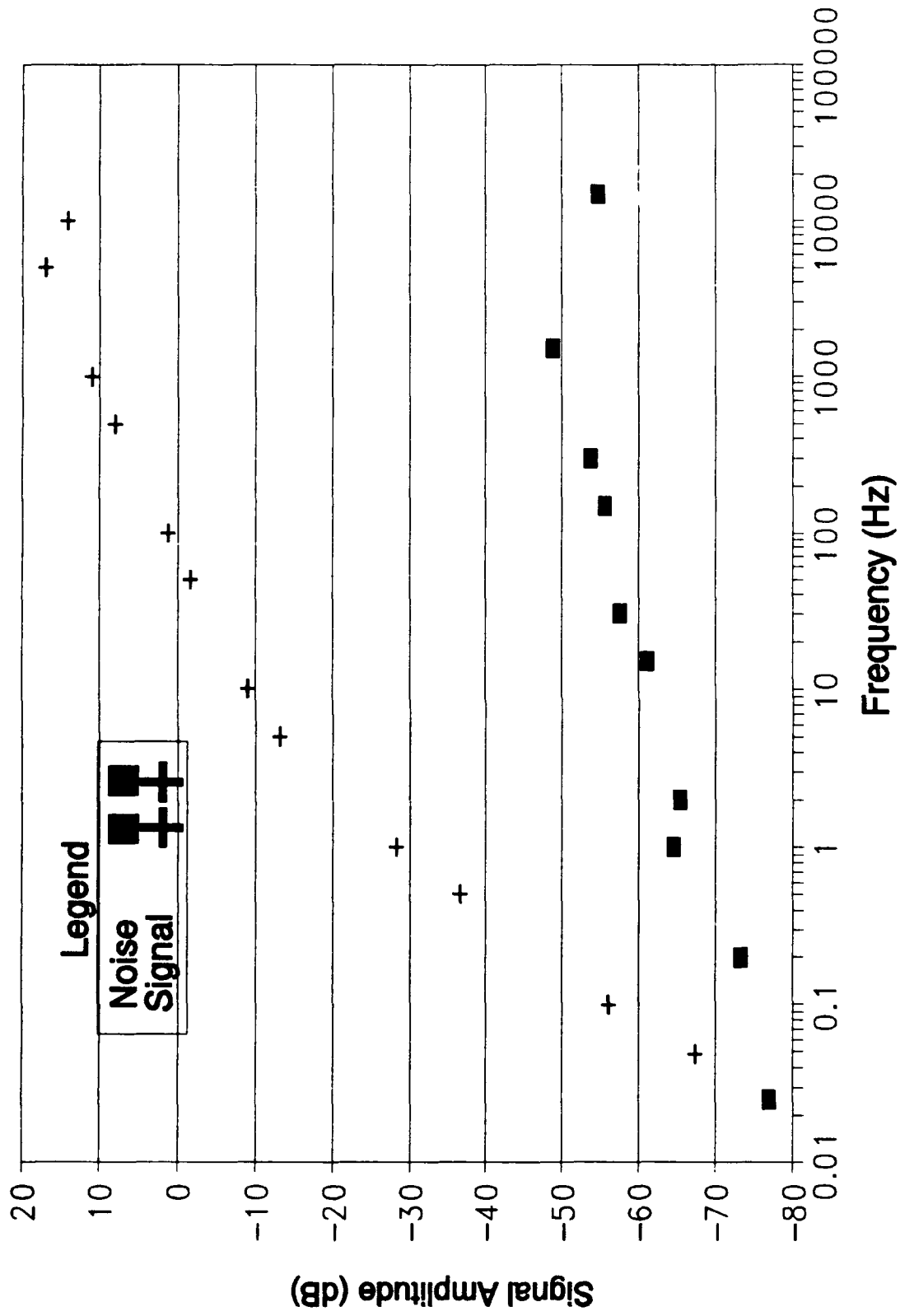
Figure 66. Signal and Noise Responses for the Oldfield Surface Mount Component Circuit.

VI. Conclusions And Recommendations

This portion of the research effort describes the significant conclusions, and the circuit and design rankings and recommendations for further research.

Conclusions

The conclusions that can be inferred from the experimental data are discussed first. No single set of data can be utilized to evaluate the overall performance of each circuit variant. The actual performance criteria has been documented in the preceding chapters. However, a subjective ranking of the circuits is presented based upon this research experience and the design specifications. That is, the circuit that satisfied both the gain and phase specifications for the largest frequency span will be ranked first, and so on.

Under these test conditions and component availability, the Oldham circuit design outperformed the Oldfield circuit design. Both the Oldham discrete component circuit and the Oldham hybrid component circuit manifested greater frequency ranges over which they satisfied the design criteria (Oldham discrete component circuit--0.05 Hz to 1.9 KHz; Oldham hybrid circuit component--0.08 Hz to 2.0 KKz). The computer simulation performance analysis also revealed that the Oldham circuit design was more robust and allowed its component values to have greater deviations relative to the

"ideal" values. The performance of the circuit variants are ranked below relative to the frequency interval over which the design criteria was satisfied.

Circuit #1. The circuit that performed the best of the four was the Oldham hybrid component variant which possessed a useful frequency range spanning 0.08 Hz to 2.0 KHz.

Circuit #2. The Oldham discrete component circuit possessed a similar operational frequency performance interval (0.05 Hz to 1.9 KHz) and phase error (Figure 55 and Figure 56), but the margin of error relative to the ideal gain (slope) was greater than the hybrid design. That is, the Oldham hybrid component variant exhibited a slope error of less than 8.5 percent over the entire interval of design criteria compliance (except endpoints, where it was 10 percent; the 8.5 percent error only occurred at 298 Hz; otherwise the error (slope) was less than 6 percent), but, the Oldham discrete component variant exhibited regions (0.09 Hz to 0.2 Hz, 2 Hz to 10 Hz, and 200 Hz to 300 Hz) in the frequency interval that pushed the design limit of a 10 percent error.

Circuit #3. The Oldfield surface mount component circuit variant performed the best of the Oldfield designs, and it possessed a useable frequency interval that spanned 0.5 Hz to 2.2 KHz.

Circuit #4. The Oldfield discrete circuit variant had the smallest operating frequency range (2.4 Hz to 1 KHz) and

the largest errors over that range. That is, the slope error was similar to that of the Oldfield surface mount component circuit (Figure 61 and Figure 62), but the phase error manifested significant differences. Specifically, over the frequency interval 2.0 Hz to 50 Hz, where the slope error ranged from a low of 4 percent to a high of 9 percent. In contrast, the Oldfield surface mount component slope error over the same interval was always less than 5 percent.

The effect of circuit implementation technology can not be determined from the experimental data measured in this research effort. Although both the surface mount and hybrid designs outperformed the respective discrete component designs, the data would be expected to be biased in that direction because of the higher quality components that were available from the hybrid and surface mount technology component vendors. Also, even though the VLSI chips could not be utilized in this circuit application, the wide variation (all components exhibited greater than a $\pm$ 20 percent deviation relative to the ideal design values) in component values that were measured suggests that the digitally-oriented VLSI technology is not compatible with precision analog circuit designs at this time.

Recommendations

Several techniques for circuit performance improvement became evident during the design and fabrication efforts of this research.

First, the Oldfield design technique affords an additional component sorting and selection step. This process involves measuring the capacitor values and using those values in the design equations (Chapter 2) to determine the resistor values [2]. When this process is utilized, the circuit's performance can be significantly improved.

Second, the operational amplifier used in this effort was a general purpose operational amplifier (ALM-741). Circuit performance could be improved by utilizing a low-noise operational amplifier that is better suited for the specific needs of the circuit design (e.g., AN-357).

Third, the Oldham circuit design equations facilitate the realization of any fractional-order differentiator. On the other hand, the Oldfield design was derived for a specific one-half order differentiator purpose, and it was used in heat transfer experiments. A mathematical development of the Oldfield design equations that would produce an arbitrary fractional-order differentiator is warranted.

Appendix A

Design Summary

for the

Low-Pass Filter

The following excerpt is from reference 14 and summarizes the Low-Pass filer design.

> ### Odd-Order Low-Pass Filter Design Summary.
> To design a first-order filter or a first-order stage of a higher odd-order filter having a given cutoff frequency f_c Hz (or $\omega_c = 2\pi f_c$ rad/s), gain K, and of Butterworth or Chebyshev type, perform the following steps.
>
> 1. Find the normalized coefficient C for the first-order stage from the appropriate table of Appendix A;
> 2. Select a standard value of C_1 (preferably near $10/f_c$ μF);
> 3. (a) If K > 1, use the circuit of Fig. 2-20(a) with resistance values given by

$$R_1 = \frac{1}{\omega_c C_1 C}$$

$$R_2 = \frac{KR_1}{K-1}$$

$$R_3 = KR_1.$$

> (b) If K = 1, use the circuit of Fig. 2-20(b) with R_1 as given in 3(a);
> 4. The second-order stages of the odd-order filter may be constructed as indicated in Section 2-10, 2-11, or 2-12, and cascaded with the first-order section to form the filter.

Figure A-1 and Figure A-2 are "Fig. 2-20(a)" and "Fig. 2-20(b)" redrawn for clarity.
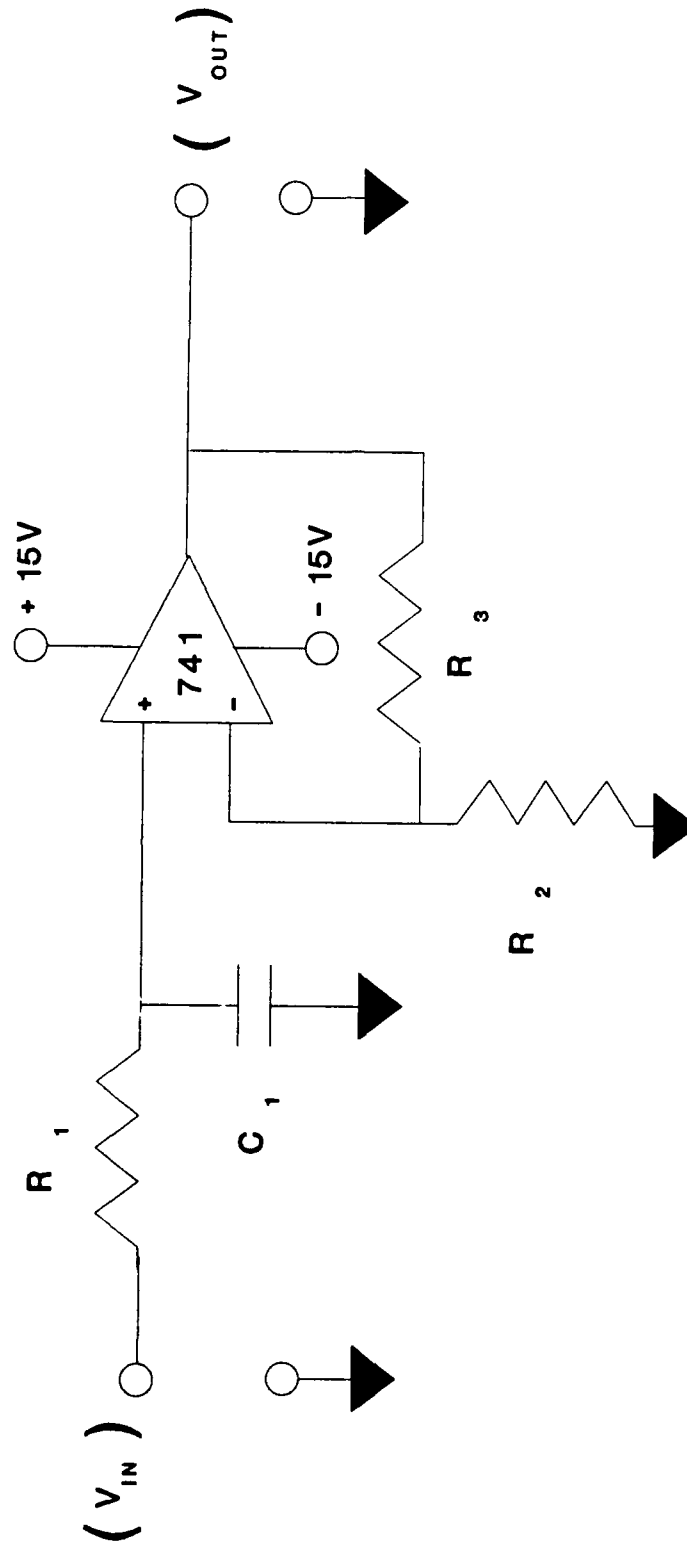
Figure A-1. Circuit Design of a Low-Pass Filter With Amplification [14].
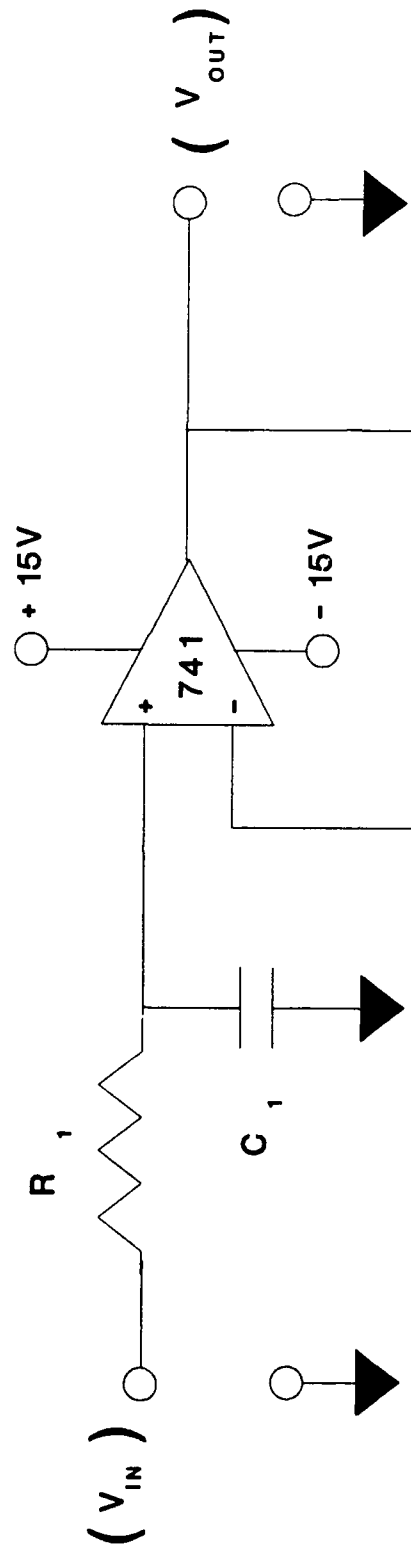
Figure A-2. Circuit Design of a Low-Pass Filter Without Amplification [14].

Appendix B

Oldham Circuit

Computer Simulation

Results

The computer simulation results for the Oldham circuit design are presented in this appendix. The results are documented in four sections. The first three sections document the systematic variation of the component values, and Section 4 displays the HSPICE simulation deck. Section 1 documents the effect on the circuit's response when each component is varied from its "ideal" value with the other component values held constant (at their "ideal" values). Section 2 summarizes the effect on the circuit's response when each cell's component values (a resistor and capacitor pair) are varied with respect to their "ideal" values while holding the components in the other cells at their ideal (calculated) values (Table 1). Section 3 documents the effect on the circuit's performance when all of the component values are systematically varied by ± 20 percent. Finally, the baseline HSPICE deck for the Oldham circuit is presented.

Figure B-0 shows the relative position of each component and cell.
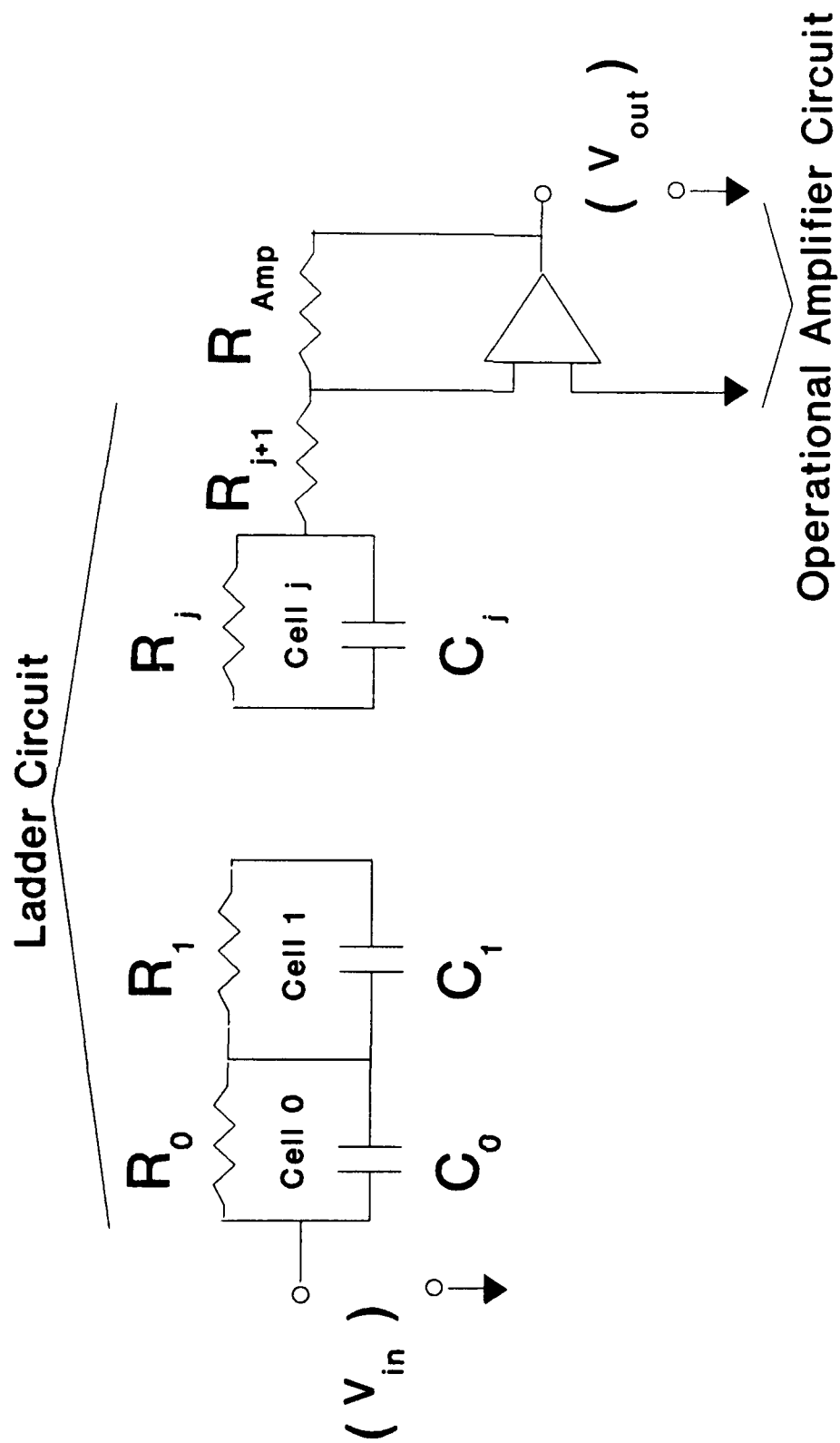
Figure B-0. Oldham Circuit Design Component and Cell Notation.

Section 1

Oldham Circuit Responses to Systematic
Resistor and Capacitor Value Variations

Resistor Values for Figure B-1						
Symbol	——	-+-	-*-	-□-	-x-	-▲-
Resis-tor Value (MΩ)	6.899	27.596	68.99 Ideal	110.38	137.98	344.95

Figure B-1. Graphical Symbol Legend and Resistor Value Correlation for Figure B-1 (cont);
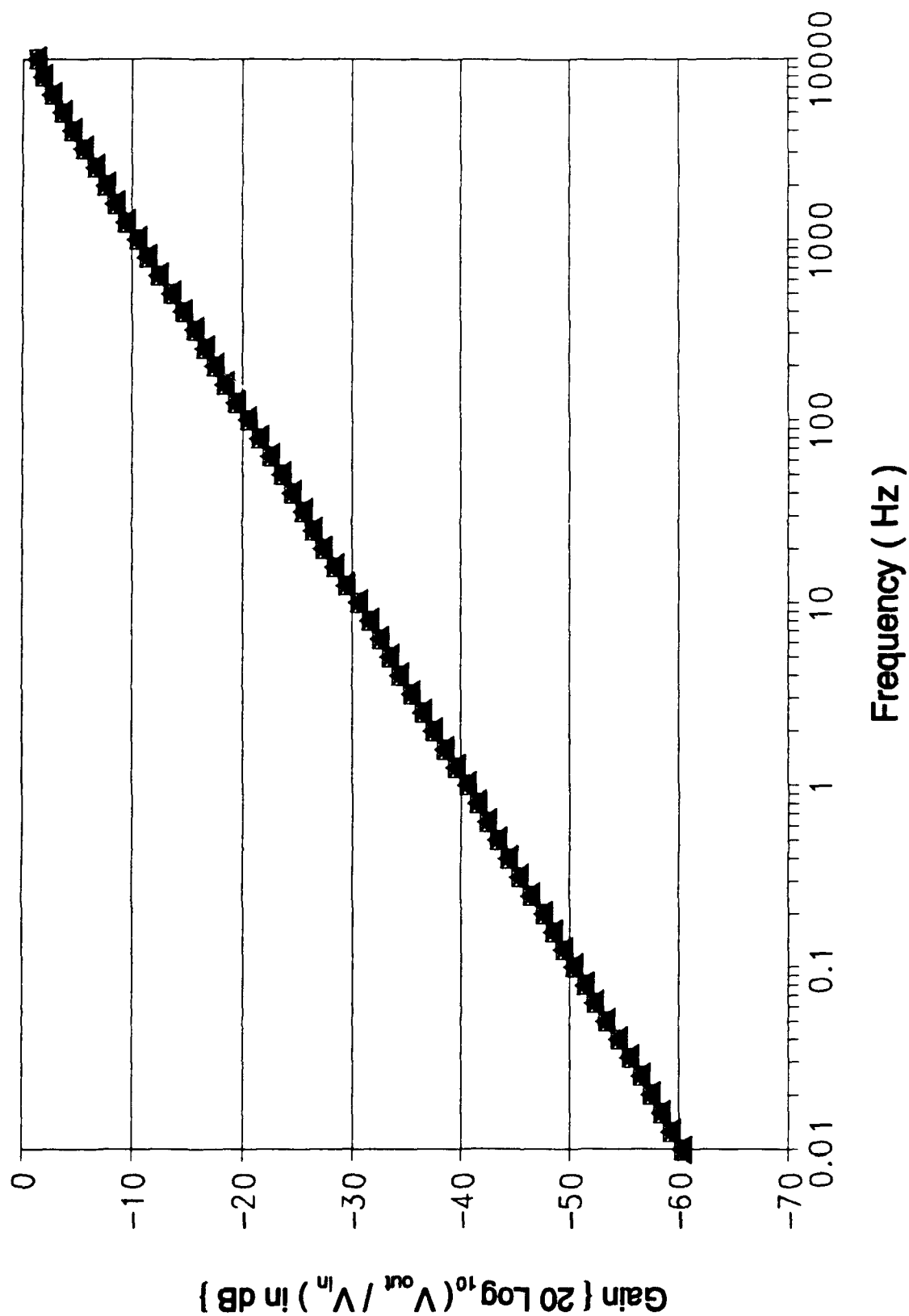
Figure B-1 (cont). Gain Response of the Oldham Circuit Design Using an HSPICE Computer Variation of Resistor 0 (cont);
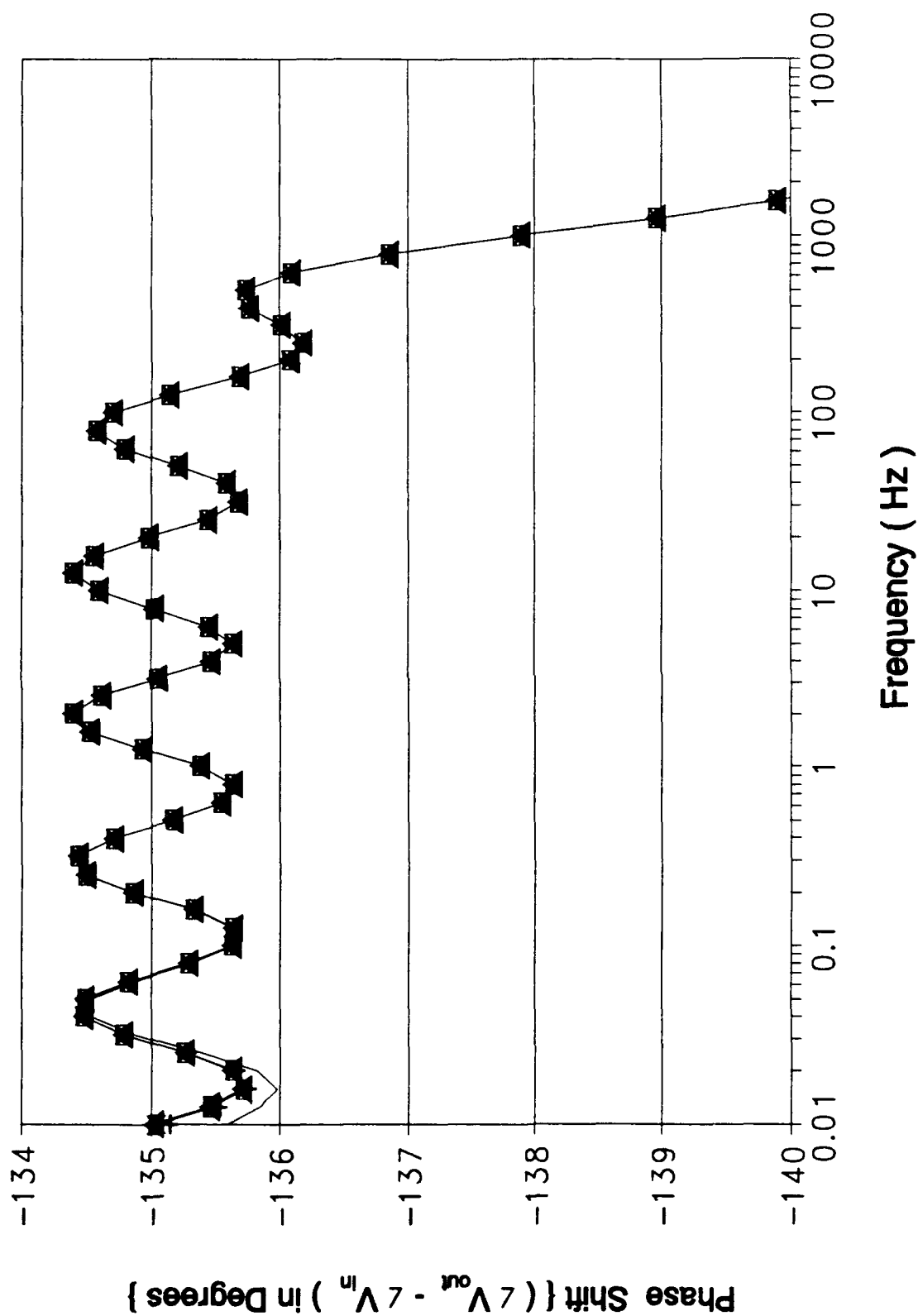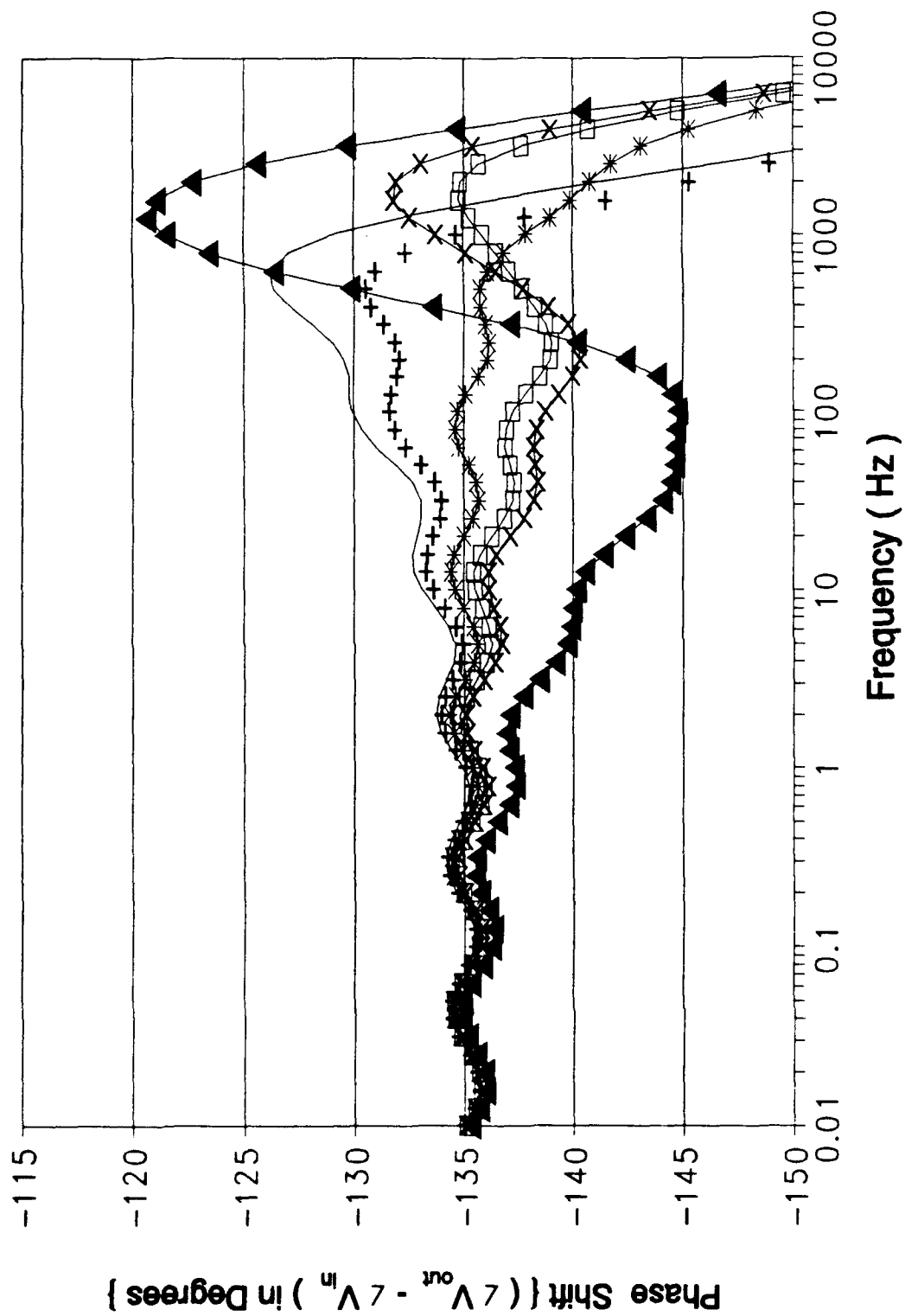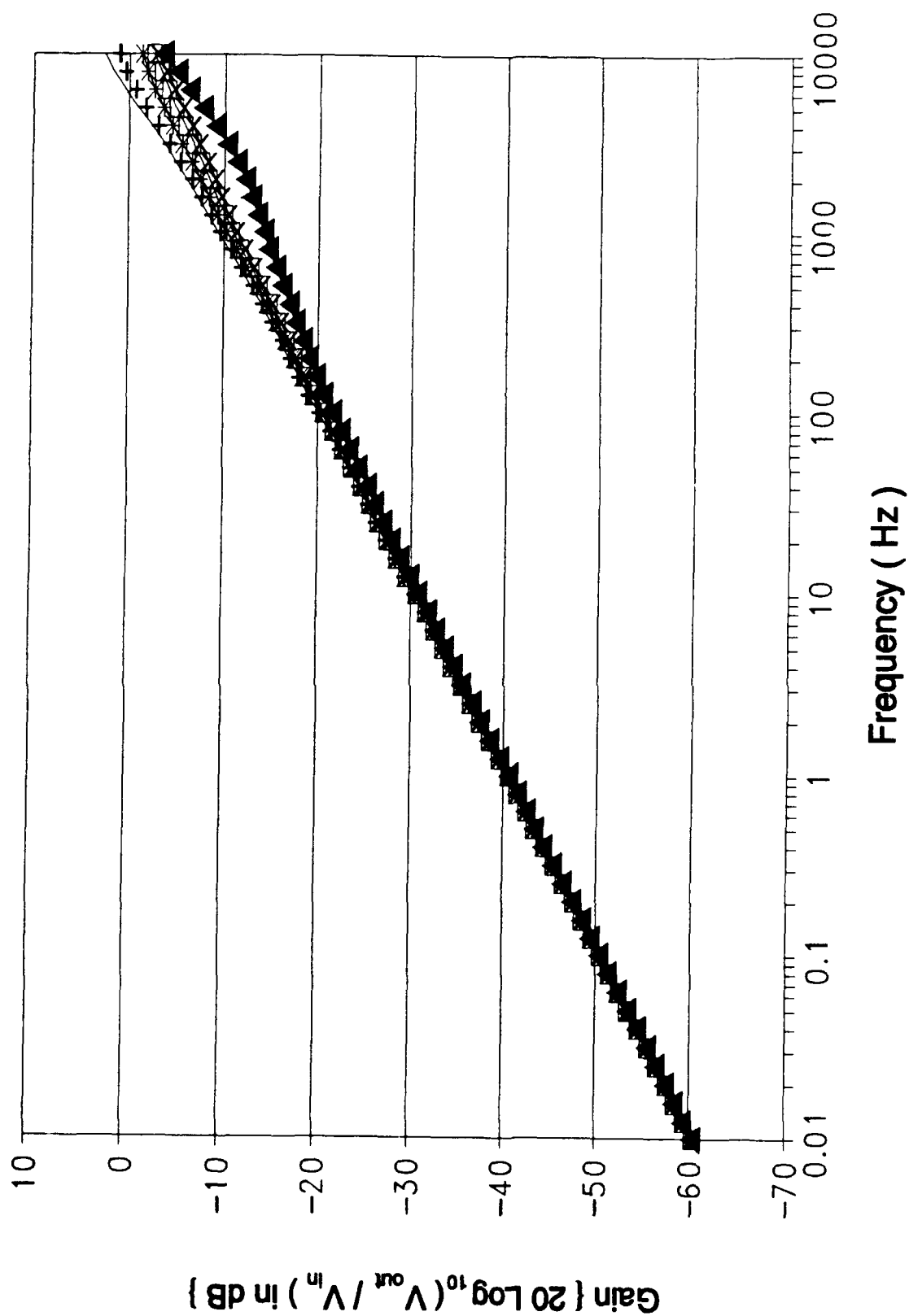
Figure B-1 (cont). Phase Response of the Oldham Circuit Design Using an HSPICE Computer Variation of Resistor 0.

Resistor Values for Figure B-2						
Symbol	——	-+-	-*-	—☐—	—×—	-▲-
Resis- tor Value (MΩ)	2.54	10.16	25.4 Ideal	40.64	50.8	127

Figure B-2. Graphical Symbol Legend and Resistor Value Correlation for Figure B-2 (cont);
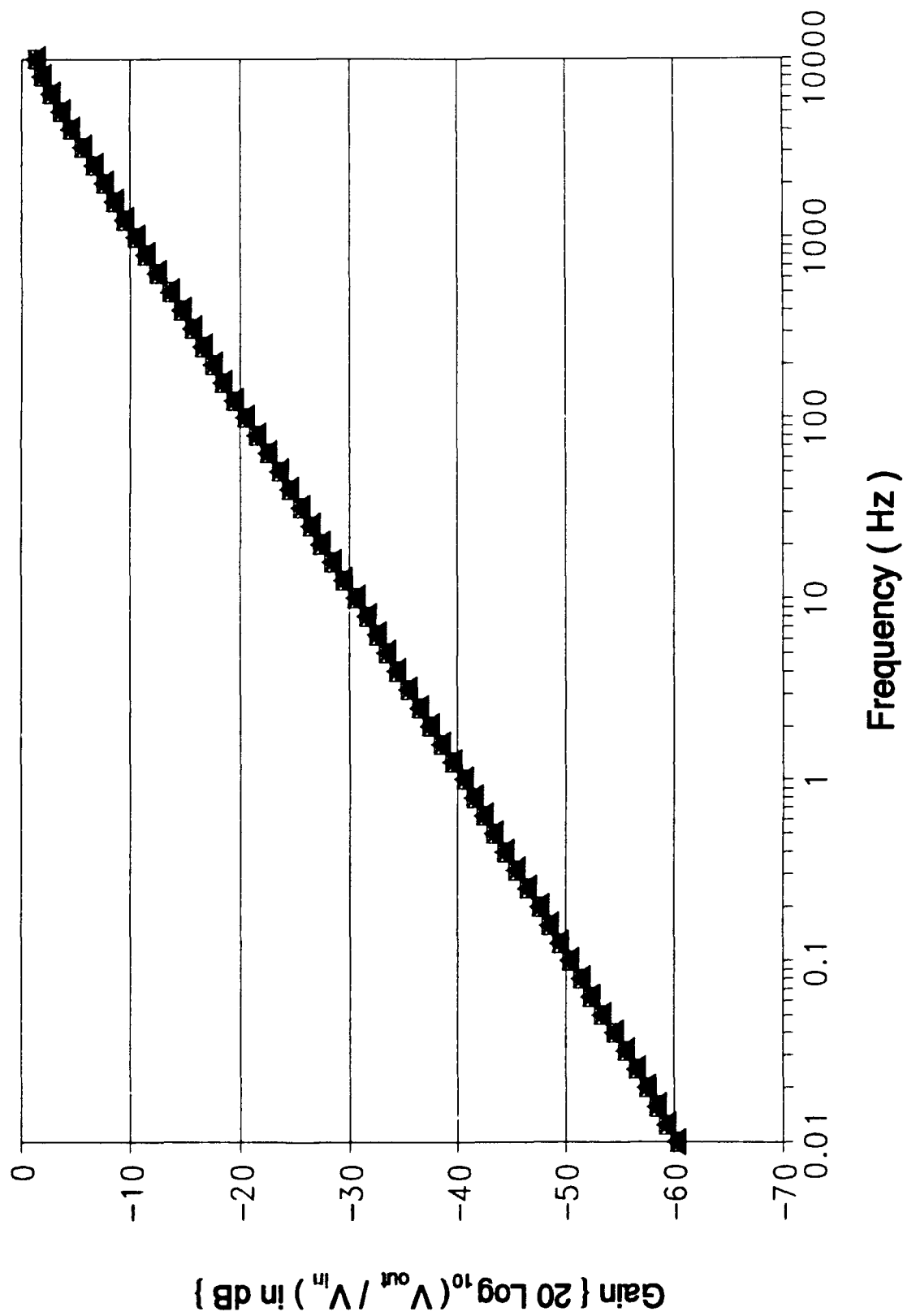
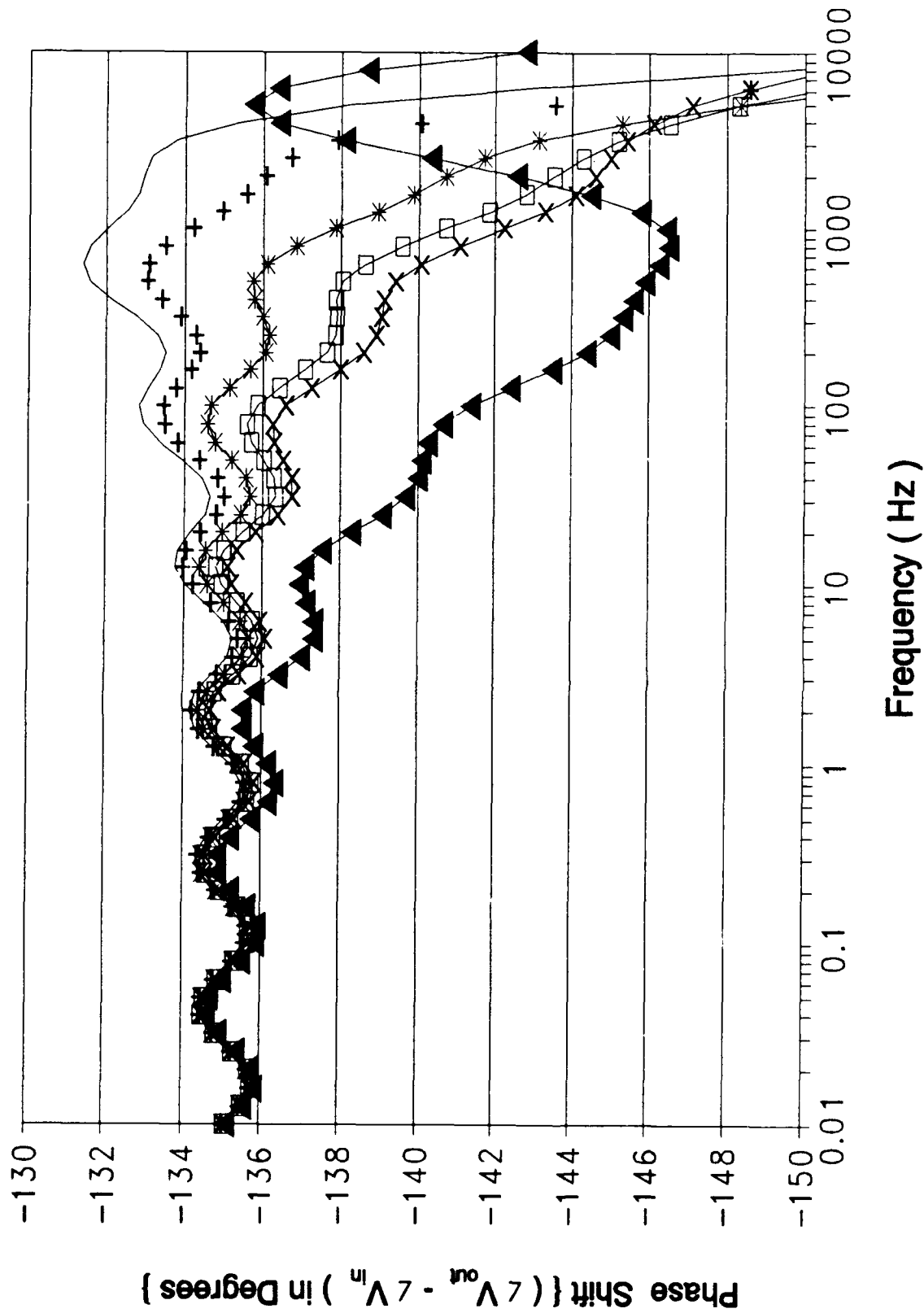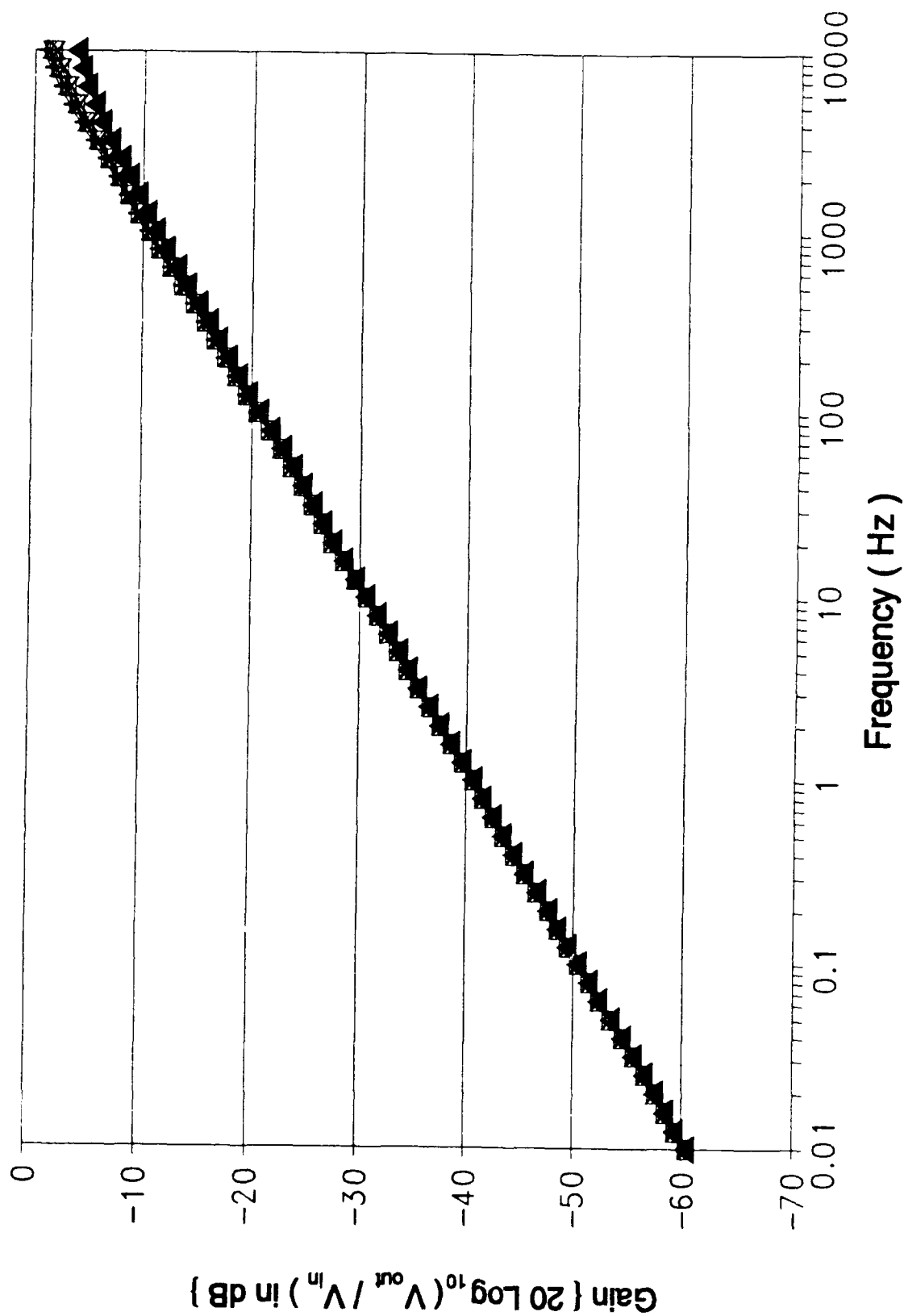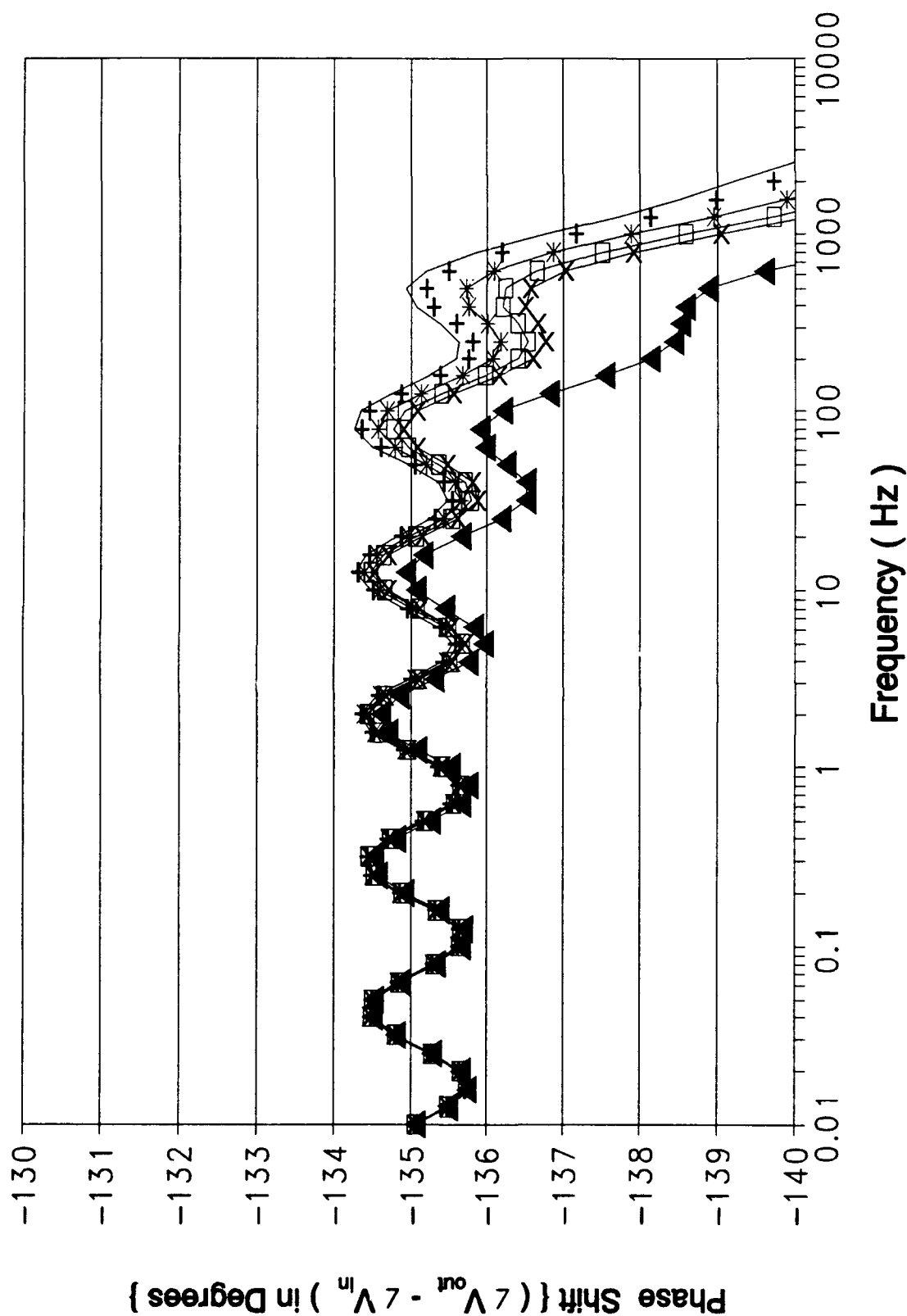Figure B-2 (cont). Gain Response of the Oldham Circuit Design Using an HSPICE Computer Variation of Resistor 1 (cont);
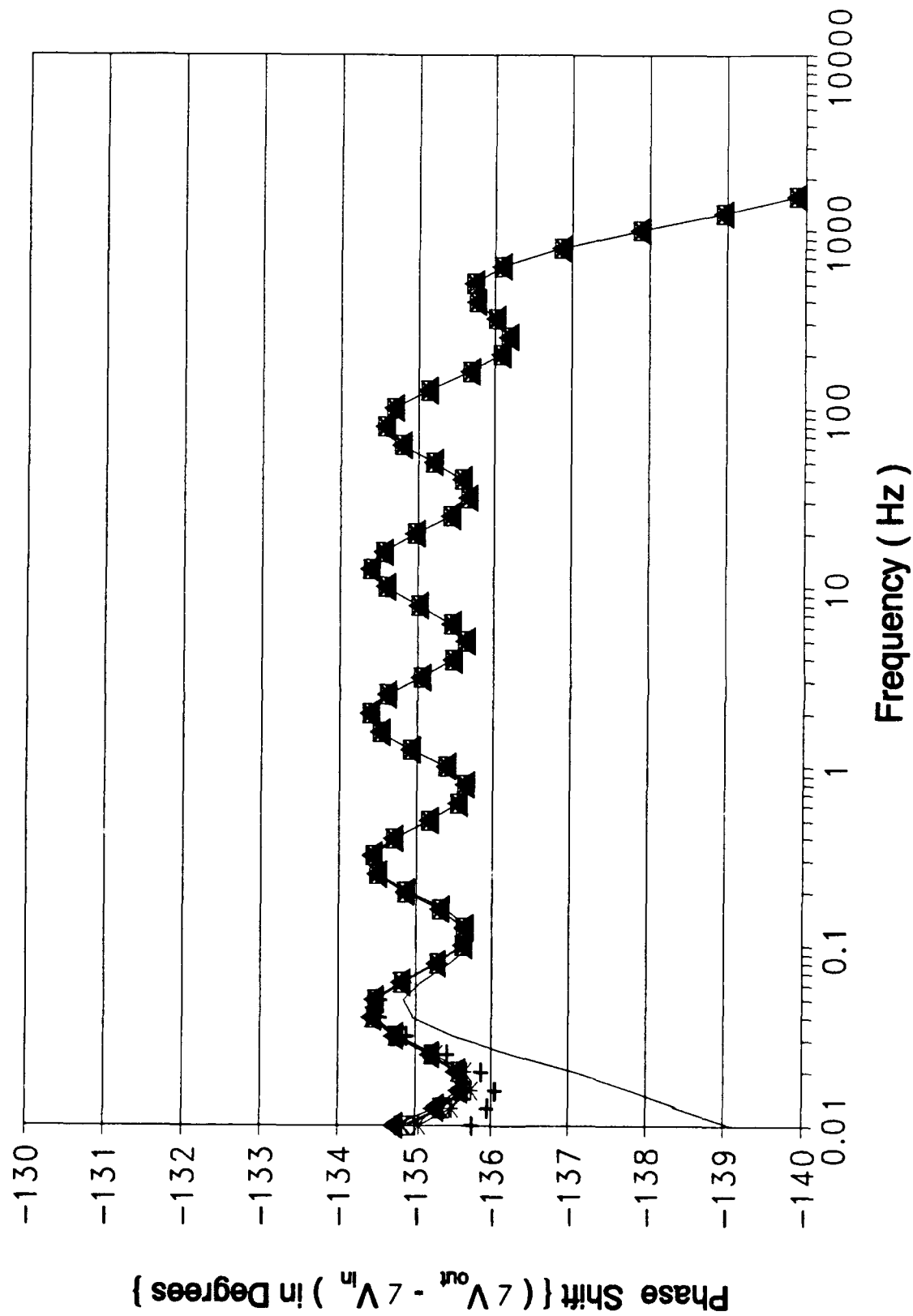
Figure B-2 (cont). Phase Response of the Oldham Circuit Design Using an HSPICE Computer Variation of Resistor 1.

Resistor Values for Figure B-3						
Symbol	——	-+-	-*-	-□-	-x-	-▲-
Resis- tor Value (MΩ)	0.985	3.94	9.85 Ideal	15.76	19.7	49.25

Figure B-3. Graphical Symbol Legend and Resistor
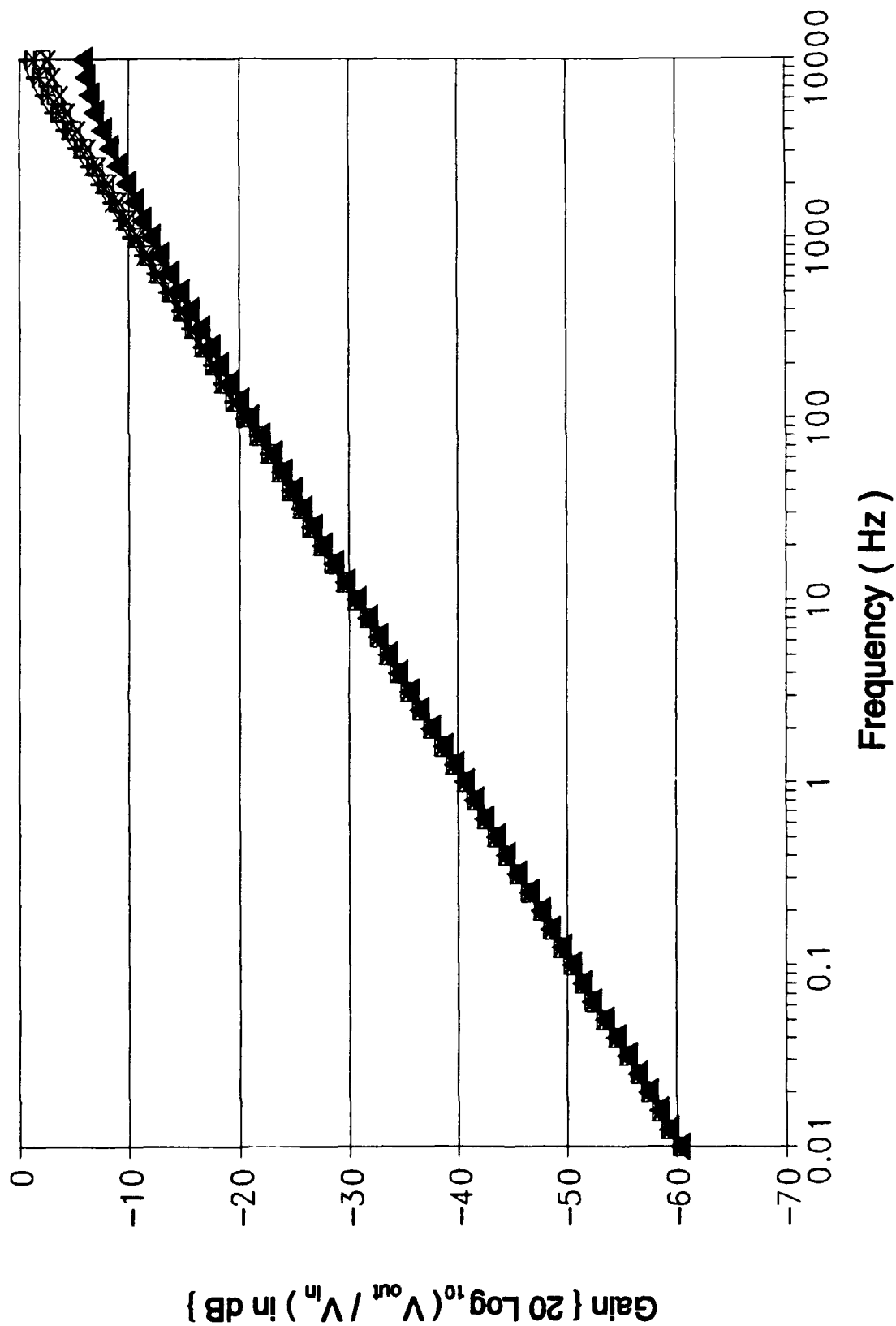**Value Correlation for Figure B-3 (cont);**
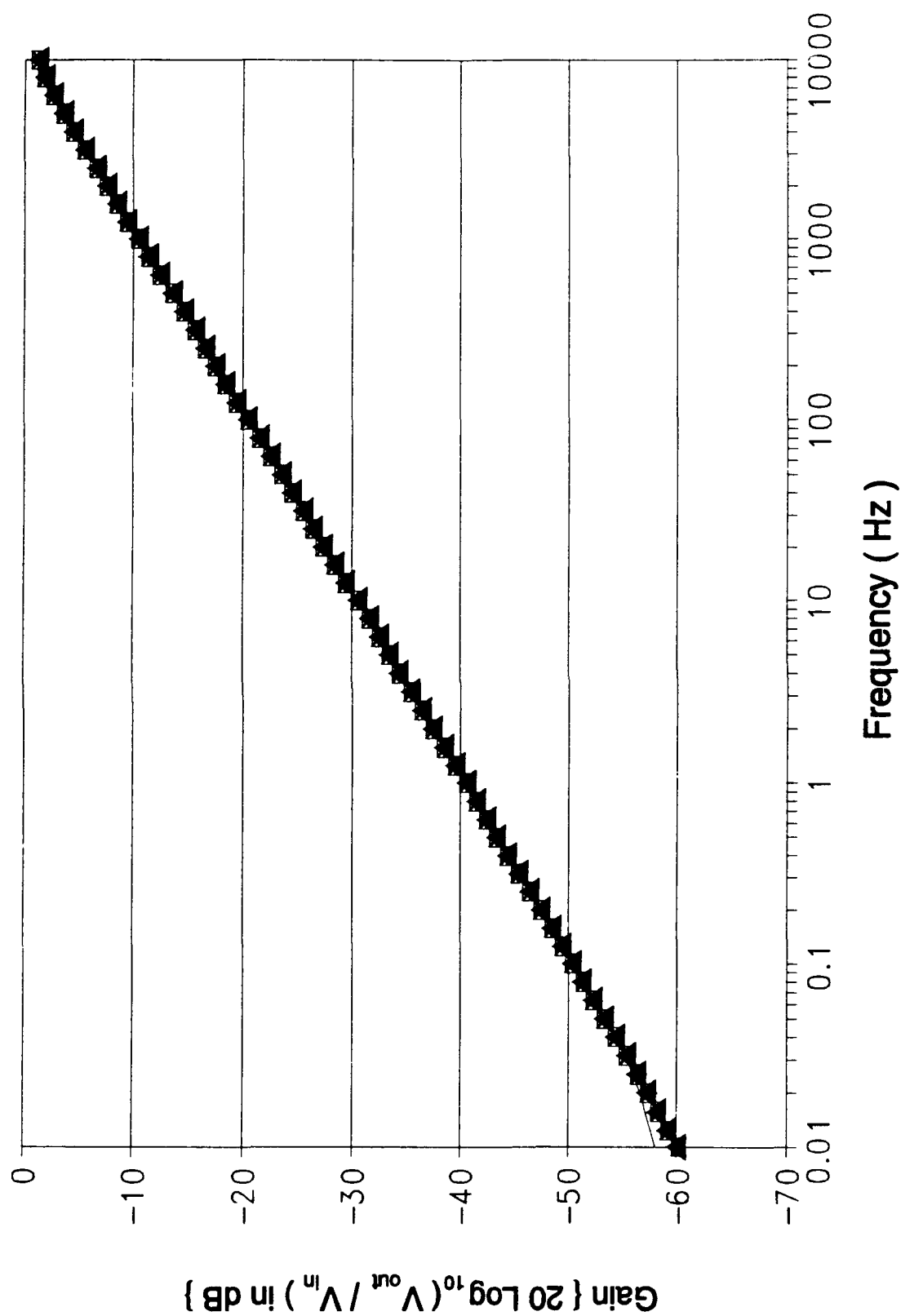
Figure B-3 (cont). Gain Response of the Oldham Circuit Design Using an HSPICE Computer Variation of Resistor 2 (cont);
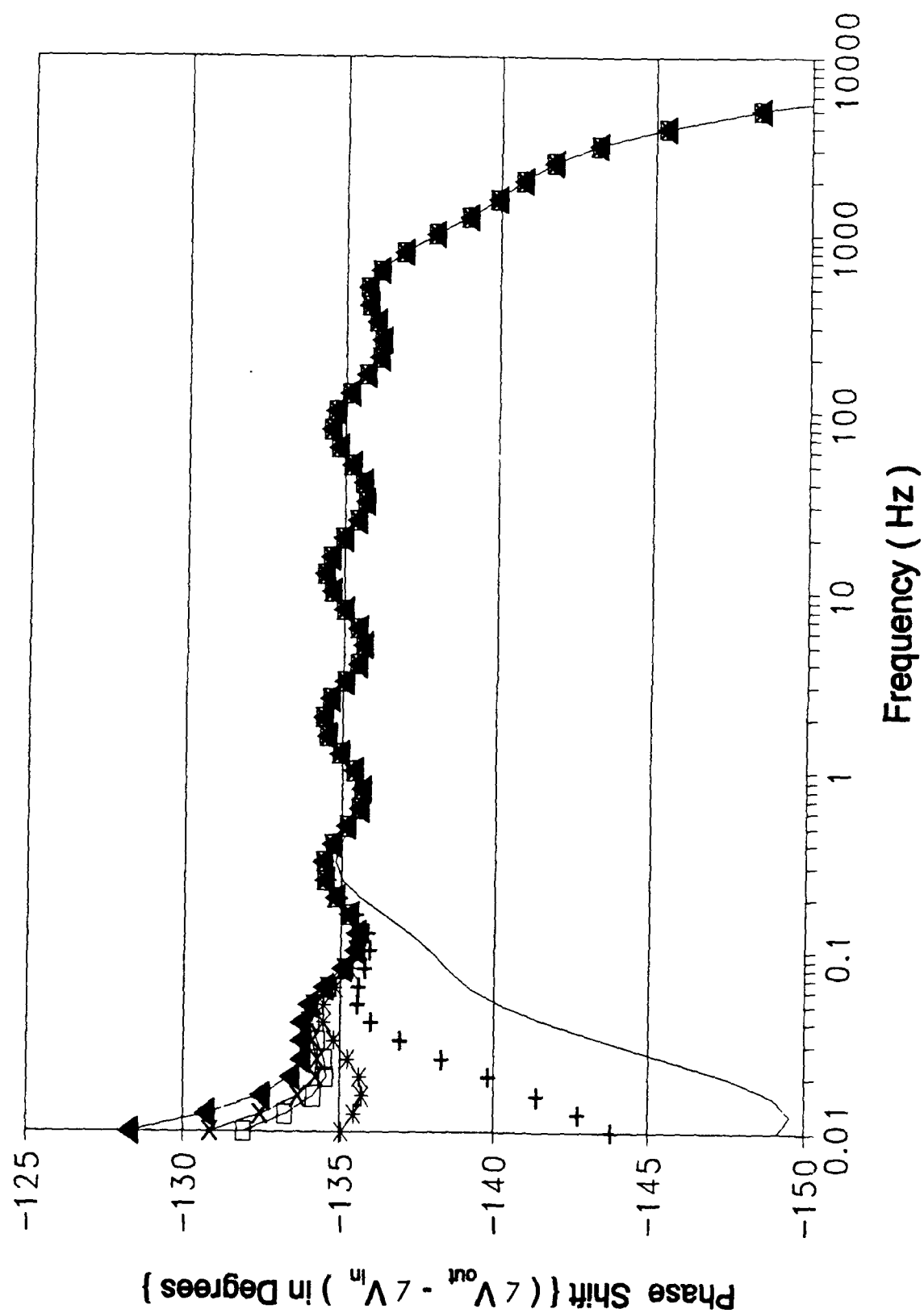
Figure B-3 (cont). Phase Response of the Oldham Circuit Design Using an HSPICE Computer Variation of Resistor 2.

Resistor Values for Figure B-4						
Symbol	——	-+-	-*-	—□—	—×—	-▲-
Resis- tor Value (MΩ)	0.383	1.532	3.83 Ideal	6.128	7.66	19.15

**Figure B-4. Graphical Symbol Legend and Resistor
Value Correlation for Figure B-4 (cont);**
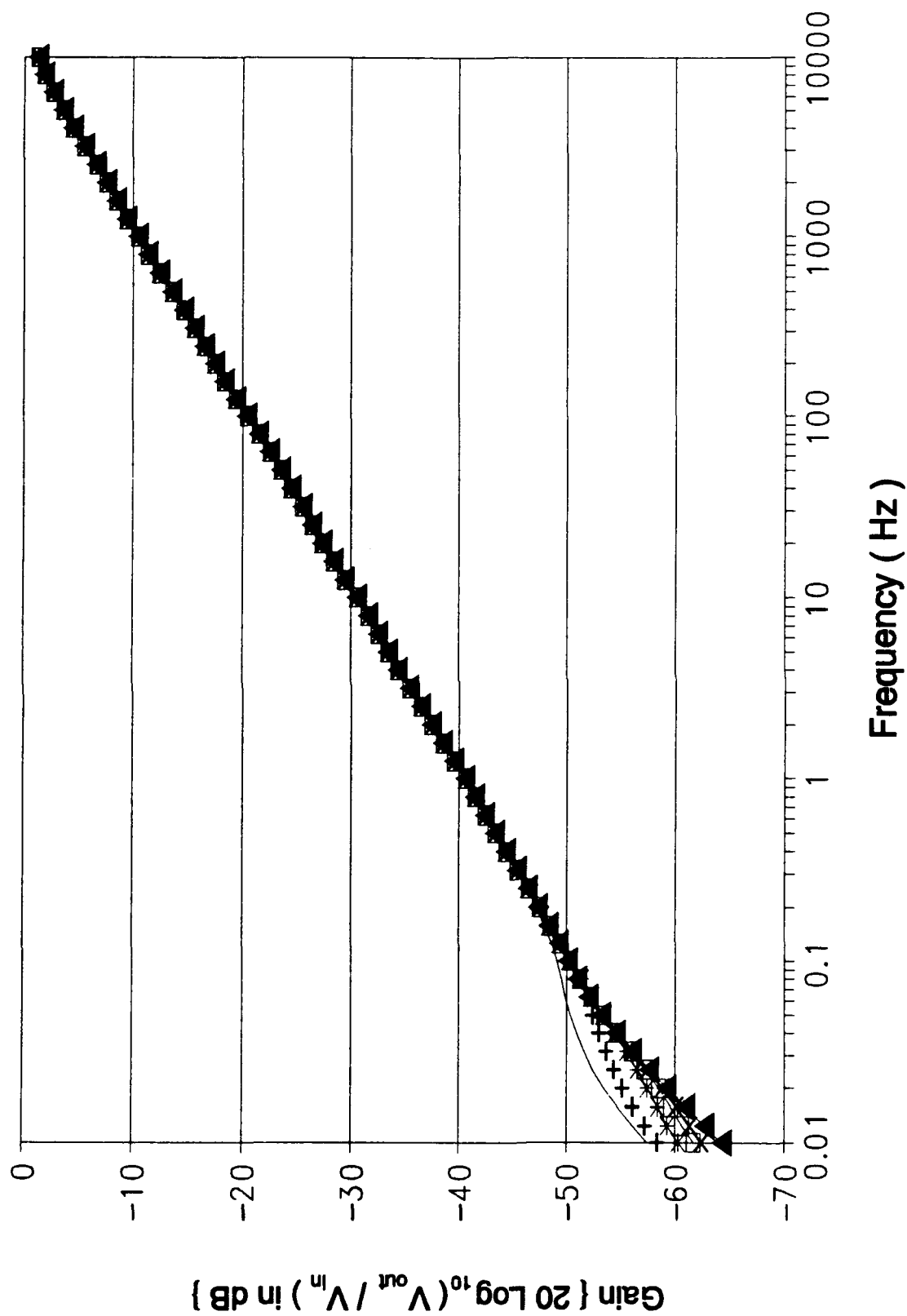
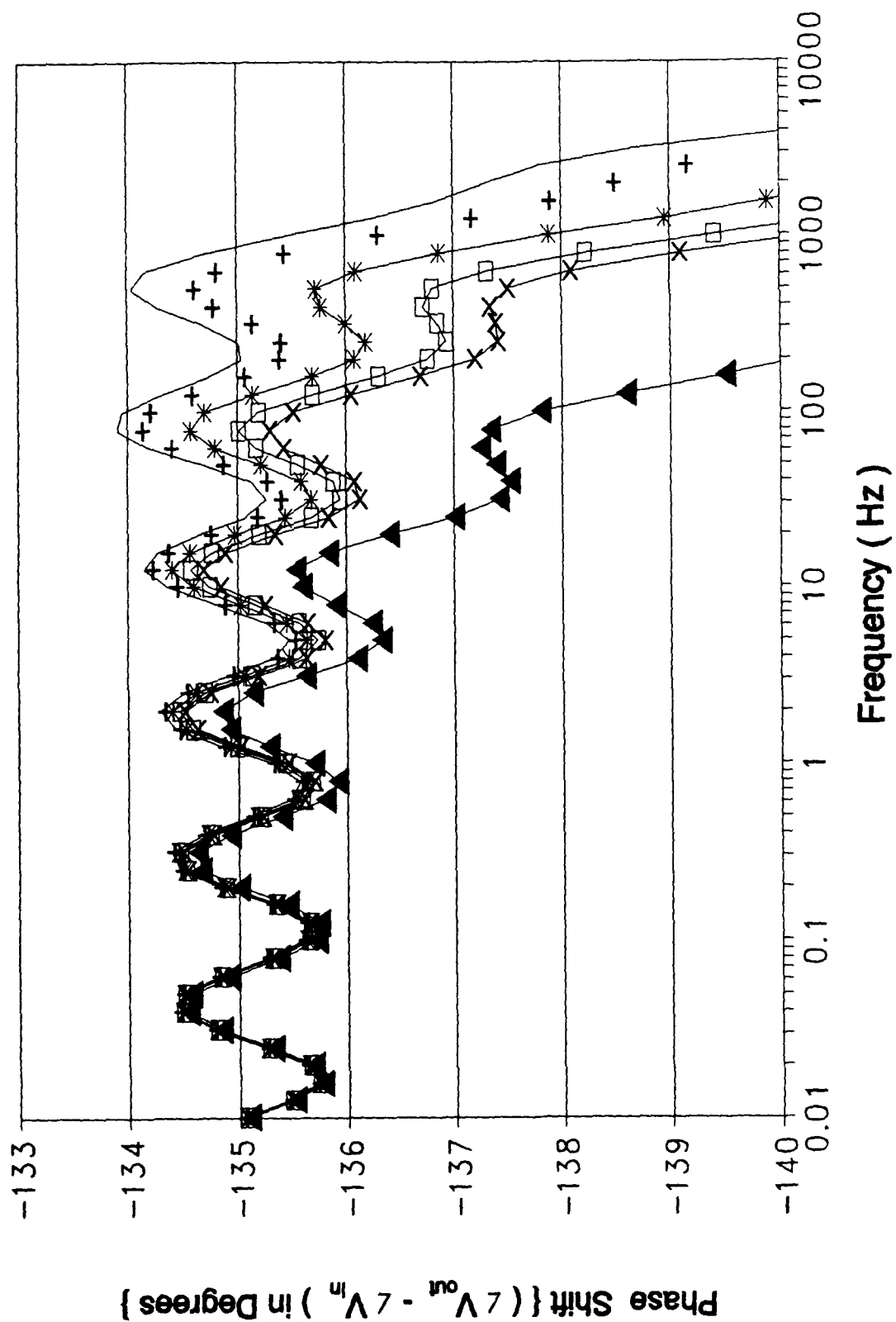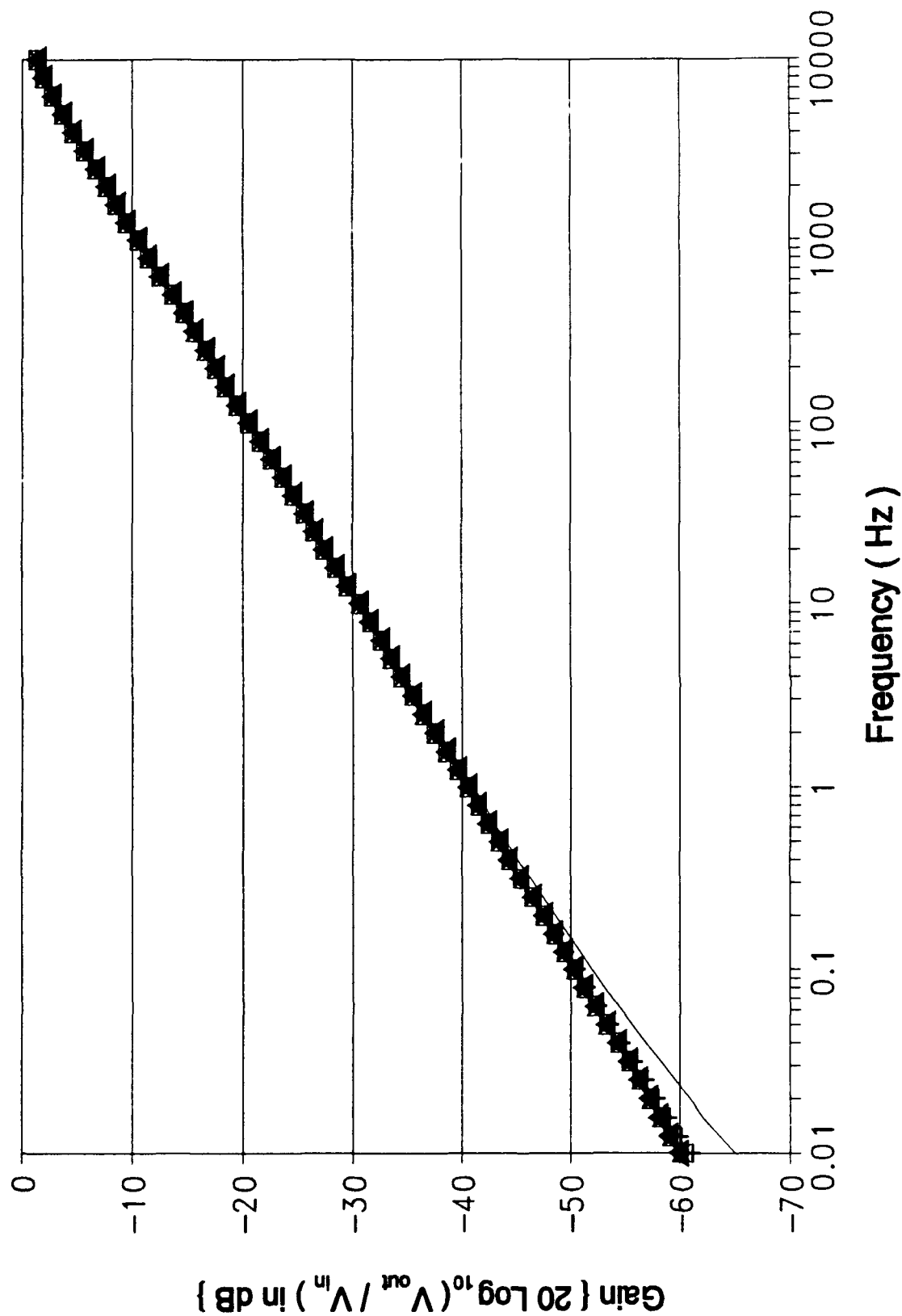Figure B-4 (cont). Gain Response of the Oldham Circuit Design Using an HSPICE Computer Variation of Resistor 3 (cont);

B-15
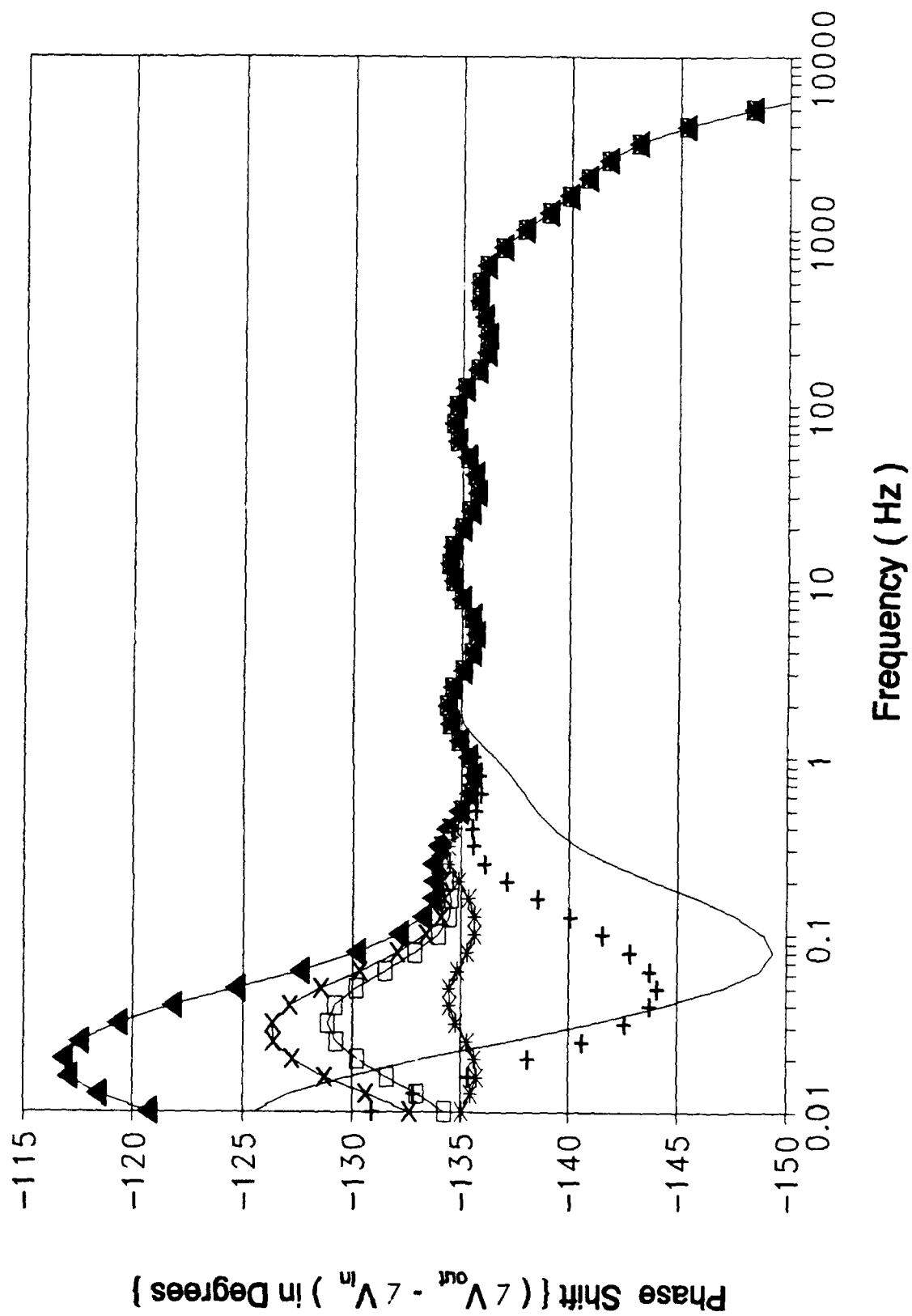
Figure B-4 (cont). Phase Response of the Oldham Circuit Design Using an HSPICE Computer Variation of Resistor 3.

Resistor Values for Figure B-5						
Symbol	——	-+-	-*-	-□-	-×-	-▲-
Resis- tor Value (MΩ)	0.1488	0.5952	1.488 Ideal	2.381	2.976	7.44

Figure B-5. Graphical Symbol Legend and Resistor
Value Correlation for Figure B-5 (cont);
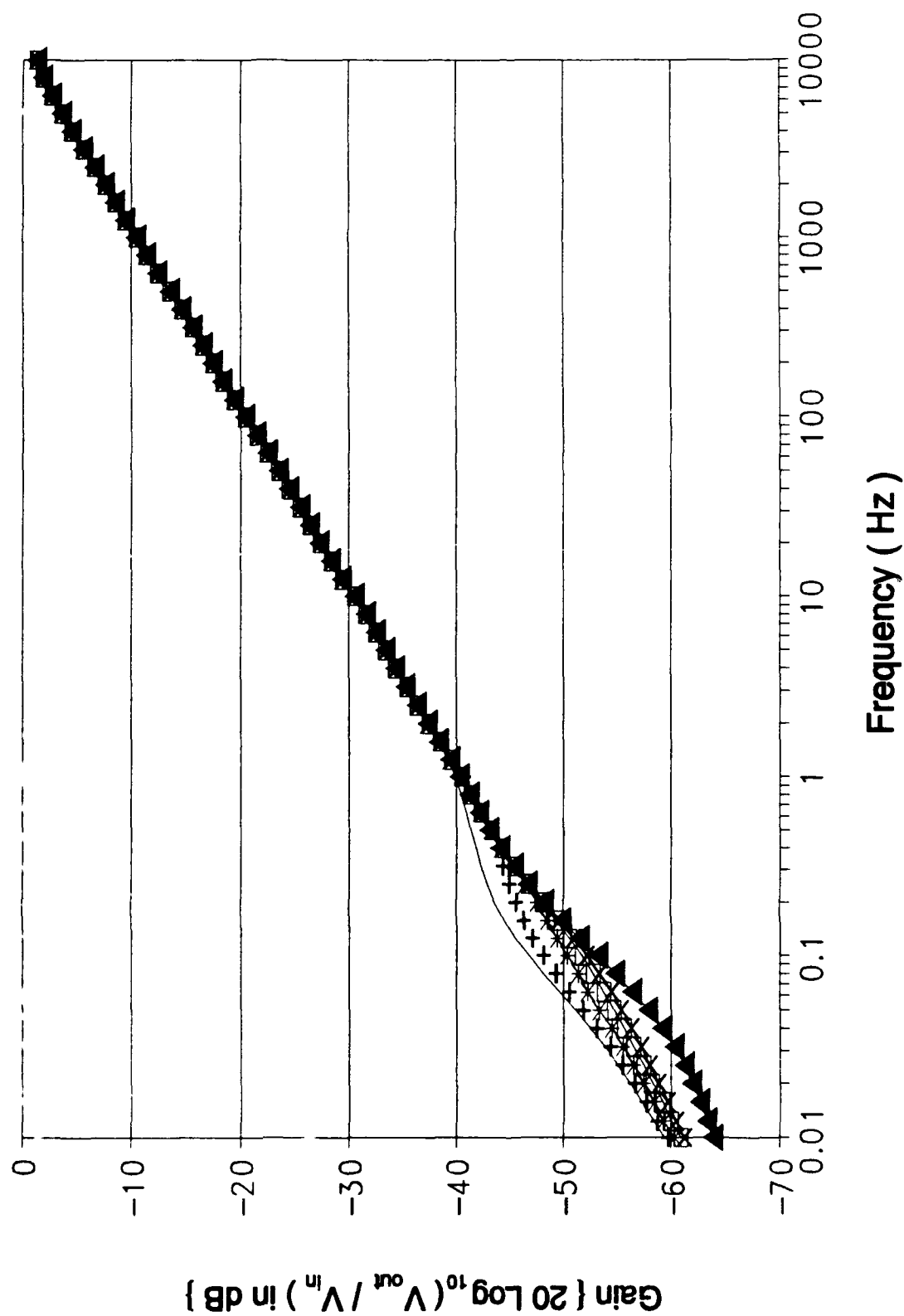
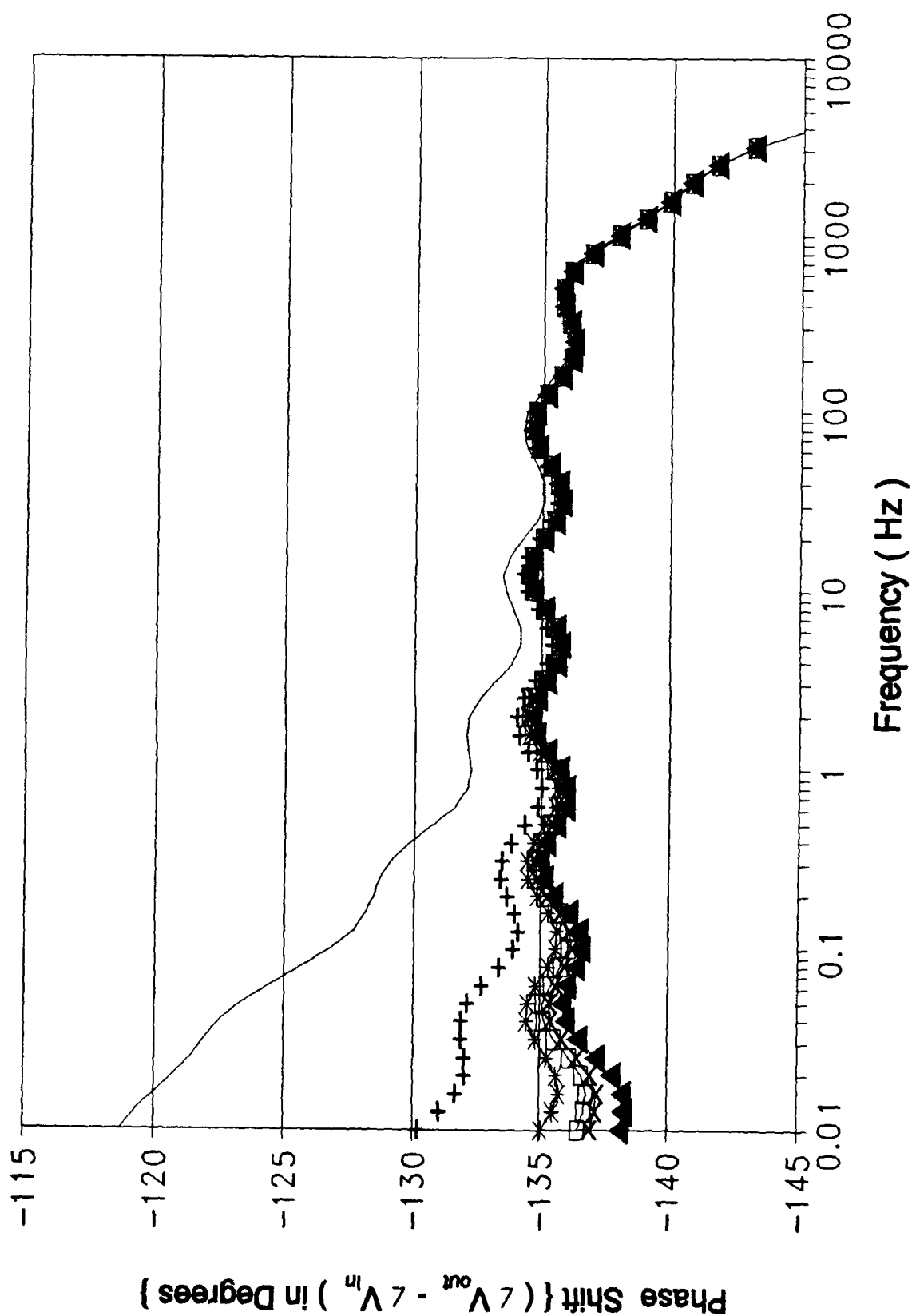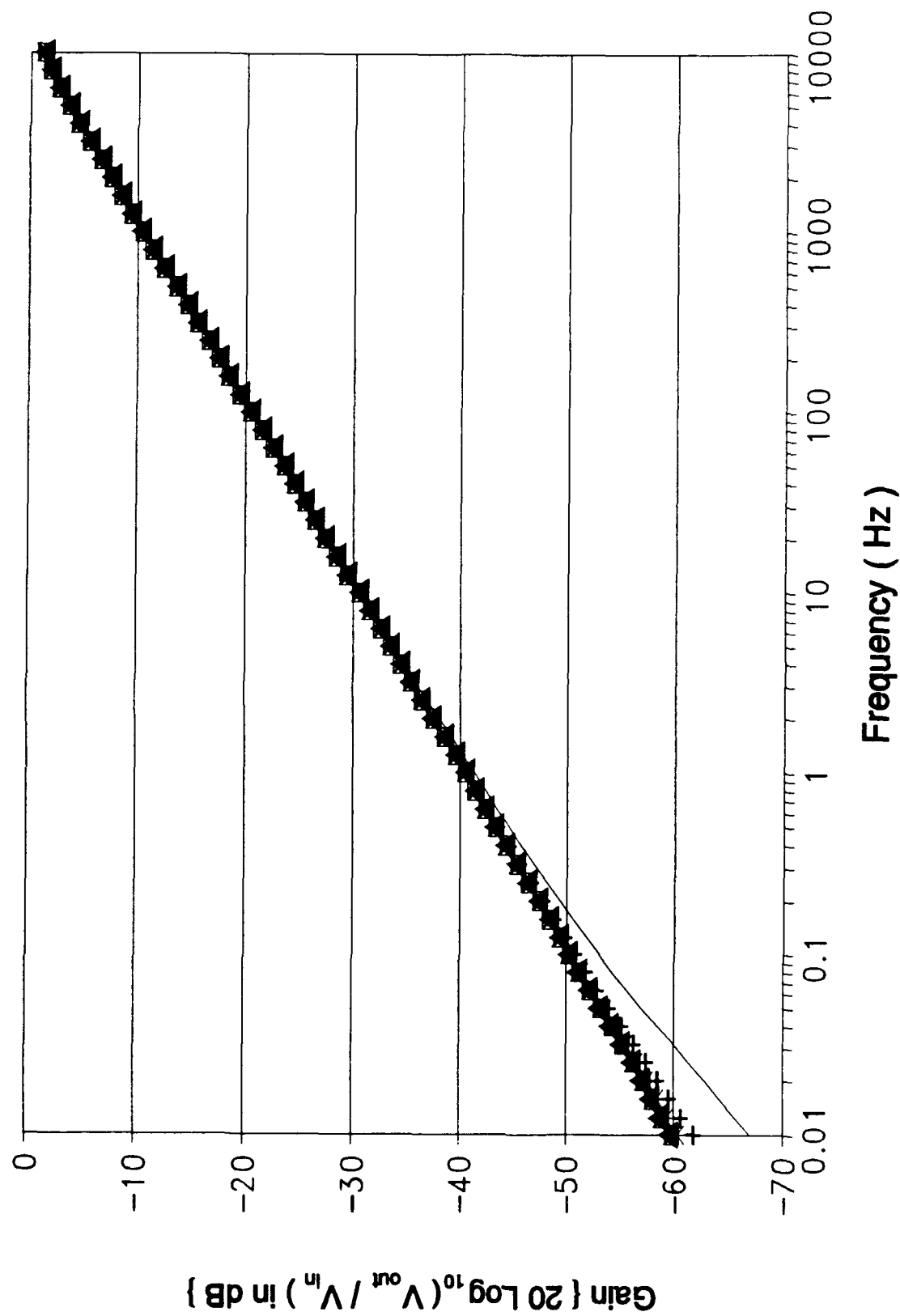**Figure B-5 (cont). Gain Response of the Oldham Circuit Design Using an HSPICE Computer Variation of Resistor 4 (cont);**

B-18
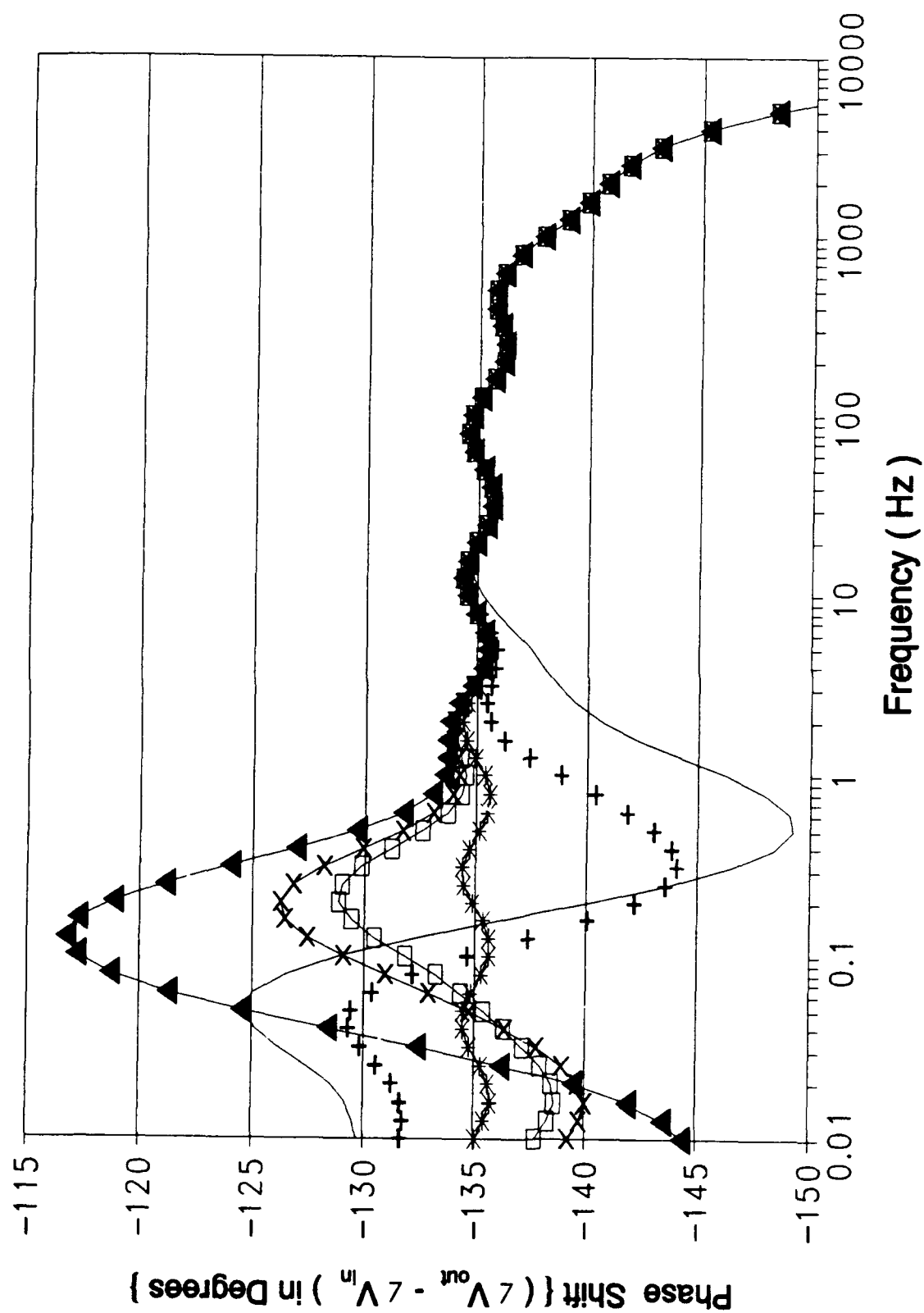
Figure B-5 (cont). Phase Response of the Oldham Circuit Design Using an HSPICE Computer Variation of Resistor 4.

Resistor Values for Figure B-6						
Symbol	———	-+-	-*-	-▢-	-✕-	-▲-
Resis- tor Value (KΩ)	57.85	231.4	578.5 Ideal	925.6	1157	2892.5

**Figure B-6. Graphical Symbol Legend and Resistor
Value Correlation for Figure B-6 (cont);**
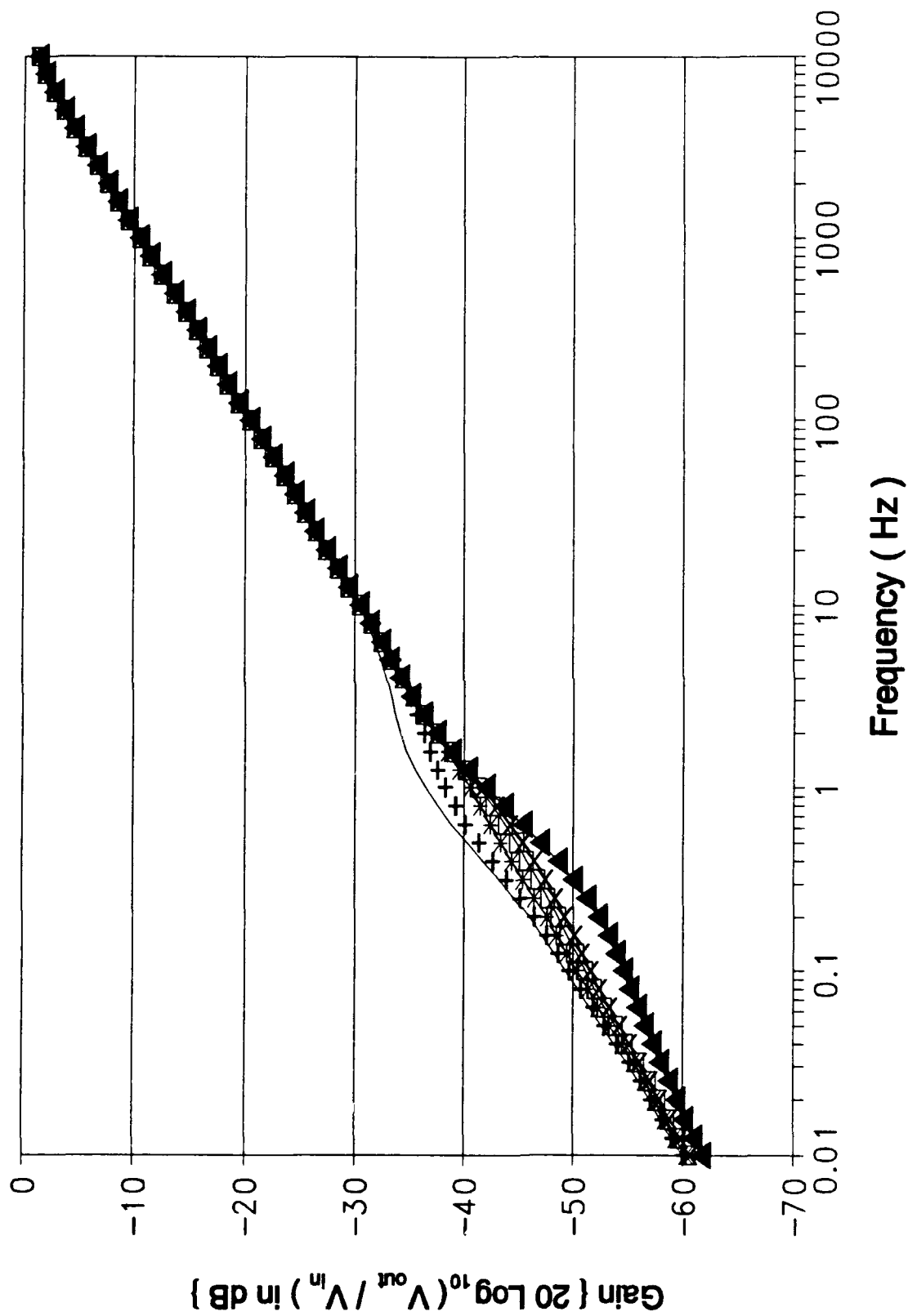
Figure B-6 (cont). Gain Response of the Oldham Circuit Design Using
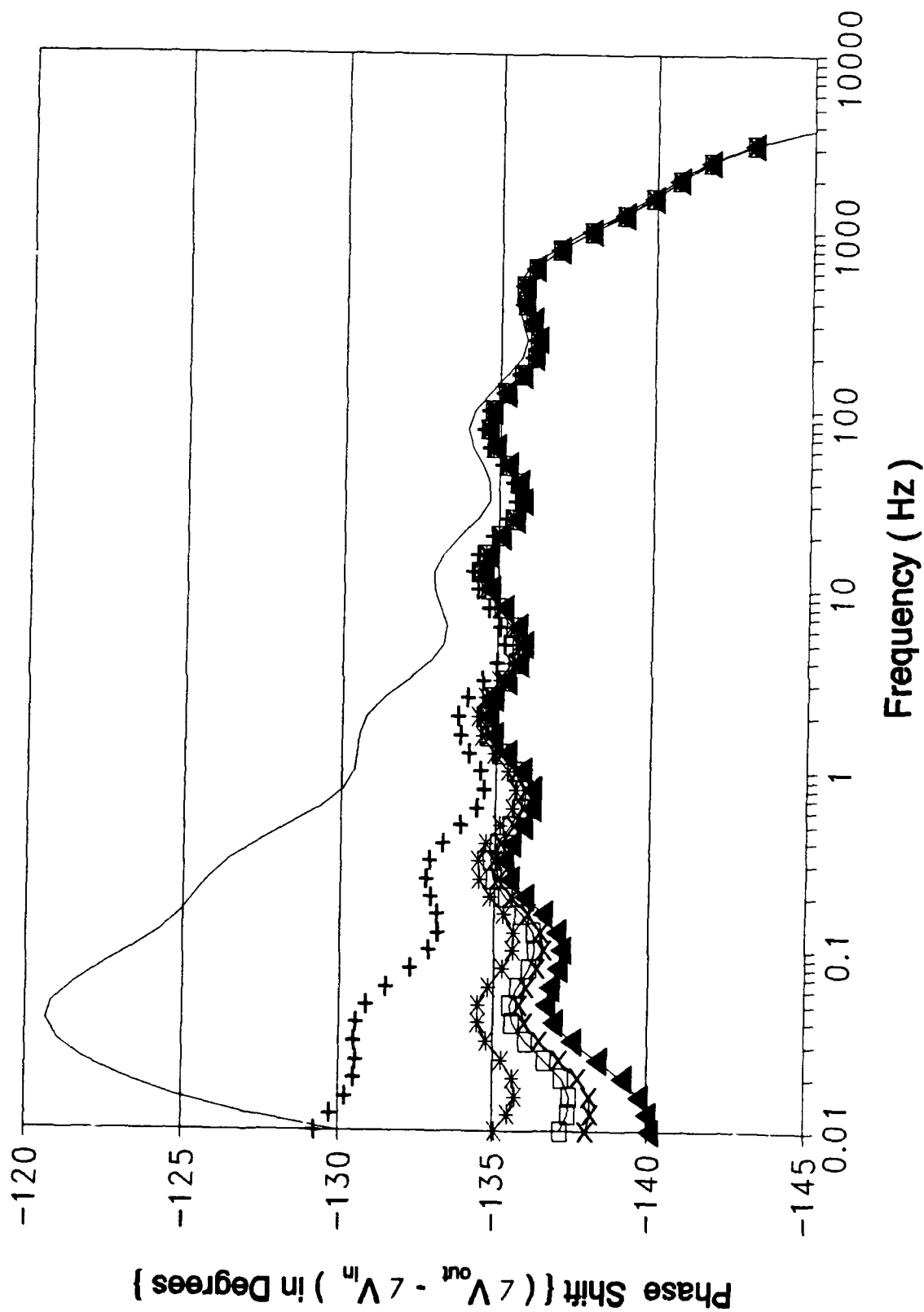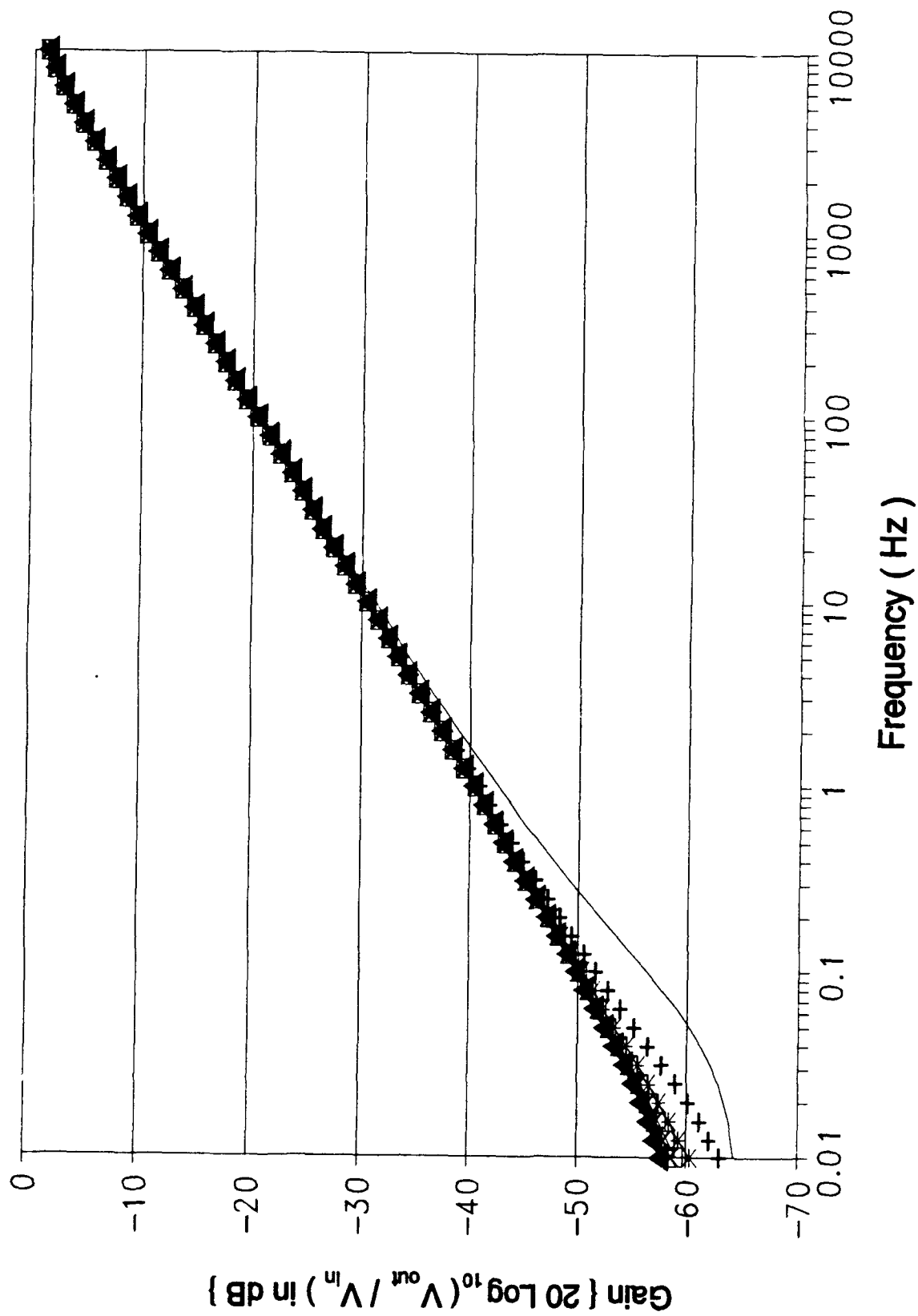an HSPICE Computer Variation of Resistor 5 (cont);
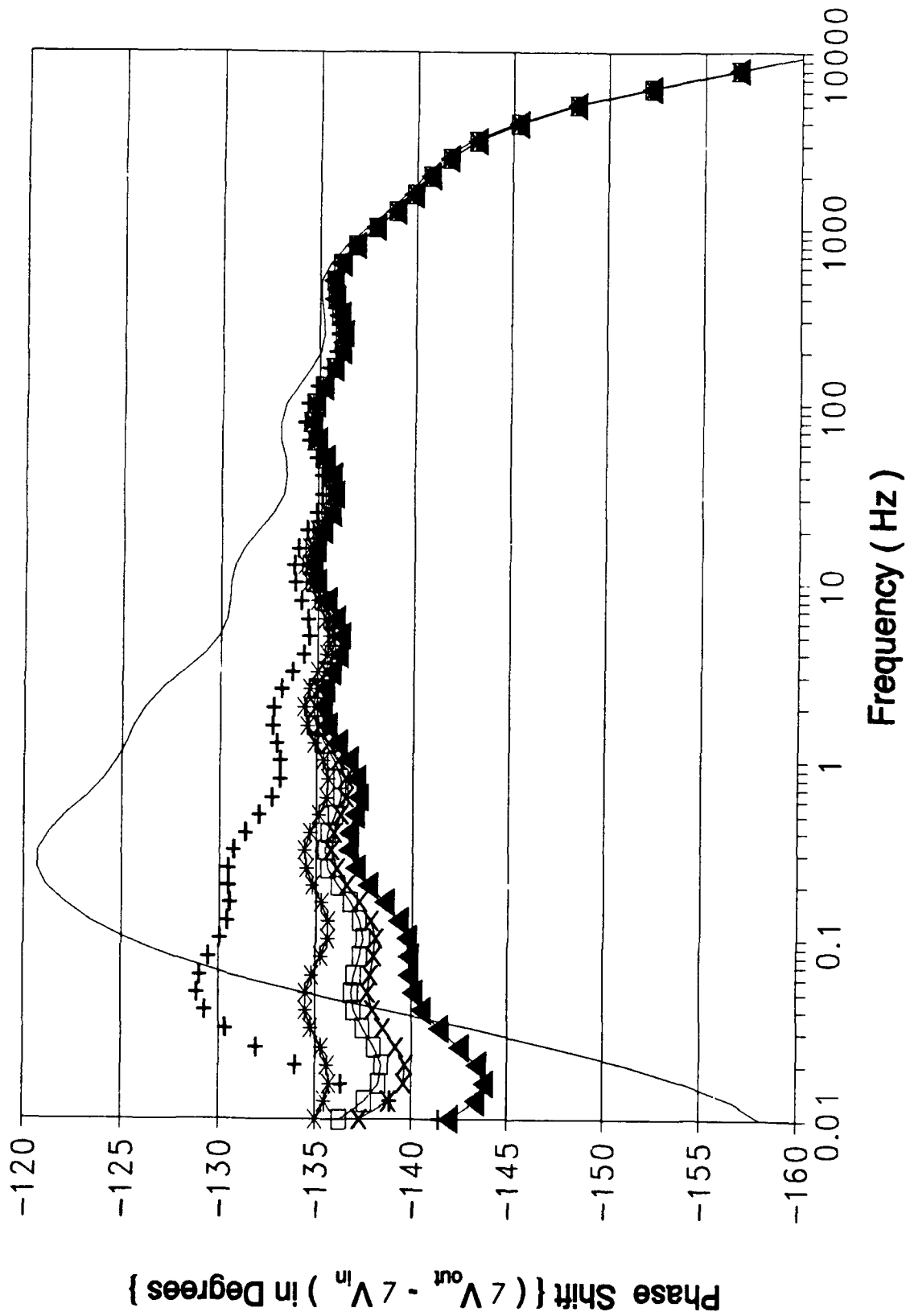
B-21
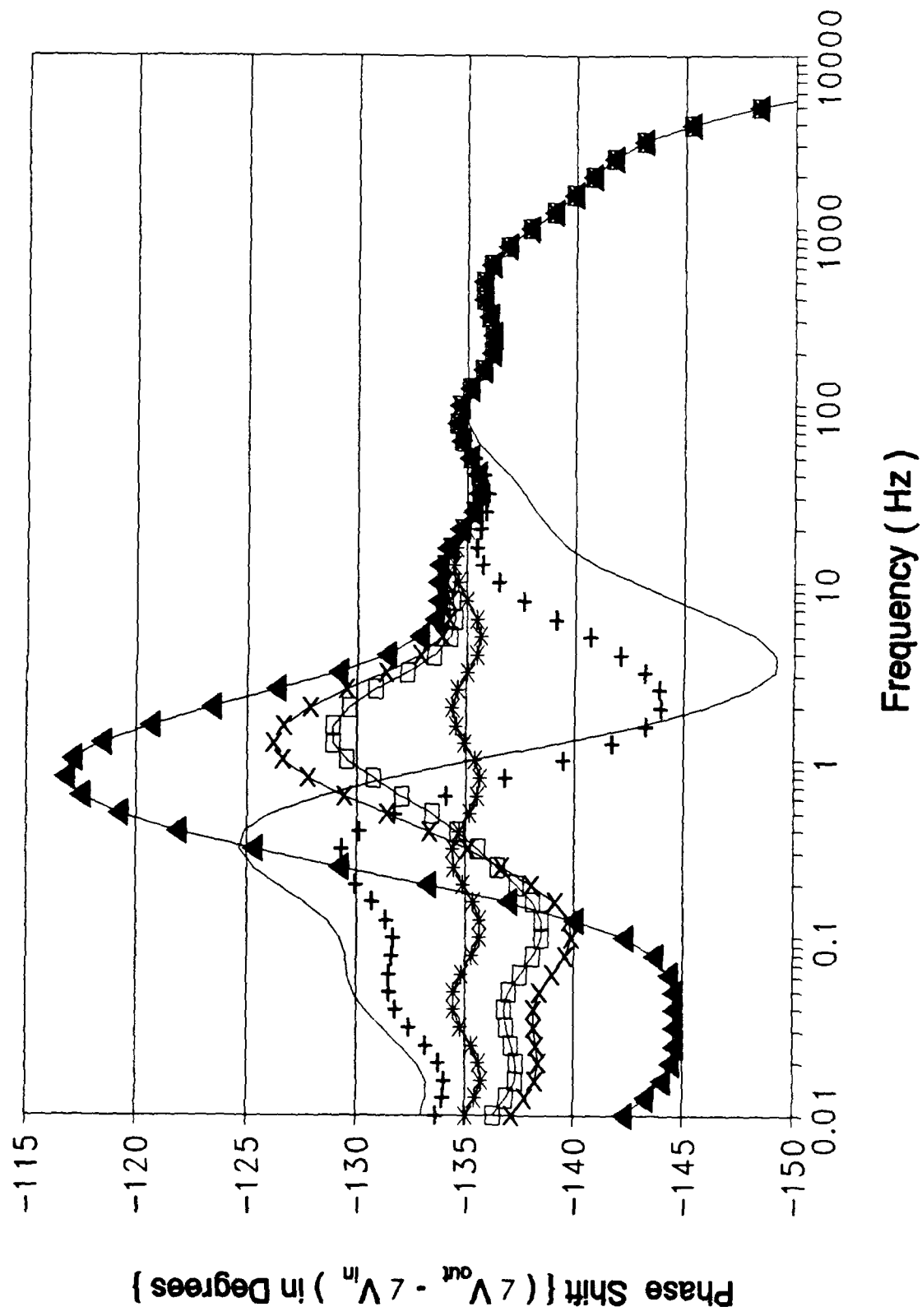
Figure B-6 (cont). Phase Response of the Oldham Circuit Design Using an HSPICE Computer Variation of Resistor 5.

B-22

Resistor Values for Figure B-7						
Symbol	——	-+-	-*-	–⎕–	—×—	-▲-
Resis- tor Value (KΩ	22.49	89.96	224.6 Ideal	359.84	449.8	1124.5

**Figure B-7. Graphical Symbol Legend and Resistor
Value Correlation for Figure B-7 (cont);**

Frequency (Hz)

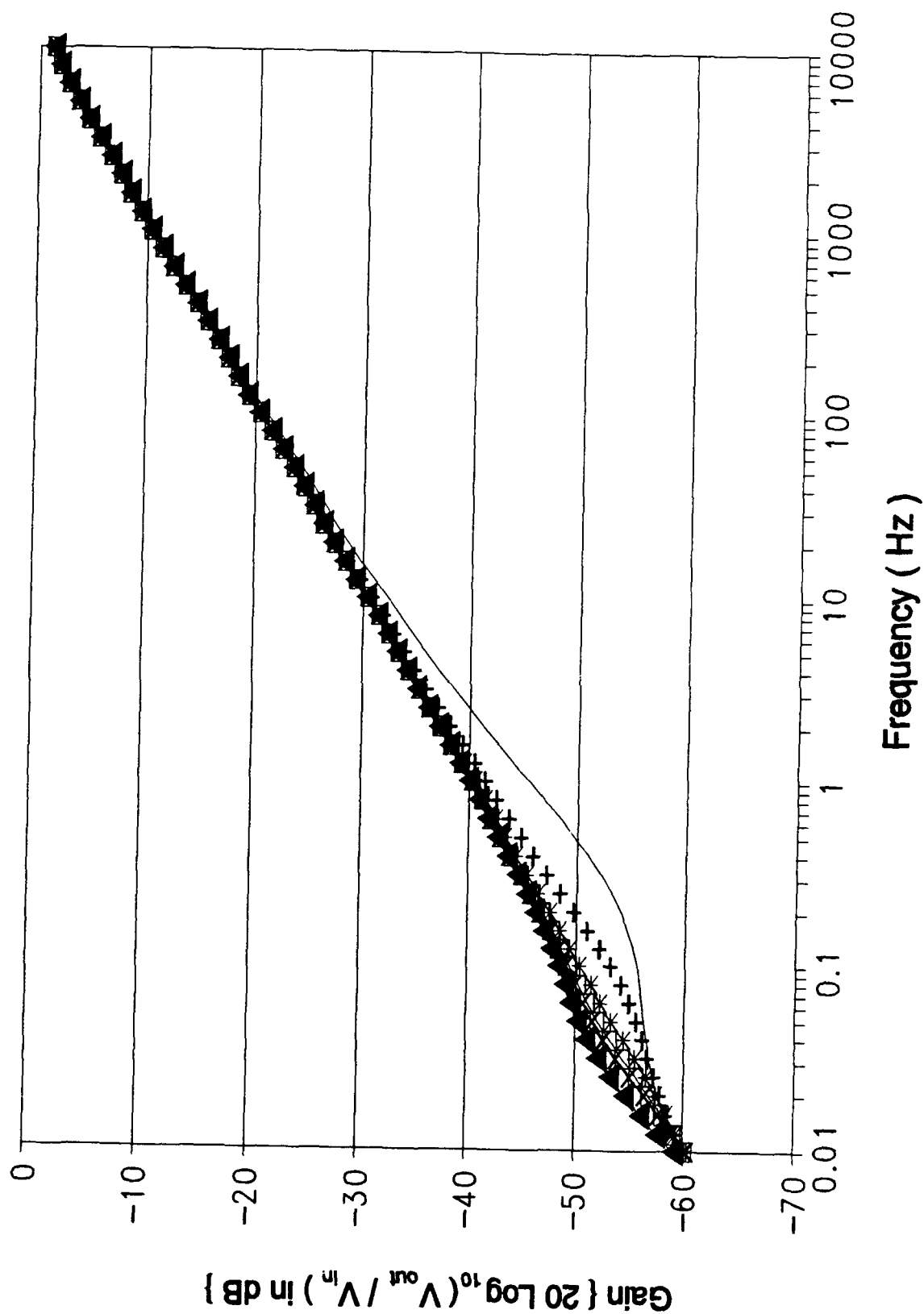Gain { 20 Log$_{10}$ (V$_{out}$ / V$_{in}$) in dB }
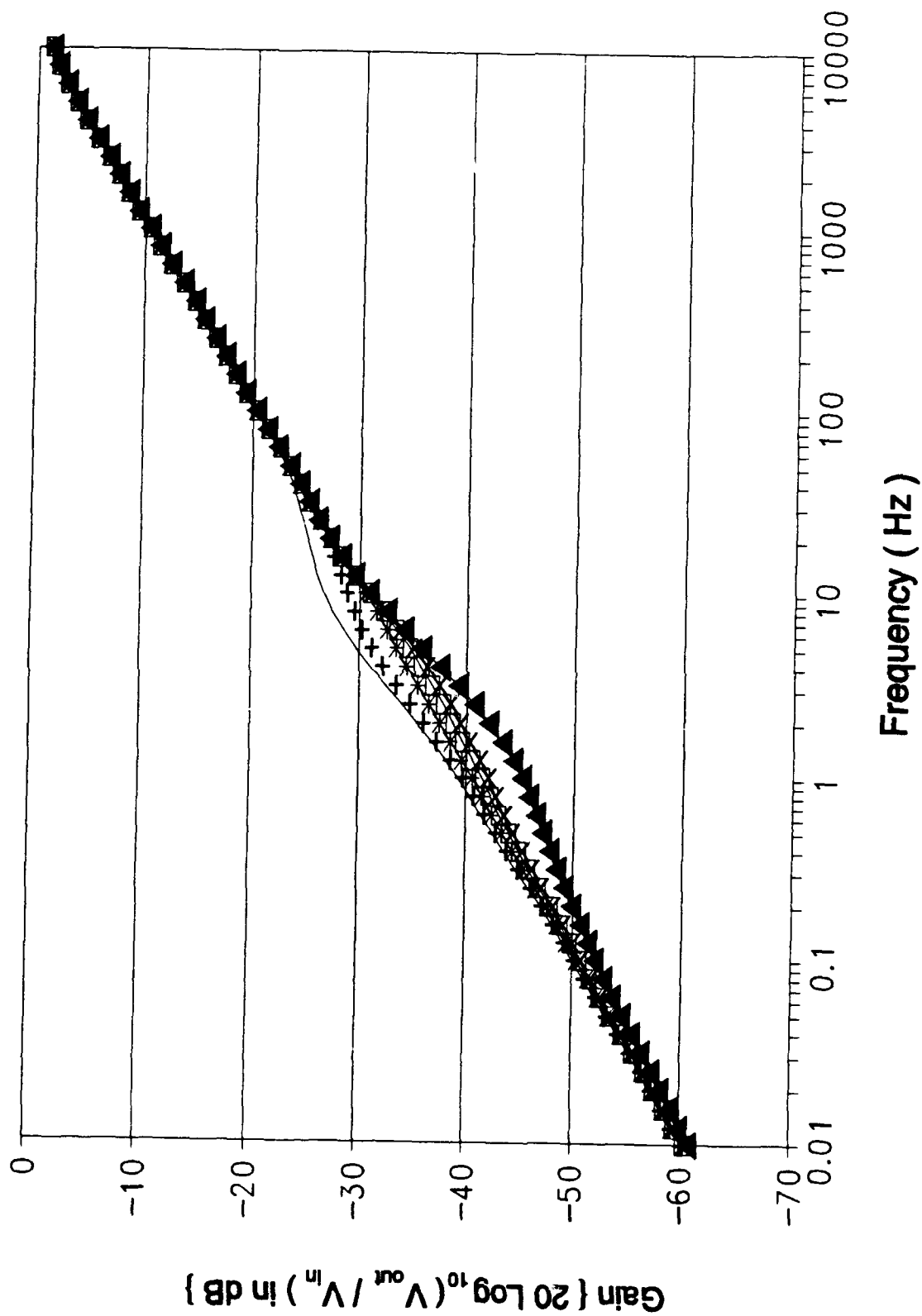
Figure B-7 (cont). Gain Response of the Oldham Circuit Design Using an HSPICE Computer Variation of Resistor 6 (cont);
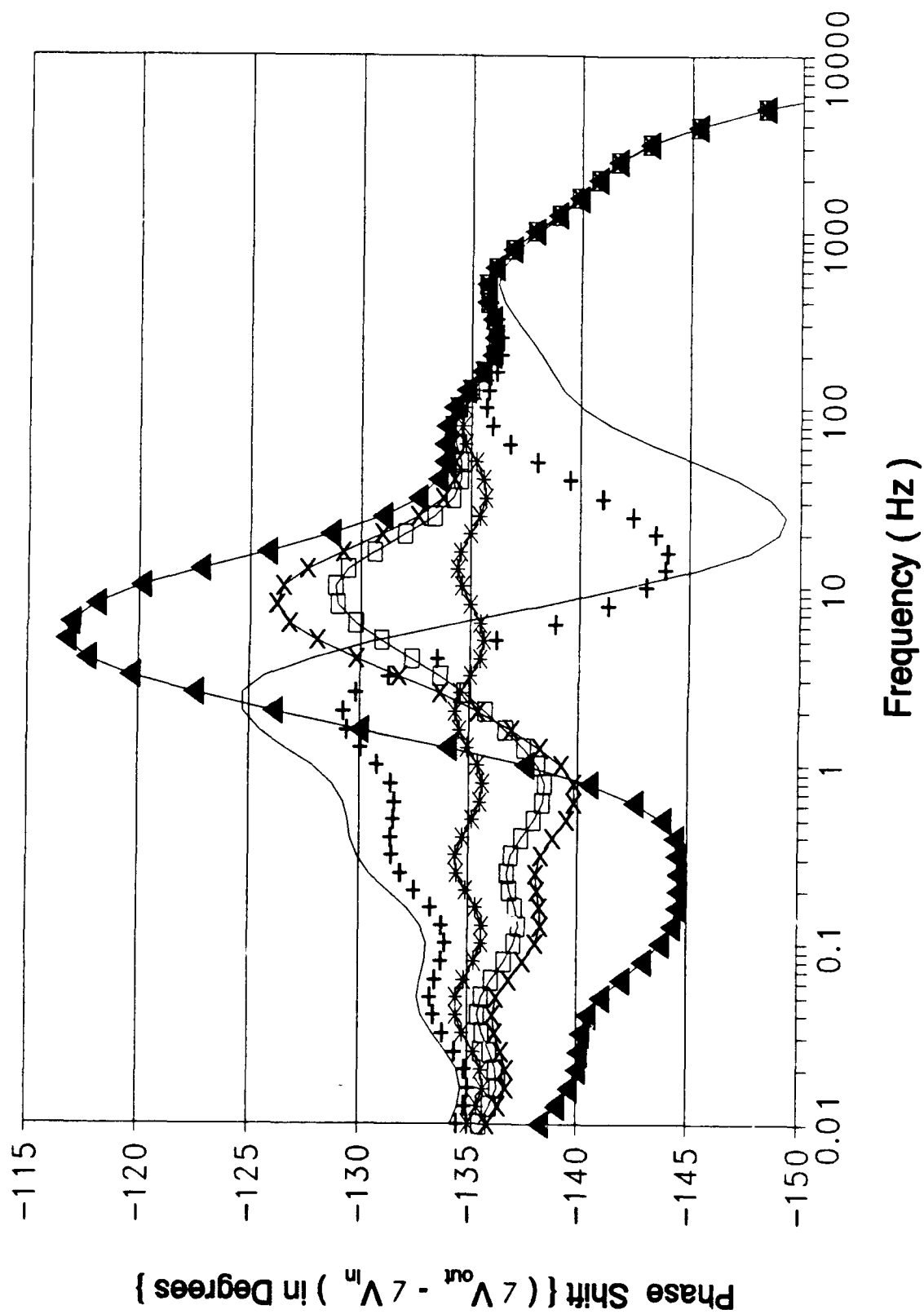
Figure B-7 (cont). Phase Response of the Oldham Circuit Design Using an HSPICE Computer Variation of Resistor 6.

Resistor Values for Figure B-8						
Symbol	——	-+-	-*-	-☐-	—✕—	-▲-
Resis- tor Value (KΩ)	8.74	34.96	87.4 Ideal	139.84	174.8	437

**Figure B-8.   Graphical Symbol Legend and Resistor
Value Correlation for Figure B-8 (cont);**

B-26
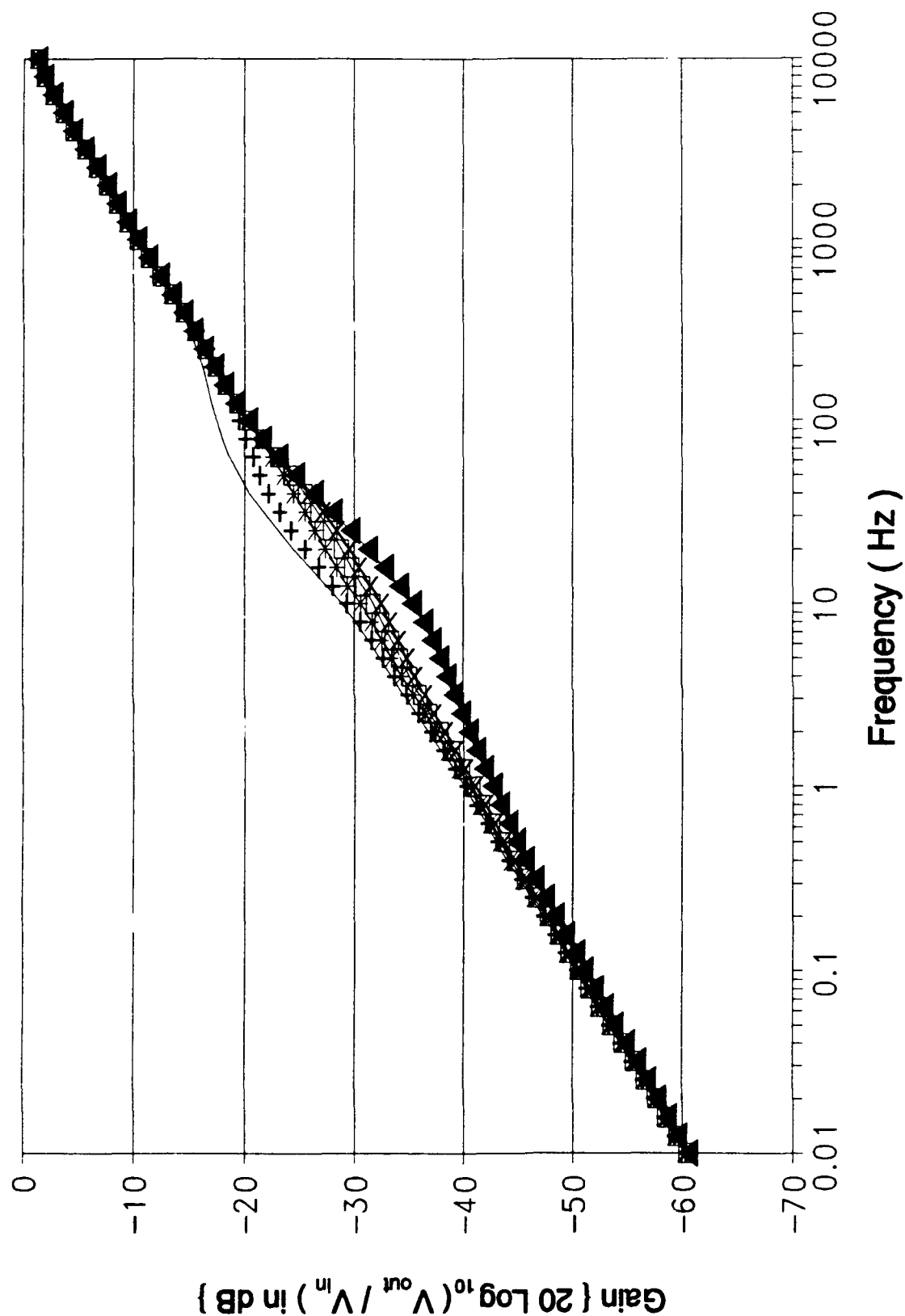
Figure B-8 (cont). Gain Response of the Oldham Circuit Design Using an HSPICE Computer Variation of Resistor 7 (cont).
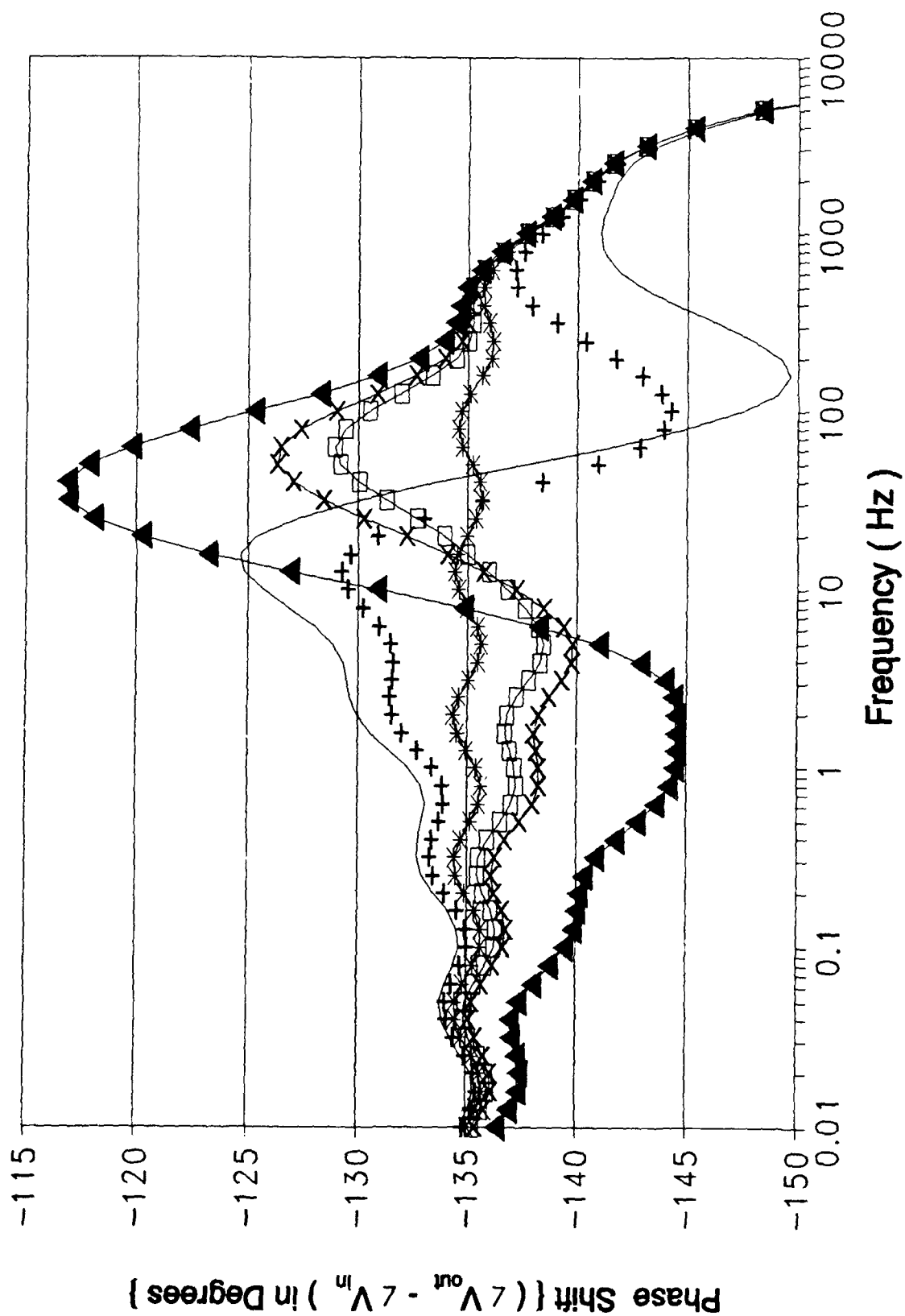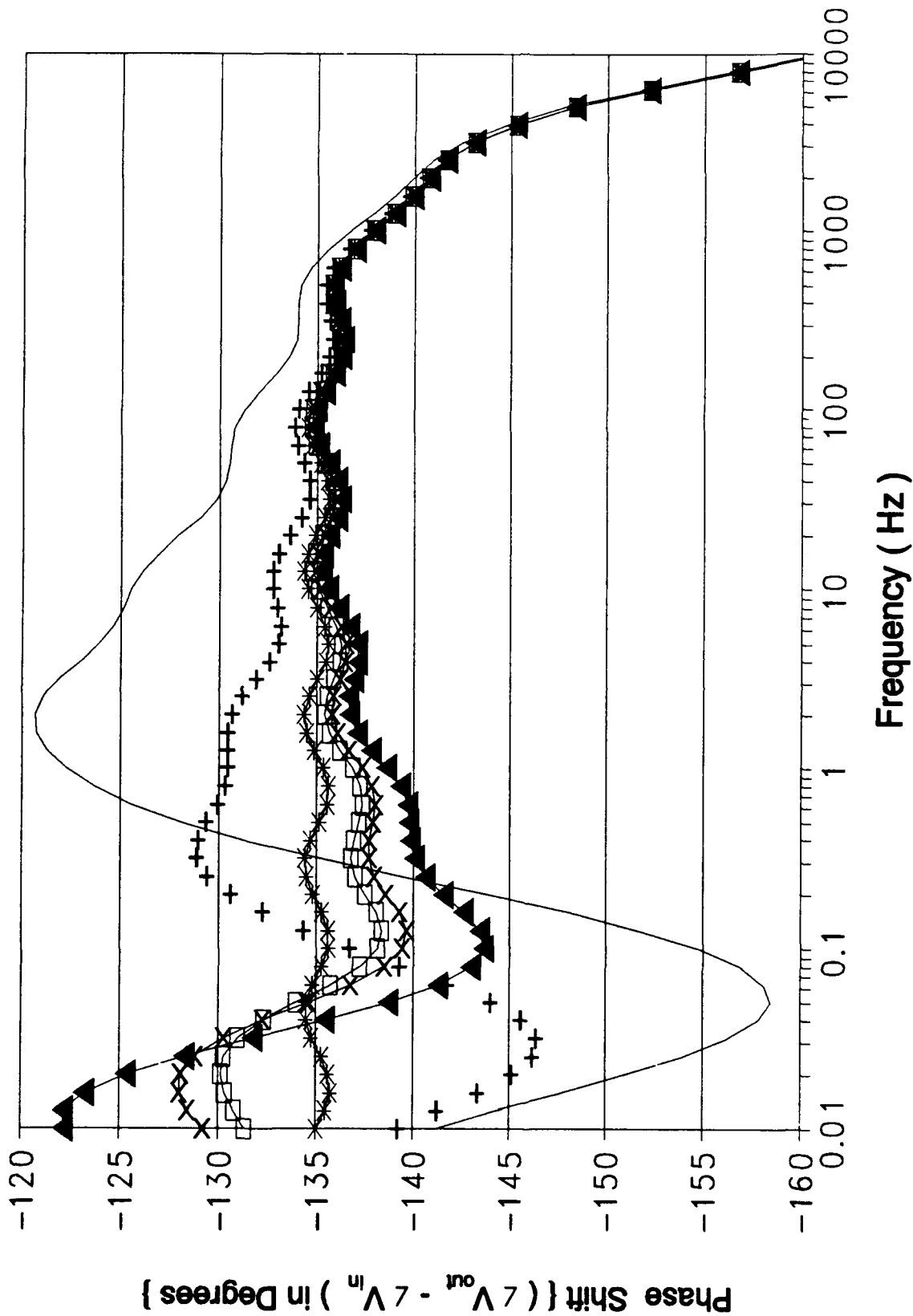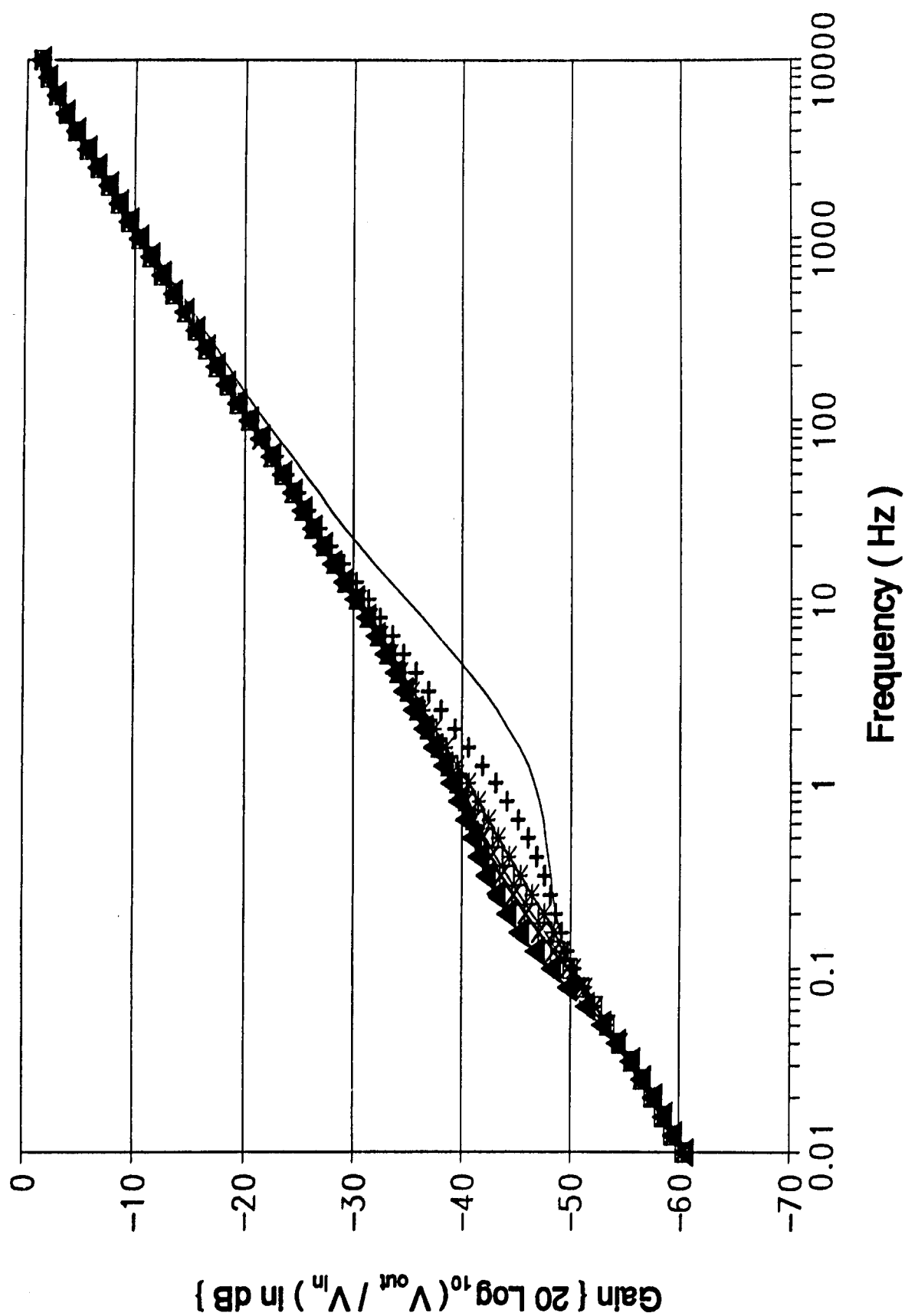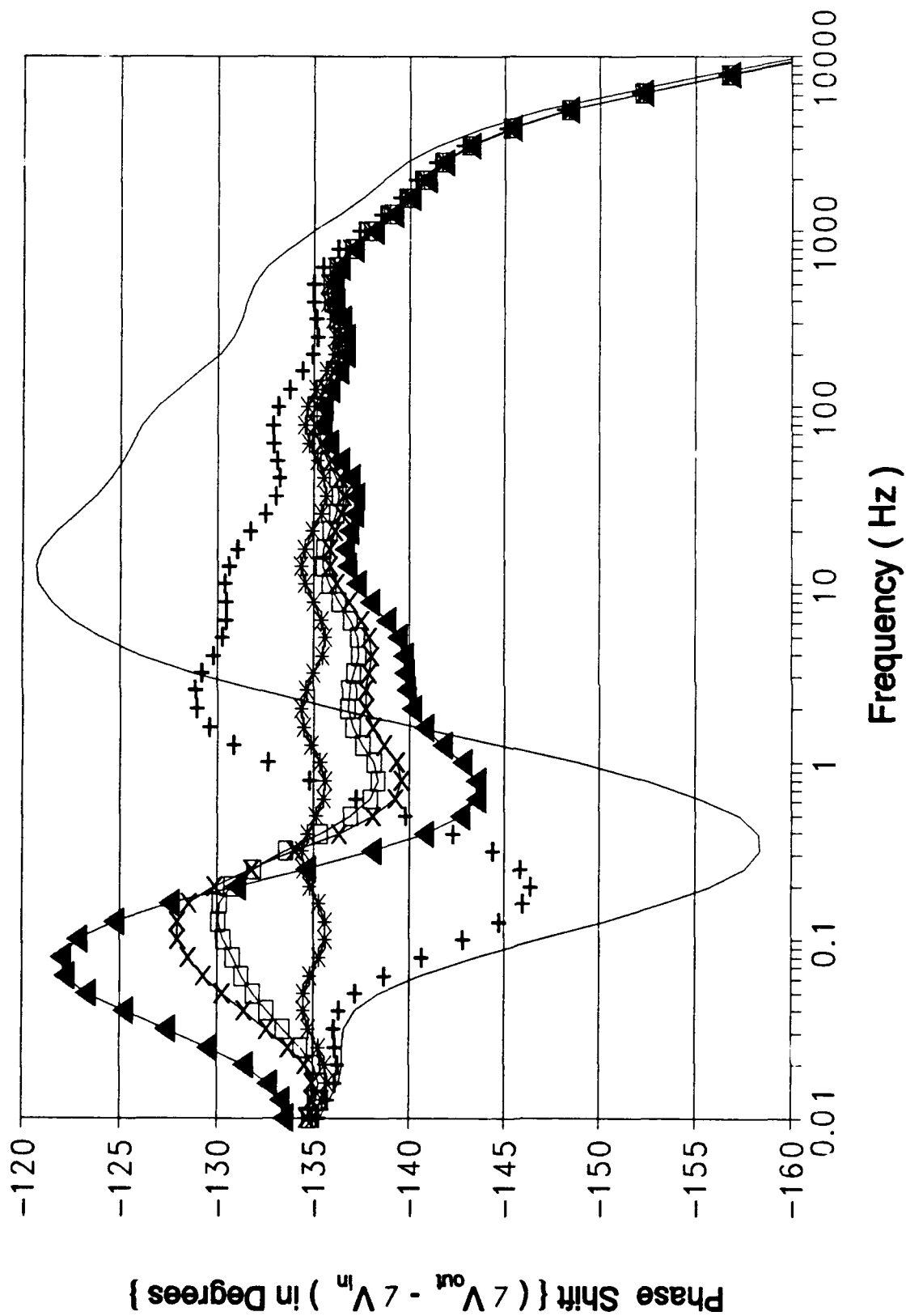
Figure B-8 (cont). Phase Response of the Oldham Circuit Design Using an HSPICE Computer Variation of Resistor 7.

B-28

Resistor Values for Figure B-9						
Symbol	——	-+-	-*-	-▯-	—×—	-▲-
Resis-tor Value (KΩ)	3.397	13.588	33.97 Ideal	54.352	67.94	169.85

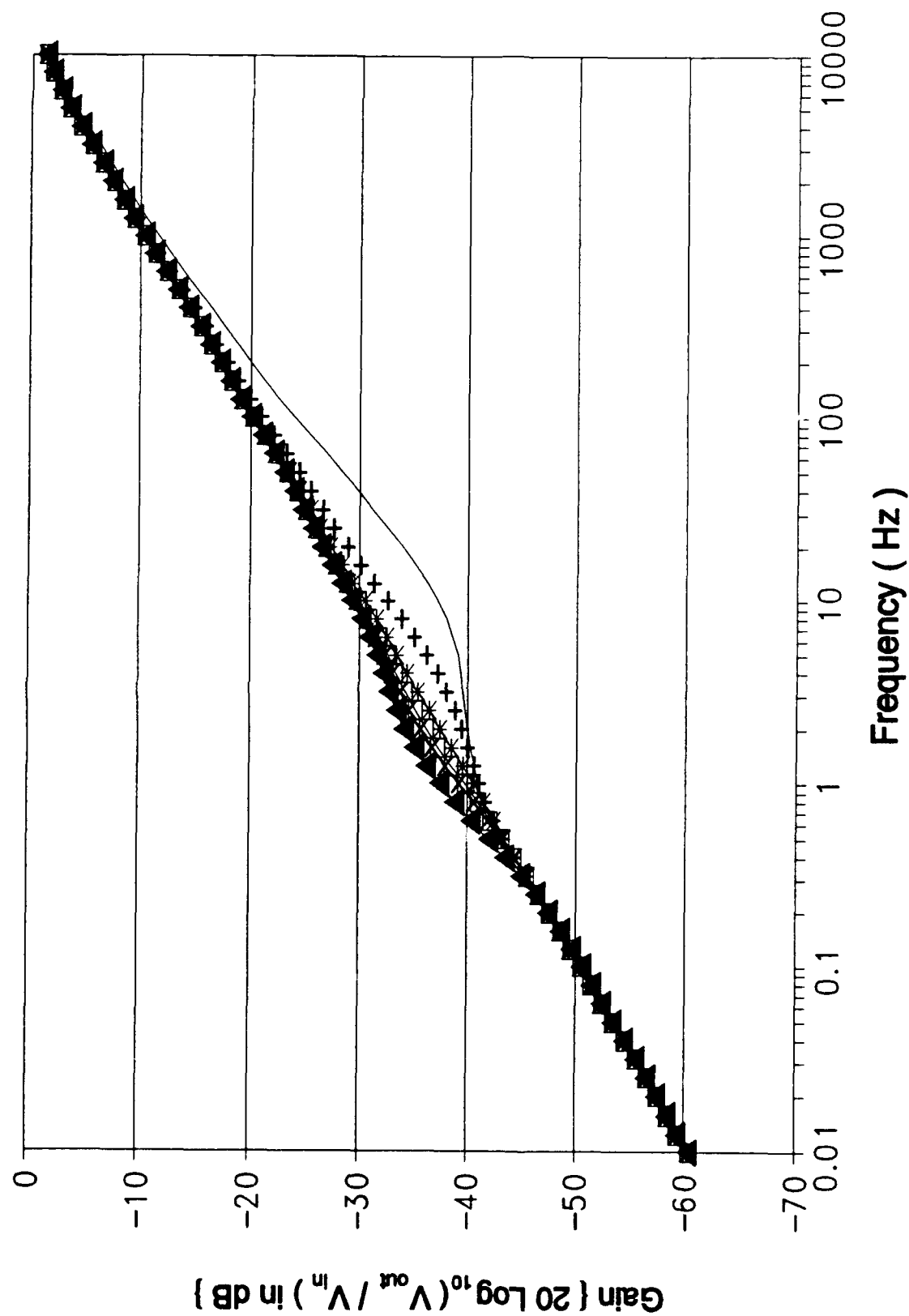**Figure B-9. Graphical Symbol Legend and Resistor Value Correlation for Figure B-9 (cont);**

B-29
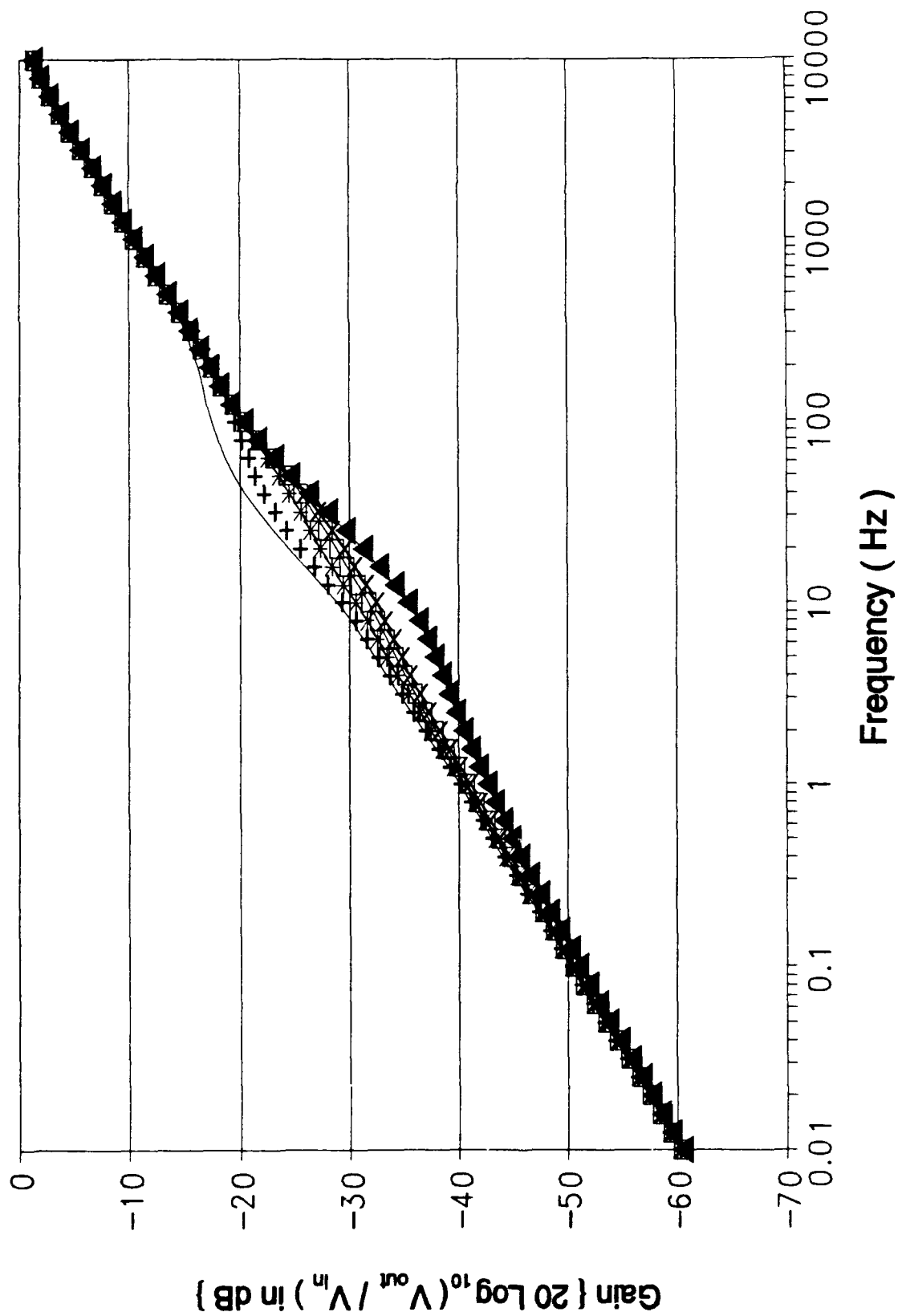
Figure B-9 (cont). Gain Response of the Oldham Circuit Design Using an HSPICE Computer Variation of Resistor 8 (cont);
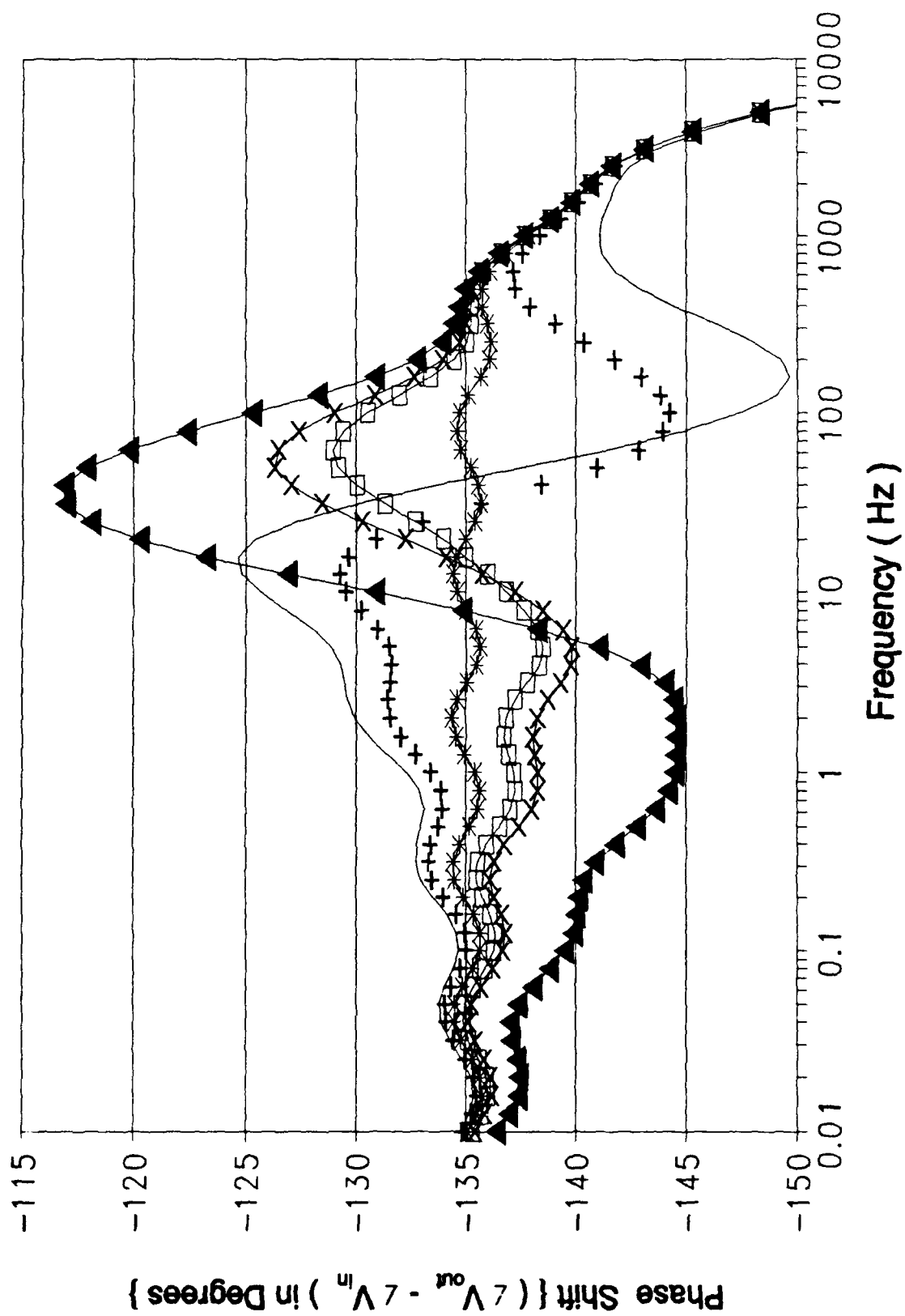
Figure B-9 (cont). Phase Response of the Oldham Circuit Design Using an HSPICE Computer Variation of Resistor 8.

Resistor Values for Figure B-10						
Symbol	——	-+-	-*-	—□—	—×—	-▲-
Resis-tor Value (KΩ)	1.321	5.284	13.21 Ideal	21.136	26.42	66.05

**Figure B-10.   Graphical Symbol Legend and Resistor Value
          Correlation for Figure B-10 (cont);**
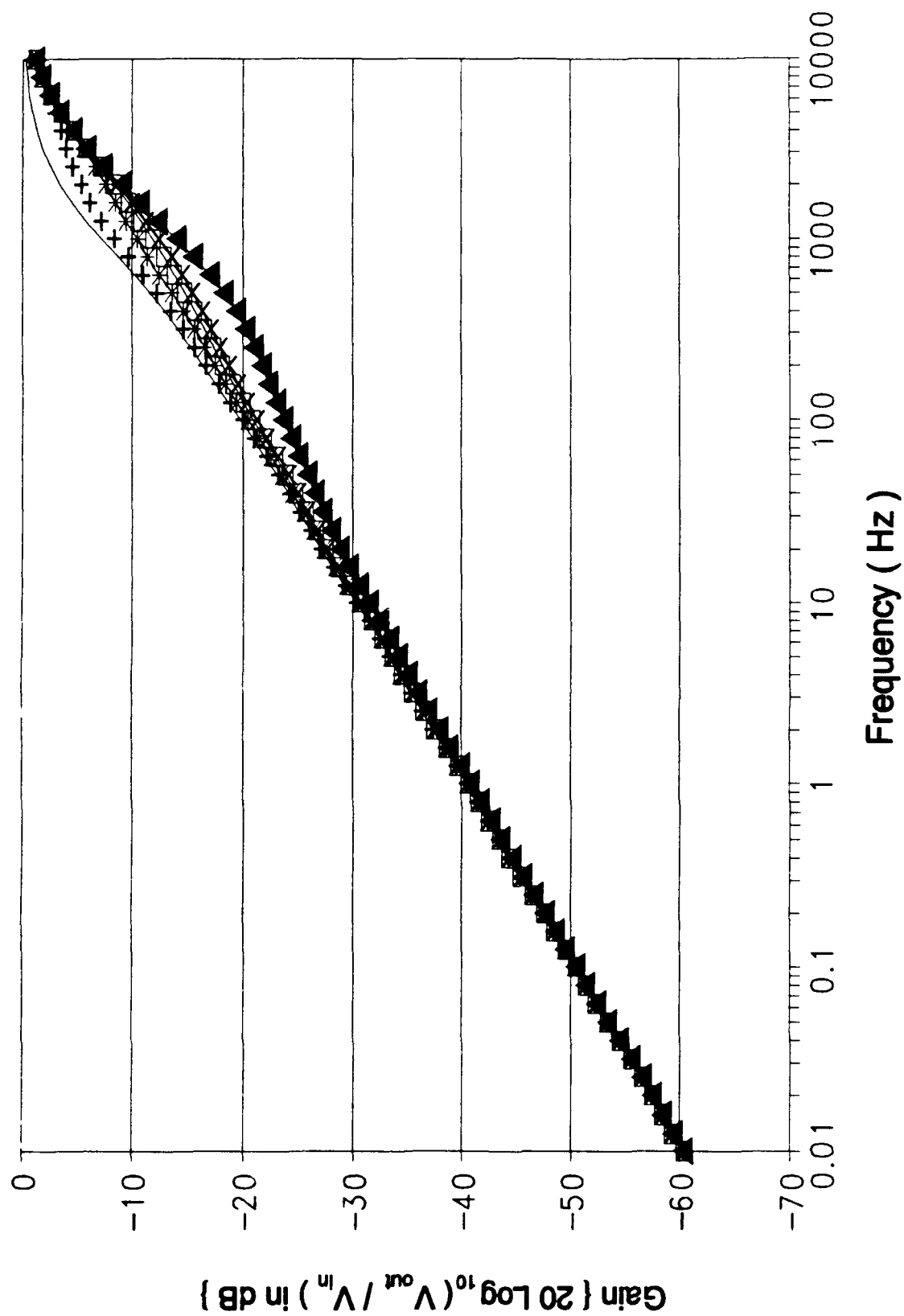
Figure B-10 (cont). Gain Response of the Oldham Circuit Design Using an HSPICE Computer Variation of Resistor 9 (cont);
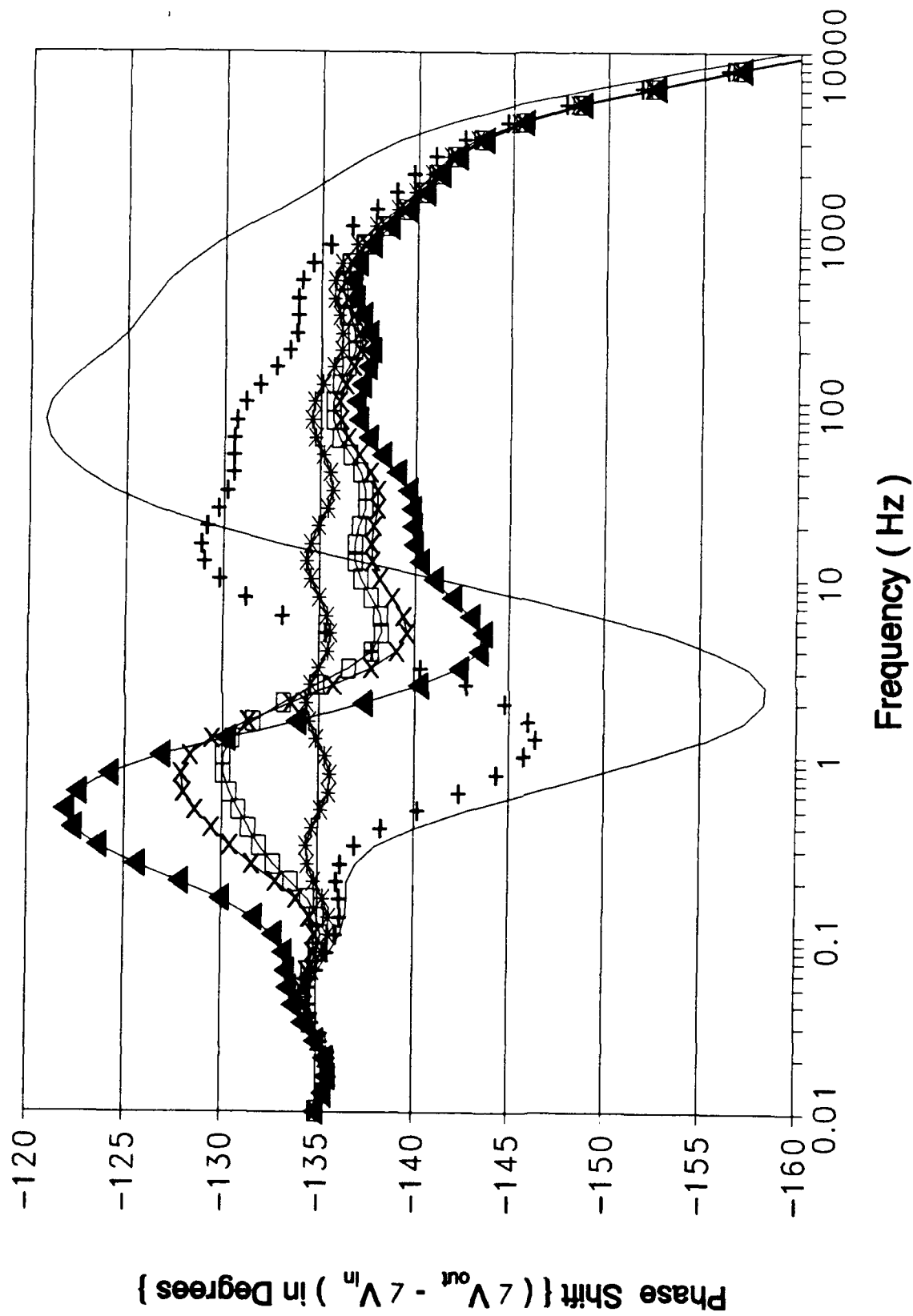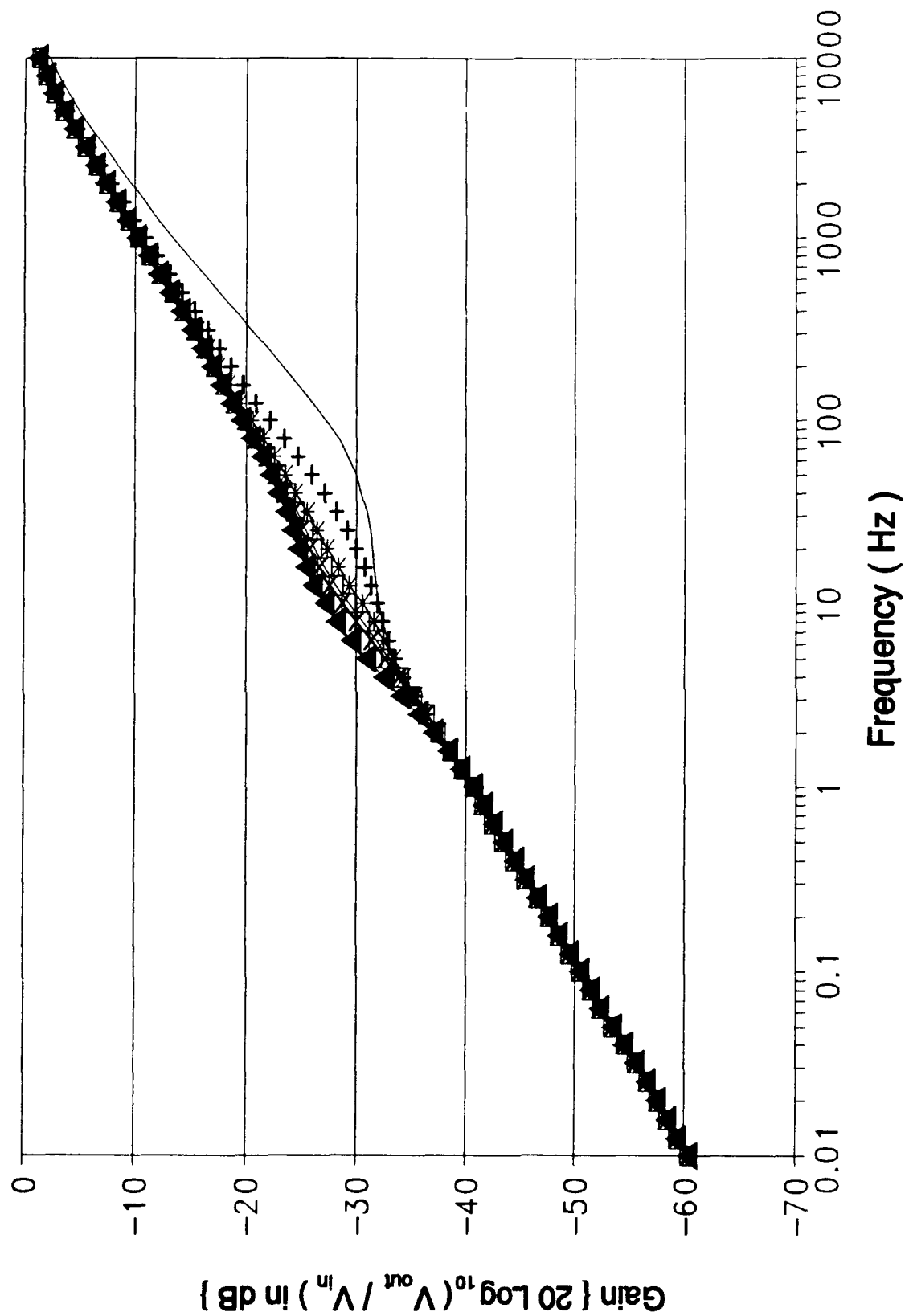
Figure B-10 (cont). Phase Response of the Oldham Circuit Design Using an HSPICE Computer Variation of Resistor 9.

Resistor Values for Figure B-11						
Symbol	——	-+-	-*-	—◻—	—✕—	-▲-
Resis-tor Value (KΩ)	0.5133	2.0532	5.133 Ideal	8.2128	10.27	25.67

Figure B-11.   Graphical Symbol Legend and Resistor Value Correlation for Figure B-11 (cont);

Figure B-11 (cont).   Gain Response of the Oldham Circuit Design Using
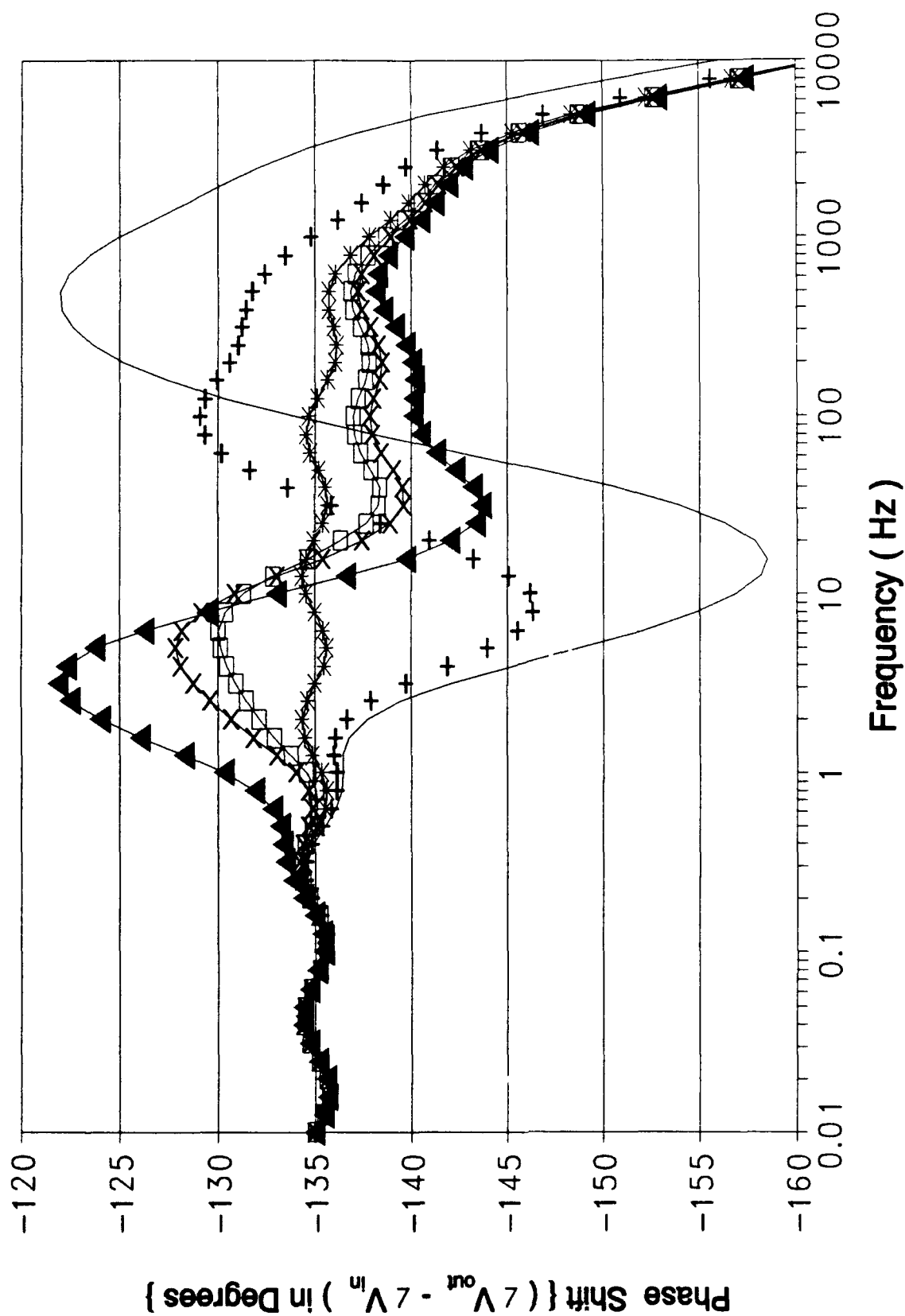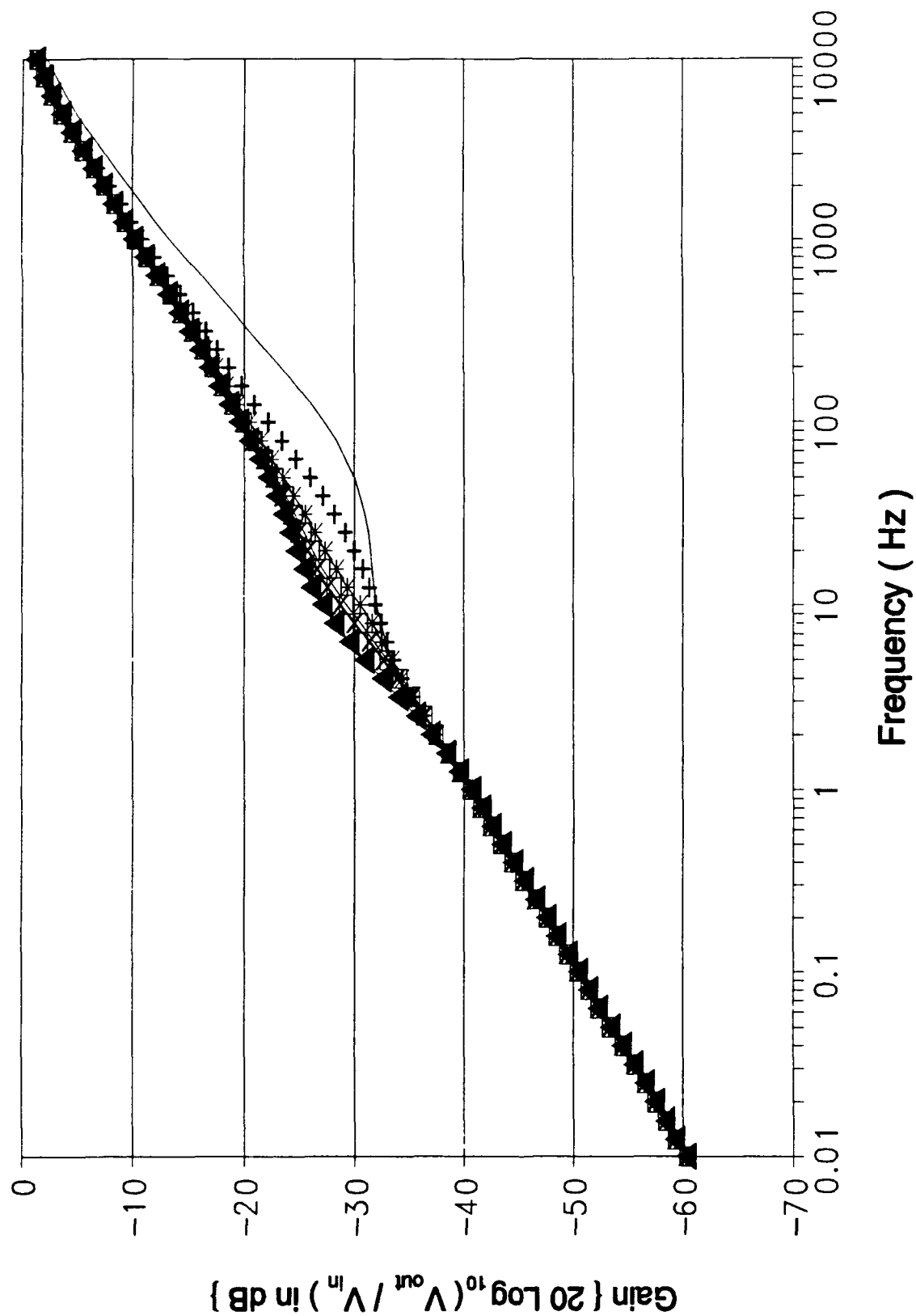an HSPICE Computer Variation of Resistor 11 (cont);

Figure B-11 (cont). Phase Response of the Oldham Circuit Design Using an HSPICE Computer Variation of Resistor 10.

Resistor Values for Figure B-12						
Symbol	——	-+-	-*-	-□-	-x-	-▲-
Resis-tor Value (Ω)	99.75	399	997.5 Ideal	1596	1995	4987.5

Figure B-12.   Graphical Symbol Legend and Resistor Value Correlation for Figure B-12 (cont);

Figure B-12 (cont). Gain Response of the Oldham Circuit Design Using an HSPICE Computer Variation of Resistor 11 (cont);
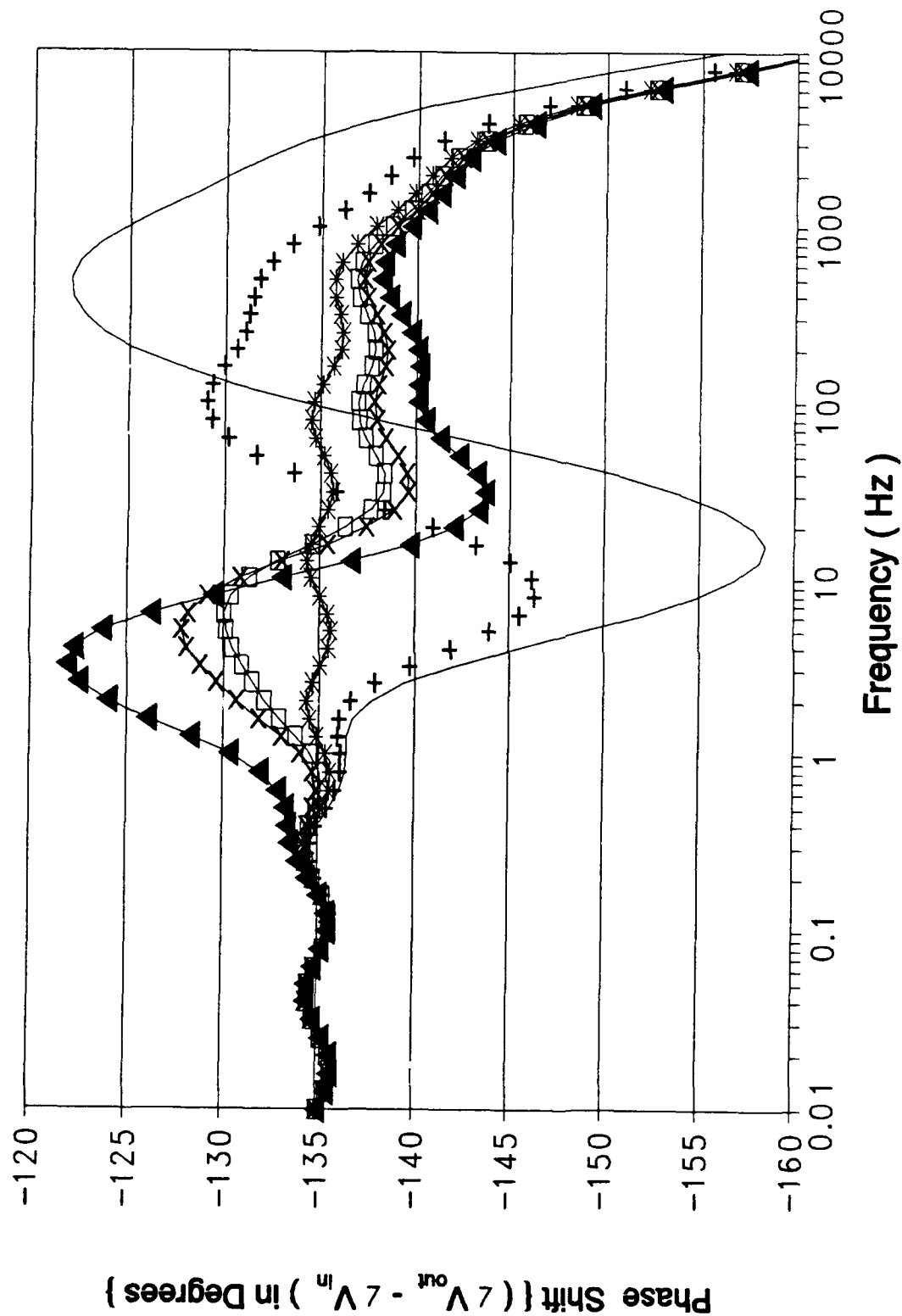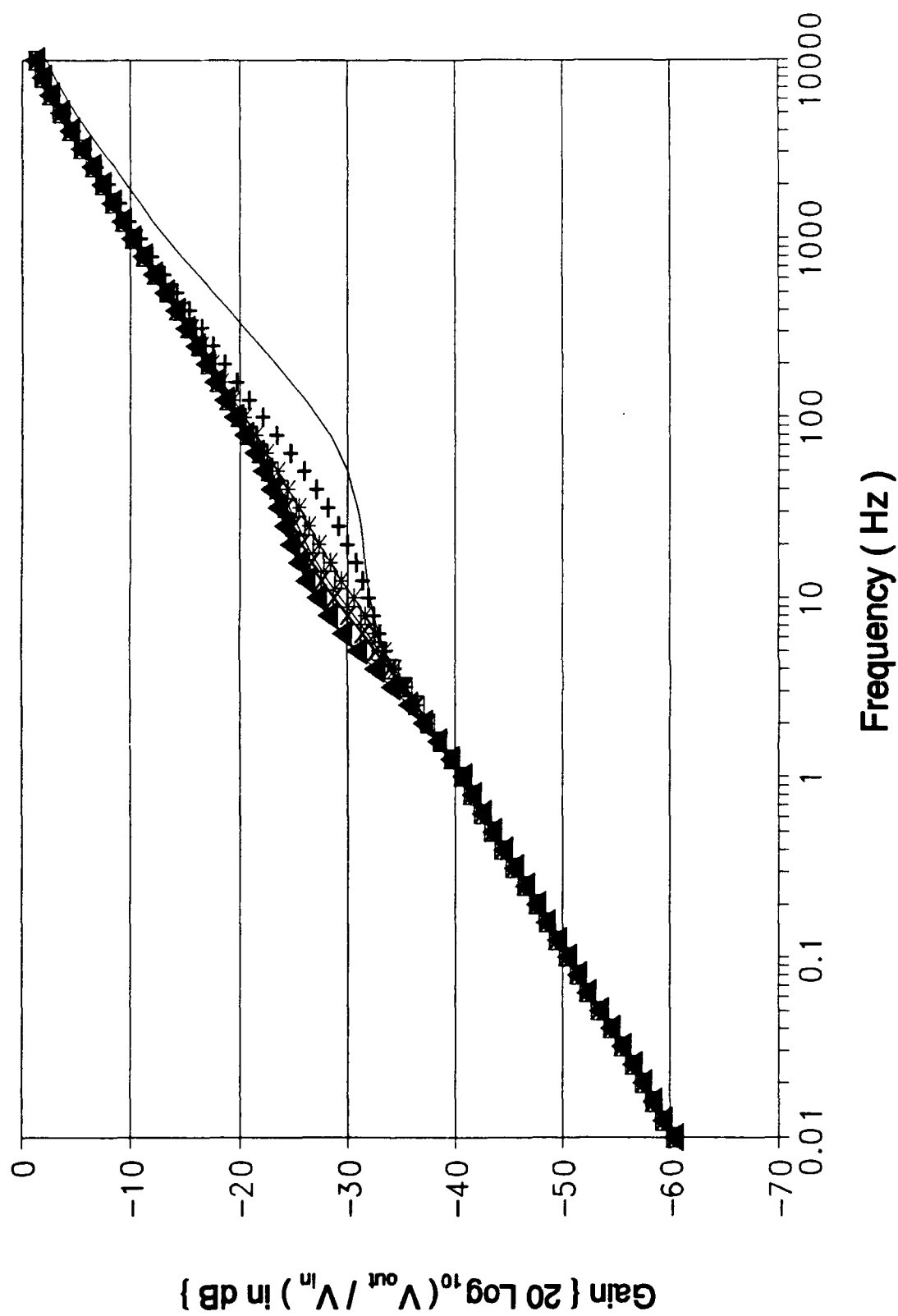
B-39

Figure B-12 (cont). Phase Response of the Oldham Circuit Design Using an HSPICE Computer Variation of Resistor 11.

Resistor Values for Figure B-13						
Symbol	——	-+-	-*-	—□—	—×—	-▲-
Resis-tor Value (KΩ)	0.211	0.844	2.11

Ideal | 3.376 | 4.22 | 10.55 |

**Figure B-13. Graphical Symbol Legend and Resistor Value
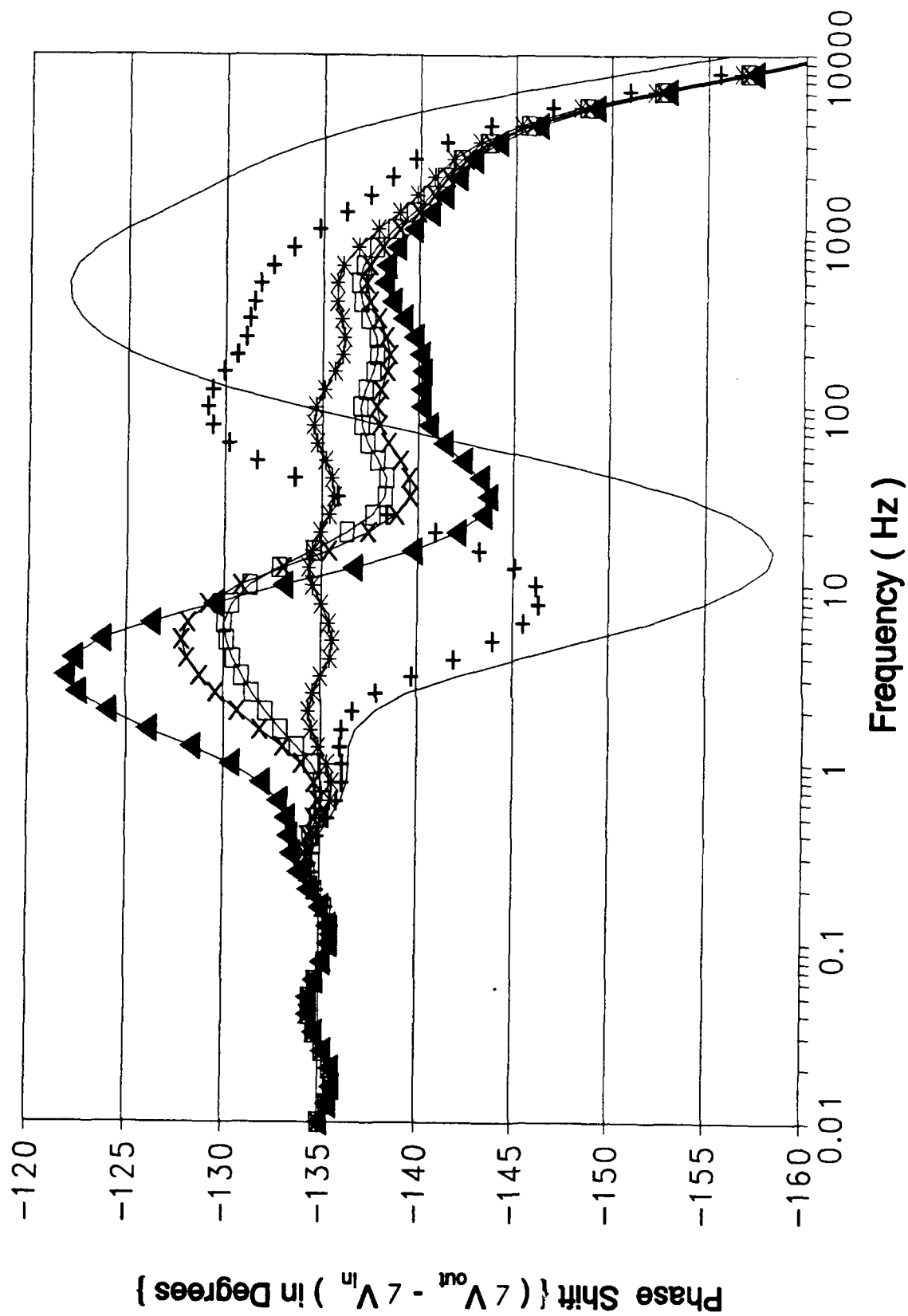Correlation for Figure B-13 (cont);**

Figure B-13 (cont). Gain Response of the Oldham Circuit Design Using an HSPICE Computer Variation of Resistor 12 (cont);

Figure B-13(cont). Phase Response of the Oldham Circuit Design Using an HSPICE Computer Variation of Resistor 12.

B-43

Capacitor Values for Figure B-14						
Symbol	——	-+-	-*-	-□-	-x-	-▲-
Capaci -tor Value (μf)	1.651	6.604	16.51 Ideal	26.416	33.02	82.55

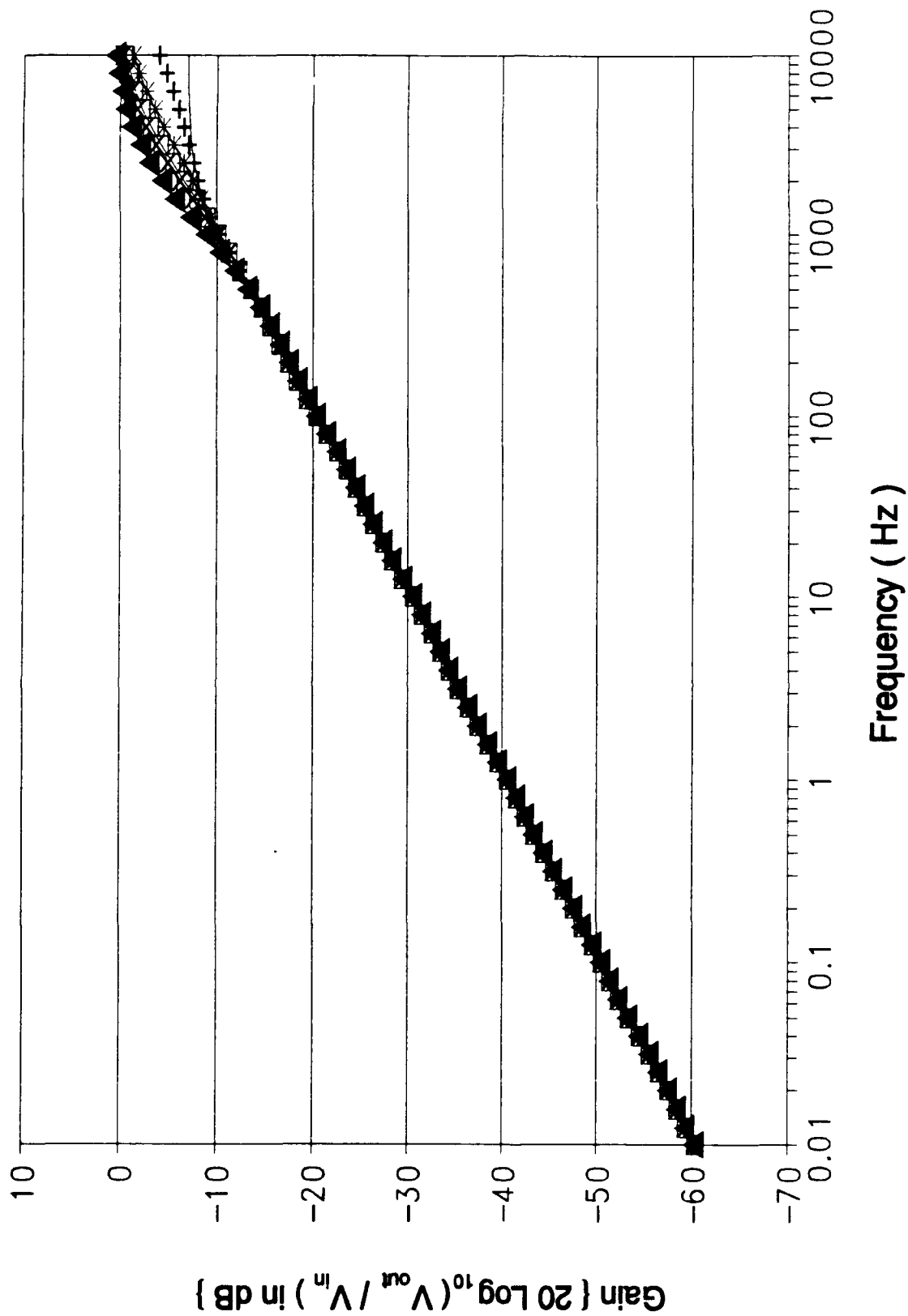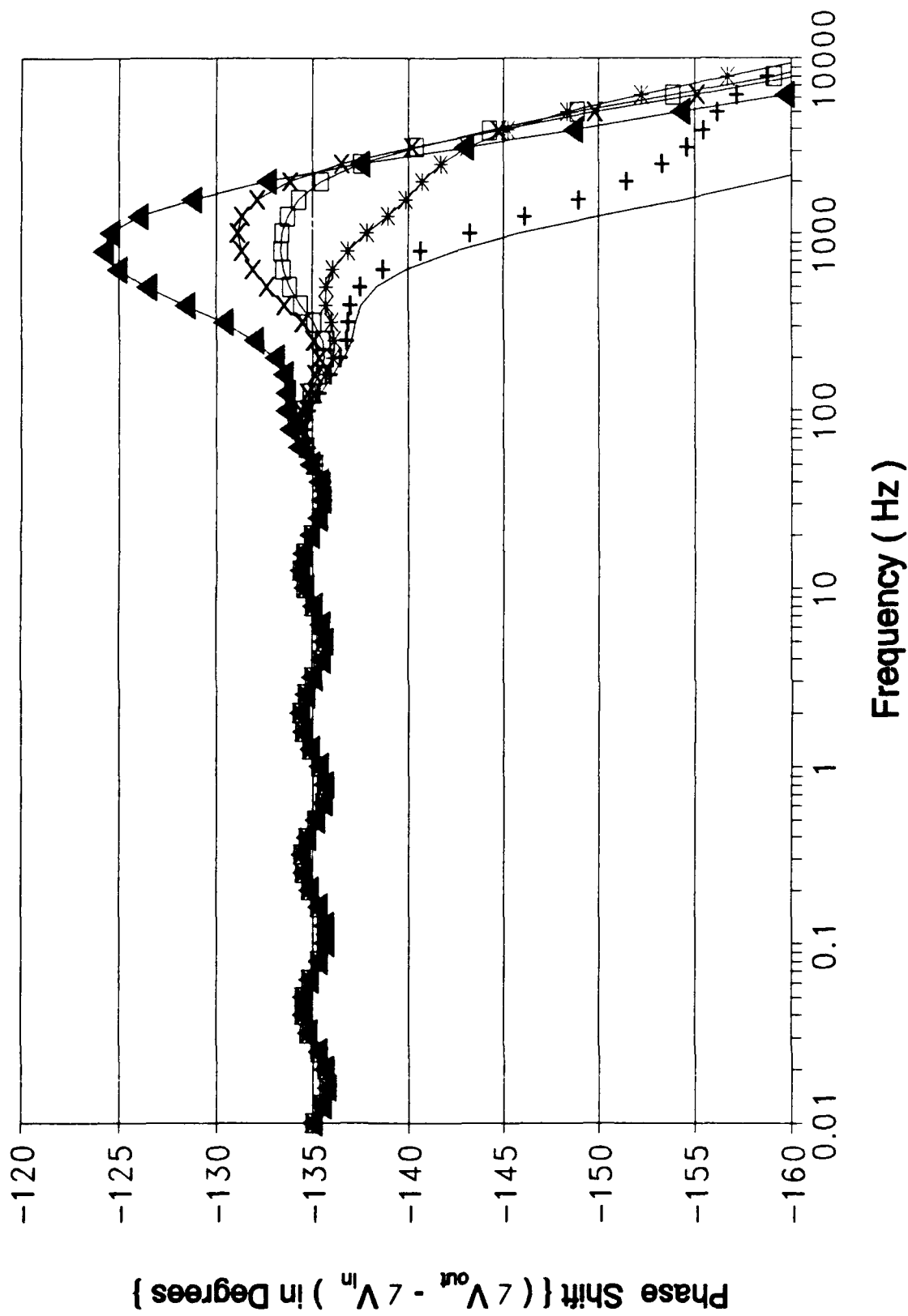**Figure B-14. Graphical Symbol Legend and Capacitor Value Correlation for Figure B-14 (cont);**

Figure B-14 (cont). Gain Response of the Oldham Circuit Design Using an HSPICE Computer Variation of Capacitor O (cont);

Figure B-14 (cont). Phase Response of the Oldham Circuit Design Using an HSPICE Computer Variation of Capacitor 0.

B-46

Capacitor Values for Figure B-15						
Symbol	——	-+-	-*-	-◻-	-×-	-▲-
Capaci -tor Value (μf)	1.000	4.00	10.00 Ideal	16.00	20.00	50.00

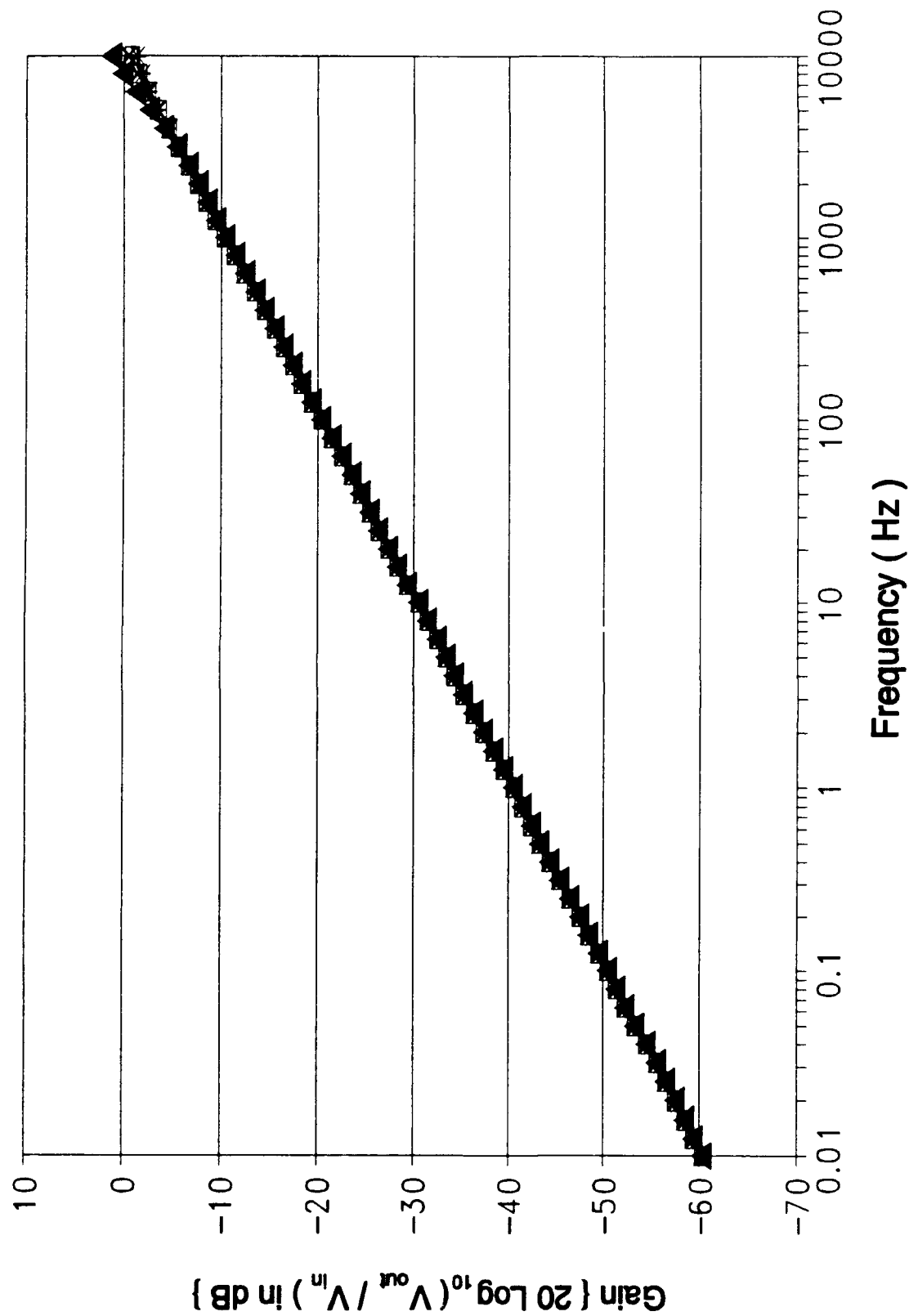**Figure B-15.   Graphical Symbol Legend and Capacitor Value Correlation for Figure B-15 (cont);**

Figure B-15 (cont). Gain Response of the Oldham Circuit Design Using an HSPICE Computer Variation of Capacitor 1 (cont).

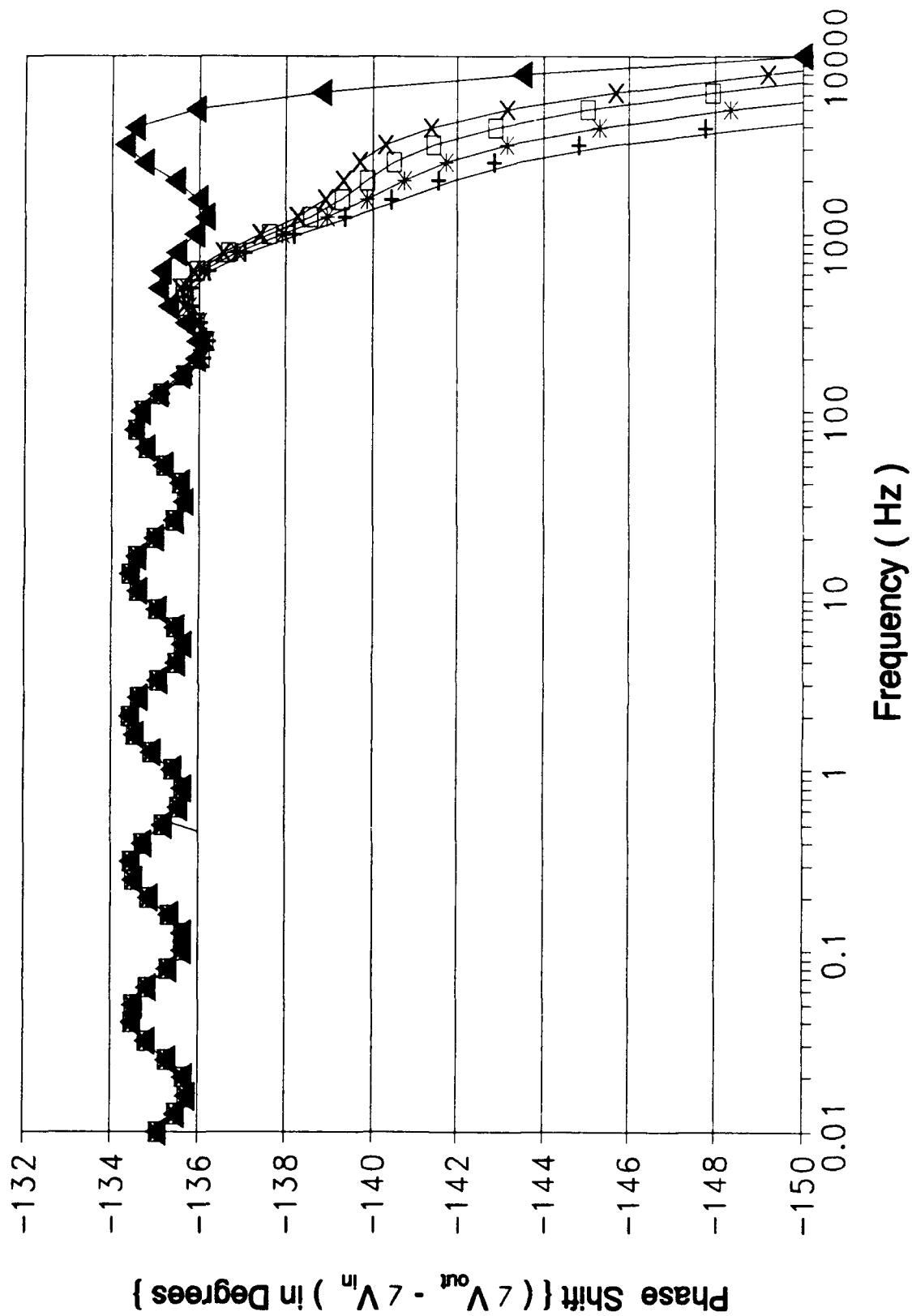Figure B-15 (cont). Phase Response of the Oldham Circuit Design Using an HSPICE Computer Variation of Capacitor 1.

Capacitor Values for Figure B-16						
Symbol	——	-+-	-*-	—▯—	—×—	-▲-
Capaci -tor Value (μf)	0.388	1.552	3.88 Ideal	6.208	7.76	19.4

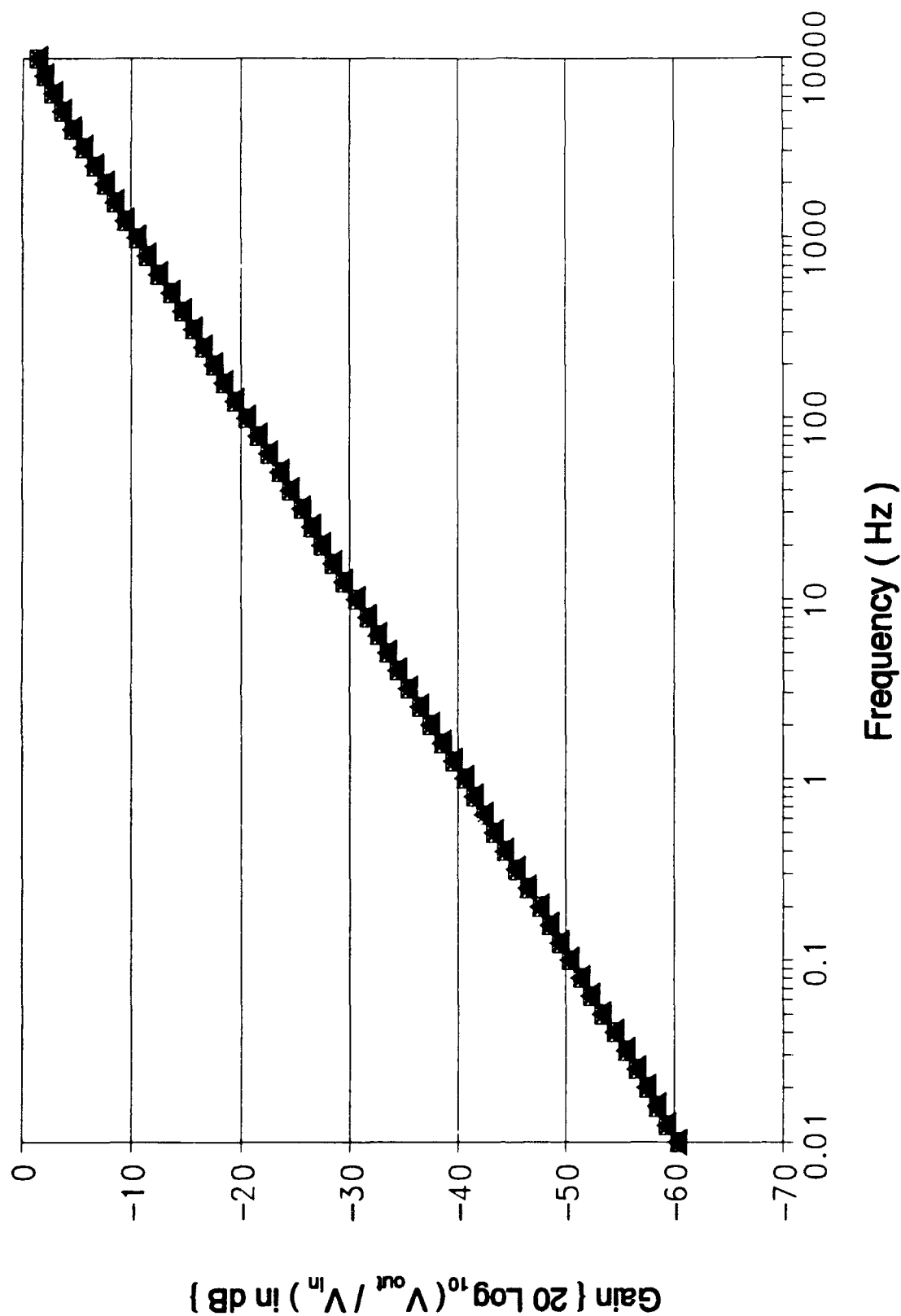**Figure B-16. Graphical Symbol Legend and Capacitor Value Correlation for Figure B-16 (cont);**

Figure B-16 (cont). Gain Response of the Oldham Circuit Design Using an HSPICE Computer Variation of Capacitor 2 (cont).
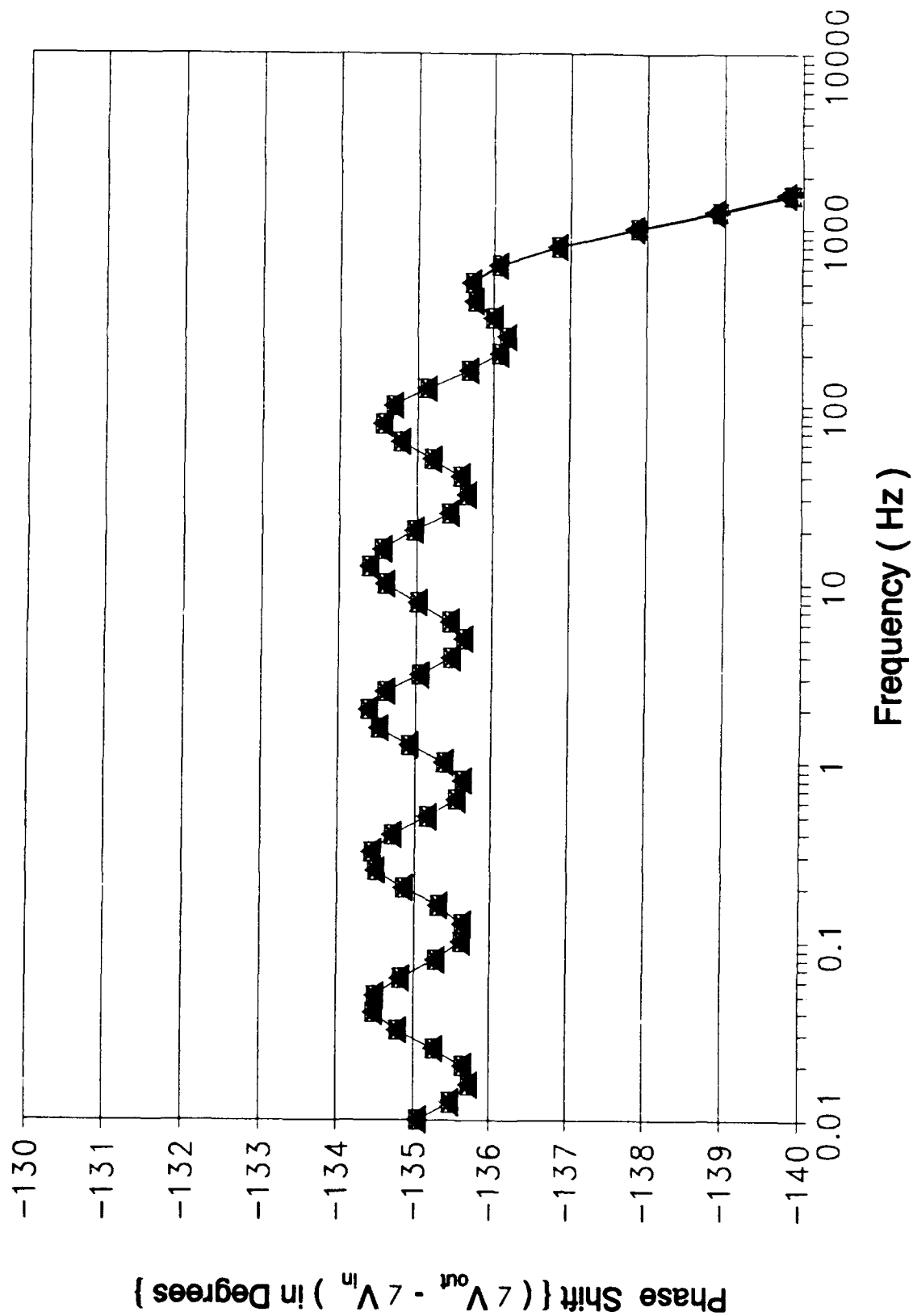
Figure B-16 (cont). Phase Response of the Oldham Circuit Design Using an HSPICE Computer Variation of Capacitor 2.

Capacitor Values for Figure B-17						
Symbol	——	-+-	-*-	—□—	—×—	-▲-
Capaci-tor Value (μf)	0.1514	0.6056	1.514 Ideal	2.4224	3.028	7.57

Figure B-17.   Graphical Symbol Legend and Capacitor Value
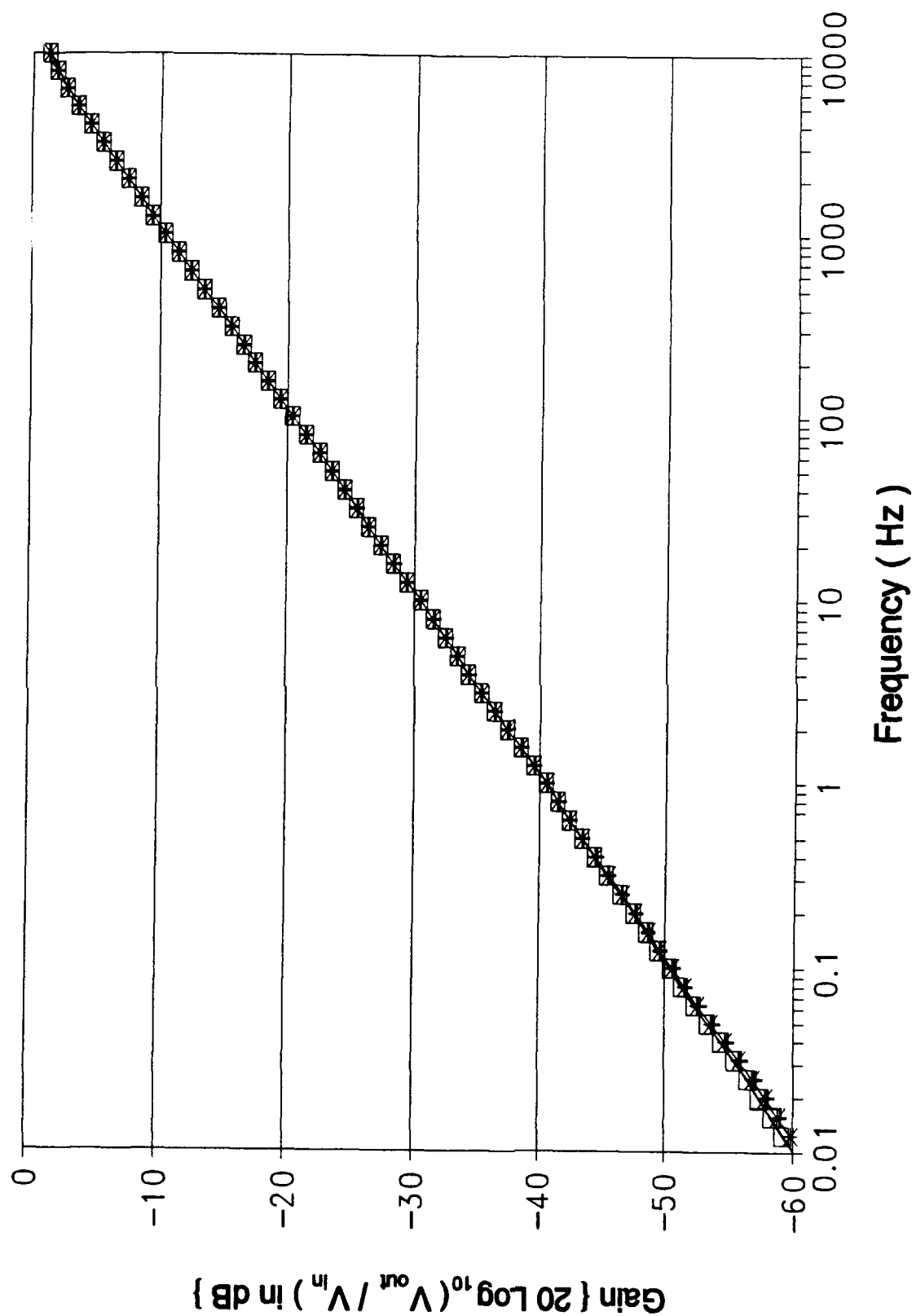   Correlation for Figure B-17 (cont);

Figure B-17 (cont). Gain Response of the Oldham Circuit Design Using an HSPICE Computer Variation of Capacitor 3 (cont).
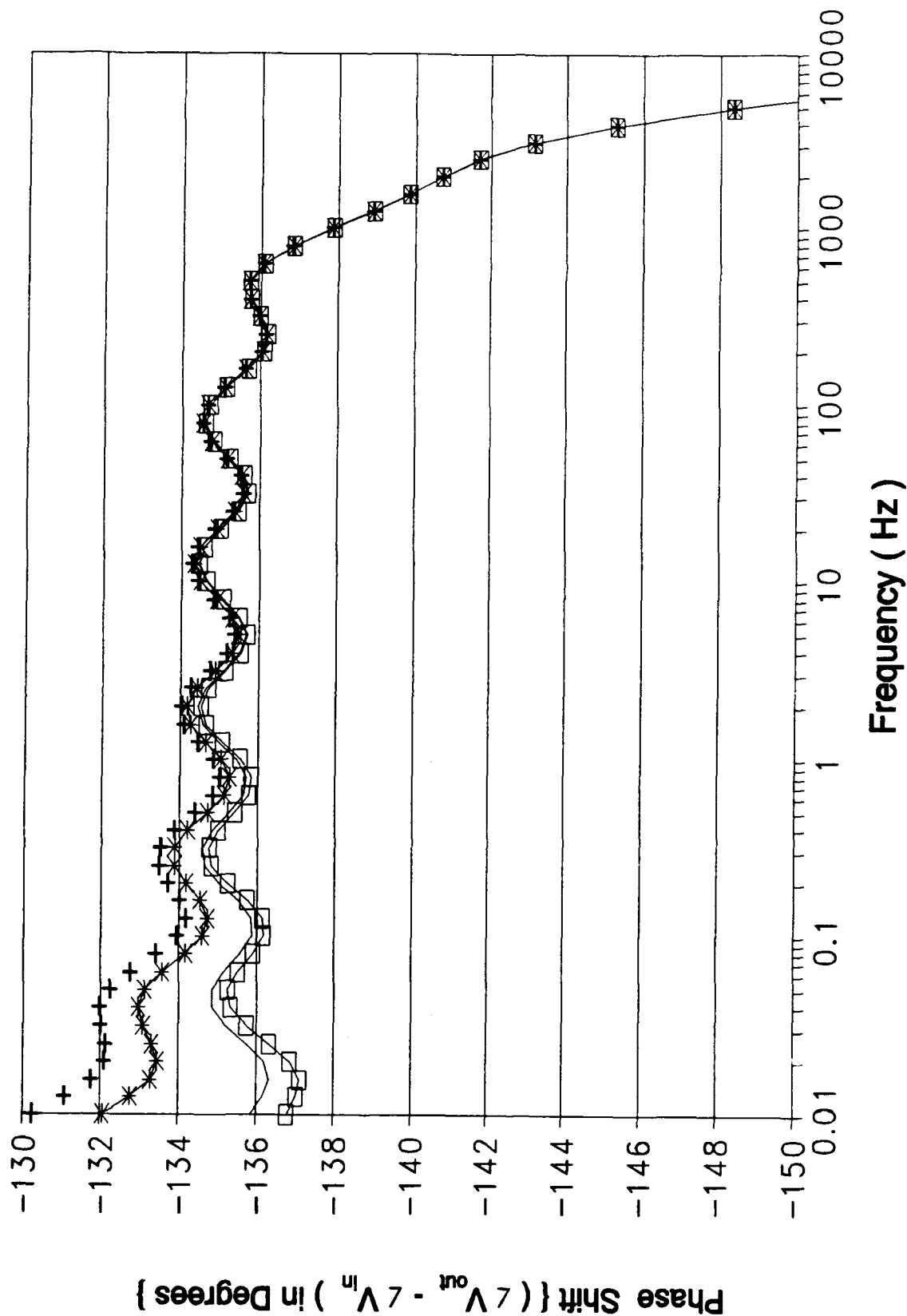
Figure B-17(cont). Phase Response of the Oldham Circuit Design Using an HSPICE Computer Variation of Capacitor 3.

Capacitor Values for Figure B-18						
Symbol	——	-+-	-*-	-□-	-×-	-▲-
Capaci -tor Value (nf)	58.73	234.92	587.3 Ideal	939.68	1174.6	2936.5

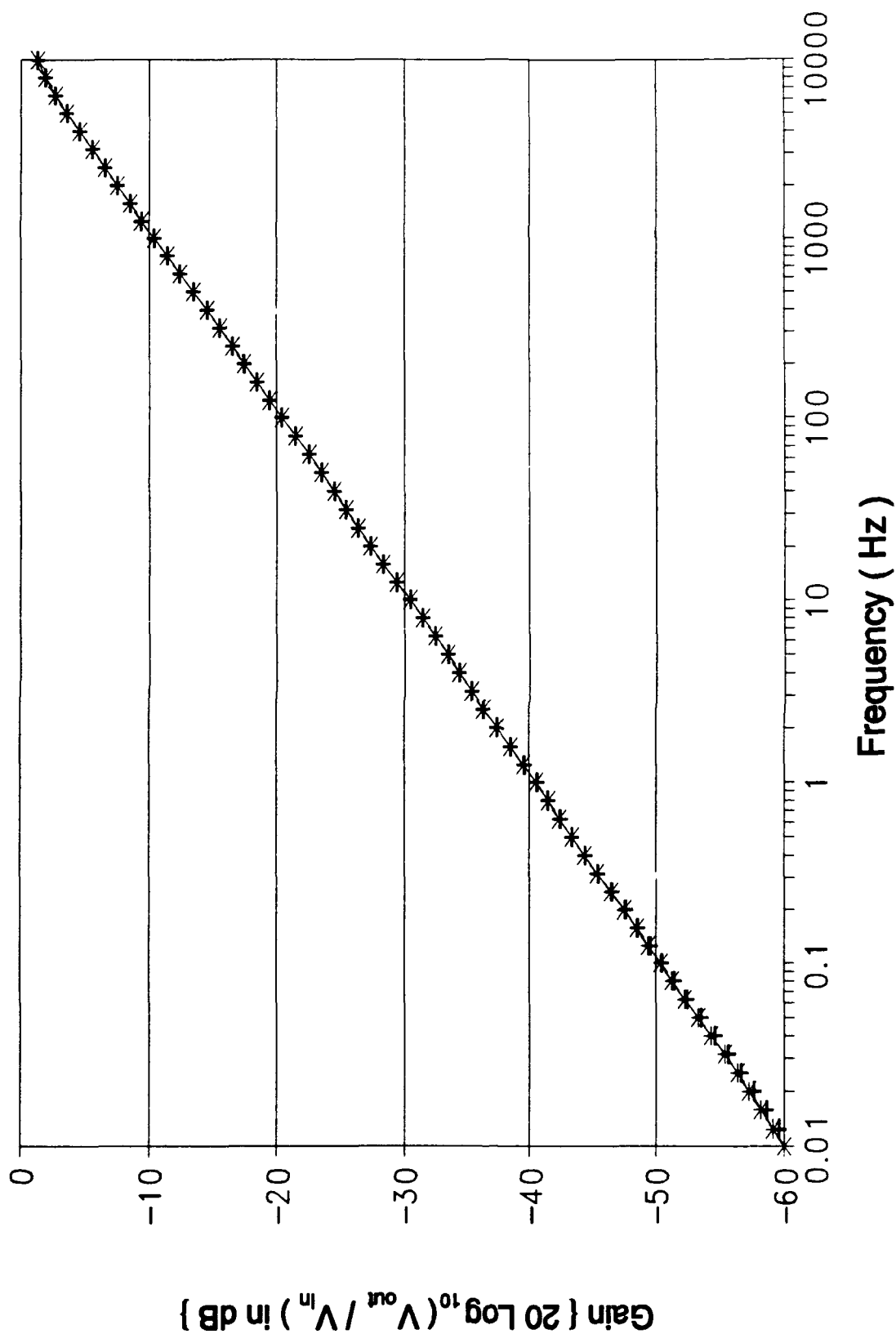**Figure B-18.** **Graphical Symbol Legend and Capacitor Value Correlation for Figure B-18 (cont);**

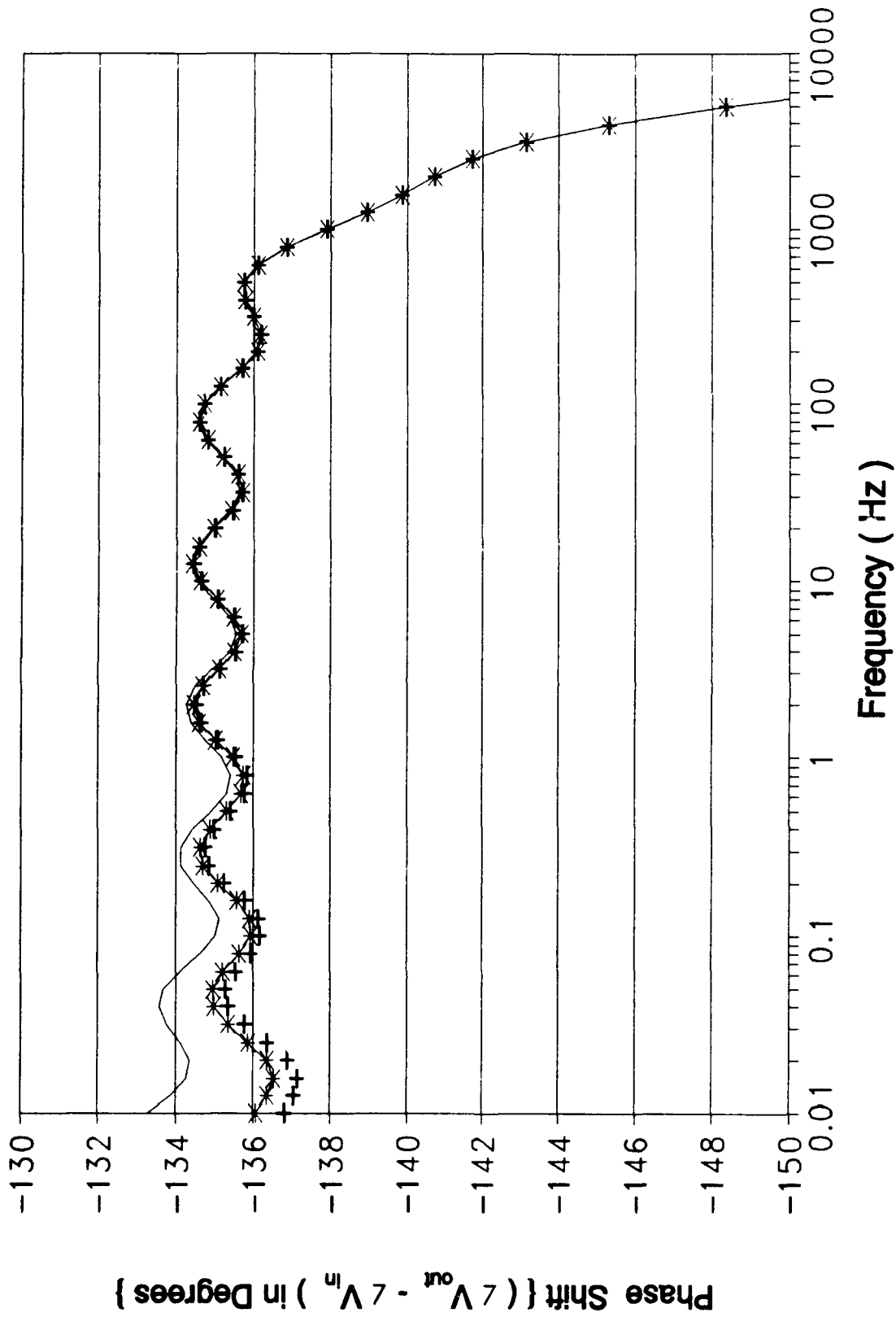Figure B-18 (cont). Gain Response of the Oldham Circuit Design Using an HSPICE Computer Variation of Capacitor 4 (cont);

Figure B-18 (cont). Phase Response of the Oldham Circuit Design Using an HSPICE Computer Variation of Capacitor 4.

Capacitor Values for Figure B-19						
Symbol	——	-+-	-*-	-□-	-×-	-▲-
Capaci -tor Value (nf)	22.83	91.32	228.3 Ideal	365.28	456.6	1141.5

Figure B-19. Graphical Symbol Legend and Capacitor Value Correlation for Figure B-19 (cont);

Frequency (Hz)

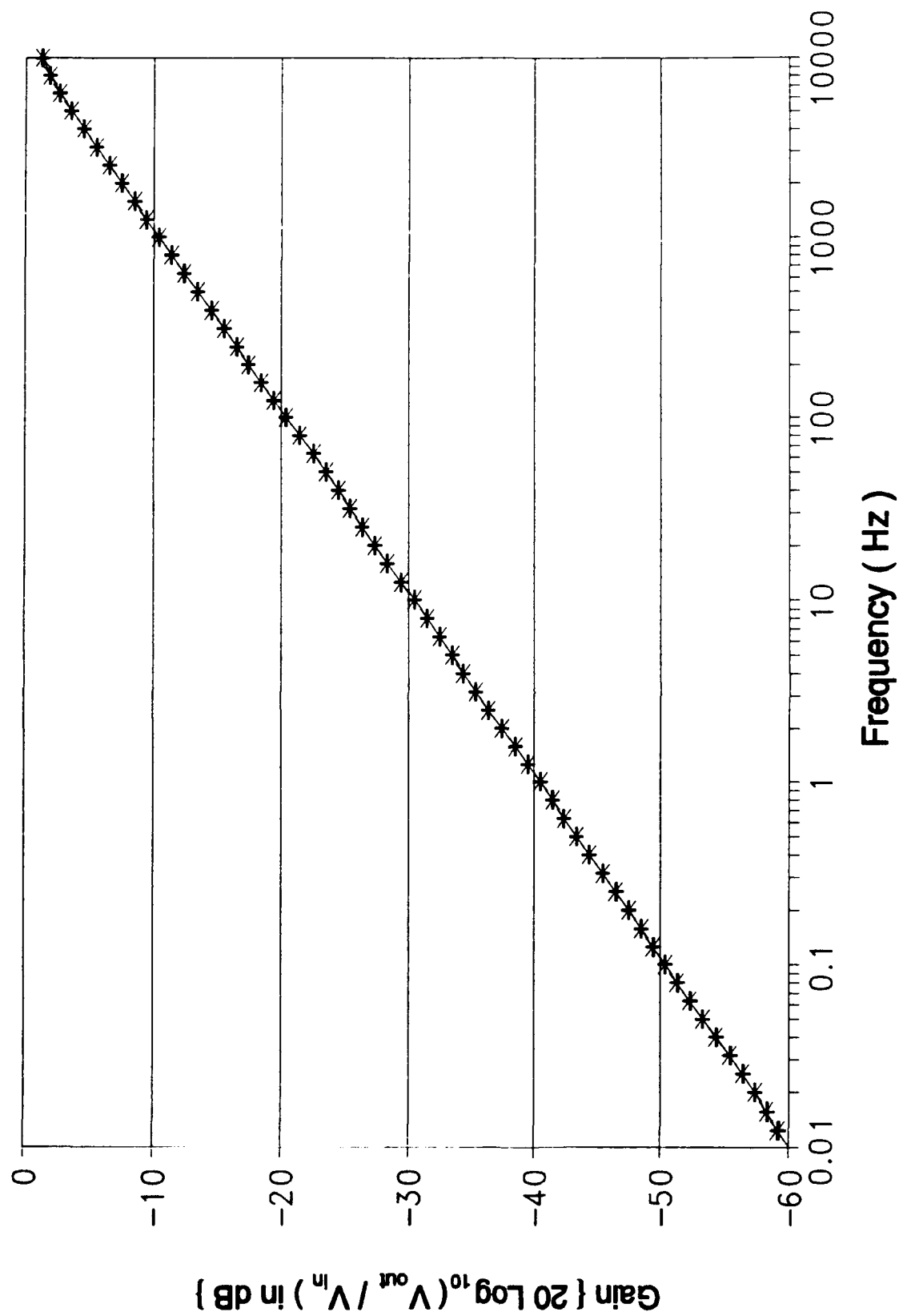Gain { 20 Log$_{10}$ (V$_{out}$ / V$_{in}$) in dB }

Figure B-19 (cont). Gain Response of the Oldham Circuit Design Using an HSPICE Computer Variation of Capacitor 5 (cont);
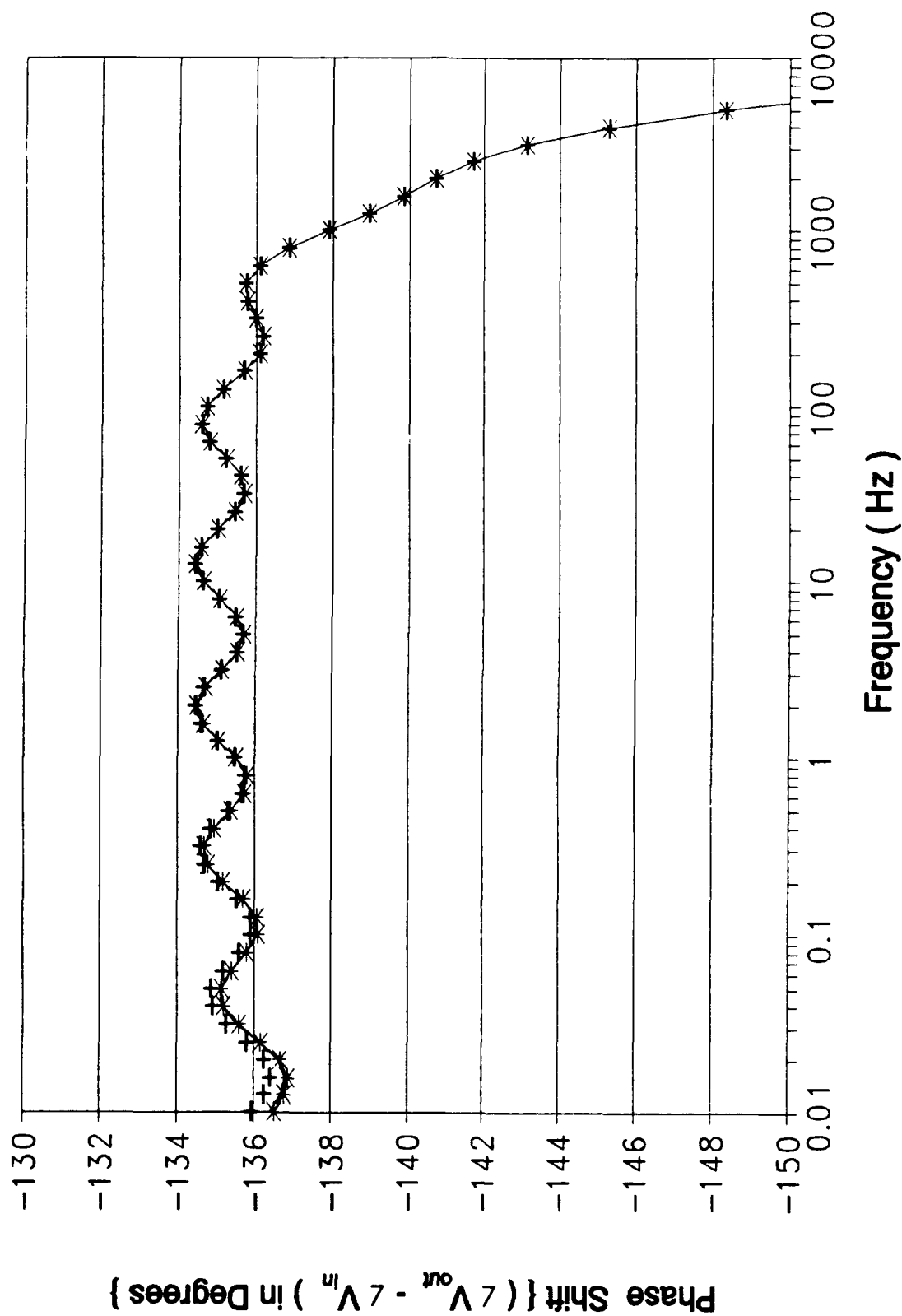
Figure B-19 (cont). Phase Response of the Oldham Circuit Design Using an HSPICE Computer Variation of Capacitor 5.

Capacitor Values for Figure B-20						
Symbol	——	-+-	-*-	-▢-	-×-	-▲-
Capaci-tor Value (nf)	8.873	35.492	88.73 Ideal	141.97	177.46	43.65

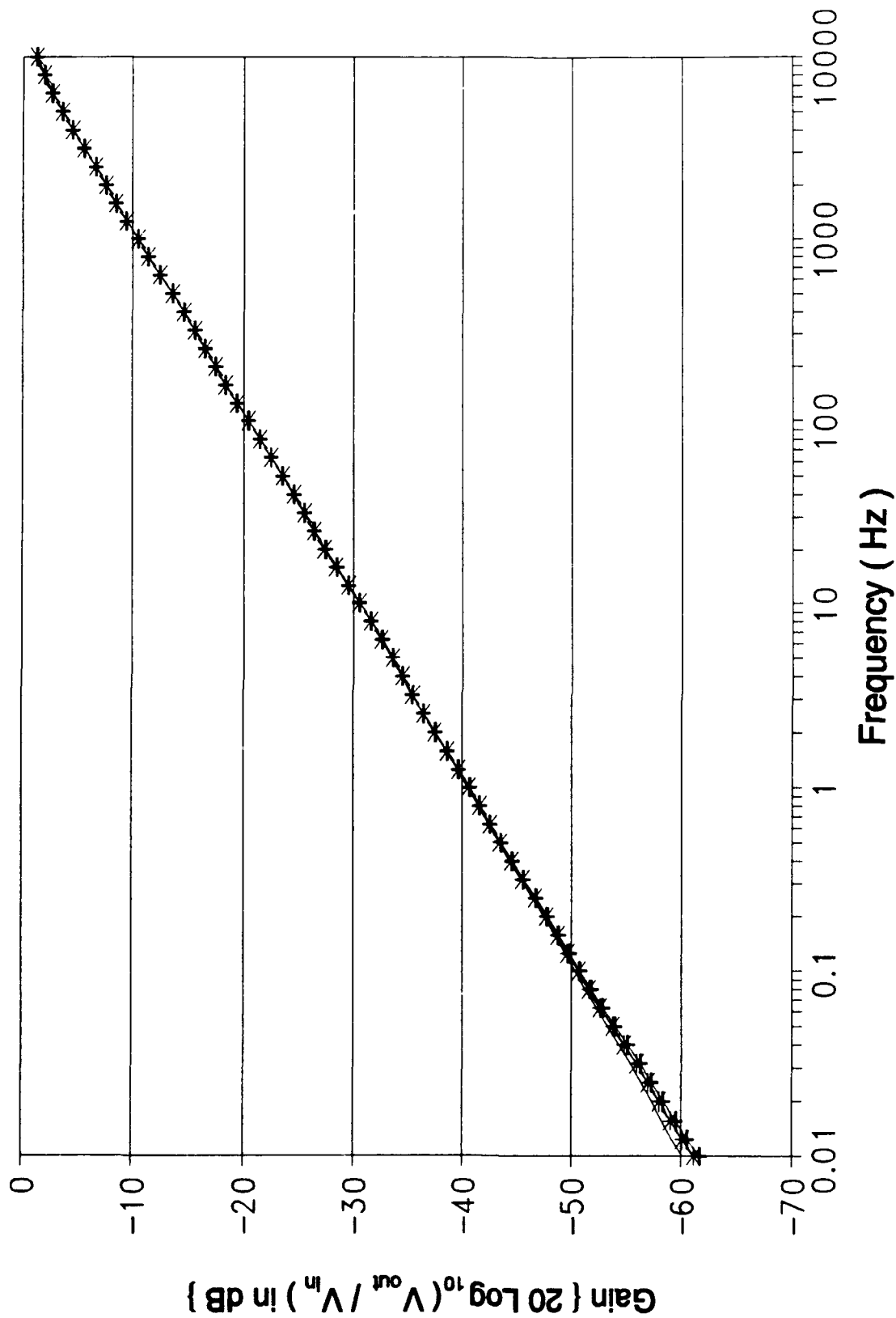**Figure B-20.   Graphical Symbol Legend and Capacitor Value
Correlation for Figure B-20 (cont);**

Figure B-20 (cont). Gain Response of the Oldham Circuit Design Using an HSPICE Computer Variation of Capacitor 6 (cont);
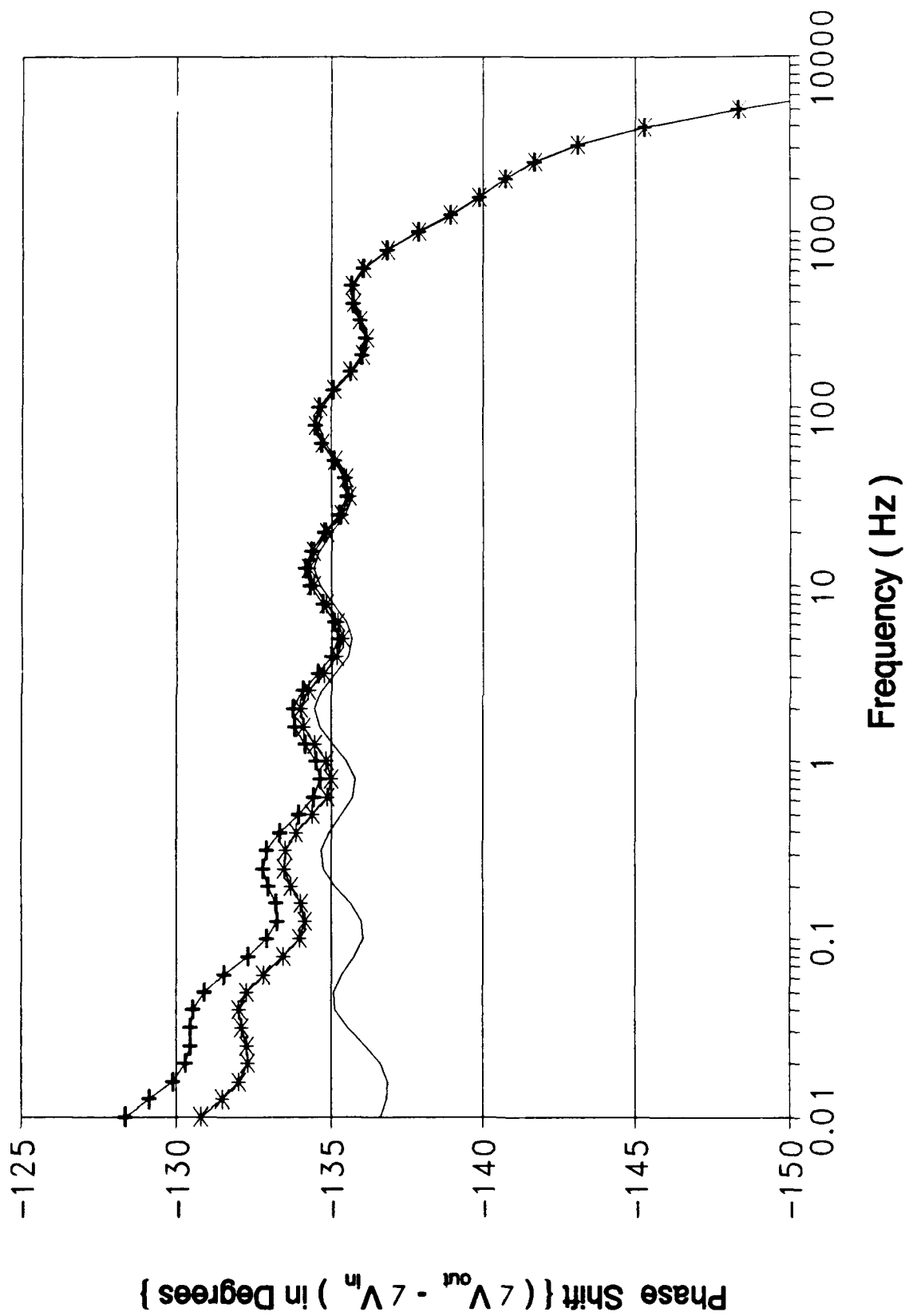
Figure B-20 (cont). Phase Response of the Oldham Circuit Design Using an HSPICE Computer Variation of Capacitor 6.

Capacitor Values for Figure B-21						
Symbol	——	-+-	-*-	-□-	-x-	-▲-
Capaci-tor Value (nf)	3.449	13.796	34.49 Ideal	55.184	68.98	172.45

Figure B-21.   Graphical Symbol Legend and Capacitor Value Correlation for Figure B-21 (cont);

Frequency (Hz)

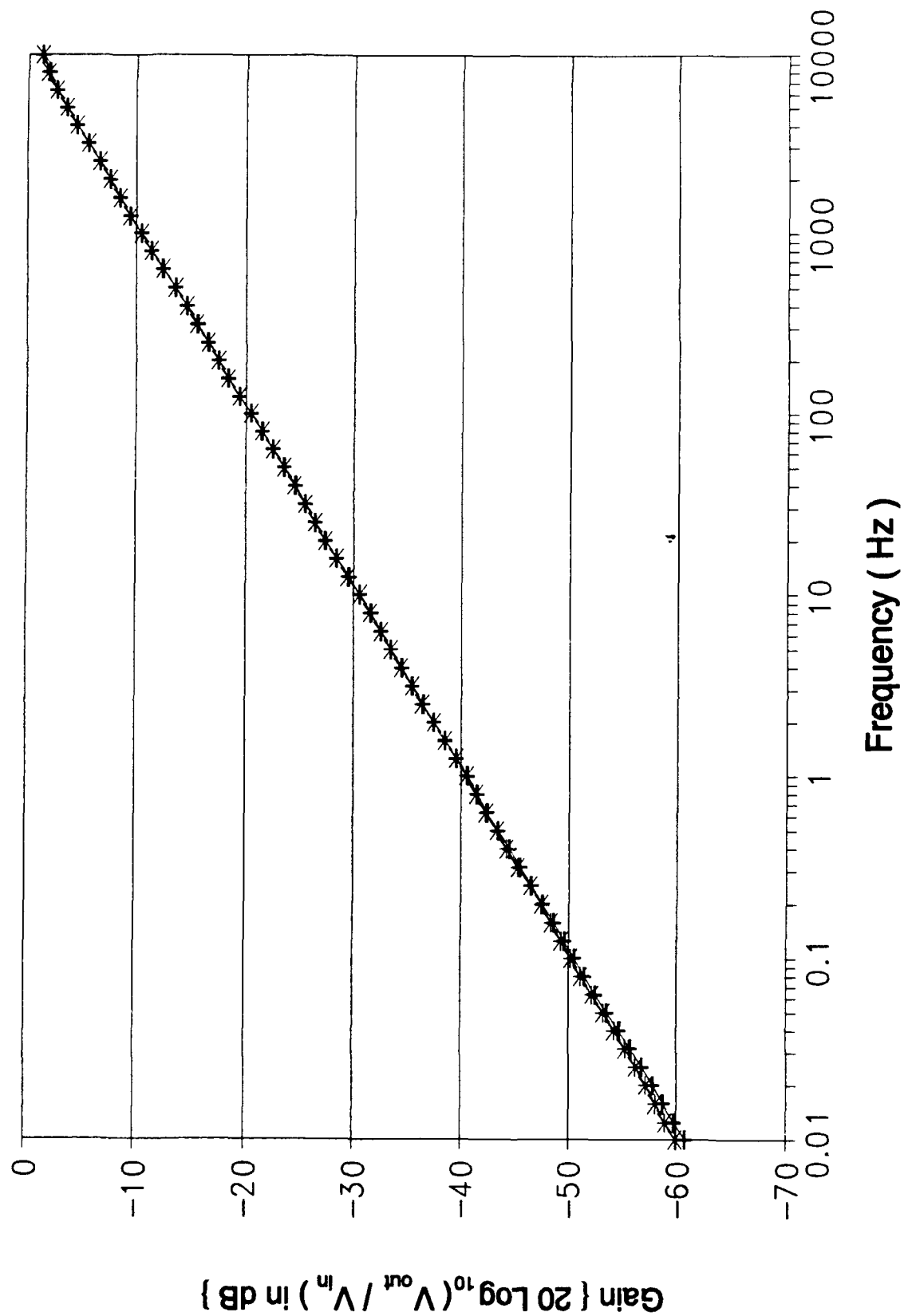Gain { 20 Log$_{10}$(V$_{out}$ / V$_{in}$) in dB }

Figure B-21 (cont). Gain Response of the Oldham Circuit Design Using an HSPICE Computer Variation of Capacitor 7 (cont);

Figure B-21 (cont). Phase Response of the Oldham Circuit Design Using an HSPICE Computer Variation of Capacitor 7.

B-67

Capacitor Values for Figure B-22						
Symbol	——	-+-	-*-	-▯-	—×—	-▲-
Capaci-tor Value (nf)	1.346	5.364	13.41 Ideal	21.456	26.82	67.05

**Figure B-22.   Graphical Symbol Legend and Capacitor Value
Correlation for Figure B-22 (cont);**

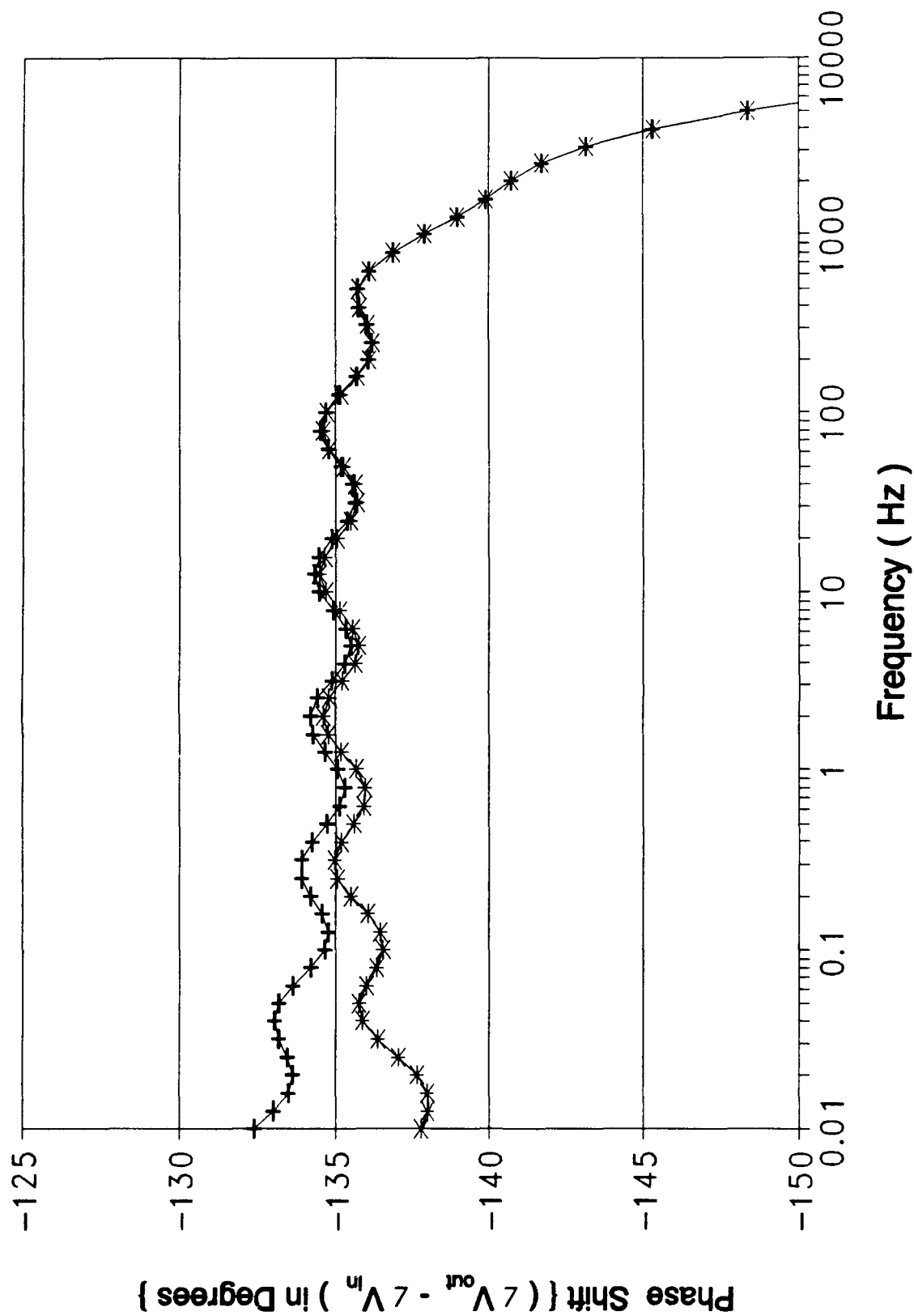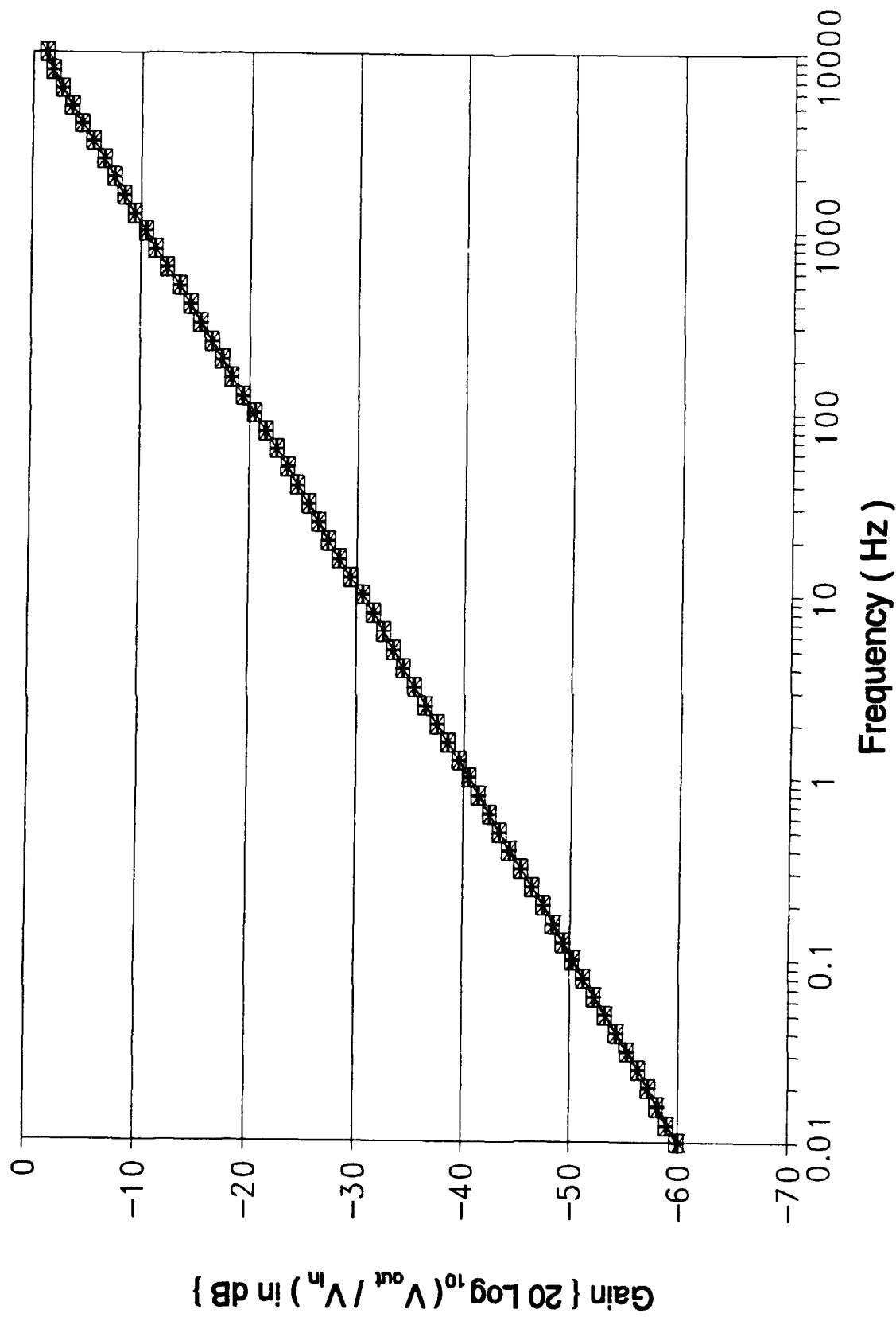Figure B-22 (cont). Gain Response of the Oldham Circuit Design Using an HSPICE Computer Variation of Capacitor 8 (cont);
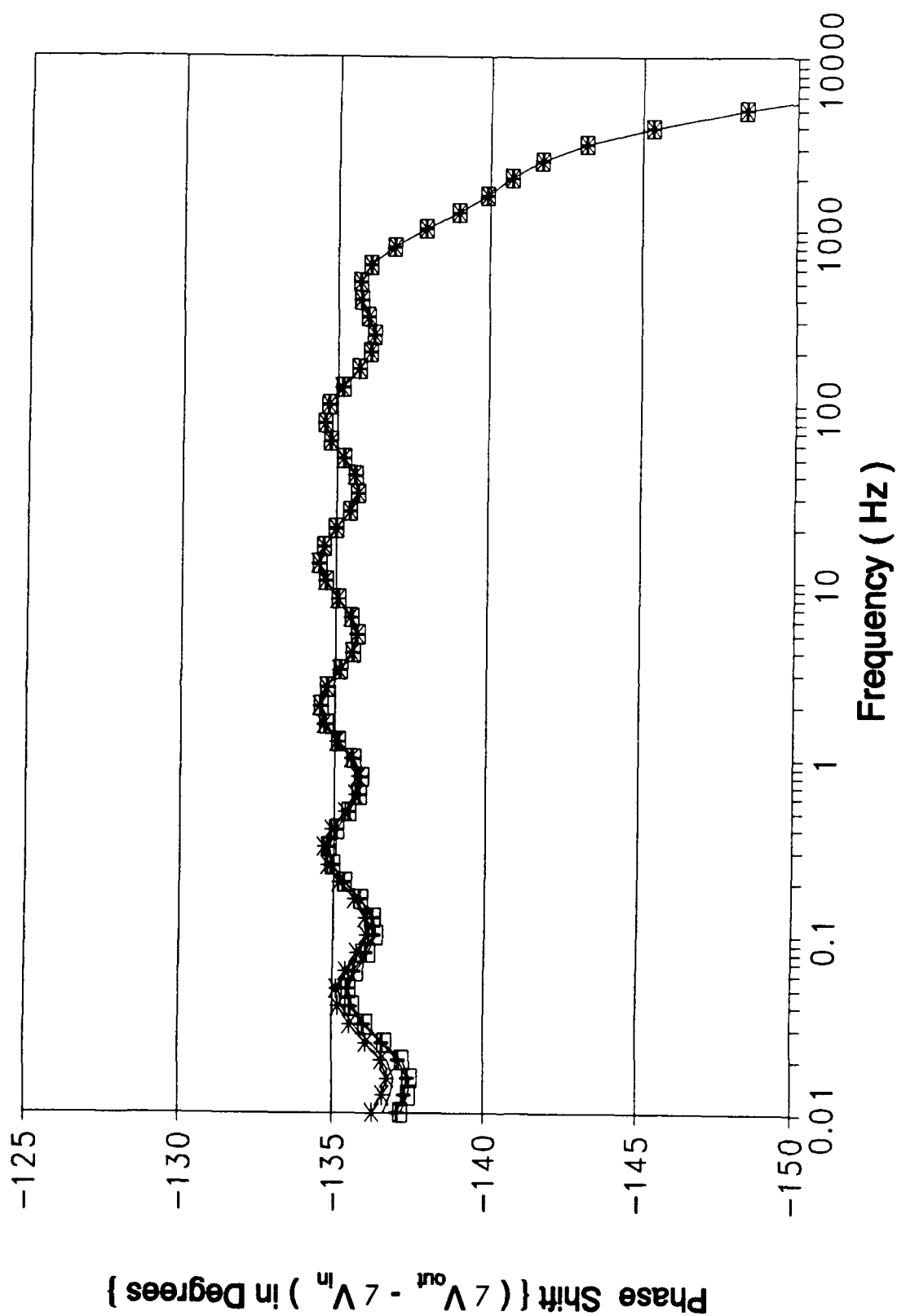
Figure B-22 (cont). Phase Response of the Oldham Circuit Design Using an HSPICE Computer Variation of Capacitor 8.

Capacitor Values for Figure B-23						
Symbol	—	-+-	-*-	-□-	-×-	-▲-
Capaci-tor Value (nf)	0.5211	2.084	5.211 Ideal	8.337	10.422	26.055

Figure B-23.   Graphical Symbol Legend and Capacitor Value Correlation for Figure B-23 (cont);

Frequency (Hz)

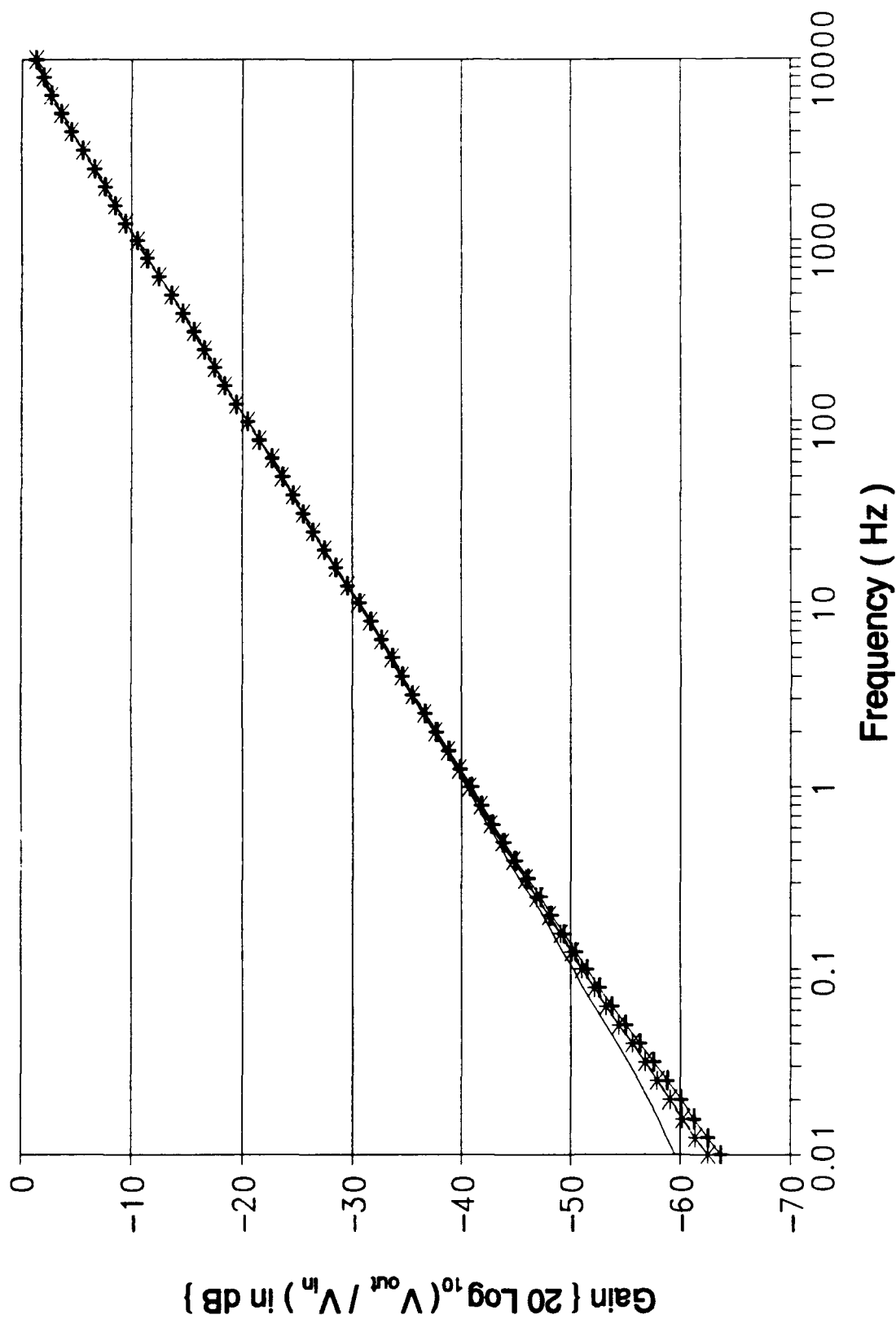Gain { 20 Log₁₀ (V_out / V_in) in dB }

Figure B-23 (cont). Gain Response of the Oldham Circuit Design Using an HSPICE Computer Variation of Capacitor 9 (cont);

Figure B-23 (cont). Phase Response of the Oldham Circuit Design Using an HSPICE Computer Variation of Capacitor 9.

Capacitor Values for Figure B-24						
Symbol	——	-+-	-*-	-□-	-×-	-▲-
Capaci -tor Value (nf)	0.2026	0.8104	2.026 Ideal	3.242	4.052	10.13

Figure B-24.   Graphical Symbol Legend and Capacitor Value Correlation for Figure B-24 (cont);

Figure B-24 (cont). Gain Response of the Oldham Circuit Design Using
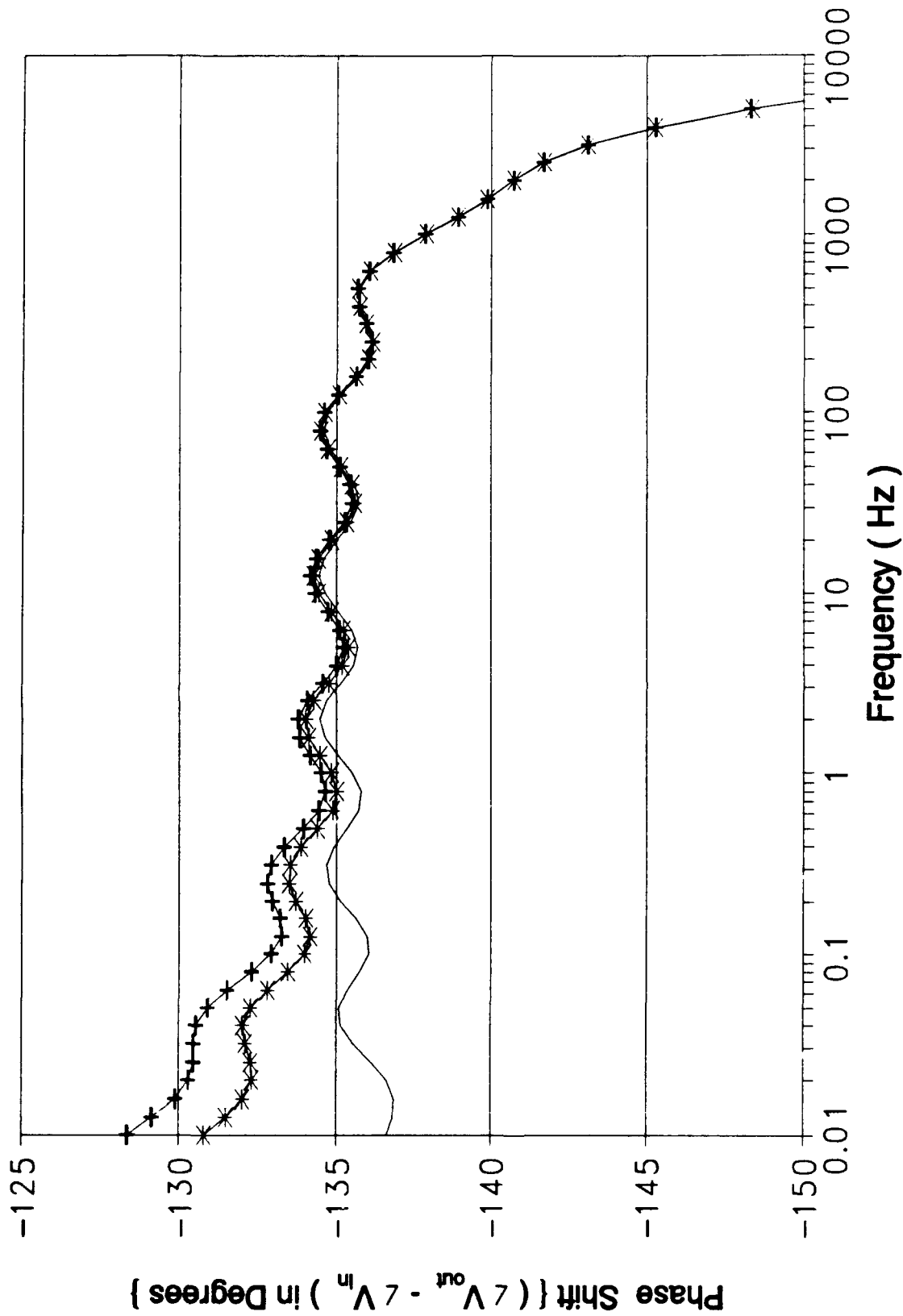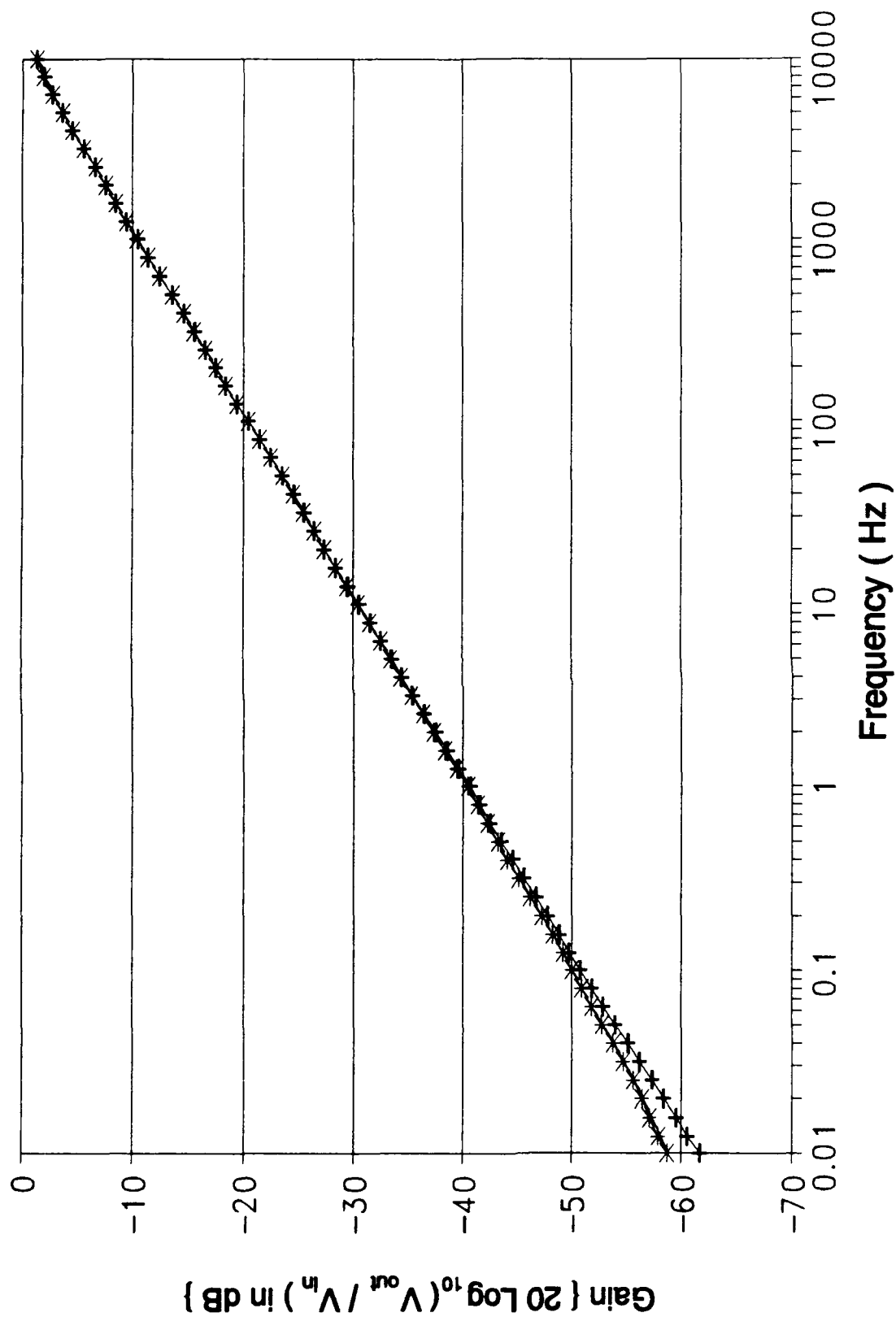an HSPICE Computer Variation of Capacitor 10 (cont);
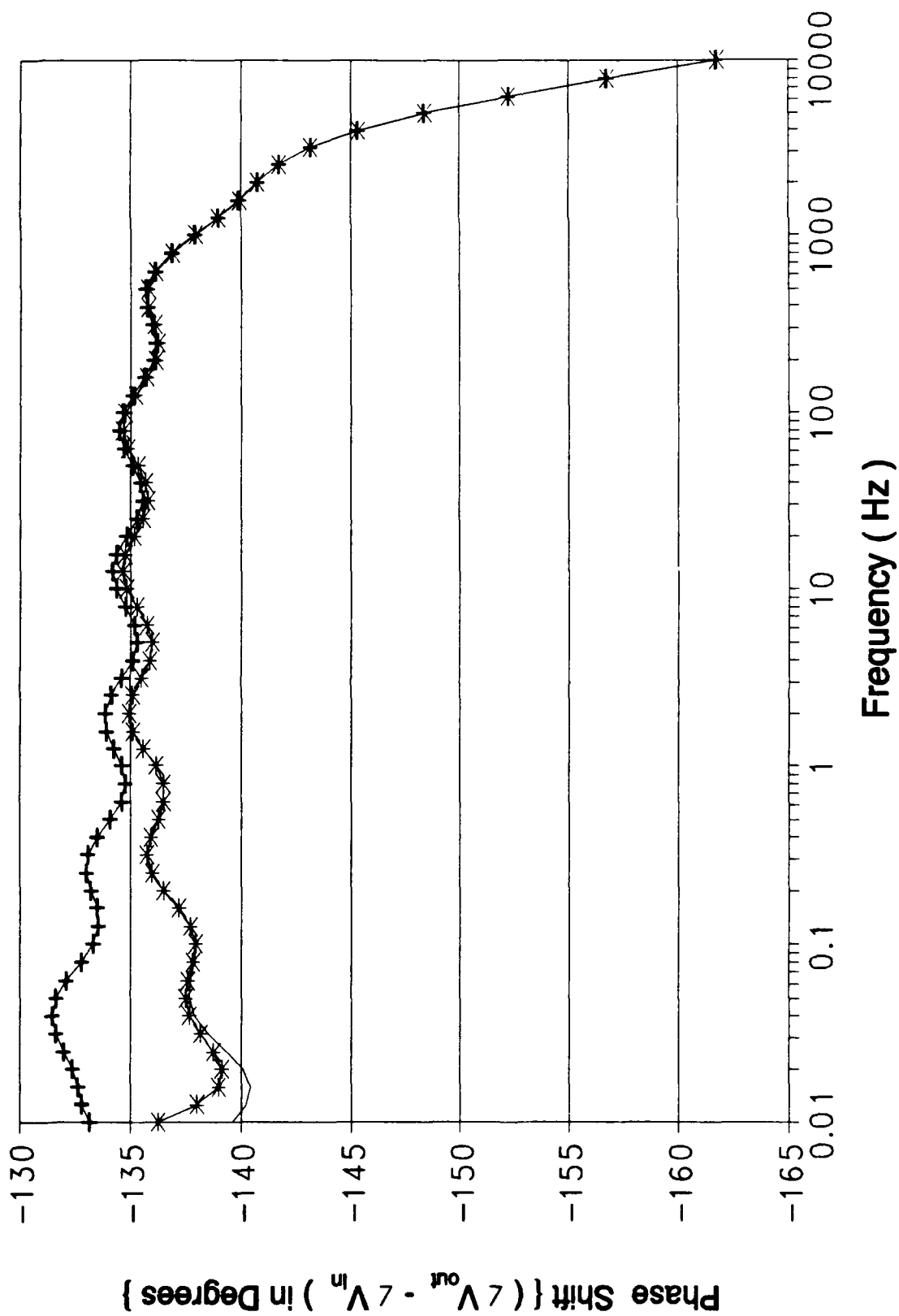
Figure B-24 (cont). Phase Response of the Oldham Circuit Design Using an HSPICE Computer Variation of Capacitor 10.

Capacitor Values for Figure B-25						
Symbol	——	-+-	-*-	—▢—	—×—	-▲-
Capaci -tor Value (nf)	0.1575	0.63	1.575 Ideal	2.52	3.15	7.875

Figure B-25. Graphical Symbol Legend and Capacitor Value Correlation for Figure B-25 (cont);

Frequency (Hz)

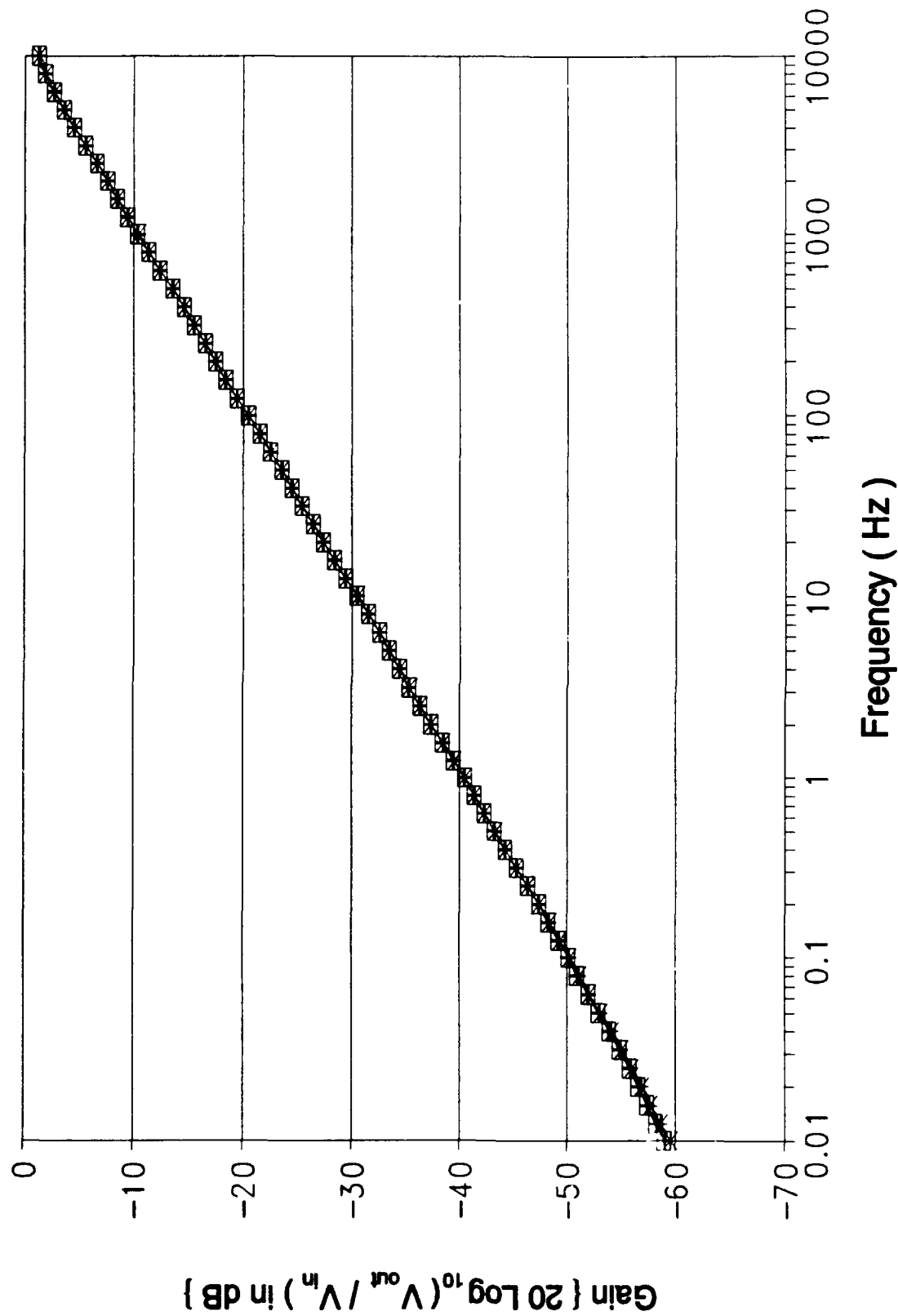Gain { 20 Log₁₀ (V_out / V_in) in dB }

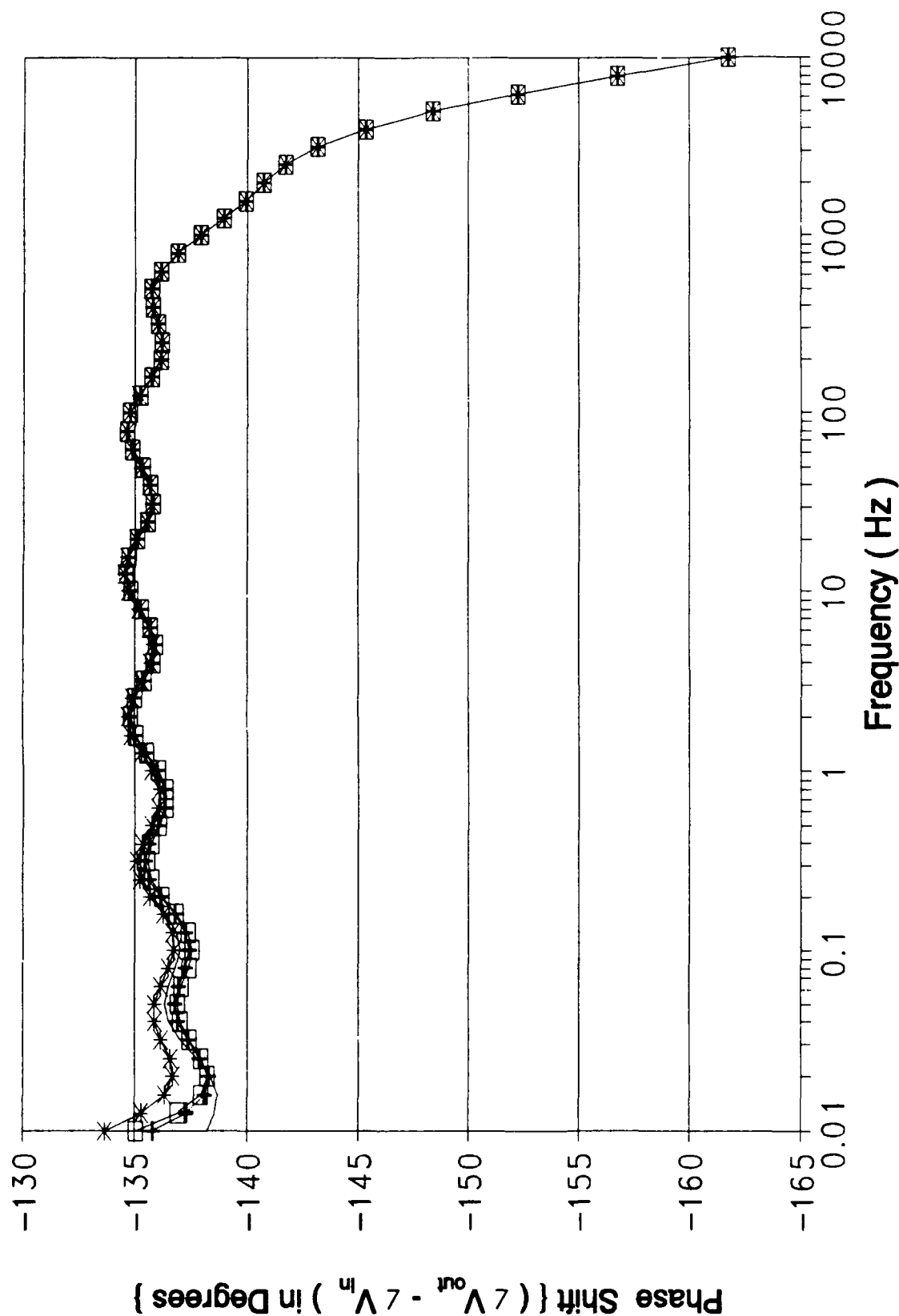Figure B-25 (cont). Gain Response of the Oldham Circuit Design Using an HSPICE Computer Variation of Capacitor 11 (cont);

B-78

Figure B-25 (cont). Phase Response of the Oldham Circuit Design Using an HSPICE Computer Variation of Capacitor 11.

Section 2

Oldham Circuit Responses to Cell Component
(Resistor and Capacitor pairs) Value Variations

Resistor And Capacitor Values For Figure B-26.1					
Symbol	▬	-+-	-*-	–⊡–	
Resis- tor Value (MΩ)	36.1	105.88	88.32	42.17	
Capaci- tor Value (μF)	20.7	6.7199	8.799	30.342	

**Figure B-26.1. Graphical Symbol Legend and Component Value
Correlation for Figure B-26.1 (cont);**

Figure B-26.1 (cont). Gain Response of the Oldham Circuit Design Using an HSPICE Computer Variation of Cell 0 (cont);

Figure B-26.1 (cont). Phase Response of the Oldham Circuit Design Using an HSPICE Computer Variation of Cell 0.
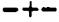
Resistor And Capacitor Values For Figure B-26.2					
Symbol	——	-+-	-*-		
Resis-tor Value (MΩ)	86.127	91.23	49.67		
Capaci-tor Value (μF)	10.96	31.064	22.51		

Figure B-26.2. Graphical Symbol Legend and Component Value Correlation for Figure B-26.2 (cont);
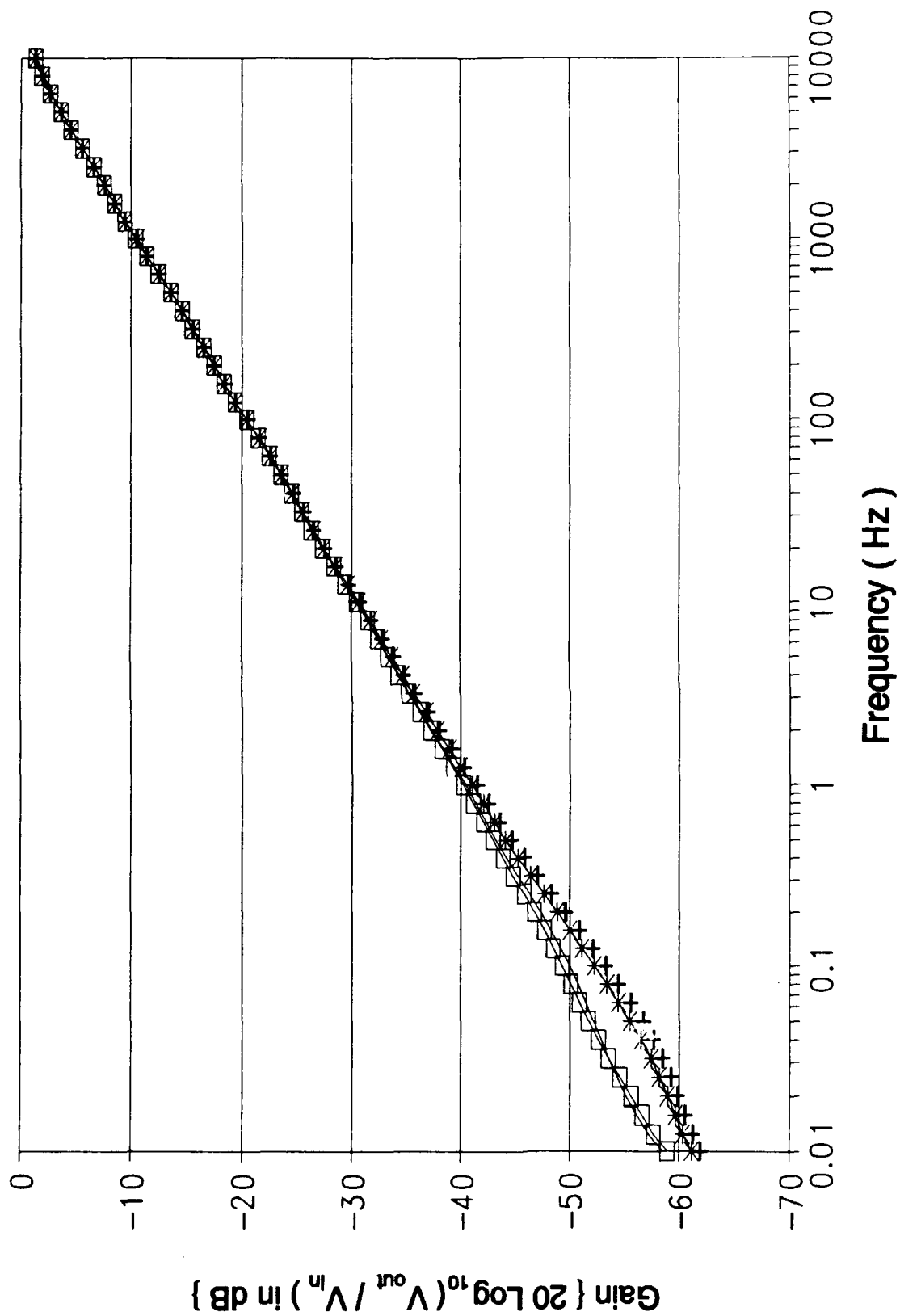
Figure B-26.2 (cont). Gain Response of the Oldham Circuit Design Using an HSPICE Computer Variation of Cell 0 (cont);
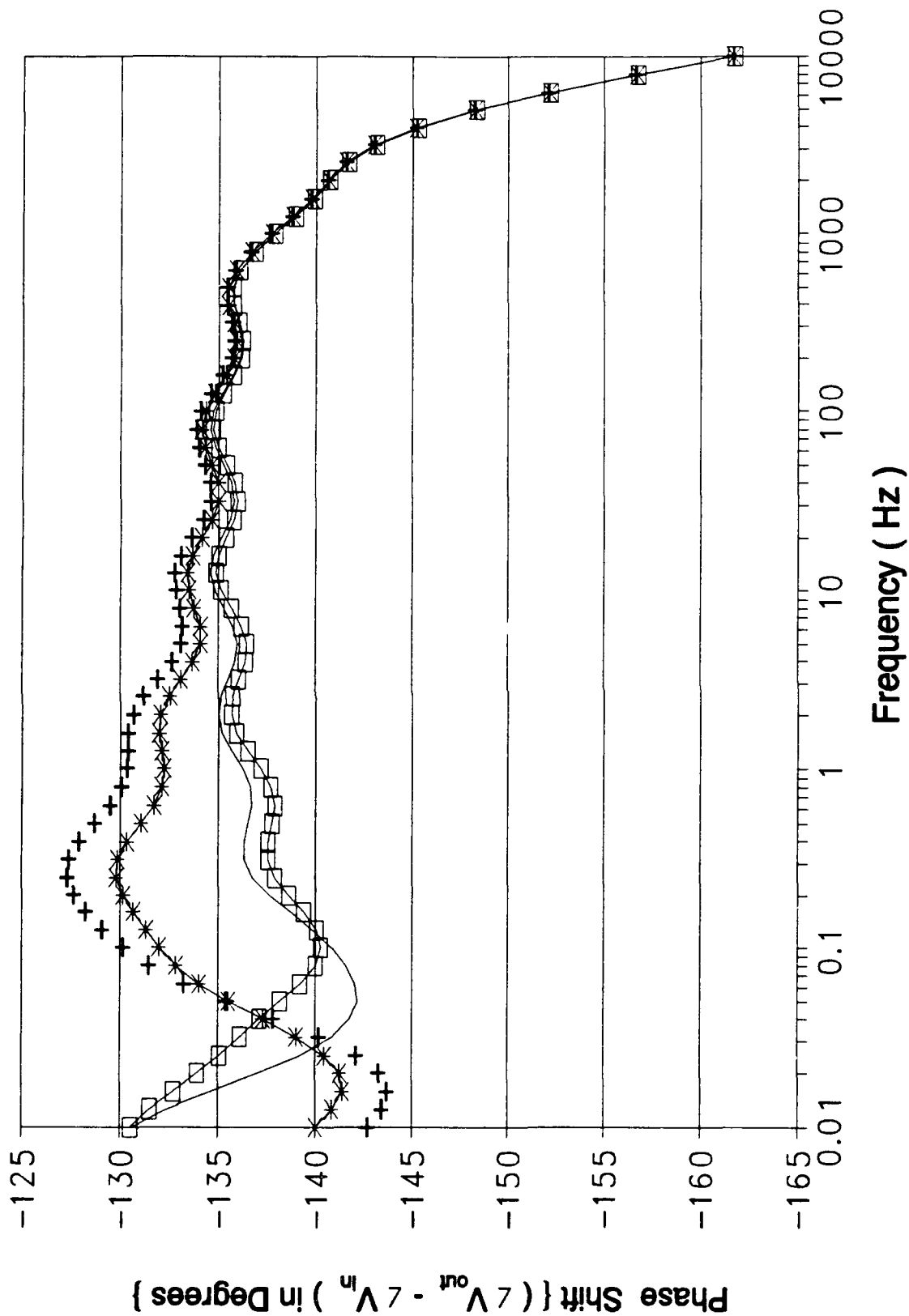
Figure B-26.2 (cont). Phase Response of the Oldham Circuit Design Using an HSPICE Computer Variation of Cell 0.

Resistor And Capacitor Values For Figure B-26.3					
Symbol	———	-+-	-*-		
Resis- tor Value (MΩ)	75.21	99.03	102.79		
Capaci- tor Value (μF)	26.06	21.71	27.2		

Figure B-26.3. Graphical Symbol Legend and Component Value
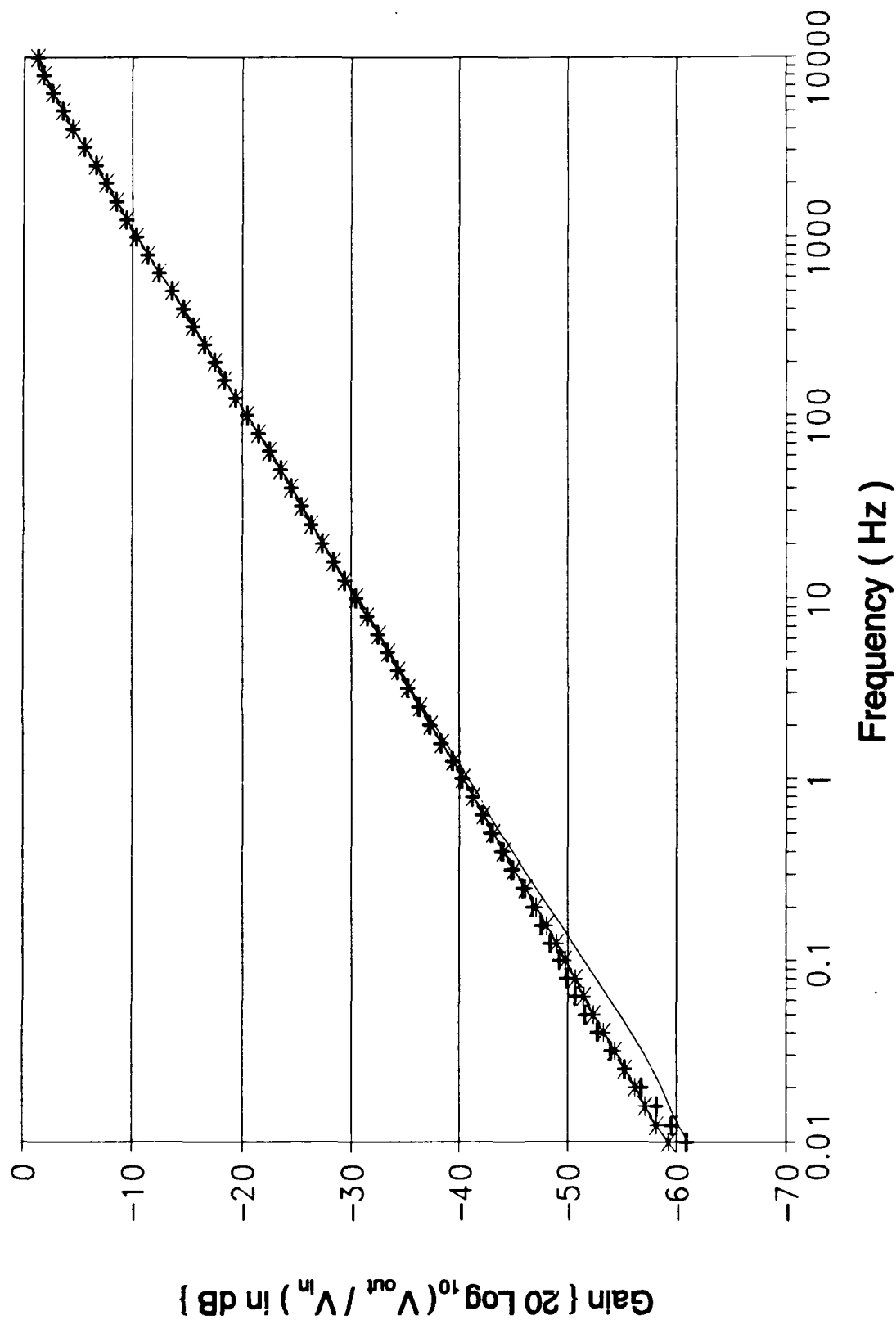**Correlation for Figure B-26.3 (cont);**

Figure B-26.3 (cont). Gain Response of the Oldham Circuit Design Using an HSPICE Computer Variation of Cell 0 (cont);
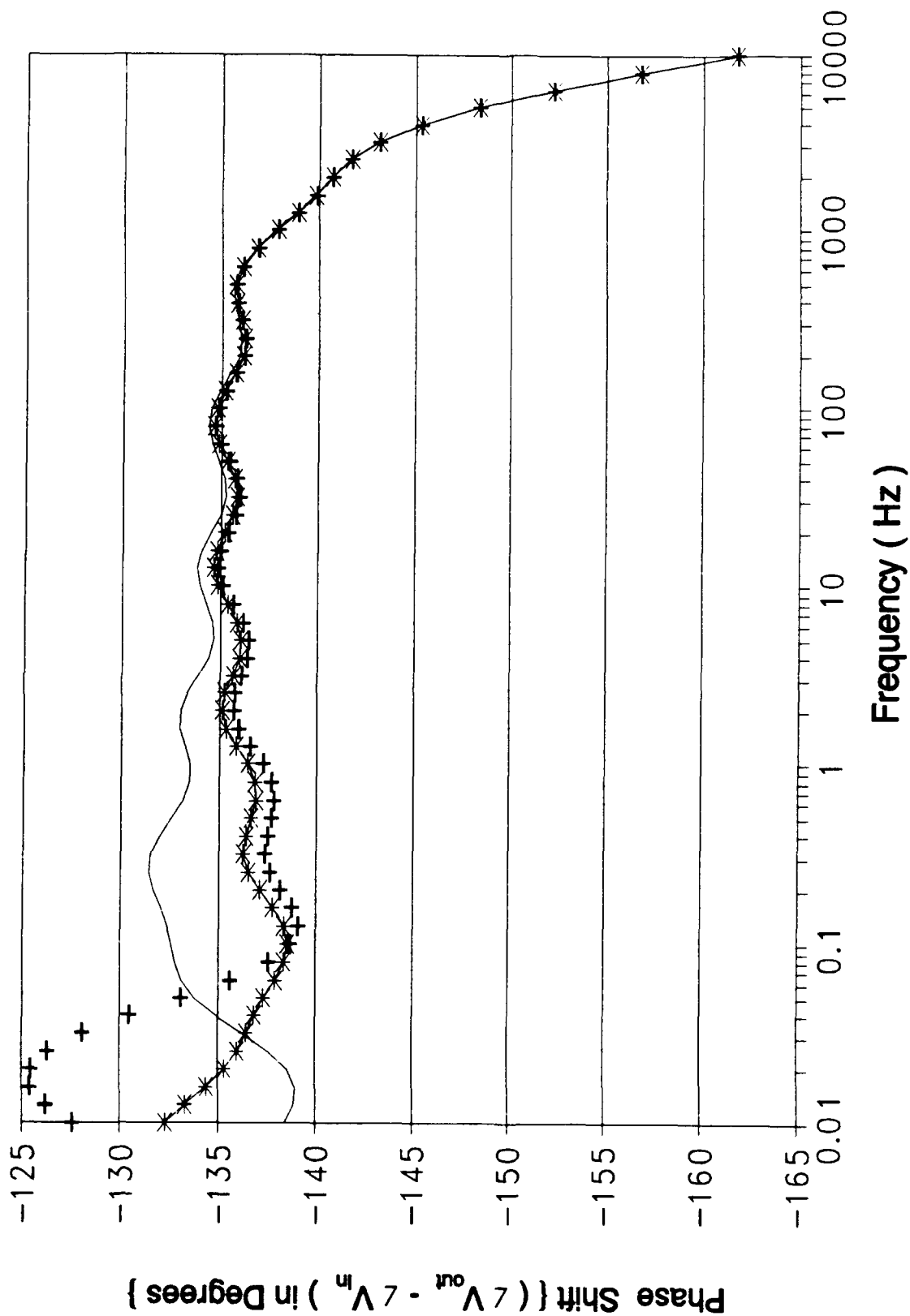
Figure B-26.3 (cont). Phase Response of the Oldham Circuit Design Using an HSPICE Computer Variation of Cell 0.

Resistor And Capacitor Values For Figure B-27.1					
Symbol	——	-+-	-*-		
Resis-tor Value (MΩ)	10.27	42.36	34.29		
Capaci-tor Value (μF)	12.56	4.070	5.329		

Figure B-27.1. Graphical Symbol Legend and Component Value Correlation for Figure B-27.1 (cont);
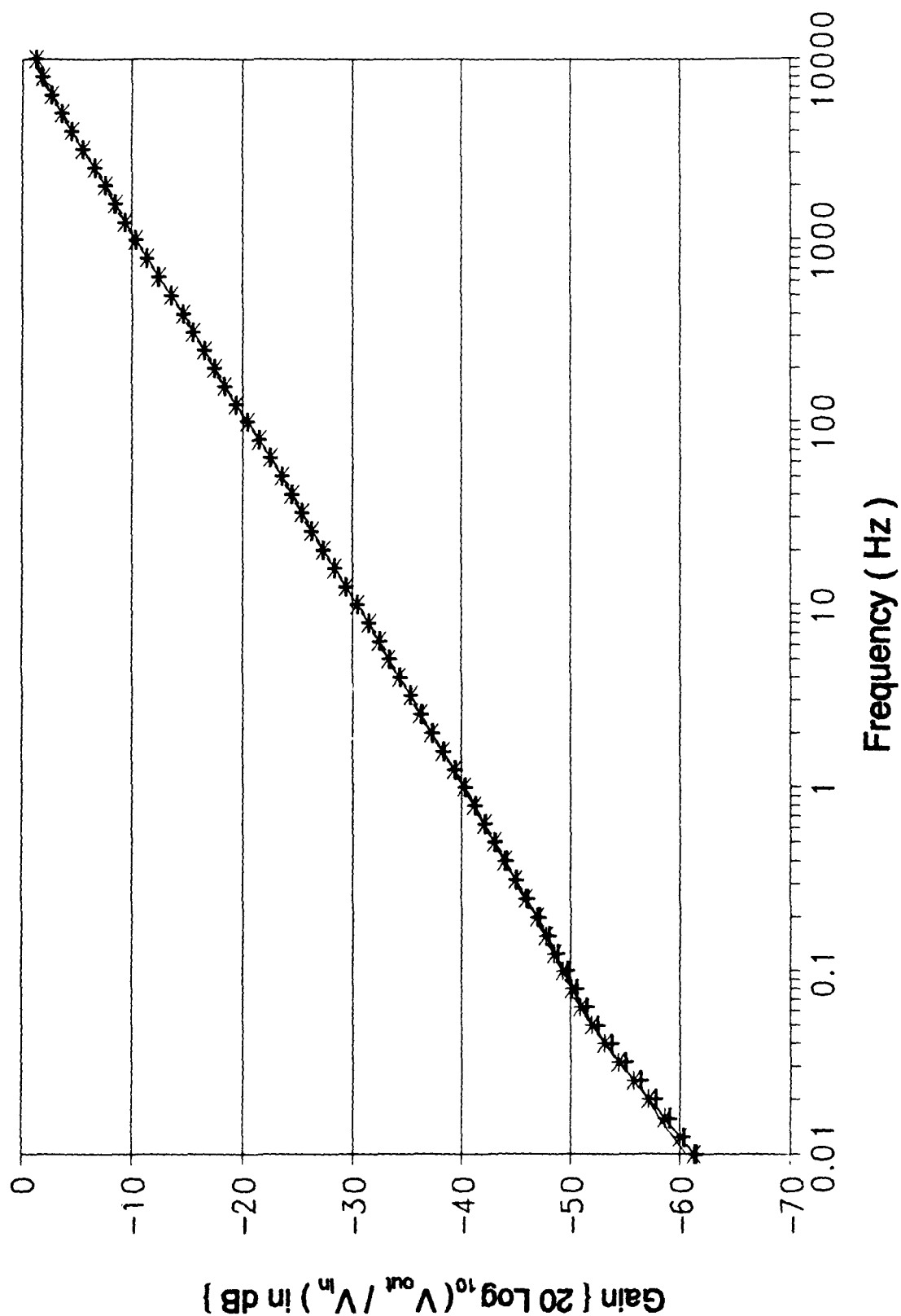
Figure B-27.1 (cont). Gain Response of the Oldham Circuit Design Using an HSPICE Computer Variation of Cell 1 (cont);
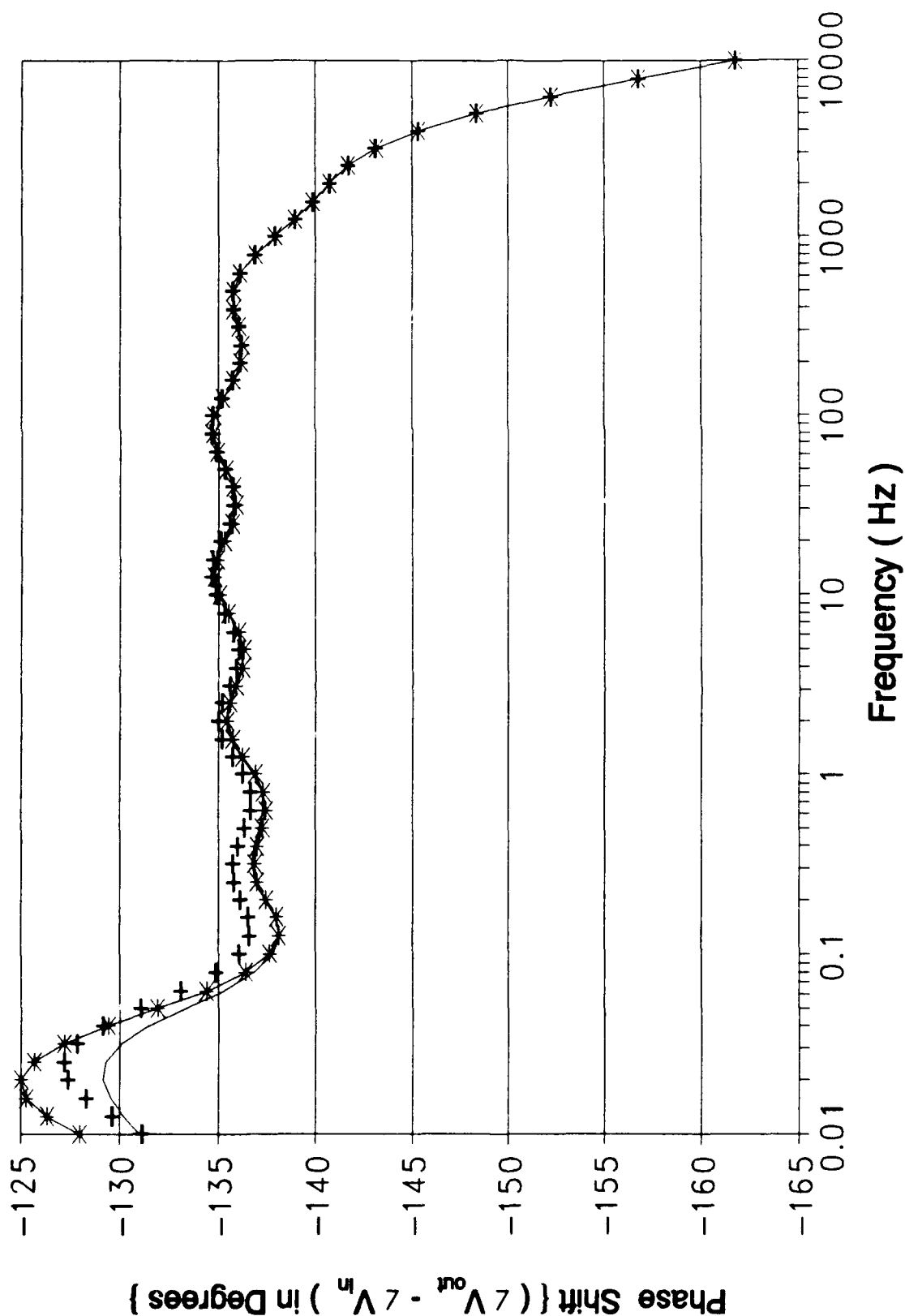
Figure B-27.1 (cont). Phase Response of the Oldham Circuit Design Using an HSPICE Computer Variation of Cell 1.

B-92

Resistor And Capacitor Values For Figure B-27.2					
Symbol	▬	−+−	−*−		
Resis-tor Value (MΩ)	13.06	33.28	35.63		
Capaci-tor Value (μF)	18.37	6.639	1.881		

Figure B-27.2.   Graphical Symbol Legend and Component Value Correlation for Figure B-27.2 (cont);

B-93

Figure B-27.2 (cont). Gain Response of the Oldham Circuit Design Using
an HSPICE Computer Variation of Cell 1 (cont);

Figure B-27.2 (cont). Phase Response of the Oldham Circuit Design Using an HSPICE Computer Variation of Cell 1.
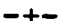
Resistor And Capacitor Values For Figure B-27.3					
Symbol	——	-+-	-*-	-□-	
Resis-tor Value (MΩ)	16.51	28.26	39.22	40.94	
Capaci-tor Value (μF)	13.63	15.78	13.15	16.47	

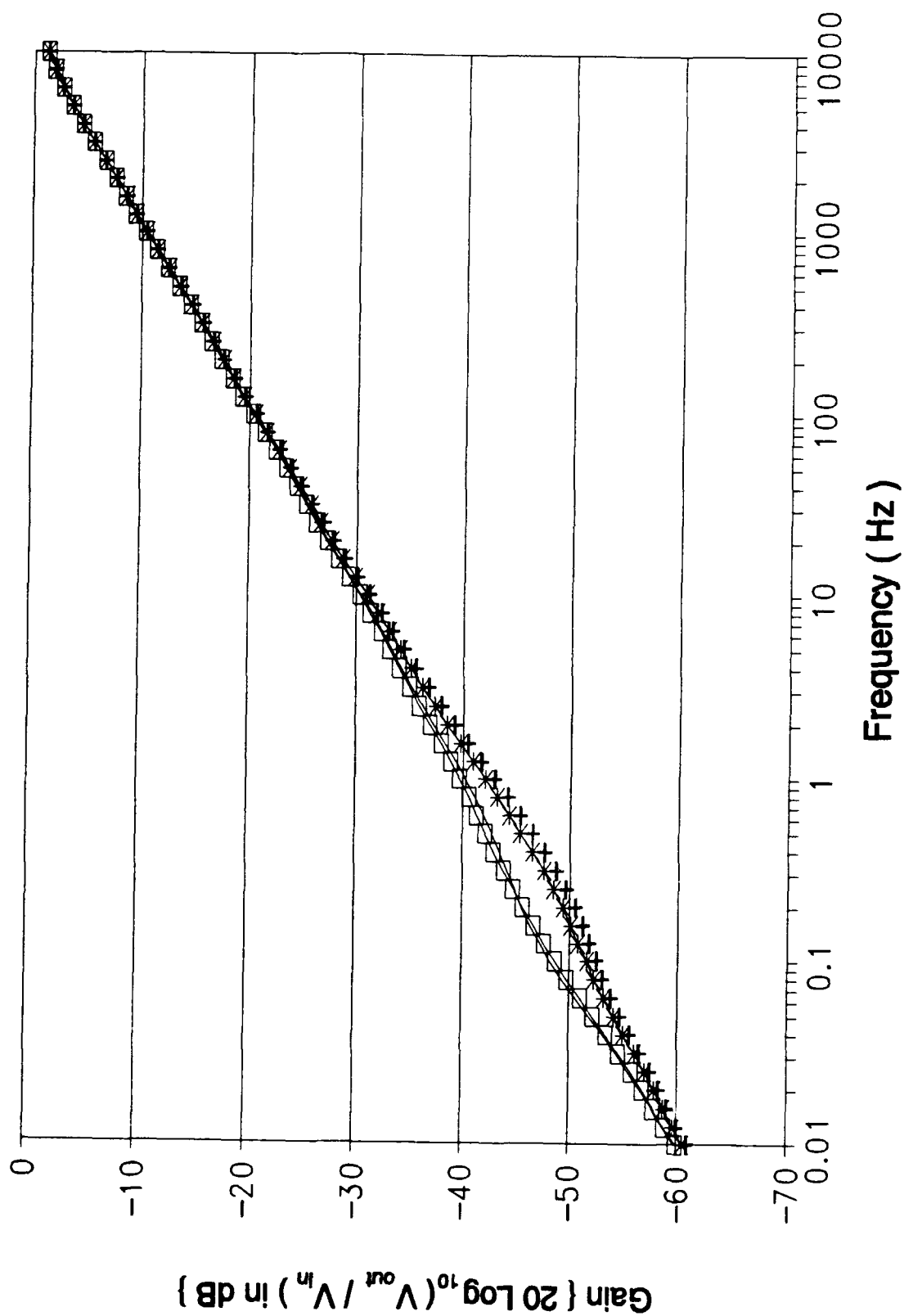**Figure B-27.3. Graphical Symbol Legend and Component Value Correlation for Figure B-27.3 (cont);**

Figure B-27.3 (cont). Gain Response of the Oldham Circuit Design Using an HSPICE Computer Variation of Cell 1 (cont);
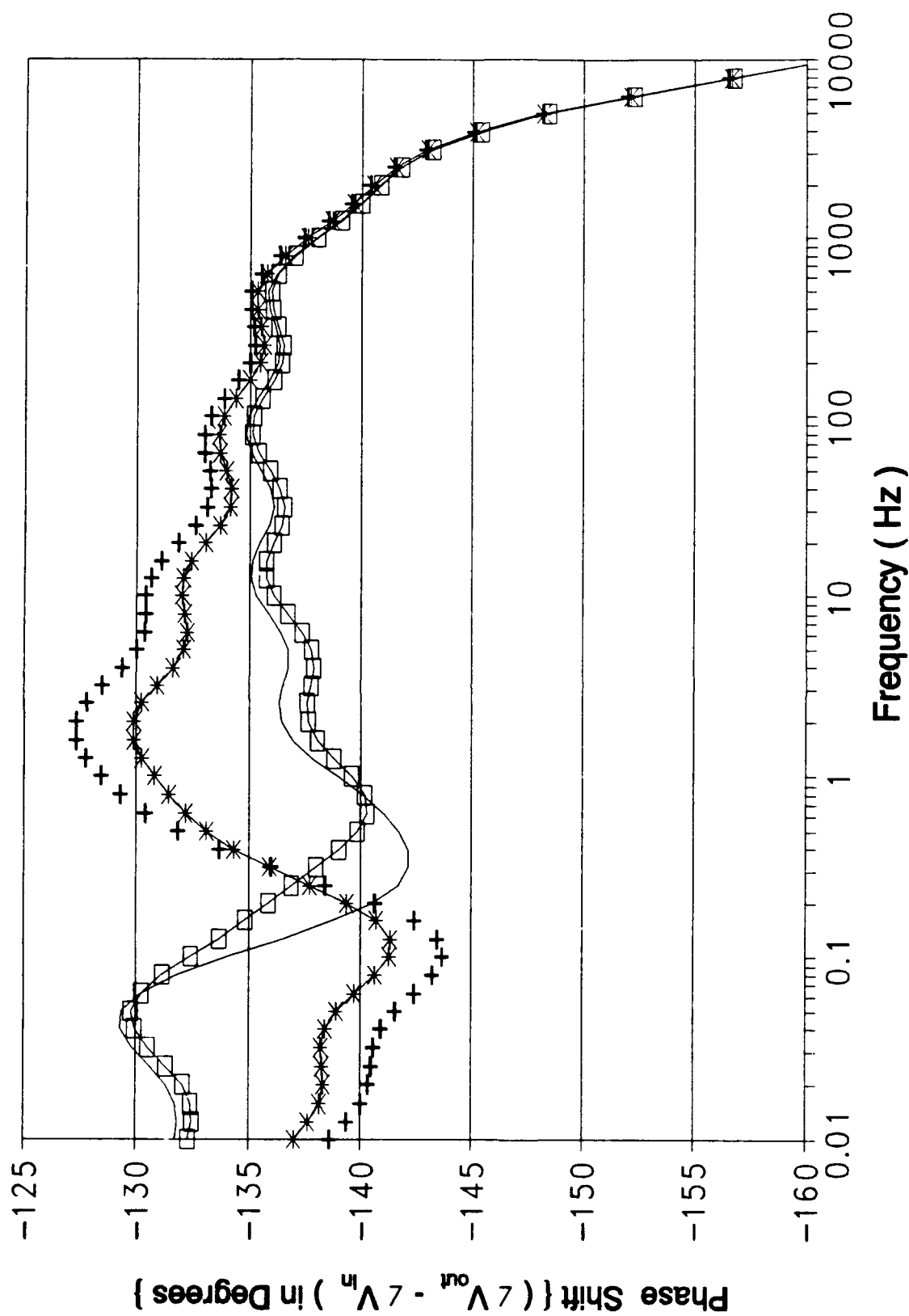
Figure B-27.3 (cont). Phase Response of the Oldham Circuit Design Using an HSPICE Computer Variation of Cell 1.

Resistor And Capacitor Values For Figure B-28.1					
Symbol	——	-+-	-*-		
Resis-tor Value (MΩ)	4.019	16.39	13.27		
Capaci-tor Value (μF)	4.874	1.579	2.068		

Figure B-28.1. **Graphical Symbol Legend and Component Value Correlation for Figure B-28.1 (cont);**
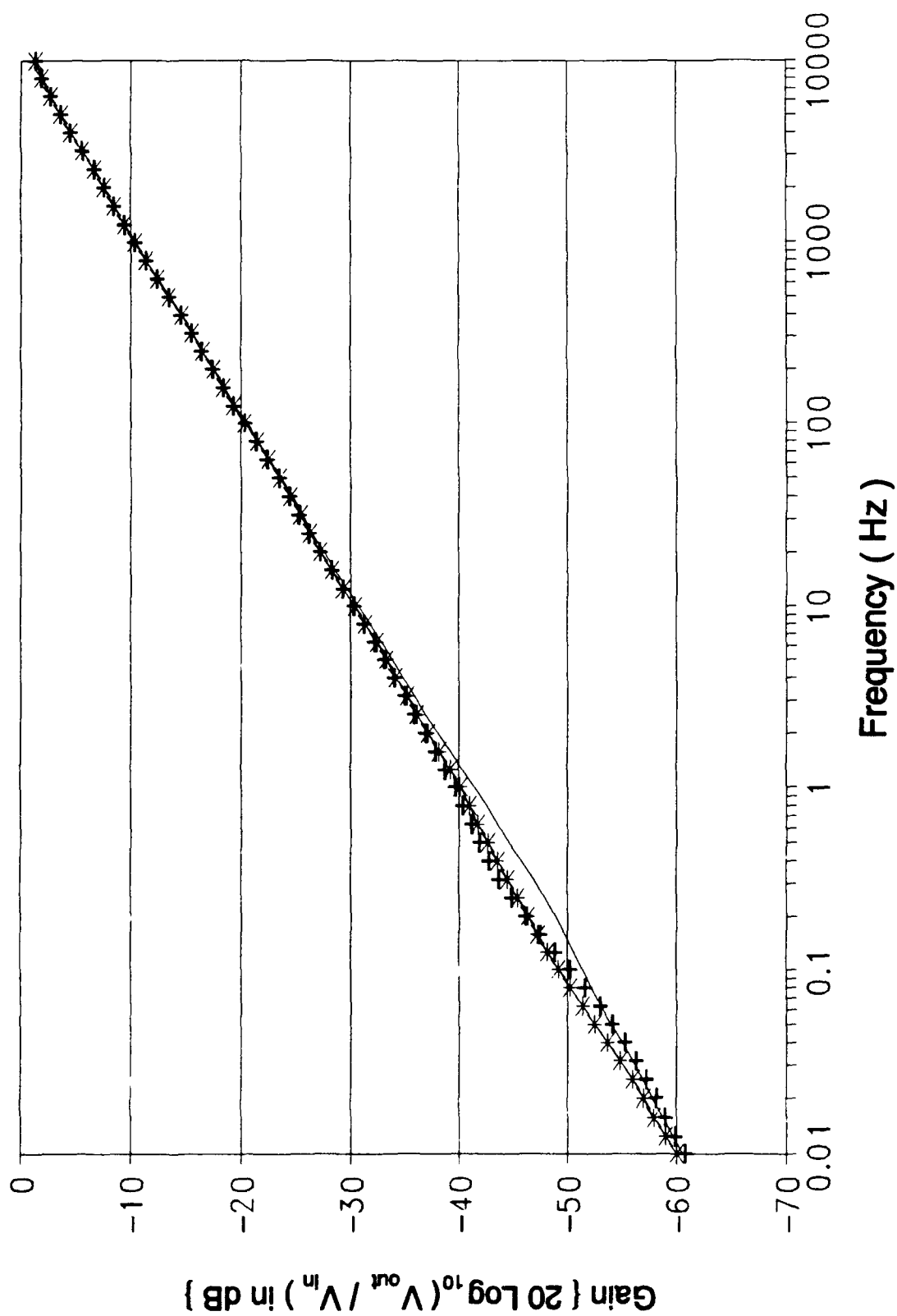
Figure B-28.1 (cont). Gain Response of the Oldham Circuit Design Using
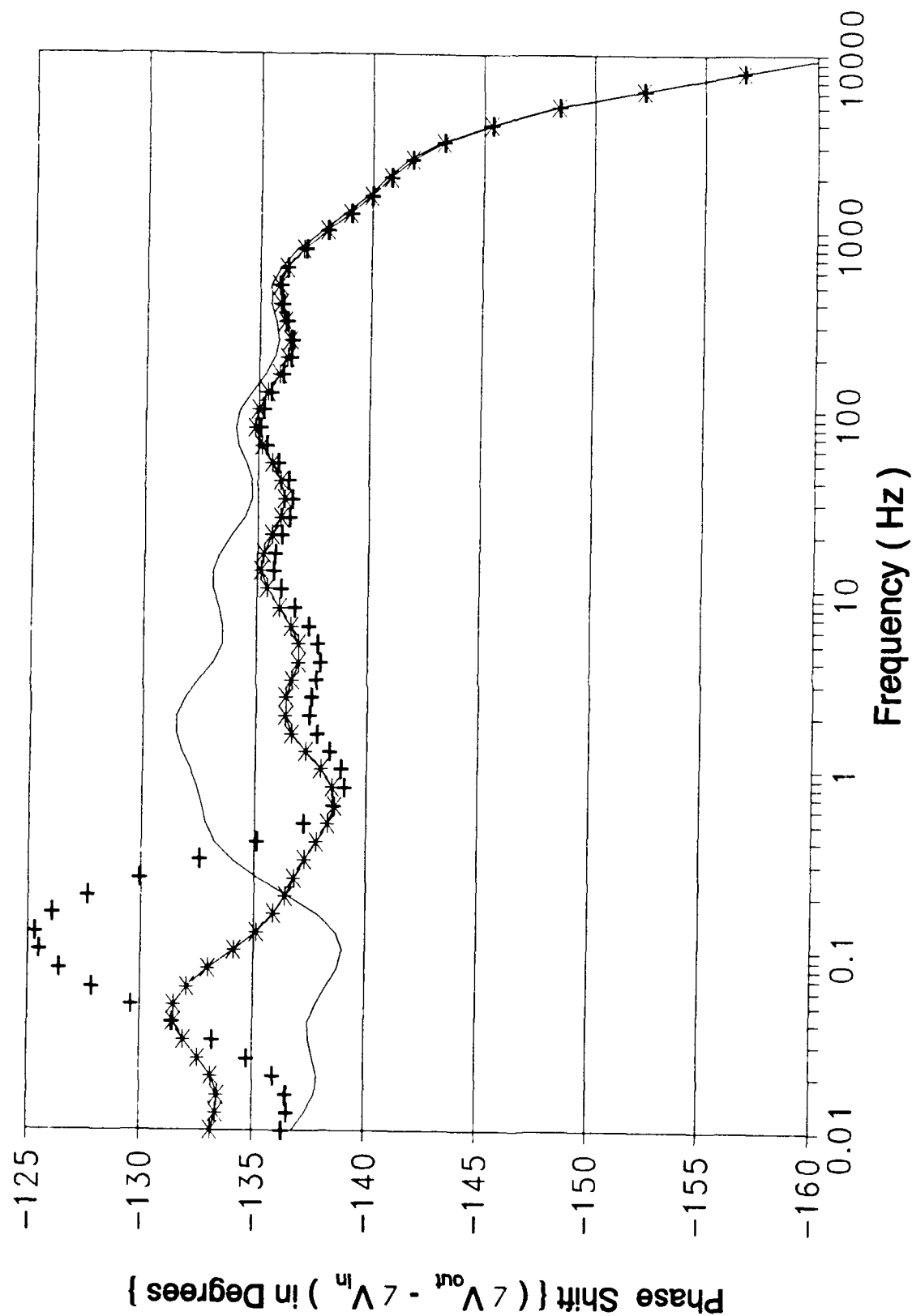an HSPICE Computer Variation of Cell 2 (cont);

Figure B-28.1 (cont). Phase Response of the Oldham Circuit Design Using an HSPICE Computer Variation of Cell 2.

Resistor And Capacitor Values For Figure B-28.2					
Symbol	▬	-+-	-*-		
Resis- tor Value (MΩ)	5.095	12.88	13.79		
Capaci- tor Value (μF)	7.13	2.576	7.3		

Figure B-28.2. Graphical Symbol Legend and Component Value
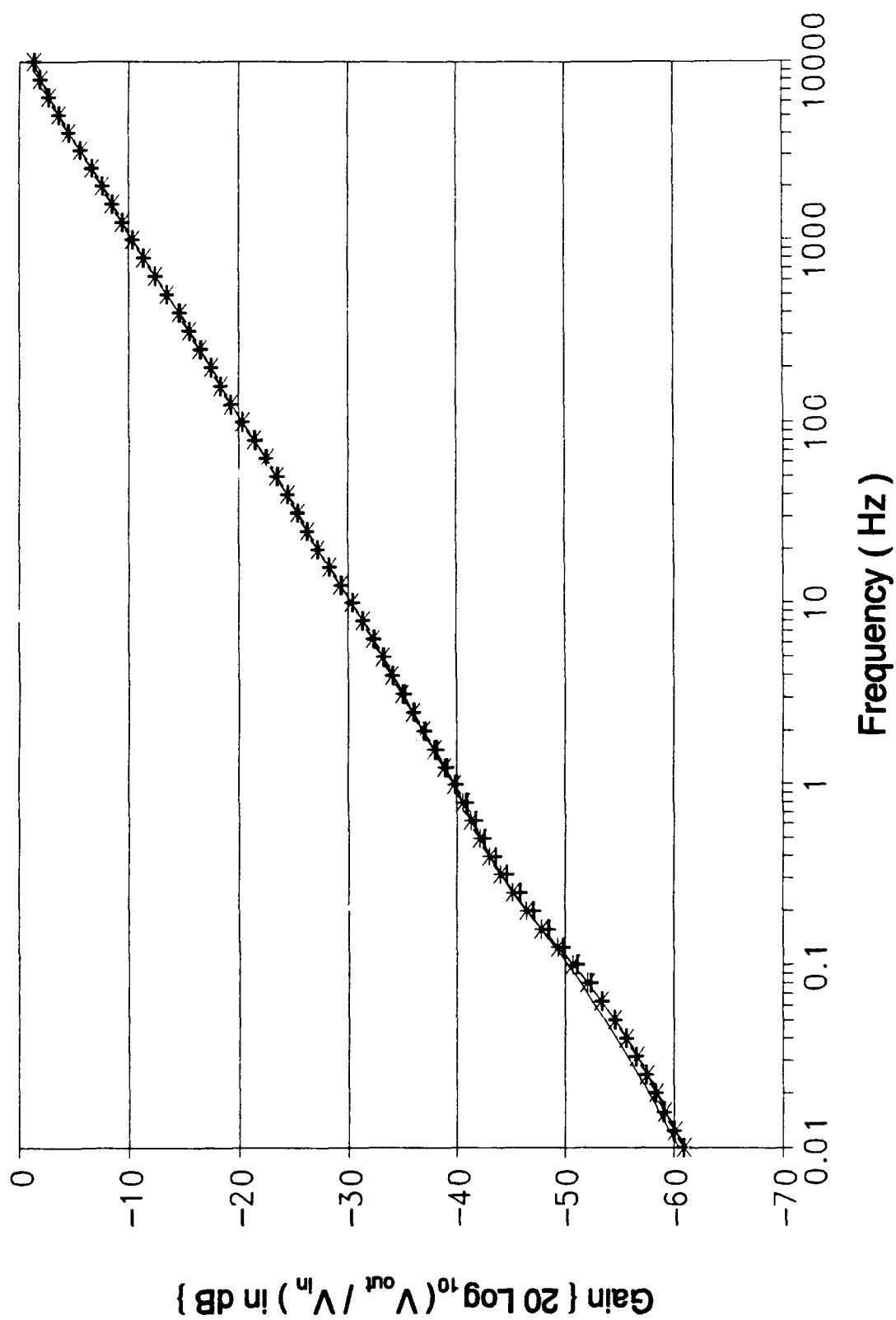Correlation for Figure B-28.2 (cont);

Figure B-28.2 (cont). Gain Response of the Oldham Circuit Design Using an HSPICE Computer Variation of Cell 2 (cont);
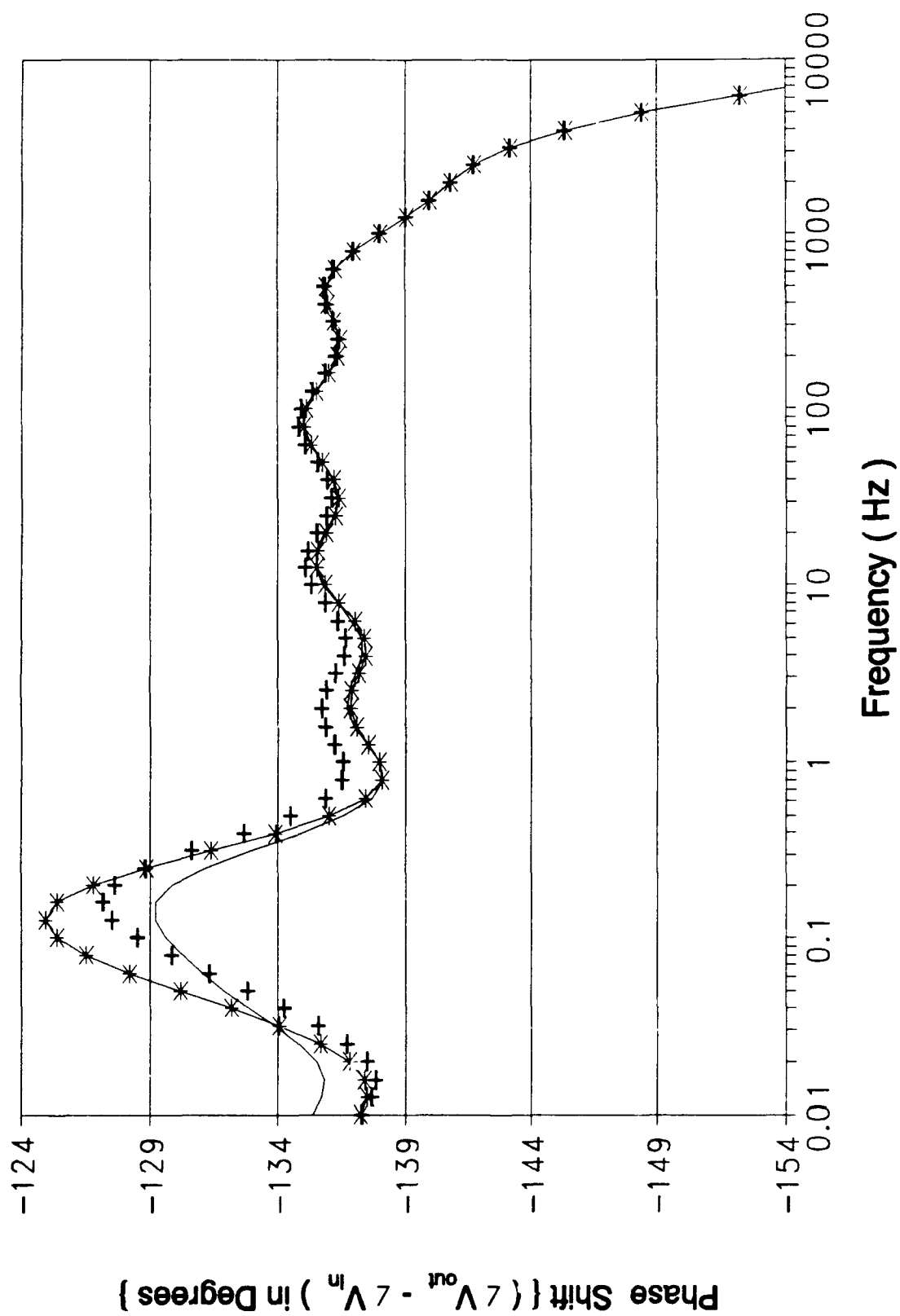
B-103

Figure B-28.2 (cont). Phase Response of the Oldham Circuit Design Using an Hspice Computer Variation of Cell 2.

Resistor And Capacitor Values For Figure B-28.3					
Symbol	——	-+-	-*-	-□-	
Resis- tor Value (MΩ)	6.425	10.95	15.177	15.84	.
Capaci- tor Value (μF)	5.29	6.125	5.1043	6.393	

Figure B-28.3. Graphical Symbol Legend and Component Value
               Correlation for Figure B-28.3 (cont);

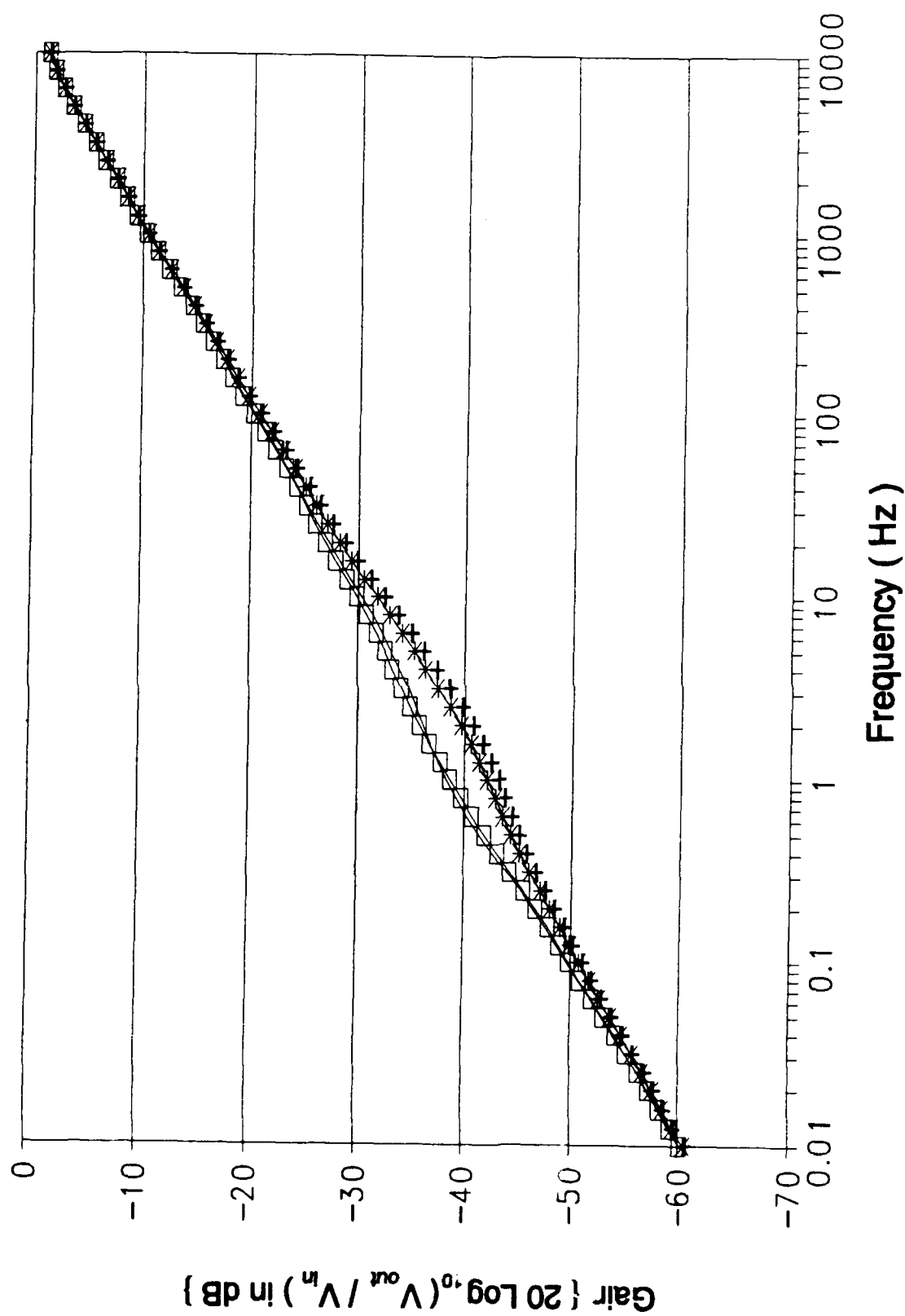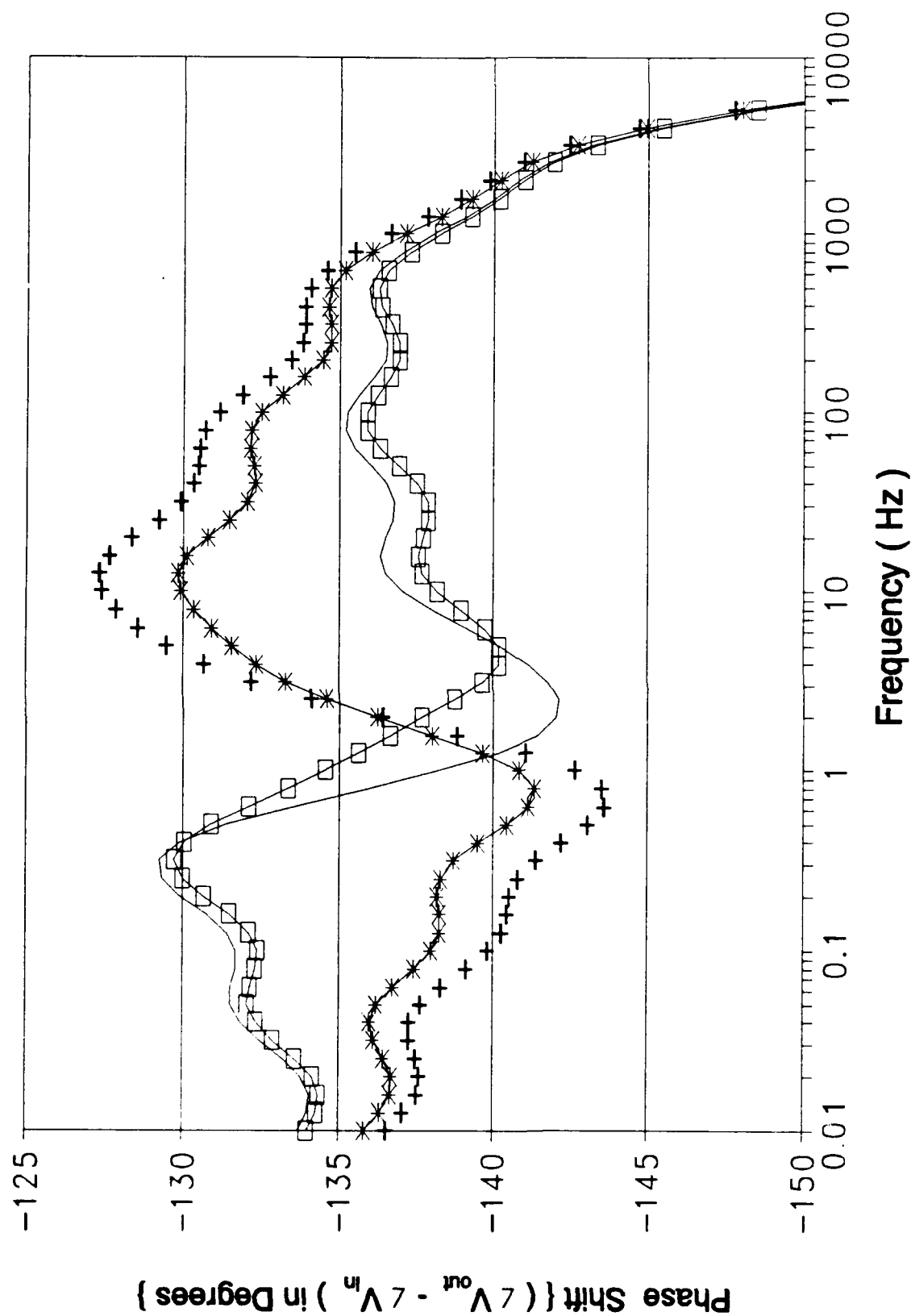Figure B-28.3 (cont). Gain Response of the Oldham Circuit Design Using an HSPICE Computer Variation of Cell 2 (cont);

Figure B-28.3 (cont). Phase Response of the Oldham Circuit Design Using an HSPICE Computer Variation of Cell 2.

Resistor And Capacitor Values For Figure B-29.1					
Symbol	——	-+-	-*-	-□-	
Resis- tor Value (MΩ)	1.5629	6.372	5.163	1.981	
Capaci- tor Value (μF)	1.902	6.162	8.069	2.782	

Figure B-29.1. Graphical Symbol Legend and Component Value Correlation for Figure B-29.1 (cont);
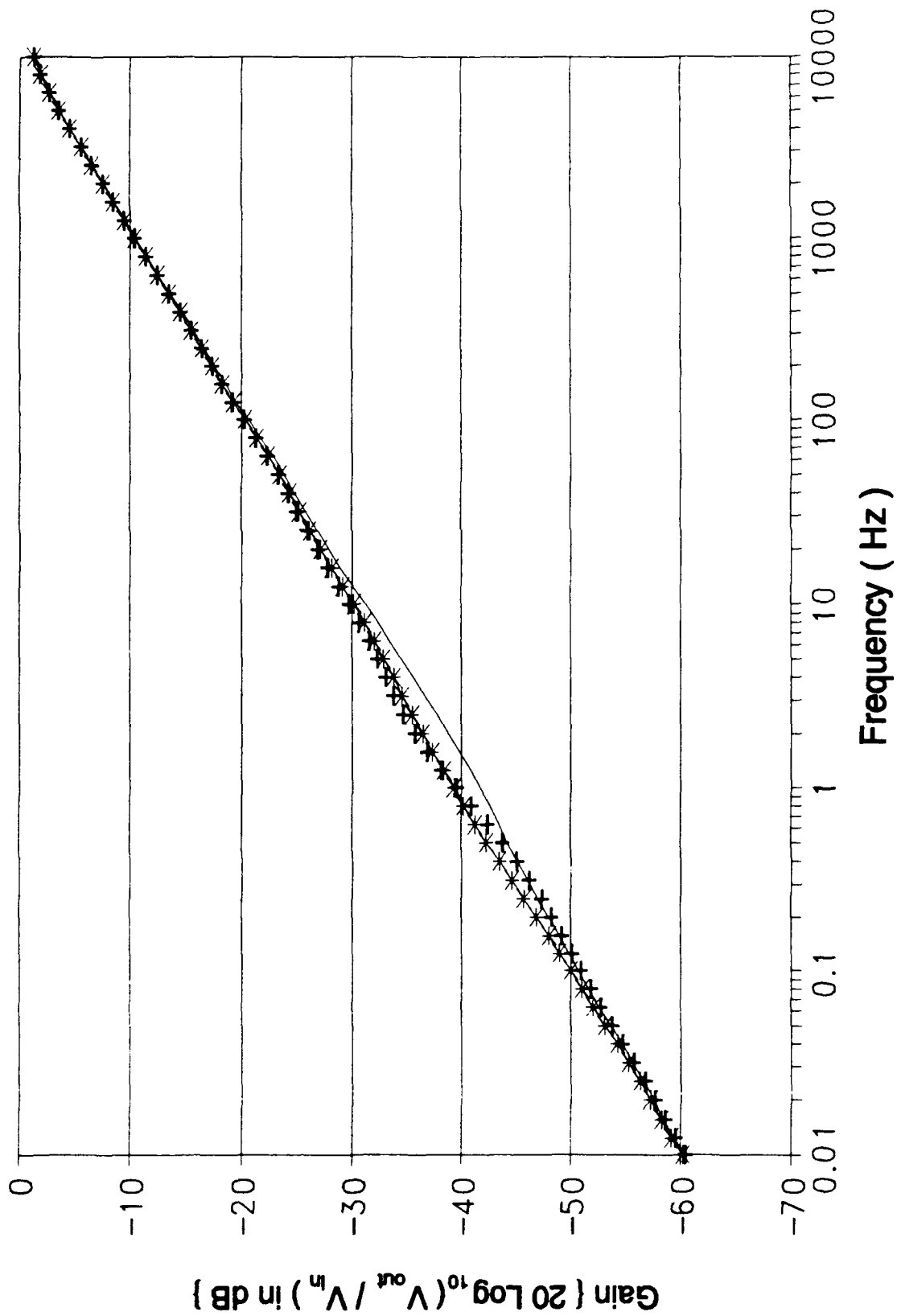
Figure B-29.1 (cont). Gain Response of the Oldham Circuit Design Using an HSPICE Computer Variation of Cell 3 (cont);
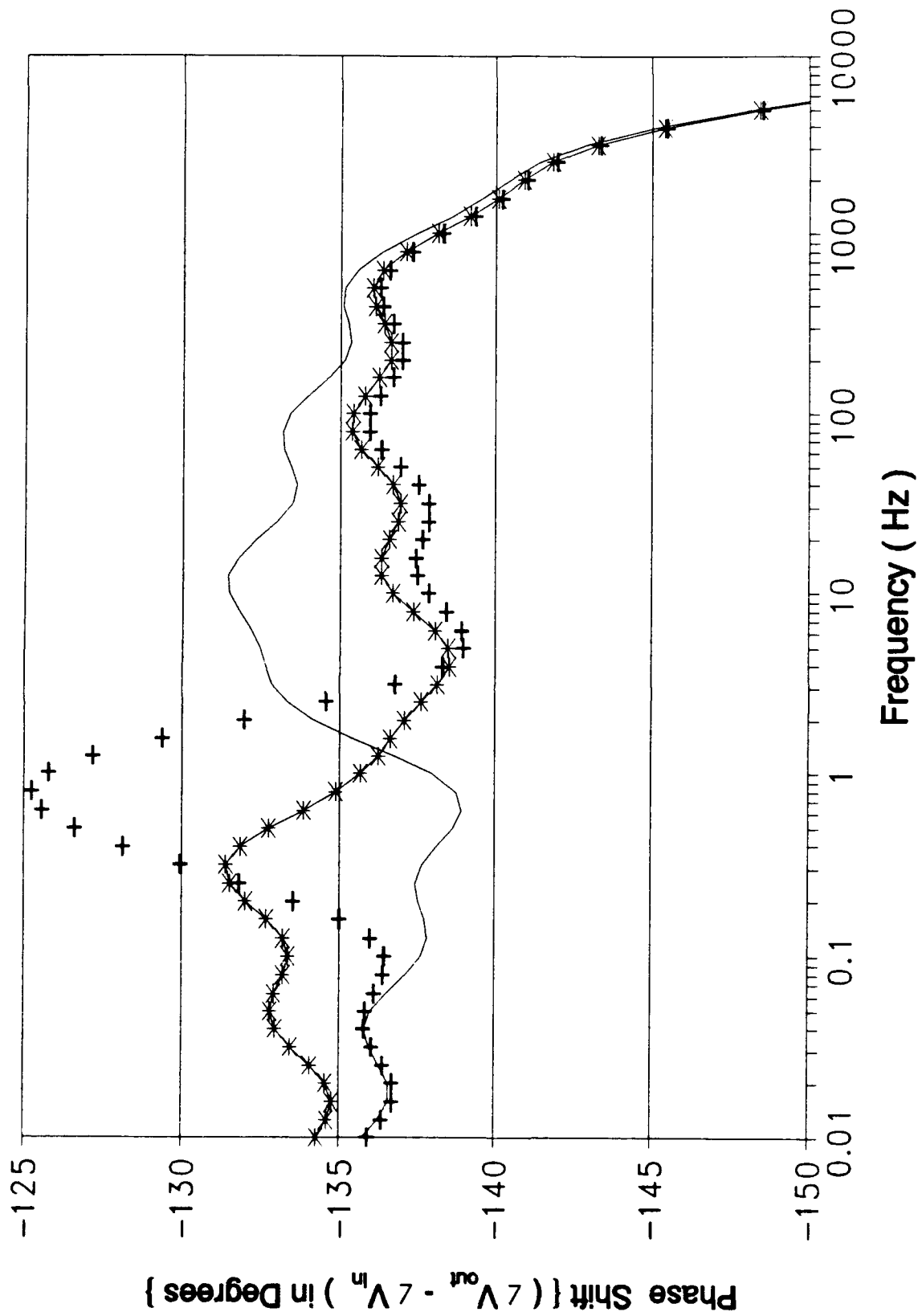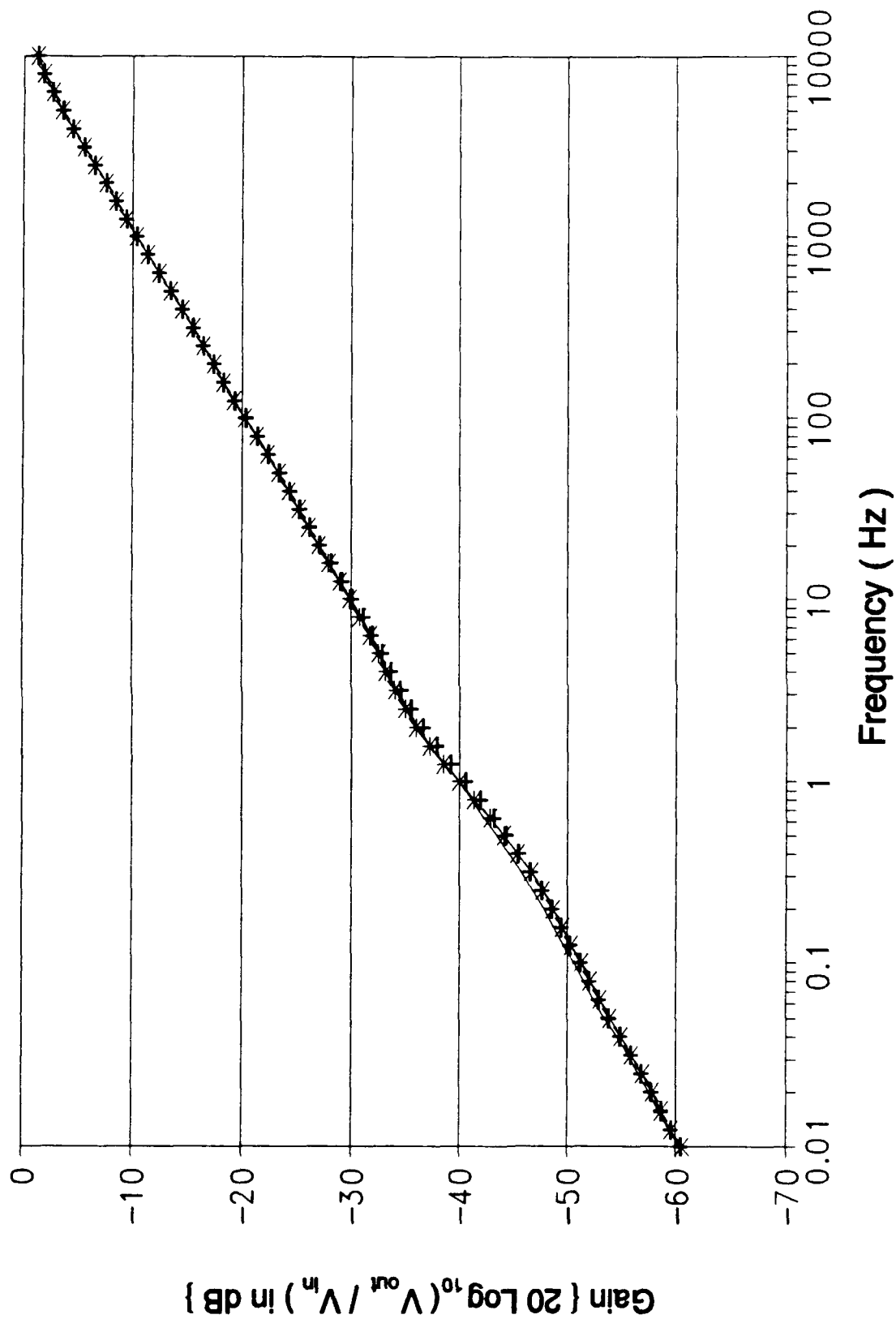
Figure B-29.1 (cont). Phase Response of the Oldham Circuit Design Using an HSPICE Computer Variation of Cell 3.

Resistor And Capacitor Values For Figure B-29.2					
Symbol	——	-+-	-*-		
Resis-tor Value (MΩ)	5.011	5.363	2.498		
Capaci-tor Value (μF)	1.005	2.848	2.0642		

Figure B-29.2. Graphical Symbol Legend and Component Value
Correlation for Figure B-29.2 (cont);

Figure B-29.2 (cont). Gain Response of the Oldham Circuit Design Using an HSPICE Computer Variation of Cell 3 (cont);
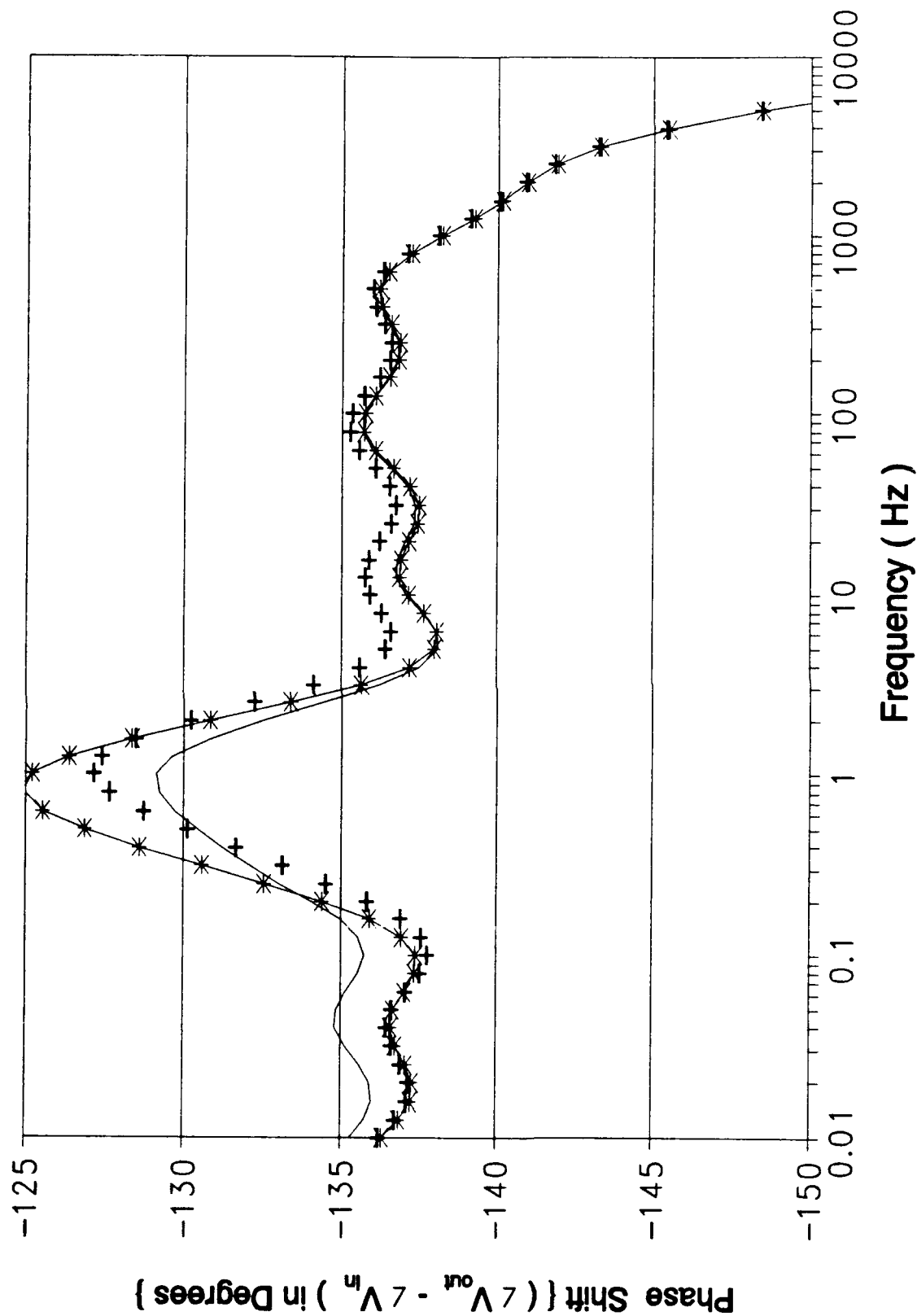
Figure A-29.2. Phase Response of Oldham Circuit Design Using Hspice Computer Variation of Cell 3 (cont);

Resistor And Capacitor Values For Figure B-29.3					
Symbol	——	-+-	-*-		
Resis- tor Value (MΩ)	4.259	5.901	6.159		
Capaci- tor Value (μF)	2.39	1.99	2.494		

Figure B-29.3.   Graphical Symbol Legend and Component Value
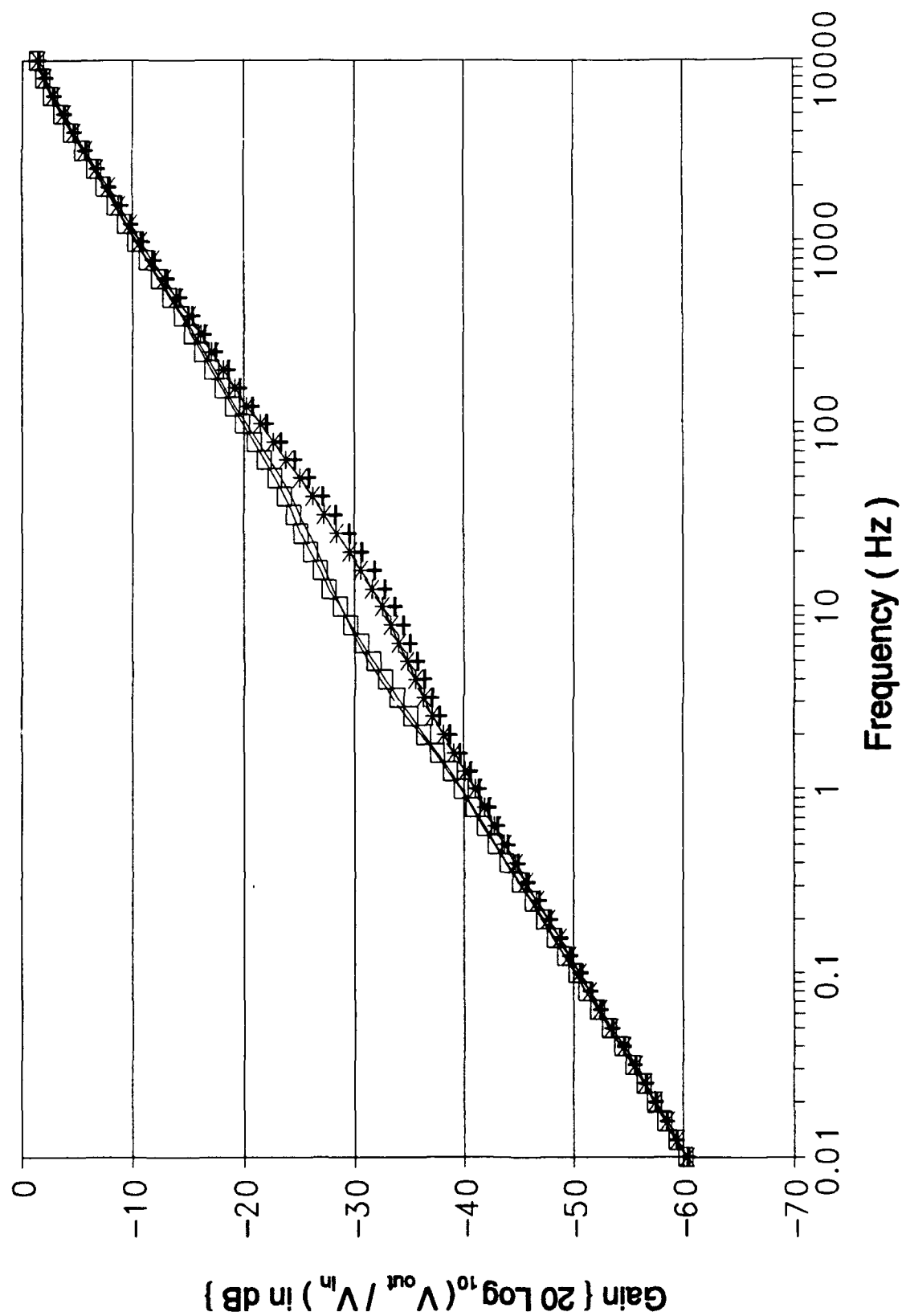   Correlation for Figure B-29.3 (cont);

Figure B-29.3 (cont). Gain Response of the Oldham Circuit Design Using an HSPICE Computer Variation of Cell 3 (cont);
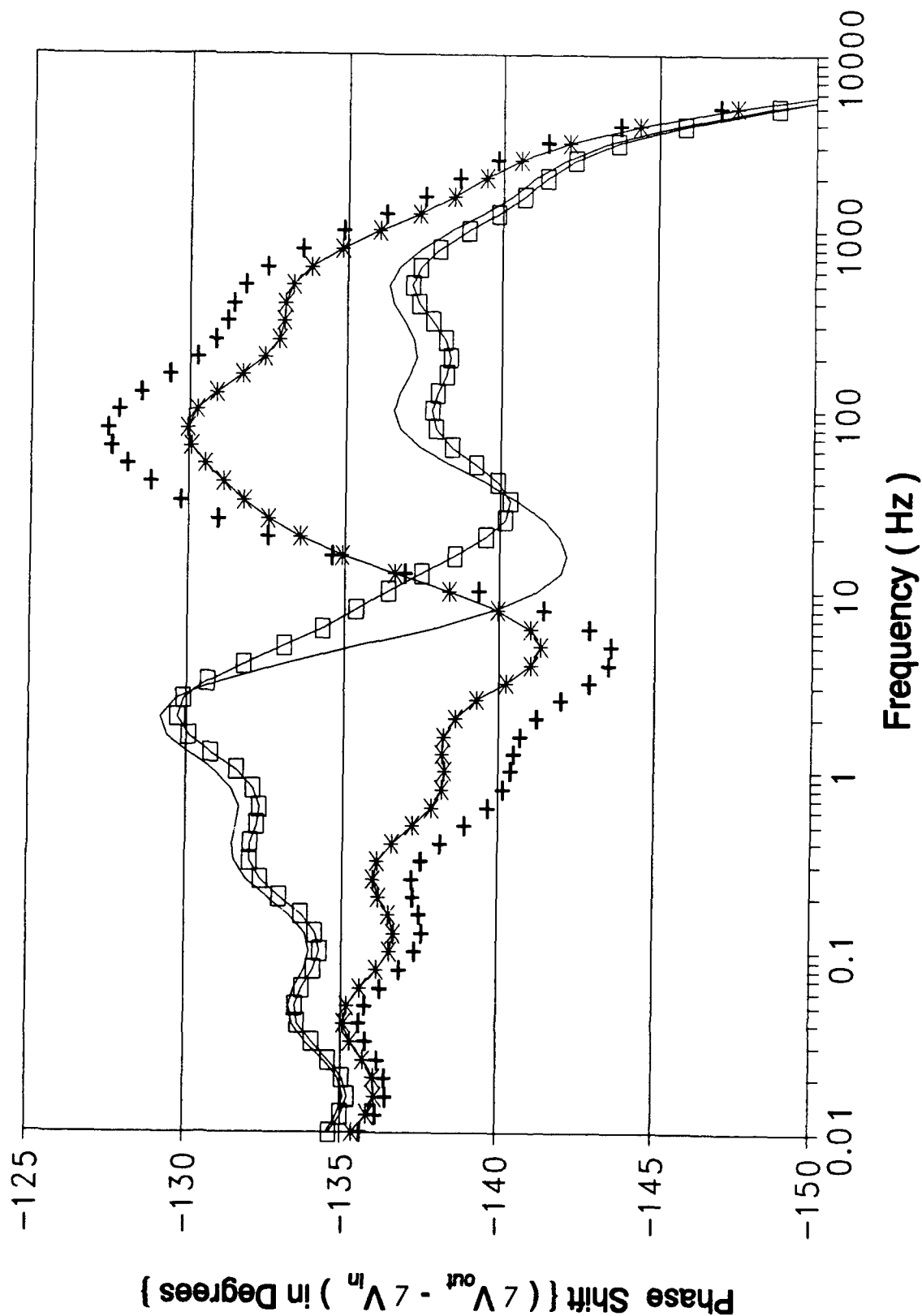
Figure B-29.3 (cont). Phase Response of the Oldham Circuit Design Using an HSPICE Computer Variation of Cell 3.

Resistor And Capacitor Values For Figure B-30.1					
Symbol	———	-+-	-*-	—◻—	
Resis-tor Value (MΩ)	0.0672	2.475	2.005	0.7697	
Capaci-tor Value (nF)	737.8	239	313	1079	

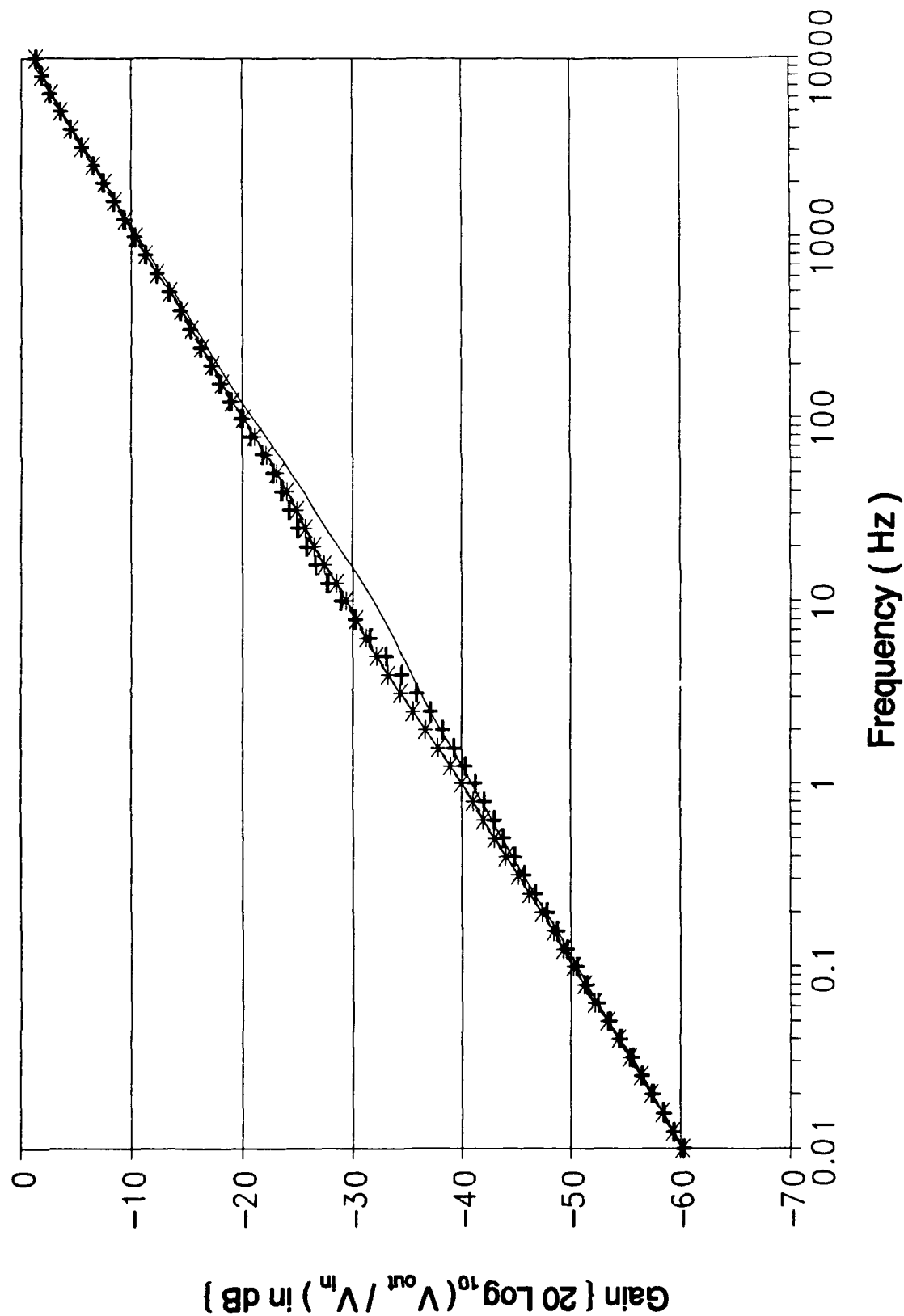**Figure B-30.1.** **Graphical Symbol Legend and Component Value Correlation for Figure B-30.1 (cont);**

Figure B-30.1 (cont). Gain Response of the Oldham Circuit Design Using an HSPICE Computer Variation of Cell 4 (cont);
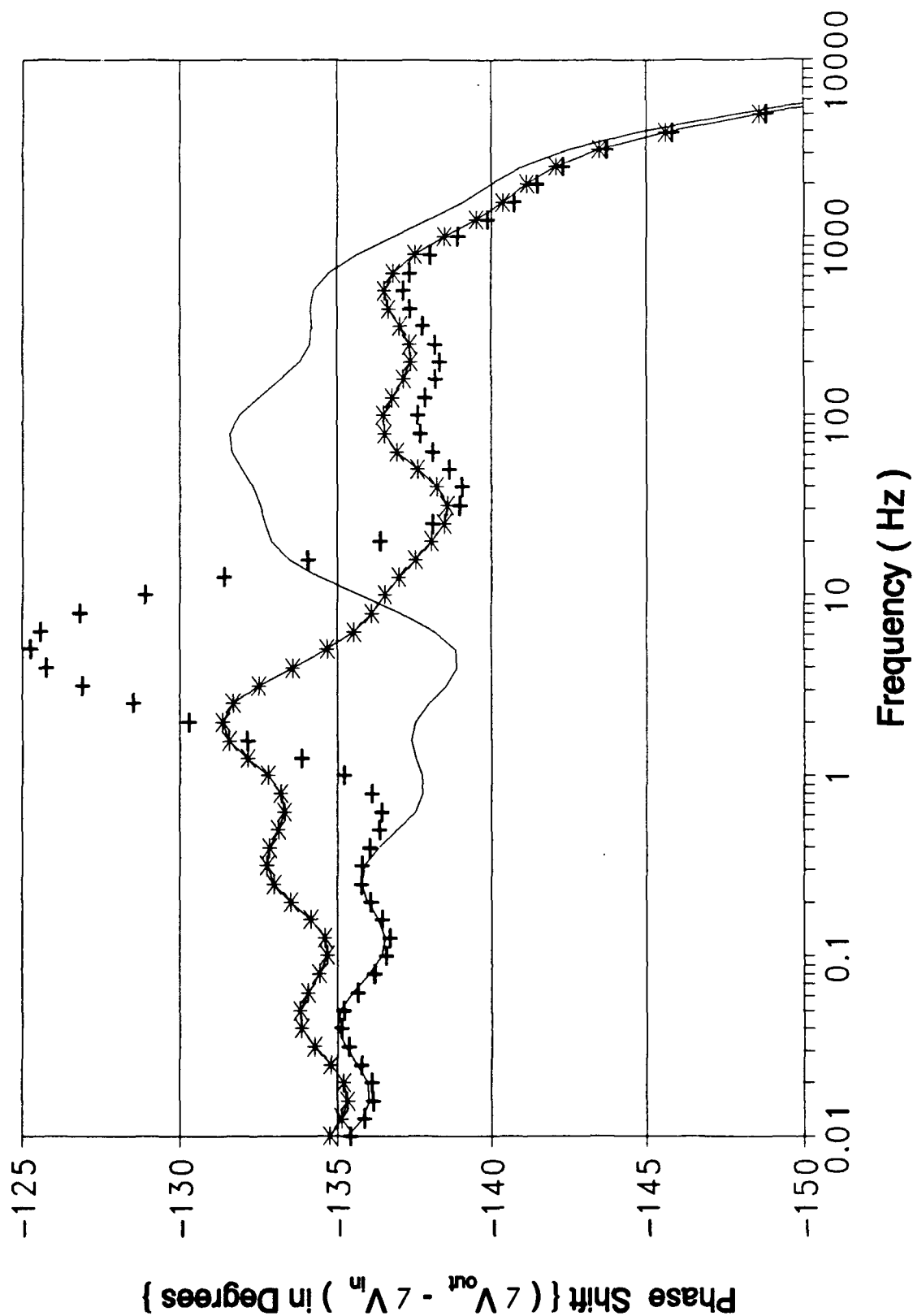
Figure B-30.1 (cont). Phase Response of the Oldham Circuit Design Using an HSPICE Computer Variation of Cell 4.

Resistor And Capacitor Values For Figure B-30.2				
Symbol	——	-+-	-*-		
Resis- tor Value (MΩ)	1.947	2.083	0.970		
Capaci- tor Value (nF)	389.9	1105	800.7		

Figure B-30.2. Graphical Symbol Legend and Component Value
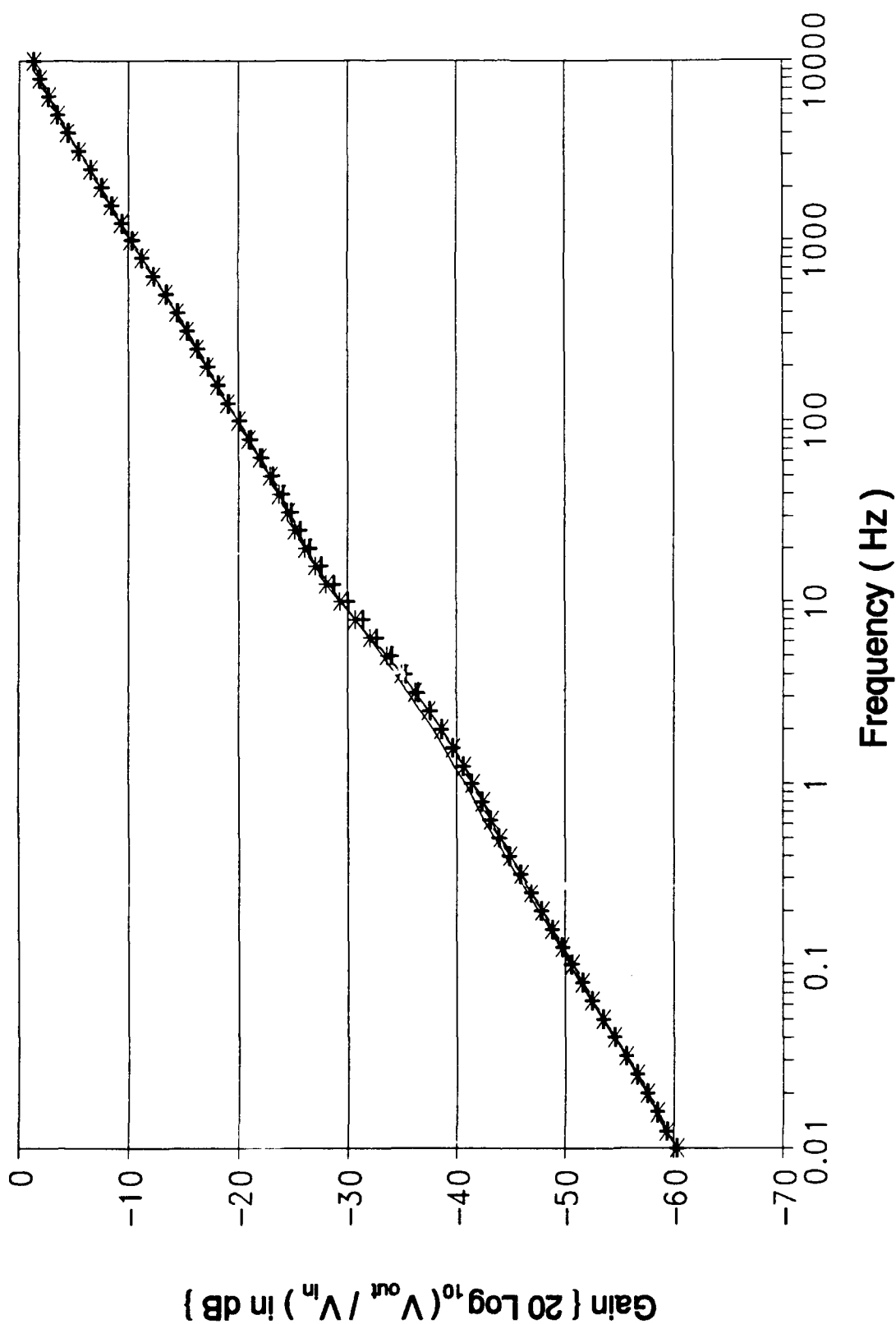**Correlation for Figure B-30.2 (cont);**

Figure B-30.2 (cont). Gain Response of the Oldham Circuit Design Using an HSPICE Computer Variation of Cell 4 (cont);
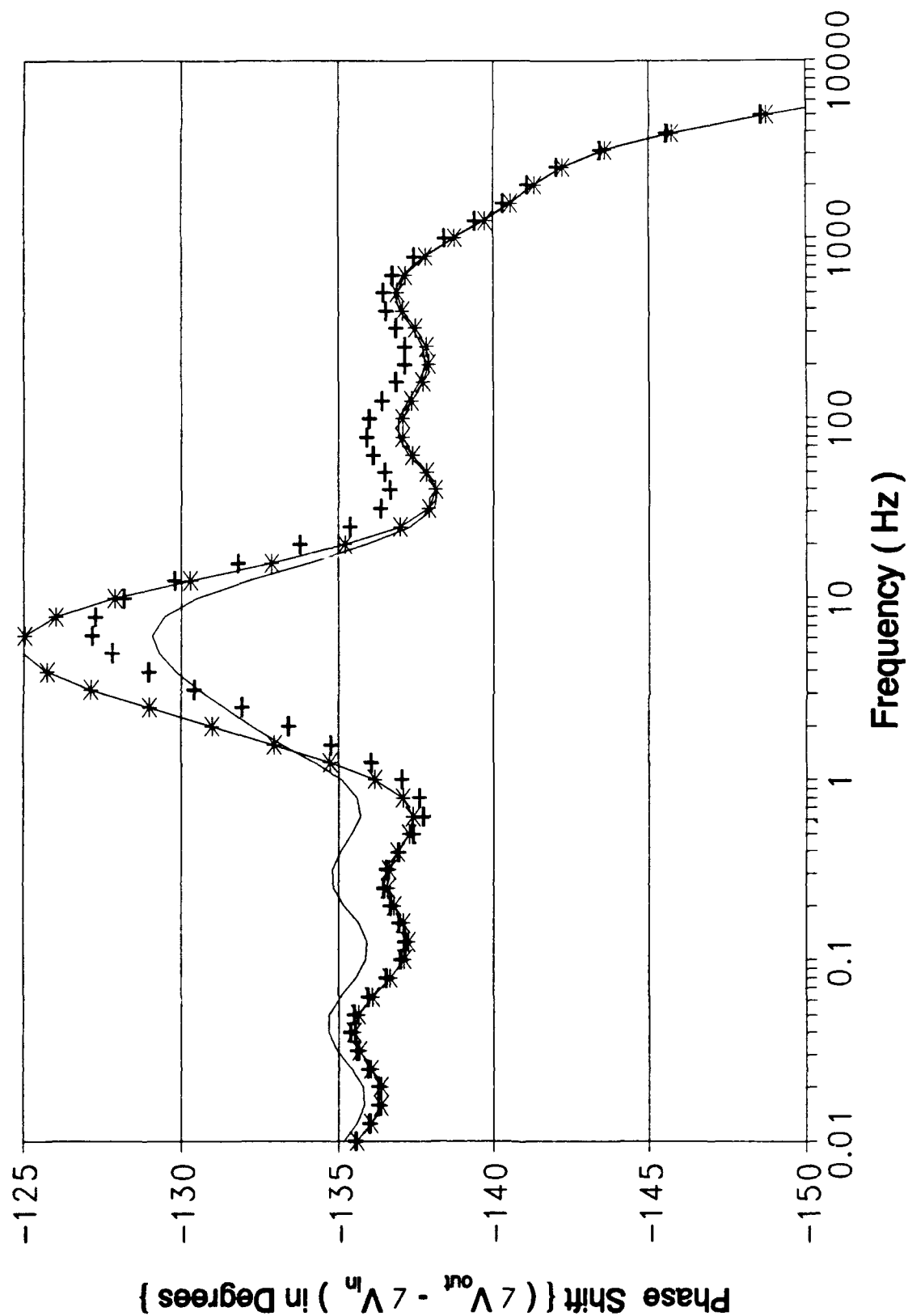
Figure B-30.2 (cont). Phase Response of the Oldham Circuit Design Using an HSPICE Computer Variation of Cell 4.

Resistor And Capacitor Values For Figure B-30.3				
Symbol	▬	-+-	-*-		
Resis-tor Value (MΩ)	1.654	2.292	2.392		
Capaci-tor Value (nF)	927.2	772.6	967.7		

Figure B-30.3. Graphical Symbol Legend and Component Value Correlation for Figure B-30.3 (cont);

Frequency (Hz)

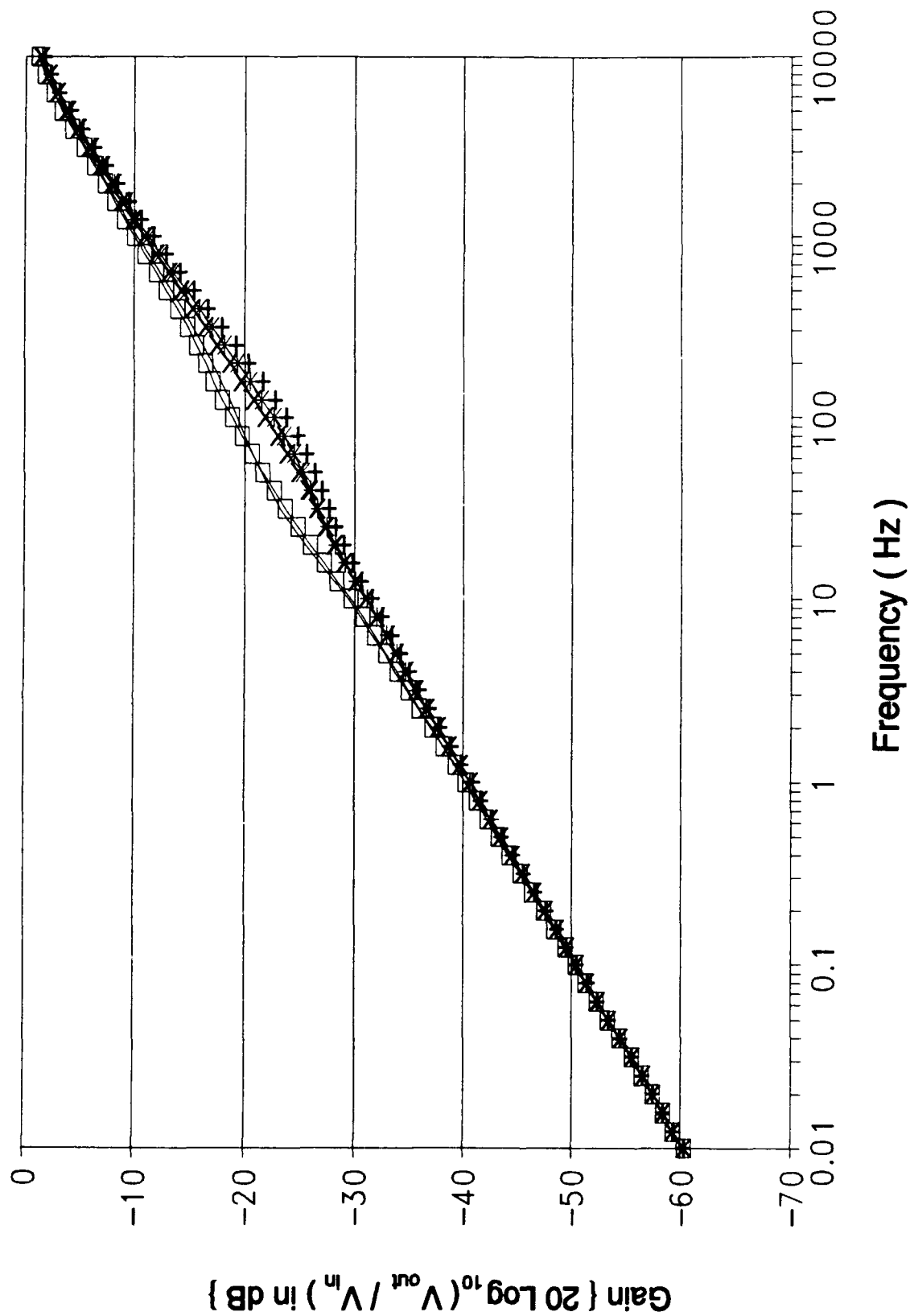Gain { 20 Log₁₀ (V_out / V_in) in dB }

Figure B-30.3 (cont). Gain Response of the Oldham Circuit Design Using an HSPICE Computer Variation of Cell 4 (cont);
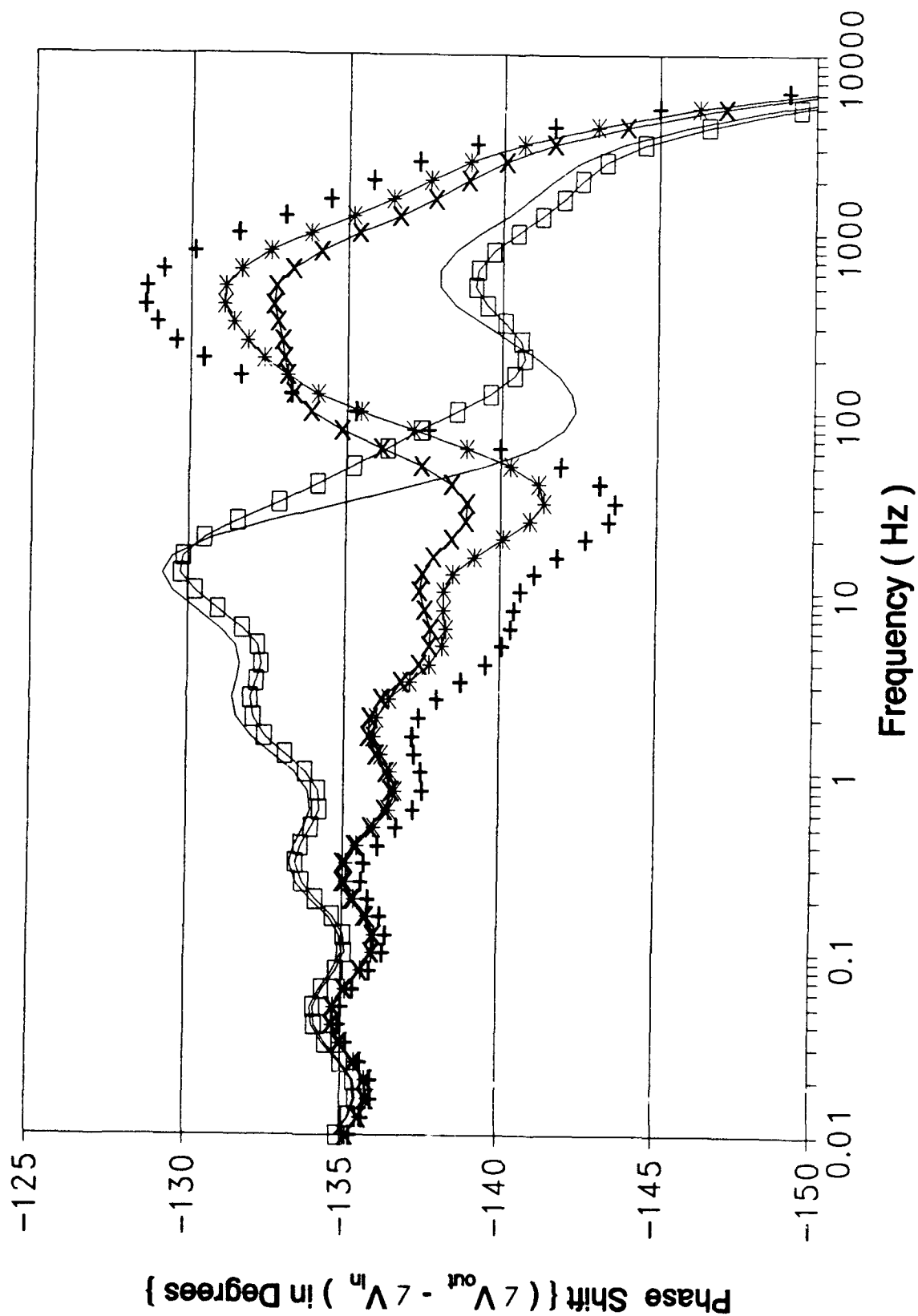
Figure B-30.3 (cont). Phase Response of the Oldham Circuit Design Using an HSPICE Computer Variation of Cell 4.

B-125

Resistor And Capacitor Values For Figure B-31.1					
Symbol	──	-+-	-*-	-□-	
Resis-tor Value (KΩ)	236	962.5	779.8	299.2	
Capaci-tor Value (nF)	286.8	92.92	121.6	419.5	

**Figure B-31.1.   Graphical Symbol Legend and Component Value Correlation for Figure B-31.1 (cont);**

Figure B-31.1 (cont). Gain Response of the Oldham Circuit Design Using an HSPICE Computer Variation of Cell 5 (cont);
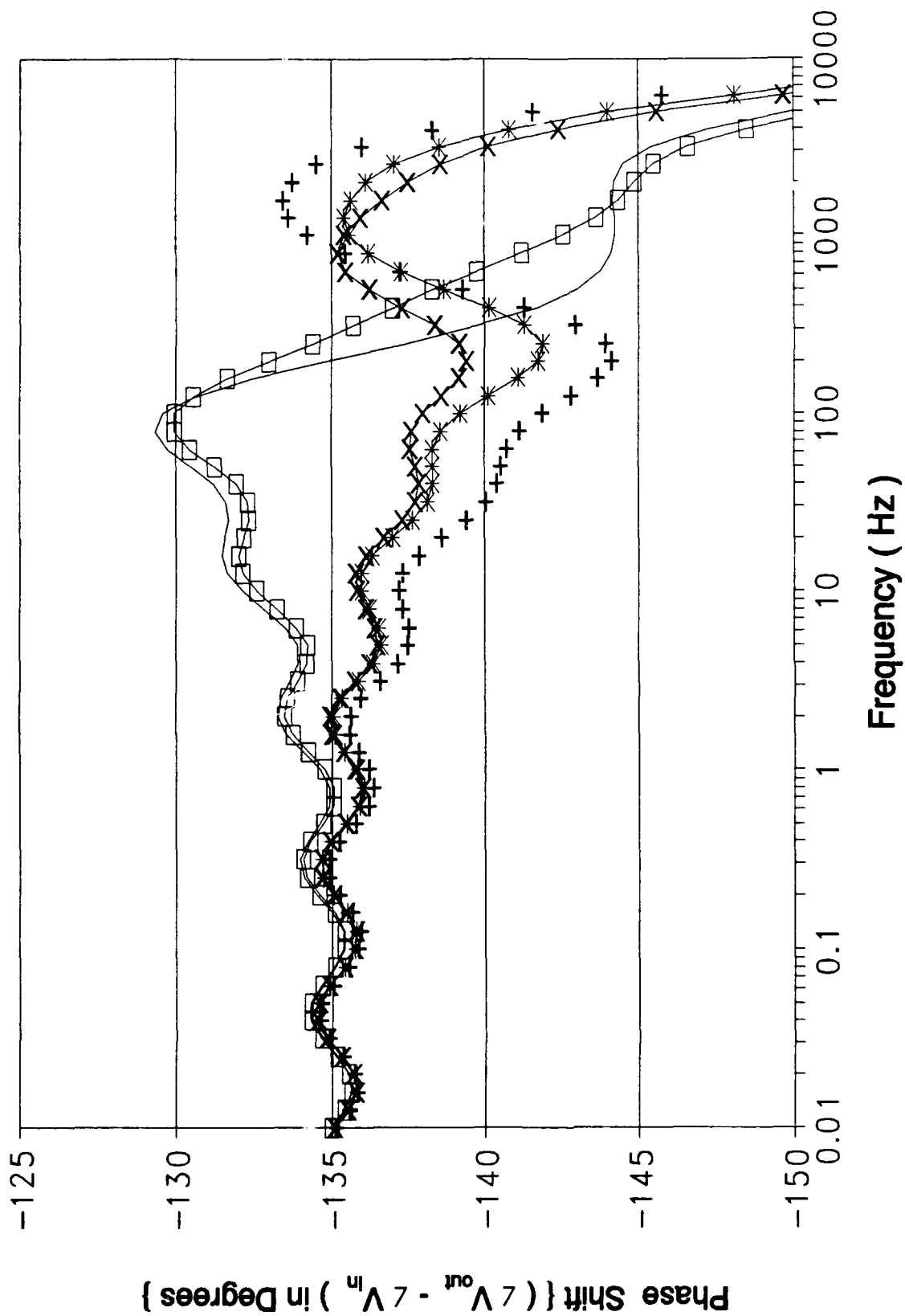
Figure B-31.1 (cont). Phase Response of the Oldham Circuit Design Using an HSPICE Computer Variation of Cell 5.

Resistor And Capacitor Values For Figure B-31.2					
Symbol	▬	-+-	-*-		
Resis- tor Value (KΩ)	756.95	810.10	377.3		
Capaci- tor Value (nF)	151.5	429.5	311.2		

Figure B-31.2. Graphical Symbol Legend and Component Value
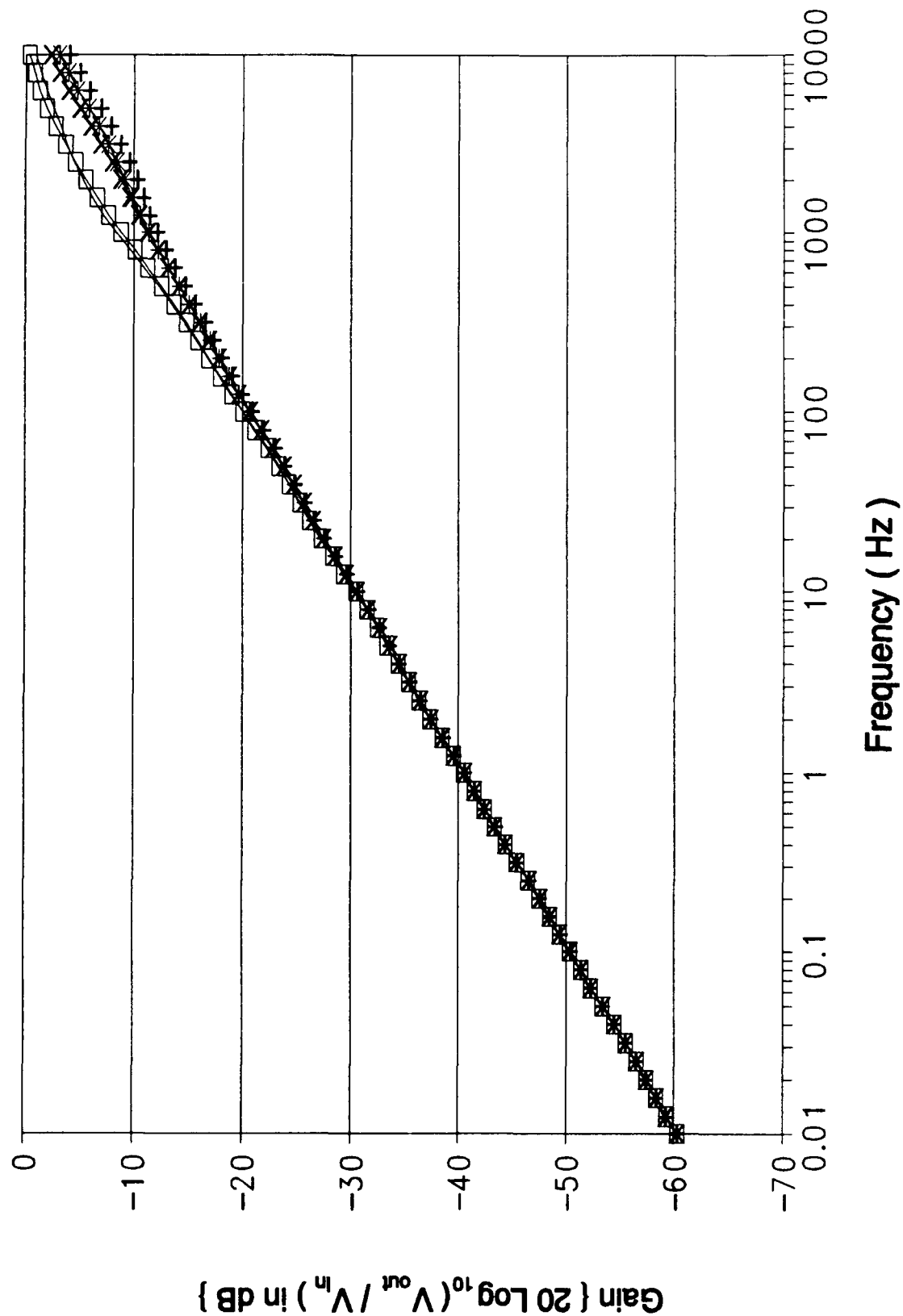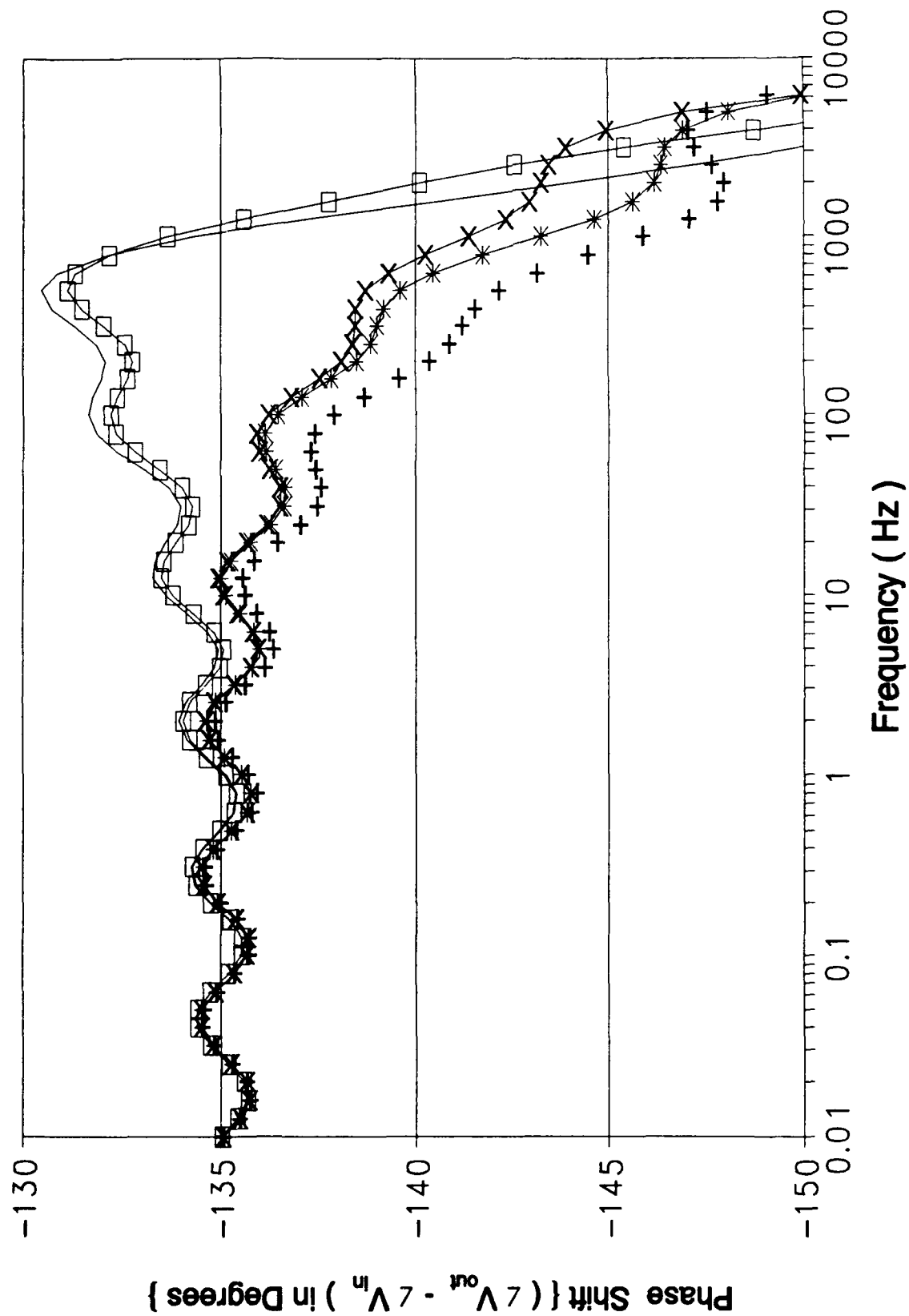**Correlation for Figure B-31.2 (cont);**

Figure B-31.2 (cont). Gain Response of the Oldham Circuit Design Using an HSPICE Computer Variation of Cell 5 (cont);

Figure B-31.2 (cont). Phase Response of the Oldham Circuit Design Using an HSPICE Computer Variation of Cell 5.

Resistor And Capacitor Values For Figure B-31.3					
Symbol	━━	-+-	-*-		
Resis- tor Value (KΩ)	643.3	891.30	930.29		
Capaci- tor Value (nF)	360.4	300.30	376.20		

Figure B-31.3. Graphical Symbol Legend and Component Value
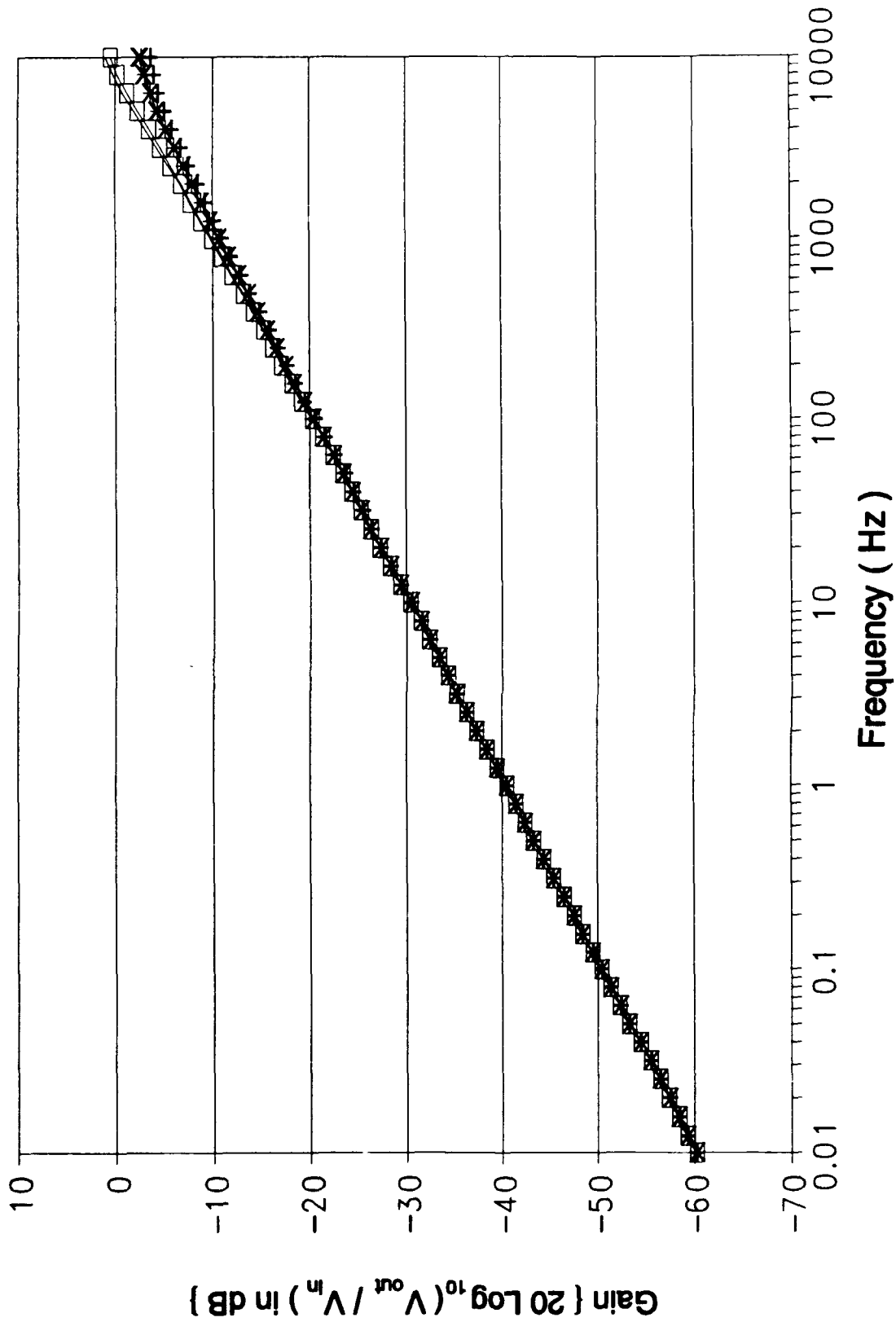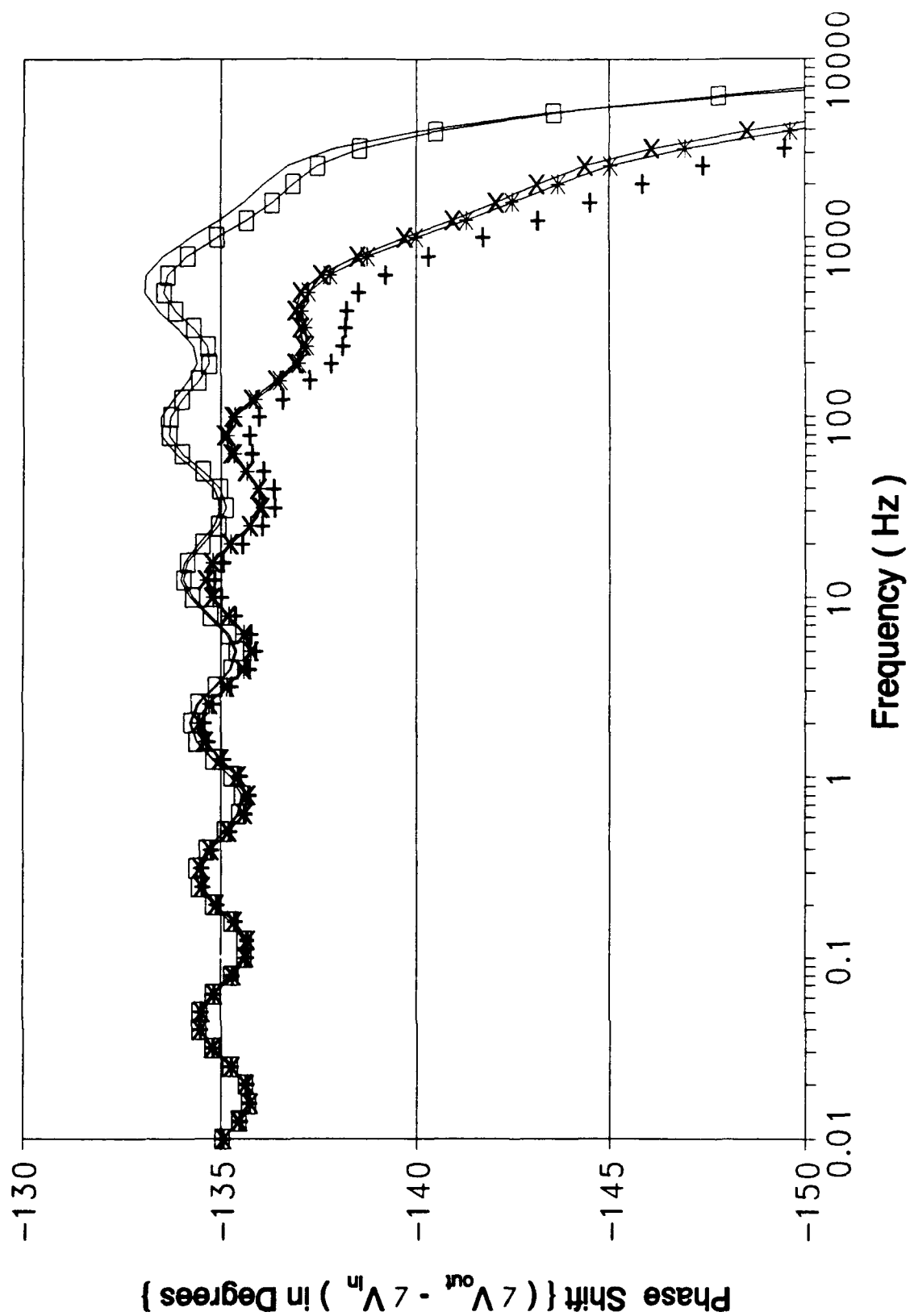**Correlation for Figure B-31.3 (cont);**

Figure B-31.3 (cont). Gain Response of the Oldham Circuit Design Using an HSPICE Computer Variation of Cell 5 (cont);

Figure B-31.3 (cont). Phase Response of the Oldham Circuit Design Using an HSPICE Computer Variation of Cell 5.

B-134

Resistor And Capacitor Values For Figure B-32.1					
Symbol	———	-+-	-*-	-▯-	
Resis-tor Value (KΩ)	91.74	374.2	303.1	116.3	
Capaci-tor Value (nF)	111.4	36.1	47.29	163.0	

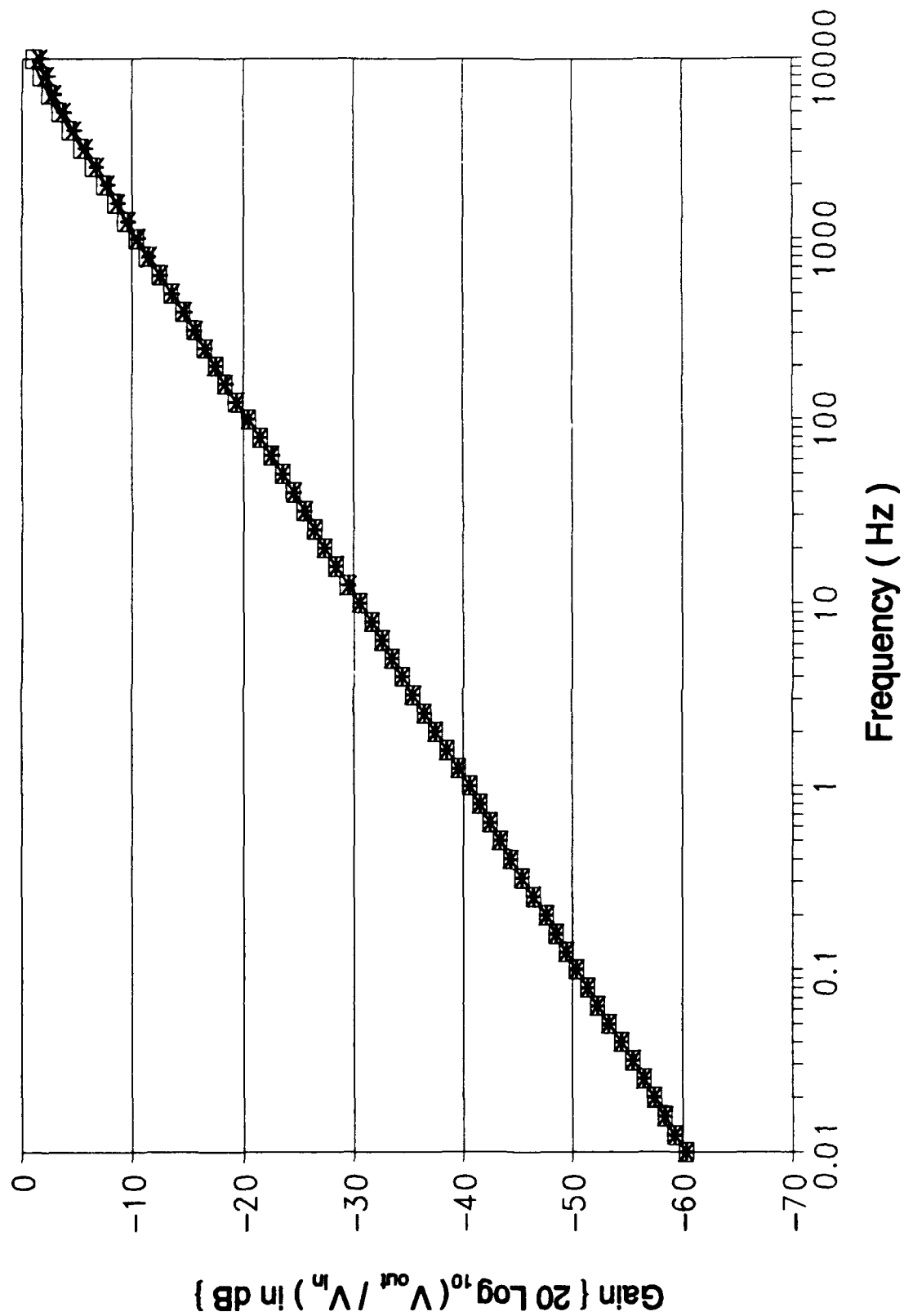**Figure B-32.1. Graphical Symbol Legend and Component Value Correlation for Figure B-32.1 (cont);**

Figure B-32.1 (cont). Gain Response of the Oldham Circuit Design Using an HSPICE Computer Variation of Cell 6 (cont);
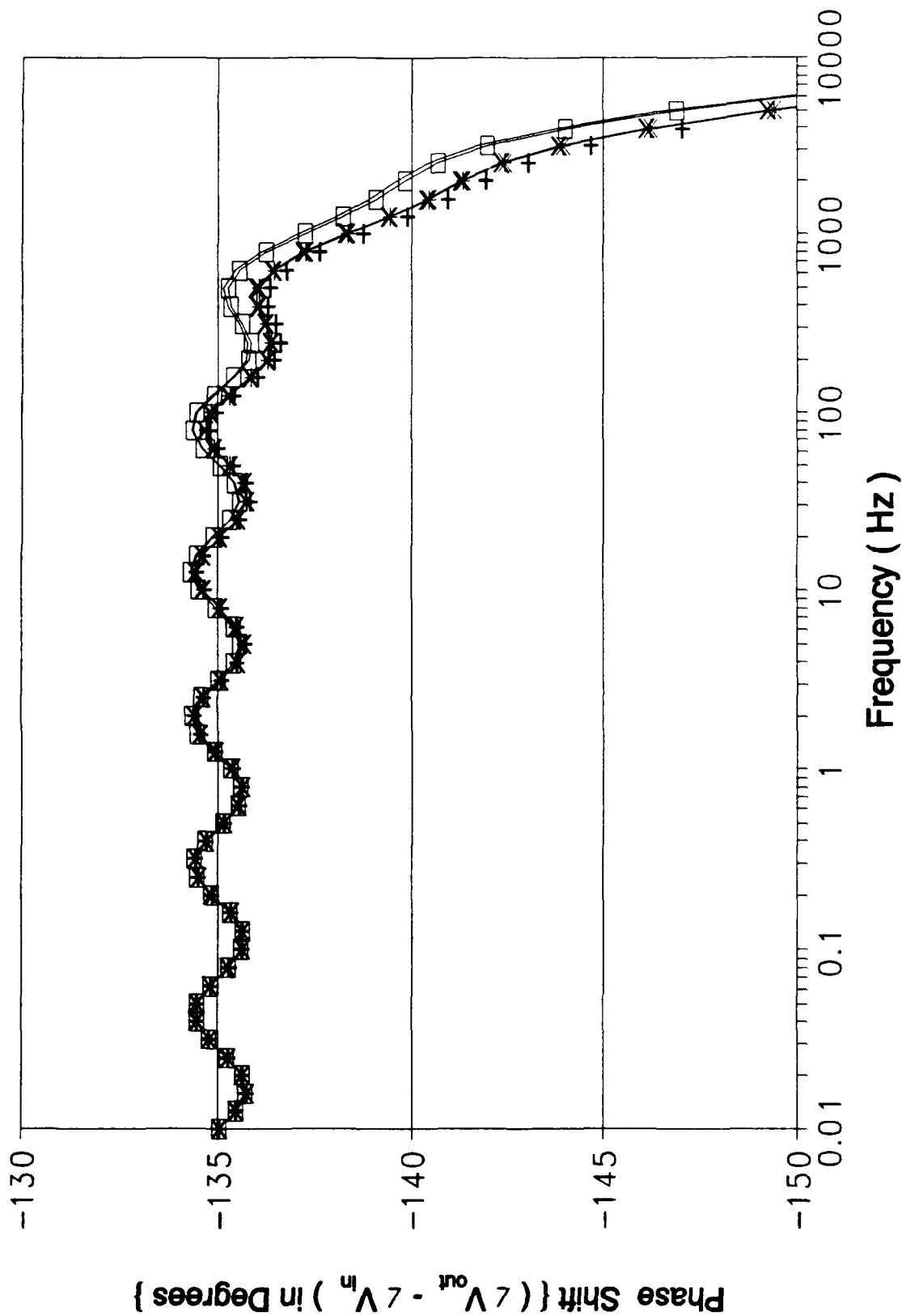
Figure B-32.1 (cont). Phase Response of the Oldham Circuit Design Using an HSPICE Computer Variation of Cell 6.

Resistor And Capacitor Values For Figure B-32.2					
Symbol	——	-+-	-*-		
Resis-tor Value (KΩ)	294.2	314.9	146.6		
Capaci-tor Value (nF)	58.91	166.9	120.9		

Figure B-32.2. **Graphical Symbol Legend and Component Value Correlation for Figure B-32.2 (cont);**

Frequency (Hz)

Gain { 20 Log$_{10}$ (V$_{out}$ / V$_{in}$) in dB }

Figure B-32.2 (cont). Gain Response of the Oldham Circuit Design Using
an HSPICE Computer Variation of Cell 6 (cont);

Figure B-32.2 (cont). Phase Response of the Oldham Circuit Design Using an HSPICE Computer Variation of Cell 6.

B-140

Resistor And Capacitor Values For Figure B-32.3					
Symbol	——	-+-	-*-		
Resis- tor Value (KΩ)	250.1	346.5	361.6		
Capaci- tor Value (nF)	140.1	116.7	146.2		

Figure B-32.3. Graphical Symbol Legend and Component Value Correlation for Figure B-32.3 (cont);

Figure B-32.3 (cont). Gain Response of the Oldham Circuit Design Using an HSPICE Computer Variation of Cell 6 (cont);

Figure B-32.3 (cont). Phase Response of the Oldham Circuit Design Using an HSPICE Computer Variation of Cell 6.

B-143

Resistor And Capacitor Values For Figure B-33					
Symbol	——	-+-	-*-	-□-	-×-
Resis-tor Value (KΩ)	35.66	145.4	117.8	45.21	114:3
Capaci-tor Value (nF)	43.32	14.03	18.38	63.38	22.9

Figure B-33. Graphical Symbol Legend and Component Value Correlation for Figure B-33 (cont);

Figure B-33 (cont). Gain Response of the Oldham Circuit Design Using an HSPICE Computer Variation of Cell 7 (cont);

Figure B-33 (cont). Phase Response of the Oldham Circuit Design Using an Hspice Computer Variation of Cell 7.

Resistor And Capacitor Values For Figure B-34					
Symbol	——	-+-	-*-	-▫-	-×-
Resis-tor Value (KΩ)	13.86	56.52	45.79	52.34	54.62
Capaci-tor Value (nF)	16.84	5.458	7.147	17.64	22.09

**Figure B-34.   Graphical Symbol Legend and Component Value Correlation for Figure B-34 (cont);**
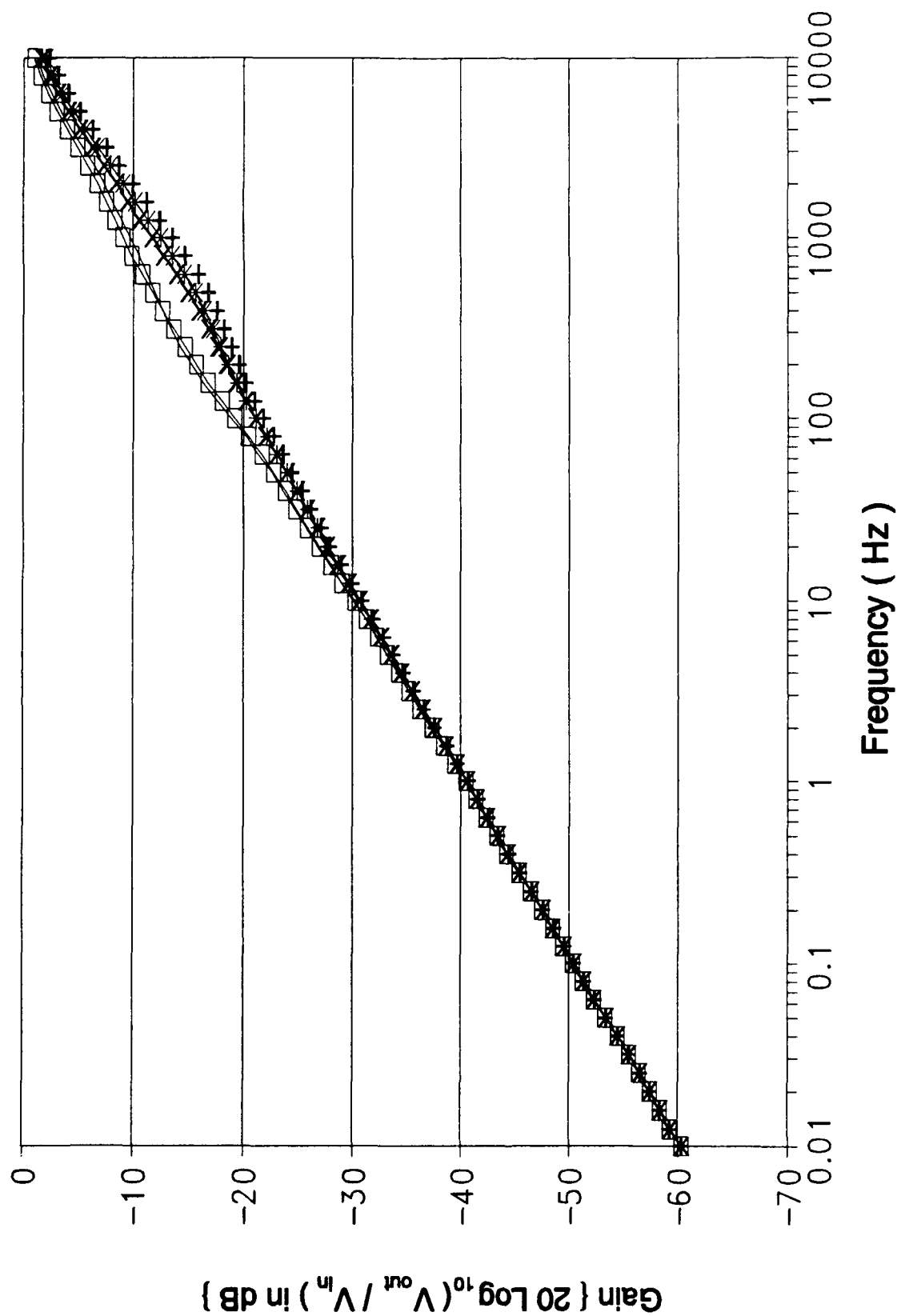
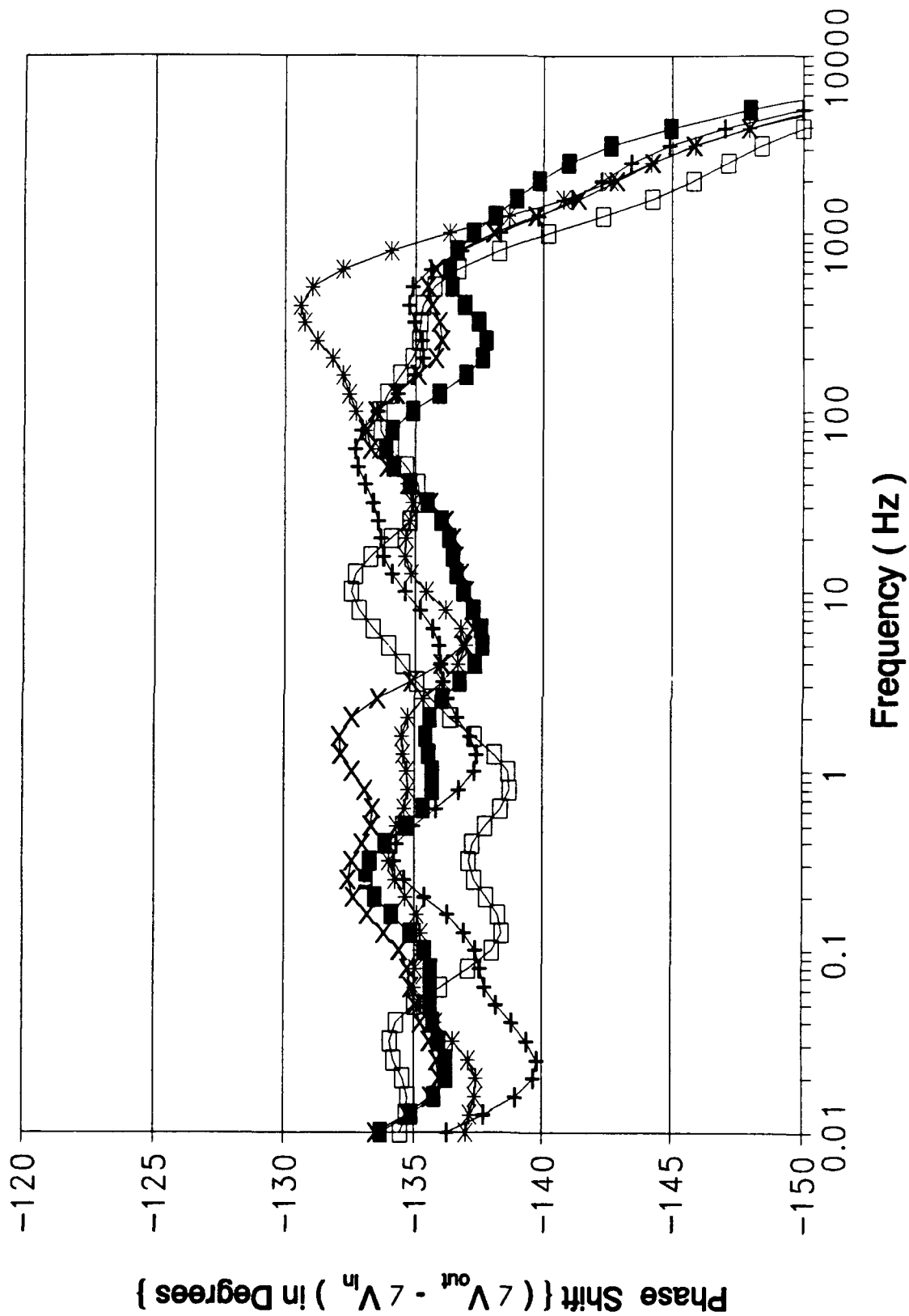Figure B-34 (cont).   Gain Response of the Oldham Circuit Design Using an HSPICE Computer Variation of Cell 8 (cont);

Figure B-34 (cont). Phase Response of the Oldham Circuit Design Using an HSPICE Computer Variation of Cell 8.

B-149

Resistor And Capacitor Values For Figure B-35					
Symbol	——	-+-	-*-	-◻-	-×-
Resis-tor Value (KΩ)	5.391	21.98	17.80	6.834	17.28
Capaci-tor Value (nF)	6.545	2.120	2.776	9.575	3.459

Figure B-35.   Graphical Symbol Legend and Component Value
              Correlation for Figure B-35 (cont);

Frequency (Hz)

Gain { 20 Log$_{10}$ (V$_{out}$ / V$_{in}$) in dB }

Figure B-35 (cont). Gain Response of the Oldham Circuit Design Using an HSPICE Computer Variation of Cell 9 (cont);

Figure B-35 (cont). Phase Response of the Oldham Circuit Design Using an HSPICE Computer Variation of Cell 9.

B-152

Resistor And Capacitor Values For Figure B-36					
Symbol	▬	–+–	–*–	–◻–	–×–
Resis-tor Value (KΩ)	2.095	8.541	6.920	2.655	6.716
Capaci-tor Value (nF)	2.545	0.8256	1.079	3.723	1.345

Figure B-36.   Graphical Symbol Legend and Component Value
Correlation for Figure B-36 (cont);

Figure B-36 (cont). Gain Response of the Oldham Circuit Design Using an HSPICE Computer Variation of Cell 10 (cont);

Figure B-36 (cont). Phase Response of the Oldham Circuit Design Using an HSPICE Computer Variation of Cell 10.

B-155

Resistor And Capacitor Values For Figure B-37					
Symbol	———	-+-	-*-	-□-	-x-
Resis- tor Value (KΩ)	0.348	1.726	1.379	0.4679	1.336
Capaci- tor Value (nF)	1.978	0.641	0.8394	2.894	1.045

**Figure B-37. Graphical Symbol Legend and Component Value
Correlation for Figure B-37 (cont);**

Figure B-37 (cont). Gain Response of the Oldham Circuit Design Using an HSPICE Computer Variation of Cell 11 (cont);

Figure B-37 (cont). Phase Response of the Oldham Circuit Design Using an HSPICE Computer Variation of Cell 11.

Section 3

Oldham Circuit Responses for "All-Cell" Component Values Varied by ± 20 Percent

Resistor and Capacitor Values for Figure B-38 and Graphical Symbol -■-		
Cell Number	Resistor (MΩ)	Capacitor (nF)
0	59.915	17844.0
1	26.847	10249.0
2	11.303	4379.1
3	3.3187	1696.0
4	1.6031	628.48
5	0.5184	259.15
6	0.20078	101.50
7	0.10367	37.327
8	0.036299	11.18
9	0.012224	6.0276
10	0.005590	2.225
11	0.001193	1.5009
12	0.001947	N/A

Figure B-38. Graphical Symbol Legend and Component Value Correlation for Figure B-38 (cont);

Resistor and Capacitor Values for Figure B-38 and Graphical Symbol -+-		
Cell Number	Resistor (MΩ)	Capacitor (nF)
0	68.526	19603.0
1	28.797	10180.0
2	9.8214	4439.2
3	3.3577	1319.0
4	1.5756	493.24
5	0.4913	187.71
6	0.20817	84.392
7	0.089286	40.013
8	0.038072	13.328
9	0.012839	4.904
10	0.004871	2.0144
11	0.001056	1.6844
12	0.002528	N/A

Figure B-38 (cont). **Graphical Symbol Legend and Component Value Correlation for Figure B-38 (cont);**

Resistor and Capacitor Values for Figure B-38 and Graphical Symbol -*-		
Cell Number	Resistor (MΩ)	Capacitor (nF)
0	78.854	13698.0
1	24.495	10788.0
2	8.3643	3358.0
3	3.6059	1255.5
4	1.3753	554.77
5	0.54143	246.57
6	0.24370	75.632
7	0.086511	34.216
8	0.039393	14.834
9	0.010652	5.1474
10	0 004385	2.231
11	0.0009216	1.5813
12	0.002517	N/A

Figure B-38 (cont). Graphical Symbol Legend and Component Value Correlation for Figure B-38 (cont);

Resistor and Capacitor Values for Figure B-38 and Graphical Symbol -▢-		
Cell Number	Resistor (MΩ)	Capacitor (nF)
0	57.823	18790.0
1	24.221	11635.0
2	10.436	4003.5
3	3.7666	1775.4
4	1.4438	538.01
5	0.54696	189.67
6	0.23229	97.711
7	0.093205	31.875
8	0.032333	14.233
9	0.011715	4.2028
10	0.005752	1.7231
11	0.0009992	1.819
12	0.002260	N/A

Figure B-38 (cont). Graphical Symbol Legend and Component Value Correlation for Figure B-38 (cont);

Resistor and Capacitor Values for Figure B-38 and Graphical Symbol -×-		
Cell Number	Resistor (MΩ)	Capacitor (nF)
0	78.577	16131.0
1	25.136	9081.0
2	11.306	4591.7
3	3.5237	1634.7
4	1.6202	680.82
5	0.62524	261.78
6	0.18056	103.70
7	0.097731	36.383
8	0.032413	13.204
9	0.010601	5.1023
10	0.004436	1.7526
11	0.001139	1.3012
12	0.001903	N/A

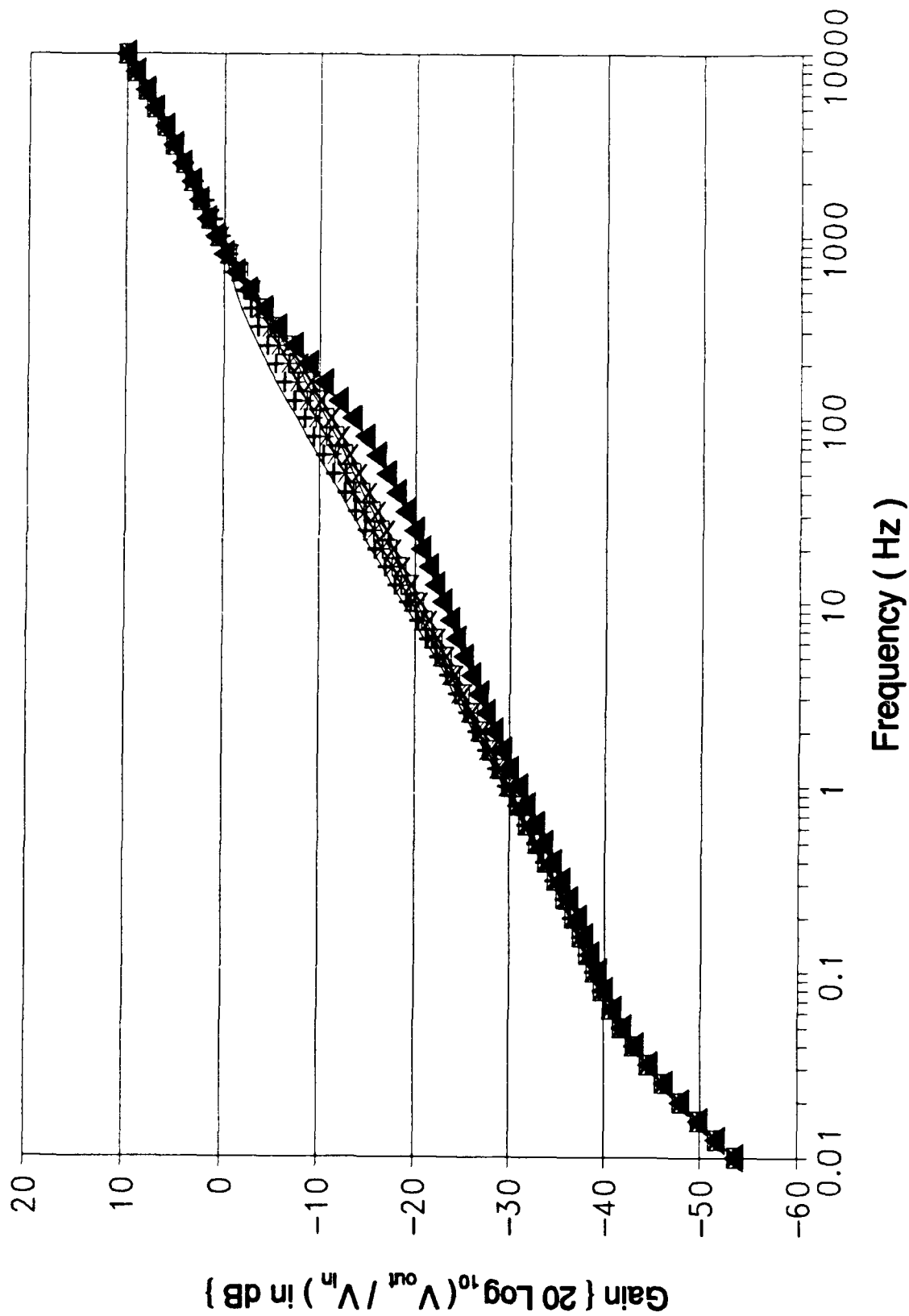Figure B-38 (cont). Graphical Symbol Legend and Component Value Correlation for Figure B-38 (cont);
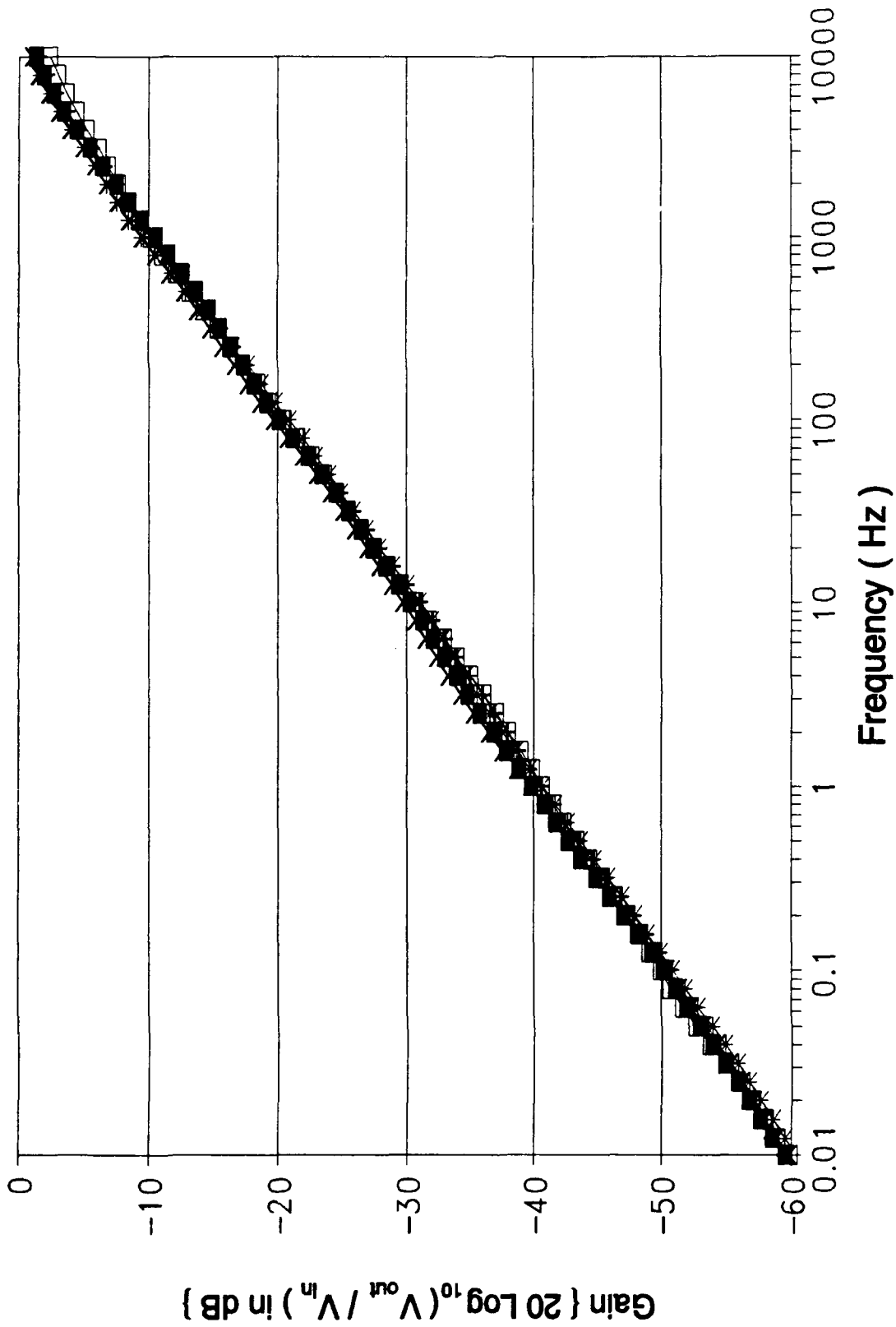
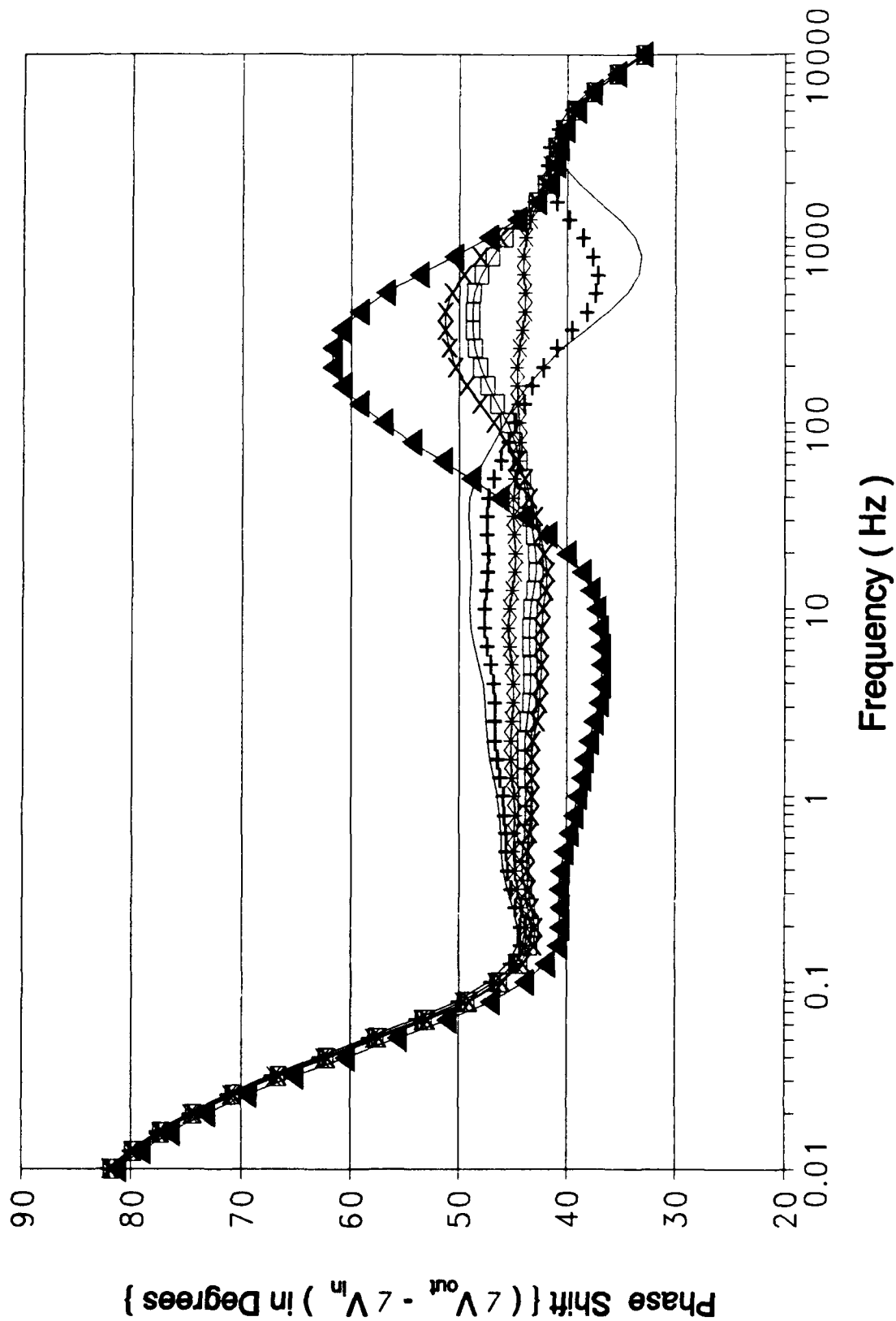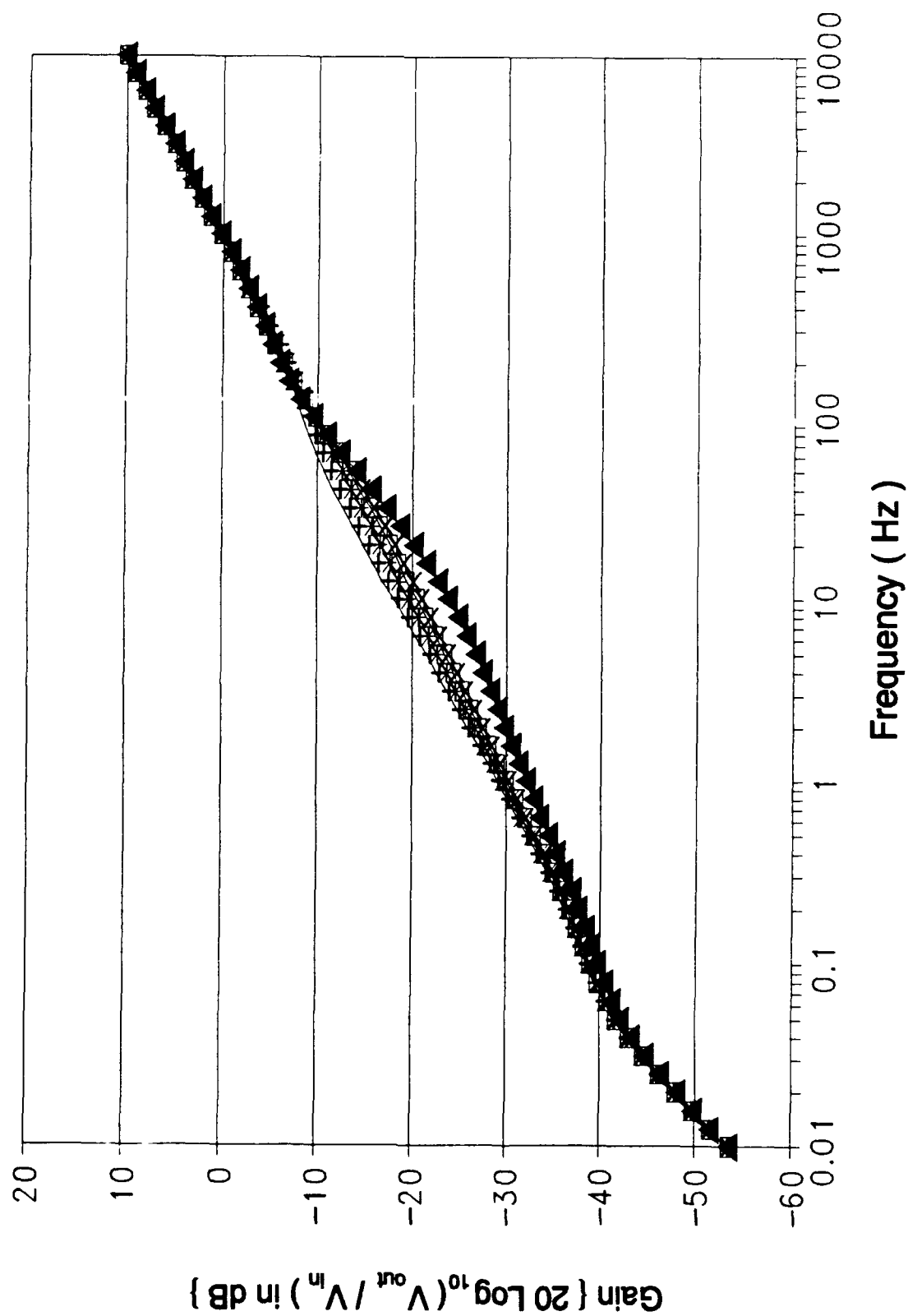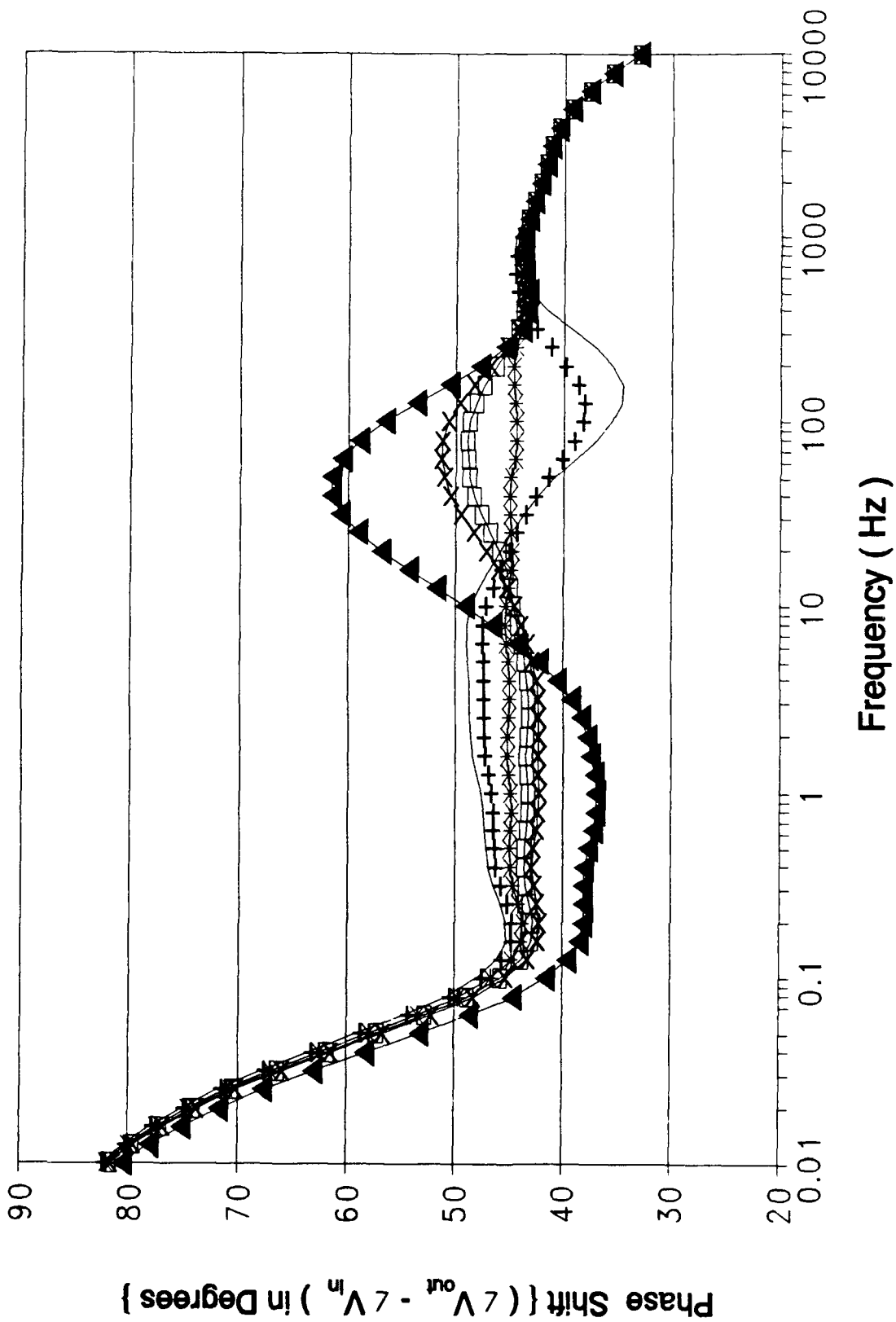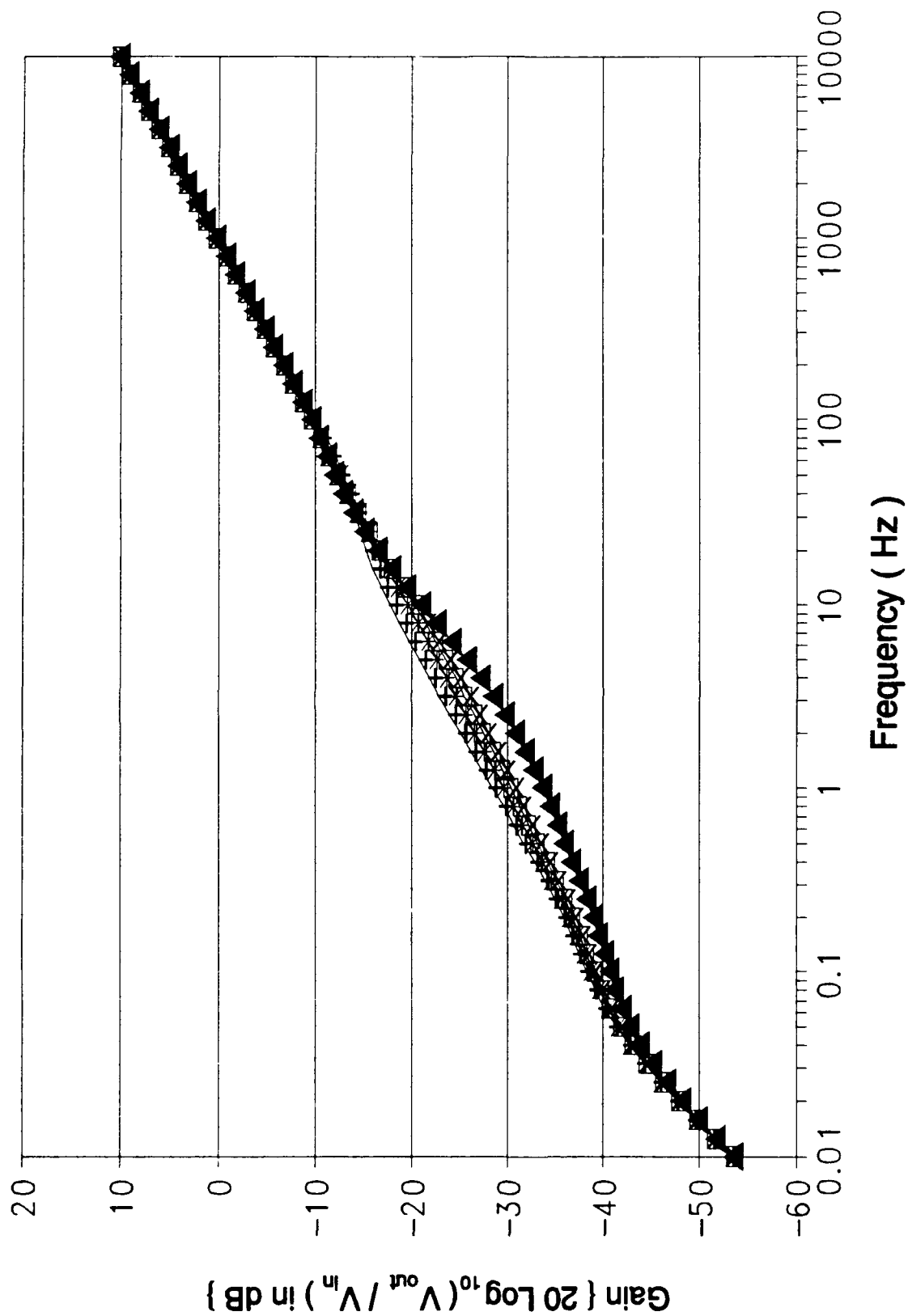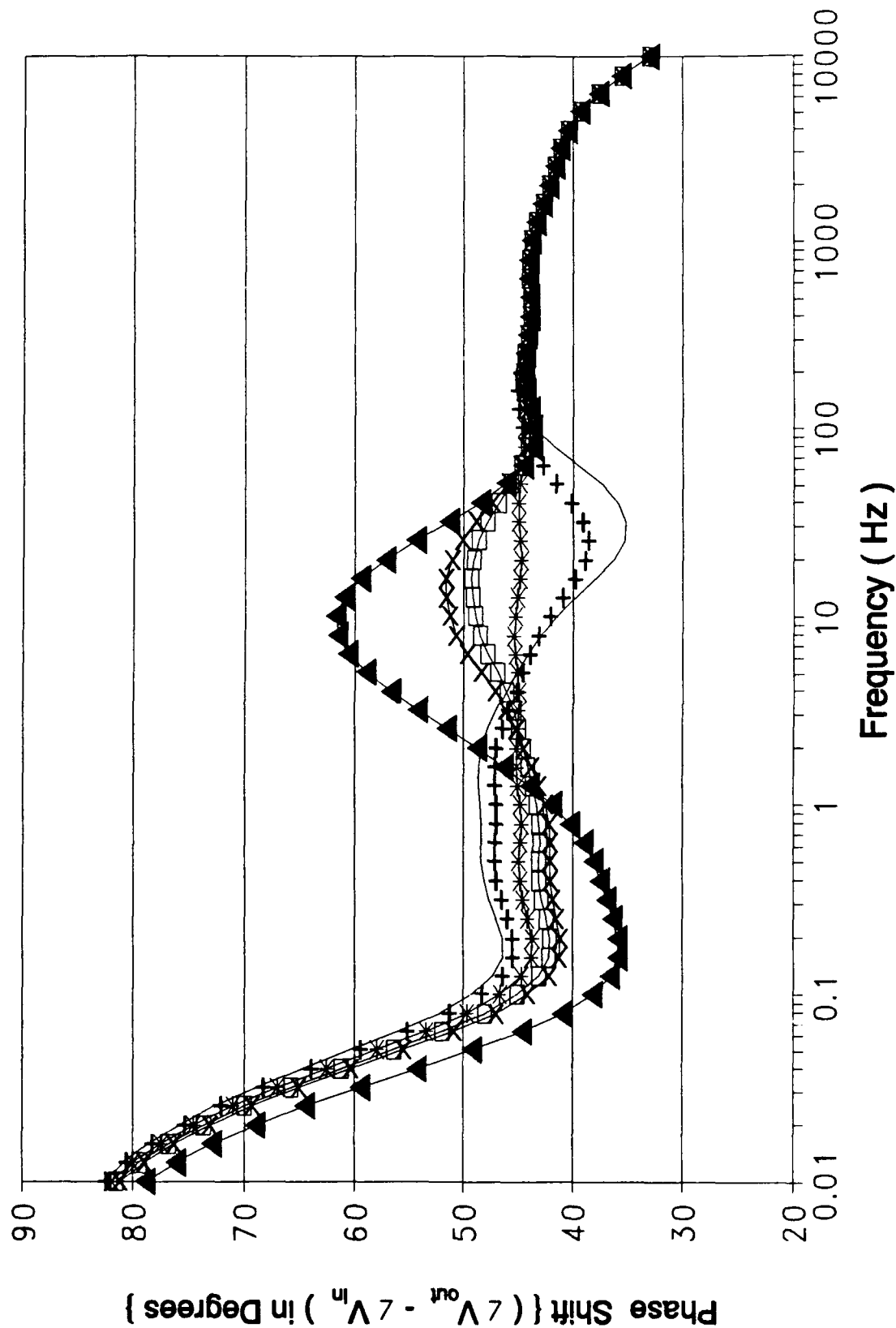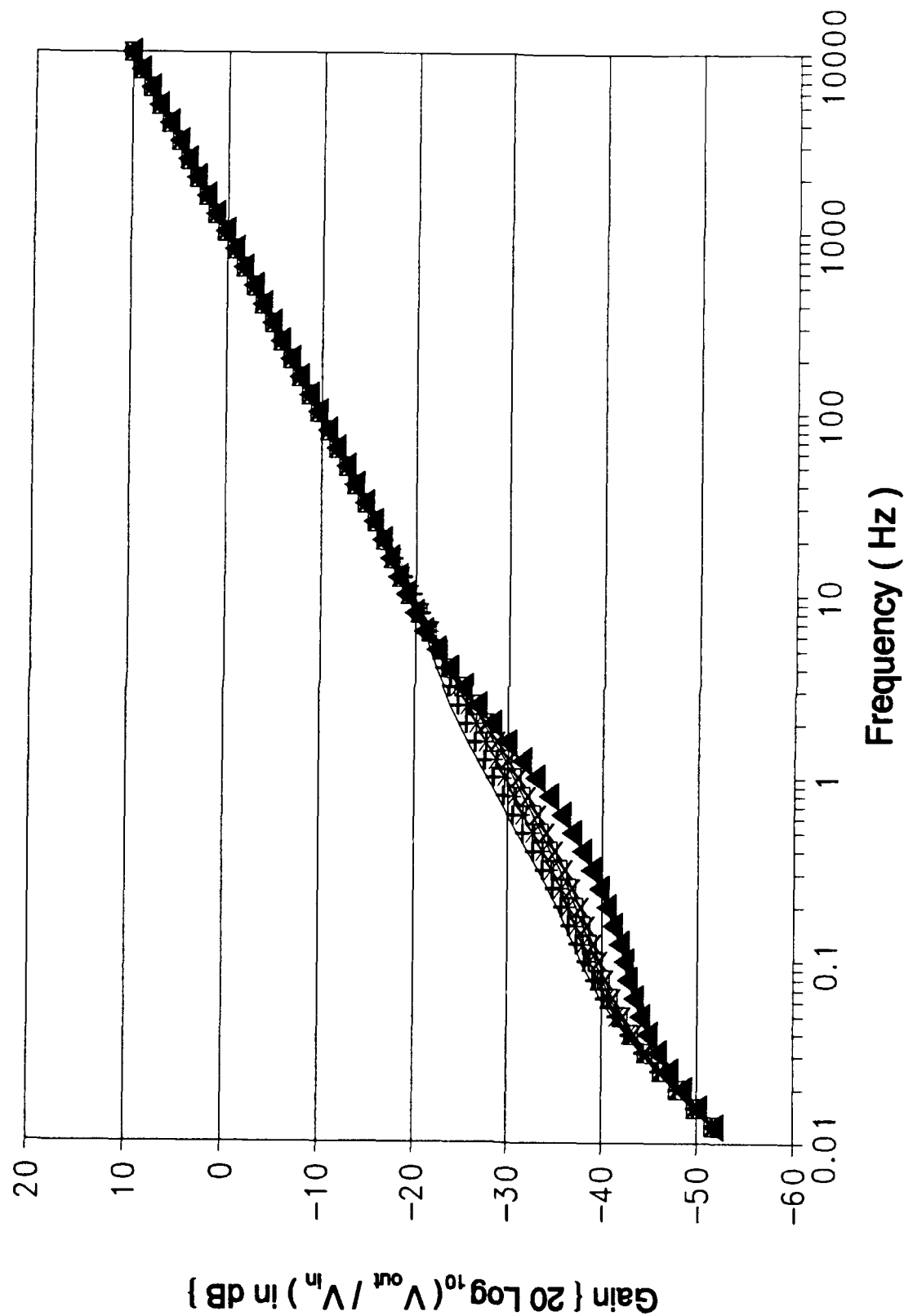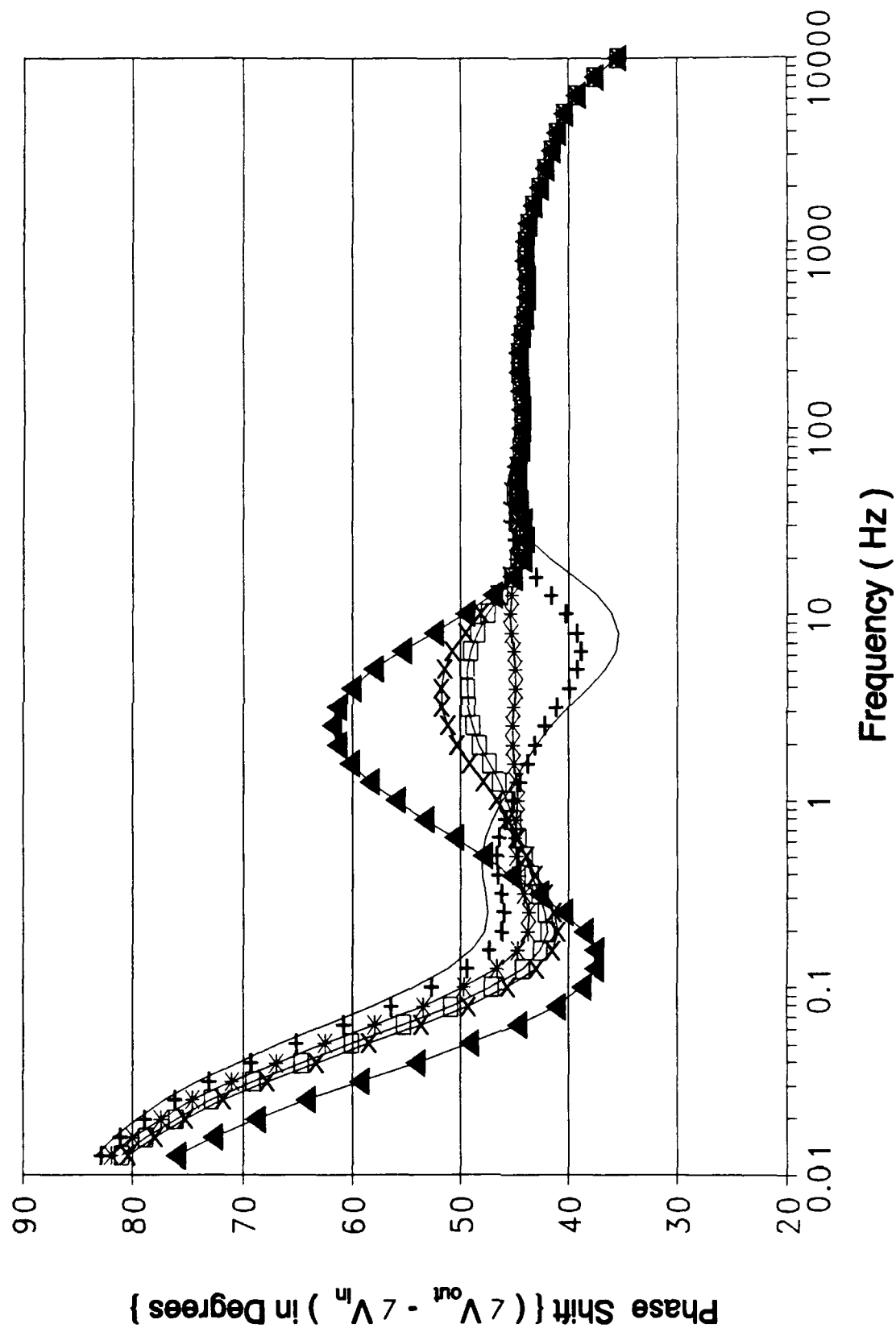Figure B-38 (cont). Gain Response of the Oldham Circuit Design Using an HSPICE Computer Variation of All Cells (cont).

Figure B-38 (cont). Phase Response of the Oldham Circuit Design Using an HSPICE Computer Variation of All Cells.

Section 4

Oldham Circuit HSPICE Baseline Simulation Deck

```
******       h s p i c e
 Half-order Differentiator Oldham/Hughes Design
****** copyright 1990 meta-software,inc.
****site:air_force_institute
******  input listing                       evaluation expires
920415
******
* hspice.ini
* compensated for high frequency and low frequency response*
* setting up for parameter tests*
.param biasr0=aunif(68.99x,13.798x)
+ biasc0=aunif(16.51u,3.303u)
+ biasr1=aunif(25.4x,5.08x)
+ biasc1=aunif(10u,2u)
+ biasr2=aunif(9.85x,1.97x)
+ biasc2=aunif(3.88u,.776u)
+ biasr3=aunif(3.83x,.776x)
+ biasc3=aunif(1.514u,.3028u)
+ biasr4=aunif(1.488x,.2976x)
+ biasc4=aunif(.5873u,.11746u)
+ biasr5=aunif(578.5k,115.7k)
+ biasc5=aunif(.2283u,.04566u)
+ biasr6=aunif(224.9k,44.98k)
+ biasc6=aunif(88.73n,17.746n)
+ biasr7=aunif(87.4k,17.48k)
+ biasc7=aunif(34.49n,6.898n)
+ biasr8=aunif(33.97k,6.794k)
+ biasc8=aunif(13.41n,2.682n)
+ biasr9=aunif(13.21k,2.642k)
+ biasc9=aunif(5.21n,1.042n)
+ biasr10=aunif(5.133k,1.0266k)
+ biasc10=aunif(2.026n,.4052n)
+ biasr11=aunif(997.5,199.5)
+ biasc11=aunif(1.575n,.315n)
+ biasr12=aunif(2.11k,.422k)
*seting output for hsplot*
.options post=2
*setting ac analysis parameters
.ac dec 10 .01hz 10meghz   sweep monte=5 $bias poi 6    .1 .4
1 1.6 2 5.0
*circuit with 11 cells
vcc vcc gnd +15v
vee vee gnd -15v
*resistors
r0 15 1 biasr0 $68.99megohm
r1 1 2 biasr1 $25.4megohm
r2 2 3 biasr2 $9.85megohm
r3 3 4 biasr3 $3.83megohm
r4 4 5 biasr4 $1.488megohm
```

```
r5 5 6 biasr5 $578.5kohm
r6 6 7 biasr6 $224.9kohm
r7 7 8 biasr7 $87.4kohm
r8 8 9 biasr8 $33.97kohm
r9 9 10 biasr9 $13.21kohm
r10 10 11 biasr10 $5.133kohm
r11 11 12 biasr11 $997.5
r12 12 13 biasr12 $2.11kohm
*capacitors
c0 15 1 biasc0 $16.51u
c1 1 2 biasc1 $10u
c2 2 3 biasc2 $3.88u
c3 3 4 biasc3 $1.514u
c4 4 5 biasc4 $.5873u
c5 5 6 biasc5 $.2283u
c6 6 7 biasc6 $88.73n
c7 7 8 biasc7 $34.49n
c8 8 9 biasc8 $13.41n
c9 9 10 biasc9 $5.211n
c10 10 11 biasc10 $2.026n
c11 11 12 biasc11 $1.575n
*opamp
x741 gnd 13 out vcc vee alm741
r13 13 out 10kohm
*inserting low pass filter for noise
r16 out 16 16.931k
c16 16 gnd 470p
x2741 out2 16 out2 vcc vee alm741
vin 15 gnd ac 5 0 sin(0 5 500)
.tran 50u 2ms sweep monte=5 $bias poi 6  .1 .4 1 1.6 2 5.0
.print ac vp(out2,15)
.print ac vdb(out2,15)
.print v(out2)
.print v(15)
.end
```

Appendix C

Oldfield Circuit

Computer Simulation

Results

The computer simulation results for the Oldfield circuit design are presented in this appendix. The results are documented in four sections. The first three sections document the systematic variation of the resistor and capacitor component values, and Section 4 presents the HSPICE simulation deck. Section 1 records the effect on the circuit's response when each component is varied relative to its "ideal" value while all the other component values are held constant (their ideal values). Section 2 summarizes the effect on the circuit's response when each cell's component values (a resistor and capacitor pair) are varied with respect to their "ideal" values while holding the components in the other cells at their "ideal" (calculated) values (Table 1). Section 3 documents the effect on the circuit's performance when all of the component values are systematically varied by ± 20 percent. Finally, the baseline HSPICE deck for the Oldfield circuit is presented.

Figure C-0 illustrates the relative position of each component and cell.
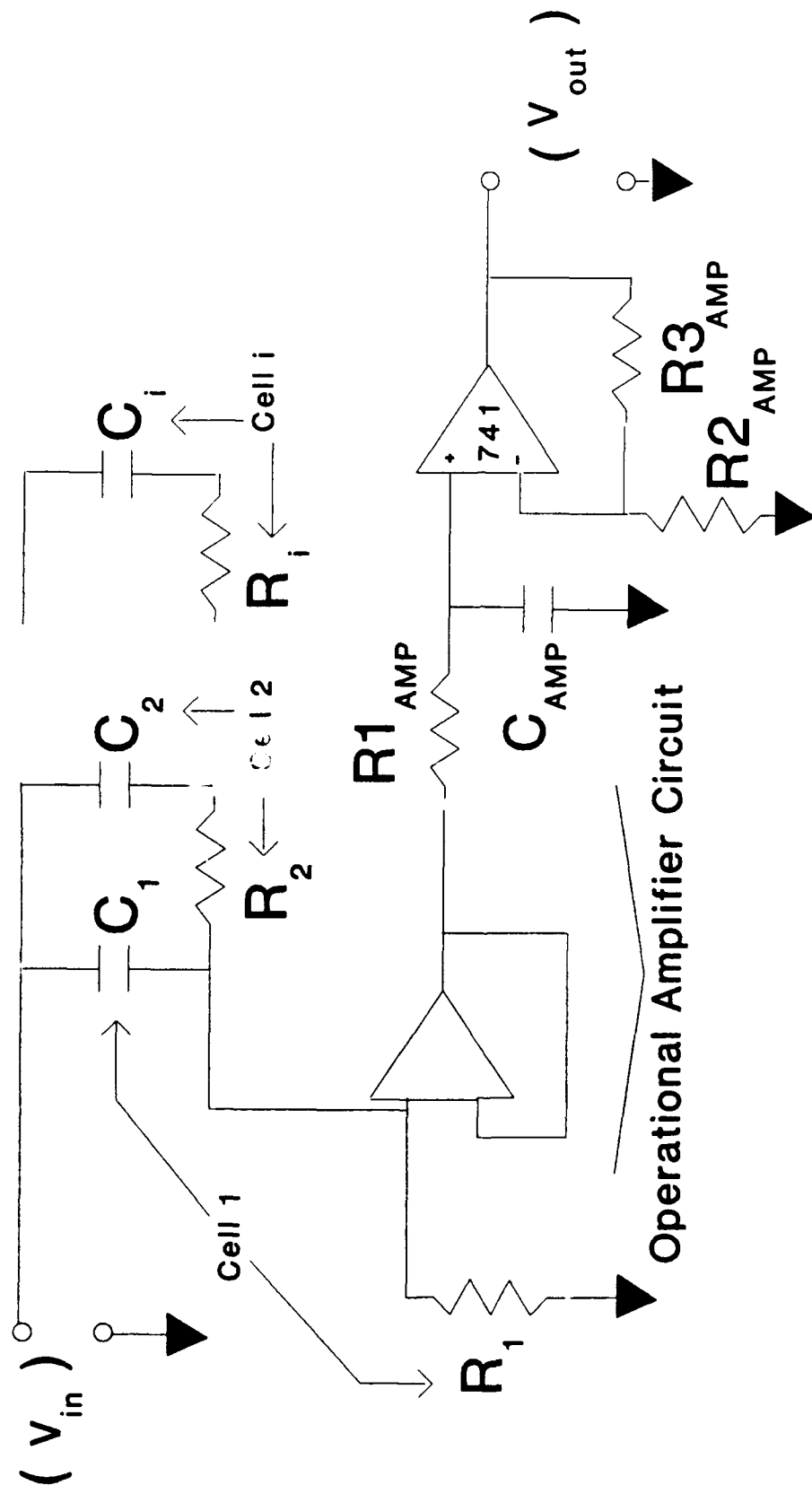
Figure C-O. Oldfield Circuit Design Component and Cell Notation.

Section 1

Oldfield Circuit Responses to Systematic

Resistor and Capacitor Value Variations

Resistor Values for Figure C-1						
Symbol	——	-+-	-*-	—□—	—×—	-▲-
Resis-tor Value (Ω)	18.02	72.08	180.2 Ideal	288.32	360.4	901

Figure C-1. Graphical Symbol Legend and Resistor Values Corresponding to Figure C-1 (cont);
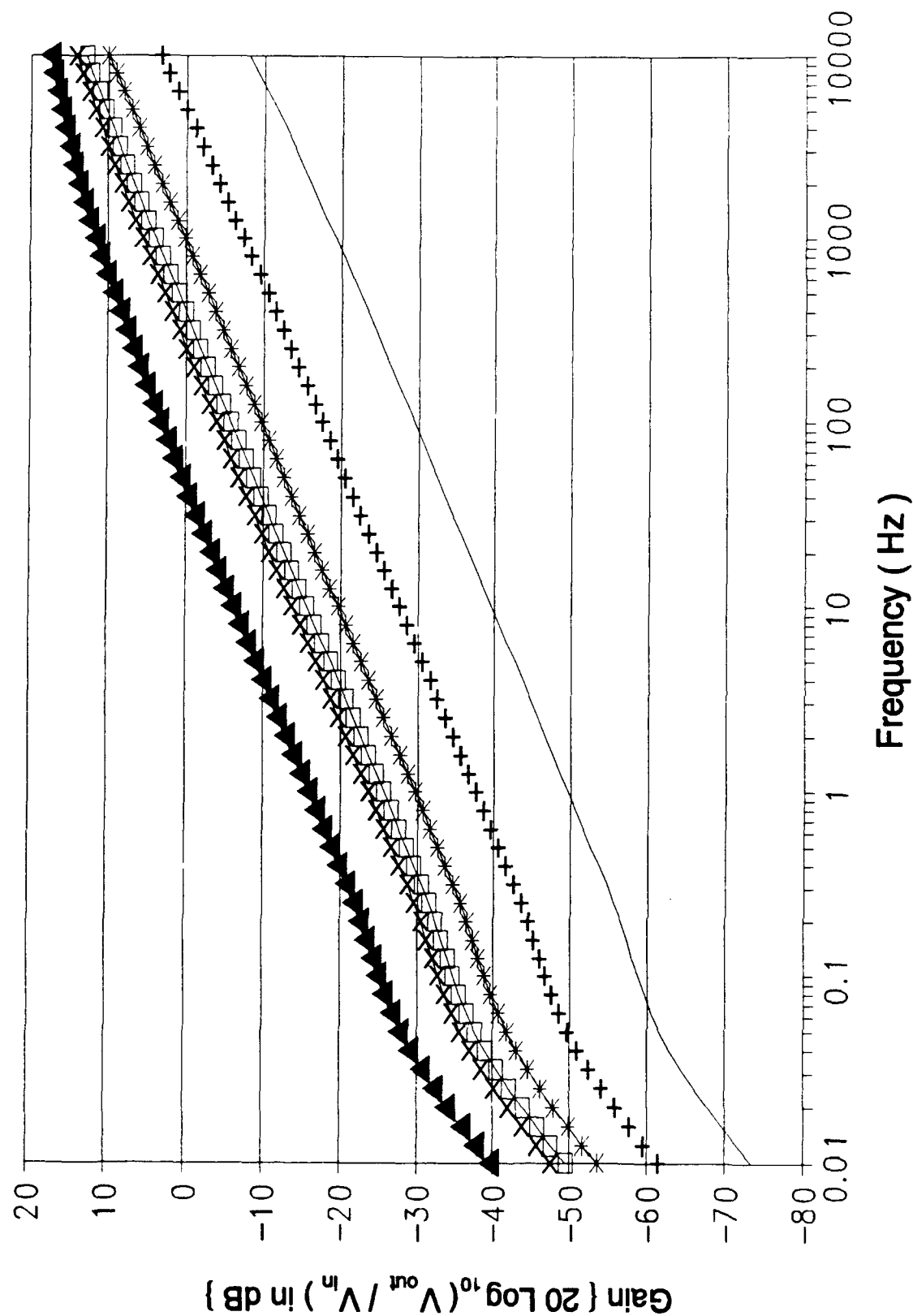
Figure C-1 (cont). Gain Response of the Oldfield Circuit Design Using an HSPICE Computer Variation of Resistor 1 (cont);
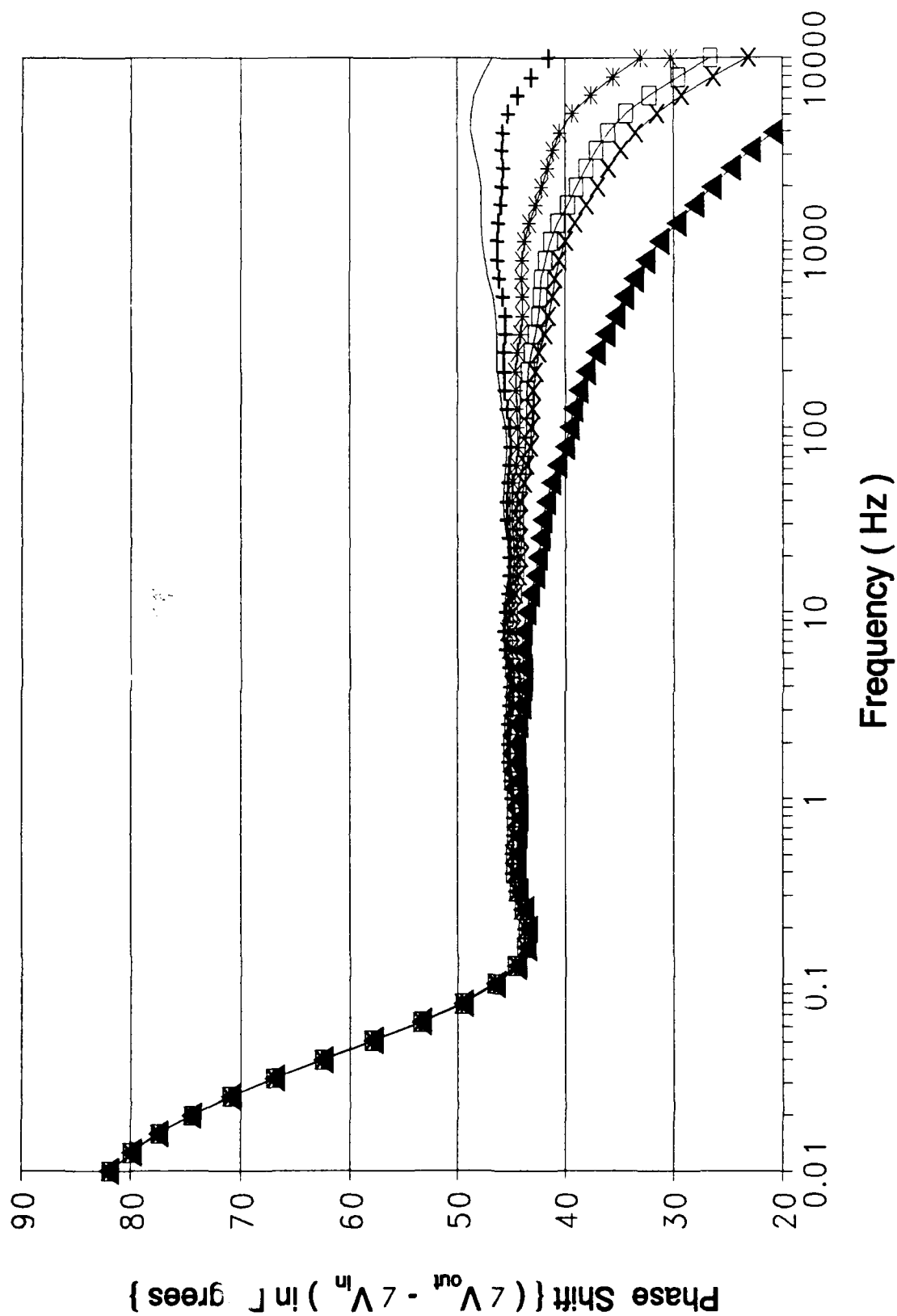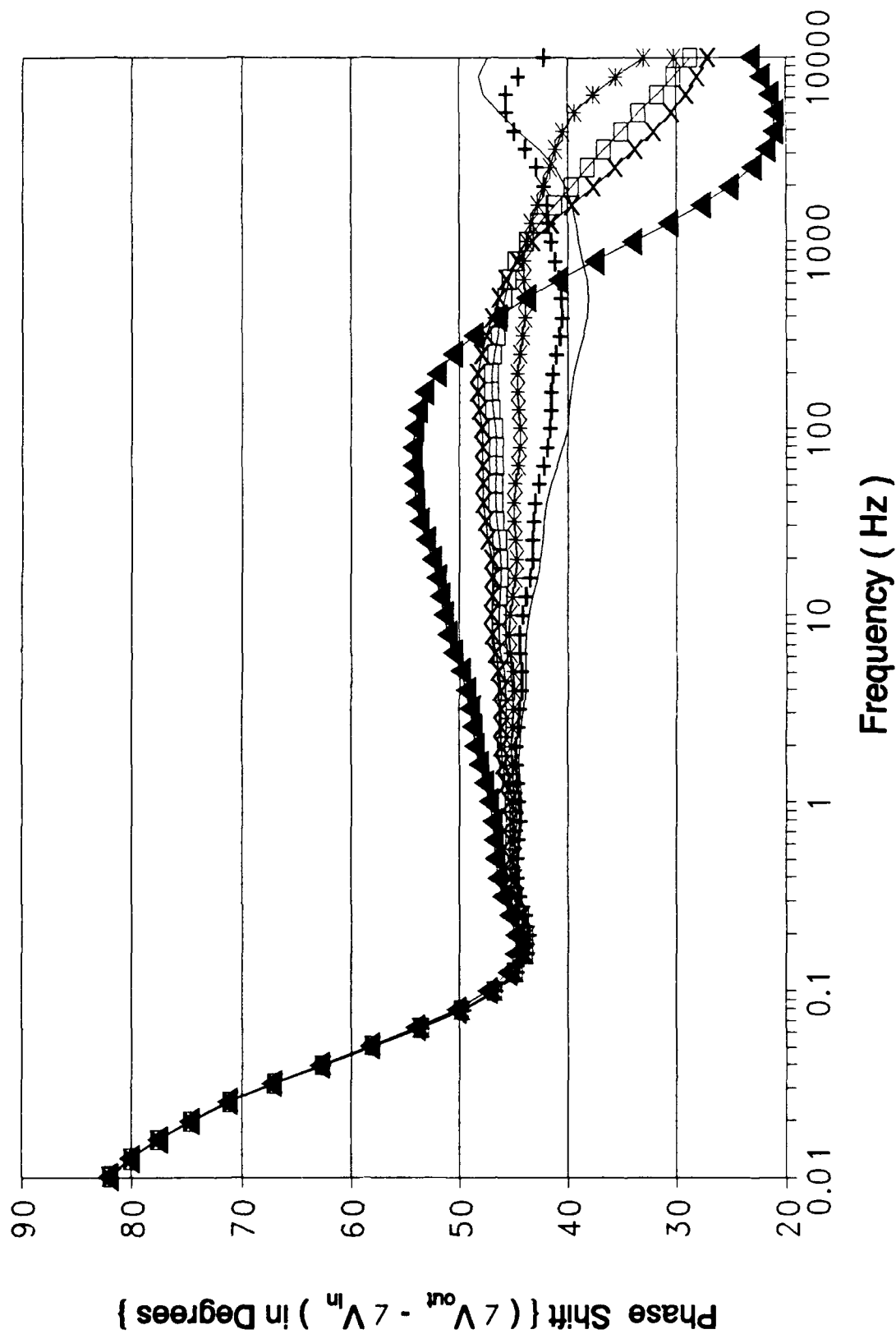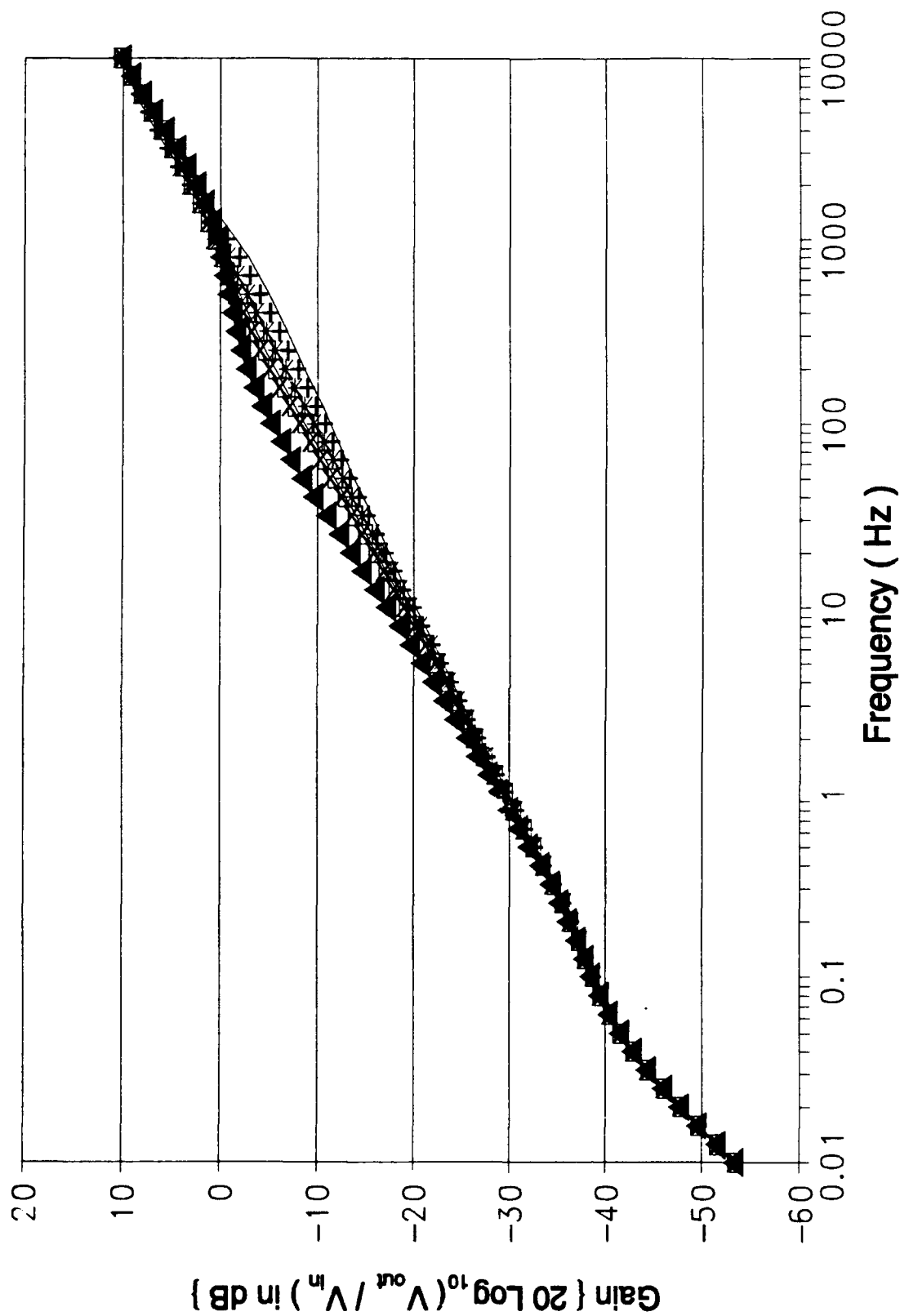
Figure C-1 (cont). Phase Response of the Oldfield Circuit Design Using an HSPICE Computer Variation of Resistor 1.

Resistor Values for Figure C-2						
Symbol	——	-+-	-*-	—□—	—×—	-▲-
Resis- tor Value (Ω)	63	252	630 Ideal	1008	1260	3150

Figure C-2. Graphical Symbol Legend and Resistor
            Values Corresponding to Figure C-2 (cont);
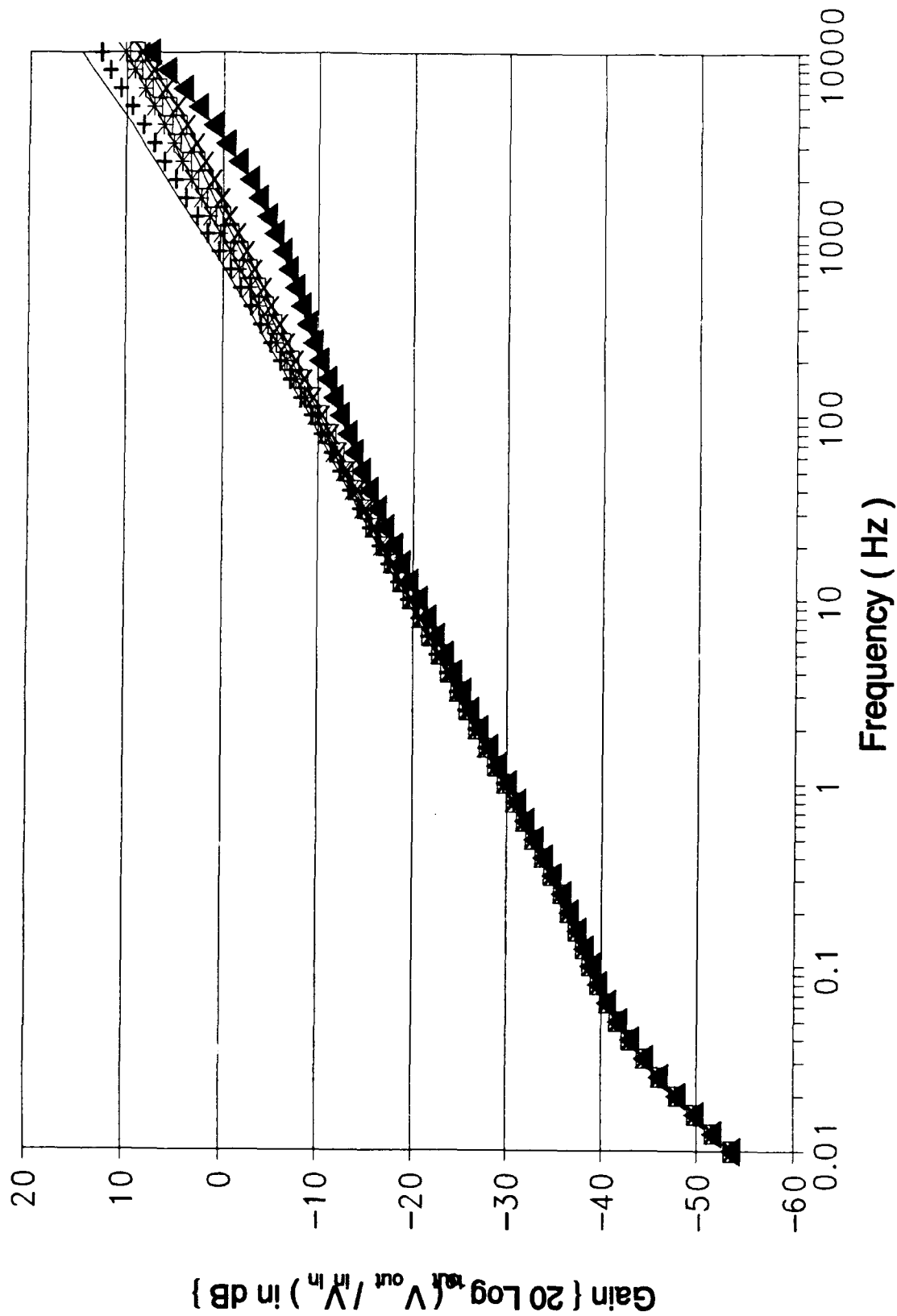
Figure C-2 (cont). Gain Response of the Oldfield Circuit Design Using an HSPICE Computer Variation of Resistor 2 (cont);
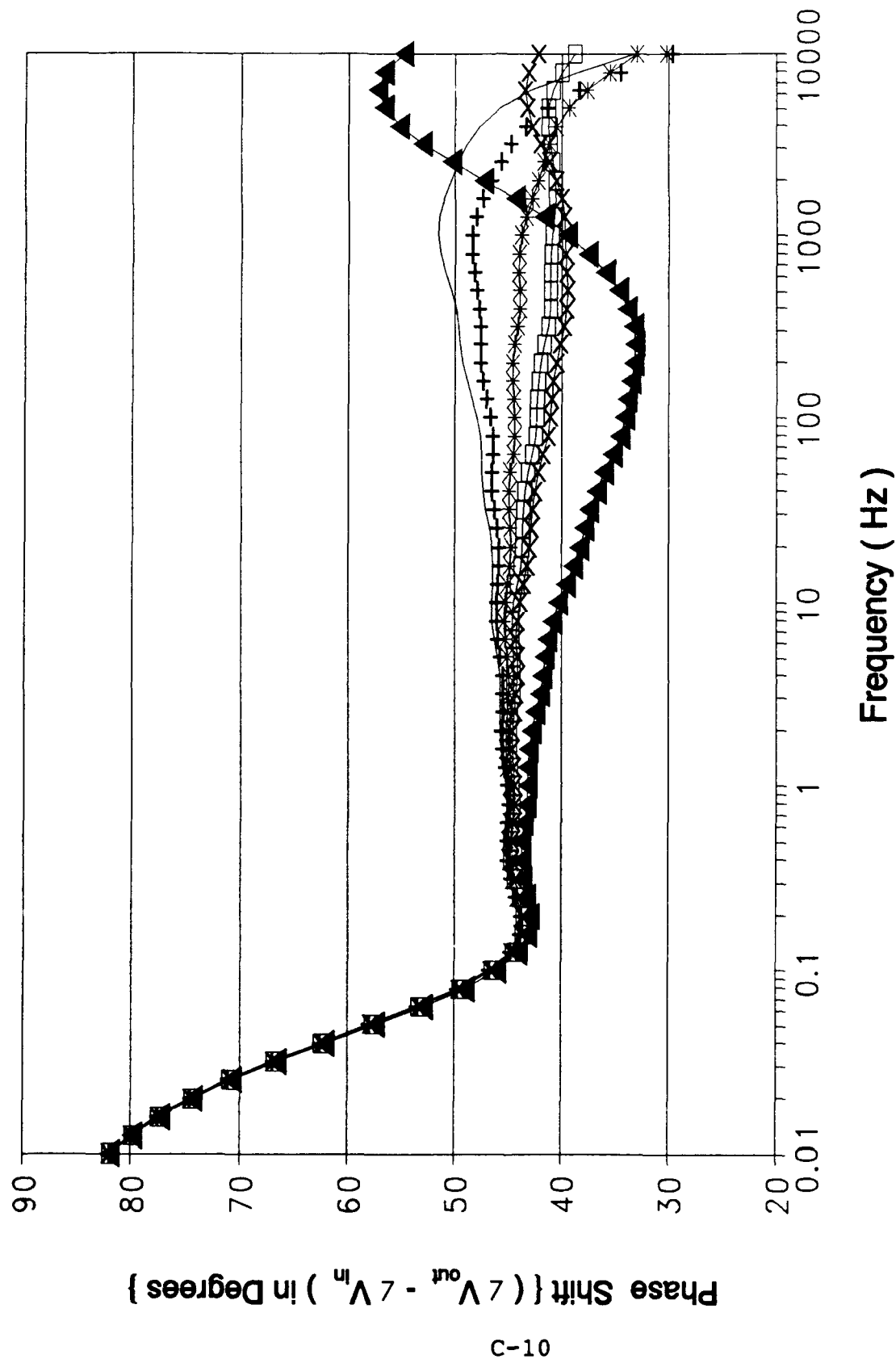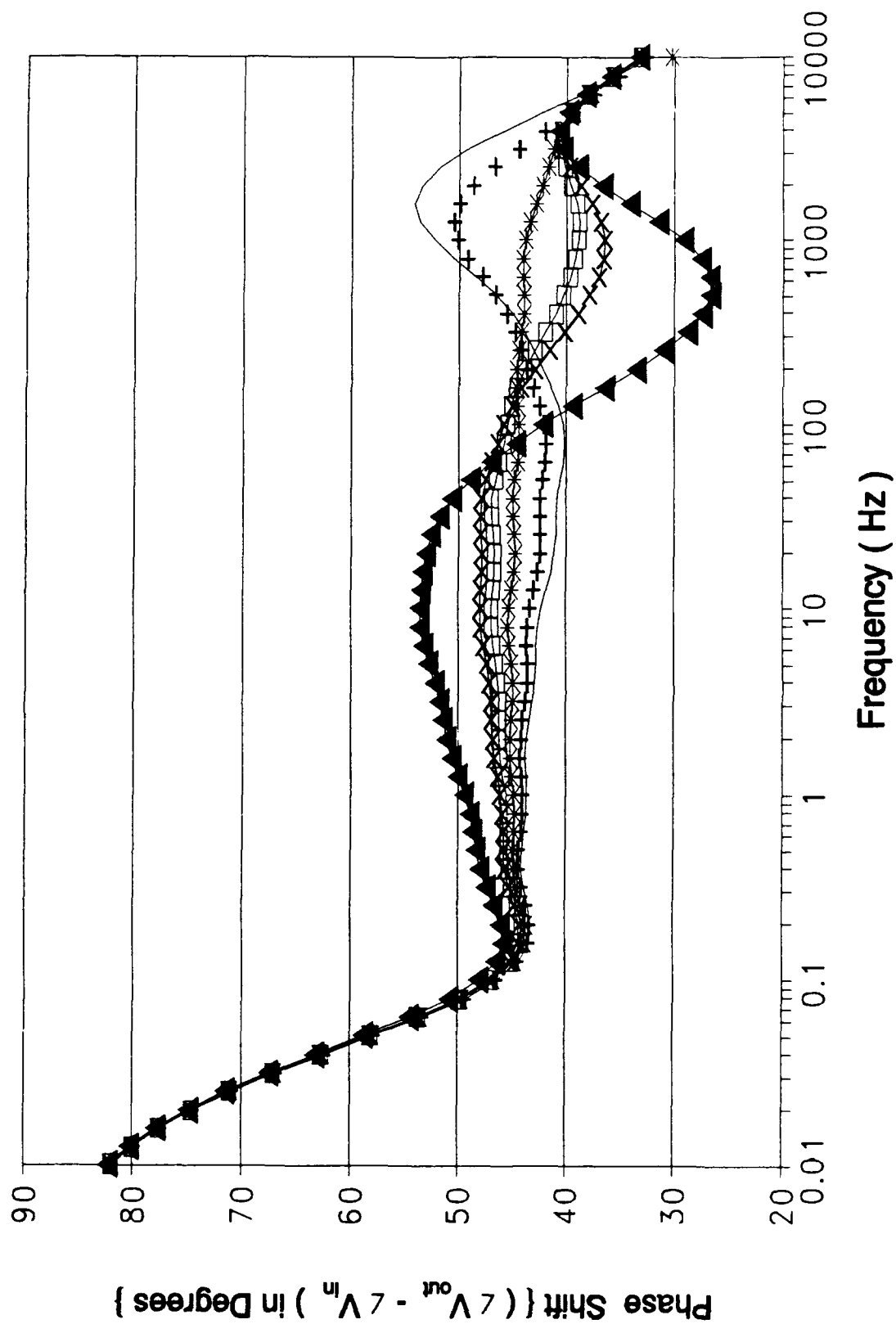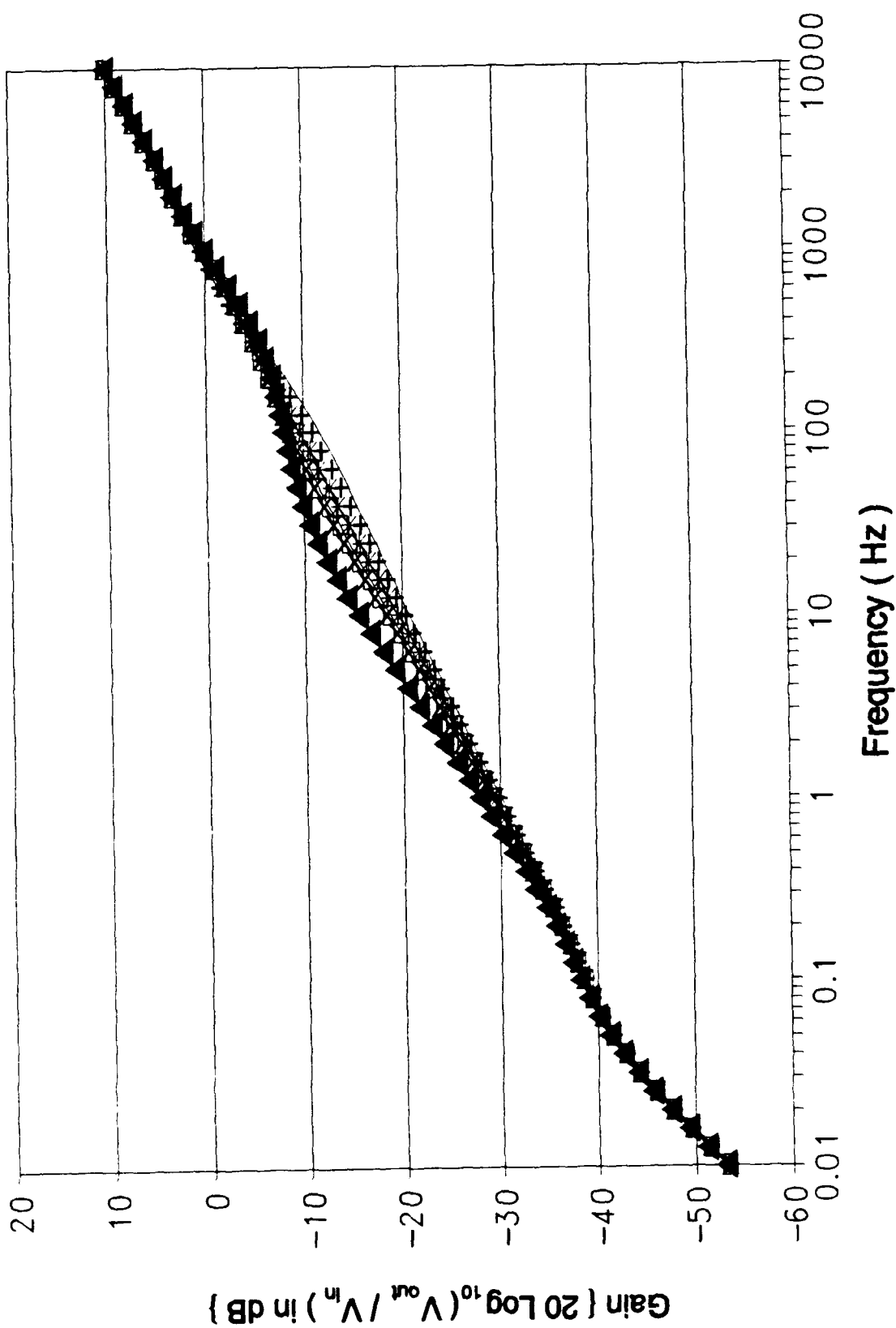
Figure C-2 (cont). Phase Response of the Oldfield Circuit Design Using an HSPICE Computer Variation of Resistor 2.

C-10

Resistor Values for Figure C-3						
Symbol	——	—+—	—*—	—☐—	—×—	—▲—
Resis- tor Value (KΩ)	0.1313	0.5252	1.313 Ideal	2.1008	2.626	6.565

Figure C-3. **Graphical Symbol Legend and Resistor**
Values Corresponding to Figure C-3 (cont);
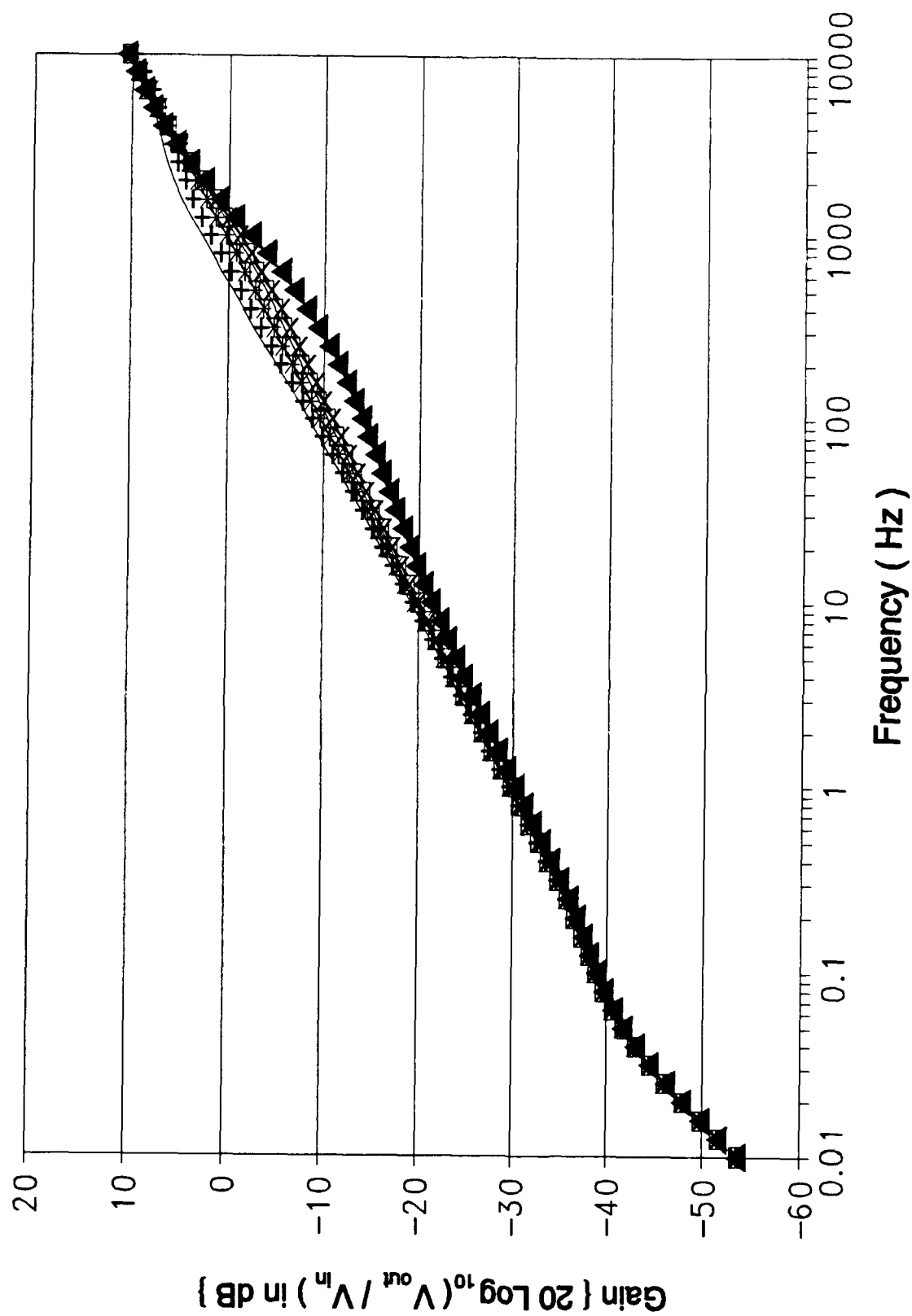
Figure C-3 (cont). Gain Response of the Oldfield Circuit Design Using an HSPICE Computer Variation of Resistor 3 (cont);
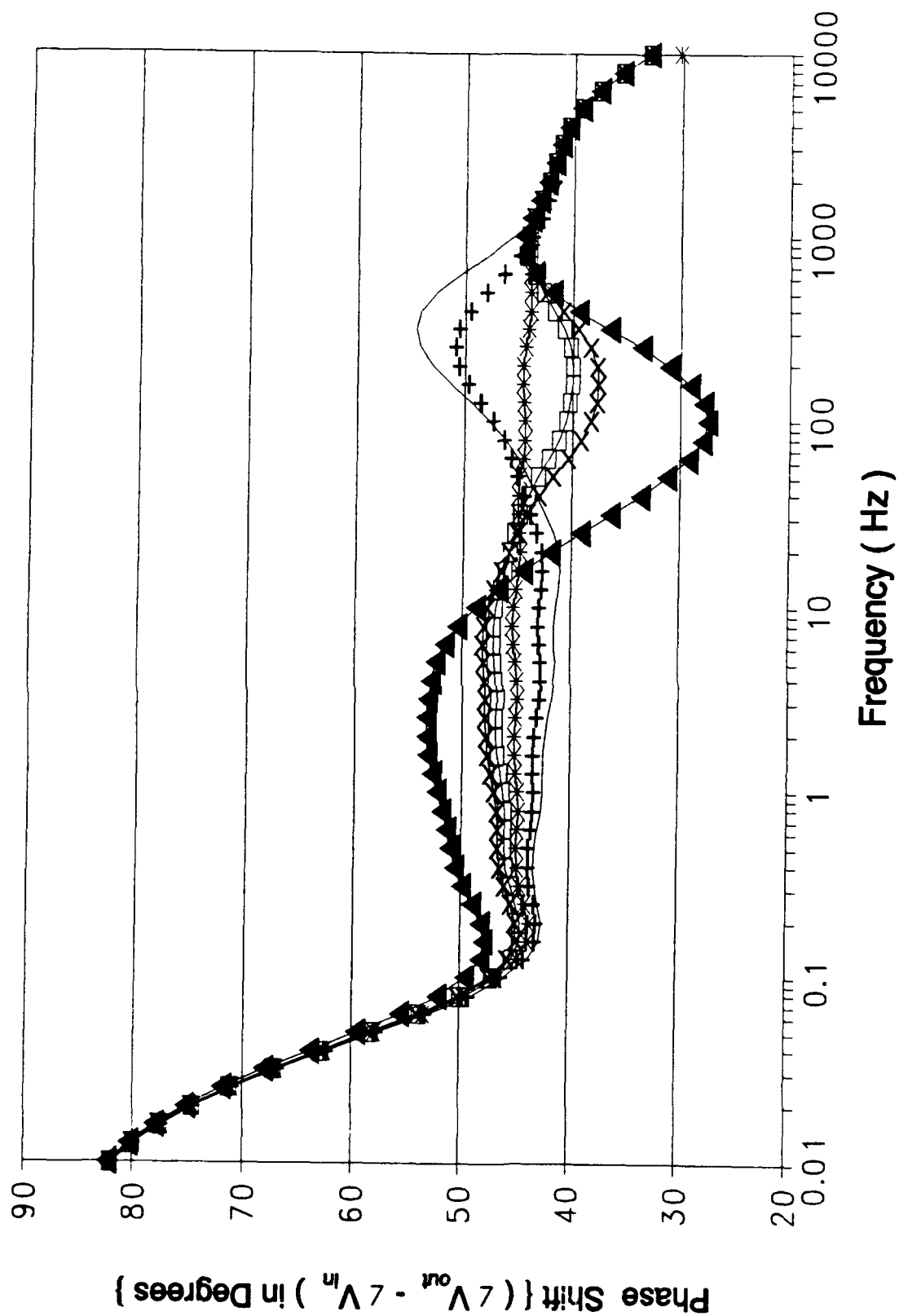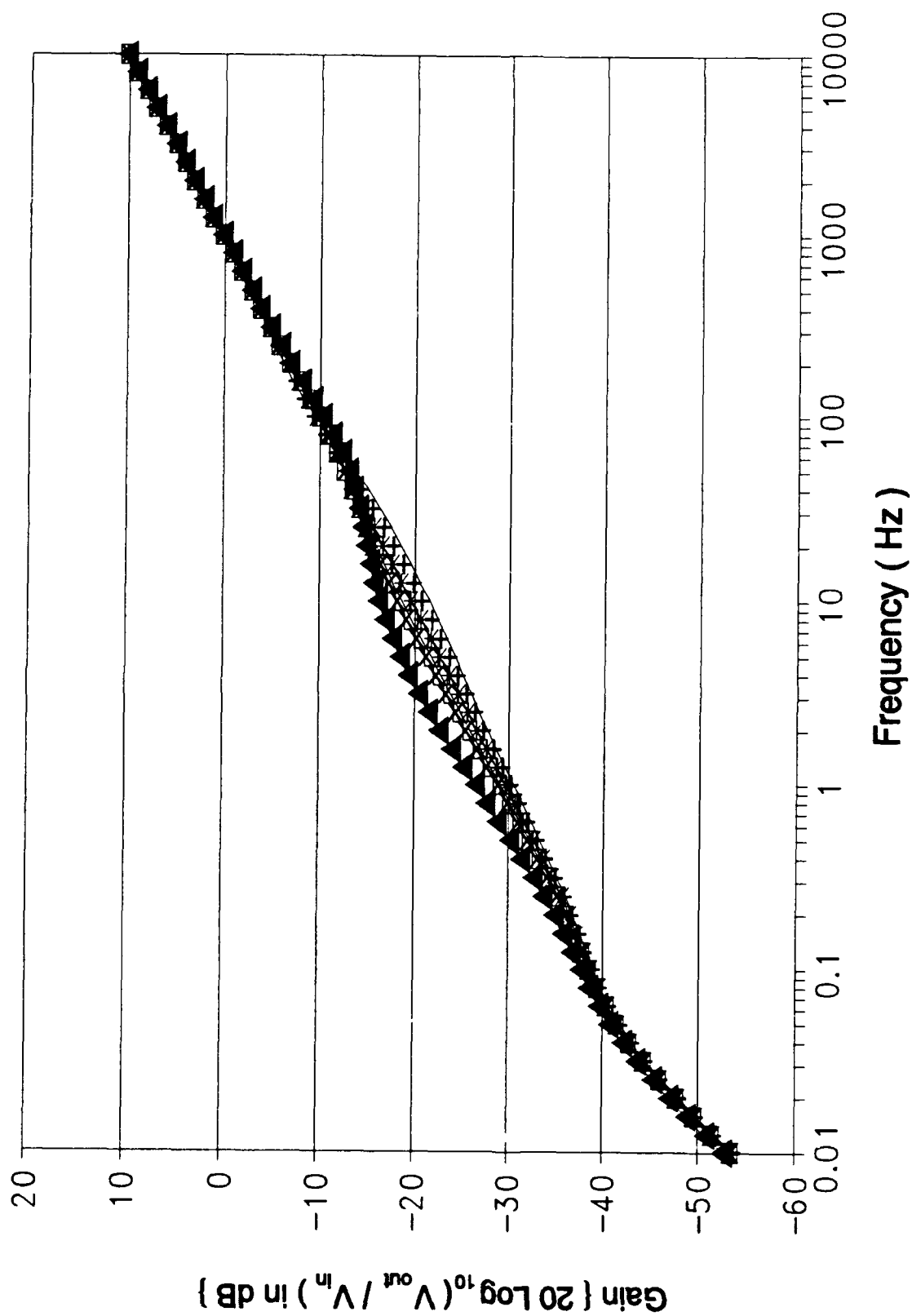
C-12
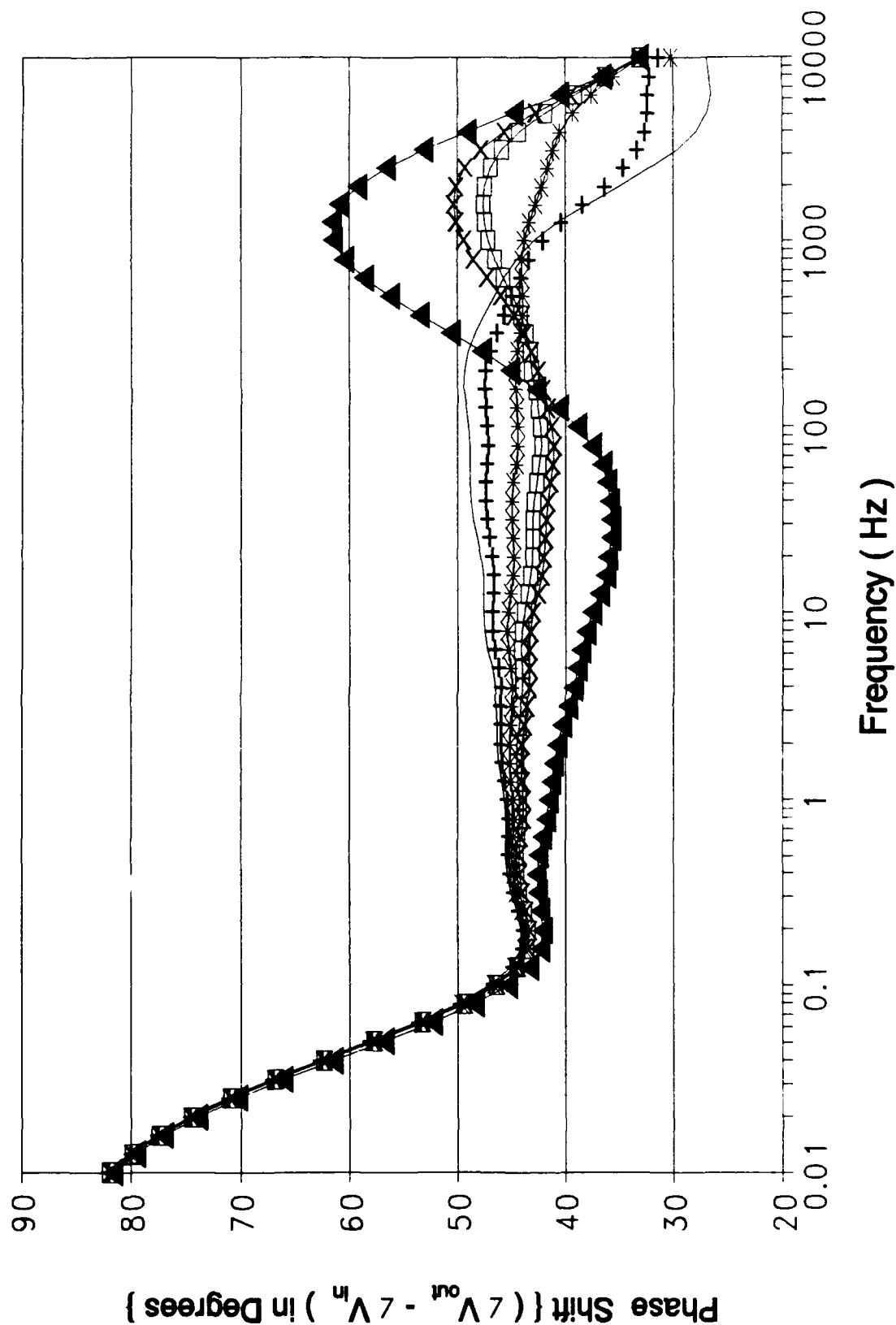
Figure C-3 (cont). Phase Response of the Oldfield Circuit Design Using an HSPICE Computer Variation of Resistor 3.

Resistor Values for Figure C-4						
Symbol	——	-+-	-*-	—▢—	—x—	-▲-
Resis- tor Value (KΩ)	0.2798	1.1192	2.798 Ideal	4.4768	5.596	13.99

Figure C-4.   Graphical Symbol Legend and Resistor
             Values Corresponding to Figure C-4 (cont);

Figure C-4 (cont). Gain Response of the Oldfield Circuit Design Using an HSPICE Computer Variation of Resistor 4 (cont);
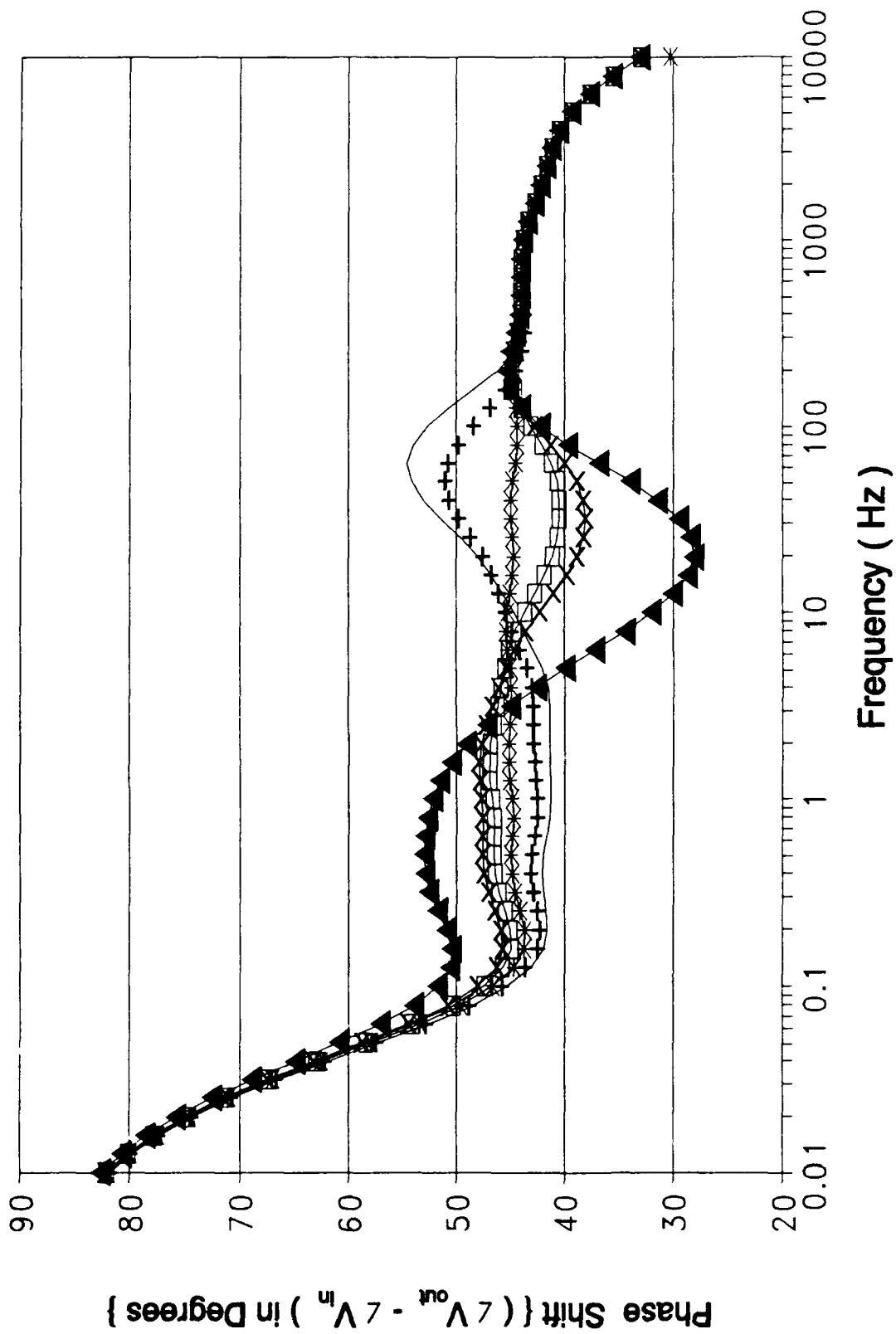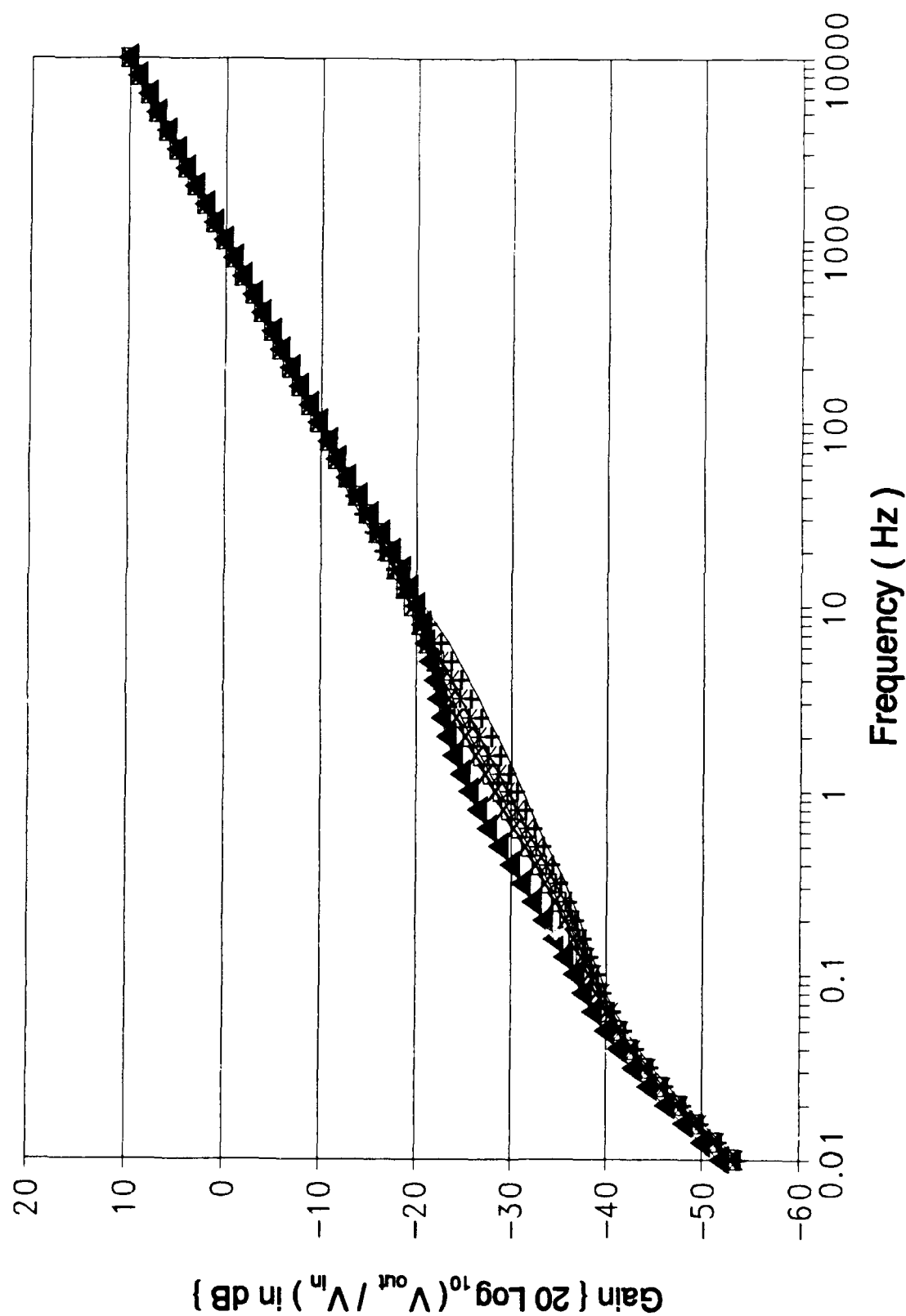
Figure C-4 (cont). Phase Response of the Oldfield Circuit Design Using an HSPICE Computer Variation of Resistor 4.

C-16

Resistor Values for Figure C-5						
Symbol	——	–+–	–*–	–▢–	–×–	–▲–
Resis- tor Value (KΩ)	0.6009	2.4024	6.009 Ideal	9.614	12.02	30.045

Figure C-5.   Graphical Symbol Legend and Resistor Values Corresponding to Figure C-5 (cont);

Figure C-5 (cont). Gain Response of the Oldfield Circuit Design Using an HSPICE Computer Variation of Resistor 5 (cont);
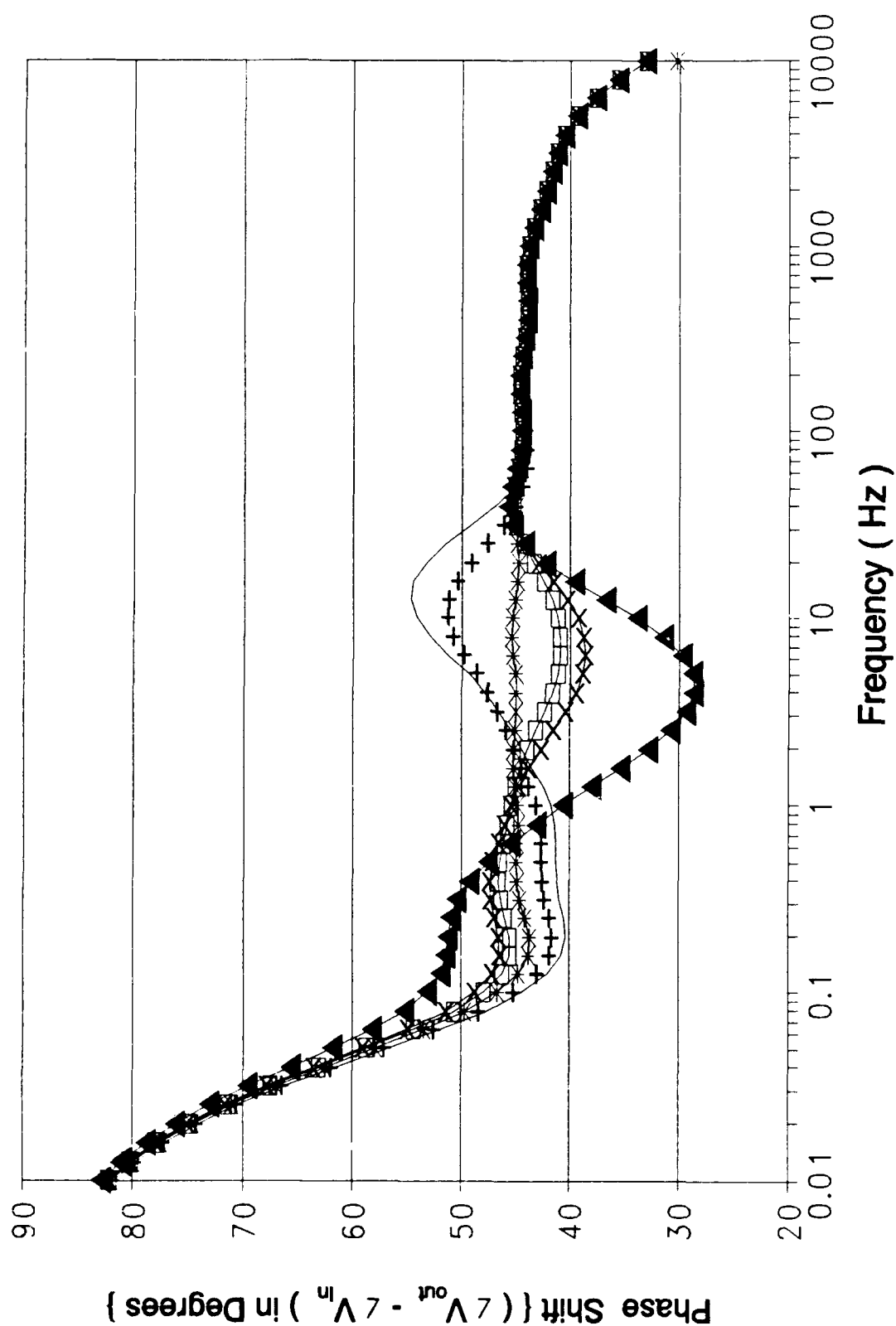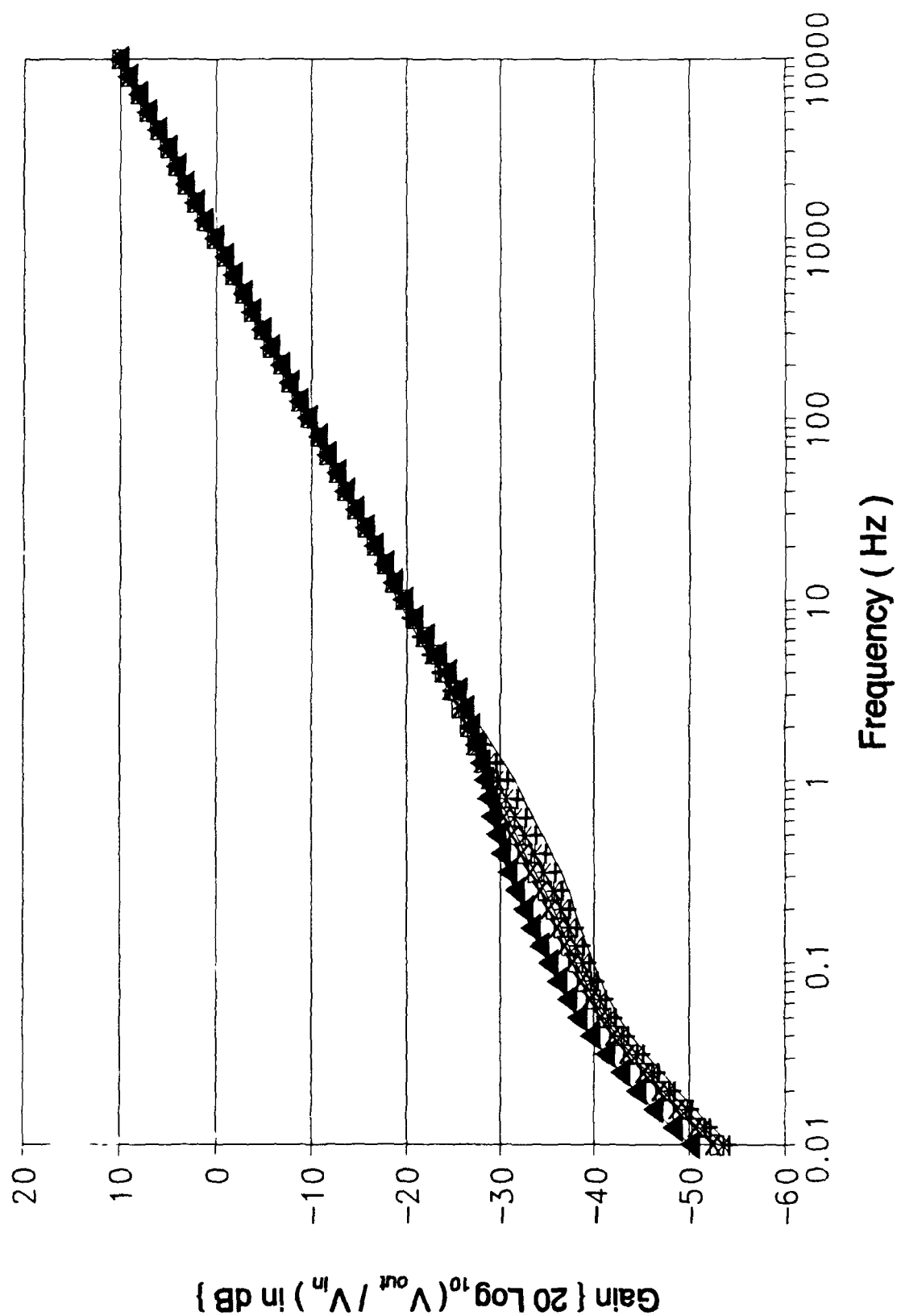
Figure C-5 (cont). Phase Response of the Oldfield Circuit Design Using an HSPICE Computer Variation of Resistor 5.

Resistor Values for Figure C-6						
Symbol	——	-+-	-*-	—□—	—×—	-▲-
Resis- tor Value (KΩ)	1.311	5.244	13.11 Ideal	20.976	26.22	65.55

Figure C-6.   Graphical Symbol Legend and Resistor
             Values Corresponding to Figure C-6 (cont);

Figure C-6 (cont). Gain Response of the Oldfield Circuit Design Using an HSPICE Computer Variation of Resistor 6 (cont);
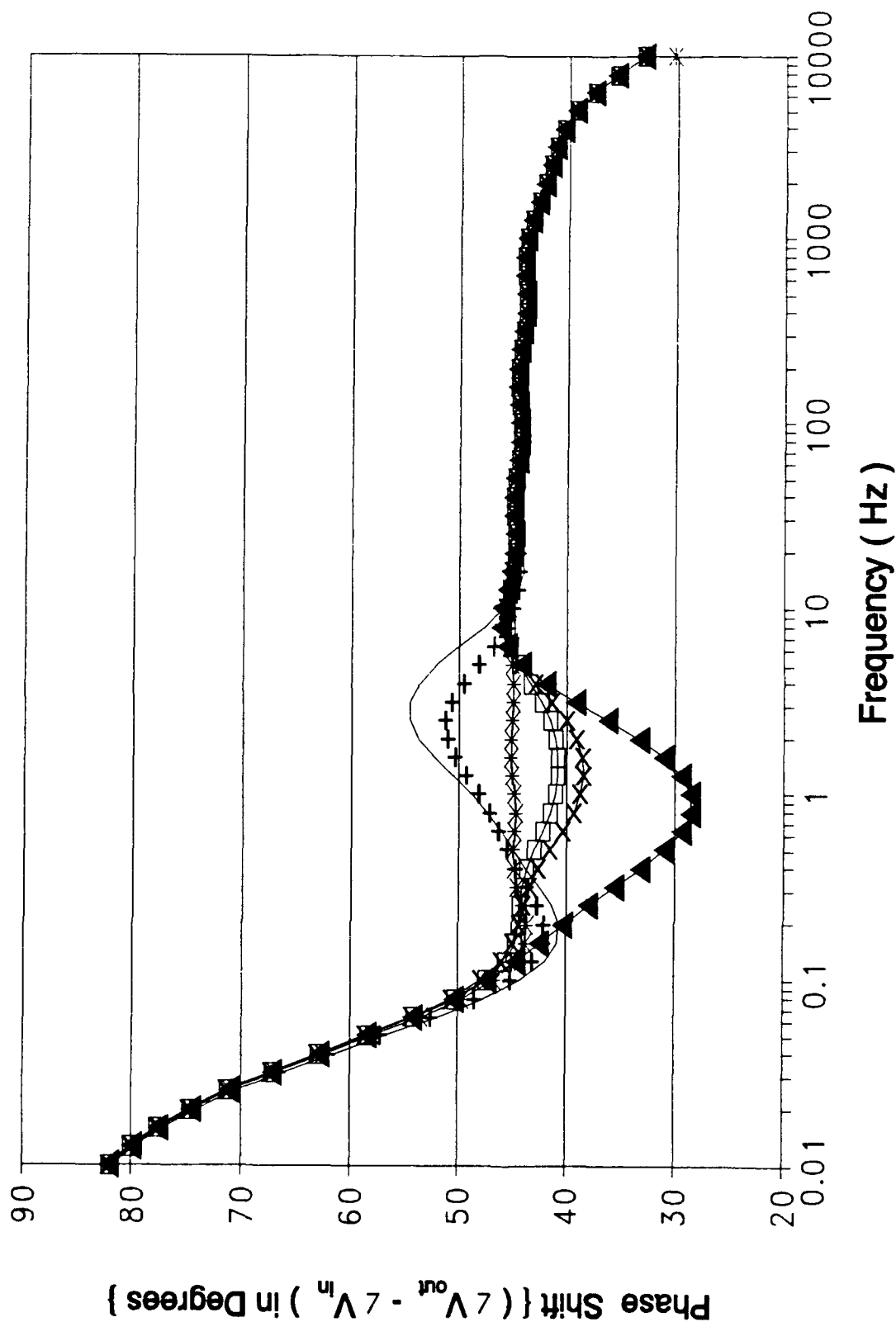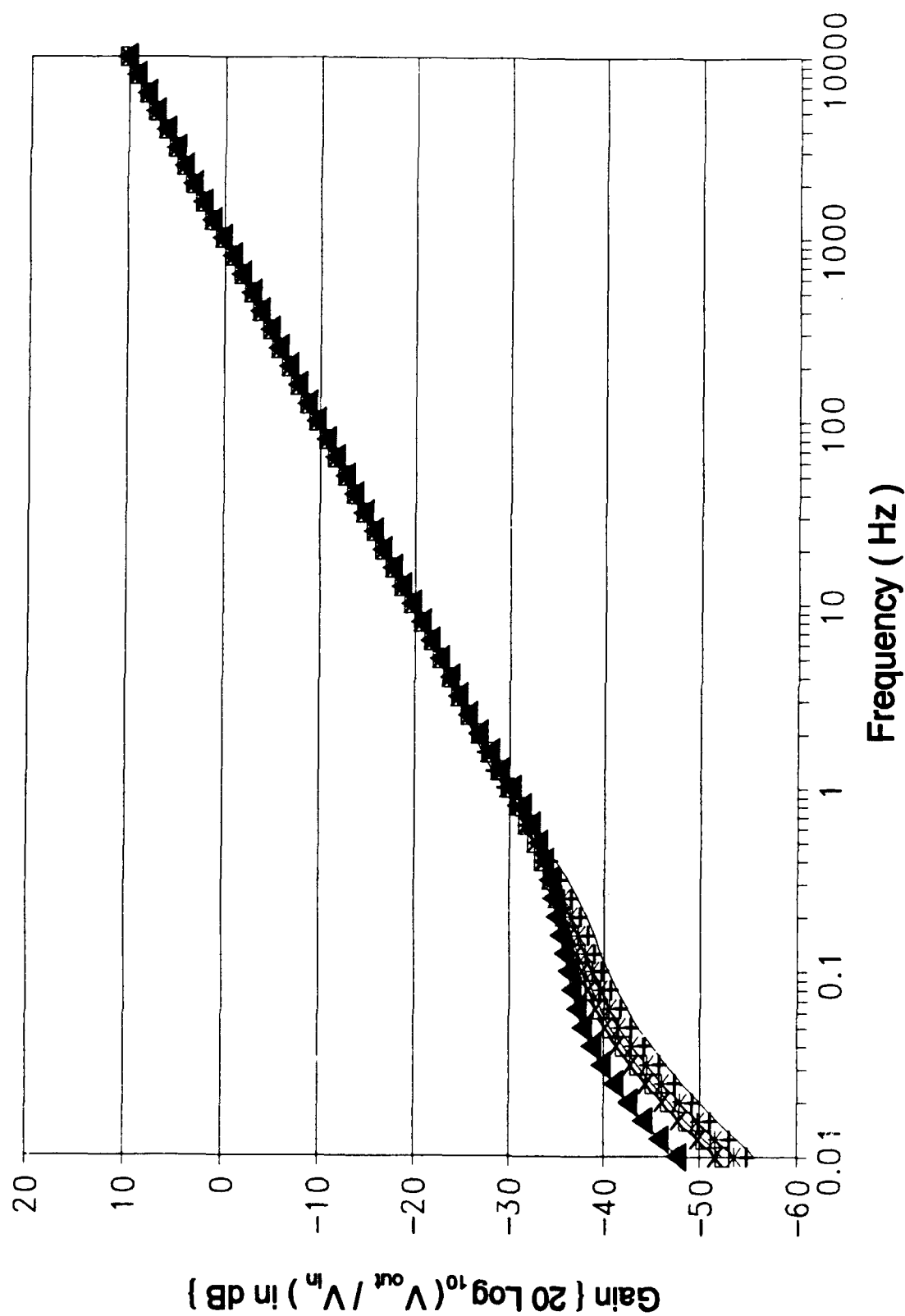
Figure C-6 (cont). Phase Response of the Oldfield Circuit Design Using an HSPICE Computer Variation of Resistor 6.

Resistor Values for Figure C-7						
Symbol	——	-+-	-*-	—□—	—×—	-▲-
Resis- tor Value (KΩ)	2.857	11.428	28.57 Ideal	345.71	57.14	142.85

Figure C-7. Graphical Symbol Legend and Resistor
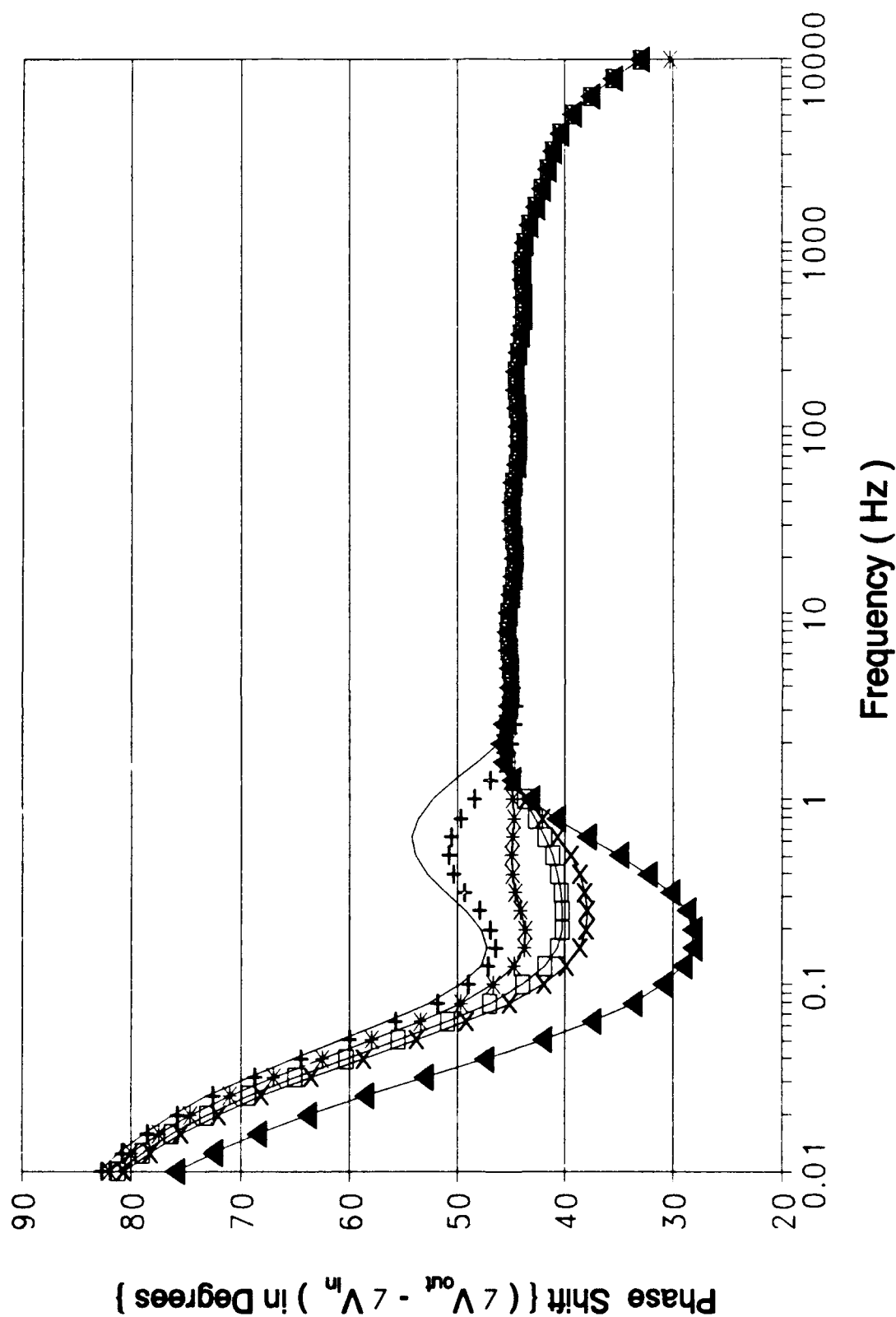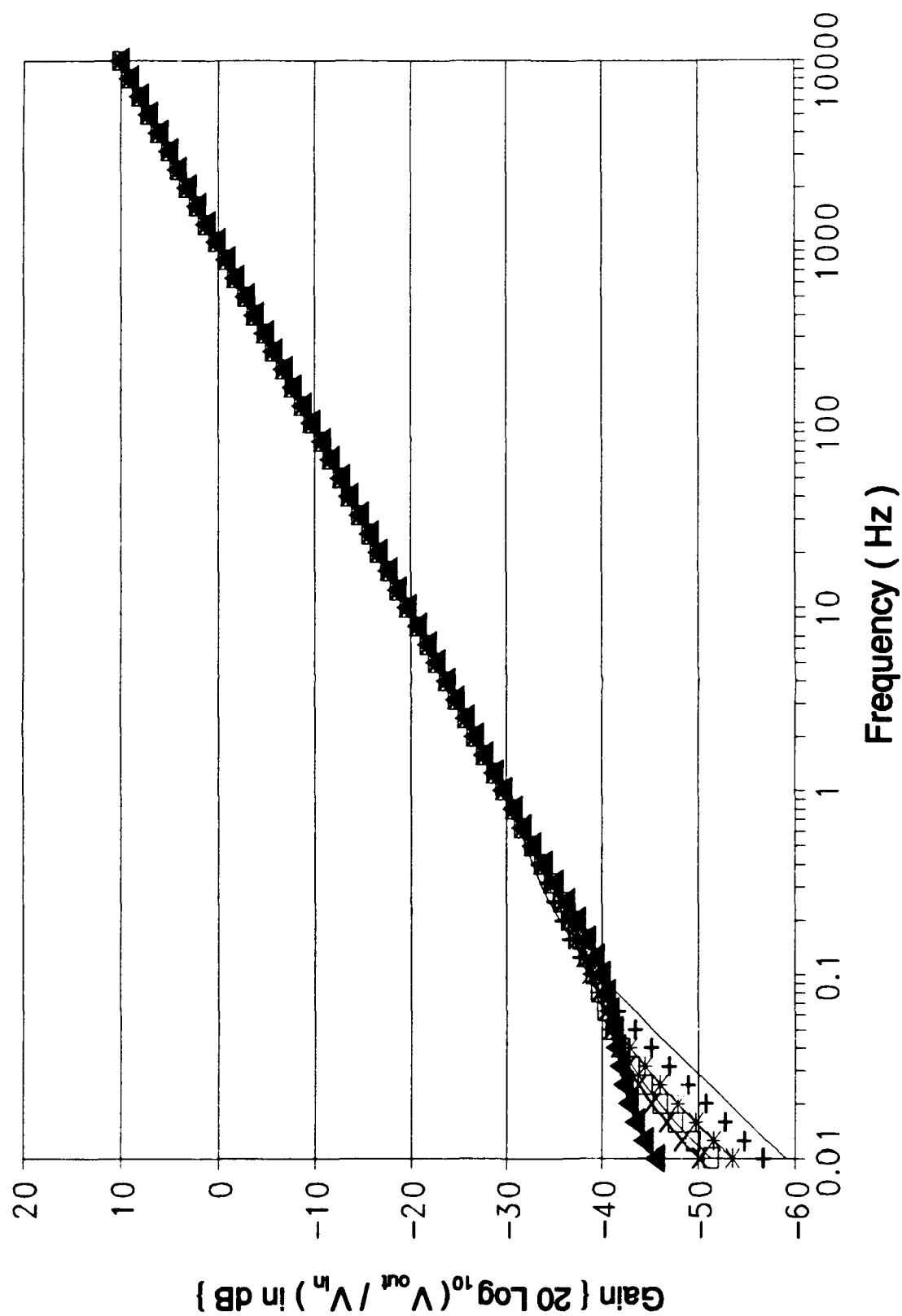**Values Corresponding to Figure C-7 (cont);**

Figure C-7 (cont). Gain Response of the Oldfield Circuit Design Using an HSPICE Computer Variation of Resistor 7 (cont);

Figure C-7 (cont). Phase Response of the Oldfield Circuit Design Using an HSPICE Computer Variation of Resistor 7.

Resistor Values for Figure C-8						
Symbol	——	-+-	-*-	—□—	—×—	-▲-
Resis-tor Value (KΩ)	6.044	24.17	60.44 Ideal	96.70	120.88	302.2

**Figure C-8. Graphical Symbol Legend and Resistor Values Corresponding to Figure C-8 (cont);**
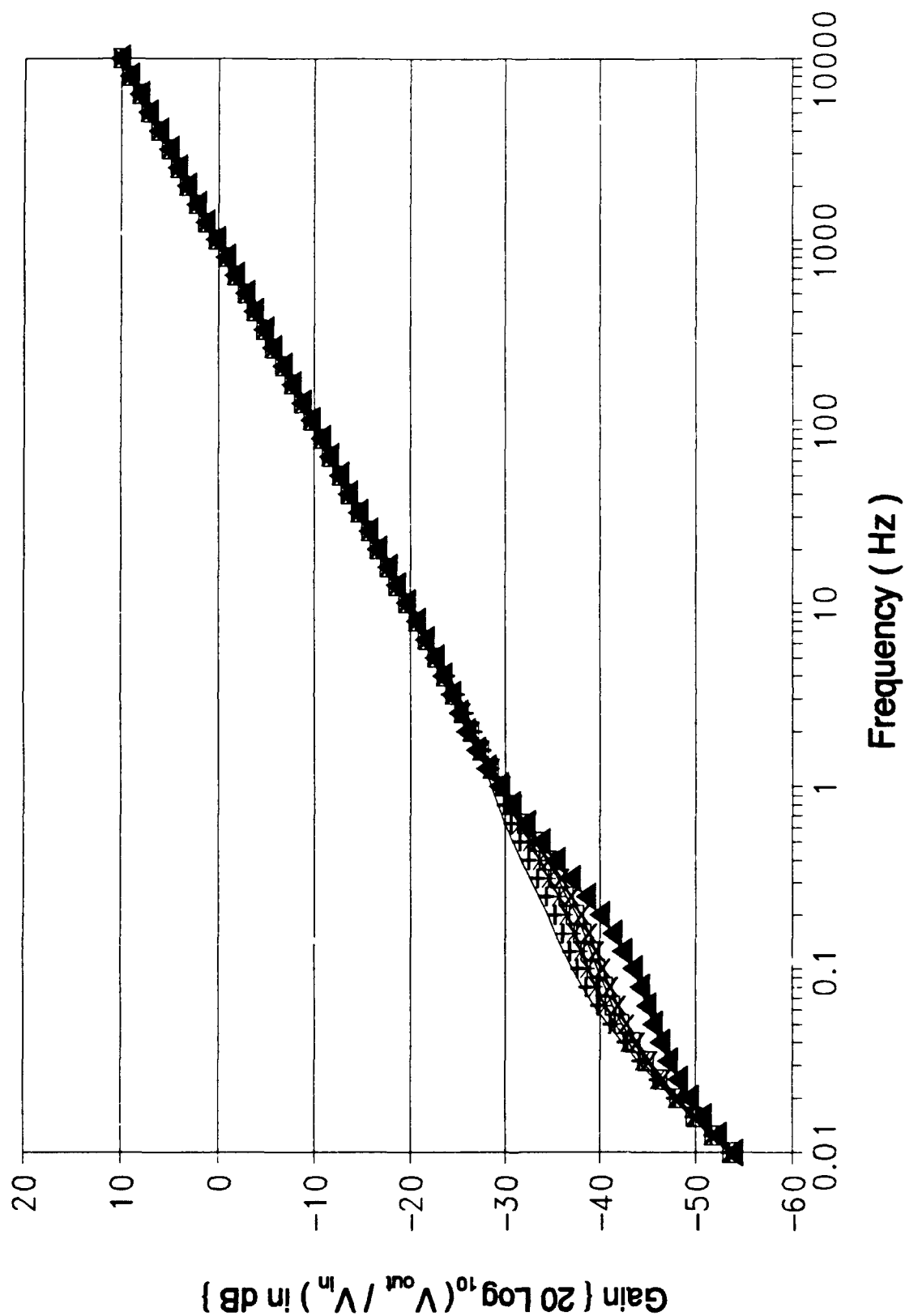
Figure C-8 (cont). Gain Response of the Oldfield Circuit Design Using an HSPICE Computer Variation of Resistor 8 (cont);
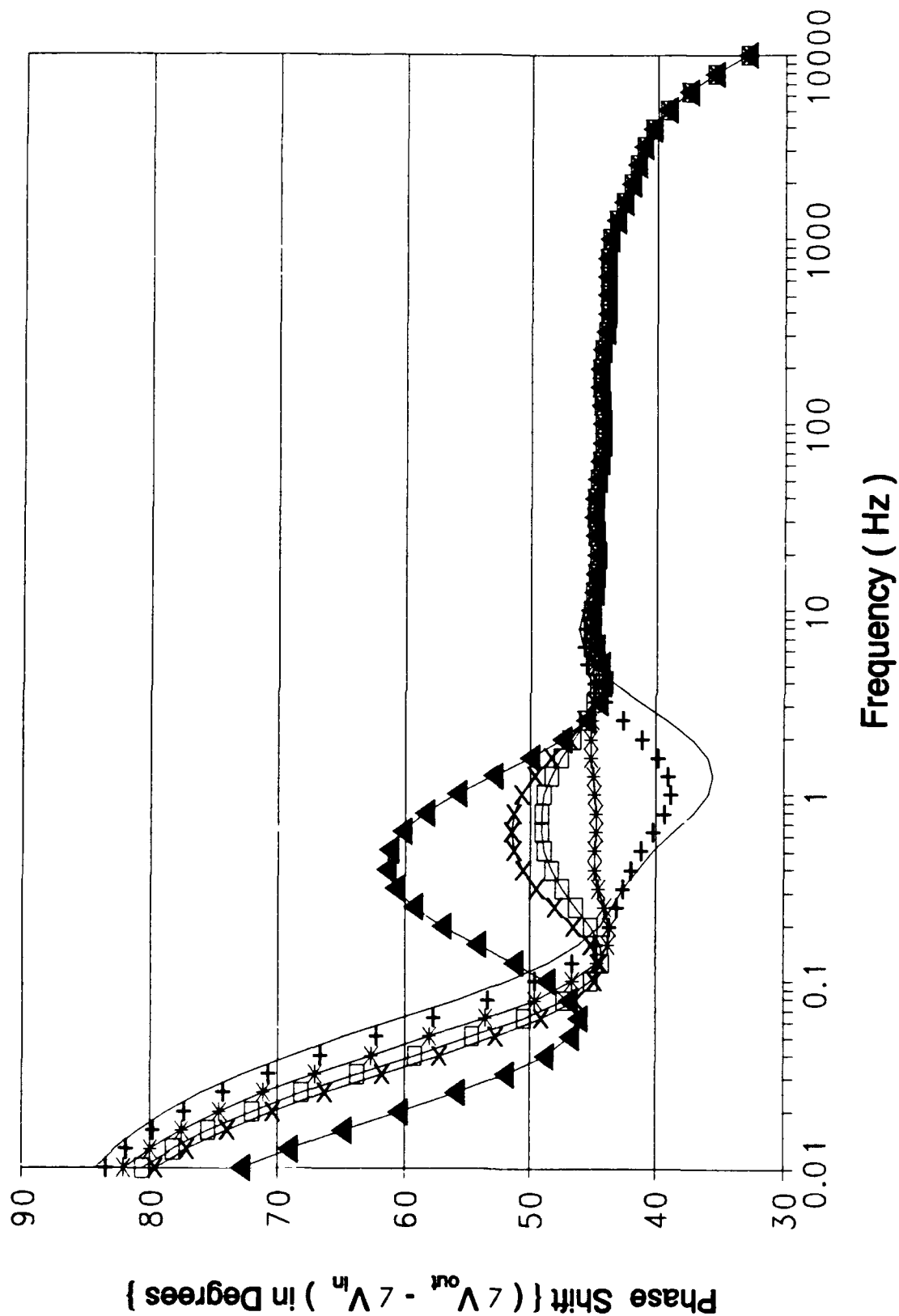
Figure C-8 (cont). Phase Response of the Oldfield Circuit Design Using an Hspice Computer Variation of Resistor 8.

C-28

Resistor Values for Figure C-9						
Symbol	——	-+-	-*-	—□—	—×—	-▲-
Resistor Value (KΩ)	12.96	51.84	129.6 Ideal	207.36	259.2	648

Figure C-9. Graphical Symbol Legend and Resistor
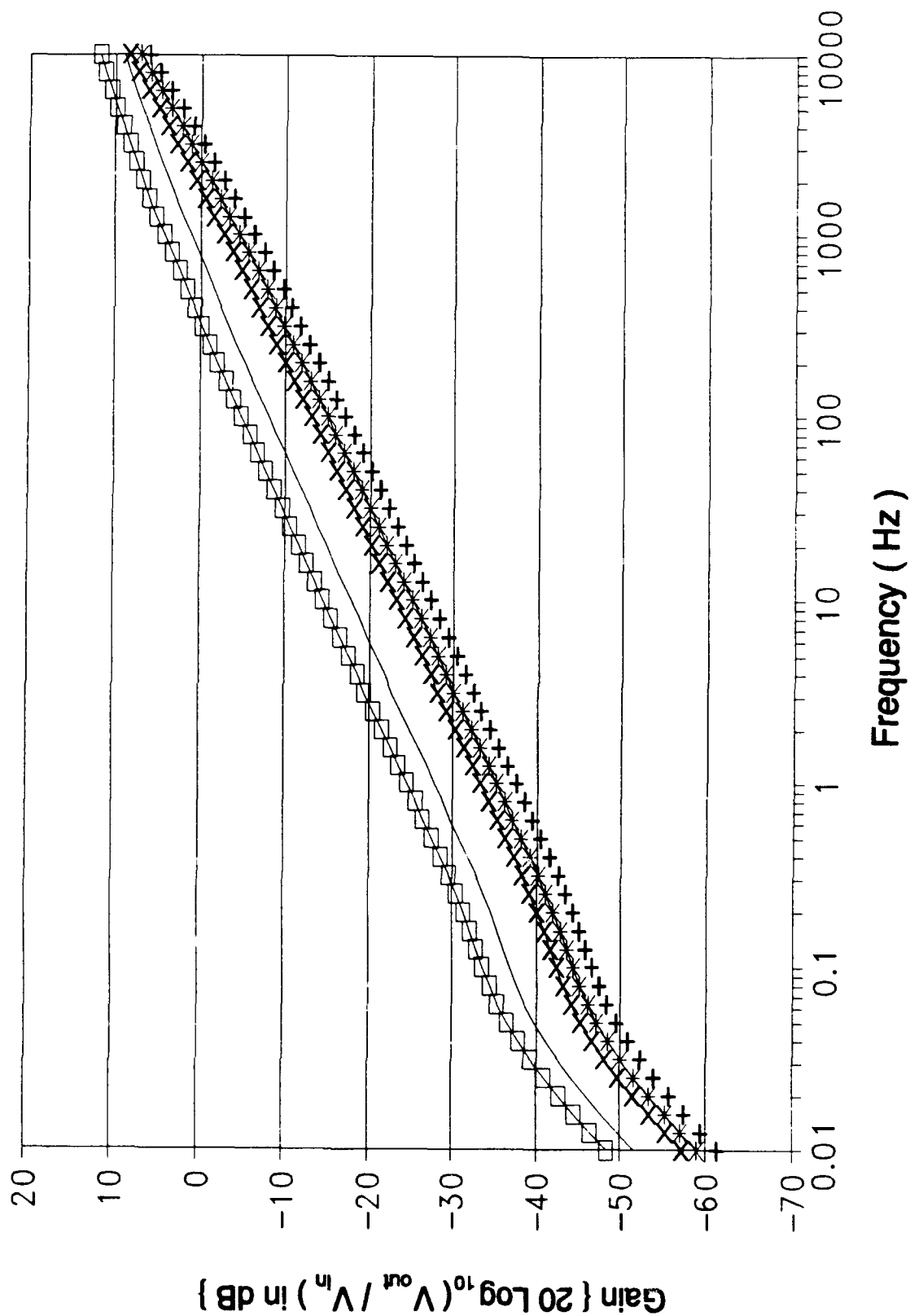   Values Corresponding to Figure C-9 (cont);
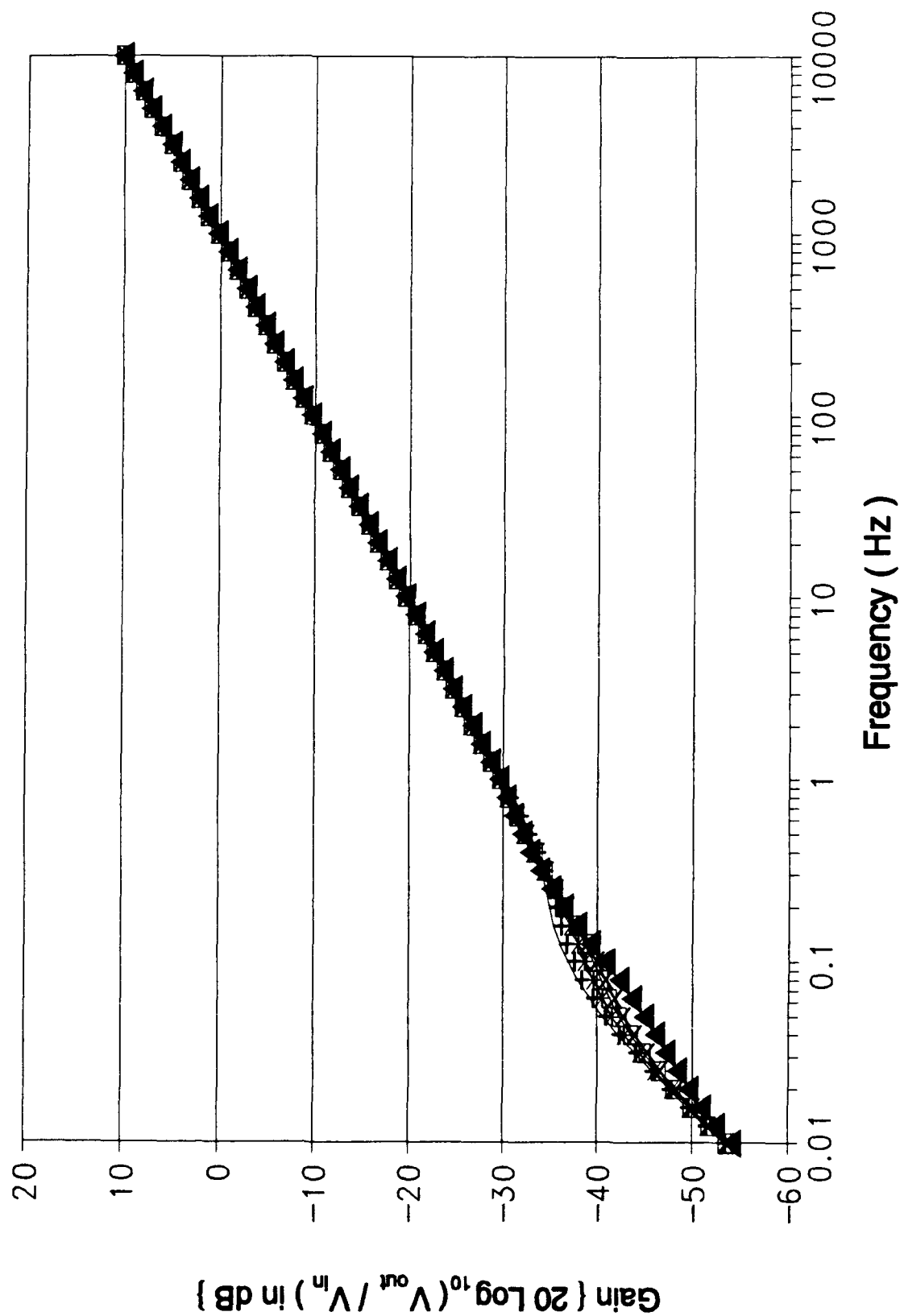
Figure C-9 (cont).   Gain Response of the Oldfield Circuit Design Using
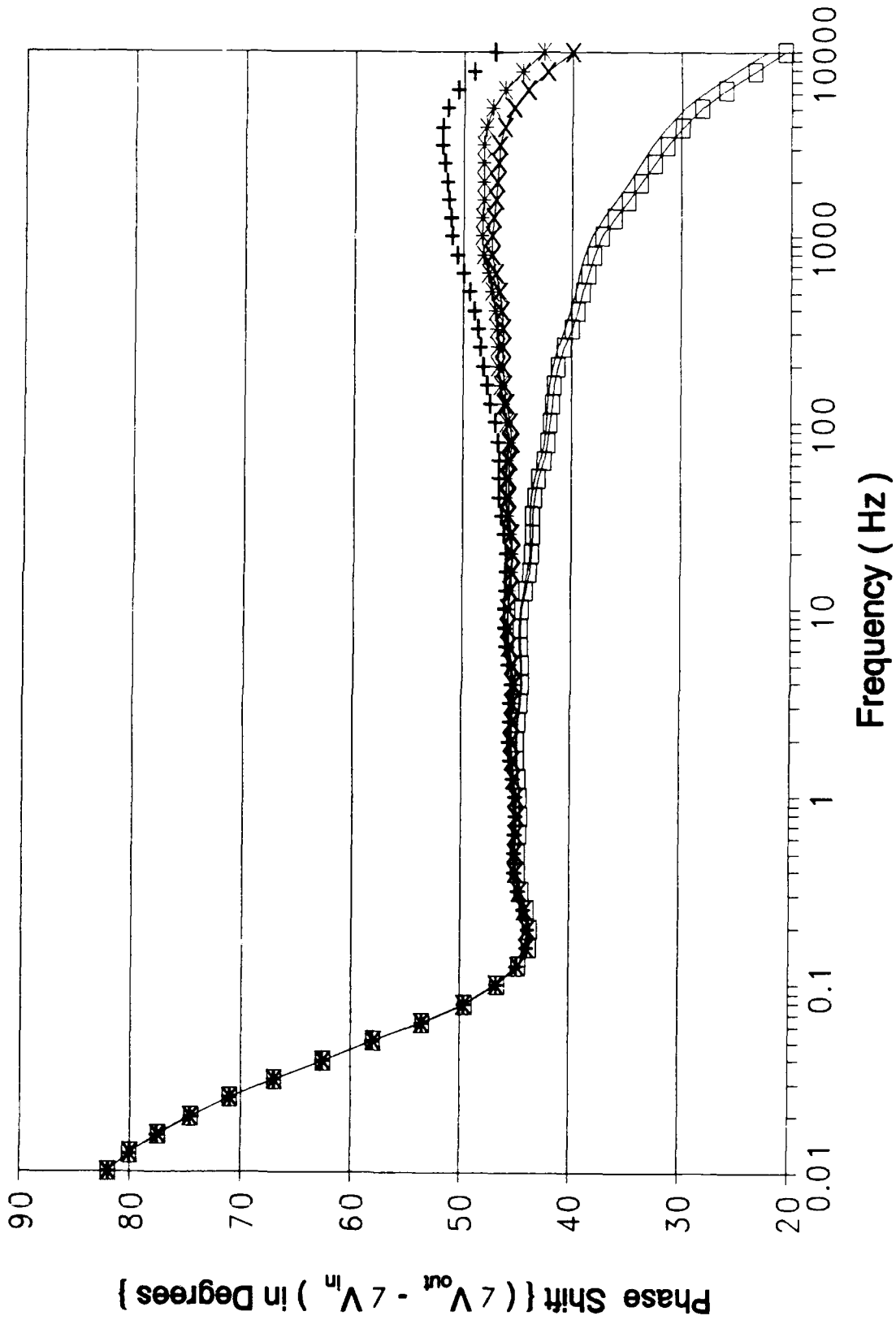an HSPICE Computer Variation of Resistor 9 (cont);
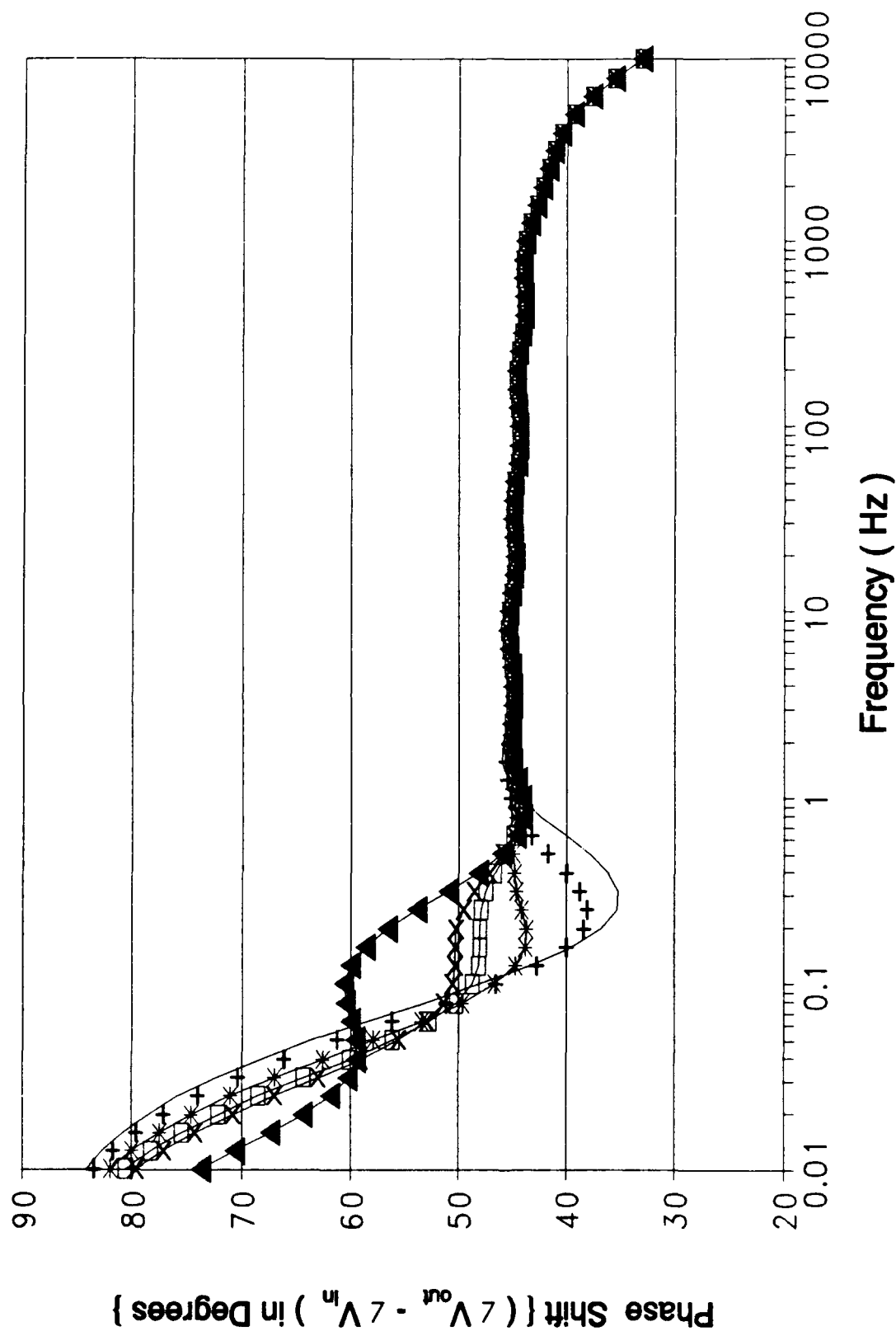
Figure C-9 (cont). Phase Response of the Oldfield Circuit Design Using an HSPICE Computer Variation of Resistor 9.

Capacitor Values for Figure C-10						
Symbol	——	-+-	-*-	—□—	—x—	-▲-
Capac-itor Value (nf)	2.2	8.8	22 Ideal	35.2	44	110

:

Figure C-10. Graphical Symbol Legend and Capacitor Values Corresponding to Figure C-10 (cont);
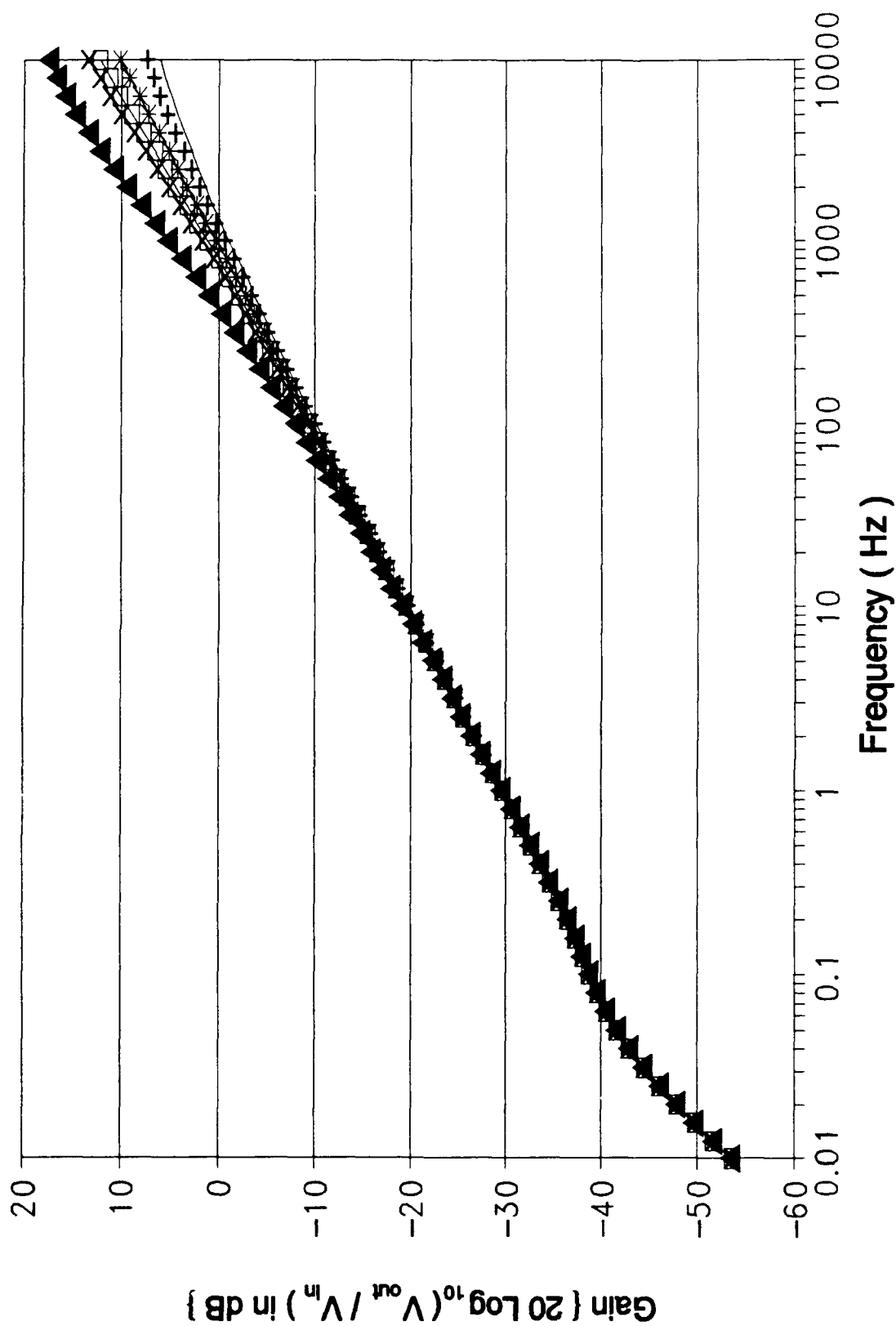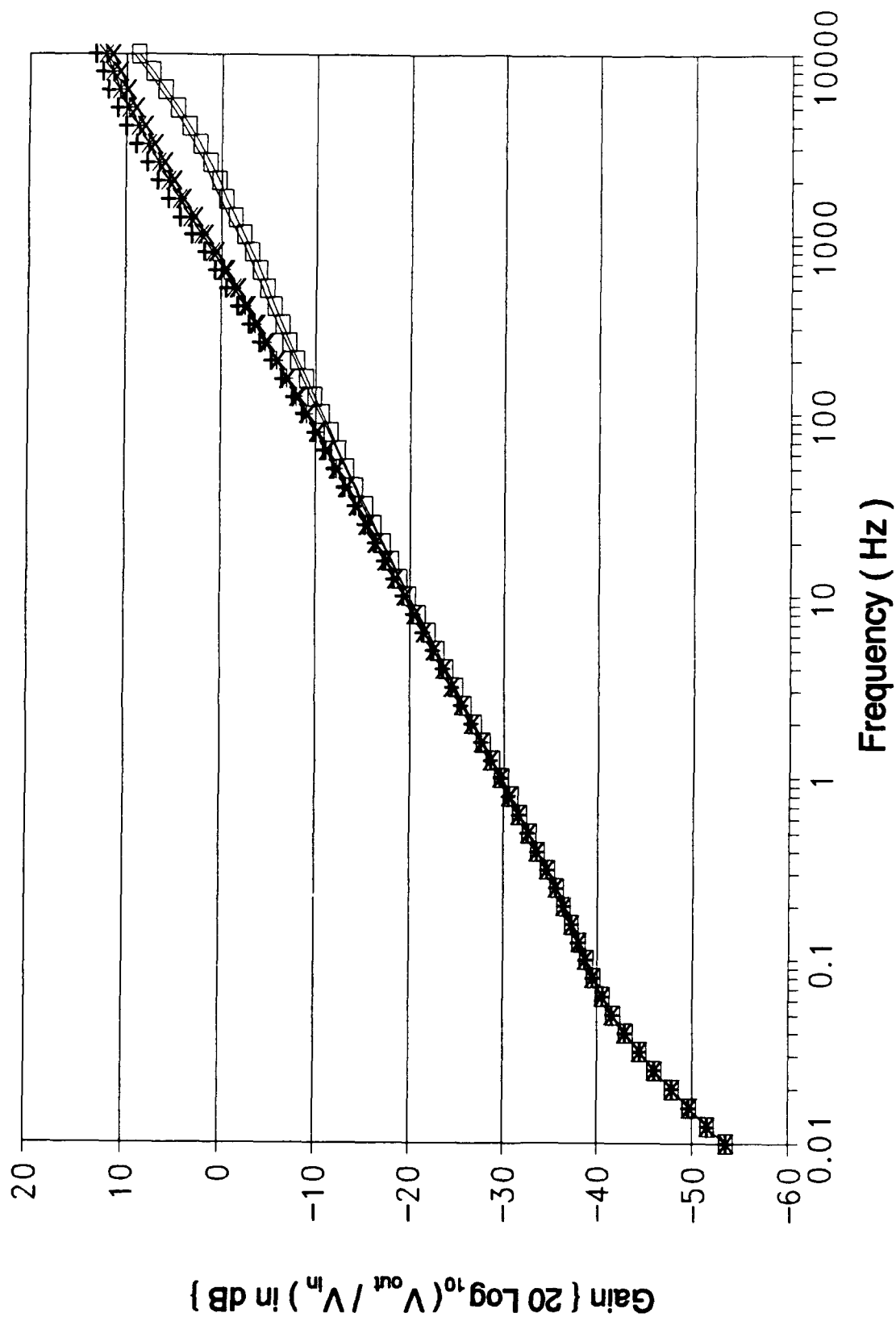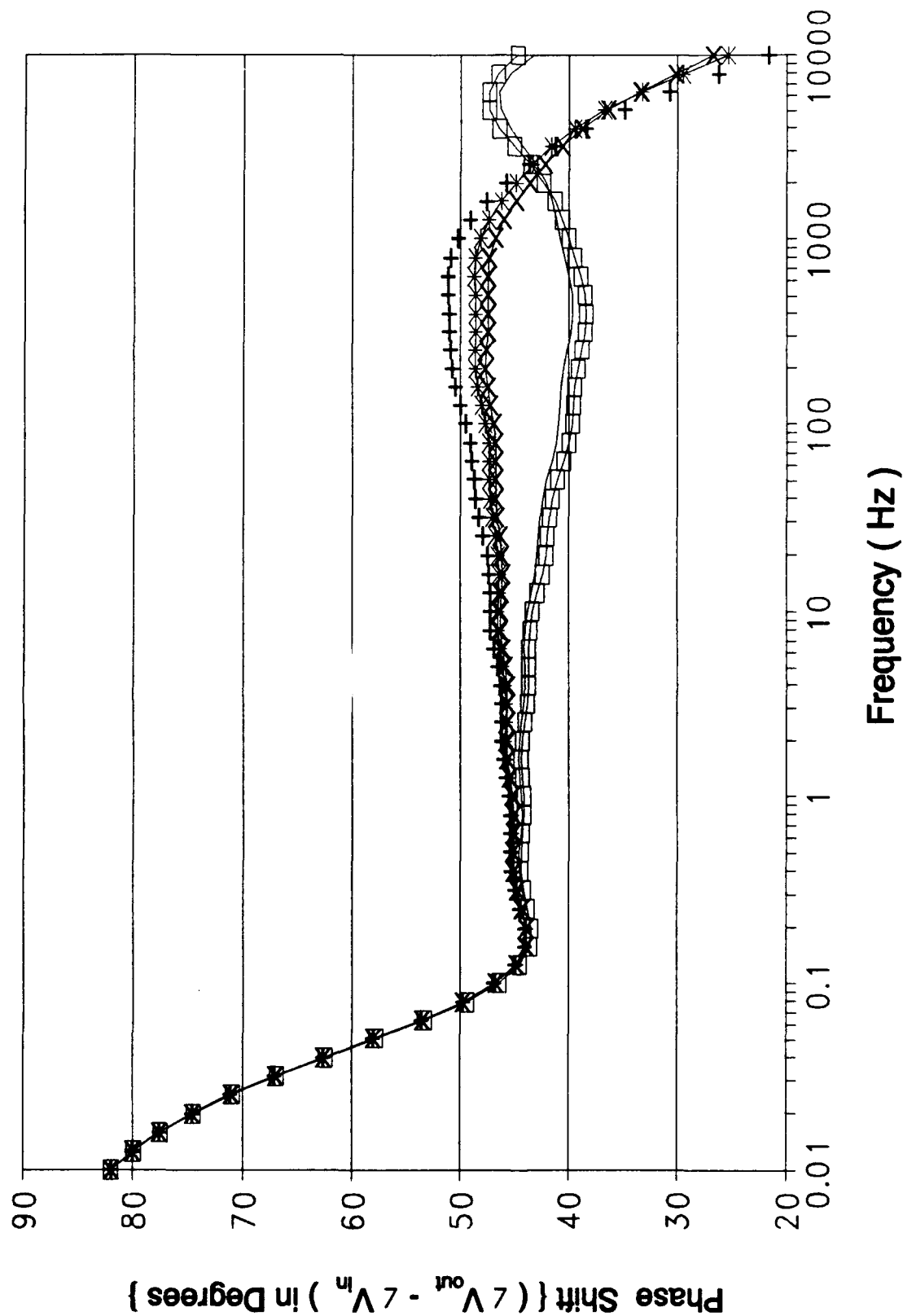
Figure C-10 (cont). Gain Response of the Oldfield Circuit Design Using
an HSPICE Computer Variation of Capacitor 1 (cont);
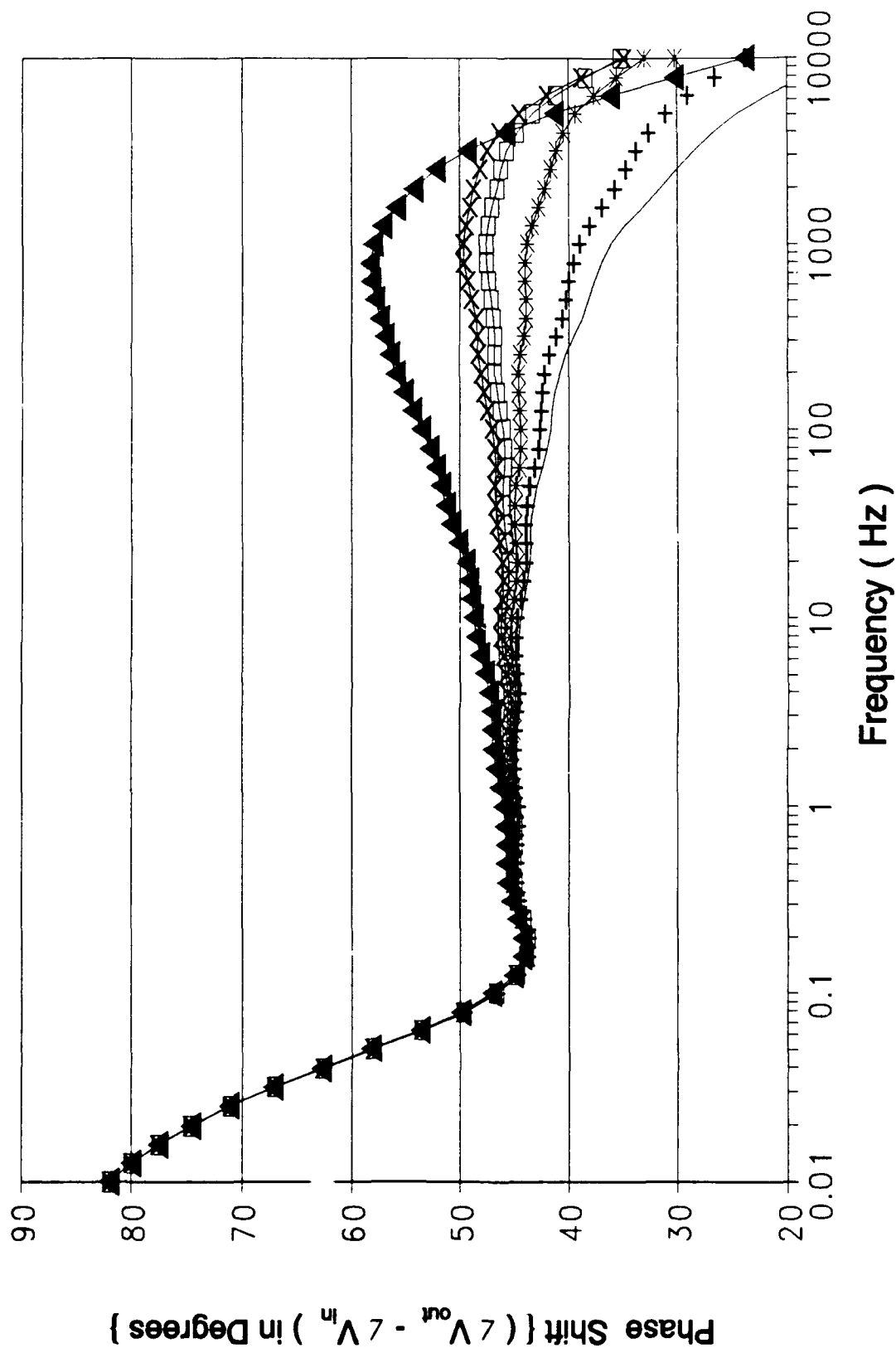
Figure C-10 (cont). Phase Response of the Oldfield Circuit Design Using an HSPICE Computer Variation of Capacitor 1.

Capacitor Values for Figure C-11						
Symbol	——	-+-	-*-	—▫—	—×—	-▲-
Capac-itor Value (nf)	4.7	18.8	47 Ideal	75.2	94	235

Figure C-11. Graphical Symbol Legend and Capacitor Values
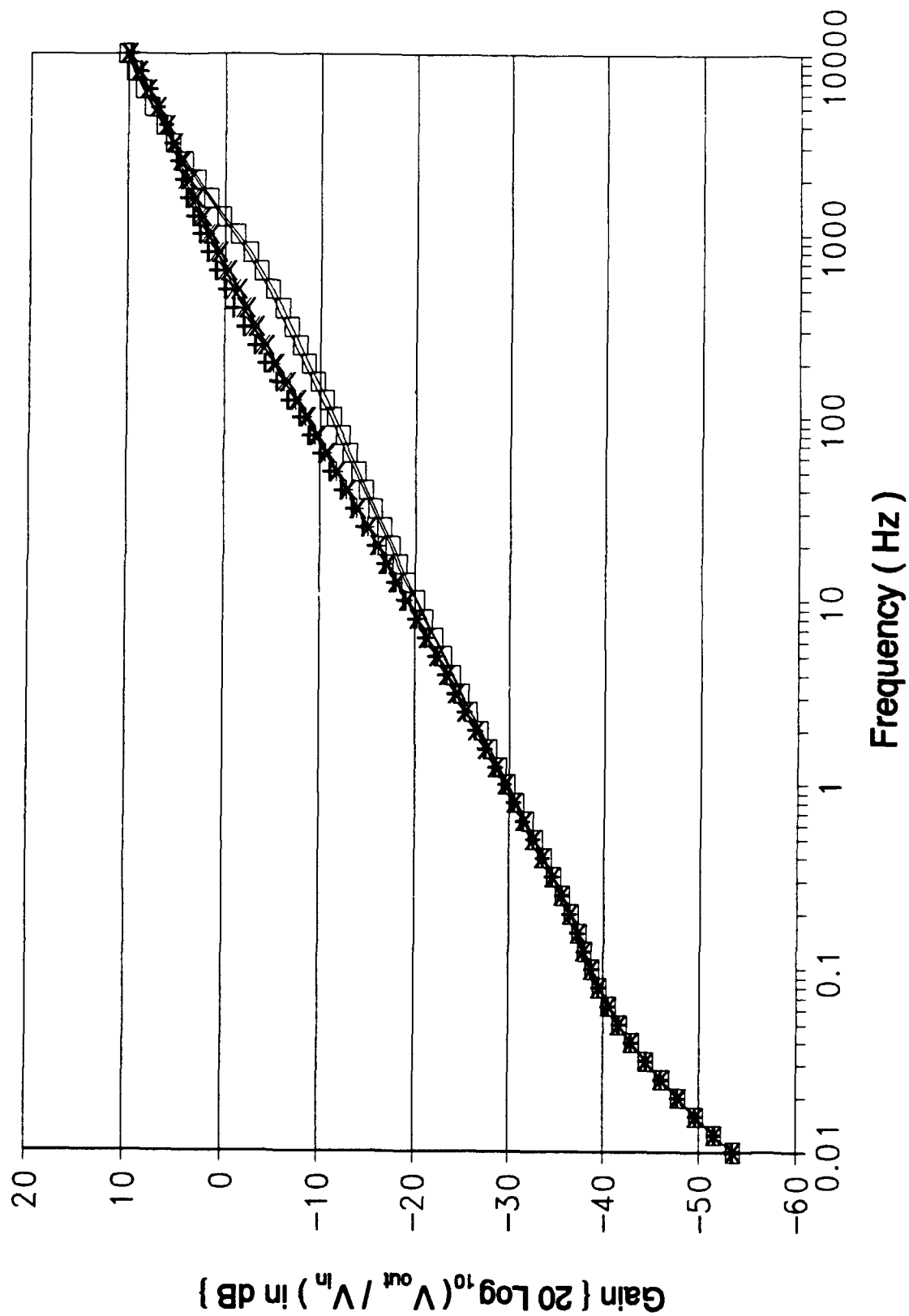Corresponding to Figure C-11 (cont);
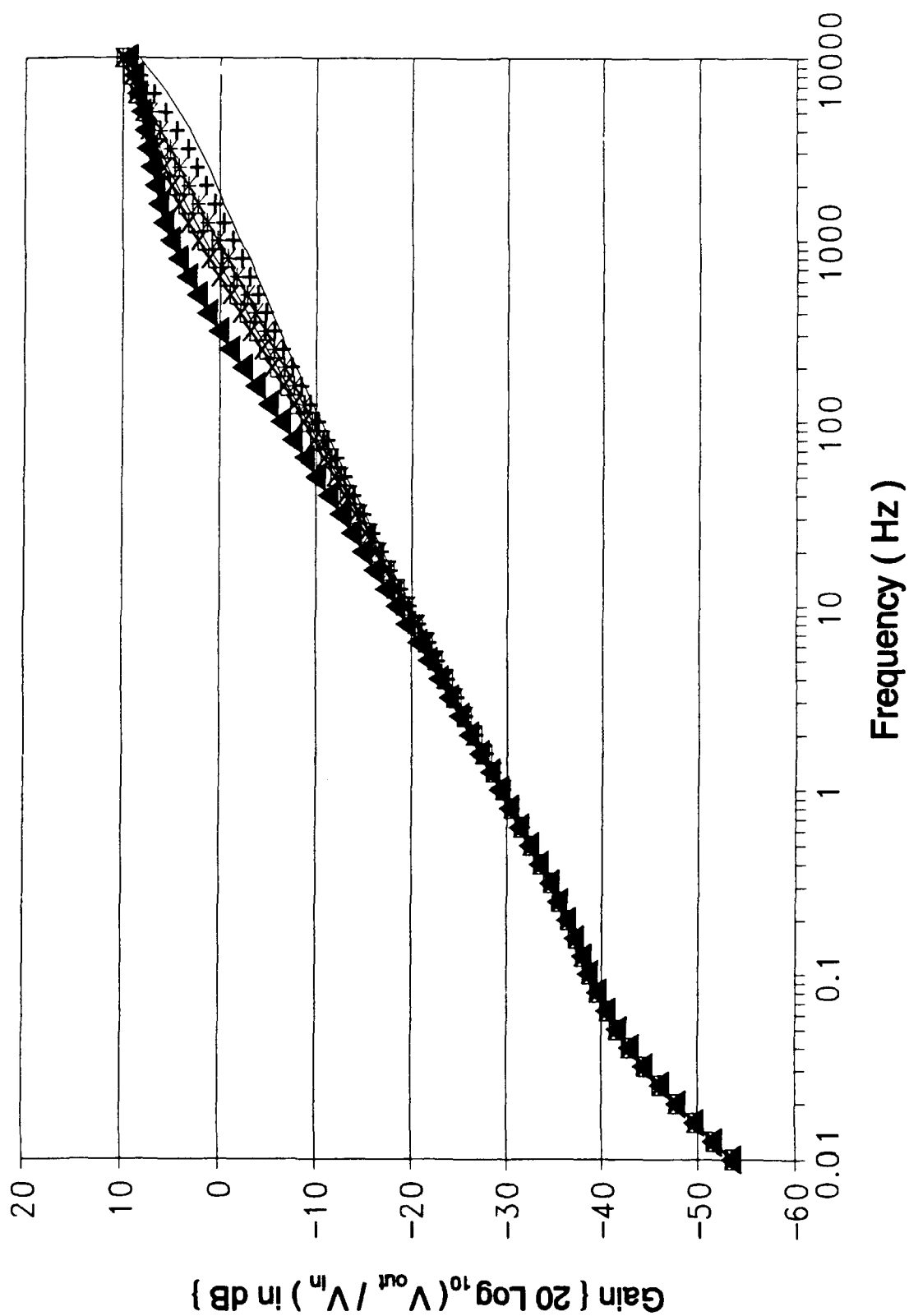
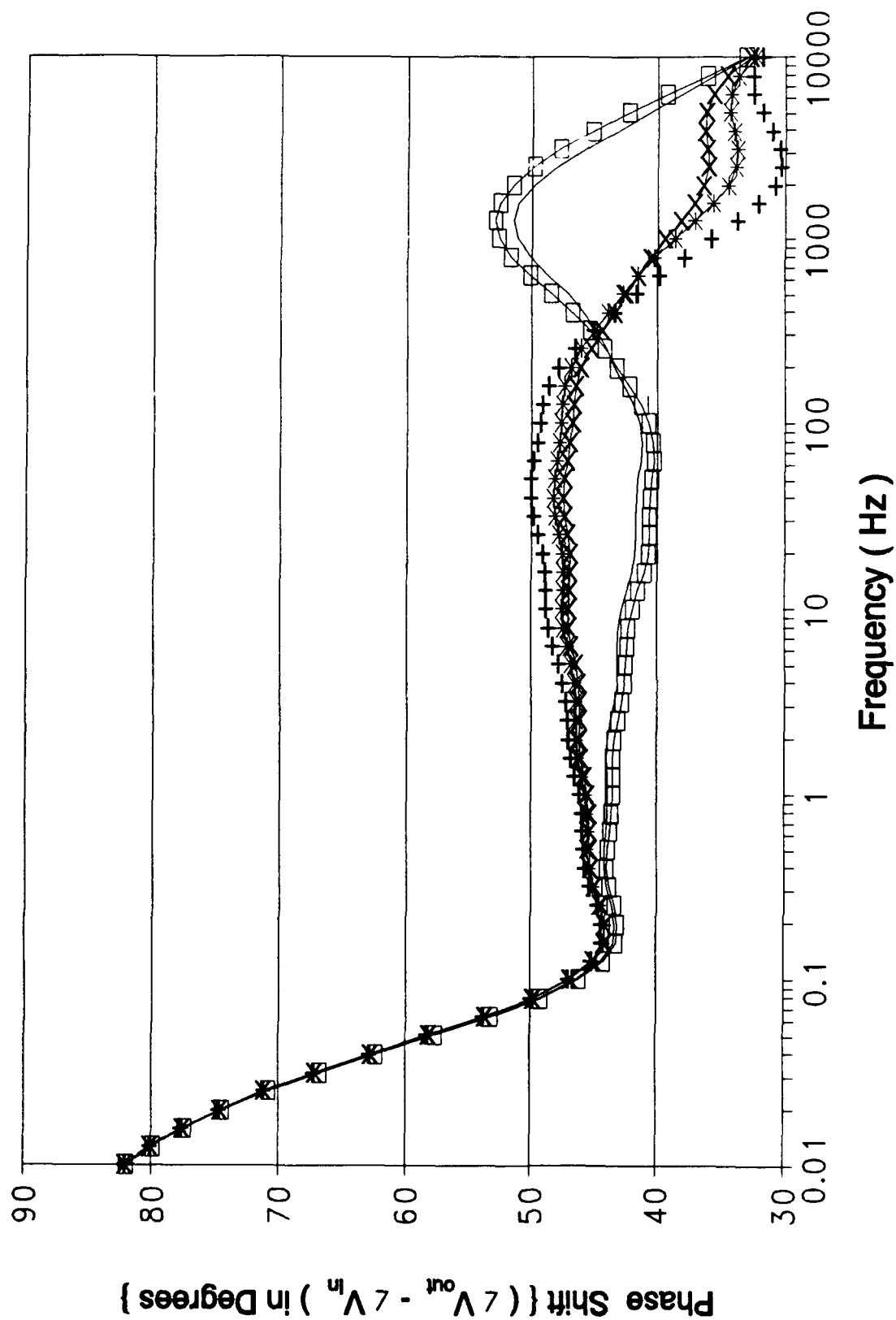Figure C-11 (cont). Gain Response of the Oldfield Circuit Design Using an HSPICE Computer Variation of Capacitor 2 (cont);

C-36

Figure C-11 (cont). Phase Response of the Oldfield Circuit Design Using an HSPICE Computer Variation of Capacitor 2.

C-37

Capacitor Values for Figure C-12						
Symbol	——	-+-	-*-	—□—	—x—	-▲-
Capac- itor Value (nf)	10	40	100 Ideal	160	200	500

Figure C-12.   Graphical Symbol Legend and Capacitor Values
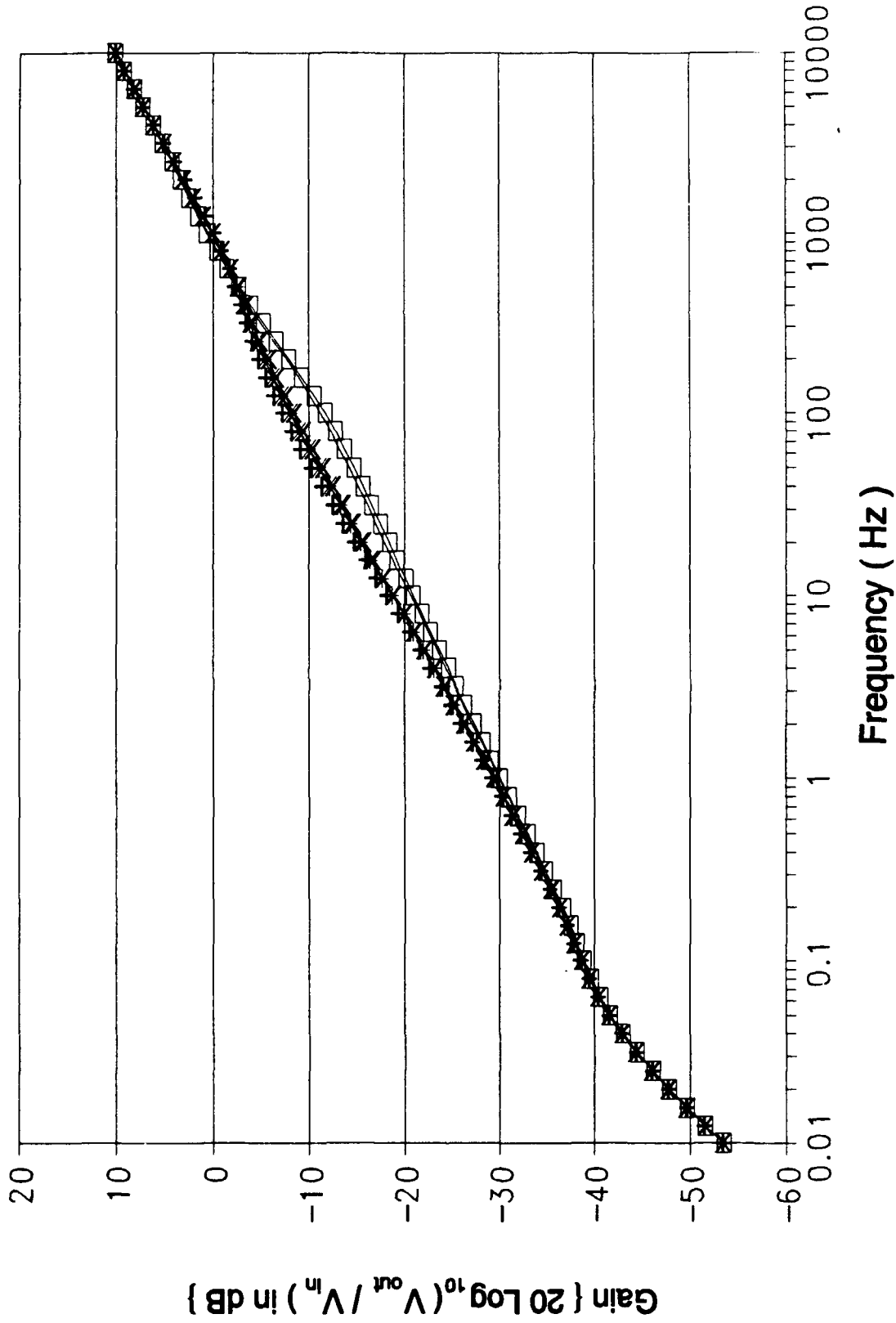Corresponding to Figure C-12 (cont);

Figure C-12 (cont). Gain Response of the Oldfield Circuit Design Using an HSPICE Computer Variation of Capacitor 3 (cont);
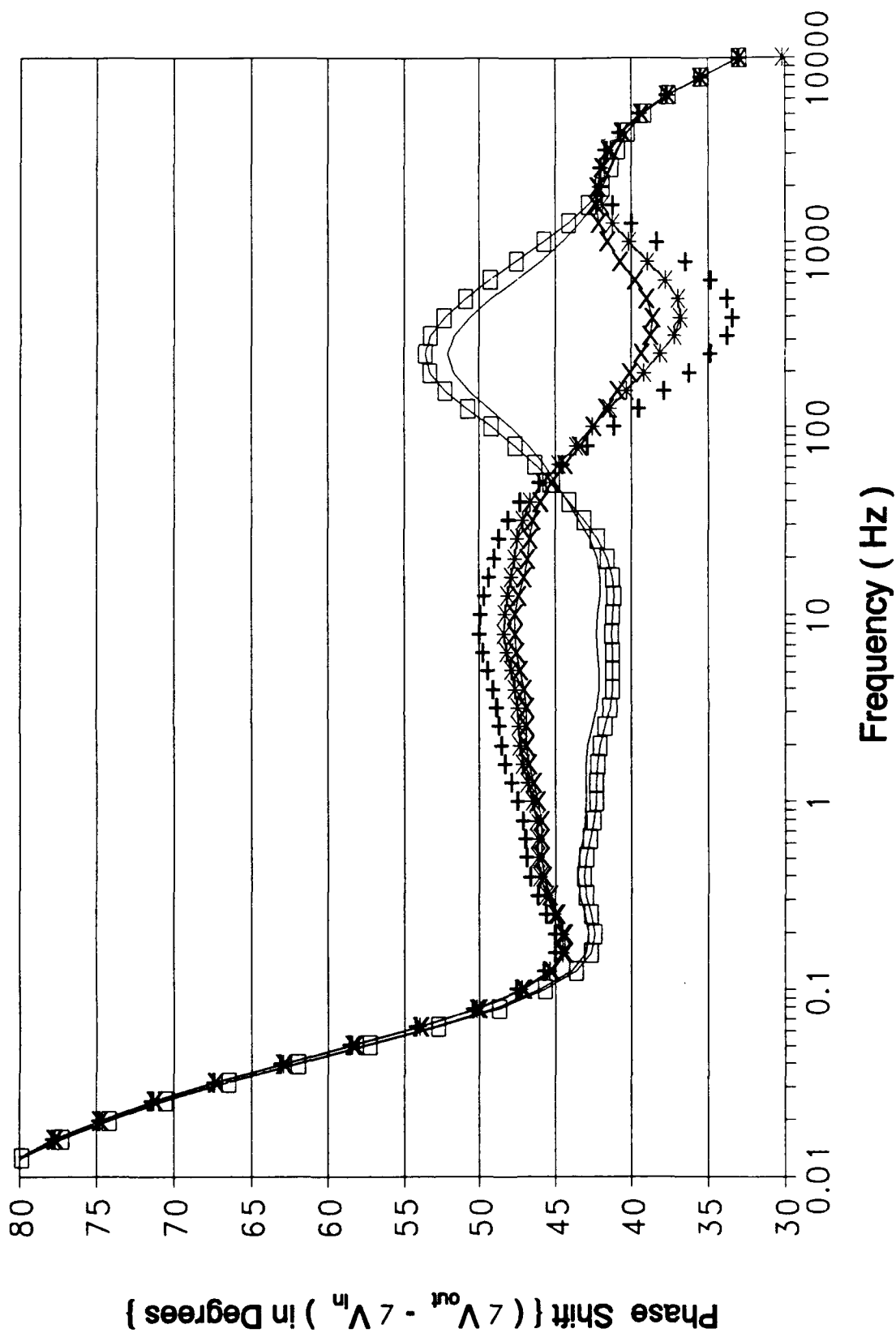
Figure C-12 (cont). Phase Response of the Oldfield Circuit Design Using an HSPICE Computer Variation of Capacitor 3.

Capacitor Values for Figure C-13						
Symbol	——	-+-	-*-	—□—	—×—	-▲-
Capac-itor Value (nf)	22	88.8	220 Ideal	352	440	1100

Figure C-13. Graphical Symbol Legend and Capacitor Values
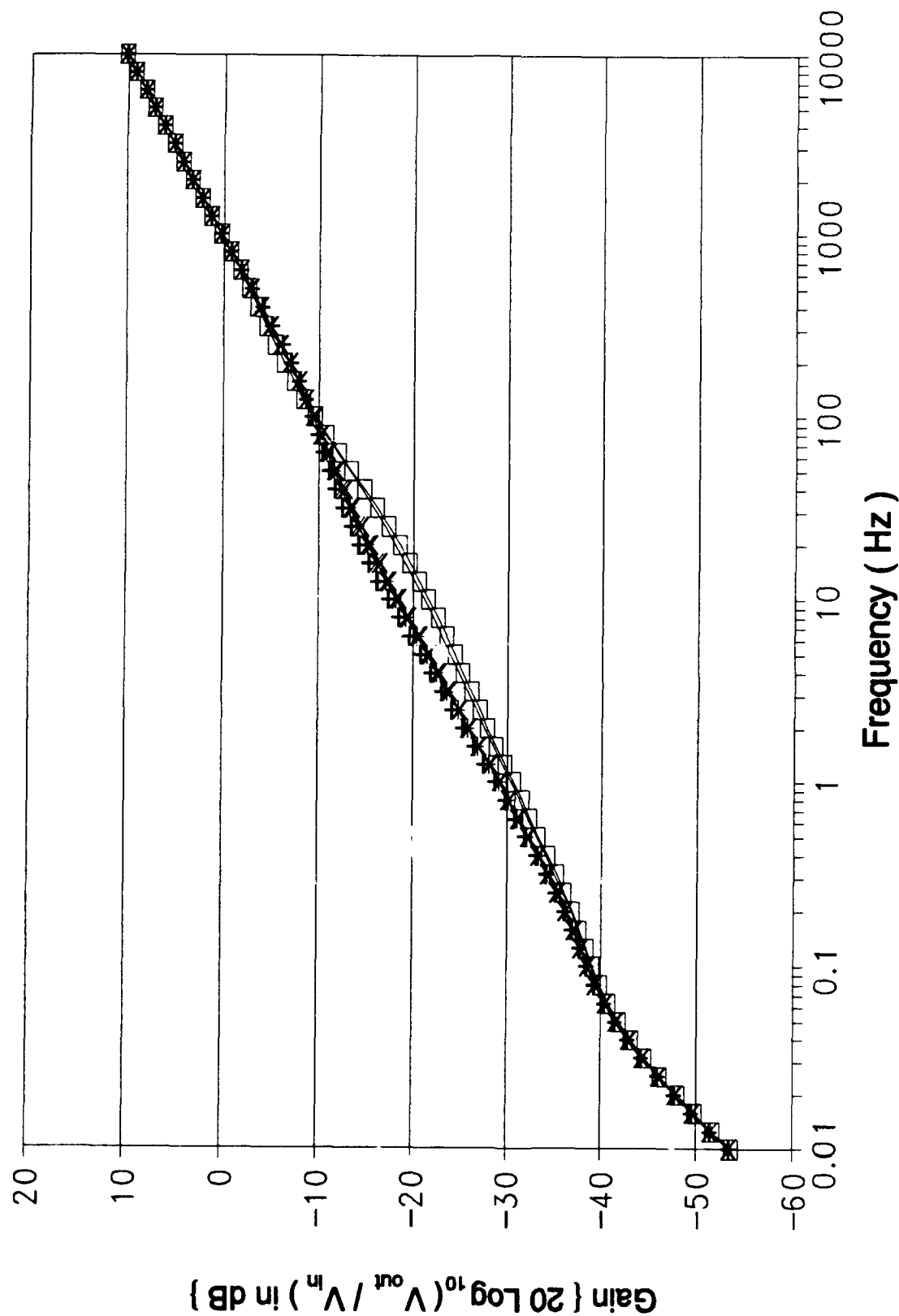Corresponding to Figure C-13 (cont);

Figure C-13 (cont). Gain Response of the Oldfield Circuit Design Using
an HSPICE Computer Variation of Capacitor 4 (cont);

C-42

Figure C-13 (cont). Phase Response of the Oldfield Circuit Design Using an HSPICE Computer Variation of Capacitor 4.

C-43

Capacitor Values for Figure C-14						
Symbol	——	-+-	-*-	—▯—	—×—	-▲-
Capac-itor Value (nf)	47	188	470 Ideal	752	940	2350

Figure C-14. Graphical Symbol Legend and Capacitor Values
Corresponding to Figure C-14 (cont);

Figure C-14 (cont). Gain Response of the Oldfield Circuit Design Using an HSPICE Computer Variation of Capacitor 5 (cont);
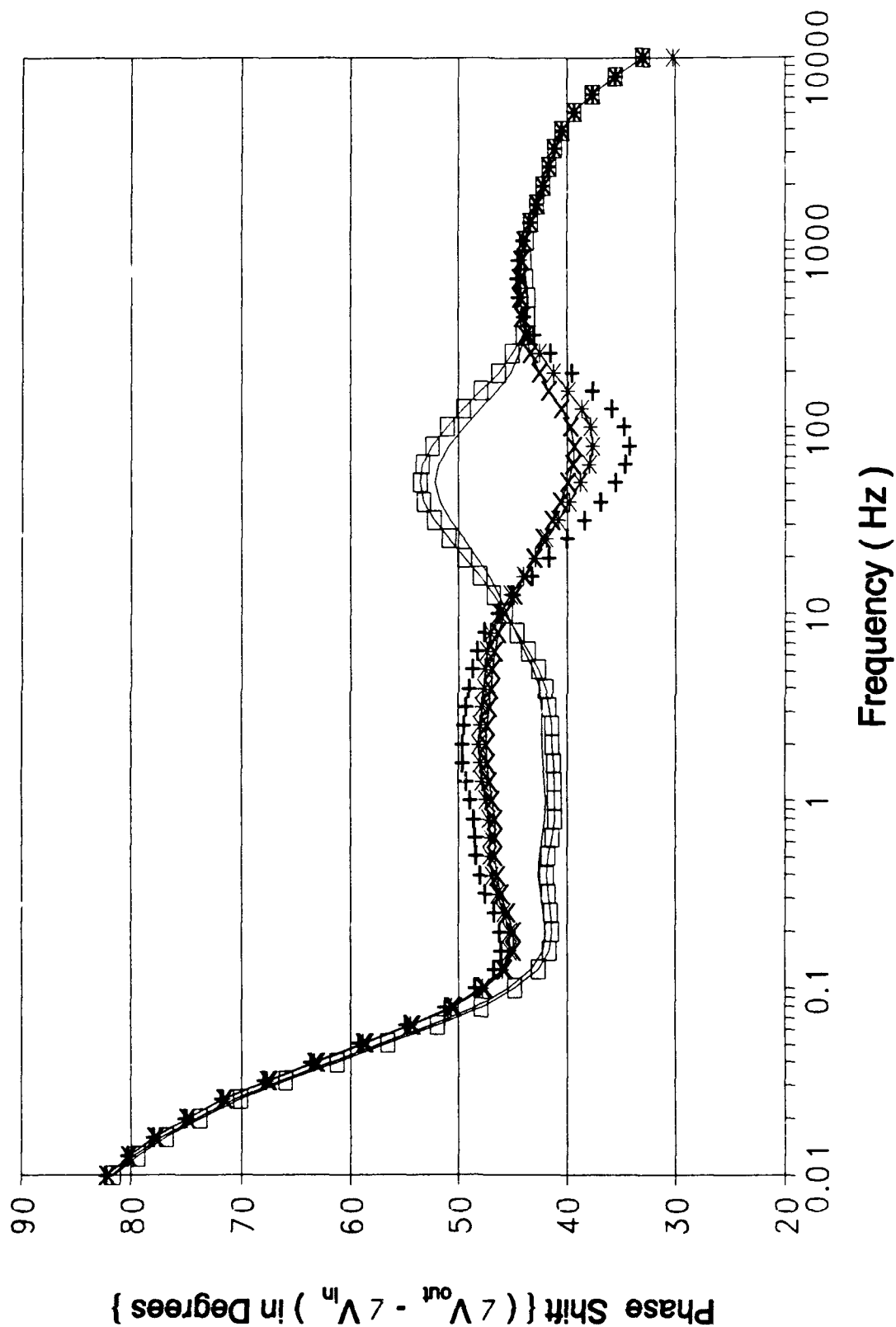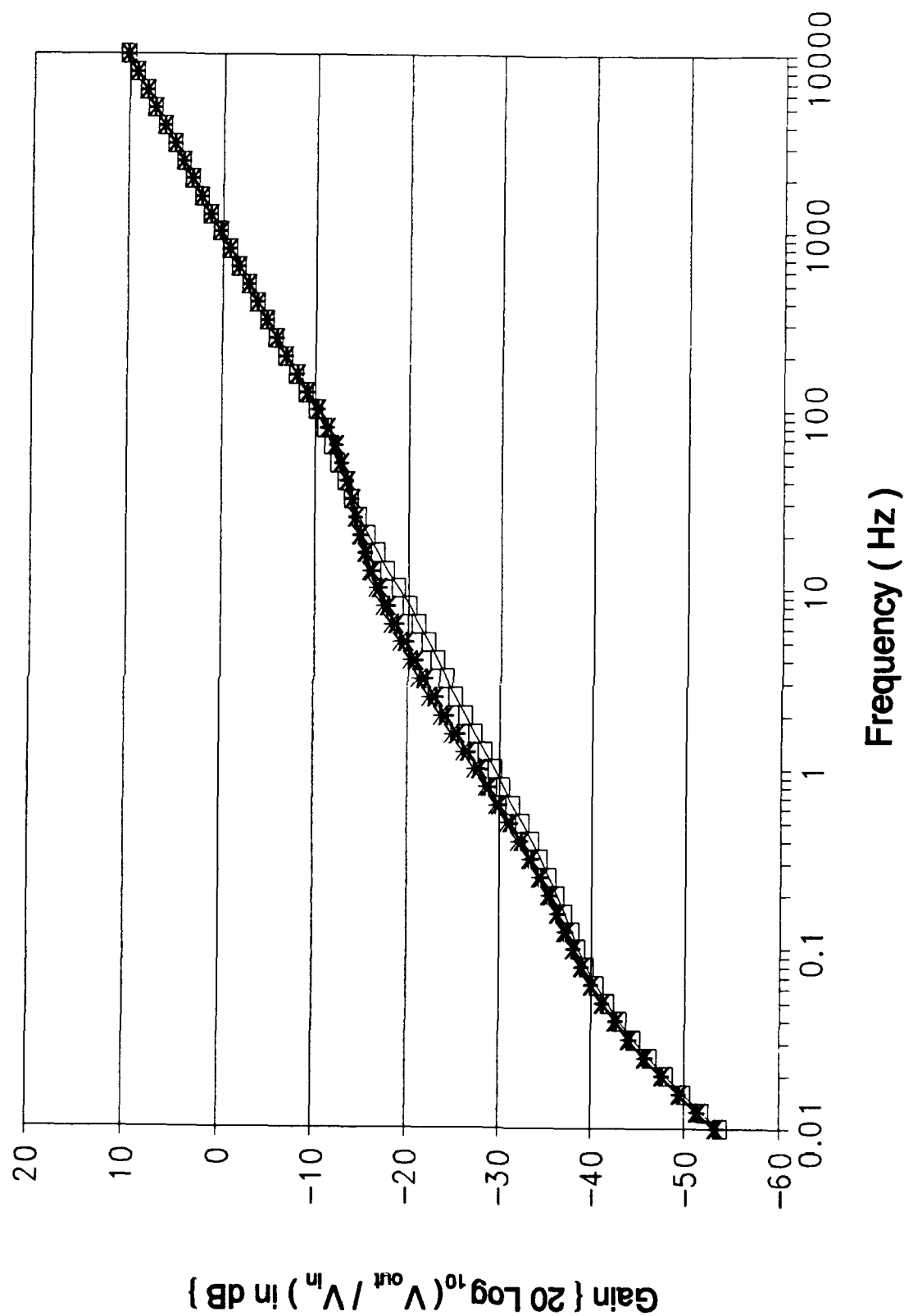
Figure C-14 (cont). Phase Response of the Oldfield Circuit Design Using an HSPICE Computer Variation of Capacitor 5.

Capacitor Values for Figure C-15						
Symbol	——	—+—	—*—	—□—	—×—	—▲—
Capac-itor Value (μf)	0.1	0.4	1.0 Ideal	1.6	2.0	5.0

Figure C-15. Graphical Symbol Legend and Capacitor Values
Corresponding to Figure C-15 (cont);

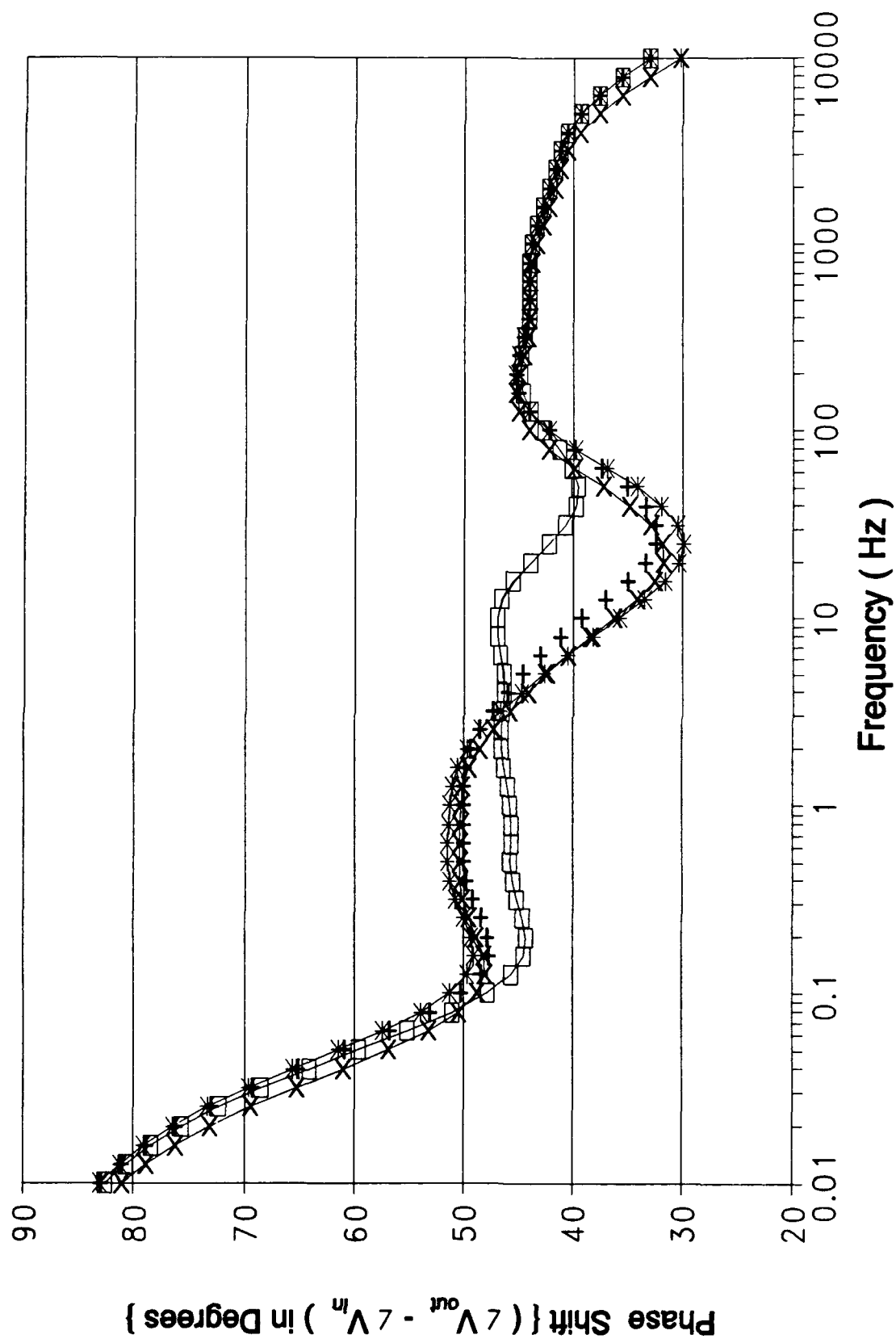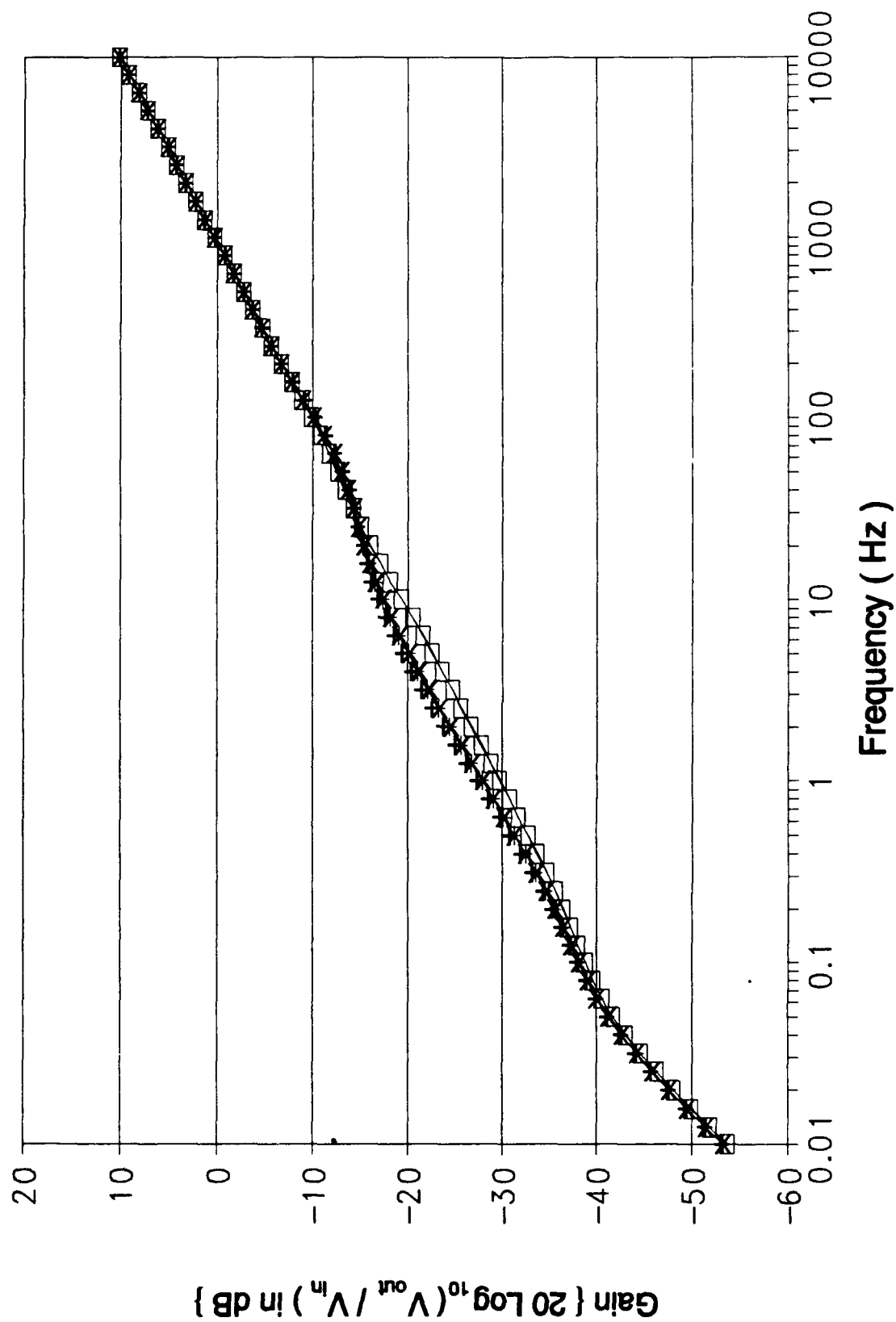Figure C-15 (cont). Gain Response of the Oldfield Circuit Design Using an HSPICE Computer Variation of Capacitor 6 (cont);

Figure C-15 (cont). Phase Response of the Oldfield Circuit Design Using an HSPICE Computer Variation of Capacitor 6.

Capacitor Values for Figure C-16						
Symbol	——	-+-	-*-	—□—	—×—	-▲-
Capac-itor Value (µf)	0.22	0.88	2.2 Ideal	3.52	4.4	11

**Figure C-16. Graphical Symbol Legend and Capacitor Values
Corresponding to Figure C-16 (cont);**

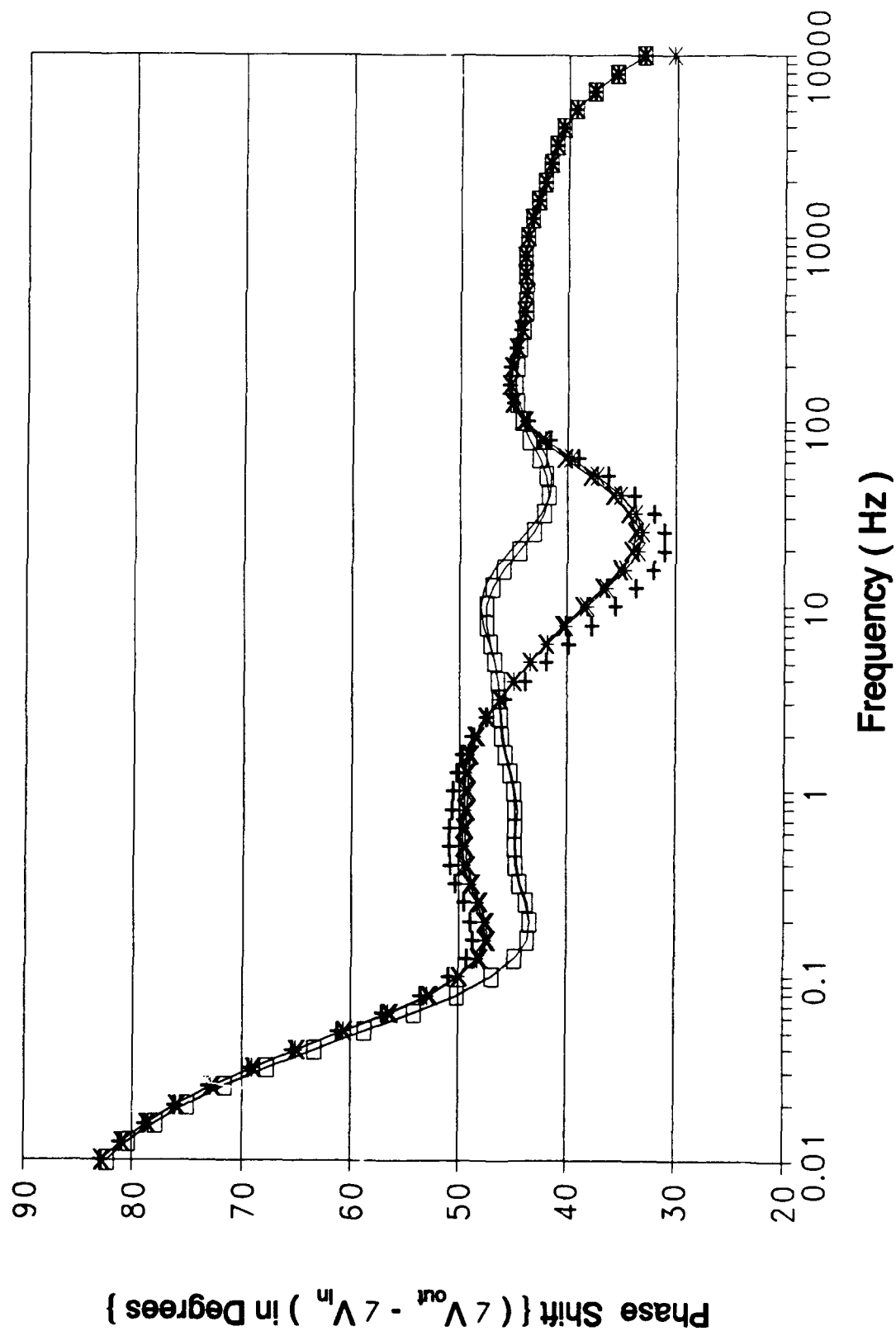Figure C-16 (cont). Gain Response of the Oldfield Circuit Design Using an HSPICE Computer Variation of Capacitor 7 (cont);

C-51

Figure C-16 (cont). Phase Response of the Oldfield Circuit Design Using an HSPICE Computer Variation of Capacitor 7.

Capacitor Values for Figure C-17						
Symbol	——	–+–	–*–	–□–	–×–	–▲–
Capac- itor Value (μf)	0.47	1.88	4.7 Ideal	7.52	9.4	23.5

Figure C-17.   Graphical Symbol Legend and Capacitor Values
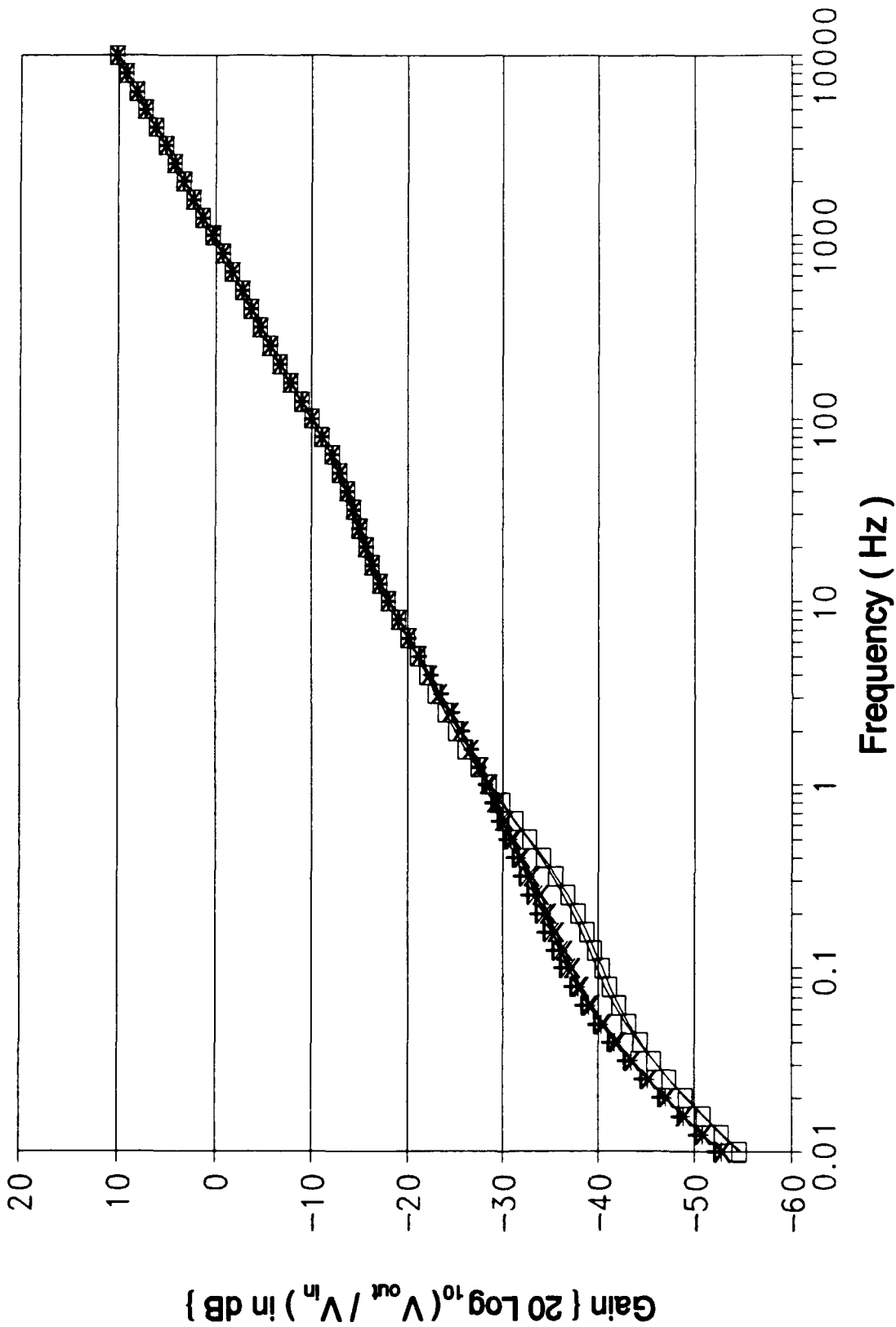**Corresponding to Figure C-17 (cont);**

Figure C-17 (cont). Gain Response of the Oldfield Circuit Design Using an HSPICE Computer Variation of Capacitor 8 (cont);
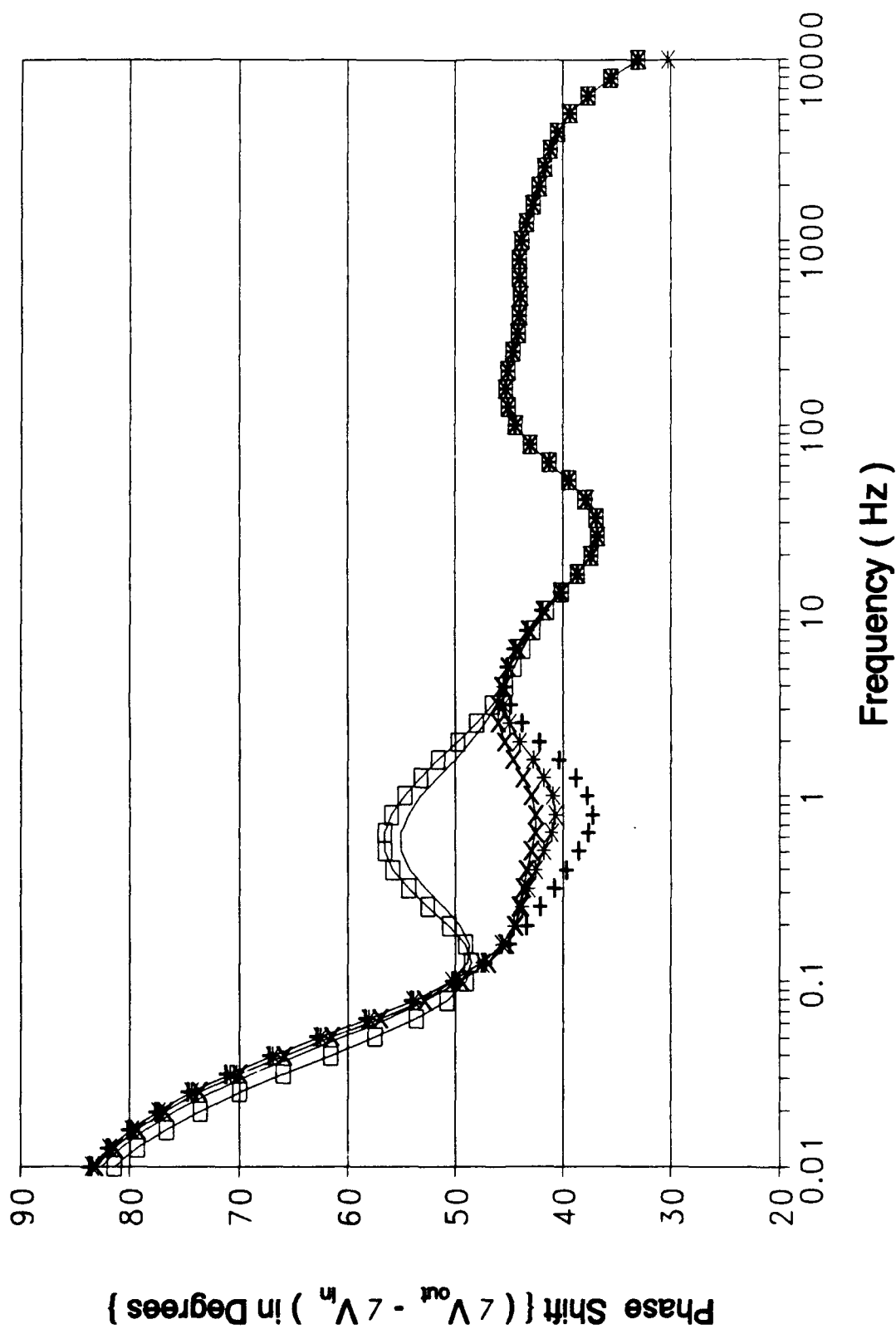
C-54

Figure C-17 (cont). Phase Response of the Oldfield Circuit Design Using an HSPICE Computer Variation of Capacitor 8.

C-55

Capacitor Values for Figure C-18						
Symbol	——	-+-	-*-	—□—	—×—	-▲-
Capac- itor Value (μf)	1.0	4.0	10.0 Ideal	16.0	20.0	50.0

Figure C-18. Graphical Symbol Legend and Capacitor Values Corresponding to Figure C-18 (cont);
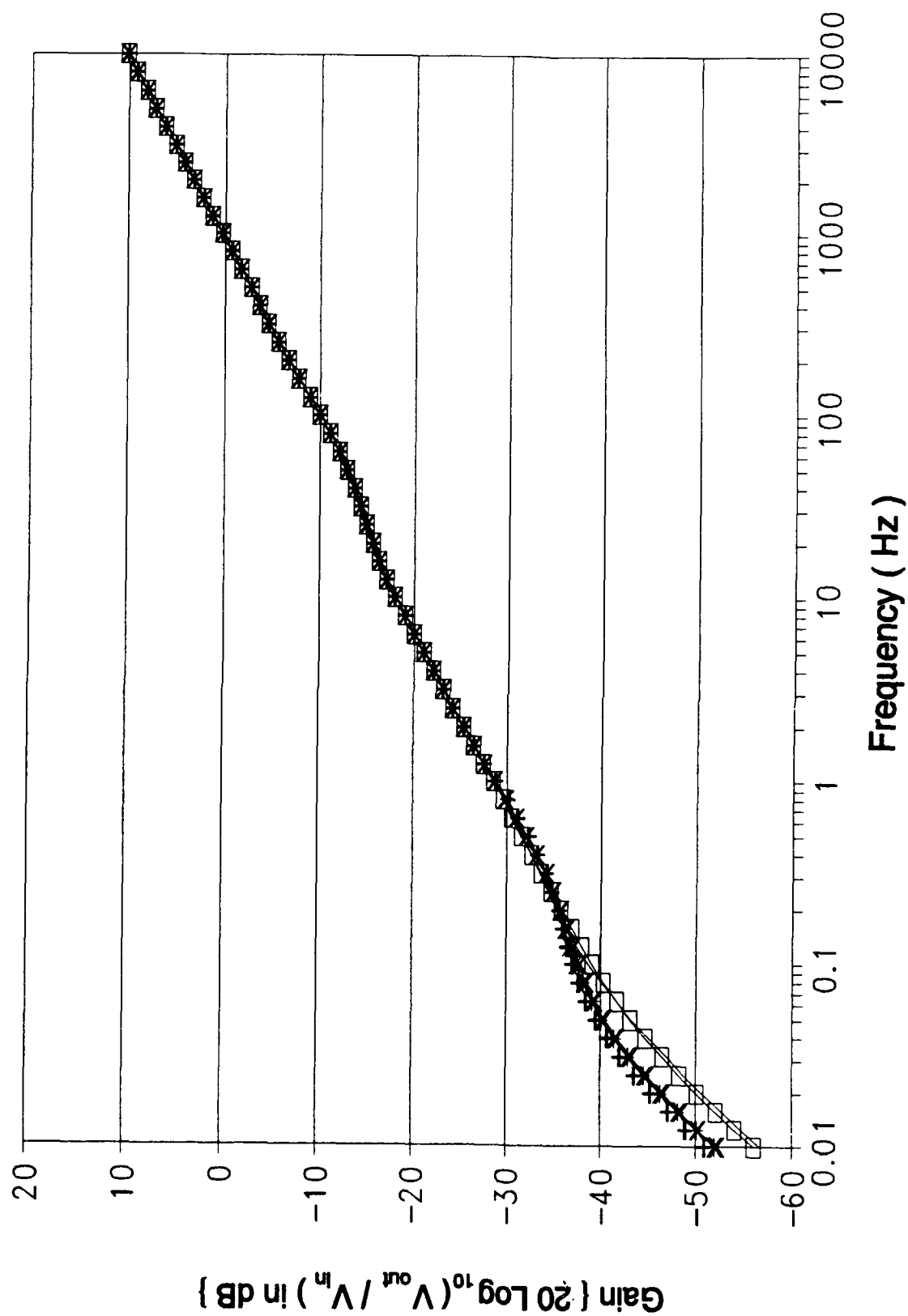
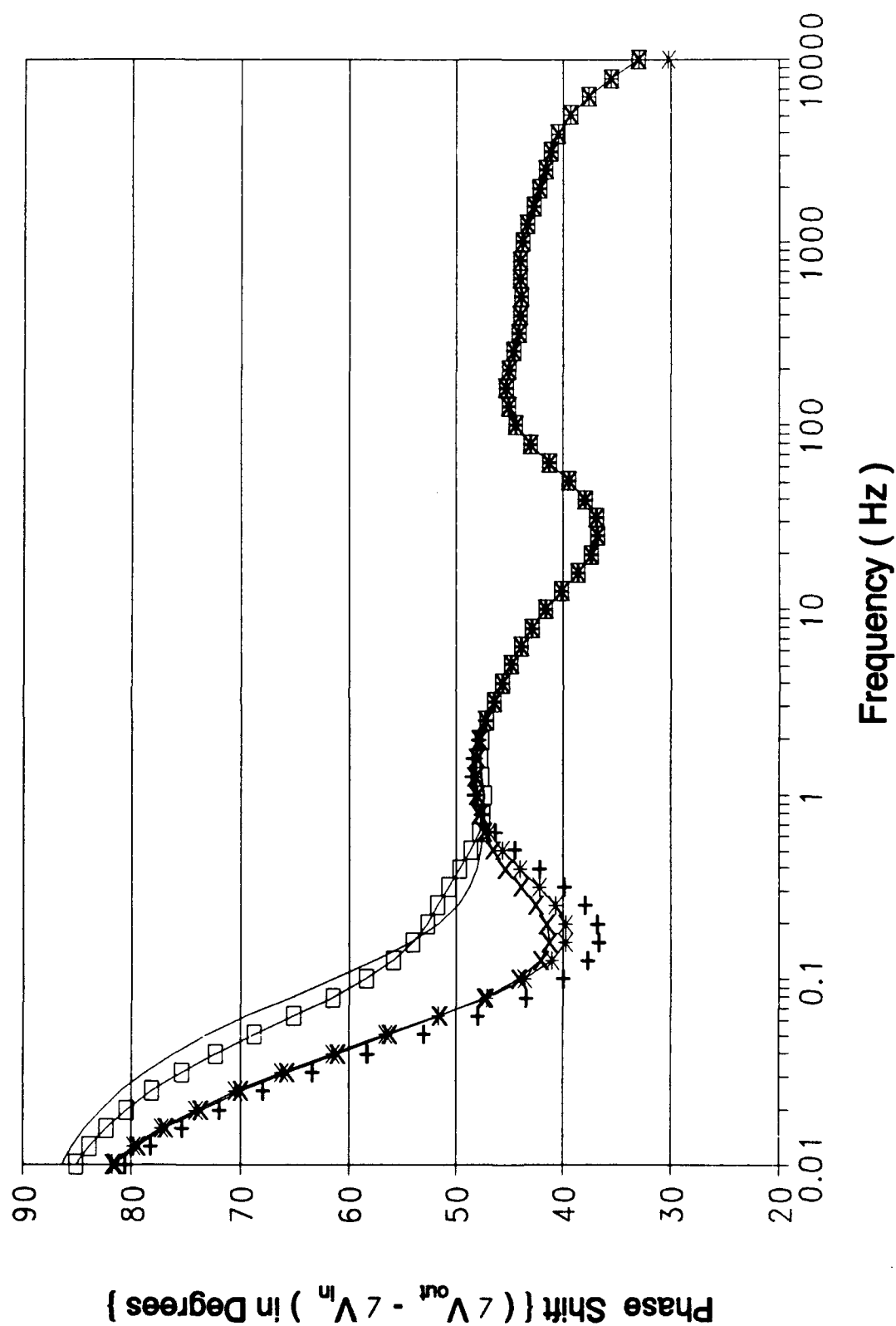Figure C-18 (cont). Gain Response of the Oldfield Circuit Design Using an HSPICE Computer Variation of Capacitor 9 (cont);
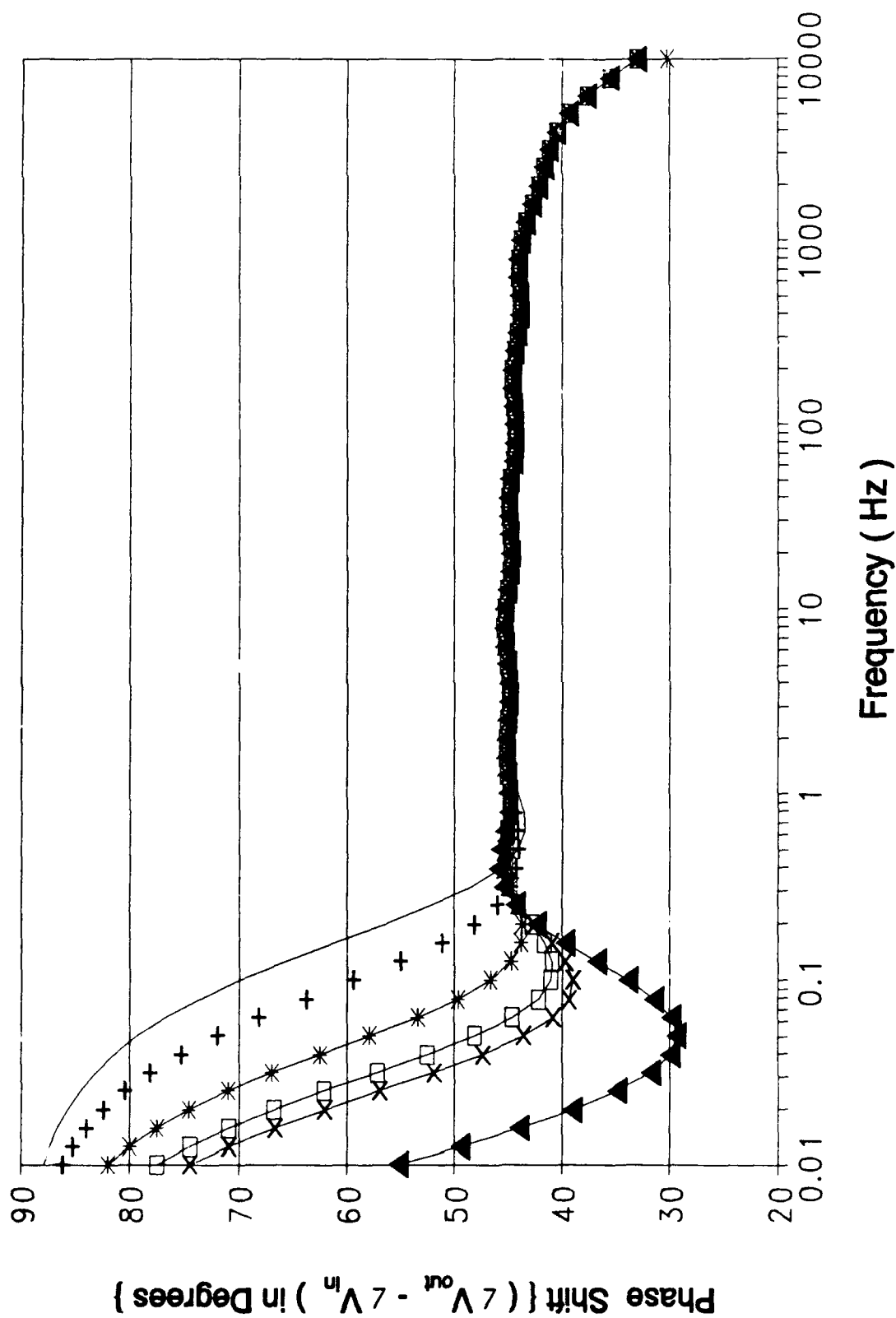
Figure C-18 (cont). Phase Response of the Oldfield Circuit Design Using an HSPICE Computer Variation of Capacitor 9.

Section 2

Oldfield Circuit Responses to Cell Component
(Resistor and Capacitor pairs) Value Variations

Resistor And Capacitor Values For Figure C-19					
Symbol	——	-+-	-*-	—▫—	—×—
Resis- tor Value (Ω)	226.4	73.35	96.04	331.2	119.7
Capac- itor Value (nF)	8.977	36.607	29.657	11.381	28.78

Figure C-19. Graphical Symbol Legend and Component Values
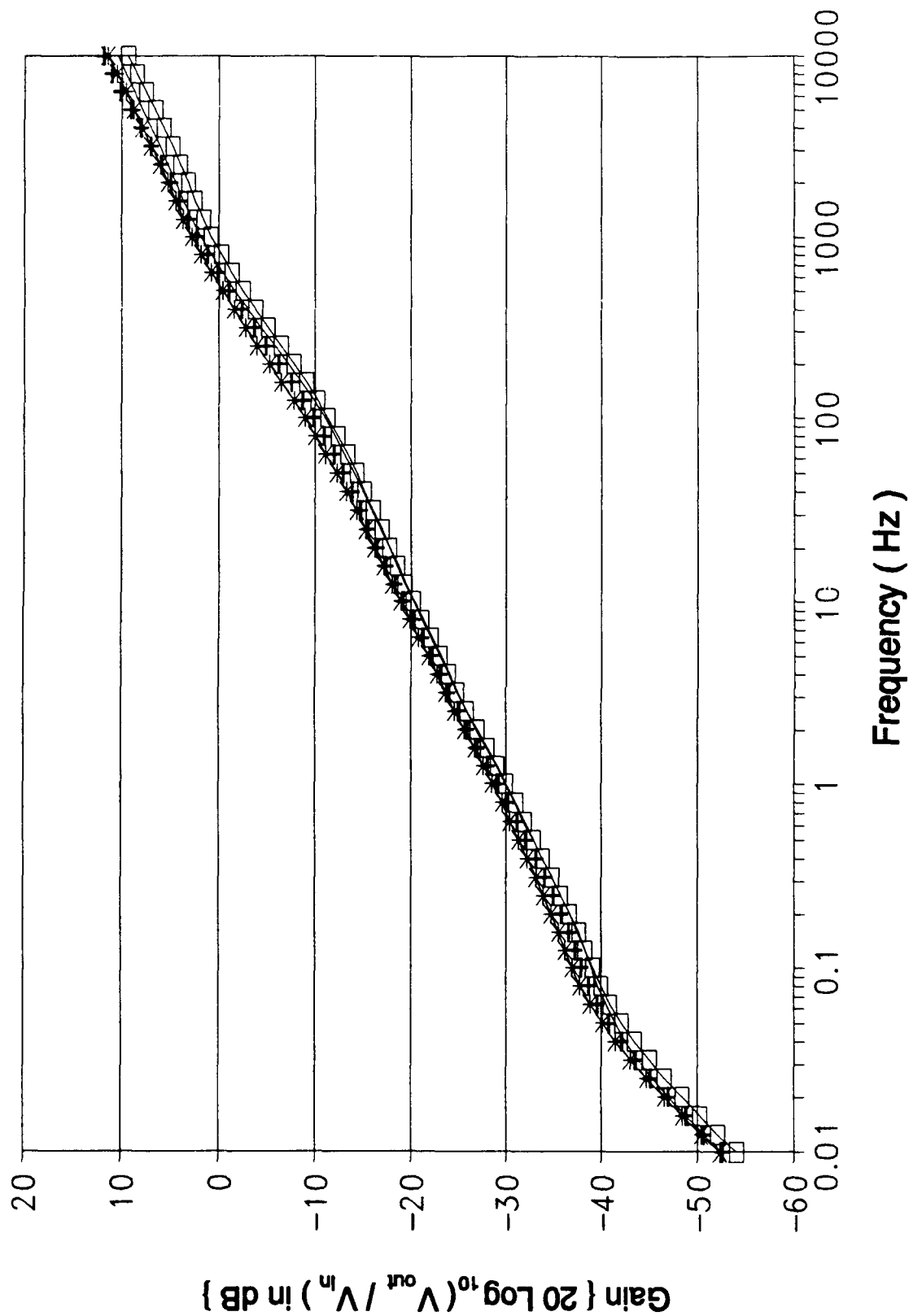**Corresponding to Figure C-19 (cont);**

Figure C-19 (cont). Gain Response of the Oldfield Circuit Design Using an HSPICE Computer Variation of Cell 1 (cont);

Figure C-19 (cont). Phase Response of the Oldfield Circuit Design Using an HSPICE Computer Variation of Cell 1.

Resistor And Capacitor Values For Figure C-20					
Symbol	——	-+-	-*-	-□-	-x-
Resis- tor Value (Ω)	791.5	256.4	335.8	1158	418.3
Capac- itor Value (nF)	19.179	78.205	63.358	24.313	61.498

Figure C-20. Graphical Symbol Legend and Component Values
Corresponding to Figure C-20 (cont);

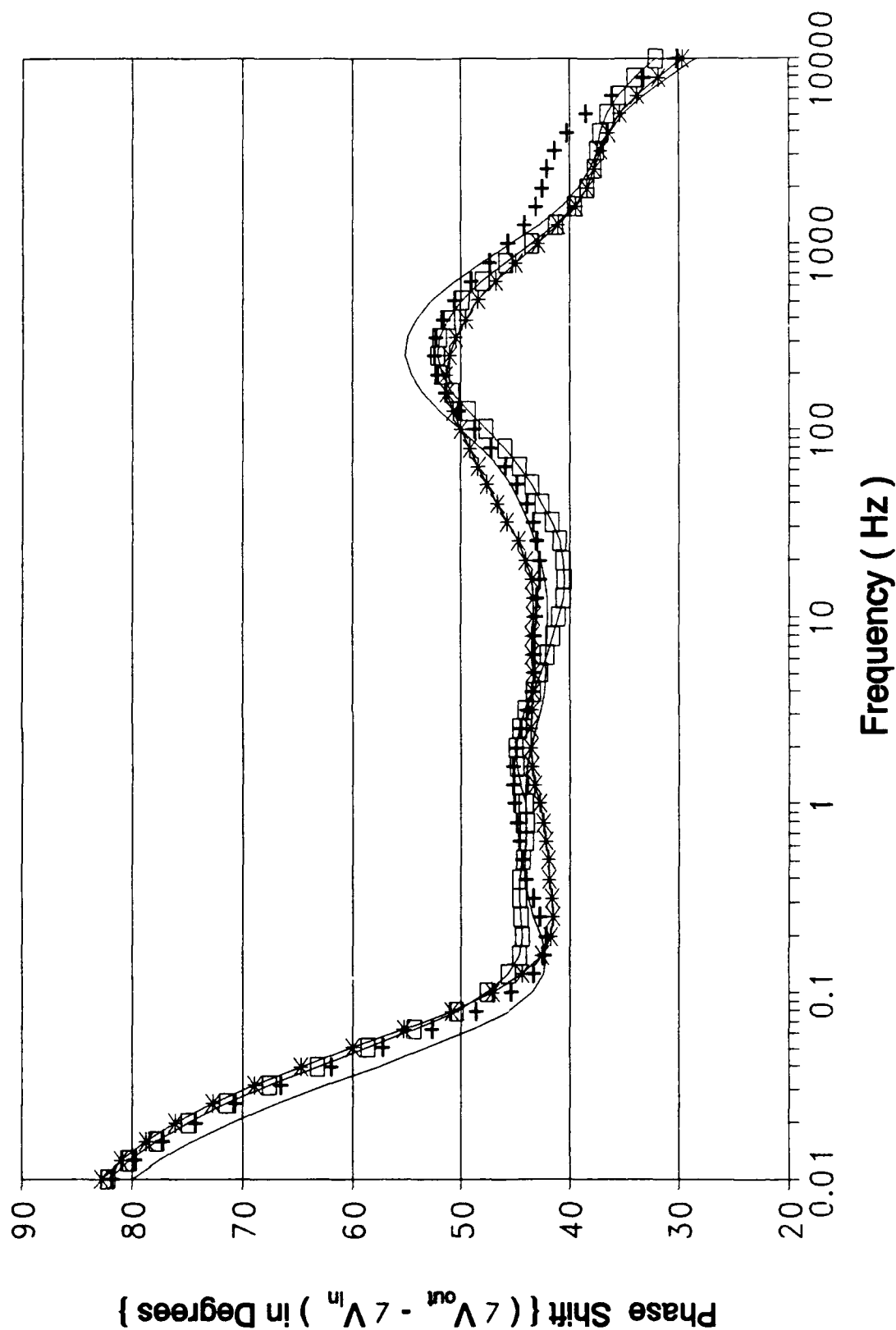Figure C-20 (cont). Gain Response of the Oldfield Circuit Design Using an HSPICE Computer Variation of Cell 2 (cont);

C-64

Frequency (Hz)

Phase Shift { ($\angle V_{out} - \angle V_{in}$) in Degrees }

Figure C-20 (cont). Phase Response of the Oldfield Circuit Design Using an HSPICE Computer Variation of Cell 2.

Resistor And Capacitor Values For Figure C-21					
Symbol	——	–+–	–*–	–□–	–×–
Resis-tor Value (Ω)	1650	534.4	699.8	2413	871.8
Capac-itor Value (nF)	40.807	166.39	134.8	51.73	130.85

**Figure C-21. Graphical Symbol Legend and Component Values
Corresponding to Figure C-21 (cont);**

Frequency (Hz)

Gain { 20 Log$_{10}$(V$_{out}$ / V$_{in}$) in dB }

Figure C-21 (cont). Gain Response of the Oldfield Circuit Design Using an HSPICE Computer Variation of Cell 3 (cont);

Figure C-21 (cont). Phase Response of the Oldfield Circuit Design Using an HSPICE Computer Variation of Cell 3.

C-68

Resistor And Capacitor Values For Figure C-22					
Symbol	——	—+—	—*—	—□—	—×—
Resis-tor Value (KΩ)	3.515	1.139	1.491	5.142	1.858
Capac-itor Value (nF)	89.725	366	296.6	113.8	287.8

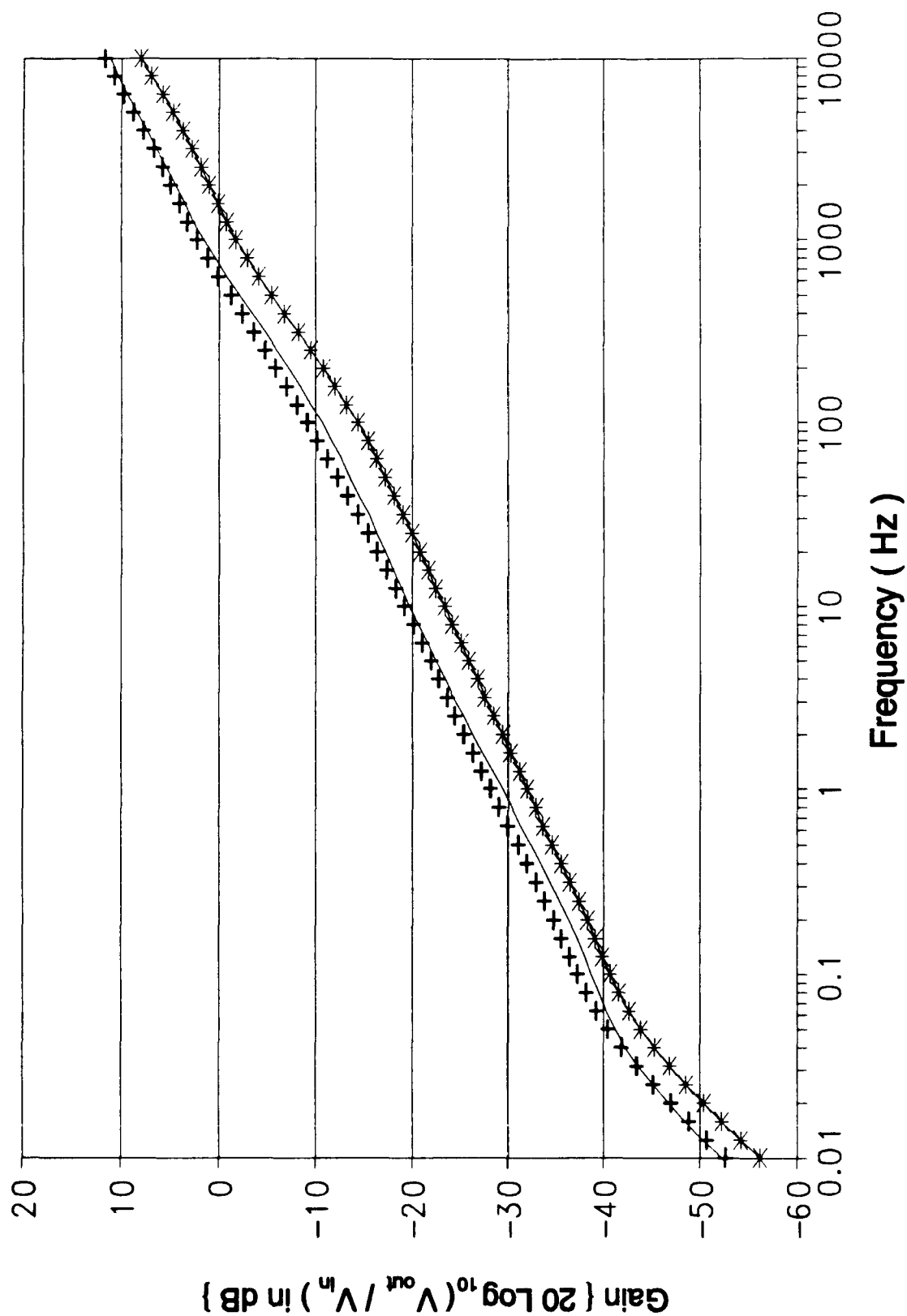**Figure C-22.** **Graphical Symbol Legend and Component Values Corresponding to Figure C-22 (cont);**

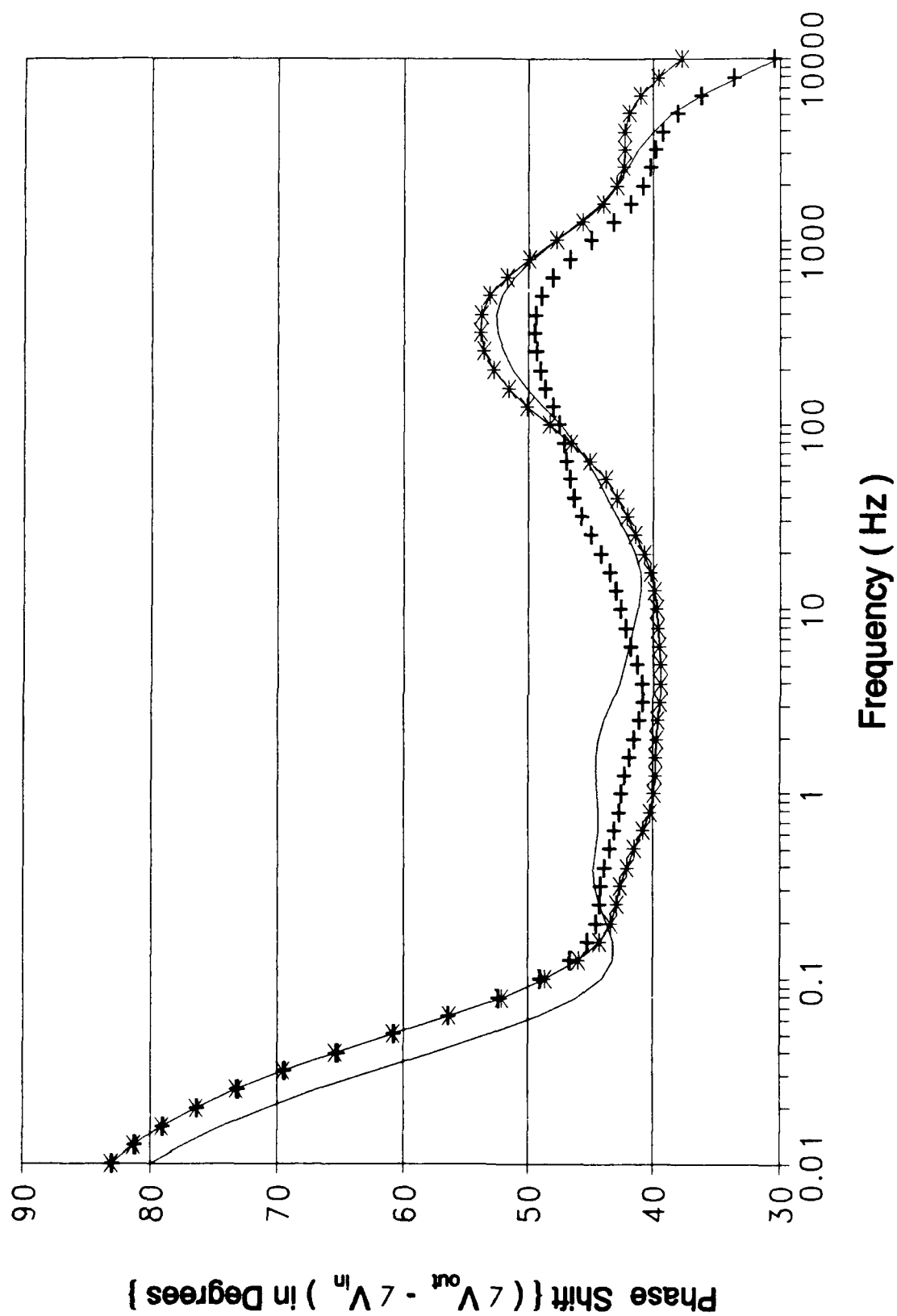Figure C-22 (cont). Gain Response of the Oldfield Circuit Design Using an HSPICE Computer Variation of Cell 4 (cont);

Figure C-22 (cont). Phase Response of the Oldfield Circuit Design Using an HSPICE Computer Variation of Cell 4.

Resistor And Capacitor Values For Figure C-23					
Symbol	──	─+─	─*─	─□─	─×─
Resis-tor Value (KΩ)	7.549	2.446	3.203	11.04	3.990
Capac-itor Value (nF)	191.79	782.05	633.5	243.13	614.98

Figure C-23. Graphical Symbol Legend and Component Values
Corresponding to Figure C-23 (cont);

Figure C-23 (cont). Gain Response of the Oldfield Circuit Design Using an HSPICE Computer Variation of Cell 5 (cont);

Figure C-23 (cont). Phase Response of the Oldfield Circuit Design Using an HSPICE Computer Variation of Cell 5.

Resistor And Capacitor Values For Figure C-24					
Symbol	——	-+-	-*-	—▫—	—×—
Resis- tor Value (KΩ)	3.907	5.715	12.66	20.65	16.58
Capac- itor Value (μF)	0.408	1.256	1.66	0.407	1.348

Figure C-24. Graphical Symbol Legend and Component Values
            Corresponding to Figure C-24 (cont);

Frequency (Hz)

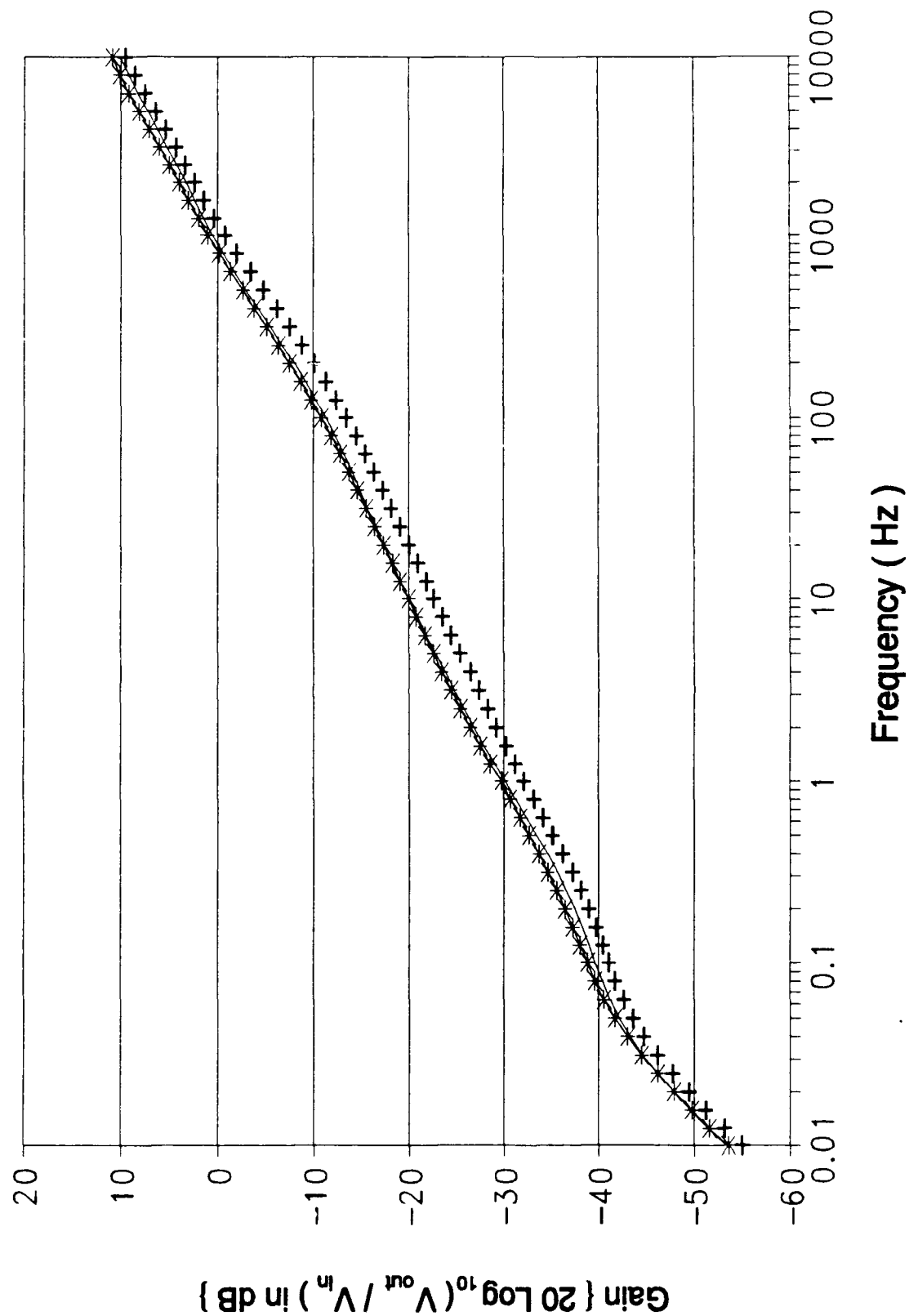Gain { 20 Log$_{10}$ (V$_{out}$ / V$_{in}$) in dB }

Figure C-24 (cont). Gain Response of the Oldfield Circuit Design Using an HSPICE Computer Variation of Cell 6 (cont);

Figure C-24 (cont). Phase Response of the Oldfield Circuit Design Using an HSPICE Computer Variation of Cell 6.

Resistor And Capacitor Values For Figure C-25					
Symbol	——	—+—	—*—	—□—	—×—
Resistor Value (KΩ)	32.064	20.486	22.203	39.99	23.989
Capacitor Value (μF)	1.476	3.011	2.625	1.61	2.577

Figure C-25. Graphical Symbol Legend and Component Values Corresponding to Figure C-25 (cont);

Figure C-25 (cont). Gain Response of the Oldfield Circuit Design Using an HSPICE Computer Variation of Cell 7 (cont);

Figure C-25 (cont). Phase Response of the Oldfield Circuit Design Using an HSPICE Computer Variation of Cell 7.

Resistor And Capacitor Values For Figure C-26					
Symbol	——	–+–	–*–	–□–	–×–
Resis- tor Value (KΩ)	75.9	24.69	32.213	111	40.132
Capac- itor Value (μF)	1.917	7.8205	6.33	2.43	6.1498

**Figure C-26. Graphical Symbol Legend and Component Values
Corresponding to Figure C-26 (cont);**

Figure C-26 (cont). Gain Response of the Oldfield Circuit Design Using an HSPICE Computer Variation of Cell 8 (cont);

Figure C-26 (cont). Phase Response of the Oldfield Circuit Design Using an HSPICE Computer Variation of Cell 8.

C-83

Resistor And Capacitor Values For Figure C-27					
Symbol	——	–+–	–*–	–□–	–×–
Resistor Value (MΩ)	162.8	52.75	69.07	238.1	86.05
Capacitor Value (μF)	4.08	16.63	13.48	5.17	13.08

Figure C-27. Graphical Symbol Legend and Component Values Corresponding to Figure C-27 (cont);

Figure C-27 (cont). Gain Response of the Oldfield Circuit Design Using an HSPICE Computer Variation of Cell 9 (cont);

C-85

Figure C-27 (cont). Phase Response of the Oldfield Circuit Design Using an HSPICE Computer Variation of Cell 9.

Section 3

Oldfield Circuit Responses for "All-Cell" Component Values Varied by $\pm$ 20 Percent Variations

Resistor and Capacitor Values for Figure C-28.1 and Graphical Symbol ——		
Cell Number	Resistor (KΩ)	Capacitor (nF)
1	0.1905	19.106
2	0.547	53.934
3	1.177	107.73
4	7.128	196.40
5	5.560	502.22
6	15.678	1089.0
7	30.877	2030.0
8	68.214	4817.0
9	138.69	11202.0

Figure C-28.1.   Graphical Symbol Legend and Component Values
Corresponding to Figure C-28.1 (cont);

Resistor and Capacitor Values for Figure C-28.1 and Graphical Symbol +		
Cell Number	Resistor (KΩ)	Capacitor (nF)
1	0.2061	24.973
2	0.5545	50.866
3	1.442	115.69
4	5.969	209.65
5	5.992	532.86
6	13.882	878.27
7	26.445	1868.4
8	67.739	4801.4
9	122.99	9719.1

Figure C-28.1. Graphical Symbol Legend and Component Values Corresponding to Figure C-28.1 (cont);

Resistor and Capacitor Values for Figure C-28.1 and Graphical Symbol -*-		
Cell Number	Resistor (KΩ)	Capacitor (nF)
1	0.2159	23.284
2	0.6413	55.802
3	1.144	114.41
4	4.941	184.77
5	6.971	447.02
6	12.34	993.85
7	30.555	2187.4
8	58.286	5372.0
9	122.12	8491.7

Figure C-28.1. Graphical Symbol Legend and Component Values Corresponding to Figure C-28.1 (cont);

Resistor and Capacitor Values for Figure C-28.1 and Graphical Symbol -□-		
Cell Number	Resistor (MΩ)	Capacitor (nF)
1	0.1687	20.334
2	0.6236	50.929
3	1.059	115.97
4	5.552	187.95
5	4.986	560.62
6	11.346	107.88
7	26.988	182.44
8	51.518	507.62
9	143.36	992.05

Figure C-28.1. Graphical Symbol Legend and Component Values Corresponding to Figure C-28.1 (cont);

Figure C-28.1 (cont). Gain Response of the Oldfield Circuit Design Using an HSPICE Computer Variation of All Cells (cont);

Figure C-28.1. Phase Response of the Oldfield Circuit Design Using an HSPICE Computer Variation of All Cells.

C-93

Resistor and Capacitor Values for Figure C-28.2 and Graphical Symbol ──		
Cell Number	Resistor (KΩ)	Capacitor (nF)
1	0.1985	21.736
2	0.528	47.189
3	1.391	95.358
4	5.830	216.41
5	6.206	444.38
6	12.478	1066.40
7	32.014	1951.1
8	64.742	4708.2
9	150.79	11381.0

Figure C-28.2. Graphical Symbol Legend and Component Values Corresponding to Figure C-28.2 (cont);

Resistor and Capacitor Values for Figure C-28.2 and Graphical Symbol +		
Cell Number	Resistor (KΩ)	Capacitor (nF)
1	0.2113	22.7
2	0.5234	43.056
3	1.213	110.12
4	4.847	233.50
5	6.940	399.74
6	12.974	1139.0
7	26.315	2525.2
8	65.323	5117.5
9	144.92	8028.3

Figure C-28.2. Graphical Symbol Legend and Component Values Corresponding to Figure C-28.2 (cont);

Resistor and Capacitor Values for Figure C-28.2 and Graphical Symbol -*-		
Cell Number	Resistor (KΩ)	Capacitor (nF)
1	0.1446	20.992
2	0.7195	40.622
3	1.283	90.196
4	7.111	199.78
5	6.966	507.47
6	15.322	1146.7
7	28.131	2320.8
8	52.284	4602.8
9	142.01	8261.5

Figure C-28.2. Graphical Symbol Legend and Component Values Corresponding to Figure C-28.2 (cont);

Figure C-28.2 (cont). Gain Response of the Oldfield Circuit Design Using an HSPICE Computer Variation of All Cells (cont);

C-97

Figure C-28.2 (cont). Phase Response of the Oldfield Circuit Design Using an HSPICE Computer Variation of All Cells.

Resistor and Capacitor Values for Figure C-28.3 and Graphical Symbol ——		
Cell Number	Resistor (KΩ)	Capacitor (nF)
1	0.183	23.399
2	0.7283	52.352
3	1.553	99.541
4	5.864	248.38
5	5.562	554.6
6	13.369	95.644
7	32.166	176.19
8	71.678	383.21
9	125.91	1125.3

Figure C-28.3. Graphical Symbol Legend and Component Values Corresponding to Figure C-28.3 (cont);

Resistor and Capacitor Values for Figure C-28.3 and Graphical Symbol +		
Cell Number	Resistor (KΩ)	Capacitor (nF)
1	0.1484	25.961
2	0.6247	48.277
3	1.362	80.758
4	6.426	258.69
5	7.175	472.66
6	15.183	1074.0
7	33.768	2155.8
8	64.683	4032.4
9	118.90	11099.0

Figure C-28.3. Graphical Symbol Legend and Component Values Corresponding to Figure C-28.3 (cont);

Resistor and Capacitor Values for Figure C-28.3 and Graphical Symbol -*-		
Cell Number	Resistor (KΩ)	Capacitor (nF)
1	0.1882	21.493
2	0.5269	49.166
3	1.559	99.366
4	5.480	245.0
5	6.35043	484.96
6	12.91	1134.4
7	29.049	1790.7
8	68.479	5320.6
9	149.47	8680.2

Figure C-28.3. Graphical Symbol Legend and Component Values Corresponding to Figure C-28.3 (cont);

Figure C-28.3 (cont). Gain Response of the Oldfield Circuit Design Using an HSPICE Computer Variation of All Cells (cont);
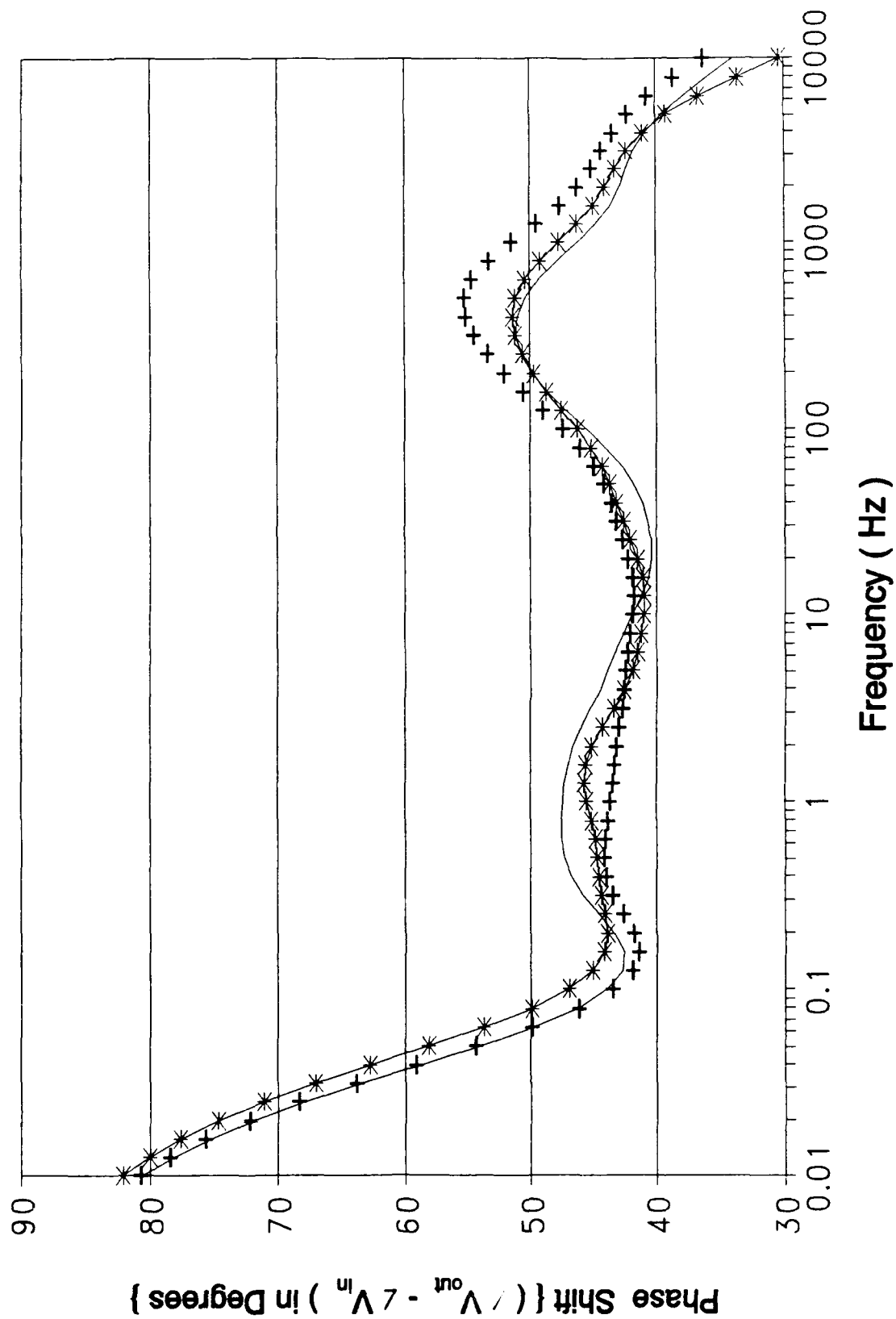
Figure C-28.3. Phase Response of the Oldfield Circuit Design Using an Hspice Computer Variation of All Cells (cont);

Frequency (Hz)

Phase Shift { (∠V_out − ∠V_in) in Degrees }

Section 4

Oldfield Circuit HSPICE Baseline Simulatior Deck

```
******     h s p i c e

Half-order Differentiator Oldfield/Hughes Design

****** copyright 1990 meta-software,inc.
****site:air_force_institute
******  input listing                    evaluation expires
920415
******
* hspice.ini
.options post=2
.param biasc1=aunif(22n,4.4n)
+ biasr1=aunif(180.2,36.04)
+ biasc2=aunif(47n,9.4n)
+ biasr2=aunif(630,126)
+ biasc3=aunif(100n,20n)
+ biasr3=aunif(1.313k,.2626k)
+ biasc4=aunif(220n,44n)
+ biasr4=aunif(2.798k,.5596k)
+ biasc5=aunif(470n,94n)
+ biasr5=aunif(6.009k,1.2018k)
+ biasc6=aunif(1u,.2u)
+ biasr6=aunif(13.11k,2.622k)
+ biasc7=aunif(2.2u,.44u)
+ biasr7=aunif(28.57k,5.714k)
+ biasc8=aunif(4.7u,.94u)
+ biasr8=aunif(60.44k,12.088k)
+ biasc9=aunif(10u,2u)
+ biasr9=aunif(129.6k,25.92k)
.ac dec 10 .01 10meghz sweep monte=10 $bias poi 6 .1 .4 1
1.6 2 5
* circuit with 9 cells
* second opamp added to compensate for time response
* opamp added
*vbias vbias gnd +15v
vcc vcc gnd +15v
vee vee gnd -15v
c1 1 2 biasc1 $22n
r1 2 gnd biasr1 $180.2
c2 1 3 biasc2 $47n
r2 2 3 biasr2 $630
c3 1 4 biasc3 $100n
r3 3 4 biasr3 $1.313k
c4 1 5 biasc4 $220n
r4 4 5 biasr5 $2.798k
c5 1 6 biasc5 $470n
r5 5 6 biasr5 $6.009k
c6 1 7 biasc6 $1u
r6 6 7 biasr6 $13.11k
```

```
c7 1 8 biasc7 $2.2u
r7 7 8 biasr7 $28.57k
c8 1 9 biasc8 $4.7u
r8 8 9 biasr8 $60.44k
c9 1 10 biasc9 $10u
r9 9 10 biasr9 $129.6k
*opamp for feedback response
.tran 50u 2ms sweep monte=10 $bias poi 6 .1 .4 1.0 1.6 2 5

x741 2 out out  vcc vee alm741
*opamp for lowpass and amplification
ramp1 out in 15.915k
camp1 in gnd .1n
x2741 neg in out2 vcc vee alm741
ramp2 neg gnd 17.683k
ramp3 neg out2 159.15k

vin 1 gnd ac 10 0 sin(0 10 500)

*.print ac  vdb(out,1)
*.print ac vp(out,1)
.print ac vdb(out2,1)
.print ac vp(out2,1)
.print v(1)
.print v(out2)
.end
```

Appendix D

Oldham And Oldfield Discrete Component Value

Variation Versus Frequency

Results

The measured discrete component values versus frequency are presented in this appendix. The results are documented in four sections. The first two sections document the variation of the component values versus frequency for the Oldham discrete circuit design option. Section 1 reports the resistor values, and Section 2 reports the capacitor values. Correspondingly, Sections 3 and 4 document the resistor and capacitor value variations for the Oldfield discrete circuit option.

Section 1

Oldham Discrete Resistor Component Value

Variations Versus Frequency

Results
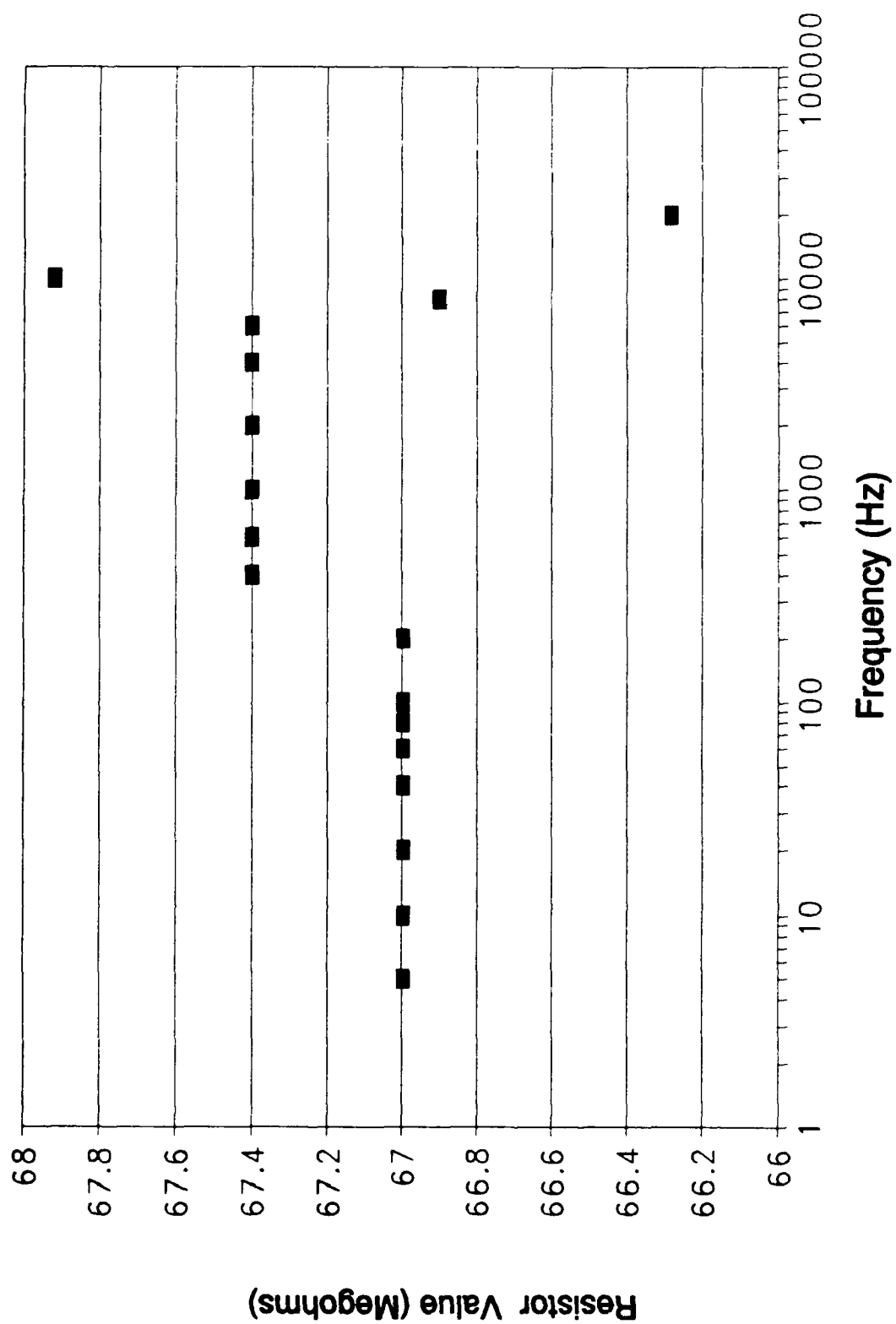
Figure D-1. Oldham Circuit Design -- the Value of
Resistor R0 versus Frequency
(Ideal Value -- 68.99 Megohms).
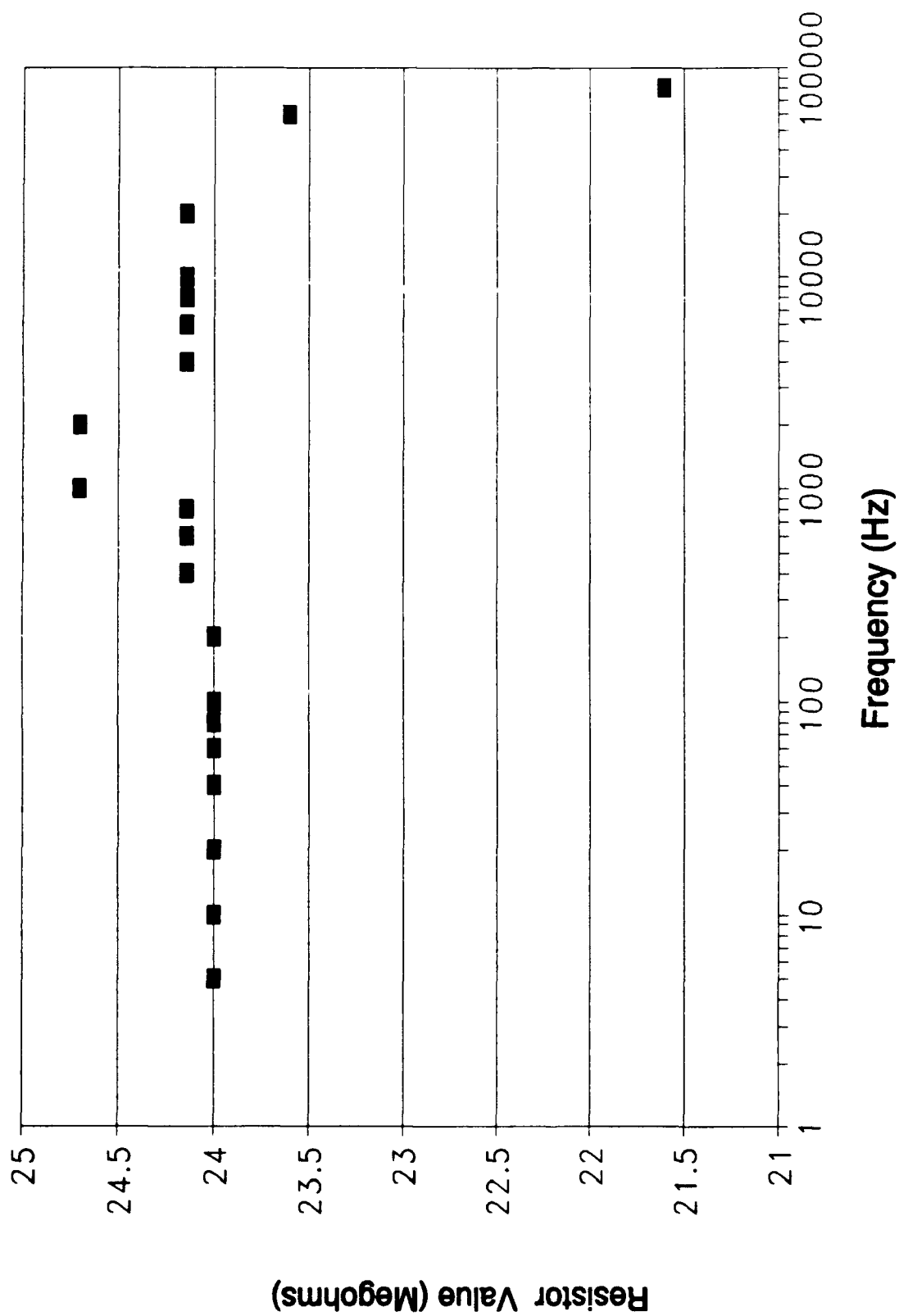
Figure D-2. Oldham Circuit Design -- the Value of
Resistor R1 versus Frequency.
(Ideal Value -- 25.4 Megohms)
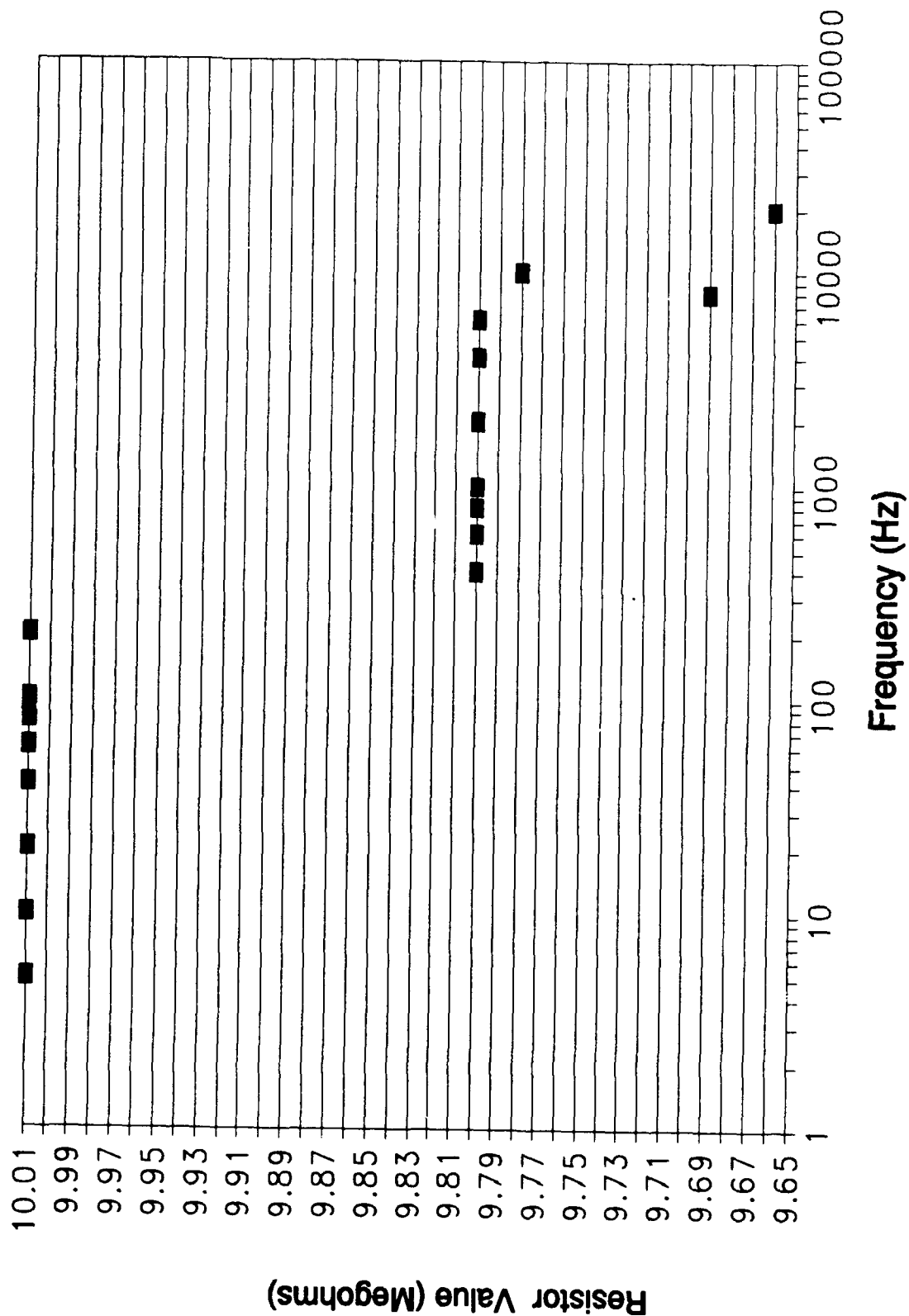
Figure D-3.   Oldham Circuit Design -- the Value of
Resistor R2 versus Frequency
(Ideal Value -- 9.85 Megohms).
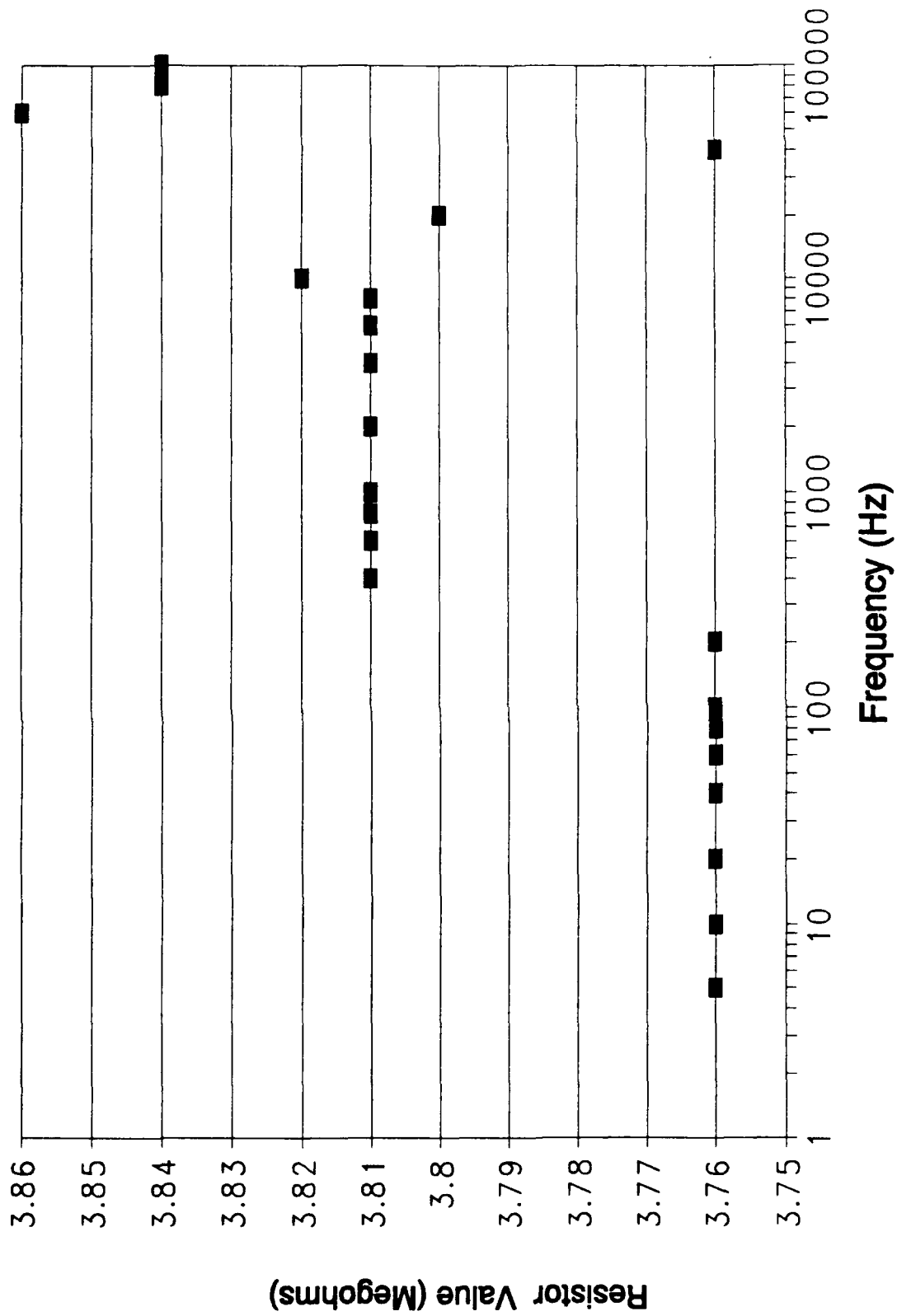
Figure D-4. Oldham Circuit Design -- the Value of Resistor R3 versus Frequency (Ideal Value -- 3.83 Megohms).
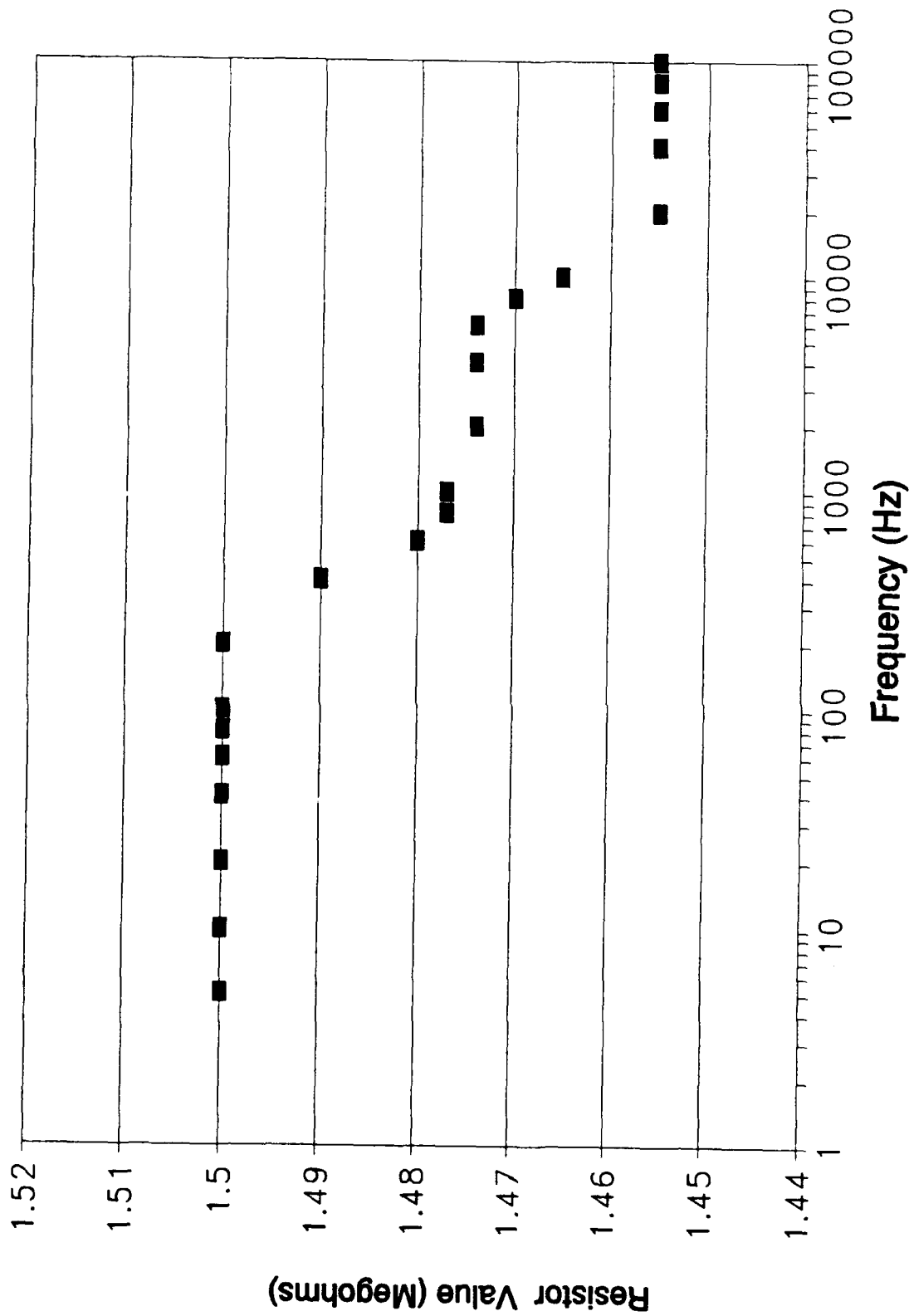
Figure D-5. Oldham Circuit Design -- the Value of Resistor R4 versus Frequency (Ideal Value -- 1.488 Megohms).
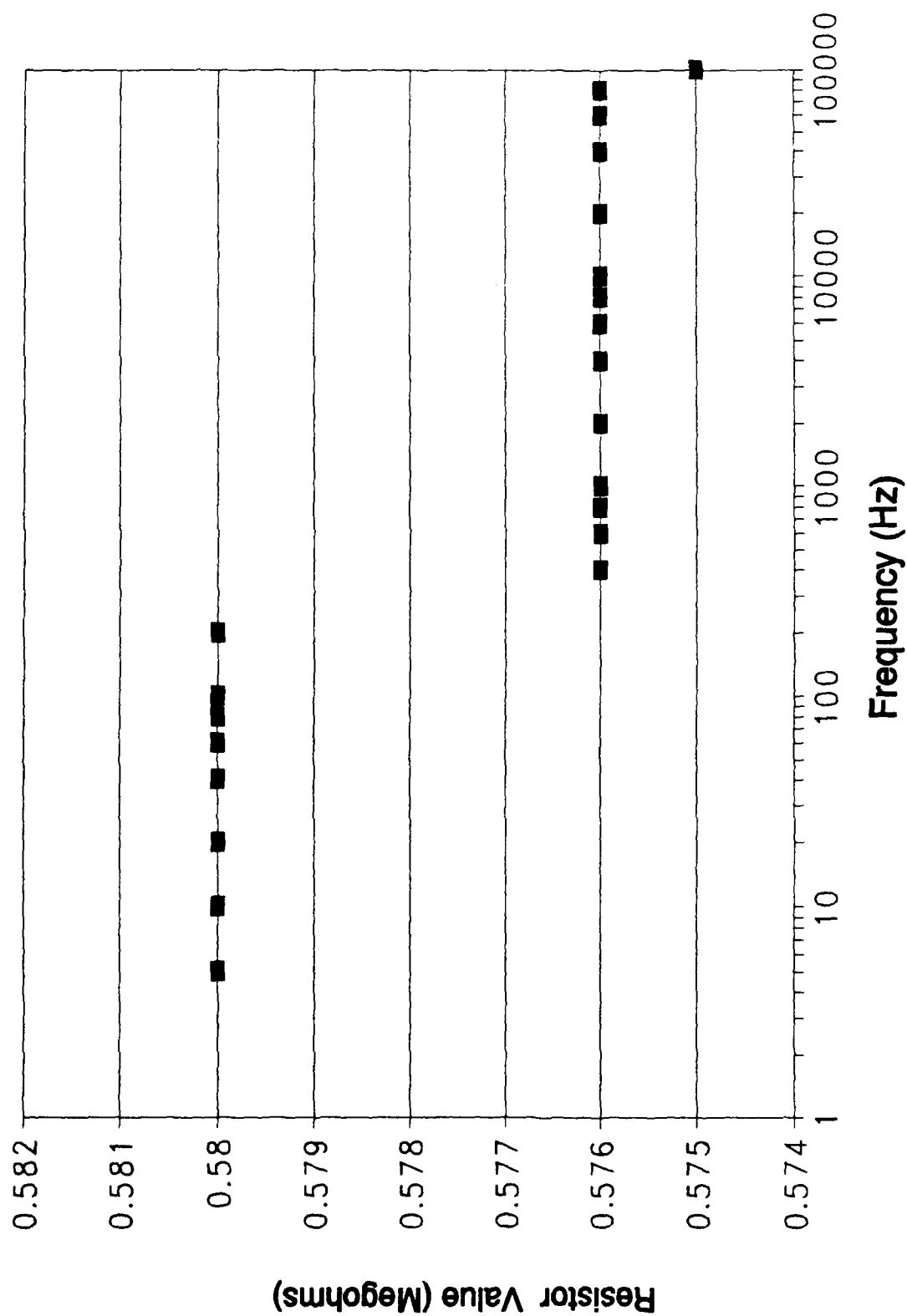
Figure D-6. Oldham Circuit Design -- the Value of Resistor R5 versus Frequency (Ideal Value -- 0.5785 Megohms).
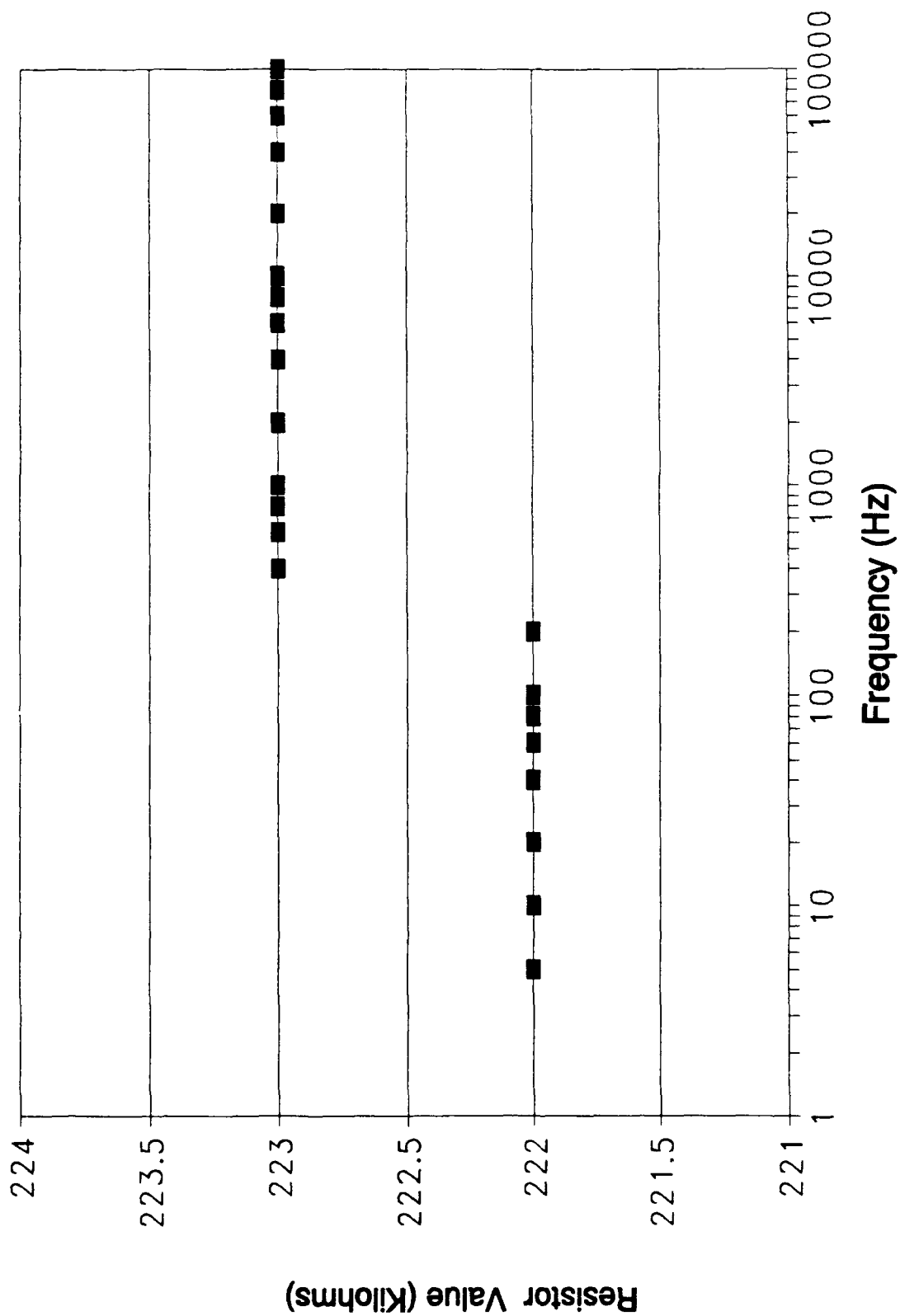
Figure D-7. Oldham Circuit Design -- the Value of Resistor R6 versus Frequency (Ideal Value -- 224.9 Kilohms).
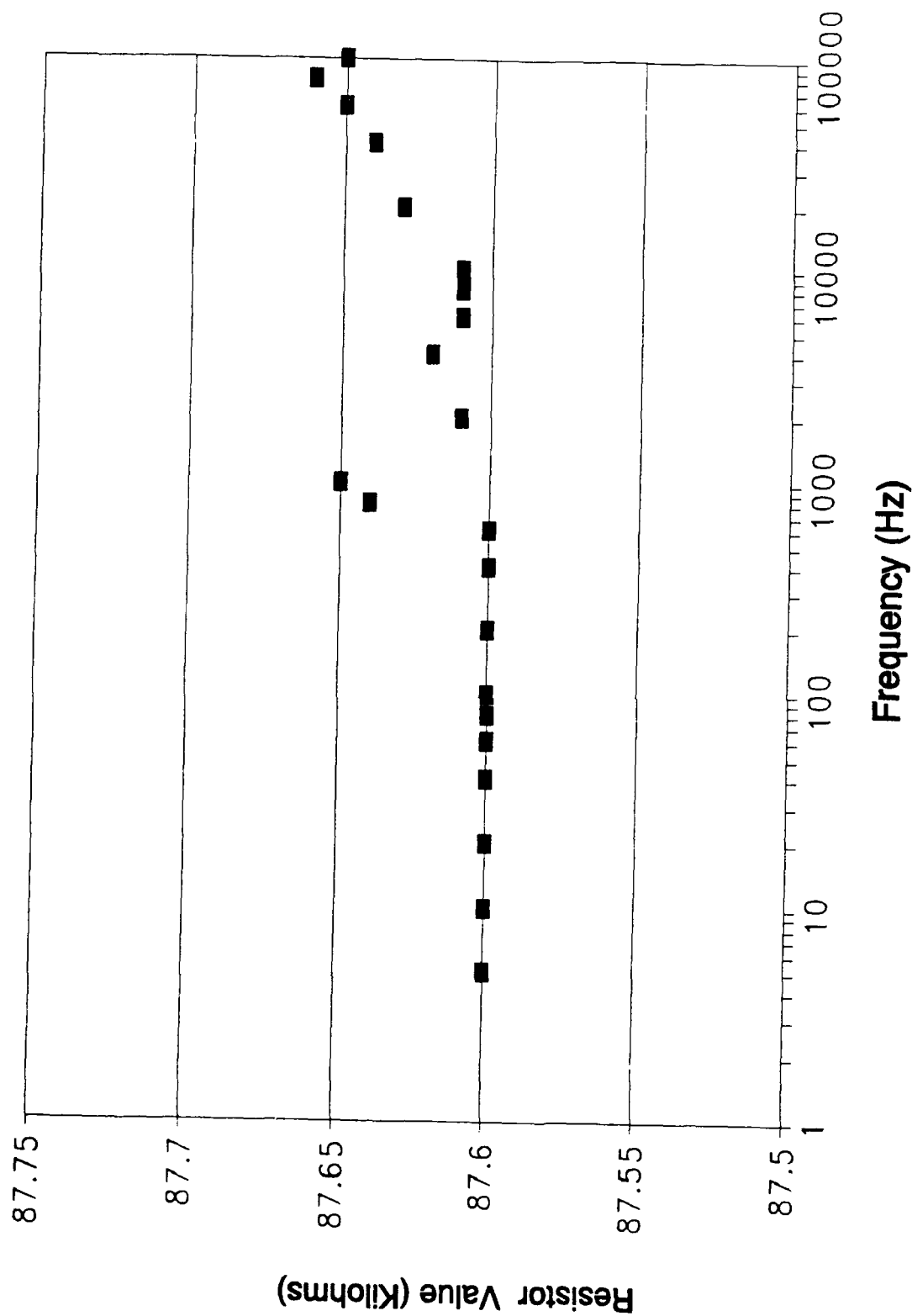
Figure D-8. Oldham Circuit Design -- the Value of Resistor R7 versus Frequency (Ideal Value -- 87.4 Kilohms).
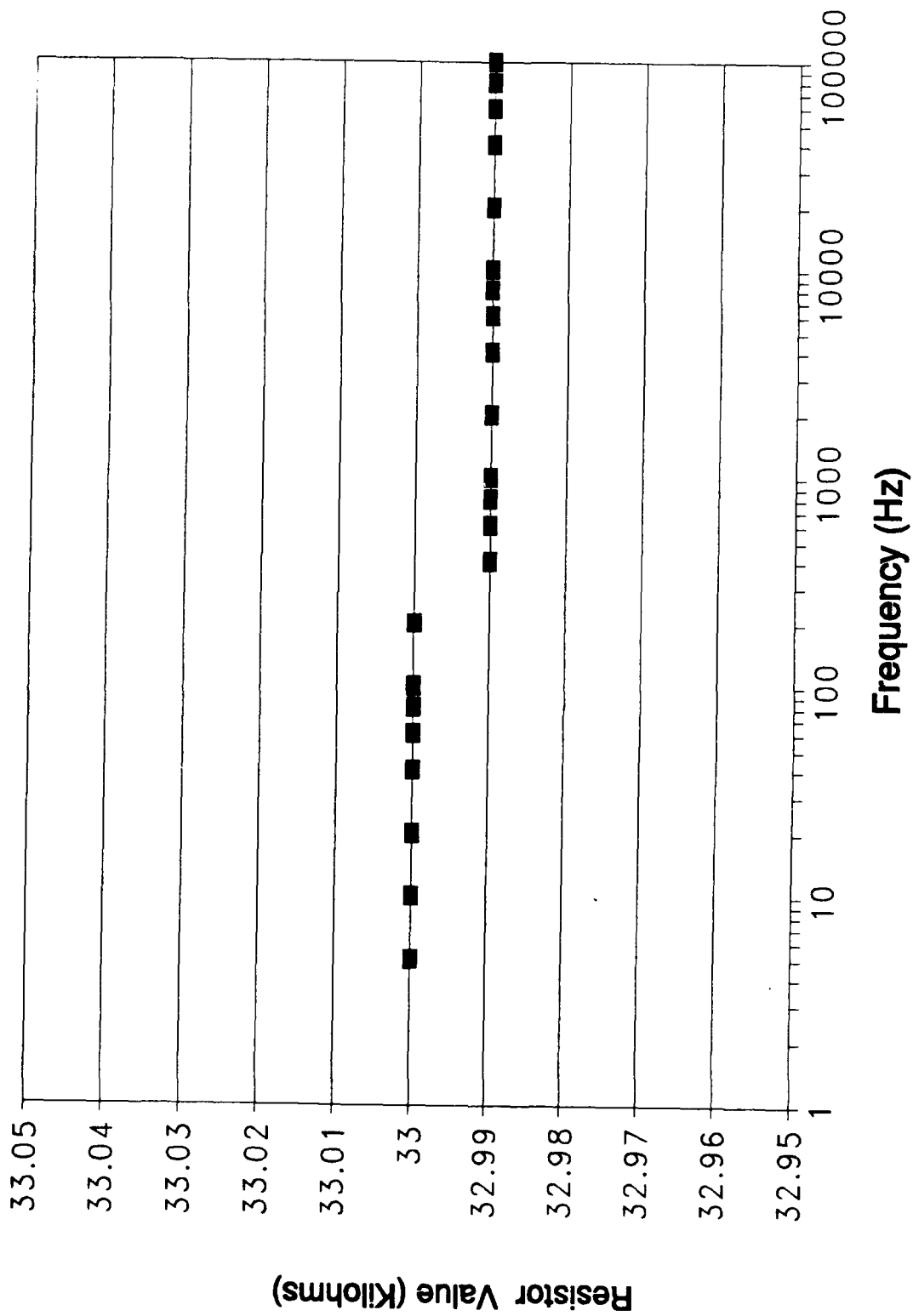
Figure D-9.   Oldham Circuit Design -- the Value of
Resistor R8 versus Frequency
(Ideal Value -- 33.97 Kilohms).
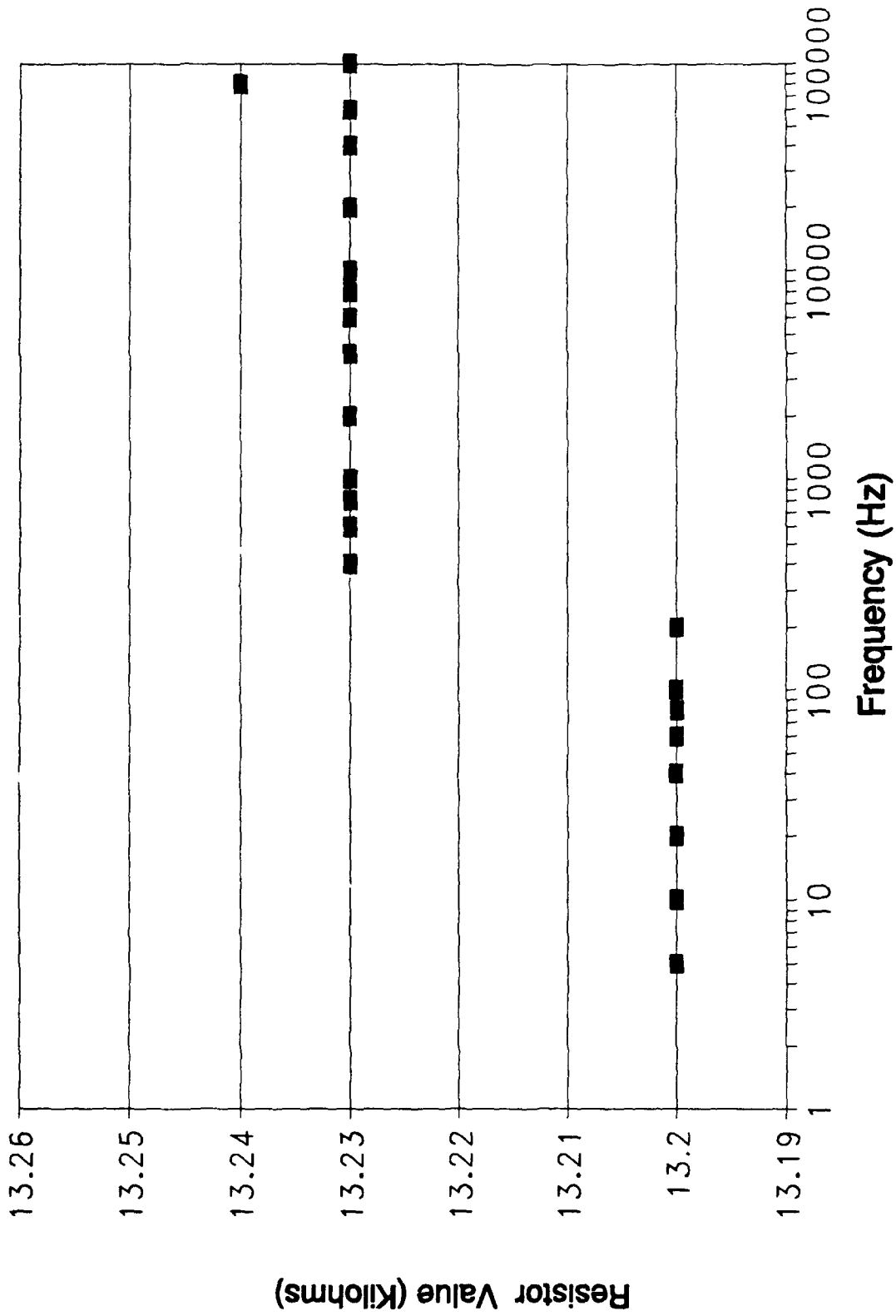
Figure D-10. Oldham Circuit Design -- the Value of Resistor R9 versus Frequency (Ideal Value -- 13.21 Kilohms).
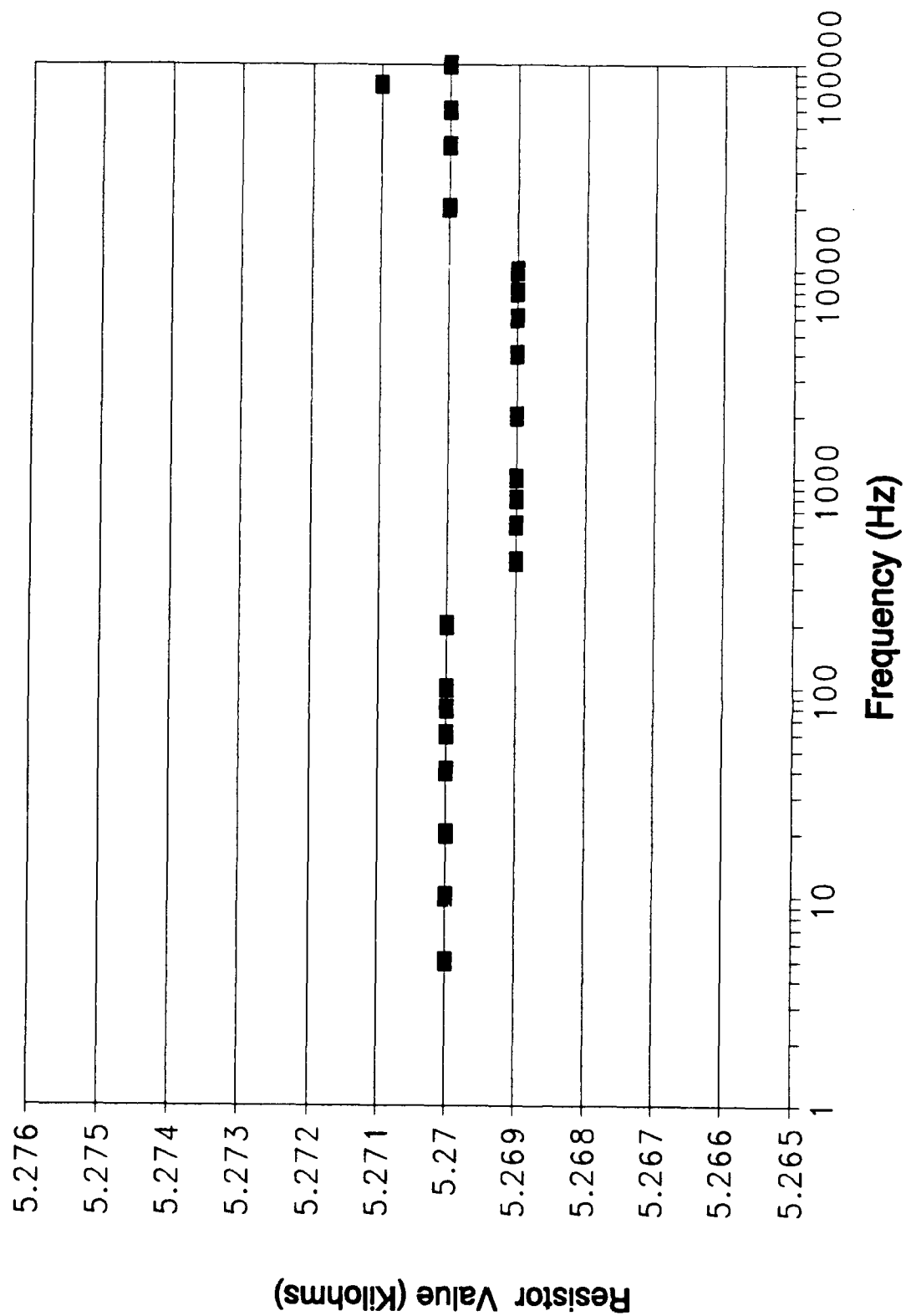
Figure D-11. Oldham Circuit Design -- the Value of Resistor R10 versus Frequency (Ideal Value -- 5.133 Kilohms).
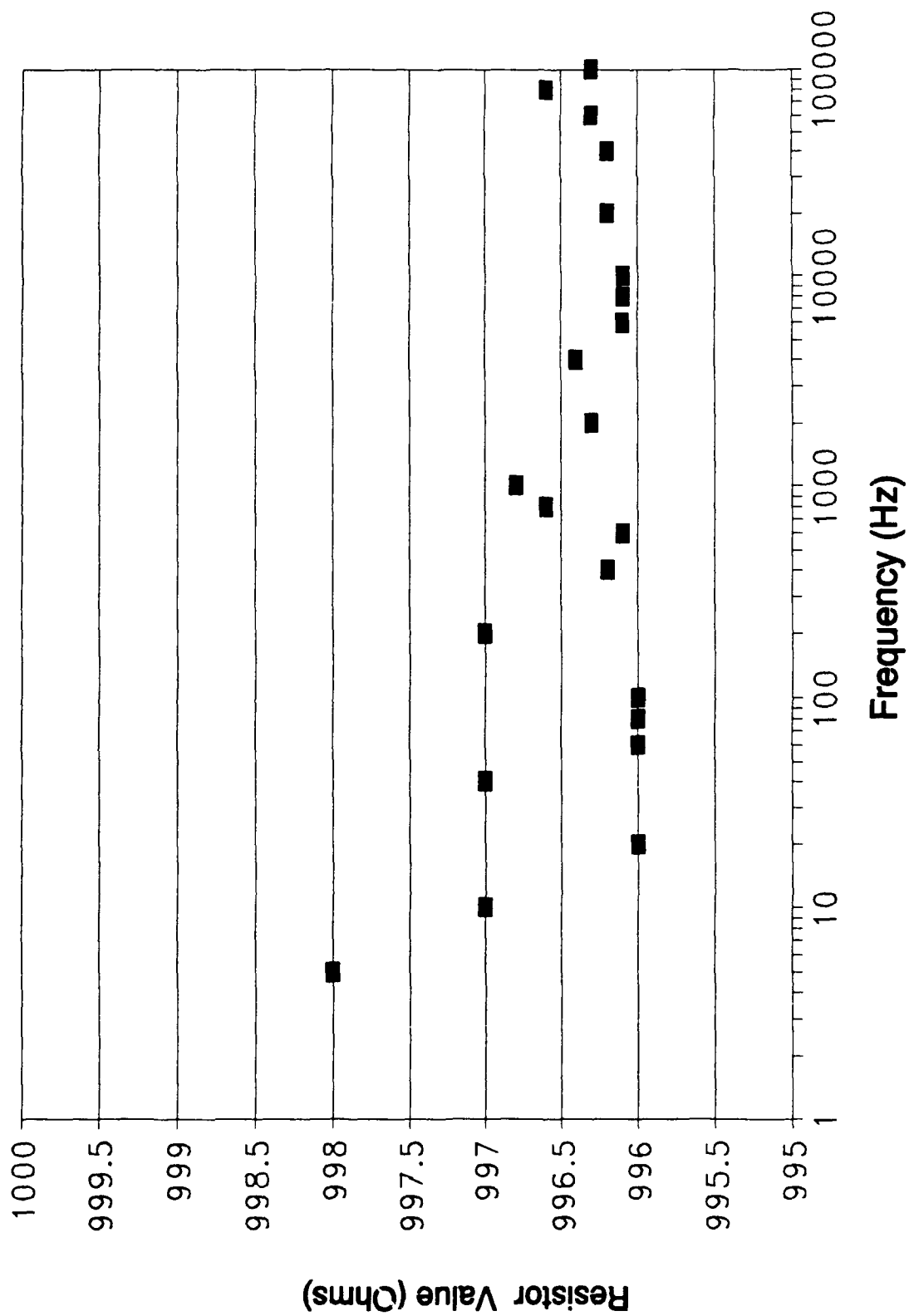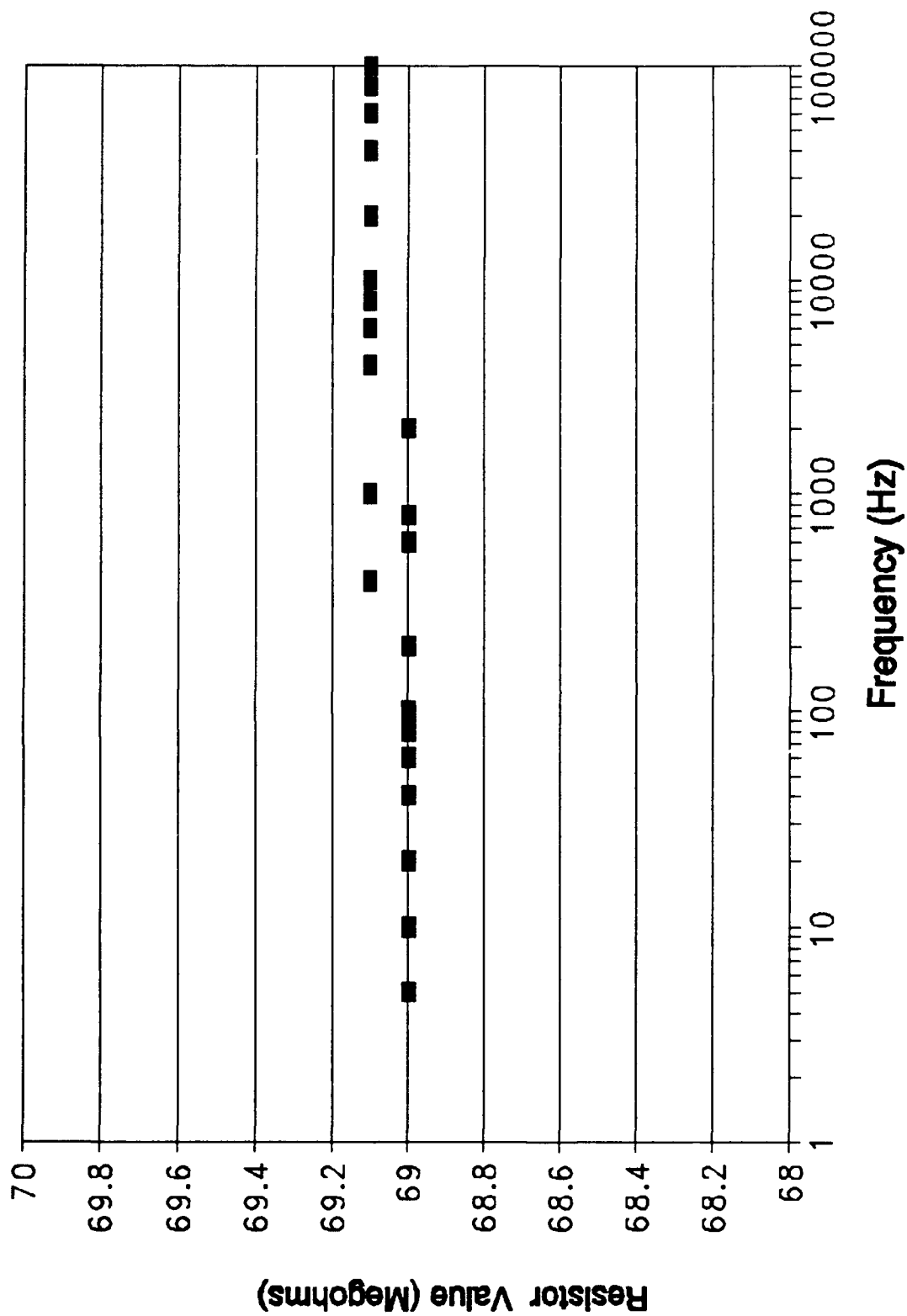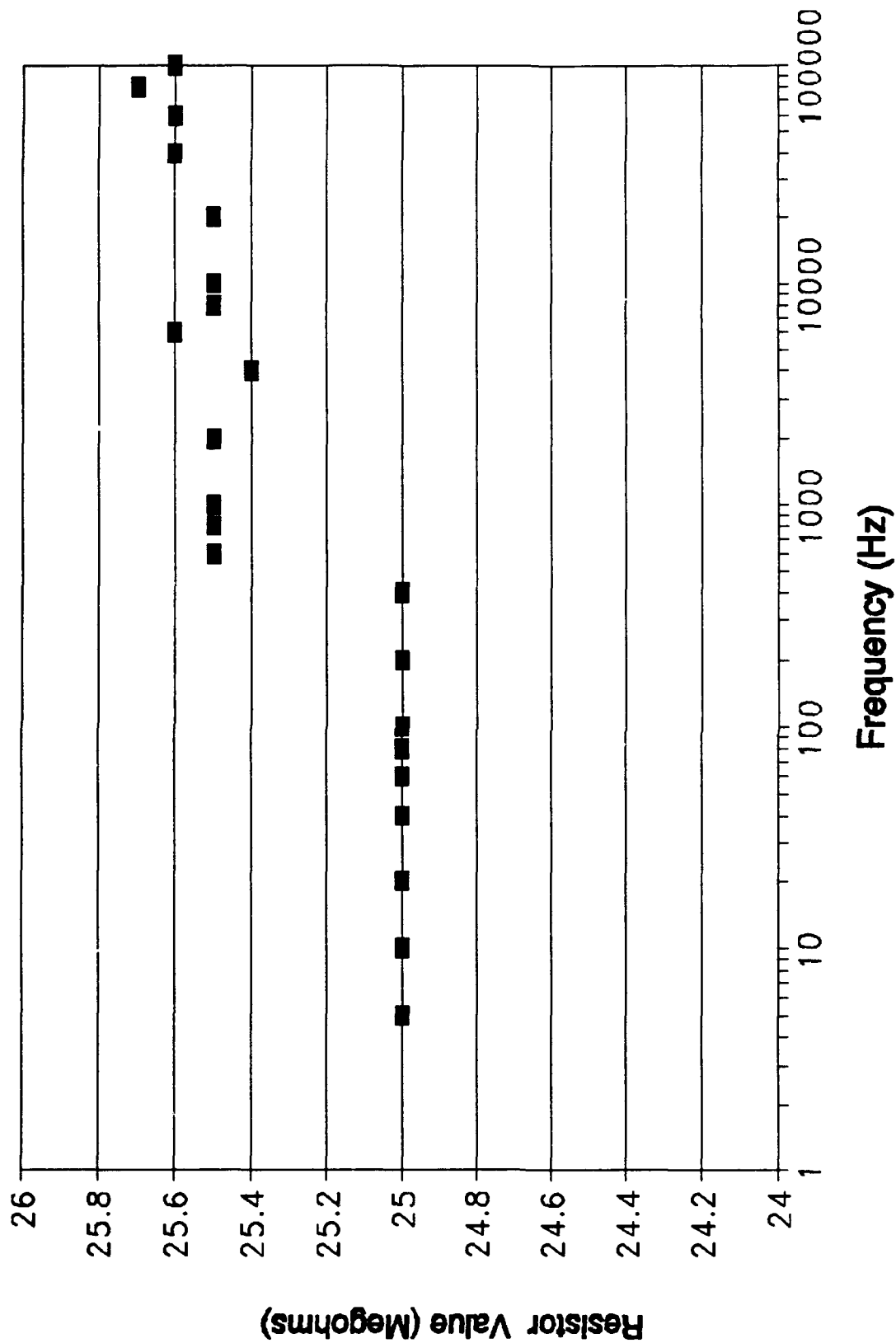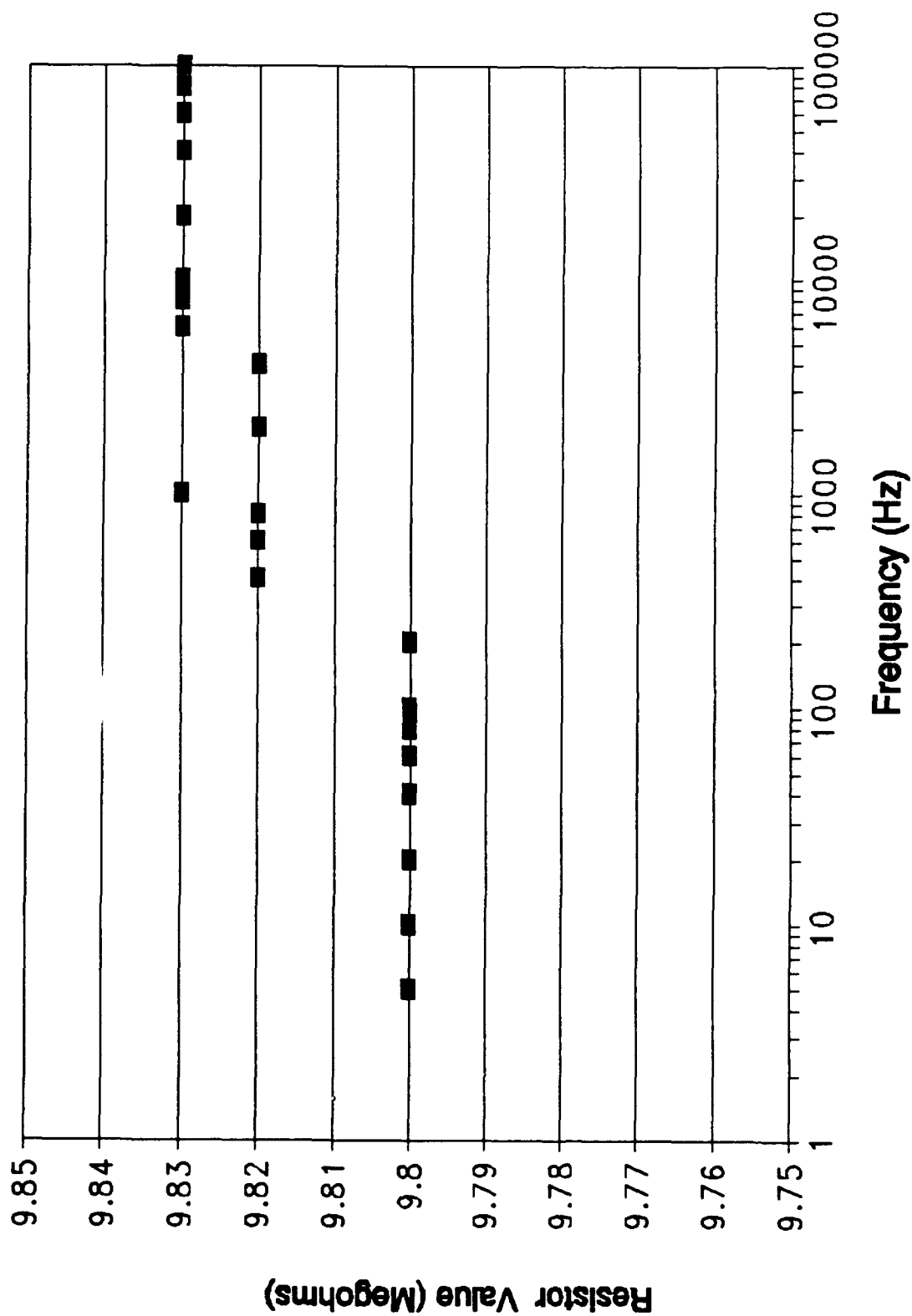
Figure D-12. Oldham Circuit Design -- the Value of Resistor R11 versus Frequency (Ideal Value -- 997.5 Ohms).
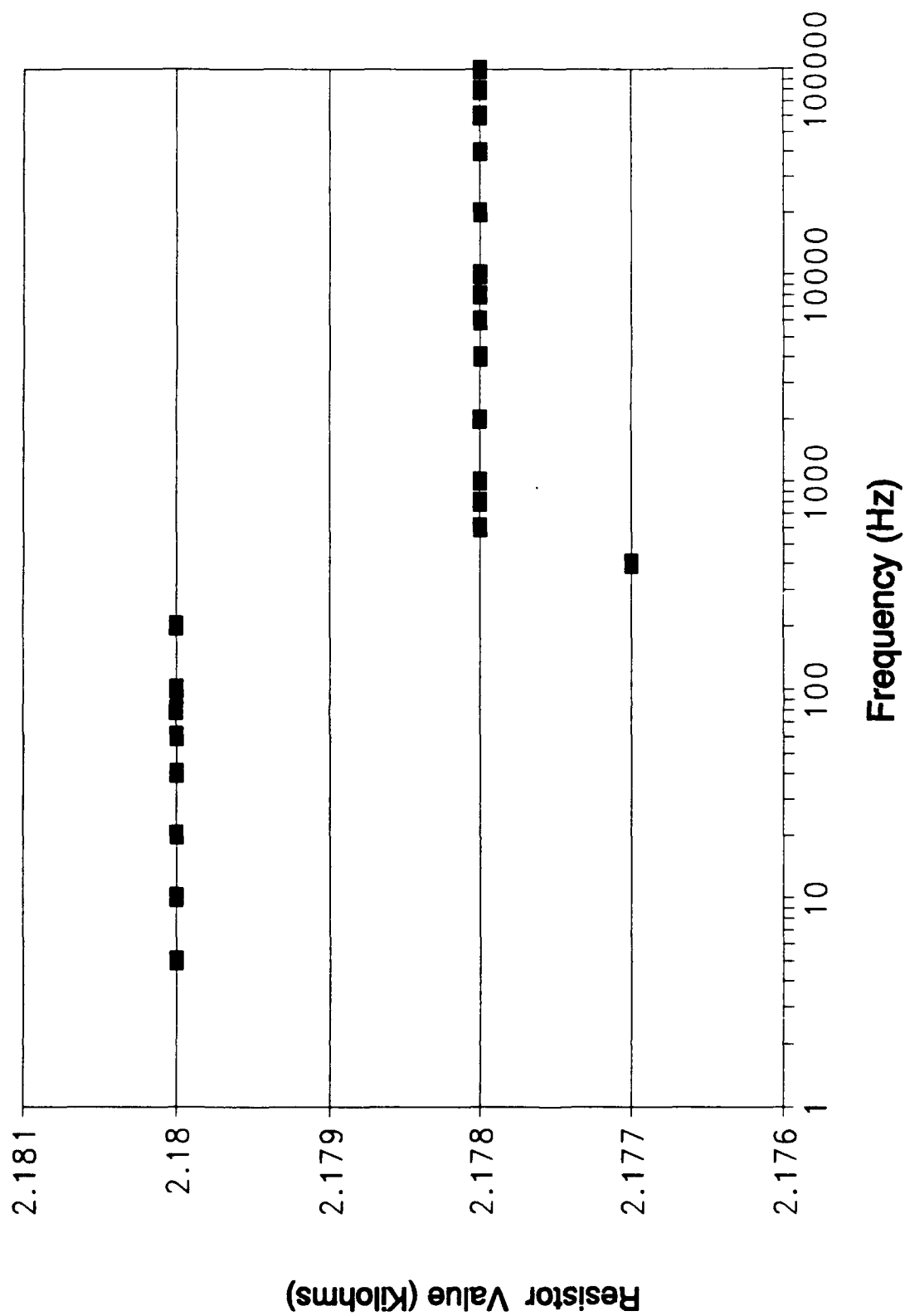
Figure D-13. Oldham Circuit Design -- the Value of Resistor R12 versus Frequency (Ideal Value -- 2.11 Kilohms).

Section 2

Oldham Discrete Capacitor Component Values

Variations Versus Frequency

Results

D-17
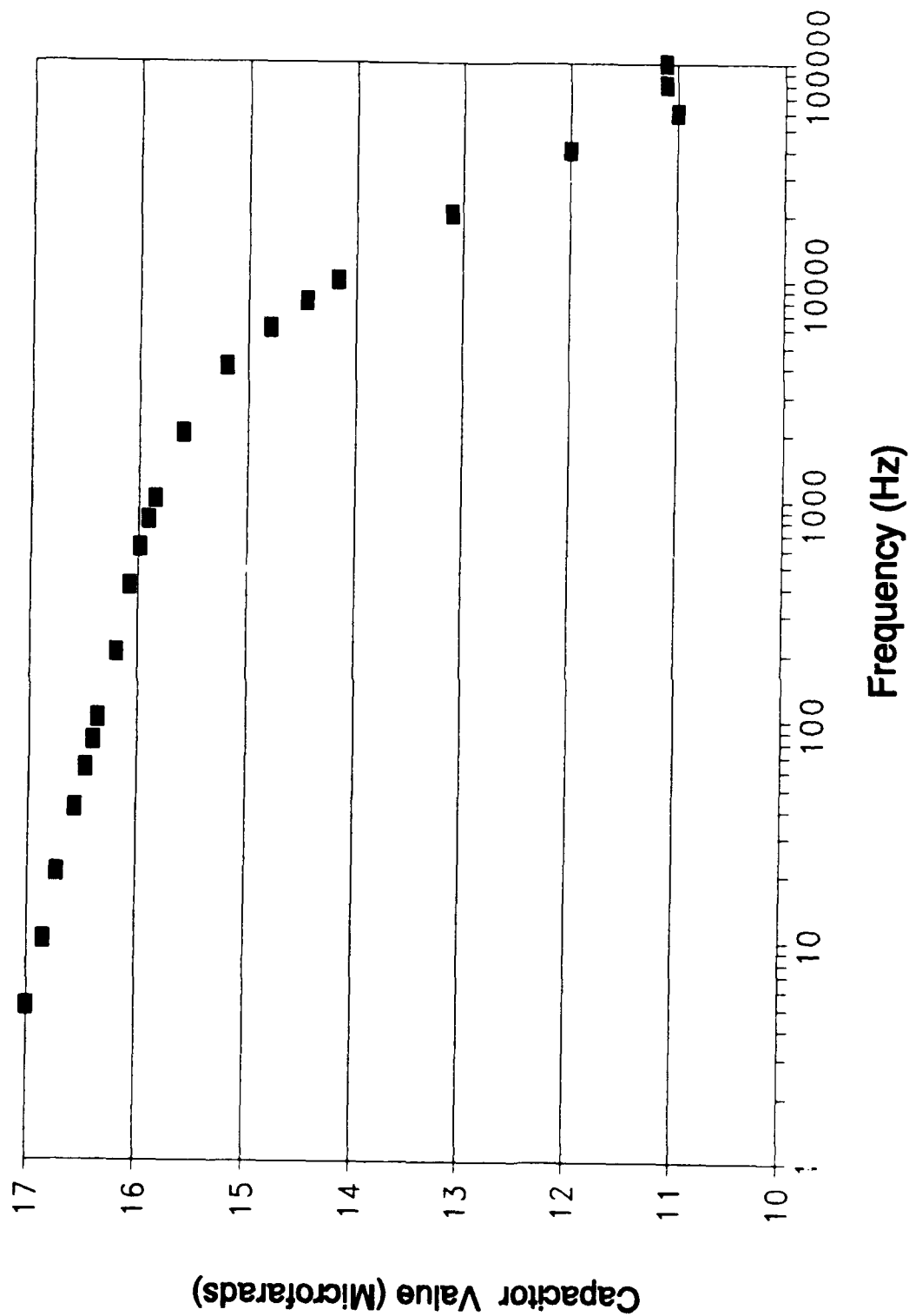
Figure D-14. Oldham Circuit Design -- of the Value of Capacitor CO versus Frequency (Ideal Value -- 16.51 µf).
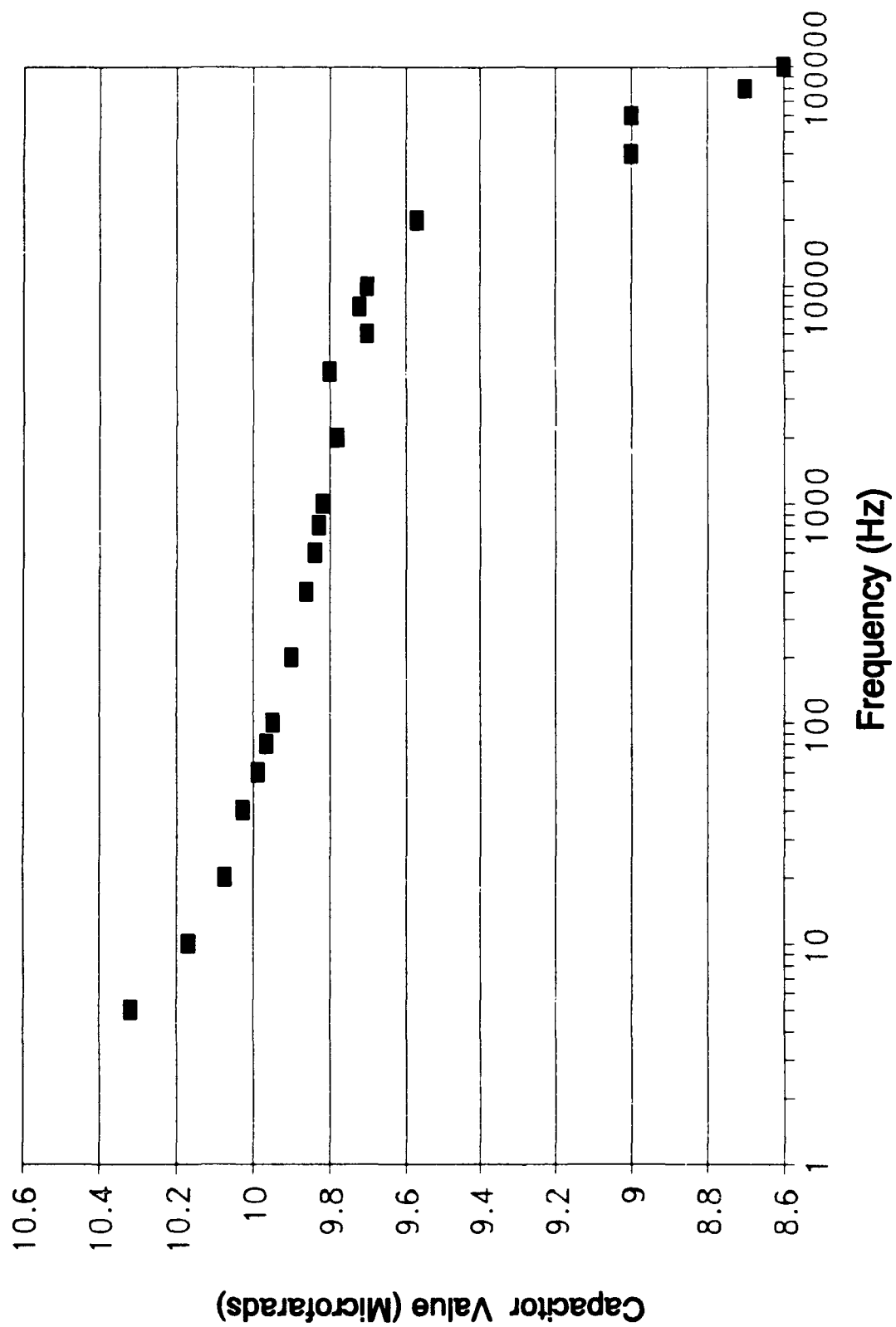
Figure D-15. Oldham Circuit Design -- the Value of Capacitor C1 versus Frequency (Ideal Value -- 10.0 μf).
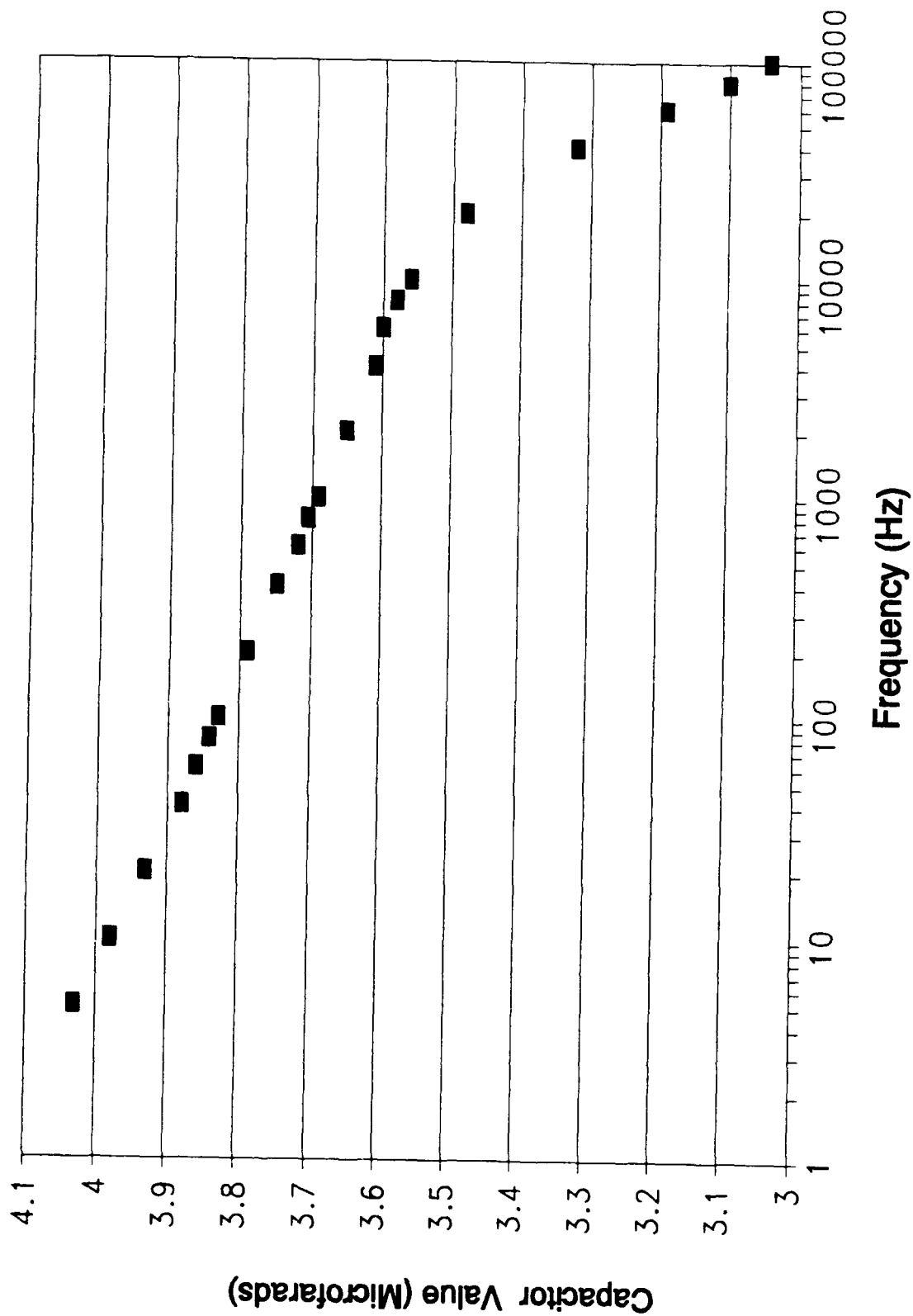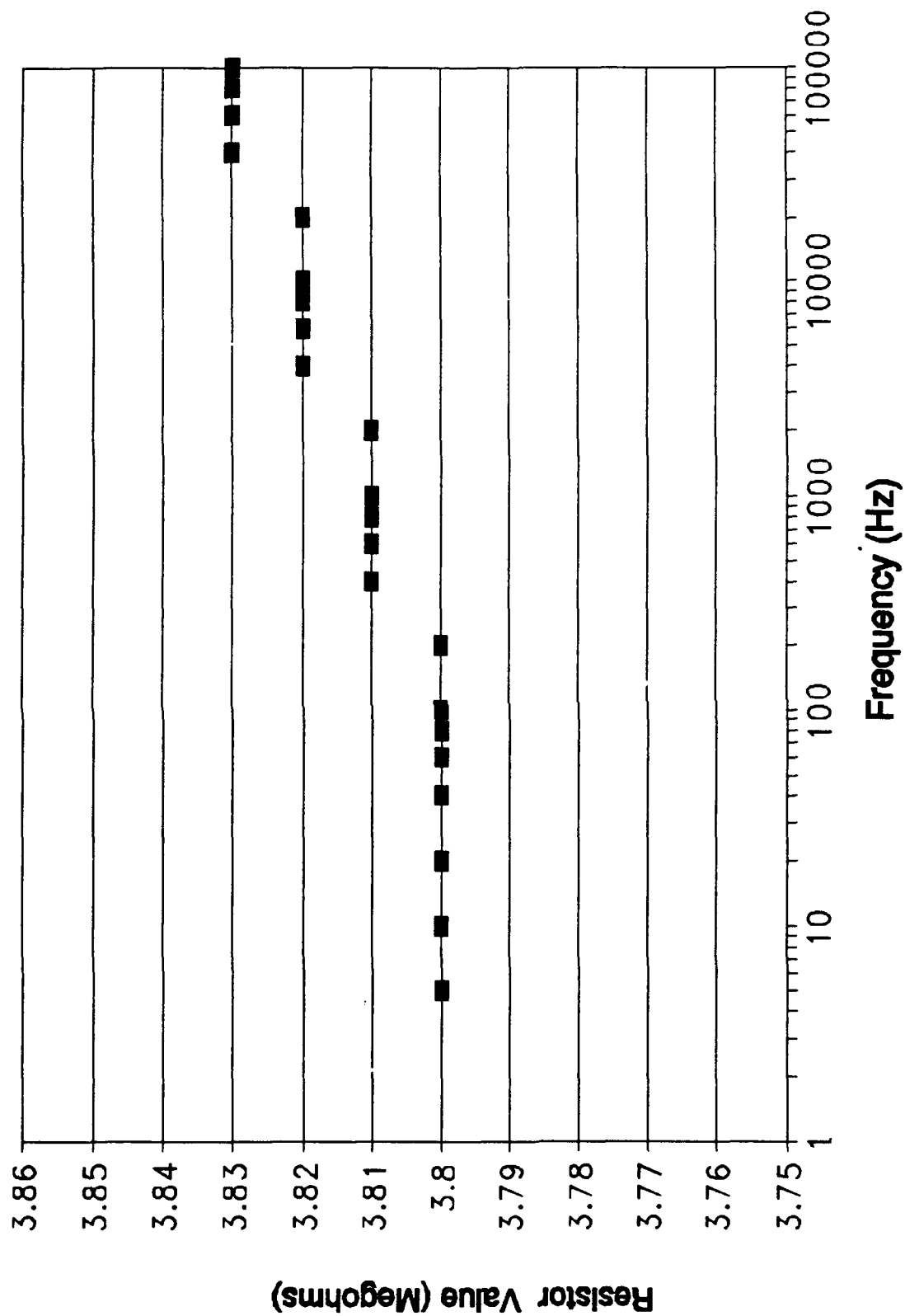
Figure D-16. Oldham Circuit Design -- the Value of Capacitor C2 versus Frequency (Ideal Value -- 3.88 µf).
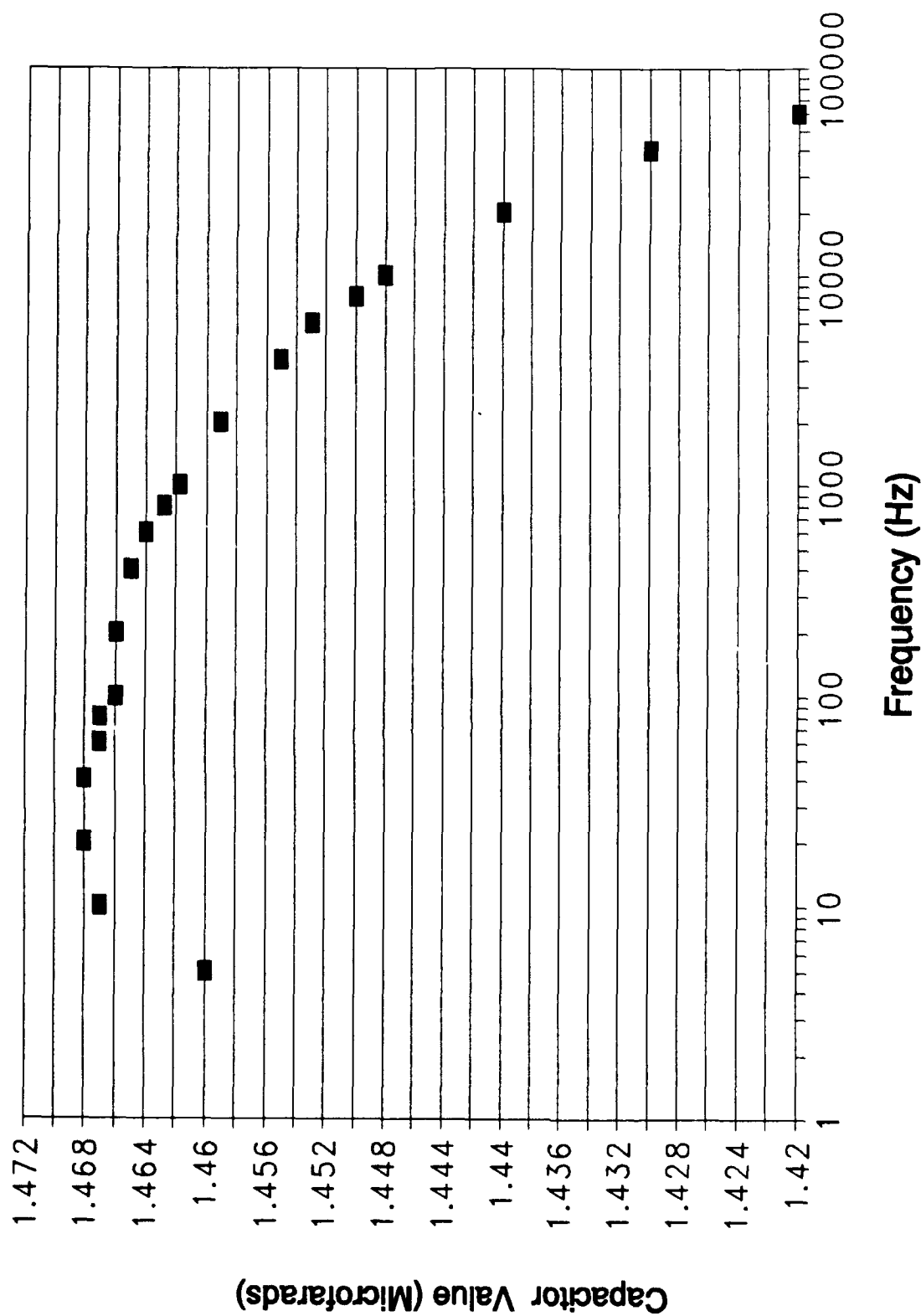
Figure D-17. Oldham Circuit Design -- the Value of Capacitor C3 versus Frequency (Ideal Value -- 1.514 μf).
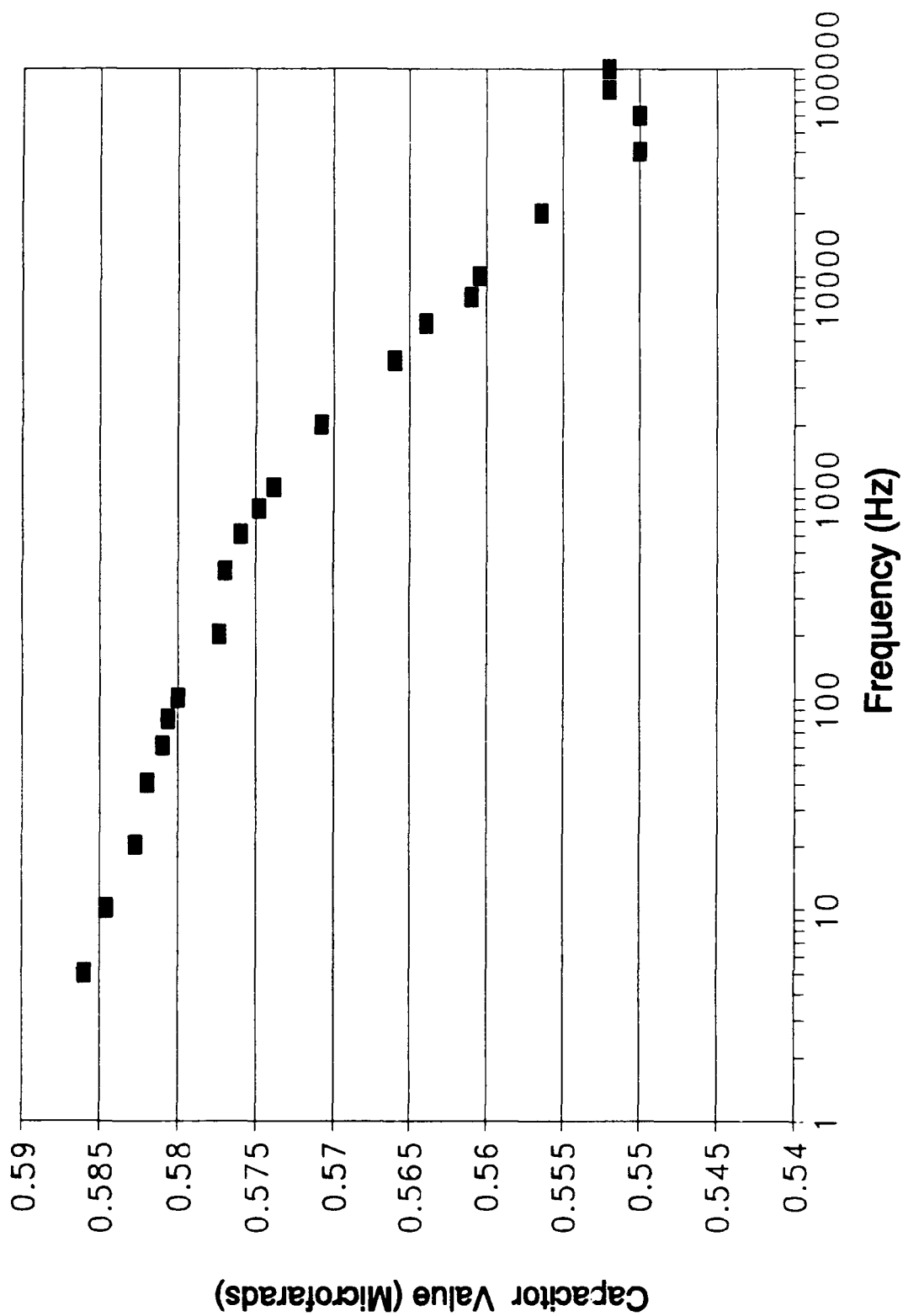
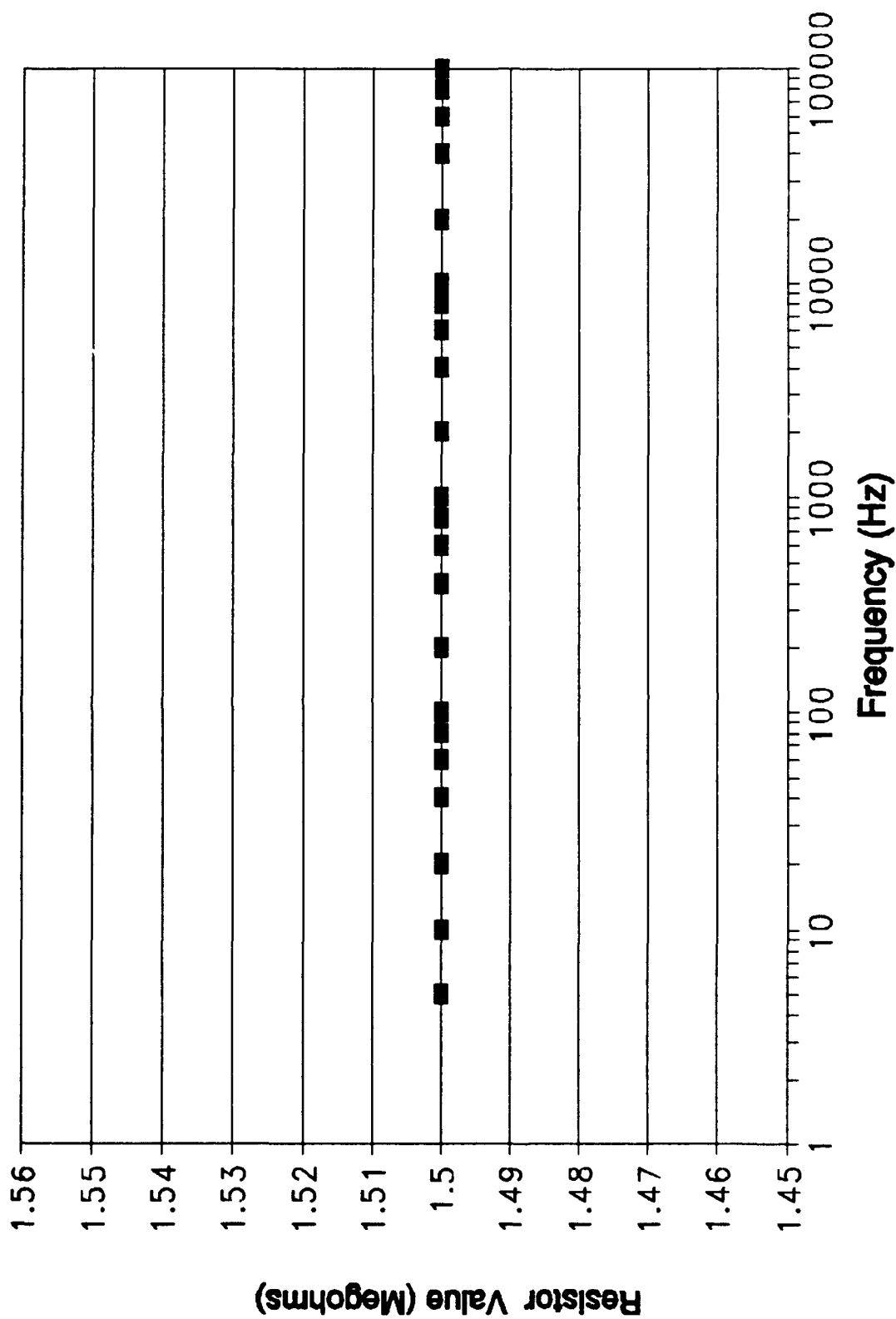Figure D-18. Oldham Circuit Design -- the Value of Capacitor C4 versus Frequency (Ideal Value -- 0.5873 µf).
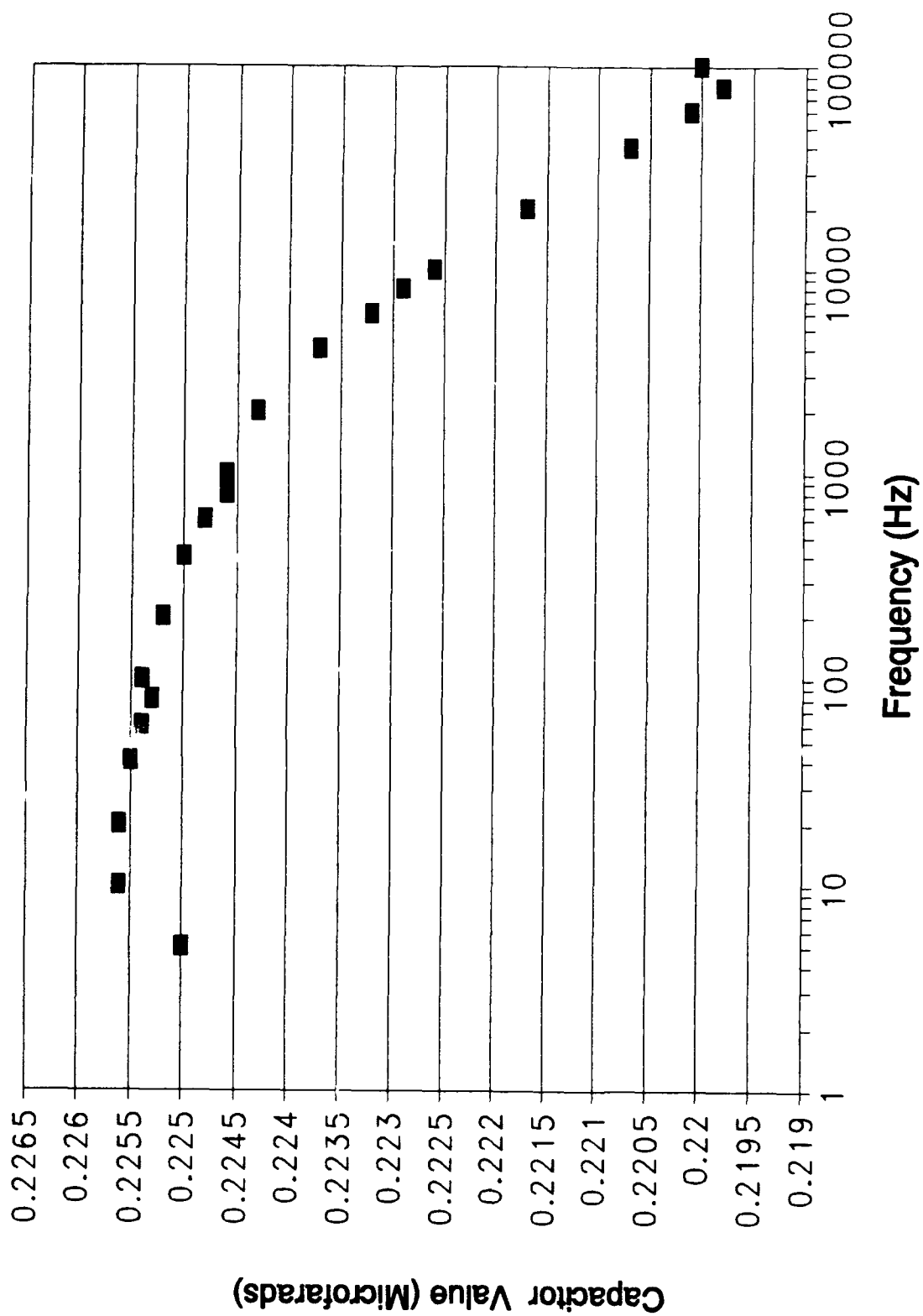
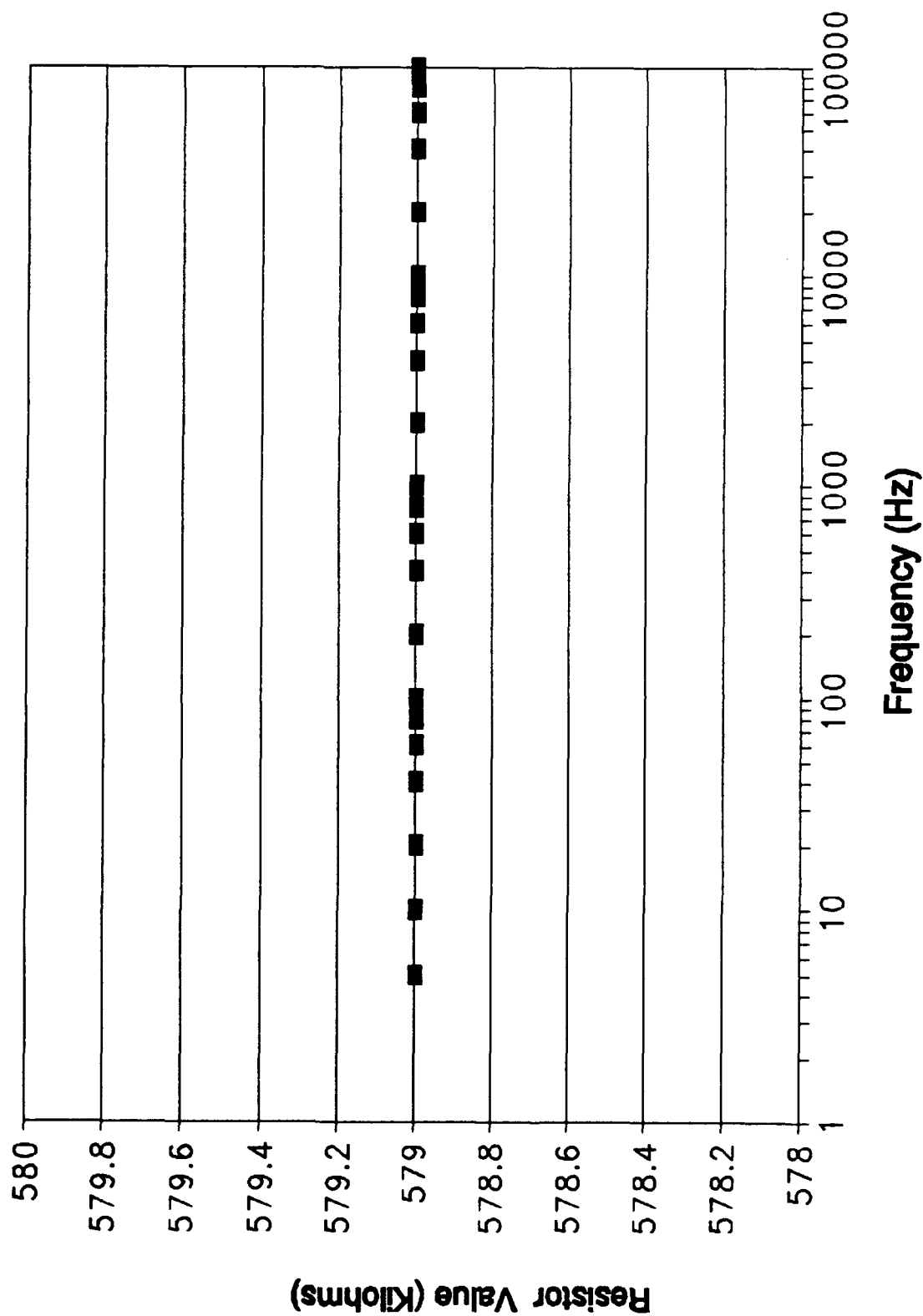Figure D-19. Oldham Circuit Design -- the Value of Capacitor C5 versus Frequency (Ideal Value -- .2283 µf).
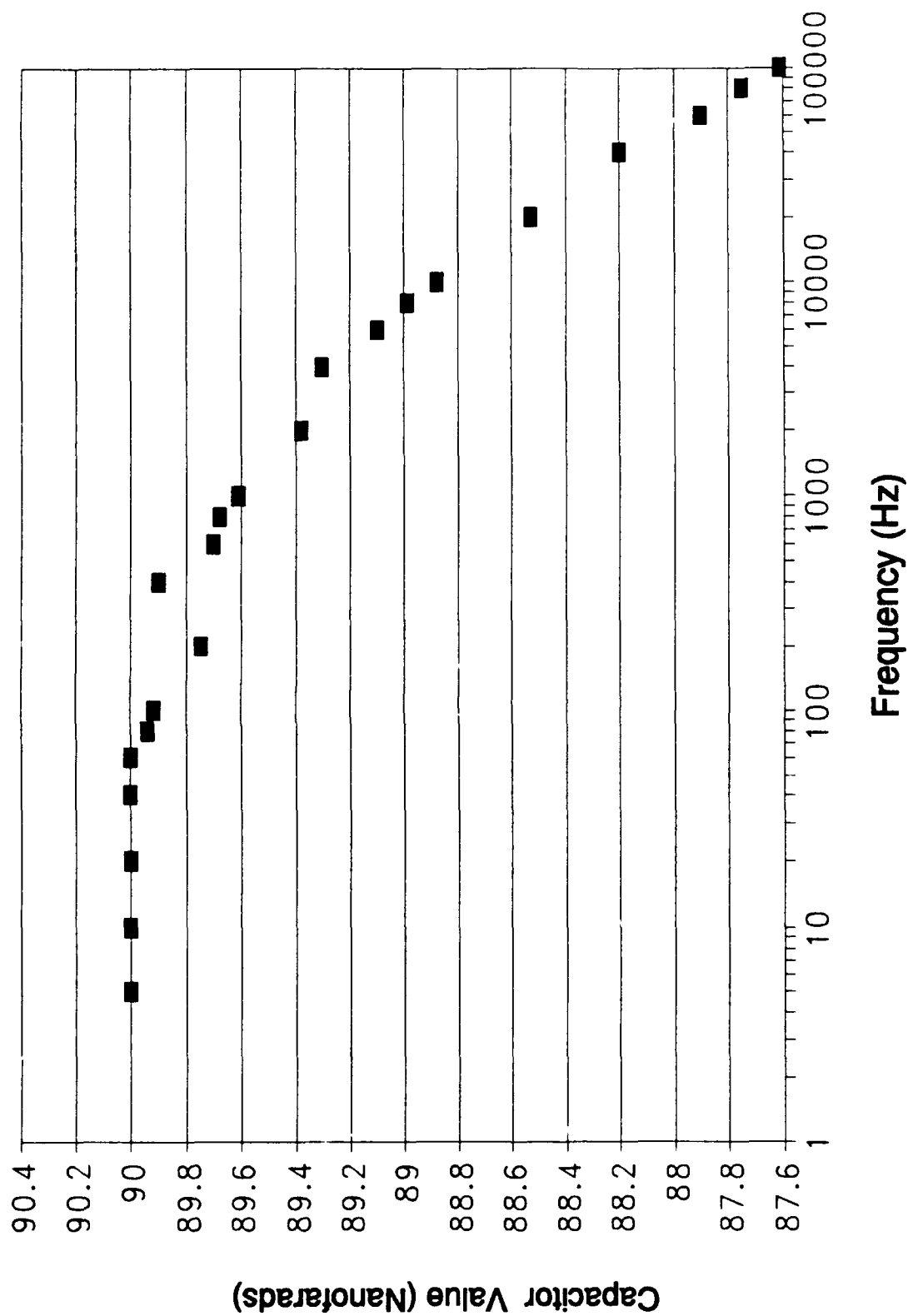
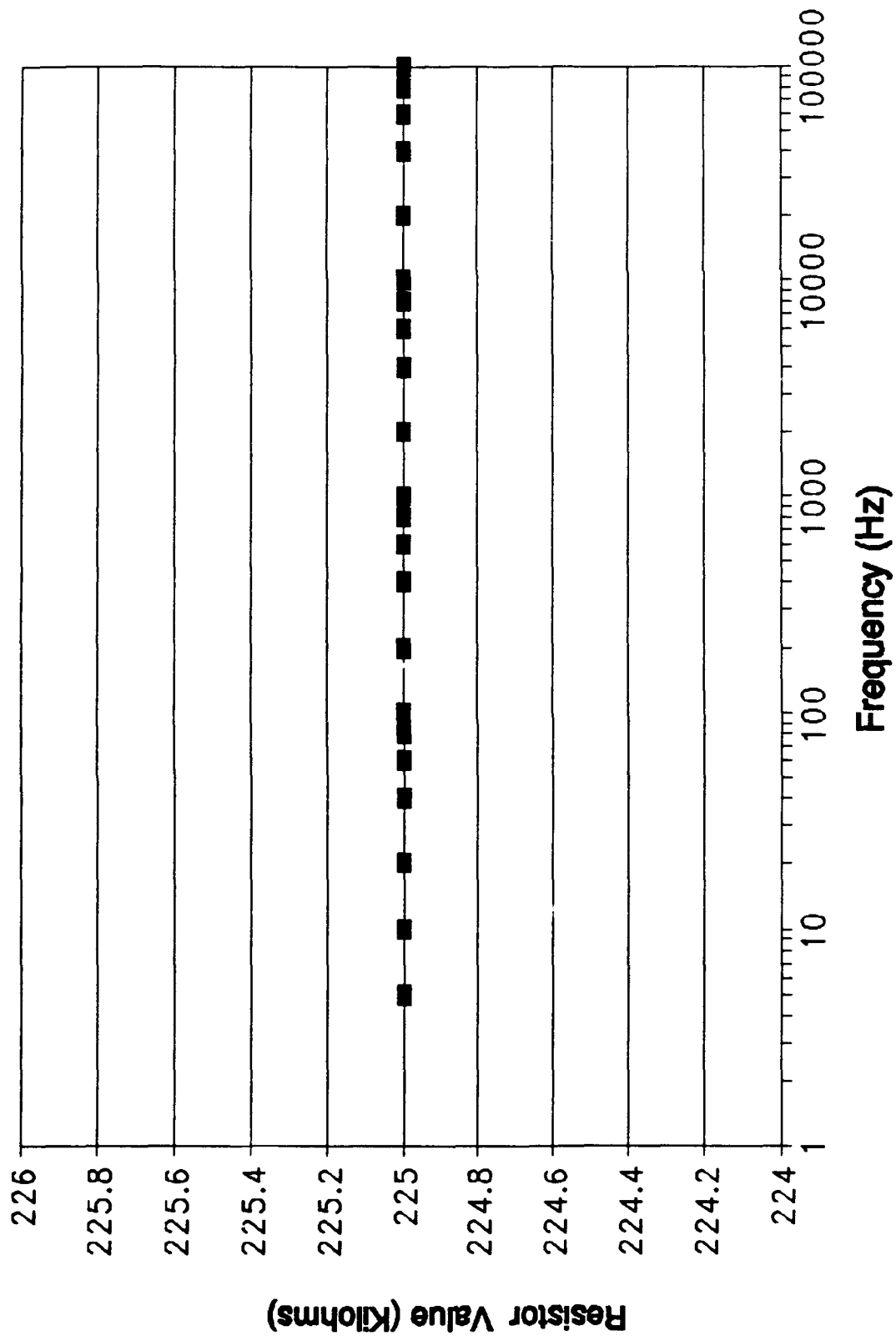Figure D-20. Oldham Circuit Design -- the Value of Capacitor C6 versus Frequency (Ideal Value -- 88.73 nf).
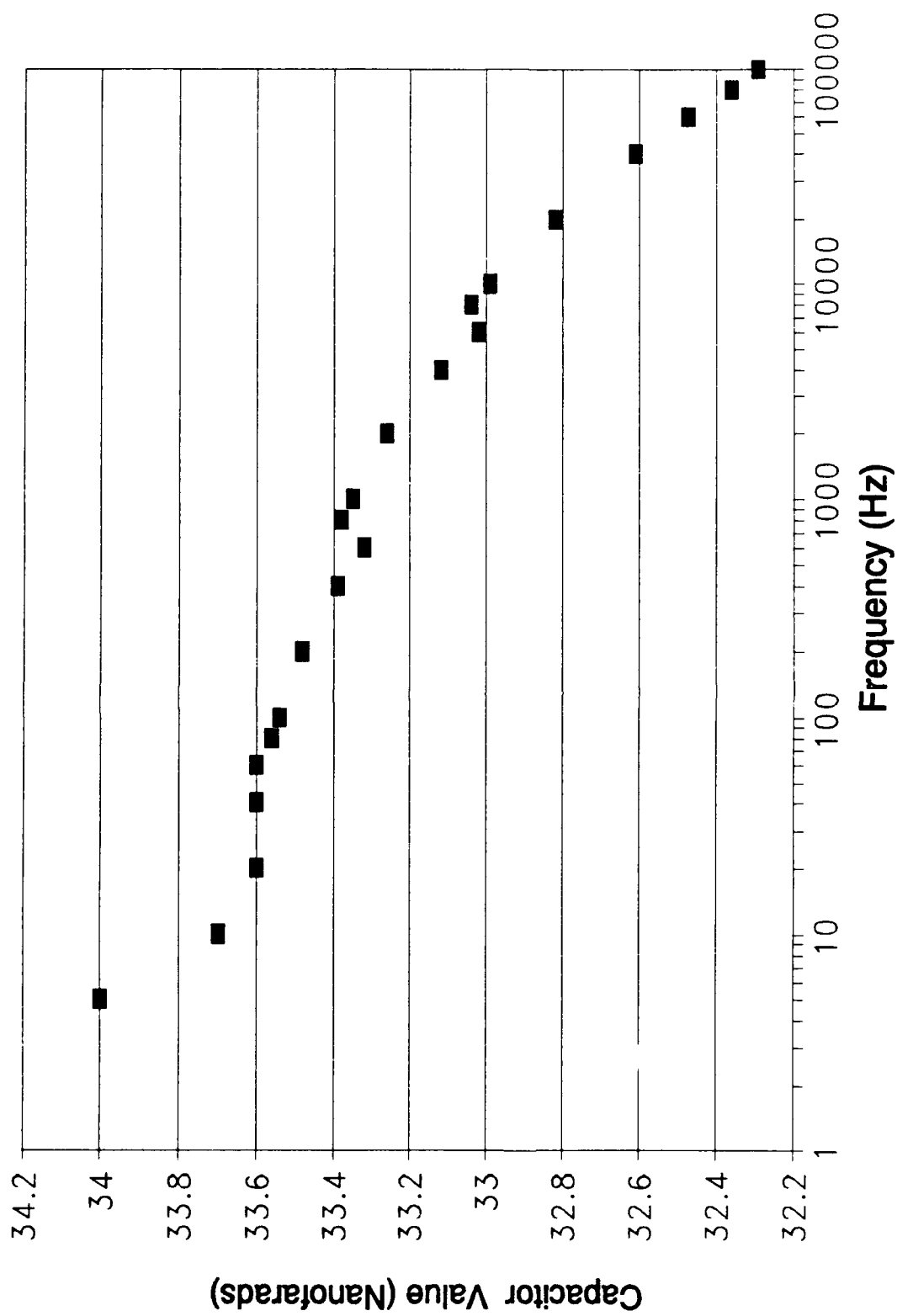
Figure D-21. Oldham Circuit Design -- the Value of Capacitor C7 versus Frequency (Ideal Value -- 34.49 nf).
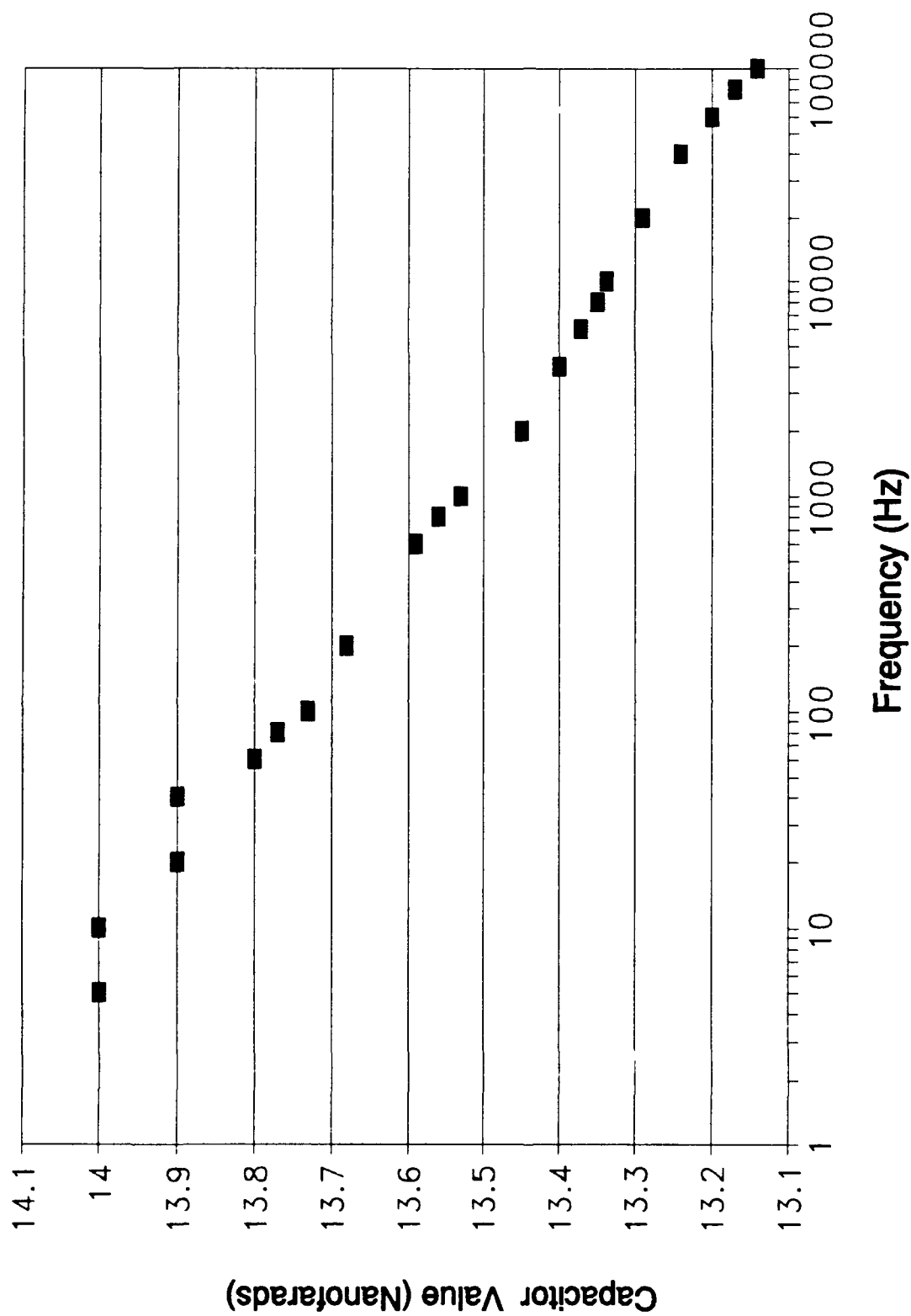
Figure D-22. Oldham Circuit Design -- the Value of Capacitor C8 versus Frequency (Ideal Value -- 13.41 nf).
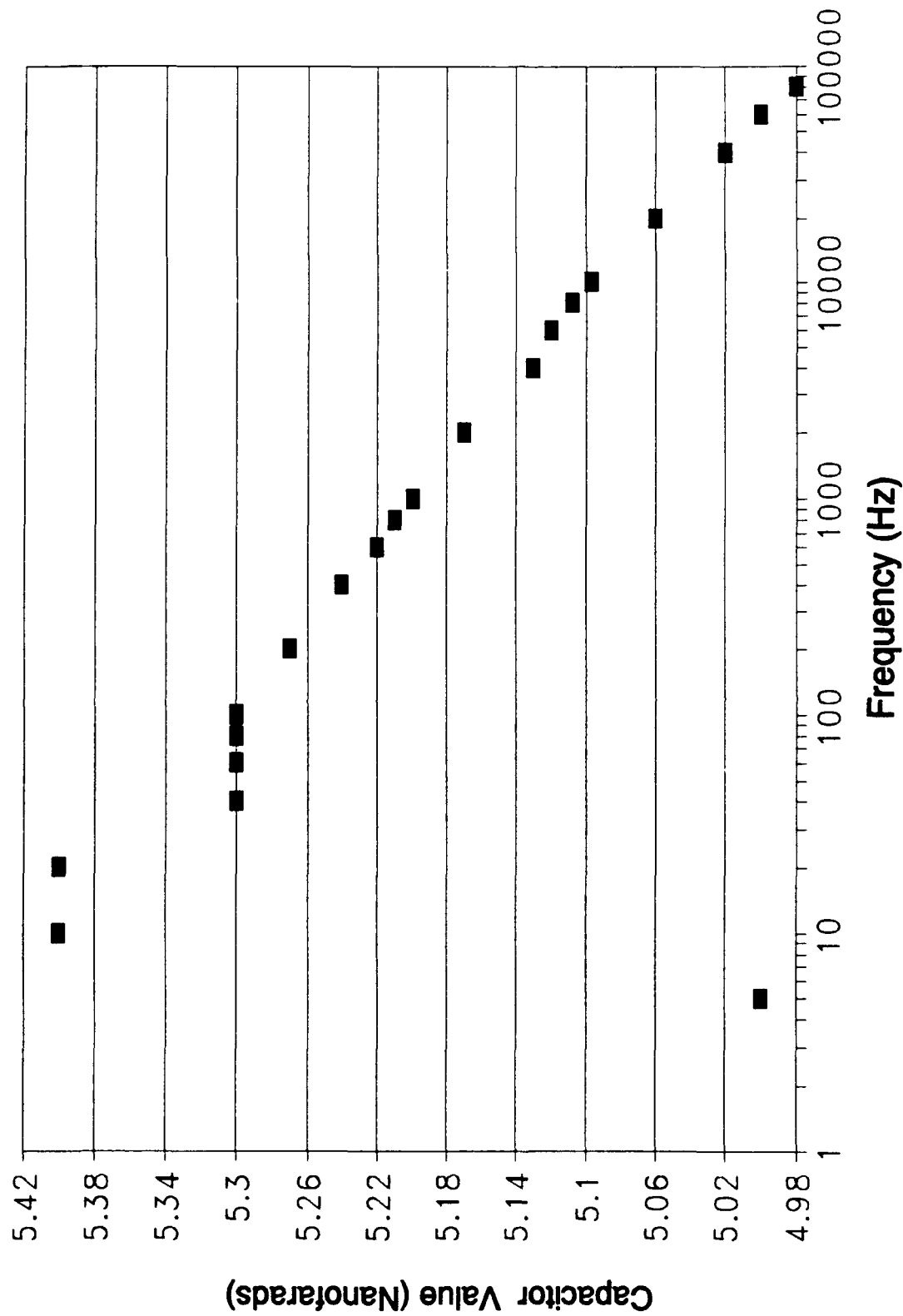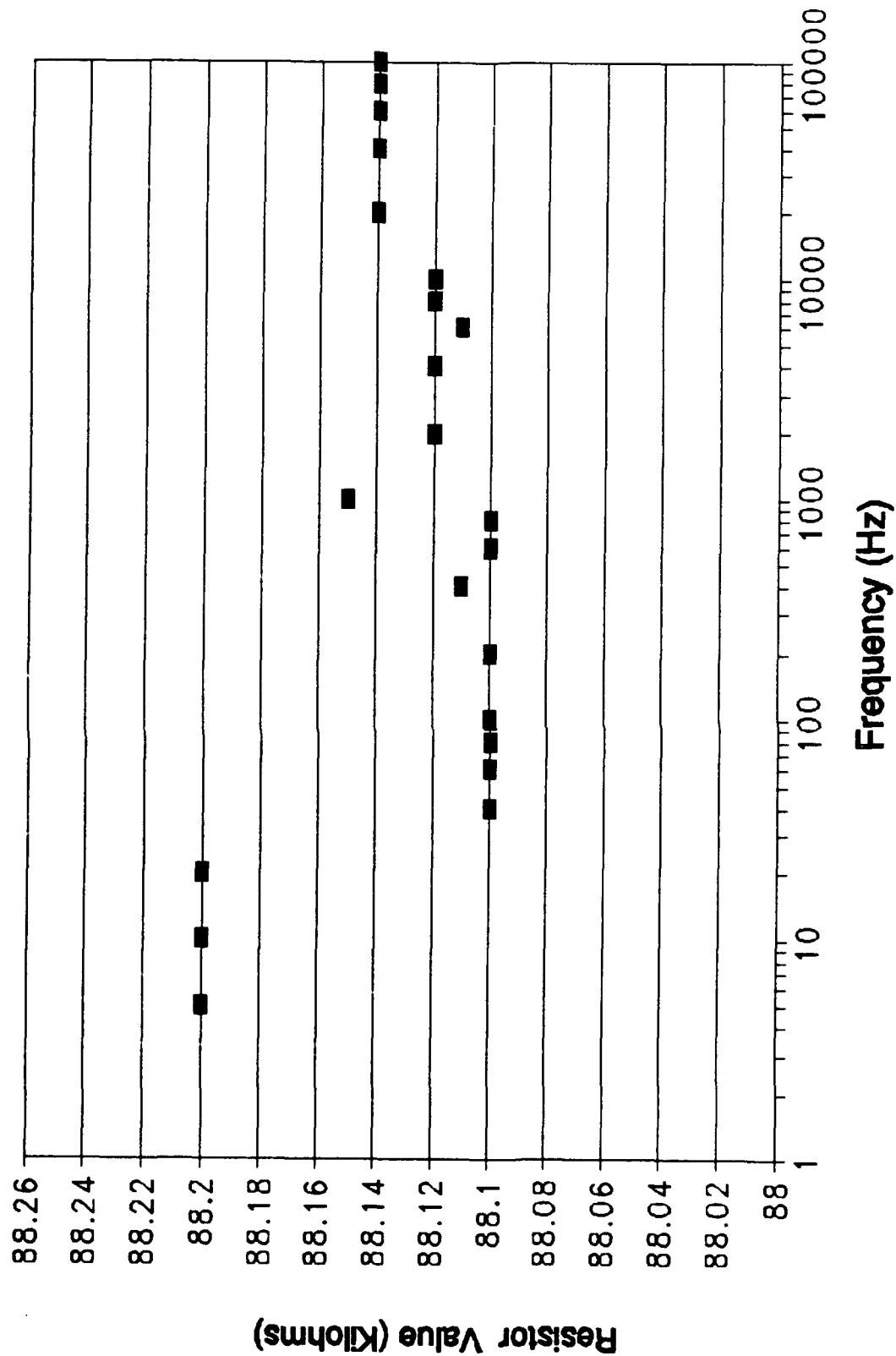
Figure D-23. Oldham Circuit Design -- the Value of Capacitor C9 versus Frequency (Ideal Value -- 5.211 nf).
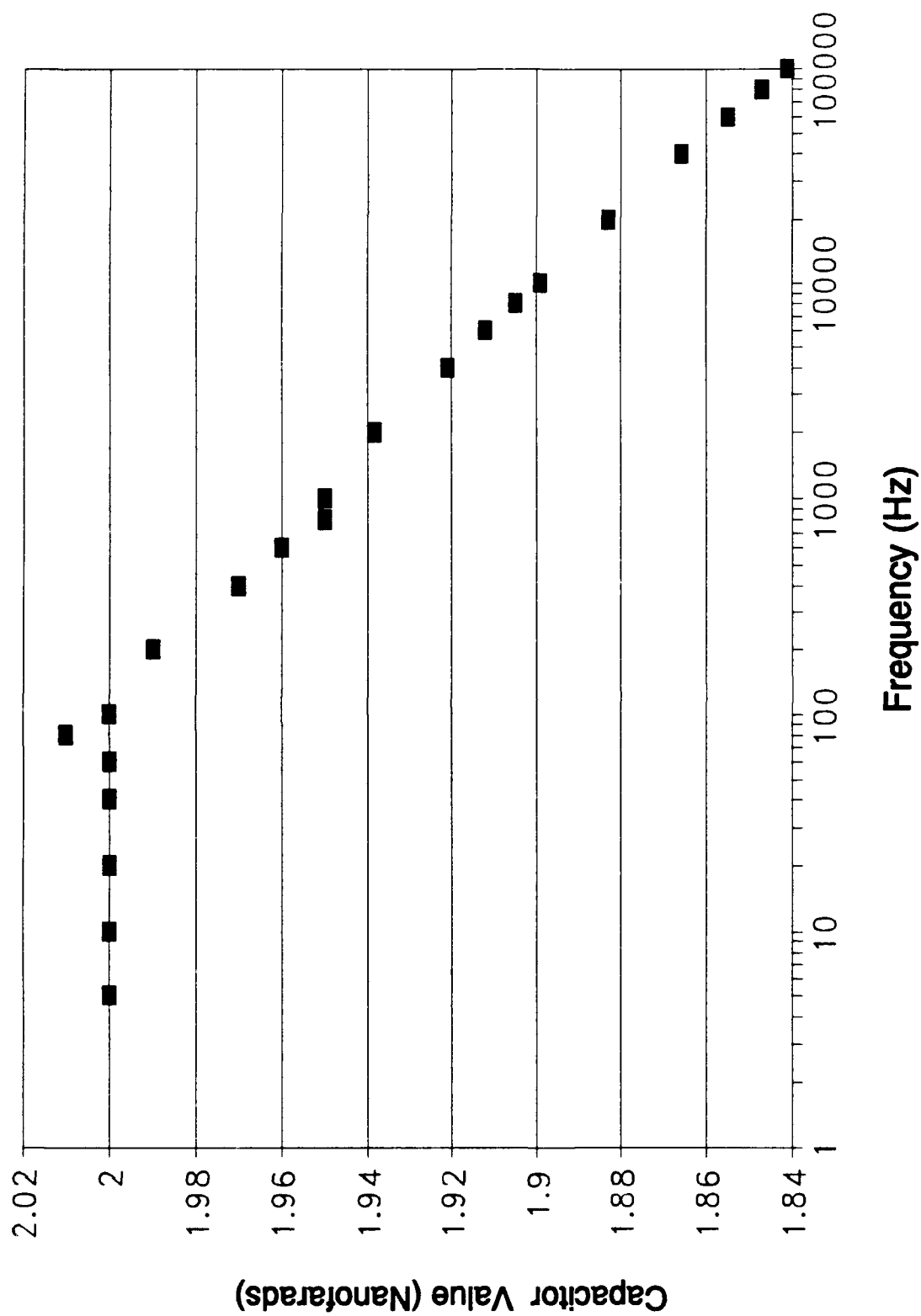
Figure D-24.   Oldham Circuit Design -- the Value of
Capacitor C10 versus Frequency
(Ideal Value -- 2.026 nf).

Figure D-25. Oldham Circuit Design -- the Value of Capacitor C11 versus Frequency (Ideal Value -- 1.575 nf).
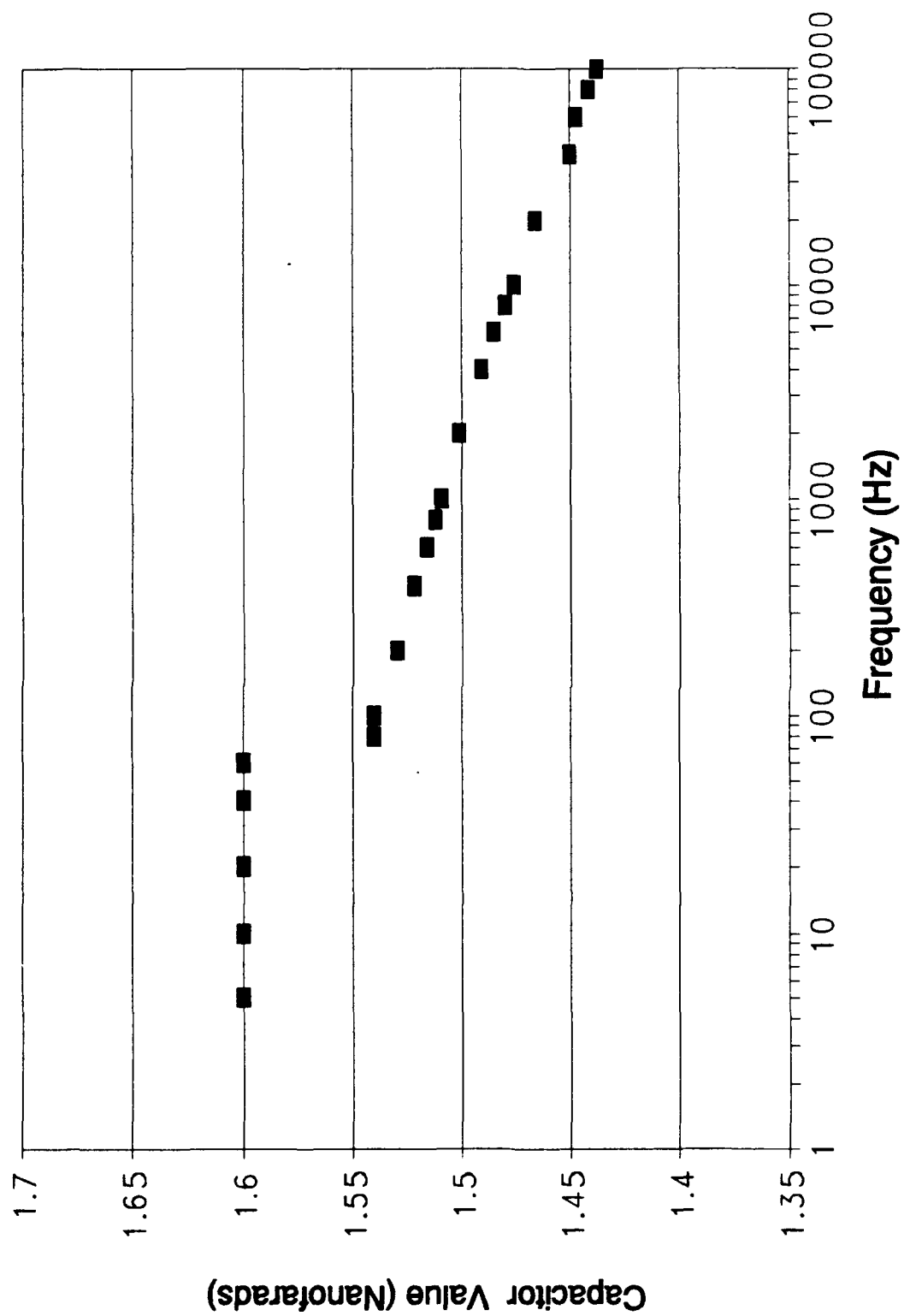
Section 3

Oldfield Discrete Resistor Component Value

Variations Versus Frequency

Results
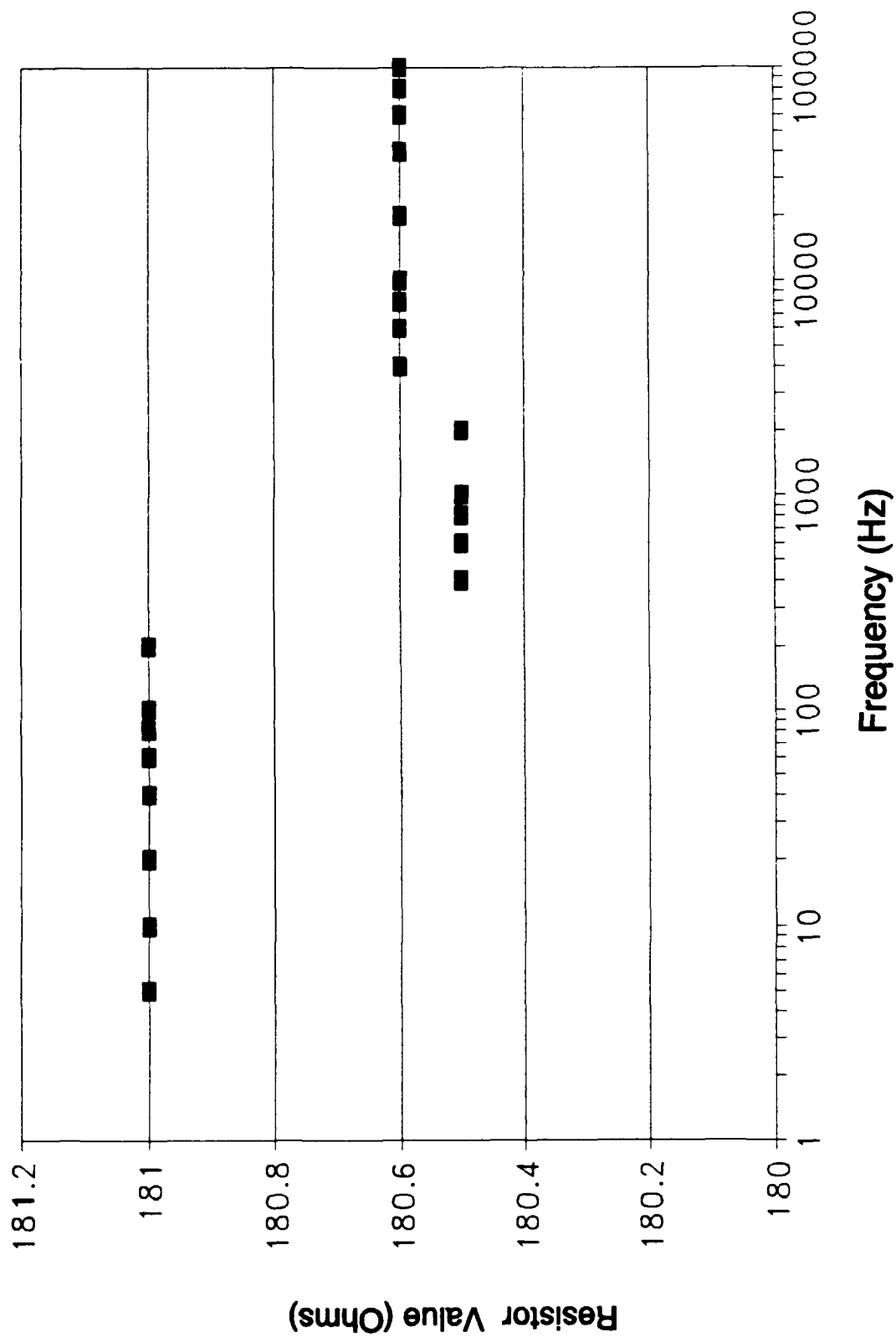
Figure D-26. Oldfield Circuit Design -- the Value of Resistor R1 versus Frequency (Ideal Value -- 180.2 Ohms).
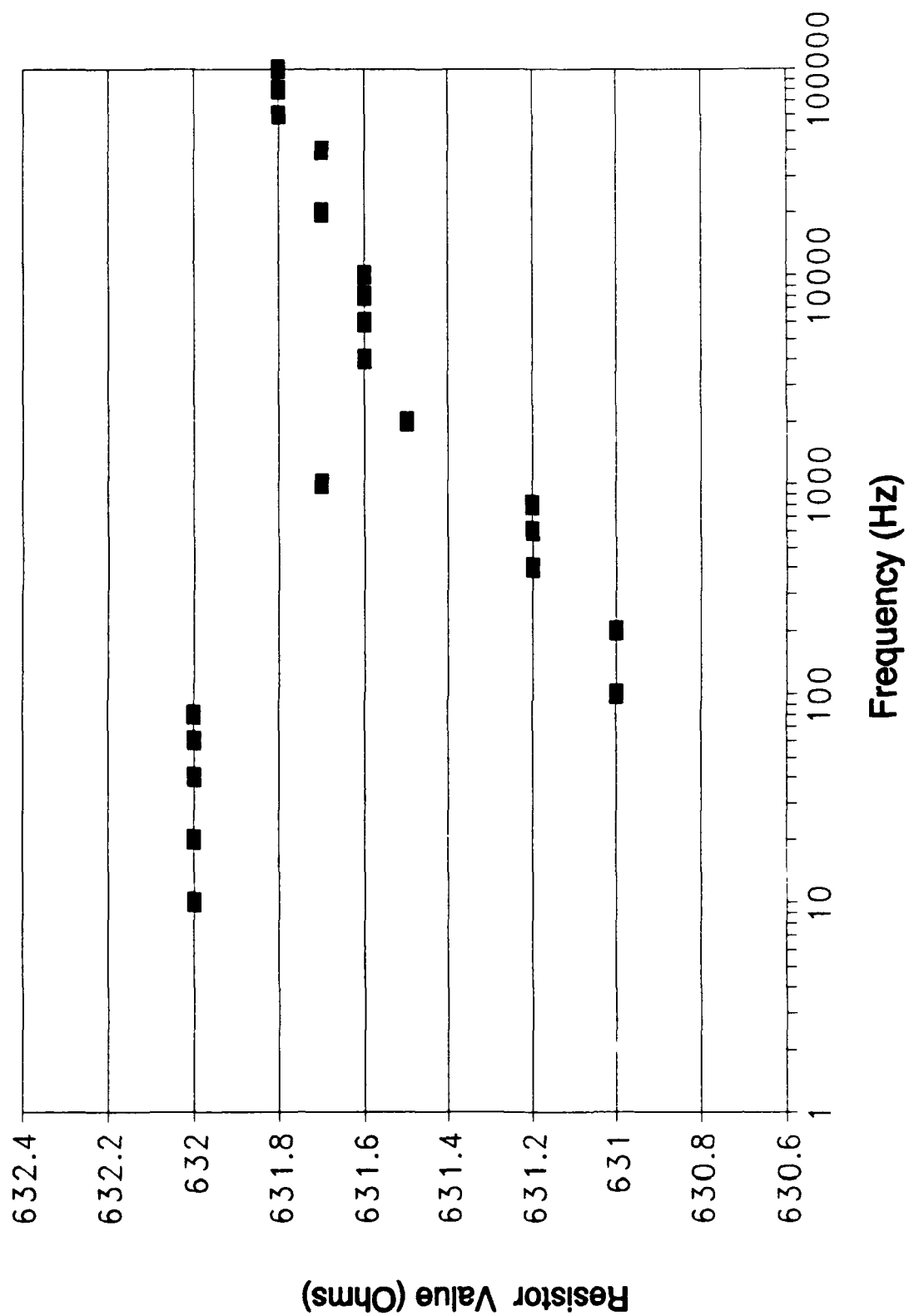
Figure D-27. Oldfield Circuit Design -- the Value of Resistor R2 versus Frequency (Ideal Value -- 630 Ohms).
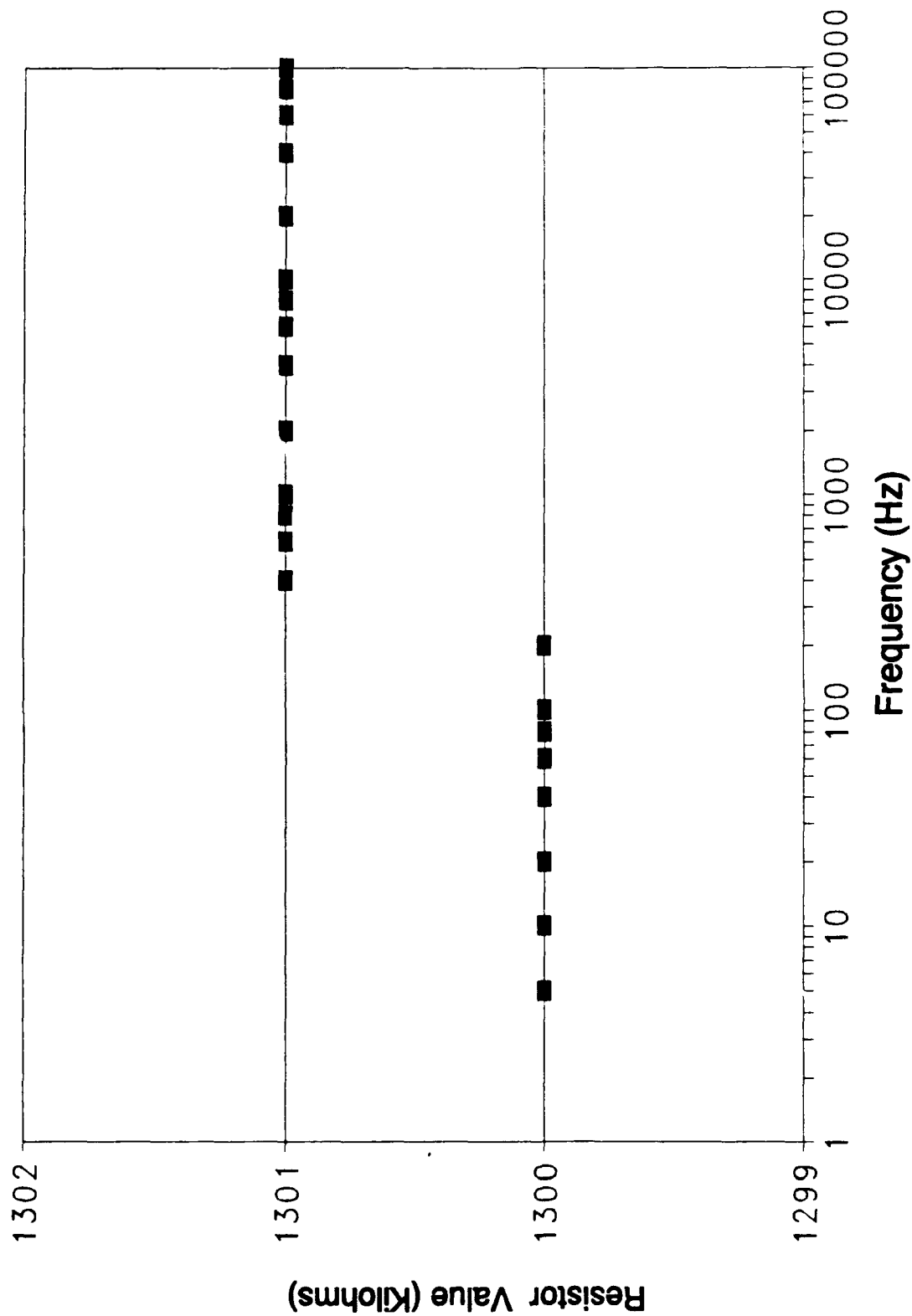
Figure D-28. Oldfield Circuit Design -- the Value of
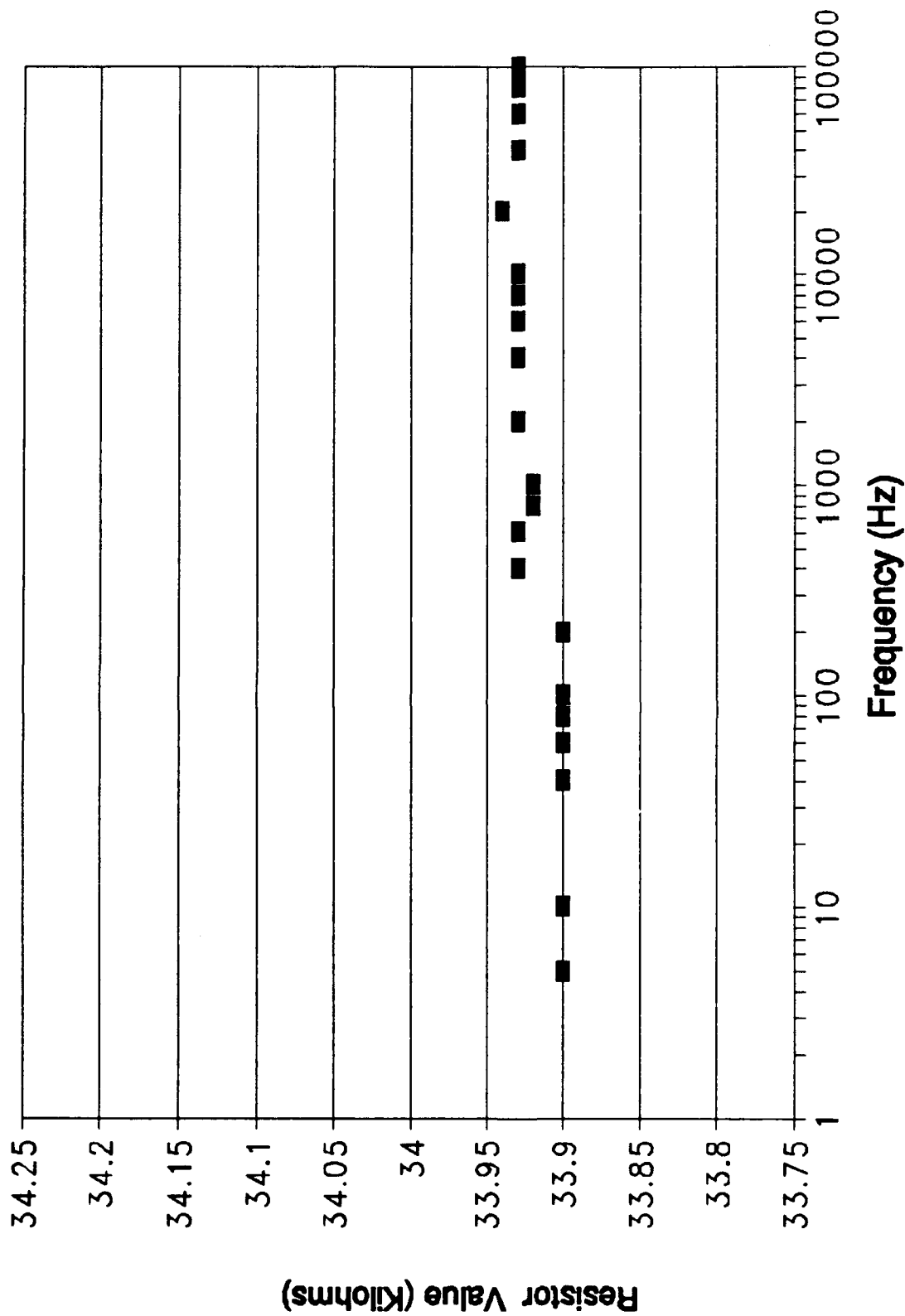Resistor R3 versus Frequency
(Ideal Value -- 1.313 Kilohms).
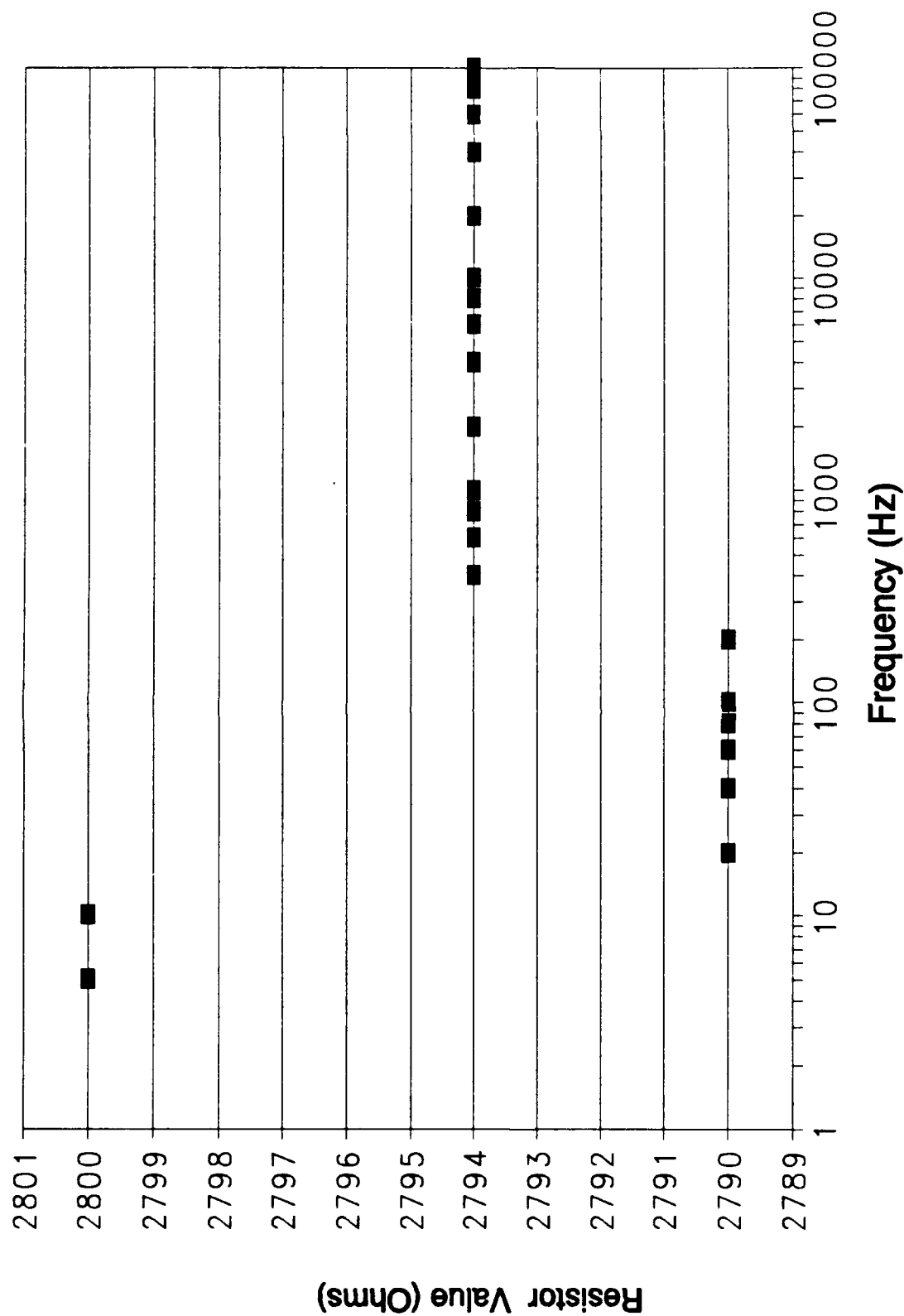
Figure D-29. Oldfield Circuit Design -- the Value of Resistor R4 versus Frequency (Ideal Value -- 2798 Ohms).
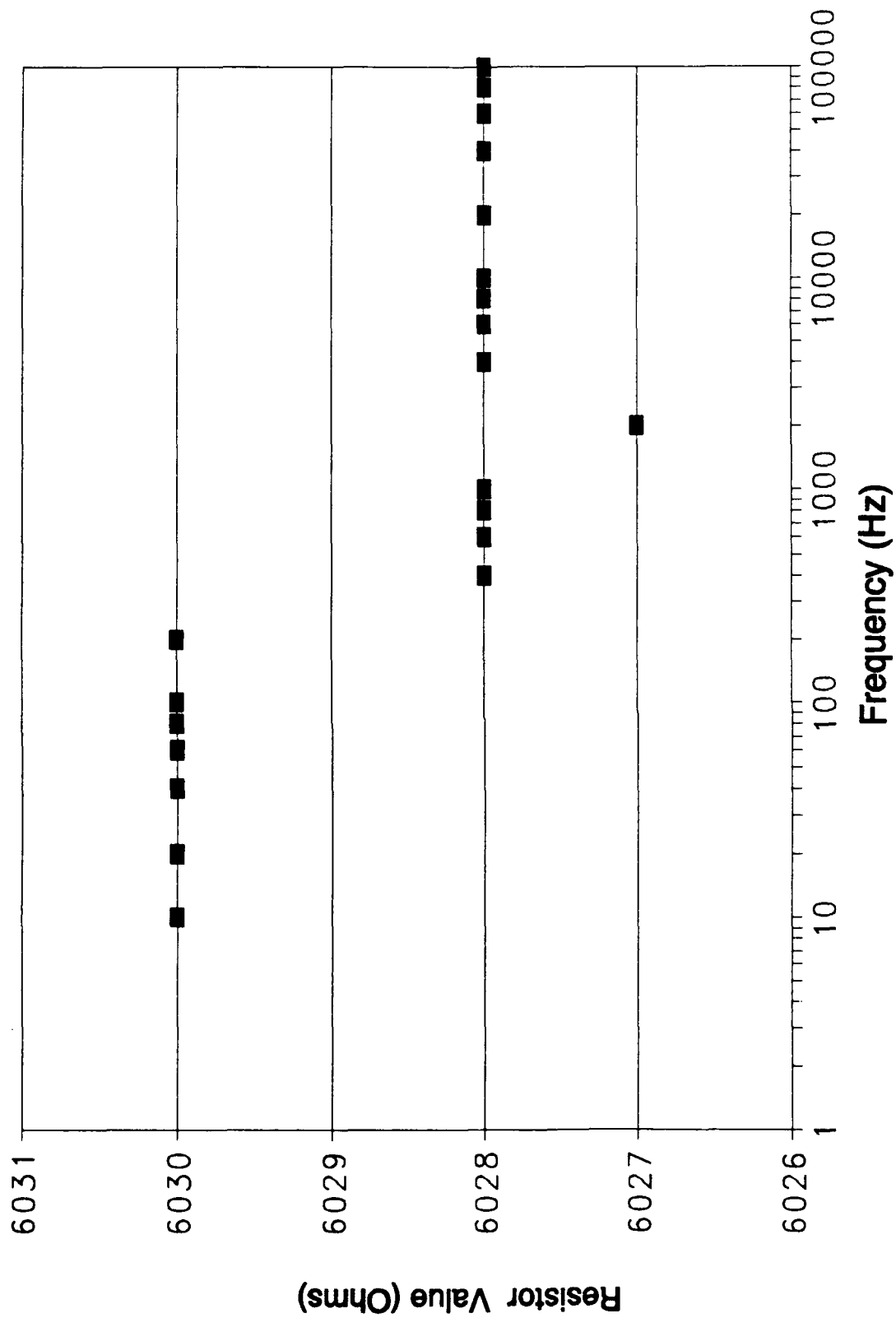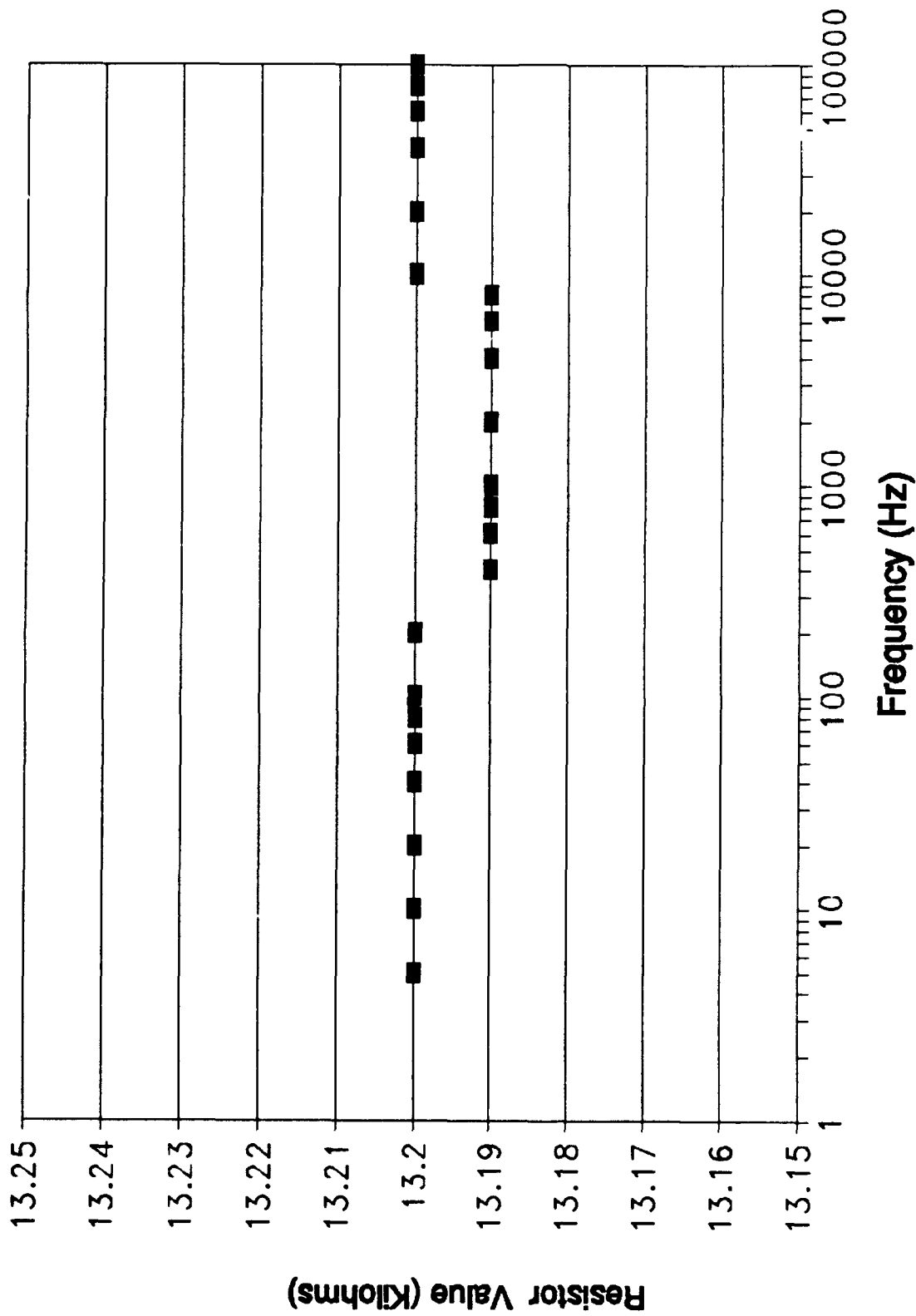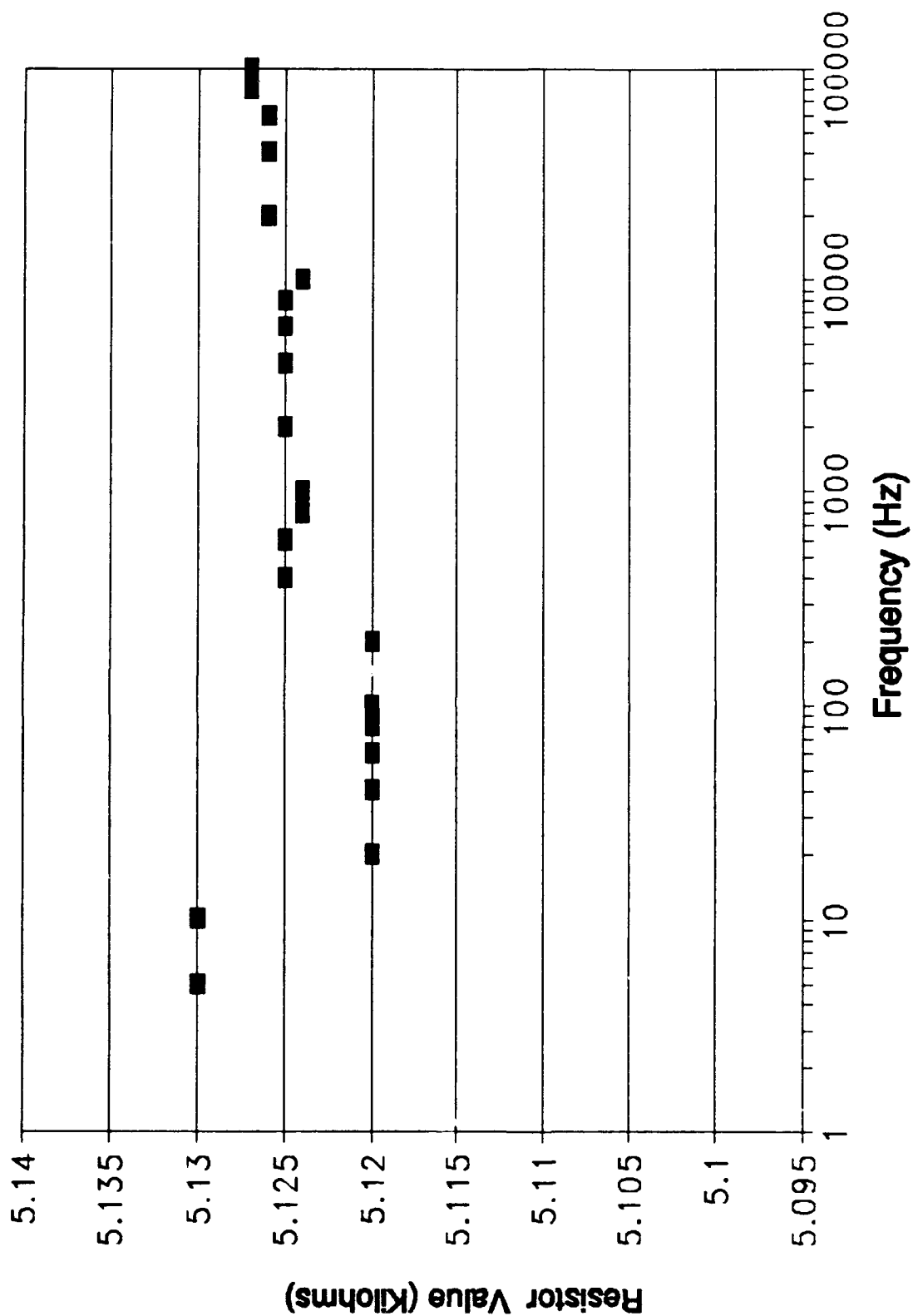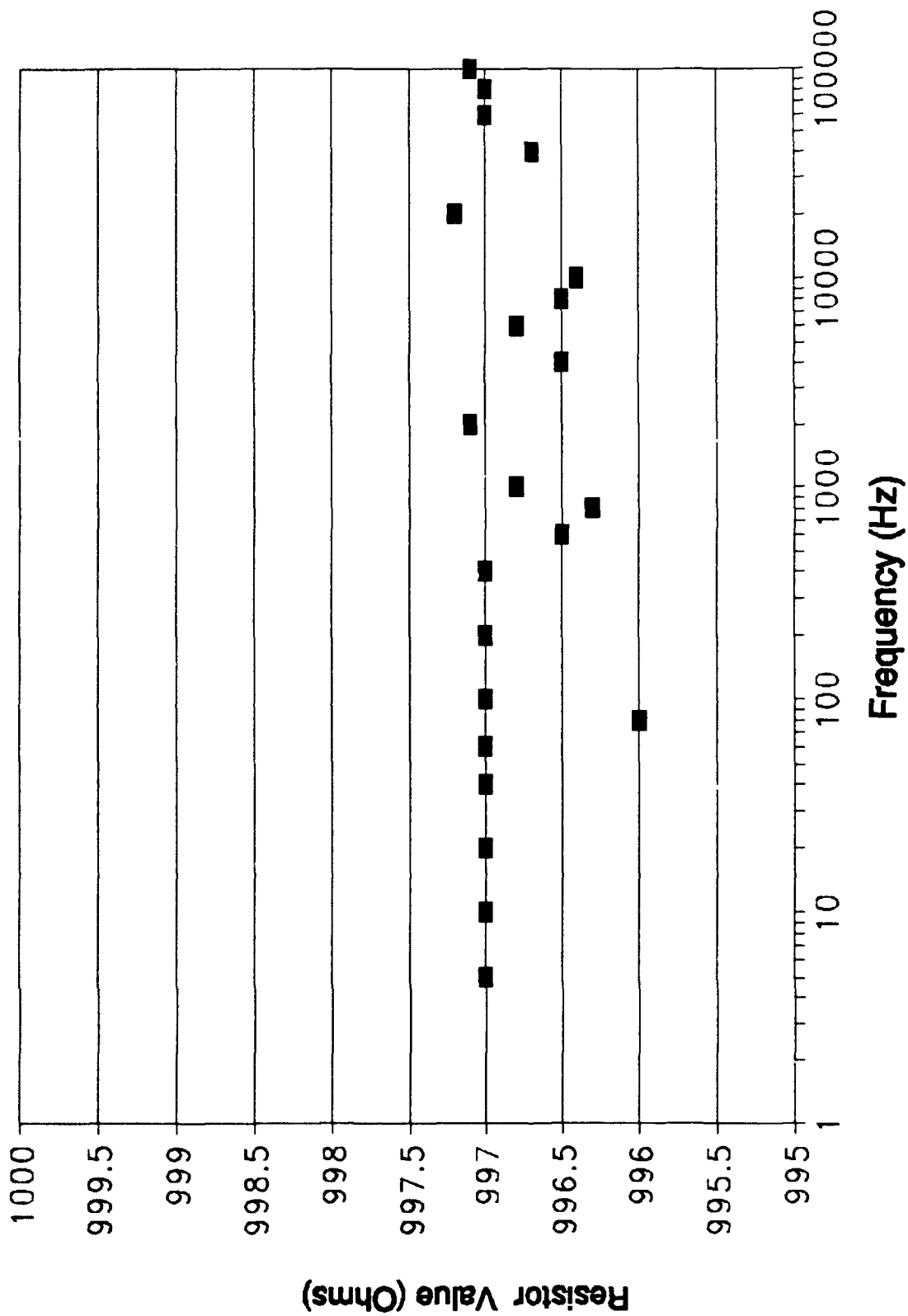
Figure D-30. Oldfield Circuit Design -- the Value of Resistor R5 versus Frequency (Ideal Value -- 6009 Ohms).
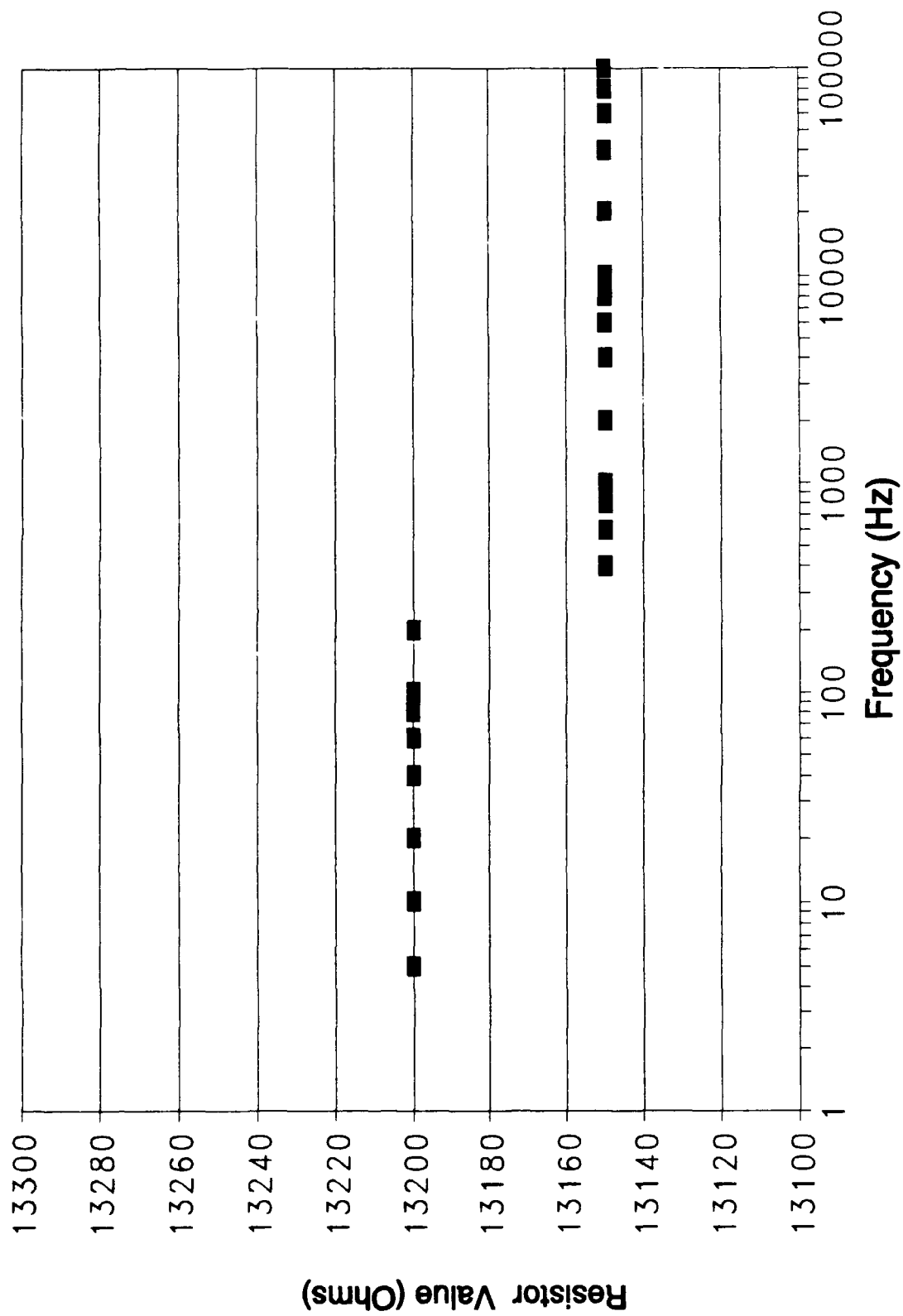
Figure D-31. Oldfield Circuit Design -- the Value of Resistor R6 versus Frequency (Ideal Value -- 13110 Ohms).
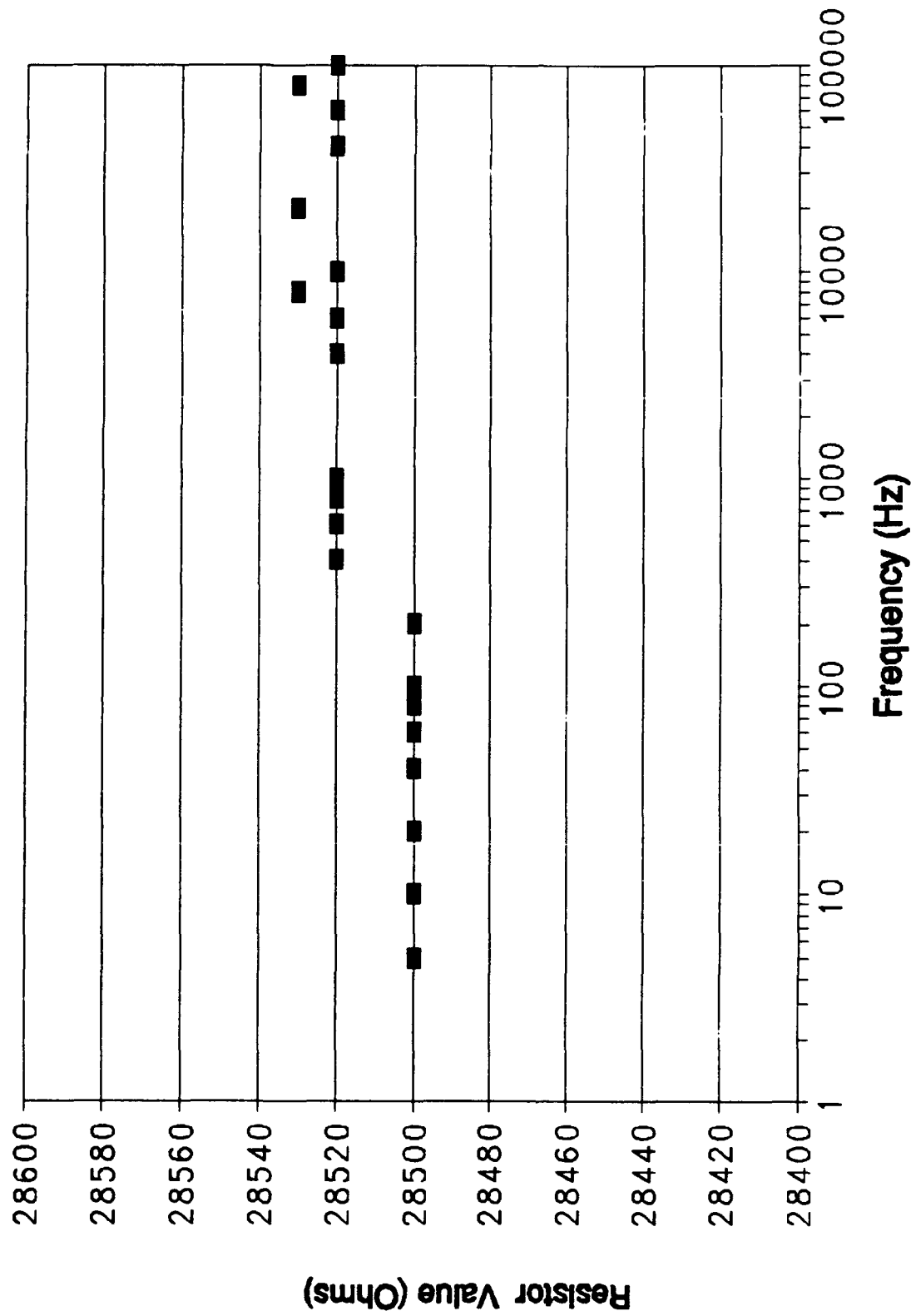
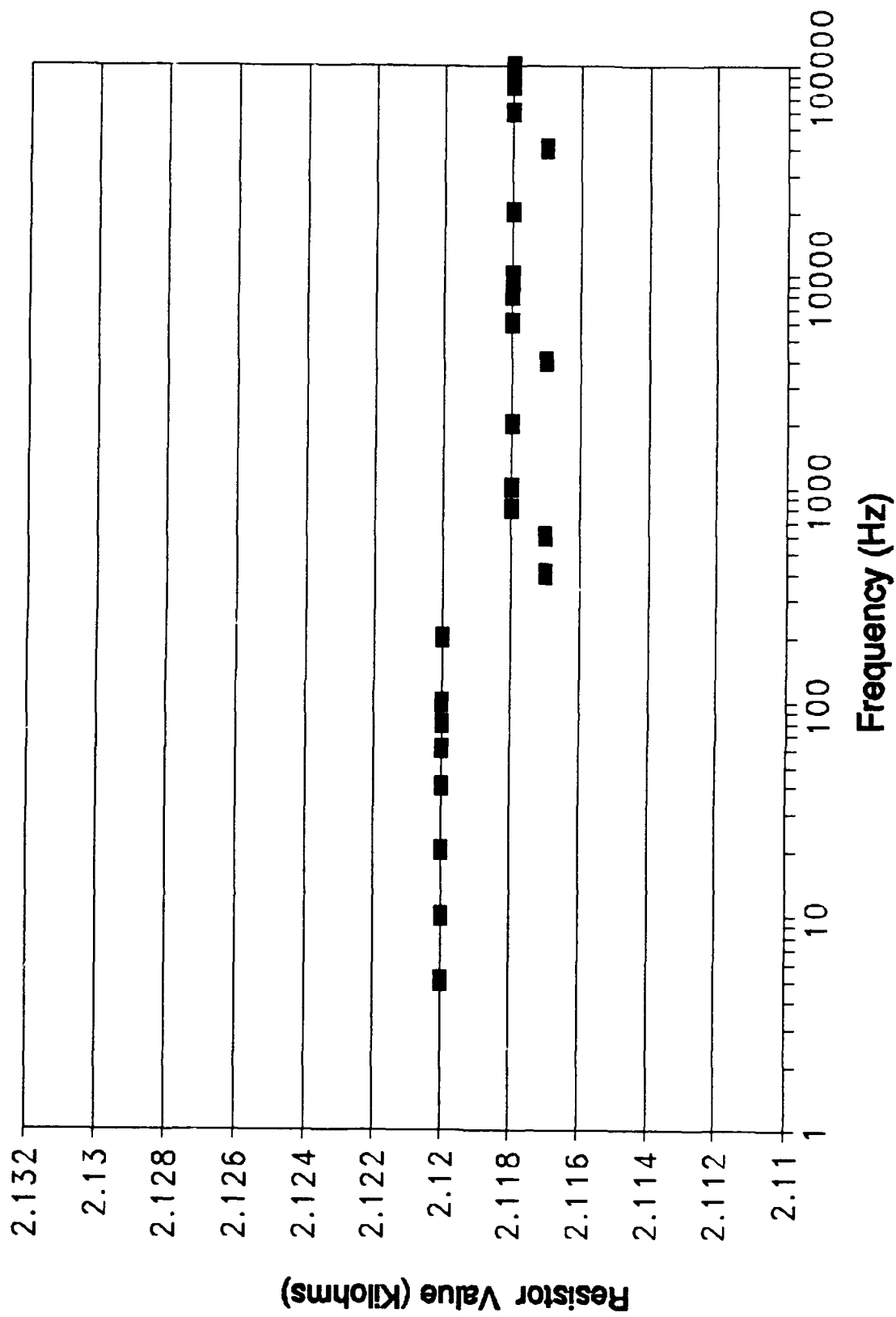Figure D-32. Oldfield Circuit Design -- the Value of Resistor R7 versus Frequency (Ideal Value -- 2857 Ohms).
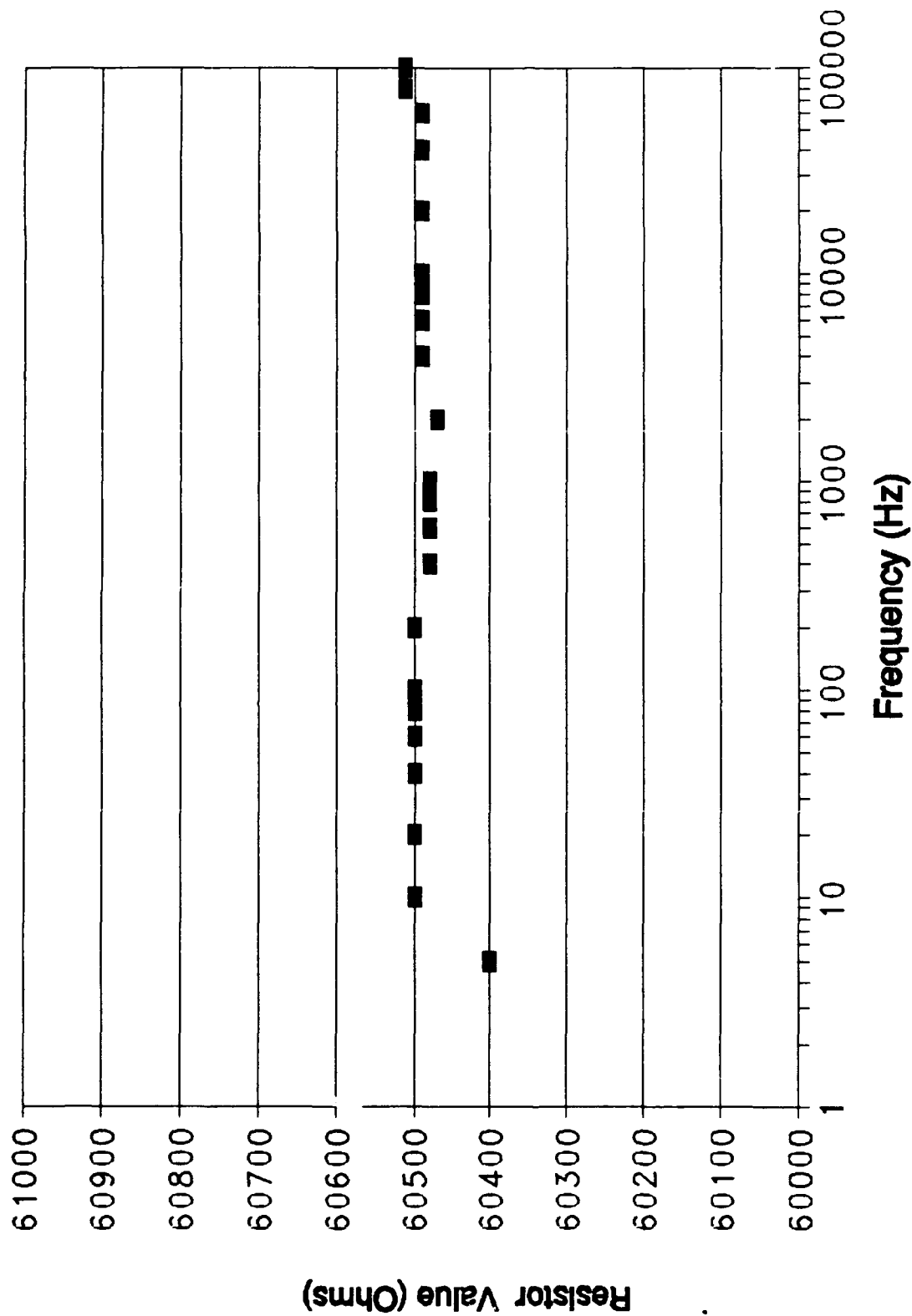
Figure D-33. Oldfield Circuit Design -- the Value of Resistor R8 versus Frequency (Ideal Value -- 60440 Ohms).
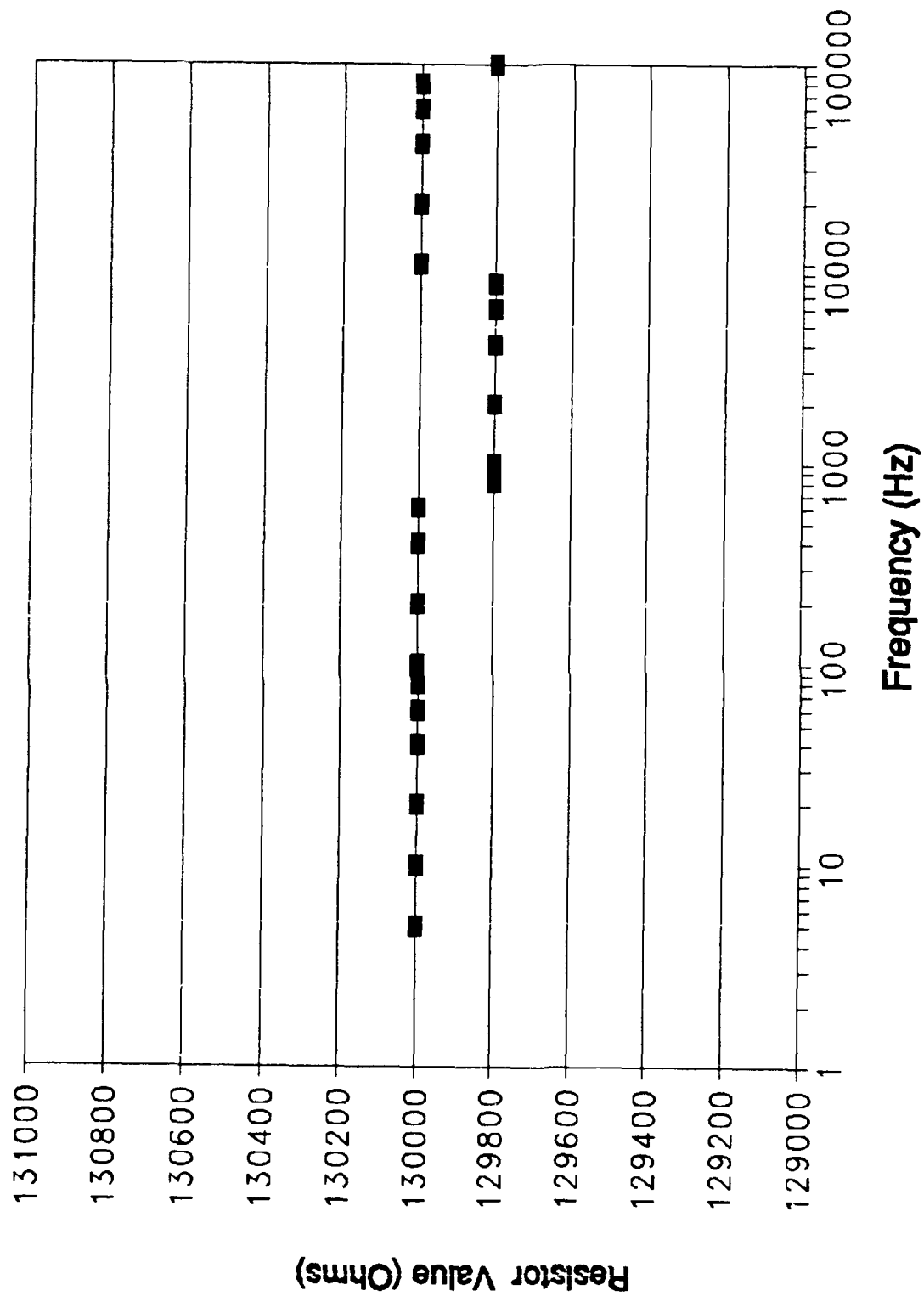
Figure D-34. Oldfield Circuit Design -- the Value of
Resistor R9 versus Frequency
(Ideal Value -- 129600 Kilohms).

Section 4

Oldfield Discrete Capacitor Component Value

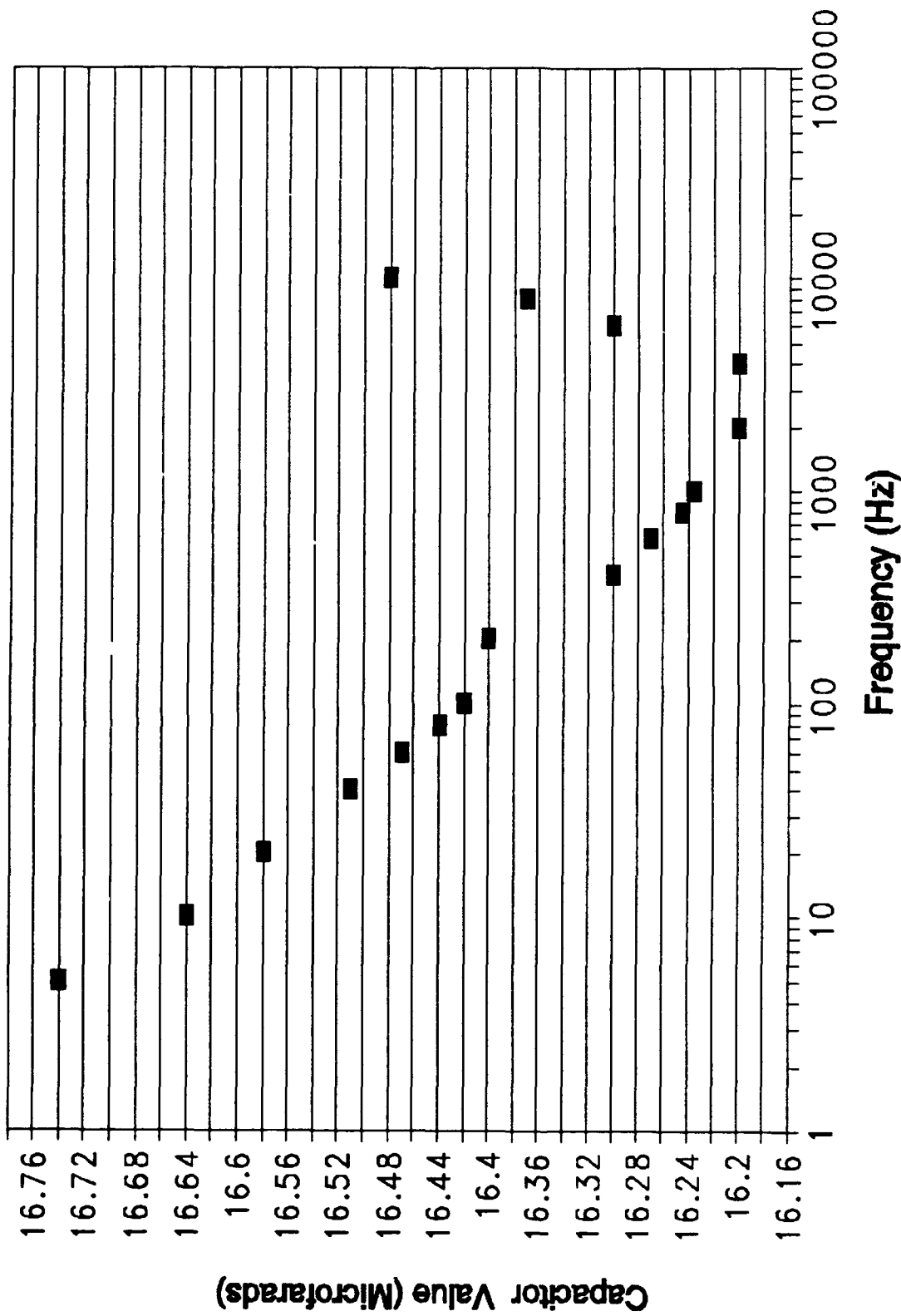Variations Versus Frequency

Results
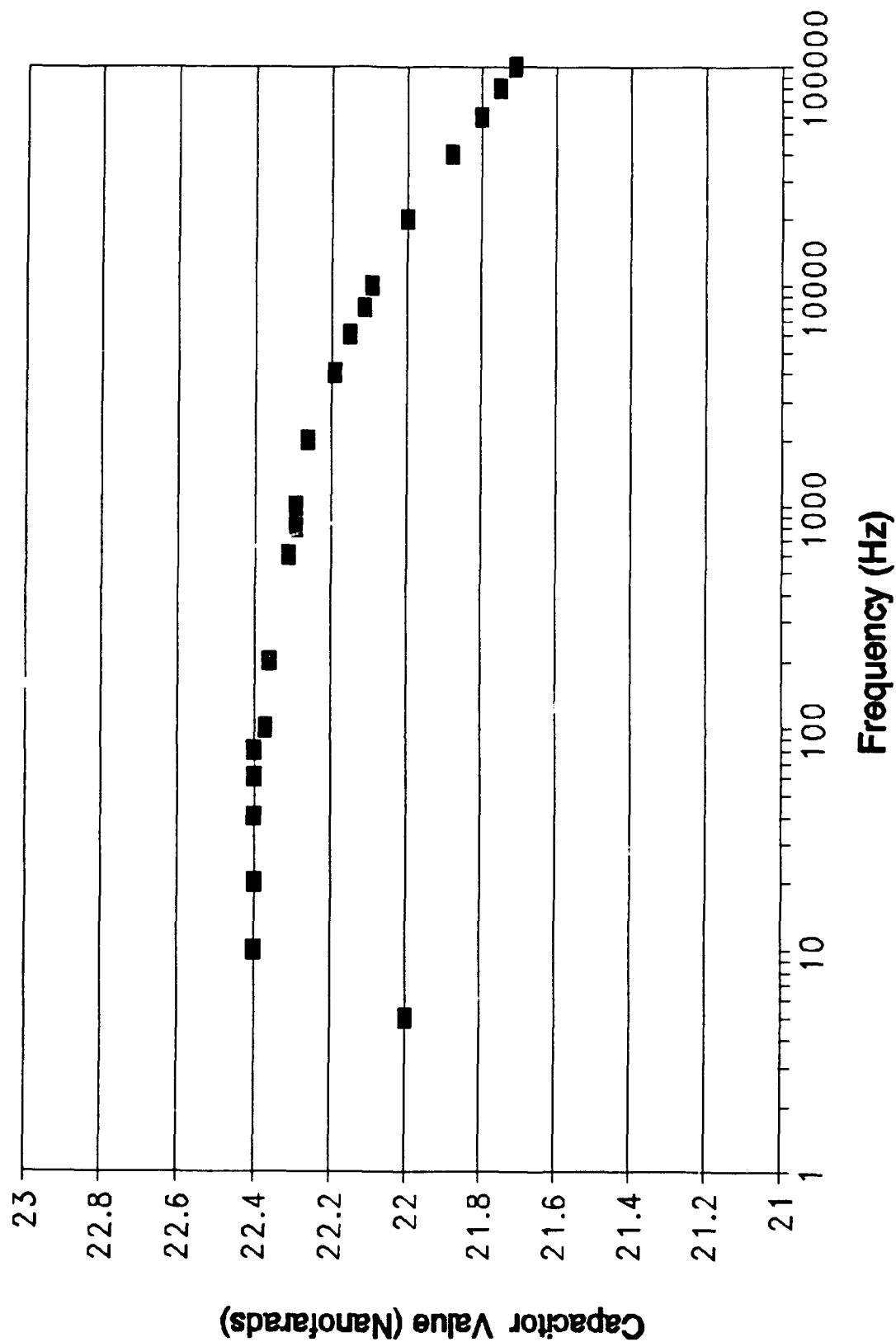
Figure D-35. Oldfield Circuit Design -- the Value of Capacitor C1 versus Frequency (Ideal Value -- 22 nf).
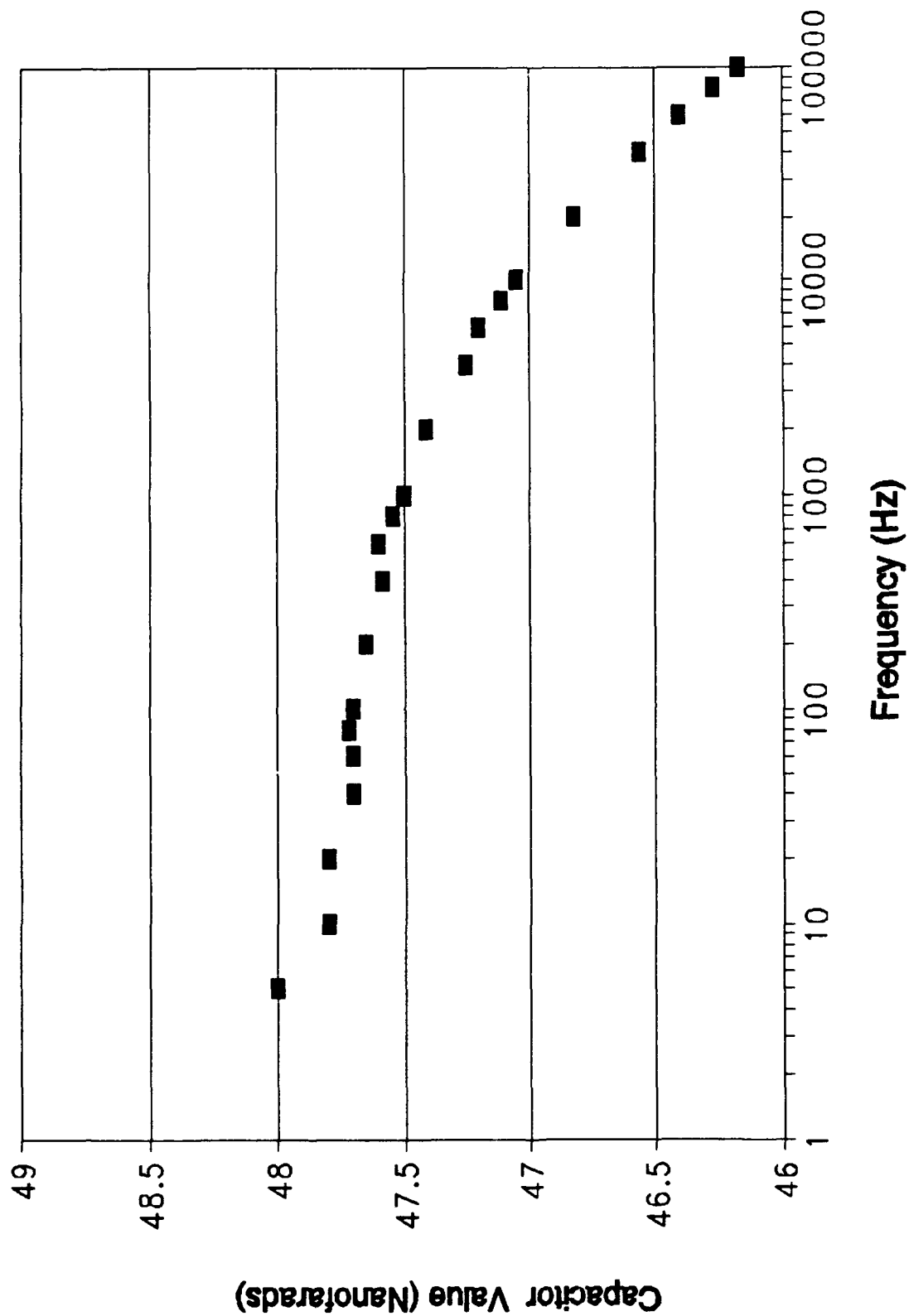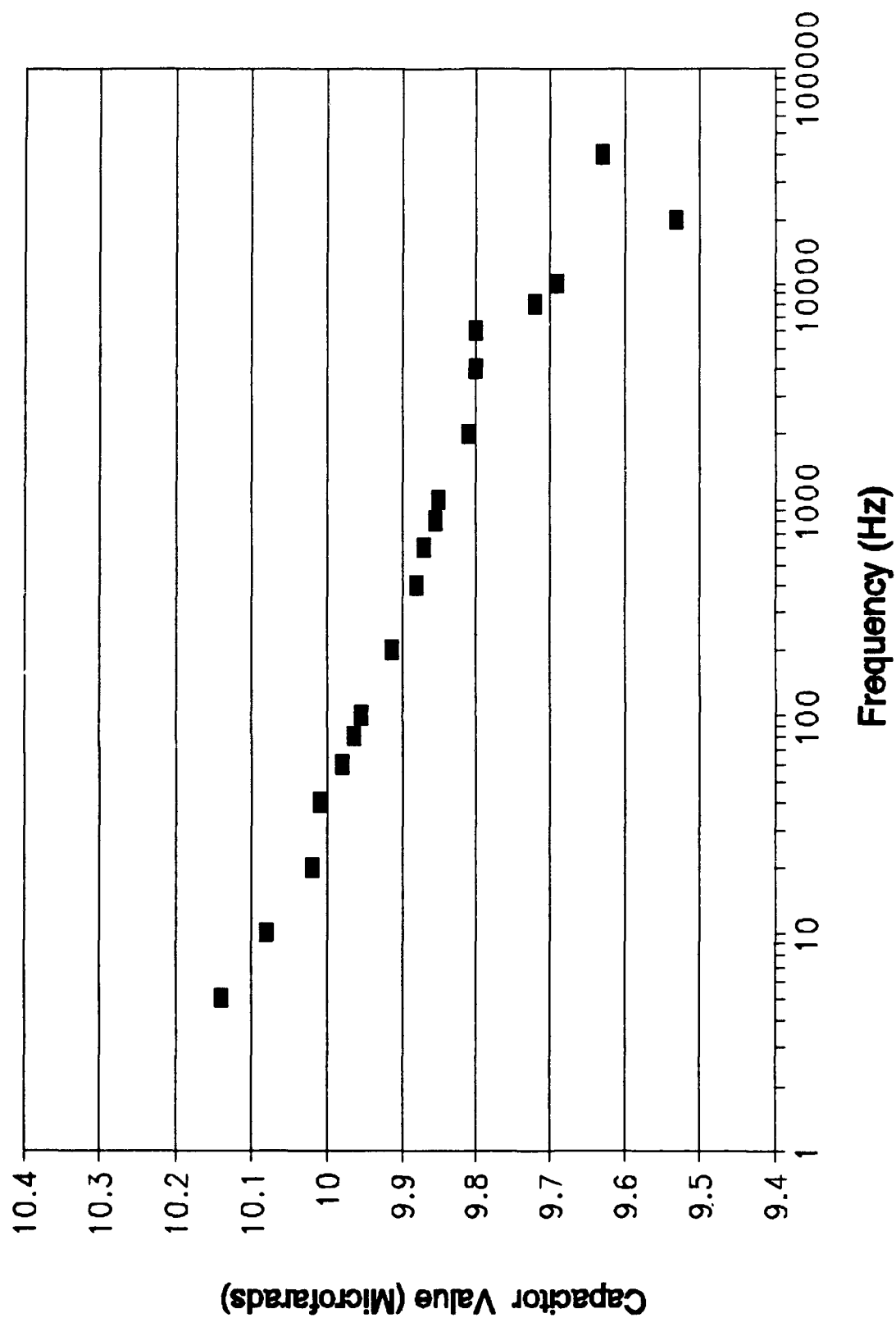
Figure D-36. Oldfield Circuit Design -- the Value of Capacitor C2 versus Frequency (Ideal Value -- 47 nf).
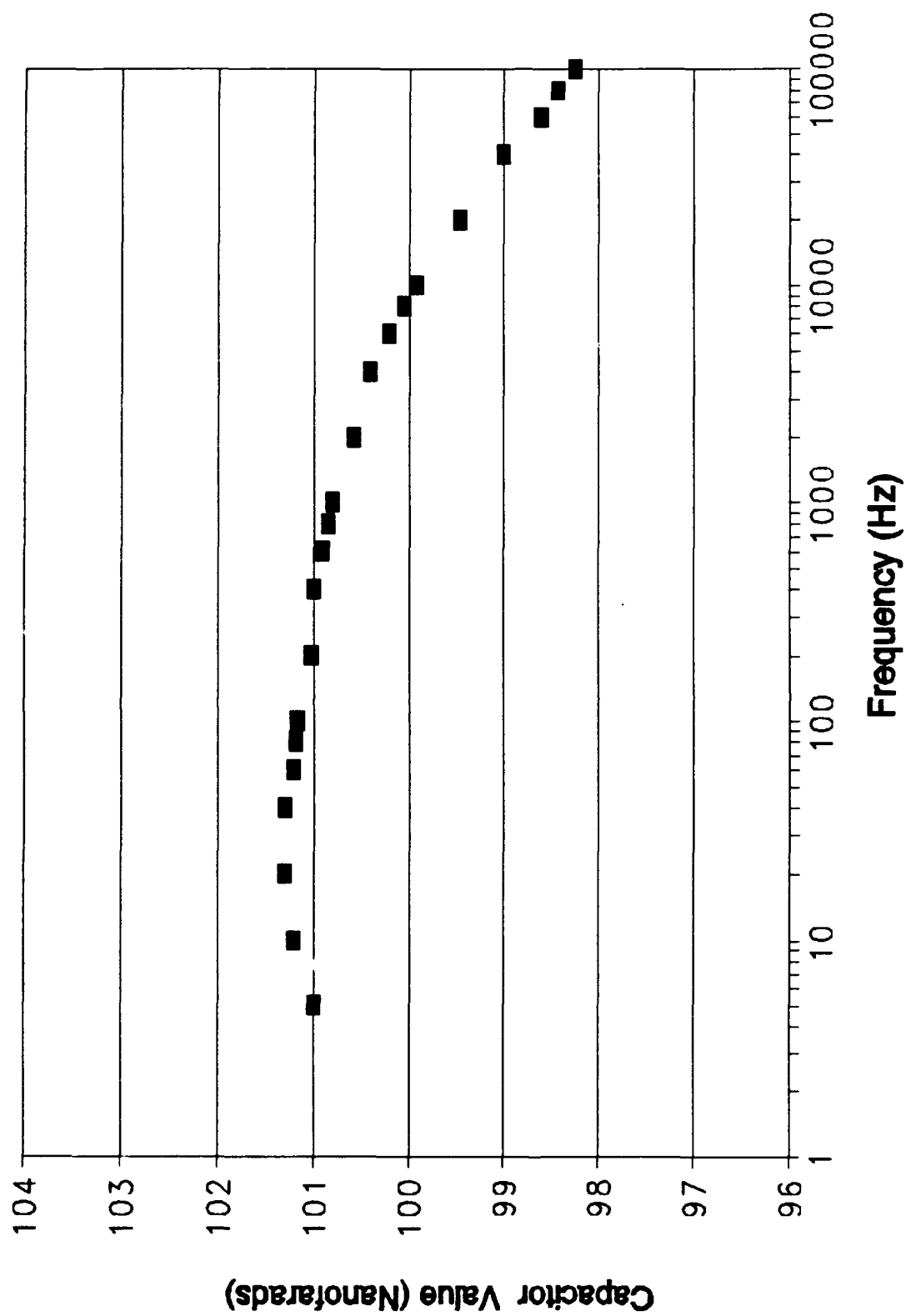
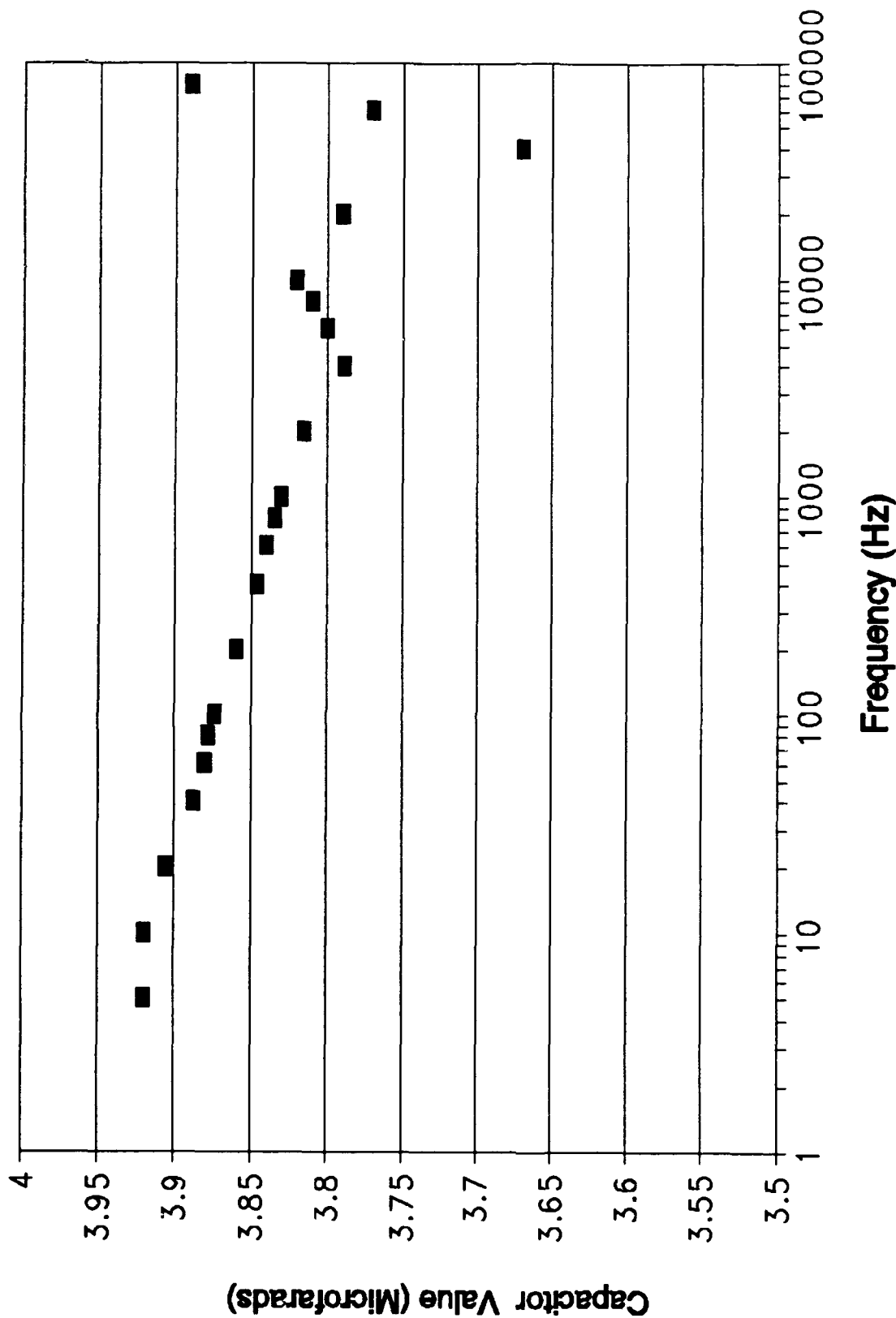Figure D-37. Oldfield Circuit Design -- the Value of Capacitor C3 versus Frequency (Ideal Value -- 100 nf).
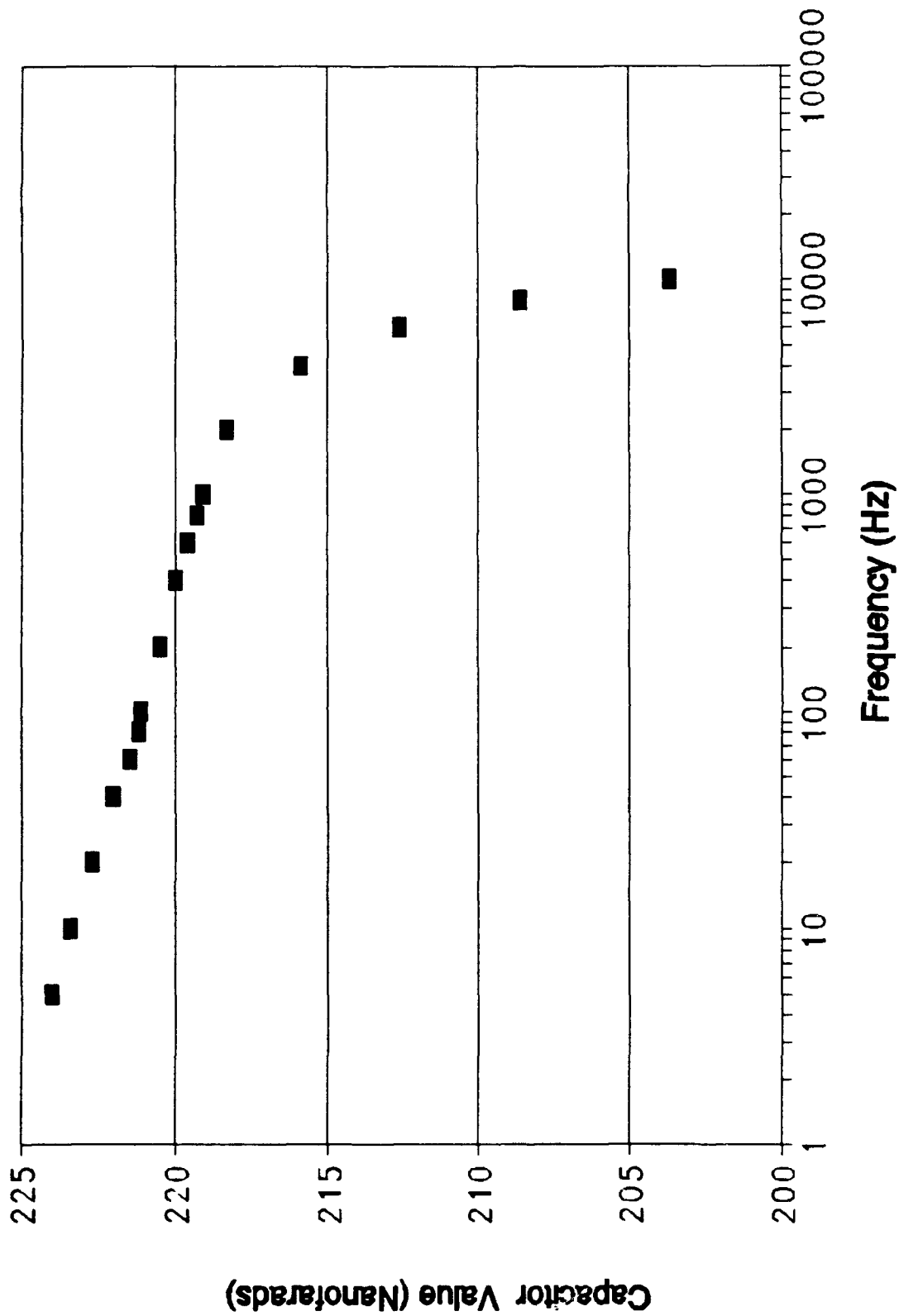
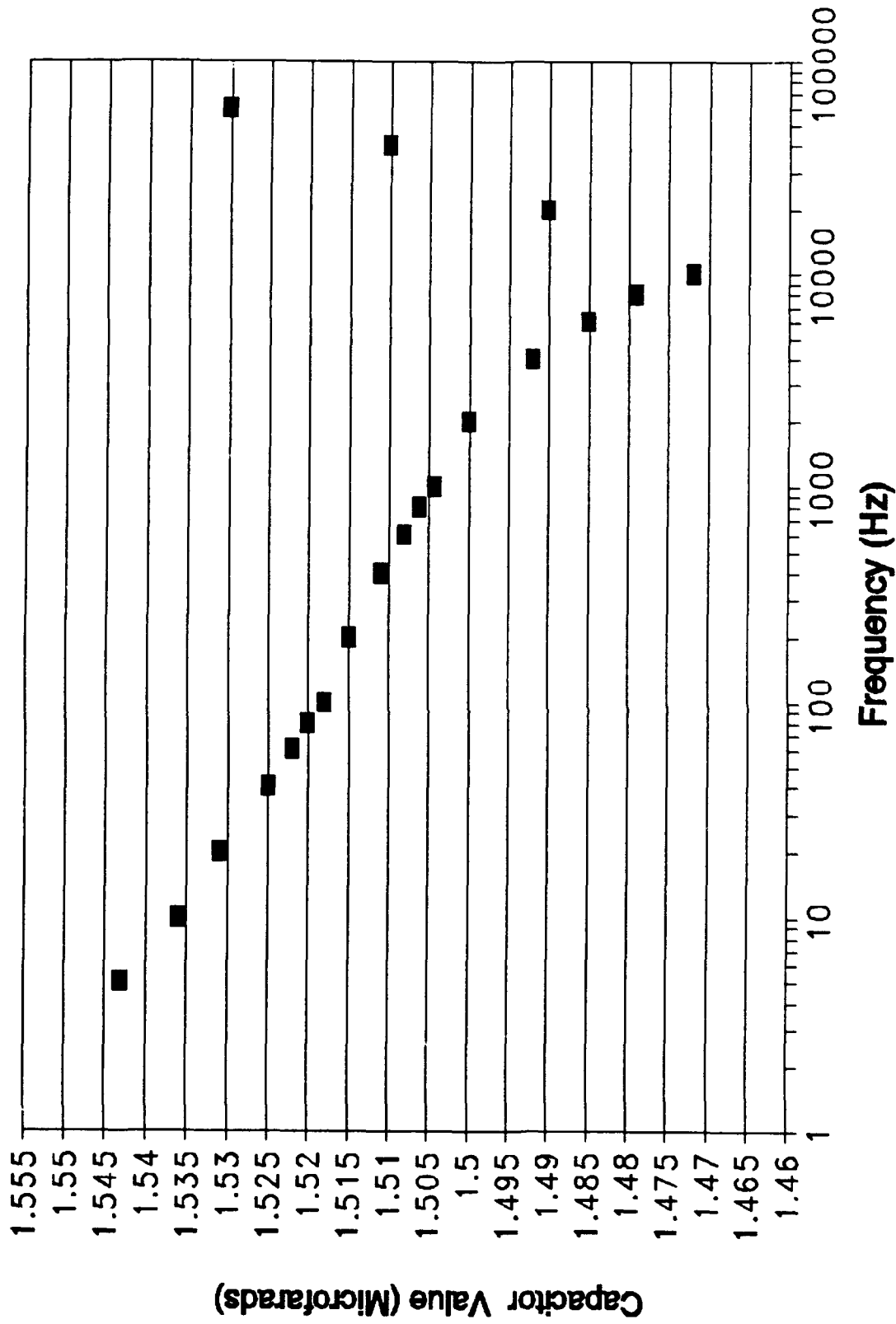Figure D-38. Oldfield Circuit Design -- the Value of Capacitor C4 versus Frequency (Ideal Value -- 220 nf).
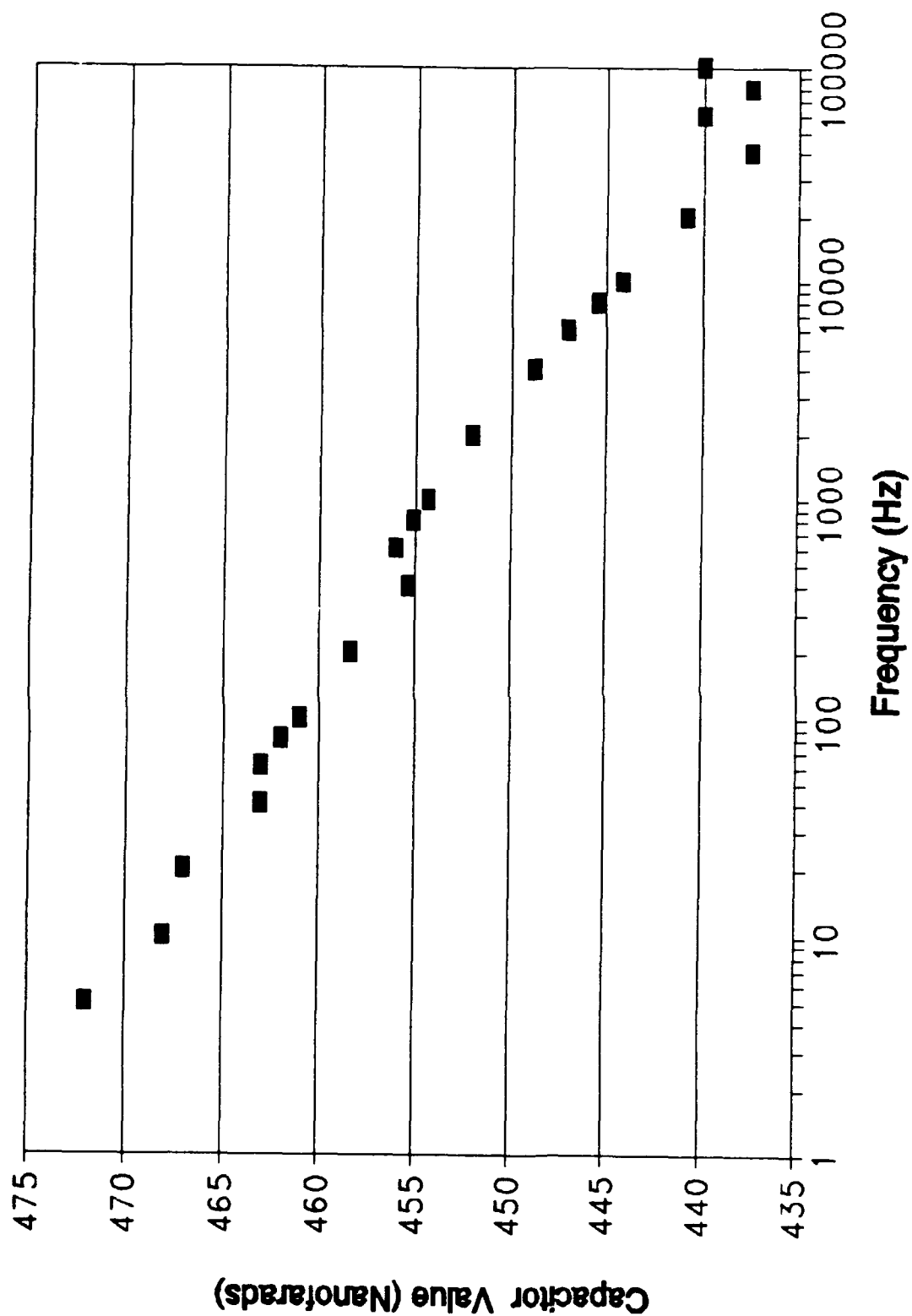
Figure D-39. Oldfield Circuit Design -- the Value of
Capacitor C5 versus Frequency
(Ideal Value -- 470 nf).
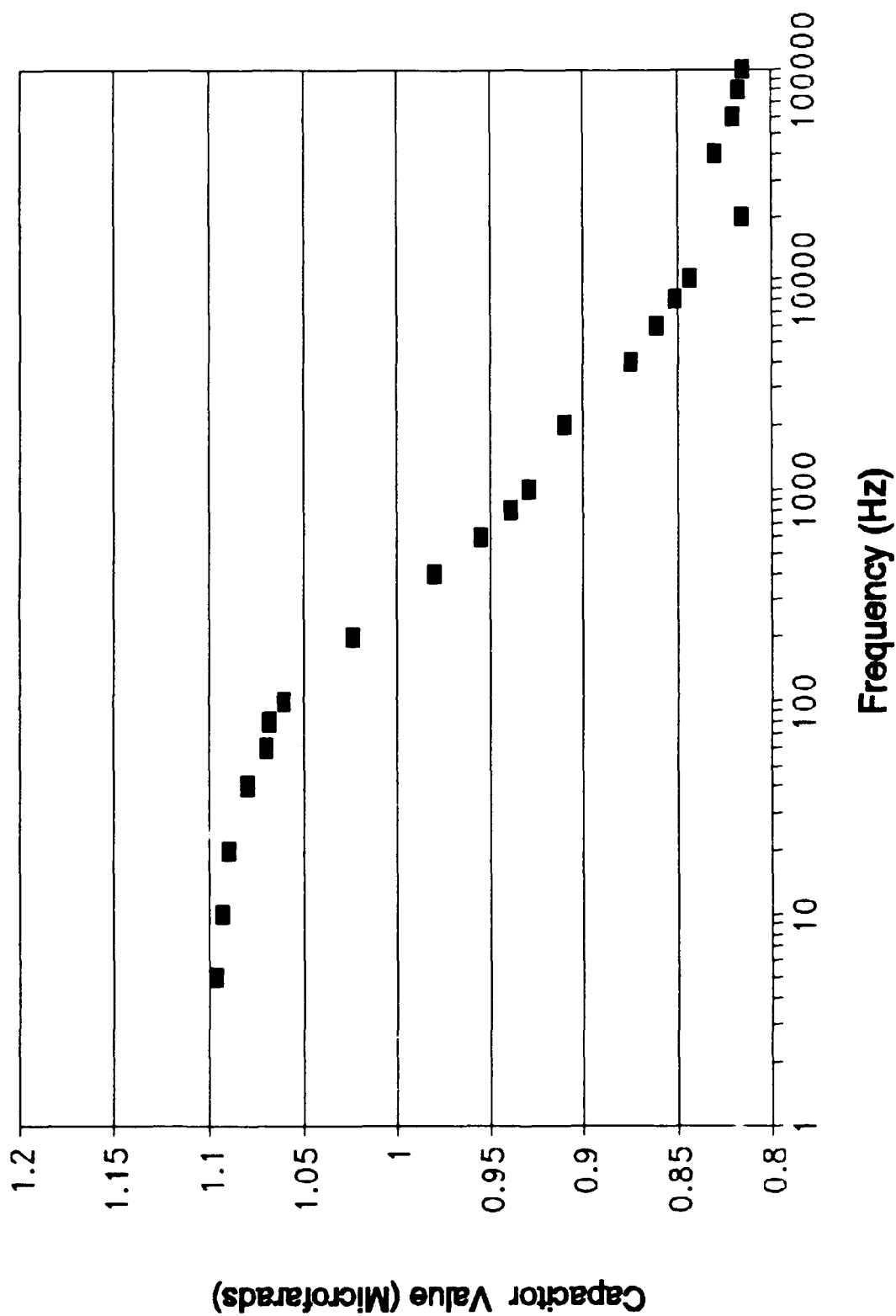
Figure D-40. Oldfield Circuit Design -- the Value of Capacitor C6 versus Frequency (Ideal Value -- 1.0 µf).
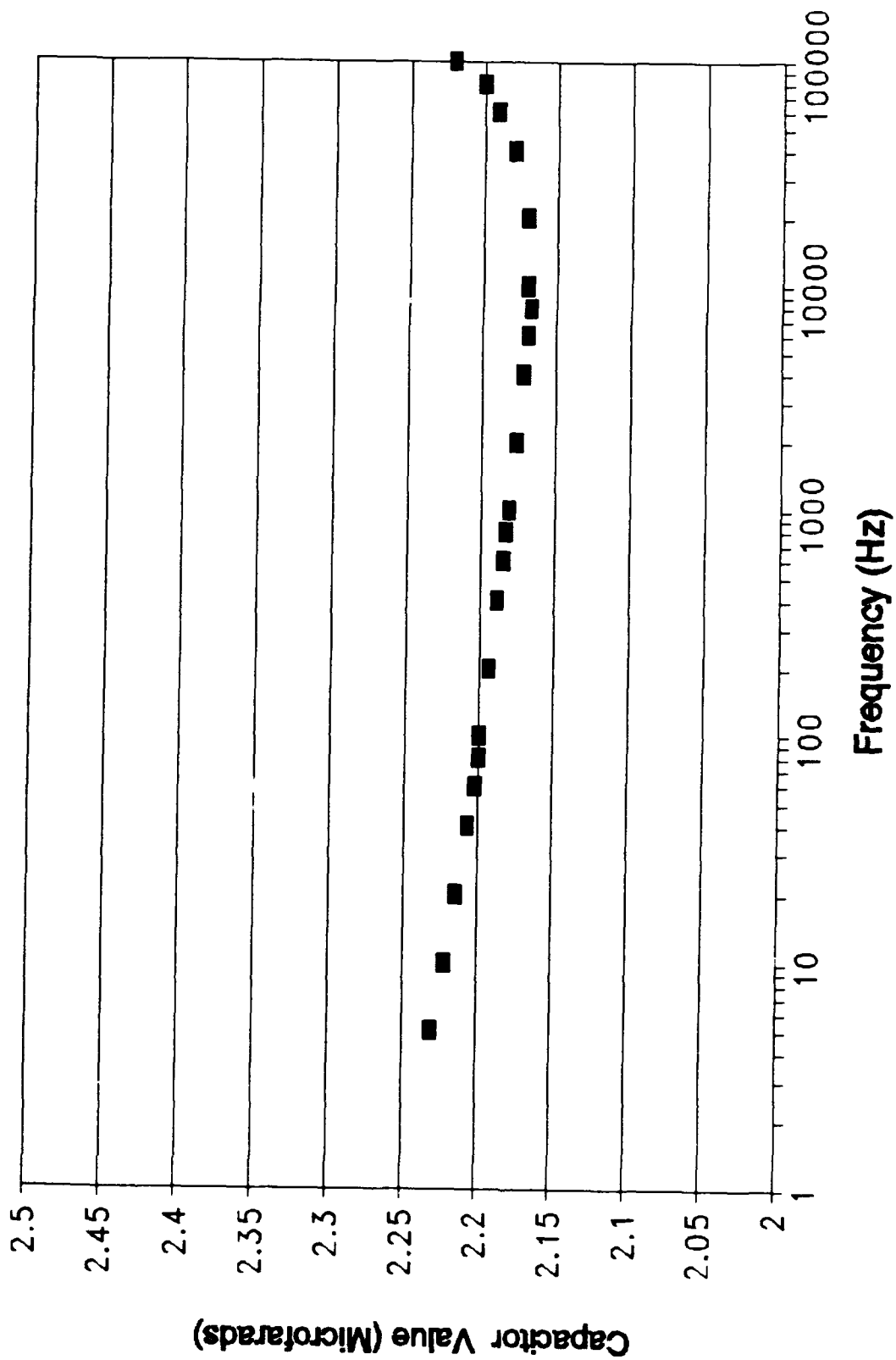
Figure D-41. Oldfield Circuit Design -- the Value of
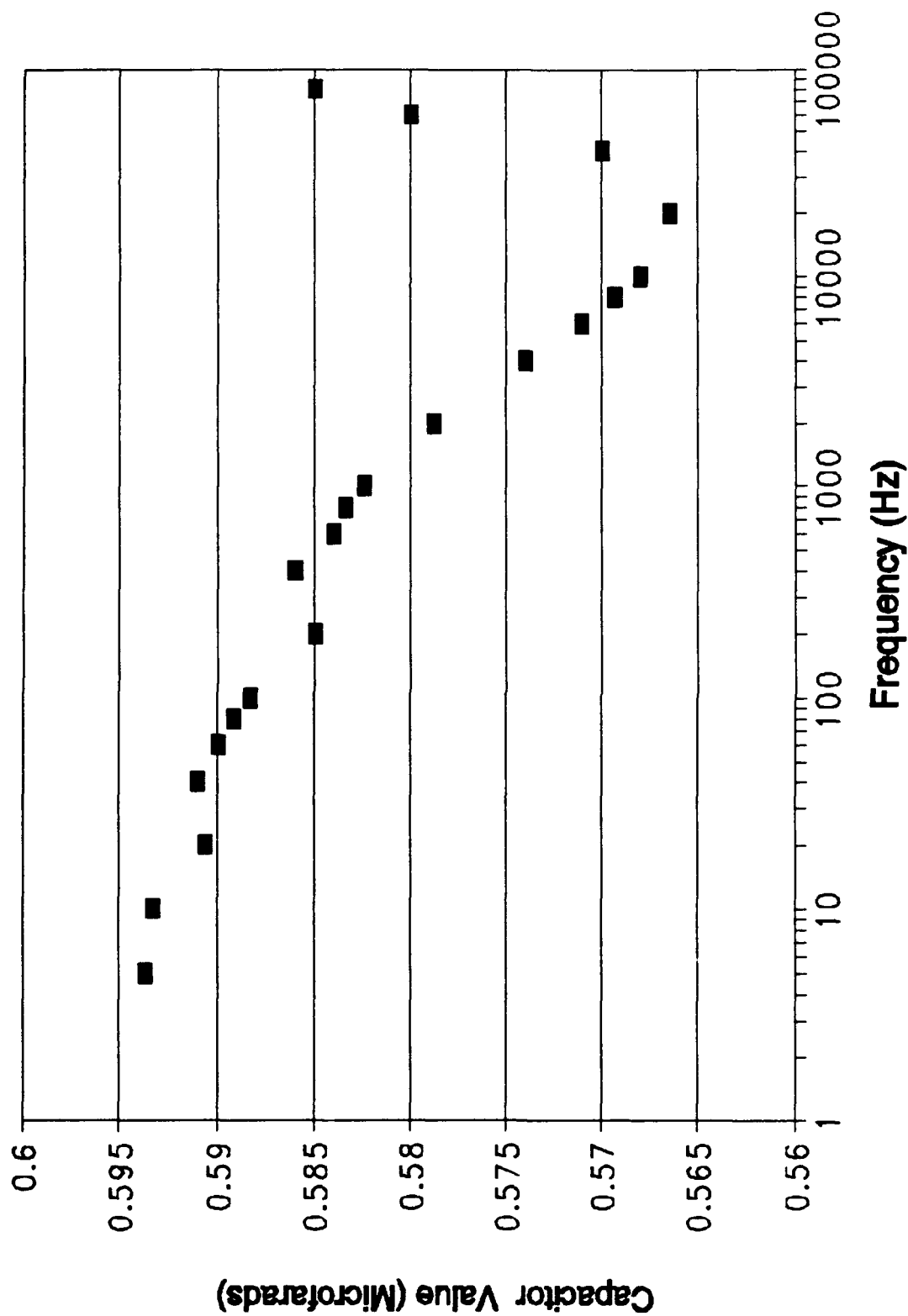Capacitor C7 versus Frequency
(Ideal Value -- 2.2 µf).
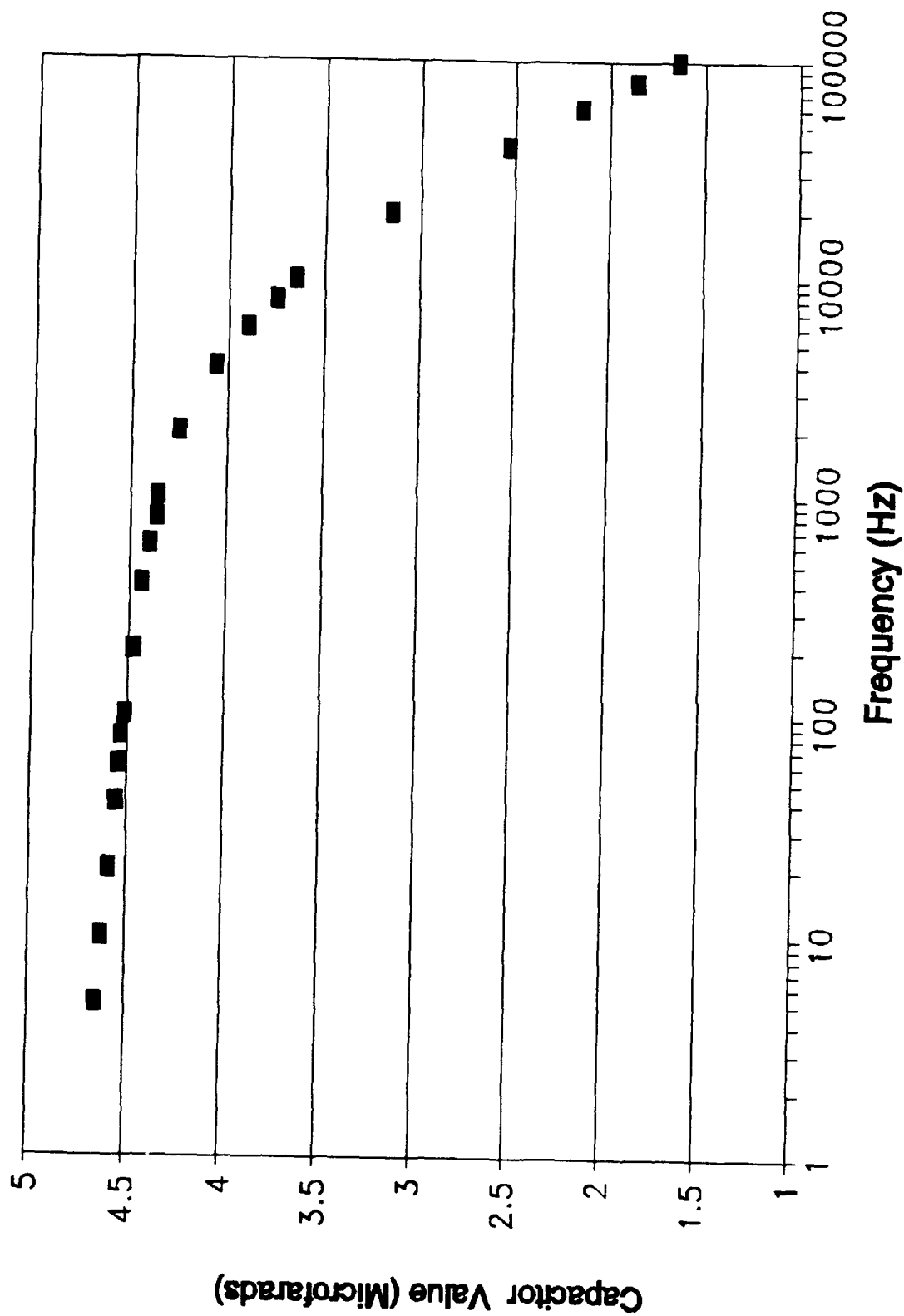
Figure D-42. Oldfield Circuit Design -- the Value of Capacitor C8 versus Frequency (Ideal Value -- 4.7 µf).
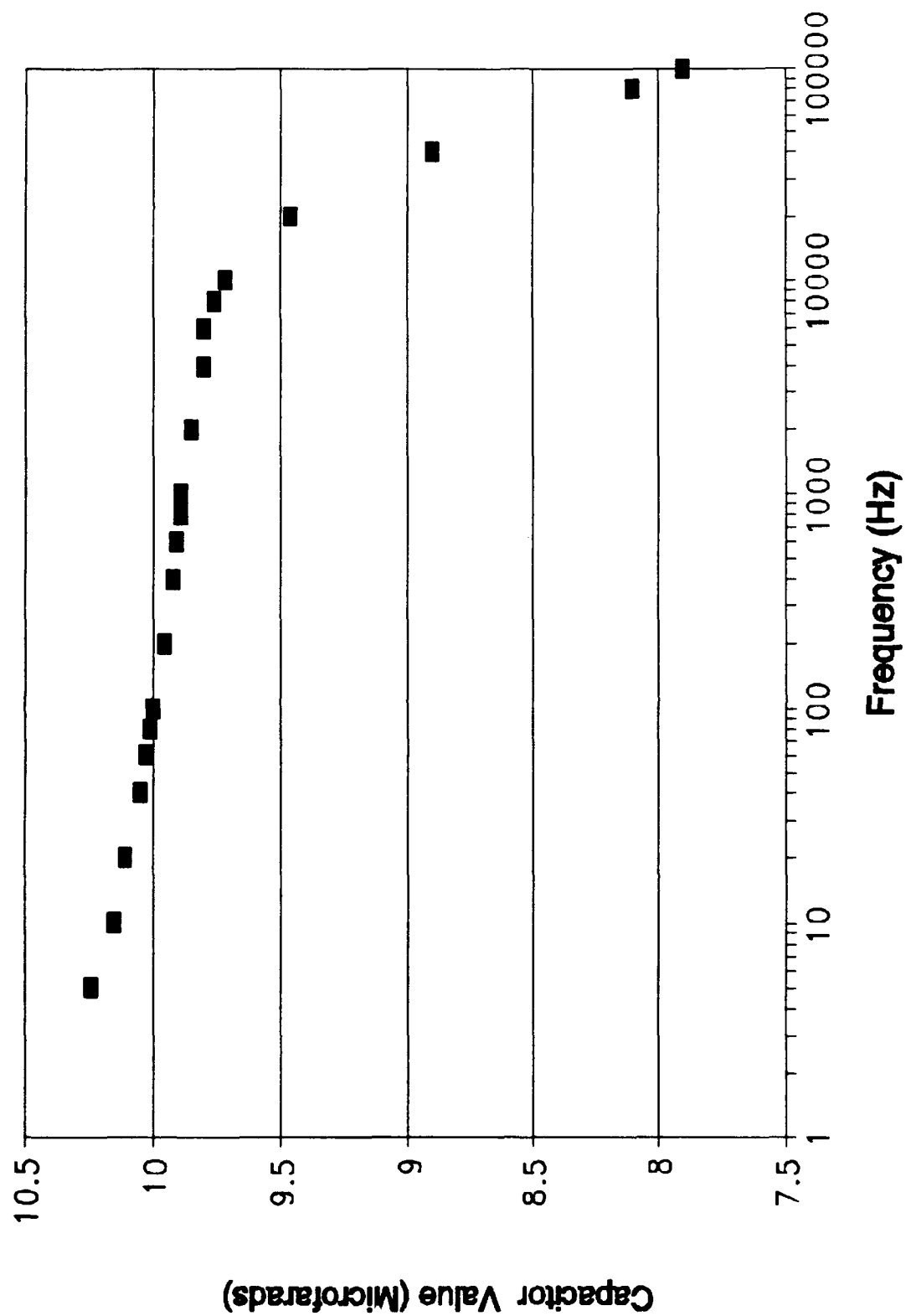
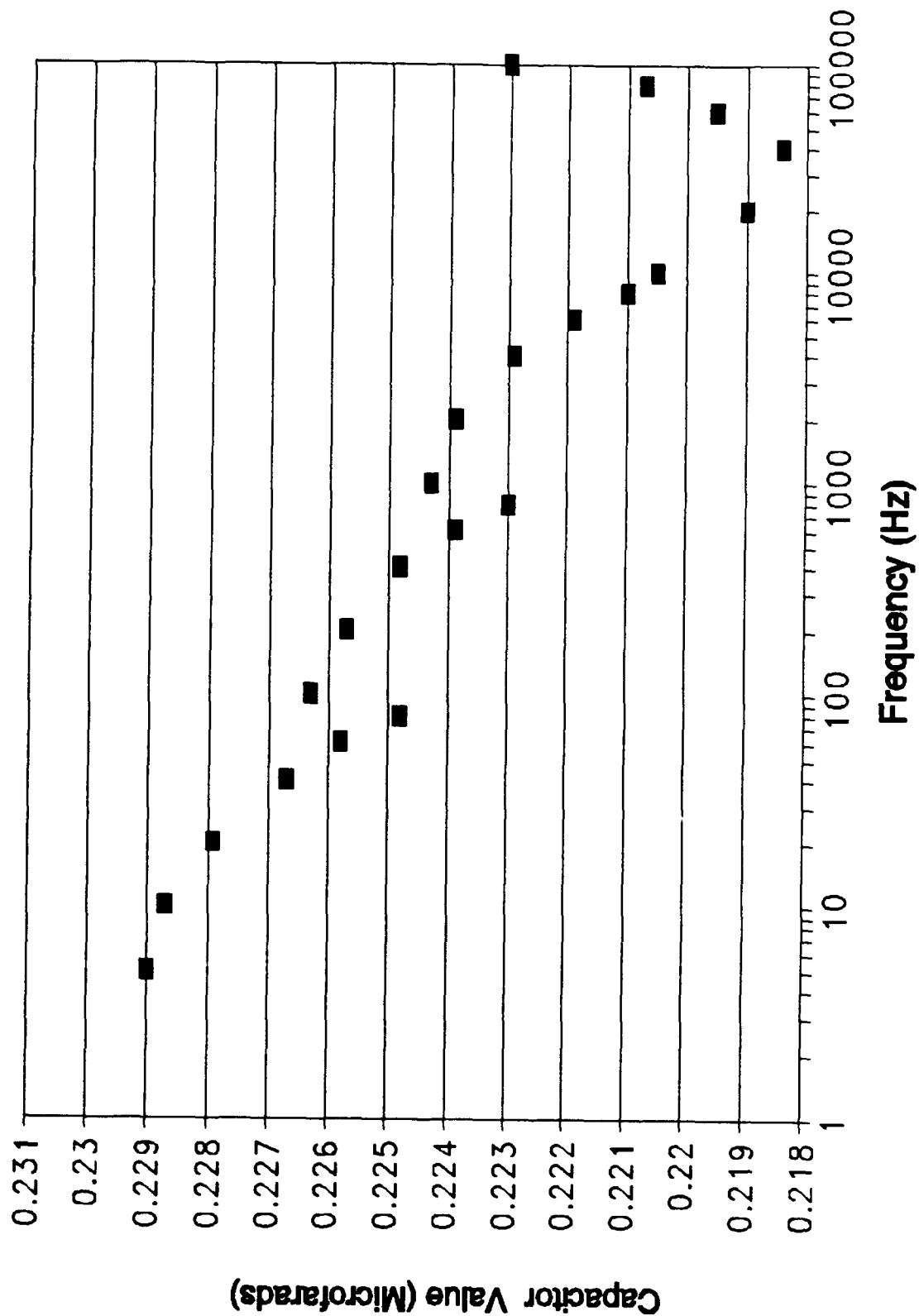Figure D-43. Oldfield Circuit Design -- the Value of
Capacitor C9 versus Frequency
(Ideal Value -- 10 µf).

Appendix E

Oldham And Oldfield Integrated Circuit Technology

Component Value

Variations Versus Frequency Results

(Oldham - Hybrid; Oldfield - Surface Mount)

The measured integrated circuit technology and hybrid component value variations versus frequency are presented in this appendix. The results are documented in four sections. The first two sections document the component value variations versus frequency for the Oldham hybrid circuit design option. Section 1 reports the resistor values, and Section 2 reports the capacitor values. Correspondingly, Sections 3 and 4 document the resistor and capacitor values for the Oldfield surface mount circuit option.

Section 1

Oldham Hybrid Resistor Component Value
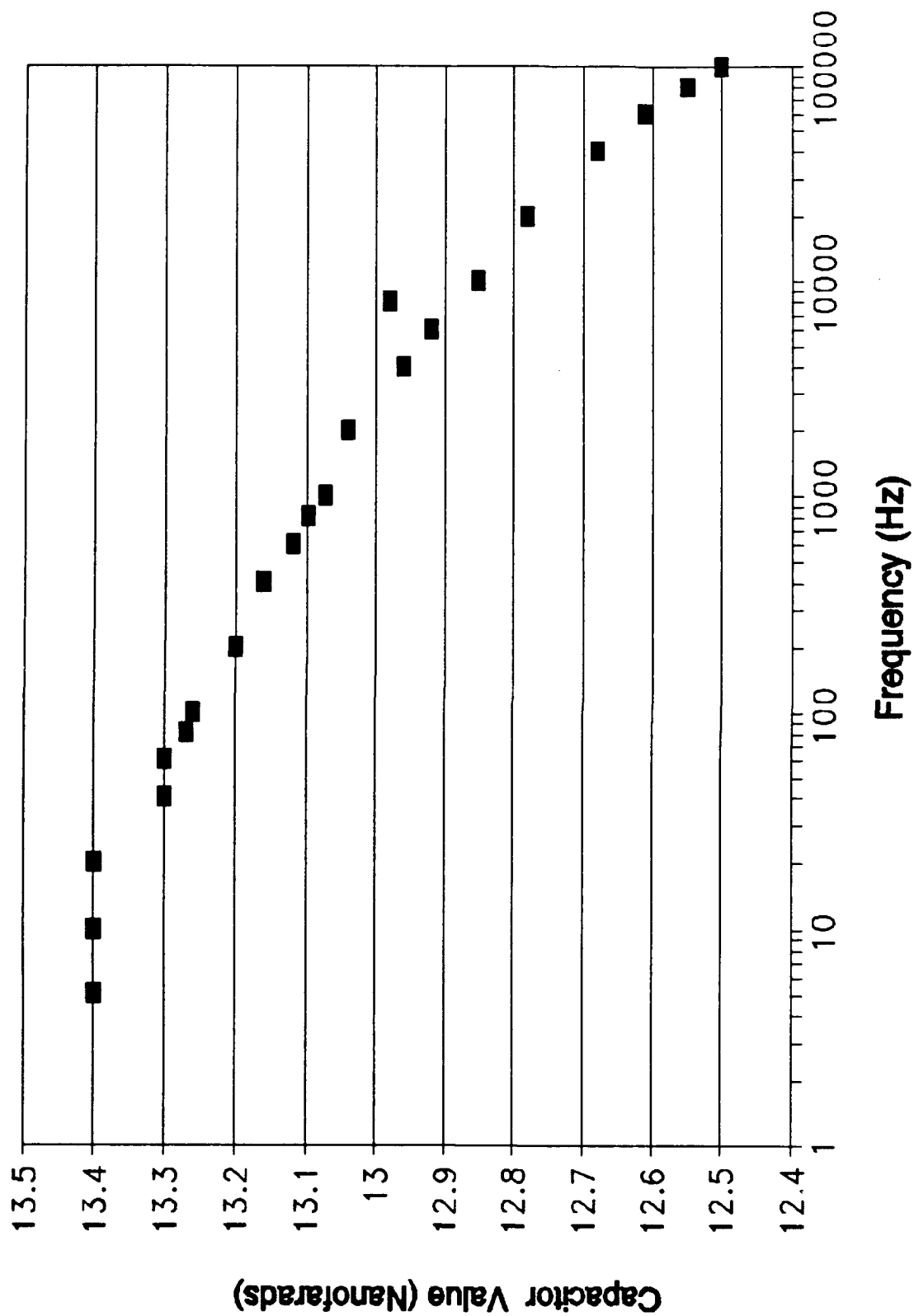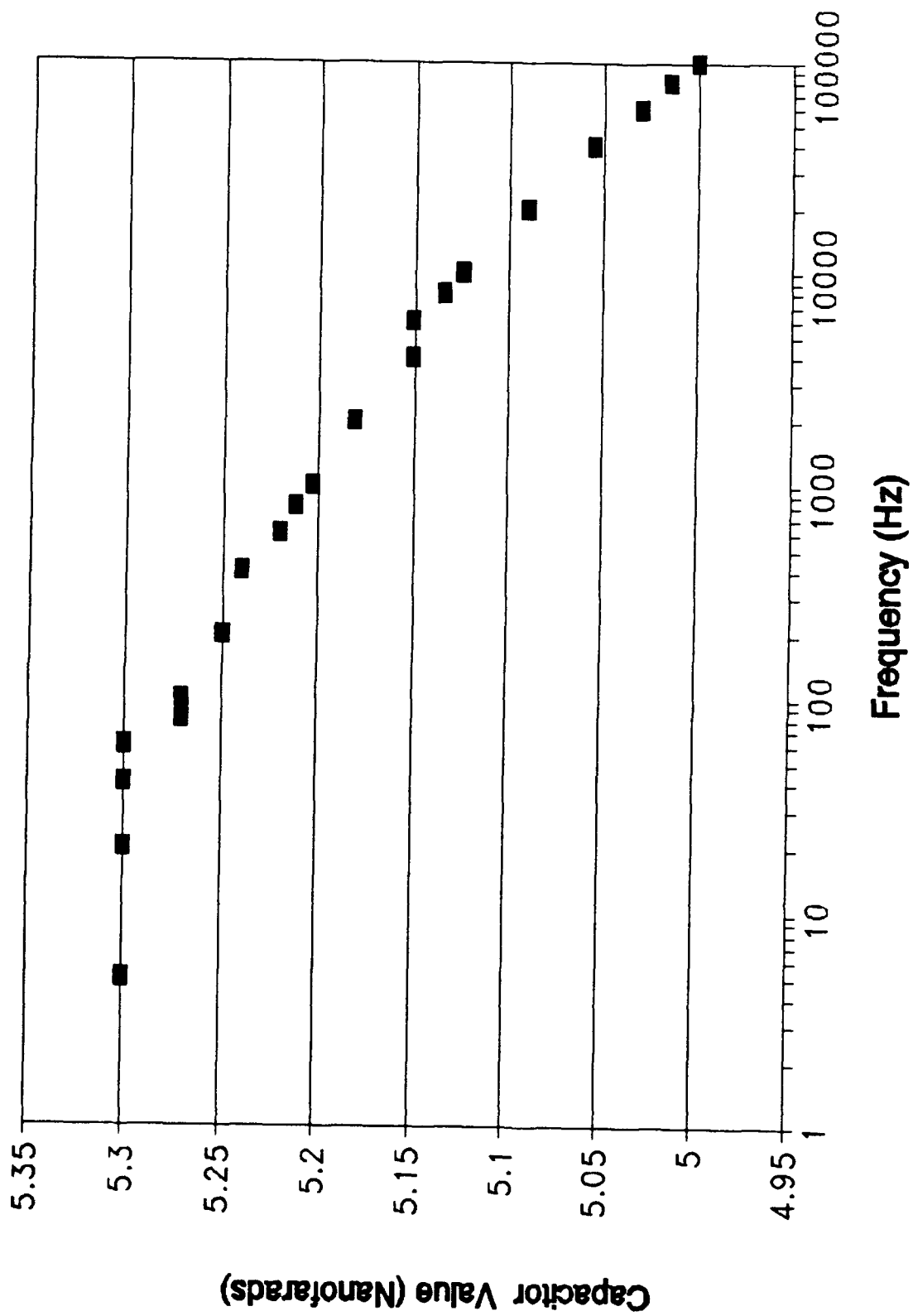
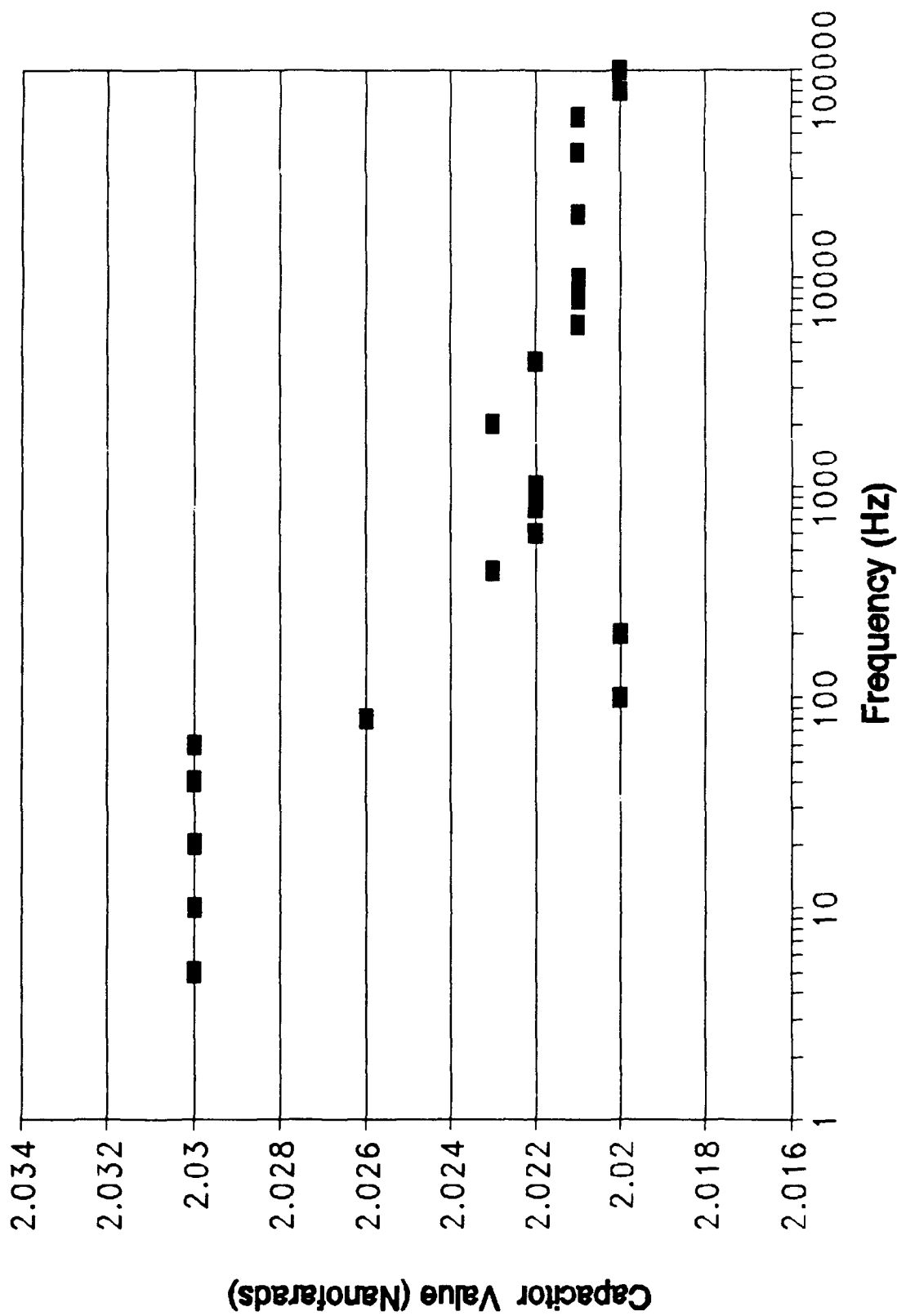## Variations Versus Frequency

Results

E-3

Figure E-1. Oldham Circuit Design -- the Value of Resistor R0 versus Frequency (Ideal Value -- 68.99 Megohms).

Figure E-2. Oldham Circuit Design -- the Value of Resistor R1 versus Frequency (Ideal Value -- 25.4 Megohms).

Figure E-3. Oldham Circuit Design -- the Value of Resistor R2 versus Frequency (Ideal Value -- 9.85 Megohms).

Figure E-4. Oldham Circuit Design -- the Value of Resistor R3 versus Frequency (Ideal Value -- 3.83 Megohms).

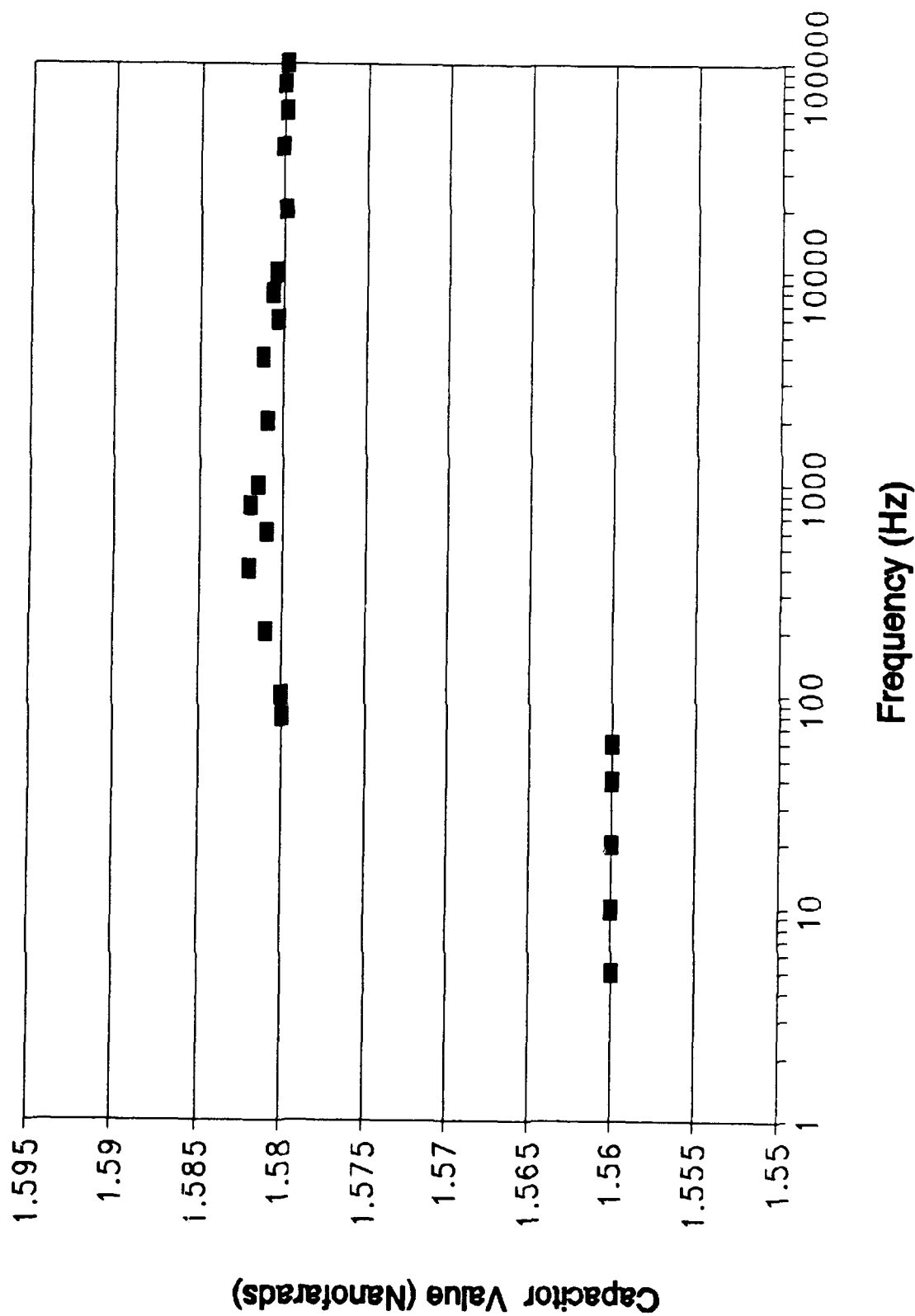Figure E-5. Oldham Circuit Design -- the Value of Resistor R4 versus Frequency (Ideal Value -- 1.488 Megohms).
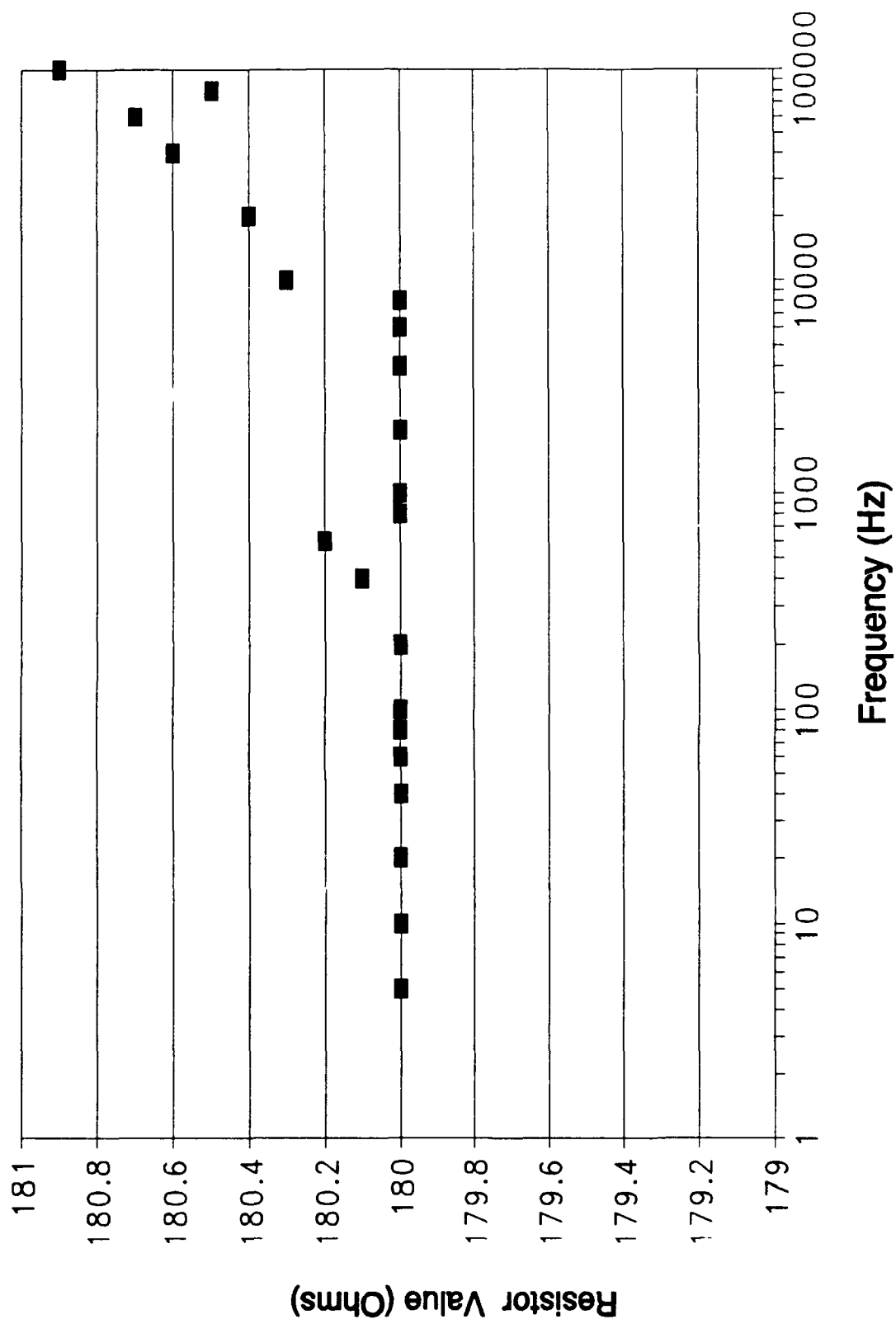
Figure E-6. Oldham Circuit Design -- the Value of Resistor R5 versus Frequency (Ideal Value -- 578.5 Kilohms).
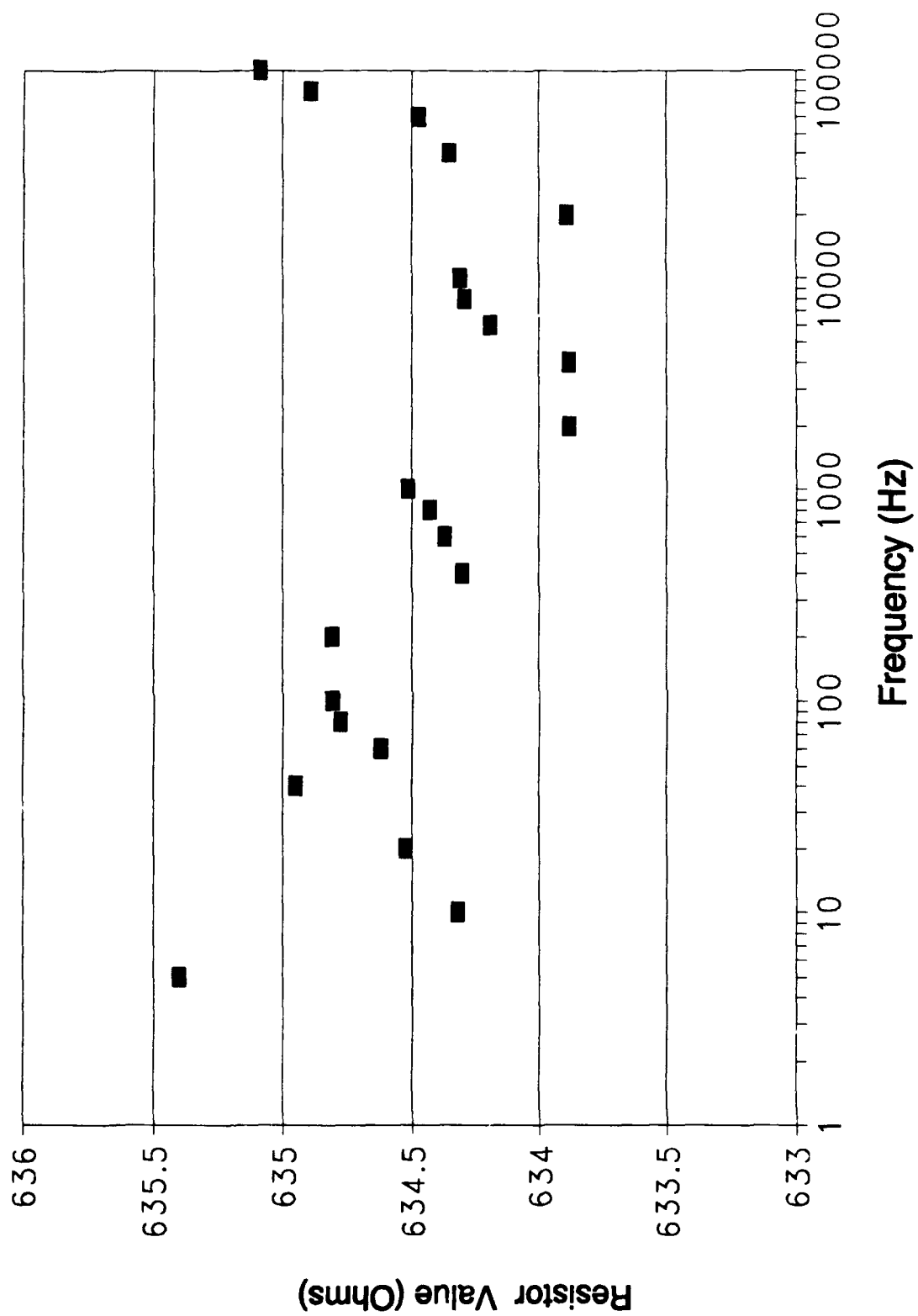
Figure E-7. Oldham Circuit Design -- the Value of Resistor R6 versus Frequency (Ideal Value -- 224.9 Kilohms).

Figure E-8. Oldham Circuit Design -- the Value of Resistor R7 versus Frequency (Ideal Value -- 87.4 Kilohms).

Figure E-9. Oldham Circuit Design -- the Value of Resistor R8 versus Frequency (Ideal Value -- 33.97 Kilohms).
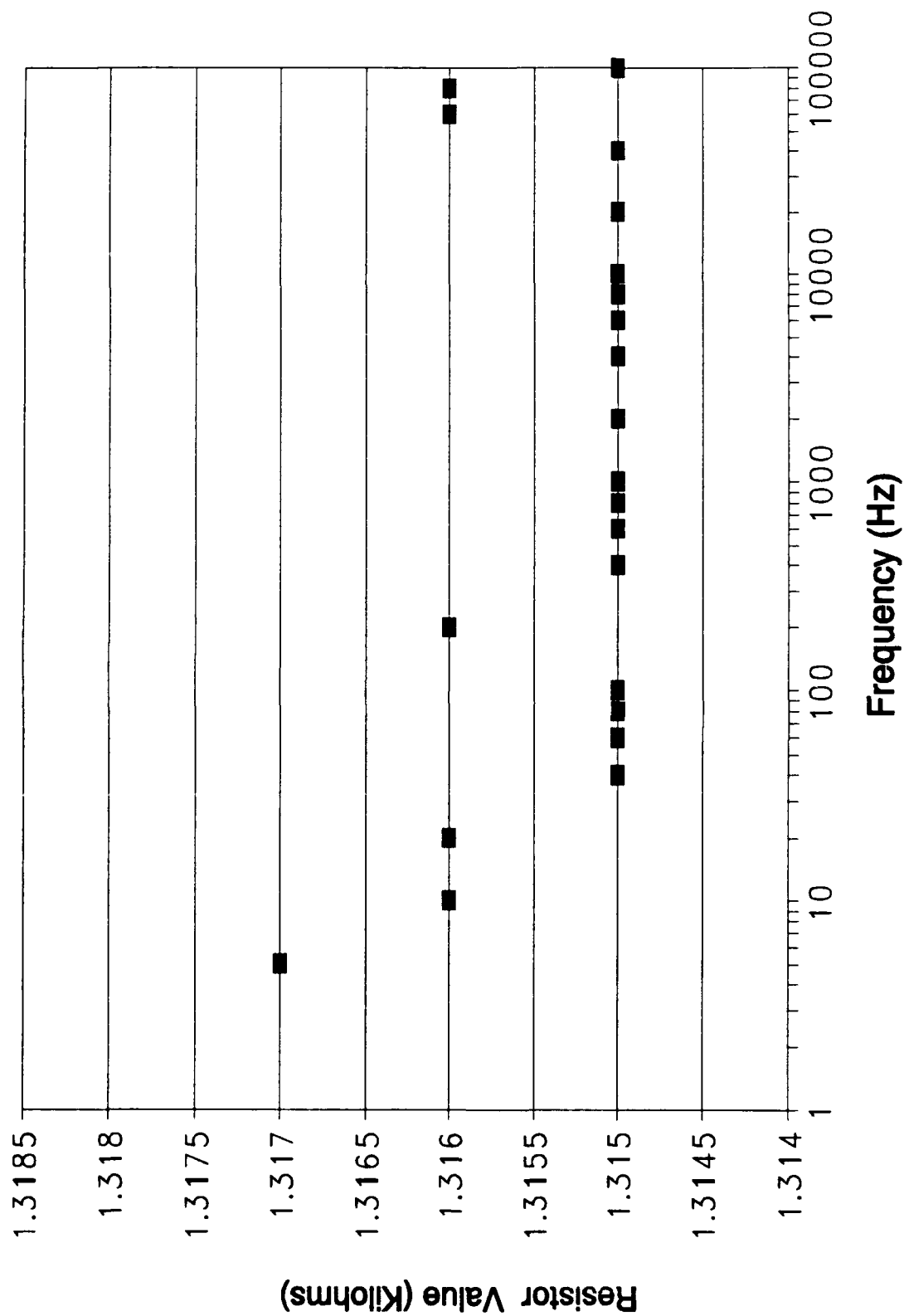
Figure E-10. Oldham Circuit Design -- the Value of
Resistor R9 versus Frequency
(Ideal Value -- 13.21 Kilohms).

Figure E-11. Oldham Circuit Design -- the Value of
Resistor R10 versus Frequency
(Ideal Value -- 5.133 Kilohms).

Figure E-12. Oldham Circuit Design -- the Value of Resistor R11 versus Frequency (Ideal Value -- 997.5 Ohms).

Figure E-13.   Oldham Circuit Design -- the Value of
Resistor R12 versus Frequency
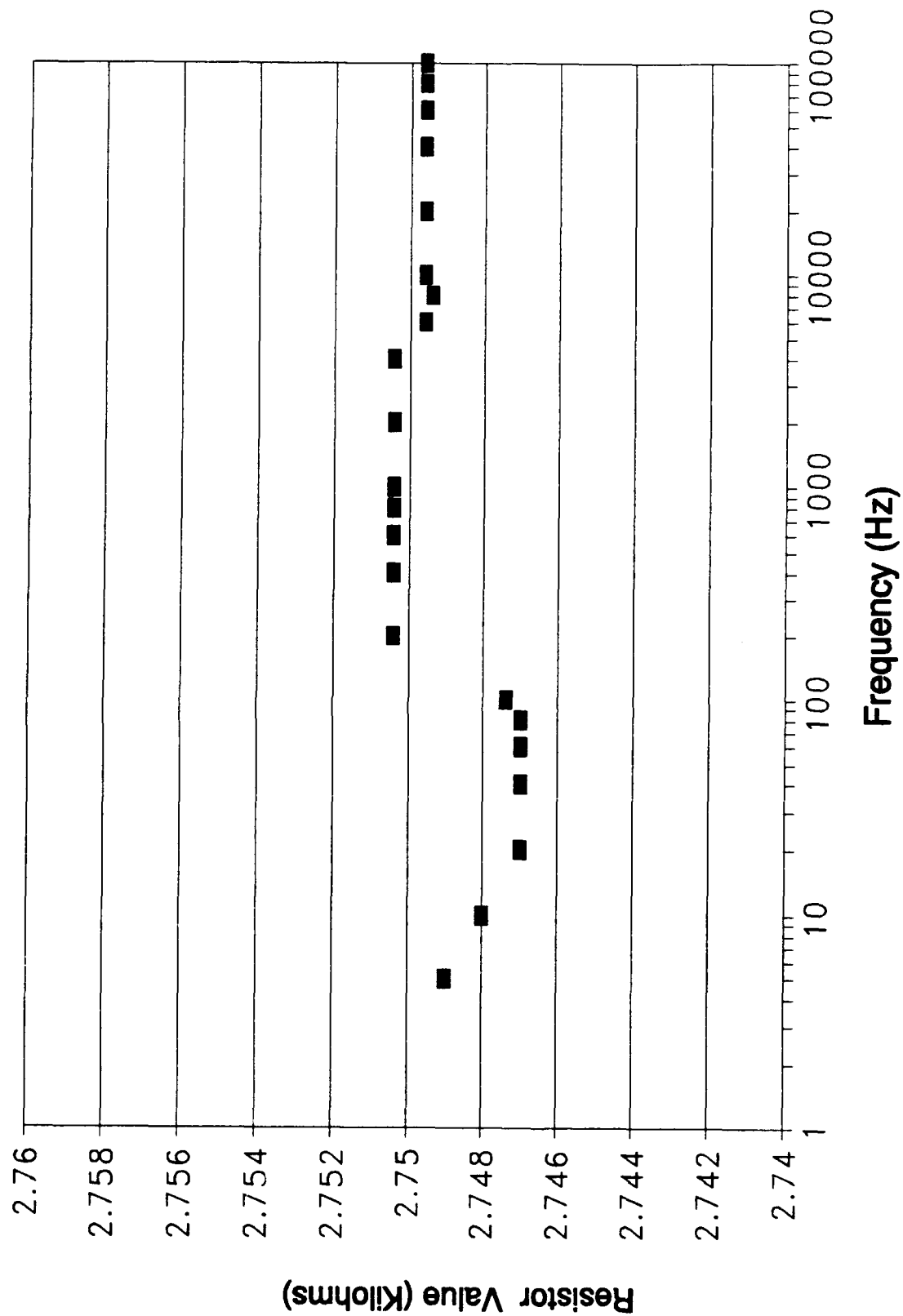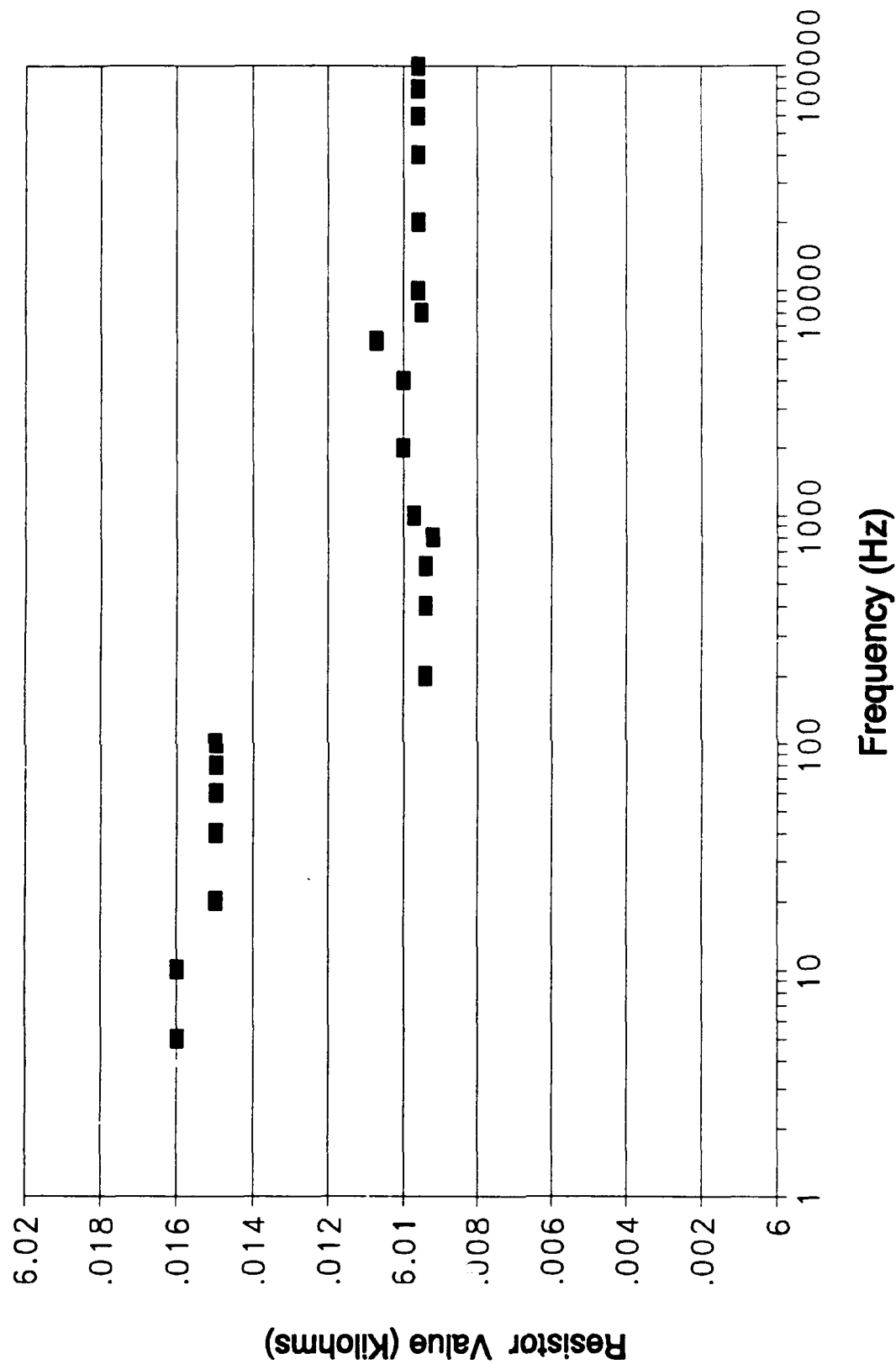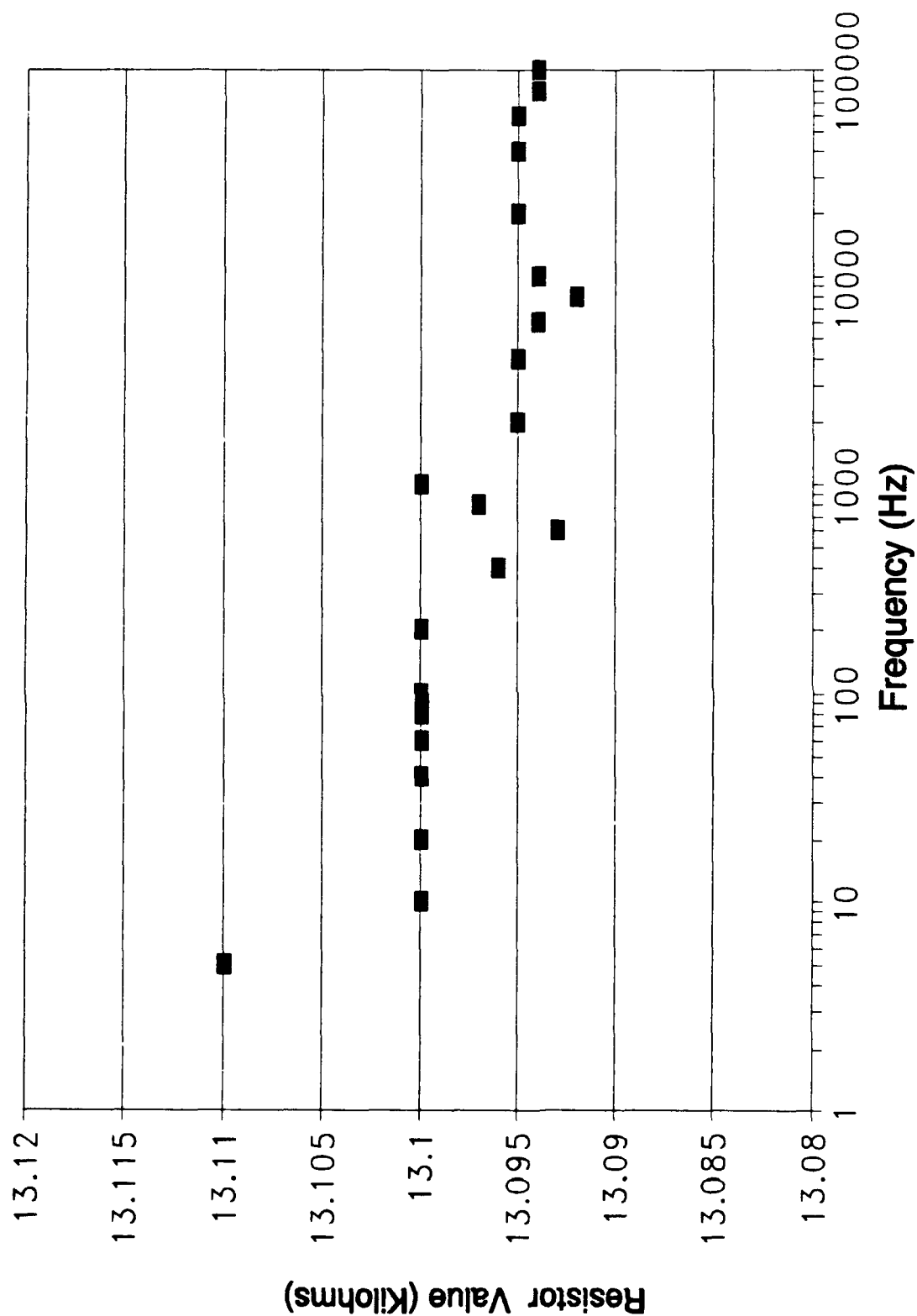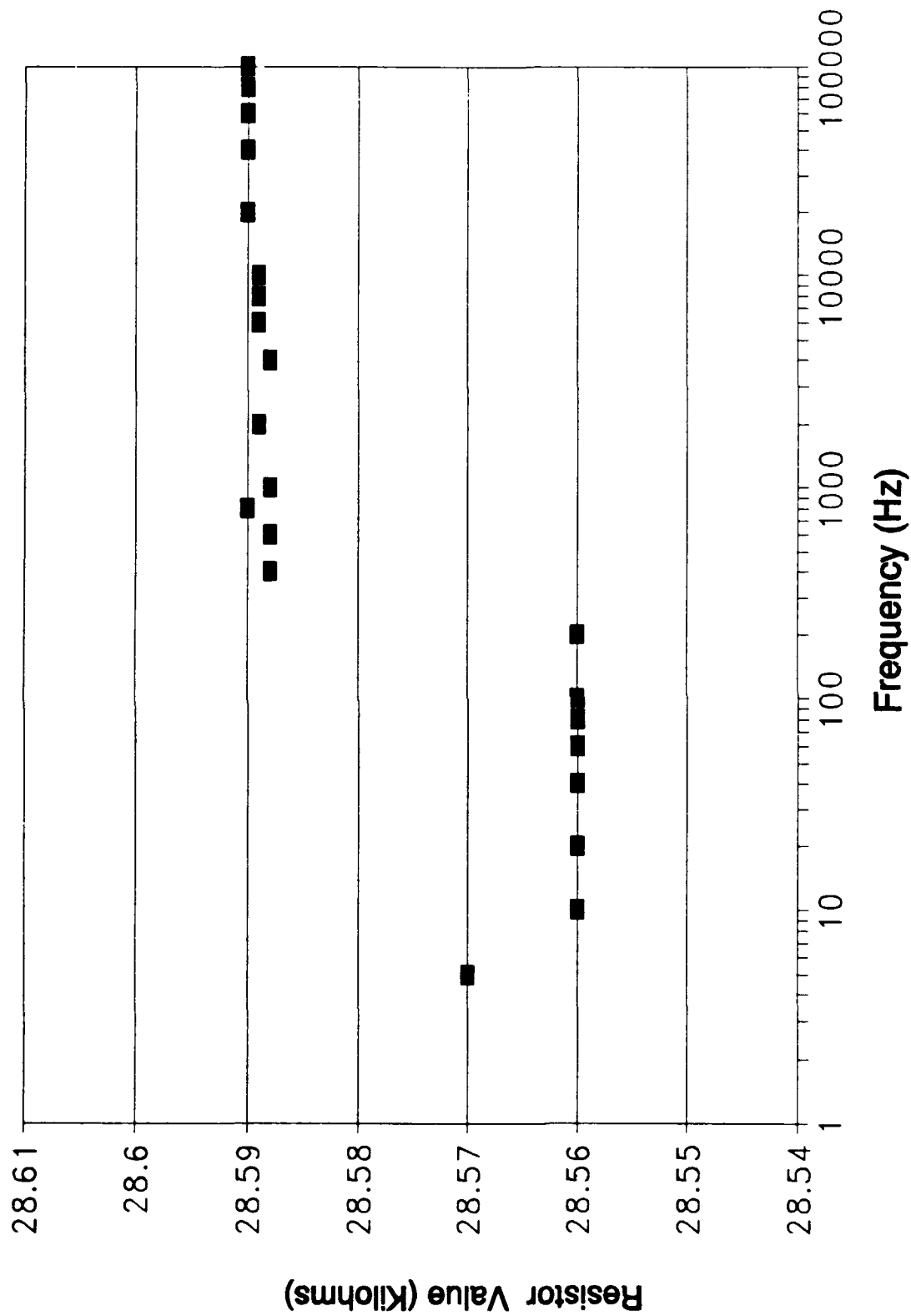(Ideal Value -- 2.11 Kilohms).

Section 2

Oldham Hybrid Capacitor Component Value

Variations Versus Frequency

Results

Figure E-14. Oldham Circuit Design -- the Value of Capacitor C0 versus Frequency (Ideal Value -- 16.51 µf).

Figure E-15. Oldham Circuit Design -- the Value of Capacitor C1 versus Frequency (Ideal Value -- 10.0 µf).

Figure E-16. Oldham Circuit Design -- the Value of Capacitor C2 versus Frequency (Ideal Value -- 3.88 µf).

Figure E-17. Oldham Circuit Design -- the Value of Capacitor C3 versus Frequency (Ideal Value -- 1.514 μf).

Figure E-18. Oldham Circuit Design -- the Value of Capacitor C4 versus Frequency (Ideal Value -- .5873 μf).

Figure E-19. Oldham Circuit Design -- the Value of
Capacitor C5 versus Frequency
(Ideal Value -- .2283 µf).
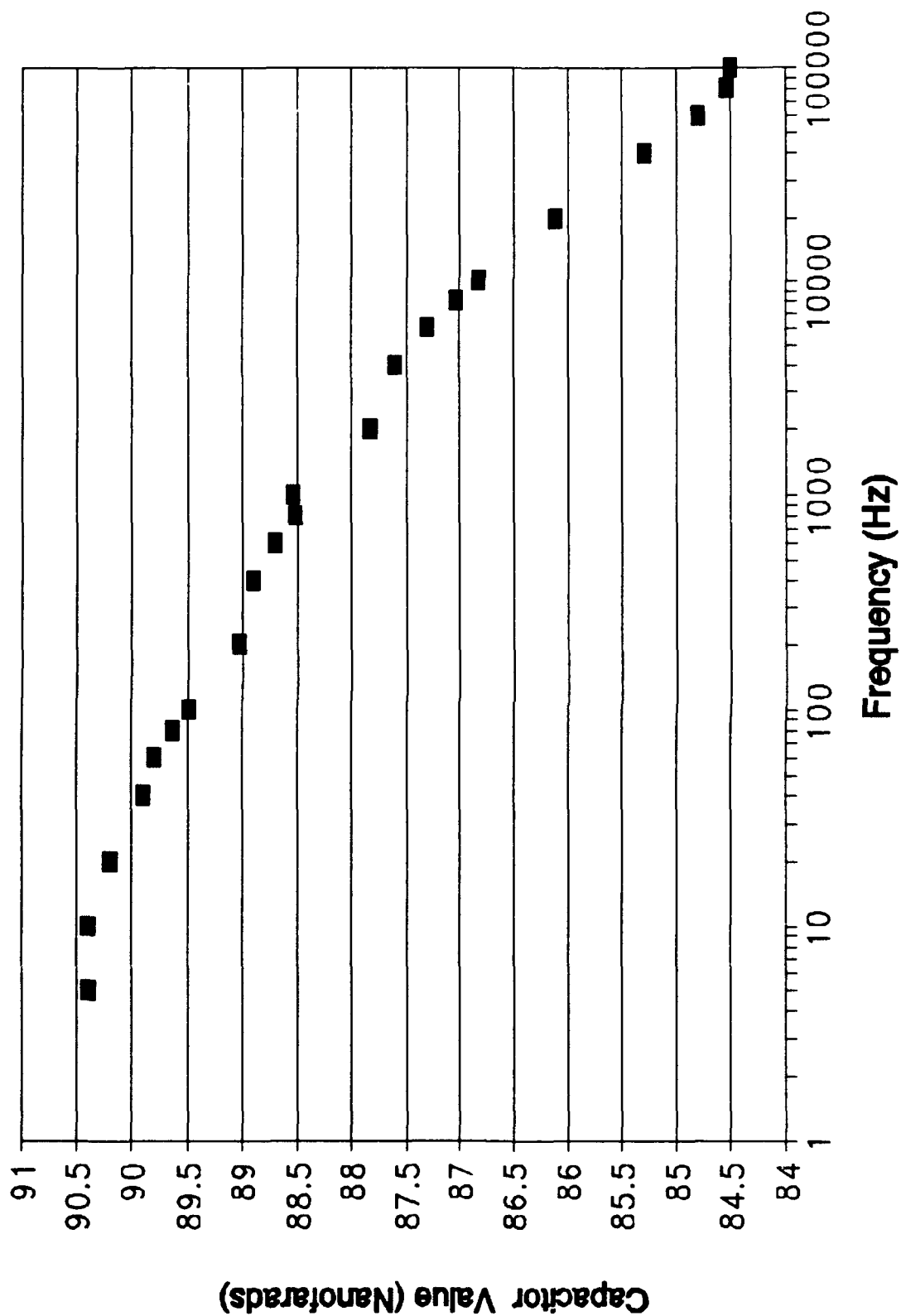
Figure E-20. Oldham Circuit Design -- the Value of Capacitor C6 versus Frequency (Ideal Value -- 88.73 nf).
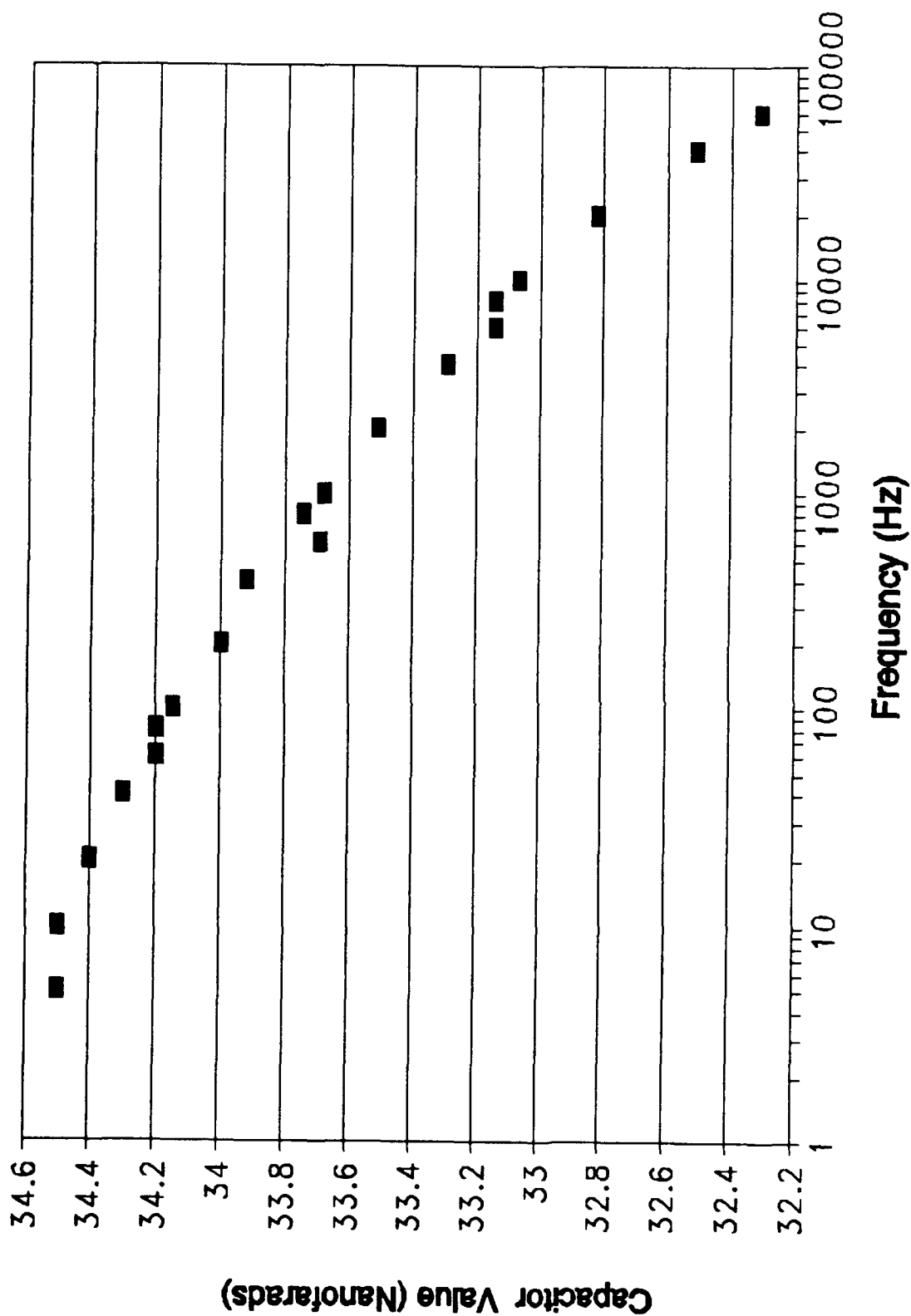
Figure E-21. Oldham Circuit Design -- the Value of Capacitor C7 versus Frequency (Ideal Value -- 34.49 nf).

Figure E-22. Oldham Circuit Design -- the Value of
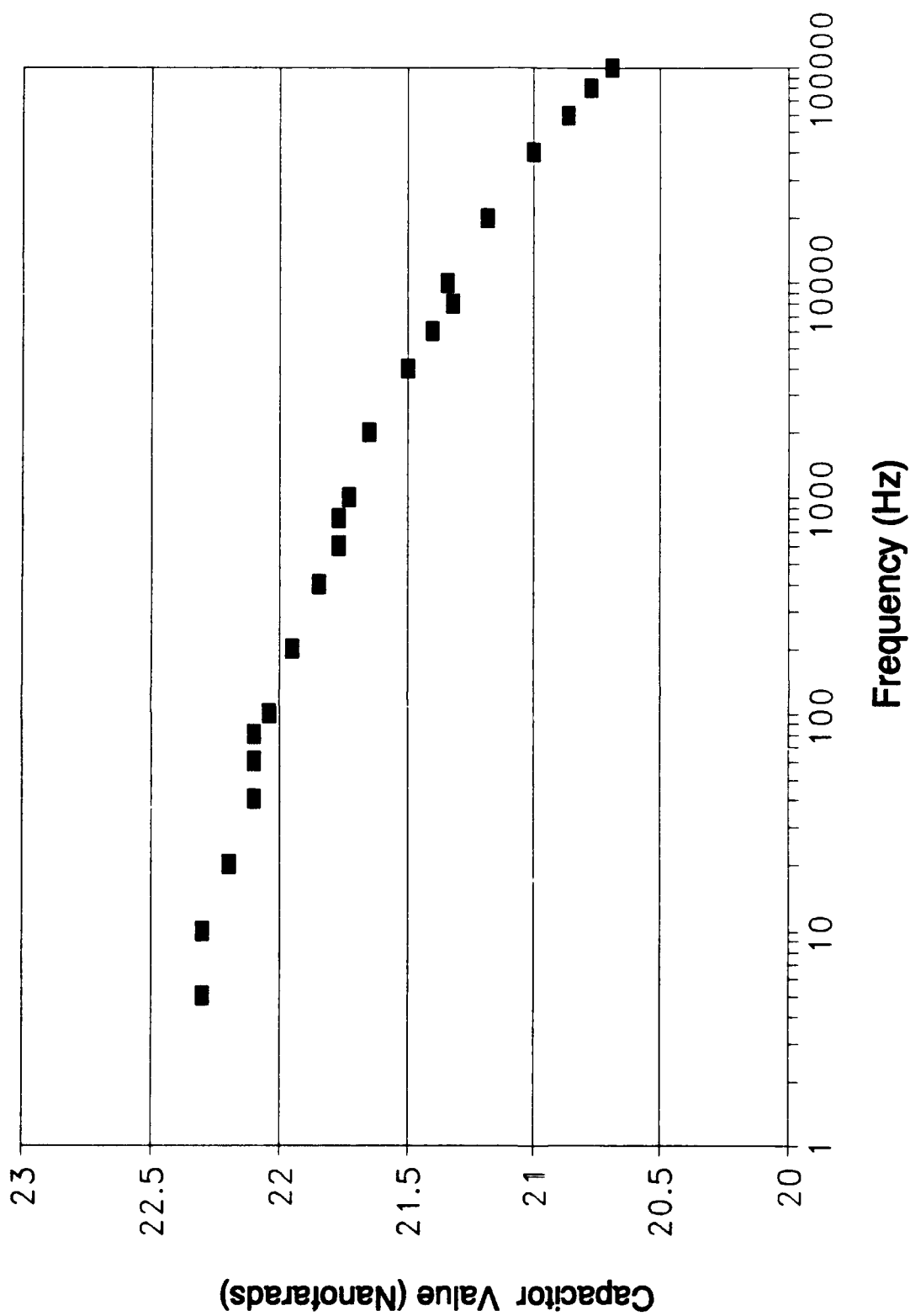Capacitor C8 versus Frequency
(Ideal Value -- 13.41 nf).

Figure E-23. Oldham Circuit Design -- the Value of Capacitor C9 versus Frequency (Ideal Value -- 5.211 nf).
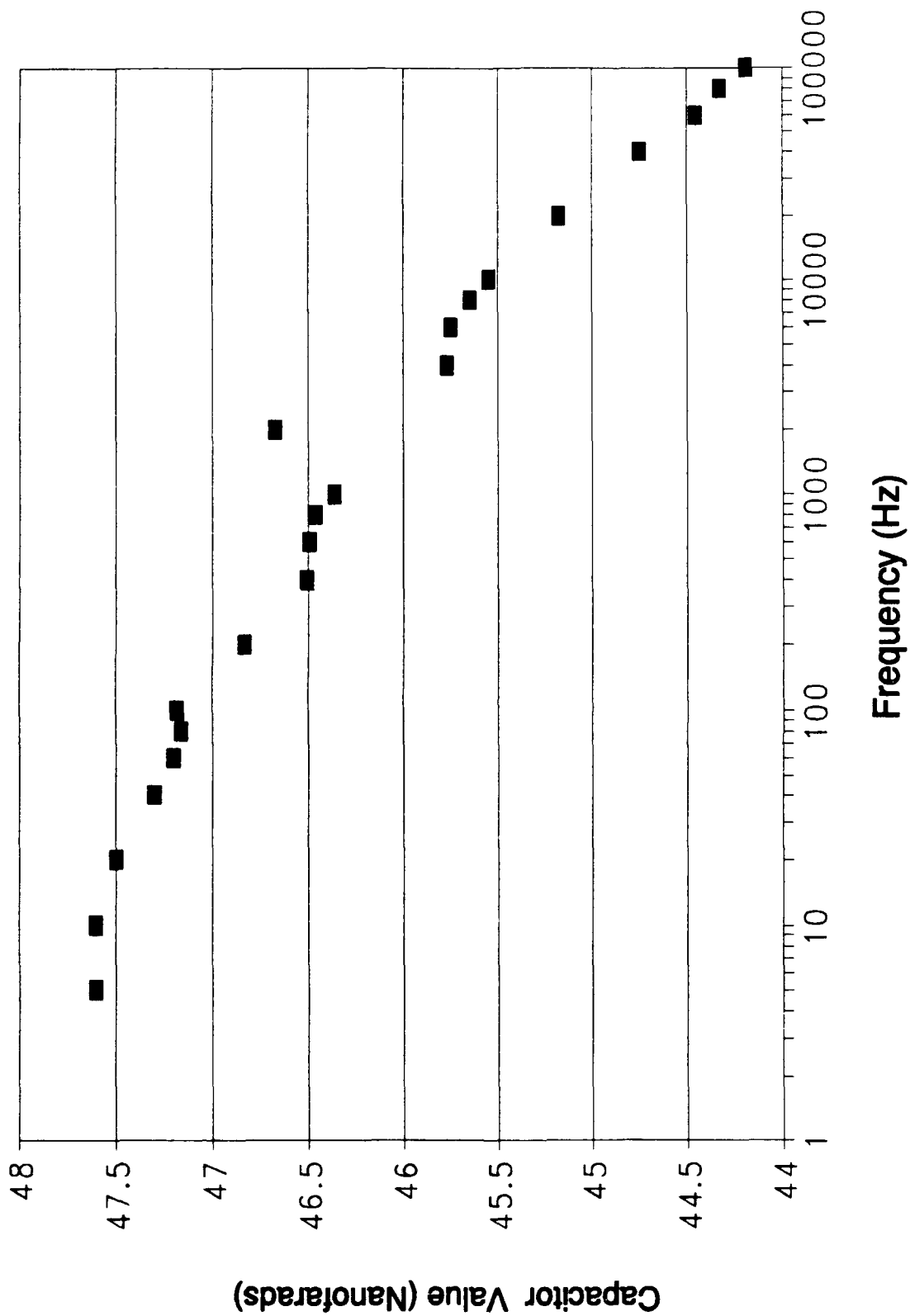
Figure E-24. Oldham Circuit Design -- the Value of Capacitor C10 versus Frequency (Ideal Value -- 2.026 nf).

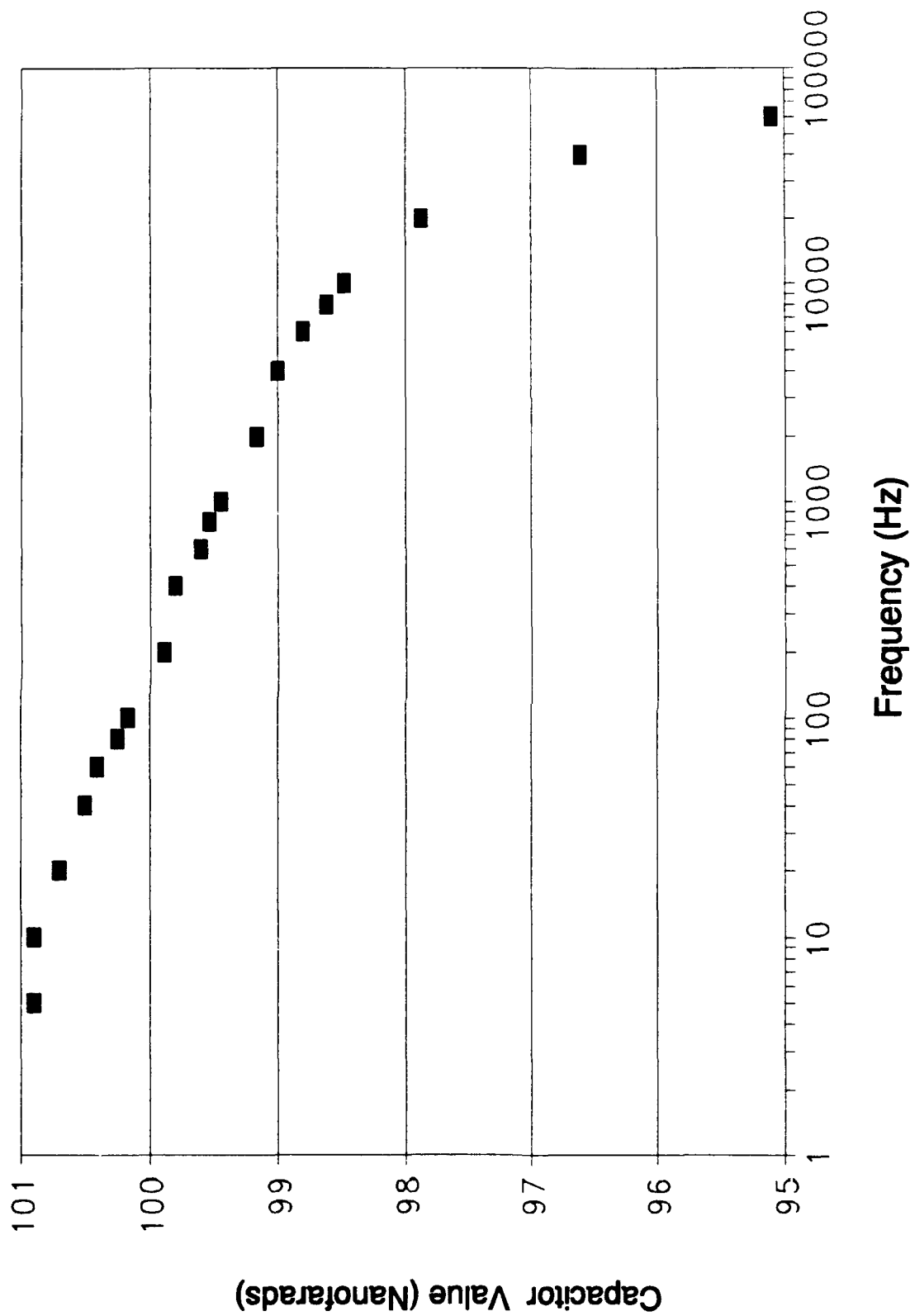Figure E-25. Oldham Circuit Design -- the Value of Capacitor C11 versus Frequency (Ideal Value -- 1.575 nf).

Section 3

Oldfield Surface Mount Resistor Component Value

Variations Versus Frequency

Results

Figure E-26. Oldfield Circuit Design -- the Value of
Resistor R1 versus Frequency
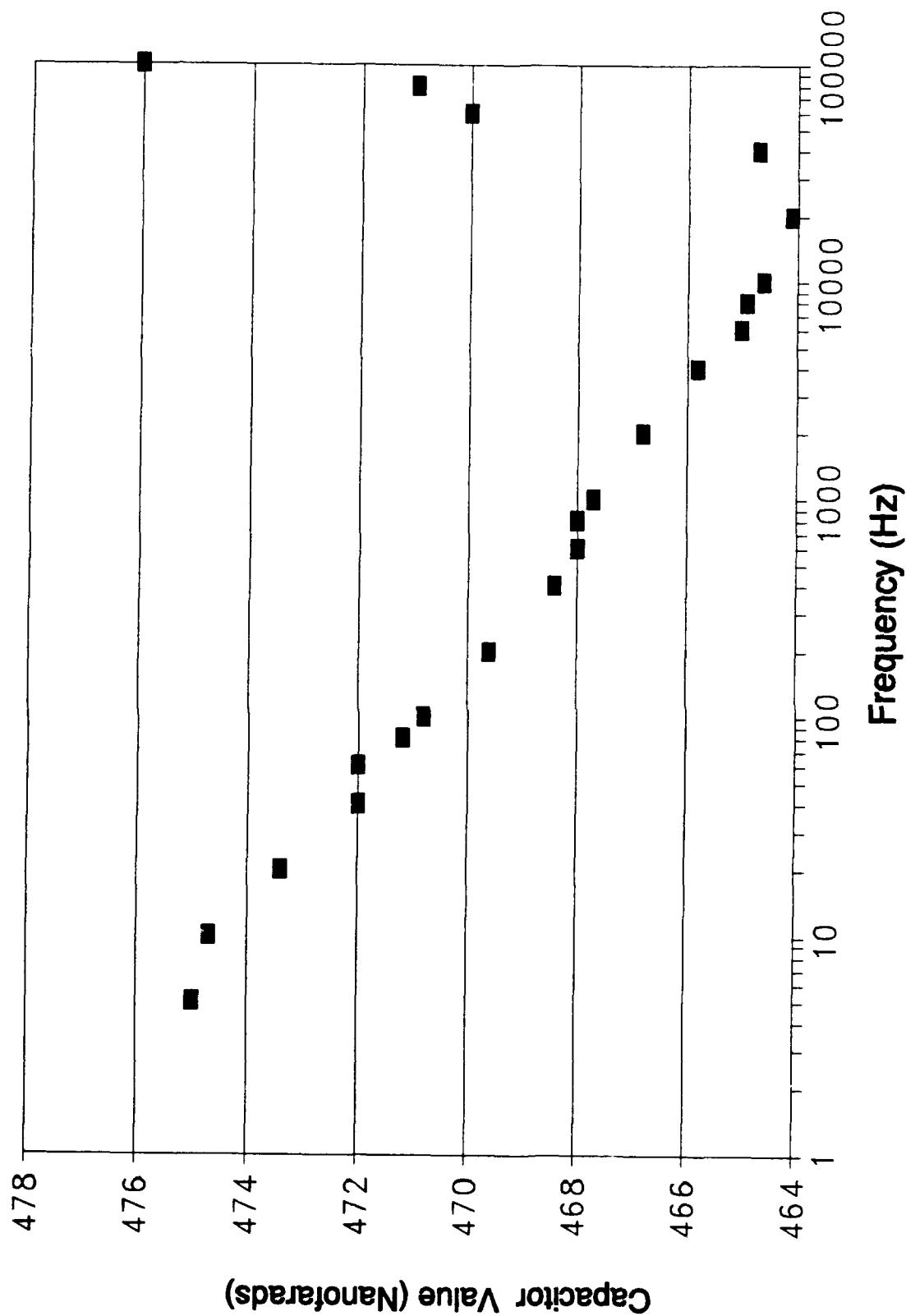(Ideal Value -- 180.2 Ohms).

Figure E-27. Oldfield Circuit Design -- the Value of
Resistor R2 versus Frequency
(Ideal Value -- 630 Ohms).

Figure E-28. Oldfield Circuit Design -- the Value of Resistor R3 versus Frequency (Ideal Value -- 1.313 Kilohms).

Figure E-29. Oldfield Circuit Design -- the Value of Resistor R4 versus Frequency (Ideal Value -- 2.798 Kilohms).
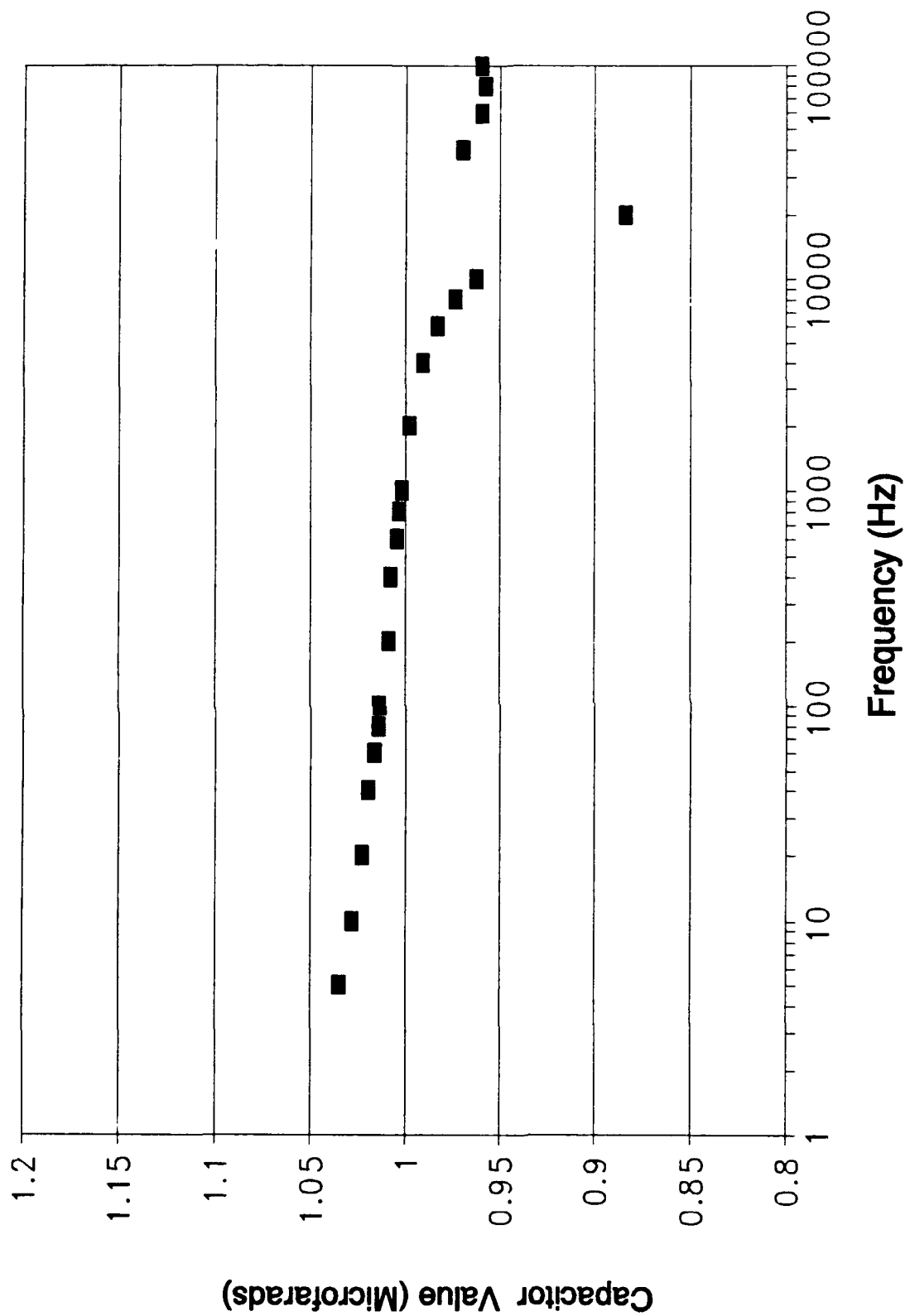
Figure E-30. Oldfield Circuit Design -- the Value of Resistor R5 versus Frequency (Ideal Value -- 6.009 Kilohms).
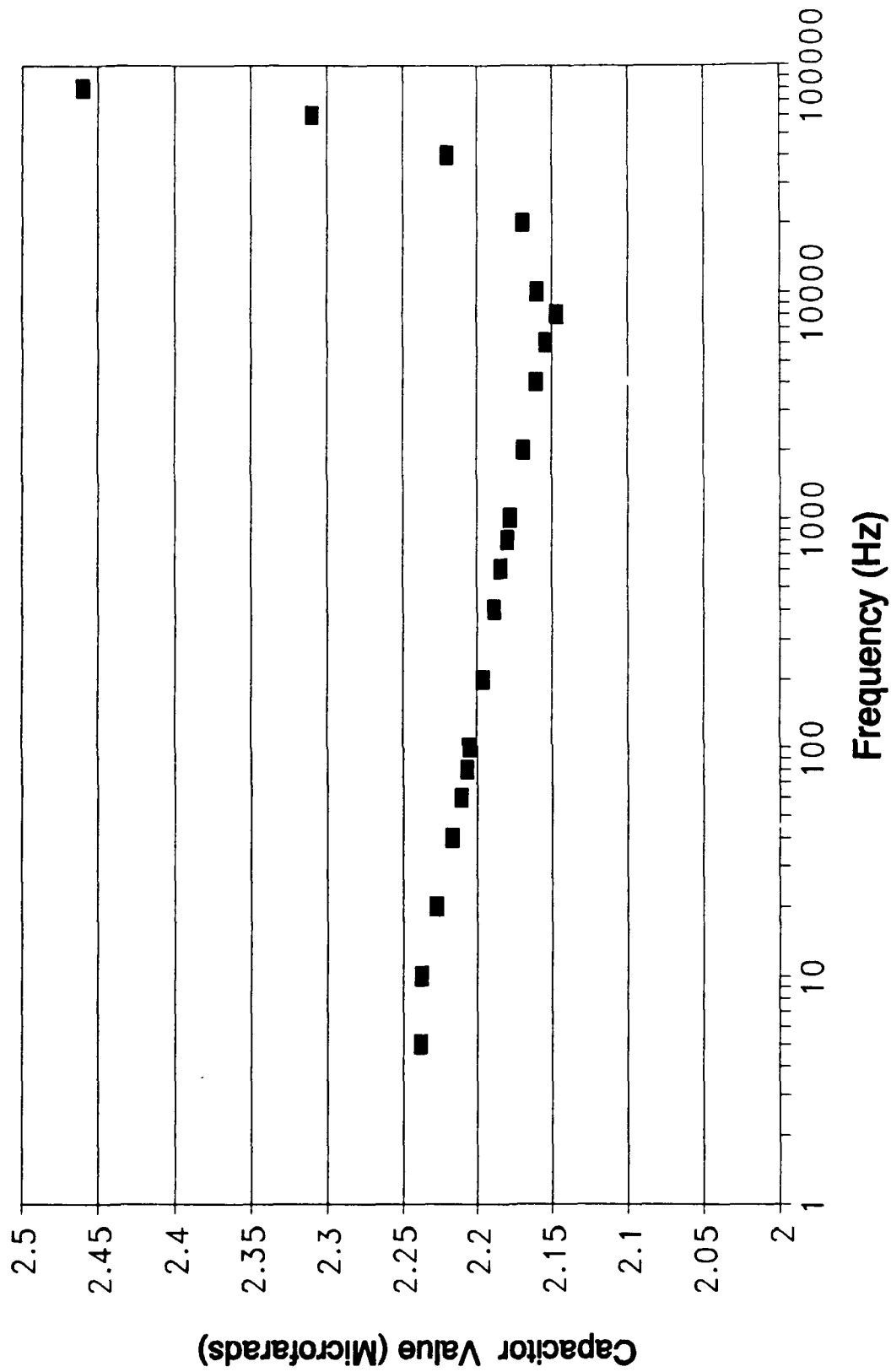
Figure E-31. Oldfield Circuit Design -- the Value of Resistor R6 versus Frequency (Ideal Value -- 13.11 Kilohms).
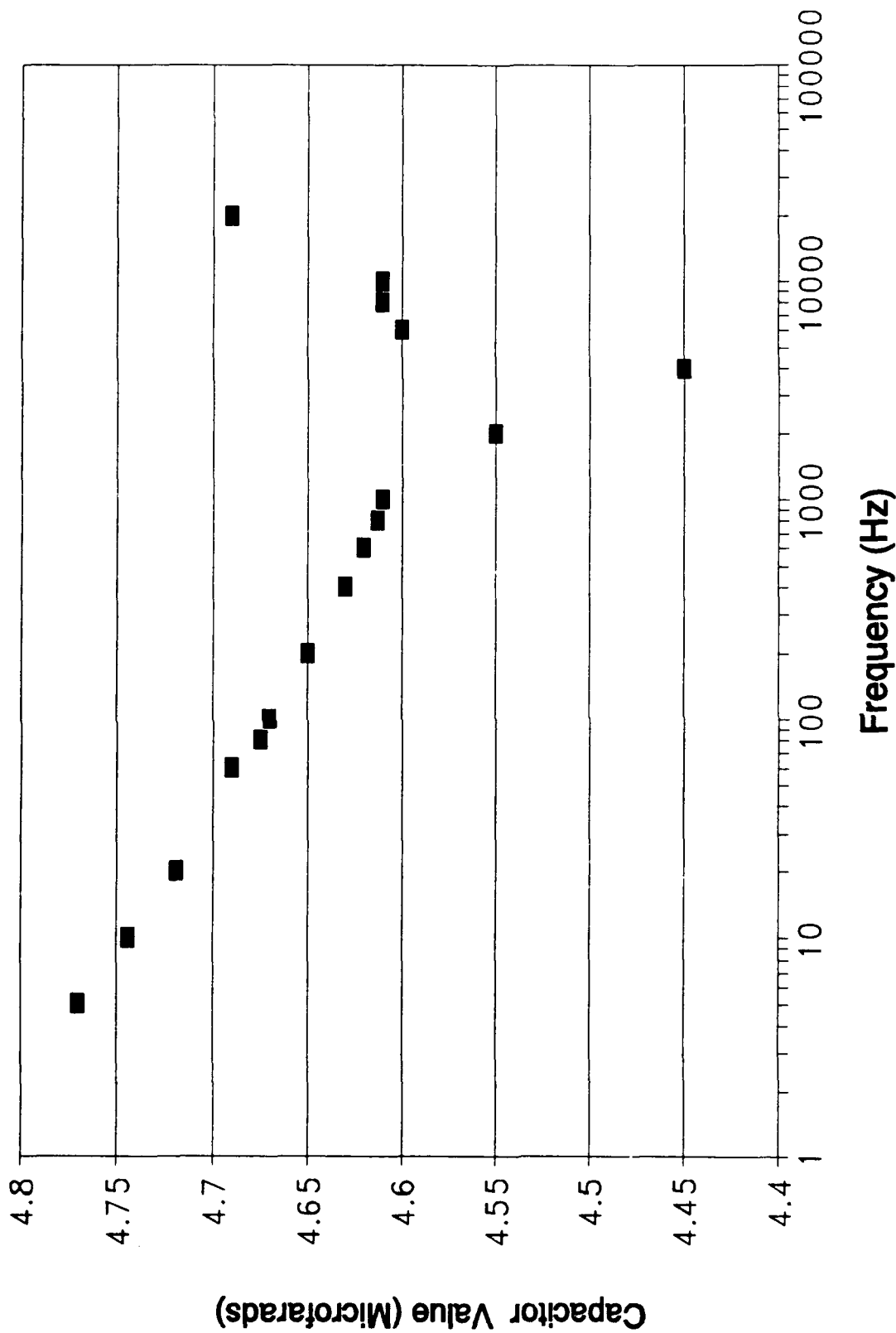
Figure E-32. Oldfield Circuit Design -- the Value of
Resistor R7 versus Frequency
(Ideal Value -- 28.57 Kilohms).
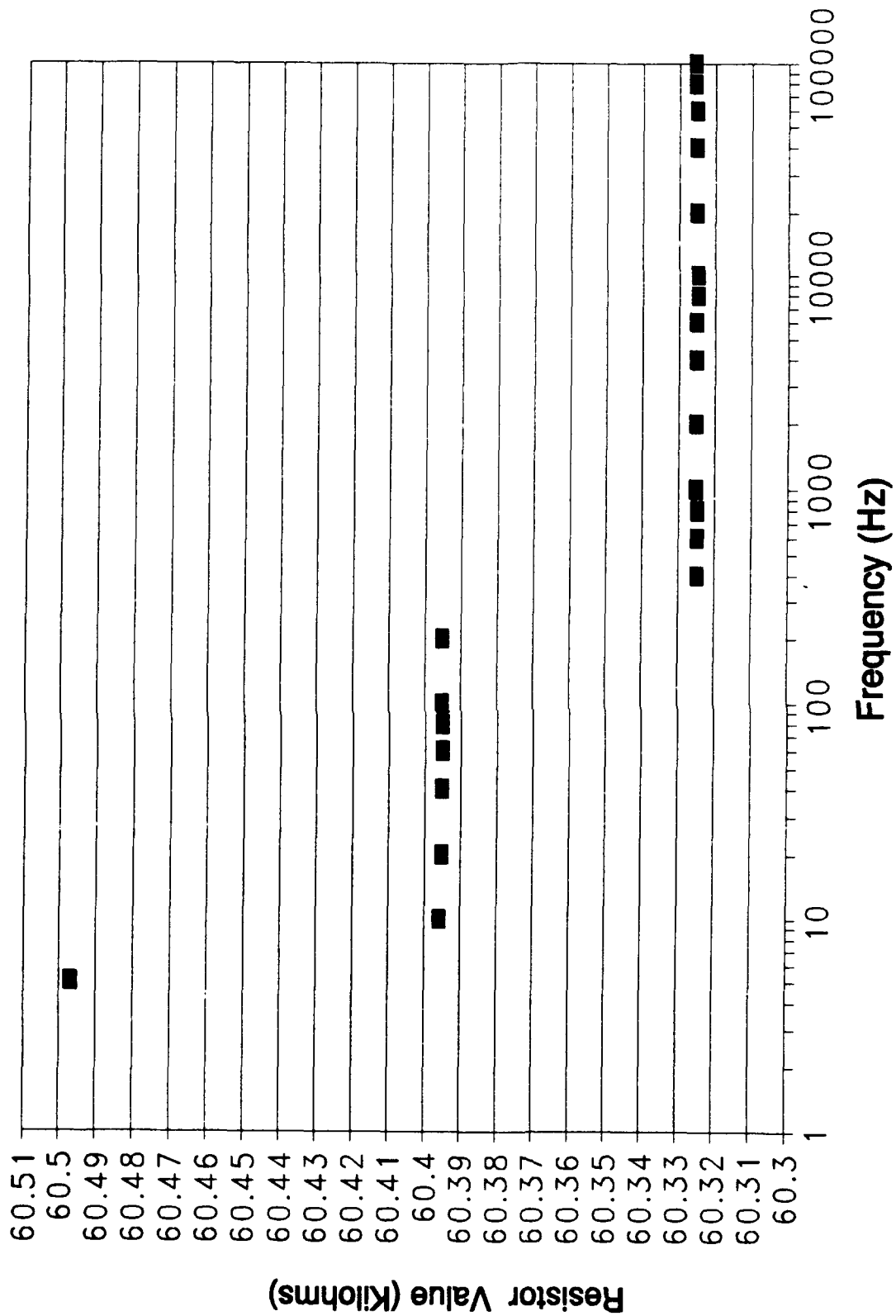
Figure E-33. Oldfield Circuit Design -- the Value of Resistor R8 versus Frequency (Ideal Value -- 60.44 Kilohms).

Figure E-34. Oldfield Circuit Design -- the Value of
Resistor R9 versus Frequency
(Ideal Value -- 129.6 Kilohms).
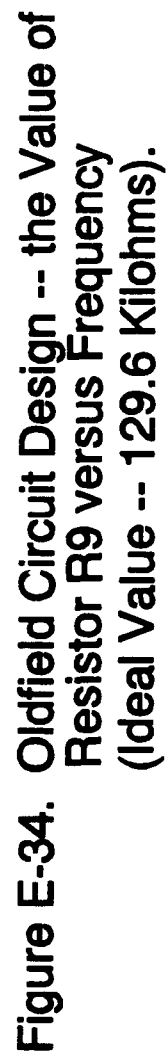
Section 4

Oldfield Surface Mount Capacitor Component Value

Variations Versus Frequency

Results

Figure E-35. Oldfield Circuit Design -- the Value of Capacitor C1 versus Frequency (Ideal Value -- 22 nf).

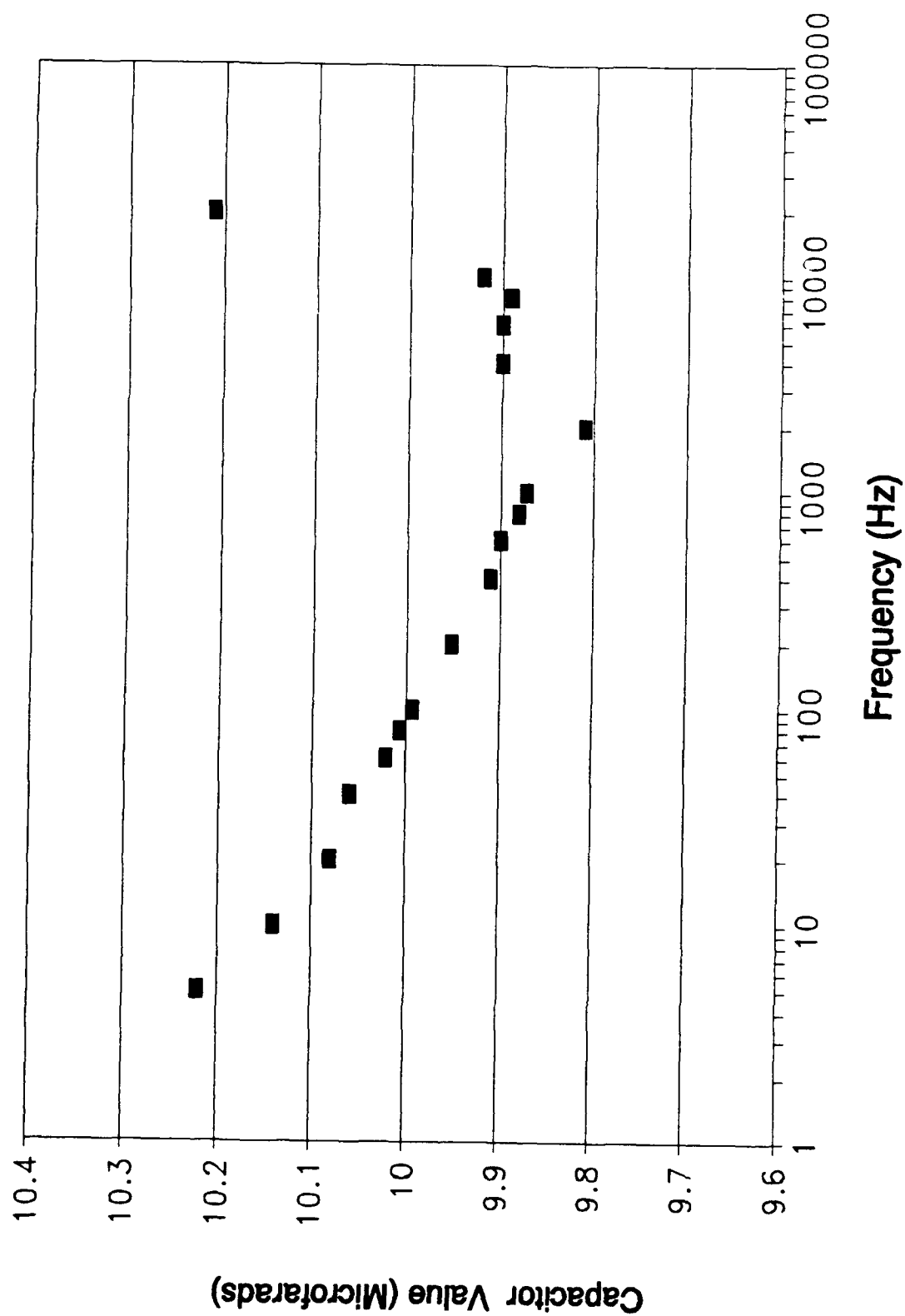Figure E-36. Oldfield Circuit Design -- the Value of Capacitor C2 versus Frequency (Ideal Value -- 47 nf).

Figure E-37. Oldfield Circuit Design -- the Value of Capacitor C3 versus Frequency (Ideal Value -- 100 nf).
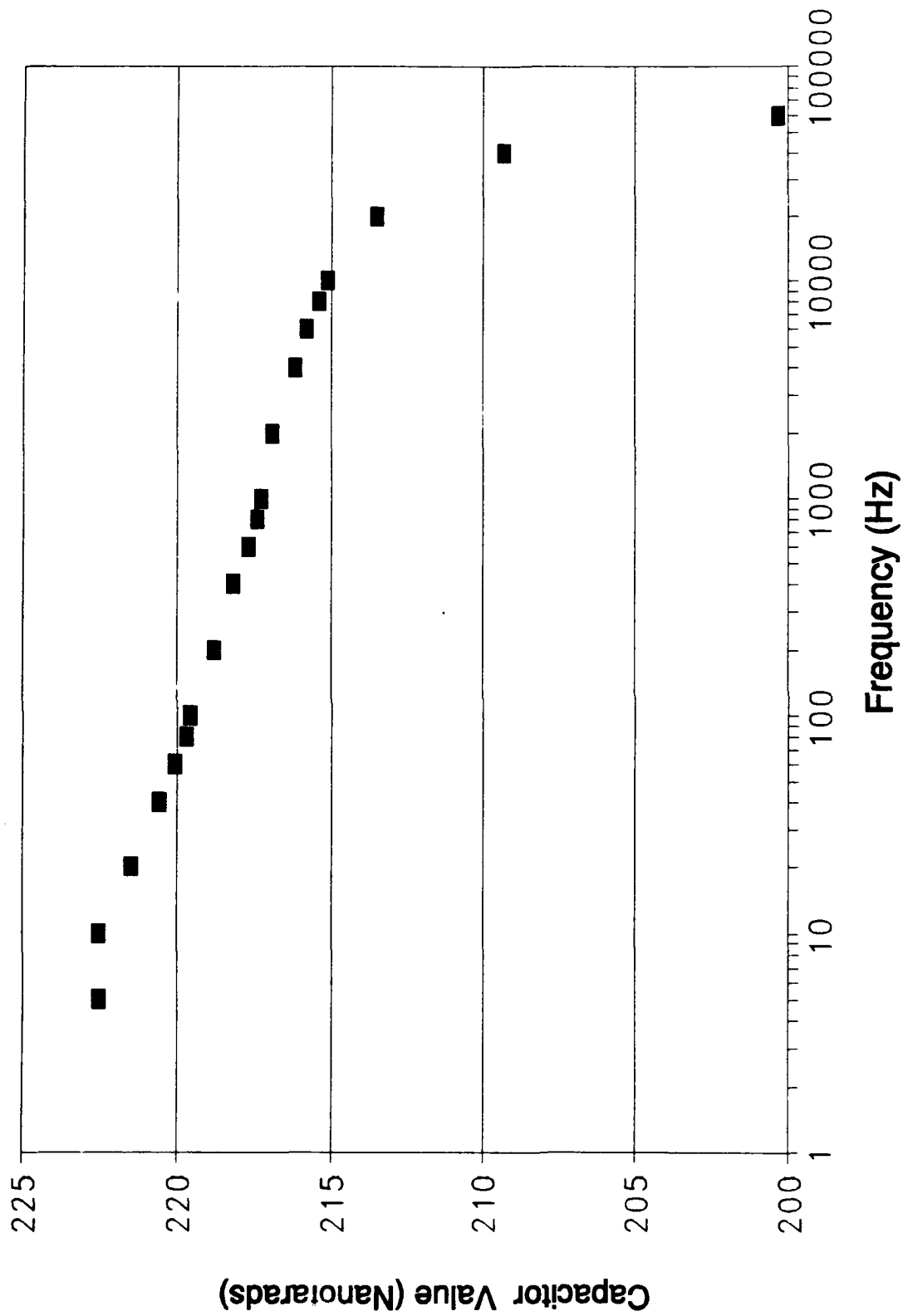
Figure E-38. Oldfield Circuit Design -- the Value of Capacitor C4 versus Frequency (Ideal Value -- 220 nf).

Figure E-39. Oldfield Circuit Design -- the Value of Capacitor C5 versus Frequency (Ideal Value -- 470 nf).

Figure E-40. Oldfield Circuit Design -- the Value of Capacitor C6 versus Frequency (Ideal Value -- 1.0 µf).

Figure E-41. Oldfield Circuit Design -- the Value of Capacitor C7 versus Frequency (Ideal Value -- 2.2 μf).

Figure E-42.   Oldfield Circuit Design -- the Value of Capacitor C8 versus Frequency (Ideal Value -- 4.7 μf).

Figure E-43. Oldfield Circuit Design -- the Value of Capacitor C9 versus Frequency (Ideal Value -- 10.0 μf).

Appendix F

Electrical Performance Results for

the Oldham and Oldfield

Discrete Component Circuits Realized

With a Breadboard Format

This appendix documents the electrical performance results obtained for the Oldham and Oldfield discrete component circuits realized with a breadboard fornmat. As stated in Chapter 4, a limited number of data points were acquired for these circuit configurations. The data presented for each circuit consists of gain and phase plots and the time-domain response due to a 500 Hz excitation signal. The Oldham circuit responses are documented in Section 1, and the Oldfield circuit responses are documented in Section 2.

Section 1

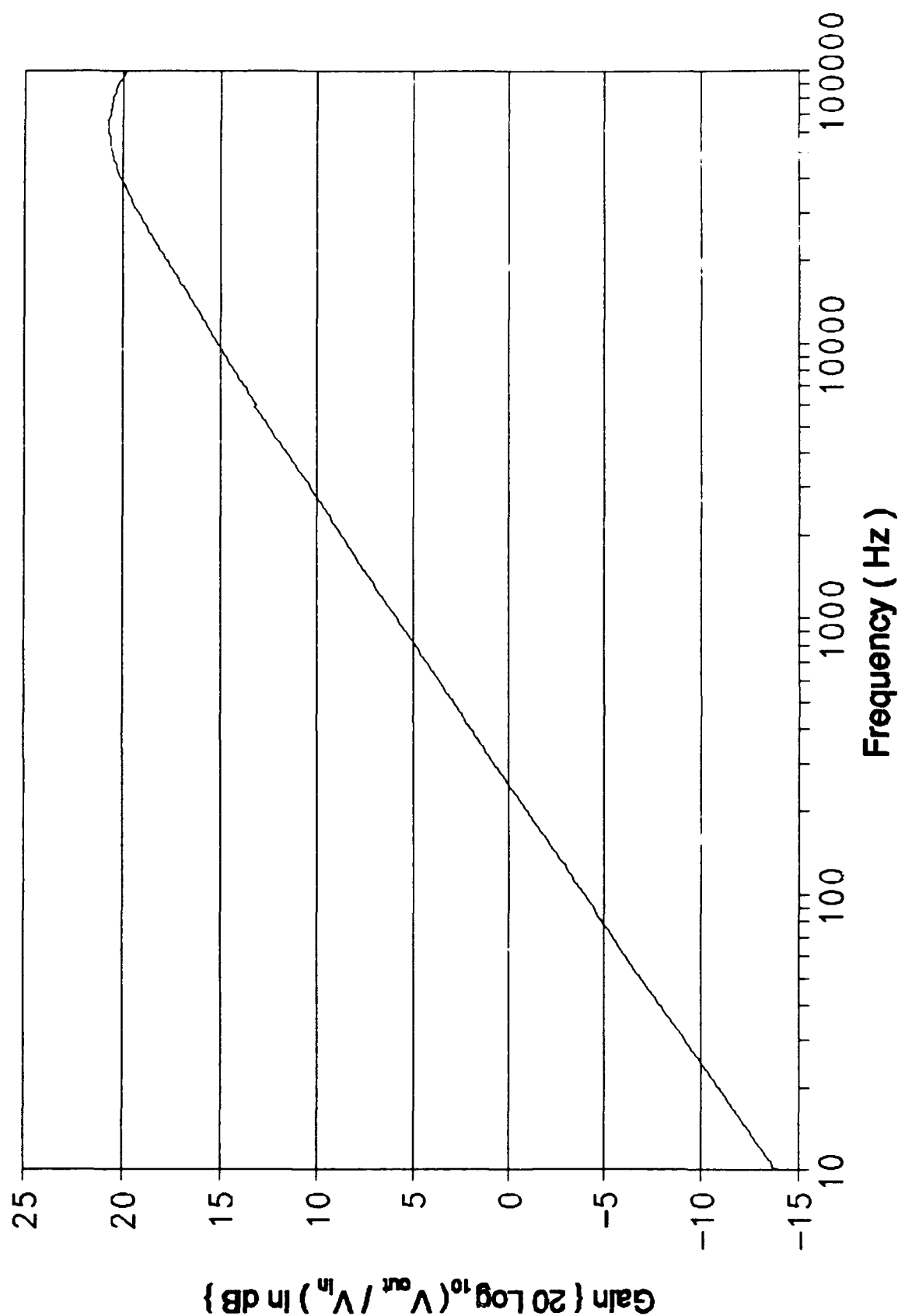## Electrical Performance Results for the Oldham Discrete Component Circuit Realized with a Breadboard Format
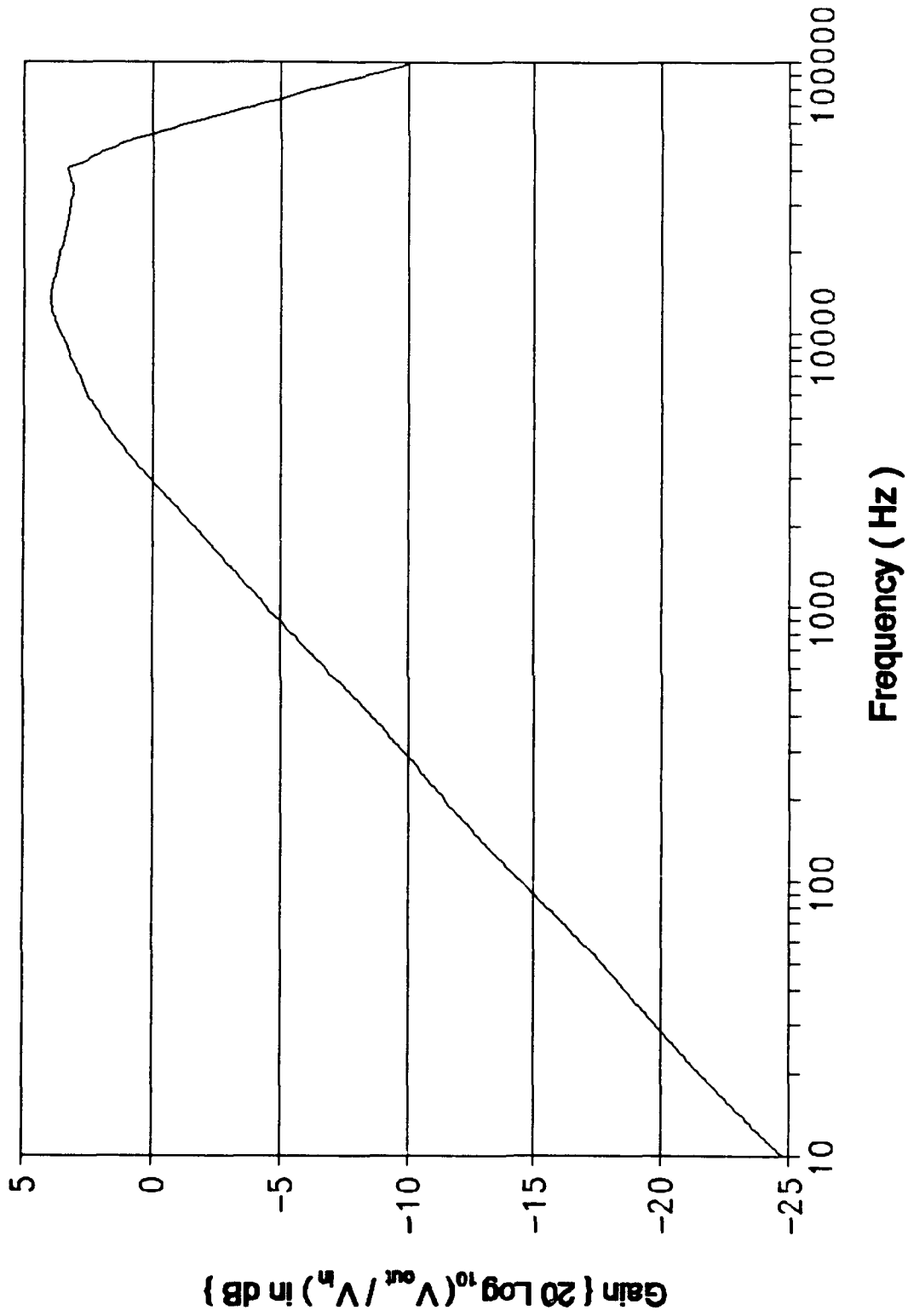
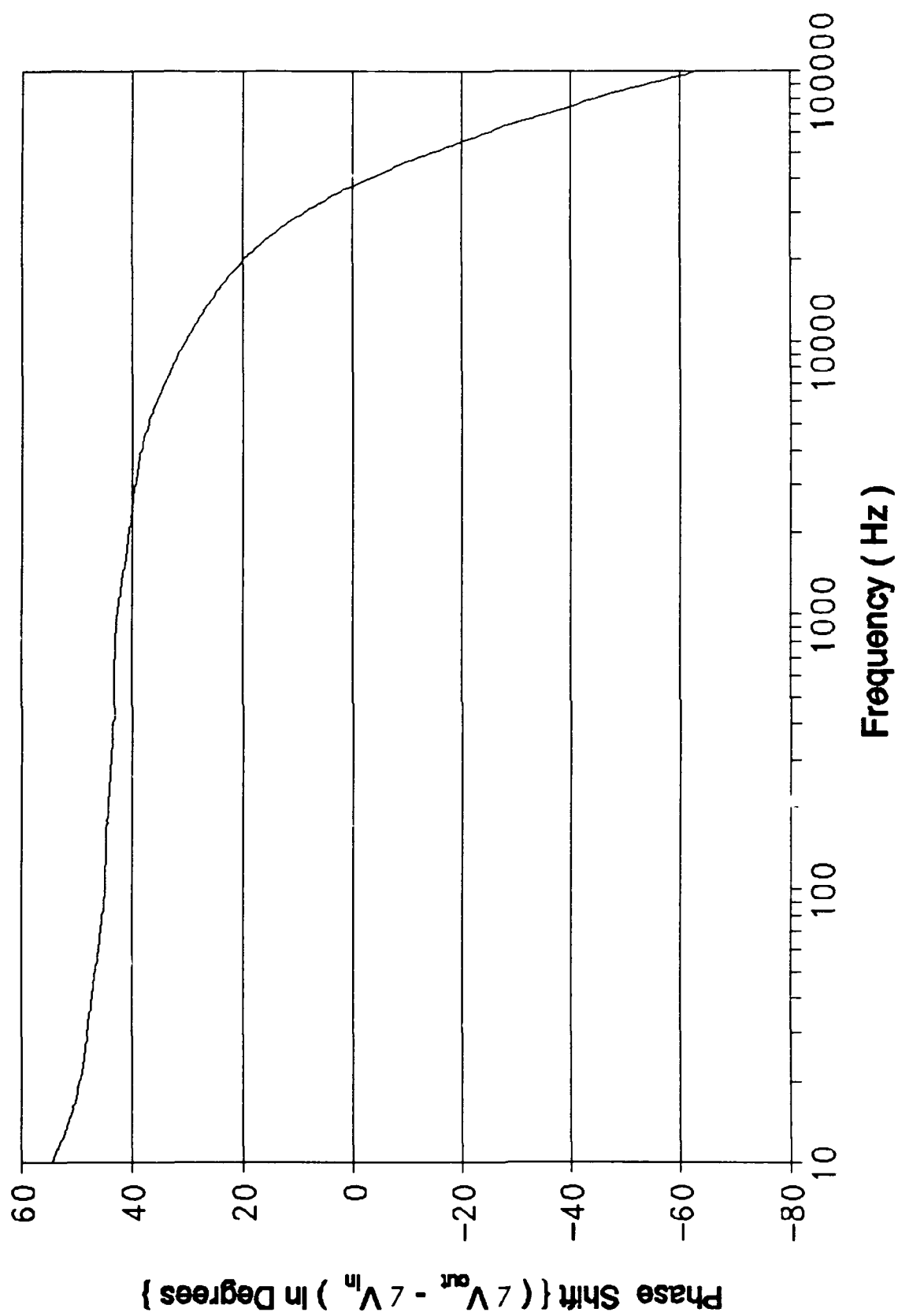**Figure F-1.** Gain Response of the Oldham Discrete Component Circuit Realized on a Breadboard.
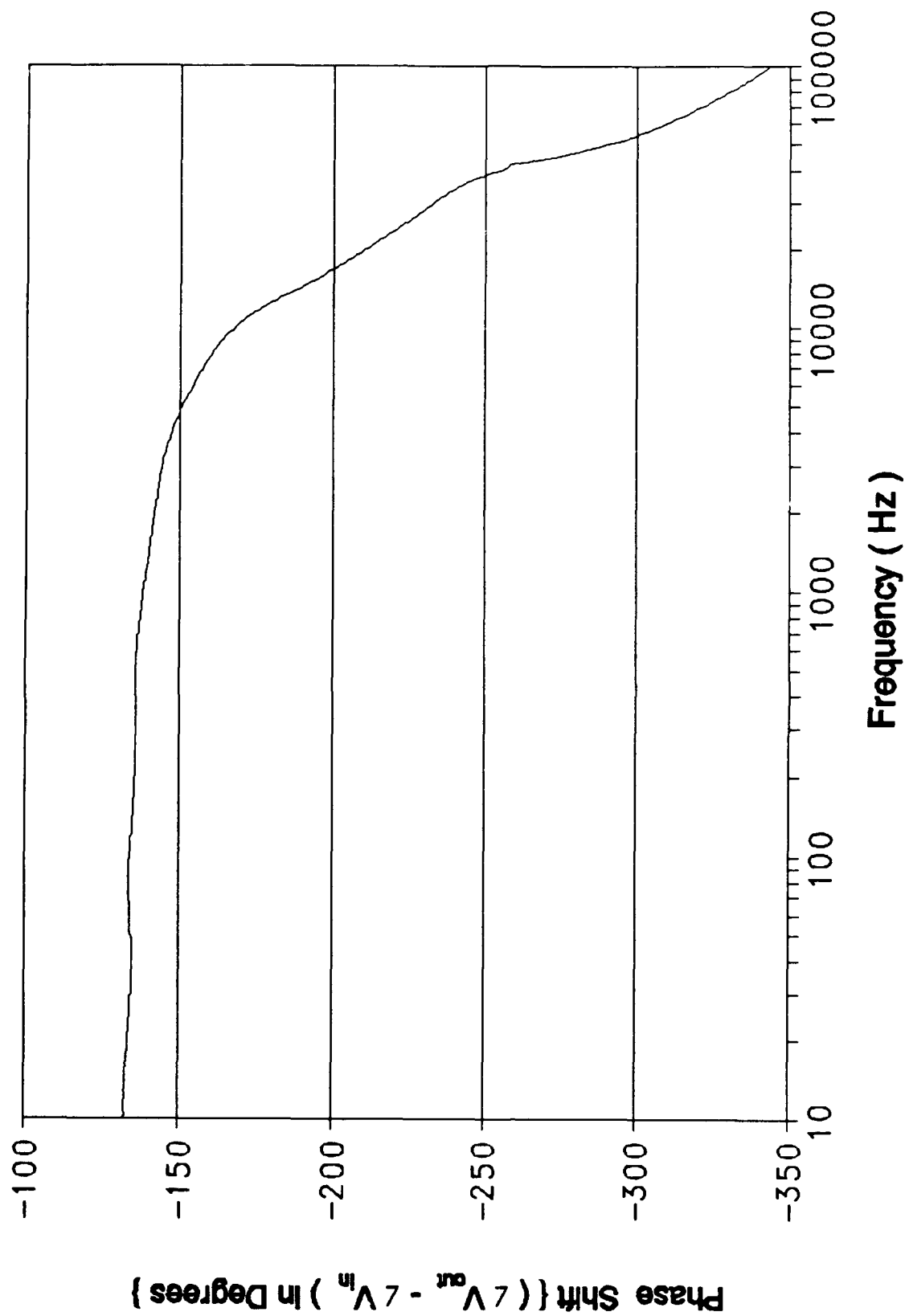
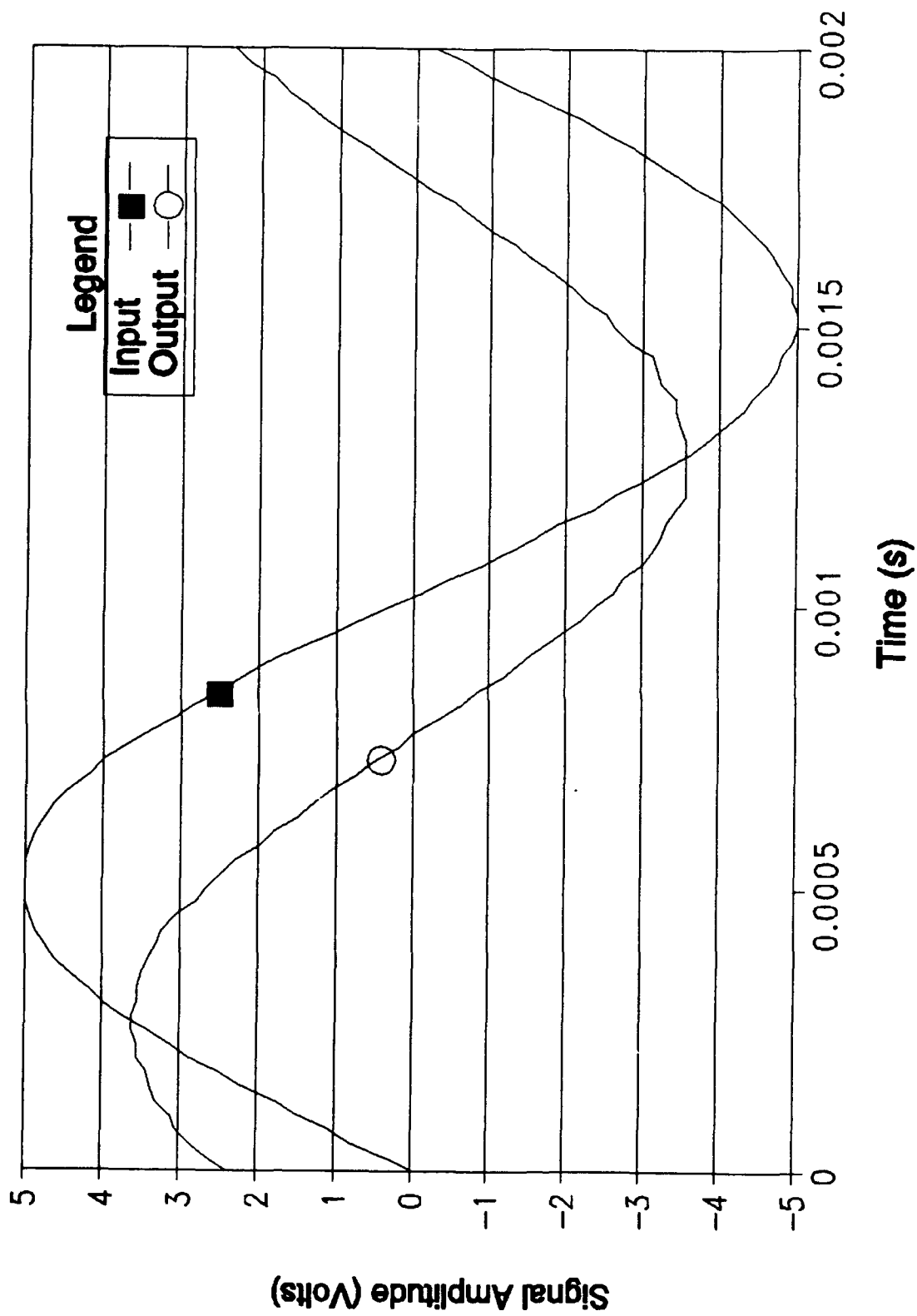Figure F-2. Phase Response of the Oldham Discrete Component Circuit Realized on a Breadboard.
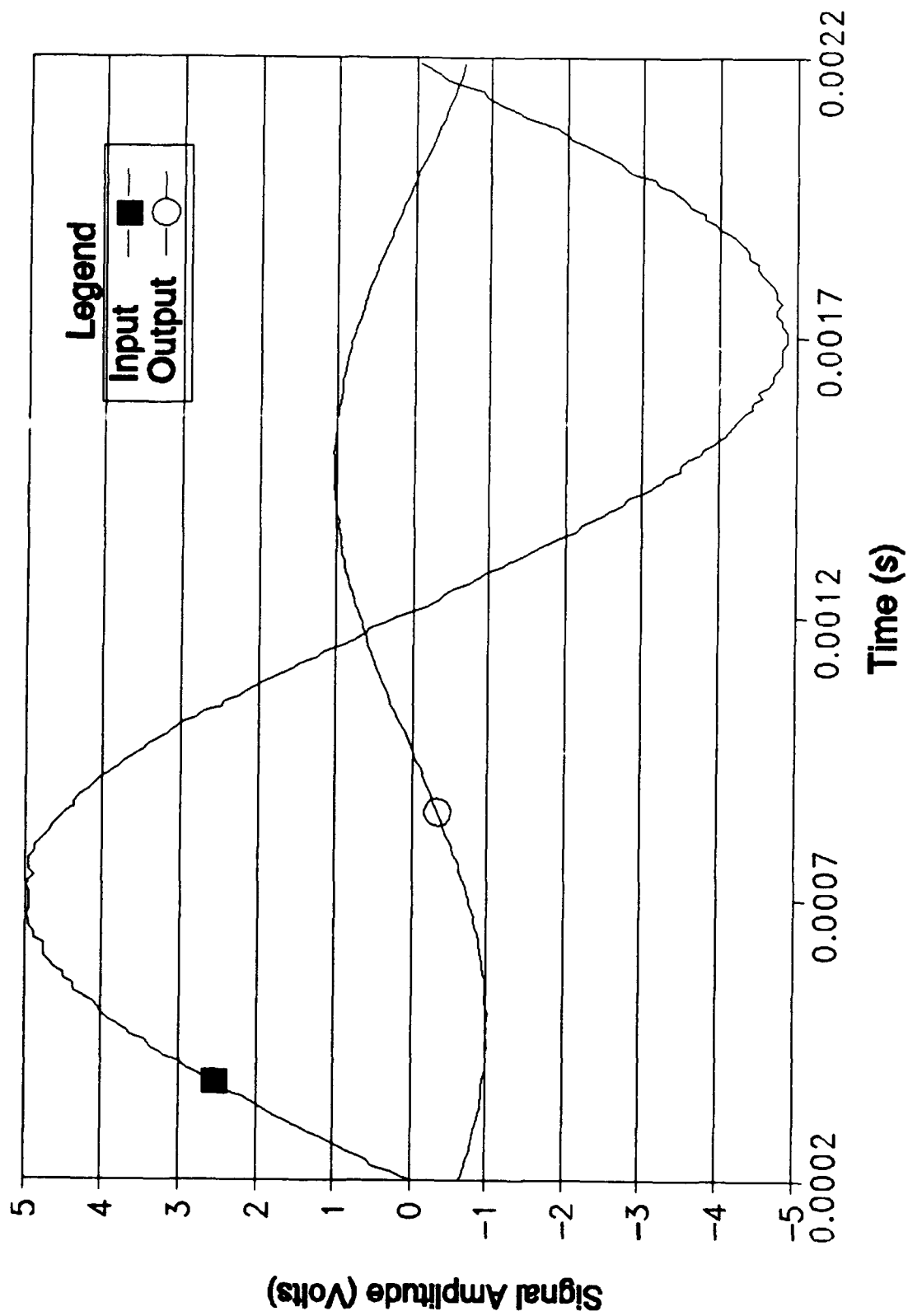
Figure F-3. Time Response of the Oldham Discrete Component
Circuit Realized on a Breadboard.

Section 2

Electrical Performance Results for the

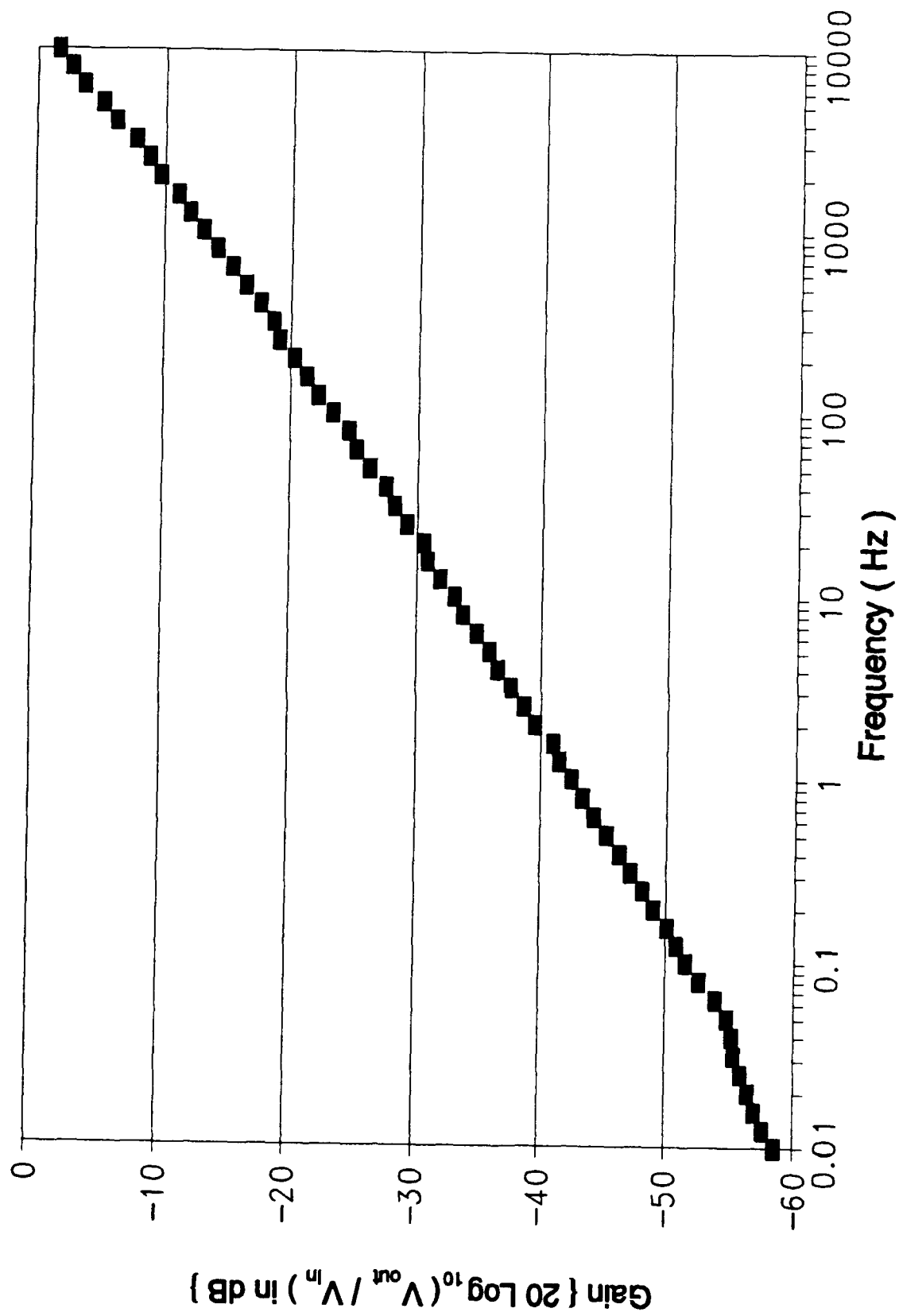Oldfield Discrete Component Circuit

Realized with a Breadboard Format

Figure E-4. Gain Response of the Oldfield Discrete Component Circuit Realized on a Breadboard.

Figure F-5. Phase Response of the Oldfield Discrete Component Circuit Realized on a Breadboard.

Figure F-6. Time Response of the Oldfield Discrete Component Circuit Realized on a Breadboard.

Appendix G

Electrical Performance Results for

the Oldham and Oldfield

Circuits Realized

With a Printed Circuit Board Format

This appendix documents the electrical performance results obtained for the Oldham and Oldfield discrete, hybrid and surface mount component circuits realized with a printed circuit board fornmat. The Oldham and Oldfield discrete component circuit responses are documented in Section 1. Corresspondingly, the Oldham hybrid and the Oldfield surface mount component circuits are documented in Section 2.

Section 1

Electrical Performance Results for

the Oldham and Oldfield Discrete Component Circuit

Realized with a Printed Circuit Board Format

Figure G-1. Oldham Circuit Discrete Component Gain Response.
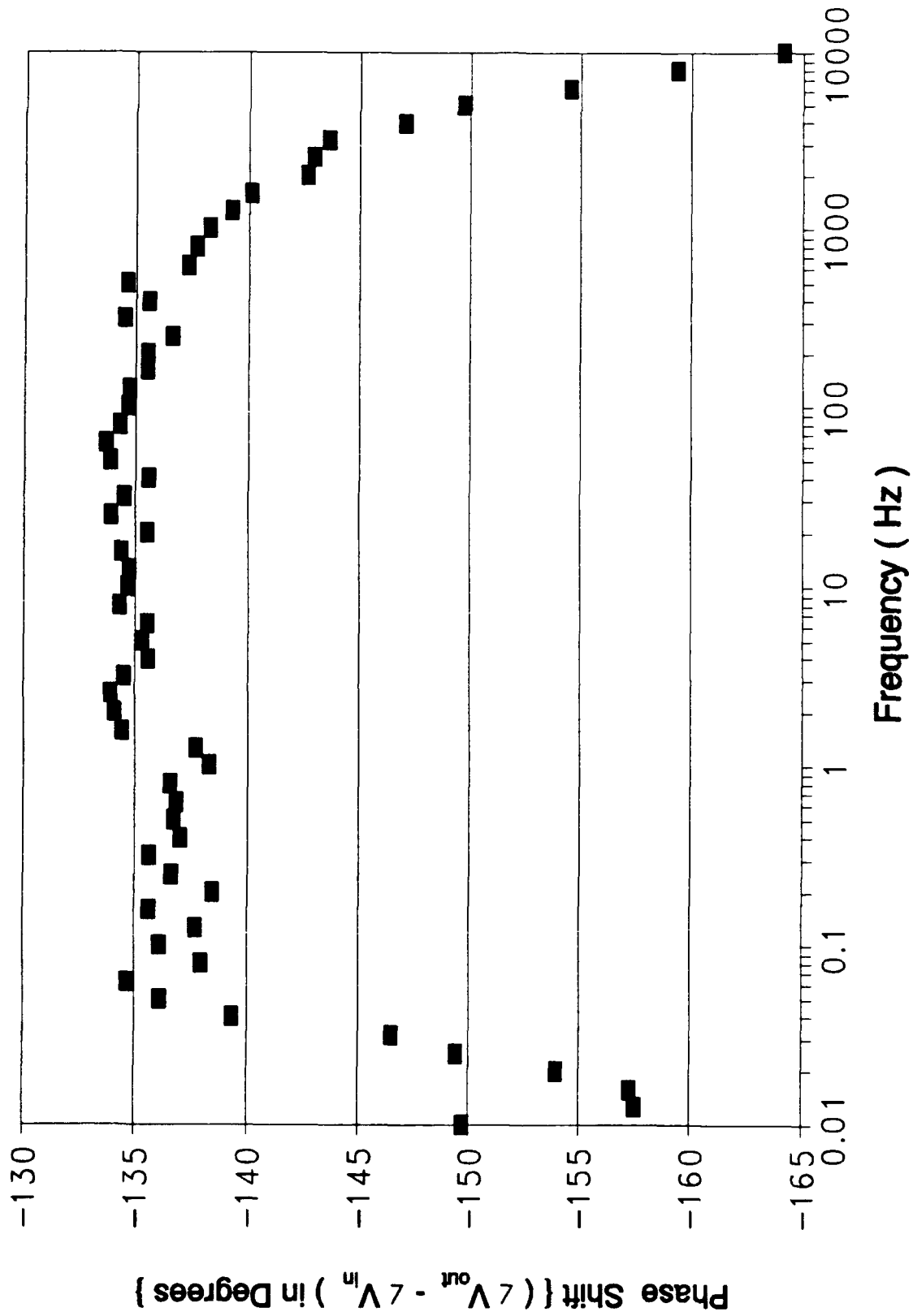
Figure G-2. Oldham Circuit Discrete Component Phase Response.
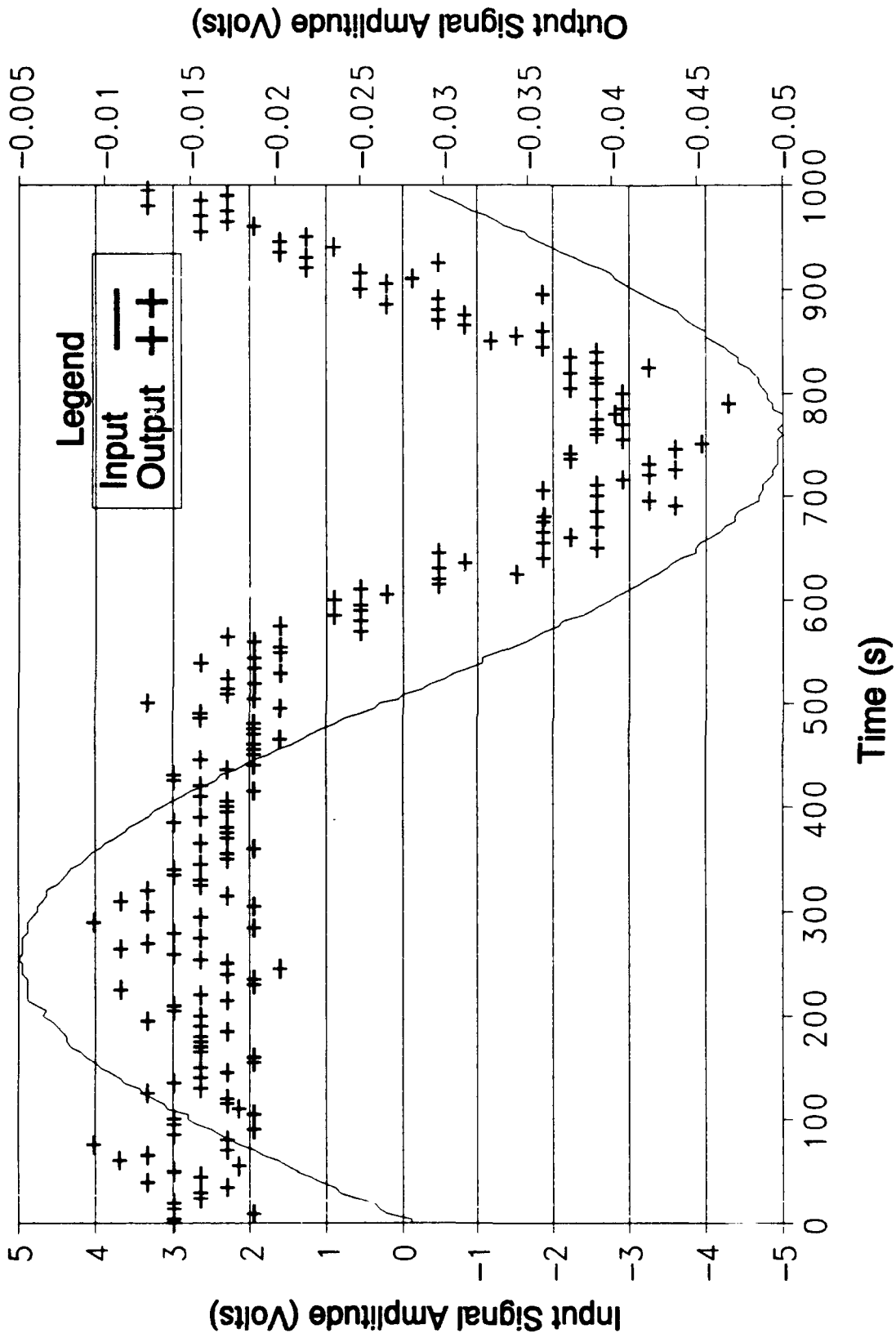
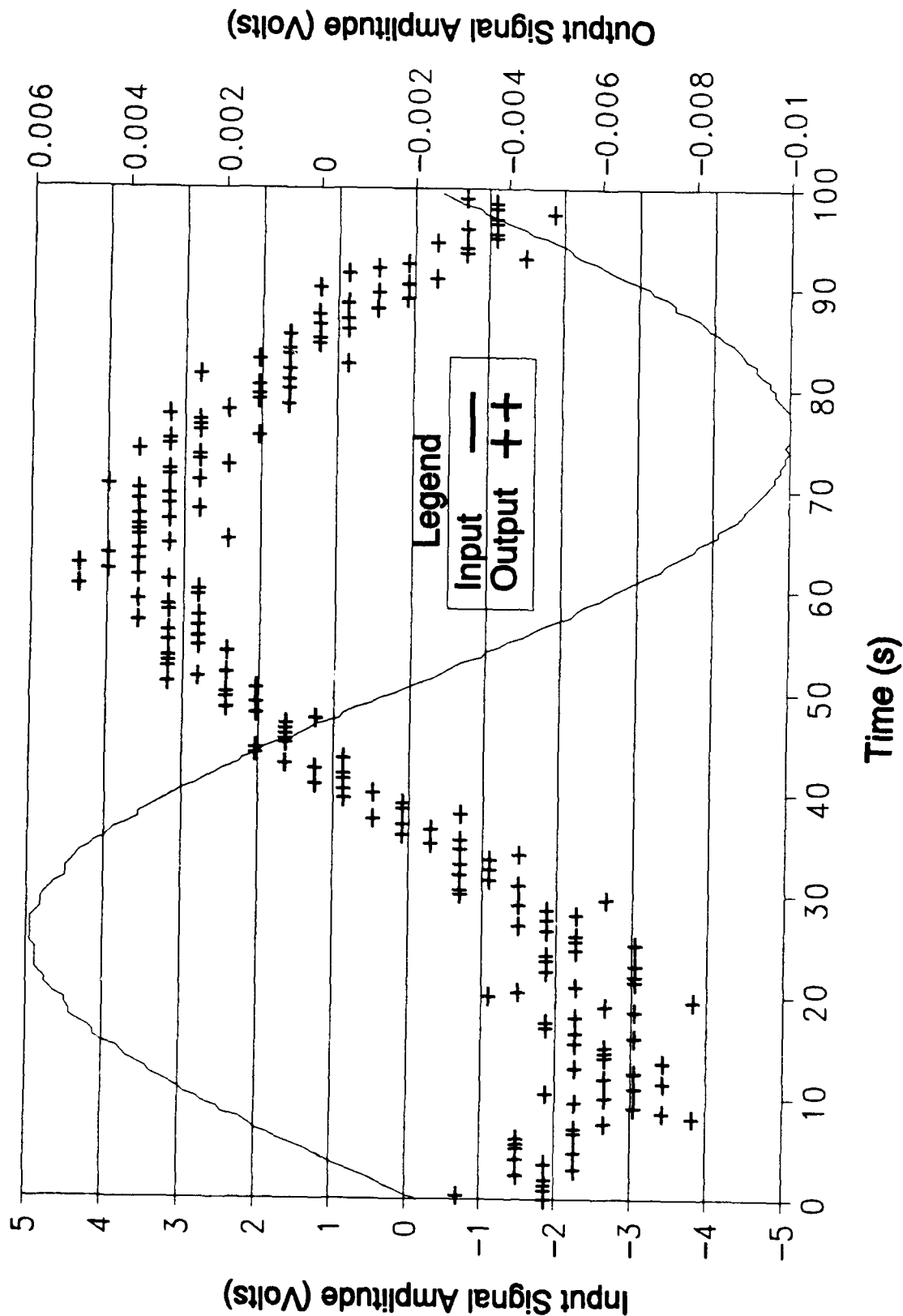Figure G-3. Time Response of the Oldham Discrete Component Circuit Design with a 0.001 Hz Excitation Signal.

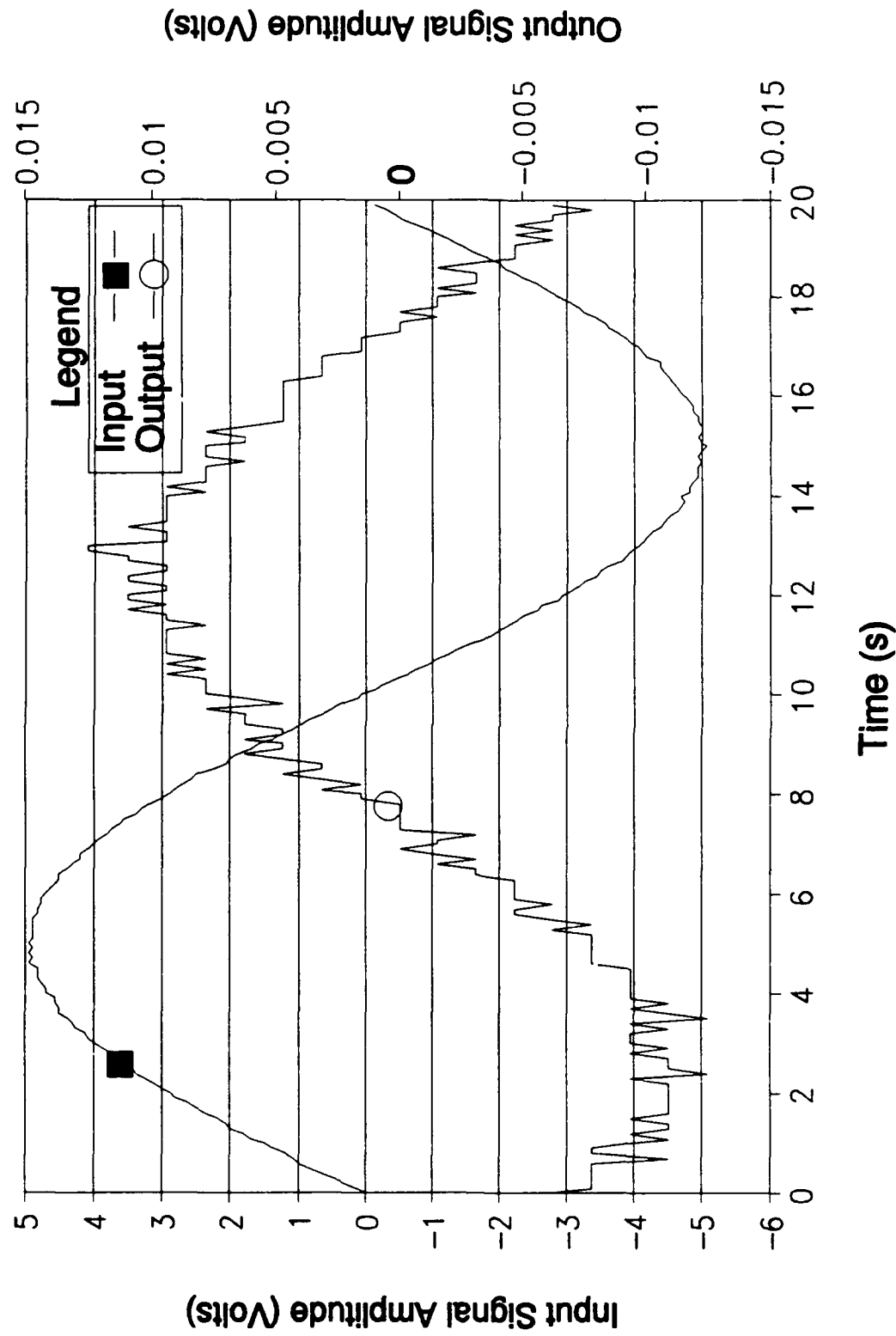Figure G-4. Time Response of the Oldham Discrete Component Circuit Design with a 0.01 Hz Excitation Signal.

Figure G-5. Time Response of the Oldham Discrete Component Circuit Design with a 0.05 Hz Excitation Signal.
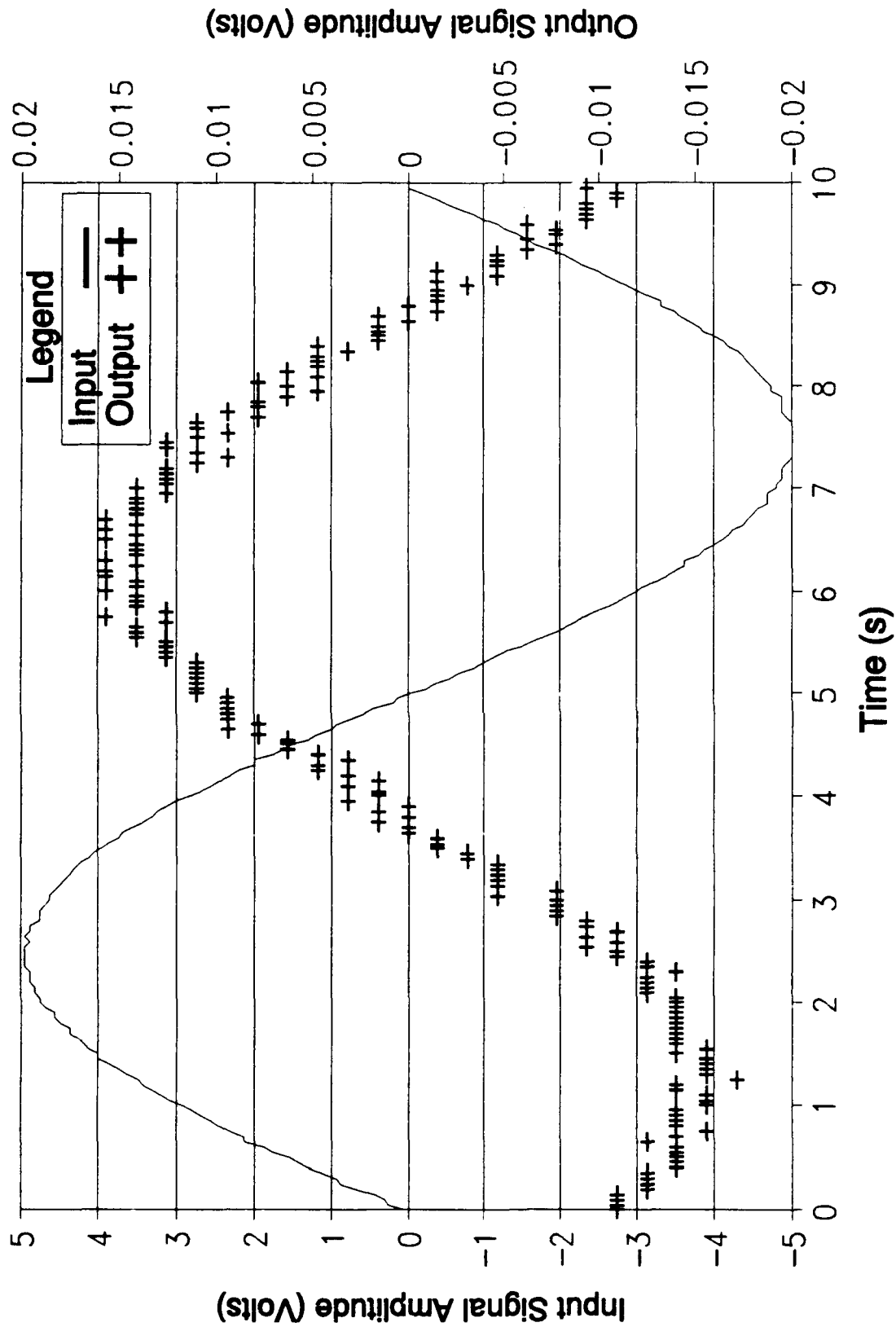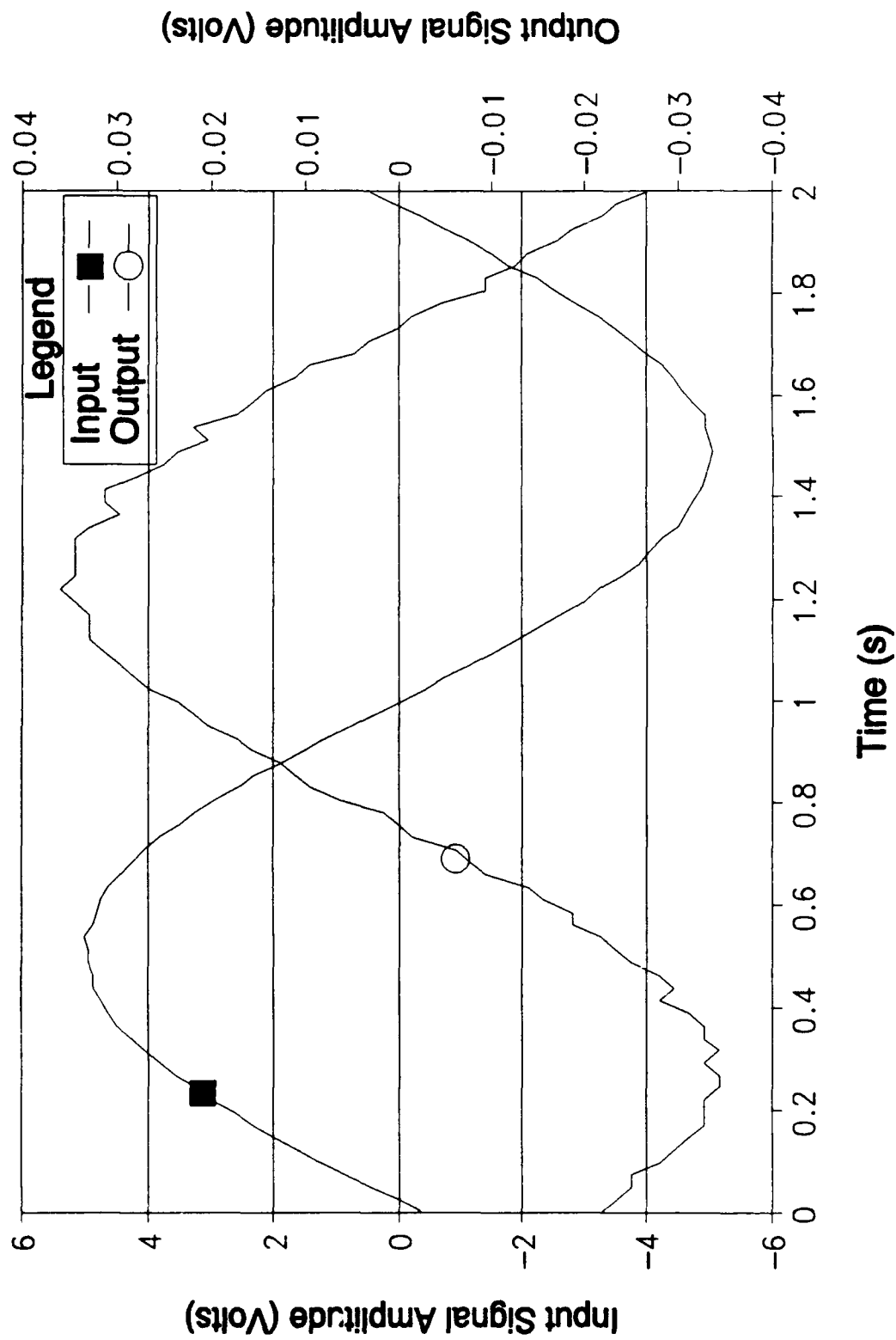
Figure G-6. Time Response of the Oldham Discrete Component Circuit Design with a 0.1 Hz Excitation Signal.

Figure G-7. Time Response of the Oldham Discrete Component Circuit Design with a 0.5 Hz Excitation Signal.
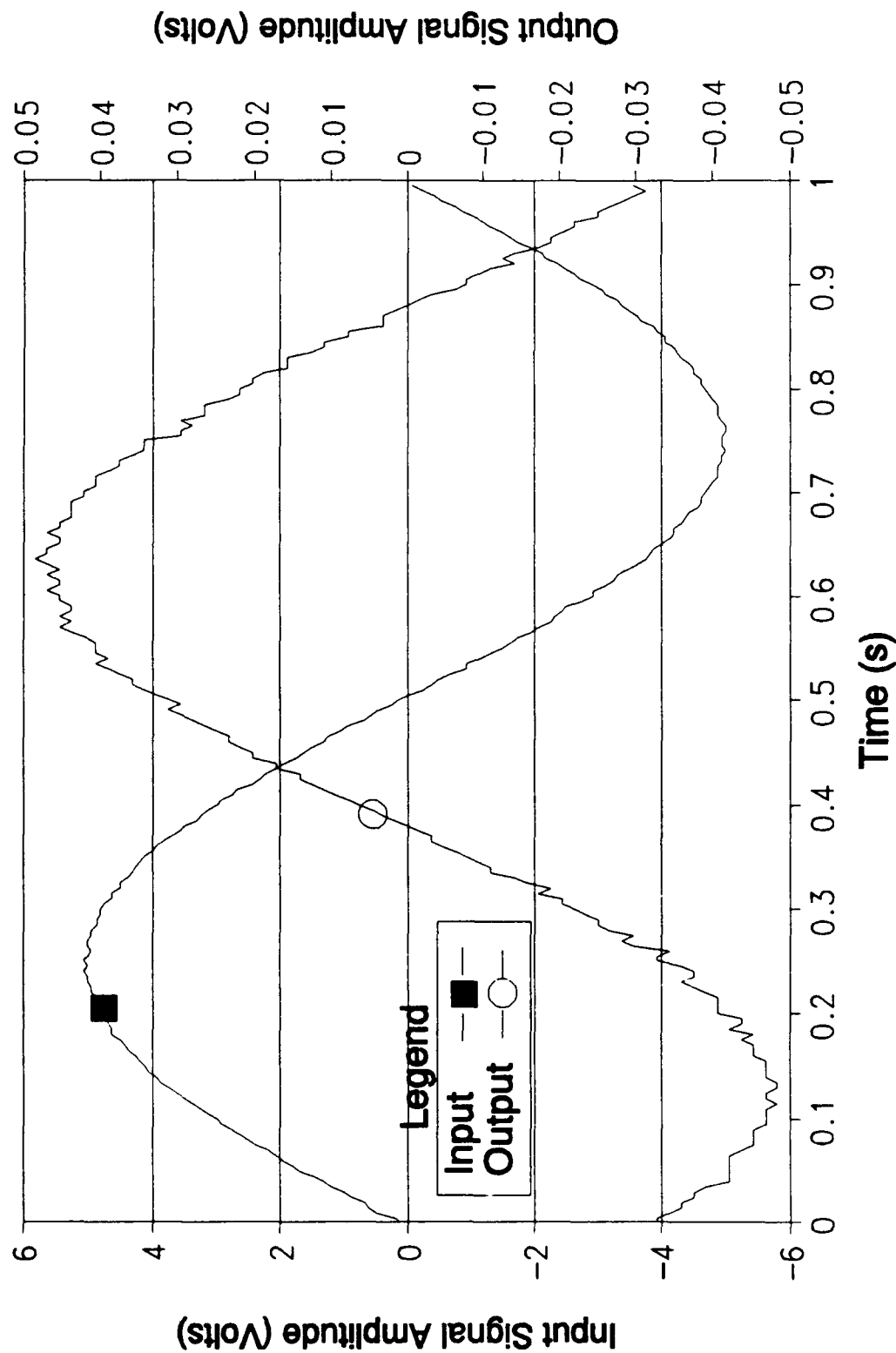
Figure G-8. Time Response of the Oldham Discrete Component Circuit Design with a 1 Hz Excitation Signal.
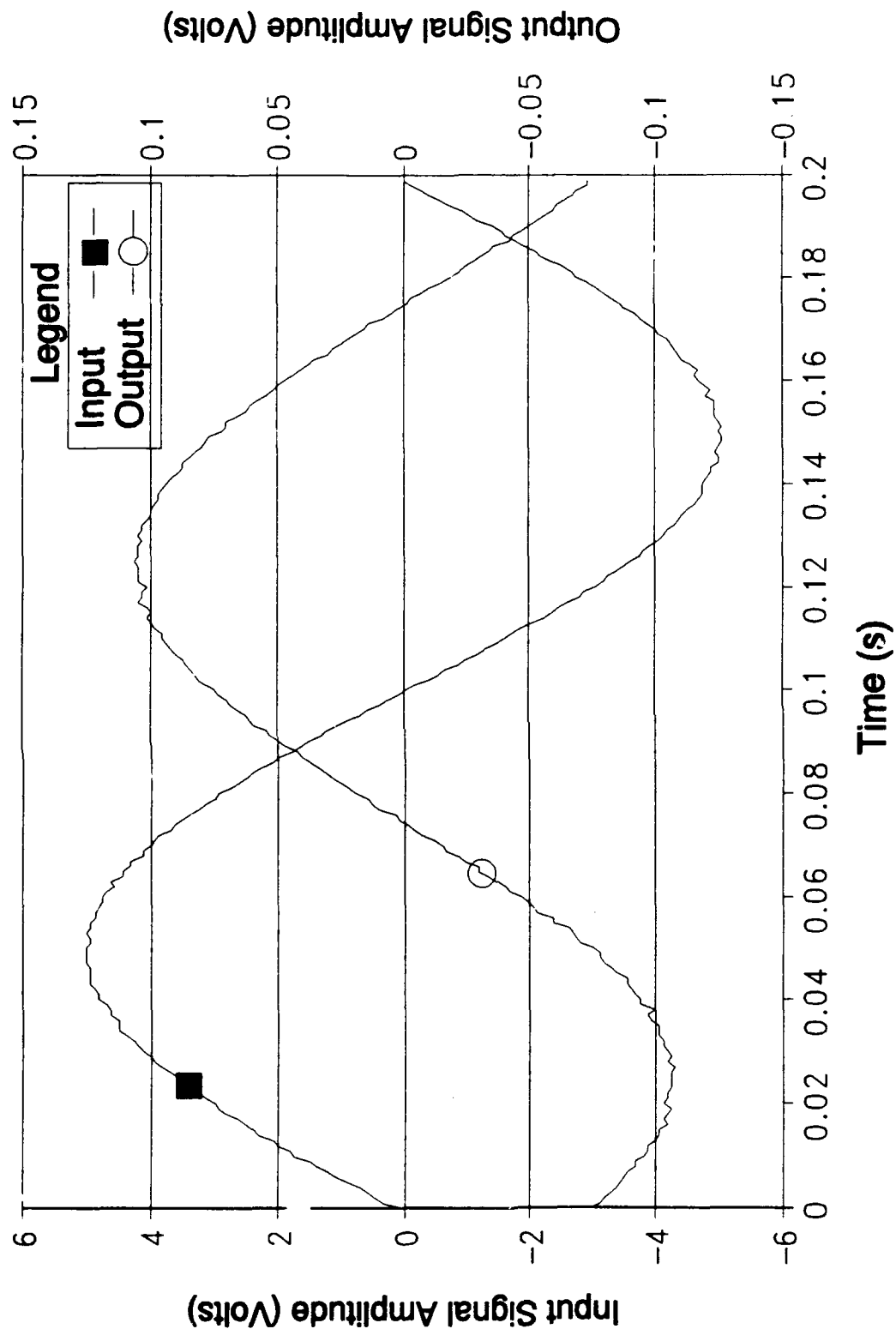
Figure G-9. Time Response of the Oldham Discrete Component Circuit Design with at 5 Hz Excitation Signal.
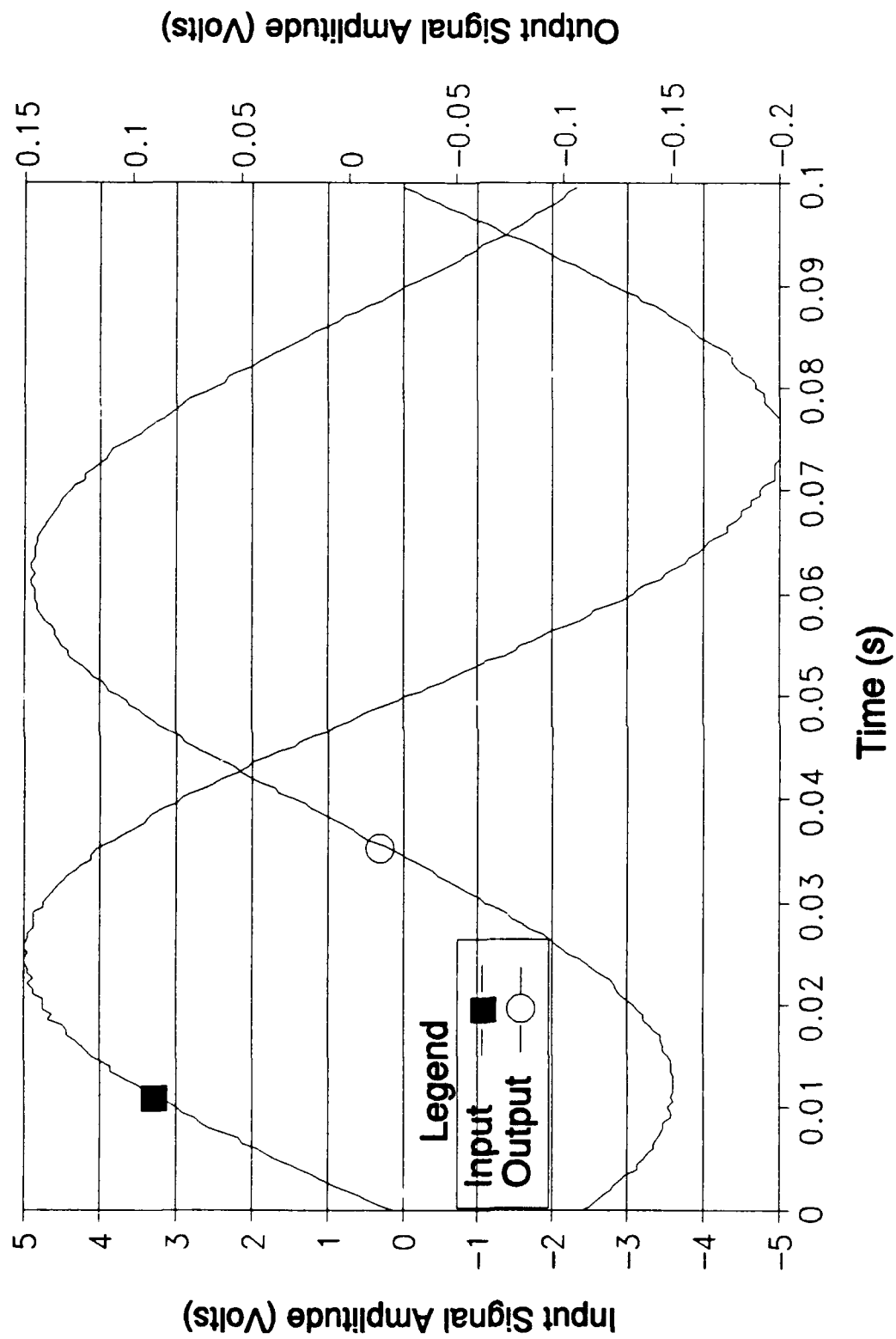
Figure G-10. Time Response of the Oldham Discrete Component Circuit Design with a 10 Hz Excitation Signal.

Figure G-11. Time Response of the Oldham Discrete Component Circuit Design with a 50 Hz Excitation Signal.

Figure G-12. Time Response of the Oldham Discrete Component Circuit Design with a 100 Hz Excitation Signal.
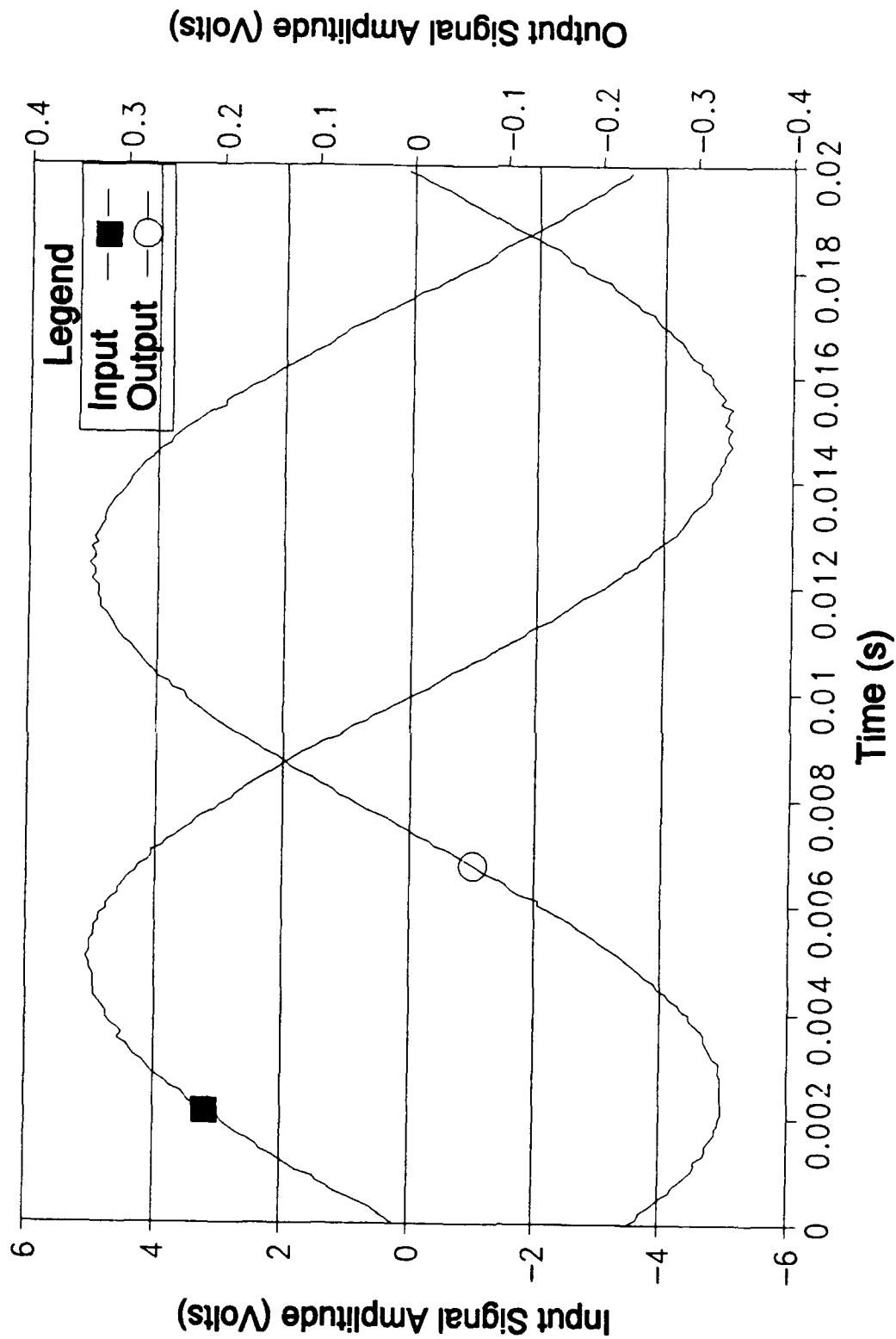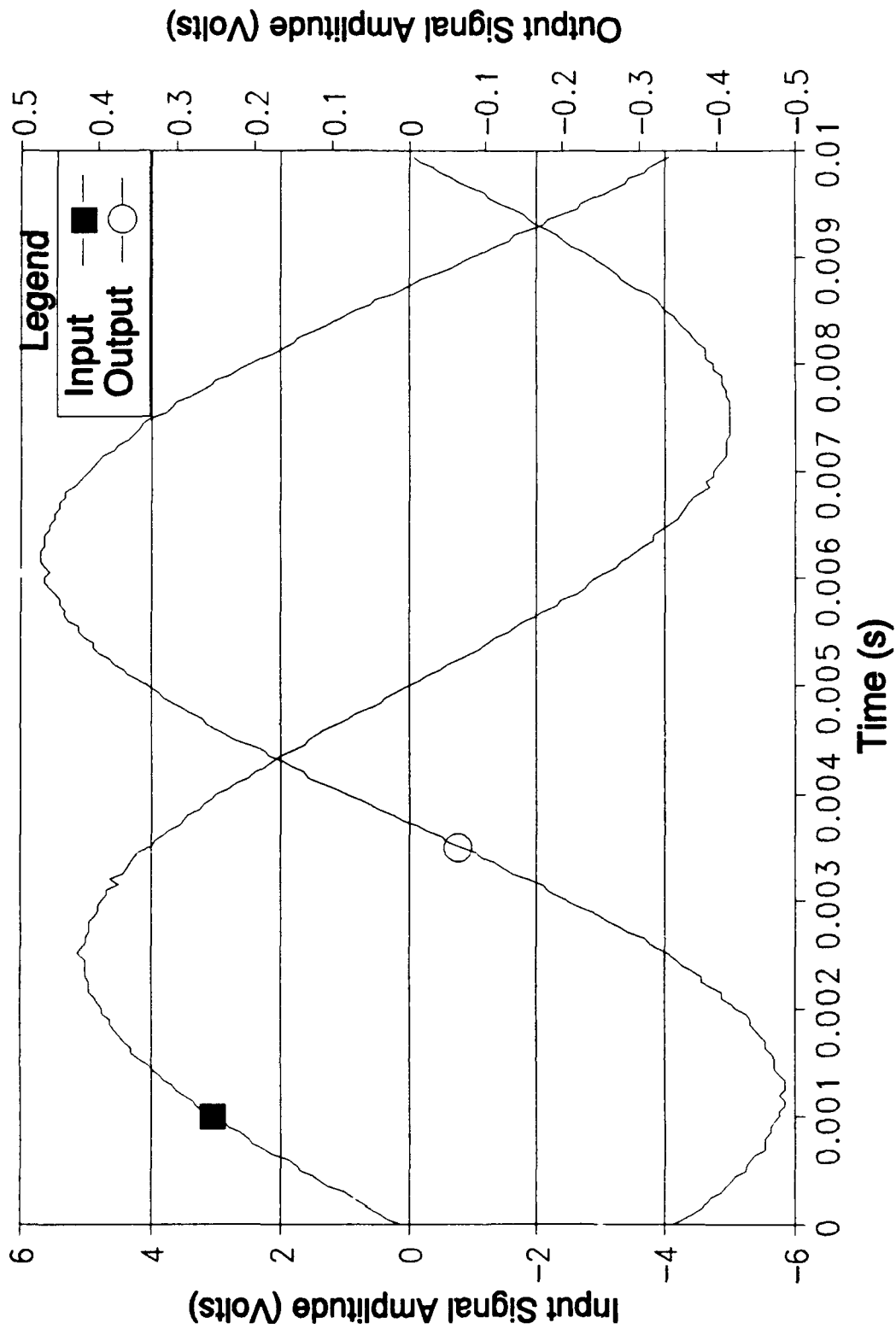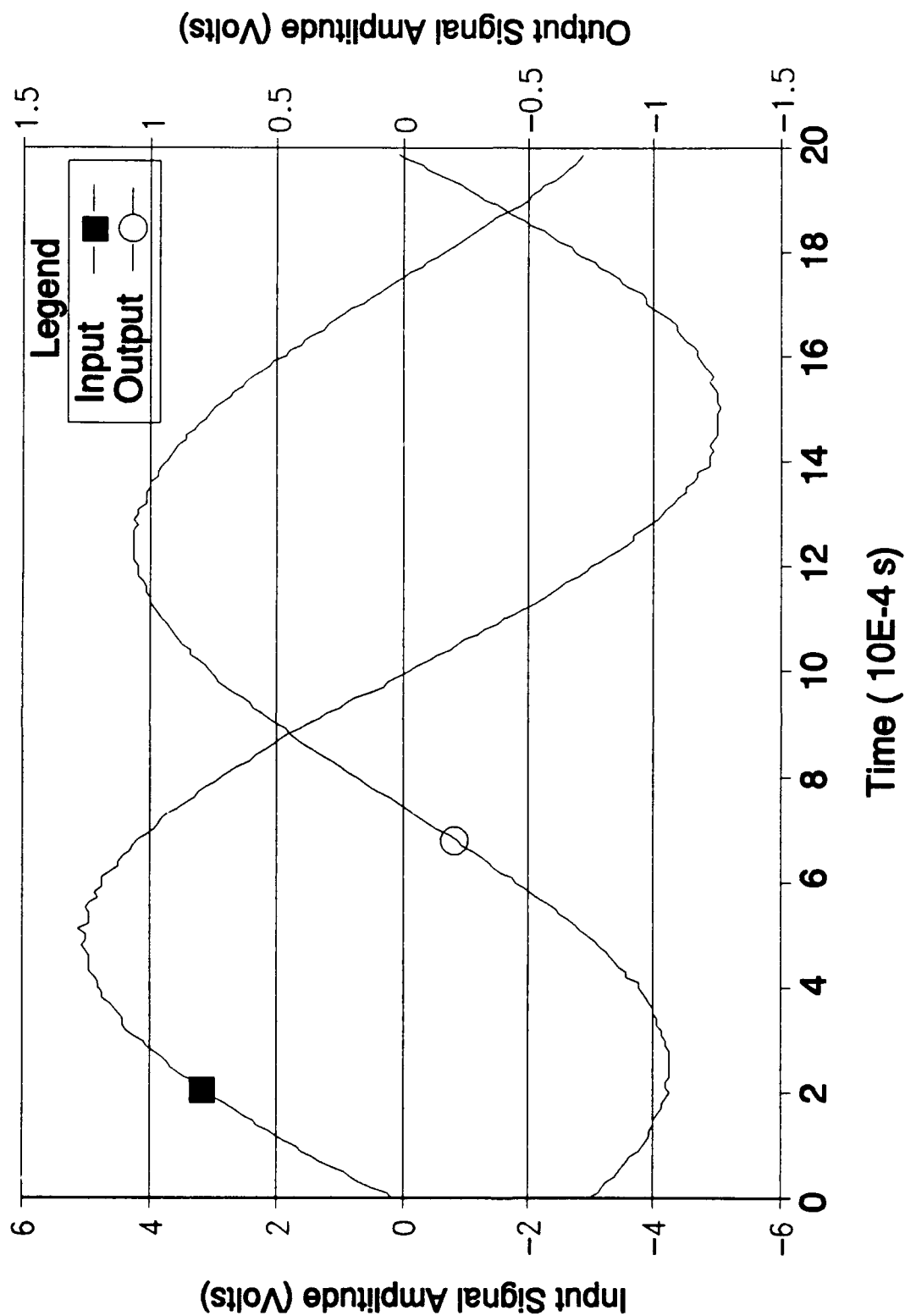
Figure G-13. Time Response of the Oldham Discrete Component Circuit Design with a 500 Hz Excitation Signal.
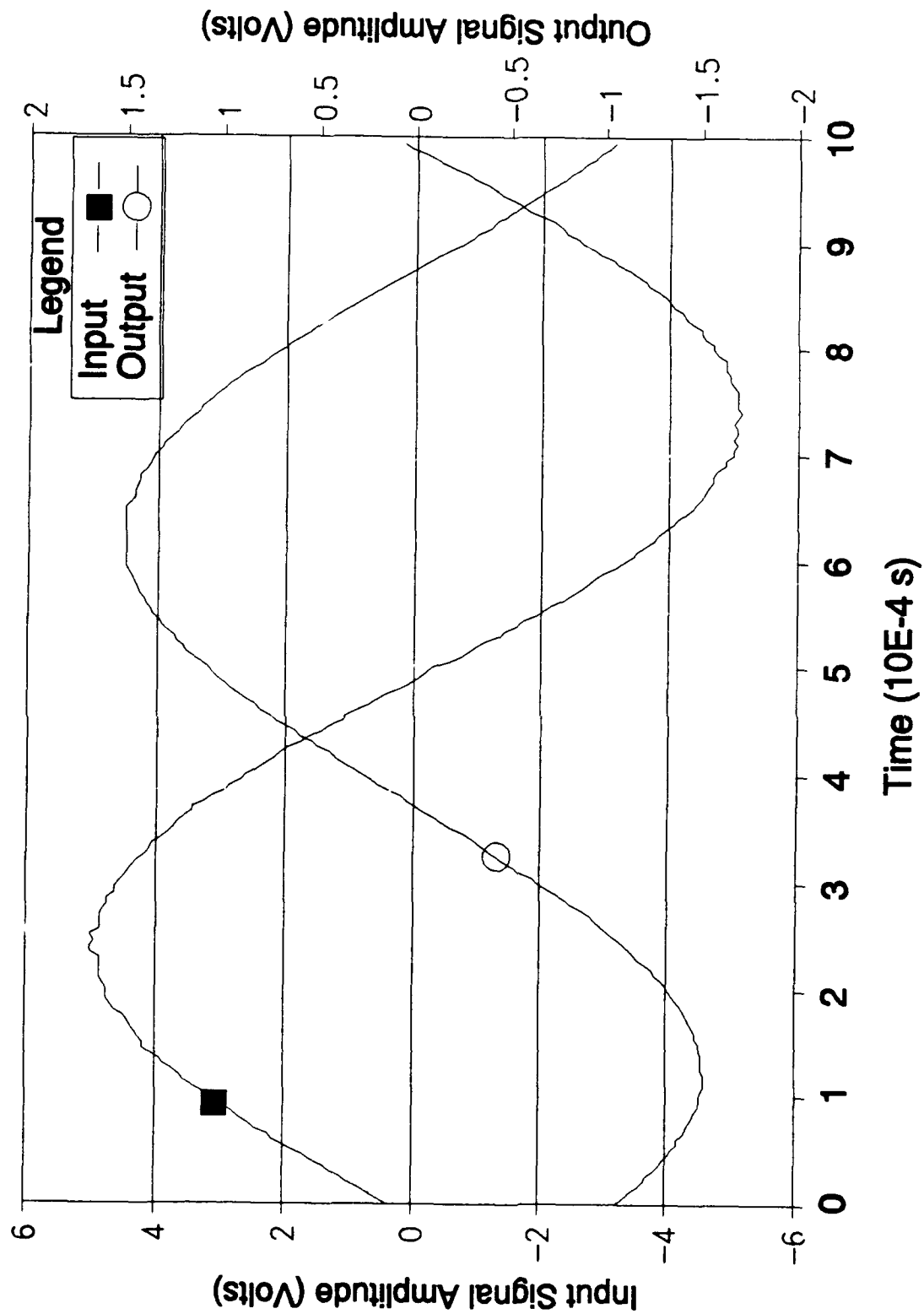
Figure G-14. Time Response of the Oldham Discrete Component Circuit Design with a 1000 Hz Excitation.
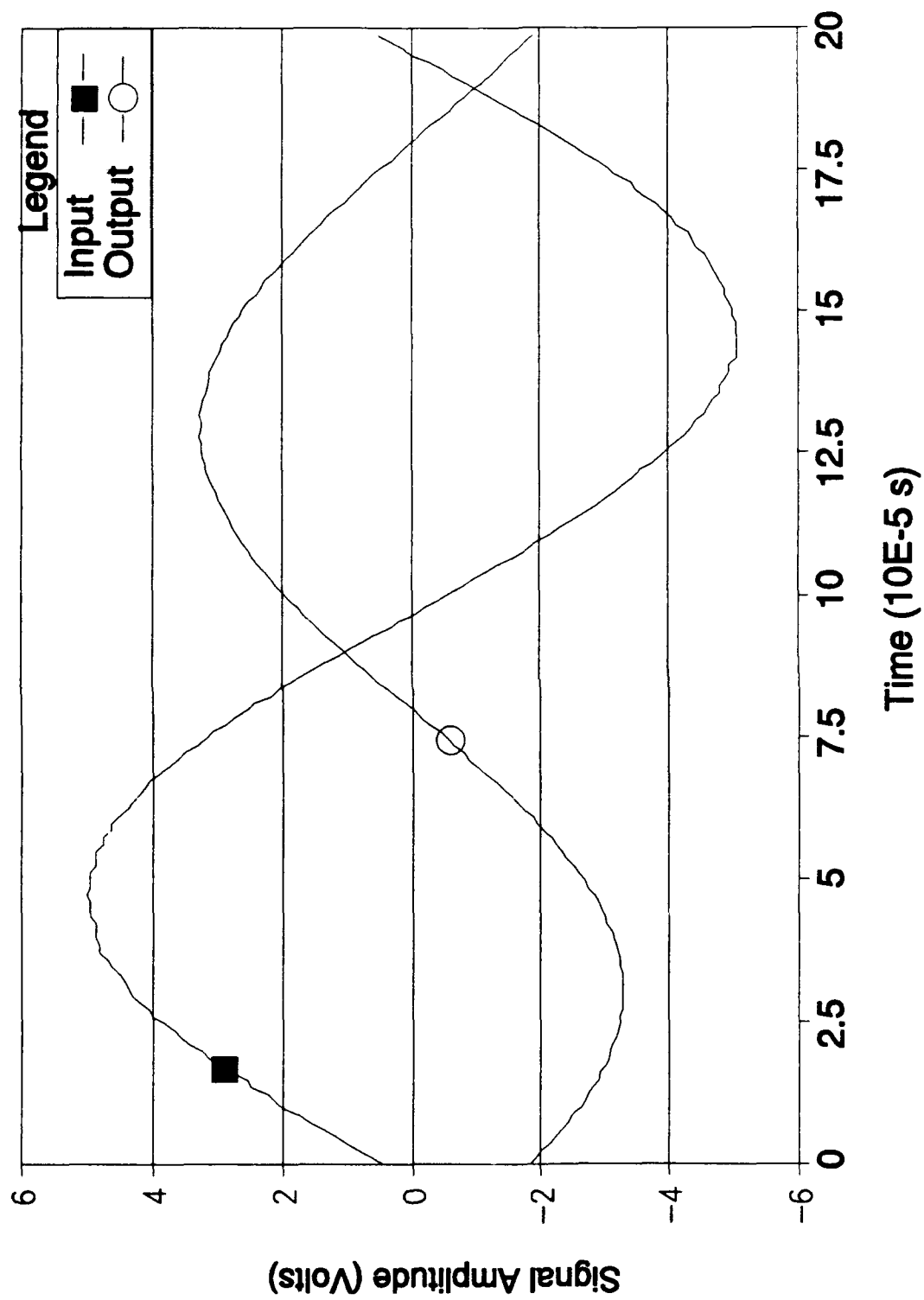
Figure G-15. Time Response of the Oldham Discrete Component Circuit Design with a 5000 Hz Excitation Signal.

G-18

Figure G-16. Oldfield Circuit Discrete Component Gain Response.
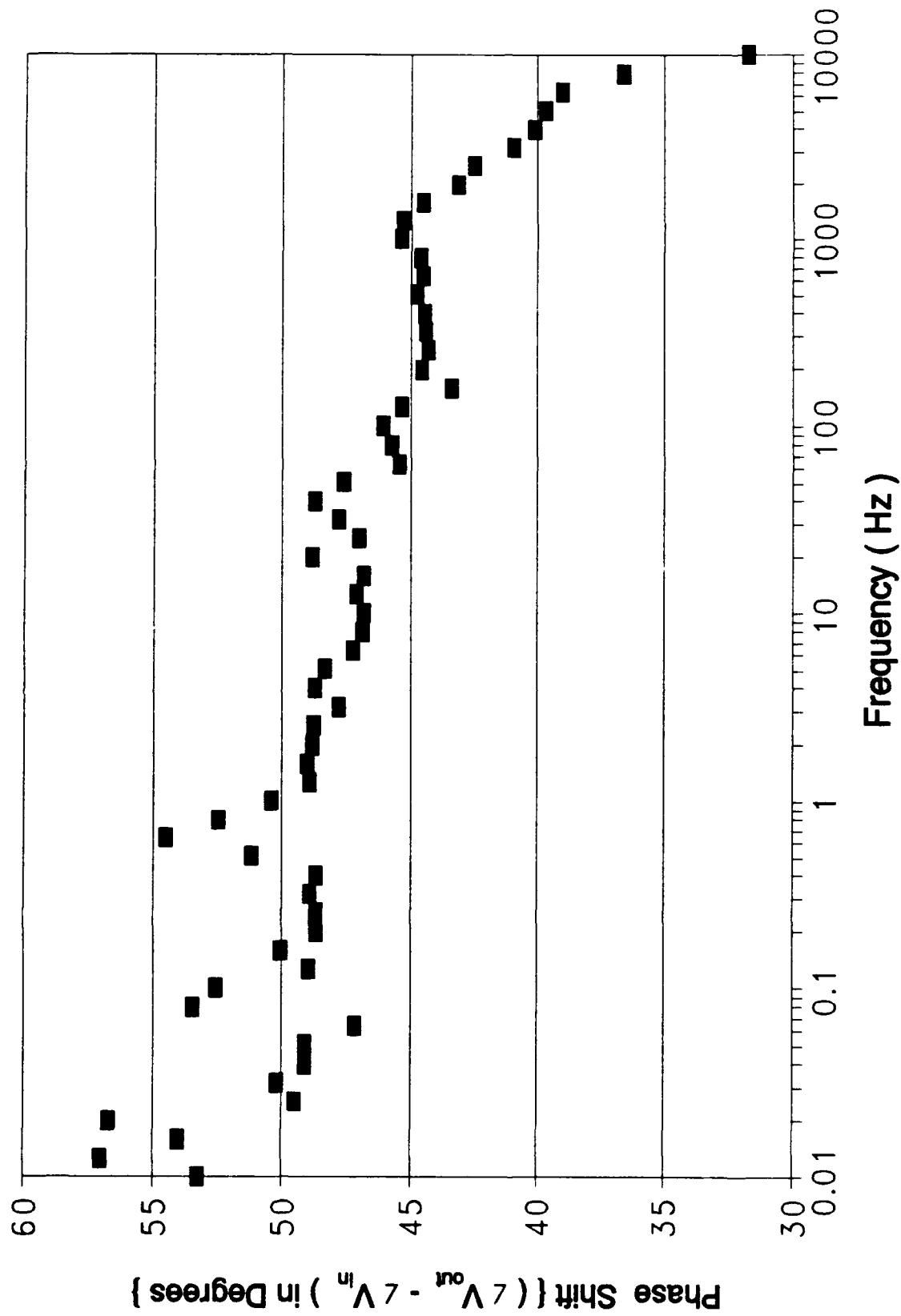
Figure G-17. Oldfield Circuit Discrete Component Phase Response.

Figure G-18. Time Response of the Oldfield Discrete Component Circuit Design with a a 0.001 Hz Excitation Signal.

Figure G-19. Time Response of the Oldfield Discrete Component Circuit Design with a 0.01 Hz Excitation Signal.

Figure G-20. Time Response of the Oldfield Discrete Component Circuit Design with a 0.05 Hz Excitation Signal.

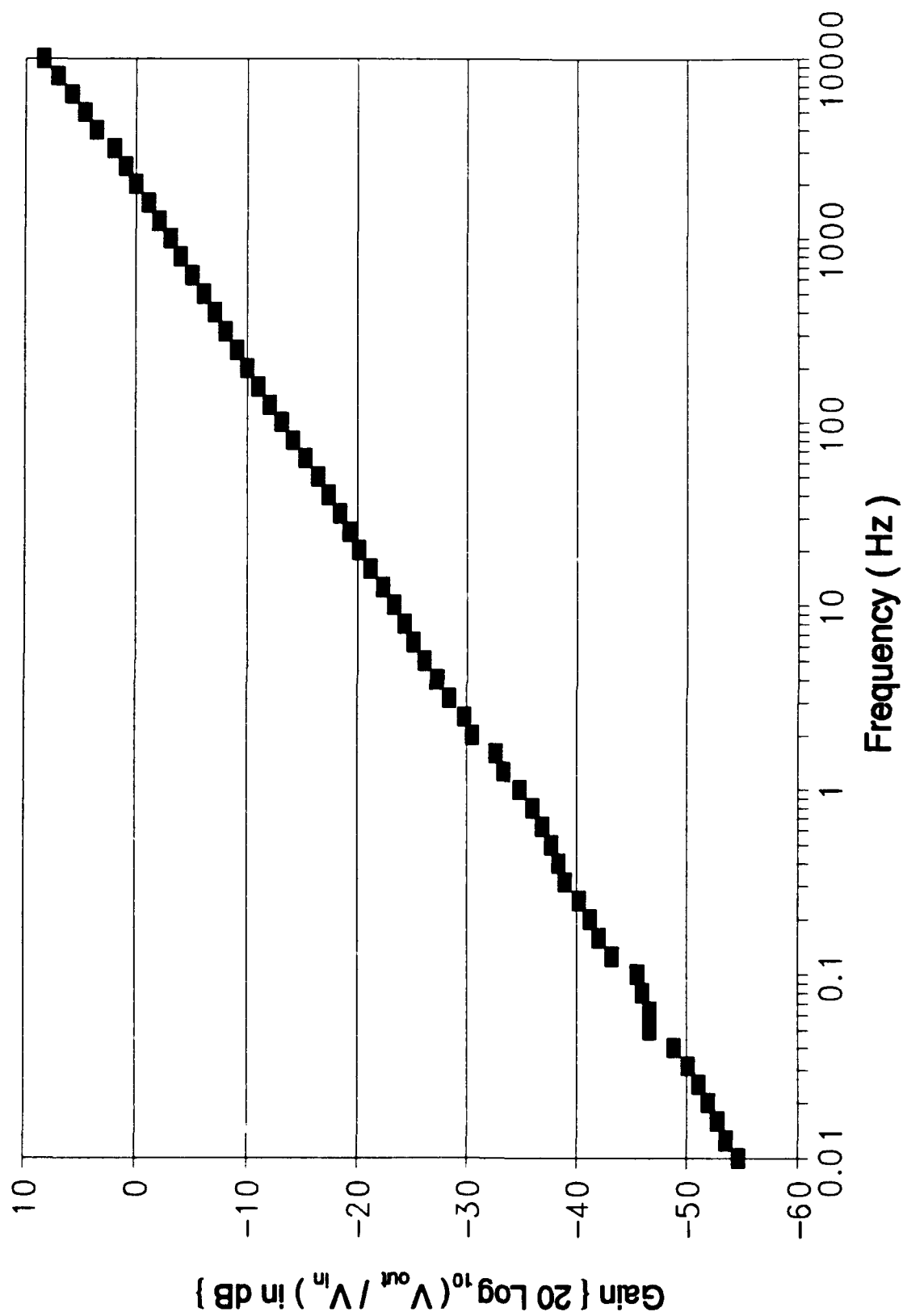Figure G-21. Time Response of the Oldfield Discrete Component Circuit Design with a 0.1 Hz Excitation Signal.

G-24

Figure G-22. Time Response of the Oldfield Discrete Component Circuit Design with a 0.5 Hz Excitation Signal.

Figure G-23. Time Response of the Oldfield Discrete Component Circuit Design with a 1 Hz Excitation Signal.

Figure G-24. Time Response of the Oldfield Discrete Comonent Circuit Design with a 5 Hz Excitation Signal.

Figure G-25. Time Response of the Oldfield Discrete Component Circuit Design with a 10 Hz Excitation Signal.

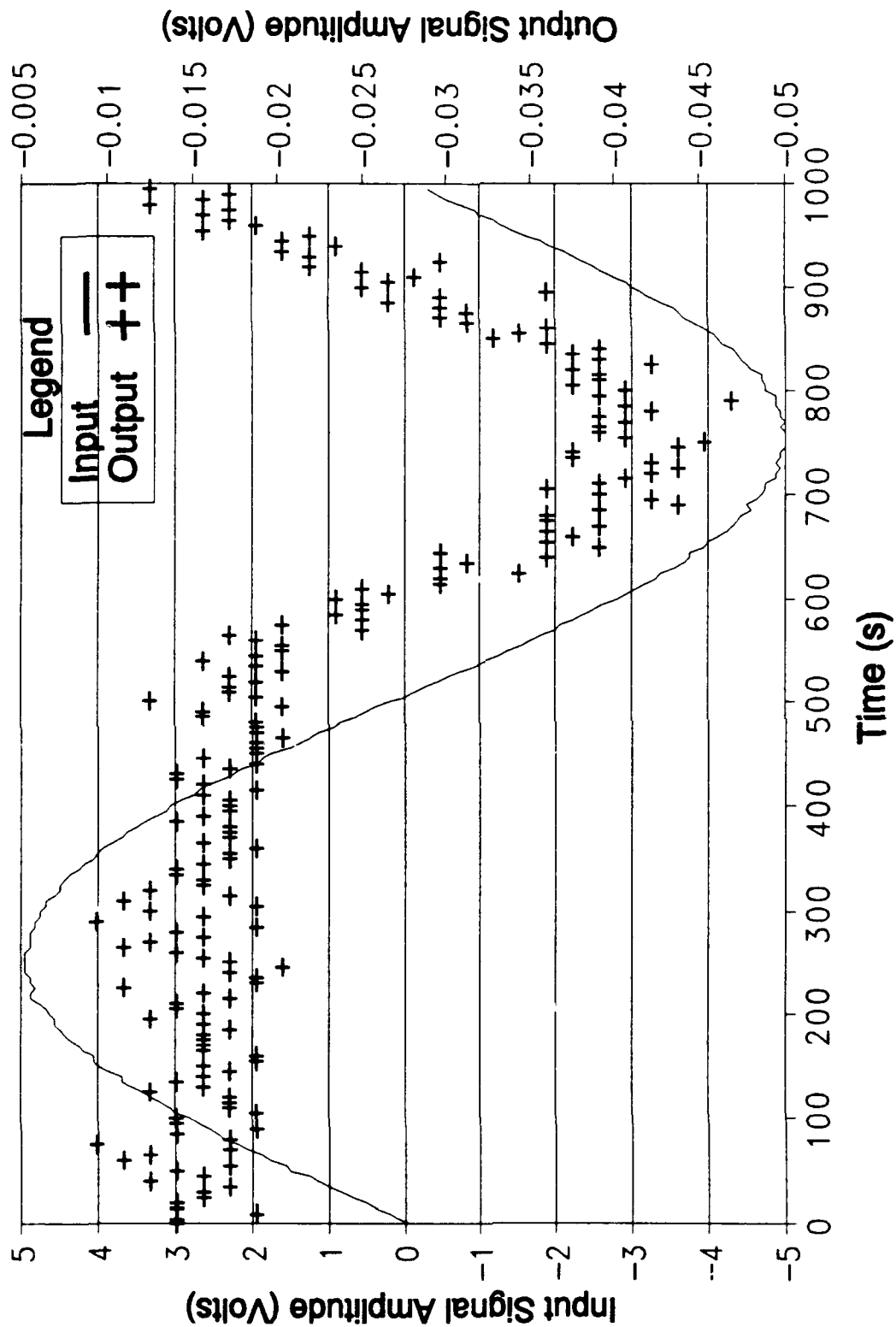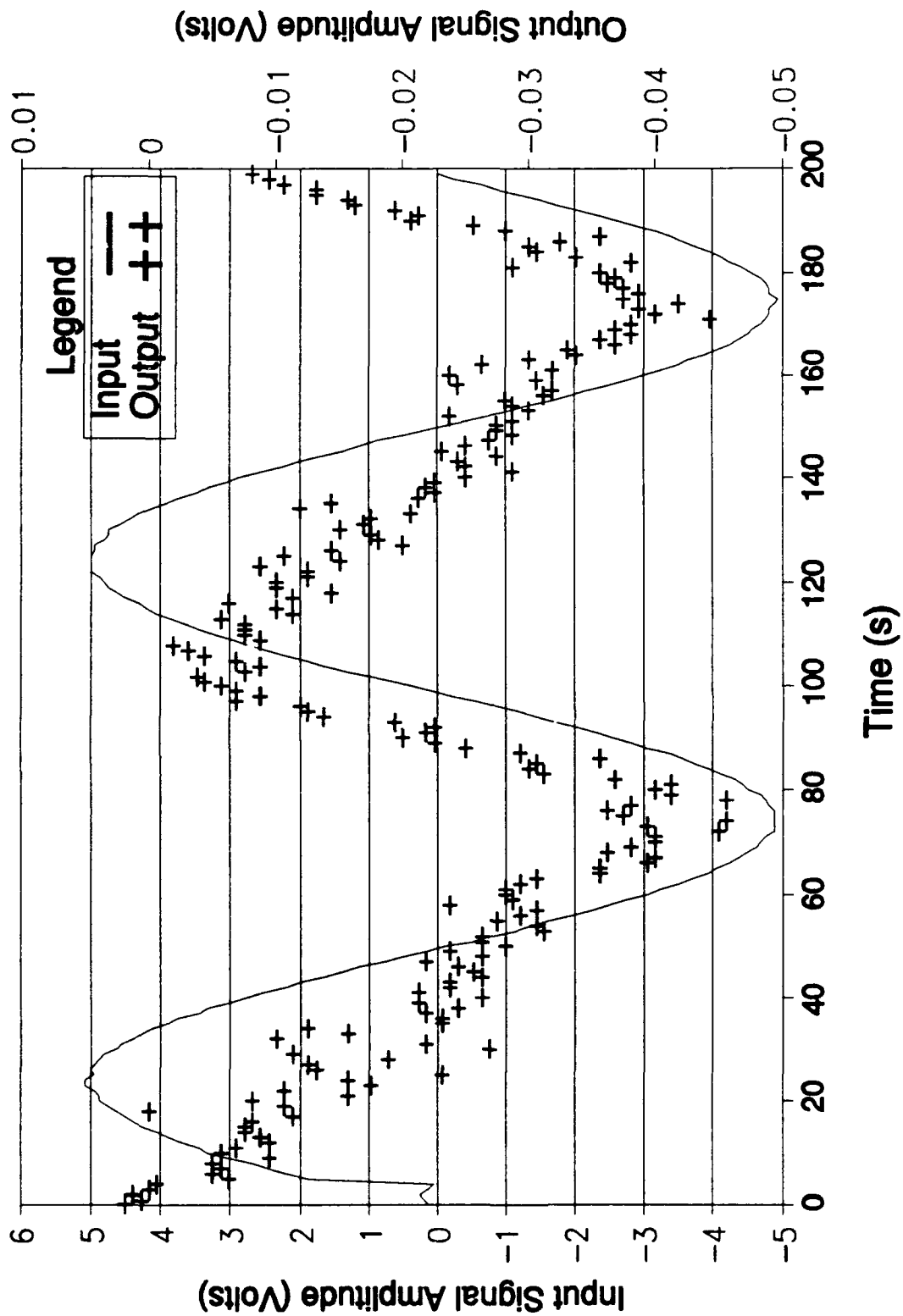Figure G-26. Time Response of the Oldfield Discrete Component Circuit Design with a 50 Hz Excitation Signal.

Figure G-27. Time Response of the Oldfield Discrete Component Circuit Design with a 100 Hz Excitation Signal.

Figure G-28. Time Response of the Oldfield Discrete Component Circuit Design with a 500 Hz Excitation Signal.

Figure G-29. Time Response of the Oldfield Discrete Component Circuit Design with a 1000 Hz Excitation Signal.
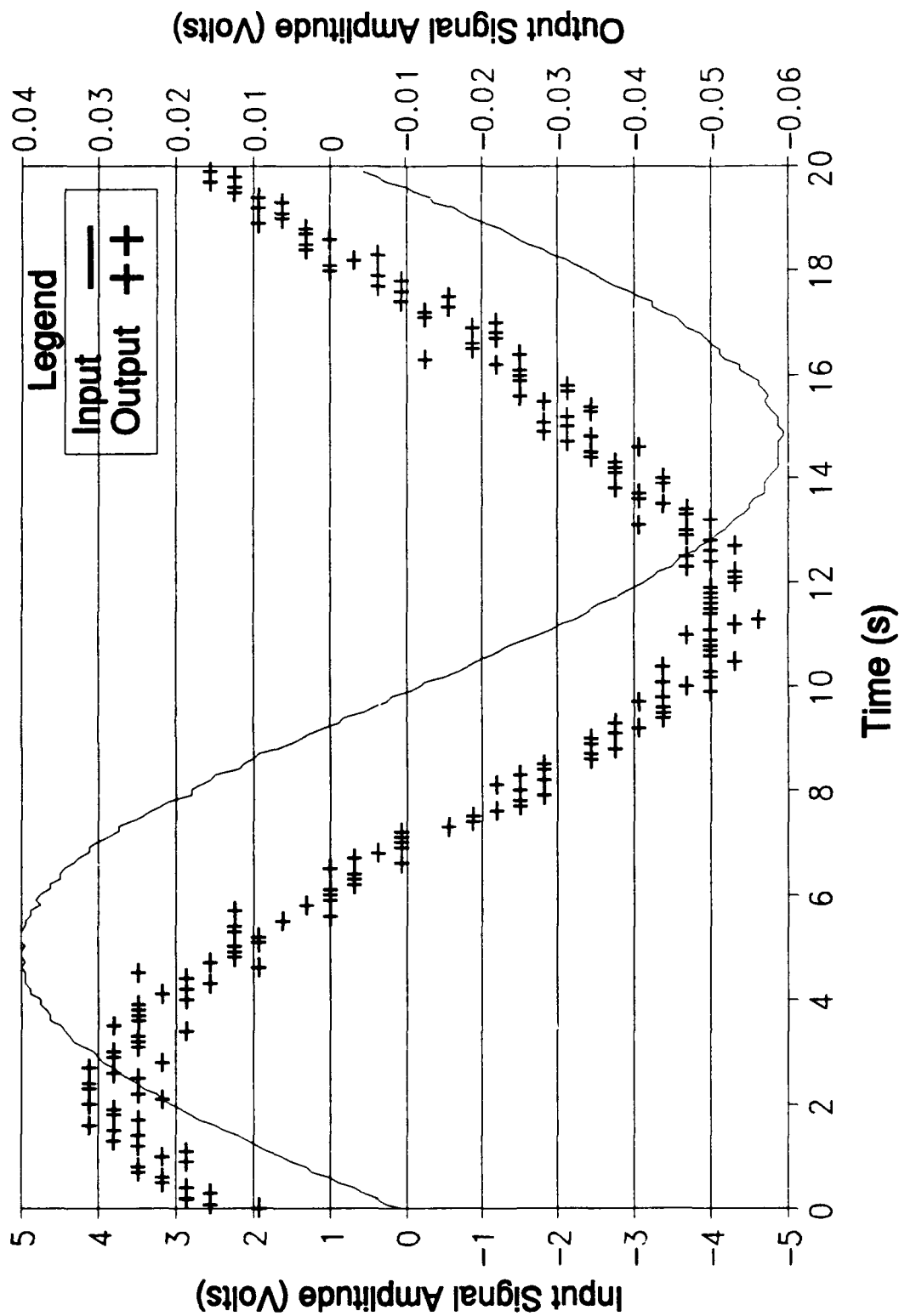
Figure G-30. Time Response of the Oldfield Discrete Component Circuit Design with a 5000 Hz Excitation Signal.

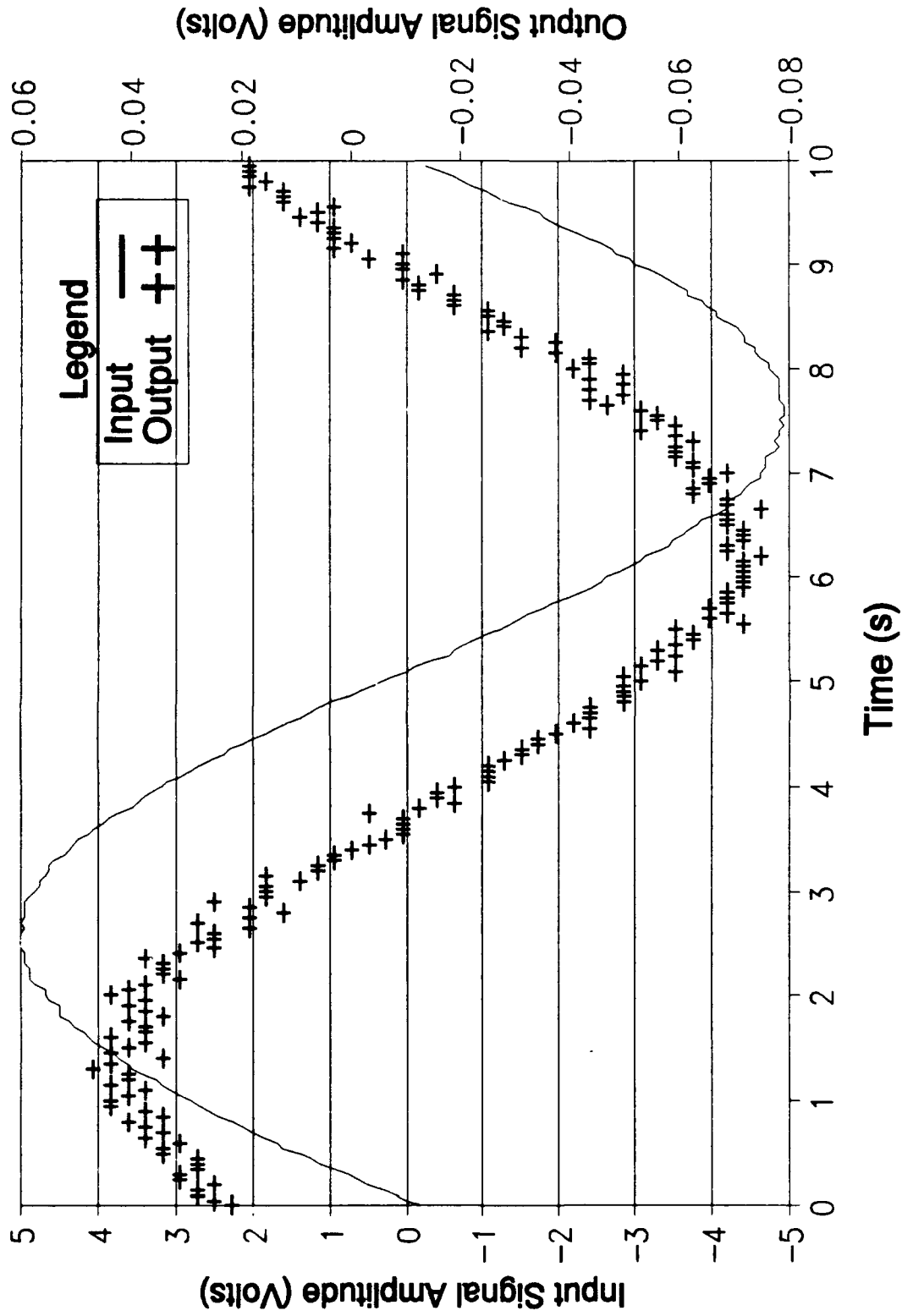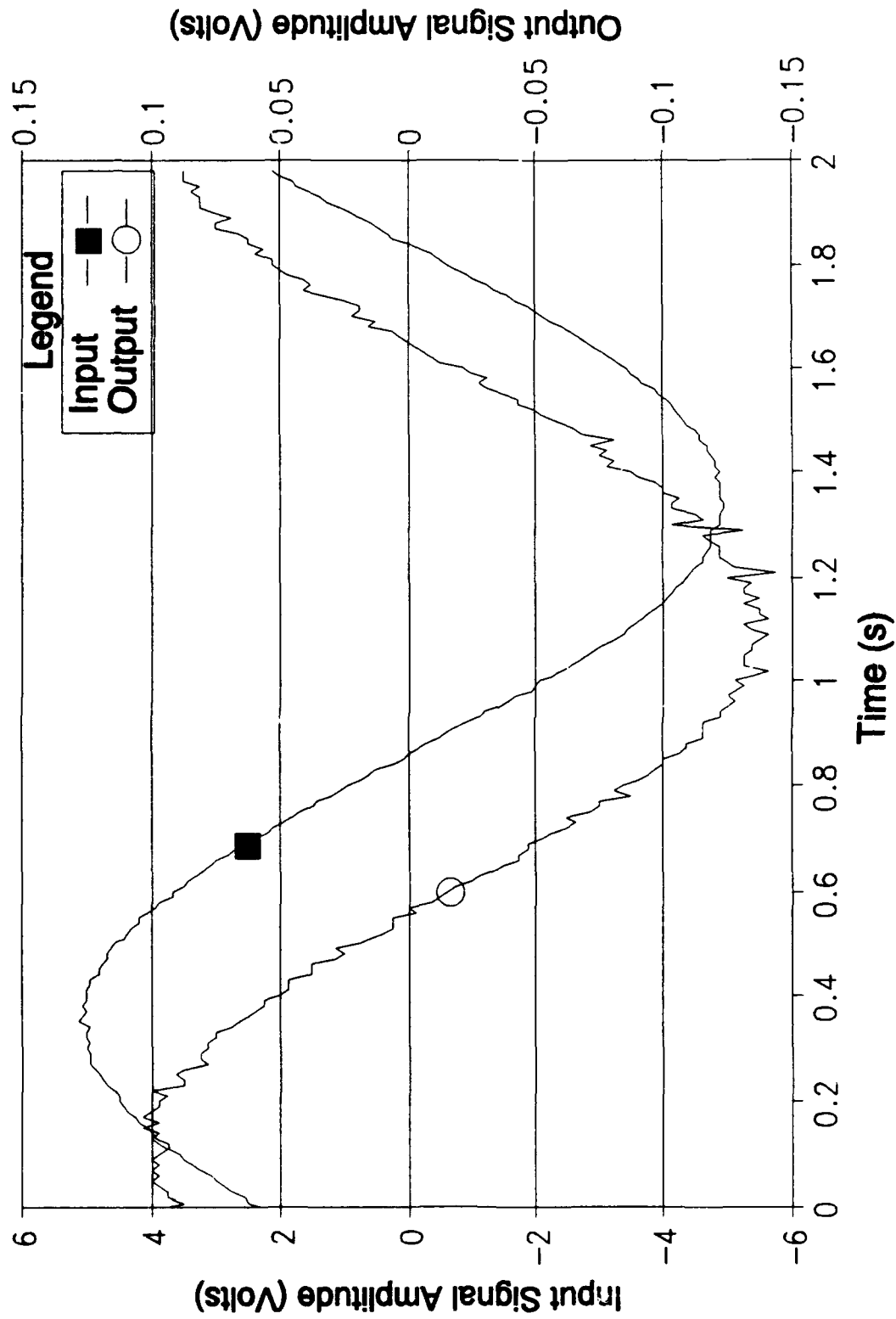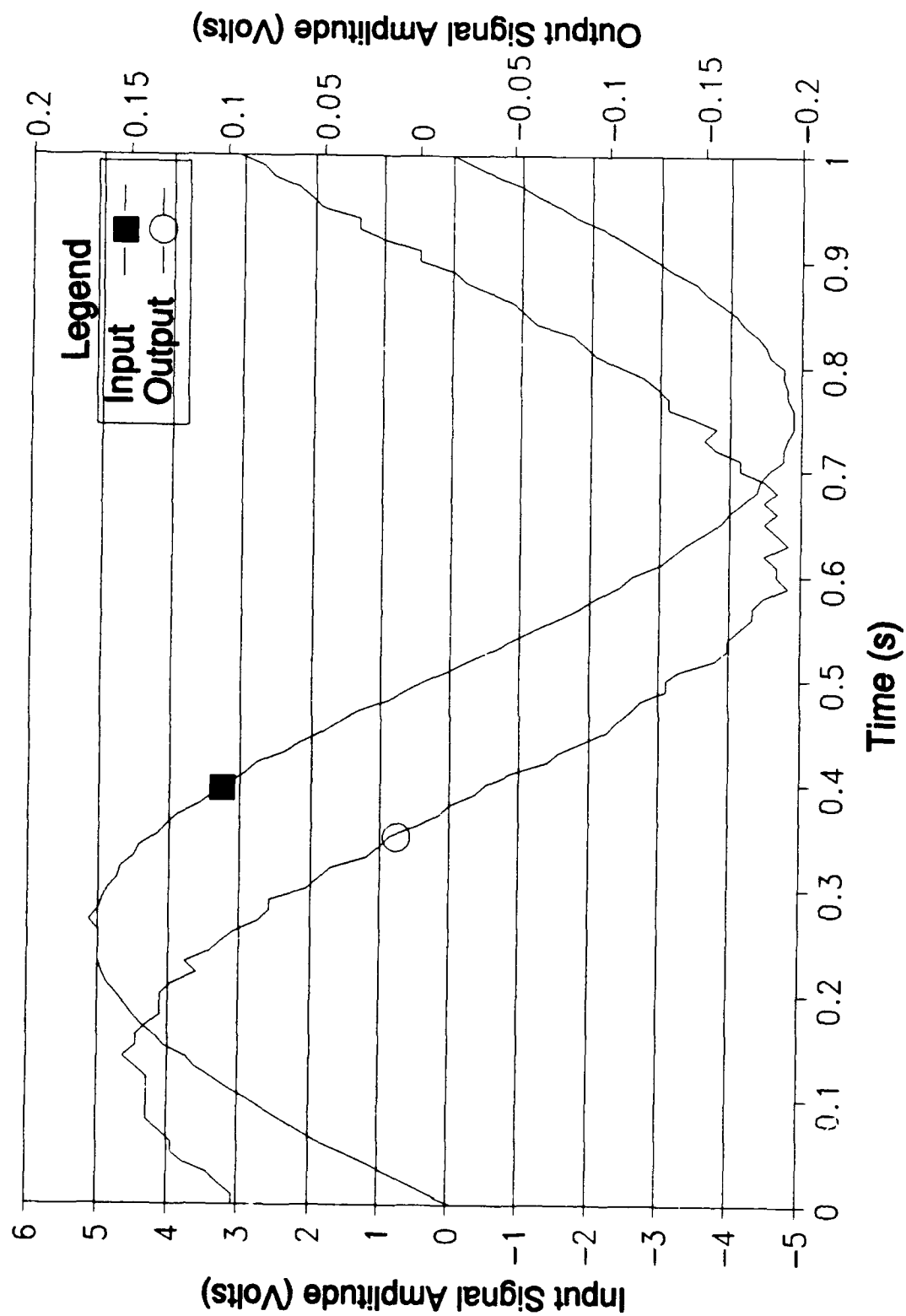Figure G-31. Time Response of the Oldfield Discrete Component Circuit Design with a 10 KHz Excitation Signal.

Section 2

Electrical Performance Results for the

Oldham Hybrid and Oldfield Surface Mount Component Circuits

Realized with a Printed Circuit Board Format
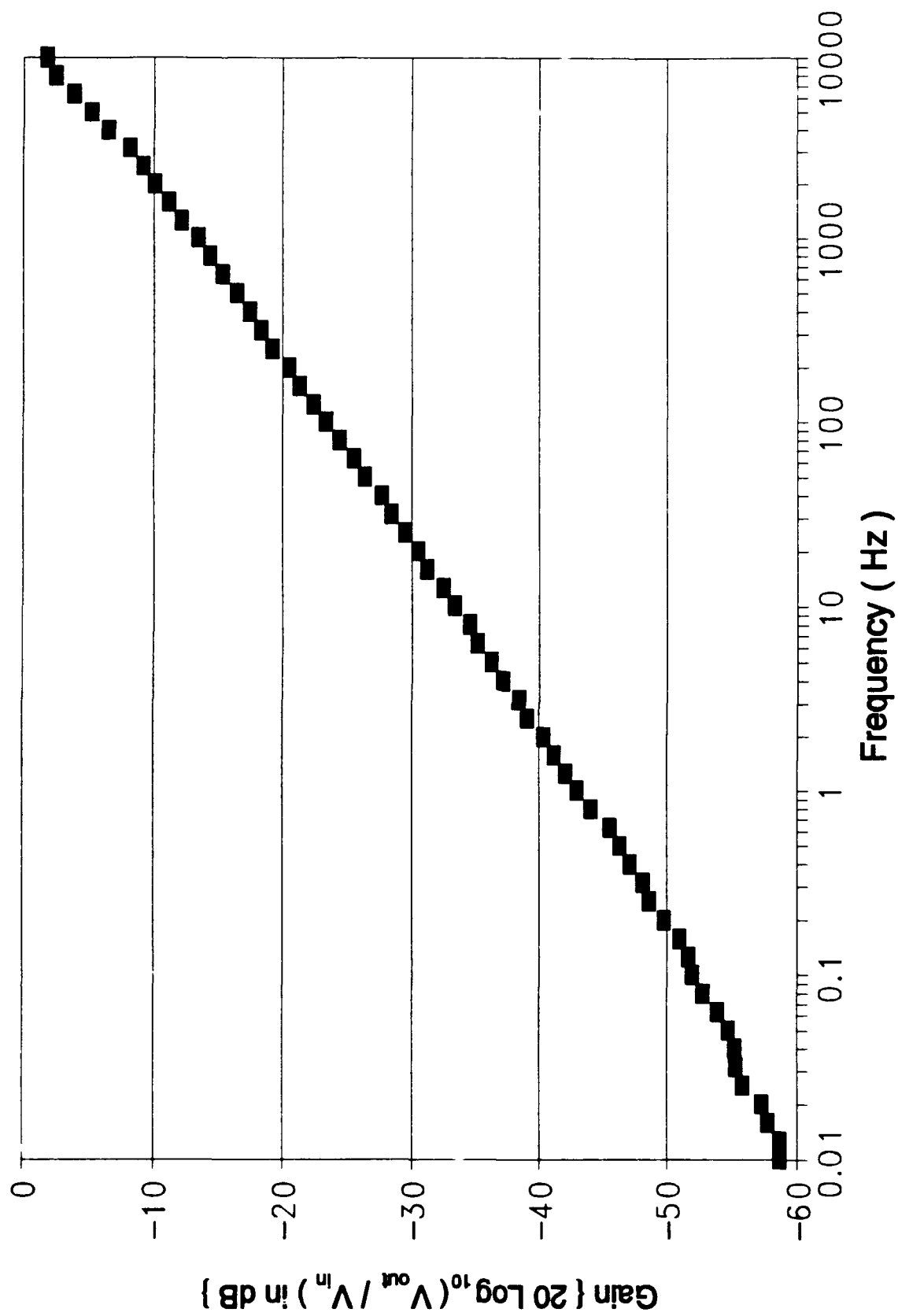
Figure G-32. Oldham Circuit Hybrid Component Gain Response.
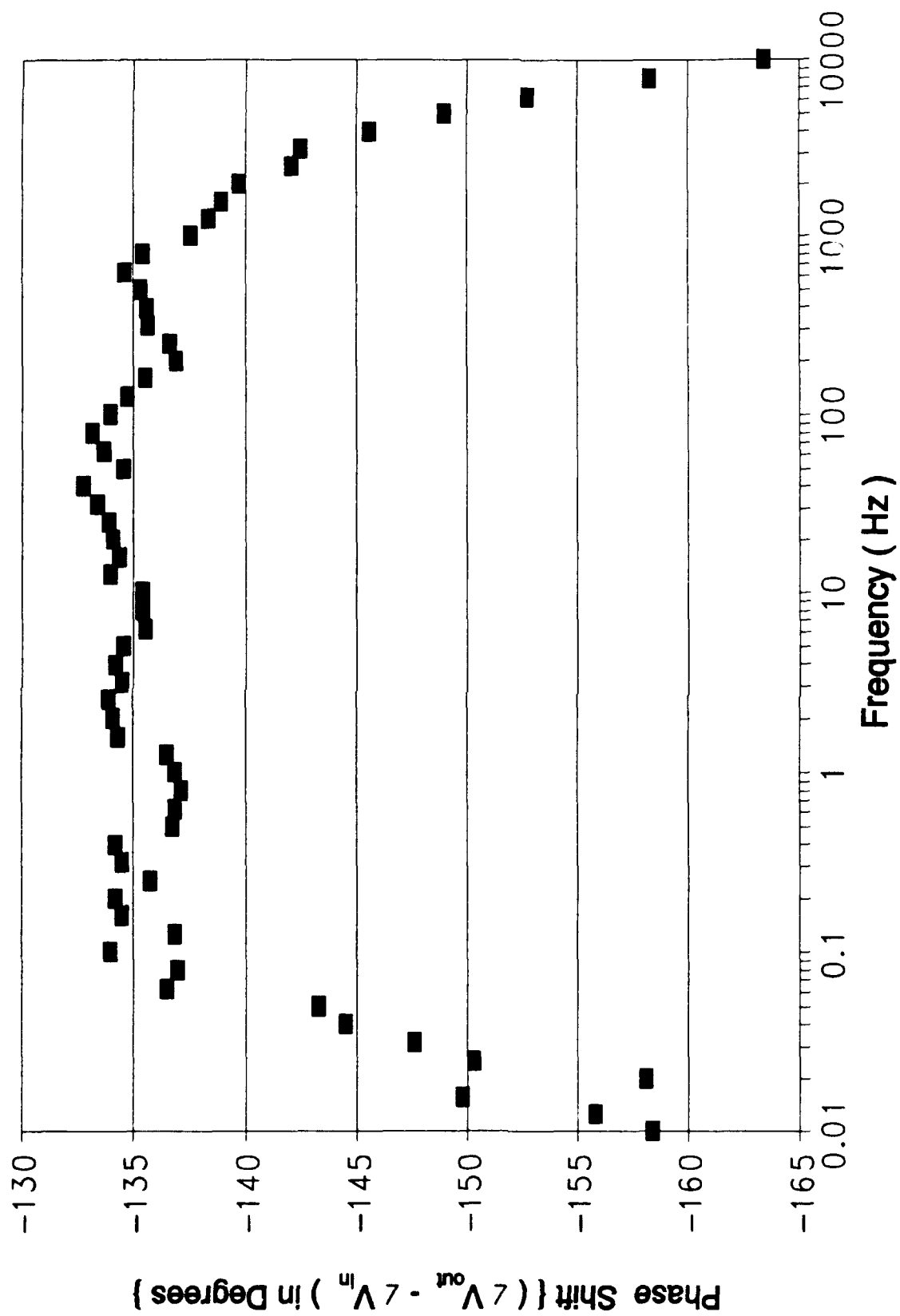
Figure G-33. Oldham Circuit Hybrid Component Phase Response.

Figure G-34. Time Response of the Oldham Hybrid Component Circuit Design with a 0.001 Hz Excitation Signal.
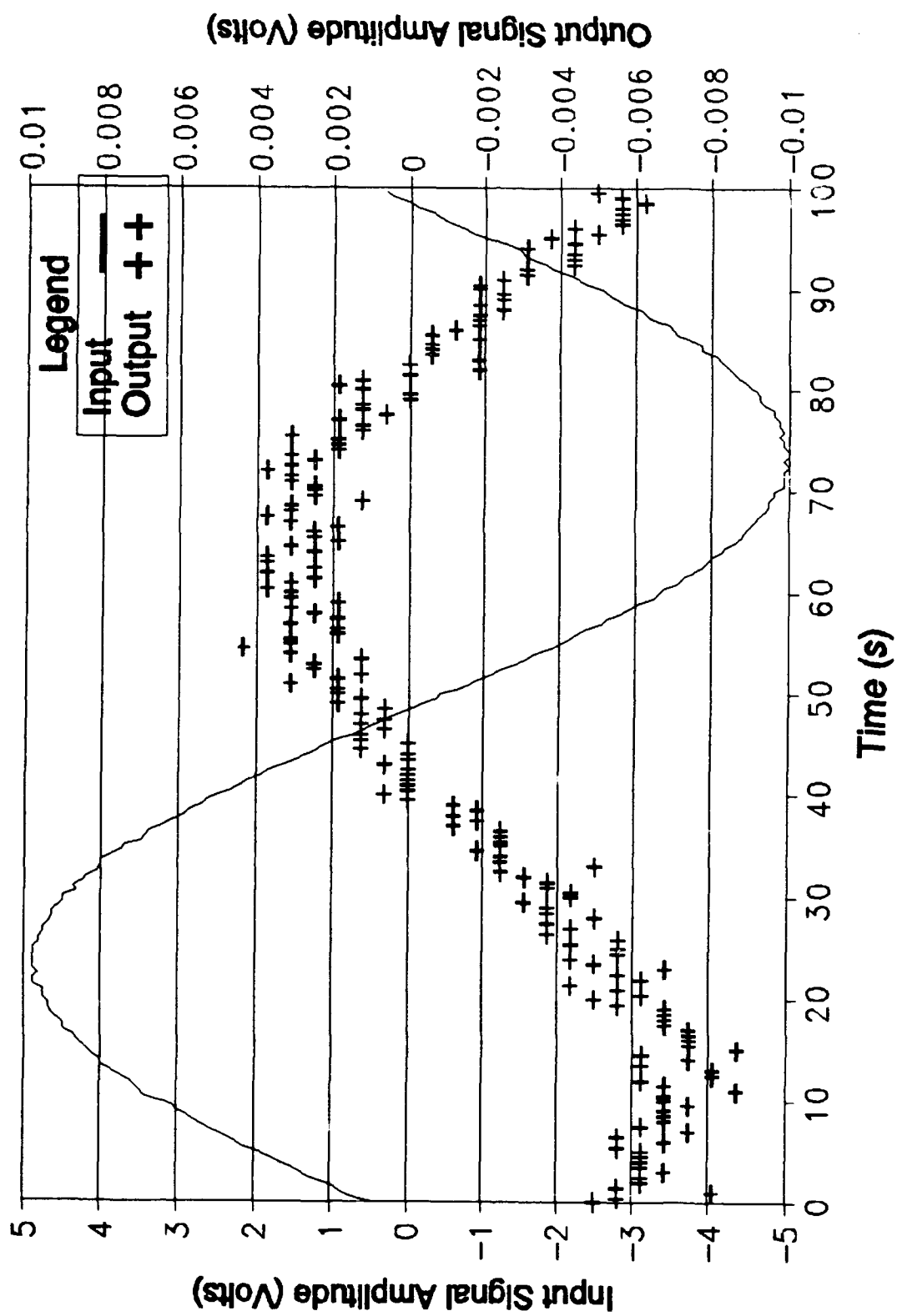
Figure G-35. Time Response of the Oldham Hybrid Component Circuit Design with a 0.01 Hz Excitation Signal.
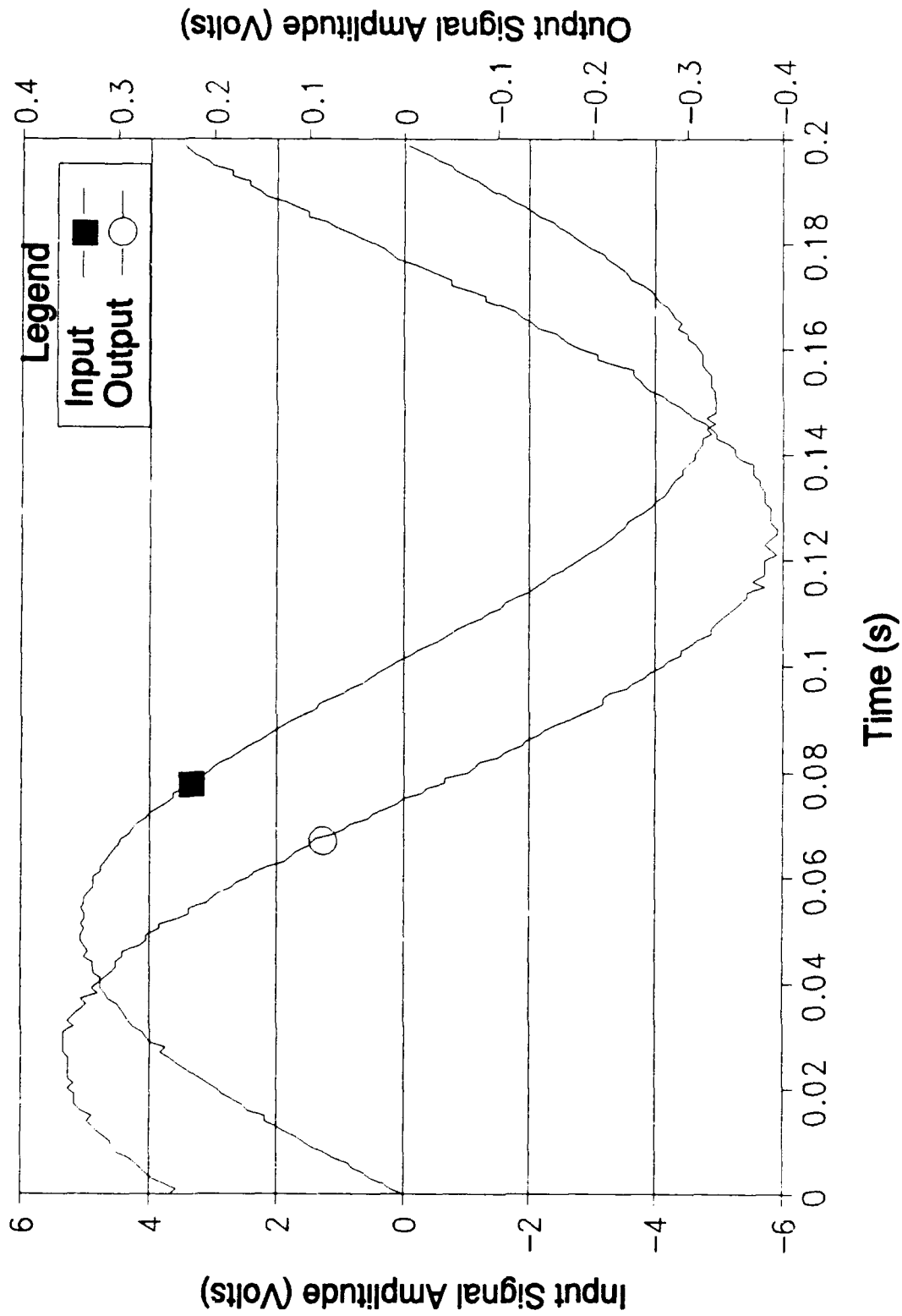
Figure G-36. Time Response of the Oldham Hybrid Component
Circuit Design wit a 0.05 Hz Excitation Signal.
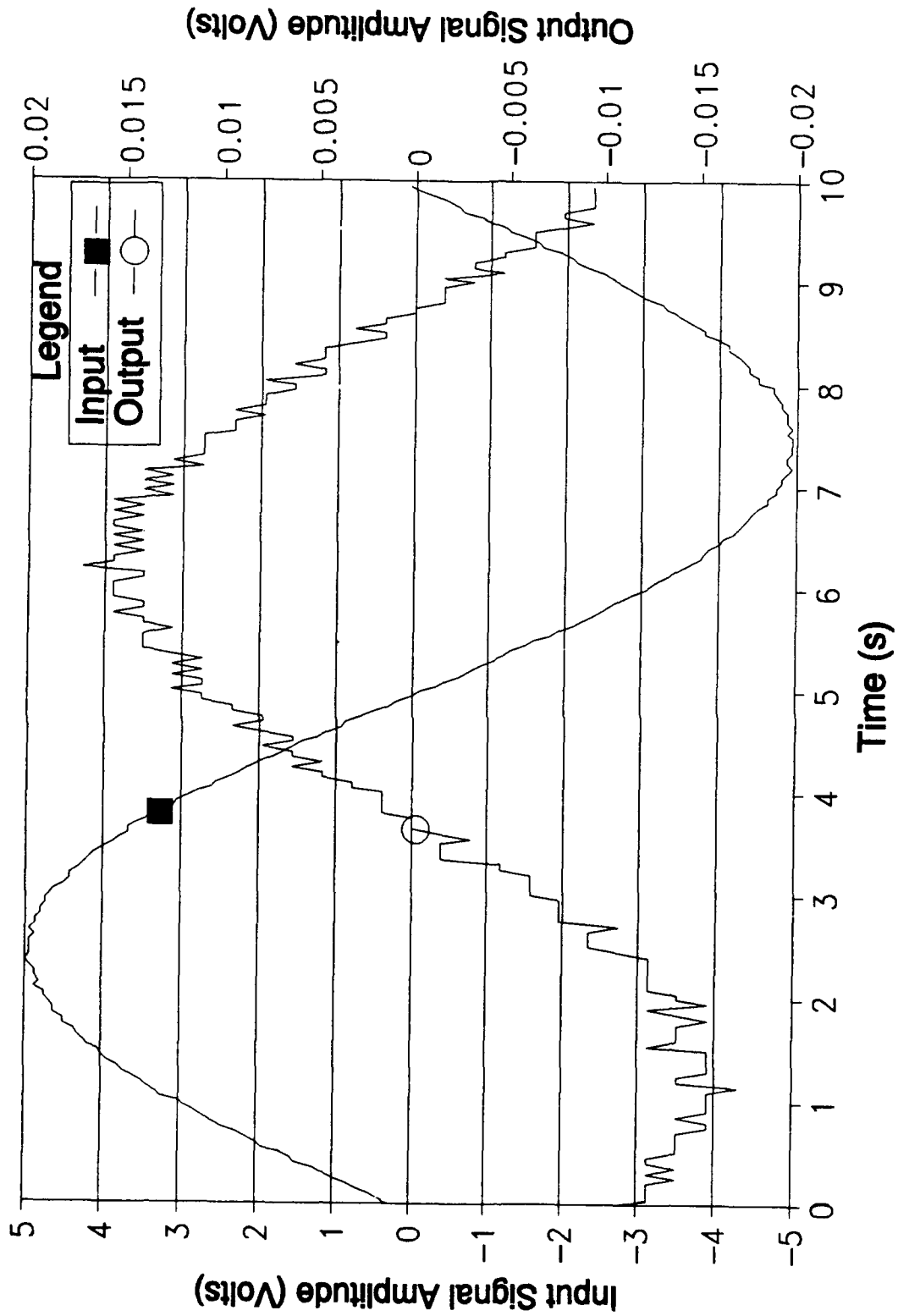
Figure G-37. Time Response of the Oldham Hybrid Component Circuit Design with a 0.1 Hz Excitation Signal.
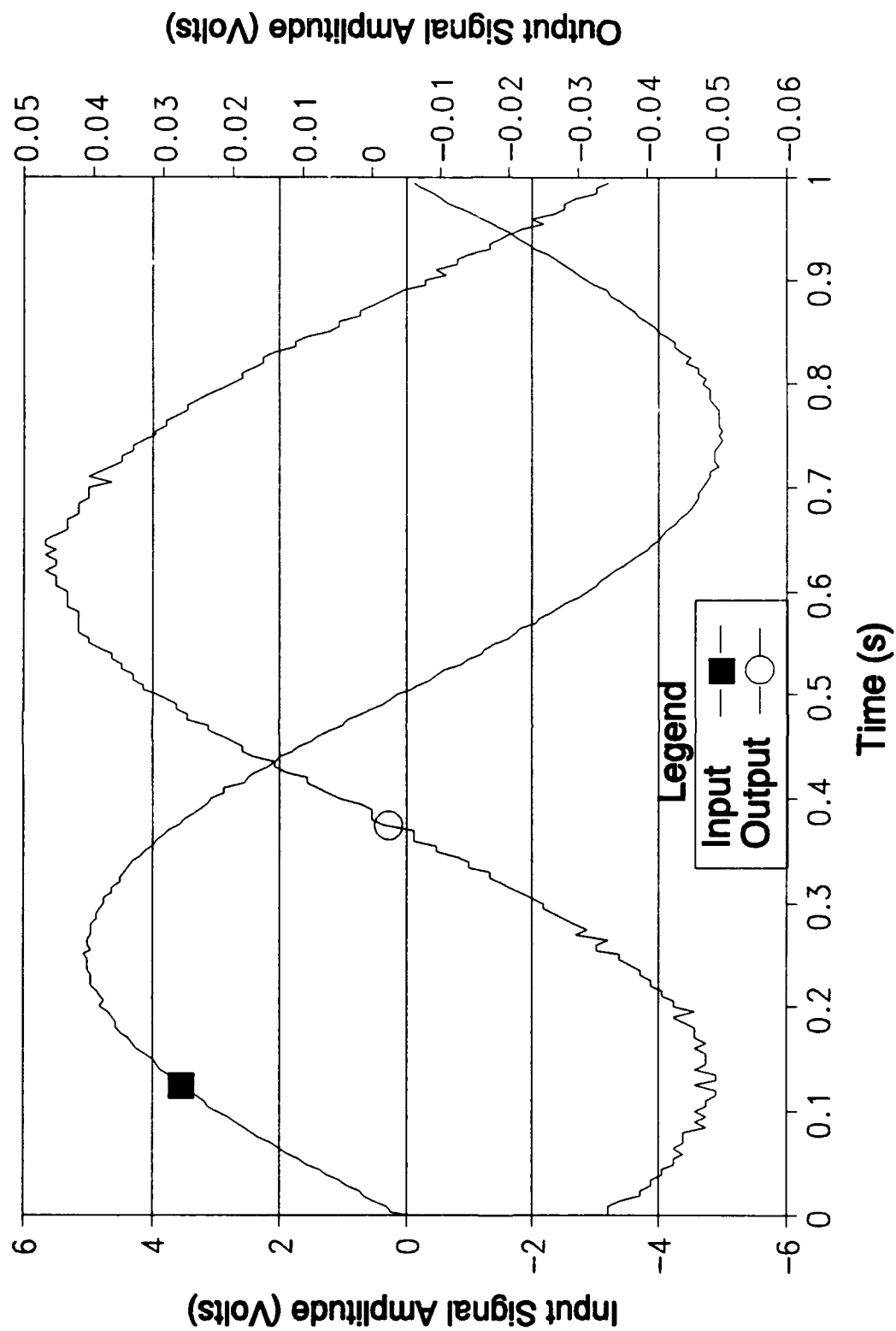
Figure G-39. Time Response of the Oldham Hybrid Component Circuit Design with a 1 Hz Excitation Signal.
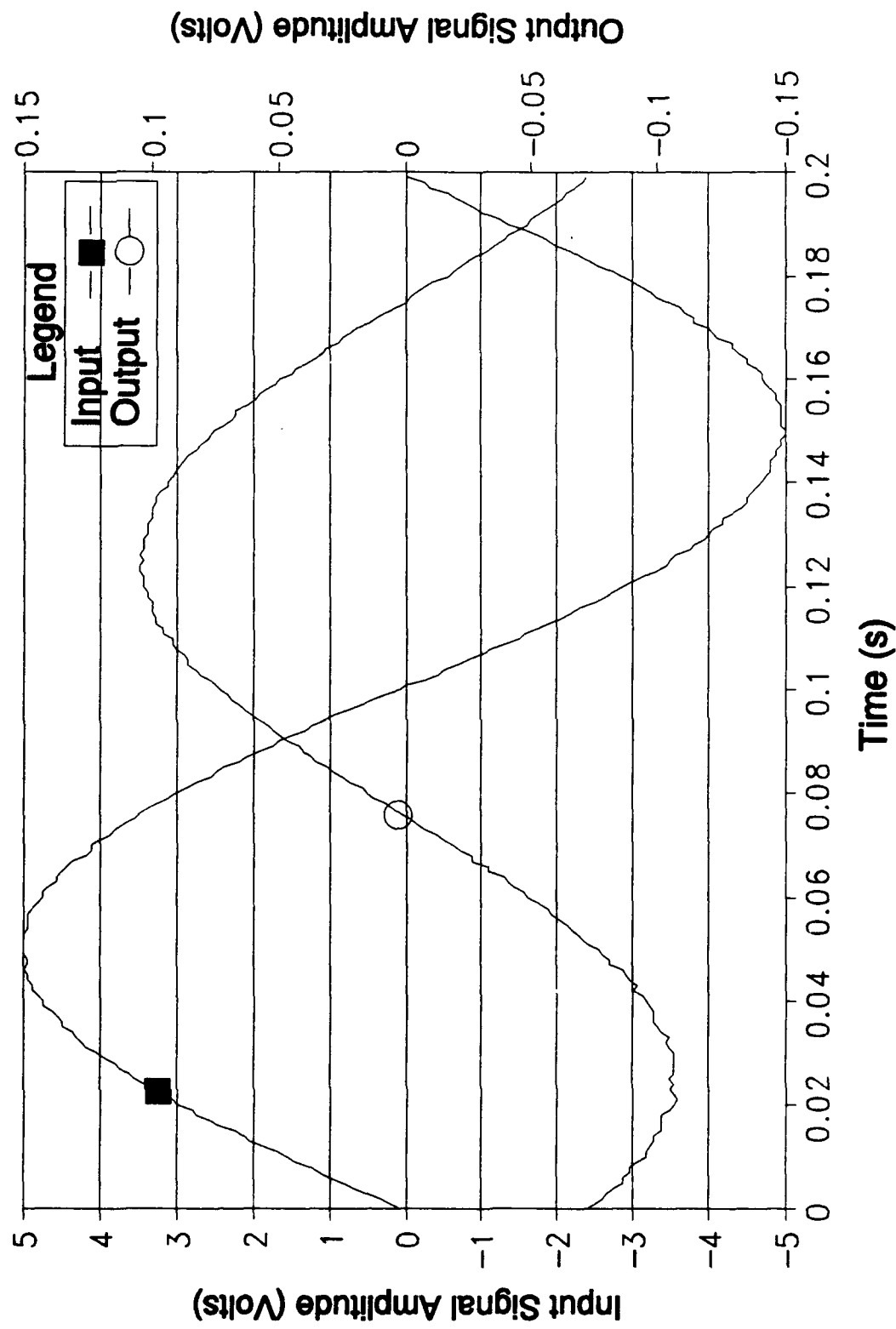
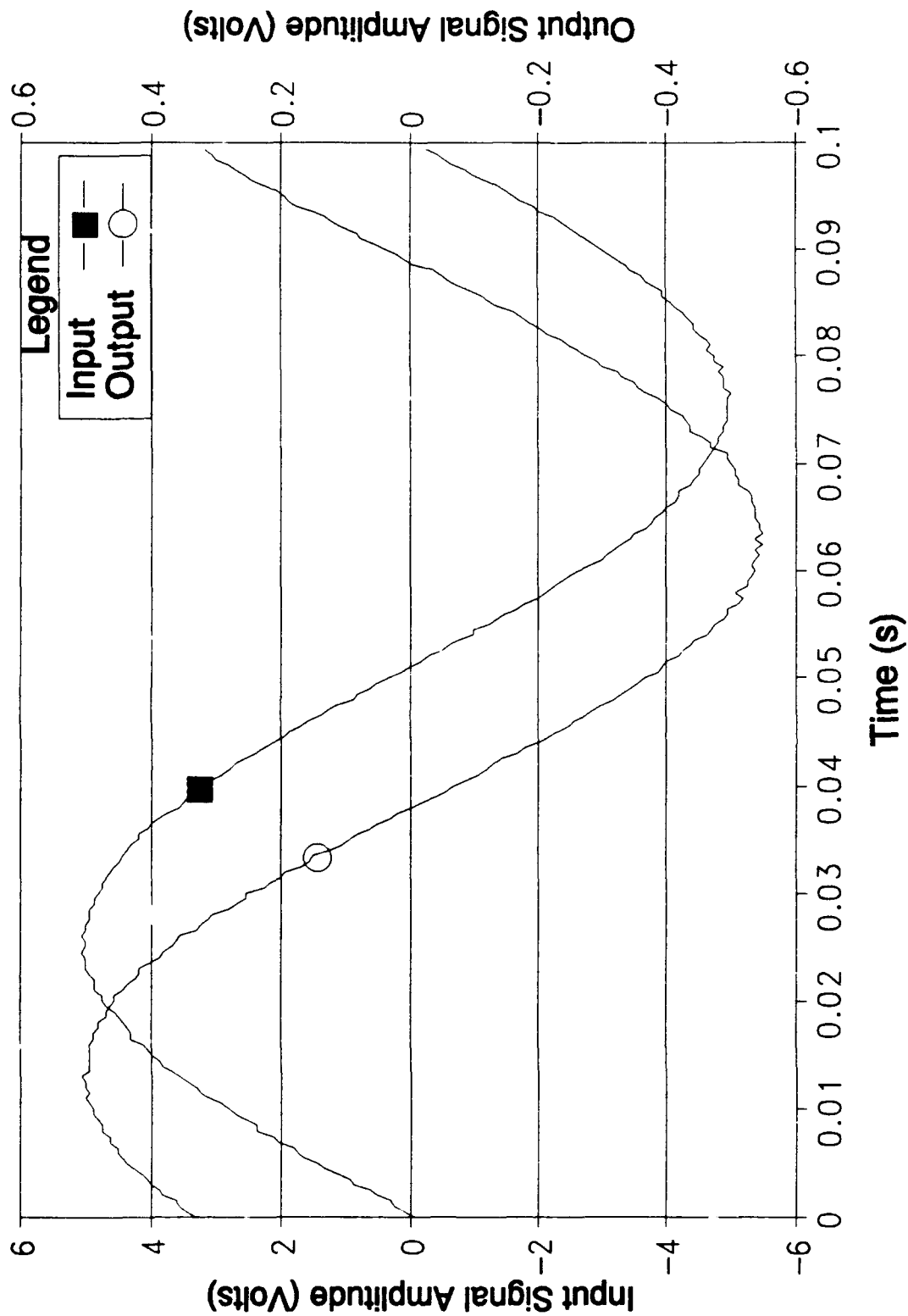**Figure G-40. Time Response of the Oldham Hybrid Component Circuit Design with a 5 Hz Excitation Siganl.**
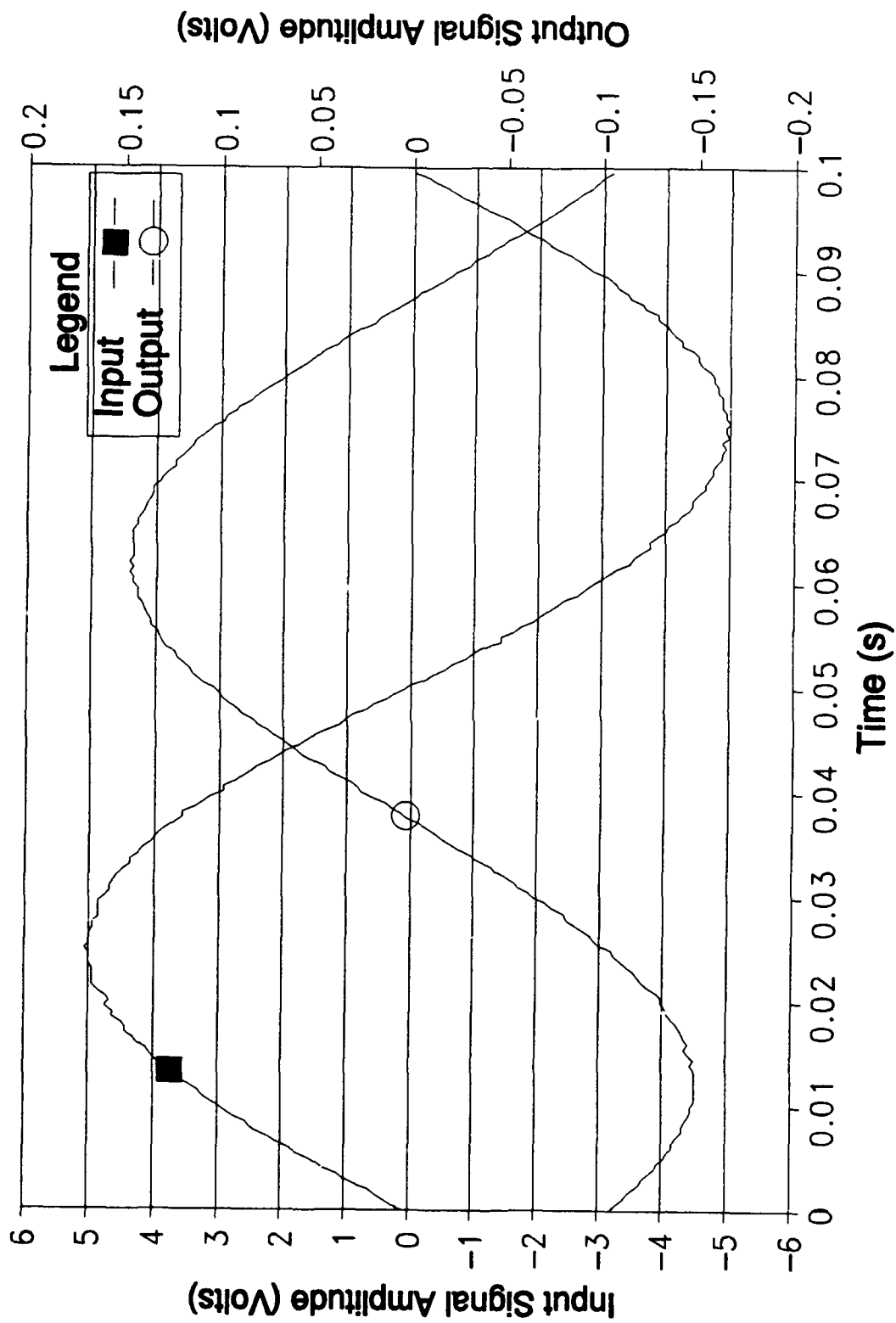
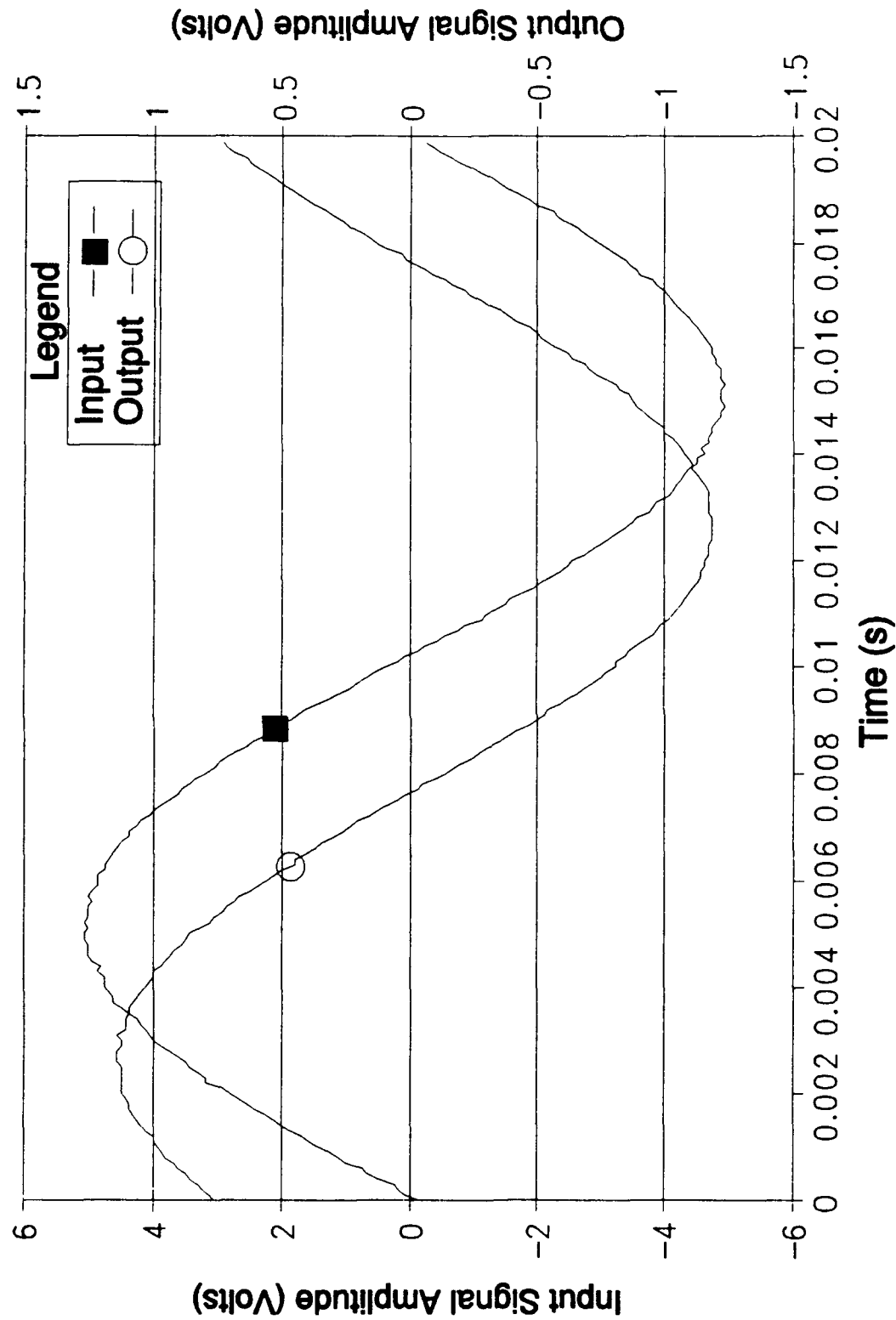Figure G-41.   Time Response of the Oldham Hybrid Component Circuit Design with a 10 Hz Excitation Signal.
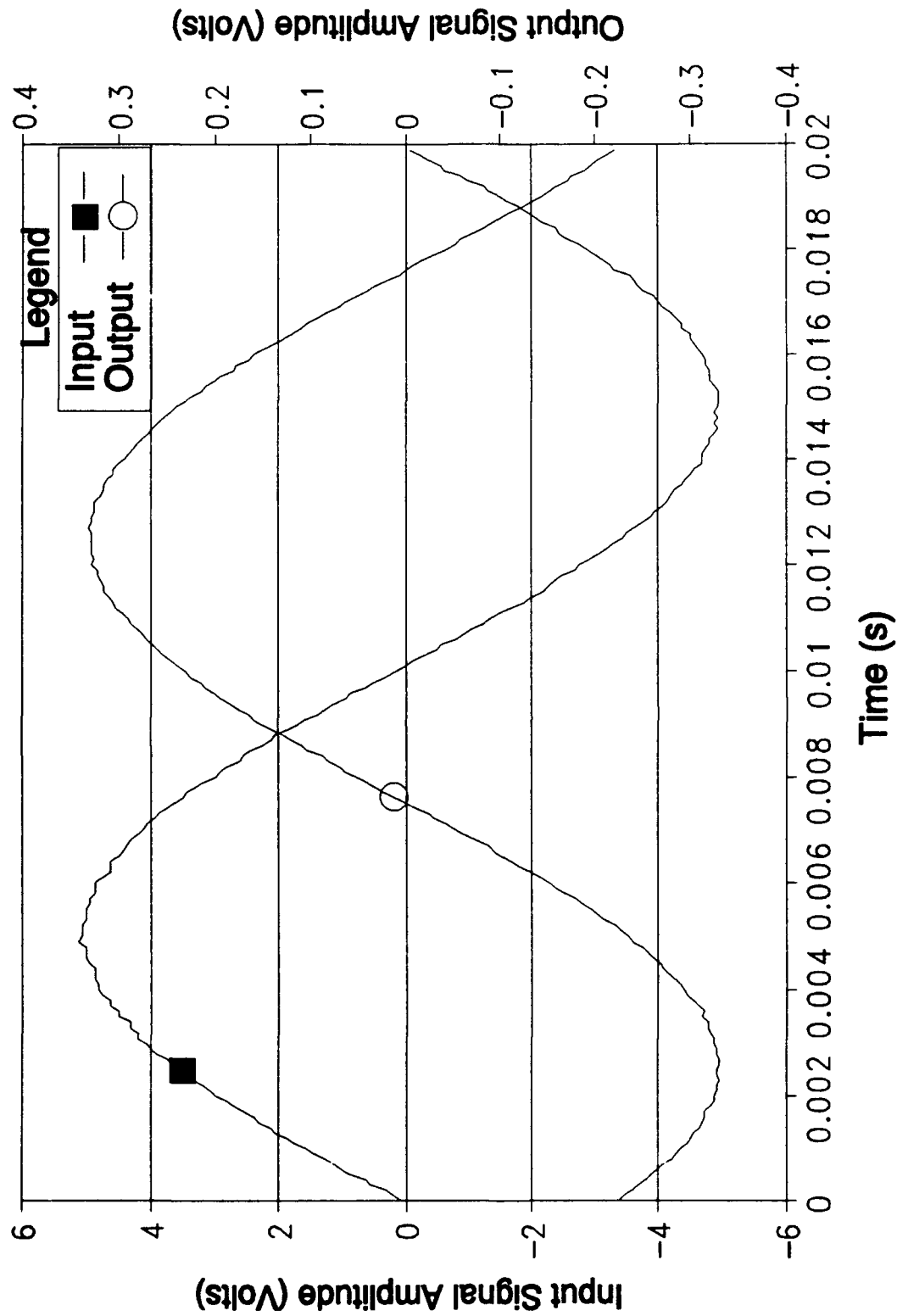
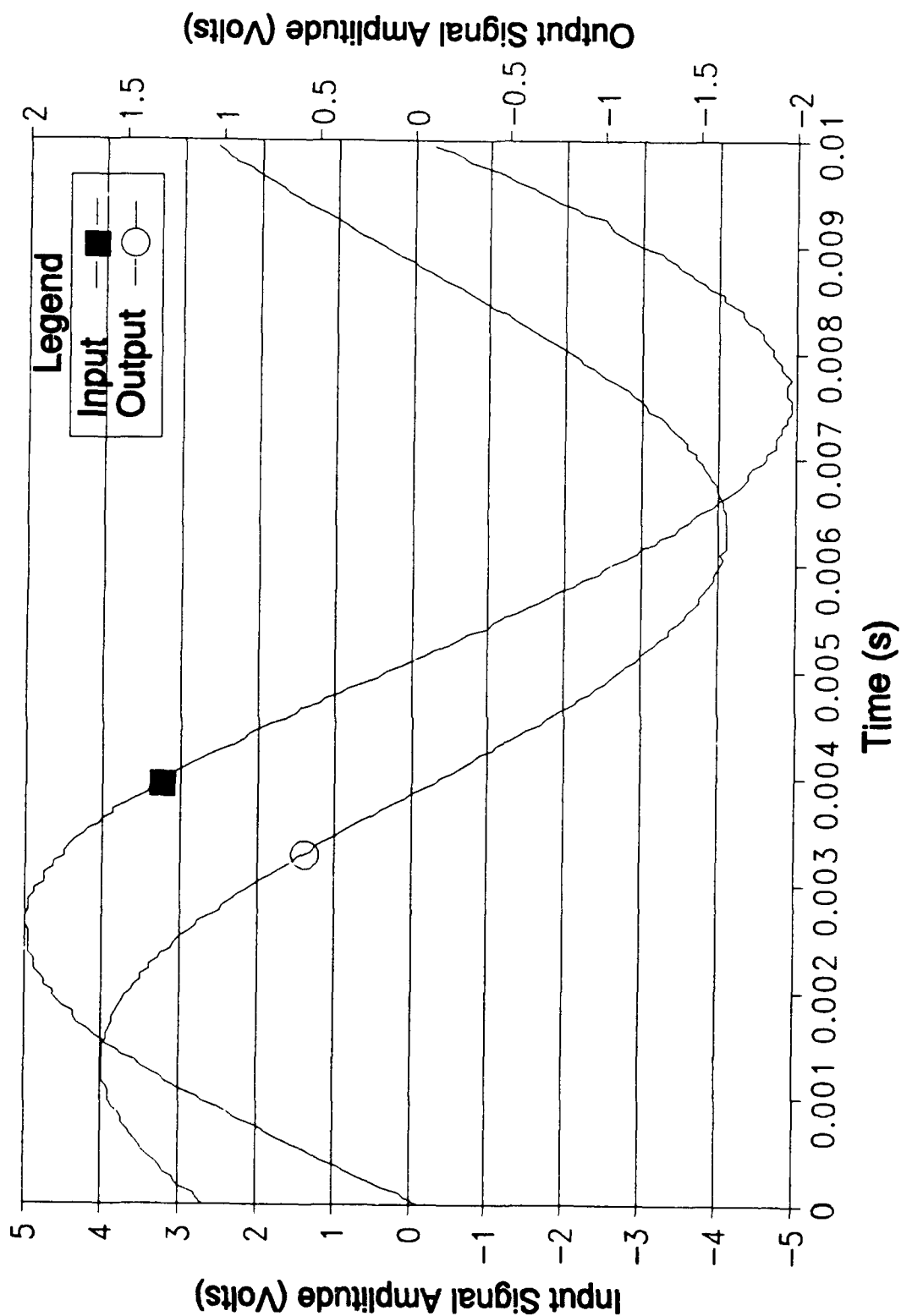Figure G-42. Time Response of the Oldham Hybrid Component Circuit Design with a 50 Hz Excitation Signal.
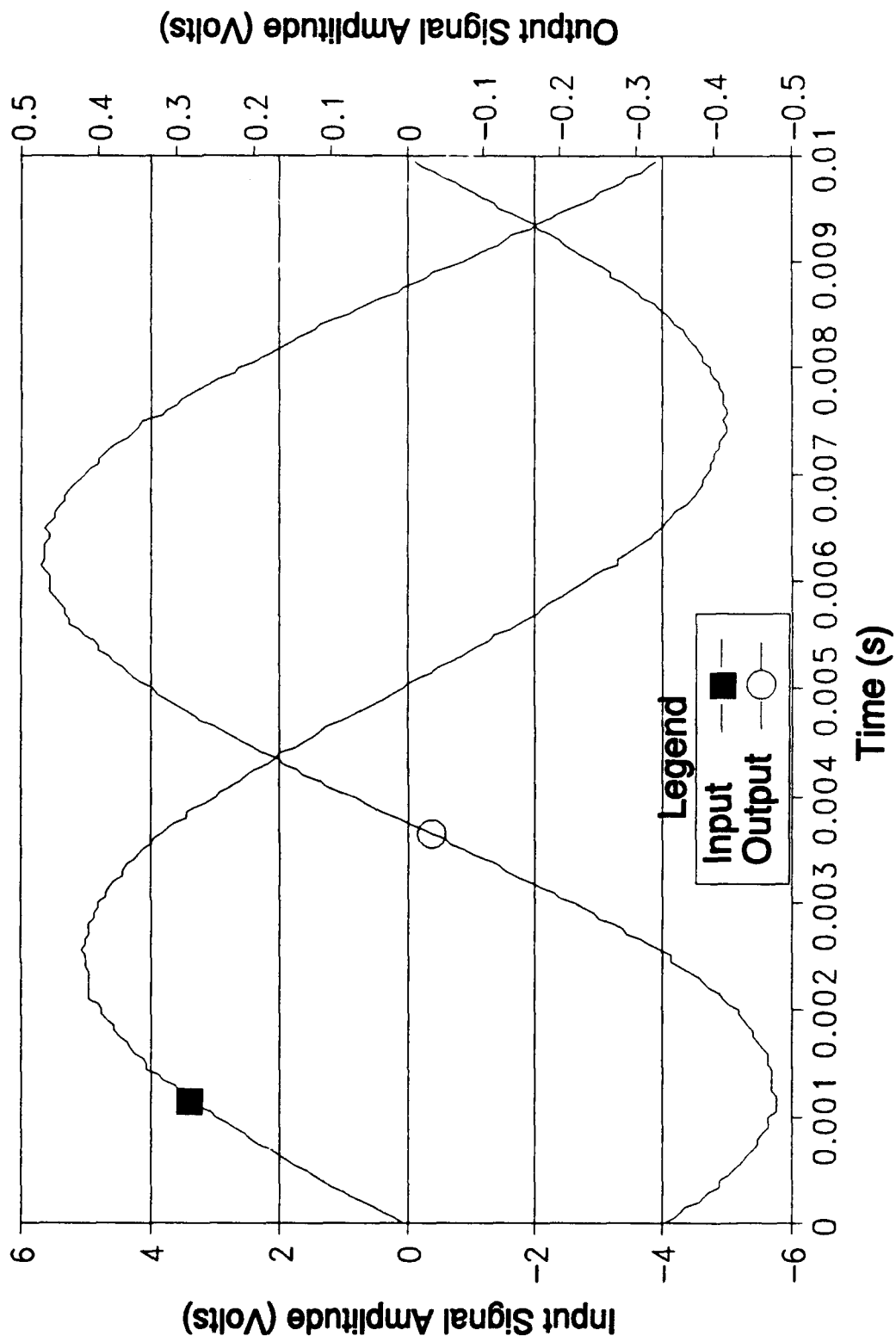
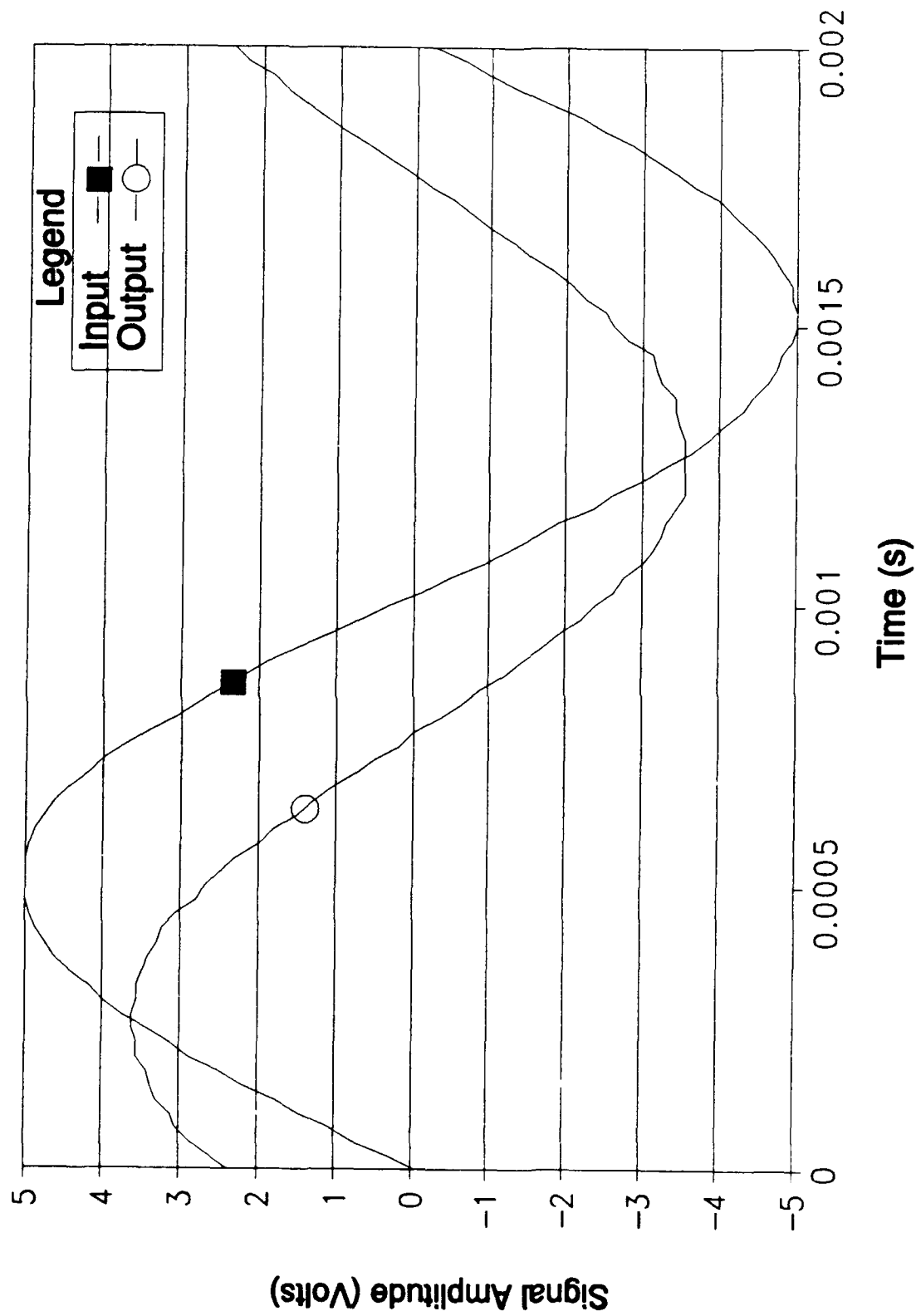**Figure G-43. Time Response of the Oldham Hybrid Component Circuit Design with a 100 Hz Excitation Signal.**
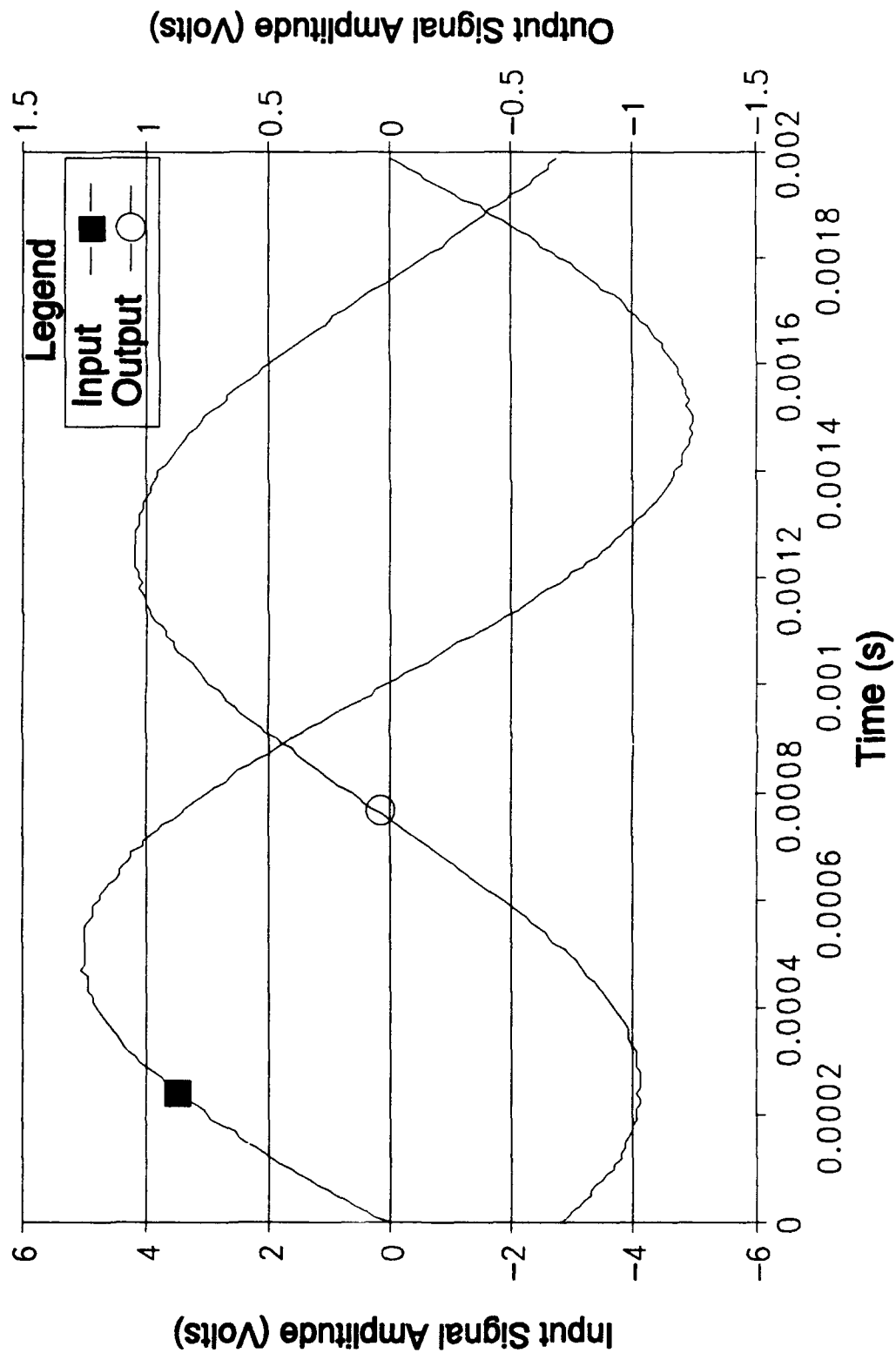
Figure F-42. Time Response of the Oldham Hybrid Component Circuit Design with a 500 Hz Excitation Signal.
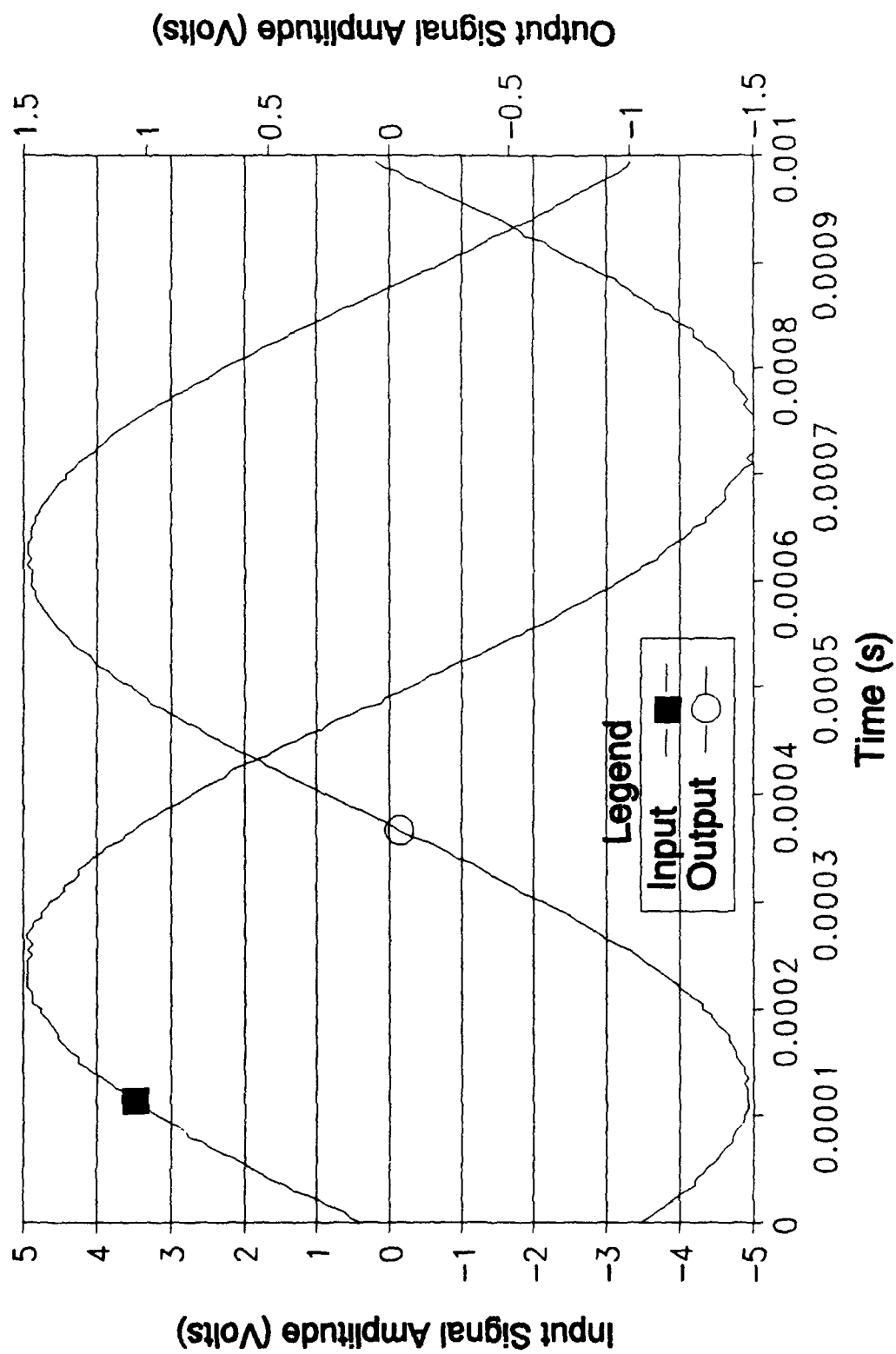
Figure G-45.   Time Response of the Oldham Hybrid Component
Circuit Design wth a 1000 Hz Excitation Signal.
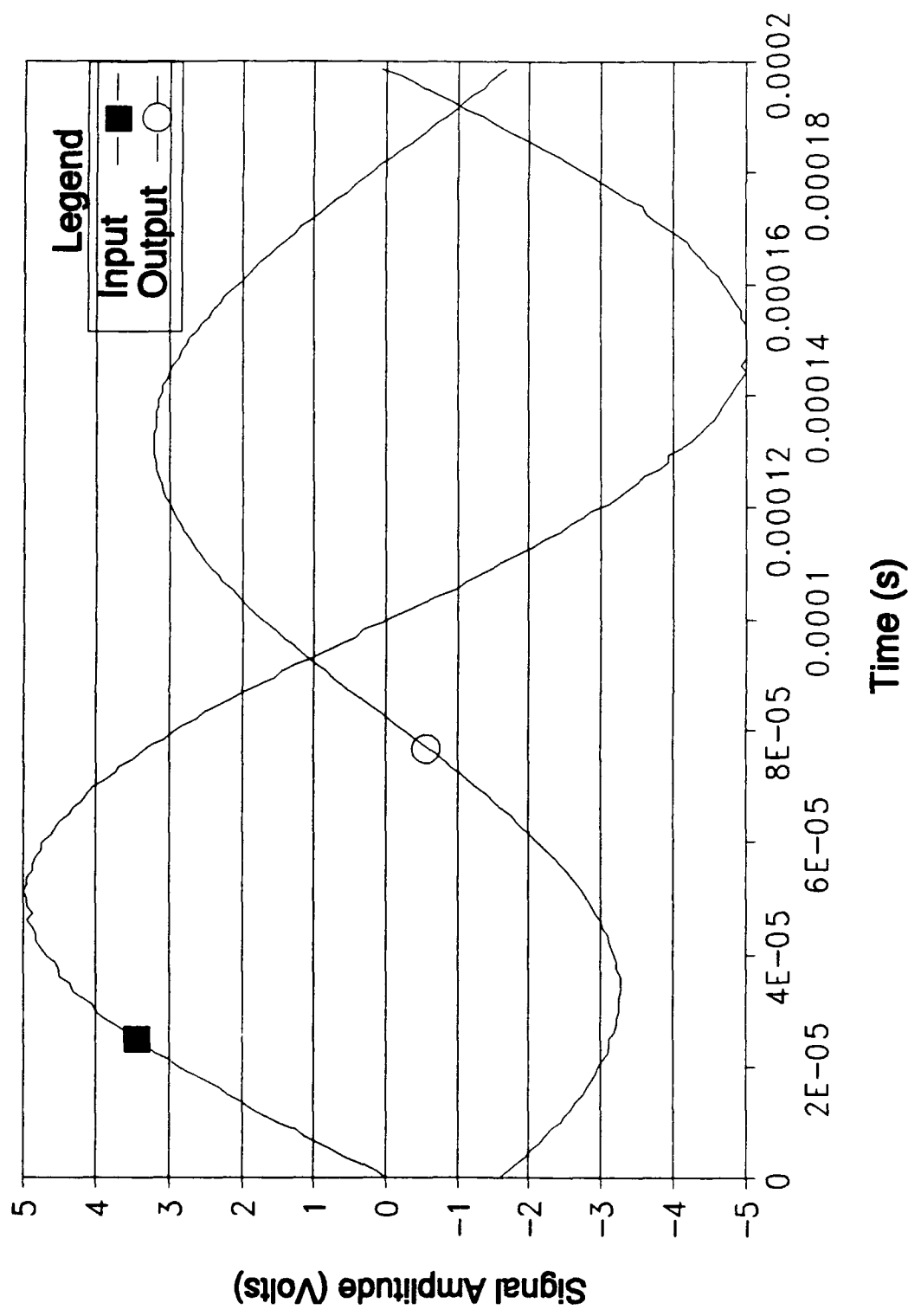
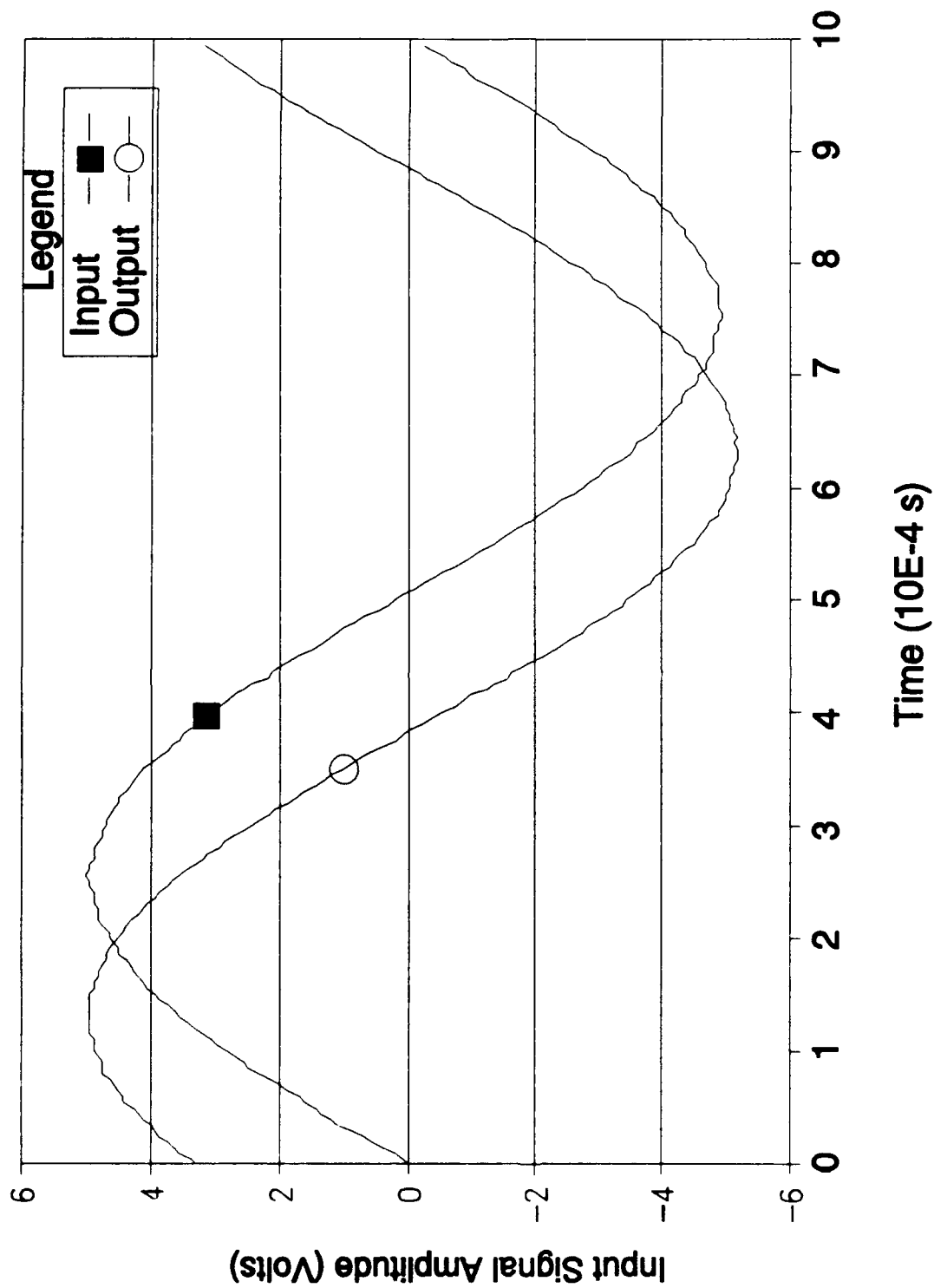Figure G-46. Time Response of the Oldham Discrete Component Circuit Design with a 5000 Hz Excitation Signal.
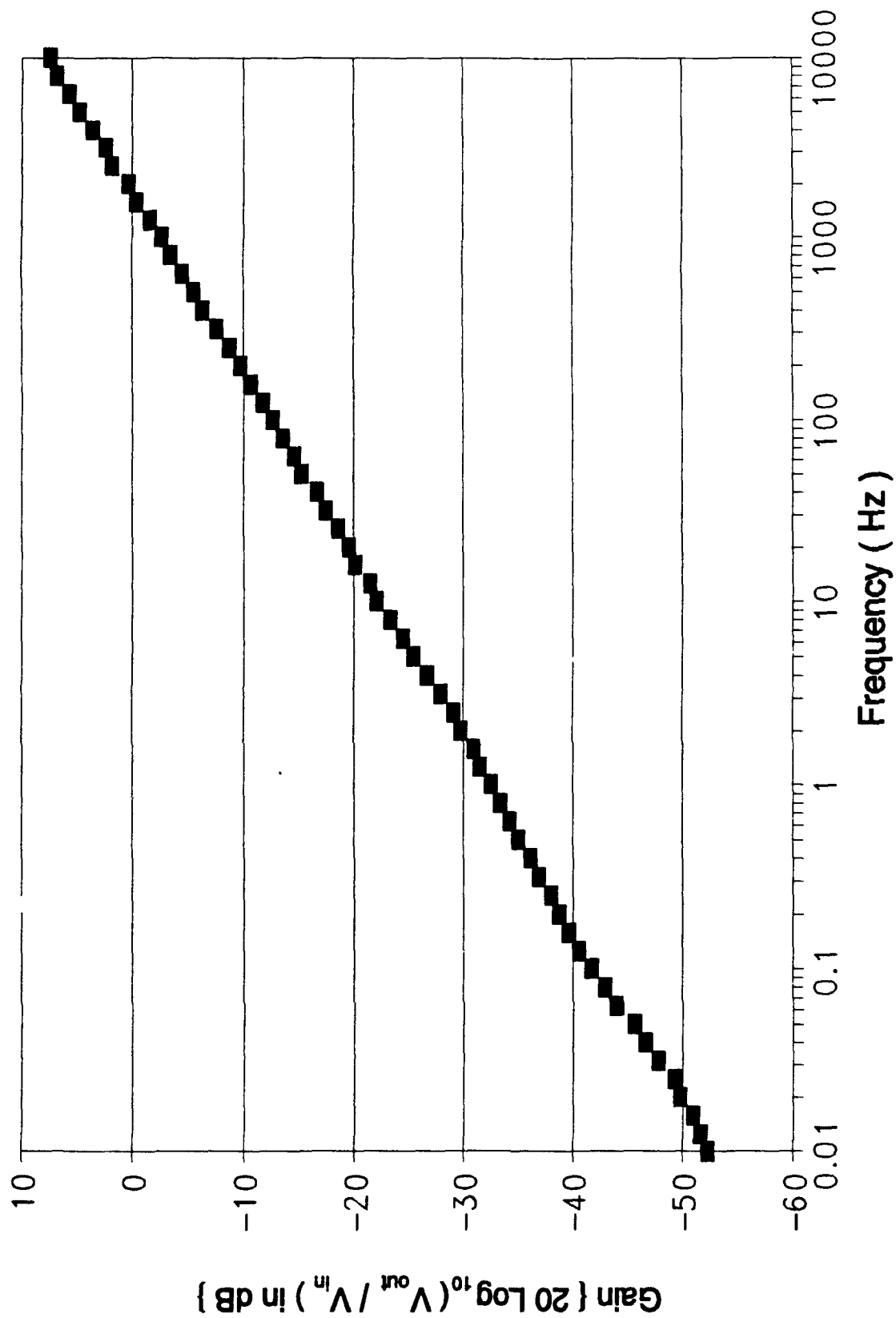
Figure G-47. Oldfield Circuit Surface Mount Component Gain Response.
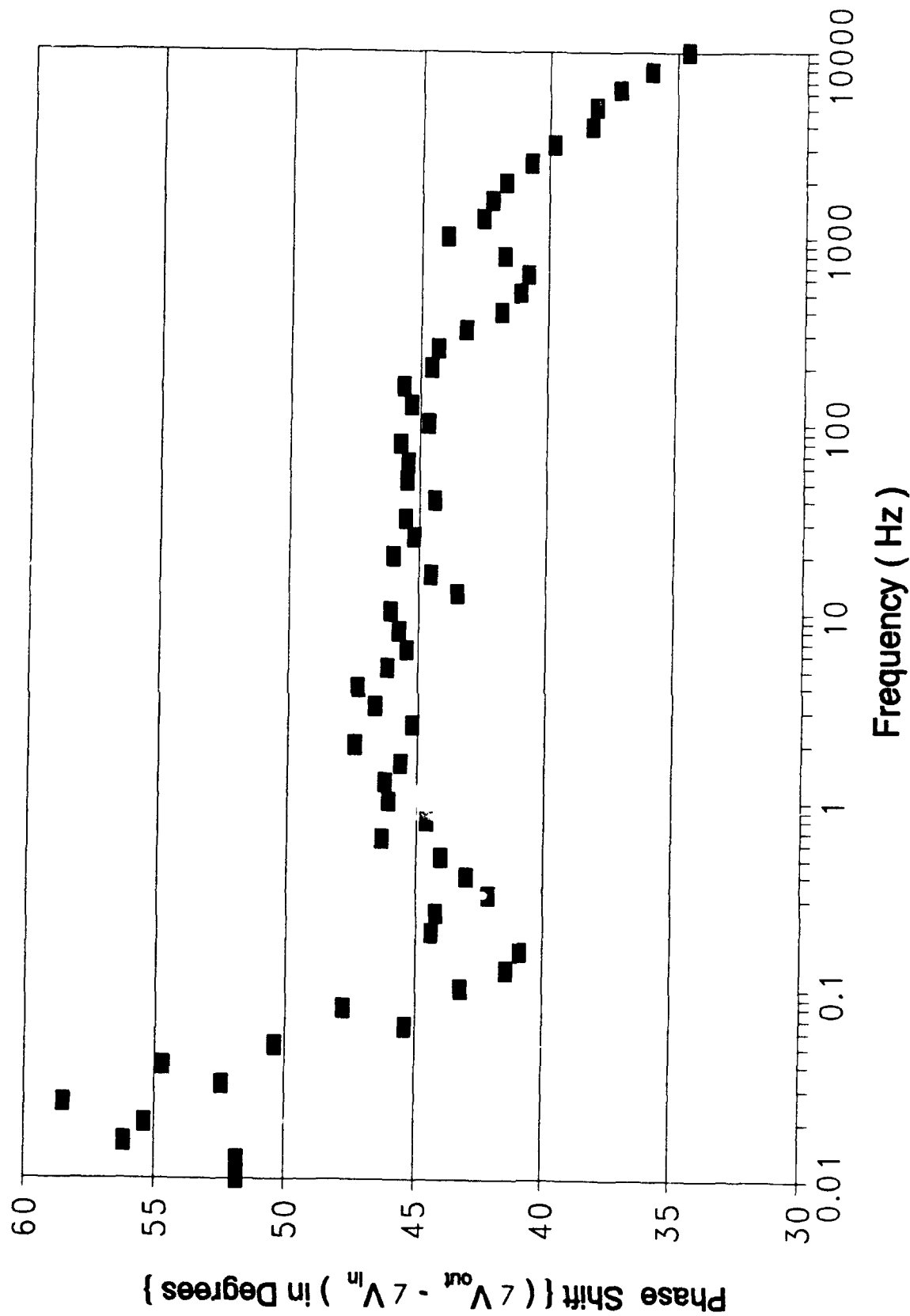
Figure G-48. Oldfield Circuit Surface Mount Component Phase Response.

G-52
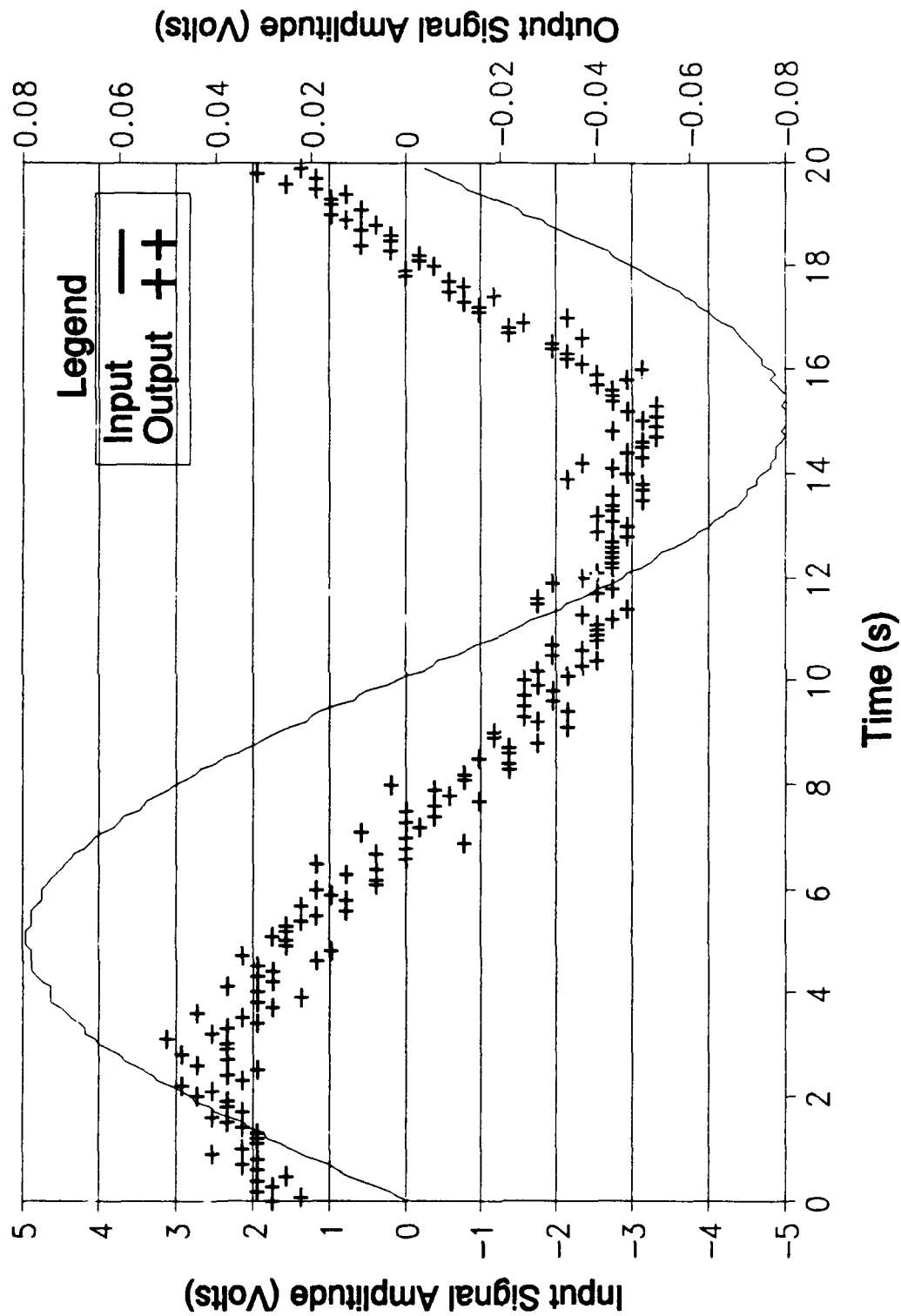
Figure G-49. Time Response of the Oldfield Surface Mount Component Circuit Design with a 0.05 Hz Excitation Signal.
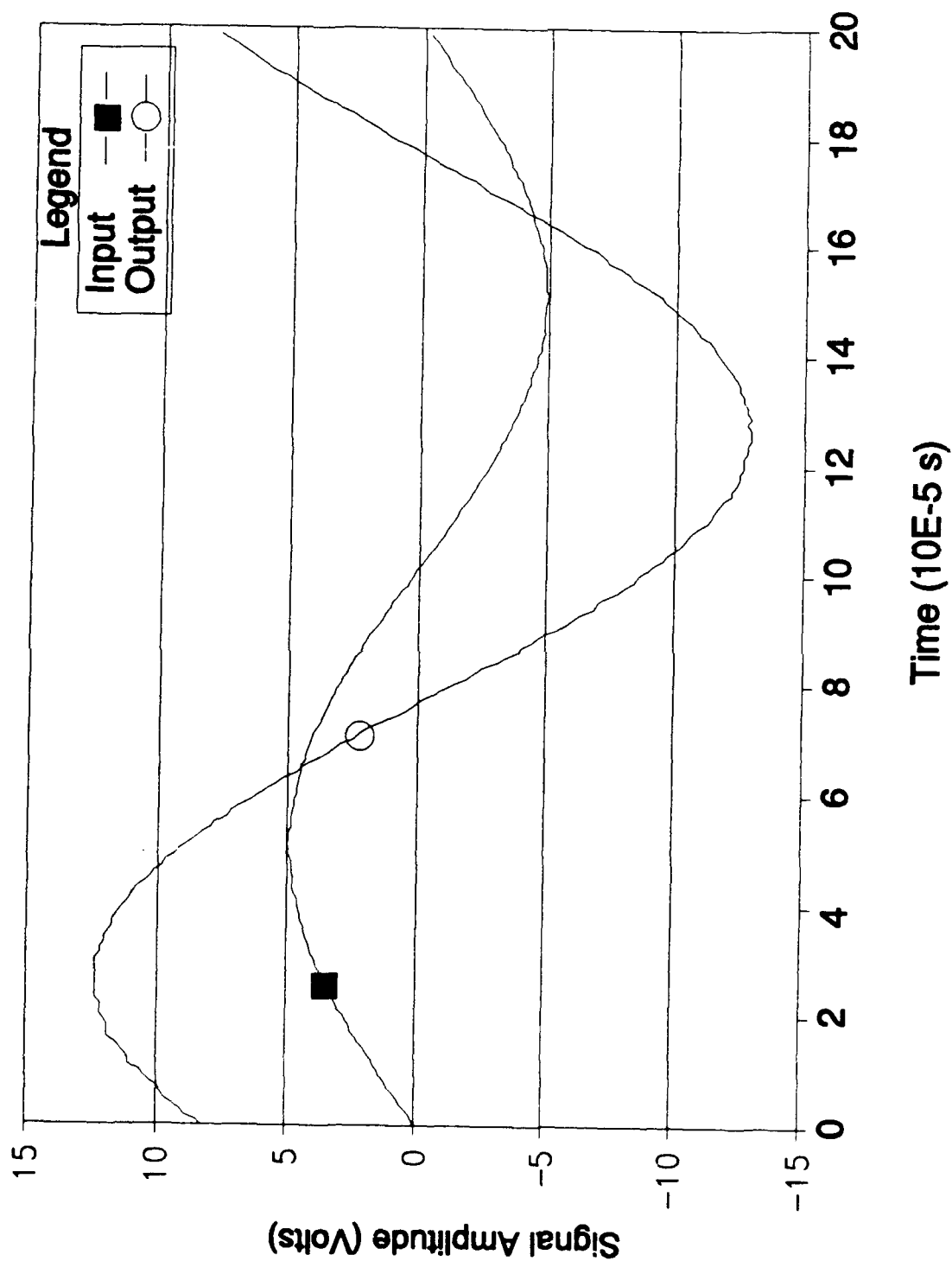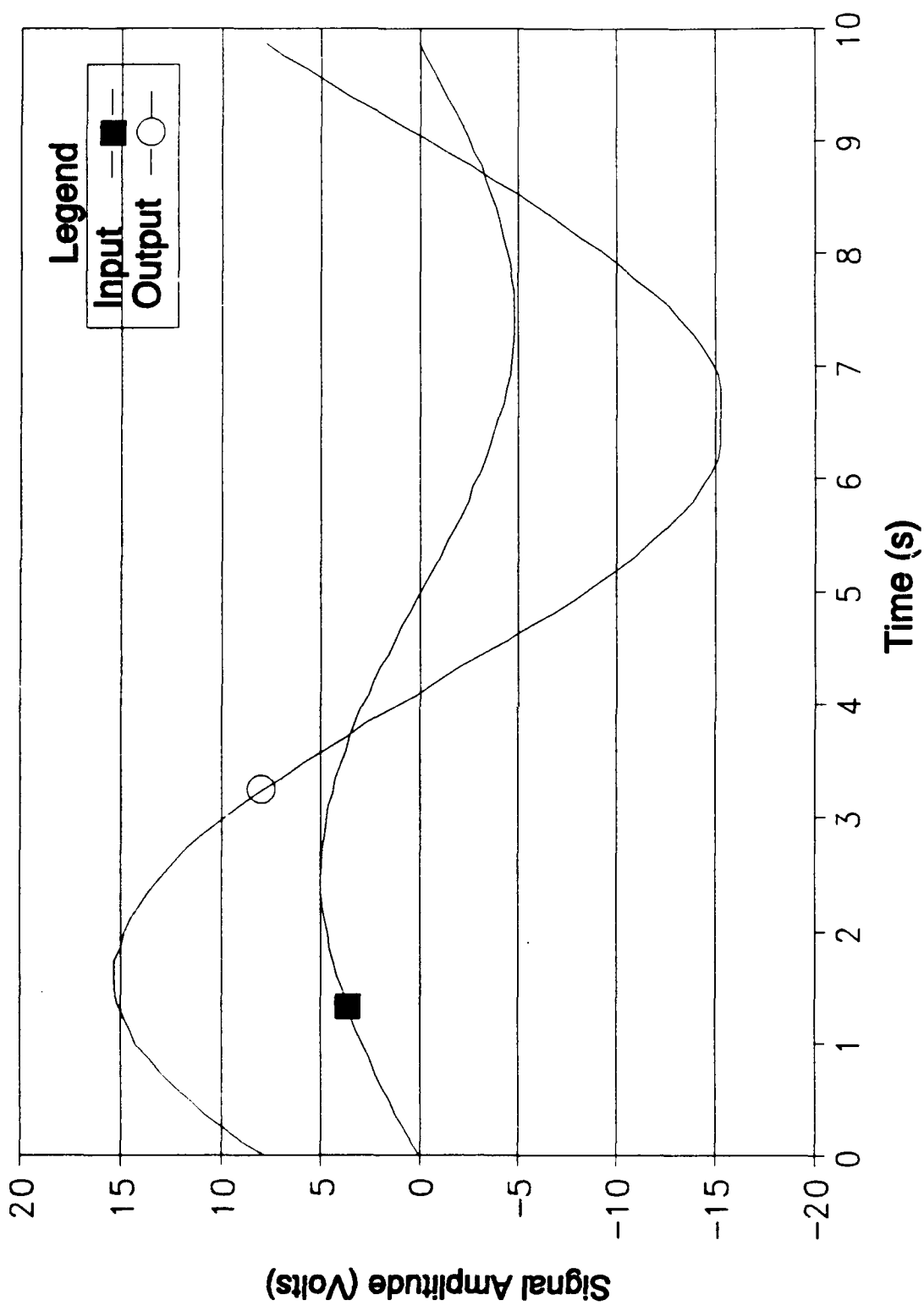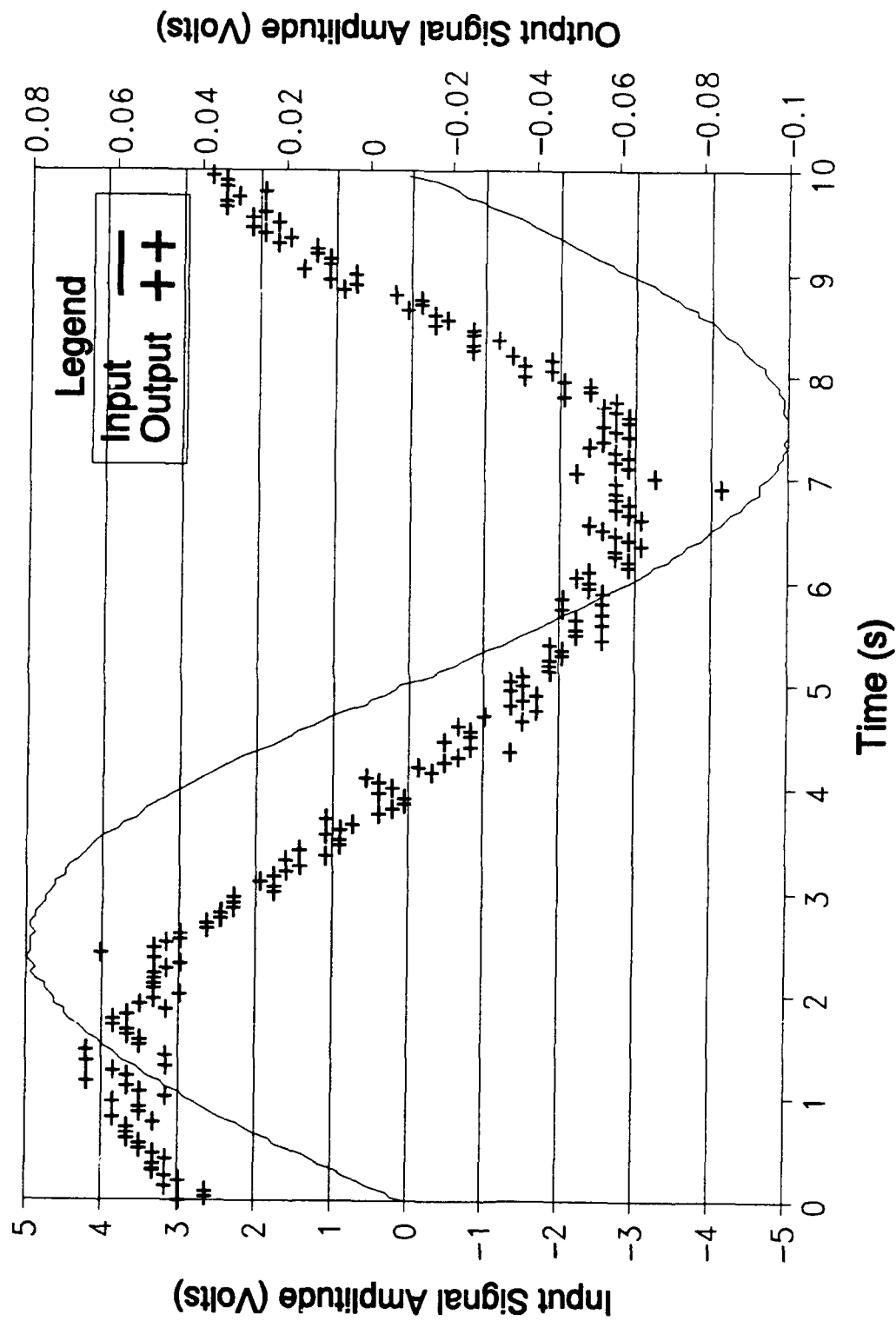
Figure G-50. Time Response of the Oldfield Surface Mount Component Circuit Design with a 0.1 Hz Excitation Signal.
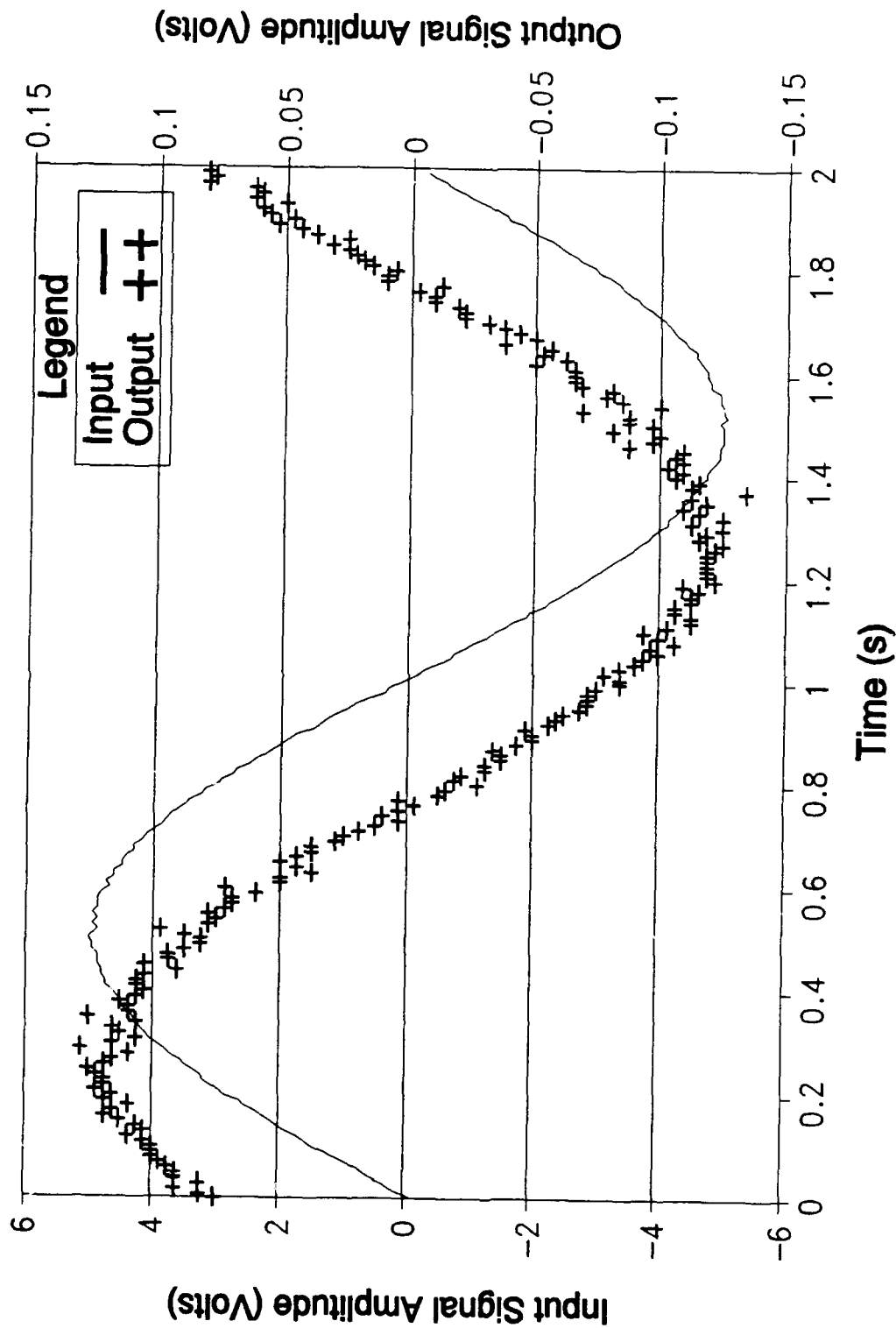
Figure G-51. Time Response of the Oldfield Surface Mount Component Circuit Design with a 0.5 Hz Excitation Signal.
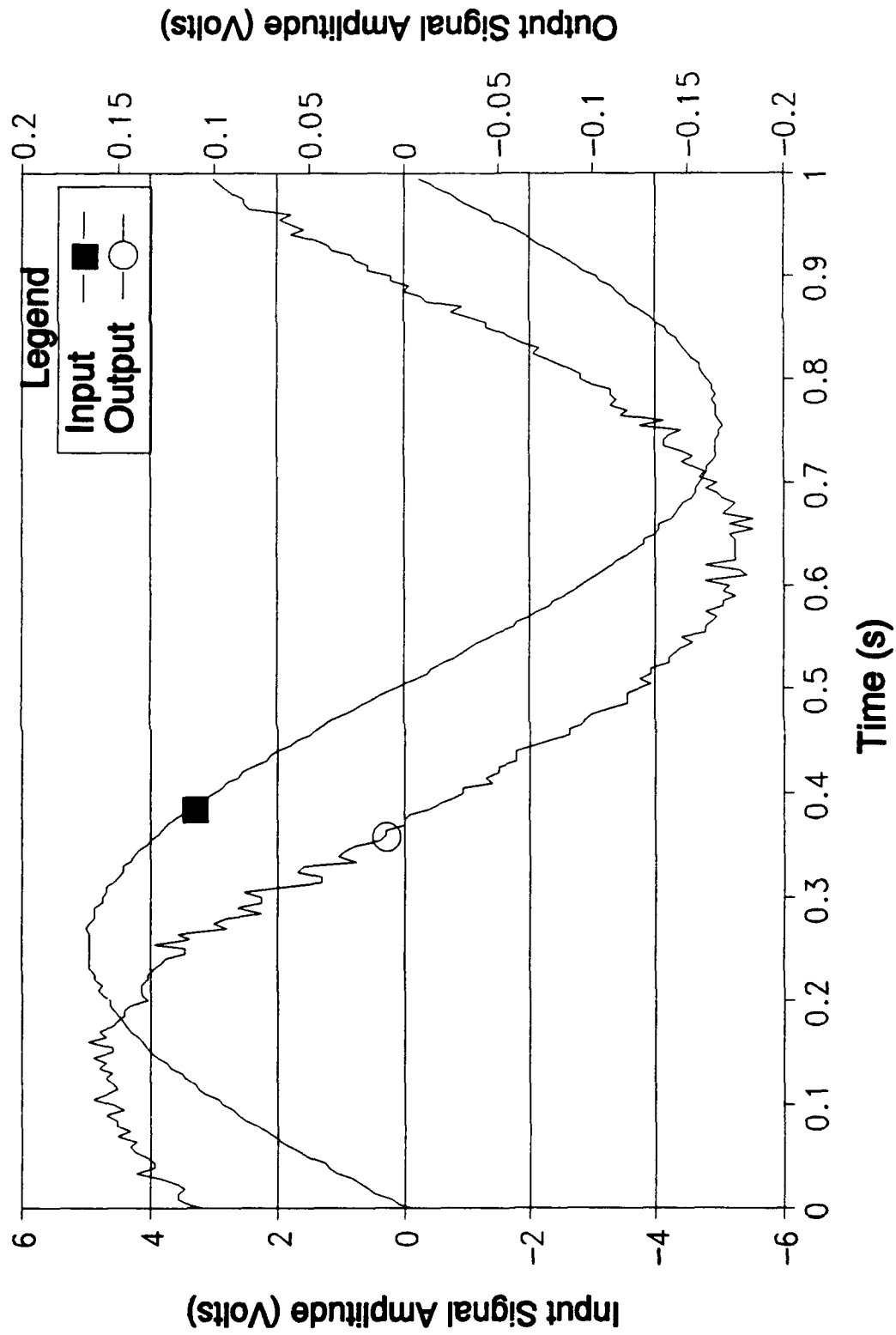
Figure G-52. Time Response of the Oldfield Surface Mount Component Circuit Design with a 1 Hz Excitation Signal.
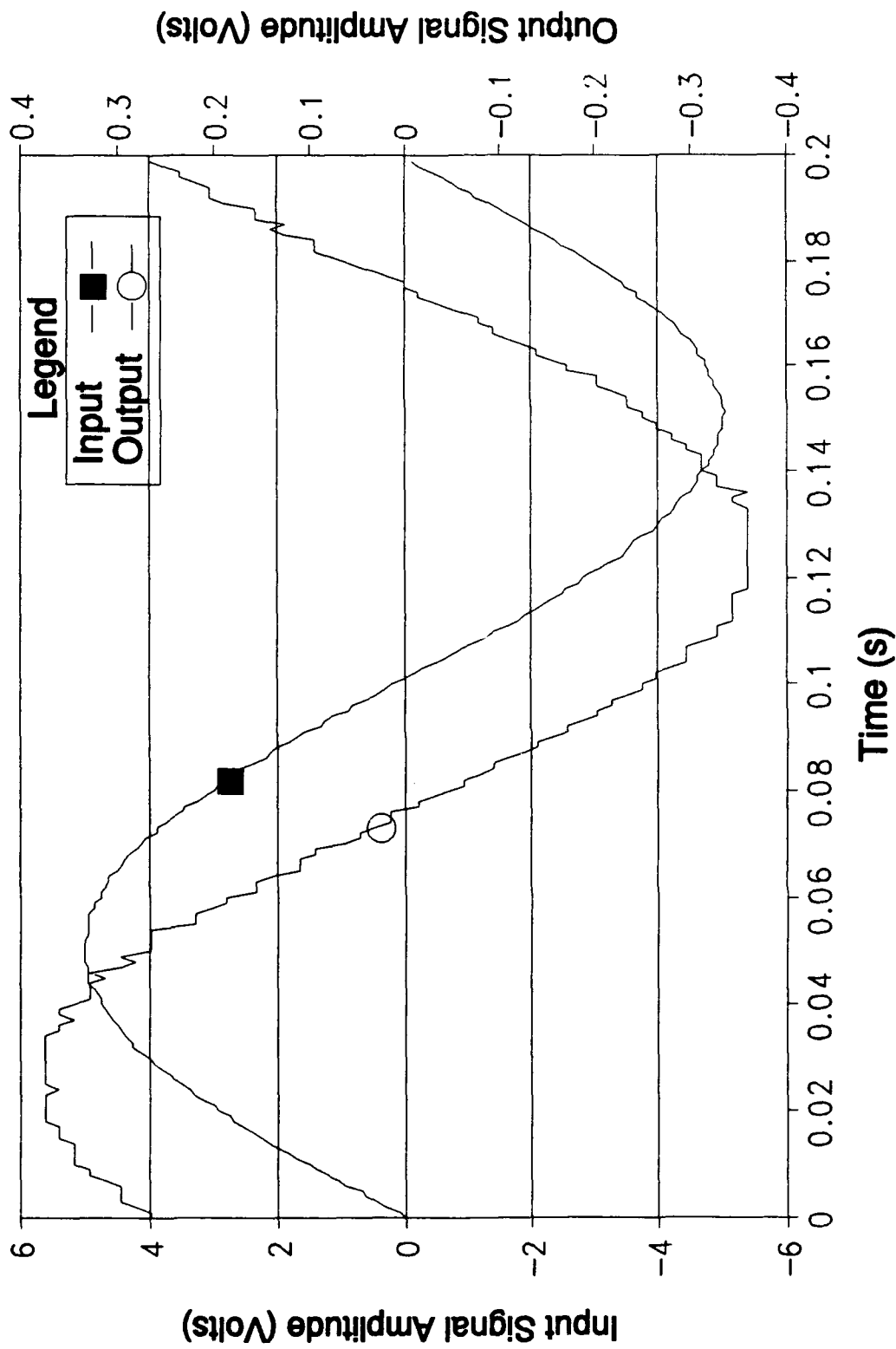
Figure G-53. Time Response of the Oldfield Surface Mount Component Circuit Design with a 5 Hz Excitation Signal.
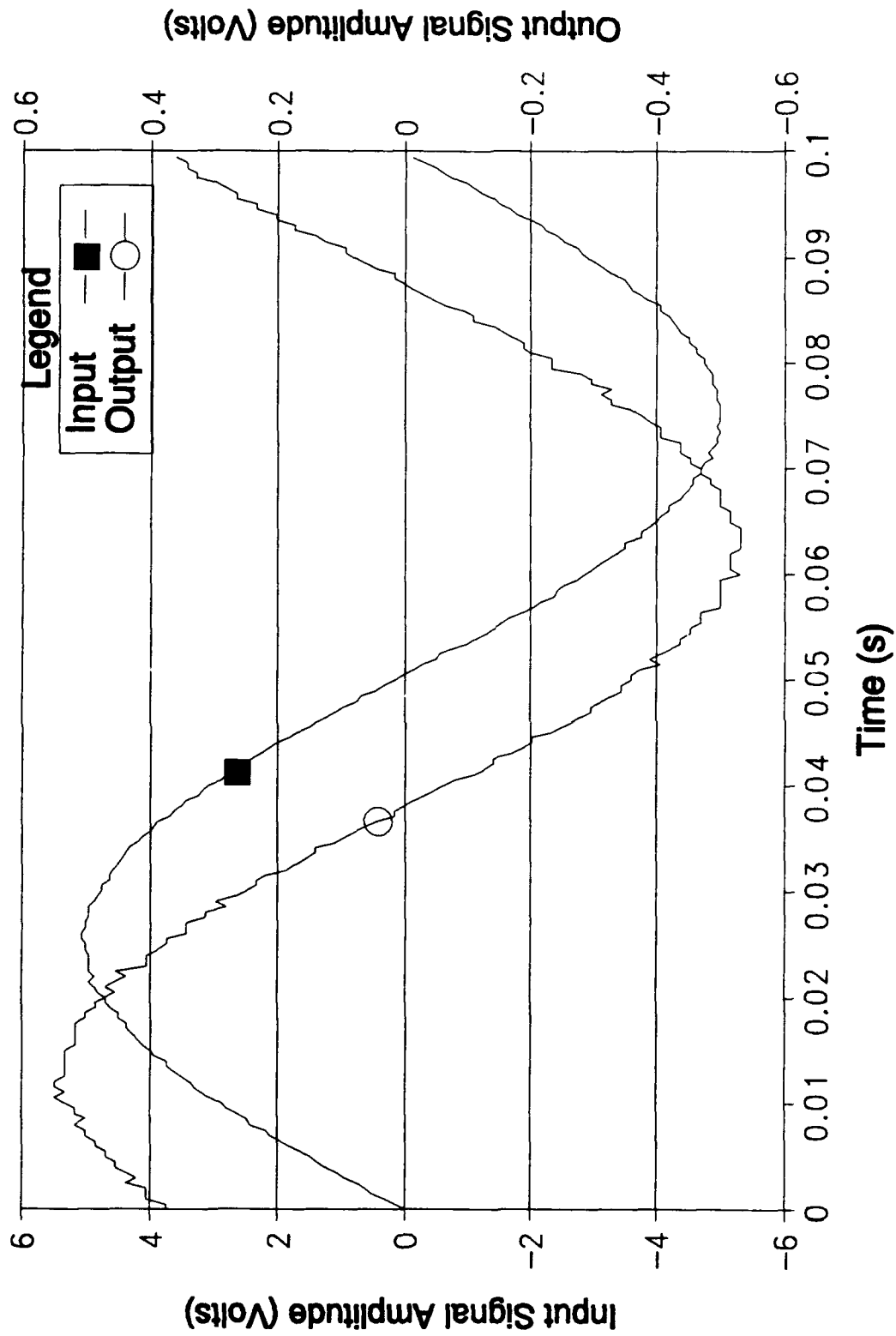
Figure G-54. Time Response of the Oldfield Surface Mount Component Circuit Design with a 10 Hz Excitation Signal.
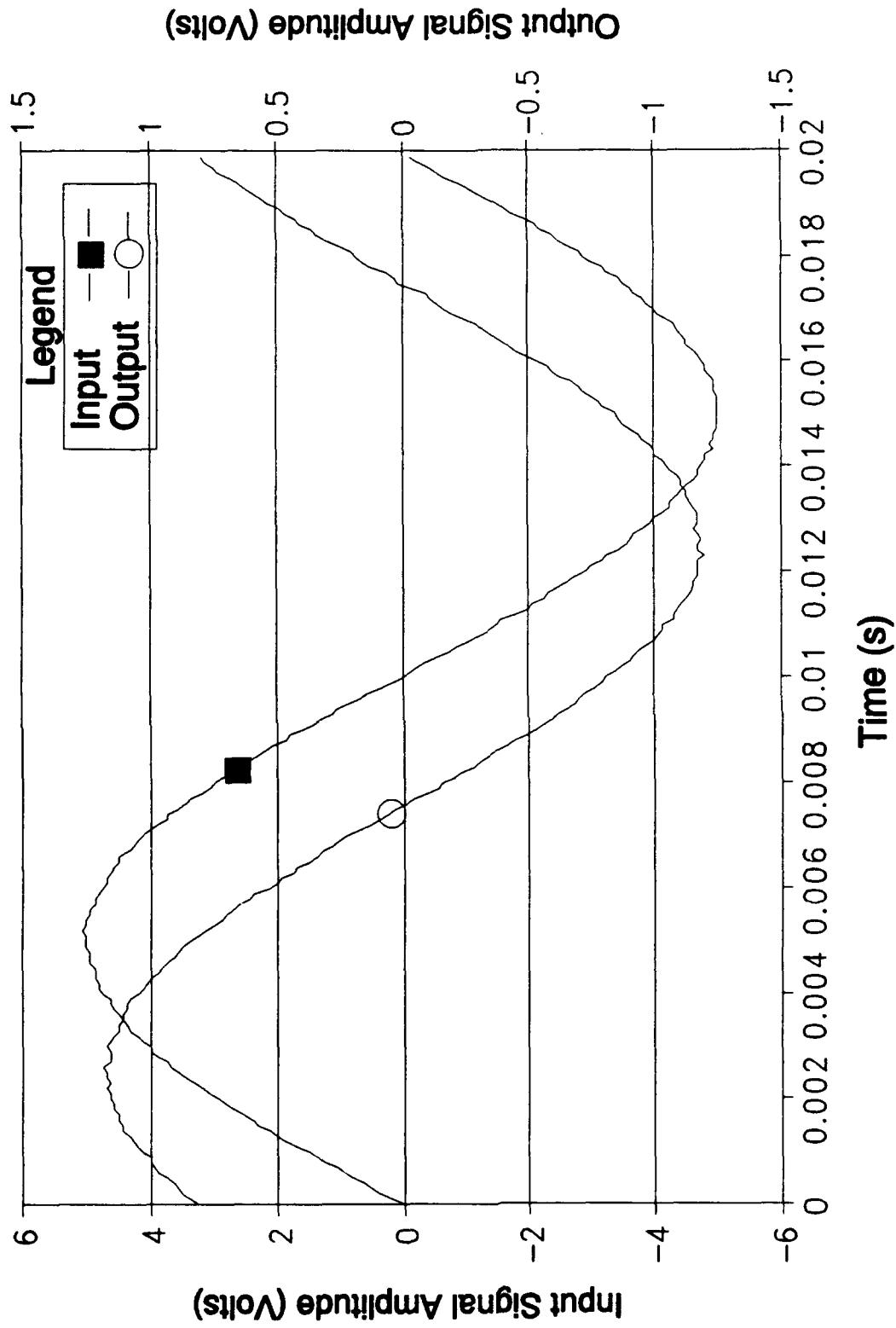
Figure G-55. Time Response of the Oldfield Surface Mount Component Circuit Design with a 50 Hz Excitation Signal.
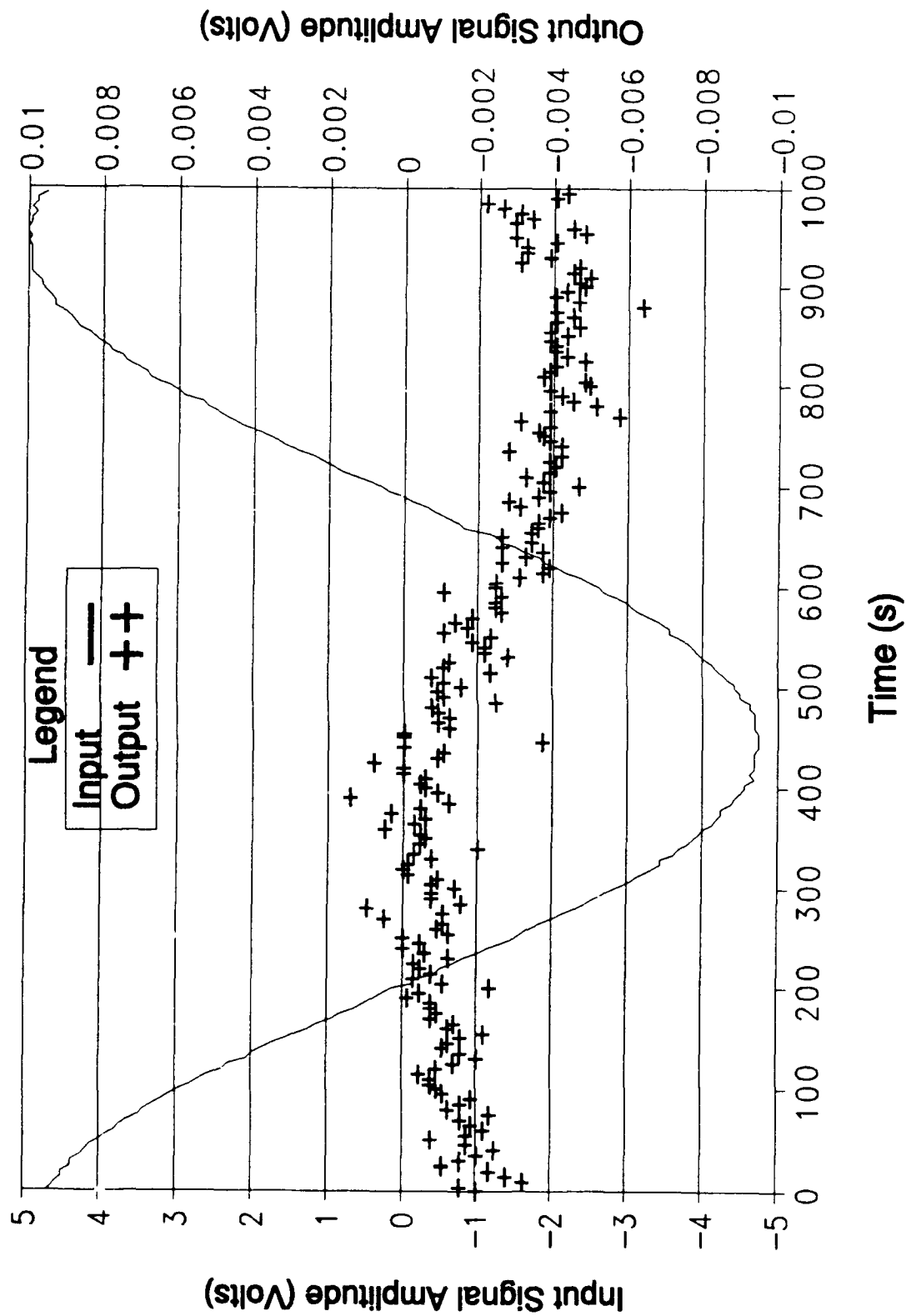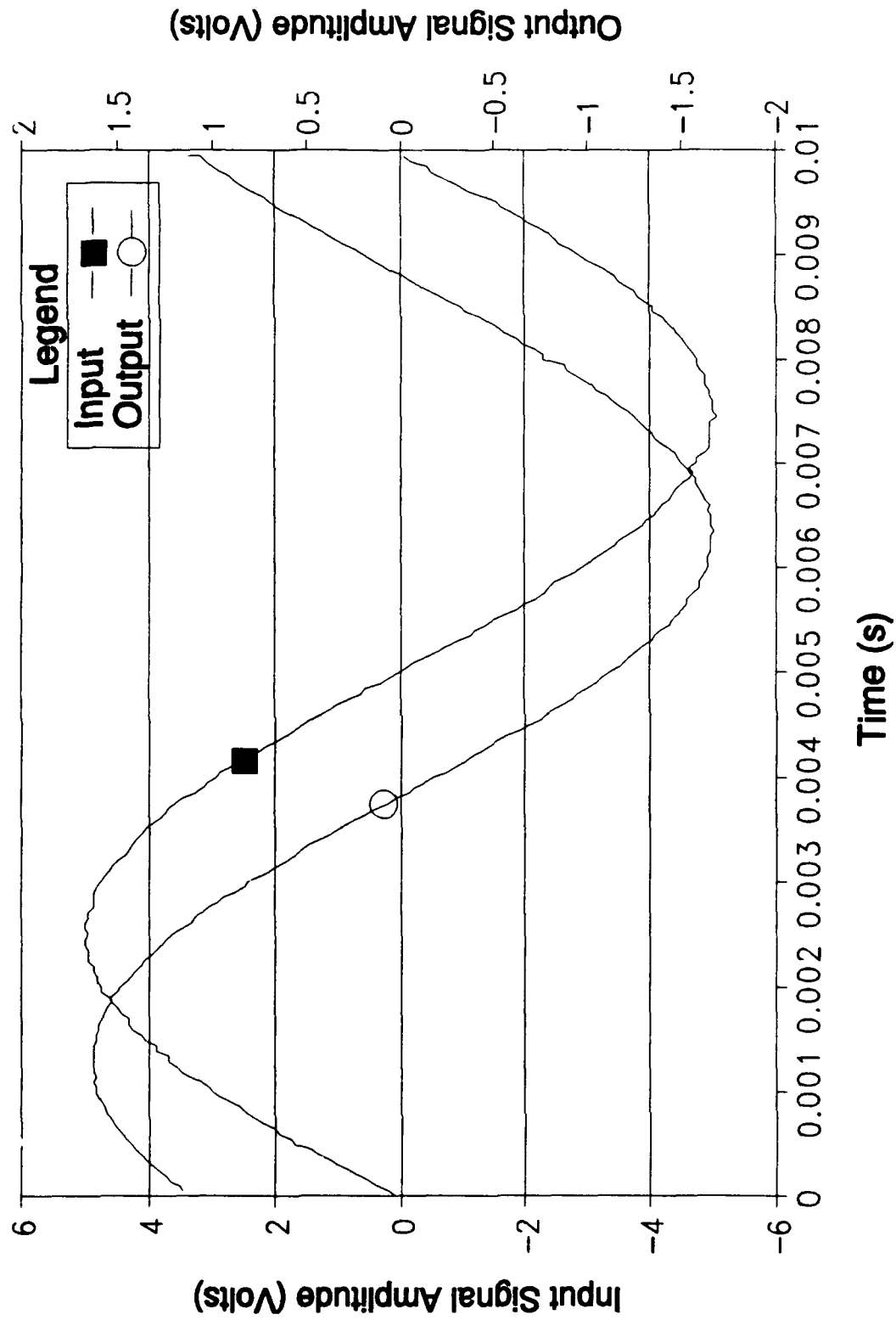
Figure G-52. Time Response of the Oldfield Surface Mount Component Circuit Design with a 100 Hz Excitation Signal.
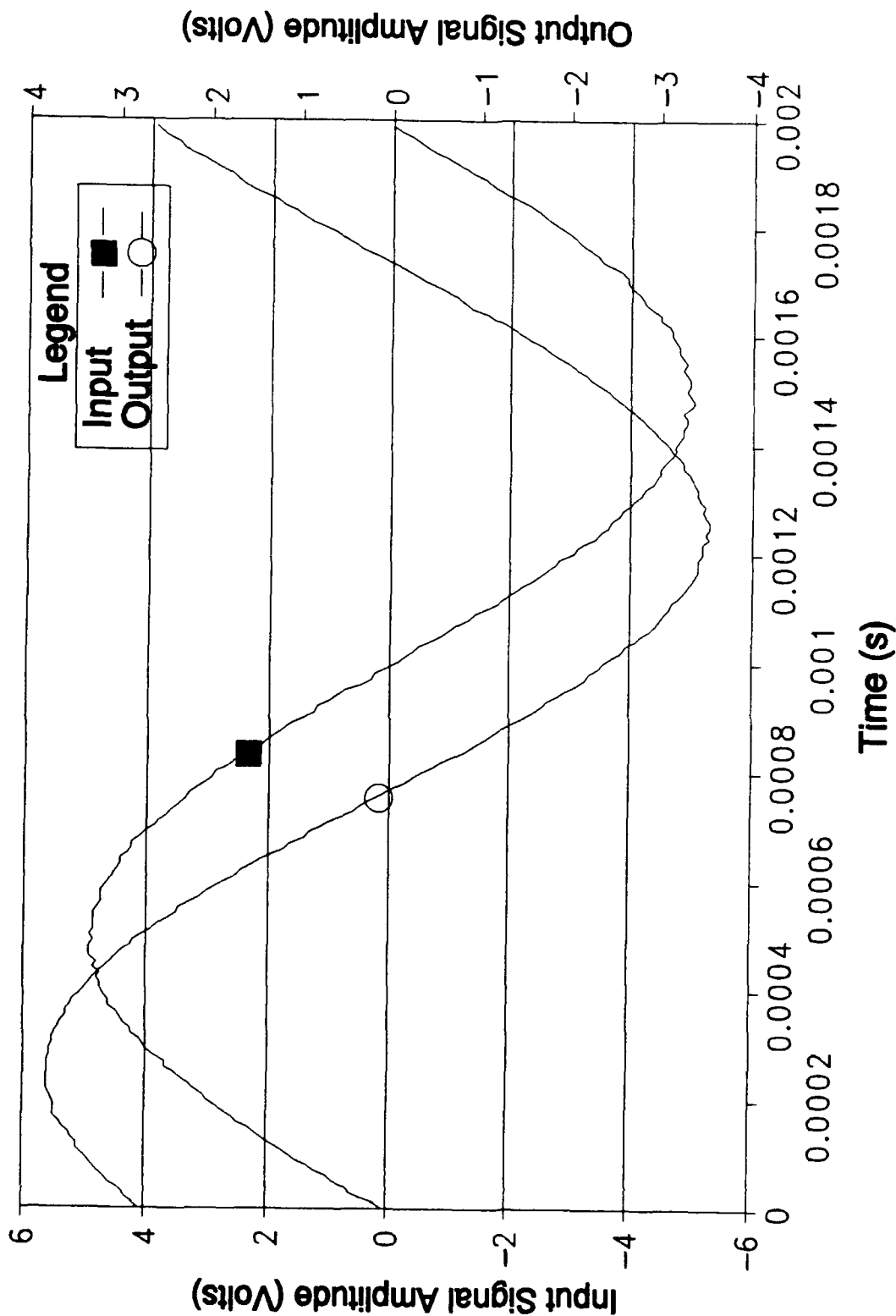
Figure G-57. Time Response of the Oldfield Surface Mount Component Circuit Design with a 500 Hz Excitation Signal.
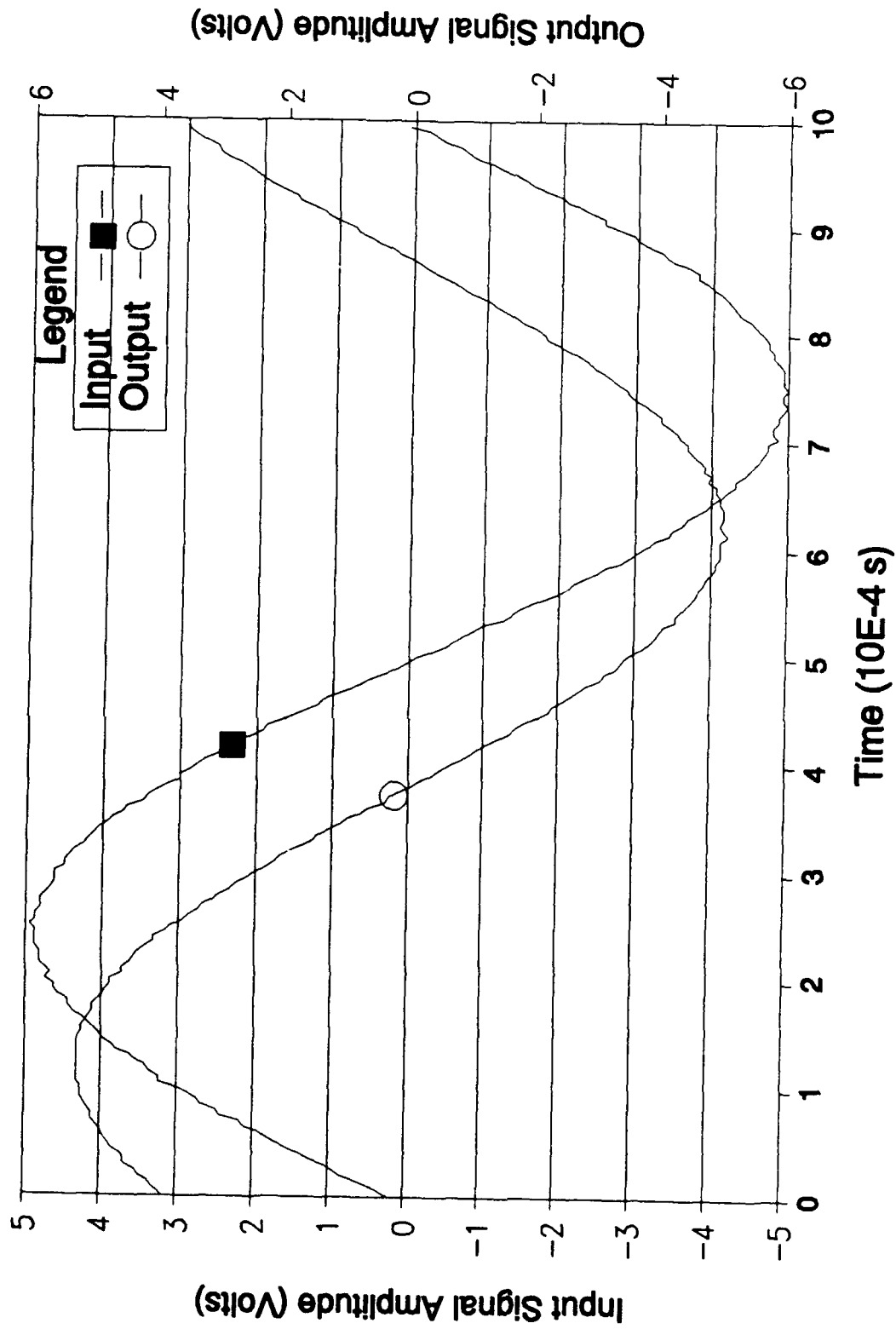
Figure G-58. Time Response of the Oldfield Surface Mount Component Circuit Design with a 1000 Hz Excitation Signal.
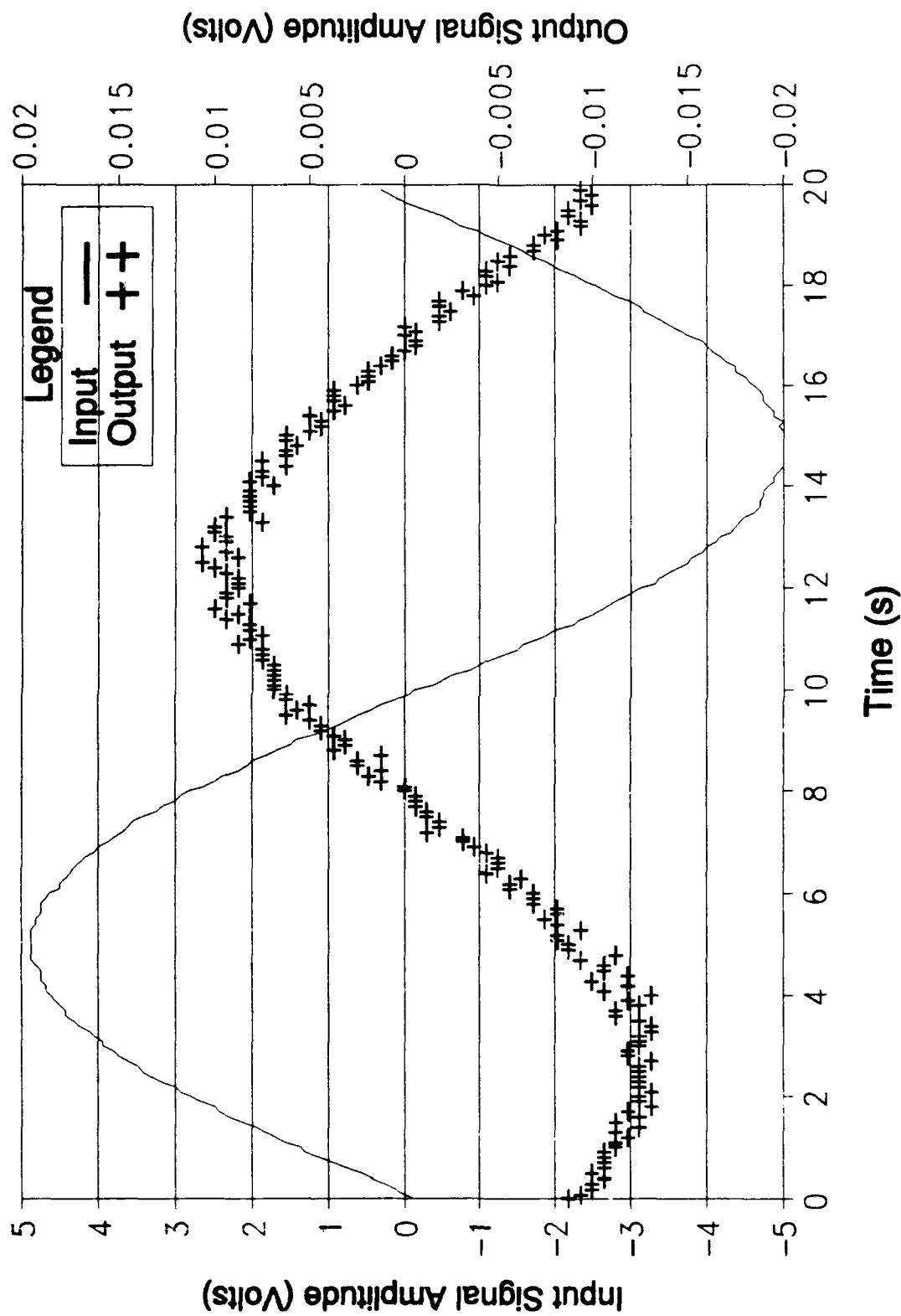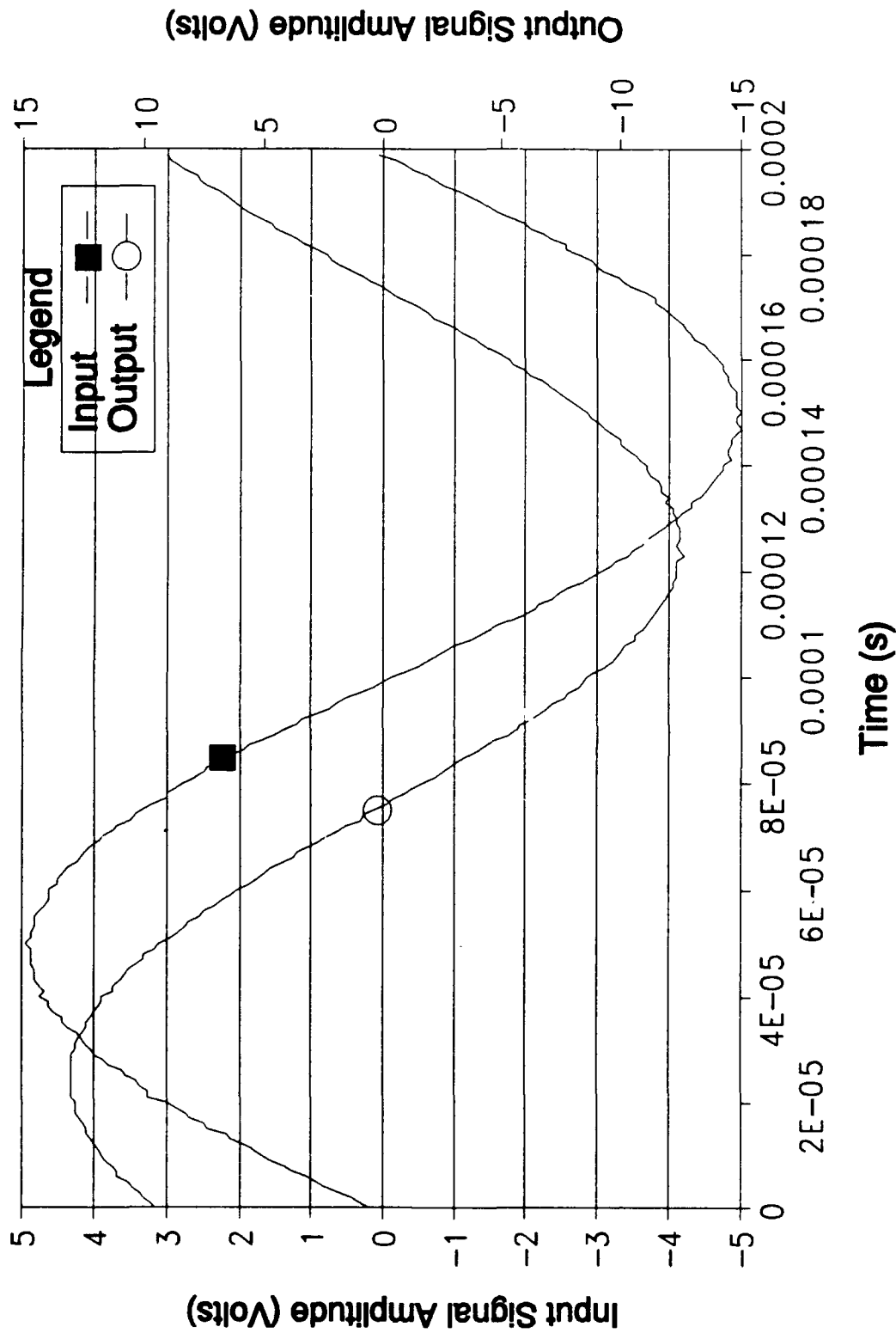
Figure G-59. Time Response of the Oldfield Surface Mount Component Circuit Design with a 5 KHz Excitation Signal.
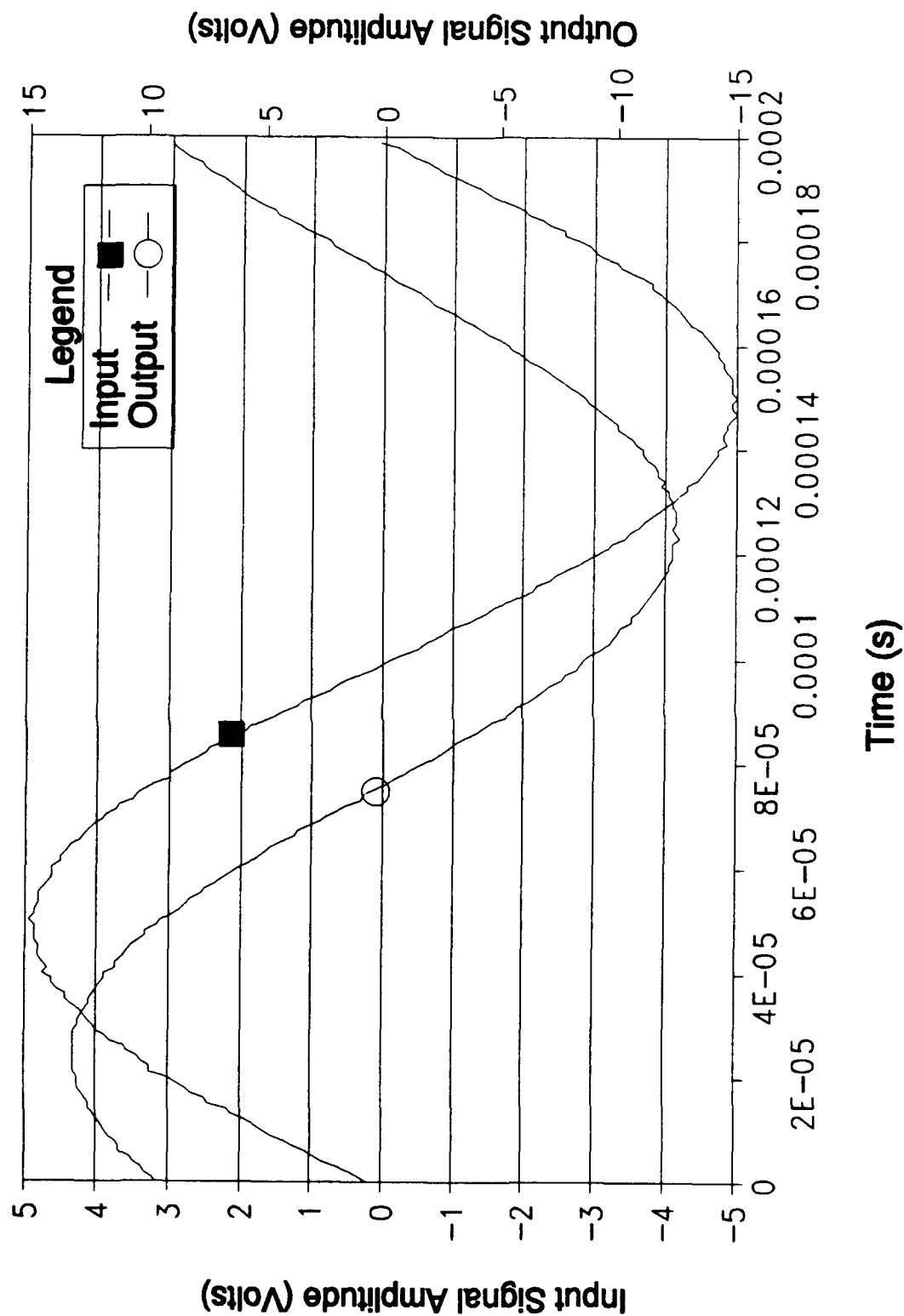
Figure G-60. Time Response of the Oldfield Surface Mount Component Circuit Design with a 10 KHz Excitation Signal.

Appendix H

Nichols Plots for

the Oldham and Oldfield

Circuits Realized

With a Printed Circuit Board Format

This appendix documents the Nichols Plots obtained for the Oldham and Oldfield discrete, hybrid and surface mount component circuits realized with a printed circuit board format.
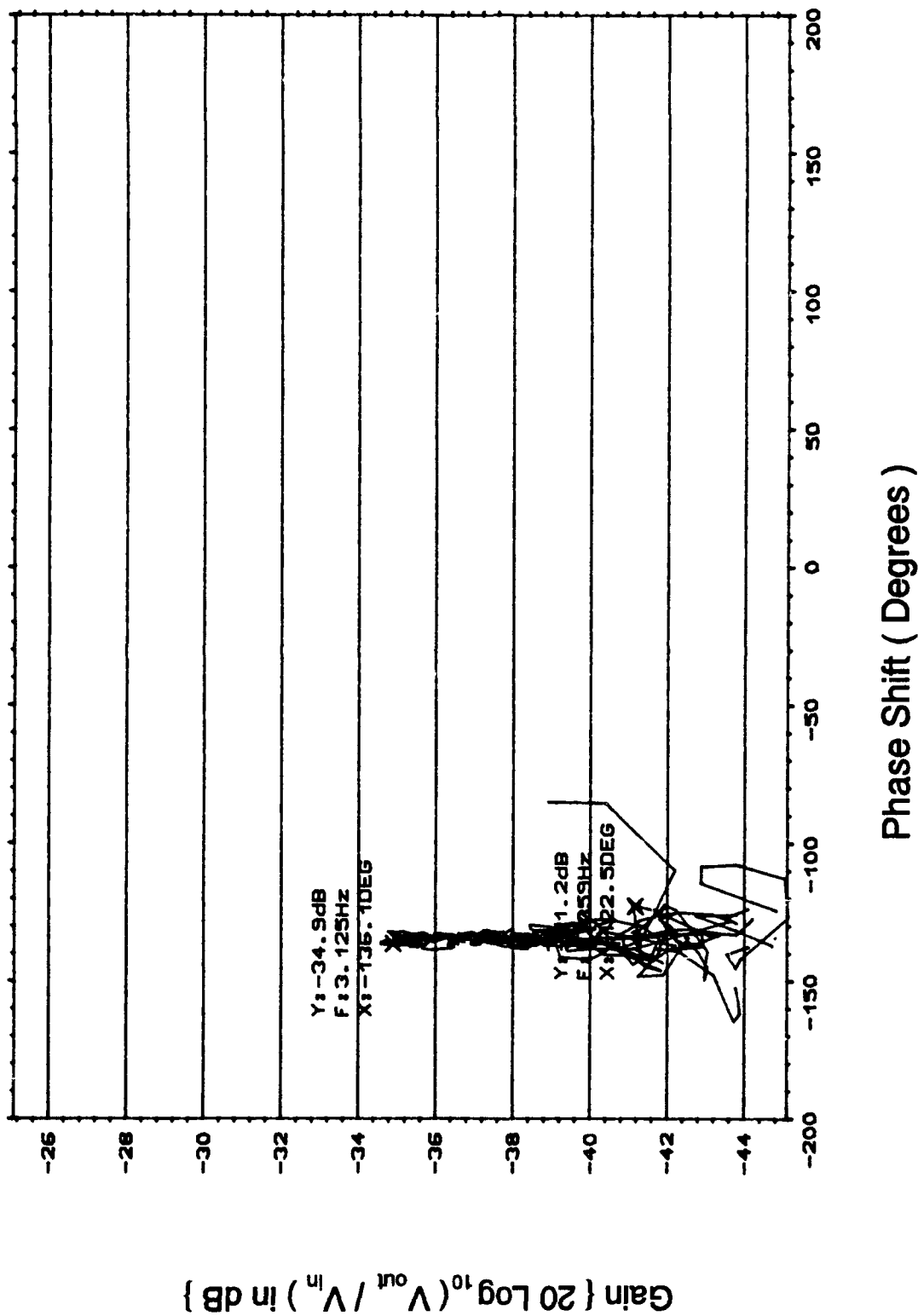
Figure H-1. Nichols Plot for the Oldham Discrete Component Circuit (Frequency Range 0.059 Hz to 3.125 Hz).

Phase Shift (Degrees)

Gain { 20 Log₁₀ (V_out / V_in) } in dB
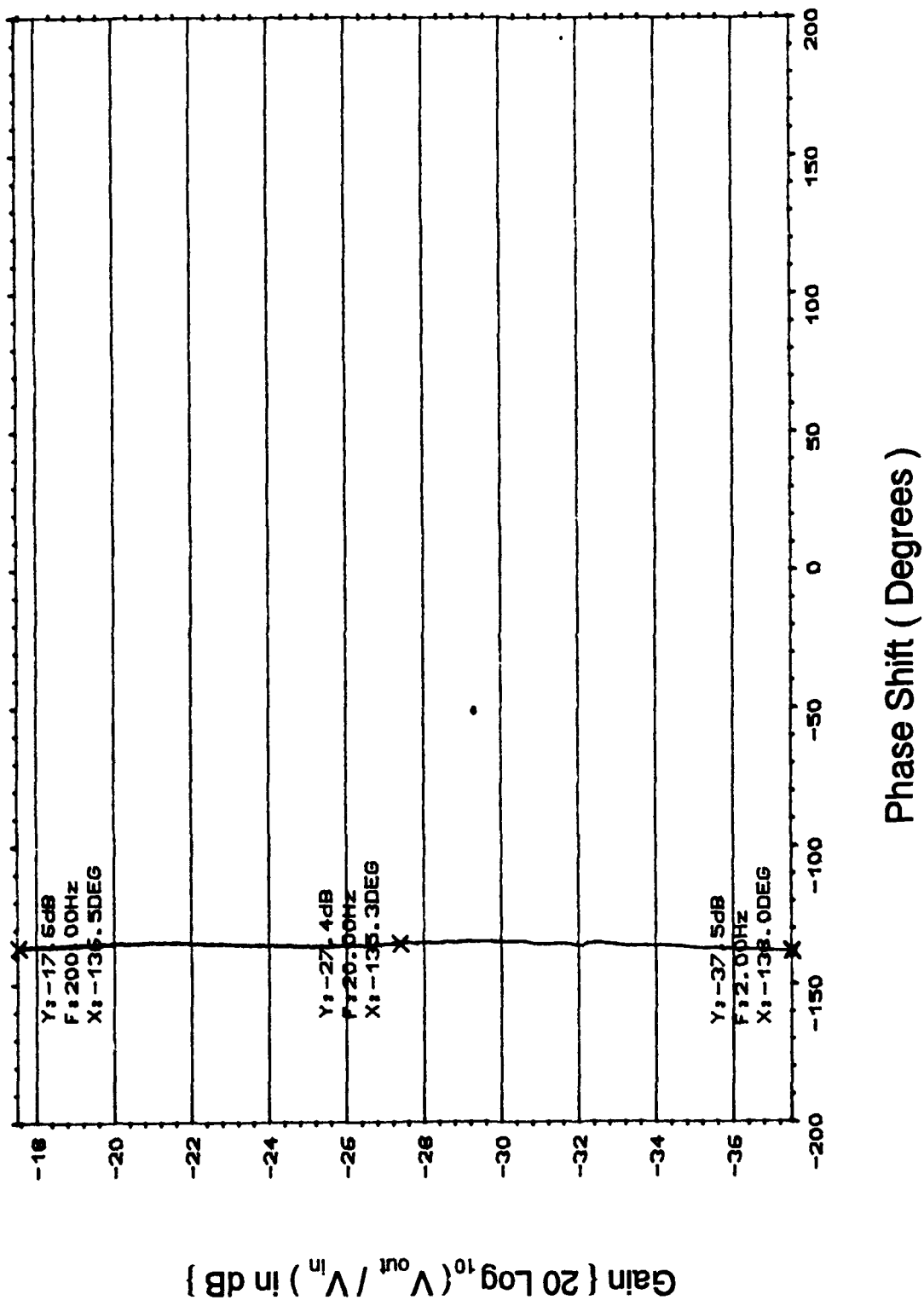
Figure H-2. Nichols Plot for the Oldham Discrete Component Circuit (Frequency Range 2.0 Hz to 200 Hz).

Phase Shift (Degrees)
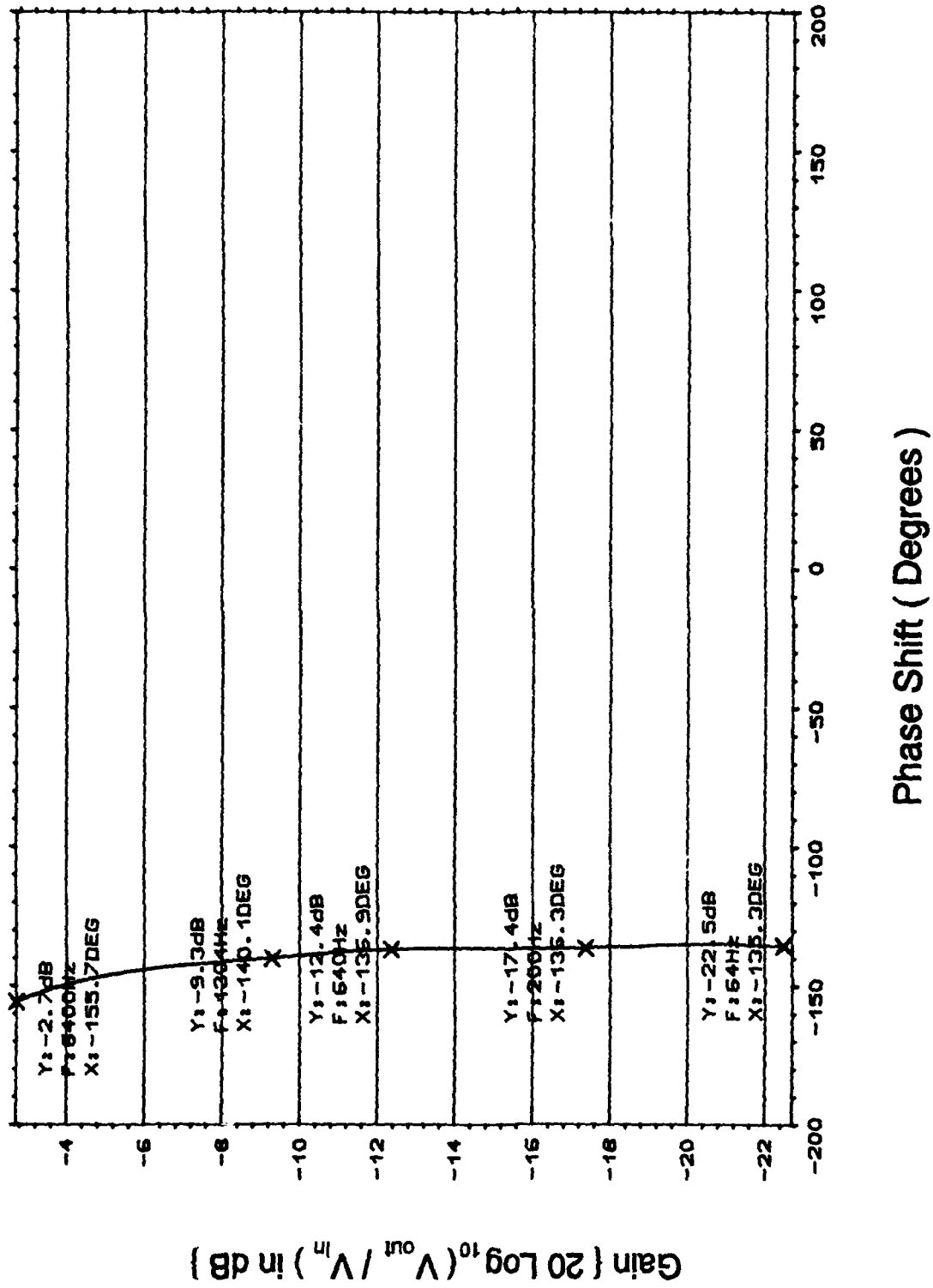
Figure H-3. Nichols Plot for the Oldham Discrete Component Circuit
(Frequency Range 64 Hz to 6400 Hz).

Gain (20 Log₁₀ (V_out / V_in) in dB)

Phase Shift (Degrees)

Gain { 20 Log₁₀(V_out / V_in) in dB }
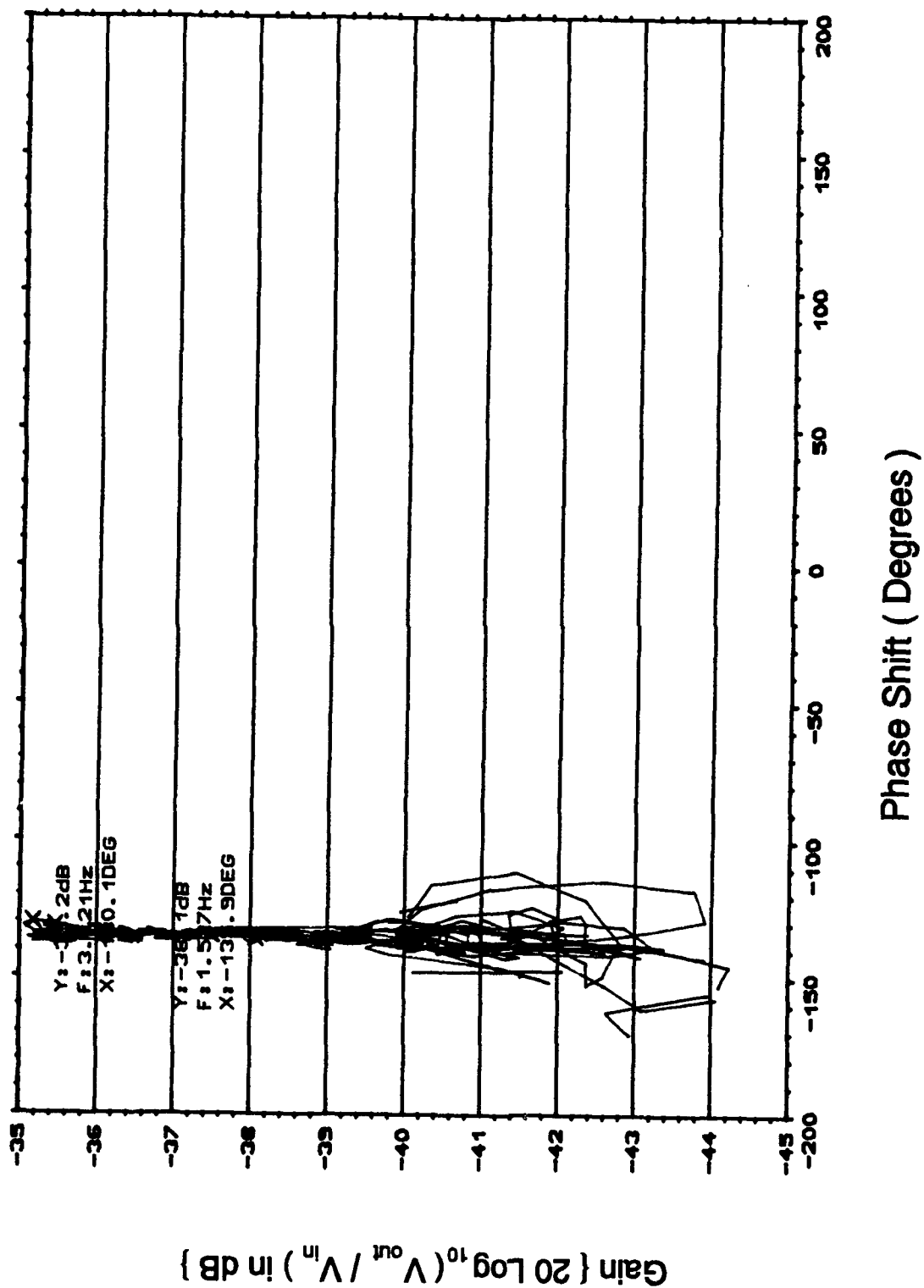
Figure H-4. Nichols Plot for the Oldham Hybrid Component Circuit
(Frequency Range 1.57 Hz to 3.21 Hz).

Phase Shift (Degrees)
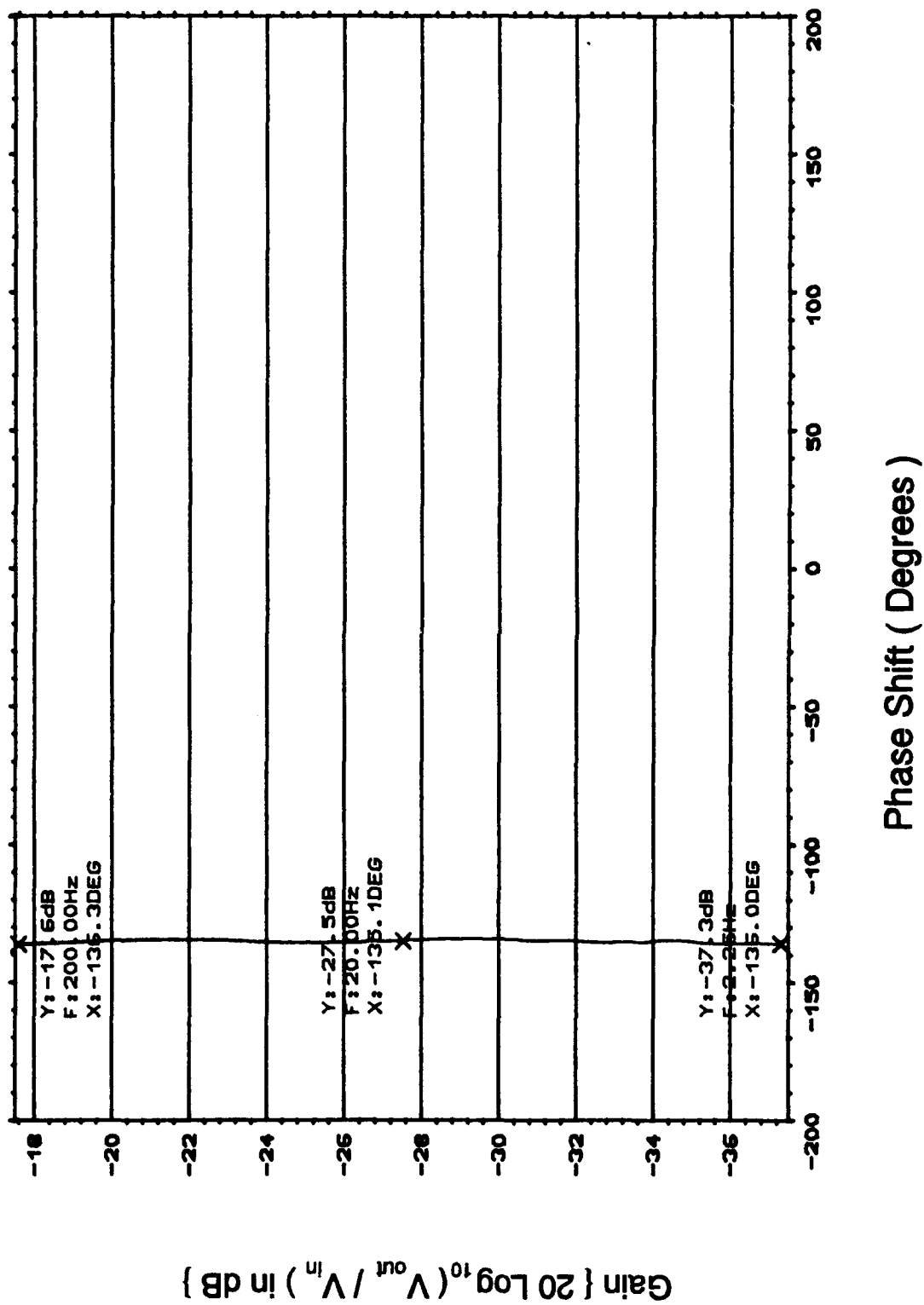
Figure H-5. Nichols Plot for the Oldham Hybrid Component Circuit. (Frequency Range 2.25 Hz to 200 Hz).

Gain { 20 Log$_{10}$ (V$_{out}$ / V$_{in}$) in dB }

Phase Shift (Degrees)

Gain { 20 Log₁₀ (Vₒᵤₜ / Vᵢₙ) in dB }
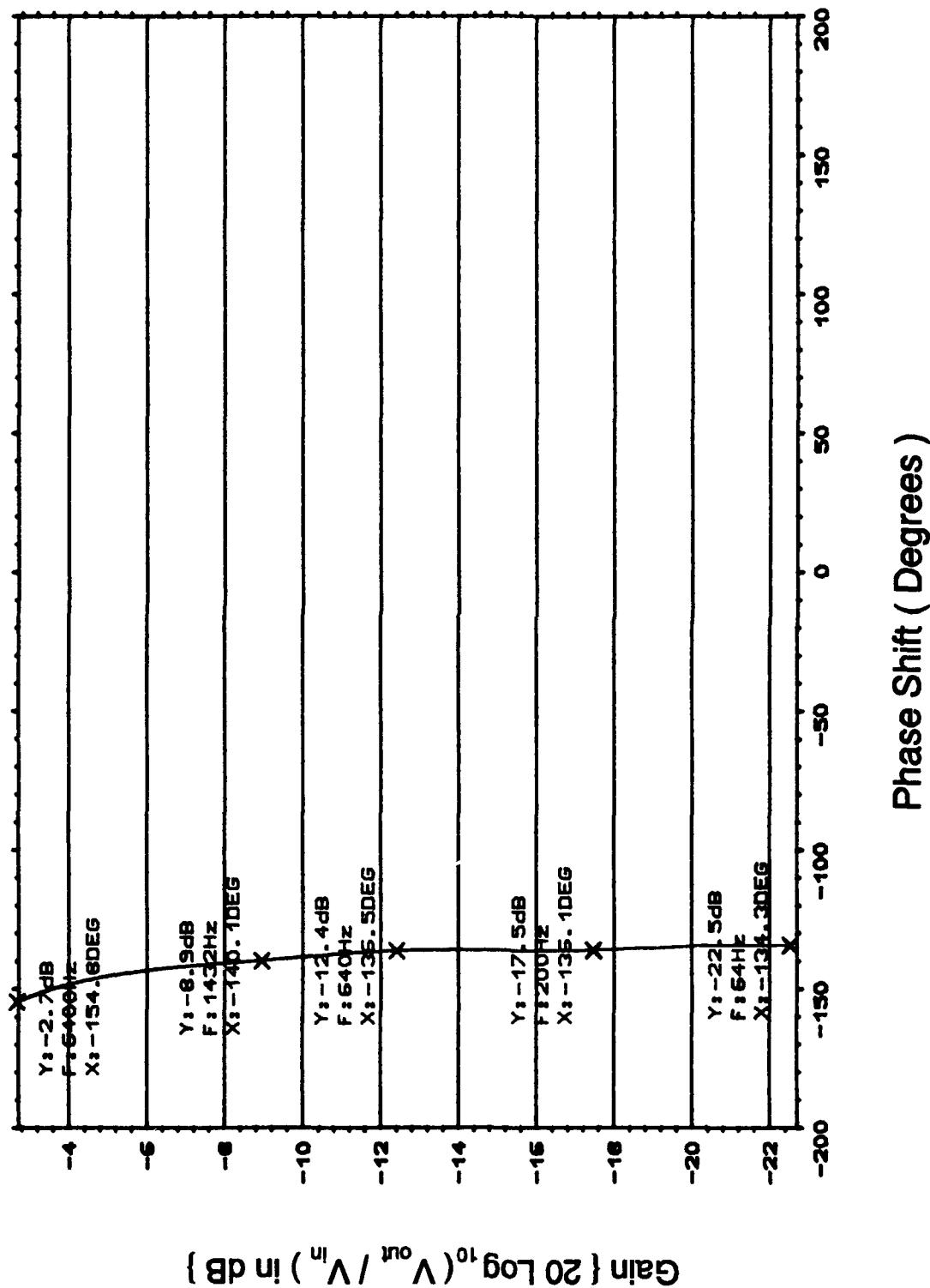
Figure H-6. Nichols Plot for the Oldham Hybrid Component Circuit (Frequency Range 64 Hz to 6400 Hz).
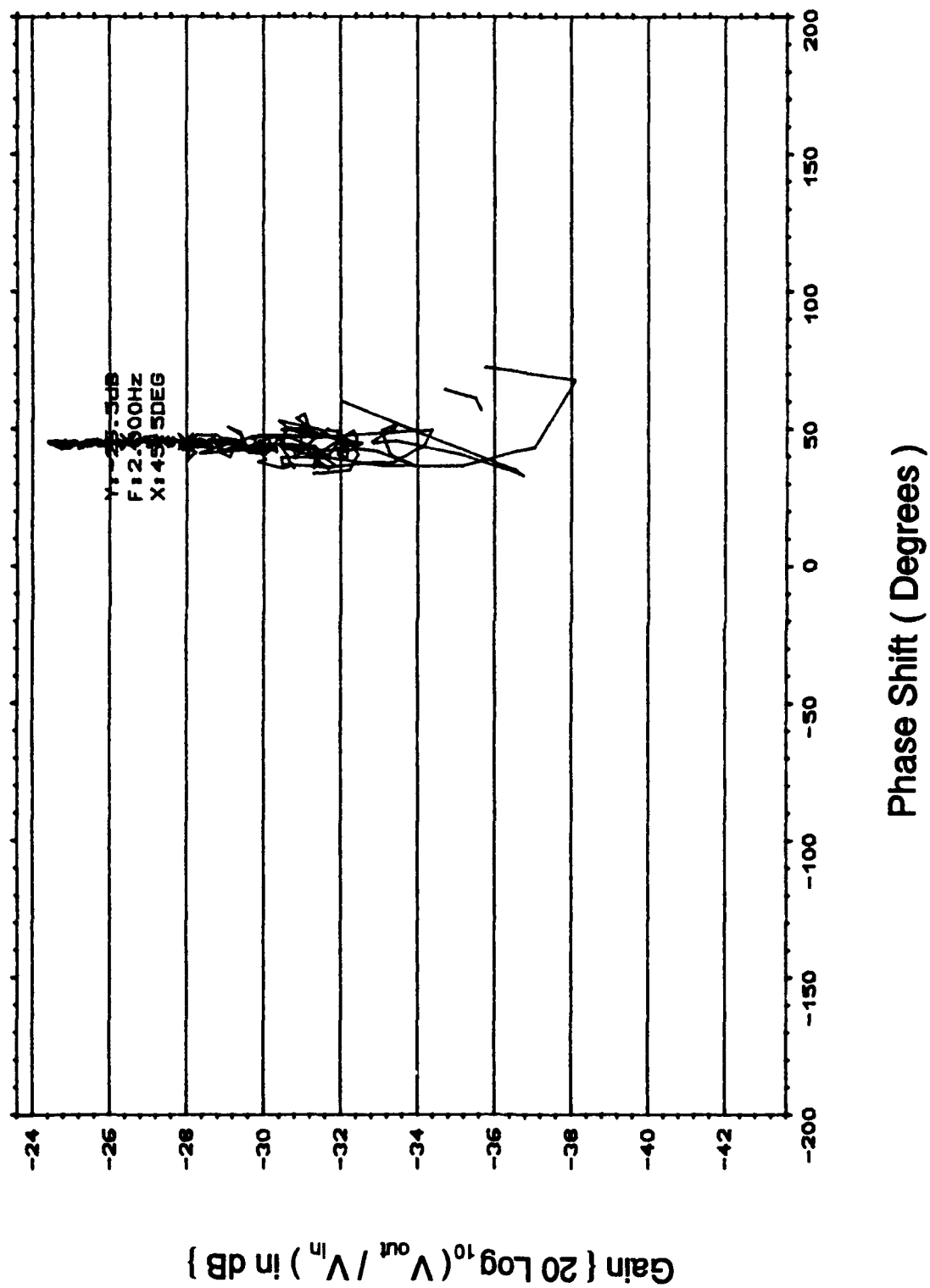
Figure H-7. Nichols Plot for the Oldfield Discrete Component Circuit
(Frequency Range 2.0 Hz to 3.125 Hz).

Phase Shift (Degrees)

Gain { 20 Log$_{10}$ (V$_{out}$ / V$_{in}$) in dB }
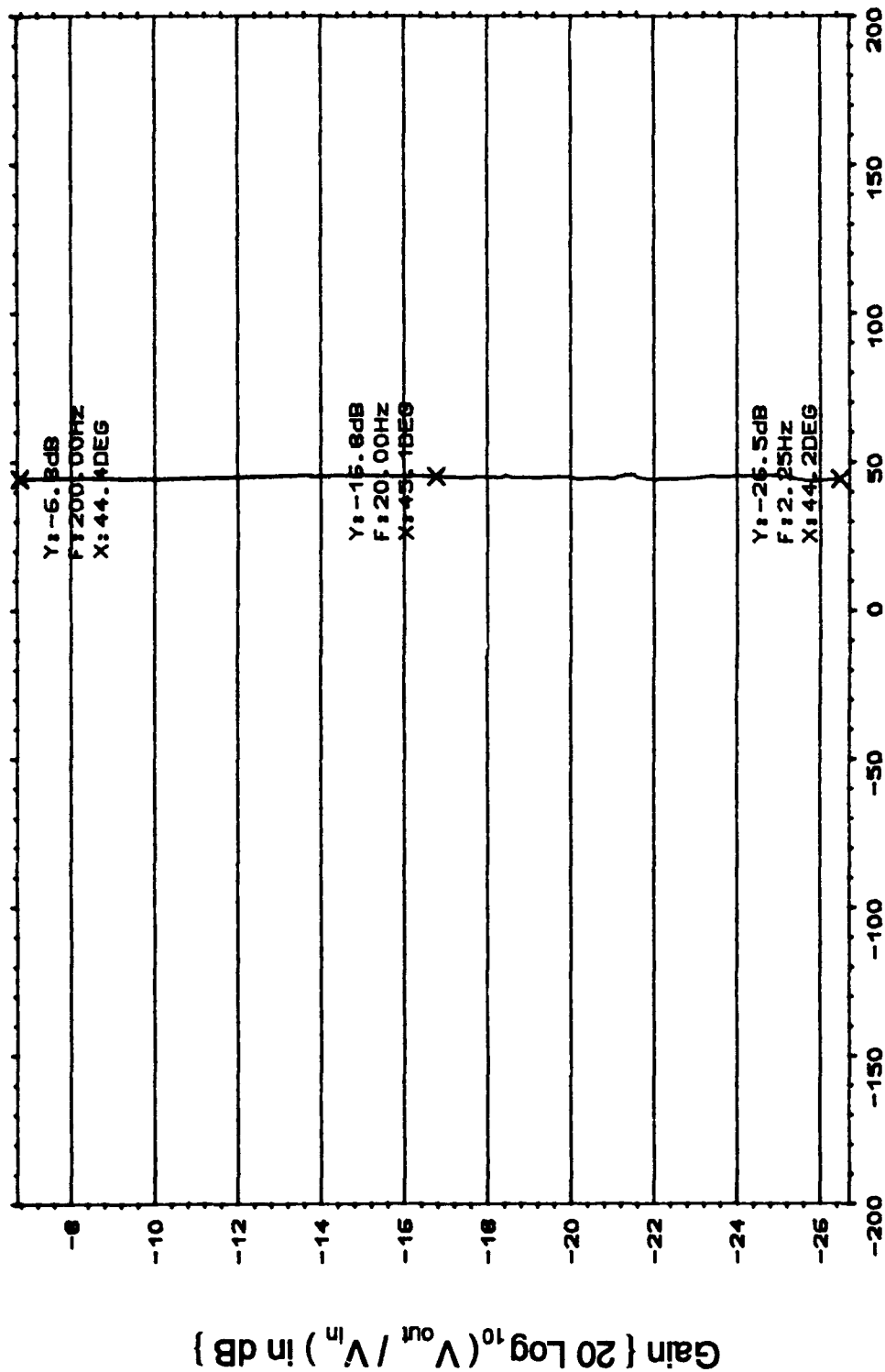
Figure H-8. Nichols Plot for the Oldfield Discrete Component Circuit
(Frequency Range 2.25 Hz to 200 Hz).

Phase Shift (Degrees)

Gain { 20 Log₁₀(Vₒᵤₜ / Vᵢₙ) in dB }
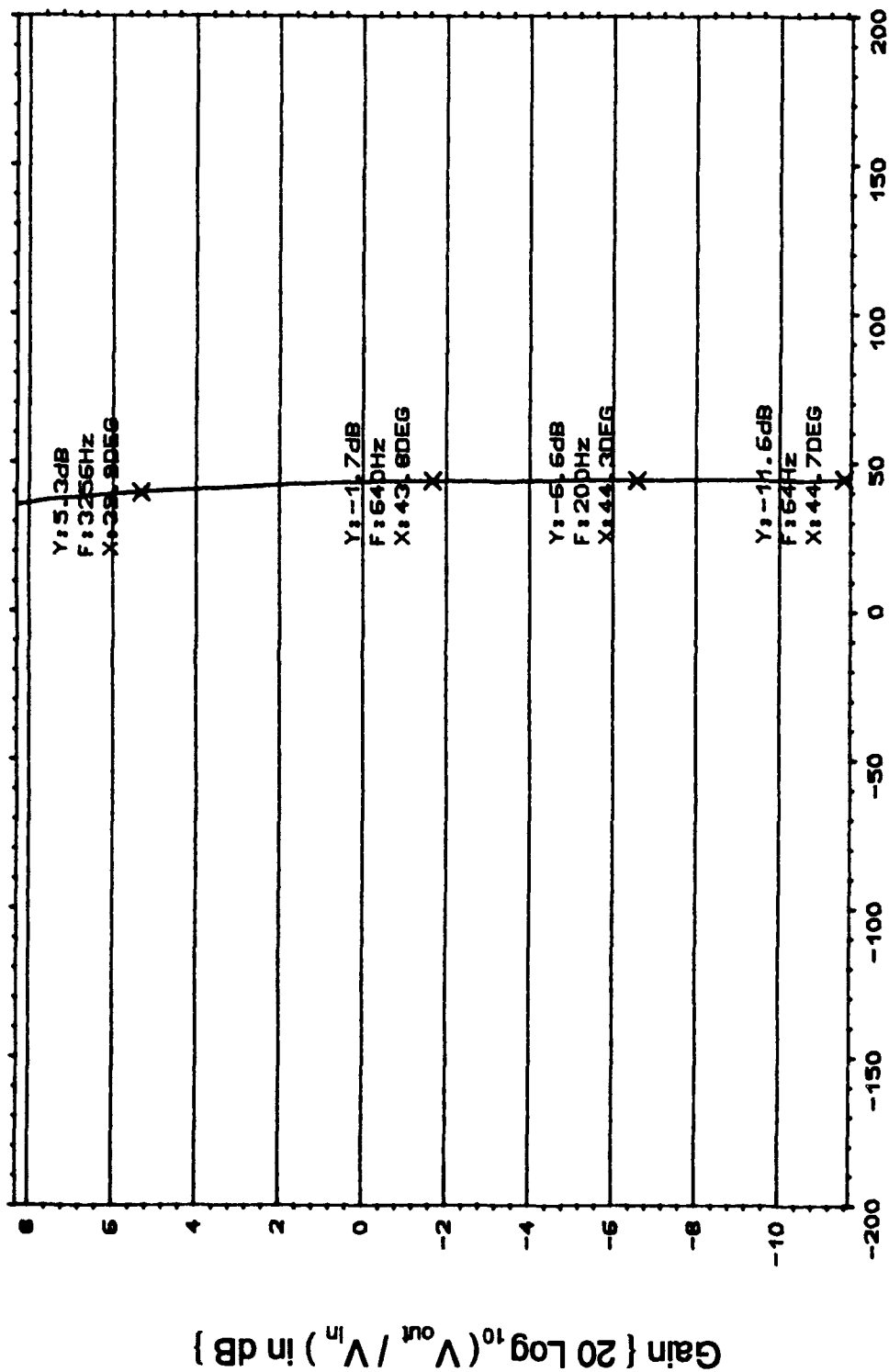
Figure H-9.   Nichols Plot for the Oldfield Discrete Component Circuit
(Frequency Range 64 Hz to 3256 Hz).

Phase Shift (Degrees)

Gain { 20 Log$_{10}$ (V$_{out}$ / V$_{in}$) in dB }
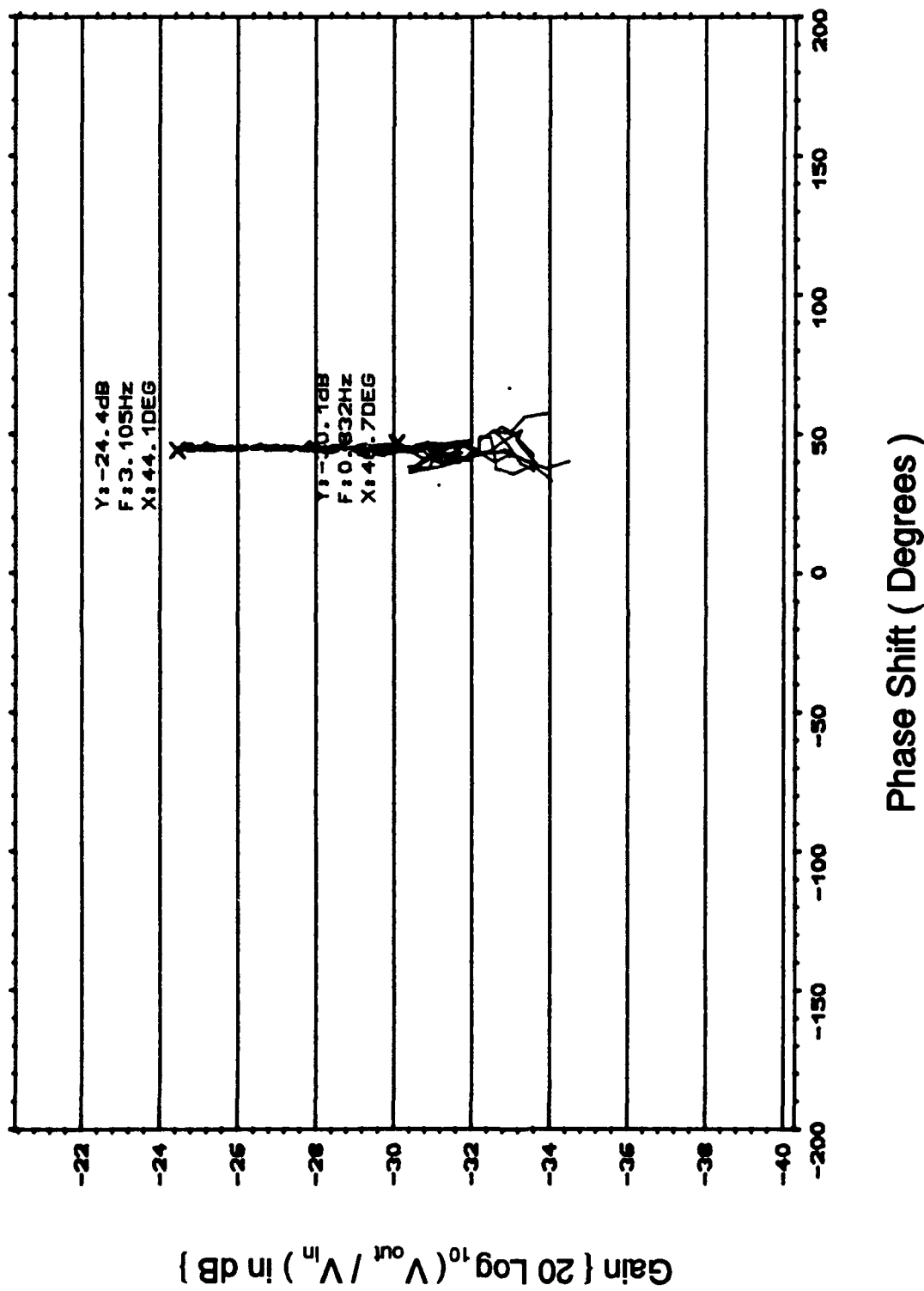
Figure H-10. Nichols Plot for the Oldfield Surface Mount Component Circuit (Frequency Range 0.832 Hz to 3.105 Hz).

Phase Shift (Degrees)

Gain { 20 Log$_{10}$ (V$_{out}$ / V$_{in}$) in dB }
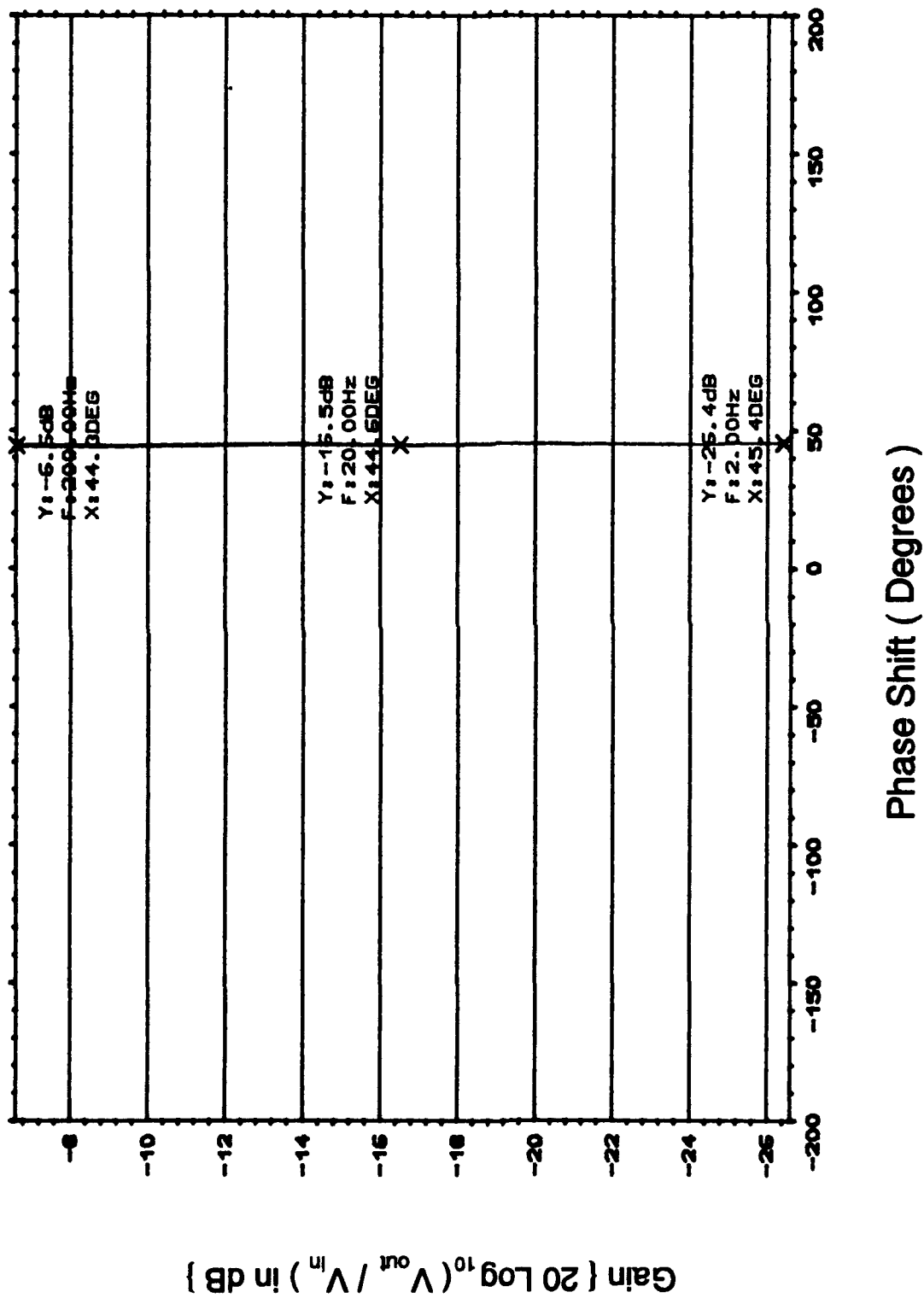
Figure H-11. Nichols Plot for the Oldfield Surface Mount Component Circuit (Frequency Range 2.0 Hz to 200 Hz).
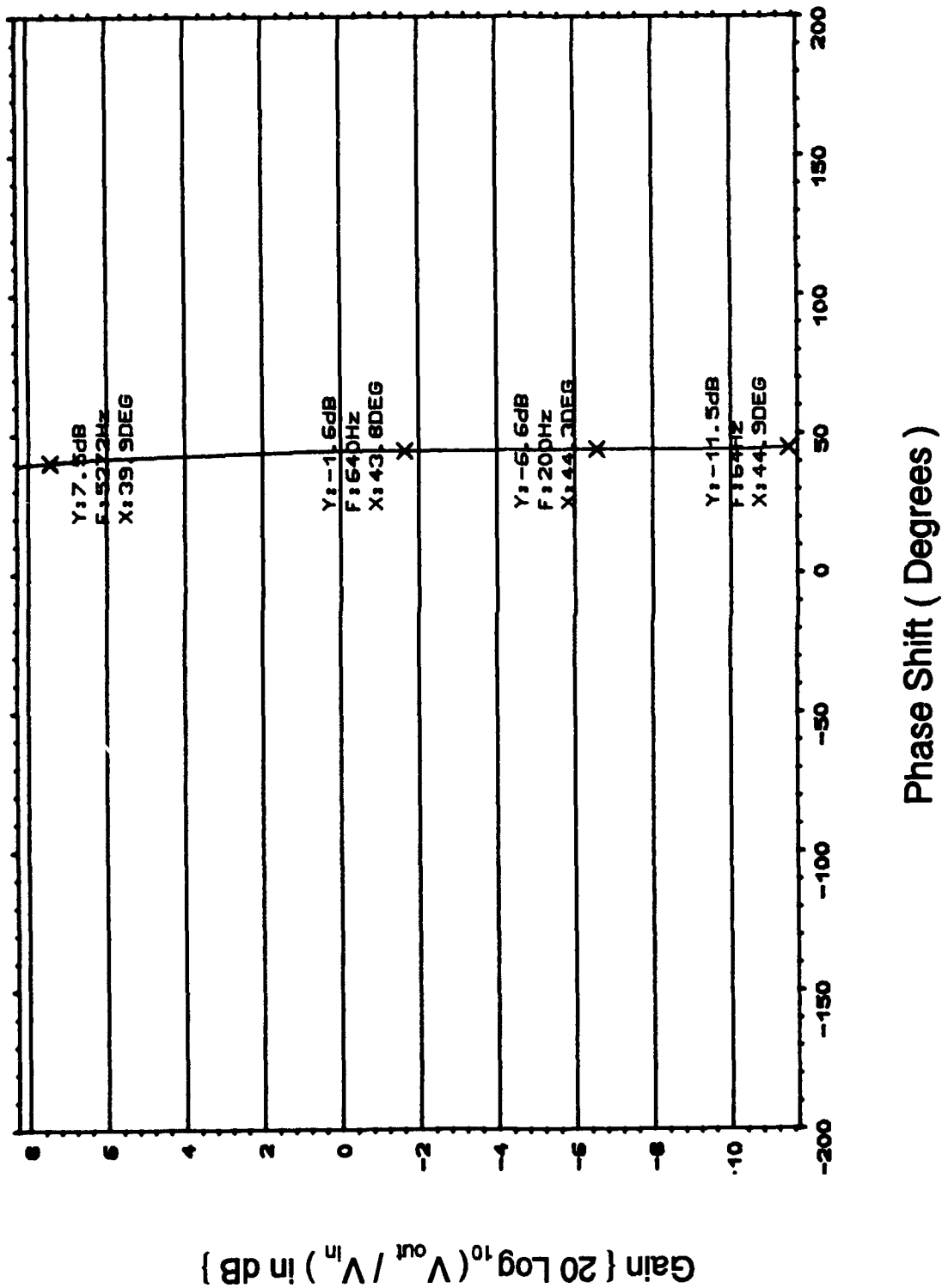
Figure H-12. Nichols Plot for the Oldfield Surface Mount Component Circuit (Frequency Range 64 Hz to 5272 Hz).

Appendix I

Spectrum Data for

the Oldham and Oldfield

Circuits Realized

With a Printed Circuit Board Format

This appendix documents the experimentally measured spectrum data obtained for the Oldham and Oldfield discrete, hybrid and surface mount component circuits realized with a printed circuit board format. The data is arranged according to circuit variant. That is, Section 1 documents the Oldham discrete component spectrum data, Section 2 documents the Oldham hybrid component spectrum data, Section 3 documents the Oldfield discrete component spectrum data, and Section 4 documents the Oldfield surface mount data.

Section 1

Spectrum Plots for
the Oldham Discrete Component Circuit

Figure I-1. Spectrum Analysis of the Oldham Discrete Component Circuit With a 0.05 Hz Excitation Signal.

Figure I-2. Spectrum Analysis of the Oldham Discrete Component Circuit With a 0.099 Hz Excitation Signal.

Figure I-3.   Spectrum Analysis of the Oldham Discrete Component Circuit
With a 0.5 Hz Excitation Signal.

Figure I-4.   Spectrum Analysis of the Oldham Discrete Component Circuit
With a 1 Hz Excitation Signal.

Figure I-5. Spectrum Analysis of the Oldham Discrete Component Circuit
With a 5 Hz Excitation Signal.

Figure I-6. Spectrum Analysis of the Oldham Discrete Component Circuit With a 10 Hz Excitation Signal.

Figure I-7. Spectrum Analysis of the Oldham Discrete Component Circuit With a 50 Hz Excitation Signal.

Frequency (Hz)
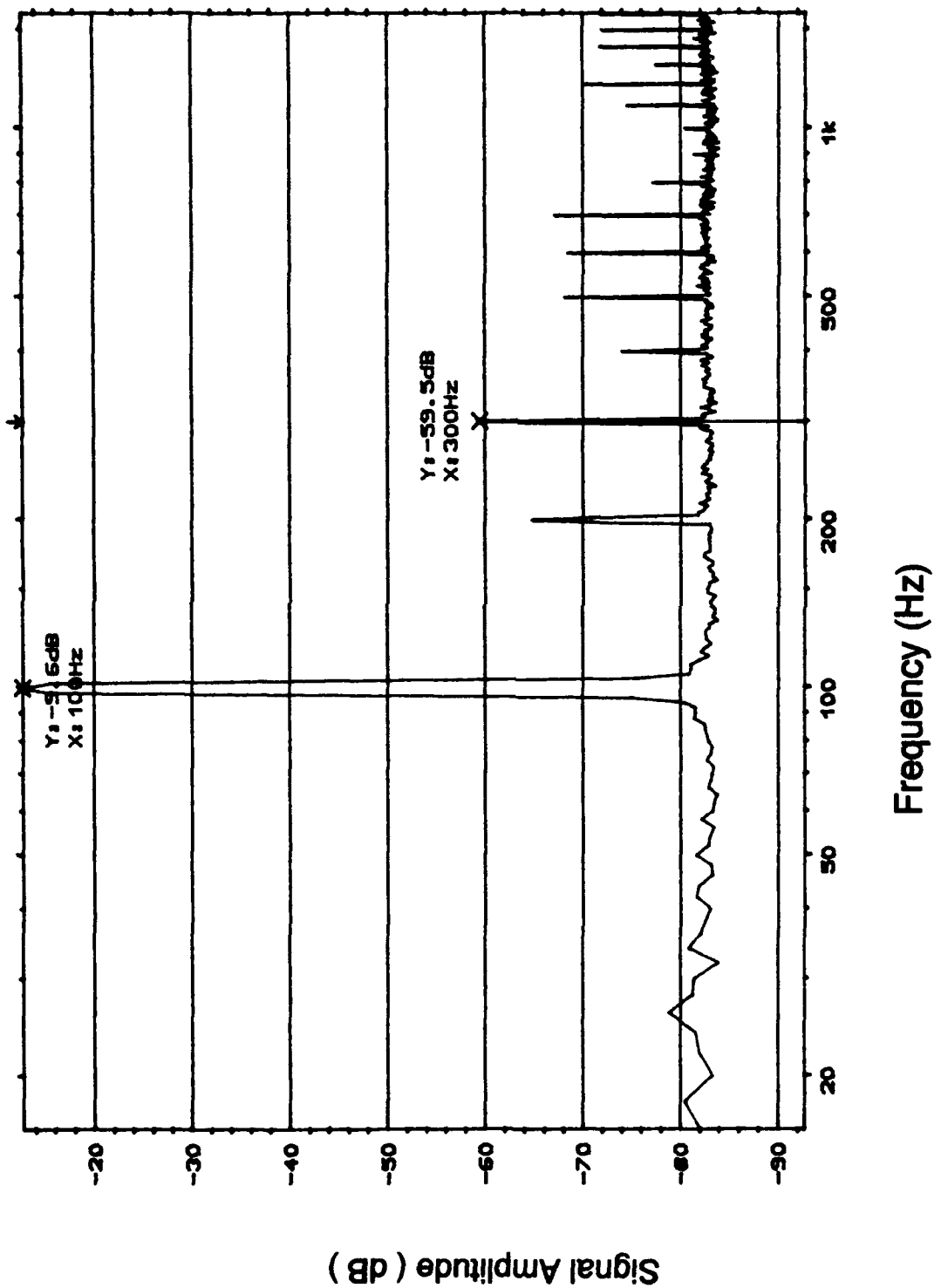
Figure I-8. Spectrum Analysis of the Oldham Discrete Component Circuit With a 100 Hz Excitation Signal.
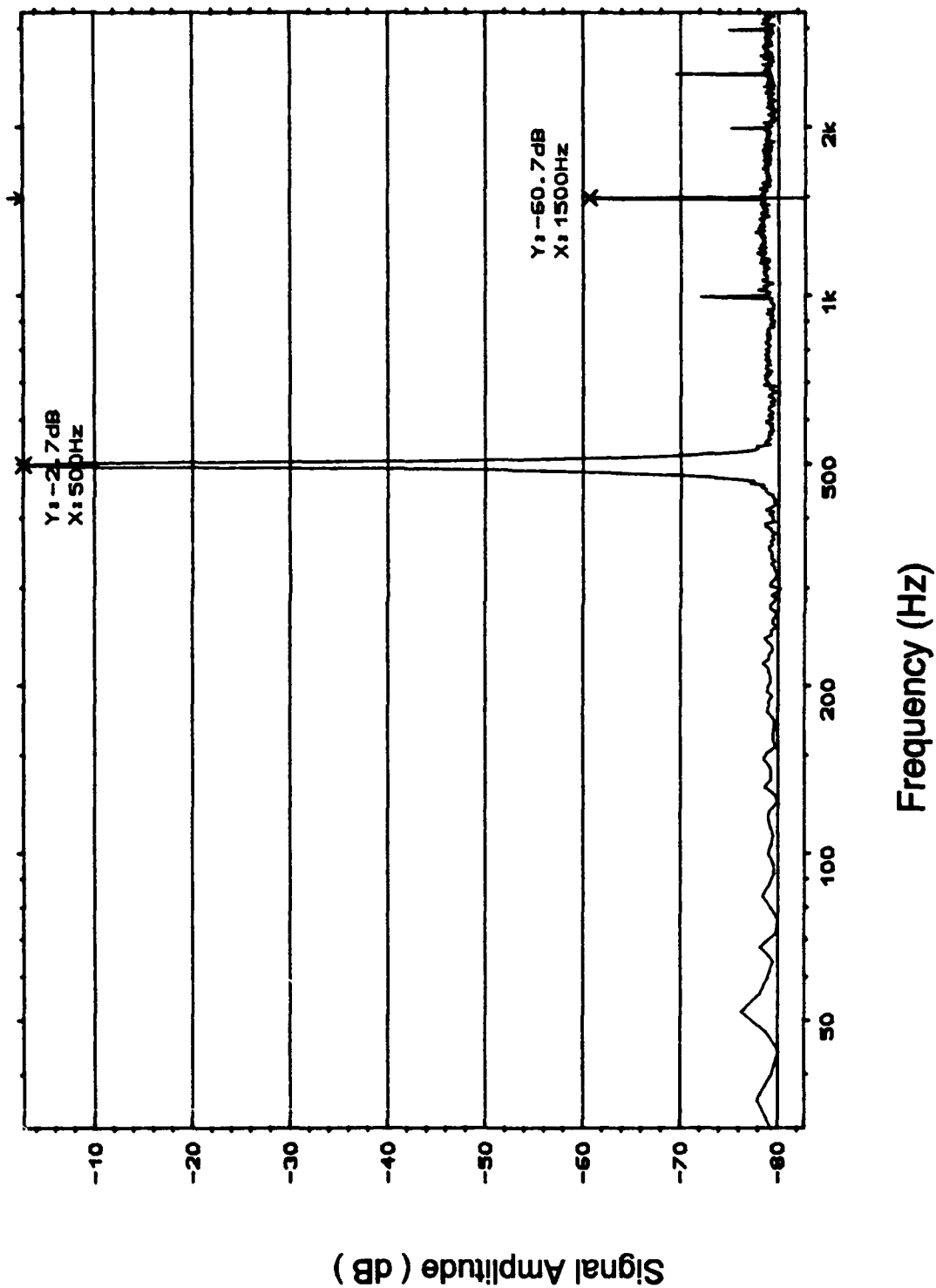
Figure I-9. Spectrum Analysis of the Oldham Discrete Component Circuit With a 500 Hz Excitation Signal.
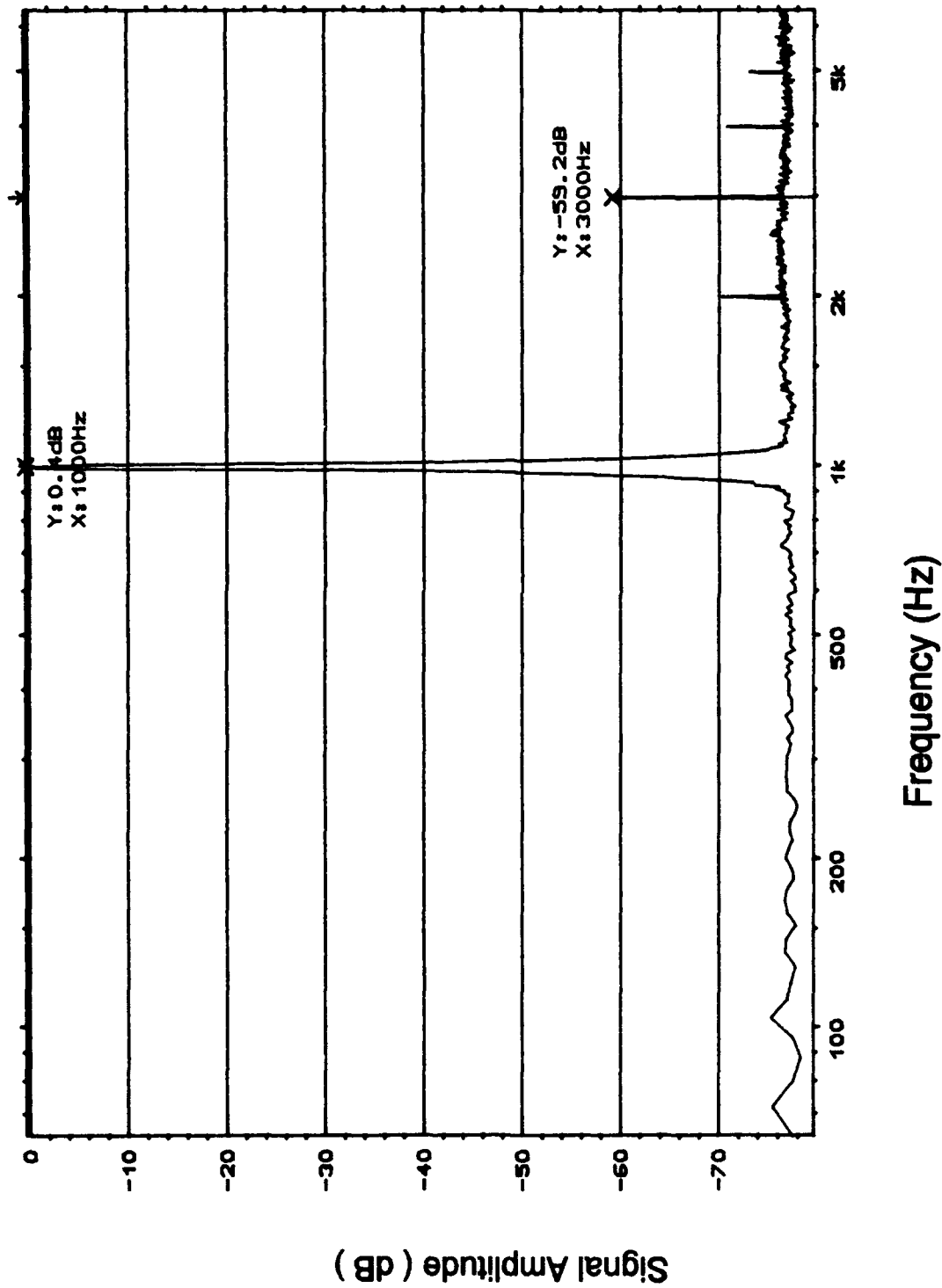
Figure I-10. Spectrum Analysis of the Oldham Discrete Component Circuit With a 1 KHz Excitation Signal.

Y:6.3dB
X:4992Hz

Y:-61.1dB
X:15008Hz

Frequency (Hz)

Signal Amplitude (dB)
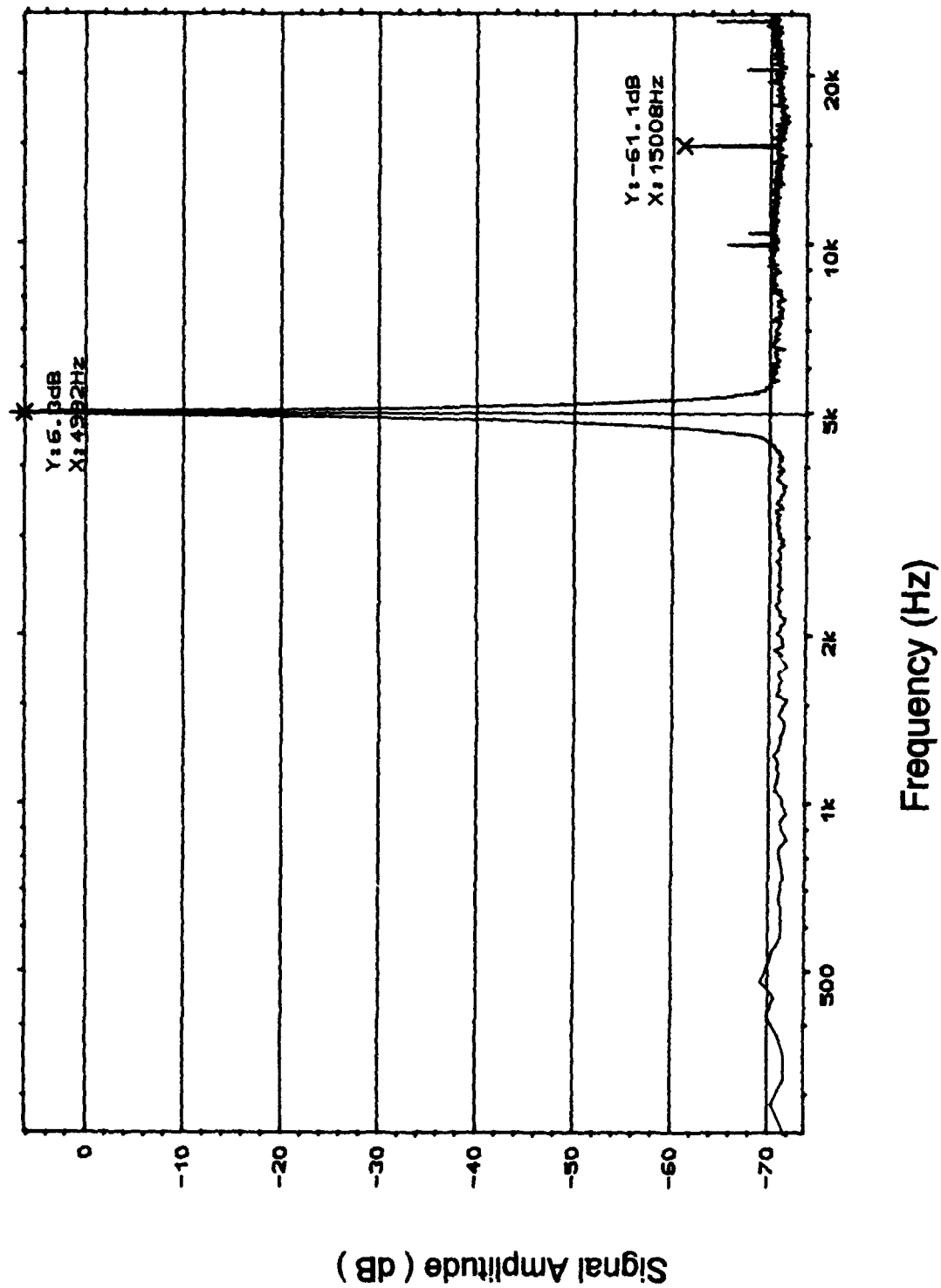
Figure I-11. Spectrum Analysis of the Oldham Discrete Component Circuit With a 4.982 KHz Excitation Signal.
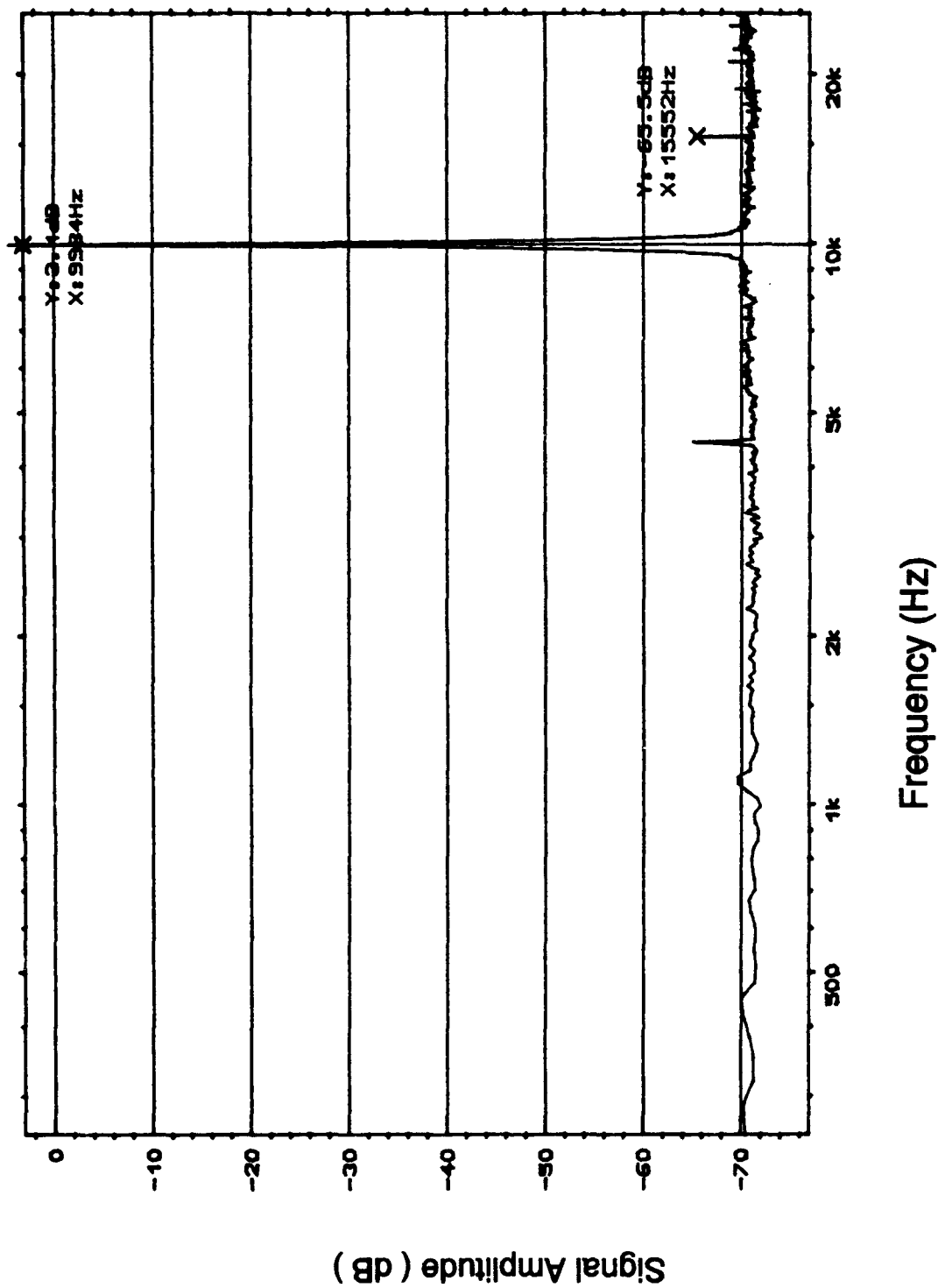
Figure I-12. Spectrum Analysis of the Oldham Discrete Component Circuit With a 9.984 KHz Excitation Signal.

Section 2

Spectrum Plots for

the Oldham Hybrid Component Circuit
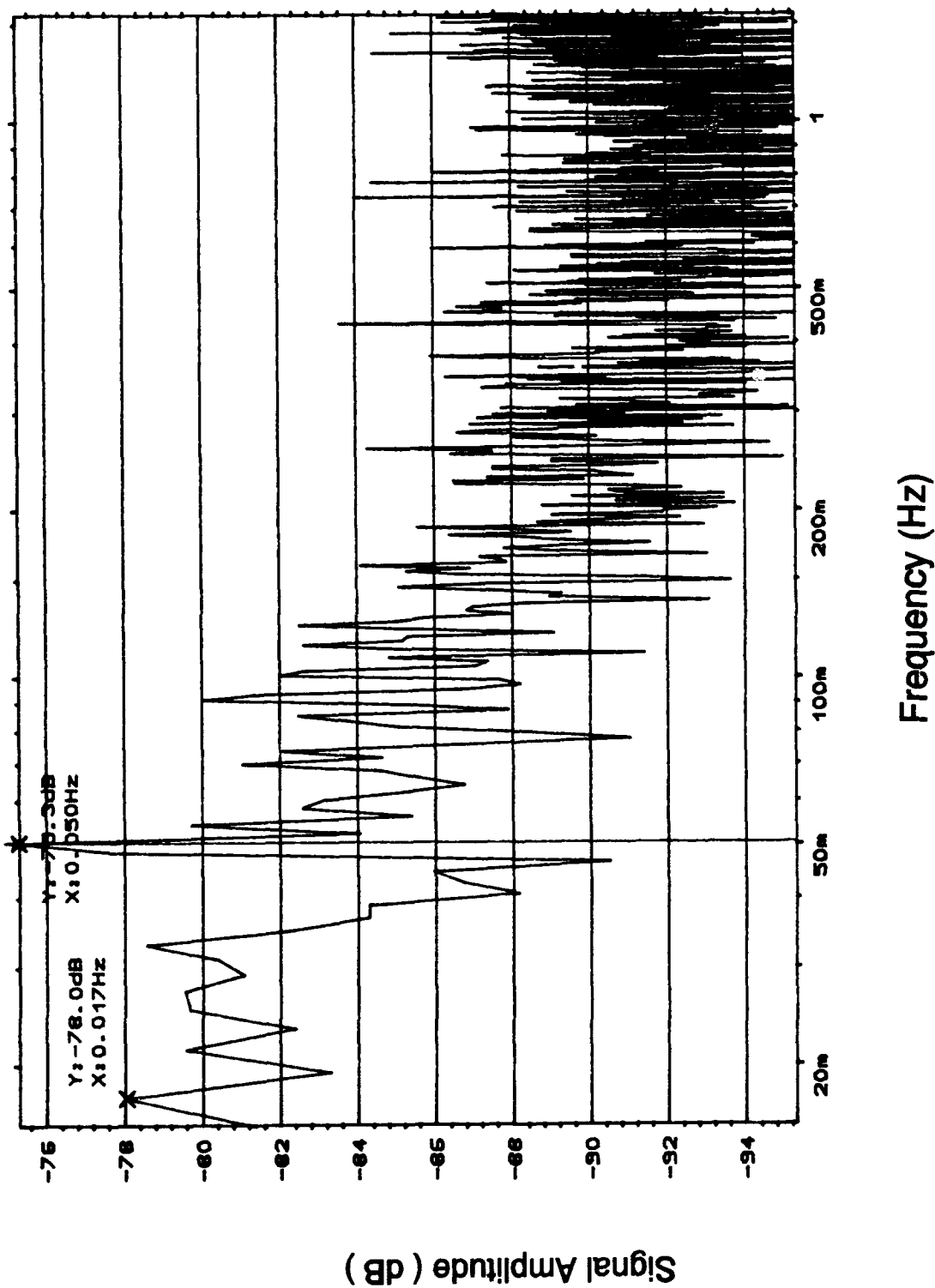
Figure I-13. Spectrum Analysis of the Oldham Hybrid Component Circuit With a 0.05 Hz Excitation Signal.
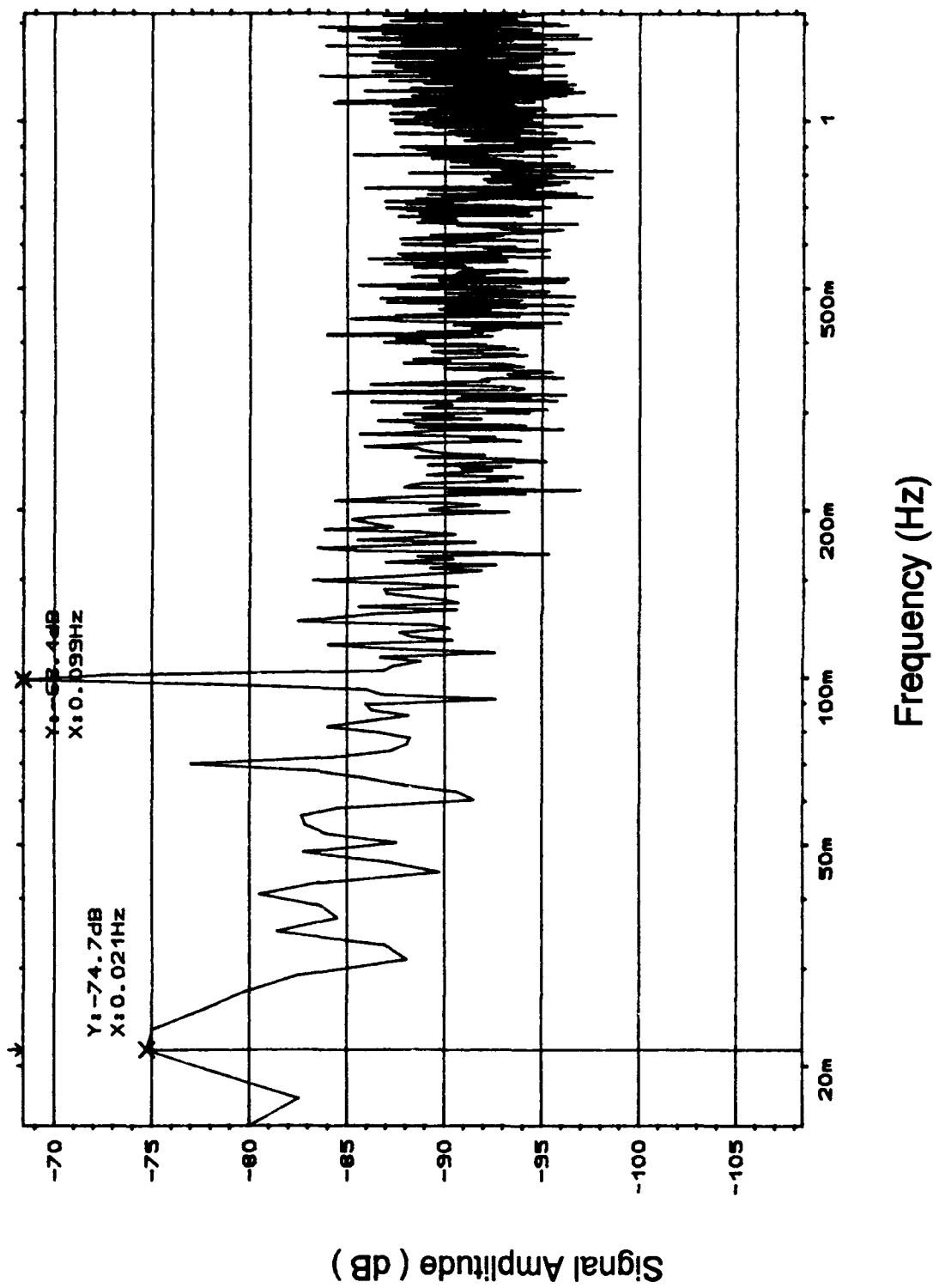
Figure I-14. Spectrum Analysis of the Oldham Hybrid Component Circuit
With a 0.099 Hz Excitation Signal.
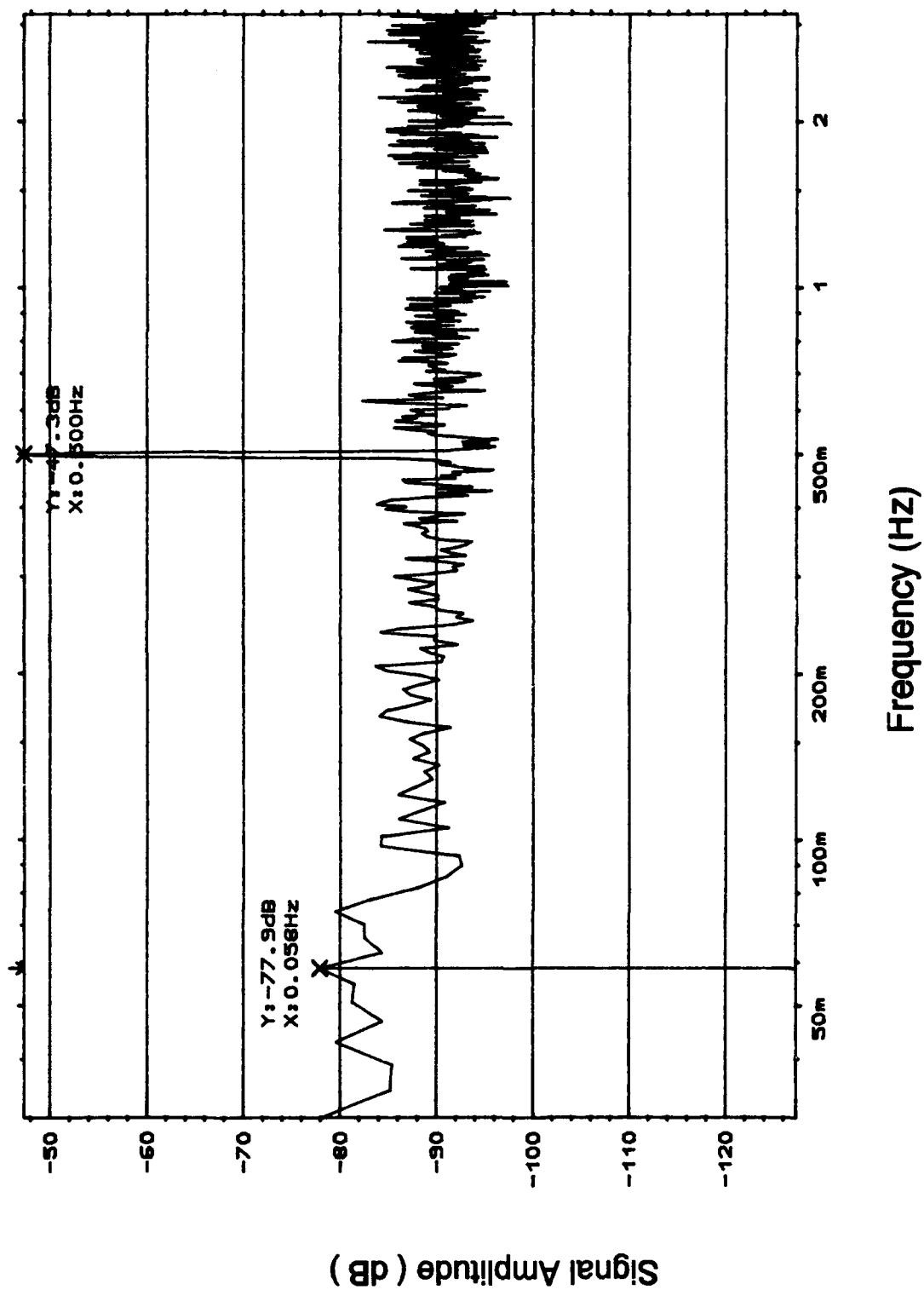
Figure I-15. Spectrum Analysis of the Oldham Hybrid Component Circuit With a 0.5 Hz Excitation Signal.
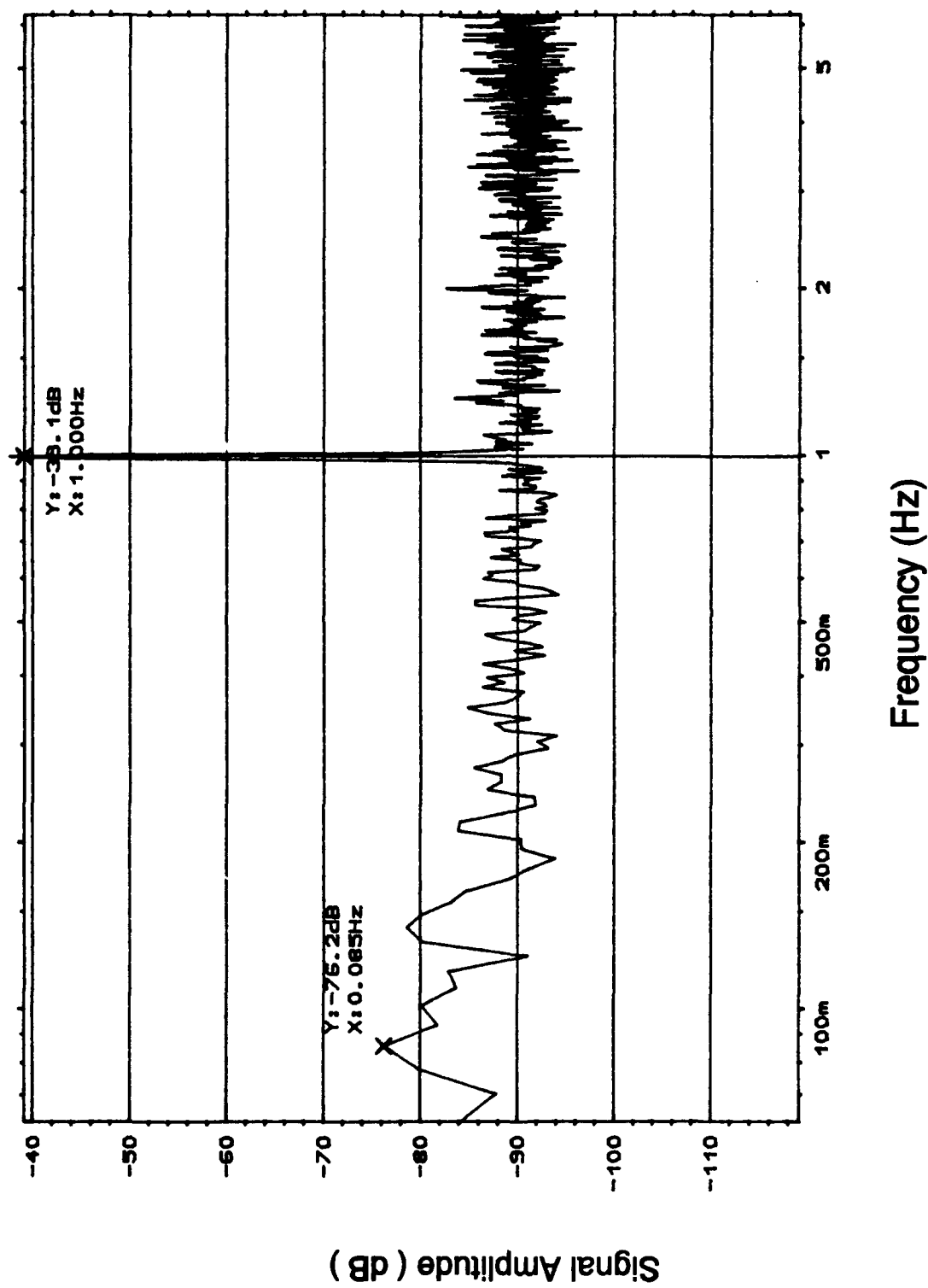
Figure I-16.   Spectrum Analysis of the Oldham Hybrid Component Circuit
With a 1 Hz Excitation Signal.
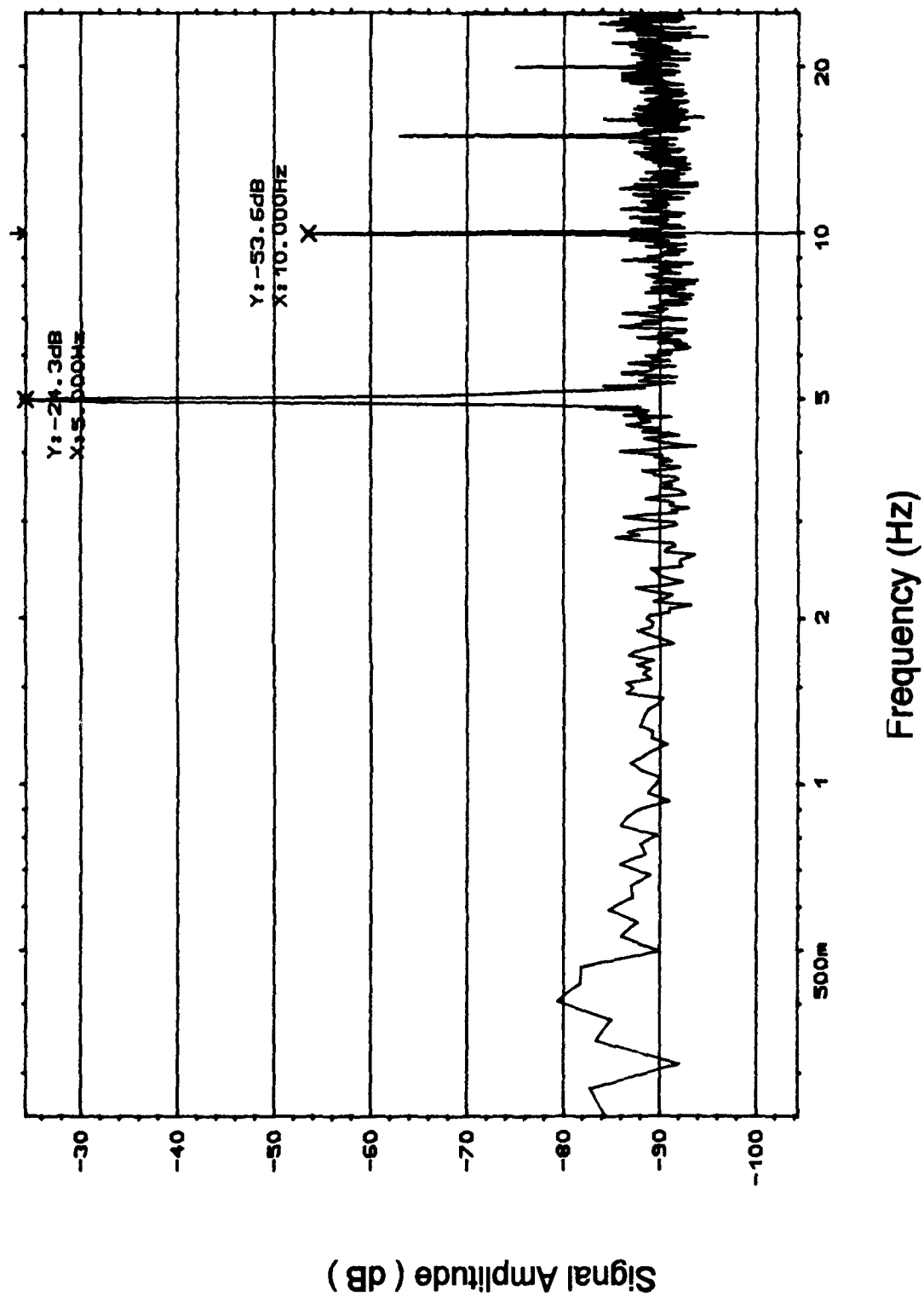
Figure I-17. Spectrum Analysis of the Oldham Hybrid Component Circuit With a 5 Hz Excitation Signal.
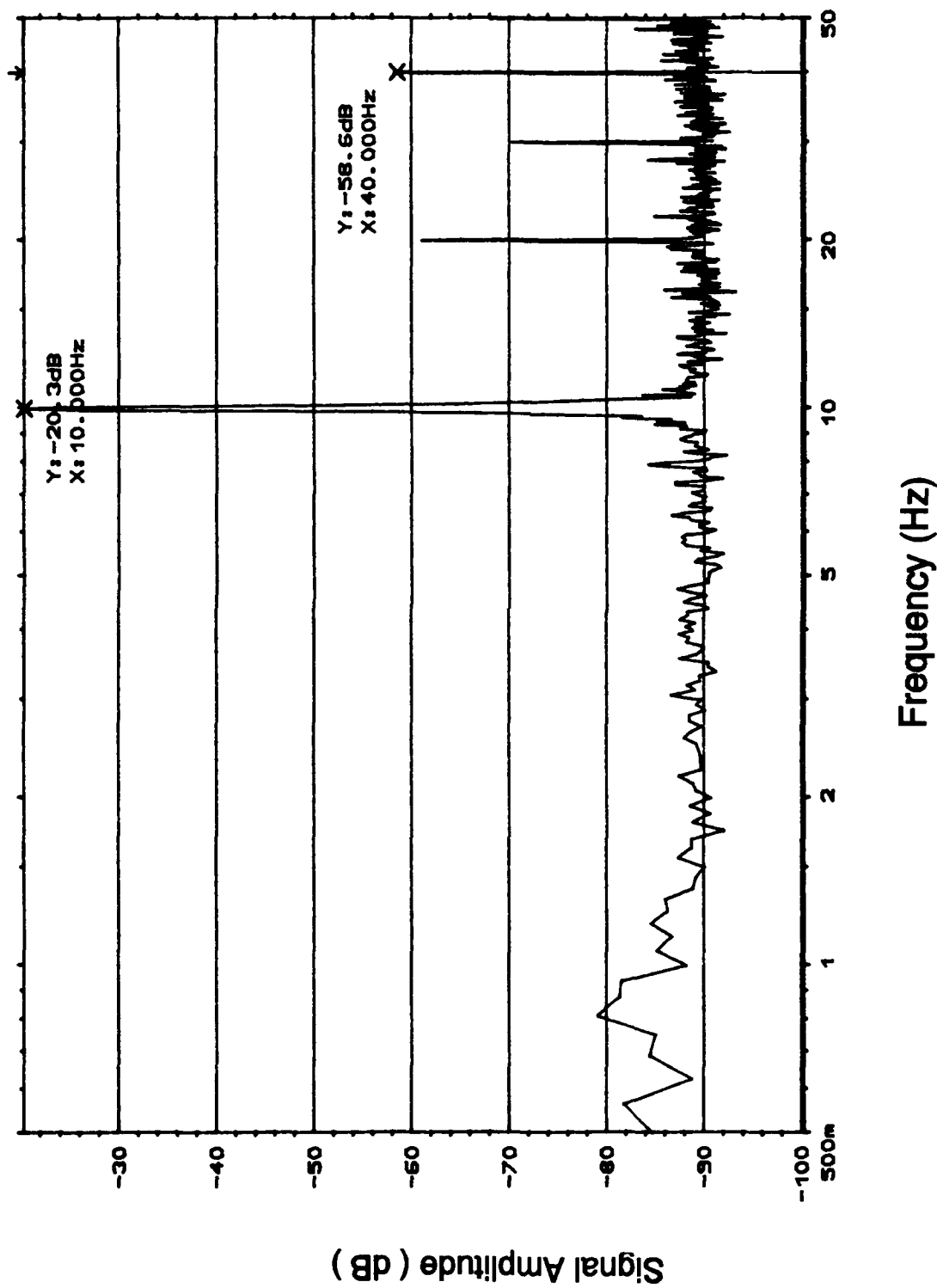
Figure I-18. Spectrum Analysis of the Oldham Hybrid Component Circuit With a 10 Hz Excitation Signal.
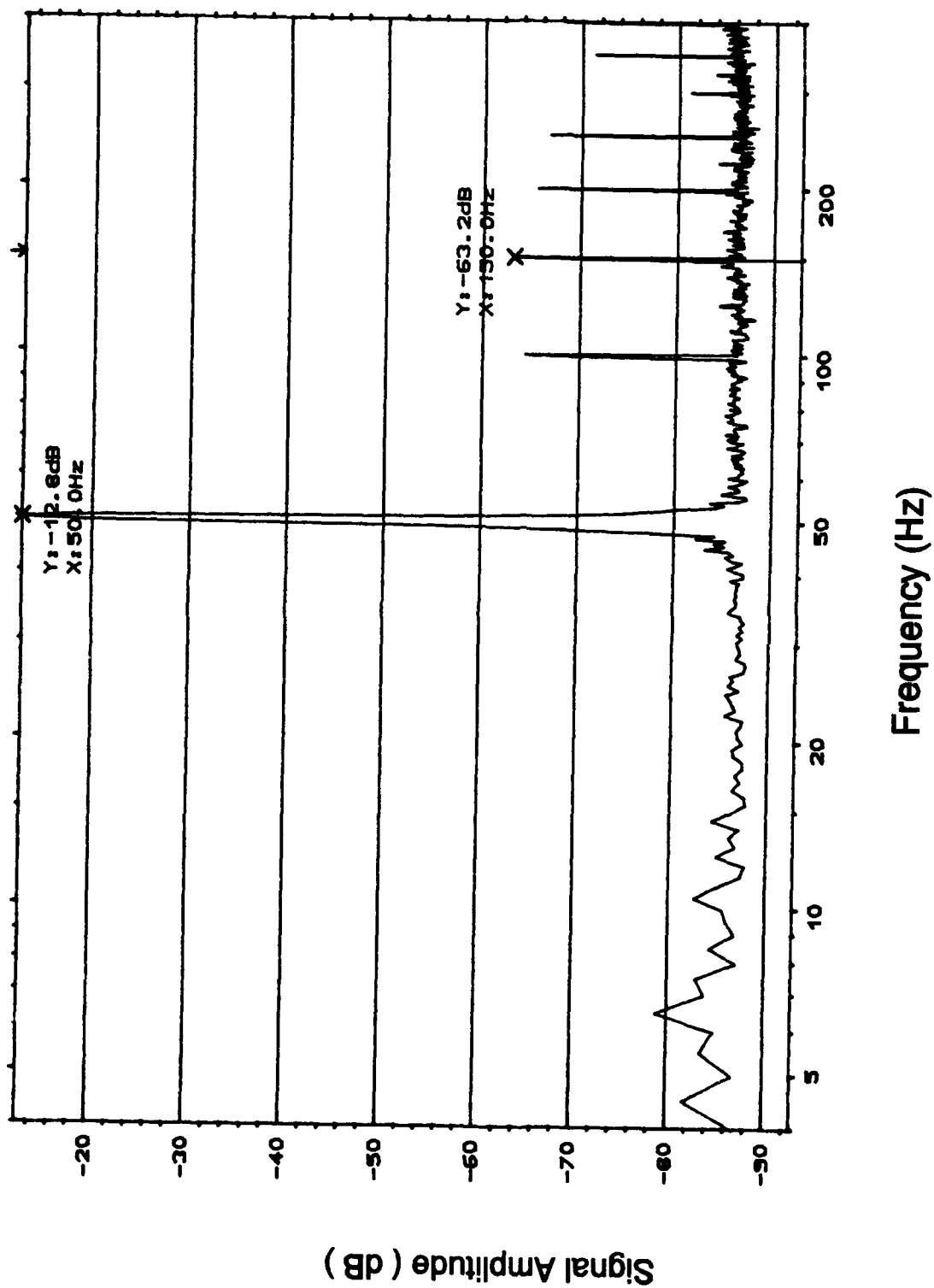
Figure I-19. Spectrum Analysis of the Oldham Hybrid Component Circuit With a 50 Hz Excitation Signal.
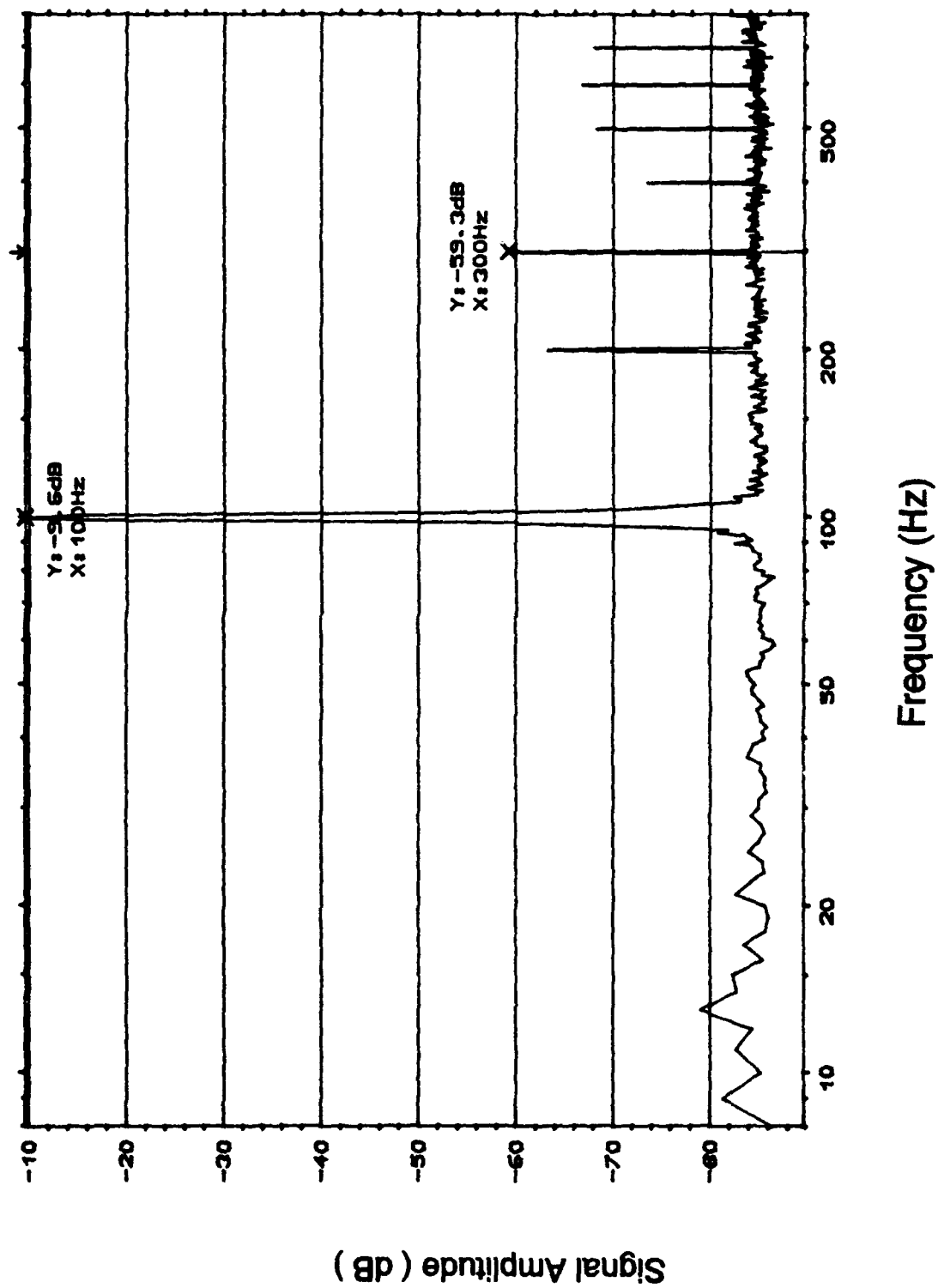
Figure I-20. Spectrum Analysis of the Oldham Hybrid Component Circuit
With a 100 Hz Excitation Signal.
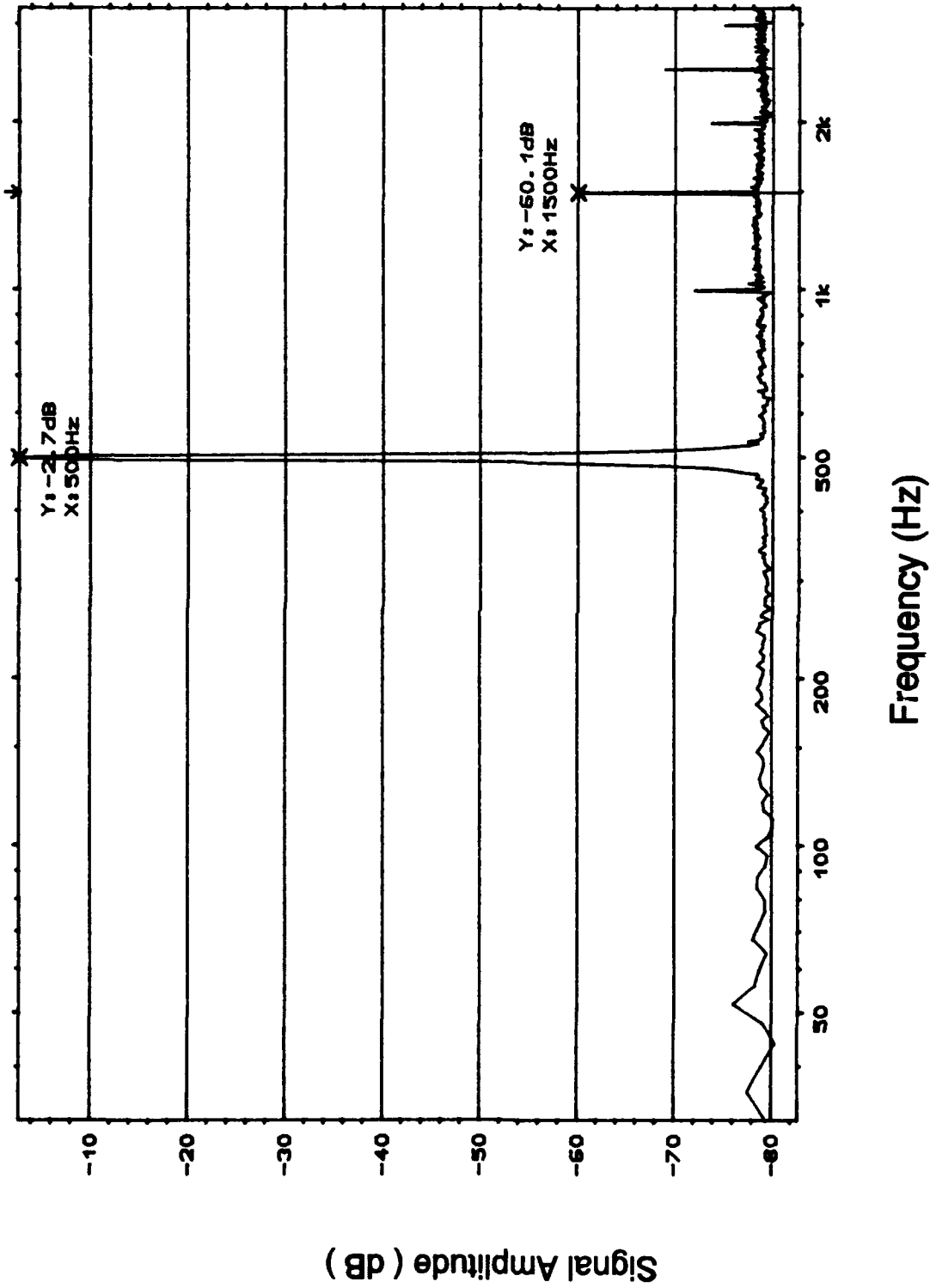
Figure I-21. Spectrum Analysis of the Oldham Hybrid Component Circuit With a 500 Hz Excitation Signal.
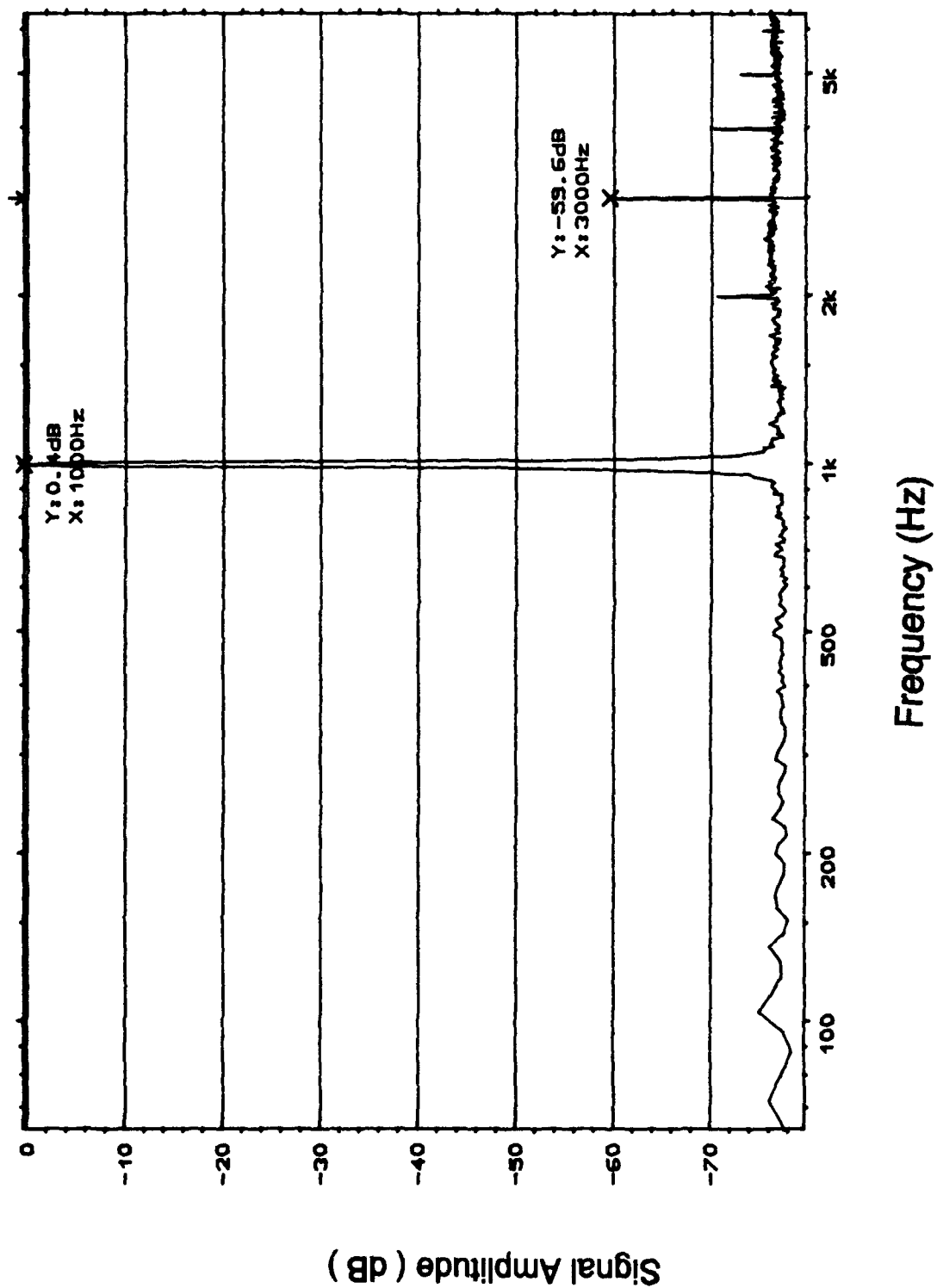
Figure I-22. Spectrum Analysis of the Oldham Hybrid Component Circuit With a 1 KHz Excitation Signal.
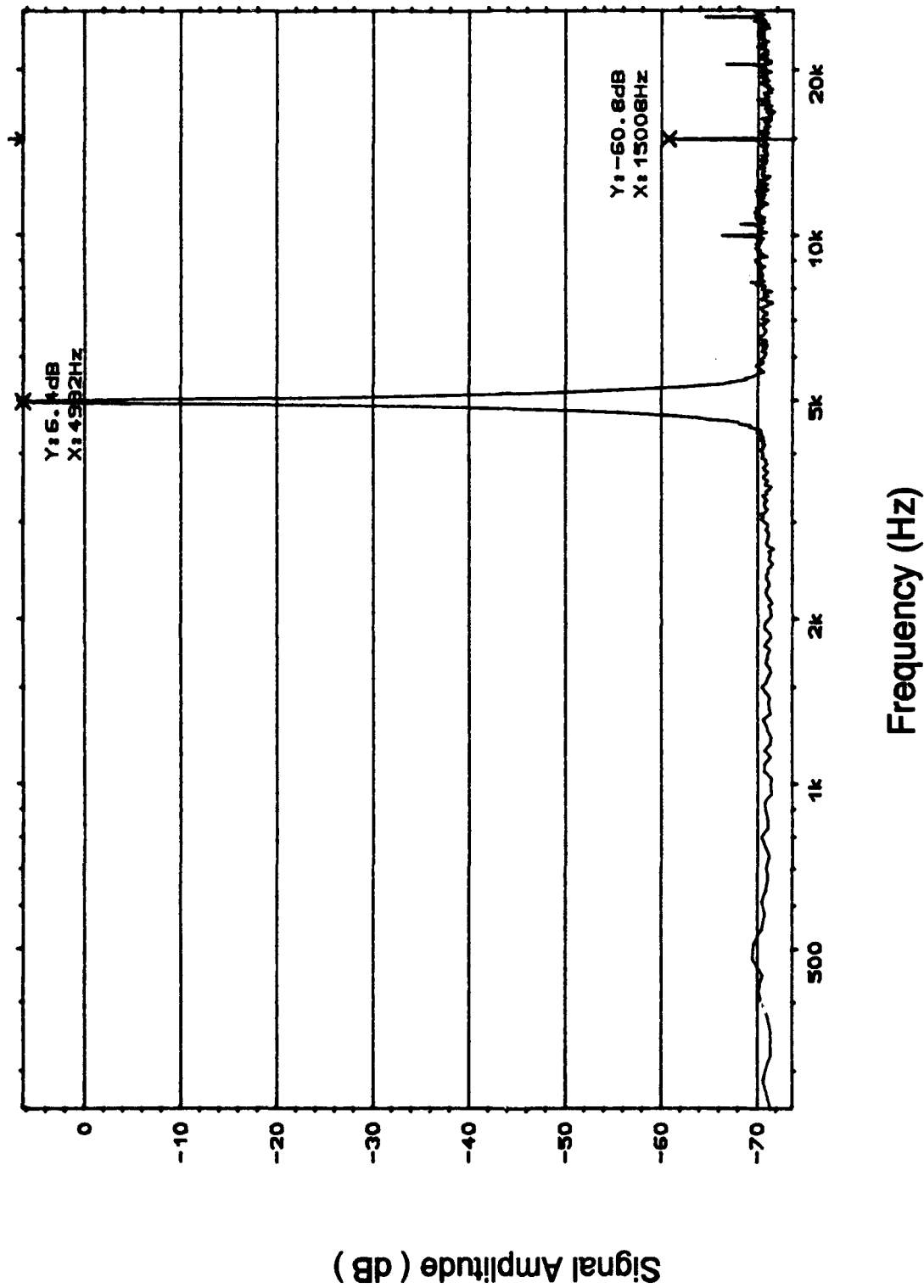
Figure I-23. Spectrum Analysis of the Oldham Hybrid Component Circuit With a 4.982 KHz Excitation Signal.

Frequency (Hz)

Signal Amplitude (dB)
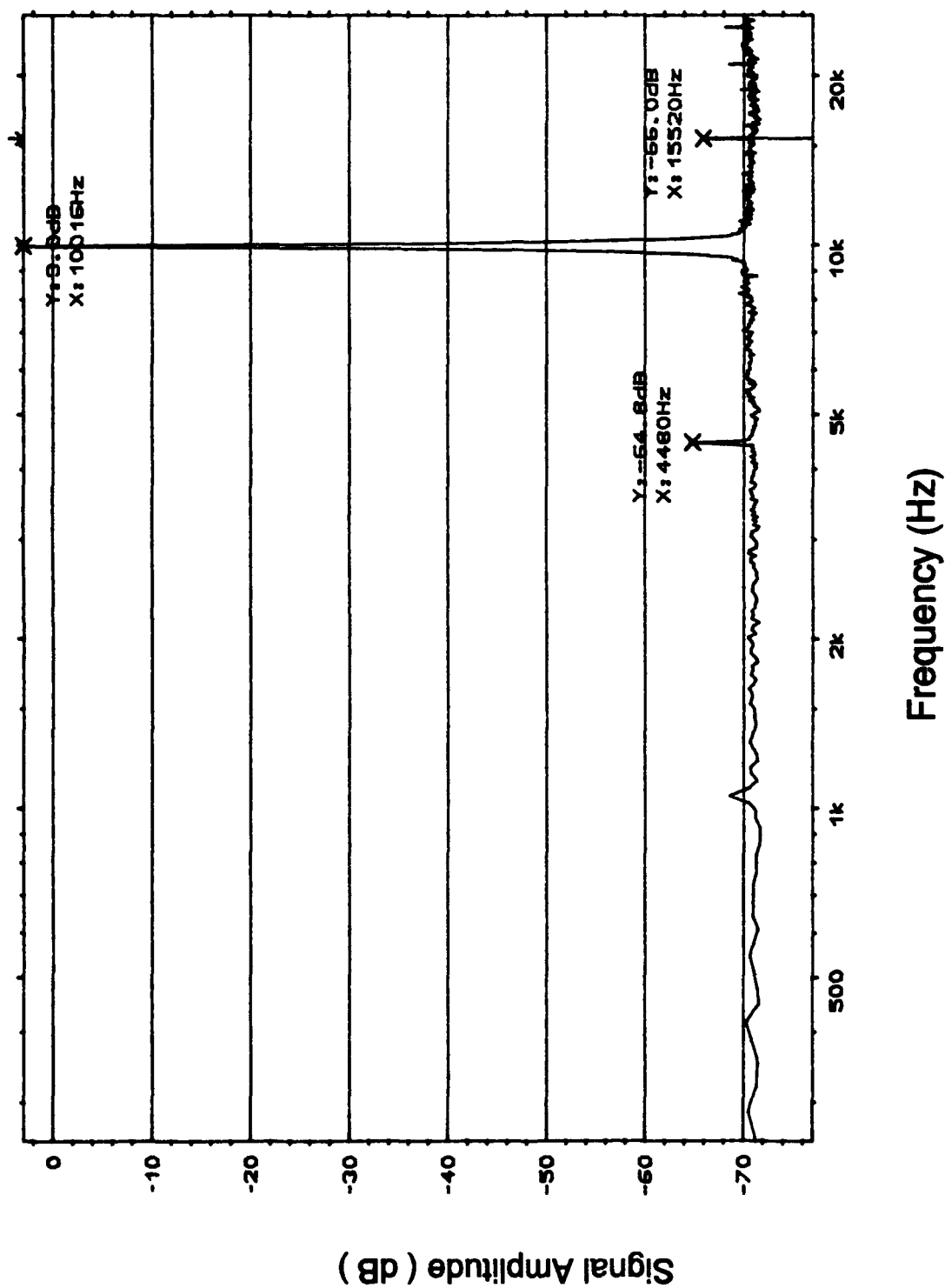
Figure I-24. Spectrum Analysis of the Oldham Hybrid Component Circuit With a 10.016 KHz Excitation Signal.

Section 3

Spectrum Plots for

the Oldfield Discrete Component Circuit
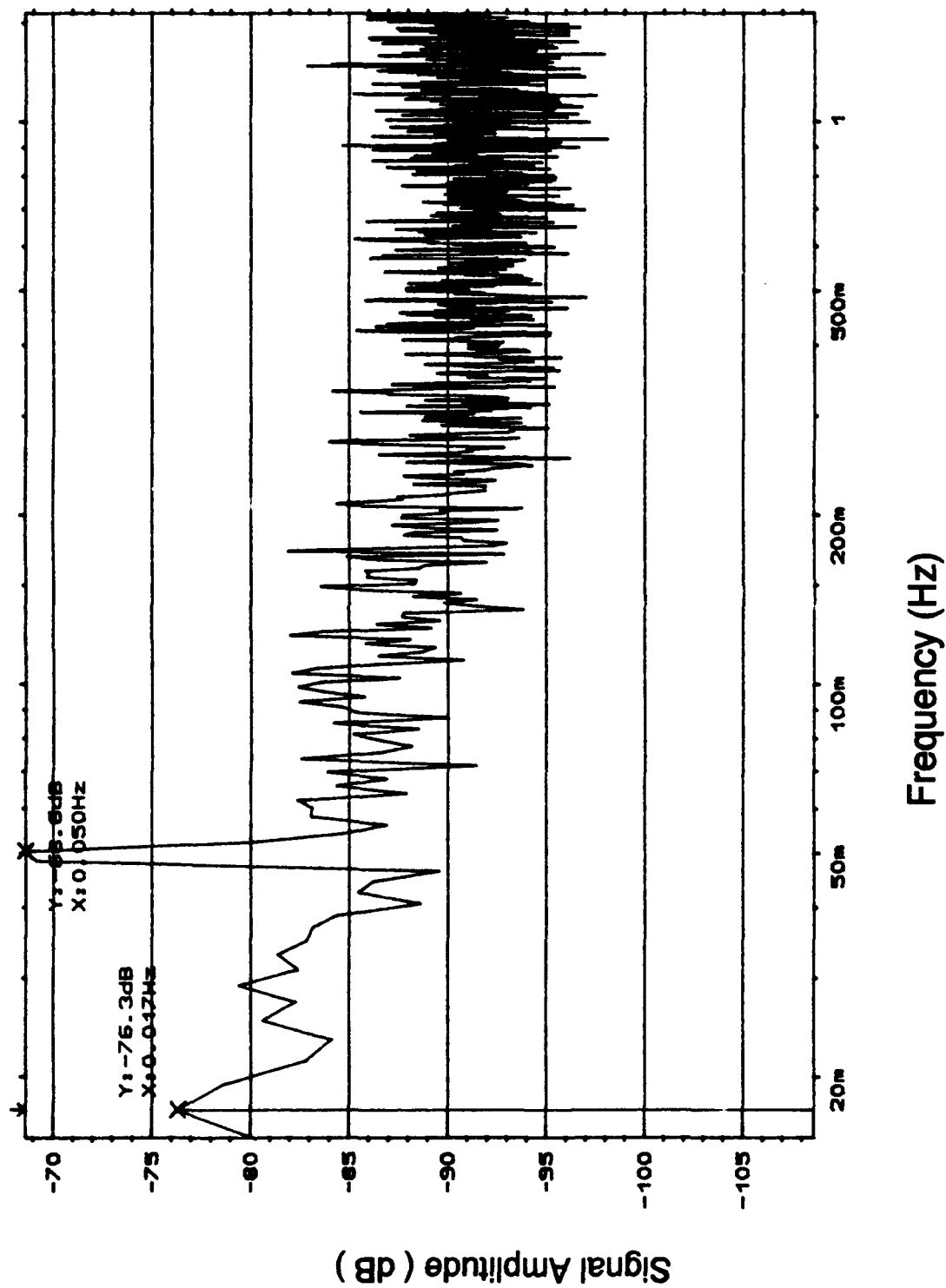
Figure I-25. Spectrum Analysis of the Oldfield Discrete Component Circuit With a 0.05 Hz Excitation Signal.
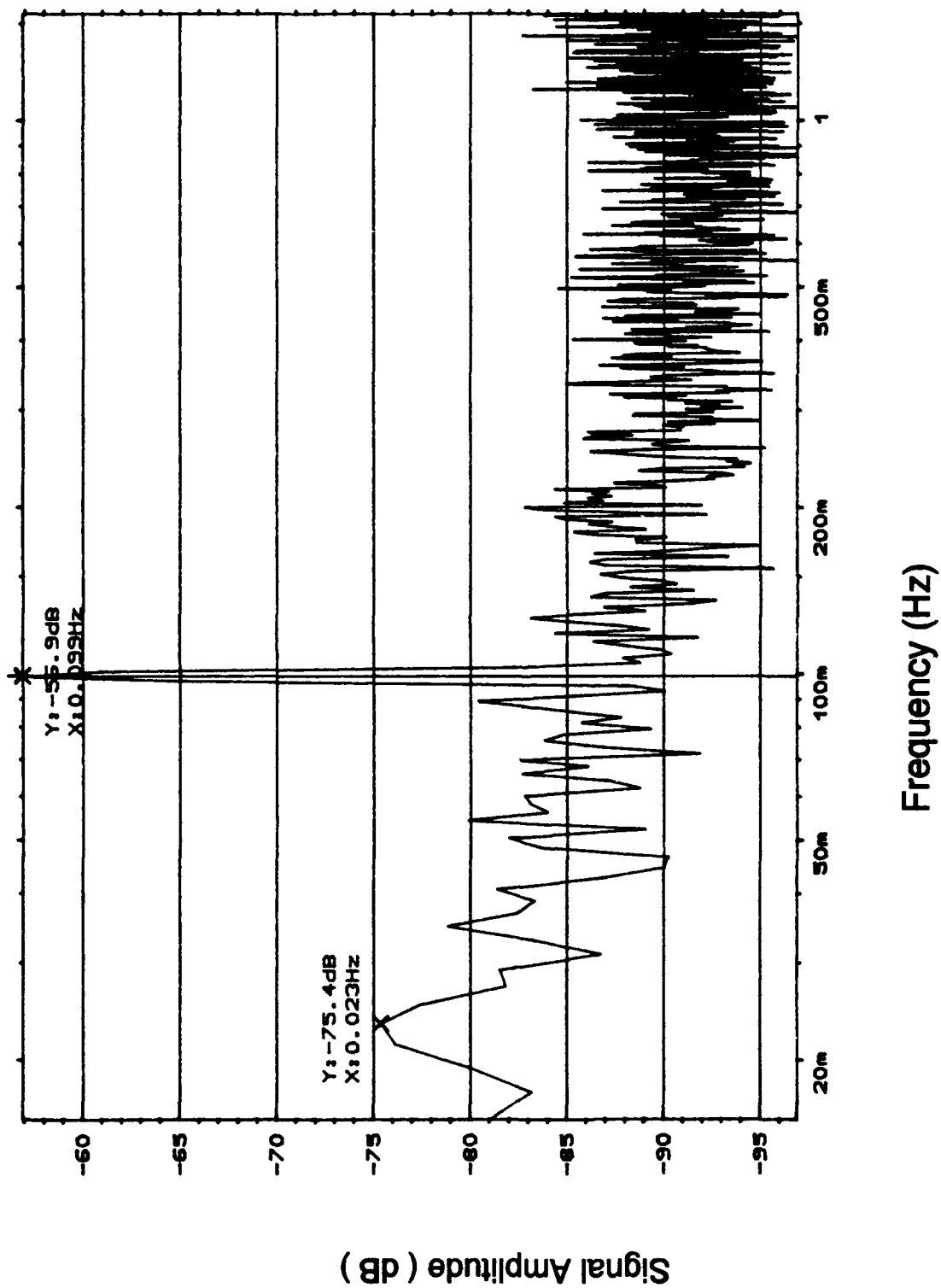
Figure I-26. Spectrum Analysis of the Oldfield Discrete Component Circuit With a 0.099 Hz Excitation Signal.

Frequency (Hz)
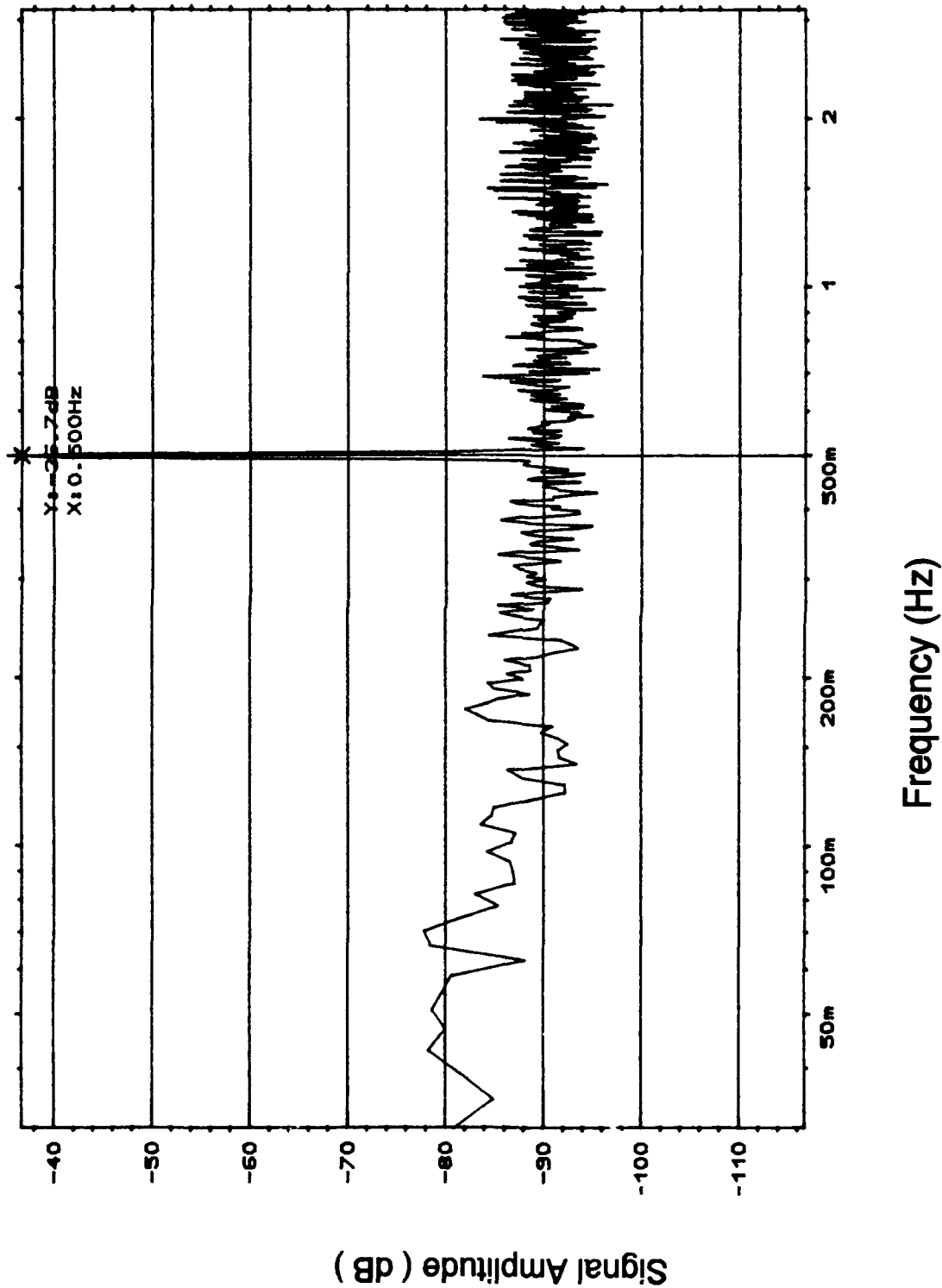
Figure I-27. Spectrum Analysis of the Oldfield Discrete Component Circuit
With a 0.5 Hz Excitation Signal.
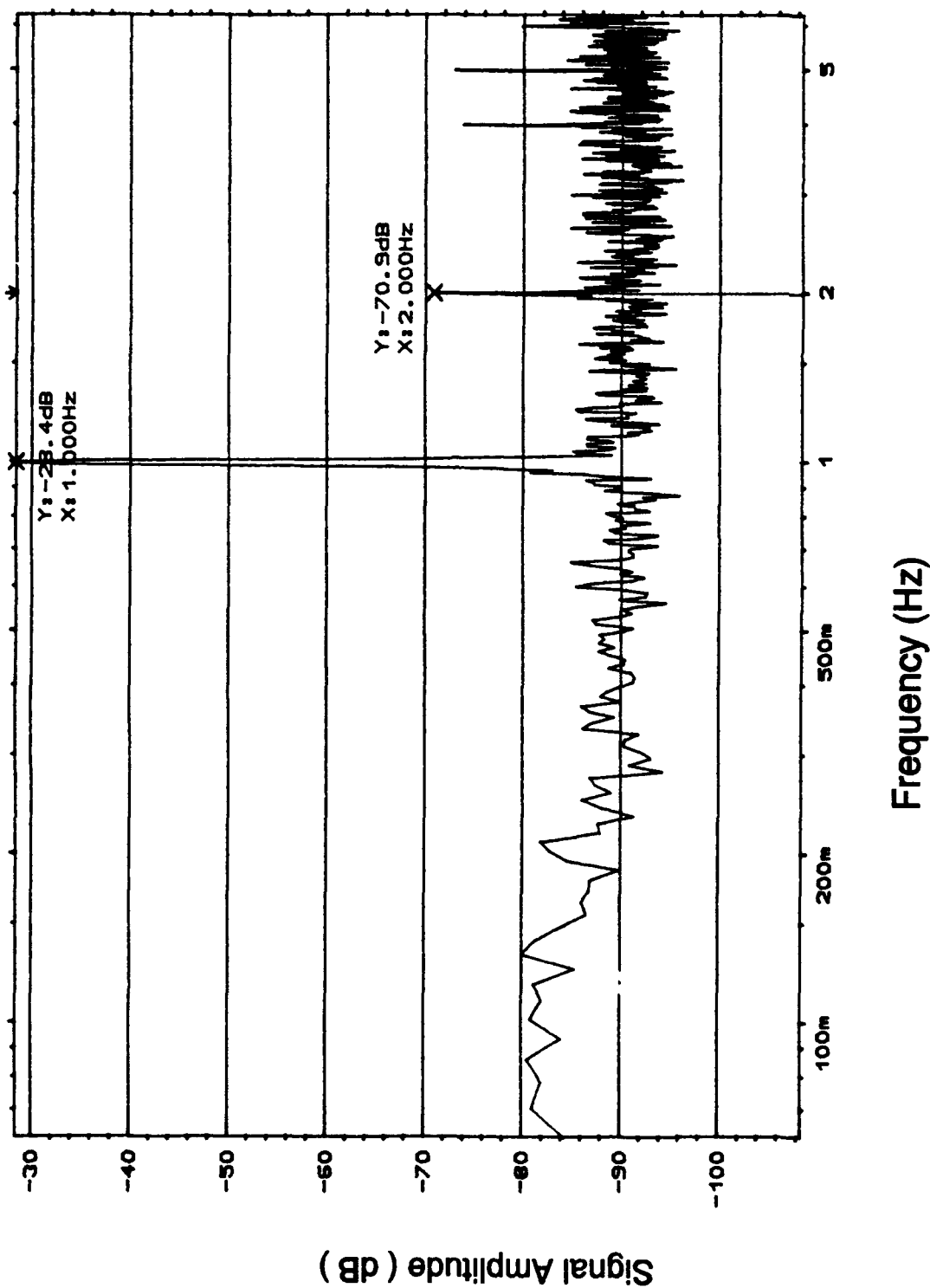
Figure I-28. Spectrum Analysis of the Oldfield Discrete Component Circuit With a 1 Hz Excitation Signal.

Frequency (Hz)
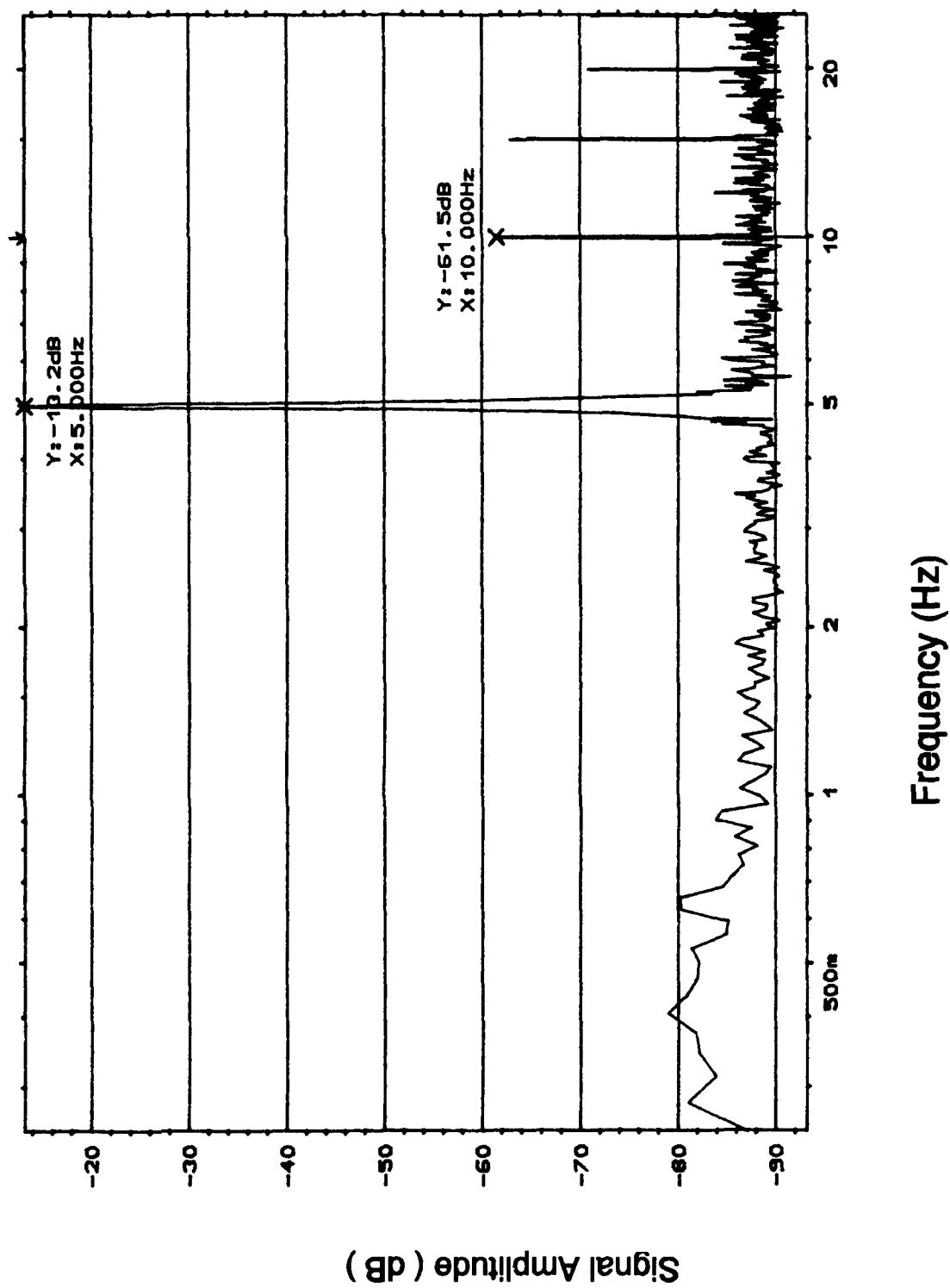
Figure I-29. Spectrum Analysis of the Oldfield Discrete Component Circuit
With a 5 Hz Excitation Signal.

Signal Amplitude (dB)
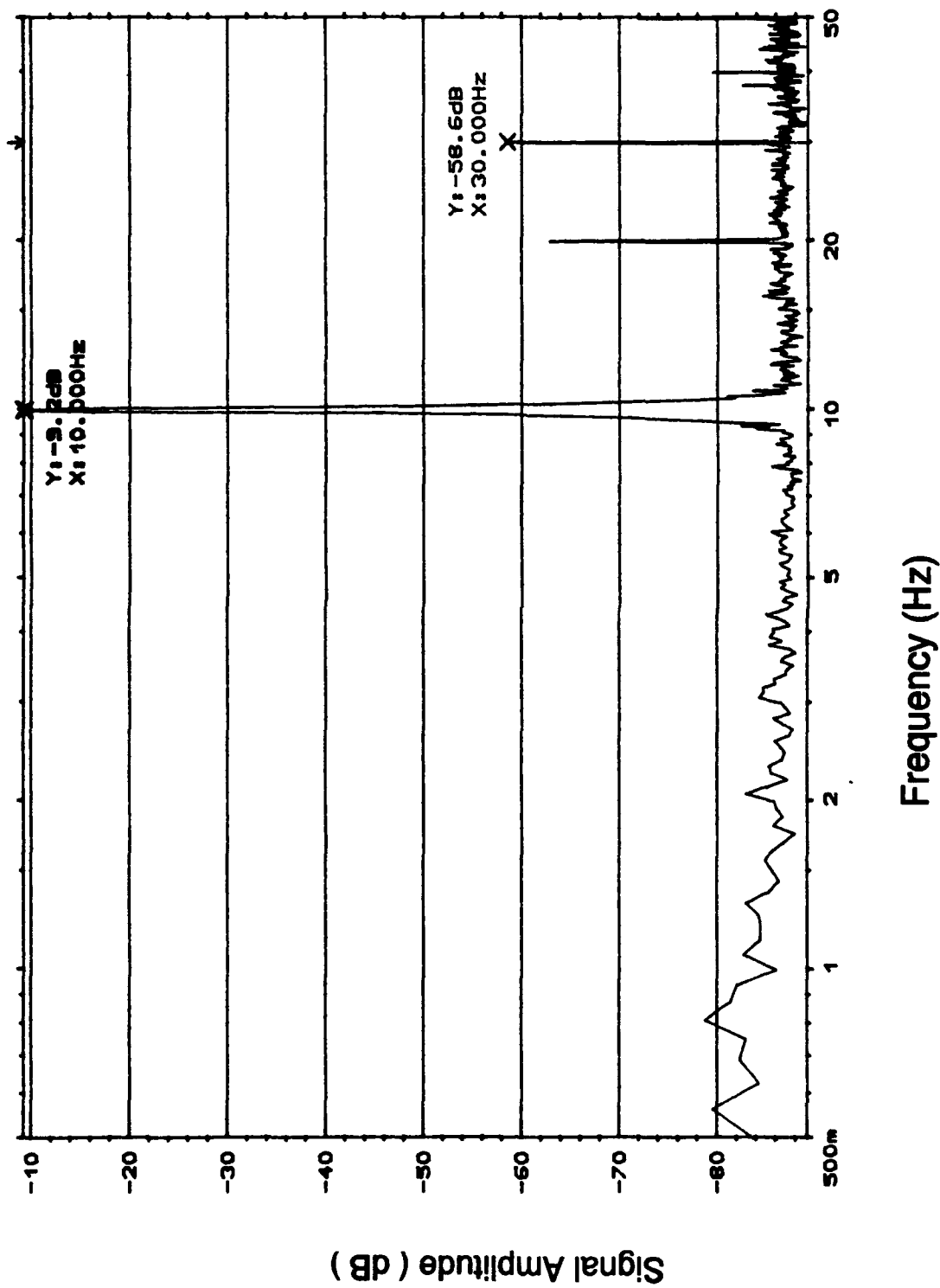
Figure I-30. Spectrum Analysis of the Oldfield Discrete Component Circuit With a 10 Hz Excitation Signal.

Frequency (Hz)
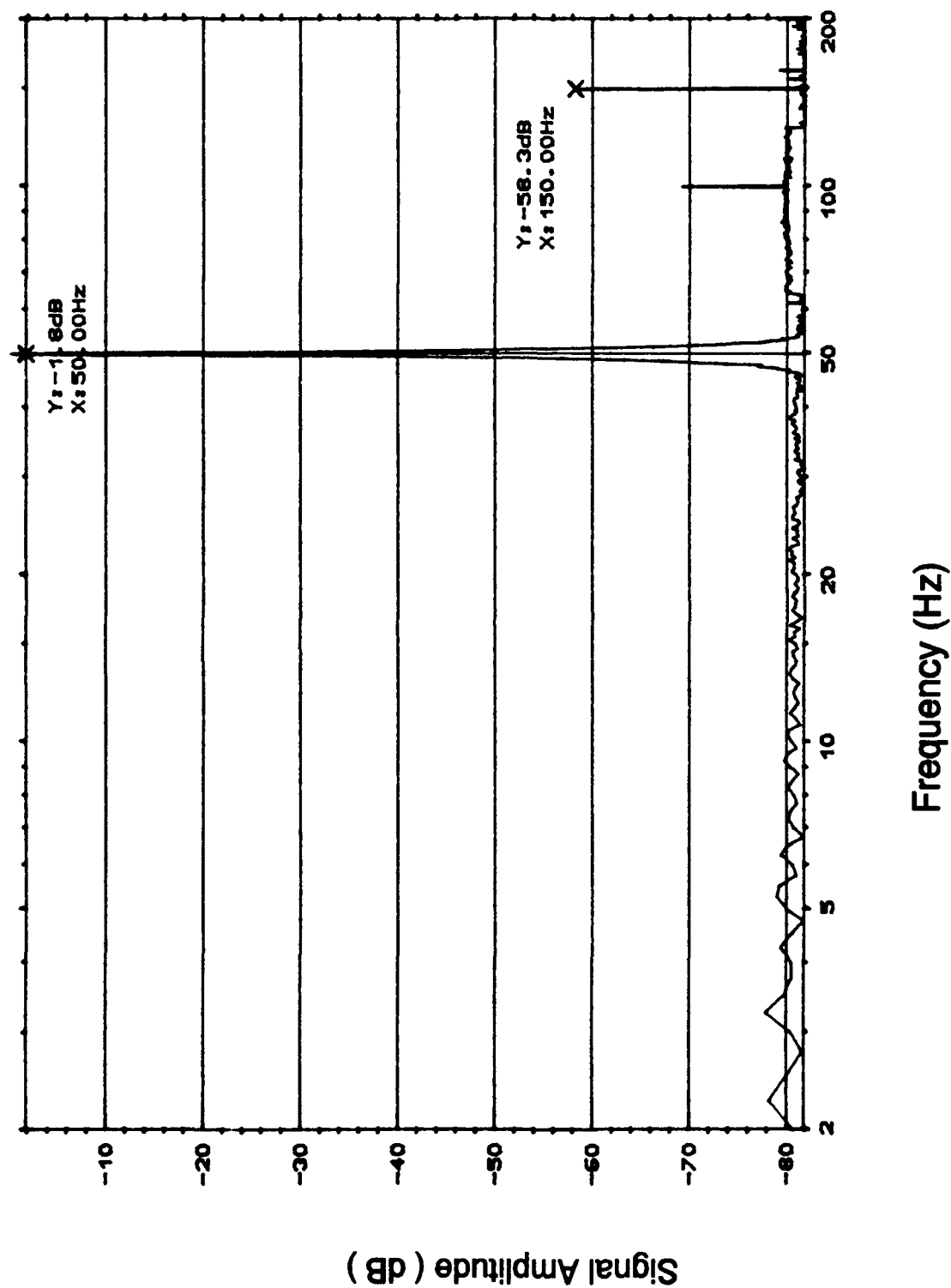
Figure I-31. Spectrum Analysis of the Oldfield Discrete Component Circuit With a 50 Hz Excitation Signal.

Signal Amplitude (dB)

I-36
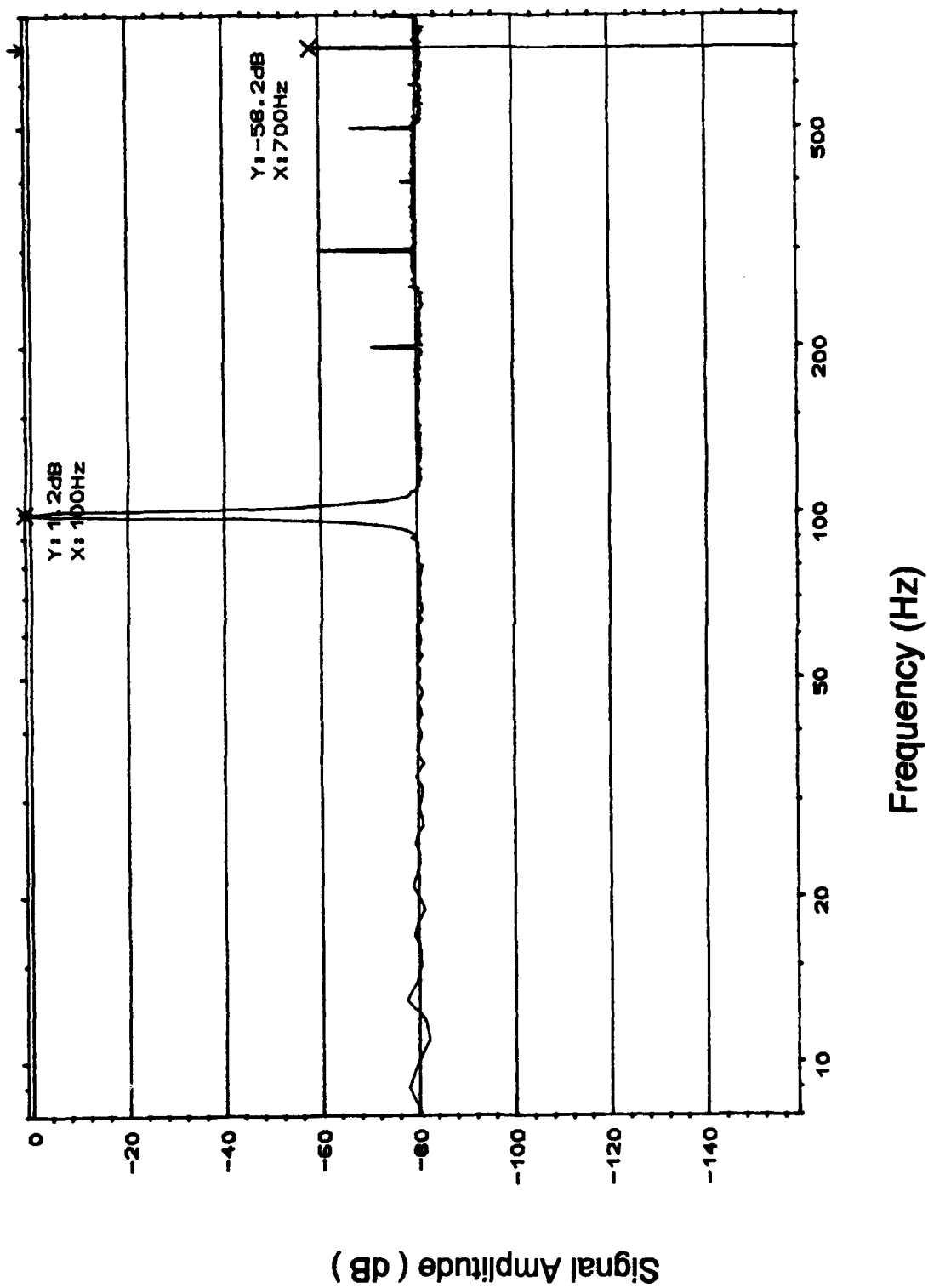
Figure I-32. Spectrum Analysis of the Oldfield Discrete Component Circuit With a 100 Hz Excitation Signal.
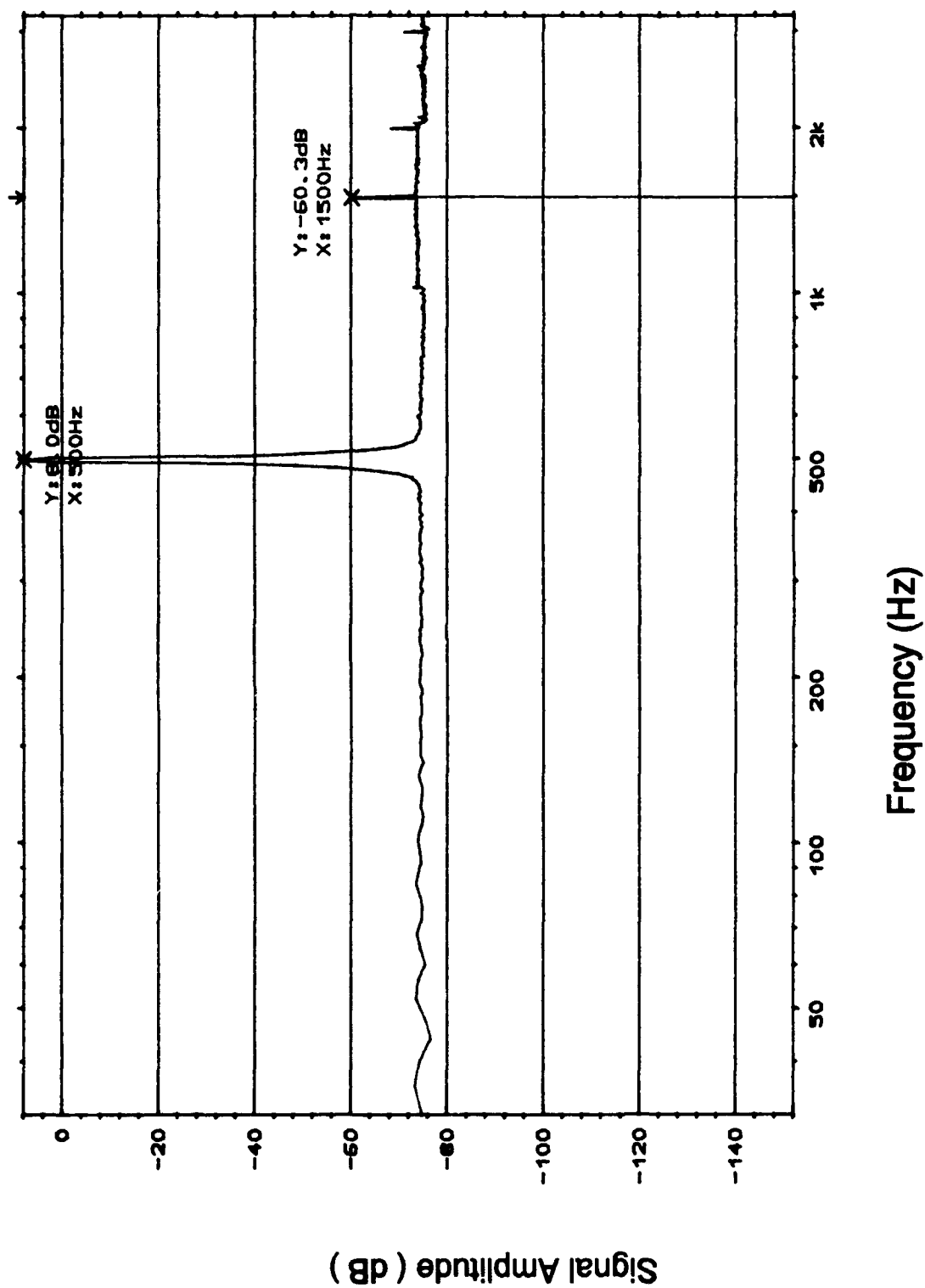
Figure I-33. Spectrum Analysis of the Oldfield Discrete Component Circuit With a 500 Hz Excitation Signal.

Frequency (Hz)

Signal Amplitude (dB)
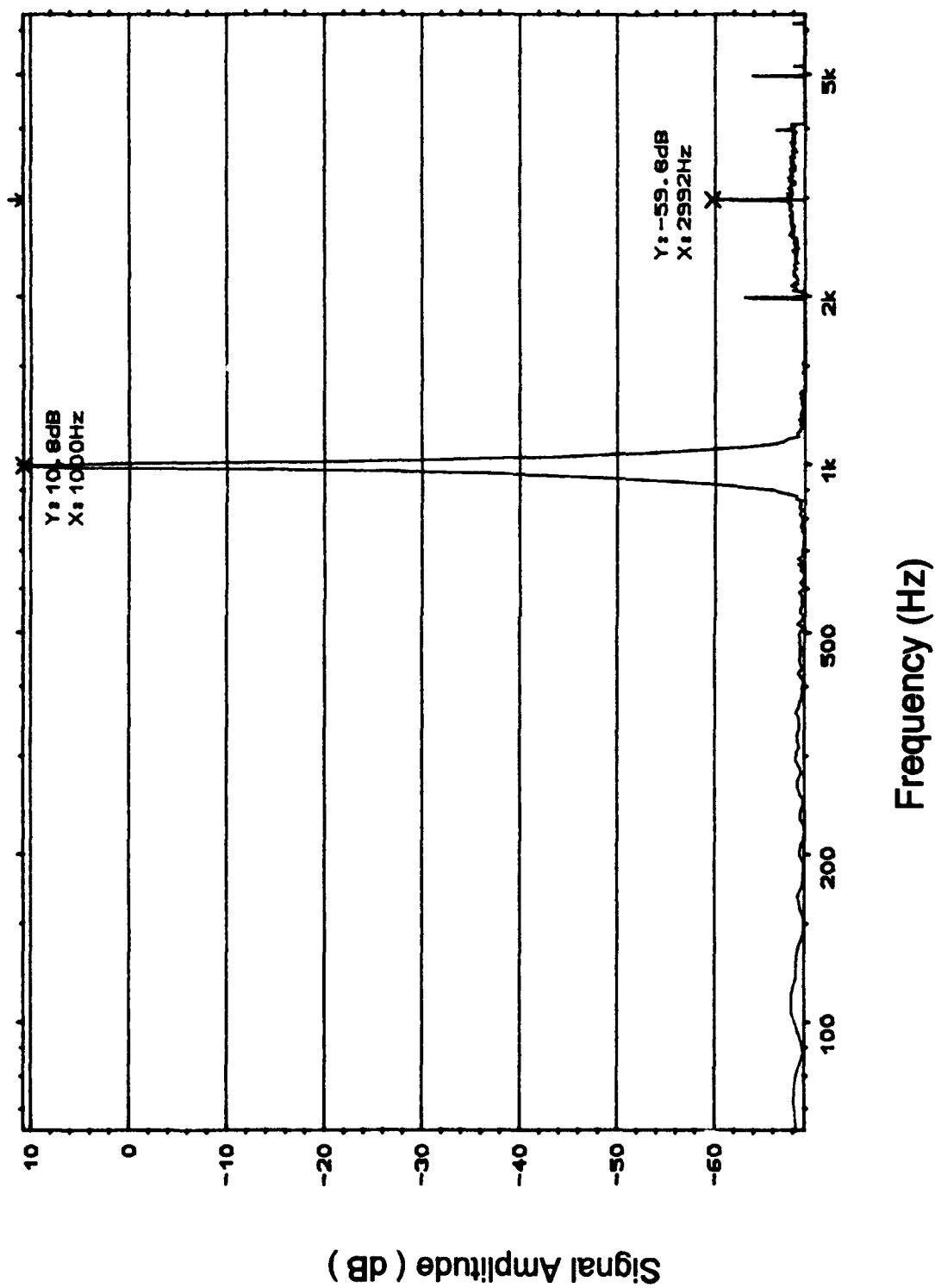
Figure I-34. Spectrum Analysis of the Oldfield Discrete Component Circuit With a 1 KHz Excitation Signal.

Frequency (Hz)
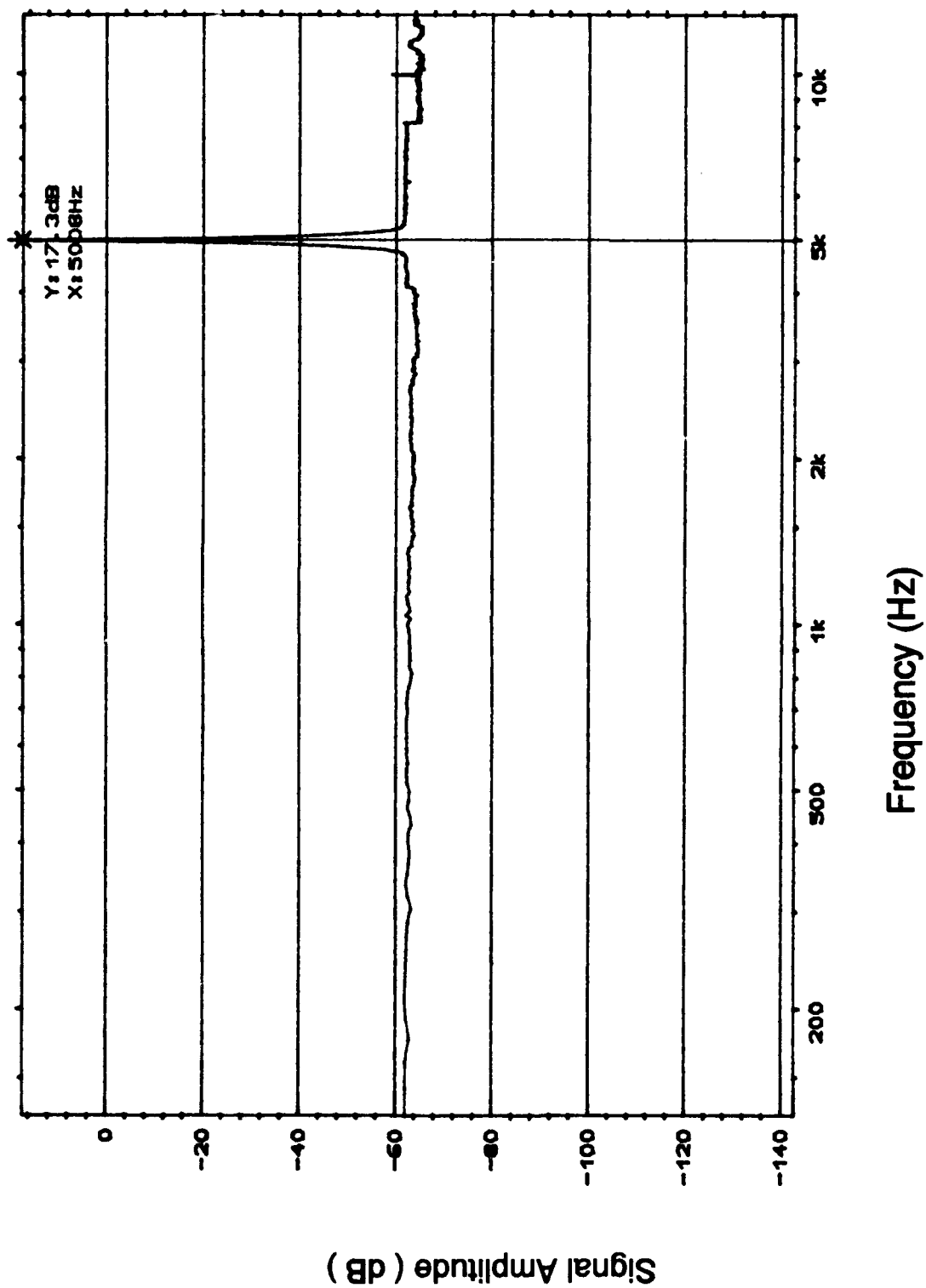
Figure I-35. Spectrum Analysis of the Oldfield Discrete Component Circuit
With a 5.008 KHz Excitation Signal.
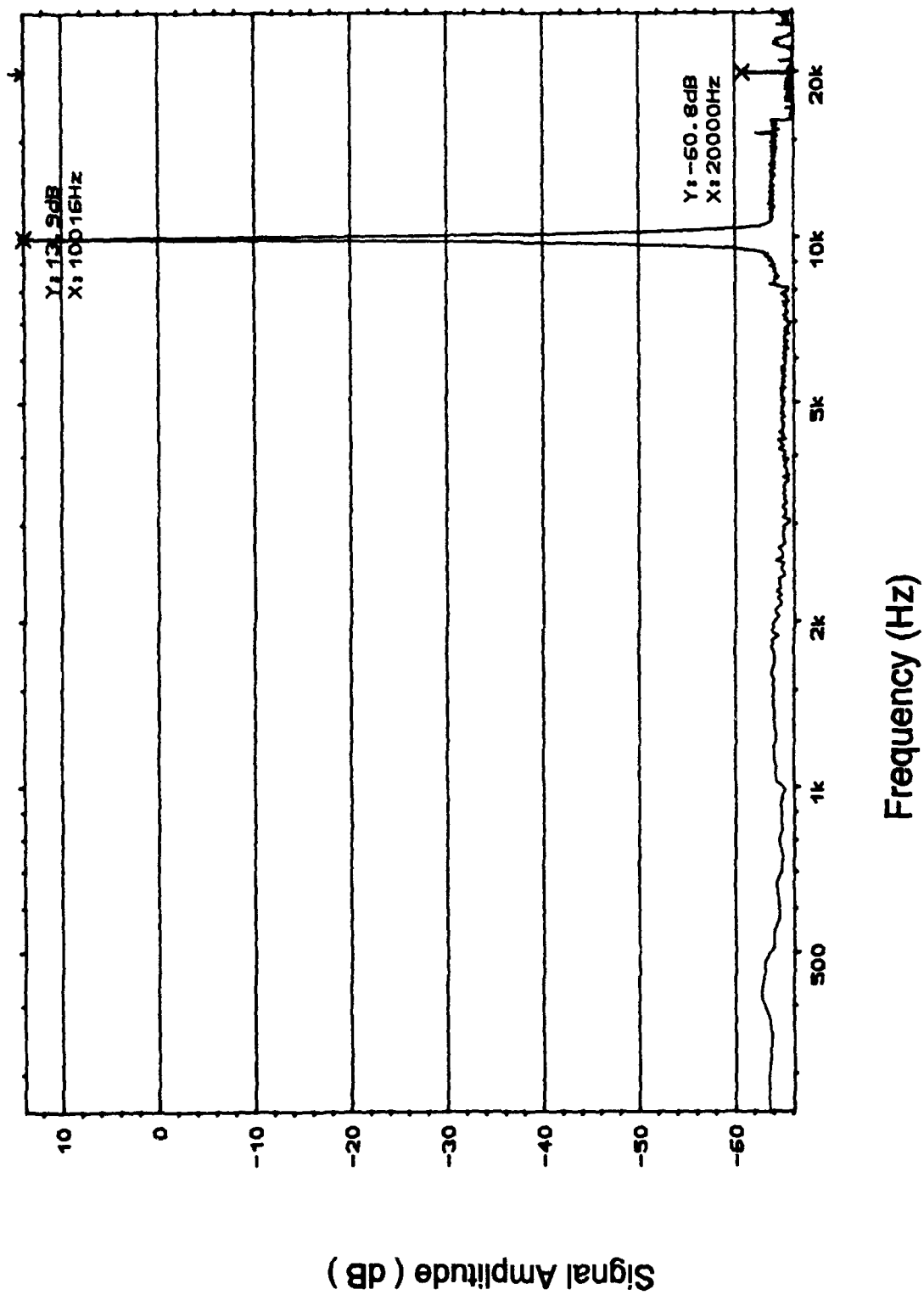
Figure I-36. Spectrum Analysis of the Oldfield Discrete Component Circuit With a 10.016 KHz Excitation Signal.

Section 4

Spectrum Plots for

the Oldfield Surface Mount Component Circuit
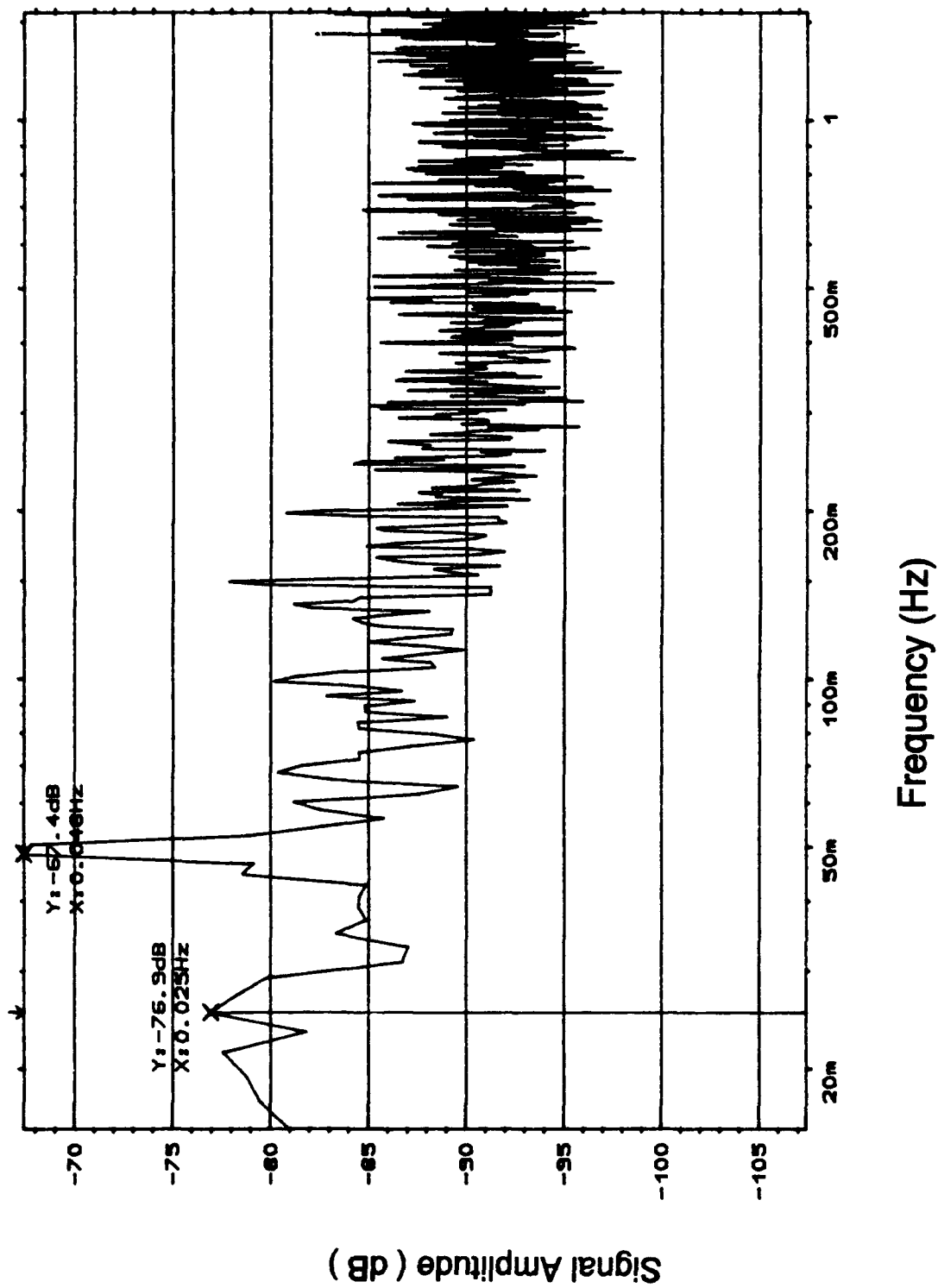
Figure I-37. Spectrum Analysis of the Oldfield Surface Mount Component Circui With a 0.048 Hz Excitation Signal.
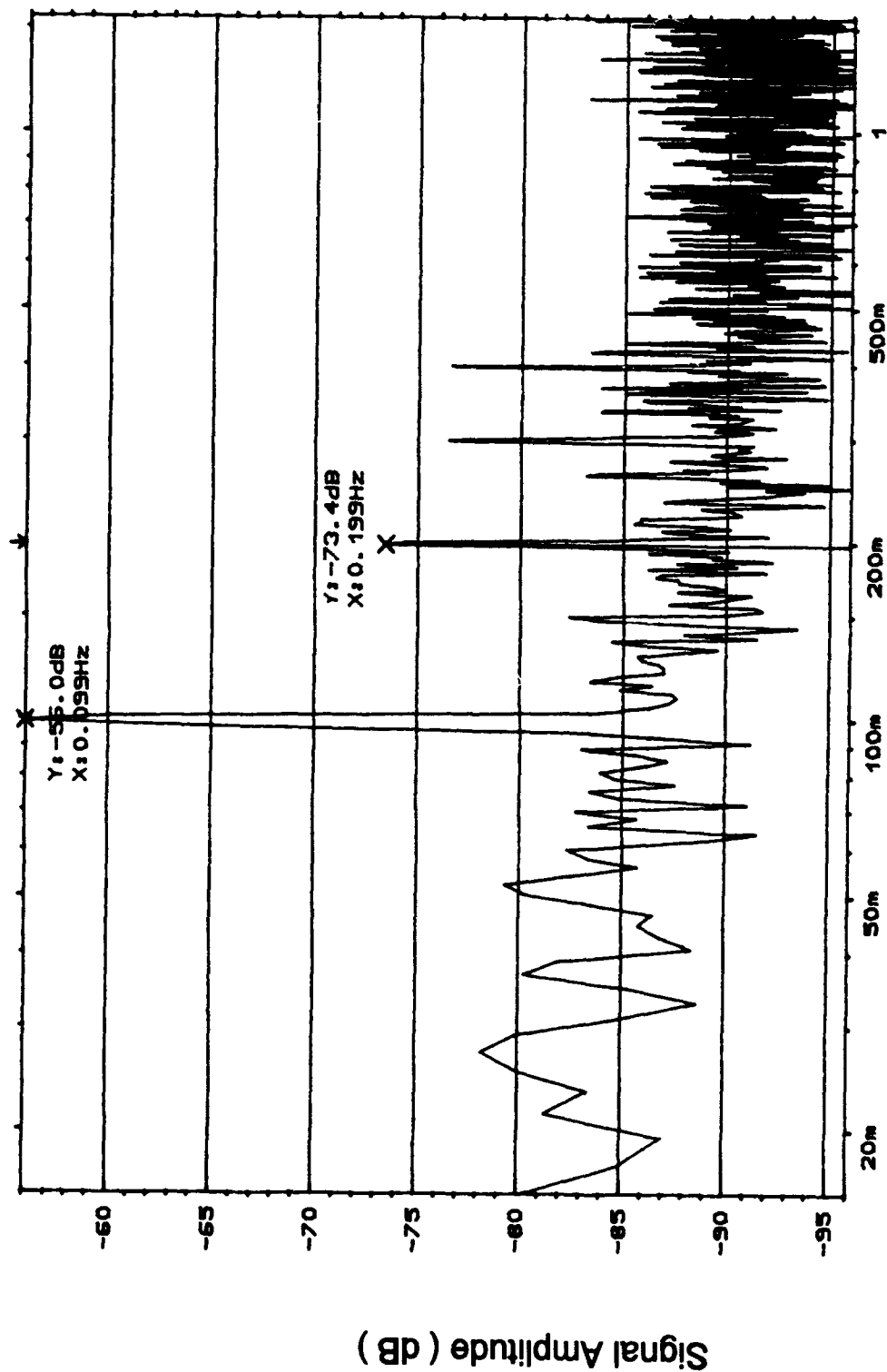
Figure I-38. Spectrum Analysis of the Oldfield Surface Mount Component Circui
With a 0.099 Hz Excitation Signal.
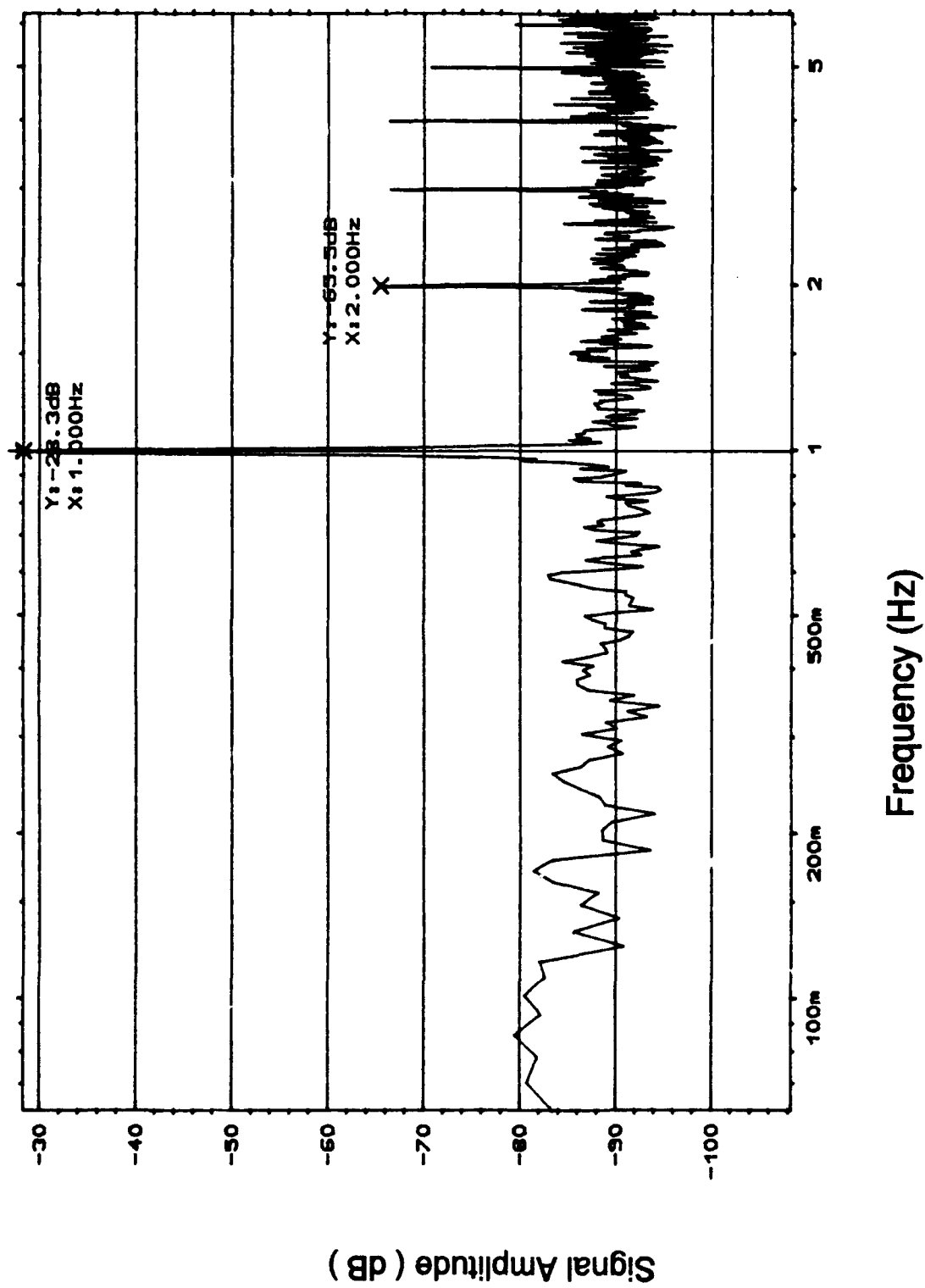
Figure I-40. Spectrum Analysis of the Oldfield Surface Mount Component Circui
With a 1 Hz Excitation Signal.
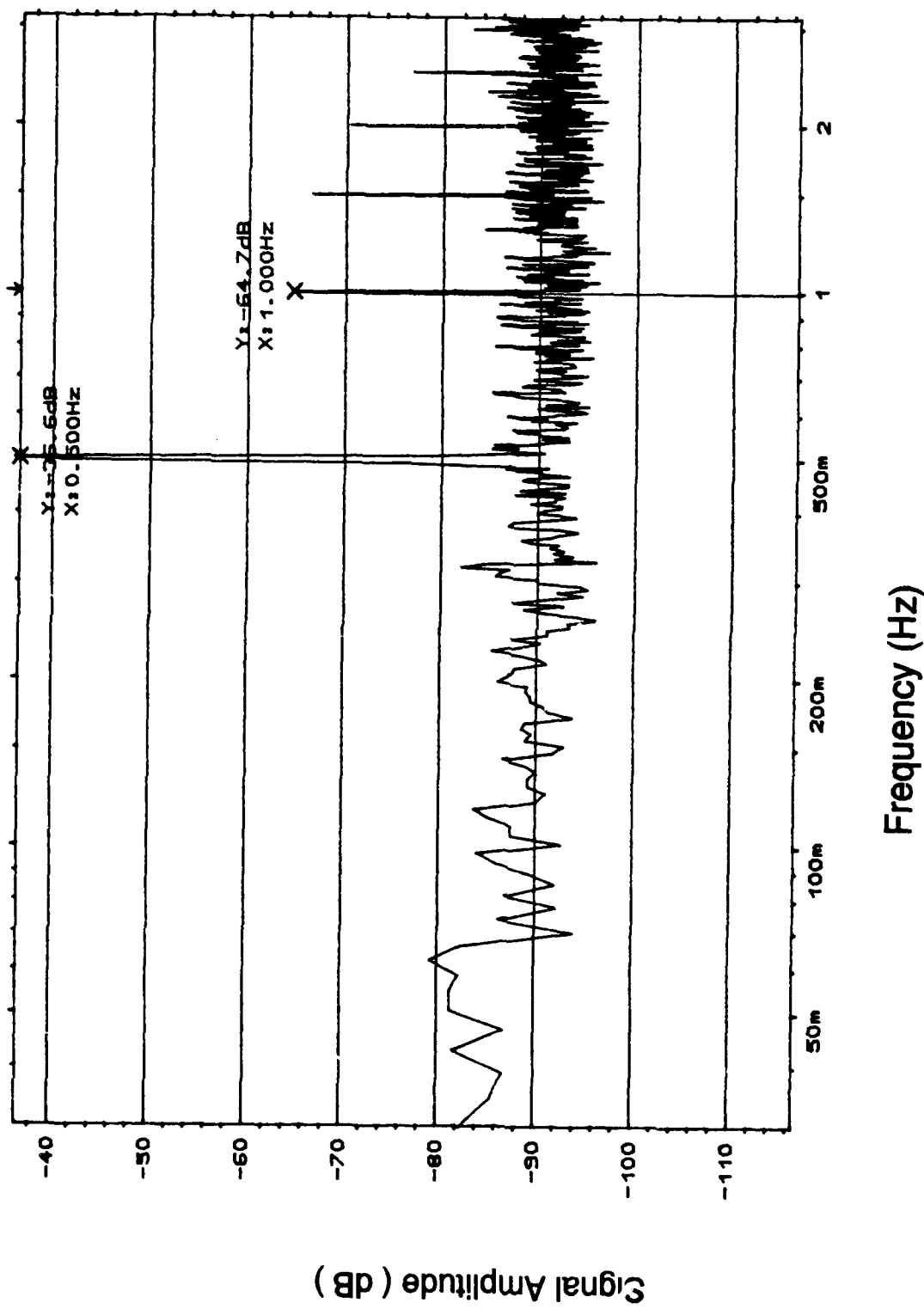
Figure I-39. Spectrum Analysis of the Oldfield Surface Mount Component Circui With a 0.5 Hz Excitation Signal.
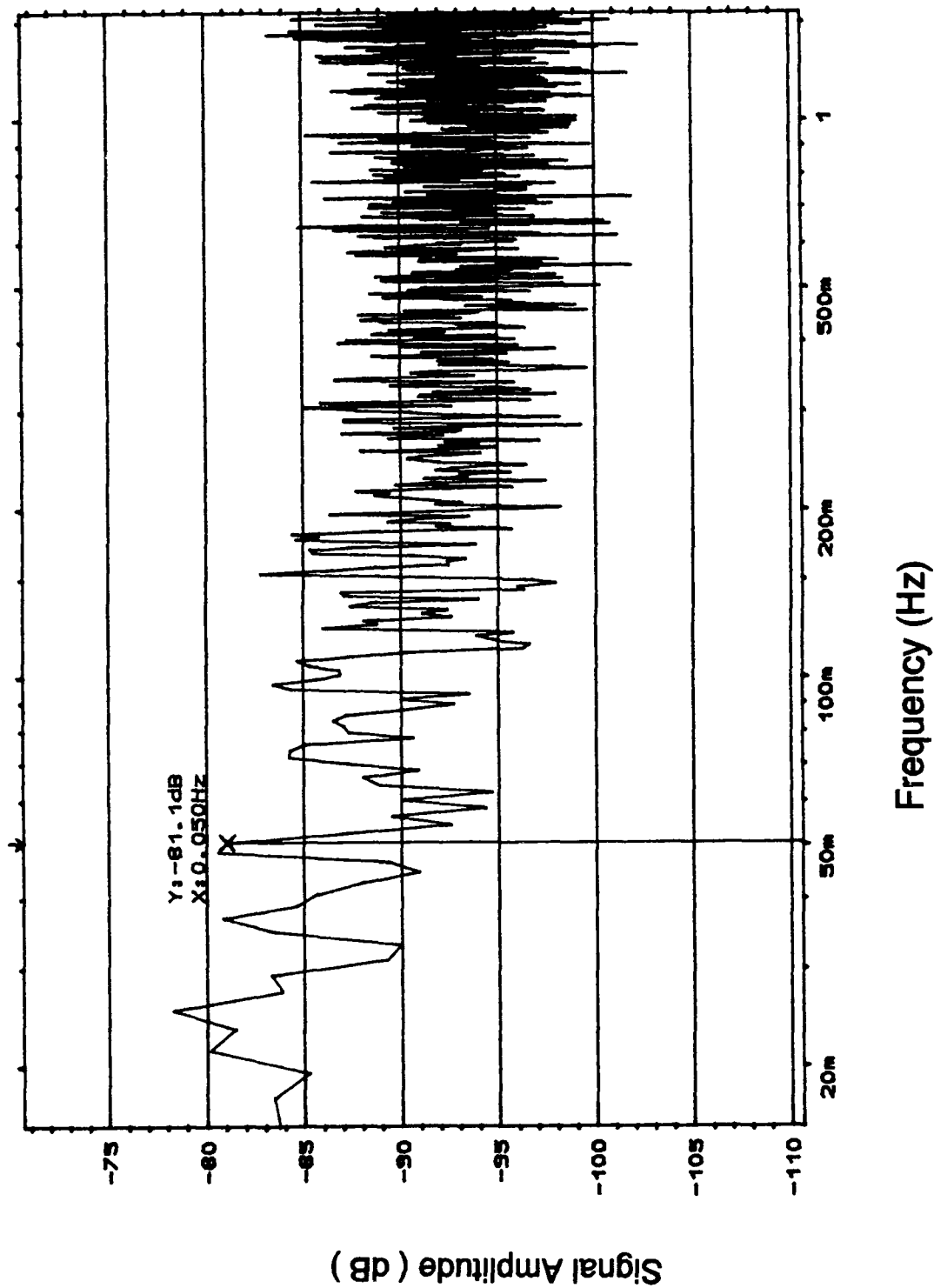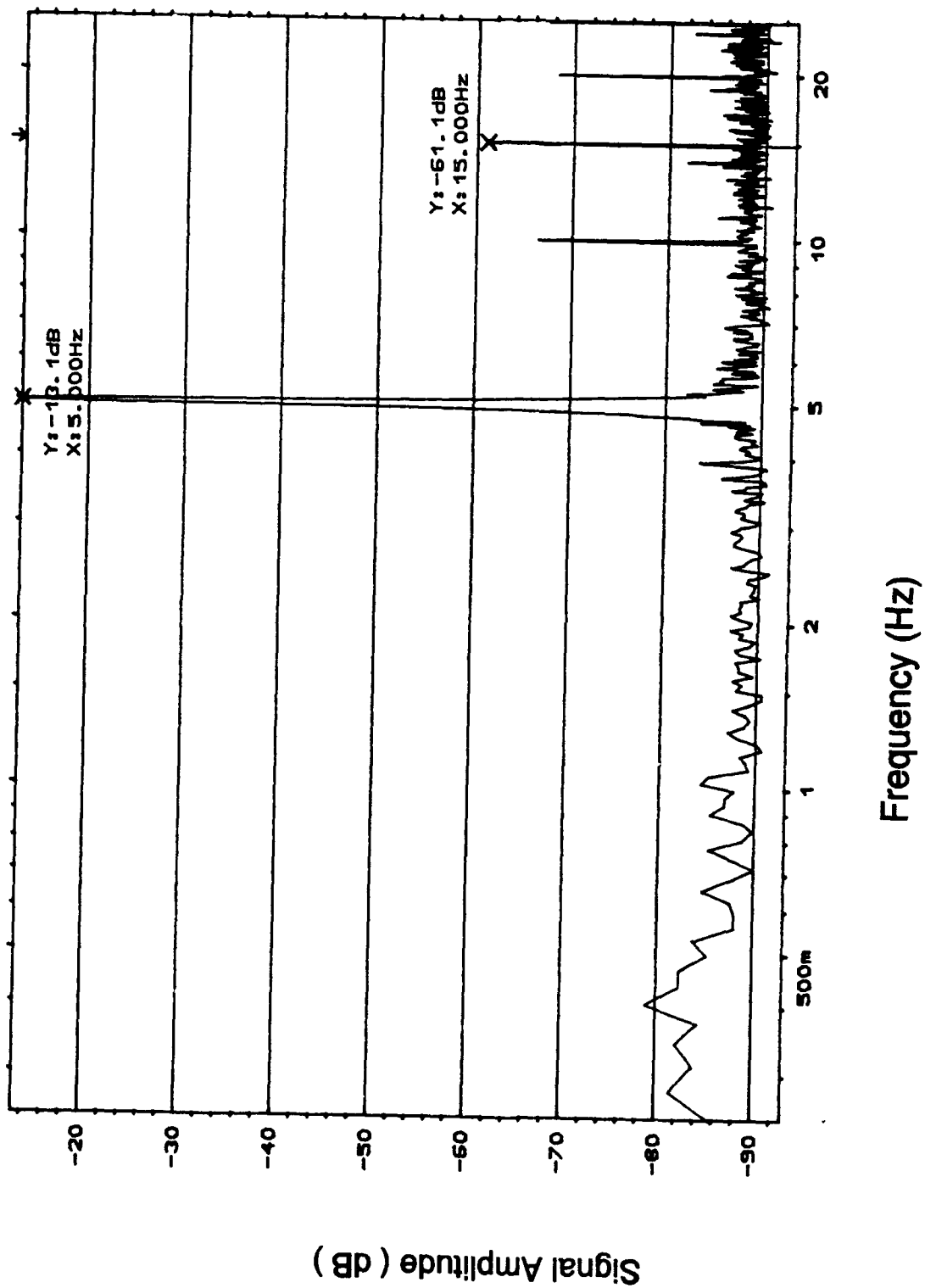
Figure I-41. Spectrum Analysis of the Oldfield Surface Mount Component Circui
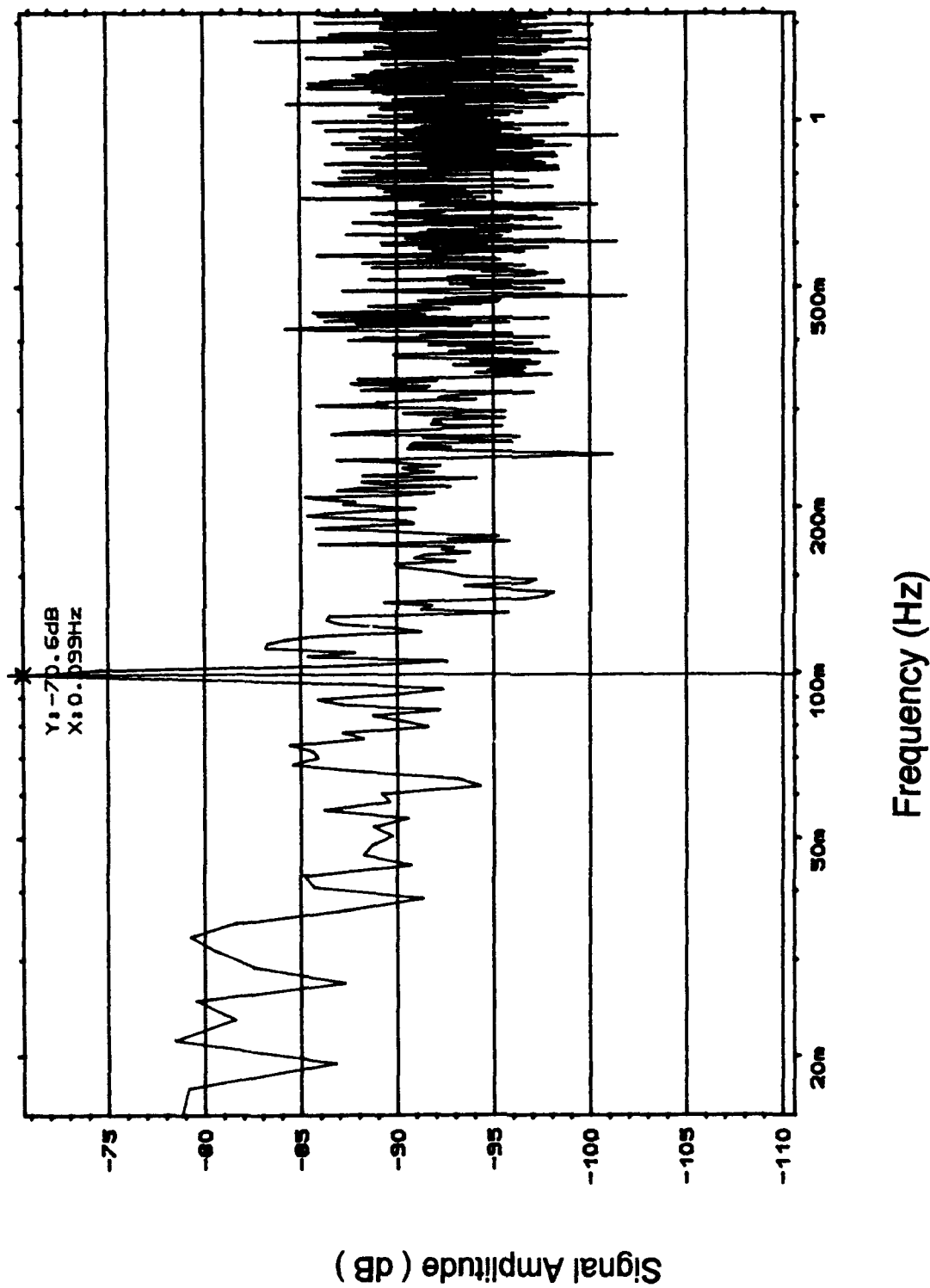With a 5 Hz Excitation Signal.
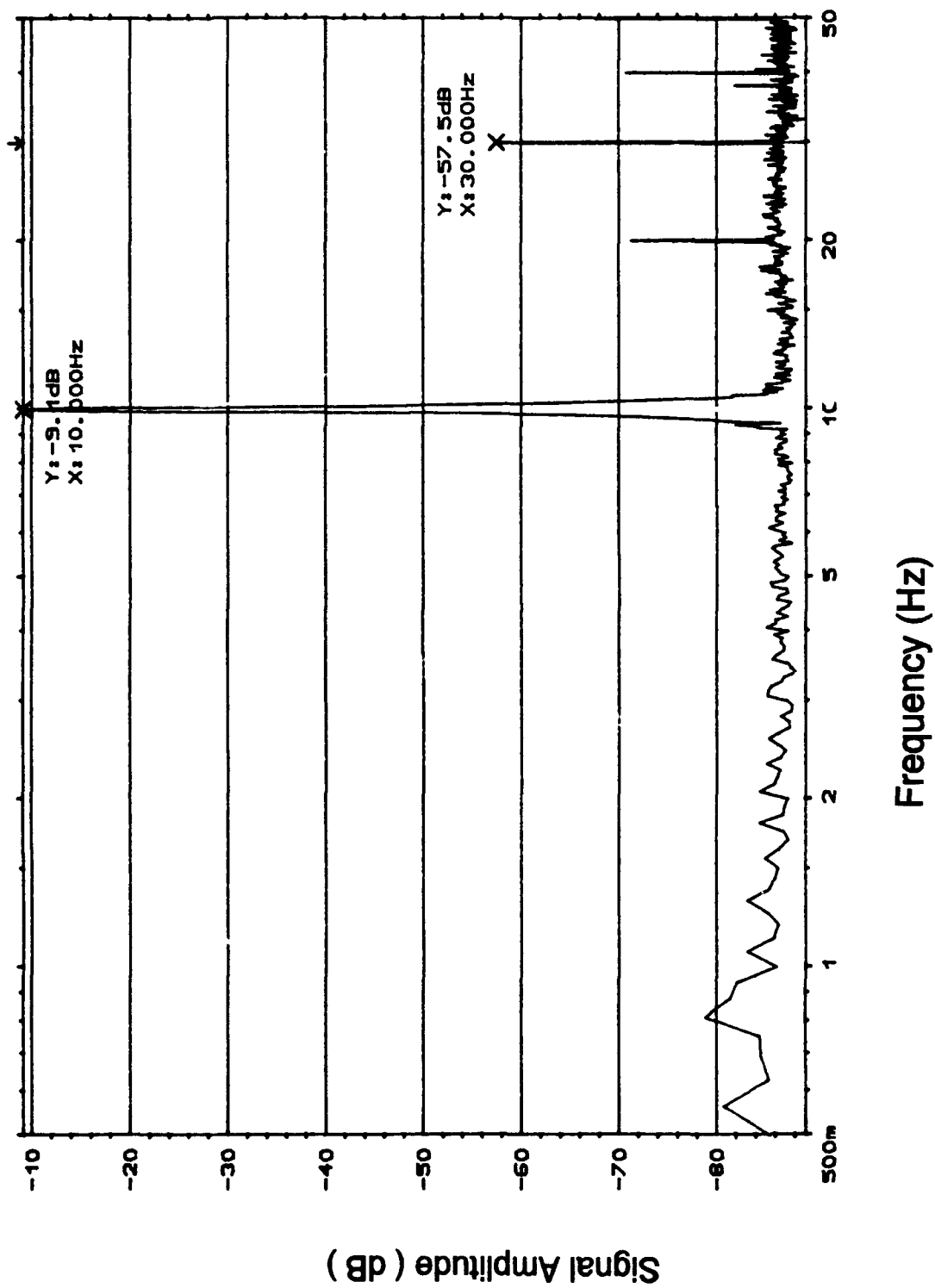
Figure I-42. Spectrum Analysis of the Oldfield Surface Mount Component Circui
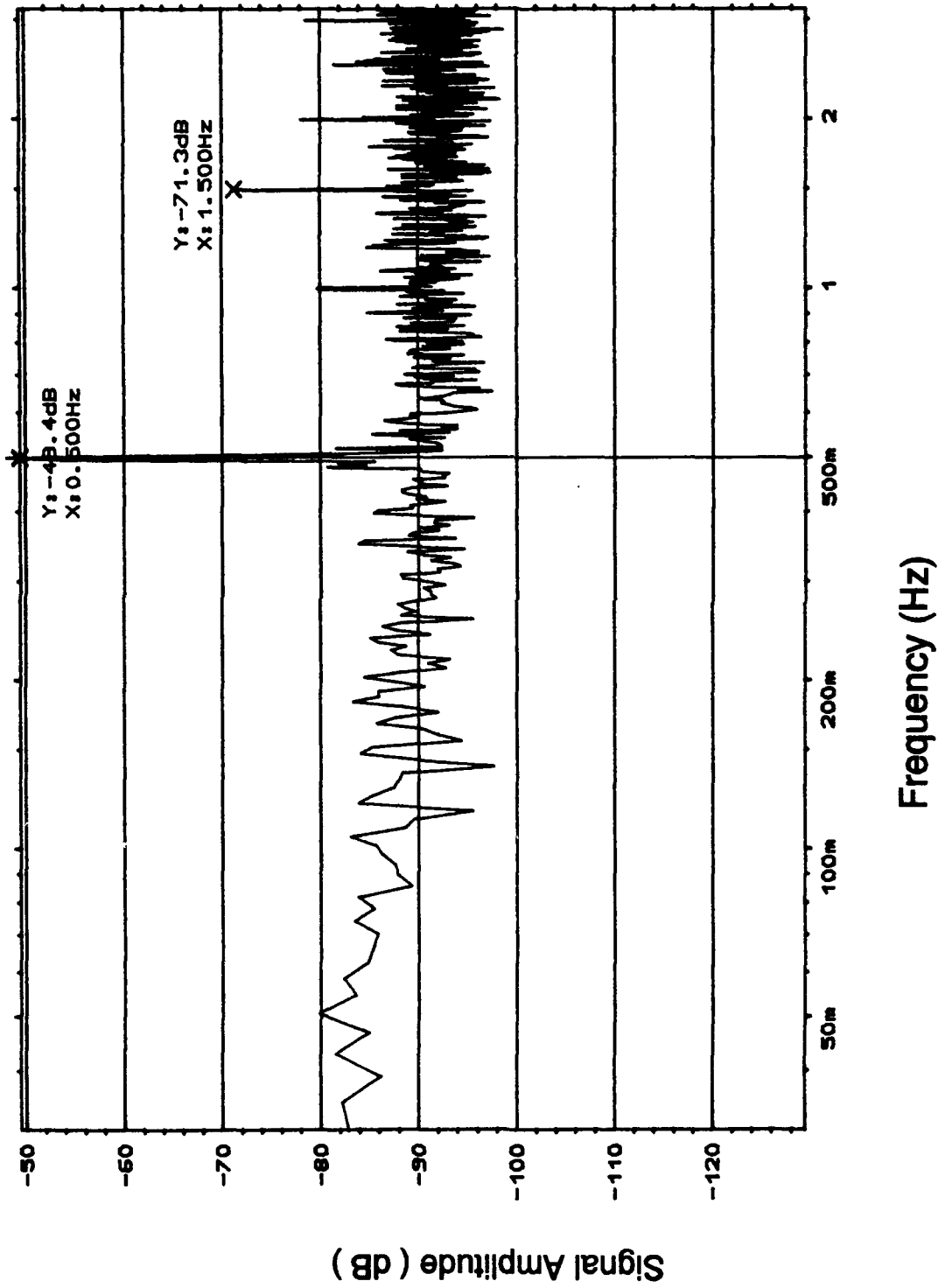With a 10 Hz Excitation Signal.
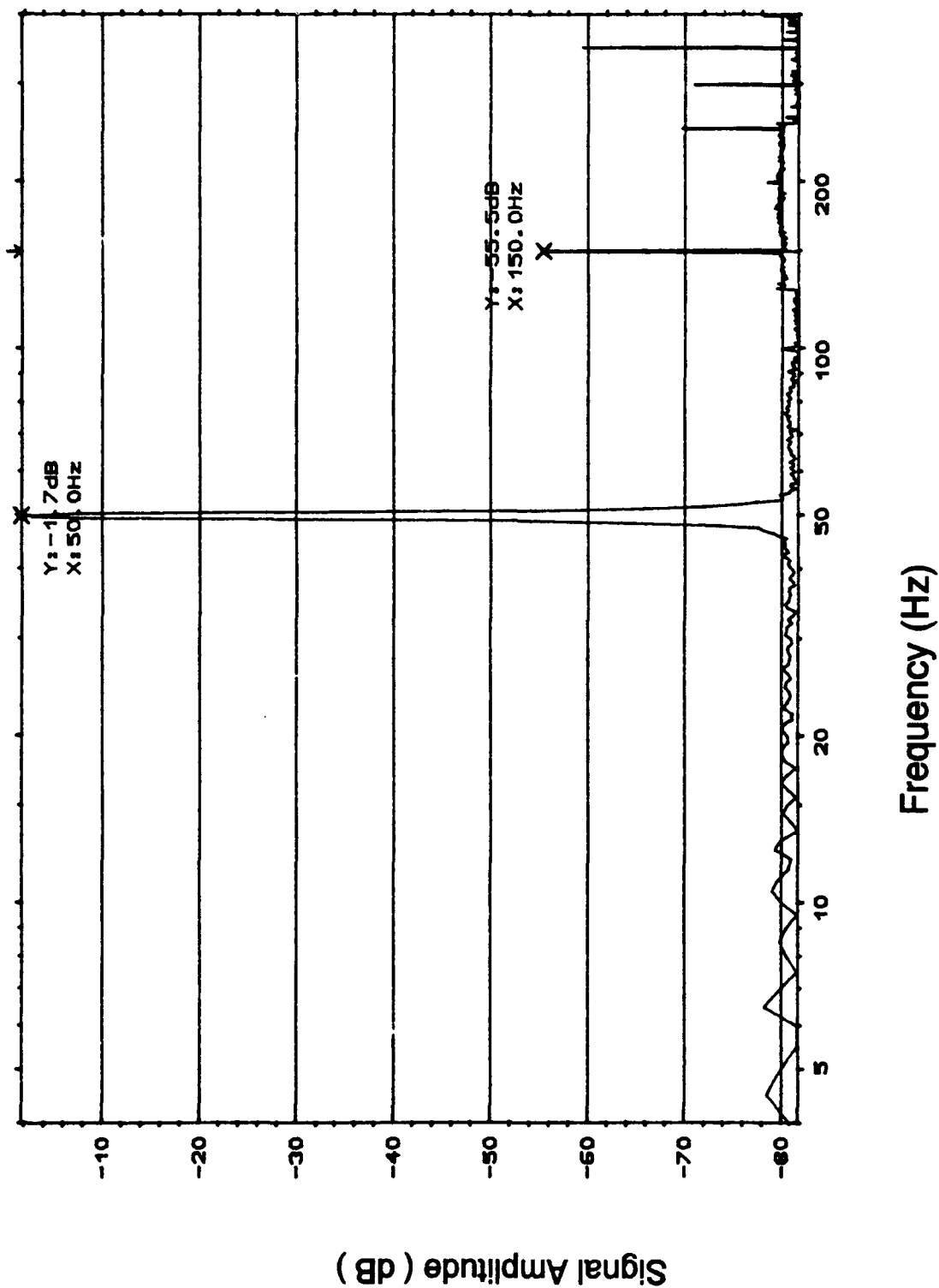
Figure I-43. Spectrum Analysis of the Oldfield Surface Mount Component Circui
With a 50 Hz Excitation Signal.
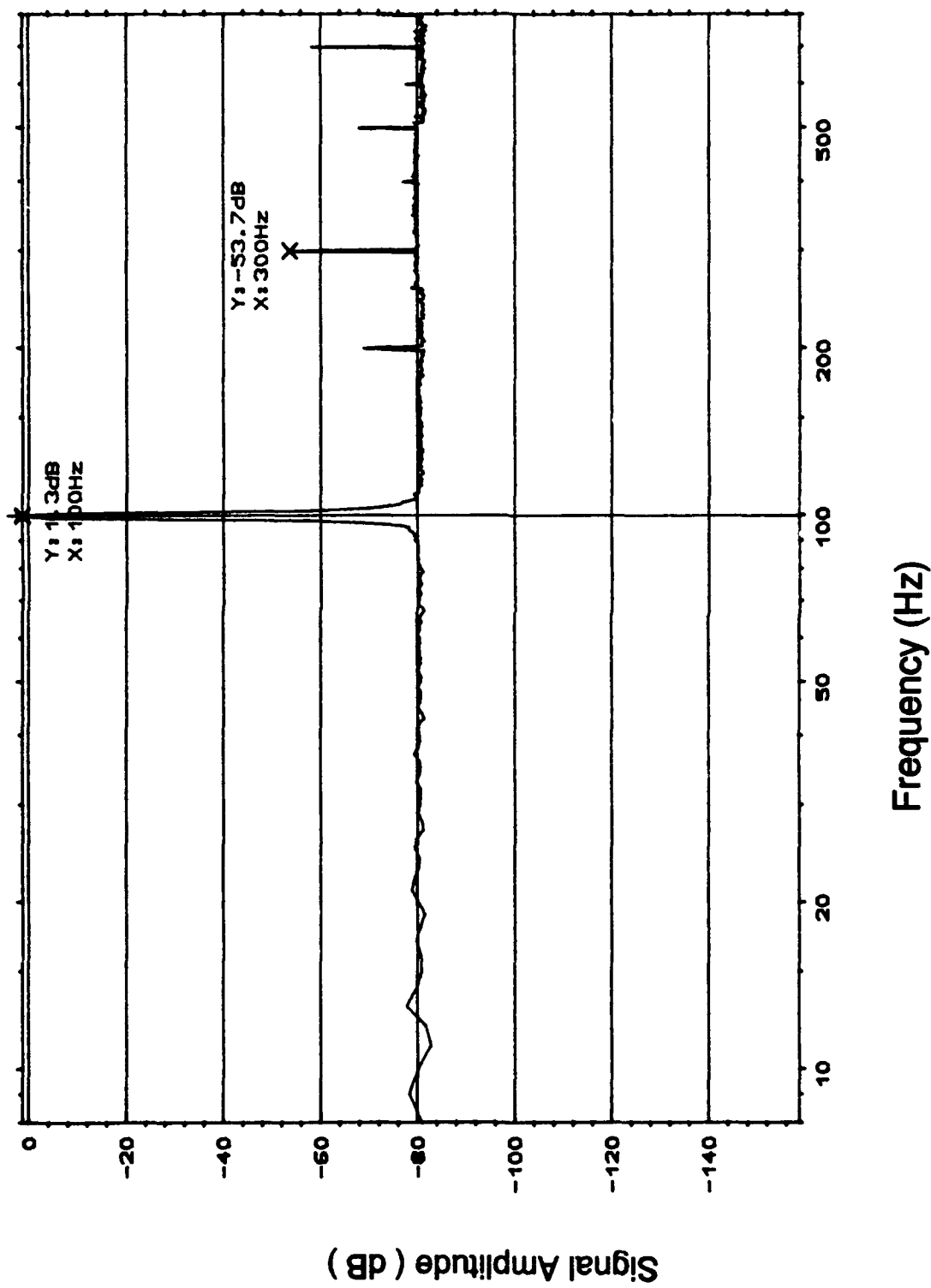
Figure I-44. Spectrum Analysis of the Oldfield Surface Mount Component Circui
With a 100 Hz Excitation Signal.
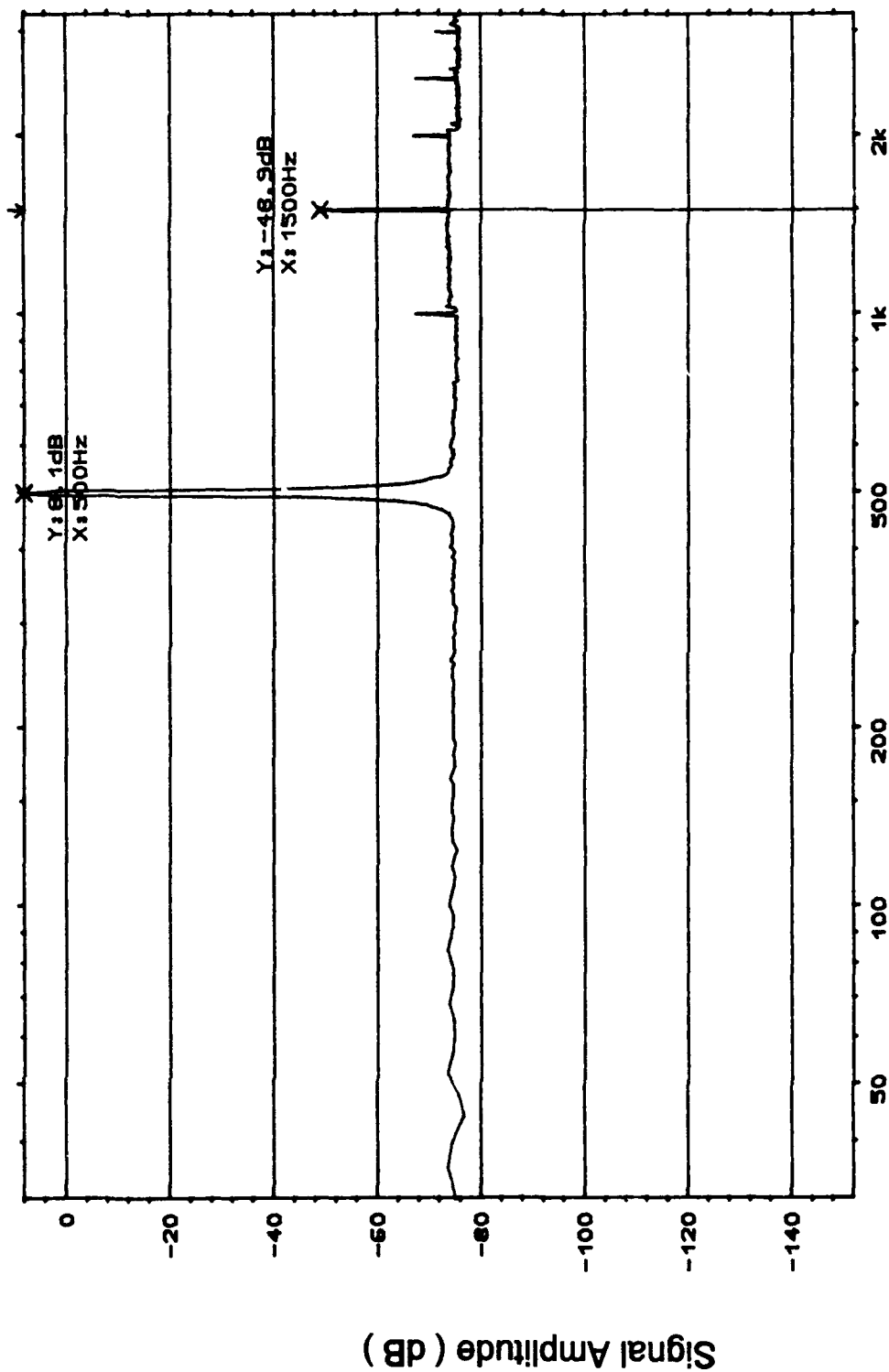
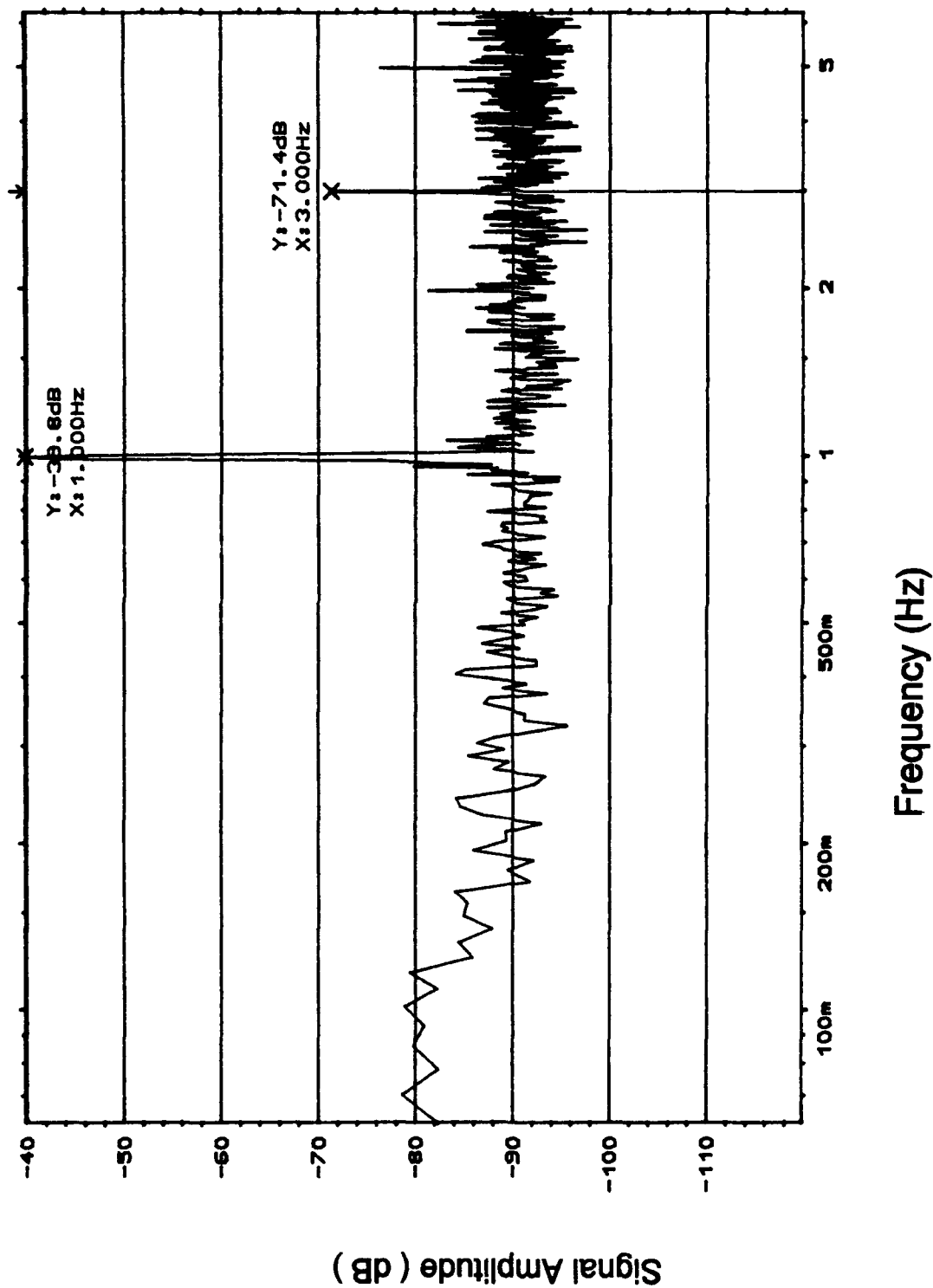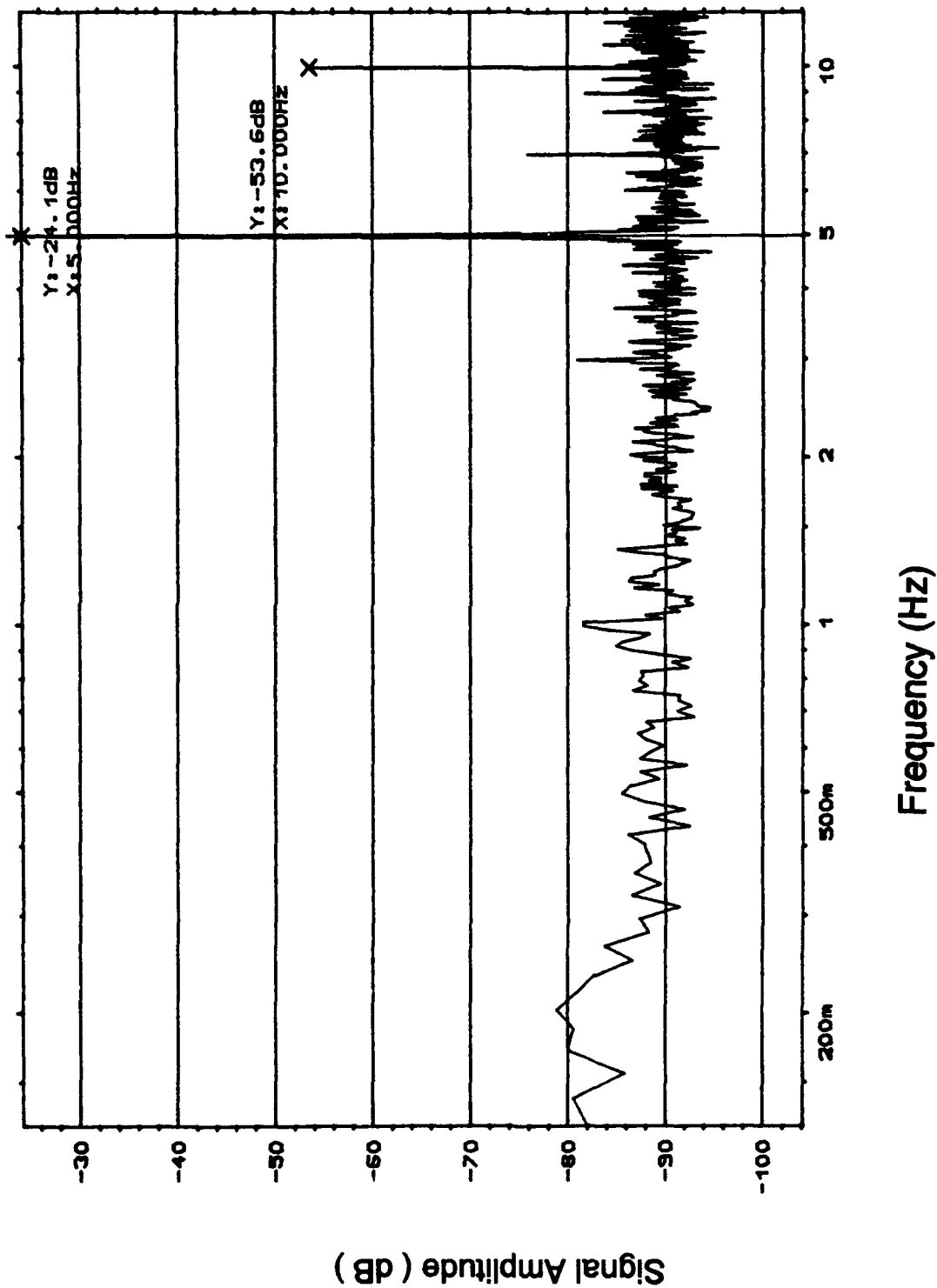Figure I-45. Spectrum Analysis of the Oldfield Surface Mount Component Circui With a 500 Hz Excitation Signal.
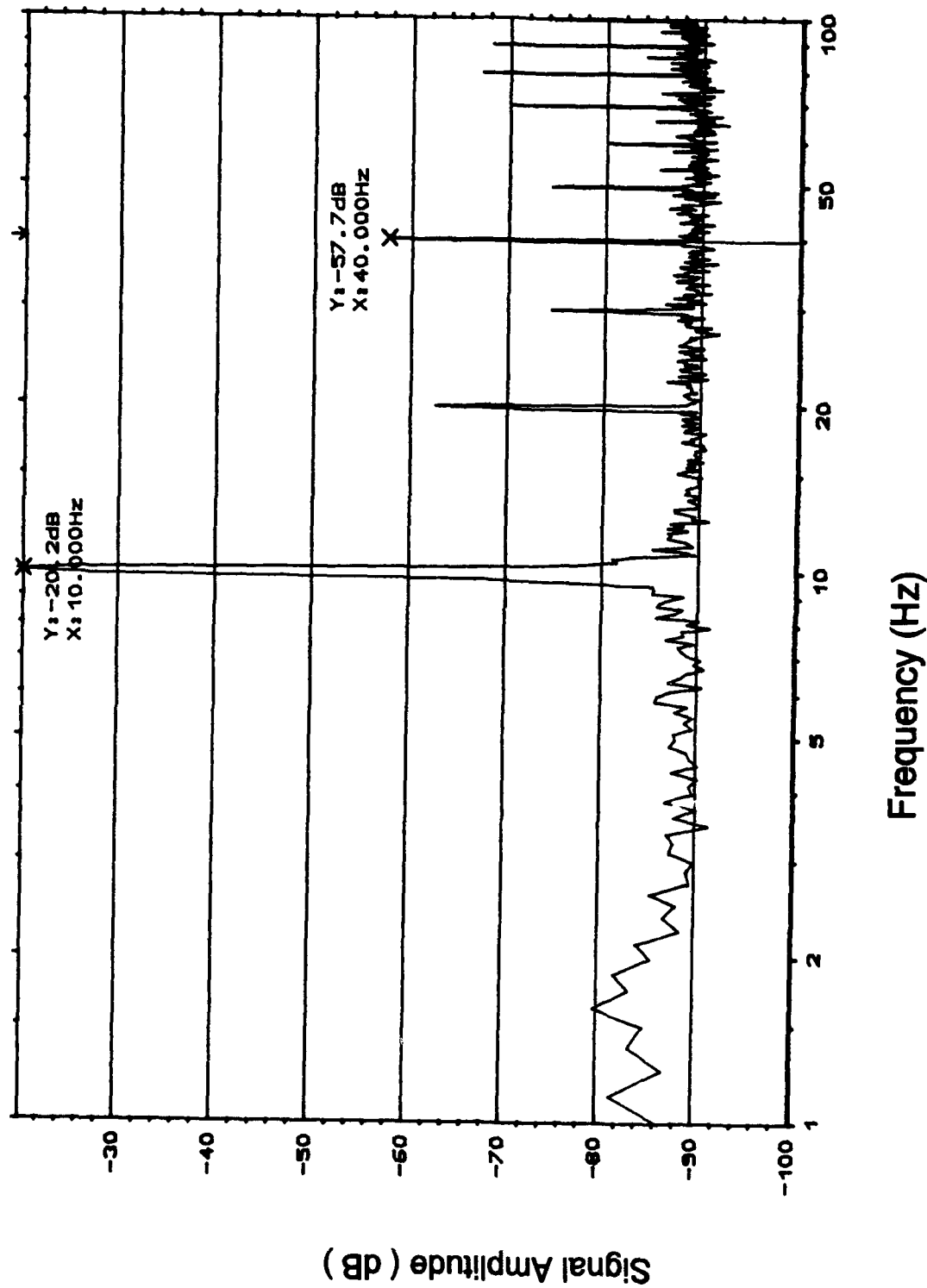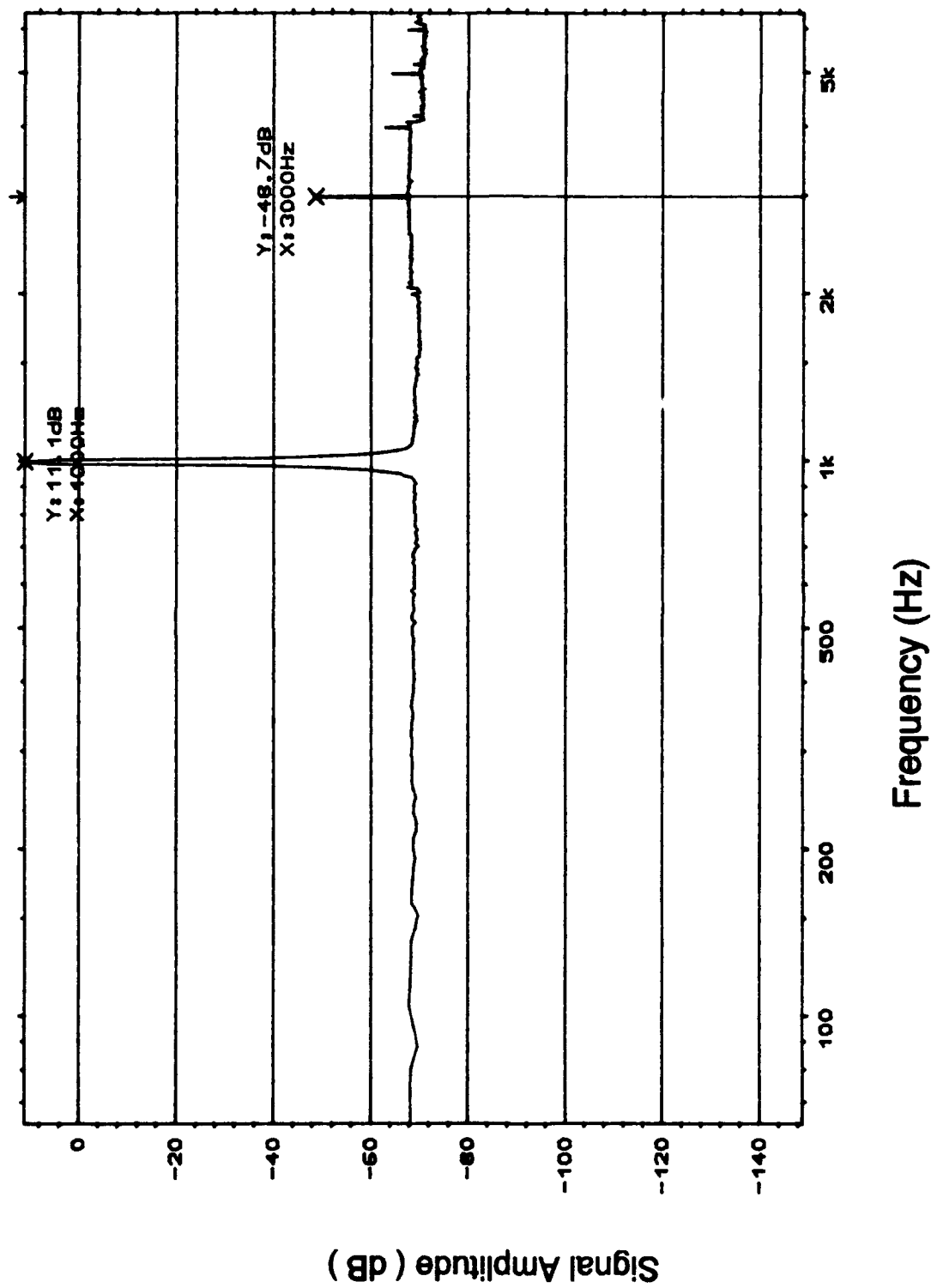
Figure I-46. Spectrum Analysis of the Oldfield Surface Mount Component Circui With a 1 KHz Excitation Signal.
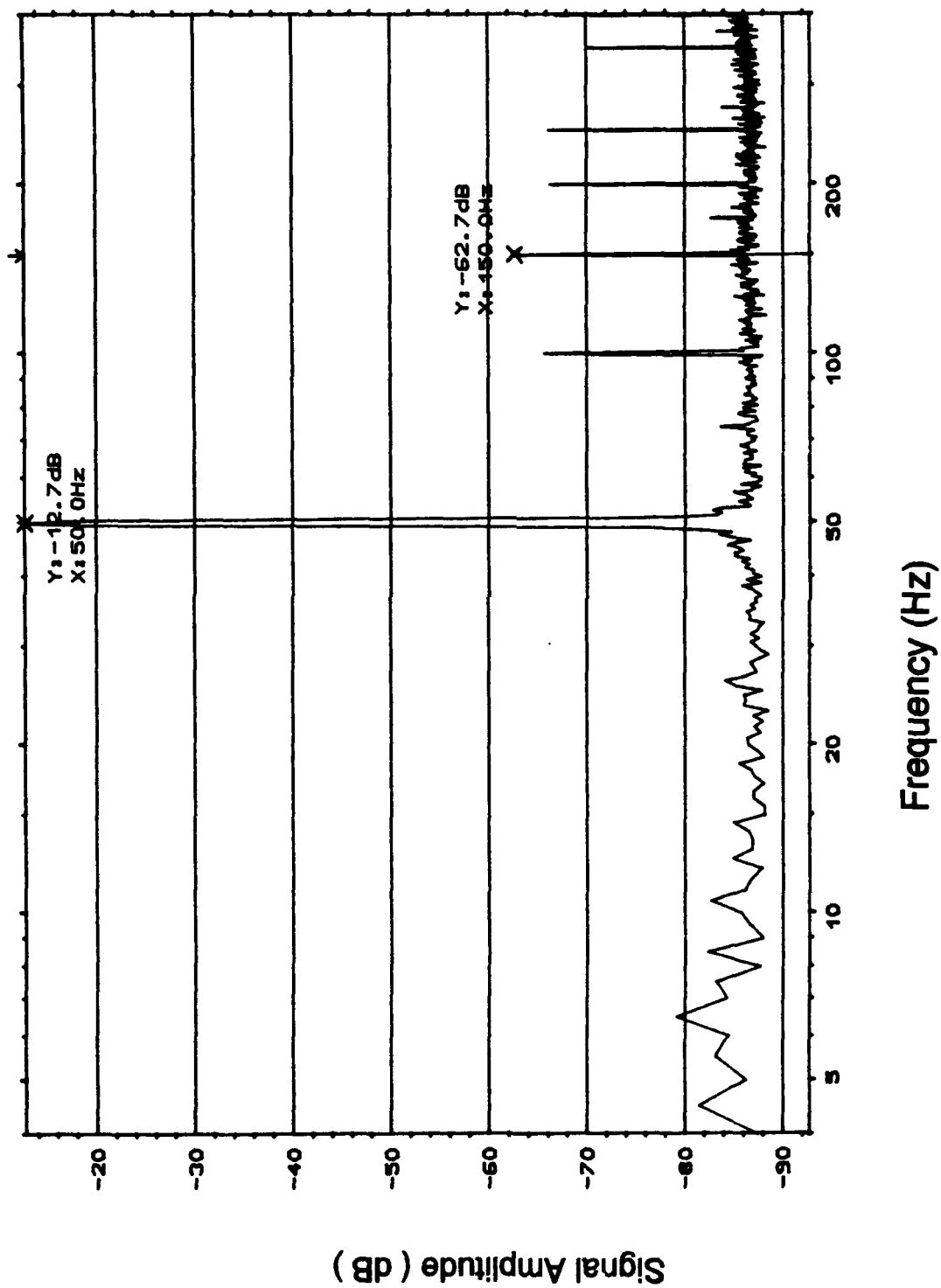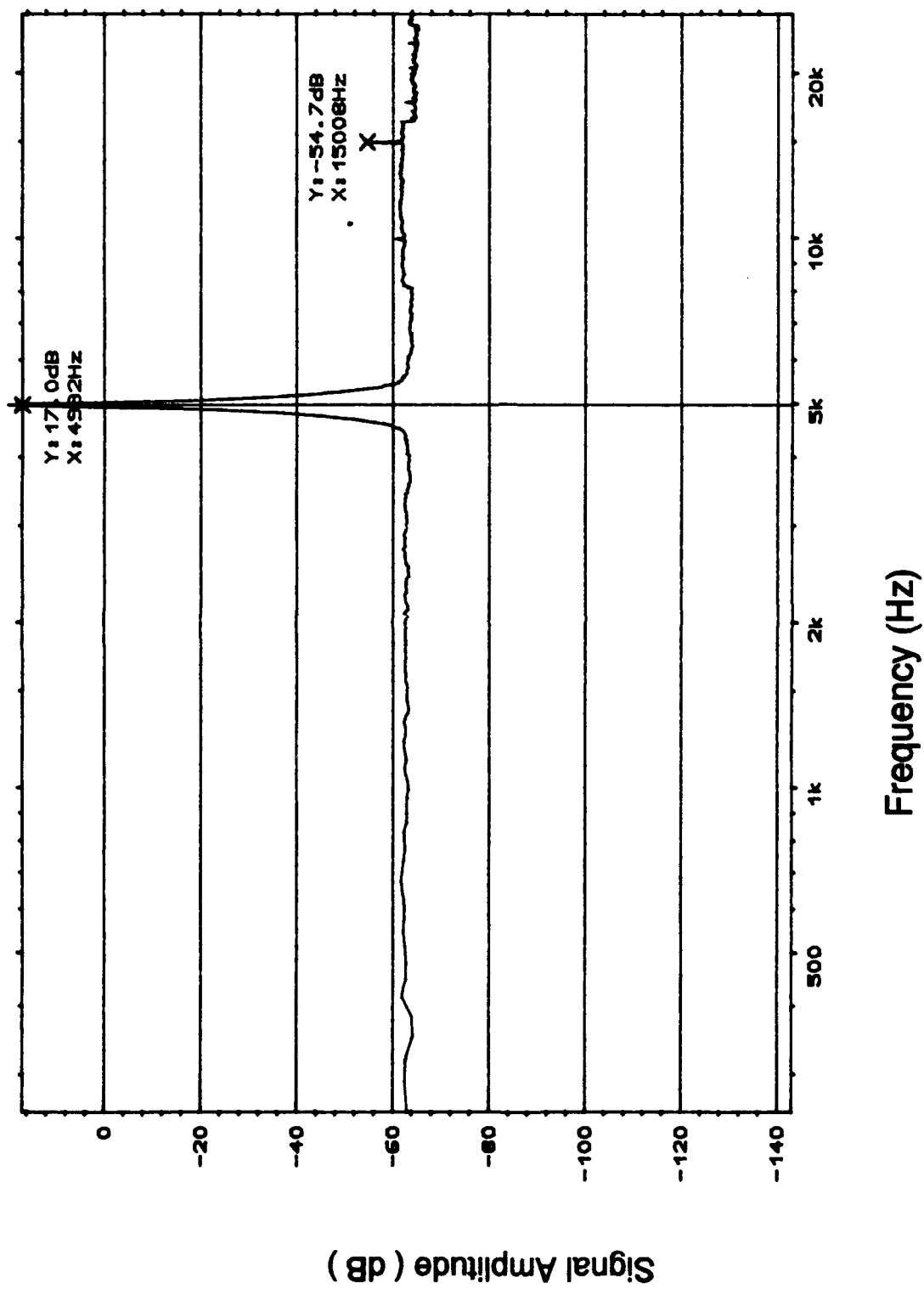
Figure I-47. Spectrum Analysis of the Oldfield Surface Mount Component Circui With a 4.982 KHz Excitation Signal.
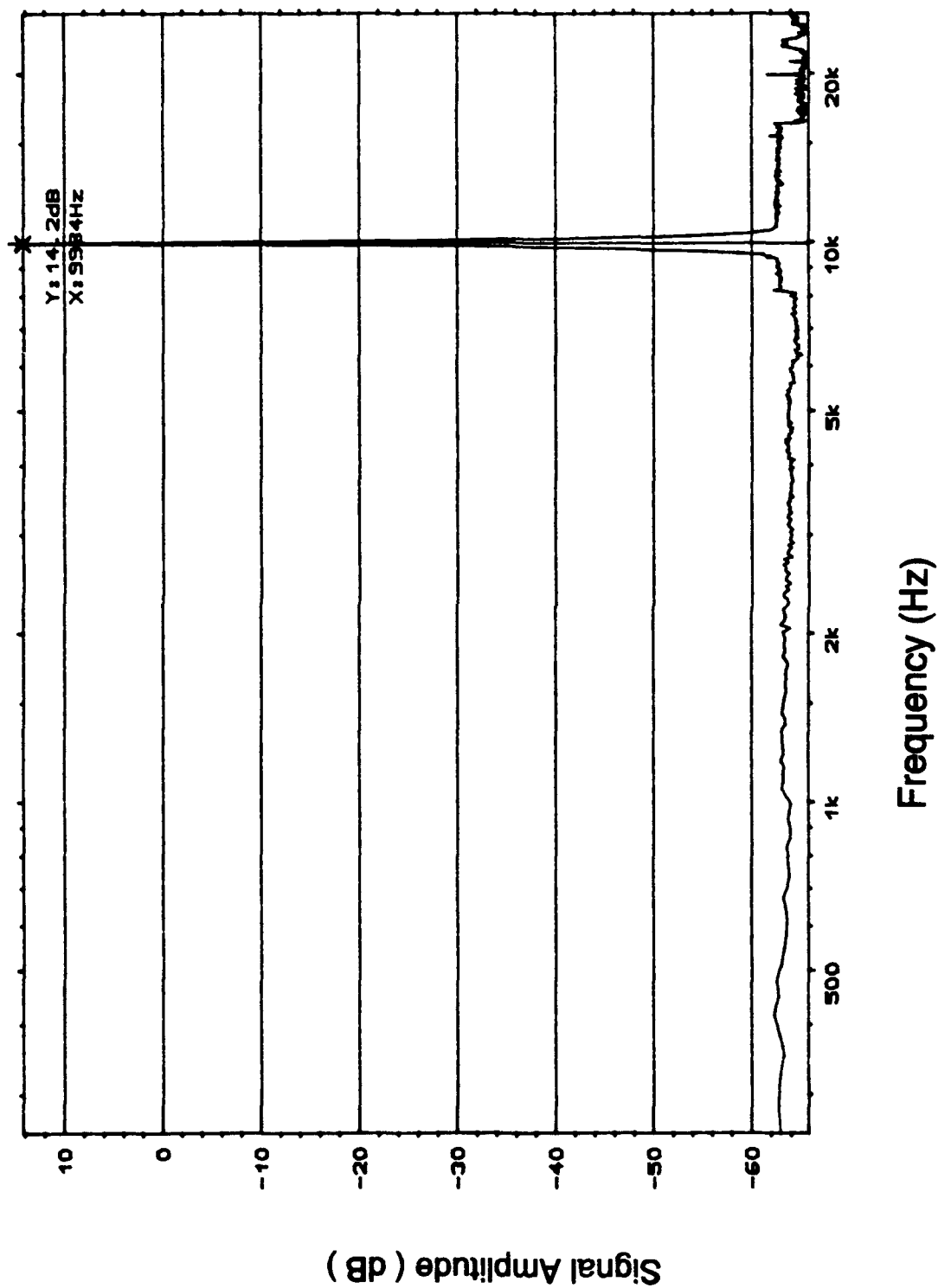
Figure I-48. Spectrum Analysis of the Oldfield Surface Mount Component Circui With a 9.984 KHz Excitation Signal.

I-54

Appendix J

Gain and Phase Data

Collected With the B & K Signal Analyzer

for

the Oldham and Oldfield

Circuits Realized

With a Printed Circuit Board Format

This appendix documents the experimentally measured gain and phase data obtained for the Oldham and Oldfield discrete, hybrid and surface mount component circuits realized with a printed circuit board format. The data is arranged according to circuit variant. That is, the Oldham discrete component circuit gain and phase data is displayed first, followed by the data for the Oldham hybrid component circuit, then, the Oldfield discrete component circuit data, and finally, the Oldfield surface mount circuit gain and phase data.
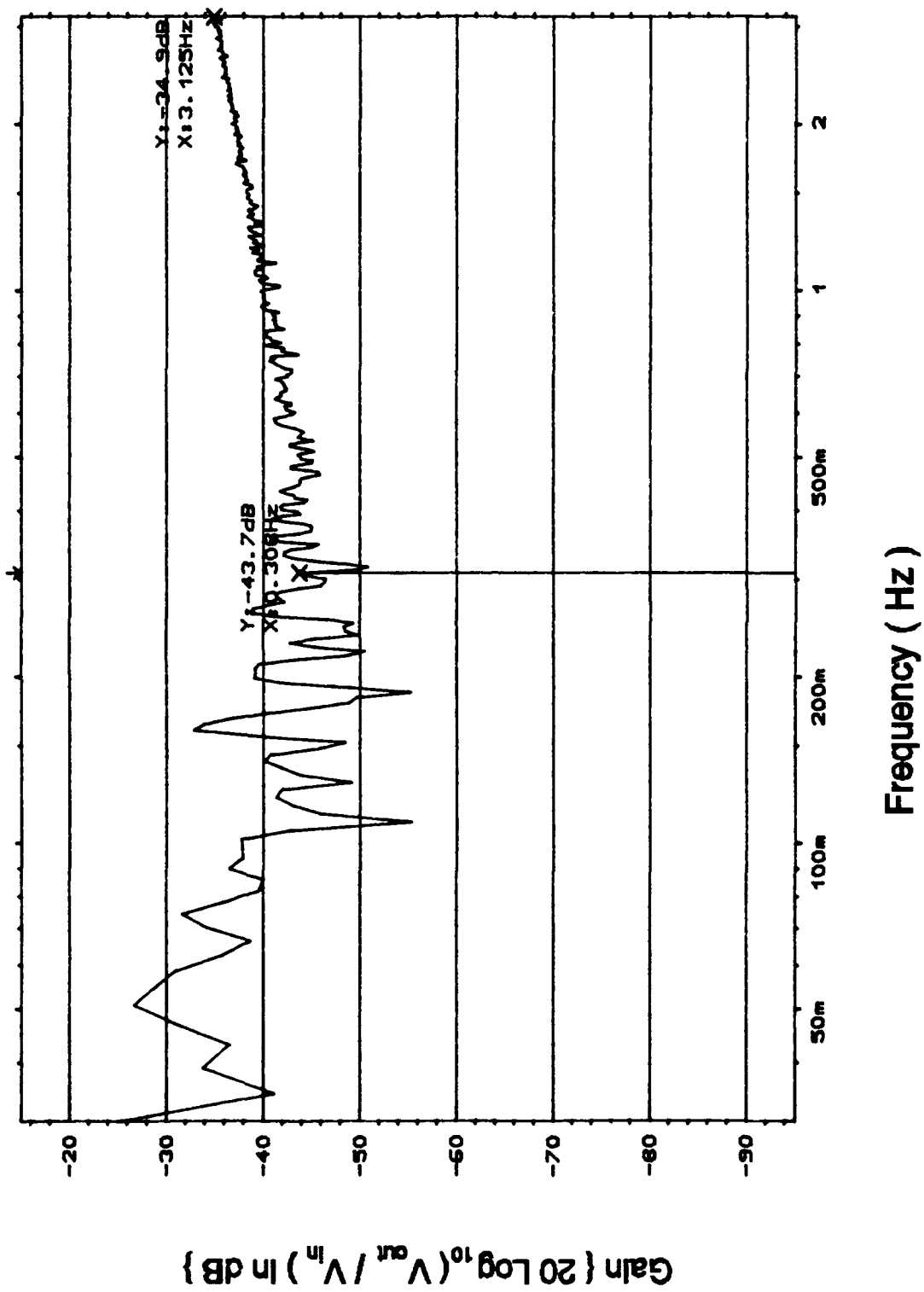
Figure J-1. Gain Response of the Oldham Discrete Component Circuit (cont);
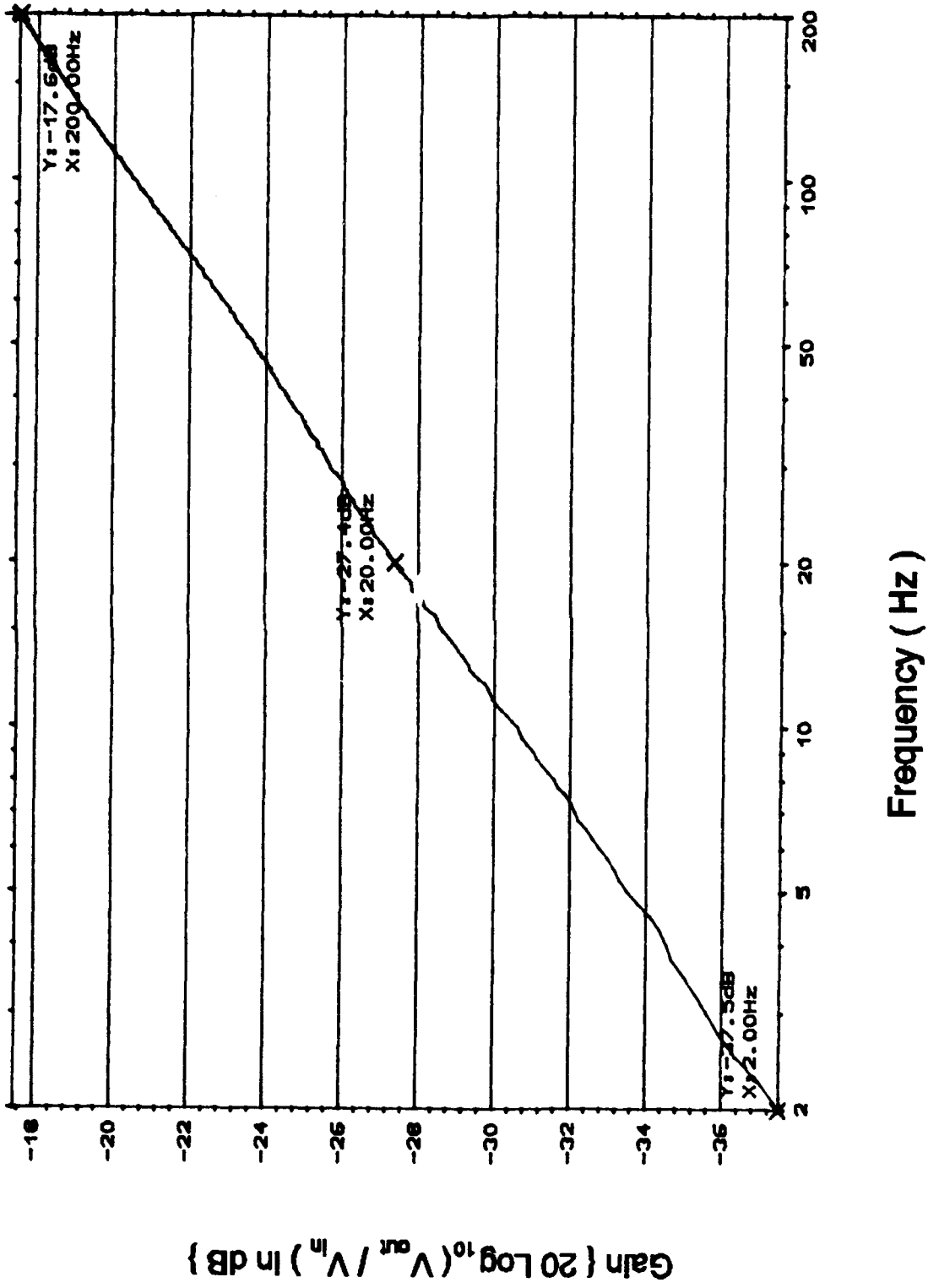
Figure J-1 (cont). Gain Response of the Oldham Discrete Component Circuit (cont):
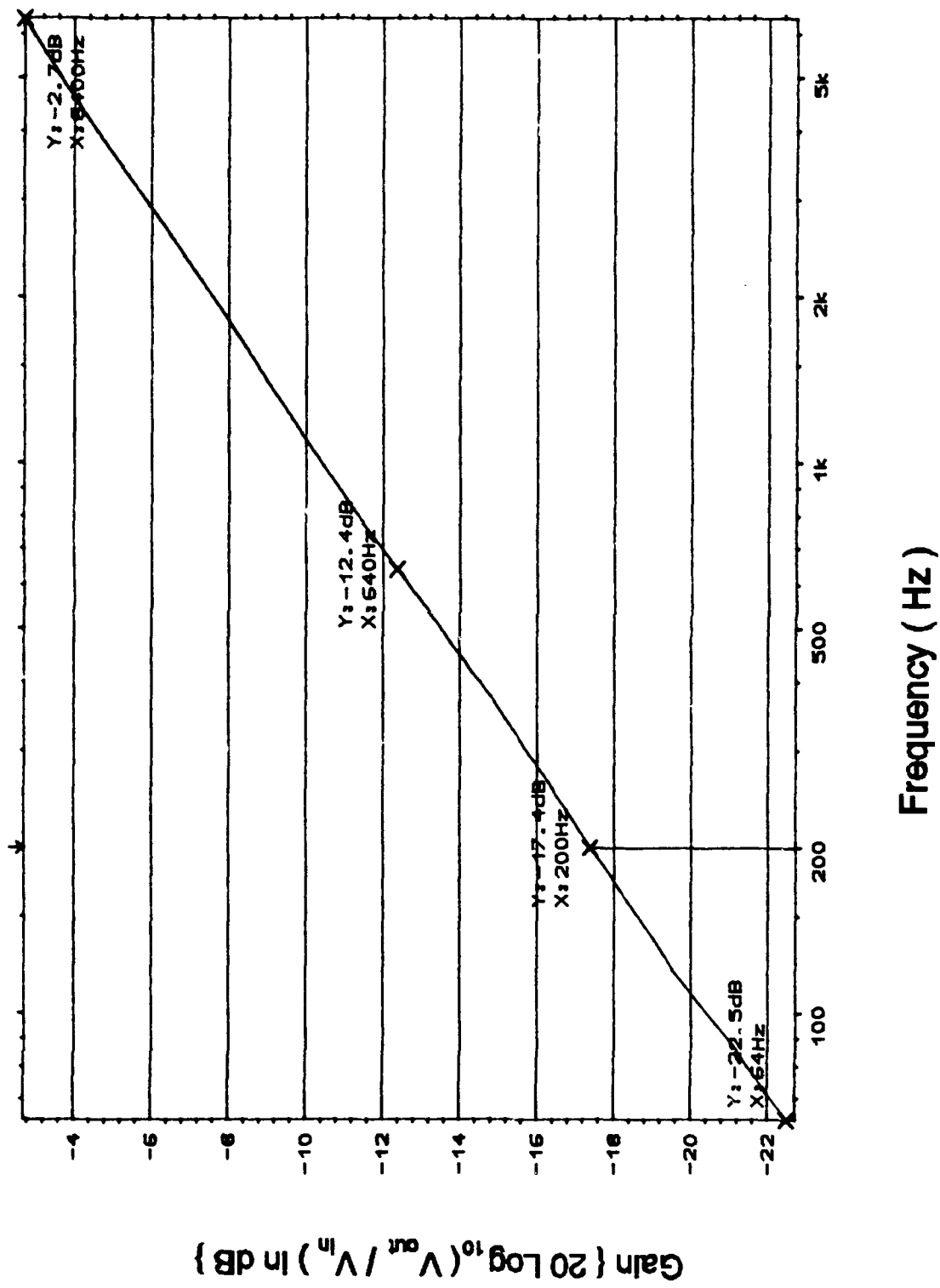
Figure J-1 (cont). Gain Response of the Oldham Discrete Component Circuit.
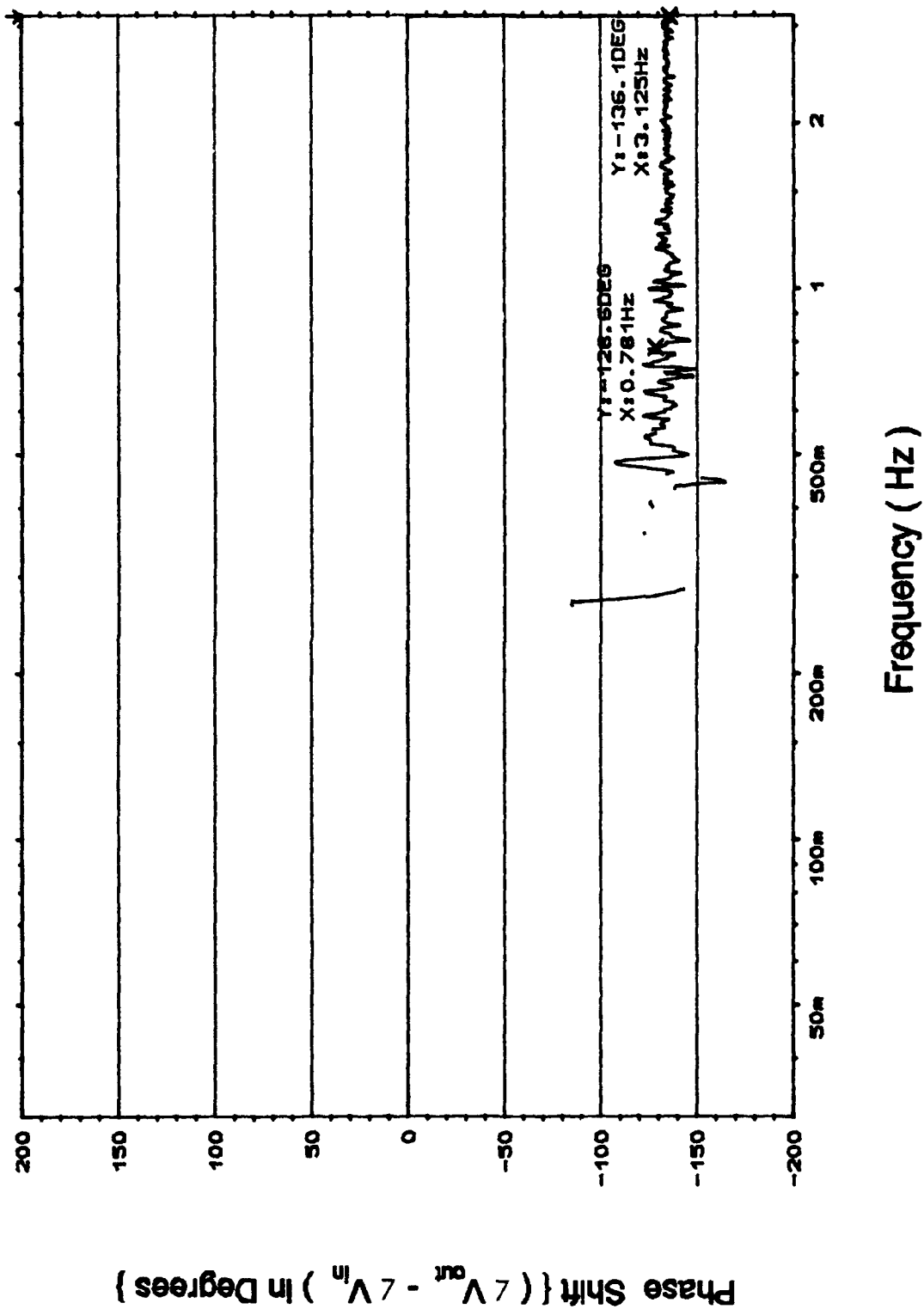
Figure J-2. Phase Response of the Oldham Discrete Component Circuit (cont);
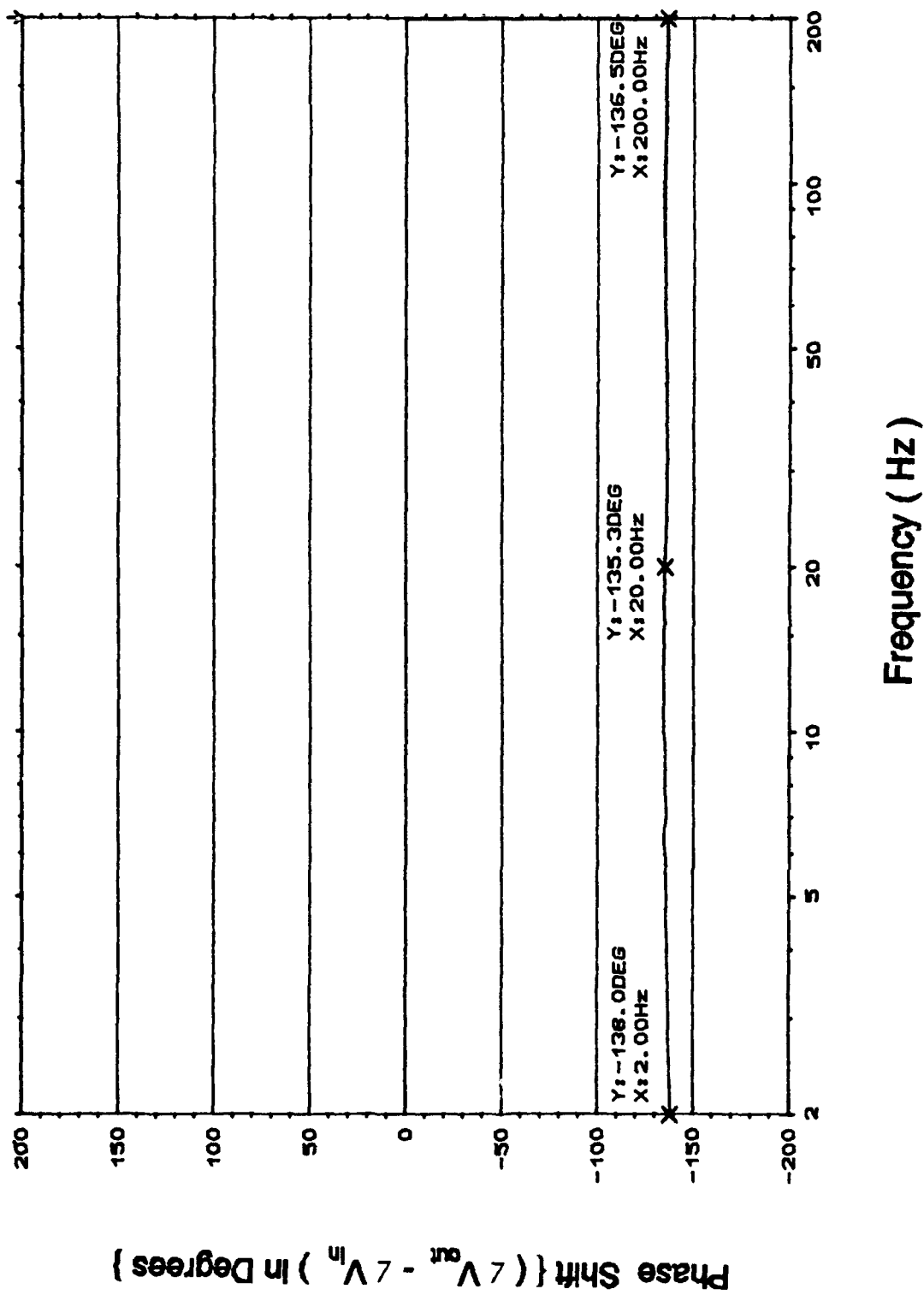
Figure J-2 (cont). Phase Response of the Oldham Discrete Component Circuit (cont);
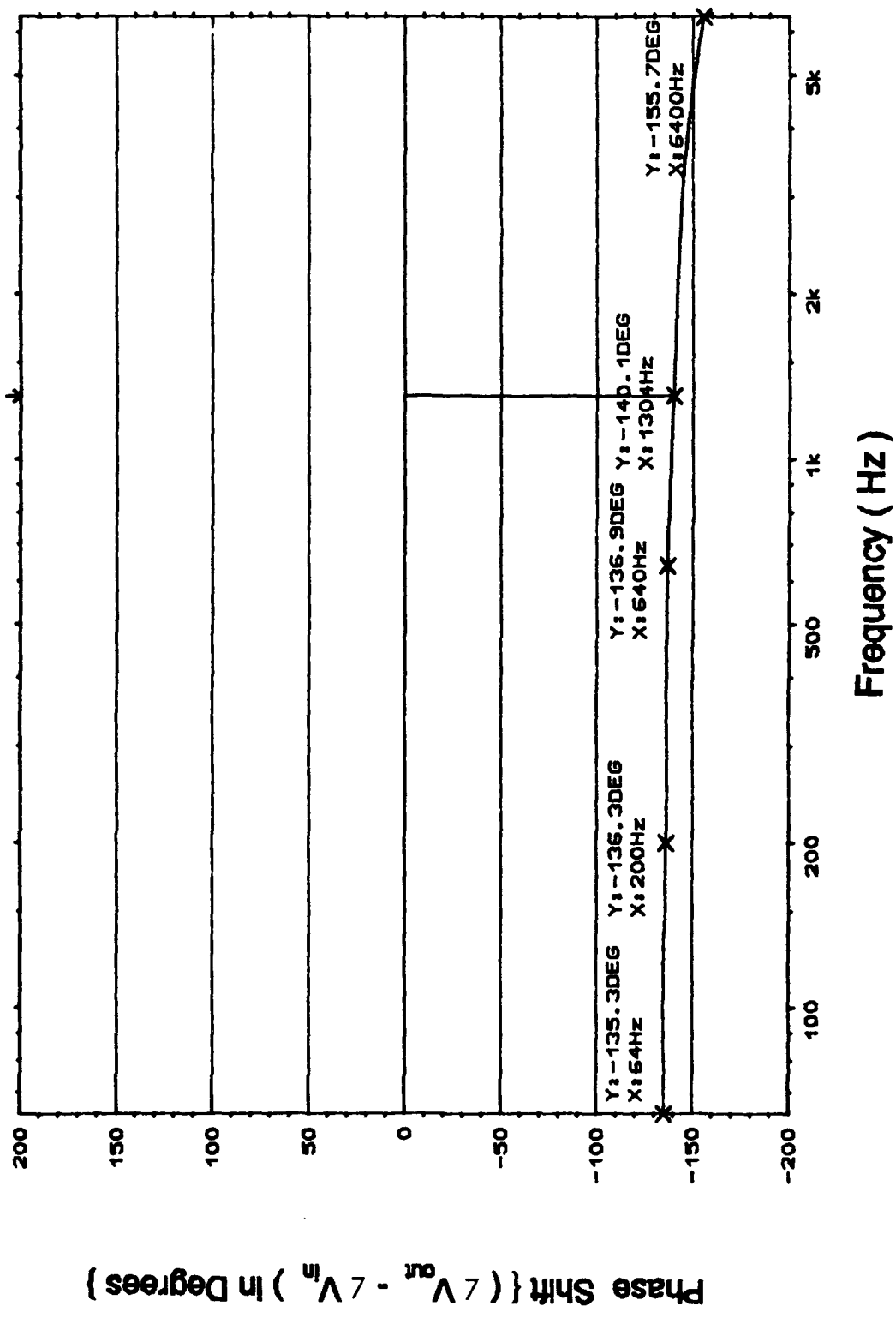
Figure J-2 (cont). Phase Response of the Oldham Discrete Component Circuit.
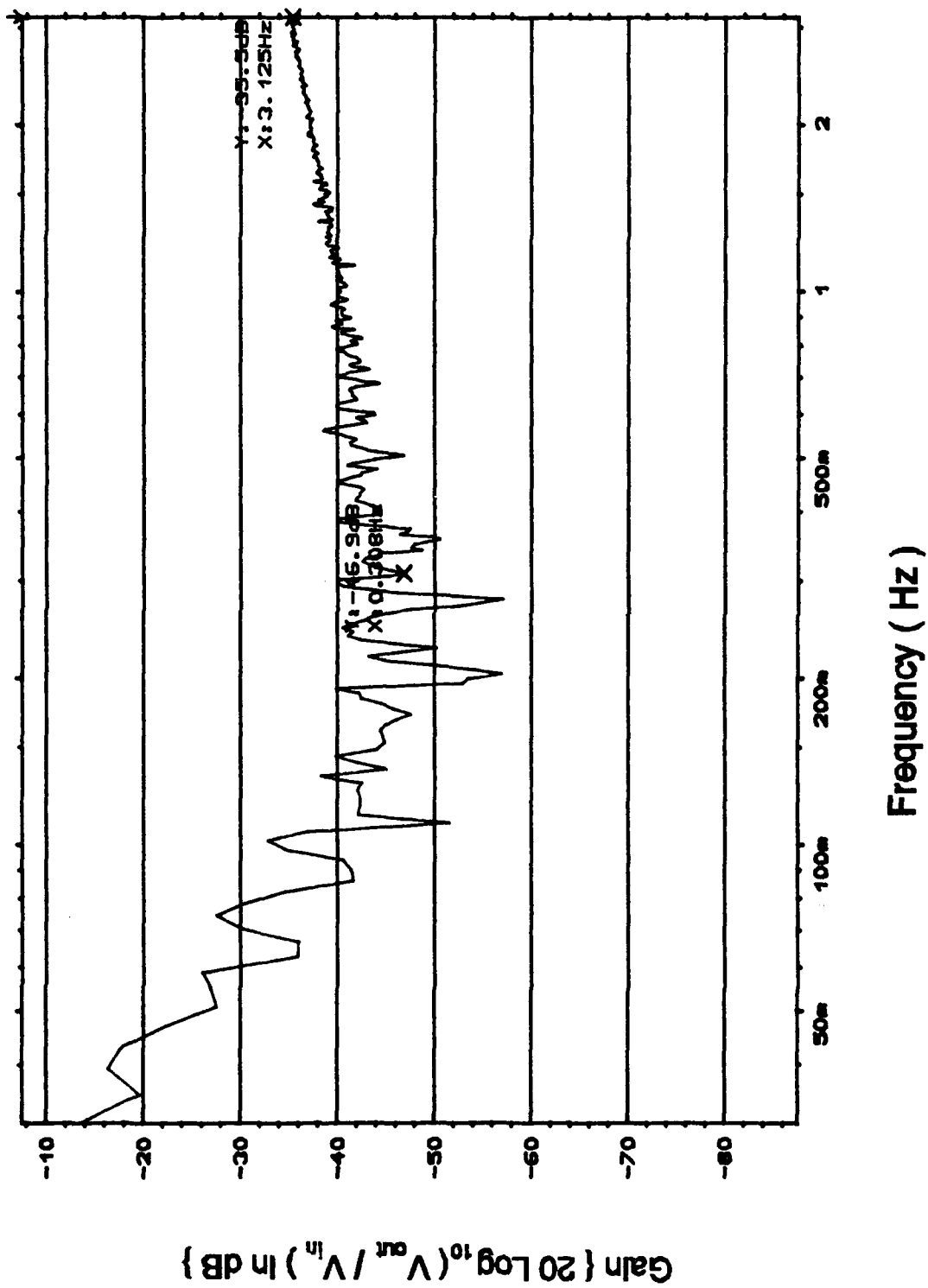
Figure J-3. Gain Response of the Oldham Hybrid Component Circuit (cont);
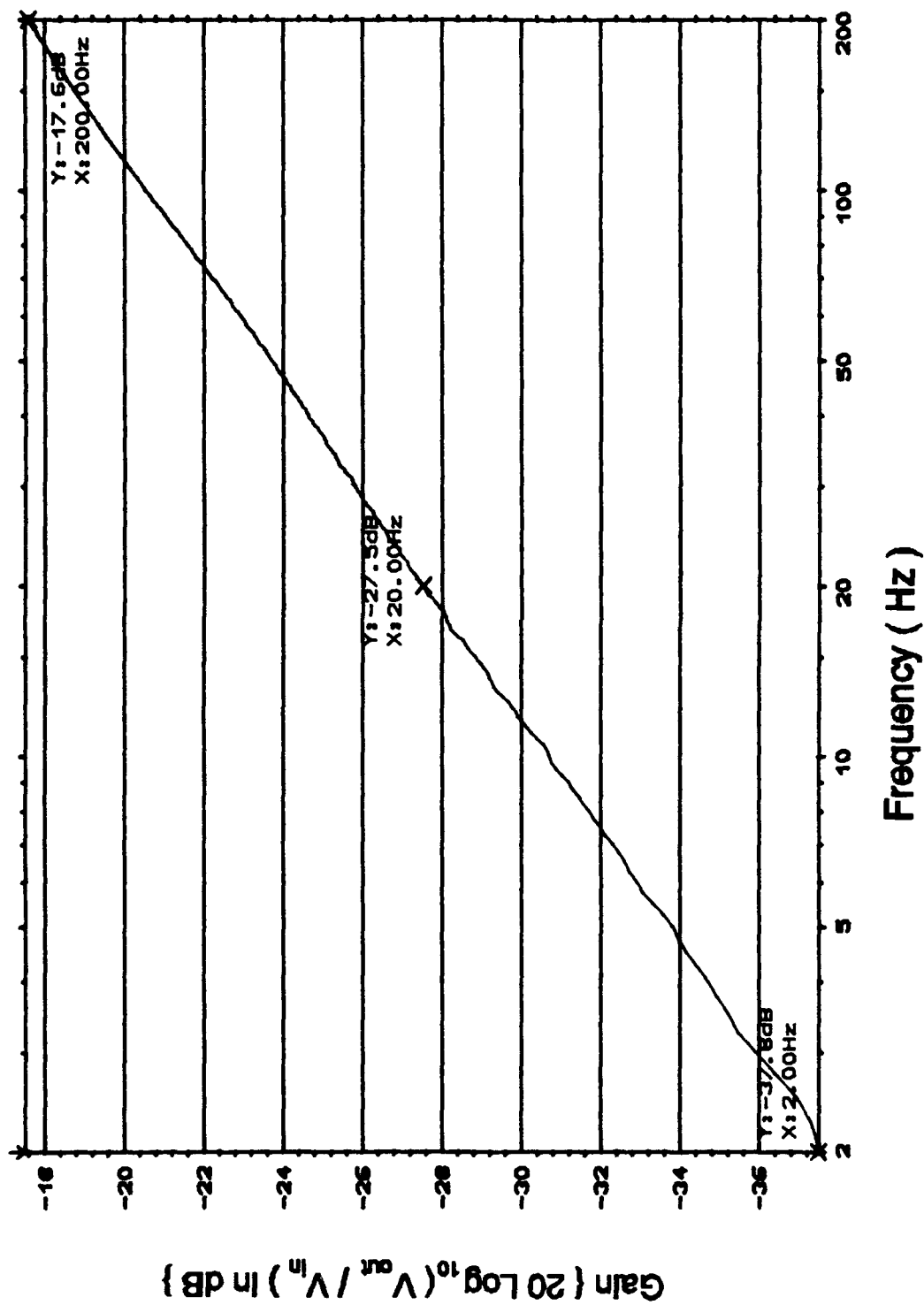
Figure J-3 (cont). Gain Response of the Oldham Hybrid Component Circuit (cont);
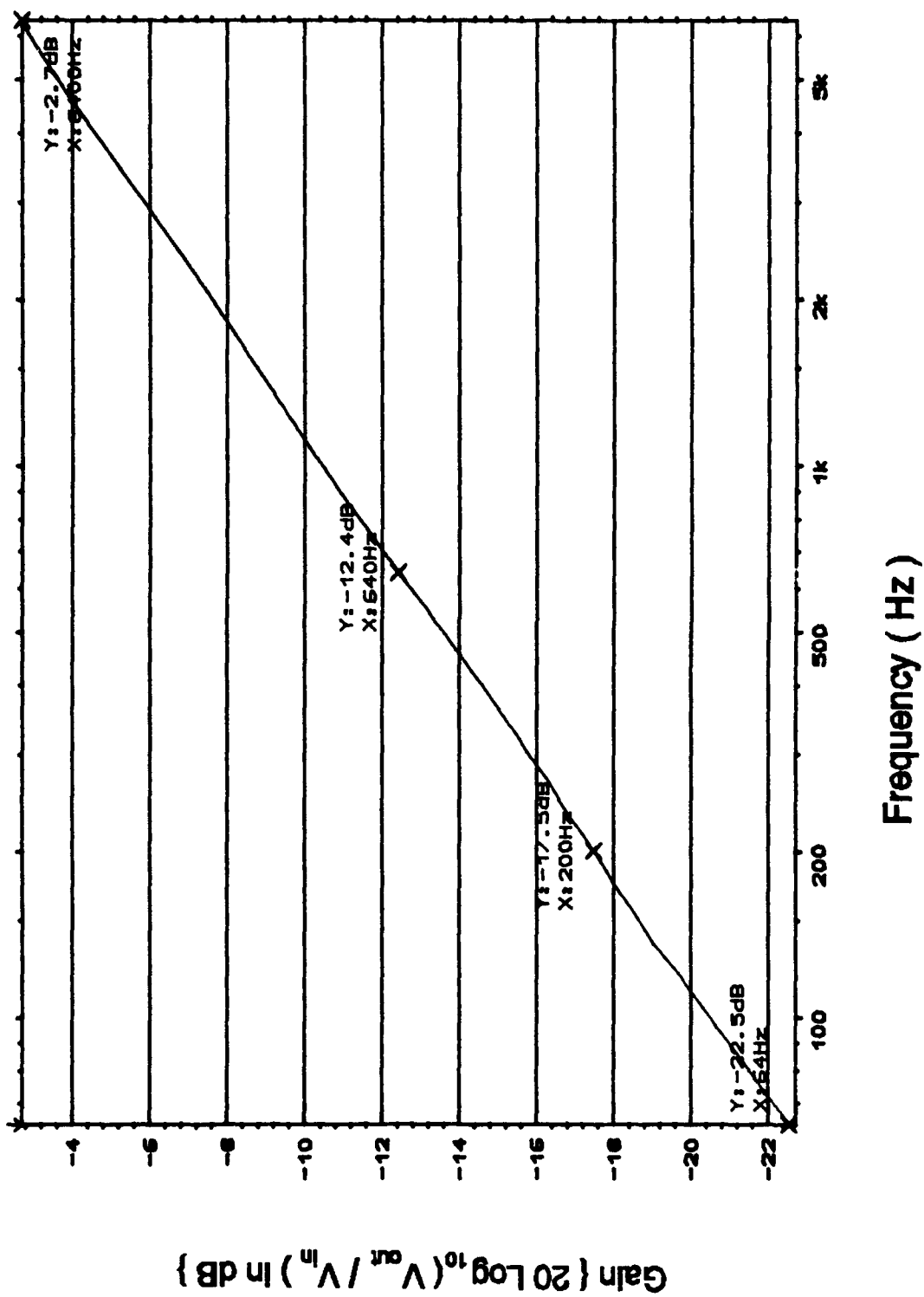
Figure J-3 (cont). Gain Response of the Oldham Hybrid Component Circuit.
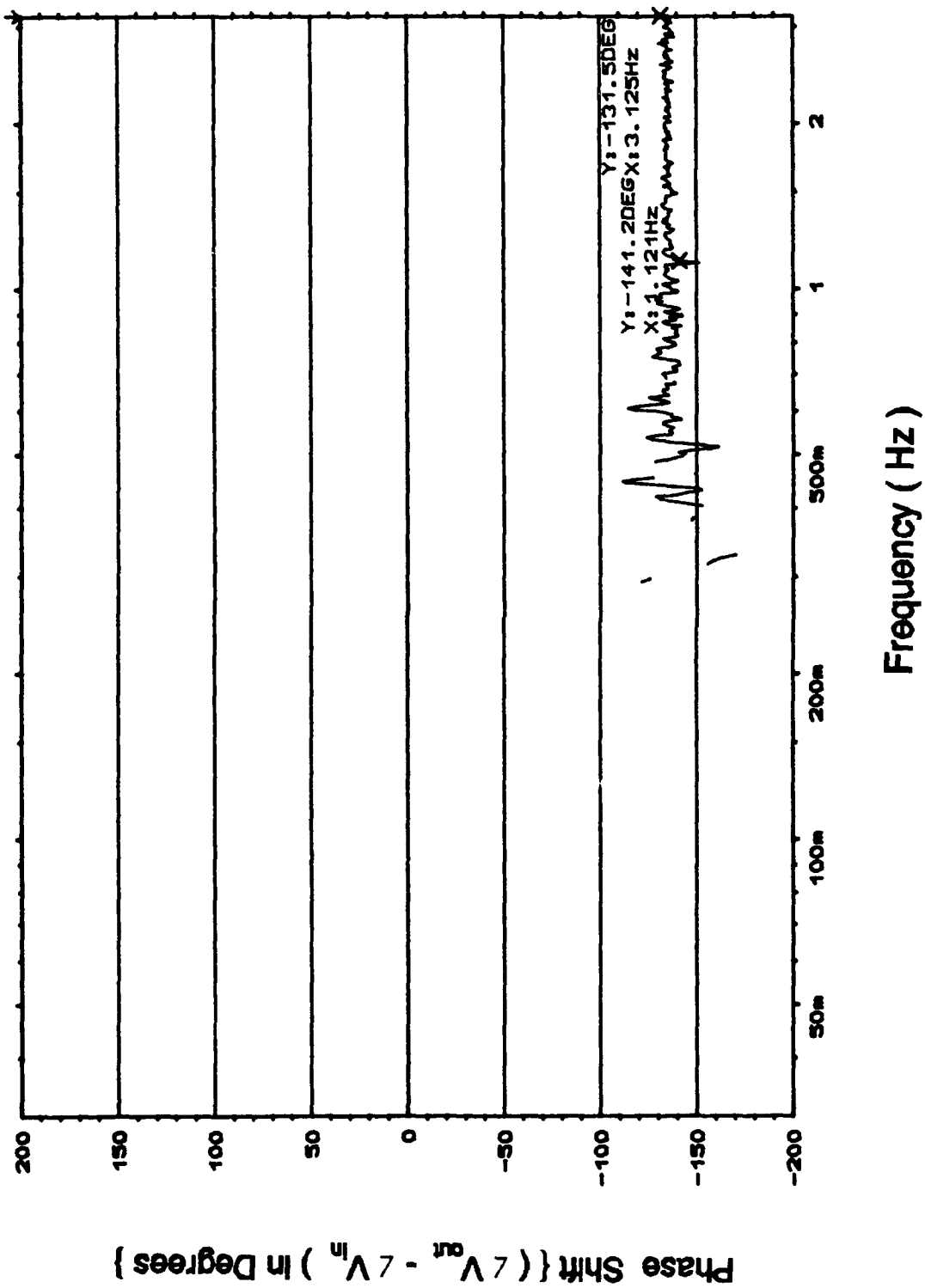
Figure J-4. Phase Response of the Oldham Hybdid Component Circuit (cont);
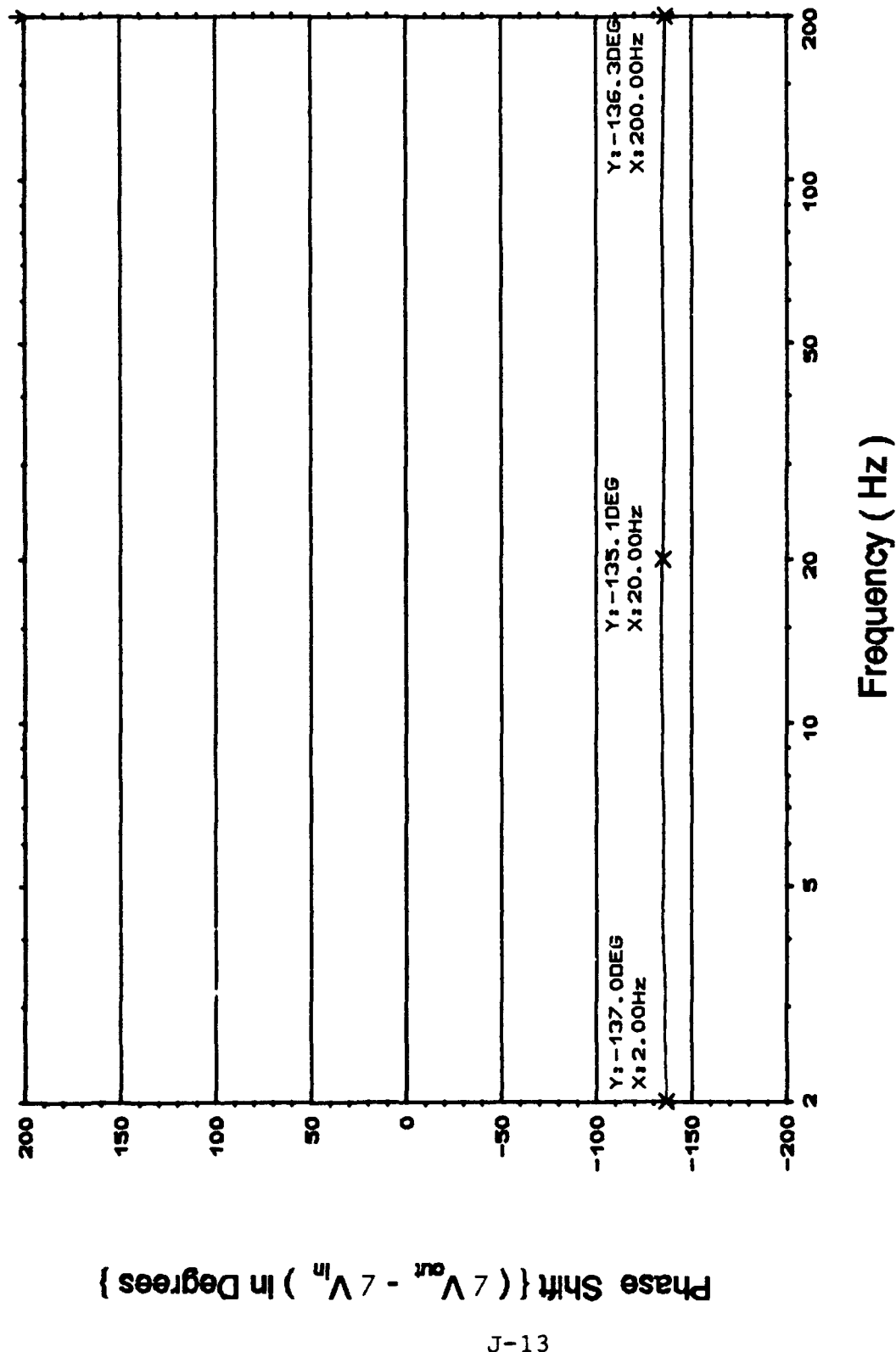
Figure J-4 (cont). Phase Response of the Oldham Hybrid Component Circuit (cont);

J-13
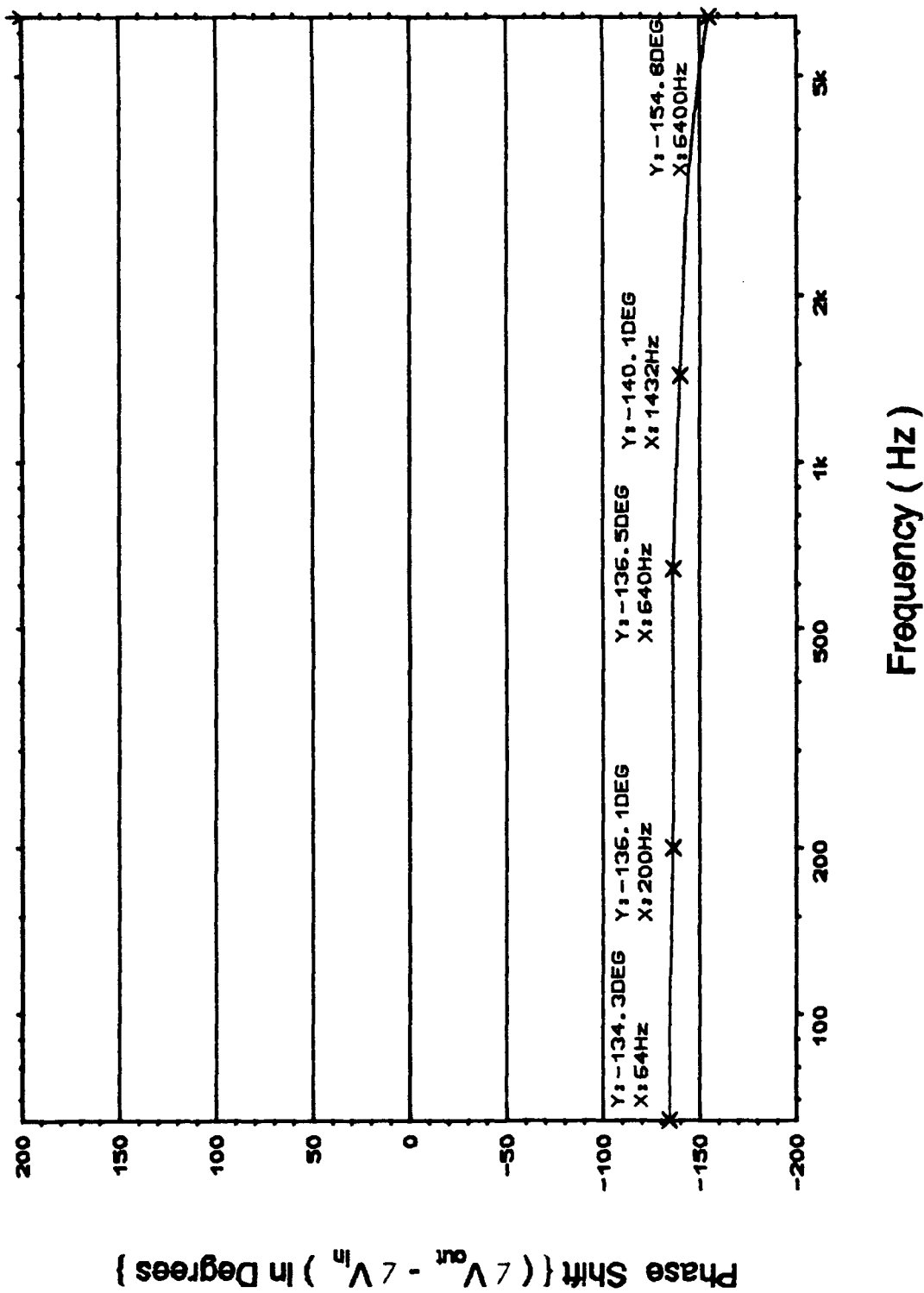
Figure J-4 (cont). Phase Response of the Oldham Hybrid Component Circuit.
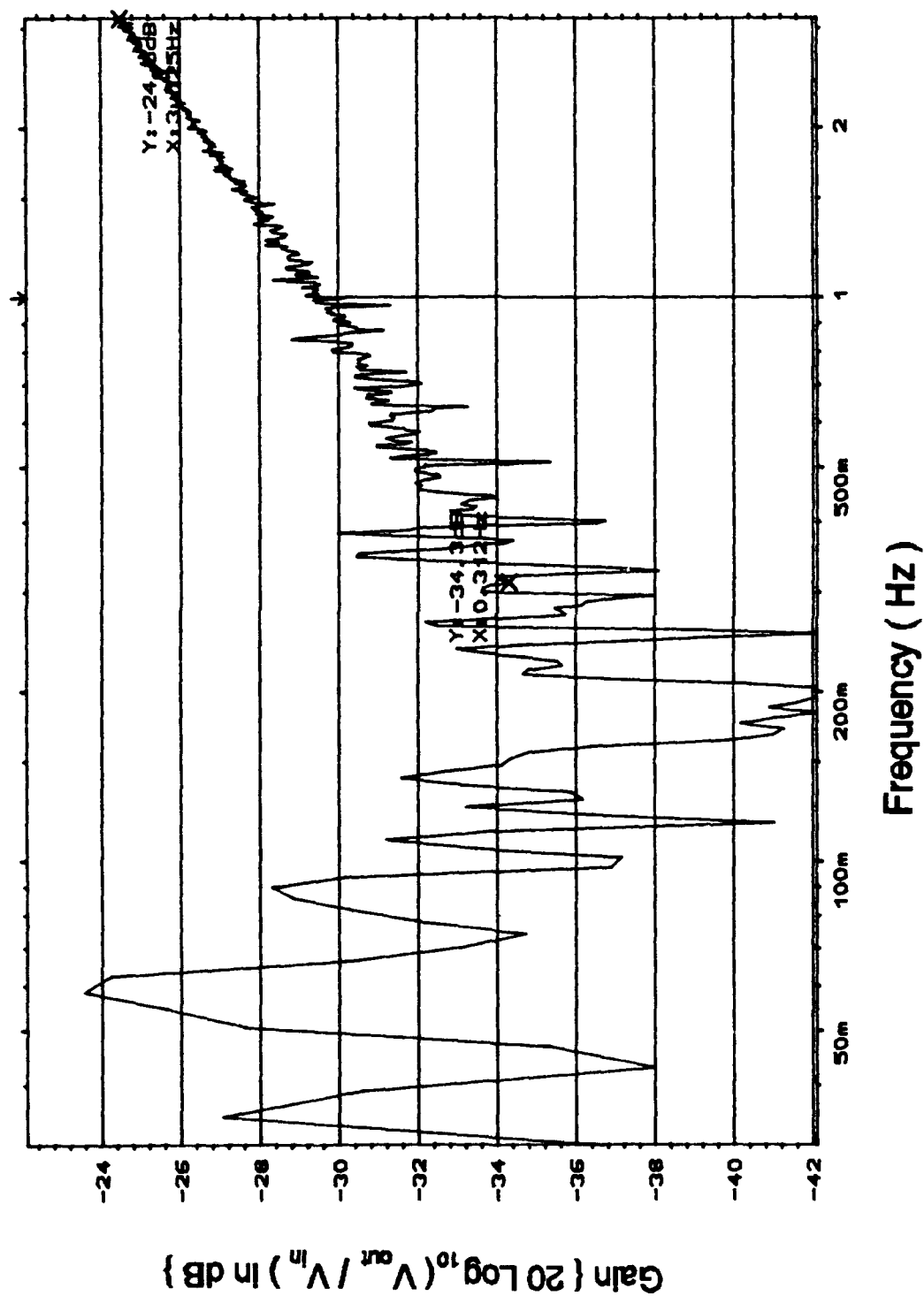
Figure J-5. Gain Response of the Oldfield Discrete Component Circuit (cont);
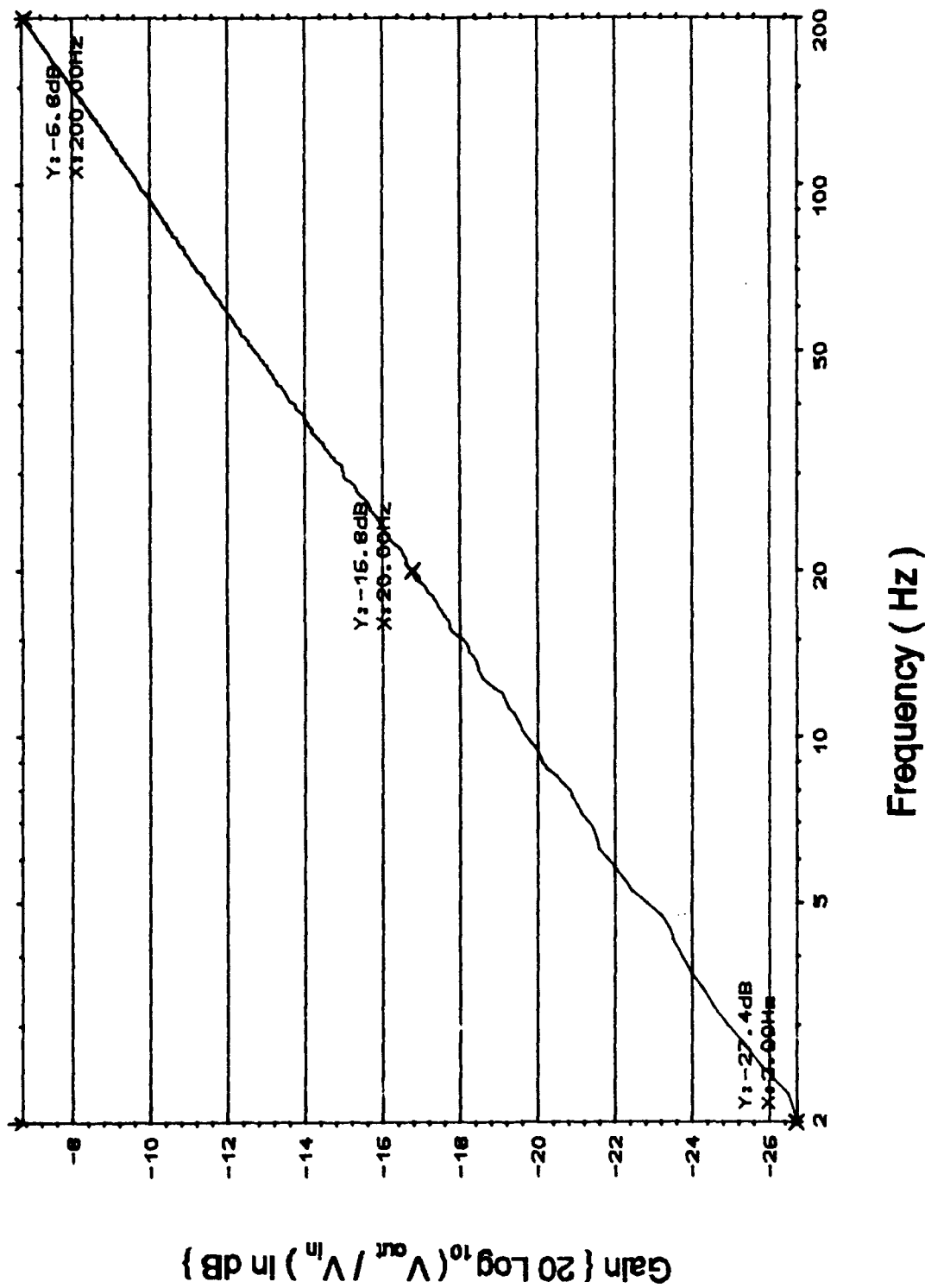
Figure J-5 (cont). Gain Response of the Oldfield Discrete Component Circuit (cont);
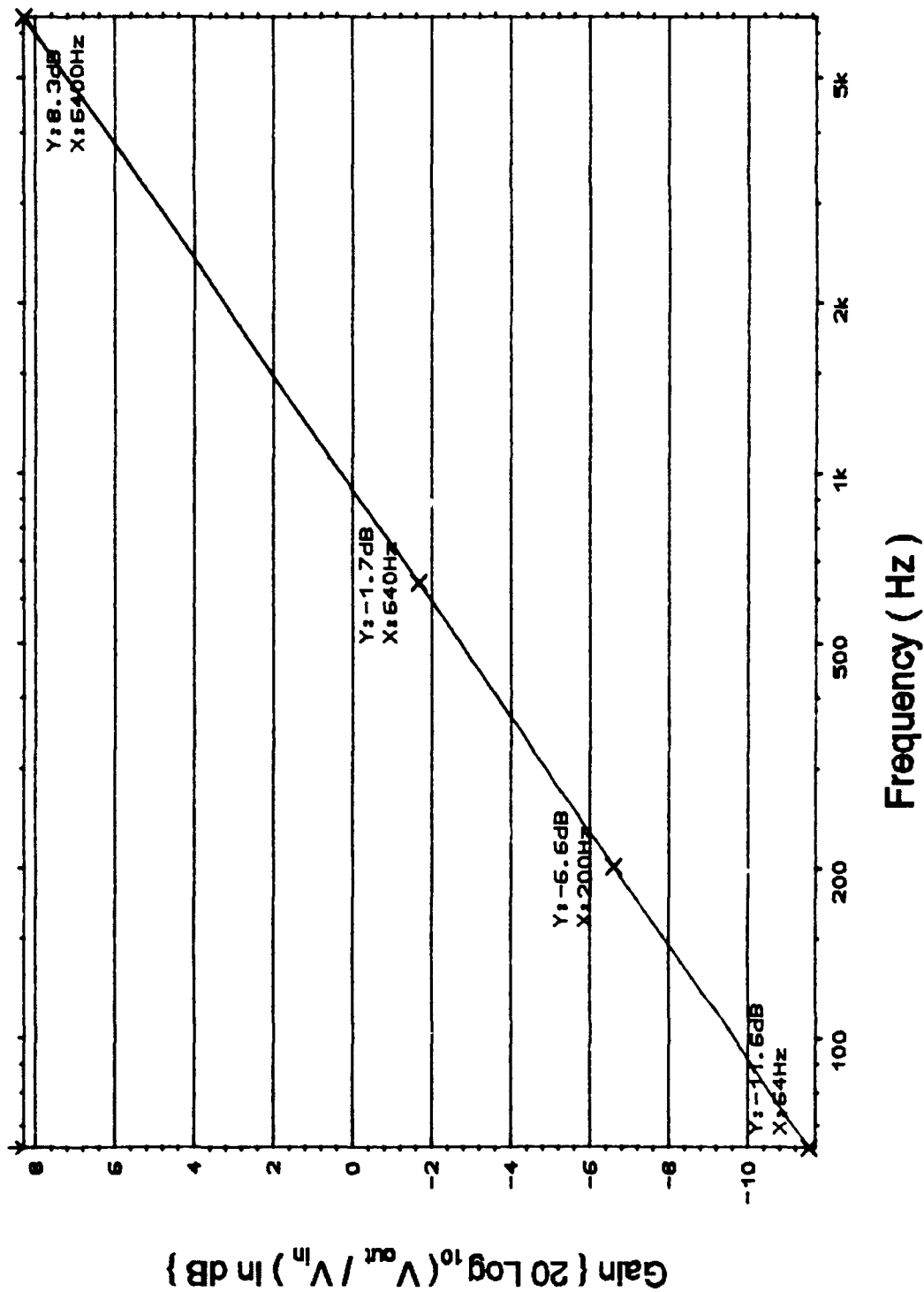
Figure J-5 (cont). Gain Response of the Oldfield Discrete Component Circuit.
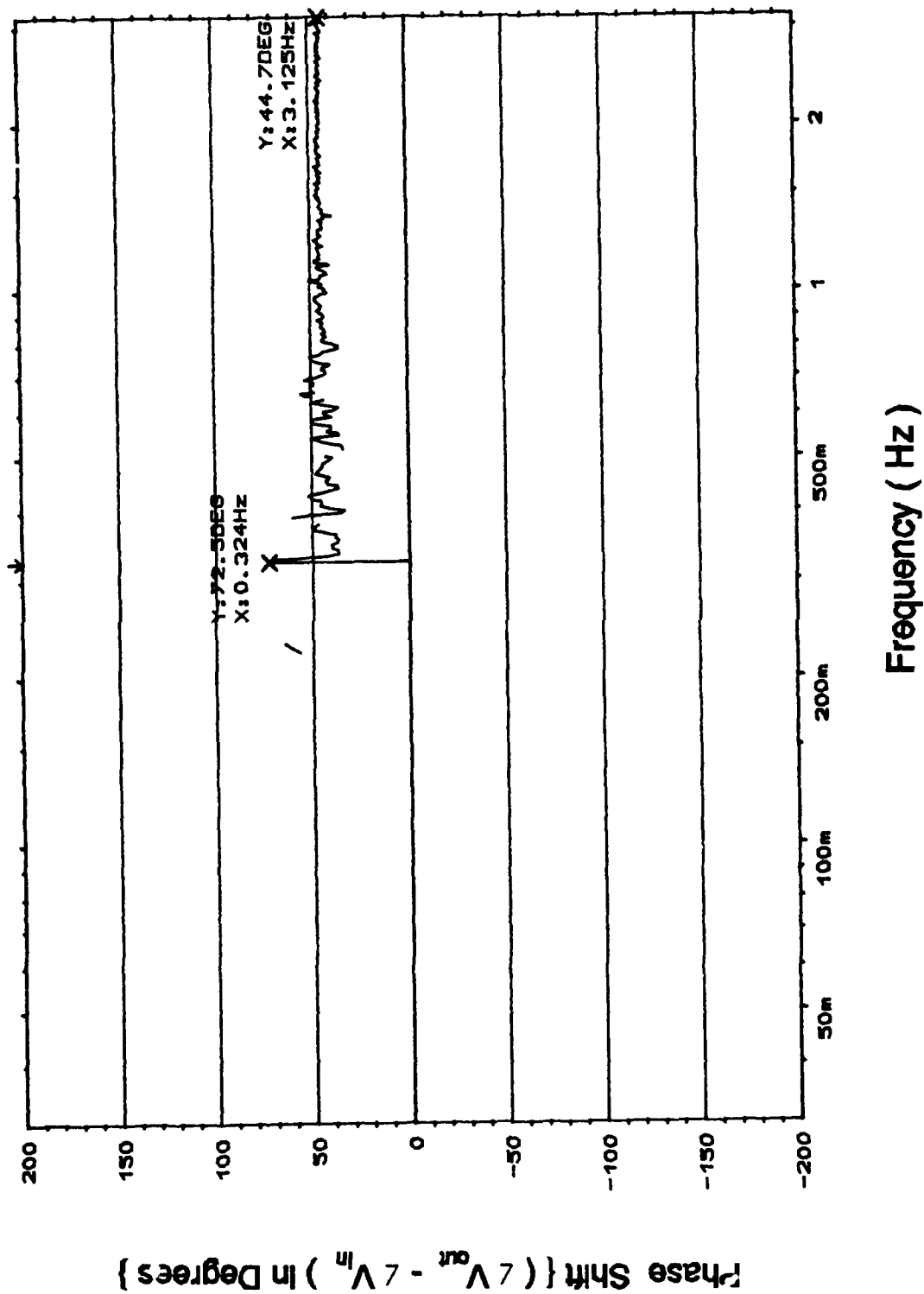
Figure J-6. Phase Response of the Oldfield Discrete Component Circuit (cont):
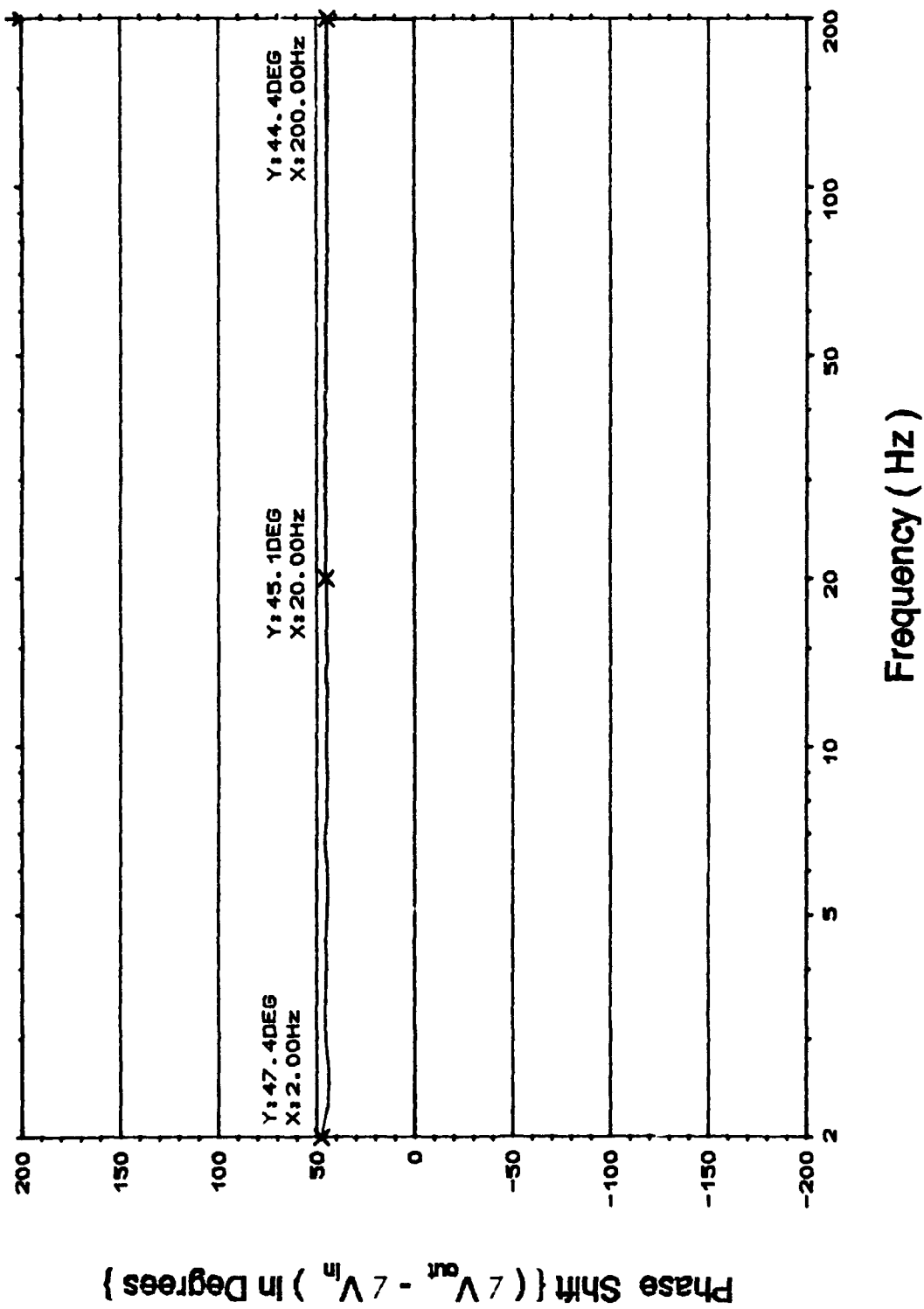
Figure J-6 (cont). Phase Response of the Oldfield Discrete Component Circuit (cont);
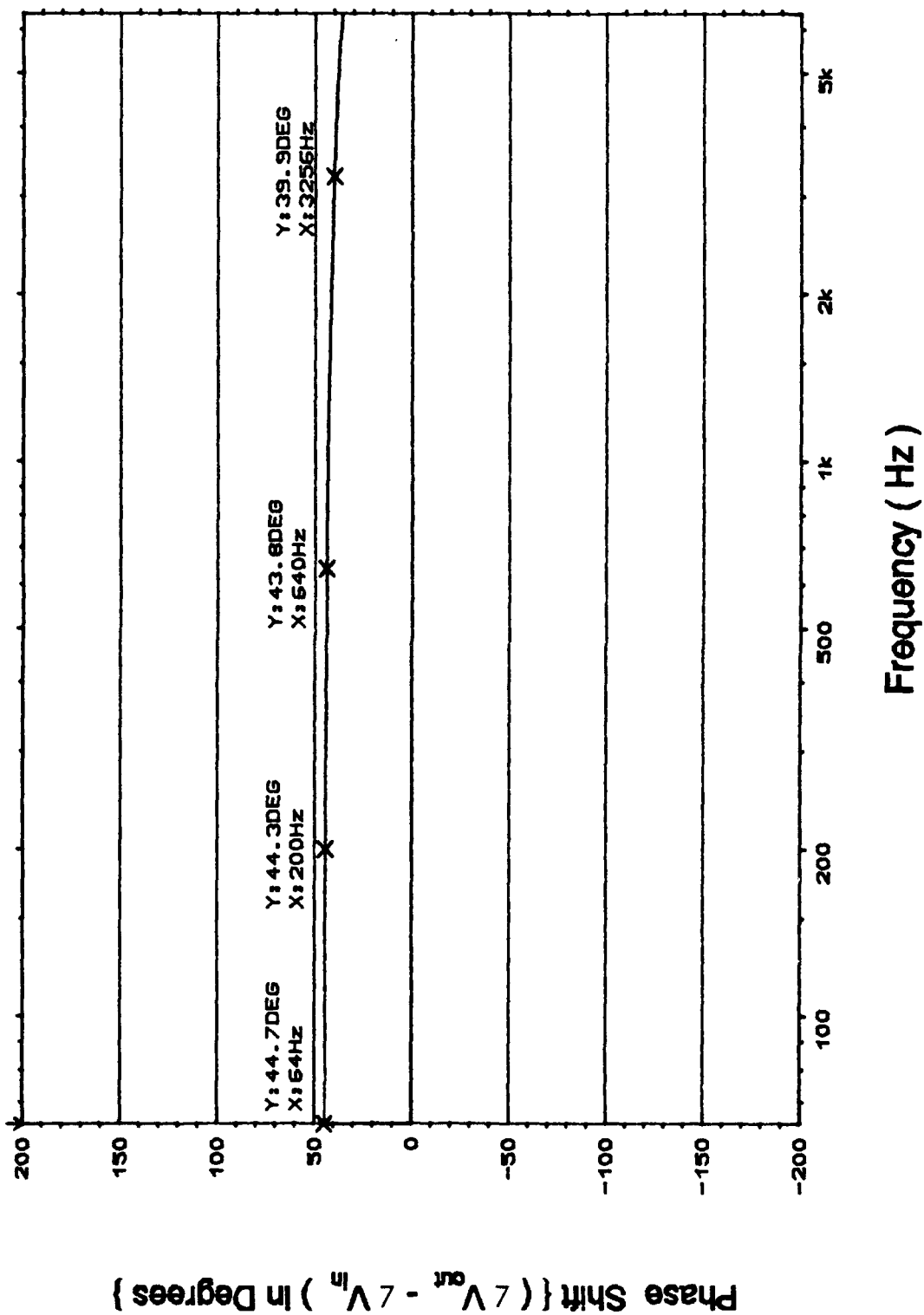
Figure J-6 (cont). Phase Response of the Oldfield Discrete Component Circuit.
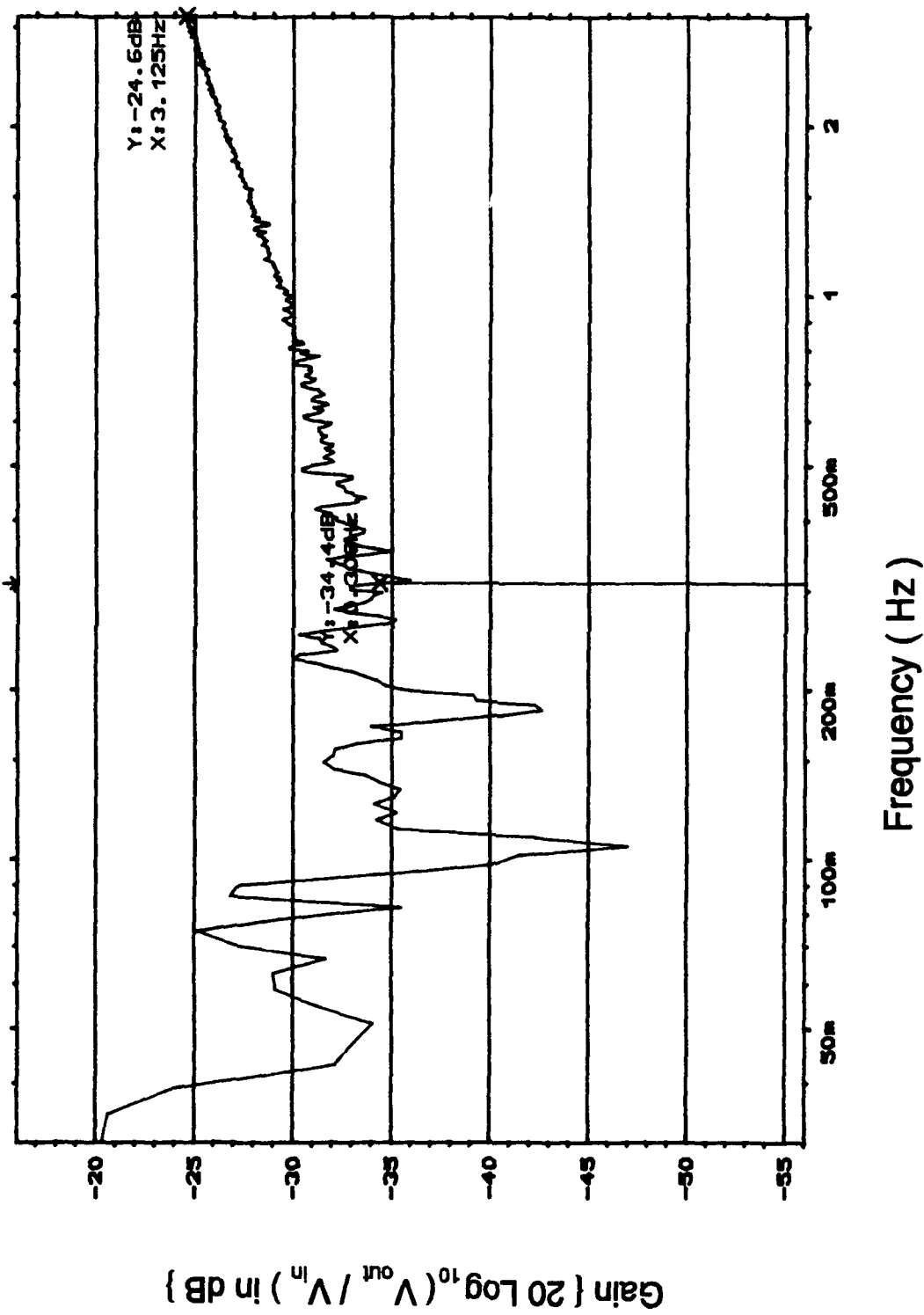
Figure J-7. Gain Response of the Oldfield Surface Mount Component Circuit (cont);
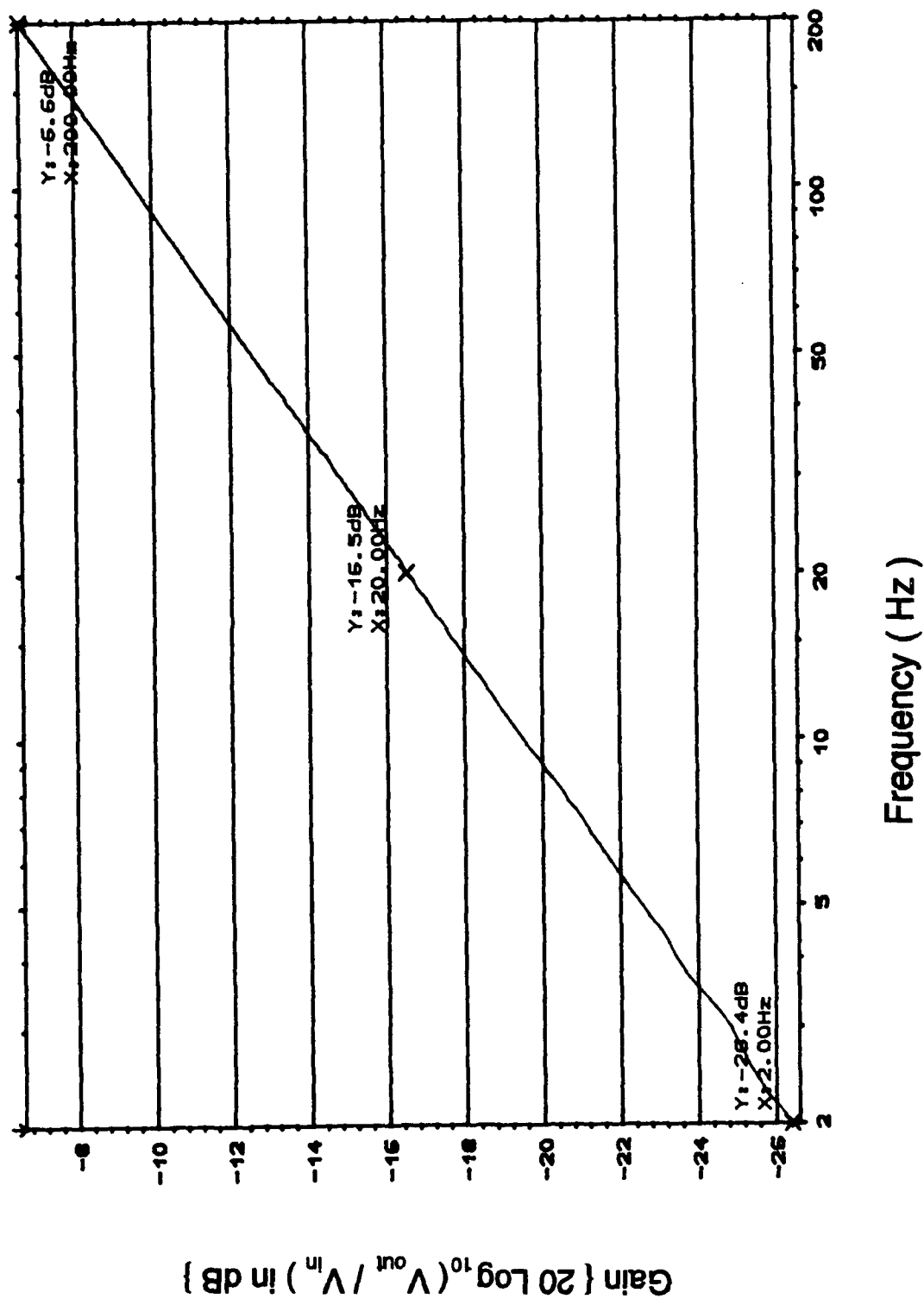
J-21

Figure J-7 (cont). Gain Response of the Oldfield Surface Mount Component Circuit (cont)
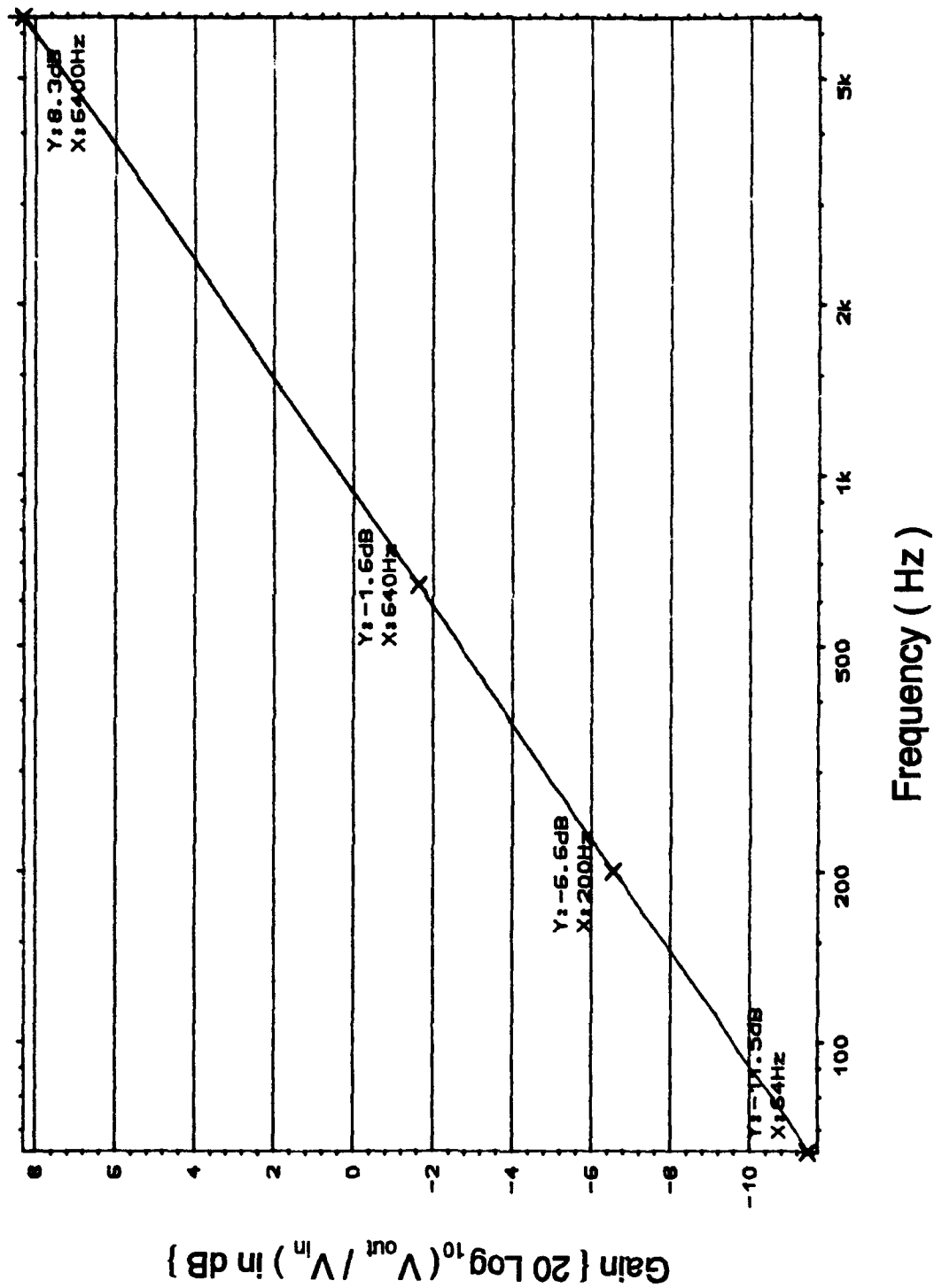
Figure J-7 (cont). Gain Response of the Oldfield Surface Mount Component Circuit.
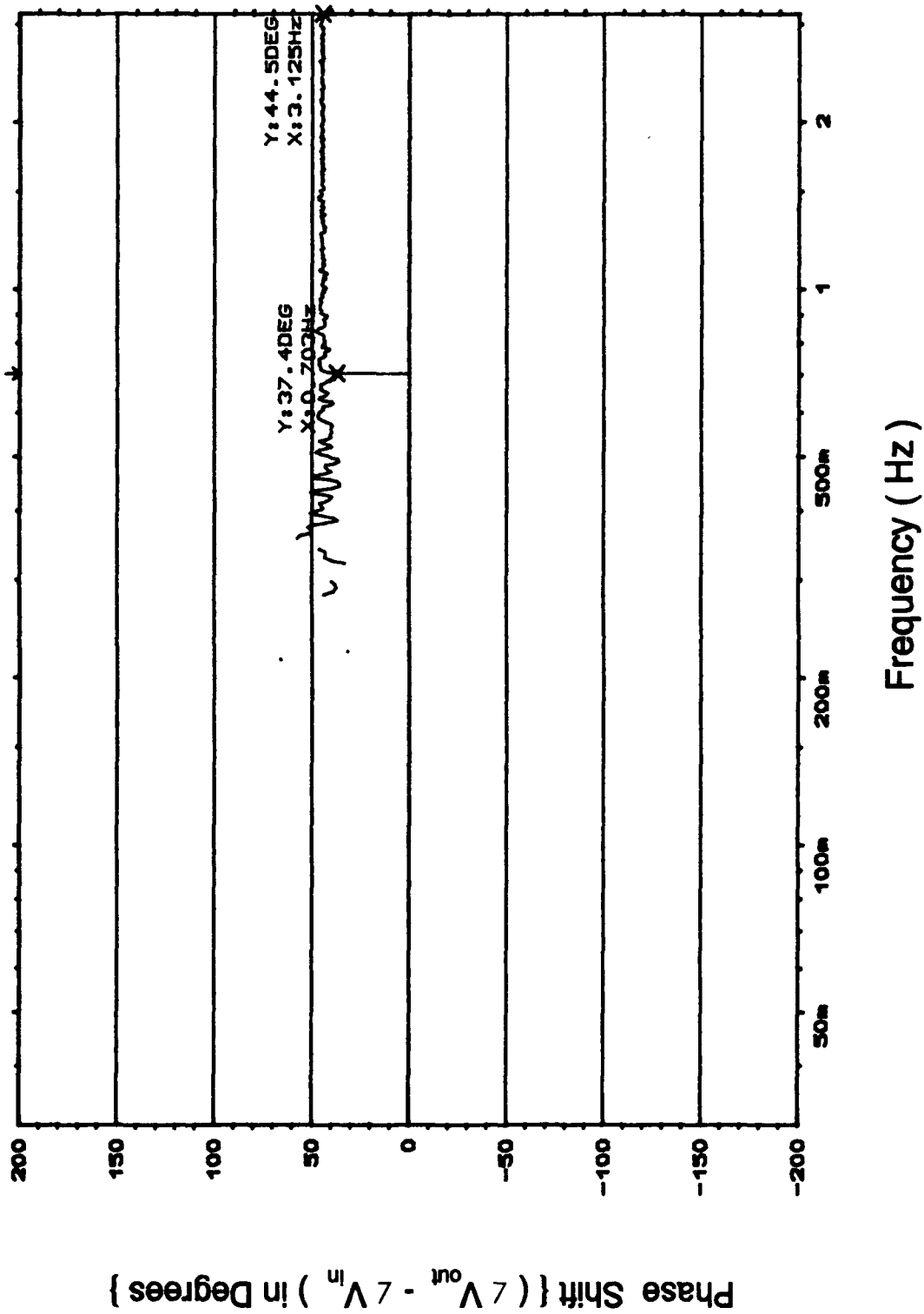
Figure J-8. Phase Response of the Oldfield Surface Mount Component Circuit (cont);
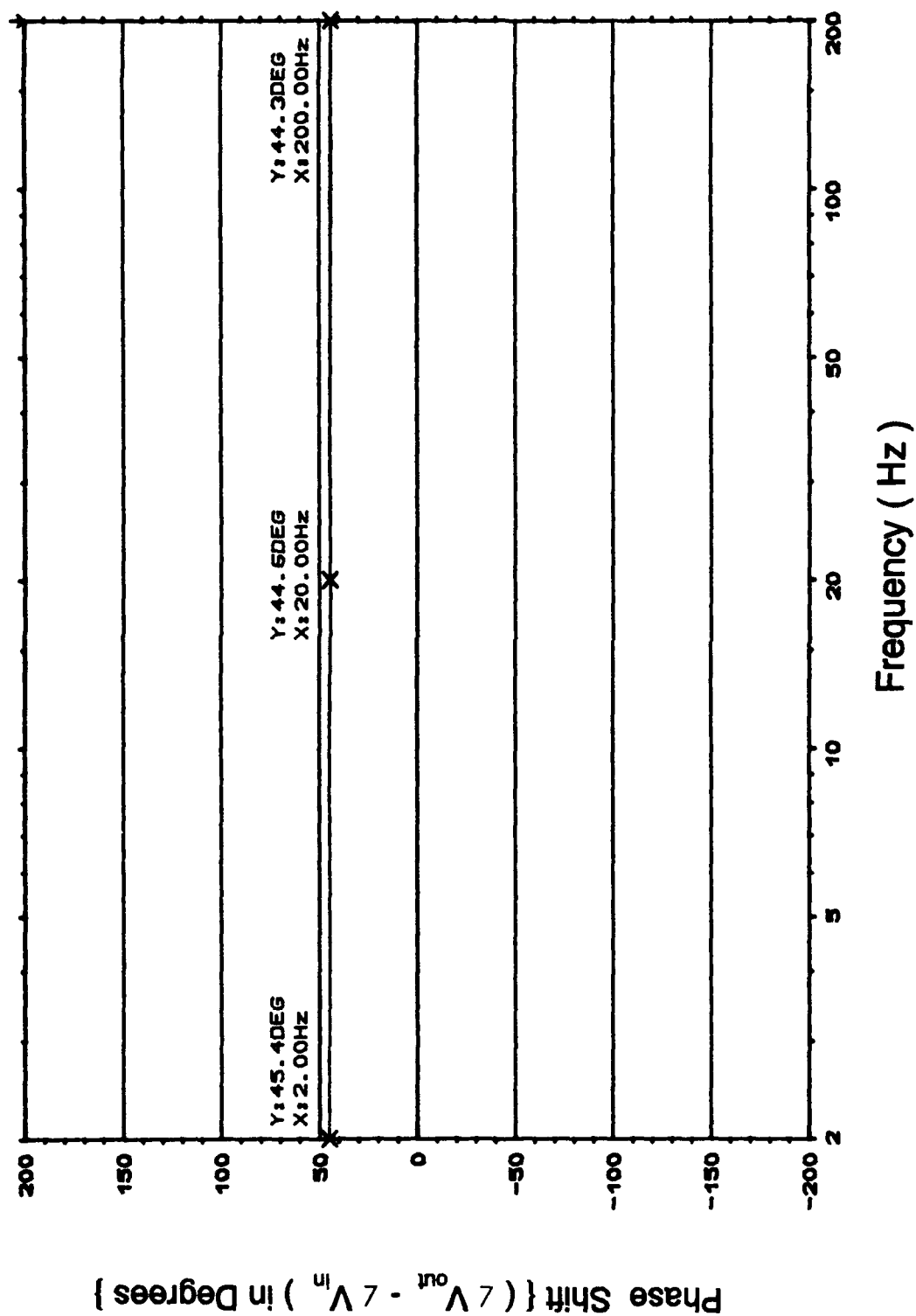
Figure J-8 (cont). Phase Response of the Oldfield Surface Mount Component Circuit (cont);
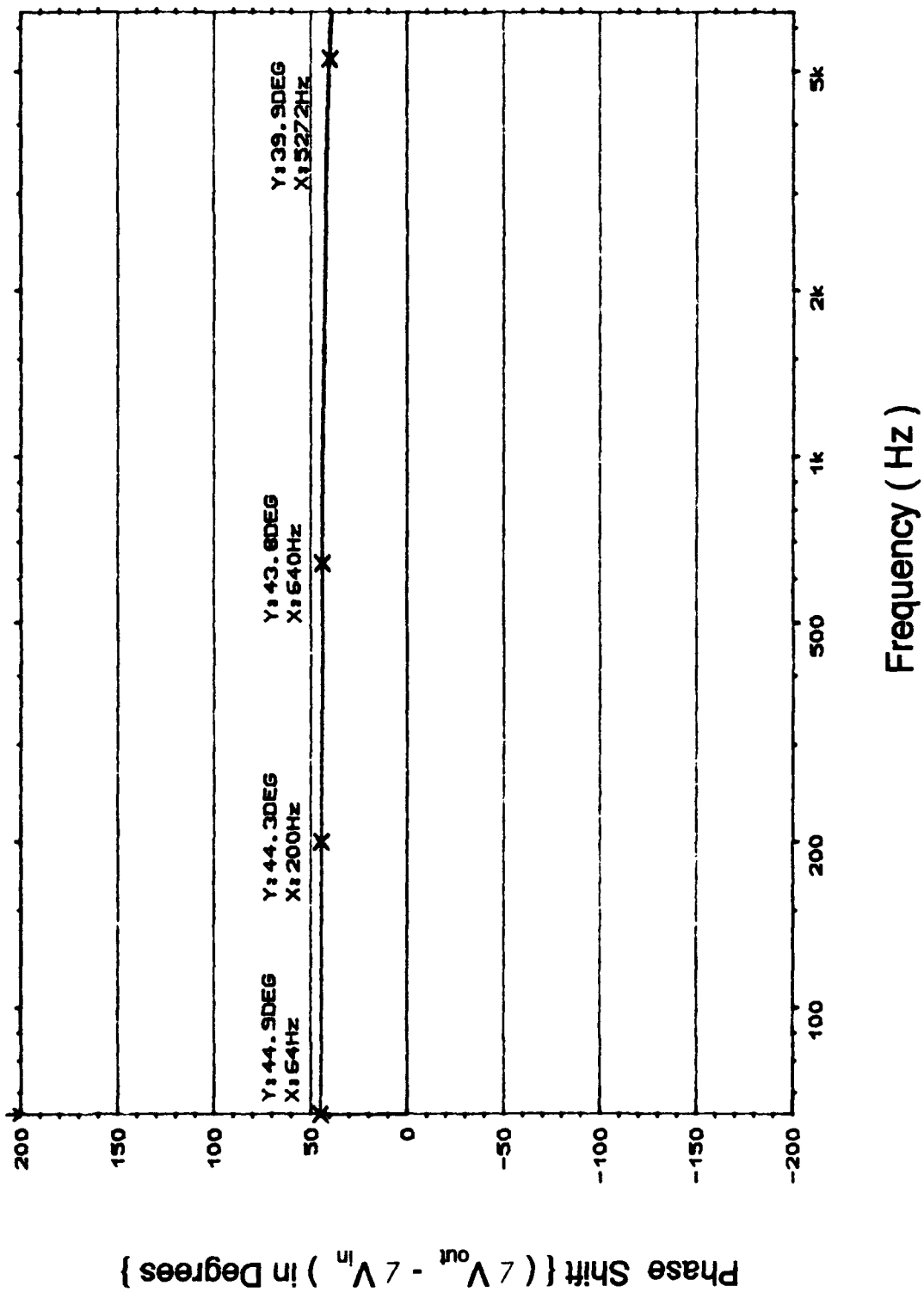
Figure J-8 (cont). Phase Response of the Oldfield Surface Mount Component Circuit.

Appendix K. Analysis of the Oldham Computer Simulation Results for the Oldham Circuit Design

This appendix records the detailed electrical performance of the Oldham circuit which resulted from the computer simulation data. (A helpful reminder for the reader -- the graphical form of this data is presented in Appendix B).

Oldham Circuit Component Value Variation. The value of each component was varied by the factors outlined in Chapter 5. The frequency interval undesirably affected by the component value's variance is recorded relative to the upper and lower design tolerance limits of the bode plot parameters (gain and phase).

Resistor R0. The value variation of resistor R0 had negligible effect on the phase response. Only at the 0.1 factor variation was there a deviation from the "ideal" performance response, and it only effected the frequency interval 0.01 Hz to 0.04 Hz. This effect was classified as being minimal, because the circuit's response was still well within the design tolerance criteria of $\pm$ 5 degrees for the phase shift. The value variation of R0 produced no detectable effect on the gain response.

Resistor R1. The value variation of resistor R1 had a negligible effect on the circuit's performance except at the 0.1 factor variation level. The circuit phase response was effected from 0.01 Hz to 0.1 Hz; however, the design

specifications were still satisfied. The value variation of resistor R1 also had no detectable effect on the circuit's gain response.

Resistor R2. The value variation of resistor R2 affected the phase response from 0.01 Hz to 0.52 Hz. At the 0.1 factor variation, the phase response did not satisfy the design specifications from 0.01 Hz to 0.52 Hz. The phase shift limits were -149 degrees at 0.01 to -140 degrees at 0.52 Hz. The 0.4 and 5.0 scaling factors also produced undesirable results. Specifically, at the 0.4 level the phase was undesirably affected from 0.01 Hz to 0.04 Hz with a phase shift variation range of -144 degrees to -140 degrees. At the 5.0 scaling factor, the undesirable effect spanned 0.01 Hz to 0.018 Hz and the phase response varied from --127 degrees to -130 degrees. Again, there was no detectable effect on the gain response.

Resistor R3. The value variation of resistor R3 had a more pronounced effect on the circuit's performance and degraded both the phase and gain responses. The frequency range affected spanned 0.01 Hz to 2 Hz. All variation factors produced responses in excess of the design tolerances with the most prominent effect being for the 0.1 scaling factor. The gain response was effected from 0.01 Hz to 0.3 Hz. However, the gain response slope was still within design specifications.

Resistor R4. The value variation of resistor R4 had an

undesirable frequency range effect that spanned 0.01 Hz to 10.5 Hz for the phase response and from 0.01 Hz to 1 Hz for the gain response. The phase response varied from -150 degrees to -116.1 degrees, while the gain response slope varied from 9.1 dB/decade to 10.6 dB/decade. All variation factors produced responses in excess of the design tolerances with the most prominent effect being for the 0.1 scaling factor.

Resistor R5. The value variation of resistor R5 affected the frequency range of 0.01 hz to 100 Hz for the phase response and from 0.02 hz to 6.5 Hz for the gain response. All variation factors produced responses in excess of the design tolerances with the most prominent effect being for the 5.0 scaling factor. The affected phase shift spanned -150 degrees to -116 degrees. The corresponding gain plot slope varied from 6.67 dB/decade to 12.33 dB/decade.

Resistor R6. The value variation of resistor R6 produced an undesirable effect for the phase shift over almost the entire frequency range of concern. The frequency interval affected spanned 0.01 Hz to 650 Hz, with a corresponding phase shift range of -115.9 degrees to -149 degrees. The undesirable gain plot frequency affect spanned 0.03 Hz to 35 Hz with a slope range of 8.9 dB/decade to 17 dB/decade. All variation factors produced responses in excess of the design tolerances with the most prominent

effect being from the 0.1 scaling factor for the phase shift and from the 5.0 scaling factor for the gain slope.

Resistor R7. The value variation of resistor R7 affected the frequency interval 0.01 Hz to 4 KHz for phase shift. The undesirable affect spanned 0.1 hz to 4 KHz with a corresponding phase shift of -116.5 degrees to -149.9 degrees. The gain response was only affected from 0.1 Hz to 450 Hz with a corresponding slope range of 6 dB/decade to 18 dB/decade. All variation factors produced responses in excess of the design tolerances with the most prominent effect being the from 0.1 scaling factor for the phase shift and from the 5.0 scaling factor for the gain slope.

Resistor R8. The value variation of resistor R8 affected the frequency interval 0.01 Hz to 4 KHz for phase shift. The undesirable effect spanned 0.1 Hz to 4 KHz with a corresponding phase shift of -116.5 degrees to -149.9 degrees. The gain response was undesirably affected from 0.2 Hz to 290 Hz with a corresponding slope range of 6.2 dB/decade to 19 dB/decade. All variation factors produced responses in excess of the design tolerances with the most prominent effect being from the 0.1 scaling factor for the phase shift and from the 5.0 scaling factor for the gain slope.

Resistors R9. The value variation of resistor R9 phase affected the frequency interval 0.2 Hz to 10 KHz for the phase shift. The undesirable effect spanned 8.2 Hz to 10

KHz with a corresponding phase shift range of -121 degrees to -144.9 degrees. The gain response was undesirably affected from 10 Hz to 10 KHz with a slope range of 9 dB/decade to 16 dB/decade. All variation factors produced responses in excess of the design tolerances with the most prominent effect being from the 5.0 scaling factor for the phase shift and from the 0.1 scaling factor for the gain slope.

Resistor R10. The value variation of resistor R10 affected the frequency interval 0.5 Hz to 10 KHz for the phase shift. The undesirable effect spanned 11 Hz to 10 KHz with a corresponding phase shift of -131.3 degrees to -150 degrees. The gain response was undesirably affected from 900 Hz to 10 KHz with a slope range of 5 dB/decade to 13.1 dB/decade. All variation factors produced responses in excess of the design tolerances with the most prominent effect being from the 5.0 scaling factor for the phase shift and from the 0.1 scaling factor for the gain slope.

Resistor R11. The value variation of resistor R11 affected the frequency interval 3 Hz to 2.5 KHz. The undesirable effect spanned 690 Hz to 1.3 KHz where the phase shift response dropped below -140 degrees. All variation factors produced responses in excess of the design tolerances with the most prominent effect being from the 5.0 scaling factor for the phase shift. The gain response was affected from 300 Hz to 10 KHz with a slope range of 9.1

dB/decade to 10.8 dB/decade (within design tolerances).

Resistor R12. The value variation of resistor R12 affected the frequency interval 4 Hz to 3.9 KHz. The undesirable effect spanned 195 Hz to 3.9 KHz, where the phase shift response dropped below -140 degrees. All variation factors produced responses in excess of the design tolerances with the most prominent effect being from the 5.0 scaling factor for the phase shift. The gain response was affected from 600 Hz to 10 KHz with a slope range of 9.8 dB/decade to 10.2 dB/decade (within design tolerances).

Capacitor C0. The value variation of capacitor C0 affected the frequency interval 0.01 Hz to 70 Hz for the phase shift response. The undesirable effect spanned 0.01 Hz to 0.41 Hz with a corresponding phase shift of -119 degrees to -130 degrees. The gain response was undesirably affected from 0.01 Hz to 0.41 Hz with a slope range of 6 dB/decade to 9.9 dB/decade. Only the 0.1 variation factor produced responses in excess of the design tolerances.

Capacitor C1. The value variation of capacitor C1 affected the frequency interval 0.01 Hz to 200 Hz for the phase shift response. The undesirable effect was from 0.01 Hz to 0.82 Hz with a corresponding phase shift of -121 degrees to -140 degrees. The gain response was undesirably affected from 0.01 to 0.6 Hz with a corresponding slope range of 9.2 dB/decade to 13.1 dB/decade. Only the 0.1 variation factor produced responses in excess of the design

tolerances.

Capacitor C2. The value variation of capacitor C2 affected the frequency interval 0.01 Hz to 700 Hz for the phase shift response. The undesirable effect spanned 0.01 Hz to 5.2 Hz with a corresponding phase shift of -121 degrees to -158 degrees. The gain response was undesirably affected from 0.01 Hz to 5.2 Hz with a corresponding slope range of 4.5 dB/decade to 14.9 dB/decade. Only the 1.6 variation factor did not produce responses in excess of the design tolerances with the most prominent effect being from the 0.1 scaling factor for the phase shift.

Capacitor C3. The value variation of capacitor C3 affected the frequency interval 0.01 Hz to 1 KHz for the phase response. The undesirable effect was from 0.01 Hz to 32 Hz with a corresponding phase shift range -120.5 degrees to -157.5 degrees. The gain response was undesirably affected from 0.02 Hz to 32 Hz with a slope range of 4.5 dB/decade to 13.1 dB/decade. All variation factors produced responses in excess of the design tolerances with the most prominent effect being from the 0.1 scaling factor for the phase shift.

Capacitor C4. The value variation of capacitor C4 affected the frequency interval 0.02 Hz to 4 KHz for the phase response. The undesirable effect also spanned 0.02 Hz to 4 KHz with a corresponding phase shift range of -120.4 degrees to -157.5 degrees. The gain response was

undesirably affected from 0.08 Hz to 300 Hz with a corresponding slope range of 3.0 dB/decade to 12.4 dB/decade. All variation factors produced responses in excess of the design tolerances with the most prominent effect being from the 0.1 scaling factor for the phase shift.

Capacitor C5. The value variation of capacitor C5 affected the frequency interval 0.042 Hz to 10 KHz for the phase response. The undesirable effect spanned 0.18 Hz to 10 KHz with a corresponding phase shift of -121 degrees to -158 degrees. The gain response was undesirably affected from 0.62 Hz to 2 KHz with a corresponding slope range of 3.1 dB/decade to 14.0 dB/decade. All variation factors produced responses in excess of the design tolerances with the most prominent effect being from the 0.1 scaling factor for the phase shift.

Capacitor C6. The value variation of capacitor C6 affected the frequency interval 0.3 Hz to 10 KHz for the phase response. The undesirable effect spanned 1.0 Hz to 10 KHz with a corresponding phase shift of -122 degrees to -157 degrees. The gain response was undesirably affected from 0.3 Hz to 10 KHz with a corresponding slope range of 3.9 dB/decade to 14 dB/decade. All variation factors produced responses in excess of the design tolerances with the most prominent effect being from the 0.1 scaling factor for the phase shift.

Capacitor C7. The value variation of capacitor C7
affected the frequency interval 0.36 Hz to 10 KHz for the
phase response. The undesirable effect spanned 1.0 Hz to 10
KHz with a corresponding phase shift of -122 degrees to
-158 degrees. The gain response was undesirably affected
from 3.6 Hz to 10 KHz with a corresponding slope range of
4.0 dB/decade to 13.9 dB/decade. All variation factors
produced responses in excess of the design tolerances with
the most prominent effect being from the 0.1 scaling factor
for the phase shift.

Capacitor C8. The value variation of capacitor C8
affected the frequency interval 0.3 Hz to 10 KHz for the
phase response. The undesirable effect spanned 1.1 Hz to 10
KHz with a corresponding phase shift of -122.8 degrees to
-157.5 degrees. The gain response was undesirably affected
from 4.0 Hz to 10 KHz with a corresponding slope range of
6.6 dB/decade to 12.9 dB/decade. All variation factors
produced responses in excess of the design tolerances with
the most prominent effect being from the 0.1 scaling factor
for the phase shift.

Capacitor C9. The value variation of capacitor C9
affected the frequency interval 90 Hz to 10 KHz for the
phase response. The undesirable effect spanned 200 Hz to 10
KHz with a corresponding phase shift of -124 degrees to -160
degrees. The gain response was undesirably affected from
800 Hz to 10 KHz with a corresponding slope range of 7.0

dB/decade to 12.0 dB/decade. All variation factors produced responses in excess of the design tolerances with the most prominent effect being from the 0.1 scaling factor for the phase shift.

Capacitor C10. The value variation of capacitor C10 affected the frequency interval 220 Hz to 10 KHz for the phase response. The undesirable effect spanned 1.2 KHz to 10 KHz with a corresponding phase shift of -140 degrees to -150 degrees. All variation factors produced responses in excess of the design tolerances with the most prominent effect being from the 0.1 scaling factor for the phase shift. The gain response was effect negligible.

Capacitor C11. The value variation of capacitor C11 had no detectable effect on either the phase shift or gain response.

Oldham Circuit Individual Cell Component Value Variation. The component values in each cell (resistor and capacitor pair) were varied by the factors outlined in Chapter 5. Each cell's dominant frequency is recorded along with the upper and lower limits of the bode plot parameters (gain and phase).

Cell 0. The value variation of the zeroth Cell's components affected the frequency interval 0.01 Hz to 5.8 Hz for the phase response. There was no detectable undesirable effect on the phase response, and the gain response frequency effect was also negligible.

Cell 1. The value variation of the first Cell's components affected the frequency interval 0.01 Hz to 7.0 Hz for the phase response. The undesirable effect spanned 0.01 Hz to 0.02 Hz with a corresponding phase shift of -127 degrees to -130 degrees. The gain response was undesirably affected from 0.01 Hz to 0.04 Hz with a corresponding slope range of 8.6 dB/decade to 9.9 dB/decade. Only the 0.4 variation factor produced responses in excess of the design tolerances.

Cell 2. The value variation of the second Cell's components affected the frequency interval 0.01 Hz to 30 Hz for the phase response. The undesirable effect spanned 0.01 Hz to 0.12 KHz with a corresponding phase shift of -127 degrees to -142 degrees. The gain response was undesirably affected from .01 Hz to 0.2 Hz with a corresponding slope range of 8.9 dB/decade to 11.1 dB/decade. Only the 0.4 and 0.5 variation factors produced responses in excess of the design tolerances.

Cell 3. The value variation of the third Cell's components affected the frequency interval 0.01 Hz to 300 Hz for the phase response. The undesirable effect spanned 0.01 Hz to 0.9 Hz with a corresponding phase shift of -126.5 degrees to -144 degrees. The gain response was undesirably affected from 0.01 Hz to 3.0 Hz with a corresponding slope range of 8.0 dB/decade to 12.0 dB/decade. All variation factors produced responses in excess of the design

tolerances with the most prominent effect being from the 0.4 scaling factor for the phase shift.

Cell 4. The value variation of the fourth Cell's components affected the frequency interval 0.01 Hz to 1 KHz for the phase response. The undesirable effect spanned 0.019 Hz to 5.0 Hz with a corresponding phase shift of -125 degrees to -144 degrees. The gain response was undesirably affected from 0.01 Hz to 20 Hz with a corresponding slope range of 7.0 dB/decade to 11.5 dB/decade. All variation factors produced responses in excess of the design tolerances with the most prominent effect being from the 0.4 scaling factor for the phase shift.

Cell 5. The value variation of the fifth Cell 's components affected the frequency interval 0.01 Hz to 3.0 KHz for the phase response. The undesirable effect spanned 0.1 Hz to 50 Hz with a corresponding phase shift of -127.5 degrees to -143 degrees. The gain response was undesirably affected from 0.04 Hz to 200 Hz with a corresponding slope range of 6.0 dB/decade to 12.9 dB/decade. All variation factors produced responses in excess of the design tolerances with the most prominent effect being from the 0.4 scaling factor for the phase shift.

Cell 6. The value variation of the sixth Cell's components affected the frequency interval 0.01 Hz to 10 KHz for the phase response. The undesirable effect spanned 0.7 Hz to 200 Hz with a corresponding phase shift of -127.5

degrees to -144 degrees. The gain response was undesirably affected from 0.1 Hz to 1 KHz with a corresponding slope range of 6.5 dB/decade to 12.0 dB/decade. All variation factors produced responses in excess of the design tolerances with the most prominent effect being from the 0.4 scaling factor for the phase shift.

Cell 7. The value variation of the seventh Cell's affected the frequency interval 0.03 Hz to 10 KHz for the phase response. The undesirable effect spanned 5.0 Hz to 900 Hz with a corresponding phase shift range of -128 degrees to -142.5 degrees. The gain response frequency effect was from 1.0 Hz to 2 KHz with a slope range of 7.0 dB/decade to 11.9 dB/decade. All variation factors produced responses in excess of the design tolerances with the most prominent effect being from the 0.4 scaling factor for the phase shift.

Cell 8. The value variation of the eighth Cell's components affected the frequency interval 0.08 Hz to 10 KHz for the phase response. The undesirable effect spanned 30 Hz to 10 KHz with a corresponding phase shift of -129.5 degrees to -150 degrees. The gain response was undesirably affected from 10 Hz to 10 KHz with a corresponding slope range of 7.5 dB/decade to 12.9 dB/decade. All variation factors produced responses in excess of the design tolerances with the most prominent effect being from the 0.4 scaling factor for the phase shift.

Cell 9. The value variation of the ninth Cell's components affected the frequency interval 0.08 Hz to 10 KHz for the phase response. The undesirable effect spanned 200 Hz to 10 KHz with a corresponding phase shift of -130 degrees to -150 degrees. The gain response was undesirably affected from 50 Hz to 10 KHz with a corresponding slope range of 6.2 dB/decade to 13.0 dB/decade. All variation factors produced responses in excess of the design tolerances with the most prominent effect being from the 0.4 scaling factor for the phase shift.

Cell 10. The value variation of the tenth Cell's components affected the frequency interval 2 Hz to 10 KHz for the phase shift response. The undesirable effect spanned 800 Hz to 10 KHz with a corresponding phase shift of -130 degrees to -150 degrees. The gain response was undesirably affected from 200 Hz to 10 KHz with a corresponding slope range of 5.0 dB/decade to 10.5 dB/decade. Only the 1.3, 1.33 and 1.8 variation factors produced responses in excess of the design tolerances.

Cell 11. Cell 11 had no detectable undesirable effect on either the phase shift or gain response.

Appendix L.   Analysis of the Computer Simulation
Results for the Oldfield Design

This appendix records the detailed effects relative to the
operating frequency which resulted from the Oldfield circuit
performance computer simulation data.   (A helpful reminder
for the reader; the graphical form of this data is presented
in Appendix C).

Oldfield Circuit Component Value Variation.   The value of
each component was varied by the factors outlined in Chapter
5.   The frequency interval undesirably affected by the
component value's variance is recorded relative to the upper
and lower design tolerance limits of the bode parameters
(gain and phase).

Resistor R1.   The value variation of resistor R1
affected the frequency interval 0.2 Hz to 10 KHz for the
phase response.   The undesirable effect spanned 62 Hz to 10
KHz with a corresponding phase shift of 20 degrees to 40
degrees.   The gain response was affected from 0.01 Hz to 10
KHz with a corresponding slope range of 7.8 dB/decade to
17.7 dB/decade.   All variation factors produced responses in
excess of the design tolerances with the most prominent
effect being the relative shift of the gain plots.

Resistor R2.   The value variation of resistor R2
affected the frequency interval 0.13 Hz to 10 KHz for the
phase response.   The undesirable effect spanned 8.0 Hz to 10

KHz with a corresponding phase shift of 33 degrees to 57 degrees. The gain response was undesirably affected from 3.0 Hz to 10 KHz with a corresponding slope range of 7.0 dB/decade to 16.0 dB/decade. All variation factors produced responses in excess of the design tolerances with the most prominent effect being from the 1.6 and 5.0 scaling factors for the phase shift.

Resistor R3. The value variation of resistor R3 affected the frequency interval 0.08 Hz to 10 KHz for the phase response. The undesirable effect spanned 2.0 Hz to 10 KHz with a corresponding phase shift range of 28 degrees to 61 degrees. The gain response was undesirably affected from 0.3 Hz to 5.0 KHz with a corresponding slope range of 8.9 dB/decade to 16.0 dB/decade. All variation factors produced responses in excess of the design tolerances with the most prominent effect being from the 0.1 and 5.0 scaling factors for the phase shift.

Resistor R4. The value variation of resistor R4 affected the frequency interval 0.05 Hz to 2.0 KHz for the phase response and the interval 0.1 Hz to 2.0 KHz for the gain response. The phase response varied from 33 degrees to 61 degrees. The corresponding gain response slope varied from 7.5 dB/decade to 15.0 dB/decade. All variation factors produced responses in excess of the design tolerances with the most prominent effect being from the 0.1 scaling factor for the phase shift and from the 5.0 scaling factor for the

gain slope.

Resistor R5. The value variation of resistor R5 affected the frequency interval 0.05 Hz to 2.0 KHz for phase the response and the interval 0.1 Hz to 500 Hz for the gain response. The phase response varied from 36 degrees to 61 degrees. The corresponding gain response slope varied from 7.0 dB/decade to 14.8 dB/decade. All variation factors produced responses in excess of the design tolerances with the most prominent effect being from the 5.0 scaling factor for the phase shift.

Resistor R6. The value variation of resistor R6 affected the frequency interval 0.05 Hz to 200 Hz for the phase response. The undesirable effect spanned 0.9 Hz to 70 Hz with a corresponding phase shift of 35.5 degrees to 61 degrees. The gain response was undesirably affected from 0.05 Hz to 60 Hz with a corresponding slope range of 7.5 dB/decade to 14.5 dB/decade. All variation factors produced responses in excess of the design tolerances with the most prominent effect being from the 5.0 scaling factor for the phase shift.

Resistor R7. The value variation of resistor R7 affected the frequency interval 0.05 Hz to 60 Hz for the phase response. The undesirable effect spanned 0.9 Hz to 18 Hz with a corresponding phase shift of 37 degrees to 61 degrees. The gain response was undesirably affected from 0.03 Hz to 20 Hz with a corresponding slope range of 5.0

dB/decade to 16 dB/decade. All variation factors produced responses in excess of the design tolerances with the most prominent effect being from the 5.0 scaling factor for the phase shift.

Resistor R8. The value variation of resistor R8 affected the frequency interval 0.05 Hz to 20 Hz for the phase response. The undesirable effect spanned 0.12 Hz to 3.0 Hz with a corresponding phase shift of 36.5 degrees to 61 degrees. The gain response was undesirably affected from 0.018 Hz to 4.0 Hz with a corresponding slope range of 7.0 dB/decade to 17 dB/decade. All variation factors produced responses in excess of the design tolerances with the most prominent effect being from the 5.0 scaling factor for the phase shift.

Resistor R9. The value variation of resistor R9 affected the frequency interval 0.05 Hz to 3 Hz for the phase response. The undesirable effect spanned 0.05 Hz to 0.64 Hz with a corresponding phase shift of 36 degrees to 60.5 degrees. The gain response was undesirably affected from 0.01 Hz to 0.9 Hz with a corresponding slope range of 8.8 dB/decade to 16 dB/decade. All variation factors produced responses in excess of the design tolerances with the most prominent effect being from the 0.1 and 5.0 scaling factors for the phase shift.

Capacitor C1. The value variation of capacitor C1 affected the frequency range was 0.4 Hz to 10 KHz for the

phase response. The undesirable effect spanned 11.4 Hz to 10 KHz with a corresponding phase shift of 20 degrees to 58 degrees. The gain response was undesirably affected from 10 Hz to 10 KHz with a corresponding slope range of 6.0 dB/decade to 10.5 dB/decade. All variation factors produced responses in excess of the design tolerances with the most prominent effect being from the 5.0 scaling factor for the phase response and from the 0.1 scaling factor for the gain slope.

Capacitor C2. The value variation of capacitor C2 affected the frequency interval 0.1 Hz to 10 KHz for the phase response. The undesirable effect spanned 5.7 Hz to 10 KHz with a corresponding phase shift of 20.5 degrees to 55 degrees. The gain response was undesirably affected from 7.0 Hz to 10 KHz with a corresponding slope range of 6.0 dB/decade to 12.2 dB/decade. All variation factors produced responses in excess of the design tolerances the with most prominent effect being from the 5.0 scaling factor for the phase response.

Capacitor C3. The value variation of capacitor C3 affected the frequency interval 0.05 Hz to 10 KHz for the phase response. The undesirable effect spanned 1.4 Hz to 4 KHz with a corresponding phase shift of 27 degrees to 54 degrees. The gain response was undesirably affected from 0.6 Hz to 3.0 KHz with a slope range of 8.9 dB/decade to 10.8 dB/decade. All variation factors produced responses in

excess of the design tolerances with the most prominent effect being from the 5.0 scaling factor for the phase response.

Capacitor C4. The value variation of capacitor C4 affected the frequency interval 0.05 Hz to 1.4 KHz for the phase response. The undesirable effect also spanned 0.4 Hz to 700 Hz with a corresponding phase shift range of 28 degrees to 54.5 degrees. The gain response was undesirably affected from 0.3 Hz to 700 Hz with a corresponding slope range of 6.0 dB/decade to 10.8 dB/decade. All variation factors produced responses in excess of the design tolerances with the most prominent effect being from the 5.0 scaling factor for the phase response.

Capacitor C5. The value variation of capacitor C5 affected the frequency interval 0.05 Hz to 500 Hz for the phase response. The undesirable effect spanned 0.05 Hz to 140 Hz with a corresponding phase shift range of 28 degrees to 54 degrees. The gain response was undesirably affected from 0.1 Hz to 160 Hz with a corresponding slope range of 7.0 dB/decade to 10.5 dB/decade. All variation factors produced responses in excess of the design tolerances with the most prominent effect being from the 5.0 scaling factor for the phase response.

Capacitor C6. The value variation of capacitor C6 affected the frequency interval 0.05 Hz to 100 Hz for the phase response. The undesirable effect spanned 0.05 Hz to

100 Hz with a corresponding phase shift of 28.5 degrees to 54.5 degrees. The gain response was undesirably affected from 0.01 Hz to 20 KHz with a corresponding slope range of 5.5 dB/decade to 17 dB/decade. All variation factors produced responses in excess of the design tolerances with the most prominent effect being from the 5.0 scaling factor for the phase response.

Capacitor C7. The value variation of capacitor C7 affected the frequency interval 0.05 Hz to 4 Hz for the phase response. The undesirable effect spanned 0.2 Hz to 6 Hz with a phase shift of 28.5 degrees to 54 degrees. The gain response frequency effect was from 0.01 Hz to 4 Hz with a slope range of 6.5 dB/decade to 19.3 dB/decade. All variation factors produced responses in excess of the design tolerances with the most prominent effect being from the 5.0 scaling factor for the phase response.

Capacitor C8. The value variation of capacitor C8 affected the frequency interval 0.05 Hz to 4 Hz for the phase response. The undesirable effect spanned 0.06 Hz to 1.2 Hz with a corresponding phase shift of 29 degrees to 53.8 degrees. The gain response was undesirably affected was 0.01 Hz to 2.0 Hz with a slope range of 6.5 dB/decade to 20 dB/decade. All variation factors produced responses in excess of the design tolerances with the most prominent effect being from the 5.0 scaling factor for the phase response.

Capacitor C9. The value variation of capacitor C9 affected the frequency interval 0.01 Hz to 2 Hz for the phase response. The undesirable effect spanned 0.01 Hz to 0.3 Hz with a corresponding phase shift of 29.5 degrees to 89 degrees. The gain response was undesirably affected from 0.01 Hz to 0.6 Hz with a slope range of 5.5 dB/decade to 20 dB/decade. All variation factors produced responses in excess of the design tolerances with the most prominent effect being from the 5.0 scaling factor for the phase response.

Oldfield Circuit Individual Cell Component Value Variation. The component values in each cell (resistor and capacitor pair) were varied by the factors outlined in Chapter 5. Each cells dominant frequency is recorded along with the upper and lower limits of bode plot parameters (gain and phase).

Cell 1. The value variation of the first Cell's components affected the frequency interval 0.08 Hz to 10 KHz for the phase response. The undesirable effect spanned 300 Hz to 10 KHz with a corresponding phase shift of 20 degrees to 52 degrees. The gain response was undesirably affected from 0.01 Hz to 10 KHz with a corresponding slope range of 8.8 dB/decade to 18 dB/decade. All variation factors produced responses in excess of the design tolerances with the most prominent effect being from the 1.8 scaling factor for the phase response.

Cell 2. The value variation of the second Cell 2's components affected the frequency interval 0.2 Hz to 10 KHz for the phase response. The undesirable effect spanned 80 Hz to 1.4 KHz with a corresponding phase shift range of 38.5 degrees to 51 degrees. The gain response was undesirably affected from 10 Hz to 10 KHz with a corresponding gain slope range of 8.0 dB/decade to 11 dB/decade. All variation factors produced responses in excess of the design tolerances with the most prominent effect being from the 1.8 scaling factor for the phase response.

Cell 3. The value variation of the third Cell's components affected the frequency interval 0.05 Hz to 10 KHz for the phase response. The undesirable effect spanned 620 Hz to 10 KHz with a corresponding phase shift of 20 degrees to 53 degrees. The gain response was undesirably affected from 1.0 Hz to 4.0 KHz with a corresponding gain slope range of 8.0 dB/decade to 11.8 dB/decade. All variation factors produced responses in excess of the design tolerances with the most prominent effect being from the 1.8 scaling factor for the phase response.

Cell 4. The value variation of the fourth Cell's components affected the frequency interval 0.05 Hz to 10 KHz for the phase response. The undesirable effect spanned 100 Hz to 1.2 KHz with a corresponding phase shift of 33 degrees to 54 degrees. The gain response was undesirably affected from 0.1 Hz to 1 KHz with a corresponding gain slope range

of 7.5 dB/decade to 10.5 dB/decade. All variation factors produced responses in excess of the design tolerances with the most prominent effect being from the 1.8 scaling factor for the phase response.

Cell 5. The value variation of the fifth Cell's components affected the frequency interval 0.05 Hz to 1.0 KHz for the phase response. The undesirable effect spanned 21 Hz to 200 Hz with a corresponding phase shift range of 34 degrees to 54 degrees. The gain response was undesirably affected from .09 Hz to 500 Hz with a corresponding gain slope range of 6.5 dB/decade to 12 dB/decade. All variation factors produced responses in excess of the design tolerances with the most prominent effect being from the 1.8 scaling factor for the phase response.

Cell 6. The value variation of the sixth Cell's components affected the frequency interval 0.05 Hz to 200 Hz for the phase response. The undesirable effect spanned 0.25 Hz to 82 Hz with a corresponding phase shift of 30 degrees to 50.5 degrees. The gain response was undesirably affected from 0.8 Hz to 100 Hz with a corresponding gain slope range of 5.5 dB/decade to 11 dB/decade. All variation factors produced responses in excess of the design tolerances with the most prominent effect being from the 1.8 scaling factor for the phase response.

Cell 7. The value variation of the seventh Cell's components affected the frequency interval 0.05 Hz to 130 Hz

for the phase response. The undesirable effect spanned 0.3 Hz to 62 Hz with a corresponding phase shift range of 30.5 degrees to 50.5 degrees. The gain response was undesirably affected from 0.05 Hz to 800 Hz with a corresponding gain slope range of 5.5 dB/decade to 11.5 dB/decade. All variation factors produced responses in excess of the design tolerances with the most prominent effect being from the 1.8 scaling factor for the phase response.

Cell 8. The value variation of the eighth Cell's components affected the frequency interval 0.05 Hz to 60 Hz for the phase response. The undesirable effect spanned 0.25 Hz to 82 Hz with a corresponding phase shift range of 30 degrees to 50.5 degrees. The gain response was undesirably affected from 0.01 Hz to 60 Hz with a corresponding gain slope range of 8.5 dB/decade to 14 dB/decade. All variation factors produced responses in excess of the design tolerances with the most prominent effect being from the 1.8 scaling factor for the phase response.

Cell 9. The value variation of the ninth Cell's components affected the frequency interval 0.05 Hz to 60 Hz for the phase response. The undesirable effect spanned 0.05 Hz to 52 Hz with a corresponding phase shift range of 37 degrees to 60 degrees. The gain response was undesirably affected from 0.01 Hz to 5.0 Hz with a corresponding gain slope range of 5.5 dB/decade to 14 dB/decade. All variation factors produced responses in excess of the design

tolerances with the most prominent effect being from the 1.8

scaling factor for the phase response.

Bibliography

1. Oldham Keith B. and Cynthia G. Zoski. "Analogue Instrumentation for the Process of Polarographic Data," _Journal of Electroanalytical Chemistry 157_: 27-51 (1983).

2. Oldfield M. L. et al. "Design of Wide-Bandwidth Analogue Circuits for Heat Transfer Instrumentation in Transient Tunnels", _16th Symposium of the International Centre for Heat and Mass Transfer (Heat and Mass Transfer in Rotating Machinery) Dubrovnik_, D. E. Metzger, Ed. Hemisphere Publishing Corp., NY, 1984, 233-258.

3. Klonoski, Capt Kevin D. _Fractional-Order Feedback in Linear Systems_, MS Thesis, AFIT/GA/ENY/88D-05, School of Engineering, Air Force Institute of Technology (AU), Wright-Patterson AFB, OH (Mar 1989).

4. Ross, Bertram. "Fractional Calculus," _Mathematics Magazine 50_: 115-122 (May 1977).

5. Fowler, Annelle F. _A Study of Fractional Calculus: Its Definitions and Properties_, PhD Dissertation, East Texas State University, TX, University Microfilms International, Ann Arbor, MI, document number 75-19, 970, (May 1975).

6. Torvik, P. J. and R. L. Bagley. "On the Appearance of the Fractional Derivative in the Behavior of Real Materials," _Journal of Applied Mechanics 51_: 234-238 (1984).

7. Walker, Capt Richard. _Linear Quadratic Control Theory for Viscoelastically Damped Structures Using a Fractional-Derivative Viscoelasticity Model_, MS Thesis, AFIT/GA/EN/88D-13, School of Engineering, Air Force Institute of Technology (AU), Wright-Patterson AFB, OH (Dec 1988).

8. Torvik, P. J. and R. L. Bagley. "Fractional Derivatives in the Description of Damping Materials and Phenomena," _The Role in Damping in Vibration and Noise Control, DE Vol 5, ASME Book No. H00405:_ 125-135, Edited by L. Rogers and J. C. Simonis, NY.

9. Bagley R. L. and P. J. Torvik. "Fractional Calculus - A Different Approach to the Analysis of Viscoelastically Damped Structures," _AIAA Journal 21:_ 741-748 (May 1983).

10. Bagley, R. L. <u>Applications of Generalized Derivatives to Viscoelasticity</u>, PhD Dissertation, AFIT/DS/AA/79S-2, School of Engineering, Air Force Institute of Technology (AU), Wright-Patterson AFB, OH (Jun 1979).

11. Bagley, R. L., and R. Calico. "The Fractional Order State Equations for the Control of Viscoelastically Damped Structures," <u>Proceedings of the 30th AIAA Structures, Structural Dynamics and Materials Conference:</u> 487-496 (April 1989).

12. Bagley, R. L. et al. "A New Approach to Modeling Unsteady Aerodynamic Forces," <u>Proceedings of the 29th Aerospace Sciences Meeting:</u> 1-10 (January 1991).

13. Millman, Jacob. <u>Microelectronics</u>, McGraw-Hill Book Co., NY, 1979.

14. Johnson, D. E. et al. <u>A Handbook of Active Filters</u>, Prentice-Hall Inc., Englewood Cliffs, NJ, 1980.

15. <u>HSPICE Users Manual</u>, Meta-Software Inc., Campbell, CA, 1990.

16. The MOSIS Project, USC/Information Sciences Institute, Marina del Rey, CA, Data Sheets (ID 33532, ID 33533), Fab ID N15SMA1, Fab ID N15SMB1, May 1991.

17. Weste, Neil H. E. and Kamran Eshraghian. <u>Principles of CMOS VLSI Design</u>, Addison-Wesley Publishing Co., Reading, MA., 1988.

18. Lindsey, Darryl. <u>The Design and Drafting of Printed Circuits</u>, Bishop Graphics Inc., Westlake, CA, 1982.

VITA

Captain Richard N. Hughes was born in a Borough of New York
City -- The Bronx. In 1971, he graduated as the class
Salutatorian from Vergennes Union High School, Vergennes,
Vermont. He enlisted in the Air Force in 1972 as an
Armament Systems Technician. During the next 12 1/2 years,
he was assigned various positions ranging from aircraft
technician and technical instructor to NCOIC of Loading
Standardization. His assignment locations spanning those
years included: 1972 - Griffiss AFB OH; 1974 - Utapao RTAFB
Thailand; 1975 - Loring AFB ME; 1978 - Spangdahlem AFB
Germany; 1981 - George AFB CA. During this time, he earned
two degrees -- an Associate of Science in Armament Systems
Technology from the Community College of the Air Force
(1983) and a Bachelor of Science in Aviation Management from
the Southern Illinois University (1985). In 1984, He earned
a scholarship through the Airmen Education and Commissioning
Program and began classes at the University of Lowell.
Subsequently, He graduated in 1987 Magna Cum Laude with a
Bachelor of Science degree in Electrical Engineering. He
received his commission through OTS in September 1987. He
was then assigned to Headquarters Air Force Logistics
Command (AFLC) as a project engineer. During this time, he
worked two major reorganizations of AFLC, developed the
technology insertion process for AFLC and worked as the
Executive Officer for the Deputy Chief of Staff for
Distribution. He entered the Air Force Institute of
Technology in June 1987.

permanent address: 2746 Coldsprings Drive

Beavercreek, OH 45434

VITA-1